# Guide to Instruments and Methods of Observation

## Volume I –Measurement of Meteorological Variables

2024 edition

WEATHER CLIMATE WATER

WORLD METEOROLOGICAL ORGANIZATION

WMO-No. 8

# Guide to Instruments and Methods of Observation

## Volume I –Measurement of Meteorological Variables

2024 edition



WORLD
METEOROLOGICAL
ORGANIZATION

WMO-No. 8

**EDITORIAL NOTE**

METEOTERM, the WMO terminology database, may be consulted at https://wmo.int/wmo-community/meteoterm.

Readers who copy hyperlinks by selecting them in the text should be aware that additional spaces may appear immediately following http://, https://, ftp://, mailto:, and after slashes (/), dashes (-), periods (.) and unbroken sequences of characters (letters and numbers). These spaces should be removed from the pasted URL. The correct URL is displayed when hovering over the link or when clicking on the link and then copying it from the browser.

WMO-No. 8

**© World Meteorological Organization, 2024**

The right of publication in print, electronic and any other form and in any language is reserved by WMO. Short extracts from WMO publications may be reproduced without authorization, provided that the complete source is clearly indicated. Editorial correspondence and requests to publish, reproduce or translate this publication in part or in whole should be addressed to:

Chair, Publications Board
World Meteorological Organization (WMO)
7 bis, avenue de la Paix
P.O. Box 2300
CH-1211 Geneva 2, Switzerland

Tel.: +41 (0) 22 730 84 03
Email: publications@wmo.int

ISBN 978-92-63-10008-5

NOTE

The designations employed in WMO publications and the presentation of material in this publication do not imply the expression of any opinion whatsoever on the part of WMO concerning the legal status of any country, territory, city or area, or of its authorities, or concerning the delimitation of its frontiers or boundaries.

The mention of specific companies or products does not imply that they are endorsed or recommended by WMO in preference to others of a similar nature which are not mentioned or advertised.

# CONTENTS


Page

**FOREWORD** ..... **xix**

**CHAPTER 1. GENERAL** ..... **1**
1.1 Meteorological observations ..... 1
1.1.1 General ..... 1
1.1.2 Representativeness ..... 2
1.1.3 Metadata ..... 3
1.2 Meteorological observing systems ..... 3
1.3 General requirements of a meteorological station ..... 3
1.3.1 Automatic weather stations ..... 4
1.3.2 Observers ..... 4
1.3.3 Siting and exposure ..... 5
1.3.3.1 Site selection ..... 5
1.3.3.2 Coordinates of the station ..... 7
1.3.3.3 Operating equipment in extreme environments ..... 7
1.3.4 Changes of instrumentation and homogeneity ..... 8
1.3.5 Inspection and maintenance ..... 8
1.3.5.1 Inspection of stations ..... 8
1.3.5.2 Maintenance ..... 8
1.4 General requirements of instruments ..... 9
1.4.1 Desirable characteristics ..... 9
1.4.2 Impact of the Minamata convention ..... 10
1.4.3 Mechanically recording instruments ..... 10
1.5 Measurement standards, traceability and units ..... 11
1.5.1 Definitions of standards of measurement ..... 11
1.5.2 Traceability assurance ..... 13
1.5.3 Symbols, units and constants ..... 13
1.5.3.1 Symbols and units ..... 13
1.5.3.2 Constants ..... 15
1.6 Uncertainty of measurements ..... 15
1.6.1 Meteorological measurements ..... 15
1.6.1.1 General ..... 15
1.6.1.2 Definitions of measurements and measurement errors ..... 15
1.6.1.3 Characteristics of instruments ..... 17
1.6.2 Sources and estimates of error ..... 18
1.6.3 The measurement uncertainties of a single instrument ..... 19
1.6.3.1 The statistical distributions of observations ..... 19
1.6.3.2 Estimating the true value ..... 20
1.6.3.3 Expressing the uncertainty ..... 22
1.6.3.4 Measurements of discrete values ..... 23
1.6.4 Accuracy requirements ..... 23
1.6.4.1 General ..... 23
1.6.4.2 Required and achievable performance ..... 24

Annex 1.A. Operational measurement uncertainty requirements and instrument performance requirements ..... 25

Annex 1.B. Strategy for traceability assurance ..... 35

Annex 1.C. Regional Instrument Centres ..... 42

Annex 1.D. Siting classifications for surface observing stations on land ..... 44

Annex 1.E. Operating equipment in extreme environments ..... 58

Annex 1.F. Station exposure description ..... 79

Annex 1.G. Measurement quality classifications for surface observing stations on land ..... 81

References and further reading ..... 88

*Page*

**CHAPTER 2. MEASUREMENT OF TEMPERATURE ..... 90**
2.1 General ..... 90
2.1.1 Definition ..... 90
2.1.2 Units and scales ..... 90
2.1.3 Meteorological requirements ..... 91
2.1.3.1 General ..... 91
2.1.3.2 Measurement uncertainty ..... 91
2.1.3.3 Response times ..... 91
2.1.3.4 Recording the circumstances in which measurements are taken ..... 91
2.1.4 Methods of measurement and observation ..... 92
2.1.4.1 General measurement principles ..... 92
2.1.4.2 General exposure requirements ..... 93
2.1.4.3 Sources of error – general comments ..... 94
2.1.4.4 Maintenance – general comments ..... 95
2.1.4.5 Implications of the Minamata Convention for temperature measurement ..... 96
2.2 Electrical thermometers ..... 96
2.2.1 General description ..... 96
2.2.1.1 Metal resistance thermometers ..... 96
2.2.1.2 Thermistors ..... 98
2.2.1.3 Thermocouples ..... 100
2.2.2 Measurement procedures ..... 101
2.2.2.1 Electrical resistance thermometers ..... 101
2.2.2.2 Thermocouples ..... 102
2.2.3 Exposure and siting ..... 103
2.2.4 Sources of error ..... 104
2.2.4.1 Electrical resistance thermometers ..... 104
2.2.4.2 Thermocouples ..... 104
2.2.5 Comparison and calibration ..... 105
2.2.5.1 Electrical resistance thermometers ..... 105
2.2.5.2 Thermocouples ..... 105
2.2.6 Corrections ..... 105
2.2.7 Maintenance ..... 106
2.3 Liquid-in-glass thermometers ..... 107
2.3.1 General description ..... 107
2.3.1.1 Ordinary (station) thermometers ..... 108
2.3.1.2 Maximum thermometers ..... 108
2.3.1.3 Minimum thermometers ..... 108
2.3.1.4 Soil thermometers ..... 108
2.3.2 Measurement procedures ..... 109
2.3.2.1 Reading ordinary thermometers ..... 109
2.3.2.2 Measuring grass minimum temperatures ..... 109
2.3.3 Thermometer siting and exposure ..... 110
2.3.4 Sources of error in liquid-in-glass thermometers ..... 110
2.3.4.1 Elastic errors ..... 110
2.3.4.2 Errors caused by the emergent stem ..... 110
2.3.4.3 Parallax and gross reading errors ..... 111
2.3.4.4 Errors due to differential expansion ..... 111
2.3.4.5 Errors associated with spirit thermometers ..... 111
2.3.5 Comparison and calibration in the field and laboratory ..... 112
2.3.5.1 Laboratory calibration ..... 112
2.3.5.2 Field checks ..... 112
2.3.6 Corrections ..... 113
2.3.7 Maintenance ..... 113
2.3.7.1 Breakage in the liquid column ..... 113
2.3.7.2 Scale illegibility ..... 114
2.3.8 Safety ..... 114

*Page*

2.4 Mechanical thermographs . . . 114
2.4.1 General description . . . 114
2.4.1.1 Bimetallic thermograph . . . 114
2.4.1.2 Bourdon-tube thermograph . . . 114
2.4.2 Measurement procedures . . . 115
2.4.3 Exposure and siting . . . 115
2.4.4 Sources of error . . . 115
2.4.5 Comparison and calibration . . . 115
2.4.5.1 Laboratory calibration . . . 115
2.4.5.2 Field comparison . . . 115
2.4.6 Corrections . . . 116
2.4.7 Maintenance . . . 116
2.5 Radiation shields . . . 116
2.5.1 Louvred screens . . . 117
2.5.2 Other artificially ventilated shields . . . 118
2.6 Traceabilitty assurance and calibration . . . 118

Annex. Defining the fixed points of the International Temperature Scale of 1990 . . . 120

References and further reading . . . 121

**CHAPTER 3. MEASUREMENT OF ATMOSPHERIC PRESSURE . . . 124**
3.1 General . . . 124
3.1.1 Definition . . . 124
3.1.2 Units and scales . . . 124
3.1.3 Meteorological requirements . . . 124
3.1.4 Methods of measurement and observation . . . 125
3.1.4.1 General measurement principles . . . 125
3.1.4.2 General exposure requirements . . . 125
3.1.4.3 Sources of error: general comments . . . 126
3.1.4.4 Maintenance: general comments . . . 127
3.1.4.5 Implications of the Minamata Convention for pressure measurement . . . 127
3.2 Electronic barometers . . . 128
3.2.1 Integrated-circuit-based variable capacitive sensors . . . 128
3.2.2 Digital piezoresistive barometers . . . 128
3.2.3 Cylindrical resonator barometers . . . 129
3.2.4 Aneroid displacement transducers . . . 129
3.2.5 Exposure of electronic barometers . . . 130
3.2.6 Reading electronic barometers . . . 130
3.2.7 Sources of error . . . 130
3.2.7.1 Drift between calibrations . . . 130
3.2.7.2 Temperature . . . 131
3.2.7.3 Electrical interference . . . 131
3.2.7.4 Nature of operation . . . 131
3.3 Aneroid barometers . . . 131
3.3.1 Construction requirements . . . 131
3.3.2 Achievable measurement uncertainty . . . 132
3.3.3 Exposure of aneroid barometers . . . 132
3.3.4 Reading aneroid barometers . . . 132
3.3.4.1 Accuracy of readings . . . 132
3.3.4.2 Reductions applied to barometers . . . 132
3.3.5 Sources of error . . . 132
3.3.5.1 Incomplete compensation for temperature . . . 132
3.3.5.2 Elasticity errors . . . 133
3.4 Barographs . . . 133
3.4.1 General requirements . . . 133
3.4.2 Construction of barographs . . . 134
3.4.3 Exposure of barographs . . . 134

*Page*

3.4.4 Sources of error . . . 134
3.4.5 Reading a barograph . . . 134
3.4.5.1 Accuracy of readings . . . 134
3.4.5.2 Corrections to be applied to barograph readings . . . 135
3.4.5 Transport . . . 135
3.5 Barometric change and Pressure tendency . . . 135
3.5.1 Pressure tendency and pressure tendency characteristics . . . 135
3.5.2 Measurement of a barometric change . . . 135
3.6 Traceability assurance and calibration . . . 135
3.6.1 General comments . . . 135
3.6.2 Laboratory calibration . . . 136
3.6.2.1 General equipment set-up . . . 136
3.6.2.2 Laboratory standards . . . 137
3.6.2.3 Method of calibration . . . 140
3.6.3 Field inspections . . . 141
3.7 Adjustment of barometer readings to standard and other levels . . . 142
3.7.1 Standard levels . . . 142
3.7.2 General reduction formula . . . 142
3.7.3 Reduction formula for low-level stations . . . 143

Annex 3.A. Methods of measurement with mercury barometers . . . 144

Annex 3.B. Correction of mercury barometer readings to standard conditions . . . 153

References and further reading . . . 157

**CHAPTER 4. MEASUREMENT OF HUMIDITY . . . 158**
4.1 General . . . 158
4.1.1 Definitions . . . 158
4.1.2 Units and scales . . . 158
4.1.3 Meteorological requirements . . . 159
4.1.4 Methods of measurement and observation . . . 159
4.1.4.1 Overview of general measurement principles . . . 159
4.1.4.4 Maintenance: general comments . . . 163
4.1.5 Implications of the Minamata Convention for humidity measurement . . . 164
4.2 Electrical capacitance hygrometers . . . 164
4.2.1 General considerations . . . 164
4.2.2 Electrical capacitance hygrometer . . . 164
4.2.3 Observation procedure . . . 165
4.2.4 Exposure and siting . . . 165
4.2.5 Sources of error . . . 165
4.2.6 Calibration and field inspection . . . 166
4.2.7 Maintenance . . . 167
4.3 The psychrometer . . . 167
4.3.1 General considerations . . . 167
4.3.1.1 Psychrometric formulae . . . 167
4.3.1.2 The specification of a psychrometer . . . 168
4.3.1.3 The wet-bulb sleeve . . . 168
4.3.1.4 Operation of the wet bulb below freezing . . . 169
4.3.1.5 General procedure for making observations . . . 170
4.3.1.6 Use of electrical resistance thermometers . . . 170
4.3.1.7 Psychrometric formulae and tables . . . 170
4.3.1.8 Sources of error in psychrometry . . . 171
4.3.2 Assmann and other aspirated psychrometers . . . 172
4.3.2.1 Description . . . 172
4.3.2.2 Observation procedure . . . 173
4.3.2.3 Exposure and siting . . . 173
4.3.2.4 Calibration . . . 173
4.3.2.5 Maintenance . . . 174

*Page*

4.3.3 Screen psychrometer . . . 175
4.3.3.1 Description . . . 175
4.3.3.2 Observation procedure . . . 175
4.3.3.3 Exposure and siting . . . 176
4.3.3.4 Calibration . . . 176
4.3.3.5 Maintenance . . . 176
4.3.4 Sling or whirling psychrometers . . . 176
4.3.4.1 Description . . . 176
4.3.4.2 Observation procedure . . . 177
4.4 The chilled-mirror dew-point hygrometer . . . 177
4.4.1 General considerations . . . 177
4.4.1.1 Theory . . . 177
4.4.1.2 Principles . . . 177
4.4.2 Description . . . 178
4.4.2.1 Sensor assembly . . . 178
4.4.2.2 Optical detection assembly . . . 178
4.4.2.3 Thermal control assembly . . . 178
4.4.2.4 Temperature display system . . . 179
4.4.2.5 Instrument format . . . 179
4.4.2.6 Auxiliary systems . . . 179
4.4.3 Observation procedure . . . 180
4.4.4 Exposure and siting . . . 180
4.4.5 Calibration and field inspection . . . 181
4.4.5.1 Calibration . . . 181
4.4.5.2 Field inspection . . . 181
4.5 Hygrometers using absorption of electromagnetic radiation . . . 182
4.6 The hair hygrograph . . . 182
4.6.1 General considerations . . . 182
4.6.2 Description . . . 183
4.6.3 Observation procedure . . . 183
4.6.4 Exposure and siting . . . 184
4.6.5 Sources of error . . . 184
4.6.5.1 Changes in zero offset . . . 184
4.6.5.2 Errors due to contamination of the hair . . . 184
4.6.5.3 Hysteresis . . . 184
4.6.6 Calibration and field inspection . . . 184
4.6.7 Maintenance . . . 185
4.7 Traceability assurance and calibration . . . 185
4.7.1 Principles involved in the calibration of hygrometers . . . 185
4.7.2 Primary standards . . . 185
4.7.2.1 Gravimetric hygrometry . . . 185
4.7.2.2 Dynamic two-pressure standard humidity generator . . . 187
4.7.2.3 Dynamic two-temperature standard humidity generator . . . 187
4.7.3 Secondary standards . . . 187
4.7.4 Working standards (and field reference instruments) . . . 187
4.7.5 Salt solutions . . . 188
4.7.6 Calibration methods . . . 189
4.7.6.1 General comments . . . 189
4.7.6.2 Laboratory calibration . . . 189
4.7.6.3 Field calibration . . . 190
4.8 Time constants, Protective filters and Safety . . . 190
4.8.1 Time constants of humidity sensors . . . 190
4.8.2 Protective filters . . . 191
4.8.3 Safety . . . 192

Annex 4.A. Definitions and specifications of water vapour in the atmosphere . . . 193

*Page*

Annex 4.B. Formulae for the computation of measures of humidity . . . . . 197
Annex 4.C. Instruments and methods in limited use, or no longer used. . . . . 199
References and further reading. . . . . 204

**CHAPTER 5. MEASUREMENT OF SURFACE WIND . . . . . 205**
5.1 General. . . . . 205
5.1.1 Definitions . . . . . 205
5.1.2 Units and scales . . . . . 206
5.1.3 Meteorological requirements . . . . . 206
5.1.4 Methods of measurement and observation . . . . . 207
5.2 Estimation of wind . . . . . 208
5.2.1 Wind speed . . . . . 208
5.2.2 Wind direction . . . . . 209
5.2.3 Wind fluctuations . . . . . 209
5.3 Simple instrumental methods . . . . . 209
5.3.1 Wind speed . . . . . 209
5.3.2 Wind direction . . . . . 209
5.4 Cup and propeller sensors . . . . . 209
5.5 Wind-direction vanes . . . . . 210
5.6 Other wind sensors. . . . . 211
5.7 Sensors and sensor combinations for component resolution . . . . . 211
5.8 Data-processing methods . . . . . 212
5.8.1 Averaging . . . . . 212
5.8.2 Peak gusts and standard deviations . . . . . 213
5.8.3 Recommendations for the design of wind-measuring systems . . . . . 214
5.9 Exposure of wind instruments . . . . . 214
5.9.1 General problems . . . . . 214
5.9.2 Anemometers over land. . . . . 215
5.9.3 Anemometers at sea . . . . . 216
5.9.4 Exposure correction . . . . . 217
5.10 Calibration and maintenance . . . . . 218

Annex. The effective roughness length . . . . . 219

References and further reading. . . . . 221

**CHAPTER 6. MEASUREMENT OF PRECIPITATION . . . . . 223**
6.1 General . . . . . 223
6.1.1 Definitions . . . . . 223
6.1.2 Units, scales, resolution, integration periods and observation times . . . . . 224
6.1.3 Methods of measurement . . . . . 224
6.2 Types of Instruments . . . . . 225
6.2.1 Non-recording (manual) precipitation gauges . . . . . 225
6.2.1.1 Calibration, field verification and maintenance . . . . . 228
6.2.1.2 Sources of error and corrections . . . . . 228
6.2.2 Weighing (automated) gauges . . . . . 229
6.2.2.1 Description of technology. . . . . 229
6.2.2.2 Calibration, field verification and maintenance . . . . . 231
6.2.2.3 Sources of error and corrections . . . . . 232
6.2.3 Tipping buckets . . . . . 233
6.2.3.1 Description of technology. . . . . 233
6.2.3.2 Sources of error and corrections . . . . . 234
6.2.3.3 Calibration, field verification and maintenance . . . . . 235
6.2.4 Float gauge . . . . . 236

*Page*

6.2.5 Non-catching technologies . . . 237
6.2.5.1 Optical instruments . . . 237
6.2.5.2 Impact instruments . . . 238
6.2.5.3 Radar instruments . . . 238
6.2.5.4 Field verification . . . 239
6.2.5.5 Other operational considerations . . . 239
6.3 Challenges of measuring precipitation . . . 239
6.3.1 Solid precipitation . . . 239
6.3.1.1 Undercatch . . . 239
6.3.1.2 Capping . . . 240
6.3.1.3 Use of antifreeze and oil . . . 243
6.3.2 Liquid precipitation . . . 246
6.3.2.1 Undercatch due to wind . . . 246
6.3.2.2 Evaporation and wetting loss . . . 246
6.3.2.3 Clogging . . . 247
6.3.2.4 Splashing . . . 247
6.4 Reference configurations . . . 247
6.4.1 Solid precipitation . . . 248
6.4.2 Liquid precipitation . . . 249
6.4.3 Intercomparison sites . . . 250
6.5 Transfer functions . . . 252
6.5.1 Liquid precipitation: rain . . . 253
6.5.2 Solid precipitation: snow . . . 253
6.5.2.1 Weighing gauges . . . 253
6.5.2.2 Heated tipping buckets . . . 256
6.6 Siting and exposure . . . 257
6.7 Precipitation data quality control (automated gauges) . . . 259
6.7.1 Environmental factors impacting precipitation data quality and mitigation approaches . . . 259
6.7.2 Post-processing approaches for precipitation accumulation data . . . 260
6.8 Measurement of Dew, Ice Accumulation and Fog Precipitation . . . 260
6.8.1 Measurement of dew and leaf wetness . . . 260
6.8.2 Measurement of ice accumulation . . . 263
6.8.2.1 Measurement methods . . . 263
6.8.2.2 Ice on pavements . . . 263
6.8.3 Measurement of fog precipitation . . . 264

Annex 6.A. Standardized procedure for laboratory calibration of catchment-type rainfall intensity gauges . . . 266

Annex 6.B. detailed field verification Procedure FOR catchment-type rainfall intensity gauges . . . 269

References . . . 271

**CHAPTER 7. MEASUREMENT OF RADIATION . . . 275**
7.1 General . . . 275
7.1.1 Definitions . . . 276
7.1.2 Units and/or scales . . . 276
7.1.2.1 Units . . . 276
7.1.2.2 Standardization of solar radiation measurements . . . 276
7.1.2.3 Standardization of terrestrial radiation measurements . . . 278
7.1.3 Meteorological requirements . . . 279
7.1.3.1 Data to be reported . . . 279
7.1.3.2 Uncertainty . . . 279
7.1.3.3 Sampling and recording . . . 279
7.1.3.4 Observation times . . . 279
7.1.4 Methods of measurement . . . 279

*Page*

7.2 Measurement of direct solar radiation . . . 281
7.2.1 Direct solar radiation . . . 282
7.2.1.1 Primary standard pyrheliometers . . . 282
7.2.1.2 Secondary standard pyrheliometers . . . 284
7.2.1.3 Field and network pyrheliometers . . . 285
7.2.1.4 Calibration of pyrheliometers . . . 286
7.2.2 Exposure . . . 286
7.3 Measurement of global and diffuse sky radiation . . . 286
7.3.1 Calibration of pyranometers . . . 287
7.3.1.1 By reference to a standard pyrheliometer and a shaded reference pyranometer . . . 289
7.3.1.2 By reference to a standard pyrheliometer . . . 290
7.3.1.3 Alternate calibration using a pyrheliometer . . . 291
7.3.1.4 By comparison with a reference pyranometer . . . 291
7.3.1.5 By comparison in the laboratory . . . 292
7.3.1.6 Routine checks on calibration factors . . . 292
7.3.2 Performance of pyranometers . . . 293
7.3.2.1 Sensor levelling . . . 293
7.3.2.2 Change of sensitivity due to ambient temperature variation . . . 293
7.3.2.3 Variation of response with orientation . . . 293
7.3.2.4 Variation of response with angle of incidence . . . 293
7.3.2.5 Uncertainties in hourly and daily totals . . . 294
7.3.3 Installation and maintenance of pyranometers . . . 294
7.3.3.1 Correction for obstructions to a free horizon . . . 295
7.3.3.2 Installation of pyranometers for measuring global radiation . . . 295
7.3.3.3 Installation of pyranometers for measuring diffuse sky radiation . . . 296
7.3.3.4 Installation of pyranometers for measuring reflected radiation . . . 296
7.3.3.5 Maintenance of pyranometers . . . 297
7.3.3.6 Installation and maintenance of pyranometers on special platforms 297
7.4 Measurement of total and long-wave radiation . . . 297
7.4.1 Instruments for the measurement of long-wave radiation . . . 298
7.4.2 Instruments for the measurement of total radiation . . . 300
7.4.3 Calibration of pyrgeometers . . . 302
7.4.4 Installation of pyrradiometers and pyrgeometers . . . 302
7.4.5 Recording and data reduction . . . 303
7.5 Measurement of special radiation quantities . . . 303
7.5.1 Measurement of daylight . . . 303
7.5.1.1 Instruments . . . 305
7.5.1.2 Calibration . . . 305
7.5.1.3 Recording and data reduction . . . 306
7.6 Measurement of Ultraviolet radiation . . . 306
7.6.1 Instruments . . . 307
7.6.1.1 Broadband sensors . . . 309
7.6.1.2 Narrowband sensors . . . 310
7.6.1.3 Spectroradiometers . . . 311
7.6.2 Calibration . . . 312

Annex 7.A. Nomenclature of radiometric and photometric quantities . . . 314

Annex 7.B. Meteorological radiation quantities, symbols and definitions . . . 316

Annex 7.C. Specifications for World, Regional and National Radiation Centres . . . 318

Annex 7.D. Guidelines for radiometer comparisons . . . 322

Annex 7.E. Governance and traceability of atmospheric longwave irradiance . . . 327

Annex 7.F. Useful formulae . . . 328

Annex 7.G. Diffuse sky radiation – correction for a shading ring . . . 331

References and further reading . . . 333

*Page*

**CHAPTER 8. MEASUREMENT OF SUNSHINE DURATION . . . . . 336**
8.1 General . . . . . 336
8.1.1 Definition . . . . . 336
8.1.2 Units and scales . . . . . 336
8.1.3 Meteorological requirements . . . . . 336
8.1.3.1 Application of sunshine duration data . . . . . 337
8.1.3.2 Correlations to other meteorological variables . . . . . 337
8.1.3.3 Requirement of automated records . . . . . 338
8.1.4 Measurement methods . . . . . 338
8.2 Instruments and sensors . . . . . 339
8.2.1 Pyrheliometric method . . . . . 339
8.2.1.1 General . . . . . 339
8.2.1.2 Sources of error . . . . . 339
8.2.2 Pyranometric method . . . . . 340
8.2.2.1 General . . . . . 340
8.2.2.2 Sources of error . . . . . 341
8.2.3 The Campbell-Stokes sunshine recorder (burn method) . . . . . 341
8.2.3.1 Adjustments . . . . . 341
8.2.3.2 Evaluation . . . . . 342
8.2.3.3 Special versions . . . . . 343
8.2.3.4 Sources of error . . . . . 343
8.2.4 Contrast-evaluating devices . . . . . 343
8.2.5 Contrast-evaluating and scanning devices . . . . . 343
8.2.5.1 General . . . . . 343
8.2.5.2 Sources of error . . . . . 343
8.3 Exposure of sunshine detectors . . . . . 344
8.4 General sources of error . . . . . 344
8.5 Calibration . . . . . 345
8.5.1 Outdoor methods . . . . . 345
8.5.1.1 Comparison of sunshine duration data . . . . . 345
8.5.1.2 Comparison of analogue signals . . . . . 346
8.5.1.3 Mean effective irradiance threshold method . . . . . 346
8.5.2 Indoor method . . . . . 346
8.6 Maintenance . . . . . 347

Annex 8.A. Algorithm to estimate sunshine duration from direct global irradiance measurements . . . . . 348

Annex 8.B. Algorithm to estimate sunshine duration from 1 min global irradiance measurements . . . . . 349

References and further reading . . . . . 350

**CHAPTER 9. MEASUREMENT OF VISIBILITY . . . . . 352**
9.1 General . . . . . 352
9.1.1 Definitions . . . . . 352
9.1.2 Units and scales . . . . . 353
9.1.3 Meteorological requirements . . . . . 353
9.1.4 Measurement methods . . . . . 354
9.2 Visual estimation of meteorological optical range . . . . . 357
9.2.1 General . . . . . 357
9.2.2 Estimation of meteorological optical range by day . . . . . 358
9.2.3 Estimation of meteorological optical range at night . . . . . 358
9.2.4 Estimation of meteorological optical range in the absence of distant objects . . 360
9.2.5 Accuracy of visual observations . . . . . 360
9.2.6 Usage of cameras . . . . . 361

*Page*

9.3 Instrumental measurement of the meteorological optical range . . . 361
9.3.1 General . . . 361
9.3.2 Instruments measuring the extinction coefficient . . . 362
9.3.3 Instruments estimating the scatter coefficient . . . 364
9.3.4 Instrument exposure and siting . . . 366
9.3.5 Calibration and maintenance . . . 367
9.3.5.1 Maintenance . . . 367
9.3.5.2 Calibration . . . 368
9.3.6 Accuracy estimates for the measurement of meteorological optical range . . . 371
9.3.6.1 General . . . 371
9.3.6.2 Accuracy of transmissometers . . . 371
9.3.6.3 Accuracy of forward-scatter meters . . . 373
9.3.6.4 Accuracy of telephotometers and visual extinction meters . . . 373

References and further reading . . . 374

**CHAPTER 10. MEASUREMENT OF EVAPORATION . . . 375**
10.1 General . . . 375
10.1.1 Definitions . . . 375
10.1.2 Units and scales . . . 375
10.1.3 Meteorological requirements . . . 375
10.1.4 Measurement methods . . . 376
10.2 Atmometers . . . 377
10.2.1 Instrument types . . . 377
10.2.2 Measurement taken by atmometers . . . 377
10.2.3 Sources of error in atmometers . . . 377
10.3 Evaporation pans and tanks . . . 378
10.3.1 United States Class A pan . . . 378
10.3.2 Russian GGI-3000 pan . . . 378
10.3.3 Russian 20 $m^2$ tank . . . 378
10.3.4 Measurements taken by evaporation pans and tanks . . . 379
10.3.5 Exposure of evaporation pans and tanks . . . 379
10.3.6 Sources of error in evaporation pans and tanks . . . 380
10.3.7 Maintenance of evaporation pans and tanks . . . 380
10.4 Evapotranspirometers (lysimeters) . . . 381
10.4.1 Measurements taken by lysimeters . . . 382
10.4.2 Exposure of evapotranspirometers . . . 382
10.4.3 Sources of error in lysimeter measurements . . . 383
10.4.4 Lysimeters maintenance . . . 383
10.5 Estimation of evaporation from natural surfaces . . . 384

References and further reading . . . 386

**CHAPTER 11. MEASUREMENT OF SOIL MOISTURE . . . 387**
11.1 General . . . 387
11.1.1 Definitions . . . 387
11.1.2 Units . . . 388
11.1.3 Meteorological requirements . . . 389
11.1.4 Measurement methods . . . 389
11.2 Gravimetric direct measurement of soil water content . . . 390
11.3 Soil water content: indirect methods . . . 391
11.3.1 Radiological methods . . . 391
11.3.1.1 Neutron scattering method . . . 392
11.3.1.2 Gamma-ray attenuation . . . 393
11.3.2 Soil water dielectrics . . . 393
11.3.2.1 Time-domain reflectometry . . . 393
11.3.2.2 Frequency-domain measurement . . . 394

*Page*

11.4 Soil water potential instrumentation . . . . . 394
11.4.1 Tensiometers . . . . . 394
11.4.2 Resistance blocks . . . . . 395
11.4.3 Psychrometers . . . . . 396
11.5 Site selection and sample size . . . . . 396
11.6 Remote-sensing of soil moisture . . . . . 397
11.6.1 Microwave remote-sensing . . . . . 397
11.6.1.1 Introduction . . . . . 397
11.6.1.2 Multi-frequency radiometers . . . . . 398
11.6.1.3 Scatterometers . . . . . 399
11.6.1.4 Synthetic aperture radars . . . . . 400
11.6.1.5 Dedicated L-band missions . . . . . 400
11.6.1.6 Soil moisture retrieval . . . . . 401
11.6.2 Thermal infrared remote-sensing . . . . . 403

References and further reading . . . . . 405

**CHAPTER 12. MEASUREMENT OF UPPER-AIR PRESSURE, TEMPERATURE AND HUMIDITY . . . . . 409**
12.1 General . . . . . 409
12.1.1 Definitions . . . . . 409
12.1.2 Units used in upper-air measurements . . . . . 409
12.1.3 Meteorological requirements . . . . . 410
12.1.3.1 Radiosonde data for meteorological operations . . . . . 410
12.1.3.2 Relationships between satellite and radiosonde upper-air measurements . . . . . 412
12.1.3.3 Maximum height of radiosonde observations . . . . . 414
12.1.4 Uncertainty requirements . . . . . 414
12.1.4.1 Geopotential height: requirements and performance . . . . . 415
12.1.4.2 Temperature: requirements and performance . . . . . 416
12.1.4.3 Relative humidity: requirements and performance . . . . . 416
12.1.5 Methods of measurement . . . . . 416
12.1.5.1 Constraints on radiosonde design . . . . . 417
12.1.5.2 Radio frequency used by radiosondes . . . . . 417
12.1.6 Radiosonde errors: general considerations . . . . . 418
12.1.6.1 Types of error . . . . . 418
12.1.6.2 Potential references . . . . . 419
12.1.6.3 Sources of additional error during radiosonde operations . . . . . 420
12.2 Radiosonde electronics . . . . . 420
12.2.1 General features . . . . . 420
12.2.2 Power supply for radiosondes . . . . . 421
12.2.3 Methods of data transmission . . . . . 421
12.2.3.1 Radio transmitter . . . . . 421
12.3 Temperature sensors . . . . . 421
12.3.1 General requirements . . . . . 421
12.3.2 Thermistors . . . . . 423
12.3.3 Thermocapacitors . . . . . 423
12.3.4 Thermocouples . . . . . 423
12.3.5 Scientific sounding instruments . . . . . 423
12.3.6 Exposure . . . . . 424
12.3.7 Temperature errors . . . . . 424
12.3.7.1 Calibration . . . . . 424
12.3.7.2 Thermal lag . . . . . 426
12.3.7.3 Radiative heat exchange in the infrared . . . . . 426
12.3.7.4 Heating by solar radiation . . . . . 426
12.3.7.5 Deposition of ice or water on the sensor . . . . . 429
12.3.7.6 Representativeness issues . . . . . 429

*Page*

12.4 Relative humidity sensors . . . 429
12.4.1 General aspects . . . 429
12.4.2 Thin-film capacitors . . . 434
12.4.3 Carbon hygristors and goldbeater's skin . . . 434
12.4.4 Scientific sounding instruments . . . 435
12.4.5 Exposure . . . 436
12.4.6 Relative humidity errors . . . 436
12.4.6.1 General considerations . . . 436
12.4.6.2 Wetting or icing in cloud . . . 438
12.4.6.3 Representativeness issues . . . 438
12.5 Pressure sensors (including height measurements) . . . 438
12.5.1 General aspects . . . 438
12.5.2 Silicon sensors . . . 438
12.5.3 Aneroid capsule (capacitive) . . . 439
12.5.4 Pressure sensor errors . . . 439
12.5.4.1 Relationship of geopotential height errors to pressure errors . . . 440
12.5.5 Use of geometric height observations instead of pressure sensor observations 441
12.5.5.1 General . . . 441
12.5.5.2 Method of calculation . . . 442
12.5.6 Sources of error in direct height measurements . . . 444
12.5.6.1 In GNSS geometric height measurements . . . 444
12.5.6.2 In radar height measurements . . . 445
12.6 Ground station equipment . . . 445
12.6.1 General features . . . 445
12.6.2 Software for data processing . . . 446
12.7 Radiosonde operations . . . 447
12.7.1 Control corrections immediately before use . . . 447
12.7.2 Deployment methods . . . 448
12.7.3 Radiosonde launch procedures . . . 448
12.7.4 Radiosonde suspension during flight . . . 449
12.7.5 Public safety . . . 449
12.8 Comparison, calibration and maintenance . . . 450
12.8.1 Comparisons . . . 450
12.8.1.1 Quality evaluation using short-term forecasts . . . 450
12.8.1.2 Comparison of water vapour measurements with remote-sensing . . . 451
12.8.1.3 Radiosonde comparison tests . . . 451
12.8.2 Calibration . . . 452
12.8.3 Maintenance . . . 453
12.9 Computations and reporting . . . 453
12.9.1 Radiosonde computations and reporting procedures . . . 454
12.9.2 Corrections . . . 454
12.10 Procurement issues . . . 455
12.10.1 Use and update of the results from the WMO Intercomparison of High-quality Radiosonde Systems . . . 455
12.10.2 Some issues to be considered in procurement . . . 455

Annex 12.A. Current breakthrough and optimum uncertainty requirements for radiosonde measurements . . . 457

Annex 12.B. Estimates of goal, breakthrough and threshold limits for upper wind, upper-air temperature, relative humidity and geopotential height (derived from the WMO Rolling Review of Requirements for upper-air observations) . . . 458

Annex 12.C. Environmentally friendly radiosondes . . . 461

Annex 12.D. Guidelines for organizing radiosonde intercomparisons and for the establishment of test sites . . . 462

References and further reading . . . 469

Page

**CHAPTER 13. MEASUREMENT OF UPPER WIND . . . . . 472**
13.1 General . . . . . 472
13.1.1 Definitions . . . . . 472
13.1.2 Units of measurement of upper wind . . . . . 472
13.1.3 Meteorological requirements . . . . . 473
13.1.3.1 Uses in meteorological operations . . . . . 473
13.1.3.2 Improvements in reporting procedures . . . . . 473
13.1.3.3 Uncertainty requirements . . . . . 474
13.1.3.4 Maximum height requirements . . . . . 476
13.1.4 Methods of measurement . . . . . 476
13.1.4.1 Tracking using radionavigation signals . . . . . 477
13.1.4.2 Tracking using a directional aerial . . . . . 478
13.2 Upper-wind sensors and instruments . . . . . 478
13.2.1 Navaid tracking systems . . . . . 479
13.2.1.1 Availability of navaid signals . . . . . 479
13.2.1.2 Global positioning system . . . . . 479
13.2.2 Radar . . . . . 481
13.2.2.1 Primary radars . . . . . 481
13.2.2.2 Secondary radars . . . . . 481
13.2.3 Radiotheodolite . . . . . 481
13.2.4 Optical theodolite . . . . . 482
13.3 Measurement methods . . . . . 483
13.3.1 General considerations concerning data processing . . . . . 483
13.3.2 Observations using radionavigation systems . . . . . 484
13.3.3 Observations using a directional aerial . . . . . 484
13.3.4 Pilot-balloon observations . . . . . 485
13.4 Exposure of ground equipment . . . . . 485
13.5 Sources of uncertainty . . . . . 486
13.5.1 General . . . . . 486
13.5.1.1 Target tracking uncertainties . . . . . 486
13.5.1.2 Height assignment uncertainties . . . . . 487
13.5.1.3 Target motion relative to the atmosphere . . . . . 487
13.5.2 Uncertainties in the global positioning system windfinding systems . . . . . 487
13.5.3 Uncertainties of systems using a directional aerial . . . . . 490
13.5.4 Uncertainties in pilot-balloon observations . . . . . 493
13.5.5 Representativeness uncertainties . . . . . 493
13.6 Comparison, calibration and maintenance . . . . . 495
13.6.1 Comparison . . . . . 495
13.6.1.1 Operational monitoring by comparison with forecast fields . . . . . 495
13.6.1.2 Comparison with other windfinding systems . . . . . 495
13.6.2 Calibration . . . . . 496
13.6.3 Maintenance . . . . . 496
13.7 Corrections . . . . . 497

References and further reading . . . . . 498

**CHAPTER 14. OBSERVATION OF PRESENT AND PAST WEATHER; STATE OF THE GROUND . . . . . 500**
14.1 General . . . . . 500
14.1.1 Definitions . . . . . 500
14.1.2 Units and scales . . . . . 500
14.1.3 Meteorological requirements . . . . . 501
14.1.4 Observation methods . . . . . 501
14.2 Observation of present and past weather . . . . . 501
14.2.1 Precipitation . . . . . 502
14.2.1.1 Objects of observation . . . . . 502
14.2.1.2 Instruments and measuring devices: precipitation type . . . . . 502

*Page*

14.2.1.3 Instruments and measuring devices: precipitation intensity and character . . . 505
14.2.1.4 Instruments and measuring devices: multi-sensor approach . . . 505
14.2.2 Atmospheric obscurity and suspensoids . . . 506
14.2.2.1 Objects of observation . . . 506
14.2.2.2 Instruments and measuring devices for obscurity and suspensoid characteristics . . . 506
14.2.3 Other weather events . . . 507
14.2.3.1 Objects of observation . . . 507
14.2.3.2 Instruments and measuring devices . . . 508
14.2.4 State of the sky . . . 508
14.2.4.1 Objects of observation . . . 508
14.2.4.2 Instruments and measuring devices . . . 508
14.3 Observation of state of the ground . . . 508
14.3.1 Objects of observation . . . 508
14.3.2 Instruments and measuring devices . . . 509
14.4 Observation of special phenomena . . . 509
14.4.1 Electrical phenomena . . . 509
14.4.2 Optical phenomena . . . 510

Annex. Criteria for slight, moderate and heavy precipitation intensity . . . 511

References and further reading . . . 513

**CHAPTER 15. OBSERVATION AND MEASUREMENT OF CLOUDS . . . 517**
15.1 General . . . 517
15.1.1 Definitions . . . 517
15.1.2 Units and scales . . . 519
15.1.3 Meteorological requirements . . . 519
15.1.4 Observation and measurement methods . . . 519
15.1.4.1 Cloud amount . . . 519
15.1.4.2 Cloud-base height . . . 520
15.1.4.3 Cloud type . . . 520
15.2 Estimation and observation of cloud amount, cloud-base height and cloud type by human observer . . . 520
15.2.1 Making effective estimations . . . 520
15.2.2 Estimation of cloud amount . . . 521
15.2.3 Estimation of cloud-base height . . . 521
15.2.4 Observation of cloud type . . . 522
15.3 Instrumental measurement of cloud amount . . . 522
15.3.1 Measurement of cloud amount by laser ceilometer . . . 523
15.3.2 Measurement of cloud amount by infrared detector . . . 524
15.3.3 Measurement of cloud amount by sky camera . . . 525
15.4 Instrumental measurement of cloud-base height . . . 525
15.4.1 Measurement of cloud-base height by laser ceilometer . . . 525
15.4.1.1 Measurement method . . . 525
15.4.1.2 Exposure and installation . . . 526
15.4.1.3 Sources of error . . . 527
15.4.1.4 Calibration and maintenance . . . 527
15.4.2 Measurement of cloud-base height by rotating-beam ceilometer . . . 528
15.4.2.1 Measurement method . . . 528
15.4.2.2 Exposure and installation . . . 529
15.4.2.3 Sources of error . . . 529
15.4.2.4 Calibration and maintenance . . . 530
15.4.3 Measurement of cloud-base height by searchlight . . . 530
15.4.3.1 Measurement method . . . 530
15.4.3.2 Exposure and installation . . . 530
15.4.3.3 Sources of error . . . 530
15.4.3.4 Calibration and maintenance . . . 531

*Page*

15.4.4 Balloon measurement of cloud-base height . . . 532
15.4.4.1 Measurement method . . . 532
15.4.4.2 Sources of error . . . 532
15.5 Instrumental measurement of cloud type . . . 532
15.6 Other cloud-related properties . . . 533
15.6.1 Vertical visibility . . . 533

References and further reading . . . 534

**CHAPTER 16. MEASUREMENT OF ATMOSPHERIC COMPOSITION . . . 536**
16.1 General . . . 536
16.1.1 Definitions and descriptions . . . 537
16.1.2 Units and scales . . . 538
16.1.3 Measurement principles and techniques . . . 539
16.1.4 Quality assurance . . . 541
16.2 (Stratospheric) ozone measurements . . . 542
16.2.1 Ozone total column . . . 542
16.2.2 Ozone profile measurements . . . 543
16.2.2.1 Umkehr method . . . 544
16.2.2.2 Ozonesonde measurements . . . 544
16.2.2.3 Other measurement techniques . . . 544
16.2.3 Aircraft and satellite observations . . . 545
16.3 Greenhouse gases . . . 545
16.3.1 Carbon dioxide (including $\Delta^{14}C$, $\delta^{13}C$ and $\delta^{18}O$ in $CO_2$, and $O_2/N_2$ ratios) . . . 545
16.3.2 Methane . . . 547
16.3.3 Nitrous oxide . . . 547
16.3.4 Halocarbons and $SF_6$ . . . 548
16.3.5 Remote-sensing of greenhouse gases . . . 548
16.4 Reactive gases . . . 548
16.4.1 Tropospheric (surface) ozone . . . 549
16.4.2 Carbon monoxide . . . 550
16.4.3 Volatile organic compounds . . . 551
16.4.4 Nitrogen oxide . . . 553
16.4.5 Sulphur dioxide . . . 554
16.4.6 Molecular hydrogen . . . 555
16.5 Atmospheric wet deposition . . . 555
16.5.1 Sample collection . . . 556
16.5.2 Chemical analysis . . . 557
16.6 Aerosols . . . 560
16.6.1 Aerosol chemical measurements . . . 560
16.6.2 In *situ* measurements of aerosol radiative properties . . . 564
16.6.3 Particle number concentration and size distribution . . . 566
16.6.4 Cloud condensation nuclei . . . 566
16.6.5 Aerosol optical depth . . . 567
16.6.6 GAW aerosol lidar . . . 568
16.7 Natural radioactivity . . . 571

Annex. GAW central facilities . . . 572

References and further reading . . . 575

# FOREWORD

WMO Guides describe the practices and procedures that Members are invited to follow or implement in establishing and conducting their arrangements for compliance with the WMO Technical Regulations.

One longstanding publication in this series is the *Guide to Instruments and Methods of Observation* (WMO-No. 8) (WMO-No. 8), which was first published in 1950. The Guide is the authoritative reference for all matters related to instrumentation and methods of observation in the context of the WMO Integrated Global Observing System (WIGOS). Uniform, traceable and high-quality observational data represent an essential input for most WMO applications, such as climate monitoring, numerical weather prediction, nowcasting and severe weather forecasting, all of which facilitate the improvement of the well-being of societies around the world.

The main purpose of the Guide is to provide guidance on the most effective practices and procedures for undertaking meteorological, hydrological and related environmental measurements and observations in order to meet specific requirements for different application areas. It also provides information on the capabilities of instruments and systems that are regularly used to perform such observations. The theoretical basis of the techniques and observational methods is outlined in the text and supported by references and further reading for additional background information and details.

The continuous evolution and standardization of measurement and observational practices and the rapid development of new measurement techniques and technologies have led to the evolution of the Guide into a significantly larger publication that constitutes a fundamental and essential source of information. Beginning with the 2018 edition, the Guide has been separated into “volumes” that can be updated and published independently.

The outline of the current guide is:

Volume I – Measurement of Meteorological Variables

Volume II – Measurement of Cryospheric Variables

Volume III – Observing Systems

Volume IV – Space-based Observations

Volume V – Quality Assurance and Management of Observing Systems

This 2024 edition of Volume I was approved by the WMO Commission for Observation, Infrastructure and Information Systems (INFCOM) at its third session (INFCOM-3). In comparison to the 2023 edition of Volume I, this edition includes updates to Chapter 6 – Measurement of precipitation and Chapter 7 – Measurement of radiation.

On behalf of WMO, I would like to express my sincere gratitude to the INFCOM Standing Committee on Measurements, Instrumentation and Traceability, and in particular, to its Expert Team on Surface and Sub-surface Measurement, Expert Team on Radiation References and Editorial Board, whose tremendous efforts have enabled the publication of this new edition.



(Prof. Celeste Saulo)
Secretary-General

# CHAPTER 1. GENERAL

## 1.1 METEOROLOGICAL OBSERVATIONS

### 1.1.1 General

Meteorological (and related environmental and geophysical) observations are made for a variety of reasons. They are used for the real-time preparation of weather analyses, forecasts and severe weather warnings, for the study of climate, for local weather-dependent operations (for example, local aerodrome flying operations, construction work on land and at sea), for hydrology and agricultural meteorology, and for research in meteorology and climatology. The purpose of the *Guide to Meteorological Instruments and Methods of Observation* is to support these activities by giving advice on good practices for meteorological measurements and observations.

There are many other sources of additional advice, and users should refer to the references at the end of each chapter for a bibliography of theory and practice relating to instruments and methods of observation. The references also contain national practices, national and international standards, and specific literature. They also include reports published by WMO for the Commission for Instruments and Methods of Observation (CIMO) on technical conferences, instrumentation, and international comparisons of instruments. Many other Manuals and Guides issued by WMO refer to particular applications of meteorological observations (see especially the *Manual on the WMO Integrated Global Observing System* (WMO-No. 1160), *Guide to the WMO Integrated Global Observing System* (WMO No. 1165), *Guide to Meteorological Observing and Information Distribution Systems for Aviation Weather Services* (WMO-No. 731), *Guide to Hydrological Practices* (WMO-No. 168), *Guide to Agricultural Meteorological Practices* (WMO-No. 134) and *Guide to Climatological Practices* (WMO-No. 100)).

Quality assurance (QA) and maintenance are of special interest for instrument measurements. Throughout the present Guide many recommendations are made to meet the stated performance requirements. These requirements are described in Annex 1.A. Particularly, Volume V of the present Guide is dedicated to QA and management of observing systems. It is recognized that quality management and training of instrument specialists is of utmost importance. Therefore, on the recommendation of CIMO,[1] regional associations of WMO have set up Regional Instrument Centres (RICs) to maintain standards and provide advice regarding meteorological measurements. These RICs play a key role in the implementation of WMO strategy for traceability assurance, which is set out in Annex 1.B. Their terms of reference are given in Annex 1.C. In addition, on the recommendation of the Joint WMO/Intergovernmental Oceanographic Commission Technical Commission for Oceanography and Marine Meteorology (JCOMM)[2] (see *Joint WMO/IOC Technical Commission for Oceanography and Marine Meteorology* (WMO-No. 1049)) a network of Regional Marine Instrument Centres has been established to provide for similar functions regarding marine meteorology and other related oceanographic measurements. Their terms of reference and locations are given in Chapter 4, Annex 4.A of Volume III of the present Guide. Also, to undertake training in meteorology, hydrology and related sciences to meet the needs of the regions, WMO Regional Training Centres[3] have been established.

The definitions and standards stated in the present Guide (see 1.5.1) will always conform to internationally adopted standards. Basic documents to be referred to are the *International Meteorological Vocabulary* (WMO-No. 182) and the *International Vocabulary of Metrology – Basic and General Concepts and Associated Terms (VIM)* (Joint Committee for Guides in Metrology (JCGM), 2012).

---

1 Recommended by the CIMO at its ninth session (1985) through Recommendation 19 (CIMO-IX).
2 Recommended by JCOMM at its third session (2009) through Recommendation 1 (JCOMM-III).
3 Recent information on Regional Training Centres and their components can be found at https://community.wmo.int/wmo-regional-training-centres.

### 1.1.2 **Representativeness**

The representativeness of an observation is the degree to which it accurately describes the value of the variable needed for a specific purpose. Therefore, it is not a fixed quality of any observation, but results from joint appraisal of instrumentation, measurement interval and exposure against the requirements of some particular application. For instance, synoptic observations should typically be representative of an area up to 100 km around the station, but for small-scale or local applications the considered area may have dimensions of 10 km or less.

In particular, applications have their own preferred timescales and space scales for averaging, station density and resolution of phenomena — small for agricultural meteorology, large for global long-range forecasting. Forecasting scales are closely related to the timescales of the phenomena; thus, shorter-range weather forecasts require more frequent observations from a denser network over a limited area to detect any small-scale phenomena and their quick development. Using various sources (*Lecture Notes for Training Agricultural Meteorological Personnel* (WMO-No. 551), *Manual on the WMO Integrated Global Observing System* (WMO-No. 1160), Orlanski (1975)), horizontal meteorological scales may be classified as follows, with a factor two uncertainty:

(a) Microscale (less than 100 m) for agricultural meteorology, for example, evaporation;

(b) Toposcale or local scale (100 $m^{-3}$ km), for example, air pollution, tornadoes;

(c) Mesoscale (3–100 km), for example, thunderstorms, sea and mountain breezes;

(d) Large scale (100–3 000 km), for example, fronts, various cyclones, cloud clusters;

(e) Planetary scale (larger than 3 000 km), for example, long upper tropospheric waves.

Section 1.6 discusses the required and achievable uncertainties of instrument systems. The stated achievable uncertainties can be obtained with good instrument systems that are properly operated, but are not always obtained in practice. Good observing practices require skill, training, equipment and support, which are not always available in sufficient degree. The measurement intervals required vary by application: minutes for aviation, hours for agriculture, and days for climate description. Data storage arrangements are a compromise between available capacity and user needs.

Good exposure, which is representative on scales from a few metres to 100 km, is difficult to achieve (see 1.3). Errors of unrepresentative exposure may be much larger than those expected from the instrument system in isolation. A station in a hilly or coastal location is likely to be unrepresentative on the large scale or mesoscale. However, good homogeneity of observations in time may enable users to employ data even from unrepresentative stations for climate studies.

Annex 1.D discusses site representativeness in further detail and provides guidelines on the classification of surface observing sites on land to indicate their representativeness for the measurement of different variables. This classification has several objectives:

(a) To improve the selection of a site and the location of an instrument within the selected site to optimize representativeness by applying some objective criteria;

(b) To help in the construction of a network and the selection of its sites:

  (i) Not only for meteorological services but also, for example, for road services;

  (ii) To avoid inappropriate positioning of instruments;

(c) To document the site representativeness with an easy-to-use criterion:

(i) It is clear that a single number is not enough to fully document the environment and representativeness of a site. Additional information is necessary such as a map, pictures or a description of the surroundings;

(ii) Despite this numerical value, the site classification is not only a ranking system. Class 1 sites are preferred, but sites in other classes are still valuable for many applications;

(d) To help users benefit from metadata when using observations data. It is recommended that the metadata be as simple as practical, as well as appropriate for the intended use.

### 1.1.3 Metadata

The purpose of the present Guide and related WMO publications is to ensure reliability of observations by standardization. However, local resources and circumstances may cause deviations from the agreed standards of instrumentation and exposure. A typical example is that of regions with much snowfall, where the instruments are mounted higher than usual so that they can be useful in winter as well as summer.

Users of meteorological observations often need to know the actual exposure, type and condition of the equipment and its operation; and perhaps the circumstances of the observations. This is now particularly significant in the study of climate, in which detailed station histories have to be examined. Metadata (data about data) should be kept concerning all of the station establishment and maintenance matters described in 1.3, and concerning changes which occur, including calibration and maintenance history and the changes in terms of exposure and staff (see *Guidelines on Climate Metadata and Homogenization* (WMO/TD-No. 1186)). Metadata are especially important for elements which are particularly sensitive to exposure, such as precipitation, wind and temperature. One very basic form of metadata is information on the existence, availability and quality of meteorological data and of the metadata about them.

## 1.2 METEOROLOGICAL OBSERVING SYSTEMS

The requirements for observational data may be met using in situ measurements or remote-sensing (including space-borne) systems, according to the ability of the various sensing systems to measure the environmental elements needed. The requirements in terms of global, regional and national scales and according to the application area are described in the *Manual on the WMO Integrated Global Observing System* (WMO-No. 1160). WIGOS, designed to meet these requirements, is composed of the surface-based subsystem and the space-based subsystem. The surface-based subsystem comprises a wide variety of types of stations according to the particular application (for example, surface synoptic station, upper-air station, climatological station, and so on). The space-based subsystem comprises a number of spacecraft with on-board sounding missions and the associated ground segment for command, control and data reception. The succeeding paragraphs and chapters in the present Guide deal with the surface-based system and, to a lesser extent, with the space-based subsystem. To derive certain meteorological observations by automated systems, for example, present weather, a so-called "multi-instrument" approach is necessary, where an algorithm is applied to compute the result from the outputs of several sensing instruments.

## 1.3 GENERAL REQUIREMENTS OF A METEOROLOGICAL STATION

The requirements for elements to be observed according to the type of station and observing network are detailed in the *Manual on the WMO Integrated Global Observing System* (WMO-No. 1160). In this section, the observational requirements of a typical climatological station or a surface synoptic network station are considered.

The following elements are observed at a station making surface observations (the chapters refer to the present volume):

- Temperature (Chapter 2)
- Soil temperature (Chapter 2)
- Atmospheric pressure (Chapter 3)
- Relative humidity (Chapter 4)
- Wind direction and speed (Chapter 5)
- Precipitation (Chapter 6)
- Snow cover (Chapter 6)
- Solar radiation and/or sunshine (Chapters Chapter 7, Chapter 8)
- Visibility (Chapter 9)
- Evaporation (Chapter 10)
- Present weather (Chapter 14)
- Past weather (Chapter 14)
- Cloud amount (Chapter 15)
- Cloud type (Chapter 15)
- Cloud-base height (Chapter 15)

Instruments exist that can measure all of these elements, with the exception of cloud type. However, with current technology, instruments for present and past weather, cloud amount and height, and snow cover are not able to make observations of the whole range of phenomena, whereas human observers are able to do so.

Some meteorological stations take upper-air measurements (the present volume, Chapter 12 and Chapter 13), measurements of soil moisture (the present volume, Chapter 11), ozone and atmospheric composition (the present volume, Chapter 16), and some make use of special instrument systems as described in Volume III of the present Guide.

Details of observing methods and appropriate instrumentation are contained in the succeeding chapters of the present Guide.

### 1.3.1 Automatic weather stations

Most of the elements required for synoptic, climatological or aeronautical purposes can be measured by automatic instrumentation (see Chapter 1 of Volume III of the present Guide).

As the capabilities of automatic systems increase, the ratio of purely automatic weather stations (AWSs) to observer-staffed weather stations (with or without automatic instrumentation) increases steadily. The guidance in the following paragraphs regarding siting and exposure, changes of instrumentation, and inspection and maintenance apply equally to AWSs and staffed weather stations.

### 1.3.2 Observers

Meteorological observers are required for a number of reasons, as follows:

(a) To make synoptic and/or climatological observations to the required uncertainty and representativeness with the aid of appropriate instruments;

(b) To maintain instruments, metadata documentation and observing sites in good condition;

(c) To code and dispatch observations (in the absence of automatic coding and communication systems);

(d) To maintain in situ recording devices, including the changing of charts when provided;

(e) To make or collate weekly and/or monthly records of climatological data where automatic systems are unavailable or inadequate;

(f) To provide supplementary or back-up observations when automatic equipment does not make observations of all required elements, or when it is out of service;

(g) To respond to public and professional enquiries.

Observers should be trained and/or certified by an authorized Meteorological Service to establish their competence to make observations to the required standards. They should have the ability to interpret instructions for the use of instrumental and manual techniques that apply to their own particular observing systems. Guidance on the instrument training requirements for observers will be given in Chapter 5 of Volume V of the present Guide.

### 1.3.3 Siting and exposure

#### 1.3.3.1 *Site selection*

Meteorological observing stations are designed so that representative measurements (or observations) can be taken according to the type of station involved. Thus, a station in the synoptic network should make observations to meet synoptic-scale requirements, whereas an aviation meteorological observing station should make observations that describe the conditions specific to the local (aerodrome) site. Where stations are used for several purposes, for example, aviation, synoptic and climatological purposes, the most stringent requirement will dictate the precise location of an observing site and its associated sensing instruments. A detailed study on siting and exposure is published in *Siting and Exposure of Meteorological Instruments* (WMO/TD-No. 589).

As an example, the following considerations apply to the selection of site and instrument exposure requirements for a typical synoptic or climatological station in a regional or national network:

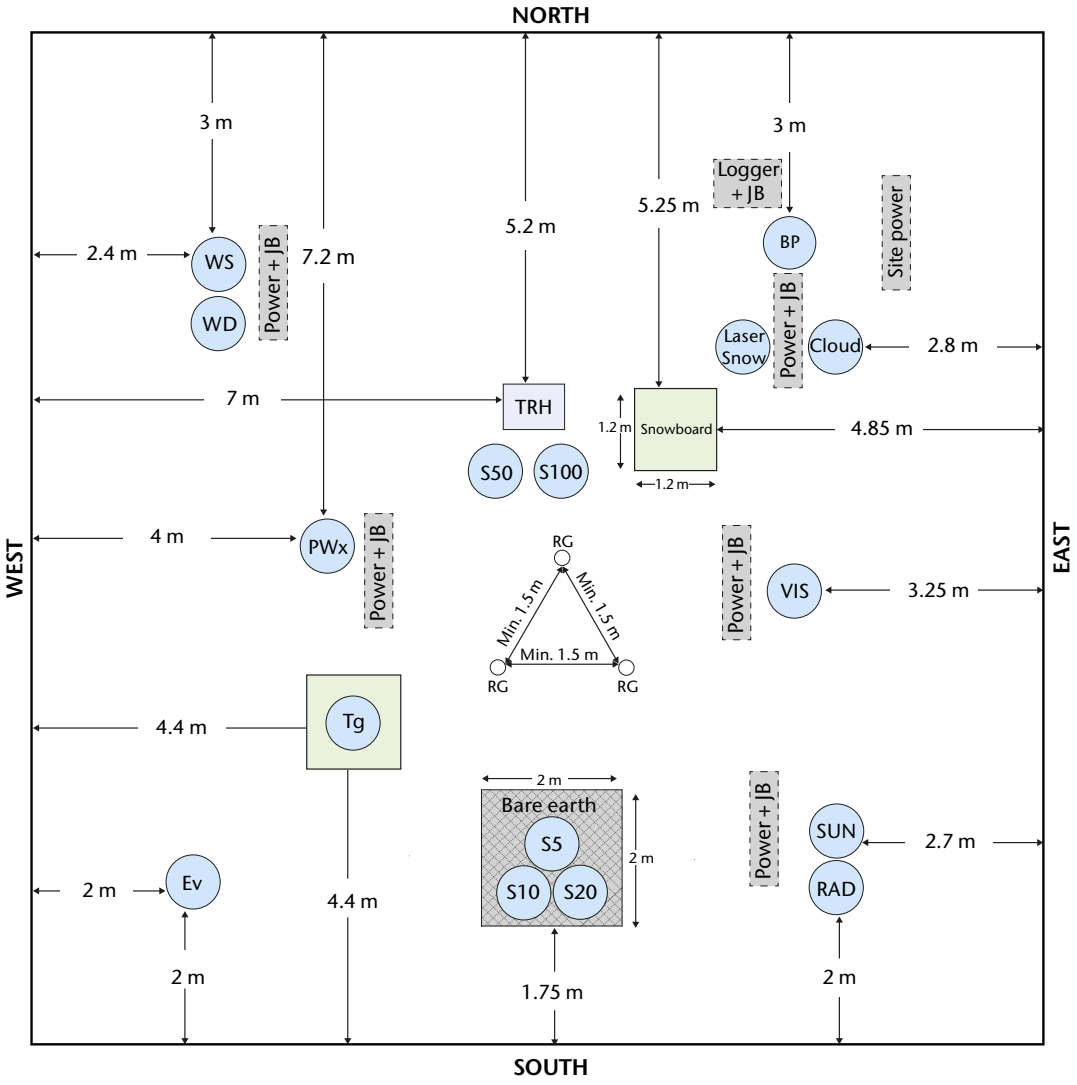
(a) Outdoor instruments should be installed on a level piece of ground, preferably no smaller than 25 m x 25 m where there are many installations, but in cases where there are relatively few installations the area may be considerably smaller. The ground should be covered with short grass or a surface representative of the locality, and surrounded by open fencing or palings to exclude unauthorized persons. Within the enclosure, a bare patch of ground of about 2 m x 2 m is reserved for observations of the state of the ground and of soil temperature at depths of equal to or less than 20 cm (see Chapter 2 of the present volume) (soil temperatures at depths greater than 20 cm can be measured outside this bare patch of ground). An example of the layout of such a station is given in Figure 1.1;

(b) There should be no steeply sloping ground in the vicinity, and the site should not be in a hollow. If these conditions are not met, the observations may show peculiarities of entirely local significance;

(c) The site should be well away from trees, buildings, walls or other obstructions. The distance of any such obstacle (including fencing) from the raingauge should not be less than twice the height of the object above the rim of the gauge, and preferably four times the height;

(d) The sunshine recorder, raingauge and anemometer must be exposed according to their requirements, preferably on the same site as the other instruments;

(e) It should be noted that the enclosure may not be the best place from which to estimate the wind speed and direction; another observing point, more exposed to the wind, may be desirable;




Notes

| | |
|---|---|
| BP | Barometric pressure |
| Ev | Evaporation |
| JB | Junction Box for data |
| PWx | Present weather |
| RG | Raingauge |
| RAD | Solar radiation (pyranometer) |
| S5 | Soil temperature 5 cm |
| S10 | Soil temperature 10 cm |
| S20 | Soil temperature 20 cm |
| S50 | Soil temperature 50 cm |
| SUN | Sunshine duration |
| Tg | Grass temperature |
| TRH | Air temperature and relative humidity in radiation shield |
| VIS | Meteorological optical range (visiometer) |
| WS | Wind speed |
| WD | Wind direction |

Fence:
Ideal = stock proof type.
Compromises may be needed to suit security needs

**Figure 1.1. Layout example of an observing station in the northern hemisphere showing typical distances between installations and the enclosure. It is important to ensure actual distances are great enough to minimize impact of surrounding obstacles.**

(f) Very open sites which are satisfactory for most instruments are unsuitable for raingauges. For such sites, the rainfall catch is reduced in conditions other than light winds and some degree of shelter is needed;

(g) If in the instrument enclosure surroundings, maybe at some distance, objects like trees or buildings obstruct the horizon significantly, alternative viewpoints should be selected for observations of sunshine or radiation;

(h) The position used for observing cloud and visibility should be as open as possible and command the widest possible view of the sky and the surrounding country;

(i) At coastal stations, it is desirable that the station command a view of the open sea. However, the station should not be too near the edge of a cliff because wind eddies created by the cliff will affect the wind and precipitation measurements;

(j) Night observations of cloud and visibility are best made from a site unaffected by extraneous lighting.

It is obvious that some of the above considerations are somewhat contradictory and require compromise solutions. Detailed information appropriate to specific instruments and measurements is given in the succeeding chapters.

#### 1.3.3.2 *Coordinates of the station*

The position of a station referred to in the World Geodetic System 1984 (WGS-84) and its Earth Geodetic Model 1996 (EGM96) must be accurately known and recorded.[4] The coordinates of a station are (as required by the *Guide to the WMO Integrated Global Observing System* (WMO-No. 1165)):

(a) The latitude in degrees, minutes and integer seconds;

(b) The longitude in degrees, minutes and integer seconds;

(c) The height of the station above mean sea level (MSL),[5] namely, the elevation of the station, in metres (up to two decimals).

These coordinates refer to the plot on which the observations are taken and may not be the same as those of the town, village or airfield after which the station is named. If a higher resolution of the coordinates is desired, the same practice applied to elevation can be followed, as explained below.

The elevation of the station is defined as the height above MSL of the ground on which the raingauge stands or, if there is no raingauge, the ground beneath the thermometer screen. If there is neither raingauge nor screen, it is the average level of terrain in the vicinity of the station. If the station reports pressure, the elevation to which the station pressure relates must be separately specified.

If a station is located at an aerodrome, other elevations must be specified (see Chapter 2 of Volume III of the present Guide and the *Guide to Meteorological Observing and Information Distribution Systems for Aviation Weather Services* (WMO-No. 731)). Definitions of measures of height and MSL are given in the *International Meteorological Vocabulary* (WMO-No. 182).

#### 1.3.3.3 *Operating equipment in extreme environments*

Continuous observations during and after extreme hydrometeorological events are extremely important, both to support recovery efforts and to prepare for future events. Mitigation strategies for common hazards are described in Annex 1.E.

---

[4] For an explanation of the WGS-84 and recording issues, see ICAO (2002).

[5] MSL is defined in WMO (1992) as the fixed reference level of MSL as described by a well-defined geoid. There are two types of models used in geodesy for defining a position in space. The first is ellipsoid, which is functionally a deformed sphere and is the base model used by many global navigation satellite systems (GNSSs). The second is the geoid, the equipotential surface of the Earth's gravity field that best fits, in a least squares sense, global MSL. GNSSs provide heights relative to the reference ellipsoid WGS-84 and must be corrected to the geoid as this difference can be as large as 100 m. The WGS-84 EGM96 includes both the WGS-84 reference ellipsoid and EGM96 geoid. For users that require local height, such as pressure or sea level, an adjustment must be applied from GNSS height to the geoid. In some jurisdictions, the national geodetic authority provides a local correction from the ellipsoid (WGS-84) that is both more precise and of finer resolution than EGM96 geoid.

### 1.3.4 Changes of instrumentation and homogeneity

The characteristics of an observing site will generally change over time, for example, through the growth of trees or erection of buildings on adjacent plots. Sites should be chosen to minimize these effects, if possible. Documentation of the geography of the site and its exposure should be kept and regularly updated as a component of the metadata (see Annex 1.F and the *Guidelines on Climate Metadata and Homogenization* (WMO/TD-No. 1186)).

It is especially important to minimize the effects of changes of instrument and/or changes in the siting of specific instruments. Although the static characteristics of new instruments might be well understood, when they are deployed operationally they can introduce apparent changes in site climatology. In order to guard against this eventuality, observations from new instruments should be compared over an extended interval (at least one year; see the *Guide to Climatological Practices* (WMO-No. 100)) before the old measurement system is taken out of service. The same applies when there has been a change of site. Where this procedure is impractical at all sites, it is essential to carry out comparisons at selected representative sites to attempt to deduce changes in measurement data which might be a result of changing technology or enforced site changes.

### 1.3.5 Inspection and maintenance

#### 1.3.5.1 *Inspection of stations*

All synoptic land stations and principal climatological stations should be inspected no less than once every two years. Agricultural meteorological and special stations should be inspected at intervals sufficiently short to ensure the maintenance of a high standard of observations and the correct functioning of instruments.

The principal objective of such inspections is to ascertain that:

(a) The siting and exposure of instruments are known, acceptable and adequately documented;

(b) Instruments are of the approved type, in good order, and regularly verified against standards, as necessary;

(c) There is uniformity in the methods of observation and the procedures for calculating derived quantities from the observations;

(d) The observers are competent to carry out their duties;

(e) The metadata information is up to date.

Further information on the standardization of instruments is given in 1.5.

#### 1.3.5.2 *Maintenance*

Observing sites and instruments should be maintained regularly so that the quality of observations does not deteriorate significantly between station inspections. Routine (preventive) maintenance schedules include regular “housekeeping” at observing sites (for example, grass cutting and cleaning of exposed instrument surfaces) and manufacturers’ recommended checks on automatic instruments. Routine quality control (QC) checks carried out at the station or at a central point should be designed to detect equipment faults at the earliest possible stage. Depending on the nature of the fault and the type of station, corrective maintenance (instrument

replacement or repair) should be conducted according to agreed priorities and timescales. As part of the metadata, it is especially important that a log be kept of instrument faults, exposure changes, and remedial action taken where data are used for climatological purposes.

Further information on station inspection and management can be found in the *Manual on the WMO Integrated Global Observing System* (WMO-No. 1160).

## 1.4 GENERAL REQUIREMENTS OF INSTRUMENTS

### 1.4.1 Desirable characteristics

The most important requirements for meteorological instruments are the following:

(a) Uncertainty, according to the stated requirement for the particular variable;

(b) Reliability and stability;

(c) Convenience of operation, calibration and maintenance;

(d) Simplicity of design which is consistent with requirements;

(e) Durability;

(f) Acceptable cost of instrument, consumables and spare parts;

(g) Safe for staff and the environment.

With regard to the first two requirements, it is important that an instrument should be able to maintain a known uncertainty over a long period. This is much better than having a high level of initial confidence (meaning low uncertainty) that cannot be retained for long under operating conditions.

Initial calibrations of instruments will, in general, reveal deviations from the ideal output, necessitating corrections to observed data during normal operations. It is important that the corrections should be retained with the instruments at the observing site and that clear guidance be given to observers for their use.

Simplicity, strength of construction, and convenience of operation and maintenance are important since most meteorological instruments are in continuous use year in, year out, and may be located far away from good repair facilities. Robust construction is especially desirable for instruments that are wholly or partially exposed to the weather. Adherence to such characteristics will often reduce the overall cost of providing good observations, outweighing the initial cost.

Appropriate safety procedures must be implemented when using instruments containing dangerous chemicals (see in particular guidance on mercury (the present volume, Chapter 3, Annex 3.A) and hazardous chemicals (Chapter 8, 8.5 and 8.6 of Volume III).

In the case of radiosondes, environmental pollution should be considered when selecting radiosonde materials; Chapter 12, Annex 12.C of the present volume describes the issues and potential near-future solutions for each radiosonde component.

An estimate of the overall quality of the measurement data can be obtained from the Measurement Quality Classifications for Surface Observing Stations on Land (Annex 1.G). This scheme, in conjunction with the Siting Classifications for Surface Observing Stations on Land (Annex 1.D), forms part of the metadata of a measurand, and provides an indication of suitability of a measurement for a particular application.

### 1.4.2 Impact of the Minamata convention

The Minamata Convention on Mercury of the United Nations Environment Programme (UNEP) came into force globally in August 2017. It bans all production, import and export of observing instruments (thermometers, barometers, and the like) containing mercury (UNEP, 2017). This agreement is a global treaty to eliminate the use of mercury to protect both human health and the environment from its adverse effects. It was agreed at the fifth session of the Intergovernmental Negotiating Committee in Geneva in January 2013.

The Convention states that "each party shall not allow, by taking appropriate measures, the manufacture, import or export of mercury-added products listed in Part I of Annex A [of the Convention] after the phase-out date specified for those products". More specifically, this list includes the following non-electronic measuring devices, except non-electronic measuring devices installed in large-scale equipment or those used for high-precision measurement, where no suitable mercury-free alternative is available:

(a) Barometers;

(b) Hygrometers;

(c) Manometers;

(d) Thermometers;

(e) Sphygmomanometers.

A similar regulation became applicable in Europe on 10 April 2014 (Commission Regulation (EU) No. 847/2012) and a number of manufacturers in Europe are already unable to provide mercury-based instruments.

Therefore, mercury-based instruments are no longer recommended and it is strongly encouraged to take appropriate measures to put in place a migration strategy to move away from the use of all instruments containing this element. Due to recent advances in electronic and digital technologies, digital electronic barometers, thermometers and hygrometers are now state of the art. They can provide an economical, accurate and reliable alternative to their dangerous, mercury-based precedents and offer other significant advantages in terms of data storage and real-time data display.

### 1.4.3 Mechanically recording instruments

In many of the mechanically recording instruments used in meteorology, the motion of the sensing element is magnified by levers that move a pen on a chart on a clock-driven drum. Such recorders should be as free as possible from friction, not only in the bearings, but also between the pen and paper. Some means of adjusting the pressure of the pen on the paper should be provided, but this pressure should be reduced to a minimum consistent with a continuous legible trace. Means should also be provided in clock-driven recorders for making time marks. In the design of recording instruments that will be used in cold climates, particular care must be taken to ensure that their performance is not adversely affected by extreme cold and moisture, and that routine procedures (time marks, and so forth) can be carried out by the observers while wearing gloves.

Recording instruments should be compared frequently with instruments of the direct-reading type.

An increasing number of instruments make use of electronic recording in magnetic media or in semiconductor microcircuits. Many of the same considerations given for bearings, friction and cold-weather servicing apply to the mechanical components of such instruments.

## 1.5 MEASUREMENT STANDARDS, TRACEABILITY AND UNITS

### 1.5.1 Definitions of standards of measurement

The term "standard" and other similar terms denote the various instruments, methods and scales used to establish the uncertainty of measurements. A nomenclature for standards of measurement is given in the *International Vocabulary of Metrology – Basic and General Concepts and Associated Terms (VIM)*, which was prepared conjointly by the Bureau international des poids et mesures (BIPM), the International Electrotechnical Commission (IEC), the International Federation of Clinical Chemistry and Laboratory Medicine, the International Laboratory Accreditation Cooperation, the International Organization for Standardization (ISO), the International Union of Pure and Applied Chemistry, the International Union of Pure and Applied Physics and the International Organization of Legal Metrology, and issued by JCGM. The current version is JCGM 200:2012, available at http://www.bipm.org/en/publications/guides/vim.html. Some of the definitions are as follows:

**International System of Units/Système international (SI).** System of units, based on the International System of Quantities, their names and symbols, including a series of prefixes and their names and symbols, together with rules for their use, adopted by the General Conference on Weights and Measures (CGPM).

**Measurement standard.** Realization of the definition of a given quantity, with stated quantity value and associated measurement uncertainty, used as a reference.

Example 1: 1 kg mass measurement standard with an associated standard measurement uncertainty of 3 μg

Example 2: 100 Ω measurement standard resistor with an associated standard measurement uncertainty of 1 μΩ

**International measurement standard (international standard).** Measurement standard recognized by signatories to an international agreement and intended to serve worldwide.

Example: The international prototype of the kilogramme

**National measurement standard (national standard).** Measurement standard recognized by national authorities to serve in a State or economy as the basis for assigning quantity values to other measurement standards for the kind of quantity concerned.

**Primary measurement standard (primary standard).** Measurement standard established using a primary reference measurement procedure, or created as an artefact, chosen by convention.

Example 1: Primary measurement standard of amount-of-substance concentration prepared by dissolving a known amount of substance of a chemical component to a known volume of solution

Example 2: Primary measurement standard for pressure based on separate measurements of force and area

**Secondary measurement standard (secondary standard).** Measurement standard established through calibration with respect to a primary measurement standard for a quantity of the same kind.

**Reference measurement standard (reference standard).** Measurement standard designated for the calibration of other measurement standards for quantities of a given kind in a given organization or at a given location.

**Working measurement standard (working standard).** Measurement standard that is used routinely to calibrate or verify measuring instruments or measuring systems.

Notes:
1. A working measurement standard is usually calibrated with respect to a reference measurement standard.
2. In relation to verification, the terms "check standard" or "control standard" are also sometimes used.

**Transfer measurement device (transfer device).** Device used as an intermediary to compare measurement standards.

Note: Sometimes, measurement standards are used as transfer devices.

**Travelling measurement standard (travelling standard).** Measurement standard, sometimes of special construction, intended for transport between different locations.

**Collective standard.** A set of similar material measures or measuring instruments fulfilling, by their combined use, the role of a standard.

Example: The World Radiometric Reference

Notes:
1. A collective standard is usually intended to provide a single value of a quantity.
2. The value provided by a collective standard is an appropriate mean of the values provided by the individual instruments.

**Traceability.** A property of the result of a measurement or the value of a standard whereby it can be related to stated references, usually national or international standards, through an unbroken chain of comparisons all having stated uncertainties.

**Metrological traceability.** A property of a measurement result whereby the result can be related to a reference through a documented unbroken chain of calibrations, each contributing to the measurement uncertainty.

**Metrological traceability chain (traceability chain).** Sequence of measurement standards and calibrations that is used to relate a measurement result to a reference.

**Calibration.** Operation that, under specified conditions, in a first step, establishes a relation between the quantity values with measurement uncertainties provided by measurement standards and corresponding indications with associated measurement uncertainties and, in a second step, uses this information to establish a relation for obtaining a measurement result from an indication.

Notes:
1. A calibration may be expressed by a statement, calibration function, calibration diagram, calibration curve, or calibration table. In some cases, it may consist of an additive or multiplicative correction of the indication with associated measurement uncertainty.
2. Calibration should not be confused with adjustment of a measuring system, often mistakenly called "self-calibration", nor with verification of calibration.

**Calibration hierarchy.** Sequence of calibrations from a reference to the final measuring system, where the outcome of each calibration depends on the outcome of the previous calibration.

### 1.5.2 Traceability assurance

Measurements have a useful meaning if the results do not vary significantly with the usage of different instruments, operators or other parameters in the measurement process. This confidence is based on regulations, international agreements and QA in the measurement process. It is universally accepted to assess the quality of measurements by a quantitative statement, which is the measurement uncertainty associated with the measurement result. The confidence in the measurement result and the stated uncertainty relies on the traceability of measurements involving an unbroken and documented chain of comparisons linking measurement result to an internationally agreed measurement standard.

Measurements should be traceable to an internationally defined and accepted reference, which is in most cases the SI. Technical and organizational infrastructure has been developed and is maintained by BIPM. Maintenance of national standards and dissemination of traceability at the national level relies on National Metrology Institutes (NMIs) or designated institutes (DIs). The concept of RICs has been established by regional associations to support National Meteorological and Hydrological Services (NMHSs) in the dissemination of traceability to their national meteorological standards and related environmental monitoring instruments. Terms of reference of RICs are presented in Annex 1.C.

The responsibility for the implementation of traceability assurance on a national level lies with the NMHS, which should ensure all necessary steps to achieve the objective of the strategy. Lack of traceability assurance strongly reduces confidence in measurements and their usage within the local and global communities.

The strategy for traceability assurance is presented in Annex 1.B.

Instruments in use face very different environmental conditions than when they are in a controlled laboratory environment. Factors that affect the measured quantity in vivo (influencing quantities, drift in time, and the like) also have to be quantified and documented for each measurement. The estimated influences will add to the uncertainty value. Only then can a measurement result be compared with any other traceable result measured in another place and/or time.

To promote standardization of meteorological and related observations and to ensure the uniform publication of observations and statistics, sets of standard procedures and recommended practices have been developed (Chapter 4 of Volume V).

### 1.5.3 Symbols, units and constants

#### 1.5.3.1 *Symbols and units*

Instrument measurements produce numerical values. The purpose of these measurements is to obtain physical or meteorological quantities representing the state of the local atmosphere. For meteorological practices, instrument readings represent variables, such as “atmospheric pressure”, “air temperature” or “wind speed”. A variable with symbol $a$ is usually represented in the form $a = \{a\} \cdot [a]$, where $\{a\}$ stands for the numerical value and $[a]$ stands for the symbol for the unit. General principles concerning quantities, units and symbols are stated in publications from ISO (2009) and International Union of Pure and Applied Physics (Cohen and Giacomo, 1987). The SI should be used as the system of units for the evaluation of meteorological elements included in reports for international exchange. This system is published and updated by BIPM (2006). Guides for the use of the SI are issued by the United States National Institute of Standards and Technology (Thompson and Taylor, 2008) and ISO (2009). Variables not defined as an international symbol by the International System of Quantities, but commonly used in meteorology can be found in the *International Meteorological Tables* (WMO-No. 188) and relevant chapters in the present Guide.

The following units should be used for meteorological observations:

(a) Atmospheric pressure, $p$, in hectopascals (hPa);[6]

(b) Temperature, $t$, in degrees Celsius (°C) or $T$ in kelvins (K);

Note: The Celsius and kelvin temperature scales should conform to the actual definition of the International Temperature Scale of 1990 (ITS-90; see BIPM, 1990).

(c) Wind speed, in both surface and upper-air observations, in metres per second (m $s^{-1}$);

(d) Wind direction in degrees clockwise from true north or on the scale 0–36, where 36 is the wind from true north and 09 the wind from true east (°);

(e) Relative humidity, $U$, in per cent (%);

Note: BIPM recommends: "When any of the terms, %, ppm, etc. are used it is important to state the dimensionless quantity whose value is being specified." For example, in Chapter 4 this recommendation is followed by using %RH.

(f) Precipitation (total amount) in millimetres (mm) or kilograms per square metre (kg $m^{-2}$);[7]

(g) Precipitation intensity, $R_i$, in millimetres per hour (mm $h^{-1}$) or kilograms per square metre per second (kg $m^{-2}$ $s^{-1}$);[8]

(h) Snow water equivalent in kilograms per square metre (kg $m^{-2}$);

(i) Evaporation in millimetres (mm);

(j) Visibility in metres (m);

(k) Irradiance in watts per square metre and radiant exposure in joules per square metre (W $m^{-2}$, J $m^{-2}$);

(l) Duration of sunshine in hours (h);

(m) Cloud height in metres (m);

(n) Cloud amount in oktas;

(o) Geopotential, used in upper-air observations, in standard geopotential metres (m').

Note: Height, level or altitude are presented with respect to a well-defined reference. Typical references are MSL, station altitude or the 1 013.2 hPa plane.

The standard geopotential metre is defined as 0.980665 of the dynamic metre; for levels in the troposphere, the geopotential is close in numerical value to the height expressed in metres.

---

[6] The unit "pascal" is the principal SI-derived unit for the pressure quantity. The unit and symbol "bar" is a unit outside the SI system; in every document where it is used, this unit (bar) should be defined in relation to the SI. Its continued use is not encouraged. By definition, 1 mbar (millibar) = 1 hPa (hectopascal).

[7] Assuming that 1 mm equals 1 kg $m^{-2}$ independent of temperature.

[8] Recommendation 3 (CBS-XII), Annex 1, adopted through Resolution 4 (EC-LIII).

#### 1.5.3.2 *Constants*

The following constants have been adopted for meteorological use:

(a) Absolute temperature of the normal ice point $T_0 = 273.15$ K ($t = 0.00$ °C);

(b) Absolute temperature of the triple point of water $T = 273.16$ K ($t = 0.01$ °C), by definition of ITS-90;

(c) Standard acceleration of gravity ($g_n$) = 9.80665 m s$^{-2}$.

The values of other constants are given in the *International Meteorological Tables* (WMO-No. 188) and the *Technical Regulations* (WMO-No. 49).

## 1.6 UNCERTAINTY OF MEASUREMENTS

### 1.6.1 Meteorological measurements

#### 1.6.1.1 *General*

This section deals with definitions that are relevant to the assessment of accuracy and the measurement of uncertainties in physical measurements, and concludes with statements of required and achievable uncertainties in meteorology. First, it discusses some issues that arise particularly in meteorological measurements.

The term *measurement* is carefully defined in 1.6.1.2, but in most of the present Guide it is used less strictly to mean the process of measurement or its result, which may also be called an "observation". A *sample* is a single measurement, typically one of a series of spot or instantaneous readings of a sensing system, from which an average or smoothed value is derived to make an observation. For a more theoretical approach to this discussion, see Chapters 2 and 3 of Volume V of the present Guide.

The terms *accuracy*, *error* and *uncertainty* are carefully defined in 1.6.1.2, which explains that accuracy is a qualitative term, the numerical expression of which is uncertainty. This is good practice and is the form followed in the present Guide. Formerly, the common and less precise use of accuracy was as in "an accuracy of $\pm x$", which should read "an uncertainty of $x$".

#### 1.6.1.2 *Definitions of measurements and measurement errors*

The following terminology relating to the accuracy of measurements is based on JCGM (2012), which contains many definitions applicable to the practices of meteorological observations. Very useful and detailed practical guidance on the calculation and expression of uncertainty in measurements is given in ISO/IEC (2008) / JCGM (2008).

**Measurement.** The process of experimentally obtaining one or more quantity values that can reasonably be attributed to a quantity.

Note: The operations may be performed automatically.

**Measuring instrument.** Device used for making measurements, alone or in conjunction with one or more supplementary devices.

Examples: Platinum resistance thermometer (PRT), electronic barometer

Note: Instrument is sometimes used without the adjective measuring. If the instrument includes a sensor the adjective sensing may be used.

**Sensor.** Element of a measuring system that is directly affected by a phenomenon, body, or substance carrying a quantity to be measured.

Examples: Sensing coil of a PRT, Bourdon tube of a pressure gauge

Note: Sometimes the term "sensing element" is used for this concept.

**Result of a measurement.** A set of quantity values being attributed to a measurand together with any other available relevant information.

Notes:
1. When a result is given, it should be made clear whether it refers to the indication, the uncorrected result or the corrected result, and whether several values are averaged.
2. A complete statement of the result of a measurement includes information about the uncertainty of the measurement.

**Corrected result.** The result of a measurement after correction for systematic error.

**Value (of a quantity).** A number and reference (unit) together expressing the magnitude of a quantity.

Example: Length of a rod: 5.34 m

**True value (of a quantity).** The quantity value consistent with the definition of a quantity.

Notes:
1. This is a value that would be obtained by a perfect measurement.
2. True values are by nature indeterminate.

**Accuracy (of a measurement).** A qualitative term referring to the closeness of agreement between a measured quantity value and a true quantity value of a measurand. The accuracy of a measurement is sometimes understood as the closeness of agreement between measured quantity values that are being attributed to the measurand. It is possible to refer to an instrument or a measurement as having a high accuracy, but the quantitative measure of the accuracy is expressed in terms of uncertainty.

**Uncertainty.** A non-negative parameter characterizing the dispersion of the quantity values being attributed to a measurand, based on the information used.

**Repeatability.** The closeness of agreement between indications or measured quantity values obtained on the same or similar objects under a set of conditions that includes the same measurement procedure, same operators, same measuring system, same operating conditions and same location, and replicate measurements over a short period of time.

Note: Relevant statistical terms are given in ISO (1994*a*) and ISO (1994*b*).

**Reproducibility.** The closeness of agreement between indications or measured quantity values obtained on the same or similar objects under a set of conditions that includes different locations, operators and measuring systems, and replicate measurements.

**Error (of measurement).** Measured quantity value minus a reference quantity value.

**Instrumental bias.** Average of replicate indications minus a reference quantity value.

**Random error.** The component of measurement error that in replicate measurements varies in an unpredictable manner.

Notes:
1. Random measurement error equals measurement error minus systematic measurement error.
2. A reference quantity value for a random measurement error is the average that would ensue from an infinite number of replicate measurements of the same measurand.

**Systematic error.** The component of measurement error that in replicate measurements remains constant or varies in a predictable manner.

Notes:
1. Systematic measurement error equals measurement error minus random measurement error.
2. Like true value, systematic error and its causes cannot be completely known.

**Correction.** Compensation for an estimated systematic effect.

Some definitions are also repeated in Chapter 4 of Volume V of the present Guide for convenience.

### 1.6.1.3 *Characteristics of instruments*

Some other properties of instruments which must be understood when considering their uncertainty are taken from JCGM (2012).

**Sensitivity.** Quotient of the change in an indication of a measuring system and the corresponding change in a value of a quantity being measured.

Note: The sensitivity of a measuring system can depend on the value of the quantity being measured.

**Discrimination threshold.** The largest change in a value of a quantity being measured that causes no detectable change in the corresponding indication.

**Resolution.** The smallest change in a quantity being measured that causes a perceptible change in the corresponding indication.

**Hysteresis.** The property of a measuring instrument whereby its response to a given stimulus depends on the sequence of preceding stimuli.

**Stability (of an instrument).** The property of a measuring instrument whereby its metrological properties remain constant in time.

**Drift.** A continuous or incremental change over time in indication due to changes in metrological properties of a measuring instrument.

**Step response time.** The duration between the instant when an input quantity value of a measuring instrument or measuring system is subjected to an abrupt change between two specified constant quantity values and the instant when a corresponding indication settles within specified limits around its final steady value.

The following other definitions are used frequently in meteorology:

**Statements of response time.** The time for 90% of the step change is often given. The time for 50% of the step change is sometimes referred to as the half-time.

**Calculation of response time.** In most simple systems, the response to a step change is:

$$Y = A(1 - e^{-t/\tau}) \tag{1.1}$$

where $Y$ is the change after elapsed time $t$; $A$ is the amplitude of the step change applied; $t$ is the elapsed time from the step change; and $\tau$ is a characteristic variable of the system having the dimension of time.

The variable $\tau$ is referred to as the time constant or the lag coefficient. It is the time taken, after a step change, for the instrument to reach $1/e$ of the final steady reading.

In other systems, the response is more complicated and will not be considered here (see also Chapter 2 of Volume V).

**Lag error.** The error that a set of measurements may possess due to the finite response time of the observing instrument.

### 1.6.2 Sources and estimates of error

The sources of error in the various meteorological measurements are discussed in specific detail in the following chapters of the present Guide, but in general they may be seen as accumulating through the chain of traceability and the measurement conditions.

It is convenient to take air temperature as an example to discuss how errors arise, but it is not difficult to adapt the following argument to pressure, wind and other meteorological quantities. For temperature, the sources of error in an individual measurement are as follows:

(a) Errors in the international, national and working standards, and in the comparisons made between them. These may be assumed to be negligible for meteorological applications;

(b) Errors in the comparisons made between the working, travelling and/or check standards and the field instruments in the laboratory or in liquid baths in the field (if that is how the traceability is established). These are small if the practice is good (say ±0.1 K uncertainty at the 95% confidence level, including the errors in (a) above), but may quite easily be larger, depending on the skill of the operator and the quality of the equipment;

(c) Non-linearity, drift, repeatability and reproducibility in the field thermometer and its transducer (depending on the type of thermometer element);

(d) The effectiveness of the heat transfer between the thermometer element and the air in the thermometer shelter, which should ensure that the element is at thermal equilibrium with the air (related to system time constant or lag coefficient). In a well-designed aspirated shelter this error will be very small, but it may be large otherwise;

(e) The effectiveness of the thermometer shelter, which should ensure that the air in the shelter is at the same temperature as the air immediately surrounding it. In a well-designed case this error is small, but the difference between an effective and an ineffective shelter may be 3 °C or more in some circumstances;

(f) The exposure, which should ensure that the shelter is at a temperature that is representative of the region to be monitored. Nearby sources and heat sinks (buildings, other unrepresentative surfaces below and around the shelter) and topography (hills, land–water boundaries) may introduce large errors. The station metadata should contain a good and regularly updated description of exposure (see Annex 1.F) to inform data users about possible exposure errors.

Systematic and random errors both arise at all the above-mentioned stages. The effects of the error sources (d) to (f) can be kept small if operations are performed very carefully and

if convenient terrain for siting is available; otherwise these error sources may contribute to a very large overall error. However, they are sometimes overlooked in the discussion of errors, as though the laboratory calibration of the instruments could define the total error completely.

Establishing the true value is difficult in meteorology (Linacre, 1992). Well-designed instrument comparisons in the field may establish the characteristics of instruments to give a good estimate of uncertainty arising from stages (a) to (e) above. If station exposure has been documented adequately, the effects of imperfect exposure can be corrected systematically for some parameters (for example, wind; see Wieringa and Rudel, 2002) and should be estimated for others.

Comparing station data against numerically analysed fields using neighbouring stations is an effective operational QC procedure, if there are sufficient reliable stations in the region. Differences between the individual observations at the station and the values interpolated from the analysed field are due to errors in the field as well as to the performance of the station. However, over a period, the average error at each point in the analysed field may be assumed to be zero if the surrounding stations are adequate for a sound analysis. In that case, the mean and standard deviation of the differences between the station and the analysed field may be calculated, and these may be taken as the errors in the station measurement system (including effects of exposure). The uncertainty in the estimate of the mean value in the long term may, thus, be made quite small (if the circumstances at the station do not change), and this is the basis of climate change studies.

### 1.6.3 The measurement uncertainties of a single instrument

ISO/IEC (2008)/JCGM (2008) should be used for the expression and calculation of uncertainties. It gives a detailed practical account of definitions and methods of reporting, and a comprehensive description of suitable statistical methods, with many illustrative examples.

#### 1.6.3.1 *The statistical distributions of observations*

To determine the uncertainty of any individual measurement, a statistical approach is to be considered in the first place. For this purpose, the following definitions are stated (ISO/IEC (2008)/JCGM (2008); JCGM, 2012):

(a) Standard uncertainty;

(b) Expanded uncertainty;

(c) Variance, standard deviation;

(d) Statistical coverage interval.

If $n$ comparisons of an operational instrument are made with the measured variable and all other significant variables held constant, if the best estimate of the true value is established by use of a reference standard, and if the measured variable has a Gaussian distribution,[9] the results may be displayed as in Figure 1.2.

In this figure, $T$ is the true value, $\bar{O}$ is the mean of the $n$ values $O$ observed with one instrument, and $\sigma$ is the standard deviation of the observed values with respect to their mean values.

In this situation, the following characteristics can be identified:

(a) The systematic error, often termed bias, given by the algebraic difference $\bar{O} - T$. Systematic errors cannot be eliminated but may often be reduced. A correction factor can be applied

[9] However, note that several meteorological variables do not follow a Gaussian distribution. See 1.6.3.2.3.

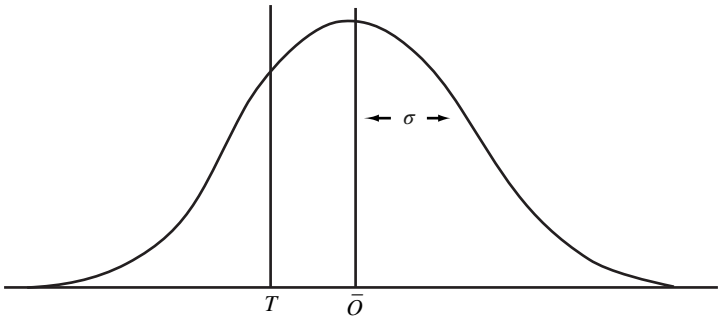



**Figure 1.2. The distribution of data in an instrument comparison**

to compensate for the systematic effect. Typically, appropriate calibrations and adjustments should be performed to eliminate the systematic errors of a measuring instrument. Systematic errors due to environmental or siting effects can only be reduced;

(b) The random error, which arises from unpredictable or stochastic temporal and spatial variations. The measure of this random effect can be expressed by the standard deviation $\sigma$ determined after $n$ measurements, where $n$ should be large enough. In principle, $\sigma$ is a measure for the uncertainty of $\bar{O}$;

(c) The accuracy of measurement, which is the closeness of the agreement between the result of a measurement and a true value of the measurand. The accuracy of a measuring instrument is the ability to give responses close to a true value. Note that "accuracy" is a qualitative concept;

(d) The uncertainty of measurement, which represents a parameter associated with the result of a measurement, that characterizes the dispersion of the values that could be reasonably attributed to the measurand. The uncertainties associated with the random and systematic effects that give rise to the error can be evaluated to express the uncertainty of measurement.

### 1.6.3.2 *Estimating the true value*

In normal practice, observations are used to make an estimate of the true value. If a systematic error does not exist or has been removed from the data, the true value can be approximated by taking the mean of a very large number of carefully executed independent measurements. When fewer measurements are available, their mean has a distribution of its own and only certain limits within which the true value can be expected to lie can be indicated. In order to do this, it is necessary to choose a statistical probability (level of confidence) for the limits, and the error distribution of the means must be known.

A very useful and clear explanation of this notion and related subjects is given by Natrella (1966). Further discussion is given by Eisenhart (1963).

#### 1.6.3.2.1 Estimating the true value – *n* large

When the number of $n$ observations is large, the distribution of the means of samples is Gaussian, even when the observational errors themselves are not. In this situation, or when the distribution of the means of samples is known to be Gaussian for other reasons, the limits between which the true value of the mean can be expected to lie are obtained from:

Upper limit:
$$L_U = \bar{X} + k \cdot \frac{\sigma}{\sqrt{n}} \tag{1.2}$$

Lower limit:
$$L_L = \bar{X} - k \cdot \frac{\sigma}{\sqrt{n}} \tag{1.3}$$

where $\bar{X}$ is the average of the observations Ō corrected for systematic error; $\sigma$ is the standard deviation of the whole population; and $k$ is a factor, according to the chosen level of confidence, which can be calculated using the normal distribution function.

Some values of $k$ are as follows:

| *Level of confidence* | *90%* | *95%* | *99%* |
|---|---|---|---|
| $k$ | 1.645 | 1.960 | 2.575 |

The level of confidence used in the table above is for the condition that the true value will not be outside the one particular limit (upper or lower) to be computed. When stating the level of confidence that the true value will lie between both limits, both the upper and lower outside zones have to be considered. With this in mind, it can be seen that $k$ takes the value 1.96 for a 95% probability, and that the true value of the mean lies between the limits $L_U$ and $L_L$.

#### 1.6.3.2.2 Estimating the true value – *n* small

When $n$ is small, the means of samples conform to Student's $t$ distribution provided that the observational errors have a Gaussian or near-Gaussian distribution. In this situation, and for a chosen level of confidence, the upper and lower limits can be obtained from:

Upper limit:
$$L_U \approx \bar{X} + t \cdot \frac{\hat{\sigma}}{\sqrt{n}} \tag{1.4}$$

Lower limit:
$$L_L \approx \bar{X} - t \cdot \frac{\hat{\sigma}}{\sqrt{n}} \tag{1.5}$$

where $t$ is a factor (Student's $t$) which depends upon the chosen level of confidence and the number $n$ of measurements; and $\hat{\sigma}$ . is the estimate of the standard deviation of the whole population, made from the measurements obtained, using:

$$\hat{\sigma}^2 = \frac{\sum_{i=1}^{n}\left(X_i - \bar{X}\right)^2}{n-1} = \frac{n}{n-1} \cdot \sigma_0^2 \tag{1.6}$$

where $X_i$ is an individual value $O_i$ corrected for systematic error.

Some values of $t$ are as follows:

| *Level of confidence* | *90%* | *95%* | *99%* |
|---|---|---|---|
| $df$ | | | |
| 1 | 6.314 | 12.706 | 63.657 |
| 4 | 2.132 | 2.776 | 4.604 |
| 8 | 1.860 | 2.306 | 3.355 |
| 60 | 1.671 | 2.000 | 2.660 |

where $df$ is the degrees of freedom related to the number of measurements by $df = n - 1$. The level of confidence used in this table is for the condition that the true value will not be outside the one particular limit (upper or lower) to be computed. When stating the level of confidence that the true value will lie between the two limits, allowance has to be made for the case in which $n$ is large. With this in mind, it can be seen that $t$ takes the value 2.306 for a 95% probability that the true value lies between the limits $L_U$ and $L_L$, when the estimate is made from nine measurements ($df = 8$).

The values of $t$ approach the values of $k$ as $n$ becomes large, and it can be seen that the values of $k$ are very nearly equalled by the values of $t$ when $df$ equals 60. For this reason, tables of $k$ (rather than tables of $t$) are quite often used when the number of measurements of a mean value is greater than 60 or so.

#### 1.6.3.2.3 **Estimating the true value – additional remarks**

Investigators should consider whether or not the distribution of errors is likely to be Gaussian. The distribution of some variables themselves, such as sunshine, visibility, humidity and ceiling, is not Gaussian and their mathematical treatment must, therefore, be made according to rules valid for each particular distribution (Brooks and Carruthers, 1953).

In practice, observations contain both random and systematic errors. In every case, the observed mean value has to be corrected for the systematic error insofar as it is known. When doing this, the estimate of the true value remains inaccurate because of the random errors as indicated by the expressions and because of any unknown component of the systematic error. Limits should be set to the uncertainty of the systematic error and should be added to those for random errors to obtain the overall uncertainty. However, unless the uncertainty of the systematic error can be expressed in probability terms and combined suitably with the random error, the level of confidence is not known. It is desirable, therefore, that the systematic error be fully determined.

### 1.6.3.3 ***Expressing the uncertainty***

If random and systematic effects are recognized, but reduction or corrections are not possible or not applied, the resulting uncertainty of the measurement should be estimated. This uncertainty is determined after an estimation of the uncertainty arising from random effects and from imperfect correction of the result for systematic effects. It is common practice to express the uncertainty as "expanded uncertainty" in relation to the "statistical coverage interval". To be consistent with common practice in metrology, the 95% confidence level, or $k = 2$, should be used for all types of measurements, namely:

$$< expanded\ uncertainty > = k \cdot \sigma = 2 \cdot \sigma \tag{1.7}$$

As a result, the true value, defined in 1.6.1.2, will be expressed as:

$$< true\ value > = < measured\ value > \pm < expanded\ uncertainty > = < measured\ value > \pm 2\sigma$$

#### 1.6.3.4 *Measurements of discrete values*

While the state of the atmosphere may be described well by physical variables or quantities, a number of meteorological phenomena are expressed in terms of discrete values. Typical examples of such values are the detection of sunshine, precipitation or lightning and freezing precipitation. All these parameters can only be expressed by "yes" or "no". For a number of parameters, all of which are members of the group of present weather phenomena, more than two possibilities exist. For instance, discrimination between drizzle, rain, snow, hail and their combinations is required when reporting present weather. For these practices, uncertainty calculations like those stated above are not applicable. Some of these parameters are related to a numerical threshold value (for example, sunshine detection using direct radiation intensity), and the determination of the uncertainty of any derived variable (for example, sunshine duration) can be calculated from the estimated uncertainty of the source variable (for example, direct radiation intensity). However, this method is applicable only for derived parameters, and not for the typical present weather phenomena. Although a simple numerical approach cannot be presented, a number of statistical techniques are available to determine the quality of such observations. Such techniques are based on comparisons of two datasets, with one set defined as a reference. Such a comparison results in a contingency matrix, representing the cross-related frequencies of the mutual phenomena. In its most simple form, when a variable is Boolean ("yes" or "no"), such a matrix is a two by two matrix with the number of equal occurrences in the elements of the diagonal axis and the "missing hits" and "false alarms" in the other elements. Such a matrix makes it possible to derive verification scores or indices to be representative for the quality of the observation. This technique is described by Murphy and Katz (1985). An overview is given by Kok (2000).

### 1.6.4 Accuracy requirements

#### 1.6.4.1 *General*

The uncertainty with which a meteorological variable should be measured varies with the specific purpose for which the measurement is required. In general, the limits of performance of a measuring device or system will be determined by the variability of the element to be measured on the spatial and temporal scales appropriate to the application.

Any measurement can be regarded as made up of two parts: the signal and the noise. The signal constitutes the quantity which is to be determined, and the noise is the part which is irrelevant. The noise may arise in several ways: from observational error, because the observation is not made at the right time and place, or because short-period or small-scale irregularities occur in the observed quantity which are irrelevant to the observations and need to be smoothed out. Assuming that the observational error could be reduced at will, the noise arising from other causes would set a limit to the accuracy. Further refinement in the observing technique would improve the measurement of the noise but would not give much better results for the signal.

At the other extreme, an instrument – the error of which is greater than the amplitude of the signal itself – can give little or no information about the signal. Thus, for various purposes, the amplitudes of the noise and the signal serve, respectively, to determine:

(a) The limits of performance beyond which improvement is unnecessary;

(b) The limits of performance below which the data obtained would be of negligible value.

This argument, defining and determining limits (a) and (b) above, was developed extensively for upper-air data by *Performance Requirements of Aerological Instruments* (WMO-No. 267). However, statements of requirements are usually derived not from such reasoning but from perceptions of practically attainable performance, on the one hand, and the needs of the data users, on the other.

### 1.6.4.2 *Required and achievable performance*

The performance of a measuring system includes its reliability, capital, recurrent and lifetime cost, and spatial resolution, but the performance under discussion here is confined to uncertainty (including scale resolution) and resolution in time.

Various statements of requirements have been made, and both needs and capability change with time. The statements given in Annex 1.A are the most authoritative at the time of writing, and may be taken as useful guides for development, but they are not fully definitive.

The requirements for the variables most commonly used in synoptic, aviation and marine meteorology, and in climatology are summarized in Annex 1.A.[10] It gives requirements only for surface measurements that are exchanged internationally. Details on the observational data requirements for Global Data-processing and Forecasting System Centres for global and regional exchange are given in the *Manual on the Global Data-processing and Forecasting System* (WMO-No. 485). The uncertainty requirement for wind measurements is given separately for speed and direction because that is how wind is reported.

The ability of individual sensing instruments or observing systems to meet the stated requirements is changing constantly as instrumentation and observing technology advance. The characteristics of typical instruments or systems currently available are given in Annex 1.A.[11] It should be noted that the achievable operational uncertainty in many cases does not meet the stated requirements. For some of the quantities, these uncertainties are achievable only with the highest quality equipment and procedures.

Uncertainty requirements for upper-air measurements are dealt with in the present volume, Chapter 12.

---

[10] Established by the Commission for Basic Systems (CBS) Expert Team on Requirements for Data from Automatic Weather Stations (2004) and approved by the president of CIMO for inclusion in the present Guide after consultation with the presidents of the other technical commissions.

[11] Established by the CIMO Expert Team on Surface Technology and Measurement Techniques (2004) and confirmed for inclusion in the present Guide by the president of CIMO.

## ANNEX 1.A. OPERATIONAL MEASUREMENT UNCERTAINTY REQUIREMENTS AND INSTRUMENT PERFORMANCE REQUIREMENTS

*(See explanatory notes at the end of the table; numbers in the top row indicate column numbers.)*

| *1* | *2* | *3* | *4* | *5* | *6* | *7* | *8* | *9* |
|---|---|---|---|---|---|---|---|---|
| *Variable* | *Range* | *Reported resolution* | *Mode of measurement/ observation* | *Required measurement uncertainty* | *Instrument time constant* | *Output averaging time* | *Achievable measurement uncertainty* | *Remarks* |
| **1. Temperature** | | | | | | | | |
| 1.1 Air temperature | –80 °C to 60 °C | 0.1 K | I | 0.3 K for ≤ –40 °C<br>0.1 K for > –40 °C and ≤ 40 °C<br>0.3 K for > 40 °C | 20 s | 1 min | 0.2 K | Achievable uncertainty and effective time constant may be affected by the design of the thermometer solar radiation screen. Time constant depends on the airflow over the sensing element |
| 1.2 Extremes of air temperature | –80 °C to 60 °C | 0.1 K | I | 0.5 K for ≤ –40 °C<br>0.3 K for > –40 °C and ≤ 40 °C<br>0.5 K for > 40 °C | 20 s | 1 min | 0.2 K | |
| 1.3 Sea-surface temperature | –2 °C to 40 °C | 0.1 K | I | 0.1 K | 20 s | 1 min | 0.2 K | |
| 1.4 Soil temperature | –50 °C to 50 °C | 0.1 K | I | | 20 s | 1 min | 0.2 K | |

| 1 | 2 | 3 | 4 | 5 | 6 | 7 | 8 | 9 |
|---|---|---|---|---|---|---|---|---|
| *Variable* | *Range* | *Reported resolution* | *Mode of measurement/ observation* | *Required measurement uncertainty* | *Instrument time constant* | *Output averaging time* | *Achievable measurement uncertainty* | *Remarks* |
| **2. Humidity** | | | | | | | | |
| 2.1 Dewpoint temperature | –80 °C to 35 °C | 0.1 K | I | 0.1 K | 20 s | 1 min | 0.25 K | Measurement uncertainty depends on the deviation from air temperature |
| 2.2 Relative humidity | 0%–100% | 1% | I | 1% | Wet-bulb temperature (psychrometer) | | | |
| | | | | | 20 s | 1 min | 0.2 K | If measured directly and in combination with air temperature (dry bulb). Large errors are possible due to aspiration and cleanliness problems (see also note 11). Threshold of 0 °C to be noticed for wet bulb |
| | | | | | Solid state and others | | | |
| | | | | | 40 s | 1 min | 3% | Time constant and achievable uncertainty of solid-state sensing instruments may show significant temperature and humidity dependence |

| 1 | 2 | 3 | 4 | 5 | 6 | 7 | 8 | 9 |
|---|---|---|---|---|---|---|---|---|
| *Variable* | *Range* | *Reported resolution* | *Mode of measurement/ observation* | *Required measurement uncertainty* | *Instrument time constant* | *Output averaging time* | *Achievable measurement uncertainty* | *Remarks* |
| **3. Atmospheric pressure** | | | | | | | | |
| 3.1 Pressure | 500–1 080 hPa | 0.1 hPa | I | 0.1 hPa | 2 s | 1 min | 0.15 hPa | Both station pressure and MSL pressure. Measurement uncertainty is seriously affected by dynamic pressure due to wind if no precautions are taken. Inadequate temperature compensation of the transducer may affect the measurement uncertainty significantly. MSL pressure is affected by the uncertainty in altitude of the barometer for measurements on board ships |
| 3.2 Tendency | Not specified | 0.1 hPa | I | 0.2 hPa | | | 0.2 hPa | Difference between instantaneous values |

| 1 | 2 | 3 | 4 | 5 | 6 | 7 | 8 | 9 |
|---|---|---|---|---|---|---|---|---|
| *Variable* | *Range* | *Reported resolution* | *Mode of measurement/ observation* | *Required measurement uncertainty* | *Instrument time constant* | *Output averaging time* | *Achievable measurement uncertainty* | *Remarks* |
| **4. Clouds** | | | | | | | | |
| 4.1 Cloud amount | 0/8–8/8 | 1/8 | I | 1/8 | n/a | | 2/8 | Period clustering algorithms may be used to estimate low cloud amount automatically |
| 4.2 Height of cloud base | 0 m–30 km | 10 m | I | 10 m for ≤ 100 m<br>10% for > 100 m | n/a | | ~10 m | Achievable measurement uncertainty can be determined with a hard target. No clear definition exists for instrumentally measured cloud-base height (e.g., based on penetration depth or significant discontinuity in the extinction profile). Significant bias during precipitation |
| 4.3 Height of cloud top | Not available | | | | | | | |

| 1 | 2 | 3 | 4 | 5 | 6 | 7 | 8 | 9 |
|---|---|---|---|---|---|---|---|---|
| *Variable* | *Range* | *Reported resolution* | *Mode of measurement/ observation* | *Required measurement uncertainty* | *Instrument time constant* | *Output averaging time* | *Achievable measurement uncertainty* | *Remarks* |
| **5. Wind** | | | | | | | | |
| 5.1 Speed | 0–75 m $s^{-1}$ | 0.5 m $s^{-1}$ | A | 0.5 m $s^{-1}$ for ≤ 5 m $s^{-1}$ 10% for > 5 m $s^{-1}$ | Distance constant 2–5 m | 2 and/or 10 min | | Average over 2 and/or 10 min Non-linear devices. Care needed in design of averaging process. Distance constant is usually expressed as response length Averages computed over Cartesian components (see Chapter 3, 3.6 of Volume V of the present Guide). When using ultrasonic anemometers, no distance constant or time constant is needed. For moving mobile stations, the movement of the station needs to be taken into account, inclusive of its uncertainty |
| 5.2 Direction | 0°–360° | 1° | A | 5° | Damping ratio > 0.3 | 2 and/or 10 min | 5° | |
| 5.3 Gusts | 0.1–150 m $s^{-1}$ | 0.1 m $s^{-1}$ | A | 10% | | 3 s | 0.5 m $s^{-1}$ for ≤ 5 m $s^{-1}$ 10% for > 5 m $s^{-1}$ | Highest 3 s average should be recorded |

| 1 | 2 | 3 | 4 | 5 | 6 | 7 | 8 | 9 |
|---|---|---|---|---|---|---|---|---|
| *Variable* | *Range* | *Reported resolution* | *Mode of measurement/ observation* | *Required measurement uncertainty* | *Instrument time constant* | *Output averaging time* | *Achievable measurement uncertainty* | *Remarks* |
| **6. Precipitation** | | | | | | | | |
| 6.1 Amount (daily) | 0–500 mm | 0.1 mm | T | 0.1 mm for ≤ 5 mm<br>2% for > 5 mm | n/a | n/a | The larger of<br>5% or 0.1 mm | Quantity based on daily amounts.<br>Measurement uncertainty depends on aerodynamic collection efficiency of gauges and evaporation losses in heated gauges |
| 6.2 Depth of snow | 0–25 m | 1 cm | I | 1 cm for ≤ 20 cm<br>5% for > 20 cm | < 10 s | 1 min | 1 cm | Average depth over an area representative of the observing site |
| 6.3 Thickness of ice accretion on ships | Not specified | 1 cm | I | 1 cm for ≤ 10 cm<br>10% for > 10 cm | | | | |
| 6.4 Precipitation intensity | 0.02–2 000 mm $h^{-1}$ | 0.1 mm $h^{-1}$ | I | (trace): n/a for 0.02–0.2 mm $h^{-1}$<br>0.1 mm $h^{-1}$ for 0.2–2 mm $h^{-1}$<br>5% for > 2 mm $h^{-1}$ | < 30 s | 1 min | Under constant flow conditions in laboratory,<br>5% above 2 mm $h^{-1}$,<br>2% above 10 mm $h^{-1}$<br>In field, 5 mm $h^{-1}$ and<br>5% above<br>100 mm $h^{-1}$ | Uncertainty values for liquid precipitation only.<br>Uncertainty is seriously affected by wind.<br>Instruments may show significant non-linear behaviour.<br>For < 0.2 mm $h^{-1}$: detection only (yes/no) instrument time constant is significantly affected during solid precipitation using catchment type of gauges |
| 6.5 Precipitation duration (daily) | 0–24 h | 60 s | T | n/a | 60 s | | | Threshold value of 0.02 mm $h^{-1}$ |

| 1 | 2 | 3 | 4 | 5 | 6 | 7 | 8 | 9 |
|---|---|---|---|---|---|---|---|---|
| *Variable* | *Range* | *Reported resolution* | *Mode of measurement/ observation* | *Required measurement uncertainty* | *Instrument time constant* | *Output averaging time* | *Achievable measurement uncertainty* | *Remarks* |
| **7. Radiation** | | | | | | | | |
| 7.1 Sunshine duration (daily) | 0–24 h | 60 s | T | 0.1 h | 20 s | n/a | The larger of 0.1 h or 2% | |
| 7.2 Net radiation, radiant exposure (daily) | Not specified | 1 J $m^{-2}$ | T | 0.4 MJ $m^{-2}$ for ≤ 8 MJ $m^{-2}$ 5% for > 8 MJ $m^{-2}$ | 20 s | n/a | 15% | Radiant exposure expressed as daily sums (amount) of (net) radiation. Best achievable operational uncertainty is obtained by combining the measurements of two pyranometers and two pyrgeometers |
| 7.3 Global downward/ upward solar radiation | Not specified | 1 J $m^{-2}$ | T | 2% | 20 s | n/a | 5% (daily) 8% (hourly) | Daily total exposure |
| 7.4 Downward/ upward long-wave radiation at Earth surface | Not specified | 1 J $m^{-2}$ | T | 5% | 20 s | n/a | 10% | |

| 1 | 2 | 3 | 4 | 5 | 6 | 7 | 8 | 9 |
|---|---|---|---|---|---|---|---|---|
| *Variable* | *Range* | *Reported resolution* | *Mode of measurement/ observation* | *Required measurement uncertainty* | *Instrument time constant* | *Output averaging time* | *Achievable measurement uncertainty* | *Remarks* |
| **8. Visibility** | | | | | | | | |
| 8.1 Meteorological optical range (MOR) | 10 m–100 km | 1 m | I | 50 m for ≤ 600 m<br>10% for > 600 m–≤ 1 500 m<br>20% for > 1 500 m | < 30 s | 1 and 10 min | The larger of 20 m or 20% | Achievable measurement uncertainty may depend on the cause of obscuration.<br>Quantity to be averaged: extinction coefficient (see Chapter 3, 3.6 of Volume V of the present Guide). Preference for averaging logarithmic values |
| 8.2 Runway visual range | 10–2 000 m | 1 m | A | 10 m for ≤ 400 m<br>25 m for > 400 m–≤ 800 m<br>10% for > 800 m | < 30 s | 1 and 10 min | The larger of 20 m or 20% | In accordance with Volume II, Attachment A of WMO-No. 49 and International Civil Aviation Organization (ICAO) Doc 9328-AN/908 (second ed., 2000).<br>New versions of these documents may exist, specifying other values. |
| 8.3 Background luminance | 0–40 000 cd $m^{-2}$ | 1 cd $m^{-2}$ | I | | 30 s | 1 min | 10% | Related to 8.2 Runway visual range |

| 1<br>*Variable* | 2<br>*Range* | 3<br>*Reported resolution* | 4<br>*Mode of measurement/ observation* | 5<br>*Required measurement uncertainty* | 6<br>*Instrument time constant* | 7<br>*Output averaging time* | 8<br>*Achievable measurement uncertainty* | 9<br>*Remarks* |
|---|---|---|---|---|---|---|---|---|
| **9. Waves** | | | | | | | | |
| 9.1 Significant wave height | 0–50 m | 0.1 m | A | 0.5 m for ≤ 5 m<br>10% for > 5 m | 0.5 s | 20 min | 0.5 m for ≤ 5 m<br>10% for > 5 m | Average over 20 min for instrumental measurements |
| 9.2 Wave period | 0–100 s | 1 s | A | 0.5 s | 0.5 s | 20 min | 0.5 s | Average over 20 min for instrumental measurements |
| 9.3 Wave direction | 0–360° | 1° | A | 10° | 0.5 s | 20 min | 20° | Average over 20 min for instrumental measurements |
| **10. Evaporation** | | | | | | | | |
| 10.1 Amount of pan evaporation | 0–100 mm | 0.1 mm | T | 0.1 mm for ≤ 5 mm<br>2% for > 5 mm | n/a | | | |

Notes:

1. Column 1 gives the basic variable.
2. Column 2 gives the common range for most variables; limits depend on local climatological conditions.
3. Column 3 gives the most stringent resolution as determined by the *Manual on Codes* (WMO-No. 306), Volumes I.1, I.2 and I.3.
4. In column 4:
   I = Instantaneous: to exclude the natural small-scale variability and the noise, an average value over a period of 1 min is considered as a minimum and most suitable; averages over periods of up to 10 min are acceptable.
   A = Averaging: average values over a fixed period, as specified by the coding requirements.
   T = Totals: totals over a fixed period, as specified by coding requirements.
5. Column 5 gives the recommended measurement uncertainty requirements for general operational use, that is, of level II data according to FM 12, 13, 14, 15 and its BUFR equivalents. They have been adopted by all eight technical commissions and are applicable for synoptic, aeronautical, agricultural and marine meteorology, hydrology, climatology, and the like. These requirements are applicable for both manned weather stations and AWSs as defined in the *Manual on the WMO Integrated Global Observing System* (WMO-No. 1160). Individual applications may have less stringent requirements. The stated value of required measurement uncertainty represents the uncertainty of the reported value with respect to the true value and indicates the interval in which the true value lies with a stated probability. The recommended probability level is 95% ($k = 2$), which corresponds to the 2 $\sigma$ level for a normal (Gaussian) distribution of the variable. The assumption that all known corrections are taken into account implies that the errors in reported values will have a mean value (or bias) close to zero. Any residual bias should be small compared with the stated measurement uncertainty requirement. The true value is the value which, under operational conditions, perfectly characterizes the variable to be measured/observed over the representative time interval, area and/or volume required, taking into account siting and exposure.

6. Columns 2 to 5 refer to the requirements established by the CBS Expert Team on Requirements for Data from AWSs in 2004.
7. Columns 6 to 8 refer to the typical operational performance established by the CIMO Expert Team on Surface Technology and Measurement Techniques in 2004.
8. Achievable measurement uncertainty (column 8) is based on instrument performance under nominal and recommended exposure that can be achieved in operational practice. It should be regarded as a practical aid to users in defining achievable and affordable requirements.
9. n/a = not applicable.
10. The term "uncertainty" has preference over "accuracy" (that is, uncertainty is in accordance with ISO/IEC/JCGM standards on the uncertainty of measurements (ISO/IEC (2008); JCGM (2008)).
11. Dewpoint temperature, relative humidity and air temperature are linked, and thus their uncertainties are linked. When averaging, preference is given to absolute humidity as the principal variable.

# ANNEX 1.B. STRATEGY FOR TRACEABILITY ASSURANCE

## 1. INTRODUCTION

Traceability of measurement and calibration results plays a key role for many application areas, ranging obviously from the assessment of climate variability and changes, but also to aspects that may have strong economic and legal impacts in the context of issuance of warnings for severe weather to protect lives and livelihoods.

Ensuring metrological traceability enables full confidence in the validity of measurement results, which leads to confidence in the implications of the measurement data: in the forecasts and warnings derived from the measurements; in climate analyses and trends derived from the measurements. And this in turn leads to improvements in disaster risk reduction (DRR), climate change mitigation, advice for policy developers, human health and safety, and property protection.

The lack of traceability of measurement results was recognized as a major concern by CIMO because the full potential of WIGOS would be brought into question without regular traceability. Therefore, CIMO stressed the need to sensitize NMHSs to the necessity of regular instrument calibrations, in addition to preventive maintenance and periodical instrument checks, as an essential tool to ensure the required traceability and quality of measurement results.

Numerous developing-country Members have no calibration laboratory at all to ensure the traceability of their instruments. Some Members are also facing challenges with the calibration of their network instruments and are replacing a comprehensive calibration strategy with a policy of carrying out field verification checks to identify instruments that do not conform to the required uncertainties and to perform complete laboratory calibrations only on these instruments. Field verification checks should cover the full measurement range, similarly to on-site regular calibrations, and they should be distinguished from the field inspections (see Chapter 4, 4.3.4 of Volume V of the present Guide), which are usually performed at one point (ambient conditions) and considered as "one-point" calibrations.

The strategy presented in this annex seeks to build upon best available practices to strengthen calibration services and improve traceability assurance across WMO Members. It focuses on providing widely acceptable guidelines to increase confidence in measurement results.

## 2. OBJECTIVE OF THE STRATEGY

The main objective of the calibration strategy for traceability assurance is to ensure the proper traceability of measurement and calibration results to the SI, through an unbroken chain of calibrations, each contributing to the measurement uncertainty.

This strategy applies to meteorological measurements for which a traceability chain to the SI is well established (for example, measurements of temperature, atmospheric pressure, humidity, wind speed, precipitation and solar radiation).

The strategy aims to provide guidance on how to effectively and efficiently achieve this objective.

## 3. RESPONSIBILITY FOR IMPLEMENTING THE STRATEGY

The responsibility for traceability assurance lies with WMO Members, who should ensure all the required calibrations as well as other necessary steps to achieve the objective of the strategy.

It is up to each NMHS to choose the most suitable approach for its traceability assurance, but ensuring the metrological traceability of all measurement results is strongly recommended.

## 4. WAYS OF TRACEABILITY ASSURANCE

Simplifying the ISO/JCGM definition, metrological traceability could be described as a direct link between a result of a measurement made in the field and a result obtained by the calibration process in a calibration laboratory. It ensures that different measurement methods and instruments used in different countries at different times produce reliable, repeatable, reproducible, compatible and comparable measurement results. When a measurement result is metrologically traceable, it can be confidently linked to the internationally accepted measurement references.

At the top of the metrological traceability chain there is an internationally defined and accepted reference, in most cases the SI, whose technical and organizational infrastructure has been developed and maintained by BIPM (www.bipm.org).

The framework through which NMIs demonstrate the international equivalence of their measurement standards and the calibration and measurement certificates they issue is called the Comité international des poids et mesures (CIPM) Mutual Recognition Arrangement (CIPM MRA). The outcomes of the MRA are the internationally recognized (peer-reviewed and approved) Calibration and Measurement Capabilities (CMCs) of the participating institutes. Approved CMCs and supporting technical data are publicly available from the CIPM MRA Key Comparison Database (http://kcdb.bipm.org/).

NMIs are responsible for maintenance of national standards and dissemination of traceability on the national level, either by themselves or by DIs. DIs are experienced institutes operating at the top of the national metrology system, but are not part of formal NMI structure. They are designated to be responsible for certain national standards and associated services that are not covered by the regular activities of NMIs.

Further dissemination of traceability relies on accredited calibration laboratories whose implemented quality management system is accredited by a national accreditation body. National accreditation bodies are usually signatories of the International Laboratory Accreditation Cooperation Mutual Recognition Arrangement, which ensures the acceptance of and confidence in calibration certificates across national borders.

Whenever possible, all the measurements within any particular country have to be traceable to the SI.

Taking into account all the aforementioned, as well as WMO Members' capabilities and needs, the following scenarios of traceability assurance (or lack of) can be identified (numbers indicate subsequent sections treating the subject):

4.1 Fully assured traceability – target, high confidence level in measurements;

4.2 Assured traceability (without accreditation) – good confidence level but some risks; improvement recommended;

4.3 Partially assured traceability – poor confidence and high risk; improvement required;

4.4 Lack of traceability – level of confidence cannot be assessed; urgent need for improvement.

## 4.1 Fully assured traceability – target, high confidence level in measurements

This traceability assurance (Figure 1.B.1) ensures fully traceable meteorological measurement results provided by particular NMHSs, to international standards. The whole traceability chain is covered by accreditation according to ISO/IEC 17025 and /or by CIPM MRA.

The NMHS field instruments have to be calibrated in the accredited calibration laboratory regularly, ensuring the highest achievable measurement uncertainties.

In the case that the calibration laboratory is also accredited for on-site calibrations that cover the whole range of meteorological parameters, those calibrations can be performed, but particular care concerning the required and achievable uncertainties must be taken into account.

If on-site calibrations are not covered by accreditation they must not be used for regular traceability assurance, but as field verification checks only. Field checks are not part of traceability assurance. They can only be used as an additional QC aiming to identify instruments performing outside of required uncertainties.

The following preconditions must be met to achieve this status:

- NMHS has a calibration laboratory;
- Laboratory personnel are well trained and competent to properly operate laboratory standards and equipment;
- Calibration standards and equipment meet the target uncertainties required for calibrations of meteorological instruments;

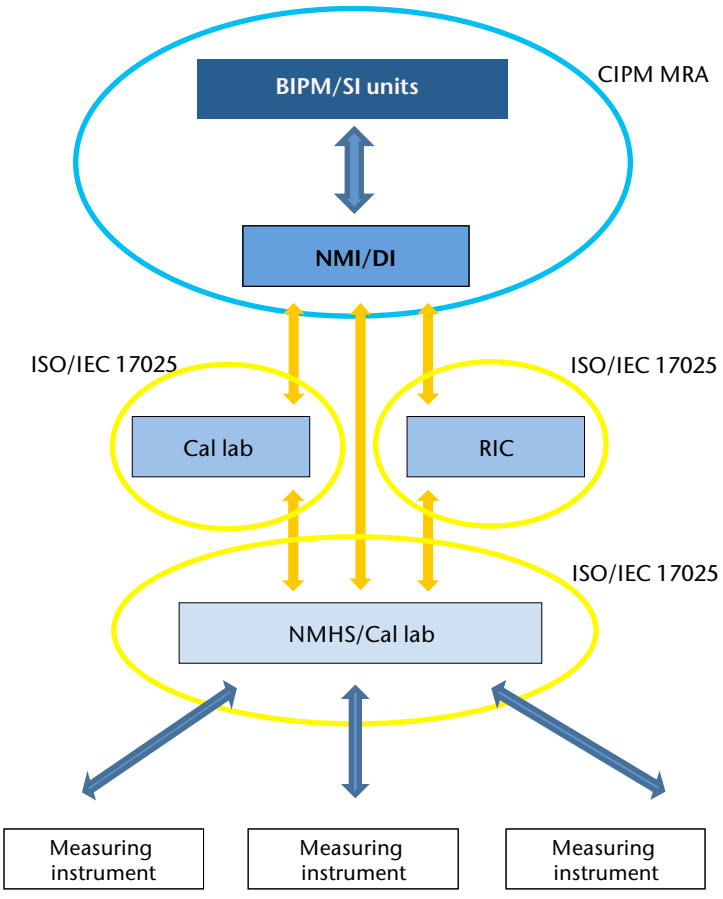



**Figure 1.B.1. Fully assured traceability – target, high confidence level in measurements**

– Calibration standards and equipment are regularly calibrated and maintained;

– Quality management system, including all the calibration procedures, working instructions and forms, is well documented and applied in laboratory work;

– Calibration laboratory is accredited according to ISO/IEC 17025;

– Calibration laboratory participates in interlaboratory comparisons.

A determined engagement of the NMHS management board to support continuous strengthening of the calibration laboratory should be stated. This should be followed by a clear policy on the needs for regular calibrations of meteorological instruments for which standards exist, under the responsibility of the NMHS, including the defined calibration intervals, as well as policy on implementation of calibration results.

Traceability of the laboratory standards and equipment has to be assured, by the means of calibrations at an NMI, DI, an accredited WMO RIC, or other accredited calibration laboratory, aiming at meeting the requirements of the Member in terms of target uncertainty.

The NMHS calibration laboratory should also, jointly with other relevant departments, develop procedures aimed at avoiding gaps in field measurements due to calibration activities. This should be achieved by a small reserve of calibrated instruments that can be used as a replacement set for the instruments in the network. Those recovered should be calibrated in the laboratory, forming, as a consequence, a new replacement set, and so on, to cover the whole network.

Additional QC could be assured by performing non-accredited on-site calibrations or field verification checks, but only to identify instruments performing outside uncertainty specifications. The instruments identified must be calibrated according to the accredited calibration methods.

A set of travelling standards and/or portable calibration devices used for non-accredited on-site calibrations or field checks must be regularly calibrated in the accredited calibration laboratory, and checked before and after field use.

### 4.2 Assured traceability (without accreditation) – good confidence level but some risks; improvement recommended

This type of traceability assurance (Figure 1.B.2) is still appropriate and acceptable, but does not ensure fully traceable meteorological measurement results. It is applicable to NMHSs with calibration facilities, but without accreditation according to ISO/IEC 17025. Although these calibration laboratories are not accredited, their calibration standards have to be calibrated by accredited calibration laboratories, accredited RICs, or by laboratories that are signatories of CIPM MRA. The least appropriate way, but still acceptable, could be a calibration done by non-accredited RIC, but that RIC must demonstrate fully assured traceability of its calibration standards.

The NMHS field instruments have to be calibrated either in the calibration laboratory (if it exists), or on site by portable calibration devices that are themselves calibrated at accredited laboratories and that cover the whole range of meteorological parameters. All calibrations have to be performed regularly ensuring the highest achievable measurement uncertainty.

Field verification checks can be used as an additional QC, aiming to identify instruments performing outside required uncertainties, but not for the traceability assurance.

The following preconditions must be met to achieve this status:

– NMHS has a calibration laboratory, or at least portable calibration devices covering the whole range of measured meteorological parameters;

– Laboratory personnel are well trained and competent to properly operate calibration standards and equipment;

– Calibration standards and equipment meet the target uncertainties required for calibrations of meteorological instruments;

– Calibration standards and equipment are regularly calibrated and maintained.

In addition, the following are highly recommended:

– Quality management system, including all the calibration procedures, working instructions and forms, should be documented and applied in laboratory work;

– Although not accredited, calibration facilities should follow the requirements of ISO/IEC 17025;

– Participation in the interlaboratory comparisons, which will be of great benefit.

Traceability of the laboratory standards and equipment has to be assured by the means of calibrations at an NMI, DI, RIC, or other accredited calibration laboratory. Non-accredited RICs must demonstrate traceability of their standards to the SI through an accredited laboratory, NMI or DI.

A determined engagement of the NMHS management board to support continuous strengthening of the calibration facilities is desired. It should be followed by a defined policy

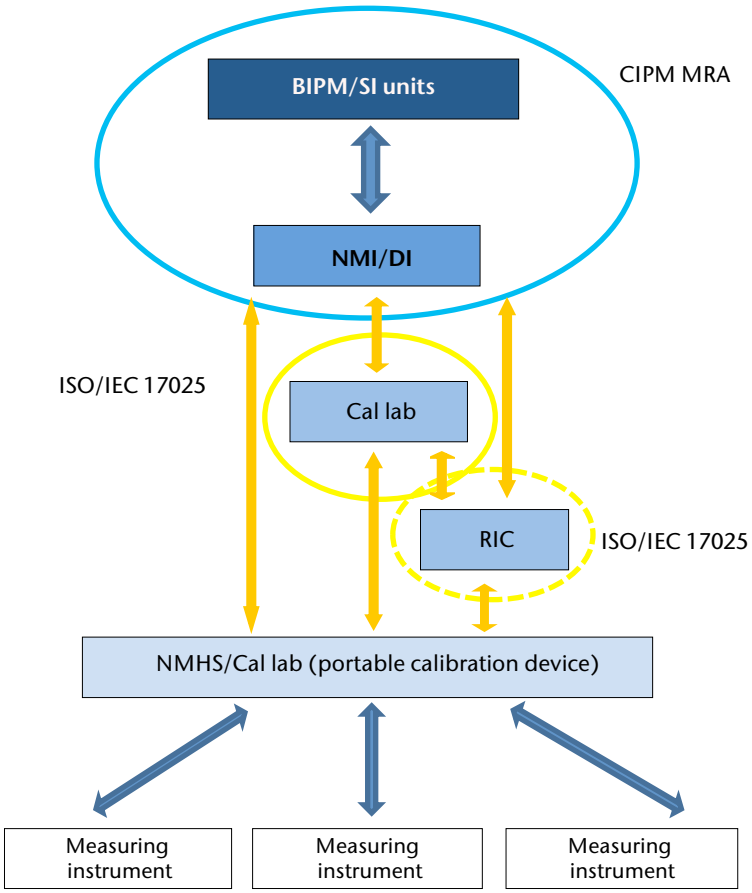



**Figure 1.B.2. Assured traceability (without accreditation) – good confidence level but some risks; improvement recommended**

on the needs for regular calibrations of all meteorological instruments under the responsibility of the NMHS, including the calibration intervals, as well as policy on implementation of calibration results.

The procedures aiming to avoid gaps in field measurements due to calibration activities should be developed. A possible solution is that the NMHS has at its disposal a small reserve of calibrated instruments that can be used as a replacement set for the instruments in the network. Those recovered should be calibrated regularly forming, as a consequence, a new replacement set, and so on, to cover the whole network.

Additional QC could be assured by performing field verification checks, but only to identify instruments out of uncertainty specifications. A set of travelling standards or portable calibration devices used for field checks has to be regularly calibrated in the calibration laboratory, and checked before and after field use.

### 4.3 Partially assured traceability – poor confidence and high risk; improvement required

This way of traceability assurance (Figure 1.B.3) is the least appropriate and should be followed only when the two aforementioned scenarios are not applicable. It is applicable to NMHSs without a calibration laboratory and portable calibration devices, but with a field inspection kit.

The field inspection kit must be regularly calibrated by accredited calibration laboratories, accredited RICs, calibration laboratories that are signatories of CIPM MRA, or in the worst case by

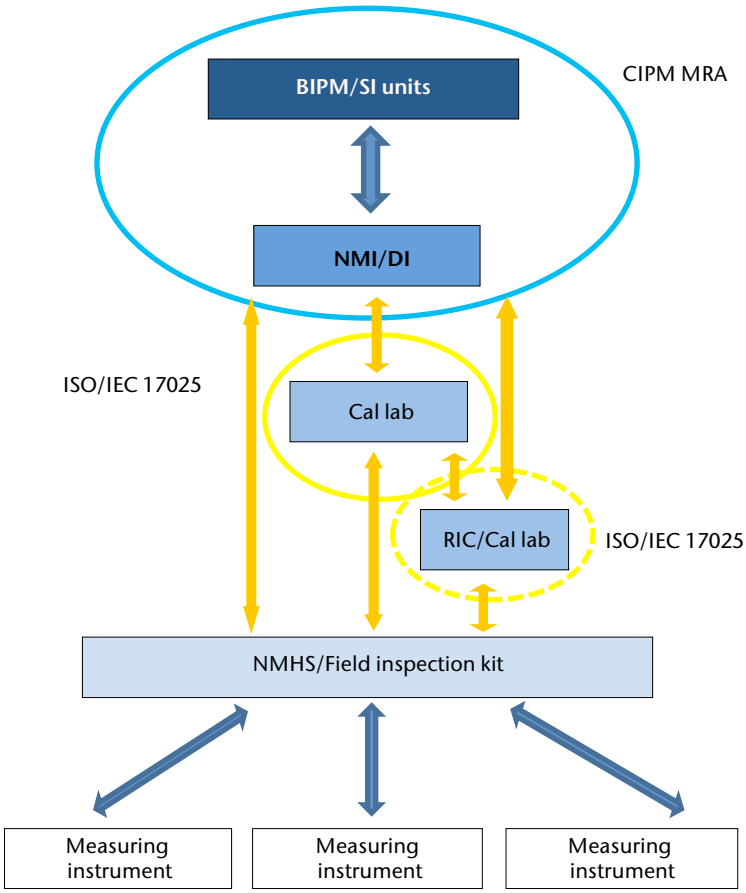



**Figure 1.B.3. Partially assured traceability – poor confidence and high risk; improvement required**

non-accredited RICs or calibration laboratories. The latter should only be used in the absence of all the aforementioned options and only when those laboratories can demonstrate fully assured traceability of their calibration standards.

A field inspection is not equivalent to a regular laboratory calibration or a field verification check, but could be an acceptable means of ensuring the quality of network observations. The field inspection can be considered as a "one-point calibration".

To enable at least partially assured traceability, Members are encouraged to achieve the following:

- A field inspection kit should be acquired with the required metrological characteristics regarding field instruments and with a calibration certificate issued by an accredited calibration laboratory;

- A cost-effective field inspection kit should include travelling instruments for the measurement of, as a minimum, pressure, temperature, humidity and rainfall;

- The field inspection kit should be regularly calibrated by an accredited calibration laboratory, accredited RIC, or by an NMI or DI. In the case that accredited calibration services are not available, the chosen calibration laboratory must demonstrate fully assured traceability;

- The field inspection kit should be checked before and after field use and cross-checked whenever more than one kit exists;

- Personnel designated to operate the field inspection kit should be well trained and competent to perform field inspections;

- Technical procedures for operating the field inspection kit should be documented;

- Field inspections should be performed on a regular time base;

- The results of field inspections must be documented.

### 4.4 Lack of traceability – not appropriate

Lack of metrological traceability leads to a lack of reliability of meteorological measurements, and consequently highly reduces confidence in the implications of measurement data such as weather forecasts, warnings and climate analyses. Ultimately, this brings into question the usefulness of meteorological measurements for the global community. So the consequences of untraceable measurement results are severe.

Therefore, measurement traceability is essential and WMO Members are urged to assure traceability of all the measurements under their responsibility.

# ANNEX 1.C. REGIONAL INSTRUMENT CENTRES

Note: Information on RIC capabilities and activities is available at https://community.wmo.int/activity-areas/imop/Regional_Instrument_Centres.

The Commission for Instruments and Methods of Observation recommended,[1] at its seventeenth session held in 2018, the following terms of reference for all RICs.

Regional Instrument Centres shall have the following capabilities to carry out their corresponding functions:

**Capabilities:**

(a) An RIC shall have the necessary facilities and laboratory equipment to perform the functions necessary for the calibration of meteorological and related environmental instruments;

(b) An RIC shall maintain a set of meteorological standard instruments and establish the traceability of its own measurement standards and measuring instruments to the SI;

(c) An RIC shall have competent managerial and technical staff to fulfil its functions;

(d) An RIC shall have technical procedures for calibration of meteorological and related environmental instruments using calibration equipment employed by the RIC;

(e) An RIC shall have and maintain a quality management system, preferably according to the ISO/IEC 17025 standard;

(f) An RIC shall participate in, and/or organize inter-laboratory comparisons of standard calibration instruments and methods;

(g) An RIC shall, as appropriate, utilize the available resources and capabilities to the Members' best interest;

(h) An RIC shall, as far as possible, apply international standards applicable for calibration laboratories, such as ISO/IEC 17025 standard;[2]

(i) An RIC shall ensure it is assessed by a recognized authority or by a WMO evaluation team, at least every four years, to verify its capabilities and performance.

**Corresponding functions:**

(a) An RIC shall assist Members of the Region, and possibly of other Regions, in calibrating their national meteorological standards and related environmental monitoring instruments;

(b) An RIC shall participate in, and/or organize, inter-laboratory comparisons, and support instrument intercomparisons following relevant WMO recommendations;

(c) According to relevant recommendations on the WMO Quality Management Framework, an RIC shall make a positive contribution to Members regarding the quality of measurements;

(d) An RIC shall advise Members on enquiries regarding instrument performance, maintenance and the availability of relevant guidance materials;

---

1 Recommendation 2 (CIMO-17).

2 RICs with accreditation for at least one parameter are called "ISO/IEC 17025-accredited RICs". Those without accreditation are strongly encouraged to achieve it as soon as possible.

(e) An RIC shall actively participate, or assist, in the organization of workshops on calibration and maintenance of meteorological and related environmental instruments;

(f) An RIC shall contribute to the standardization of meteorological and related environmental measurements;

(g) An RIC shall conduct or support the regular assessment of Members' needs for RIC services;

(h) An RIC shall regularly inform Members and report, on an annual basis, to the WMO Secretariat on the services offered to Members and activities carried out.

# ANNEX 1.D. SITING CLASSIFICATIONS FOR SURFACE OBSERVING STATIONS ON LAND

*(This annex presents the text of a common ISO/WMO standard. It is also published, with identical content, as ISO 19289:2014(E))*

Note: In this annex the word "sensor" is not used in the way it is defined in 1.6.1.2 of this chapter. According to this definition it should be replaced with the word "instrument". As this Annex is just referencing the text of the ISO standard this has not been changed.

## INTRODUCTION

The environmental conditions of a site[1] may influence measurement results. These conditions must be carefully analysed, in addition to assessing characteristics of the instrument itself, so as to avoid distorting the measurement results and affecting their representativeness, particularly when a site is supposed to be representative of a large area (that is, 100 to 1 000 $km^2$).

## 1. SCOPE

This annex[2] indicates exposure rules for various sensors. But what should be done when these conditions are not fulfilled?

There are sites that do not respect the recommended exposure rules. Consequently, a classification has been established to help determine the given site's representativeness on a small scale (impact of the surrounding environment). Hence, a class 1 site can be considered as a reference site. A class 5 site is a site where nearby obstacles create an inappropriate environment for a meteorological measurement that is intended to be representative of a wide area (at least tens of $km^2$). The smaller the siting class, the higher the representativeness of the measurement for a wide area. In a perfect world, all sites would be in class 1, but the real world is not perfect and some compromises are necessary. A site with a poor class number (large number) can still be valuable for a specific application needing a measurement in this particular site, including its local obstacles.

The classification process helps the actors and managers of a network to better take into consideration the exposure rules, and thus it often improves the siting. At least, the siting environment is known and documented in the metadata. It is obviously possible and recommended to fully document the site, but the risk is that a fully documented site may increase the complexity of the metadata, which would often restrict their operational use. That is why this siting classification is defined to condense the information and facilitate the operational use of this metadata information.

A site as a whole has no single classification number. Each parameter being measured at a site has its own class, and is sometimes different from the others. If a global classification of a site is required, the maximum value of the parameters' classes can be used.

---

1 A "site" is defined as the place where the instrument is installed.

2 Whereas this is referred to as an annex in the present Guide, it is referred to as a standard in the ISO document.

The rating of each site should be reviewed periodically as environmental circumstances can change over a period of time. A systematic yearly visual check is recommended: if some aspects of the environment have changed, a new classification process is necessary.

A complete update of the site classes should be done at least every five years.

In the following text, the classification is (occasionally) completed with an estimated uncertainty due to siting, which has to be added in the uncertainty budget of the measurement. This estimation is coming from bibliographic studies and/or some comparative tests.

The primary objective of this classification is to document the presence of obstacles close to the measurement site. Therefore, natural relief of the landscape may not be taken into account, if far away (that is, > 1 km). A method to judge if the relief is representative of the surrounding area is the following: does a move of the station by 500 m change the class obtained? If the answer is no, the relief is a natural characteristic of the area and is not taken into account.

Complex terrain or urban areas generally lead to high class numbers. In such cases, an additional flag "S" can be added to class numbers 4 or 5 to indicate specific environment or application (that is, 4S).

## 2. AIR TEMPERATURE AND HUMIDITY

### 2.1 General

Sensors situated inside a screen should be mounted at a height determined by the meteorological service (within 1.25 to 2 m as indicated in the present volume, Chapter 2, 2.1.4.2.1). The height should never be less than 1.25 m. The respect of the higher limit is less stringent, as the temperature gradient versus height is decreasing with height. For example, the difference in temperature for sensors located between 1.5 and 2 m is less than 0.2 °C.

The main discrepancies are caused by unnatural surfaces and shading:

(a) Obstacles around the screen influence the irradiative balance of the screen. A screen close to a vertical obstacle may be shaded from the solar radiation or "protected" against the night radiative cooling of the air, by receiving the warmer infrared (IR) radiation from this obstacle or influenced by reflected radiation;

(b) Neighbouring artificial surfaces may heat the air and should be avoided. The extent of their influence depends on the wind conditions, as wind affects the extent of air exchange. Unnatural or artificial surfaces to take into account are heat sources, reflective surfaces (for example buildings, concrete surfaces, car parks) and water or moisture sources (for example, ponds, lakes, irrigated areas).

Shading by nearby obstacles should be avoided. Shading due to natural relief is not taken into account for the classification (see above).

The indicated vegetation growth height represents the height of the vegetation maintained in a "routine" manner. A distinction is made between structural vegetation height (per type of vegetation present on the site) and height resulting from poor maintenance. Classification of the given site is therefore made on the assumption of regular maintenance (unless such maintenance is not practicable).

### 2.2 Class 1

(a) Flat, horizontal land, surrounded by an open space, slope less than ⅓ (19°);

(b) Ground covered with natural and low vegetation (< 10 cm) representative of the region;

(c) Measurement point situated:

(i) At more than 100 m from heat sources or reflective surfaces (buildings, concrete surfaces, car parks, and the like);

(ii) At more than 100 m from an expanse of water (unless significant of the region);

(iii) Away from all projected shade when the sun is higher than 5°.

A source of heat (or expanse of water) is considered to have an impact if it occupies more than 10% of the surface within a circular radius of 100 m surrounding the screen, makes up 5% of an annulus of 10–30 m, or covers 1% of a 10 m radius area.

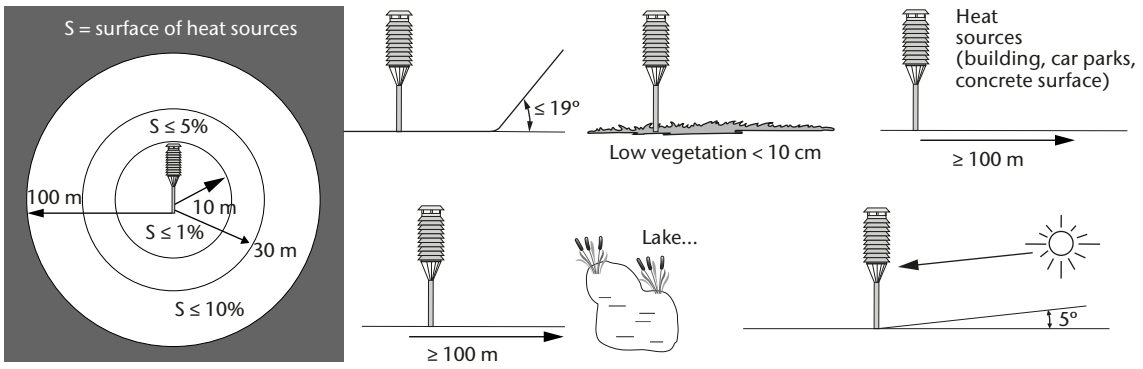



**Figure 1.D.1. Criteria for air temperature and humidity for class 1 sites**

## 2.3 Class 2

(a) Flat, horizontal land, surrounded by an open space, slope inclination less than ⅓ (19°);

(b) Ground covered with natural and low vegetation (< 10 cm) representative of the region;

(c) Measurement point situated:

(i) At more than 30 m from artificial heat sources or reflective surfaces (buildings, concrete surfaces, car parks, and the like);

(ii) At more than 30 m from an expanse of water (unless significant of the region);

(iii) Away from all projected shade when the sun is higher than 7°.

A source of heat (or expanse of water) is considered to have an impact if it occupies more than 10% of the surface within a radius of 30 m surrounding the screen, makes up 5% of an annulus of 5–10 m, or covers 1% of a 5 m radius area.

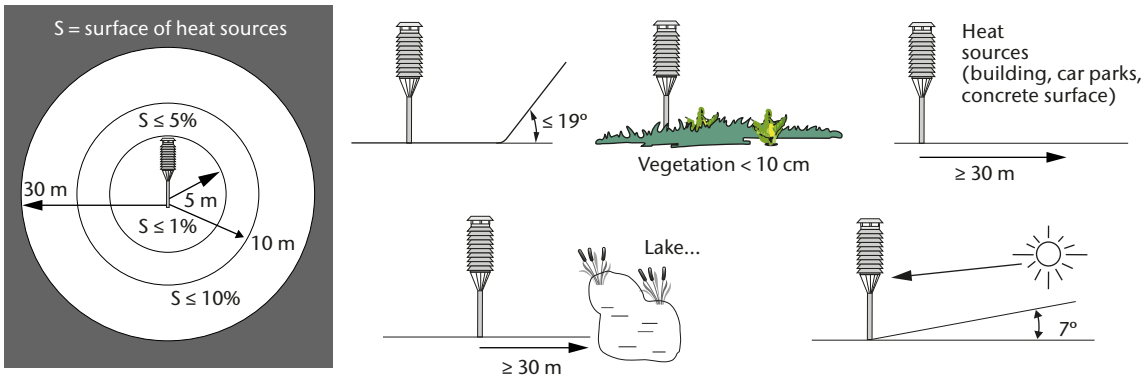



**Figure 1.D.2. Criteria for air temperature and humidity for class 2 sites**

## 2.4 Class 3 (additional estimated uncertainty added by siting up to 1 °C)

(a) Ground covered with natural and low vegetation (< 25 cm) representative of the region;

(b) Measurement point situated:

(i) At more than 10 m from artificial heat sources and reflective surfaces (buildings, concrete surfaces, car parks, and the like);

(ii) At more than 10 m from an expanse of water (unless significant of the region);

(iii) Away from all projected shade when the sun is higher than 7°.

A source of heat (or expanse of water) is considered to have an impact if it occupies more than 10% of the surface within a radius of 10 m surrounding the screen or makes up 5% of a 5 m radius area.

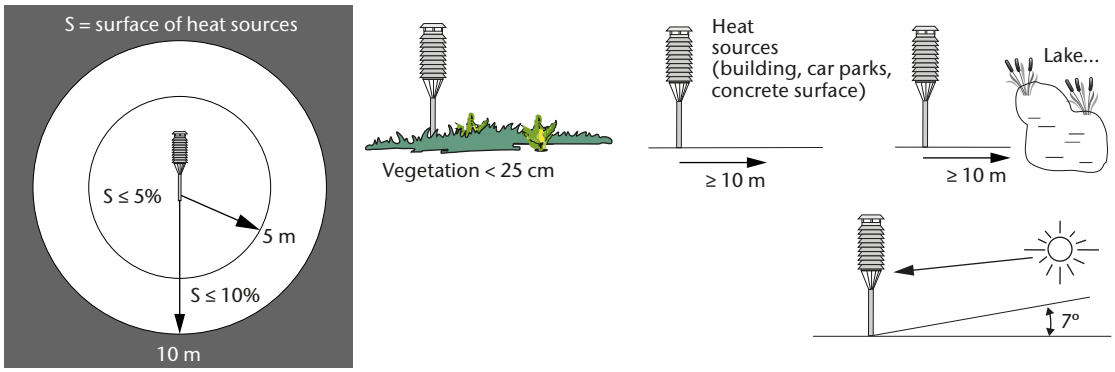



**Figure 1.D.3. Criteria for air temperature and humidity for class 3 sites**

### 2.5 Class 4 (additional estimated uncertainty added by siting up to 2 °C)

(a) Close, artificial heat sources and reflective surfaces (buildings, concrete surfaces, car parks, and the like) or expanse of water (unless significant of the region), occupying:

(i) Less than 50% of the surface within a 10 m radius around the screen;

(ii) Less than 30% of the surface within a 3 m radius around the screen;

(b) Away from all projected shade when the sun is higher than 20°.

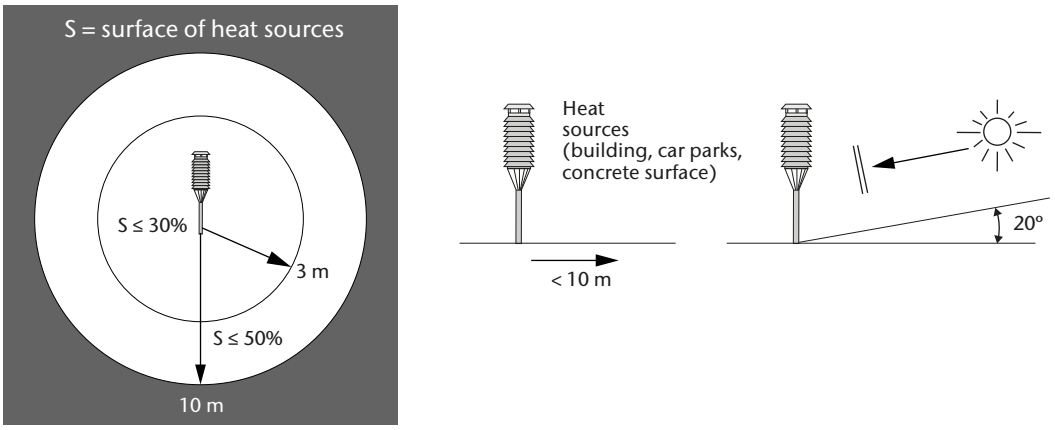



**Figure 1.D.4. Criteria for air temperature and humidity for class 4 sites**

### 2.6 Class 5 (additional estimated uncertainty added by siting up to 5 °C)

Site not meeting the requirements of class 4.

## 3. PRECIPITATION

### 3.1 General

Wind is the greatest source of disturbance in precipitation measurements, due to the effect of the instrument on the airflow. Unless raingauges are artificially protected against wind, for instance by a wind shield, the best sites are often found in clearings within forests or orchards, among trees, in scrub or shrub forests, or where other objects act as an effective windbreak for winds from all directions. Ideal conditions for the installation are those where equipment is set up in an area surrounded uniformly by obstacles of uniform height. An obstacle is an object with an effective angular width of 10° or more.

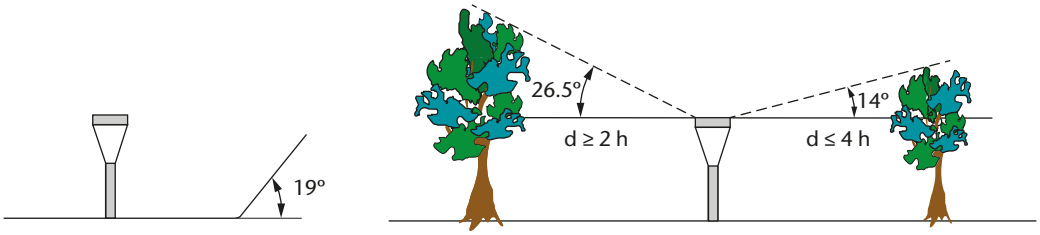
The choice of such a site is not compatible with constraints in respect of the height of other measuring equipment. Such conditions are practically unrealistic. If obstacles are not uniform, they are prone to generate turbulence, which distorts measurements; this effect is more pronounced for solid precipitation. This is the reason why more realistic rules of elevation impose a certain distance from any obstacles. The orientation of such obstacles with respect to prevailing wind direction is deliberately not taken into account. Indeed, heavy precipitation is often associated with convective factors, whereby the wind direction is not necessarily that of the prevailing wind. Obstacles are considered of uniform height if the ratio between the highest and lowest height is less than 2.

Reference for the heights of obstacles is the catchment's height of the raingauge.

3.2 **Class 1**

(a) Flat, horizontal land, surrounded by an open area, slope less than ⅓ (19°). The raingauge shall be surrounded by low obstacles of uniform height, that is subtending elevation angles between 14° and 26° (obstacles at a distance between 2 and 4 times their height);

(b) Flat, horizontal land, surrounded by an open area, slope less than ⅓ (19°). For a raingauge artificially protected against wind, the instrument does not necessarily need to be protected by obstacles of uniform height. In this case, any other obstacles must be situated at a distance of at least 4 times their height.




or:

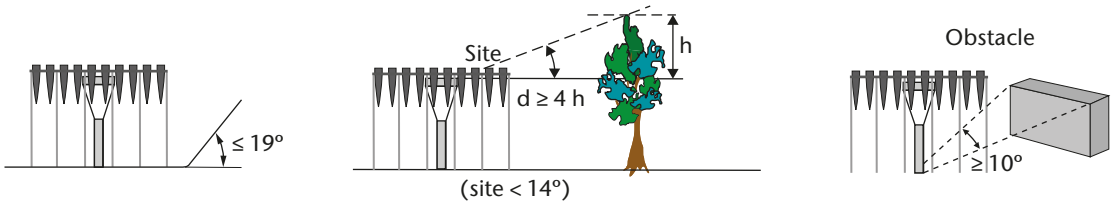



**Figure 1.D.5. Criteria for precipitation for class 1 sites**

3.3 **Class 2 (additional estimated uncertainty added by siting up to 5%)**

(a) Flat, horizontal land, surrounded by an open area, slope less than ⅓ (19°);

(b) Possible obstacles must be situated at a distance at least twice the height of the obstacle (with respect to the catchment's height of the raingauge).

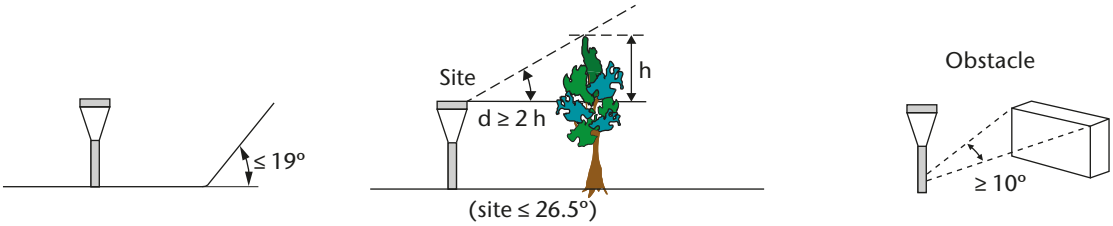



**Figure 1.D.6. Criteria for precipitation for class 2 sites**

3.4 **Class 3 (additional estimated uncertainty added by siting up to 15%)**

(a) Land is surrounded by an open area, slope less than ½ (≤ 30°);

(b) Possible obstacles must be situated at a distance greater than the height of the obstacle.

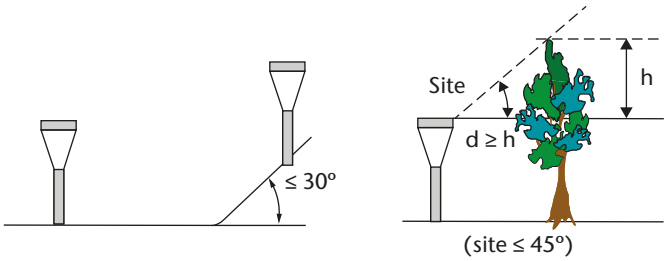



**Figure 1.D.7. Criteria for precipitation for class 3 sites**

## 3.5 Class 4 (additional estimated uncertainty added by siting up to 25%)

(a) Steeply sloping land (> 30°);

(b) Possible obstacles must be situated at a distance greater than one half (½) the height of the obstacle.

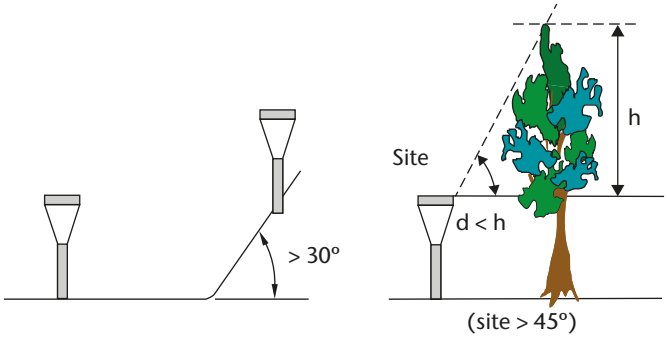



**Figure 1.D.8. Criteria for precipitation for class 4 sites**

## 3.6 Class 5 (additional estimated uncertainty added by siting up to 100%)

Obstacles situated closer than one half (½) their height (tree, roof, wall, and the like).

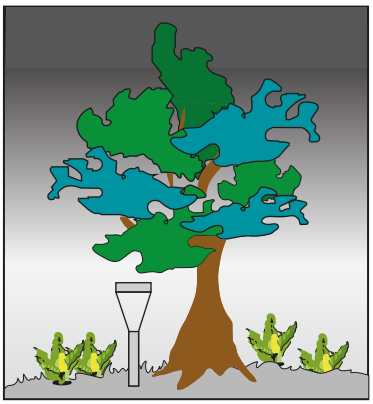


**Figure 1.D.9. Criteria for precipitation for class 5 sites**

## 4. SURFACE WIND

### 4.1 General

Conventional elevation rules stipulate that sensors should be placed 10 m above ground surface level and on open ground. Open ground here represents a surface where obstacles are situated at a minimum distance equal to at least 10 times their height.

### 4.2 Roughness

Wind measurements are disturbed not only by surrounding obstacles; terrain roughness also plays a role. WMO defines wind blowing at a geometrical height of 10 m and with a roughness length of 0.03 m as the surface wind for land stations.

This is regarded as a reference wind for which exact conditions are known (10 m height and roughness length of 0.03 m).

Therefore, roughness around the measuring site has to be documented. Roughness should be used to convert the measuring wind to the reference wind, but this procedure can be applied only when the obstacles are not too close. Roughness-related matters and correction procedure are described in the present volume, Chapter 5. The roughness classification, reproduced from the Annex of Chapter 5, is recalled here:

**Terrain classification from Davenport (1960) adapted by Wieringa (1980) in terms of aerodynamic roughness length $z_0$**

| *Class index* | *Short terrain description* | $z_0$ *(m)* |
|---|---|---|
| 1 | Open sea, fetch at least 5 km | 0.0002 |
| 2 | Mud flats, snow; no vegetation, no obstacles | 0.005 |
| 3 | Open flat terrain; grass, few isolated obstacles | 0.03 |
| 4 | Low crops; occasional large obstacles, $x/H > 20$ | 0.10 |
| 5 | High crops; scattered obstacles, $15 < x/H < 20$ | 0.25 |
| 6 | Parkland, bushes; numerous obstacles, $x/H \approx 10$ | 0.5 |
| 7 | Regular large obstacle coverage (suburb, forest) | 1.0 |
| 8 | City centre with high- and low-rise buildings | ≥ 2 |

Note: Here $x$ is a typical upwind obstacle distance and $H$ is the height of the corresponding major obstacles. For more detailed and updated terrain class descriptions see Davenport et al. (2000).

### 4.3 Environmental classification

The presence of obstacles, including vegetation, (almost invariably) means a reduction in average wind readings, but less significantly affects wind gusts.

The following classification assumes measurement at 10 m, which is the standard elevation for meteorological measurement.

When measurements are carried out at lower height (such as measurements carried out at 2 m, as is sometimes the case for agroclimatological purposes), a class 4 or 5 (see below) is to be used, with flag S (Specific situation).

Where numerous obstacles higher than 2 m are present, it is recommended that sensors be placed 10 m above the average height of the obstacles. This method allows the influence of the adjacent obstacles to be minimized. This method represents a permanent solution for partly eliminating the influence of certain obstacles. It inconveniently imposes the necessity for higher masts that are not standard and consequently are more expensive. It must be considered for certain sites and where used, the height of obstacles to be taken into account is that above the level situated 10 m below the sensors (for example, for an anemometer installed at a 13 m height, the reference "ground" level of the obstacles is at a 3 m height; an obstacle of 7 m is considered to have an effective height of 4 m).

In the following, an object is considered to be an obstacle if its effective angular width is over 10°. Tall, thin obstacles, that is with an effective angular width less than 10° and a height greater than 8 m, also need to be taken into account when considering class 1 to 3, as mentioned below. Under some circumstances, a cluster of tall, thin obstacles will have a similar effect to a single wider obstacle and will need to be considered as such.

Changes of altitude (positive or negative) in the landscape which are not representative of the landscape are considered as obstacles.

## 4.4 Class 1

(a) The mast should be located at a distance equal to at least 30 times the height of surrounding obstacles;

(b) Sensors should be situated at a minimum distance of 15 times the width of thin obstacles (mast, thin tree) higher than 8 m.

Single obstacles lower than 4 m can be ignored.

Roughness class index is less than or equal to 4 (roughness length ≤ 0.1 m).

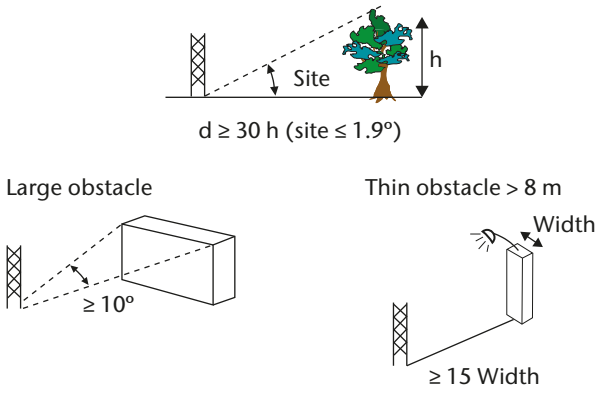



**Figure 1.D.10. Criteria for surface wind for class 1 sites**

## 4.5 Class 2 (additional estimated uncertainty added by siting up to 30%, possibility to apply correction)

(a) The mast should be located at a distance of at least 10 times the height of the surrounding obstacles;

(b) Sensors should be situated at a minimum distance of 15 times the width of thin obstacles (mast, thin tree) over 8 m high.

Single obstacles lower than 4 m can be ignored.

Roughness class index is less than or equal to 5 (roughness length ≤ 0.25 m).

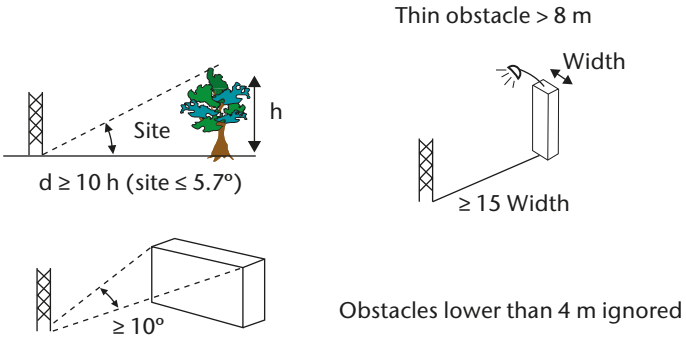



**Figure 1.D.11. Criteria for surface wind for class 2 sites**

Note: When the mast is located at a distance of at least 20 times the height of the surrounding obstacles, a correction (see the present volume, Chapter 5) can be applied. For nearer obstacles, a correction may be applied in some situations.

## 4.6 Class 3 (additional estimated uncertainty added by siting up to 50%, correction cannot be applied)

(a) The mast should be located at a distance of at least 5 times the height of surrounding obstacles;

(b) Sensors should be situated at a minimum distance of 10 times the width of thin obstacles (mast, thin tree) higher than 8 m.

Single obstacles lower than 5 m can be ignored.

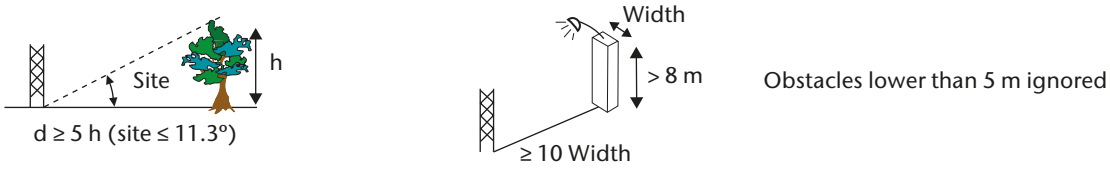



**Figure 1.D.12. Criteria for surface wind for class 3 sites**

## 4.7 Class 4 (additional estimated uncertainty added by siting greater than 50%)

(a) The mast should be located at a distance of at least 2.5 times the height of surrounding obstacles;

(b) No obstacle with an angular width larger than 60° and a height greater than 10 m, within a 40 m distance.

Single obstacles lower than 6 m can be ignored, only for measurements at 10 m or above.

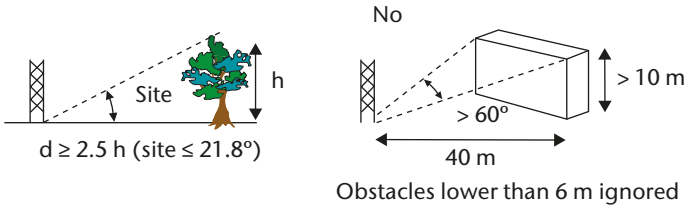



**Figure 1.D.13. Criteria for surface wind for class 4 sites**

### 4.8 Class 5 (additional estimated uncertainty cannot be defined)

Site not meeting the requirements of class 4.

## 5. GLOBAL AND DIFFUSE RADIATION

### 5.1 General

Close obstacles have to be avoided. Shading due to the natural relief is not taken into account for the classification. Non-reflecting obstacles below the visible horizon can be neglected.

An obstacle is considered as reflecting if its albedo is greater than 0.5.

The reference position for elevation angles is the sensitive element of the instrument.

### 5.2 Class 1

(a) No shade projected onto the sensor when the sun is at an angular height of over 5°. For regions with latitude ≥ 60°, this limit is decreased to 3°;

(b) No non-shading reflecting obstacles with an angular height above 5° and a total angular width above 10°.

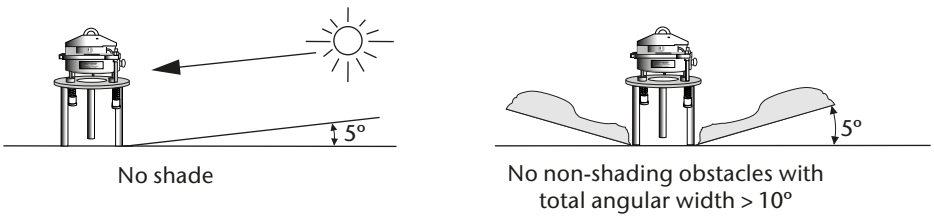



**Figure 1.D.14. Criteria for global and diffuse radiation for class 1 sites**

### 5.3 Class 2

(a) No shade projected onto the sensor when the sun is at an angular height of over 7°. For regions with latitude ≥ 60°, this limit is decreased to 5°;

(b) No non-shading reflecting obstacles with an angular height above 7° and a total angular width above 20°.

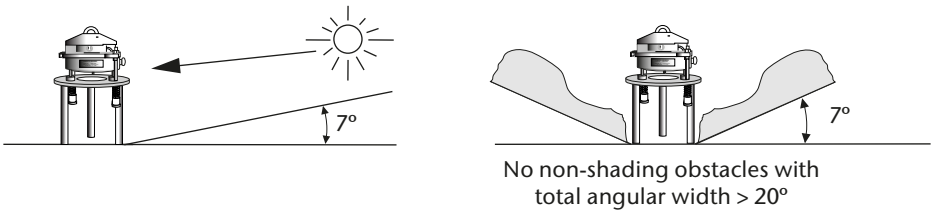



**Figure 1.D.15. Criteria for global and diffuse radiation for class 2 sites**

## 5.4 Class 3

(a) No shade projected onto the sensor when the sun is at an angular height of over 10°. For regions with latitude ≥ 60°, this limit is decreased to 7°;

(b) No non-shading reflecting obstacles with an angular height above 15° and a total angular width above 45°.

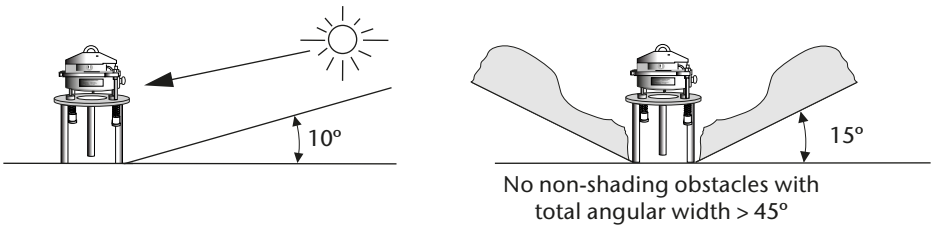



**Figure 1.D.16. Criteria for global and diffuse radiation for class 3 sites**

## 5.5 Class 4

No shade projected during more than 30% of the daytime, for any day of the year.

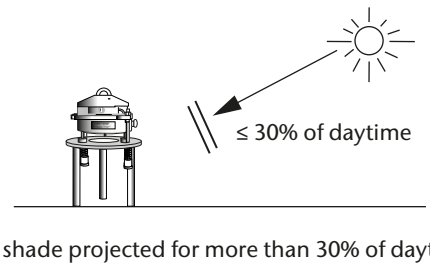



**Figure 1.D.17. Criteria for global and diffuse radiation for class 4 sites**

### 5.6 Class 5

Shade projected during more than 30% of the daytime, for at least one day of the year.

## 6. DIRECT RADIATION AND SUNSHINE DURATION

### 6.1 General

Close obstacles have to be avoided. Shading due to the natural relief is not taken into account for the classification. Obstacles below the visible horizon can be neglected.

The reference position for angles is the sensitive element of the instrument.

### 6.2 Class 1

No shade projected onto the sensor when the sun is at an angular height of over 3°.

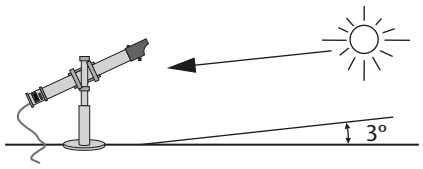



**Figure 1.D.18. Criteria for direct radiation and sunshine duration for class 1 sites**

### 6.3 Class 2

No shade projected onto the sensor when the sun is at an angular height of over 5°.

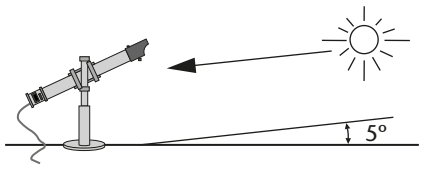



**Figure 1.D.19. Criteria for direct radiation and sunshine duration for class 2 sites**

6.4 **Class 3**

No shade projected onto the sensor when the sun is at an angular height of over 7°.

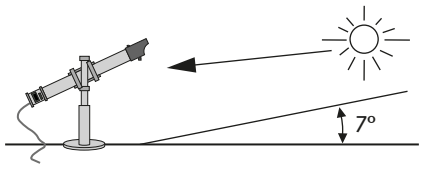



**Figure 1.D.20. Criteria for direct radiation and sunshine duration for class 3 sites**

6.5 **Class 4**

No shade projected during more than 30% of the daytime, for any day of the year.

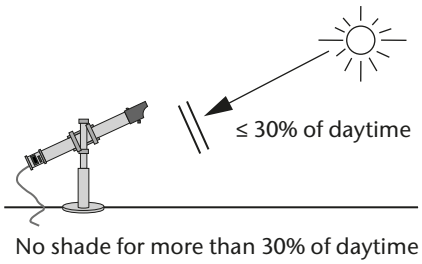



**Figure 1.D.21. Criteria for direct radiation and sunshine duration for class 4 sites**

6.6 **Class 5**

Shade projected during more than 30% of the daytime, for at least one day of the year.

## ANNEX 1.E. OPERATING EQUIPMENT IN EXTREME ENVIRONMENTS

Extreme weather events and harsh climatic environments have direct impacts on observing networks and may lead to interruption of core NMHS functions. The damage to real-time observing and monitoring systems during a weather event can severely limit the effectiveness of forecasting and warning services. The loss of delayed-mode observations affects the capacity to plan for extreme events and understand their climatology.

The WMO DRR country-level survey (2006)[1] identified droughts, flash and river floods, extreme winds, severe storms, tropical cyclones, storm surges, forest and wildfires, heatwaves, landslides and aviation hazards as the top ten hazards of concern to all Members. Maintenance of high-quality observational records (historical and real time) is critical for DRR applications. These observations are critical for:

(a) Risk identification;

(b) Risk reduction through the provision of early warnings to support emergency preparedness and response as well as climate services for medium- and long-term sectoral planning;

(c) Risk transfer through insurance and other financial tools.

Thus, interruptions in monitoring caused by damage to instruments and observing networks as a result of natural hazards hamper NMHS capacities to deliver effective services, not only during and following a disaster, but also in the long term if these systems are not rebuilt.

In this regard, CIMO stressed, at its sixteenth session, that it is critical to ensure that instrumentation and observing networks are designed according to standards that will withstand the impact of extreme weather events.

There are a number of factors that influence the robustness of equipment, both infrastructure and sensors in the field. The most straightforward and efficient way of ensuring the availability of a system is to design robustness into the system from the beginning. Factors to be considered are:

– Data availability – one of the first factors to consider. Are there other similar sources of information nearby? Is this the only information available to the forecasters and therefore critical in extreme events? If so, more effort will be needed in the design and planning of the station to ensure availability of data. What type of outages can you tolerate? Does it matter that the data are not available on a regular basis for five minutes? Does it matter if they are not available for a day? All these questions inform the way the system is designed for robustness and how the system is supported.

– Threats – what are the extreme weather events that will impact the weather station at a particular location? In an ideal world, all parameters would be monitored to the highest standard. However, funding realities generally mean that this is not possible. Identify the critical parameters and concentrate on ensuring their availability.

– Environmental impacts – every location presents its own challenges. Review topography to ensure any ground work will not be subject to water erosion. Include in your consideration soil type, local pollution sources, proximity to the sea and salt corrosion, risk of vandalism, and the like. These threats impact both the design and the maintenance requirements.

Once the need for the observation is appreciated, and the strengths and weaknesses of the location have been assessed, then a range of mitigation strategies can be considered to maximize the availability of observations and minimize operational cost. These approaches fall into one of several categories listed in Table 1.E.1.

[1] https://library.wmo.int/idurl/4/32236

**Table 1.E.1. General approaches for mitigating the impact of extreme environment on observation instrumentation and infrastructure**

| *Approach* | *Method* | *Strength* | *Weakness* |
|---|---|---|---|
| Site redundancy | Increase the density of measurement locations and equipment in critical areas | Increased density of measurements reduces the impact of the loss of information from a single site | Increase in capital costs and maintenance efforts. |
| | | Potential to use lower-cost solutions | Risk of overall lower-quality data and reliability |
| | | Allows network QC, potentially reducing maintenance costs and predicting system failures | |
| Instrument redundancy | Duplicate sensitive or vulnerable instruments at a particular site | Increased availability of data | Increase in capital costs |
| | | Greater flexibility to manage outages and maintenance | |
| Use of environmentally appropriate infrastructure materials | Choose materials that are designed to survive in extreme environments (e.g., marine and high-grade steel, UV-resistant plastics, high-oil-containing timbers) | Depending on usage, these materials will last longer and be stronger | Tend to be more expensive both as raw materials and in construction |
| | | Reduces maintenance burden | |
| | Use appropriately rated enclosures and glands | Reduces the risk of damage to equipment caused by water ingress or dust | Short-term costs can be slightly higher |
| Design | Use of structural engineers for design of infrastructure such as masts | Ensures the infrastructure will withstand extreme weather conditions | Short-term costs can be slightly higher |
| | | Lengthens the life of infrastructure by minimizing the stress caused by environmental impacts | |
| | | Reduces over engineering and associated costs | |

Specific examples of event types and the threat they pose to infrastructure and instruments in the immediate and longer term are given in Table 1.E.2. Methods of mitigation of these threats are also provided. These mitigations are in line with the four approaches of Table 1.E.1. While extensive, the mitigations are not exhaustive; they are a compilation of general knowledge and experience of a variety of NMHSs. In applying any of these methods, the user will need to consider the impact on measurements in their situation. While mitigation may work for a particular problem, it may also cause issues for other parameters. The user needs to consider the specific environment before employing any of these solutions.

**Table 1.E.2. Extreme weather hazards, examples of their associated infrastructure and sensor vulnerabilities, and mitigating actions**

| **Event type** | **Hail** | |
|---|---|---|
| Cause | Characteristic of weather systems such as thunderstorms | |
| Considerations | What size and intensity of hail would the system need to cope with?<br>* Generally hail less than 2.5 cm diameter is not considered to be significant hail, while > 4.5 cm hail will create a significant dent in a car, and > 7 cm will smash a windscreen<br>* Less than 5% of hail is greater than 2.5 cm diameter | |
| *Dominant hazard* | *Vulnerability or impact to infrastructure* | *Mitigation* |
| Impact | * Damage to: radomes - dints and holes; observer shelters - breakage of louvers; electronics enclosures - dints and holes; masts - dints, nicks or snapping | * Use high strength materials (including steel, carbon fibre) for the outer skin materials of enclosures, and the like, and that the structures are strong and well supported<br>* Use component-designed radomes, shelters, enclosures, and the like, that allow for panel changes |
| | * Deterioration of coated surfaces | * Use high strength materials that do not require painting or other coating methods |
| | * Damage to solar panels | * Install removable high-strength, stiff and structurally supported covers |
| | * Deterioration of painted surfaces | * Use high-strength and corrosion resistant materials that do not require painting or other coating methods |
| | *Vulnerability or impact to sensors* | *Mitigation* |
| Impact | * Mechanical anemometers, damage to cups in particular. Small and light weight plastic cups are particularly vulnerable | * Use heavy-duty instruments constructed from strong materials. Depending on the use, specialized materials such as carbon fibre may be considered |
| | * Ultrasonic anemometers, damage to arms and detectors causing misalignment<br>* Radiation instruments, damage to their domes | * Use heavy-duty instruments mounts and arms constructed from strong materials. Depending on the use, specialized materials such as carbon fibre may be considered<br>* Use alternate technologies such as pitot tube anemometers that rely on aerodynamic design and have minimally exposed components |

| **Event Type** | **Flood** | |
|---|---|---|
| Cause | Result of significant weather systems, including thunderstorms, cyclones, and the like. Flooding may occur well down stream of the weather event | |
| Considerations | Is the system expected to resume function post immersion?<br>What maximum rainfall amount and rate would be expected?<br>Is the site vulnerable to upstream flooding? | |
| *Dominant hazard* | *Vulnerability or impact to infrastructure* | *Mitigation* |
| Water ingress | * Ground-mounted equipment undermined or washed away | * Use mounting systems that stabilize the surrounding soil by spreading the load. There are commercial solutions that use a submerged "tripod" arrangement that minimizes soil disturbance while spreading the load |
| | | * Design and align foundations parallel to any expected surface flow to minimize hydrostatic pressure |
| Corrosion | * Equipment damaged by exposure/immersion in water | * Use materials such as marine grade stainless steel, galvanized iron or steel, appropriate plastics; avoid the use of aluminium |
| | | * Ensure all connectors are wrapped in water proofing tape to prevent corrosion |
| | | * Use preventative coatings and impregnating materials, e.g., fish oil, paint |
| | | * In marine environments, use sacrificial anodes |
| Contamination | * Corrosion of metal components, particularly connectors, welds, joints | * Perform regular data monitoring and regular inspections and maintenance of infrastructure and equipment in vulnerable environments to manage maintenance regime |
| | | * Coat welds, joints and nuts with grease, e.g., silicon, even butter |
| Power surge | * Loss of data due to power or communications failure | * Include redundant communications via an alternate supplier |
| Debris | * Damage from large debris in stream flow impacting towers and screens | * Reinforce lower sections of towers to expected flood height |
| | * Damage to protective coatings | * Ensure all powder or other coating is pit and chip free |

| **Event Type** | **Flood** | |
|---|---|---|
| *Dominant hazard* | *Vulnerability or impact to instruments* | *Mitigation* |
| Water ingress | * Any non-submersible sensor | * Mount the data acquisition system enclosure as high as practical to avoid being submerged (water stage station for example)<br>* Design and align foundations parallel to any expected surface flow to minimize hydrostatic pressure<br>* Use appropriately "IP" (ingress protection or international protection) rated seals and enclosures for equipment, typically IP67 and above for waves and splash |
| | * Equipment in close proximity to high water flow (direct contact or erosion) becomes submerged | * Use appropriately IP-rated seals and enclosures for equipment, typically IP67 and above for waves and splash |
| Corrosion | * Equipment damaged by exposure/immersion in water, particularly connectors, welds, joints | * Use appropriately IP-rated seals and enclosures for equipment, typically IP67 and above for waves and splash<br>* Avoid metals that do not passivate or are susceptible to corrosion for example low grade steel<br>* Inspect equipment regularly to ensure all paint and coated surfaces are pit and chip free<br>* Protect connectors and clamps using grease/oil impregnated tape or similar<br>* Carefully select metal types at joints or use of isolating separators and lubricants (high viscosity grease) to ensure that electrolysis is minimized |
| Contamination | * Foreign chemical or dirt build-up on sensing elements, such as relative humidity sensing elements | * Perform regular inspections and data monitoring to manage maintenance regime |
| Debris | * Damage from large debris in stream flow impacting towers and screens | * In flood prone areas, elevate instruments and enclosures above flood level |

| **Event type** | **Land/mudslide** | |
|---|---|---|
| Cause | Result of rainfall in combination with unstable ground conditions | |
| Considerations | * What is the slope of the land?<br>* Is the area subject to a long period of moderate rainfall? | |
| *Dominant hazard* | *Vulnerability or impact to infrastructure* | *Mitigation* |
| Water ingress | * Ground-mounted equipment undermined or washed away | * Use mounting systems that stabilize the surrounding soil by spreading the load. There are commercial solutions that use a submerged "tripod" arrangement that minimizes soil disturbance while spreading the load<br>* Use appropriately IP-rated seals and enclosures for equipment, typically IP67 and above for waves and splash<br>* Mount data acquisition system enclosure as high as practical when the sensor can be submerged (water stage station for example) |
| Water current | * Ground-mounted equipment undermined or washed away | * Use mounting systems that stabilize the surrounding soil by spreading the load. There are commercial solutions that use a submerged "tripod" arrangement that minimizes soil disturbance while spreading the load<br>* Design and align foundations parallel to any expected surface follow to minimize hydrostatic pressure |
| Mud | * Nearly all, total destruction | * Site equipment on local mounds, or sculpture land to redirect mud and water around equipment |
| Debris | * Nearly all, total destruction<br>See also "Flood" | * Reinforce lower sections of towers to expected land/mud slide height |
| *Dominant hazard* | *Vulnerability or impact to instruments* | *Mitigation* |
| Water ingress | * Failure of any non-submersible sensor | * Mount data-acquisition system enclosure as high as practical when the sensor can be submerged (water stage station for example)<br>* Use appropriately IP-rated sensor enclosures and seals, typically IP67 and above for waves and splash |
| Water current | * Instruments break away or are submerged in mud | * Mount instruments at height greater than expected 20- to 50-year event |
| Mud | * Nearly all, total destruction | * Perform regular inspections and data monitoring to manage maintenance regime |

| **Event type** | **High winds** | |
|---|---|---|
| Cause | Extreme weather systems such as cyclone, thunderstorm, and the like, with winds over 100 km $h^{-1}$ (approx. 27.8 m $s^{-1}$) | |
| Considerations | * What maximum average wind and maximum instantaneous wind would a system need to withstand?<br>* Is there much material that could become flying debris during an event? | |
| *Dominant hazard* | *Vulnerability or impact to infrastructure* | *Mitigation* |
| Wind | * Damage to: radomes - dints and holes; observer shelters - breakage of louvers; electronics enclosures - dints and holes; masts - dints, nicks or snapping | * Use high strength materials (including steel, carbon fibre) for the outer skin materials of enclosures, and the like, and ensure the structures are strong and well supported |
| | | * Use component-designed radomes, shelters, enclosures, and the like, that allow for panel changes |
| | * Major structural damage due to debris | * Use guy wires on tower/tripod mast to minimize damage from vibration, attached to suitable anchors, e.g., concrete or physical anchors |
| | * Structural damage due to drag and wind pressure | * Ensure all compartments/doors close securely; consider inclusion of door-open warning alarms. |
| | | * Where practical, design infrastructure to reduce wind load using curved and low profile surfaces |
| | | * Consider the aerodynamics of the design to minimize drag and to stabilize the construction |
| | * Undermining of infrastructure supports through erosion and wind stress | * Perform regular inspections, particularly after major events, to ensure the structural integrity of foundations and mounts |
| | * Creation of micro-fractures, degradation of welded joints and loosening of clamps, and the like, due to wind vibration | * Perform regular inspections, particularly after major events, to ensure the structural integrity of foundations and mounts |
| | | * Provide additional support for major infrastructure such as guy wires for masts to limit flexing during high winds |
| Debris | * Towers severely damaged | * Use towers/tripods with appropriate wind load rating |
| | | * Attach masts to suitable anchors, e.g., concrete or physical anchors |

| **Event type** | **High winds** | |
|---|---|---|
| *Dominant hazard* | *Vulnerability or impact to instruments* | *Mitigation* |
| Wind | * Damage to instruments due to wind force and small debris | * Use heavy-duty instruments<br>* Use wind instruments with few moving parts, such as "pitot tube" instruments which use pressure difference, and ultrasonic wind instruments, to eliminate vulnerabilities associated with moving parts; however, these may still be damaged by flying debris<br>* Inspect and ensure instruments are appropriately and securely mounted prior to the event, and that raingauges and screens are appropriately bolted down<br>* Tie down or remove any loose objects or material that could act as flying debris during a storm. Inspect surroundings for trees or bushes with branches that are likely to break or fall during a high wind event; arrange for their removal<br>* Use high strength rope or wire to support anemometer arm<br>* Ensure cabling is well secured and supported<br>* Consider the aerodynamics of the design to minimize drag and to stabilize the construction |
| Debris | * Damage to instruments due to flying debris | * Clean up the area around the equipment and remove any material that could become a projectile |

| **Event type** | **Thunderstorms** | |
|---|---|---|
| Cause | Strong winds, lightning and rainfall from larger storms | |
| Considerations | * Are the systems expected to operate after a lightning strike? | |
| *Dominant hazard* | *Vulnerability or impact to infrastructure* | *Mitigation* |
| Lightning | * Electrical surge | * Use electrical surge protection on the power circuit and individual surge protection on each monitored channel (e.g., temperature, wind)<br>* Use appropriate earthing of infrastructure through a collector (e.g., Franklin rod or spline ball), to a conductor for dissipation to ground. Note: all connections must maintain high conductivity and bends should be no greater than 45 degrees |
| Water | * Corrosion | * Use suitable materials such as stainless or galvanized steel and appropriate plastics<br>* Use preventative coatings and impregnating materials, e.g., fish oil, paint<br>* In marine environments use sacrificial anodes<br>* Perform regular inspection and maintenance of infrastructure and equipment in vulnerable environments |
| | See also "Flood" | |
| | See also "High wind" | |

| **Event type** | **Thunderstorms** | |
|---|---|---|
| *Dominant hazard* | *Vulnerability or impact to instruments* | *Mitigation* |
| Lightning | * Instruments with exposure and no tolerance for direct or indirect lightning strikes | * Use grounding rod/plate, finial, and the like, on weather station tower/tripod |
| | | * Use surge-suppression devices between instruments and data-acquisition system to protect the data-acquisition system |
| | * Induced noise | * Avoid long unshielded cables |
| Water | * Corrosion of connectors, and the like | * Protect connectors and clamps using grease/oil impregnated tape or similar |
| | | * Carefully select metal types at joints or use isolating separators and lubricants (high-viscosity grease) to ensure that electrolysis is minimized |
| | * Foreign chemical build-up on sensing elements, such as relative humidity sensing elements | * Perform regular inspection and data monitoring to manage maintenance regime |
| | See also "Flood" | |
| | See also "High wind" | |

| **Event type** | **Tropical cyclone** | |
|---|---|---|
| Cause | Characteristic of a weather system | |
| Considerations | * Does rotating winds present any additional risk? | |
| *Dominant hazard* | *Vulnerability or impact to infrastructure* | *Mitigation* |
| Wind | * Rotating winds | * For infrastructure that may rotate in high winds, design mounts and cables so that it does not drive or turn cables beyond limits<br>* Tie down or remove any loose objects or material that could act as flying debris during a storm. Inspect surroundings for trees or bushes with branches that are likely to break or fall during a high wind event; arrange for their removal |
| | See also "High wind" | |
| Debris | See also "High wind" | |

| **Event type** | **Tornado** | |
|---|---|---|
| Cause | A weather sub-system characterized by high winds and blowing debris | |
| Considerations | * Do rotating winds present any additional risk? | |
| *Dominant hazard* | *Impact to infrastructure examples* | *Mitigation* |
| Wind | * Rotating winds | * For infrastructure that may rotate in high winds, design mounts and cables so that it does not drive or turn cables beyond limits |
| | See also "High wind" | |
| Debris | See also "High wind" | |

| **Event type** | **Storm surge** |
|---|---|
| Cause | Results of cyclones and severe weather |
| Considerations | Constraints |
| Current | See also "Tsunami" |
| Water | See also "Flood" |
| Debris | See also "Flood" |

| **Event type** | **Tsunami** | |
|---|---|---|
| Cause | Independent of meteorological factors, resulting from geological movement, underwater land slip or meteor | |
| Considerations | | |
| *Dominant hazard* | *Vulnerability or impact to infrastructure* | *Mitigation* |
| Current | * Erosion or loss of footings | * Ensure tower and screen footings are reinforced to deal with the force of water travelling between 2 and 20 m $s^{-1}$. Note the run-up for a tsunami is significantly greater than the height of the wave<br>* Secure masts and large infrastructure to nearby structures with additional ropes<br>* Tie down or remove any loose objects or material that could act as flying debris during a storm. Inspect surroundings for trees or bushes with branches that are likely to break or fall during a high wind event; arrange for their removal |
| Water | See also "Flood" | |
| Debris | See also "Flood" | |
| *Dominant hazard* | *Vulnerability or impact to instruments* | *Mitigation* |
| Current | * Nearly all, total destruction | * In tsunami-prone areas, mount instruments above likely tsunami run-up height |
| | See also "Flood" | |
| | See also "Flood" | |

| **Event type** | **Snow/blizzard/icing** | |
|---|---|---|
| Cause | Extreme cold weather systems, and associated with prolonged cold and windy weather | |
| Considerations | * Are systems expect to operate after freeze/thaw situations?<br>* Are instruments or infrastructure specified to cope with sustained depressed temperatures? | |
| *Dominant hazard* | *Vulnerability or impact to infrastructure* | *Mitigation* |
| Cold and ice accretion | * Deterioration of shelters, masts, and the like, due to the weight of ice/snow | * Investigate the use of ice phobic coatings and materials |
| | * Weakening of screens and enclosures caused by the expansion of freezing water in joints, cracks and crevices | * Ensure screens and enclosures are well maintained; use materials that are tolerant to expansion stress and less prone to rot such as non-brittle plastics |
| | * Towers/masts | * Use towers/masts that are slightly flexible and/or that will vibrate slightly to loosen snow and ice |
| | * Snow/Ice cover on solar panels resulting in eventual loss of power | * Tilt solar panels as close to vertical as possible to prevent snow/ice accretion |
| Wind | * Failure of infrastructure (e.g., mast) in high wind due to ice accretion | * Choose materials that maintain elasticity below expected minimum temperature |
| | | * De-ice on a regular schedule |

| **Event type** | **Snow/blizzard/icing** | |
|---|---|---|
| *Dominant hazard* | *Vulnerability or impact to instruments* | *Mitigation* |
| Cold and ice accretion | * Ice build-up on instruments, e.g., mechanical anemometers, ultrasonic sensors, rain sensors and gauges | * Use heated instruments (e.g., anemometers) and heat cycling instruments (e.g., humidity) if practical. Ensure the heater does not interfere with other instruments<br>* Use a continuous flow of air (ideally dry air) to prevent water or snow to settle, or ice to form<br>* Apply heat tape directly to surfaces (electrical resistance elements embedded in a flexible sheet or nichrome wire); most effective on sensors without moving parts<br>* Use instruments that have ice phobic surfaces or coatings<br>* Spray a low freezing-point fluid (such as glycol or ethanol) on sensors during icing events; not suitable for humidity sensors<br>* Mount wind sensor on slightly flexible mast (e.g., "wind surfer" mast)<br>* In heavy icing conditions none of these methods are effective |
| | * Snow/ice cover on pyranometers/radiation sensors | * Use a continuous flow of air (ideally dry air) to prevent water or snow to settle, or ice to form |
| | * Snow/ice accretion on infrastructure impacting the measurement environment, e.g., snow/ice cover on temperature sensors and screens causes incorrect data (due to a much higher time constant), and causes turbulence around anemometers | * Prevent icing or de-ice on a regular basis using methods above such as ice-phobic materials, low freezing point fluids<br>* Minimize the surface area of the infrastructure |

| **Event type** | **Avalanche** | |
|---|---|---|
| Cause | Result of snowfall build-up in combination with certain ground and atmospheric conditions | |
| Considerations | * What is the slope of the terrain near the site? | |
| *Dominant hazard* | *Vulnerability or impact to infrastructure* | *Mitigation* |
| Mass and Debris | * Destruction of infrastructure in path of avalanche | * Site station higher on mountain sides |
| | * Snow/ice cover on solar panels resulting in eventual loss of power | * Construct tower with multiple solar cells at various height |
| | | * Include back up batteries and alarms for loss of voltage and current supply |
| | See also "Land/mudslide" | |
| *Dominant hazard* | *Vulnerability or impact to instruments* | *Mitigation* |
| Mass and debris | * Nearly all | |
| | * Snow/ice cover on optical sensors | * Construct tower with multiple sensor suites at various heights |
| | * Snow/ice cover on pyranometers/radiation sensors | * For light coverage consider automated cleaning |
| | * Snow/ice cover on temperature sensors and screens causes incorrect data (due to a much higher time constant) | * Prevent icing or de-ice on a regular basis using methods above such as ice-phobic materials, low freezing point fluids |
| | See also "Snow/blizzard/icing" | |
| | See also "Land/mudslide" | |

| **Event type** | **Dust storm** | |
|---|---|---|
| Cause | Result of high winds in combination with certain ground conditions | |
| Considerations | How long do we expect systems to operate unattended or maintained?<br>What IP rating would we expect? | |
| *Dominant hazard* | *Vulnerability or impact to infrastructure* | *Mitigation* |
| Oblation | * Equipment that can be damaged by sandblasting or burying | * Avoid the use of coated materials; choose polished metal |
| | * Failure or deterioration of protective coatings that may lead to pitting or overall corrosion | * Inspect painted, plastic or powder coasted surfaces for chips, crazing or cracking |
| Dirt | * Build-up of dust/sand in enclosures | * Use enclosures with an IP6X or higher |
| | | * Design mounts and frames to minimize the build-up of sand and dirt |
| | * Clogging of aspirated screen | * Perform regular inspections and clearing |
| | * Loss of power or communications | * Include back up batteries and alarms for loss of voltage and current supply |
| | | * Include redundant communications via an alternate supplier |
| *Dominant hazard* | *Vulnerability or impact to sensors* | *Mitigation* |
| Oblation | * Aspirated equipment drawing dust | * Stop aspiration when wind or particle count is above a set point |
| Dirt | * Clogging of non-aspirated equipment | * Increase inspection frequency of equipment to remove dust build up |
| | | * Use well-sealed (high IP-rated) enclosures for data acquisition system, e.g., IP68 |
| | | * Increase replacement frequency of filter in dusty environments |
| | | * Design sensors to minimize the surface area and presence of crevices and pockets where dirt can build up |
| | * Optical and solar radiation equipment | * For light coverage, consider daily automated cleaning |

| **Event type** | **Fire** | |
|---|---|---|
| Cause | Result of hot weather, lightning or vandalism | |
| Considerations | * How hot is a typical fire likely to burn?<br>* How long is a fire likely to keep burning? | |
| *Dominant hazard* | *Vulnerability or impact to infrastructure* | *Mitigation* |
| Heat and combustion | * Deformation of metal and plastic components | * Avoid plastics with low melting temperature and lightweight metals |
| | * Failure of electronics in extreme heat | * Use enclosures that provide some insulation such as a double skin |
| | | * Ensure electronics are correctly rated for use in the climate they are being deployed in, e.g., 20 °C–30 °C above the climatic maximum temperature |
| | * Damage reducing IP rating | * Inspect and replace seals |
| | * Destruction of any combustible materials | * Construct with non-combustible materials such as metal and concrete |
| | | * Avoid cracks and crevices in the design of housings, and the like, where embers and sparks can lodge. Openings should be screened or sealed where practical |
| | * Failure of structural integrity of masts and other infrastructure following the event | * Perform regular inspections for stress fractures, fatigue and grain growth in metal components |
| | * Failure or deterioration of protective coatings that may lead to pitting or overall corrosion | * Inspect painted, plastic or powder coated surfaces for chips, crazing or cracking |
| Debris | * Damage from falling debris | * Site equipment in fire prone areas with appropriate clearance from potential falling structures and trees |
| Dust | See also "Dust storm" | |

| **Event type** | **Fire** | |
|---|---|---|
| *Dominant hazard* | *Vulnerability or impact to instruments* | *Mitigation* |
| Heat and combustion | * Deformation of casings/enclosures and failure of electronics | * Avoid plastics with low melting temperature and lightweight metals |
| | | * Use enclosures that provide some insulation such as a double skin, but avoid combustible insulation materials |
| | * Damage reducing IP rating | * Inspect and replace seals |
| | * Destruction of any combustible materials | * Construct with non-combustible materials such as metal and concrete |
| | * Sensors damaged by heat effects (sensing elements or housings) | * Ensure sensors are correctly rated for use in the climate they are being deployed in; e.g., 20 °C–30 °C above the climatic maximum for electronics and 5 °C–10 °C above for the measurement range |
| | * Failure of structural integrity of masts and other infrastructure following the event | * Perform regular inspections for stress fractures, fatigue and grain growth in metal components |
| | * Failure or deterioration of protective coatings that may lead to pitting or overall corrosion | * Inspect painted, plastic or powder coated surfaces for chips, crazing or cracking |
| Debris | * Damage from falling debris | * Site equipment in fire prone areas with appropriate clearance from potential falling structures and trees |
| Dust | See also "Dust storm" | |
| **Event type** | **Drought** | |
| Cause | Result of prolonged periods of low or no rain | |
| Considerations | Do footings need to accommodate dynamic soils? | |
| *Dominant hazard* | *Vulnerability or impact to infrastructure* | *Mitigation* |
| Dust | * Degradation of equipment foundations in clay soils (cracking, erosion) | * Use mounting systems that stabilize the surrounding soil such as a physical anchor which causes minimal soil disturbance while spreading the load |
| Erosion | See also "Dust storm" | |
| *Dominant hazard* | *Vulnerability or impact to instruments* | *Mitigation* |
| Dust | * Failure of electronics | * Check for dry joints in electronics |
| Erosion | * Clogged filters | * Perform more frequent filter changes in dusty conditions |

| **Event type** | **Heatwave/solar radiation** | |
|---|---|---|
| Cause | Prolonged periods of elevated temperatures and/or intense sunlight | |
| Considerations | Can instruments or infrastructure cope with sustained elevated temperatures? | |
| *Dominant hazard* | *Vulnerability or impact to infrastructure* | *Mitigation* |
| Heat | * Few, unless exterior surfaces have low temperature tolerance | * Avoid plastics with low melting temperature and lightweight metals |
| | * Failure of electronics due to overheating | * Use canvas or similar to shade electronics and reduce thermal stress on systems |
| | | * Where practical, bury the electronics box. Note: Ensure that no water ingress can occur |
| | | * Use passive cooling such as with a vent and chimney design. Note: Ensure the risk of water ingress is not increased, by placing the vent above expected water levels; use filters / screens to prevent dust and animals from gaining access |
| | | * Use active cooling such as with fans (note cautions above regarding water, dust and animal ingress) |
| | | * Use active coolers such as Peltier coolers or air-conditioning |
| | * Ageing of welds and joints | * Perform more frequent inspections for metal fatigue and deterioration |
| Irradiation | * Structural deterioration due to UV exposure | * Use UV resistant materials such as metals, hardwood or UV stabilized plastics |
| | * Discolouration and ageing of plastic components | * Perform more frequent inspections to detect distortion and deterioration of enclosures and screens in particular |
| | | * Use canvas or similar to shade electronics and reduce thermal stress on systems |
| *Dominant hazard* | *Vulnerability or impact to instruments* | *Mitigation* |
| Heat | * Sensors damaged by heat effects (sensing elements or housings) | * Ensure instruments are correctly rated for use in the climate they are being deployed in; e.g., 20 °C–30 °C above the climatic maximum temperature for electronics and 5 °C–10 °C above for the measurement range |
| | * Failure of instruments due to overheating | * Where measurements will not be compromised, use Peltier coolers or airflow (passive and active) |
| Irradiation | * Structural deterioration due to UV exposure | * Use UV resistant materials such as metals, hardwood or UV stabilized plastics |

| **Event type** | **Earthquake/volcano** | |
|---|---|---|
| Cause | Independent of meteorological factors | |
| Considerations | | |
| *Dominant hazard* | *Vulnerability or impact to infrastructure* | *Mitigation* |
| Eruption | * Volcano: burying by fallout; destruction from direct contact with flow | * Maximize use of fire resistant materials |
| Land movement | * Earthquake: most infrastructure | * Use mounting systems that stabilize the surrounding soil such as a physical anchor which causes minimal soil disturbance while spreading the load |
| | * Ash cover on solar panels: eventual loss of power | * Include back up batteries and alarms for loss of voltage and current supply |
| *Dominant hazard* | *Vulnerability or impact to instruments* | *Mitigation* |
| Eruption | * Volcano: dust contamination | * See “Dust” above |
| Land movement | * Earthquake: weighing gauges, loosely mounted instruments, e.g., tipping-bucket raingauge | |
| | * Ash cover on optical sensors | * For light coverage consider automated cleaning |
| | * Ash cover on pyranometers/radiation sensors | * For light coverage consider automated cleaning |

| **Event type** | **Security** | |
|---|---|---|
| Cause | Vandalism | |
| Considerations | | |
| *Dominant hazard* | *Vulnerability or impact to infrastructure* | *Mitigation* |
| Vandalism | * Theft or wanton damage | * Use fencing |
| | | * Use non-removable fittings for high value items such as solar panels |
| | | * In remote areas, encourage engagement from the local community regarding the value of the service provided by the equipment |
| Wildlife | * Chewing of cables | * Use strong conduit or armoured cables |
| | * Crushing of infrastructure by animals rubbing against the equipment | * Use appropriate livestock fencing |
| *Dominant hazard* | *Vulnerability or impact to instruments* | *Mitigation* |
| Vandalism | * Theft or wanton damage | * Use fencing |
| | | * In remote areas, encourage engagement from the local community regarding the value of the service provided by the equipment |
| Wildlife | * Bird attacks on ultrasonic sensors | * Use bird spikes on the edges of roosting points |
| | * Contamination and corrosion by bird droppings | * Use bird spikes on the edges of roosting points |
| | * Crushing or misalignment of sensors by animals rubbing against the equipment | * Use appropriate livestock fencing |

## ANNEX 1.F. STATION EXPOSURE DESCRIPTION

The accuracy with which an observation describes the state of a selected part of the atmosphere is not the same as the uncertainty of the instrument, because the value of the observation also depends on the instrument's exposure to the atmosphere. This is not a technical matter, so its description is the responsibility of the station observer or attendant. In practice, an ideal site with perfect exposure is seldom available and, unless the actual exposure is adequately documented, the reliability of observations cannot be determined (Wieringa and Rudel, 2002).

Station metadata should contain the following aspects of instrument exposure :

(a) Height of the instruments above the surface (or below it, for soil temperature) ;

(b) Type of sheltering and degree of ventilation for temperature and humidity;

(c) Degree of interference from other instruments or objects (masts, ventilators);

(d) Microscale and toposcale surroundings of the instrument, in particular :

  (i) The state of the enclosure's surface, influencing temperature and humidity; nearby major obstacles (buildings, fences, trees) and their size;

  (ii) The degree of horizon obstruction for sunshine and radiation observations;

  (iii) Surrounding terrain roughness and major vegetation, influencing the wind;

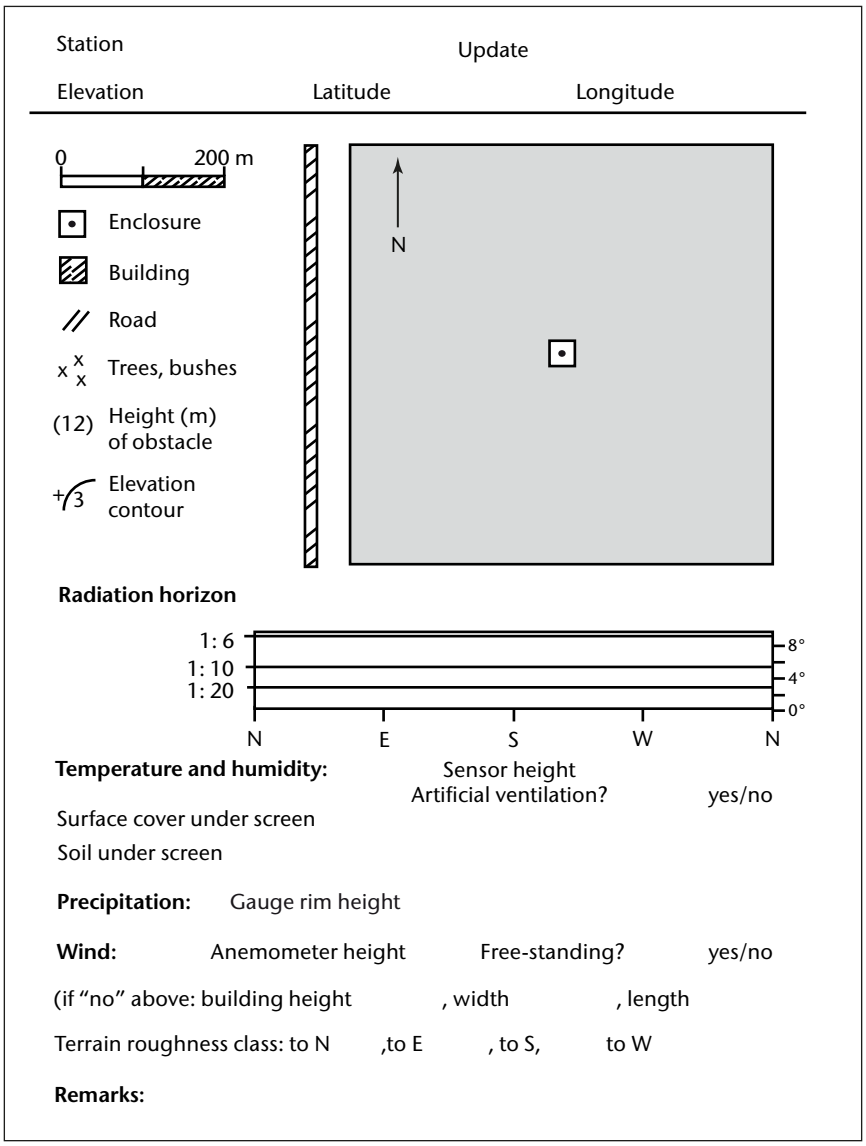
  (iv) All toposcale terrain features such as small slopes, pavements, water surfaces;

  (v) Major mesoscale terrain features, such as coasts, mountains or urbanization.

Most of these matters will be semi-permanent, but any significant changes (growth of vegetation, new buildings) should be recorded in the station logbook, and dated.

For documenting the toposcale exposure, a map with a scale not larger than 1 :25 000 showing contours of ≈ 1 m elevation differences is desirable. On this map the locations of buildings and trees (with height), surface cover and installed instruments should be marked. At map edges, major distant terrain features (for example, built-up areas, woods, open water, hills) should be indicated. Photographs are useful if they are not merely close-ups of the instrument or shelter, but are taken at sufficient distance to show the instrument and its terrain background. Such photographs should be taken from all cardinal directions.

The necessary minimum metadata for instrument exposure can be provided by filling in the template given on the next page for every station in a network (see the figure below). An example of how to do this is shown in the *Guidelines on Climate Metadata and Homogenization* (WMO/TD-No. 1186). The classes used here for describing terrain roughness are given in the present volume, Chapter 5. A more extensive description of metadata matters is given in the *Guide to the WMO Integrated Global Observing System* (WMO No. 1165).




**General template for station exposure metadata**

# ANNEX 1.G. MEASUREMENT QUALITY CLASSIFICATIONS FOR SURFACE OBSERVING STATIONS ON LAND

## 1. PURPOSE

This document is intended for use by meteorological measurement data users, network designers, implementers and managers. The aim of this document is to define a scheme for:

- Quantification of the measurement quality of data from an existing station;
- Determination of the optimal system characteristics to deliver a solution that is fit for purpose;
- Understanding of contributions to measurement quality and effective management of assets;
- Purchase and evaluation of measurement systems;
- Assisting industry to deliver solutions to meet user needs.

## 2. INTRODUCTION

2.1 This scheme, the Measurement Quality Classifications for Surface Observing Stations on Land (Measurement Quality Classification Scheme), in conjunction with the Siting Classifications for Surface Observing Stations on Land (Siting Classification Scheme) (Annex 1.D), forms part of the metadata of a measurand. The schemes assist all data users to obtain an estimate of the overall quality of the data they are using.

2.2 These schemes do not determine which measurements are good or bad, but rather indicate whether a measurement is suitable for a particular application. Furthermore, the schemes provide parameters that enable comparison between sites within, or between, observing networks using metadata that are collected in a standardized way. The schemes allow network operators to assess their stations, set appropriate goals for the quality of their observations, and identify areas that may need improvement.

2.3 This document describes a measurand-based four-level classification scheme of measurements. These levels allow network operators to focus on the required outcome and help the data users to understand the quality of the data they receive.

## 3. RELATIONSHIPS

3.1 This classification scheme creates links between various WMO publications on requirements, in particular:

- User Requirements for Observation (Observing Systems Capability Analysis and Review tool (OSCAR)/Requirements);
- Operational Measurement Uncertainty Requirements and Instrument Performance Requirements, (Annex 1.A);
- Siting Classifications for Surface Observing Stations on Land (Annex 1.D).

3.2 The user requirements are translated to an overall measurement uncertainty through the application of the Measurement Classification Scheme and the Siting Classification Scheme (see Figure 1.G.1). The measurement classification represents the realized system uncertainty, while the siting classification represents the siting measurement uncertainty. The combination of the schemes defines the overall measurement uncertainty of that measurement at the site.

3.3 All measurement uncertainties in this document are expressed at 95% confidence level ($k = 2$), unless otherwise specified.

3.4 The user requirements from OSCAR and other sources (see Note 2 to Table 1) were used to develop the Measurement Quality Classification Scheme classes (orange box in Figure 1.G.1). This scheme encompasses the following sources of uncertainty:

- Instrument and calibration – the instrument performance under controlled conditions aligned with Annex 1.A, for example, time constant, resolution and traceable calibration;

**Table 1. Criteria for Measurement Quality Classification**

| *Measurand* | *Class A* | *Class B* | *Class C* | *Class D* |
|---|---|---|---|---|
| Air temperature | 0.2 K [1a] | 0.6 K [1a] | 1.0 K [1a] | Greater than Class C or unknown |
| Relative humidity | 2% RH [1b] | 5% RH [1b] | 10% RH [1b] | |
| Atmospheric pressure | 0.2 hPa [1a] | 1.0 hPa [1a] | 2.0 hPa [1a] | |
| Wind speed and gust | Greater of<br>1 m/s or [1b]<br>5% [2b] | Greater of<br>2 m/s or [1b]<br>10% [2a] | Greater of<br>5 m/s or [1b]<br>15% [2b] | |
| Starting threshold | ≤ 0.5 m/s [2b] | ≤ 1.0 m/s [2b] | ≤ 2.5 m/s [2b] | |
| Wind direction | 5° [2a] | 10° [2b] | 15° [2b] | |
| Liquid precipitation amount (daily accumulated) | Greater of<br>1 mm or [1a]<br>2% [2a] | Greater of<br>3 mm or [1a]<br>5% [2b] | Greater of<br>5 mm or [1a]<br>10% [2b] | |
| Liquid precipitation intensity | Greater of<br>0.2 mm/h [1b]<br>or 5% [2a] | Greater of<br>0.5 mm/h [1b]<br>or 10% [2b] | Greater of<br>2 mm/h [1b]<br>or 15% [2b] | |
| Starting threshold | 0.1 mm/h [1c] | 0.3 mm/h [1c] | 1.0 mm/h [1c] | |
| Direct solar irradiance | 1% + 3 W/m² [3a] | 2% + 7 W/m² [3a] | 6% + 15 W/m² [3a] | |
| Global solar irradiance | 2% + 15 W/m² [3a] | 3% + 30 W/m² [3a] | 8% + 55 W/m² [3a] | |
| Diffuse solar irradiance | 2.5% + 15 W/m² [3a] | 4% + 30 W/m² [3a] | 10% + 55 W/m² [3a] | |
| Sunshine duration (daily integrated) | Greater of<br>0.1 h or 2% [2a] | Greater of<br>0.5 h or 5%[2b] | Greater of<br>1.0 h or 10% [2b] | |
| Sunshine duration threshold | 120 W/m² ± 10% [2d] | 120 W/m² ± 20% [2c] | 120 W/m² ± 30% [2d] | |

Notes:
1 Classifications for other measurands from the *Manual on the WMO Integrated Global Observing System* (WMO-No. 1160), Attachment 5.1, are not yet defined, due to a lack of shared knowledge on the subject or a reference.
2. The sources for the values in the table can be found in the following publications:
[1a] OSCAR/Requirements, using the lowest uncertainty of all application areas;
[1b] OSCAR/Requirements, using the nominal middle uncertainty of application areas:
[1c] OSCAR/Requirements, extrapolated to currently available technology:
[2a] Annex 1.A;
[2b] Annex 1.A, extrapolated to currently available technology;
[2c] Chapter 8 of the present volume;
[2d] Chapter 8 of the present volume, extrapolated to currently available technology;
[3a] ISO 9060:2018.

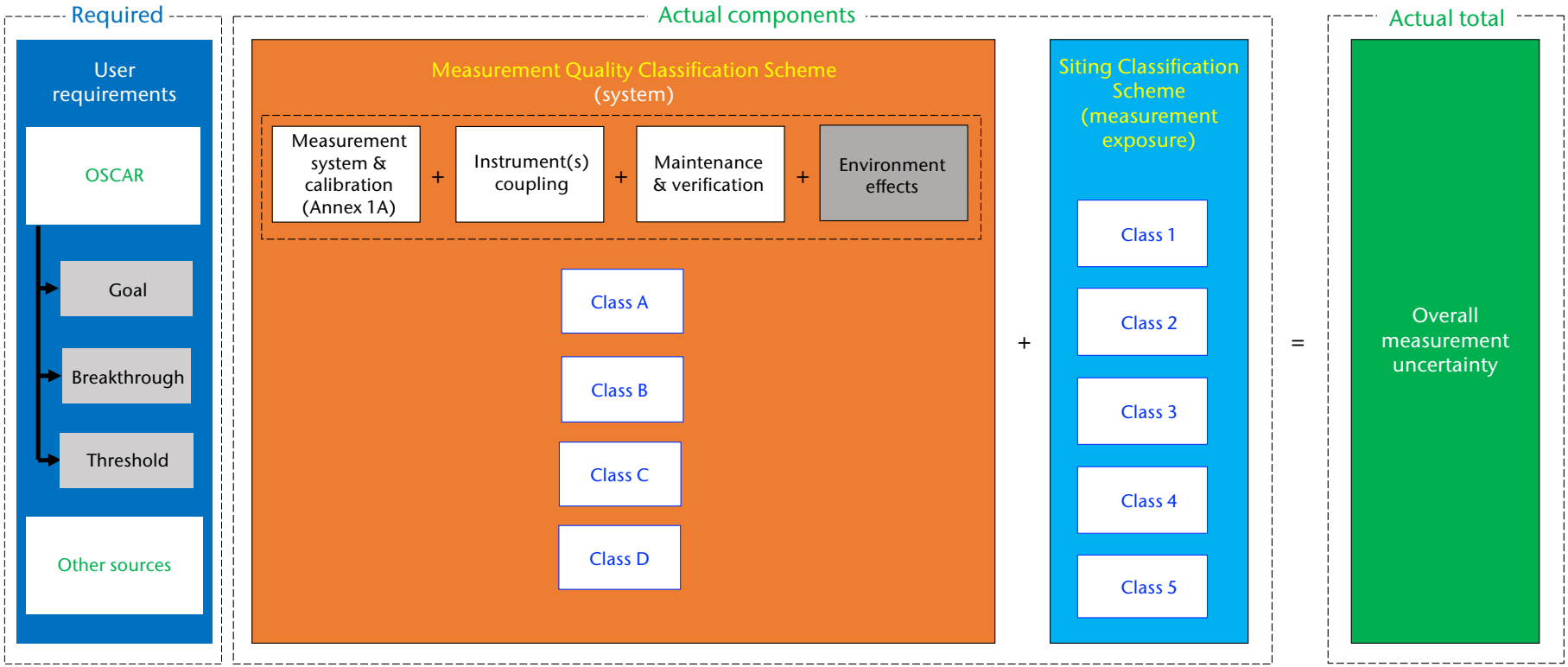



**Figure 1.G.1. User requirements and classification schemes overview**

- Instrument coupling – the effect of physical interfaces between the instrument and the environment, for example, a temperature screen, a static pressure head;

- Maintenance and verification – the influence that maintenance has on the uncertainty of a system in the field, for example, cleaning method and verification interval;

- Environment effects – the influence of field phenomena on instrument performance, for example, cooling due to water evaporating from a screen, or the effect of wind on measurements of precipitation and pressure. These effects influence instrument accuracy and are not included in the Siting Classification Scheme.

3.5 The "Environment effects" box in Figure 1.G.1 is shaded grey to indicate that this is an area of active research and not all components are well quantified.

3.6 The Measurement Quality Classification Scheme criteria are aligned with OSCAR/Requirements with an allowance for siting classification uncertainty.

## 4. DESCRIPTION OF CLASSES

4.1 The four levels of the Measurement Quality Classification Scheme are defined by target system uncertainties:

- **Class A** Aligned with OSCAR/Requirements "goal" level;

- **Class B** Aligned with OSCAR/Requirements "breakthrough" level;

- **Class C** Aligned with OSCAR/Requirements "threshold" level;

- **Class D** Greater than the uncertainty for Class C, or no information available.

4.2 Where OSCAR/Requirements exist, the lowest or nominal middle declared uncertainty of all application areas was chosen (depending on currently available technology), otherwise Annex 1.A, or the relevant standard was used (see Note 2 to Table 1).

4.3 The target system uncertainties for all classes are expressed at 95% confidence ($k = 2$). OSCAR/Requirements were adjusted accordingly from 68% confidence level ($k = 1$).

4.4 Detailed criteria for each performance class are indicated in Table 1. Table 1 covers the measurands and reports the target system uncertainty that must be fulfilled for each class. An additional threshold is required for the definition of the class for some measurands.

## 5. APPLICATION OF THE MEASUREMENT QUALITY CLASSIFICATION SCHEME

5.1 Every organization uses different sensors and implements local methods for monitoring and maintaining the quality of field measurements. This Measurement Quality Classification Scheme provides a universal approach to assist with meeting user requirements. The classification can be applied to any surface-based measurement system for measurands specified in Table 1. To maintain the realized system uncertainty over time, instruments and associate interfaces:

- Must undergo laboratory or on-site calibration, under stable, defined and known conditions, against a standard traceable to the SI, where such a traceable standard exists. Calibration must be performed over the instrument's field operational range, at time intervals consistent with the stability of the instrument., Calibration intervals should initially be as recommended by the manufacturer and then be adjusted based on analysis of calibration performance.

- Should undergo field checks or verifications using traceable transfer standards, particularly for longer calibration intervals. These are performed between laboratory calibrations. When the results of an instrument's verification fall outside its tolerance it should be replaced.

- Should have their performance verified when they are removed from the field.

- Must be maintained to retain the desired measurement uncertainty. Maintenance intervals should initially be based on manufacturers' recommendations and then be adjusted based on analysis of the system performance.

5.2 Maintaining the quality of measurements should include: monitoring of data and engineering status; having a robust fault reporting and response system; and having an overarching quality system.

5.3 Measurement quality changes with time due to internal and external influencing factors. The Measurement Quality Classification Scheme takes this into account by considering how much a measurement system changes between scheduled preventive maintenance tasks, calibrations and/or verifications during normal operation.

5.4 Three examples have been developed to demonstrate application of the scheme. Table 2 demonstrates how the measurement system, calibration, maintenance, verification and environment effects combine to determine the realized system uncertainty and therefore the class. These examples are intended to help users of Table 1 to manage and assess their decisions. The examples are not prescriptive.

5.5 The first and second scenarios in Table 2 demonstrate how a combination of different measurement system qualities, screens and maintenance intervals can result in the same class. The third scenario demonstrates that even with a well-maintained high-quality measurement system, other factors (in this particular case the screen) may impact the ability to meet a desired class. In this scenario the alternatives are to either address the factors or assess the system against a different class.

## 6. SOURCES OF UNCERTAINTY

The following is a list of some key sources of uncertainty for surface-based measurement systems. It is not exhaustive but is presented as a prompt to users. Reliable evaluation of the sources of uncertainty includes a definition of the measurand. For further guidance on the implementation of uncertainty evaluation see ISO/IEC (2008) / JCGM (2008).

**Measurement system and calibration:**

- Construction quality
- Resolution
- Instrument and logger calibration
- Linearity
- Hysteresis
- Time constant
- Drift with temperature
- Sampling method
- Sampling frequency
- Processing algorithm
- Digitization and rounding
- Response time

**Table 2. Examples of Measurement Quality Classification Scheme for Class B scenarios**

| **Scenario Class B (measurand: air temperature, target system uncertainty: 0.6 K)** | | | | | | |
|---|---|---|---|---|---|---|
| Scenario | Use of a high-quality (Class A capable) instrument in large Stevenson Screen, but reduced maintenance | | Use of a medium-quality instrument in a small Stevenson Screen and well maintained | | Use of a high-quality, well-calibrated instrument (Class A capable) in a small plastic plate screen and well maintained | |
| Resolution | 0.01 K | | 0.10 K | | 0.01 K | |
| Calibration interval | 5 years | | 2 years | | 3 years | |
| Verification interval | 3 years | | 1 year | | 1 year | |
| Maintenance interval | 3 years | | 1 year | | 1 year | |
| **Uncertainty budget** | | | | | | |
| Measurement system and calibration (k = 1) | Instrument:<br>Resolution:<br>Calibration:<br>Logger: | 0.03 K<br>0.005 K<br>0.07 K<br>0.03 K | Instrument:<br>Resolution:<br>Calibration:<br>Logger: | 0.05 K<br>0.05 K<br>0.07 K<br>0.03 K | Instrument:<br>Resolution:<br>Calibration:<br>Logger: | 0.03 K<br>0.005 K<br>0.07 K<br>0.01 K |
| Instrument coupling (k = 1) | Screen: 0.05 K | | Screen: 0.10 K | | Screen: 0.35 K | |
| Maintenance and verification (k = 1) | Maintenance:<br>Drift/aging: | 0.15 K<br>0.025 K<br>(0.005 K/y) | Maintenance:<br>Drift/aging: | 0.05 K<br>0.060 K<br>(0.030 K/y) | Maintenance:<br>Drift/aging: | 0.03 K<br>0.015 K<br>(0.005 K/y) |
| Environment effects (k = 1) | | 0.24 K | | 0.24 K | | 0.35 K |
| Combined uncertainty (k = 1) | | 0.30 K | | 0.29 K | | 0.50 K |
| Realized system uncertainty (k = 2) | | 0.60 K | | 0.58 K | | 1.00 K |
| Achieved Class B | | Pass | | Pass | | FAIL |

Notes:
1. The drift/aging values are determined by multiplying the annual rate of change, in brackets, by the calibration interval.
2. In this example, it is assumed that all individual uncertainty components are independent and follow a normal distribution. The combined uncertainty is calculated as the square root of the sum of the squared values of the individual uncertainty components.

**Instrument coupling:**

- Radiation screen
- Static pressure head
- Raingauge fence screen

**Maintenance and verification**:

- Frequency of maintenance
- Quality of maintenance
- Instrument and system drift with time
- Instrument and system aging
- Instrument and system faults (affecting data but not causing failure)
- Cleanliness of instrument and site

**Environment effects**:

- Sensor mechanical stress during transport and operation
- Evaporation of precipitation on screen
- Wind effects on measurement
- Condensation on temperature instrument
- Solar radiation effects on measurement

## 7. DEFINITIONS

For definitions of "Combined measurement uncertainty", "Coverage factor", and "Expanded measurement uncertainty" see the *Evaluation of Measurement Data – Guide to the Expression of Uncertainty in Measurement* (JCGM 100).

**Target system uncertainty** is the maximum uncertainty for a measurand to meet the particular class of the Measurement Quality Classification Scheme (see Table 1).

Note: The target system uncertainty does not include contributions from instrument exposure, as these are covered by Siting Measurement Uncertainty (see below).

**Realized system uncertainty** is the user's realization towards meeting the target system uncertainty.

Note: This estimate of uncertainty is calculated by the user taking into consideration the instrumentation, and management and maintenance processes, as outlined in the section Sources of uncertainty. The realized system uncertainty must be lower than or equal to the target system uncertainty for the designated class.

**Siting measurement uncertainty** is the uncertainty associated with instrument exposure, as described in Annex 1.D.

Note: This represents the effects from nearby objects on the environment of the measurement (for example, trees, walls, fences, large areas of water or pavement).

**Overall measurement uncertainty** is the combination of the realized system uncertainty and the siting measurement uncertainty.

## REFERENCES AND FURTHER READING


Brooks, C. E. P.; Carruthers, N. *Handbook of Statistical Methods in Meteorology*, MO 538; Meteorological Office: London, 1953.

Bureau International des Poids et Mesures. *The International System of Units (SI)*. BIPM: Sèvres/Paris, 2006.

Cohen, E. R.; Giacomo, P. *Symbols, Units, Nomenclature and Fundamental Constants in Physics*; SUNAMCO Document IUPAP-25, reprinted from Physica 146A; International Union of Pure and Applied Physics, 1987.

Davenport, A. G. Rationale for Determining Design Wind Velocities. *Journal of the Structural Division* **1960**, *86* (5), 39–68. https://doi.org/10.1061/JSDEAG.0000521.

Davenport, A. G.; Grimmond, C. S. B.; Oke, T.R.; Wieringa, J. Estimating the roughness of cities and sheltered country. In *Preprints of the Twelfth American Meteorological Society Conference on Applied Climatology*, Asheville, United States, 8–12 May 2000, pp. 96–99.

Eisenhart, C. Realistic Evaluation of the Precision and Accuracy of Instrument alibration Systems. *Journal of Research of the National Bureau of Standards–C, Engineering and Instrumentation* **1963**, *67C* (2), 161–195.

International Civil Aviation Organization (ICAO). *World Geodetic System – 1984 (WGS-84) Manual*; ICAO Doc 9674–AN/946; ICAO: Montreal, 2002.

International Organization for Standardization (ISO). *Accuracy (Trueness and Precision) of Measurement Methods and Results – Part 1: General Principles and Definitions*; ISO 5725-1:1994/Cor.1:1998, 1994a.

International Organization for Standardization (ISO). *Accuracy (Trueness and Precision) of Measurement Methods and Results – Part 2: Basic Method for the Determination of Repeatability and Reproducibility of a Standard Measurement Method*; ISO 5725-2:1994, 1994b.

International Organization for Standardization (ISO). *Quantities and Units – Part 1: General*; ISO 80000-1:2009, 2009.

International Organization for Standardization (ISO)/International Electrotechnical Commission (IEC). *Uncertainty of Measurement – Part 3: Guide to the Expression of Uncertainty in Measurement*; ISO/IEC Guide 98-3:2008, Incl. Suppl. 1:2008/Cor 1:2009, Suppl. 1:2008, Suppl. 2:2011, 2008. (Equivalent to: Joint Committee for Guides in Metrology, 2008: *Evaluation of Measurement Data – Guide to the Expression of Uncertainty in Measurement*, JCGM 100:2008, Corrected in 2010.)

Joint Committee for Guides in Metrology (JCGM). *International Vocabulary of Metrology – Basic and General Concepts and Associated Terms (VIM)*; JCGM 200:2012, 2012.

Kok, C. J. *On the Behaviour of a Few Popular Verification Scores in Yes/No Forecasting*; WR-2000-04; KNMI: De Bilt, Netherlands, 2000.

Linacre, E. *Climate Data and Resources – A Reference and Guide*; Routledge: London, 1992.

Murphy, A. H.; Katz, R. W., Eds. *Probability, Statistics and Decision Making in the Atmospheric Sciences*; Westview Press: Boulder, USA, 1985.

Natrella, M. G. *Experimental Statistics*; National Bureau of Standards Handbook 91; Washington, DC, 1966.

Orlanski, I., 1975: A rational subdivision of scales for atmospheric processes. *Bulletin of the American Meteorological Society*, 56:527–530.

Preston-Thomas, H. The International Temperature Scale of 1990 (ITS-90). *Metrologia* **1990**, *27* (1) 3–10. https://doi.org/10.1088/0026-1394/27/1/002.

Thompson, A.; Taylor, B. N. *Guide for the Use of the International System of Units (SI)*; NIST Special Publication No. 811; National Institute of Standards and Technology: Gaithersburg, USA, 2008.

United Nations Environment Programme, Minamata Convention on Mercury, 2017, https://www.mercuryconvention.org/en/documents/minamata-convention-mercury-text-and-annexes.

Wieringa, J. Representativeness of wind observations at airports. *Bulletin of the American Meteorological Society* **1980**, *61*, 962–971. https://doi.org/10.1175/1520-0477(1980)061<0962:ROWOAA>2.0.CO;2.

Wieringa, J.; Rudel, E. Station Exposure Metadata Needed for Judging and Improving the Quality of Observations of Wind, Temperature and other Parameters. In *Papers Presented at the WMO Technical Conference on Meteorological and Environmental Instruments and Methods of Observation (TECO-2002)* (WMO/TD-No. 1123). WMO: Geneva, 2002.

World Meteorological Organization (WMO). *International Meteorological Tables* (WMO-No. 188). Geneva, 1966.

World Meteorological Organization (WMO). *Performance Requirements of Aerological Instruments: An Assessment Based on Atmospheric Variability* (WMO-No. 267). Geneva, 1970.

World Meteorological Organization (WMO). *International Meteorological Vocabulary* (WMO-No. 182). Geneva, 1992.
World Meteorological Organization (WMO). *Siting and Exposure of Meteorological Instruments* (WMO/TD-No. 589). Geneva, 1993.
World Meteorological Organization (WMO). *Lecture Notes for Training Agricultural Meteorological Personnel* (WMO-No. 551), Second edition. Geneva, 2001.
World Meteorological Organization (WMO). *Guidelines on Climate Metadata and Homogenization* (WMO/TD-No. 1186). Geneva, 2003.
World Meteorological Organization (WMO). *Capacity Assessment of National Meteorological and Hydrological Services in Support of Disaster Risk Reduction*. Geneva, 2008.
World Meteorological Organization (WMO). *Guide to Hydrological Practices : Hydrology – From Measurement to Hydrological Information* (WMO-No. 168), Geneva, 2008.
World Meteorological Organization (WMO). *Guide to Agricultural Meteorological Practices* (WMO-No. 134). Geneva, 2010.
World Meteorological Organization (WMO). *Manual on the Global Data-processing and Forecasting System* (WMO-No. 485). Geneva, 2010.
World Meteorological Organization (WMO). *Guide to Climatological Practices* (WMO-No. 100). Geneva, 2011.
World Meteorological Organization (WMO). *Technical Regulations, Volume I: General Meteorological Standards and Recommended Practices* (WMO-No. 49), Geneva, 2011.
World Meteorological Organization (WMO). *Guide to Meteorological Observing and Information Distribution Systems for Aviation Weather Services* (WMO-No. 731). Geneva, 2014.
World Meteorological Organization (WMO). *Manual on the WMO Integrated Global Observing System* (WMO-No. 1160). Geneva, 2021.
World Meteorological Organization (WMO). *Guide to the WMO Integrated Global Observing System* (WMO-No. 1165). Geneva, 2019.
World Meteorological Organization (WMO)/Intergovernmental Oceanographic Commission of UNESCO (IOC). *Joint WMO/IOC Technical Commission for Oceanography and Marine Meteorology (JCOMM) –Third Session: Abridged final report with resolutions and recommendations* (WMO-No. 1049). Geneva, 2010.

# CHAPTER 2. MEASUREMENT OF TEMPERATURE

## 2.1 GENERAL

### 2.1.1 Definition

Thermodynamic temperature, $T$, is a physical quantity characterizing the average energy of random molecular motion within a substance. Direct measurement of $T$ using so-called primary thermometers is experimentally difficult and is only intermittently carried out even at national measurement institutes. Instead, the BIPM Consultative Committee for Thermometry (CCT) recommends the use of the ITS-90 to produce practical approximations to thermodynamic temperature (BIPM 1989, 1990).[1] ITS-90 summarises our knowledge of primary thermometry in 1990 and recommends the value of freezing points, melting points, or triple points of pure substances that can be used to calibrate standard PRTs (SPRTs). In the temperature range of meteorological interest (-80 °C to 60 °C), ITS-90 specifies the way in which the electrical resistance of SPRTs varies in between these fixed-point temperatures. The approximations to thermodynamic temperature produced by ITS-90 have been shown to be in error by less than ±0.01 °C over the entire range of meteorological interest (Underwood et al., 2017).

For meteorological purposes, temperatures are measured for a number of media. The most common variable measured is air temperature (at various heights). Other variables are ground surface temperature, subsurface soil temperature, minimum air temperature above grass surface and fresh- and seawater temperature. WMO (1992) defines air temperature as "the temperature indicated by a thermometer exposed to the air in a place sheltered from direct solar radiation". Although this definition cannot be used as the definition of the thermodynamic quantity itself, it is suitable for most applications.

### 2.1.2 Units and scales

Thermodynamic temperature $T$ is measured in units of kelvin (K). One K is defined as the fraction 1/273.16 of the thermodynamic temperature of the triple point of water. Thus, the triple point of water occurs at 0.01 °C and a partial water vapour pressure of 611.657 Pa exactly by definition; the temperature ($t$), in degrees Celsius defined by equation 2.1, is used for most meteorological purposes:

$$t/°\mathrm{C} = T/\mathrm{K} - 273.15 \tag{2.1}$$

Often the equilibrium between melting ice and air-saturated water (the "ice point") is used for calibration. At standard atmospheric pressure (101.325 kPa), the ice point occurs at 273.150 K (0.000 °C) and varies by $-9.91 \times 10^{-5}$ K kPa$^{-1}$. The variation thus amounts to less than ±0.001 °C for atmospheric pressure changes from 111 kPa to 92 kPa (Harvey et al., 2013).

A temperature difference of 1 °C is equal to a temperature difference of 1 K. Note that the symbol K is used without the degree symbol.

In the thermodynamic scale of temperature, measurements are expressed as differences from absolute zero (0 K), the temperature at which the molecules of any substance possess no thermal energy. ITS-90 provides a practical approximation to thermodynamic temperature (see annex), which is based on assigned values for the temperatures of a number of reproducible equilibrium states (see annex table) and on specified standard instruments calibrated at those temperatures (Nicholas and White, 1993; Quinn, 1990). Most thermometers for meteorological applications are calibrated by comparison against either a thermometer calibrated according to ITS-90, or a secondary standard that has in turn been calibrated according to ITS-90 (BIPM/CCT, 1990; Nicholas and White, 1993; Bentley, 1998).

[1] The authoritative body for this scale is BIPM; see http://www.bipm.org. CCT is the executive body responsible for establishing and realizing the ITS.

### 2.1.3 Meteorological requirements

#### 2.1.3.1 *General*

Meteorological requirements for temperature measurements primarily relate to the following:

(a) The air near the Earth's surface;

(b) The surface of the ground;

(c) The soil at various depths;

(d) The surface levels of the sea and lakes (see Volume III, Chapter 4 of the present Guide);

(e) The upper air (see Chapter 12 of the present volume).

These measurements are required, either jointly or independently and locally or globally, for input to numerical weather prediction (NWP) models, for synoptical analyses, for hydrological and agricultural purposes, and as indicators of climatic variability. Local temperature also has direct physiological significance for the day-to-day activities of the world's population. Measurements of temperature may be required as continuous records or may be sampled at different time intervals. This chapter deals with requirements relating to (a), (b) and (c).

#### 2.1.3.2 *Measurement uncertainty*

The range, reported resolution and required uncertainty for temperature measurements are detailed in Chapter 1 of the present volume. Meteorological thermometers should be calibrated against a laboratory standard and may be used with corrections being applied to their readings as necessary. It is necessary to limit the size of the corrections to keep residual errors within bounds. Also, the operational range of the thermometer will be chosen to reflect the local climatic range.

All thermometers should be issued with a certificate confirming compliance with the appropriate uncertainty or performance specification, or a calibration certificate that gives the corrections that must be applied to meet the required uncertainty. The initial, as well as regular testing and calibration, should be performed by a laboratory accredited according to ISO/IEC 17025.

#### 2.1.3.3 *Response times*

For routine meteorological observations there is no advantage in using thermometers with a very short time constant or lag coefficient, since the temperature of the air continually fluctuates up to one or two degrees within a few seconds. Thus, obtaining a representative reading with such a thermometer requires taking the mean of a number of readings, whereas a thermometer with a longer time constant tend to smooth out the rapid fluctuations. Too long a time constant, however, may result in errors when long-period changes of temperature occur. It is recommended that the time constant, defined as the time required by the thermometer to register 63.2% of a step change in air temperature, should be approximately 20 s. Nevertheless, the time constant will become shorter at high airflow over the sensor.

#### 2.1.3.4 *Recording the circumstances in which measurements are taken*

Temperature is one of the meteorological quantities whose measurements are particularly sensitive to exposure. For climate studies in particular, temperature measurements are affected by the state of the surroundings, by vegetation, sources of such as buildings and other objects, by ground cover, by the condition of, and changes in, the design of the radiation shield or screen, and by other changes in equipment (WMO, 2011). It is important that records are kept,

not only of the temperature data, but also of the circumstances in which the measurements are taken. Such information is known as metadata (data about data; see the present volume, Chapter 1, Annex 1.F).

### 2.1.4 Methods of measurement and observation

Radiation from the sun, clouds, ground and other surrounding objects passes through the air without appreciably changing its temperature, but a thermometer exposed freely in the open can absorb considerable radiation. As a consequence, its temperature may differ from the true air temperature. The difference depends on the balance between the absorption and emission of radiation and the thermal contact with the air. The effect of radiation can be minimized by using shiny thermometers – which reflect rather than absorb radiation – and which have a small diameter, so that they are effectively cooled by the air (Çengal and Ghajar, 2014; Incropera and de Witt, 2011; Erell et al., 2005; Harrison, 2015). For very fine wires used in an open-wire resistance thermometer, the difference from true air temperature may be very small or even negligible. It has been found (Harrison and Pedder, 2001; Harrison and Rogers, 2006; Harrison, 2010) that a thermometer made of 500 mm length of 0.025 mm diameter platinum wire held over a frame and exposed directly to the sun showed a warming due to irradiance of less than 0.07 °C/100 W $m^{-2}$ for wind speeds greater than 1 m $s^{-1}$. Such a thermometer would typically show less than 1 °C of error in full sunlight. Similar effects have been shown for very thin thermocouples (Bugbee et al., 1995).

However, with the more usual operational thermometers, the temperature difference may reach 25 K under extremely unfavourable conditions. Therefore, to ensure that the thermometer is as close to true air temperature as possible, it is necessary to protect it from radiation by a screen or shield that usually also serves to support the thermometer (see 2.5).

This screen also shelters the thermometer from precipitation while allowing the free circulation of air around it, and prevents accidental damage. If there is precipitation on the sensor, then evaporation will cool the sensor to an extent which depends on the local airflow. This cooling is similar to the behaviour of the wet-bulb thermometer in a psychrometer (see the present volume, Chapter 4). Maintaining free circulation may, however, be difficult to achieve under conditions of rime ice accretion. Practices for reducing observational errors under such conditions will vary and may involve the use of special designs of screens or temperature-measuring instruments, including artificial ventilation.

Nevertheless, in the case of artificial ventilation, care should be taken when moisture may be drawn onto the thermometer. In precipitation, drizzle and fog, moisture deposition in combination with evaporation may give rise to anomalous readings. An overview of concepts of temperature measurement applicable for operational practices is given by Sparks (1970). Actual best practice in thermometer exposure is exemplified by "triply redundant" aspirated sensors (Diamond et al., 2013).

#### 2.1.4.1 *General measurement principles*

Temperature measurements of an object or substance can be categorized as either contact or non-contact.

In contact thermometry a thermometer is placed in physical contact with an object, and ideally (in thermodynamic equilibrium) it attains the same temperature as the object, and so the temperature of the object can be inferred from the temperature of the thermometer itself. Any physical property of a substance that is a function of temperature can be used as the basis of a thermometer. The properties most widely used in meteorological thermometers are the change in electrical resistance of metals with temperature and thermal expansion of liquids and solids.

Electrical thermometers are the recommended instruments for temperature measurement. They are already in widespread use in meteorology for measuring temperatures and provide the potential for automatic and continuous measurements. The most frequently used measurement

principle is the temperature dependence of the electrical resistance of a metal. Thermocouples are seldom used in meteorological observation systems. They are based on the principle of the "Seebeck effect" generating a temperature-dependent voltage.

The principle of the thermal expansion of metal is used in mechanical thermographs with bimetallic or Bourdon-tube sensors. These instruments are used when accuracy is not as critical, but trends are to be observed. They are considered to be obsolete and should be replaced by alternatives if possible.

The large difference between the thermal expansion of liquids and glass is exploited in liquid-in-glass thermometers. Mercury or alcohol have been used for centuries for temperature measurement in such devices. Mercury-in-glass thermometers, used in a range of -30 °C to 50 °C, have been widespread but are no longer recommended. Taking into account the Minamata Convention on Mercury (see 2.1.4.5), NMHSs are encouraged to take appropriate measures to replace mercury-in-glass thermometers with modern alternatives as soon as possible.

In non-contact thermometry, the thermal radiation emitted from the surface of an object is used to estimate its temperature. This radiation is typically most intense in the IR or microwave region of the electromagnetic spectrum. Additionally the temperature of air may be measured without physical contact over a region of space by characterizing the transmission of sound, ultrasound or electromagnetic waves through the air (WMO, 2002*a*). Non-contact thermometers are not commonly used for meteorological measurements but can have advantages in some specialized applications.

There is considerable research aimed at developing non-contact techniques for air-temperature measurement. Ultrasonic anemometers yield a parameter called "acoustic temperature" that can follow the fluctuations in air temperature at up to 100 readings per second. These rapid measurements are useful for estimating heat flux (Schotanus et al., 1983) but the overall accuracy is poor (Richiardone et al., 2002). Other acoustic and optical techniques have been developed (for example, Underwood et al., 2017) but are not yet suitable for operational metrology.

Thermometers that indicate the prevailing temperature are often known as ordinary thermometers, while those which indicate extreme temperature over a period of time are called maximum or minimum thermometers. If the temperature measurement is taken with electrical thermometers, the maximum and minimum temperature can be determined from the measured data if a continuous recording and sufficient measuring frequency is provided. As the only liquid for liquid-in-glass maximum thermometers is mercury, electrical alternatives should be used.

There are various standard texts on instrument design and laboratory practice for the measurement of temperature (for example, Harrison, 2015; Jones, 1992). Considering the concepts of thermometry, care should be taken that, for meteorological applications, only specific technologies are applicable because of constraints determined by the typical climate or environment.

### 2.1.4.2 *General exposure requirements*

#### 2.1.4.2.1 Measuring air temperatures

In order to achieve representative results when comparing thermometer readings at different places and at different times, a standardized exposure of the screen and, hence, of the thermometer itself is also indispensable. For general meteorological work, the observed air temperature should be representative of the free air conditions surrounding the station over as large an area as possible, at a height of between 1.25 and 2 m above ground level. For reasons of comparability the measurement should be taken over natural ground, preferably over grass. The height above ground level is specified because large vertical temperature gradients may exist in the lowest layers of the atmosphere that can influence the temperature measurement. The most appropriate site for the measurements is, therefore, over level ground, freely exposed to sunshine and wind and not shielded by, or close to, trees, buildings and other obstructions.

Sites on steep slopes or in hollows are subject to exceptional conditions and should be avoided. In towns and cities, local peculiarities are expected to be more marked than in rural districts. Temperature observations on the top of buildings are of doubtful significance and use because of the variable vertical temperature gradient and the effect of the building itself on the temperature distribution.

The siting classification for surface observing stations on land (see the present volume, Chapter 1, Annex 1.D) provides additional guidance on the selection of a site and the location of a thermometer within a site to optimize representativeness.

#### 2.1.4.2.2 **Measuring soil temperatures**

The standard depths for soil temperature measurements are 5, 10, 20, 50 and 100 cm below the surface; additional depths may be included (for example, 2 cm). The site for such measurements should be a level plot of bare ground (about 2 m x 2 m) and typical of the surrounding soil for which information is required. When the ground is covered with snow, it is desirable to measure the temperature of the snow cover as well. Where snow is rare, the snow may be removed before taking the readings and then replaced.

When describing a site for soil temperature measurements, the soil type, soil cover and the degree and direction of the ground's slope should be recorded. Whenever possible, the physical soil constants, such as bulk density, thermal conductivity and the moisture content at field capacity, should be indicated. The level of the water table (if within 5 m of the surface) and the soil structure should also be included. This is important to estimate the soil heat flow in NWP.

At agricultural meteorological stations, the continuous recording of soil temperatures and air temperatures at different levels in the layer adjacent to the soil (from ground level up to about 10 m above the upper limit of prevailing vegetation) is desirable.

#### 2.1.4.2.3 **Measuring minimum temperatures (grass or bare soil)**

The grass minimum temperature is the lowest temperature reached overnight by a thermometer freely exposed to the sky just above short grass. Grass minimum temperatures should be measured at 5 cm above grass or a surface representative of the locality.

If bare soil minimum temperatures are observed, these measurements should be made at 5 cm above the natural bare-ground level.

When the ground is covered with snow, the thermometer should be supported immediately above the surface of the snow, as near to it as possible without actually touching. At a station where snow is persistent and of varying depth, it is possible to use a support that allows the thermometers to be raised or lowered to maintain the correct height above the snow surface.

### 2.1.4.3 ***Sources of error – general comments***

Errors in the measurement of temperature may be caused by the following:

(a) Direct and indirect radiation from different sources, for example, the sun, clouds, soil and surrounding objects and lakes;

(b) Uncertainty of the sensing element, the instrument and for electrical measurements made by other technical devices in the data chain;

(c) Insufficient ventilation of the screen (wind speed under 1 m $s^{-1}$) especially in conditions of high solar radiation;

(d) Psychrometric cooling due to wet surfaces on the screen and/or the sensor;

(e) Contamination of the sensor, for example, by dirt, sea spray;

(f) Incorrect operation, for example, failure to achieve stable equilibrium or reading errors from the observer.

The time constant of the sensor, the time averaging of the output and the data requirement should be consistent.

The different types of temperature sensors vary in their susceptibility to, and the significance of, each of the above; further discussion will be found in the appropriate sections of this chapter.

Due to its high relevance for temperature measurements, radiation errors are discussed in more detail in the following paragraphs.

Radiation errors are caused by direct heating of a thermometer by electromagnetic radiation (EMR) that passes freely through the air. The heating effects arise from both direct irradiation – due to visible light leaking into a thermometer enclosure – and thermal irradiation due to differences in temperature between the thermometer and its surroundings. The absorption of radiation in these two bands determines the magnitude of the radiative "load" on a sensor. The load is determined by the intensity of the irradiation in each band, and the emissivity of the sensor surface – which generally varies with the wavelength of the irradiation. However, the heating load is always minimized by having a low-emissivity, polished (that is, shiny) surface.

The measurement of air temperature with contact sensors is particularly sensitive to radiative loading because of the weak thermal contact between the sensors and the air, especially when the air is slow moving. The heat flow between the thermometer and the air is characterized by a heat transfer coefficient $h$ (Çengal and Ghajar, 2014; Incropera and de Witt, 2011) which depends on the speed of the air flowing past the thermometer and the diameter of the thermometer. For a wide range of thermometers with a cylindrical or spherical form, the heat transport improves as the square root of the air speed past the thermometer and inversely as the square root of the diameter of the thermometer (Ney et al., 1960; Erell et al., 2005; Harrison, 2015). Thus for any air speed, the error caused by a radiant heat load will be reduced by a factor of two if the diameter of the sensor is reduced by a factor of four.

The strength of radiative coupling between a thermometer and its environment is stronger than is often considered. For cylindrical sensors with a stainless steel case, a screen that is 3 °C warmer than the air, in a wind speed of 0.1 m $s^{-1}$ will result in ~0.5 °C error for a 6 mm-diameter sensor, but only ~0.2 °C error for a 1 mm-diameter sensor.

#### 2.1.4.4 ***Maintenance – general comments***

The following maintenance procedures should be considered:

(a) Sensors and housings should be kept clean to reduce radiation errors;

(b) If artificially ventilated screens are used, the fan status should be checked regularly, either manually or, preferably, automatically;

(c) Regular calibration is required for all temperature sensors and, if applicable, for the electrical interfaces. Field checks should be performed between calibration intervals;

(d) If analog–digital converters (ADCs) are used they should be checked regularly with ohmic resistance to determine whether they still fulfil requirements.

Detailed maintenance requirements specific to each type of thermometer described in this chapter are included in the appropriate section.

#### 2.1.4.5 *Implications of the Minamata Convention for temperature measurement*

The UNEP Minamata Convention on Mercury came into force globally in August 2017 and bans all production, import and export of mercury-in-glass thermometers (see the present volume, Chapter 1, 1.4.1). Therefore, mercury-in-glass thermometers are no longer recommended and it is strongly encouraged to take appropriate measures to replace them with modern alternatives as soon as possible. Electrical resistance thermometers provide an economical, accurate and reliable alternative to their dangerous, mercury-based precedents and offer significant advantages in terms of data storage and real-time data display.

## 2.2 ELECTRICAL THERMOMETERS

### 2.2.1 General description

Electrical instruments are in widespread use in meteorology for measuring temperatures. Their main virtue lies in their ability to provide an output signal suitable for use in remote indication, recording, storage, or transmission of temperature data. The most frequently used sensors are PRTs, but semiconductor thermometers (thermistors) and thermocouples are also used.

#### 2.2.1.1 *Metal resistance thermometers*

Across the entire meteorological temperature range from –80 °C to 60 °C the electrical resistance of most pure metals is an almost linear function of temperature. Although many pure metals could be used for thermometry, platinum metal is most widely used for electrical resistance thermometers because of its exceptional resistance to corrosion. Ultra-pure, strain-free platinum is used for so-called SPRTs that are used for interpolating between fixed points in realizations of ITS-90 in standard laboratories. However, these thermometers are too delicate for use in the field.

The most common format of PRT is called a Pt100 because the sensors are engineered to have a resistance $R_0$ close to 100 Ω at 0 °C. These sensors use slightly less pure platinum and are much more robust that SPRTs. Typically, the sensors consist of platinum wires wound around a ceramic core and held inside a ceramic, glass, or stainless steel outer casing (Figure 2.1(a)). Alternatively, thin films of platinum can be deposited in a labyrinthine pattern onto a ceramic substrate and then typically packaged in stainless steel (Figure 2.1(b)).

From – 80 °C to 60 °C, the electrical resistance of a PRT can be represented by the Callender-van Dusen equation:

$$R = R_0\left(1 + At + Bt^2 + C\left(t - 100\right)t^3\right) \tag{2.2}$$

where $t$ is the temperature in °C.

Pt100 sensors are commonly specified by the tolerance within which they conform to standards such as IEC 60751 (DIN EN 60751) or ASTM E1137. For a thermometer that conforms closely to the

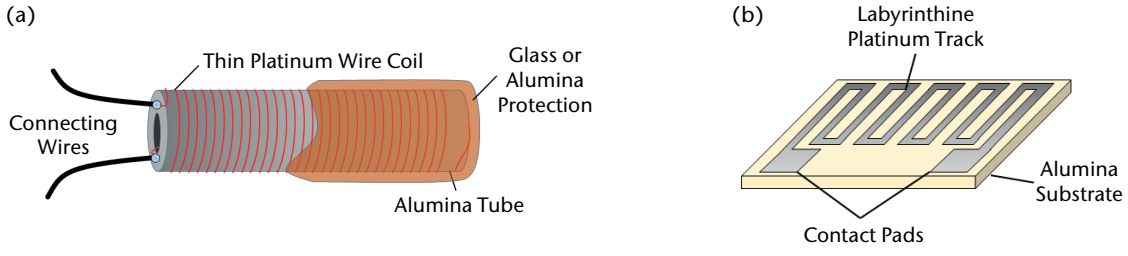



**Figure 2.1. (a) Wire-wound PRT; (b) thin-film PRT**

IEC 60751 specification, the Callendar–van Dusen coefficients are $R_0$ = 100 Ω, A = 3.908 x $10^{-3}$ °$C^{-1}$ and B = -5.80 x $10^{-7}$ °$C^{-2}$, while the $C$ coefficient takes different values above and below 0 °C. Below 0 °C, its value is C = 4.27 x $10^{-12}$ °$C^{-4}$, while $C$ is exactly zero above 0 °C.

The resistance and sensitivity of an IEC standard Pt100 sensor are shown in Figure 2.2.

The sensitivity of Pt100 thermometers describes the change in resistance due to temperature change and is commonly specified by an $\alpha$ (alpha) value defined by:

$$\alpha = \frac{R_{100} - R_0}{100°C * R_0} \tag{2.3}$$

The sensitivity (Figure 2.2(b)) is almost independent of temperature, being 0.3952 Ω °$C^{-1}$ at -40 °C, 0.3909 Ω °$C^{-1}$ at 0 °C and 0.3863 Ω °$C^{-1}$ at 40 °C, a variation of just 2.3% across a range of 80 K. For IEC 60751-compliant thermometers, $\alpha$ has a value close to 3 850 x $10^{-6}$ °$C^{-1}$.

The tolerance classes of IEC 60751 or ASTM E1137 are shown in Table 2.1 and graphed in Figure 2.3. Sensors are also available with smaller tolerance typically specified as a fraction of one of the standards shown in Table 2.1.

For example, an IEC 60751 W0.3 (old Class B) sensor describes a wirewound sensor which conforms to the IEC 60751 curve within ±(0.3 + 0.005$t$) °C, so at 20 °C a class B sensor would be guaranteed to fall within 0.400 °C of the IEC curve.

The Callendar–van Dusen equation (equation 2.2) has no simple inverse equation expressing temperature as a function of resistance, $t(R)$. There are two solutions to this difficulty. First, for temperatures greater than -40 °C, the $C$ term in equation 2.2 corresponds to less than 0.01 °C and may reasonably be neglected in many applications. In this case, the Callendar–van Dusen equation may be approximated as:

$$R = R_0\left(1 + At + Bt^2\right) \tag{2.4}$$

**Table 2.1. The tolerance classes of IEC 60751 or ASTM E1137.**

| *IEC 60751 (2008)* | | *ASTM E1137* | |
|---|---|---|---|
| Tolerance class | Definition | Tolerance grade | Definition |
| F0.3 (Old Class B) | ±(0.3 + 0.005 \|$t$\|) | B | ±(0.25 + 0.0042 \|$t$\|) |
| F0.15 (Old Class A) | ±(0.15 + 0.002 \|$t$\|) | A | ±(0.13 + 0.0017\|$t$\|) |

Note: In the IEC specification the F indicates a thin-film sensor and is replaced with a W for a wirewound sensor. |$t$| indicates the absolute value of the temperature in degrees Celsius.

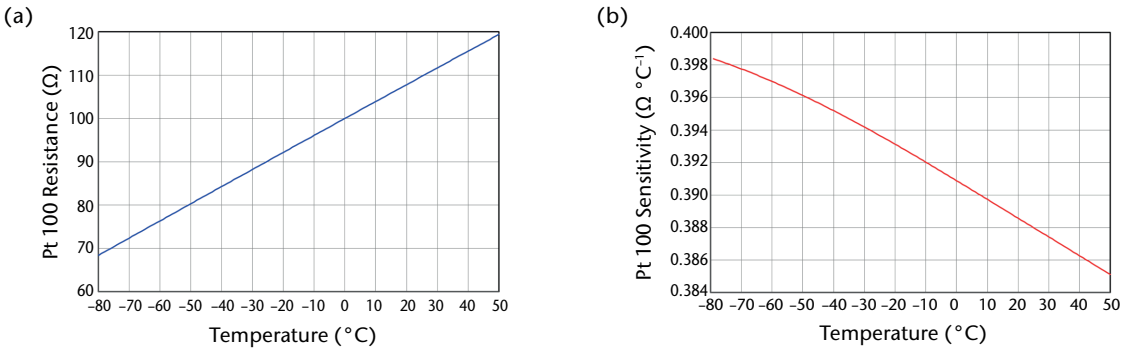



**Figure 2.2. (a) The resistance versus temperature for an IEC 60751-compliant Pt 100 sensor; (b) the sensitivity versus temperature for an IEC 60751-compliant Pt 100 sensor**

Moreover, its inverse can be calculated using the standard quadratic formulae:

$$t = -\frac{A}{2B} + \frac{A}{2B}\sqrt{1 - \frac{4B}{A^2}\left(1 - \frac{R}{R_0}\right)} \tag{2.5}$$

The error from using this formula is still less than 0.1 °C at -80 °C. Alternatively, equation 2.4 may be used to generate an initial estimate of the temperature, which is then iteratively refined by repeated use of the forward equation for $R$.

Before calibration for deployment in a meteorological setting, Pt100 sensors are usually "aged" (by manufacturers) by temperature cycling the sensor between, typically, the ice point and 20 °C. The aim of this procedure is to discover any manufacturing faults before deployment and to relieve any strain in the wires that will eventually be released in the field.

### 2.2.1.2 *Thermistors*

Another type of resistance element in common use is the thermistor. Although thermistors are available with positive temperature coefficients of resistance, the most common and useful form has large negative coefficients of resistance. The composition of thermistors is a proprietary secret, but they typically consist of sintered metallic oxides in the form of small discs, rods or spheres and are often glass-coated to prevent chemical reactions with the air, particularly moisture.

The temperature dependence of the resistance, $R$, of a thermistor can be qualitatively described by:

$$R = R_0 \exp\left(-\beta\left[\frac{1}{T_0} - \frac{1}{T}\right]\right) \tag{2.6}$$

where $R_0$ is the resistance of the thermistor at absolute temperature $T_0$ (in kelvin), and $T$ is the temperature of the thermistor in kelvin. Thermistors are typically specified for the value $R_0$ at a temperature of 25 °C, that is, $T_0 = 25 + 273.15 = 298.15$ K, and $\beta$ is specified in kelvin. Typical values are $R_0 \approx 1$ kΩ and $\beta \approx 4\,000$ K (for example, see Figure 2.4).

There are three key differences in the behaviour of thermistors when compared with Pt100 sensors.

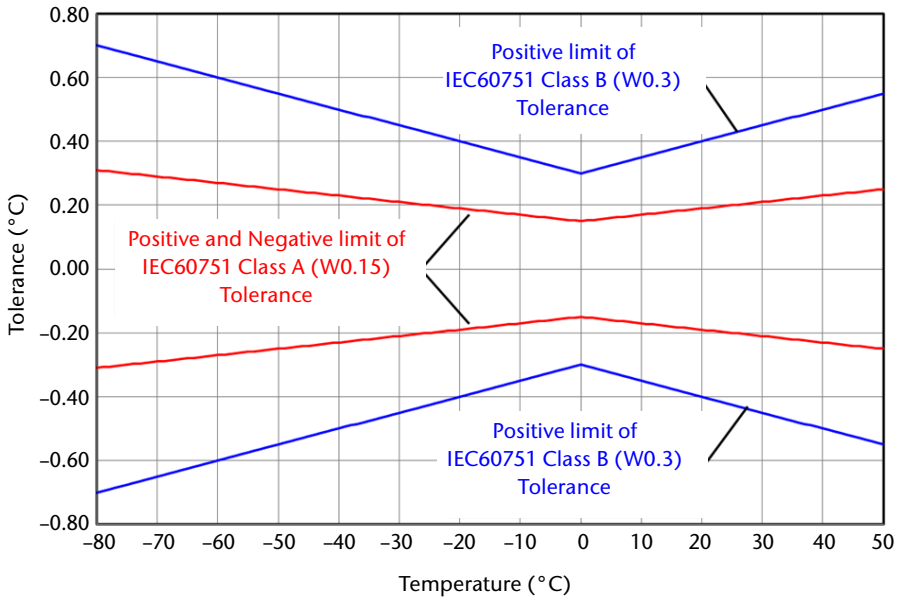



**Figure 2.3. Tolerance bands for an IEC 60751 compliant Pt100 sensor.**

The first is the high resistance of the thermistors, often sufficiently high that the resistance of the connecting wires may be neglected. This is almost never true for Pt100 sensors for which a four-wire measurement technique is always necessary.

The second is the high sensitivity compared with Pt100 sensors. Although this is an advantage at any specific temperature, the fact that the sensitivity varies with temperature is problematic and leads to a non-linear behaviour, and the very high dynamic range of the sensors also presents signal processing problems.

Finally, the sensors can be very small, and so they can have a small time constants and high heat-transfer coefficients (Erell et al., 2005). However, very small thermistors have the disadvantage that, for a given power dissipation, the self-heating effect is greater than for larger thermometers. Thus, care must be taken to keep the power dissipation small.

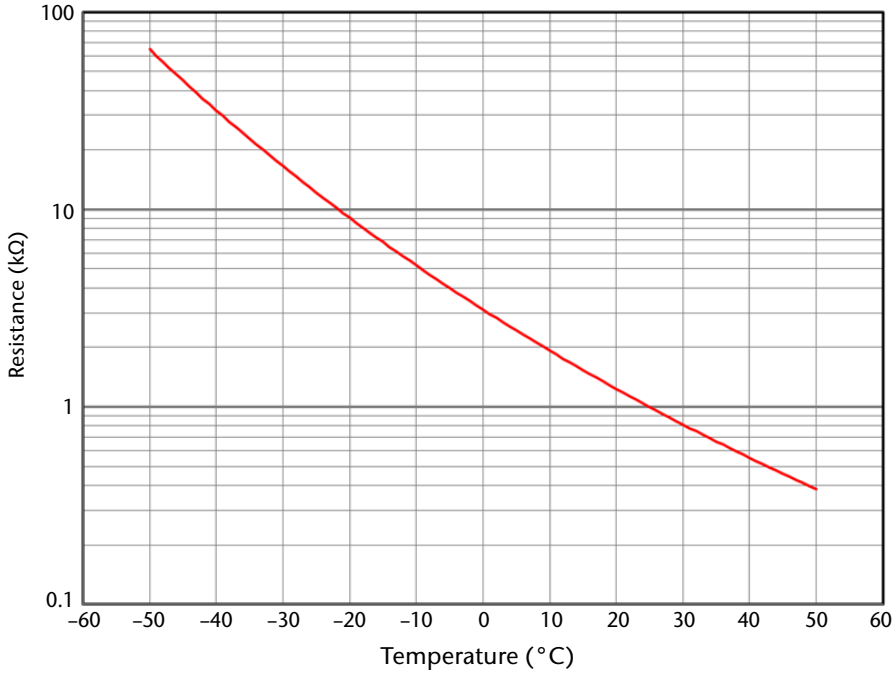



**Figure 2.4. The resistance versus temperature for a thermistor $R_0$ = 1 kΩ and $\beta \approx 3\,700$ K. (Note the vertical axis is logarithmic.)**

It should be noted that although equation 2.6 describes the general behaviour of thermistors and is useful for interpolation across small temperature intervals, it is not accurate enough to be used for meteorological applications. Several expressions of the general form:

$$R = R_0 \exp\left(A + \frac{B}{T} + \frac{C}{T^2} + \frac{D}{T^3}\right) \tag{2.7}$$

are commonly used to describe the behaviour of thermistors more accurately than equation 2.6. One special case of equation 2.7 where the coefficient $C$ is set to zero is known as the Steinhart–Hart equation. The coefficients $R_0$, $A$, $B$, $C$ (if used) and $D$ must be determined for each sensor by calibration. An equivalent inverse expression for the temperature is:

$$T = \left(A' + B'\ln\left(\frac{R}{R_0}\right) + C'\ln\left(\frac{R}{R_0}\right)^2 + D'\ln\left(\frac{R}{R_0}\right)^3\right)^{-1} \tag{2.8}$$

where the parameters $A'$, $B'$, $C'$ and $D'$ are completely different from the parameters from the parameters $A$, $B$, $C$ and $D$ in equation 2.7. In both equations 2.7 and 2.8, it must be remembered that the temperature $T$ must be expressed in kelvin.

In general the inverse formula is not as accurate as the forward formula, and if a computer is used to calculate the temperature, it is often advantageous to iterate the forward formula (equation 2.7) to find the correct result. Many iteration schemes have been devised, and optimized for accuracy and speed, but a typical approach is outlined below. In this procedure, the correct temperature is first guessed as being in the midpoint of the calibration range, and the resistance corresponding to this guess is calculated using equation 2.7.

If this resistance is greater than the measured resistance, then a new temperature guess is made in the upper half of the calibration range.

If this resistance is less than the measured resistance, then a new temperature guess is made in the lower half of the calibration range.

A new resistance is calculated from the second temperature guess and depending on the value of this resistance compared to the measured resistance, a third temperature guess is made. Iteration criteria must be met to stop the iteration process. In this way, the temperature may be inferred from a measured resistance using only the forward formula 2.7.

### 2.2.1.3 *Thermocouples*

The Seebeck effect describes the phenomenon whereby a temperature gradient in a metal gives rise to an accompanying electric field. The magnitude of the accompanying electric field is always proportional to the temperature gradient, but depends on a material-dependent and temperature-dependent Seebeck coefficient (Nicholas and White, 1993; Bentley, 1998). Thus, a wire of pure material in a temperature gradient spontaneously acquires a voltage across its ends, the magnitude of which is equal to the integrated Seebeck voltage along the wire.

A thermocouple (Figure 2.5) is made from two wires of different materials with differing Seebeck coefficients joined at one end – the so-called "hot junction". Typically the open ends of the junctions are connected to the terminals of a high-resolution voltmeter.

The thermo-voltage of a thermocouple is generated continuously along the entire length of the wires. We can consider each wire in the thermocouple to experience a sequence of small temperature changes, $\Delta T_i$ (Figure 2.5(a)). Each small temperature difference $\Delta T_i$ gives rise to a voltage $\Delta V_i$ that is proportional to $\Delta T_i$ and a material and temperature dependent Seebeck coefficient, $S$ (Figure 2.5(b)). The thermo-voltage measured across the open ends of the thermocouples is proportional to the temperature difference between the open ends of the wire and the thermocouple junction, even though no voltage is generated at the junction. Notice that terms "hot" and "cold" junctions are entirely conventional as thermocouples can measure temperatures even when the "hot junction" is colder than the "cold junction".

It is important to stress that the thermo-voltage is generated along the entire length of the thermocouple wires and that no voltage is generated at the junction itself – where the

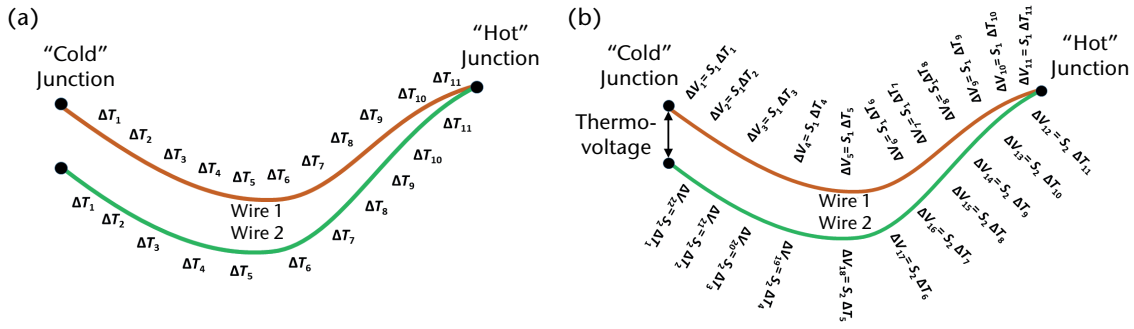



**Figure 2.5. In a temperature gradient (a) voltages are generated (b) along the entire length of both wires.**

temperature is measured. The thermocouple junction merely joins the two wires in the thermocouple together and may be made by welding or soldering together the two wires. All that is required is to create a suitably robust electrical connection between the wires.

Thermocouple wires can be made very narrow and the junctions can be made very small, with three potential benefits. First, thermocouples can be made with response times in air much less than one second. Second, the small size also improves heat exchange with the air resulting in lower errors when the thermocouple is irradiated (Bugbee et al., 1996). Finally, the effect of thermal conduction along the thermocouple wires is reduced.

Thermocouples are characterized as being made from either "base metals" (typically alloys of either copper or nickel) or "noble metals" (typically alloys of platinum, rhodium or gold). In meteorological applications there is no advantage to the use of noble metal thermocouples. Thermocouples are typically purchased as a manufactured item with the two wires preselected from standard alloy combinations which are specified by a "letter-type".

The most commonly used types in meteorological applications according to IEC 60584-1:2013 are:

– Type K: made from two nickel alloys, chromel and alumel;

– Type J: made from iron and constantan (copper–nickel alloy);

– Type T: made from copper and constantan.

In the meteorological temperature range there is little advantage to using one type over another. Type K is the most common specification, and at 20 °C it produces a signal of approximately 40 μV $°C^{-1}$. Type J has a slightly higher sensitivity (approximately 50 μV $°C^{-1}$) but the pure iron leg is potentially subject to corrosion if exposed for long periods. Type T has a similar sensitivity to Type K but the copper wire has a high thermal conductivity, which can lead to errors in some circumstances.

Tables of thermo-voltage versus temperature for standard thermocouple types are available from manufacturers and standards bodies.

## 2.2.2 Measurement procedures

### 2.2.2.1 *Electrical resistance thermometers*

Electrical resistance thermometers may be connected to a variety of electrical measurement circuits. Historically, many variations of resistance bridge circuits were used in either balanced or unbalanced form. In such circuits, a single voltage or current measurement enables the comparison of the unknown resistance of the thermometer with known temperature-independent standard resistors.

The excellent resolution and linearity of modern ADCs, and the measurement component within voltmeters and multimeters, enables alternative approaches. The unknown resistance of the thermometer is estimated from two measurements; a measurement of the current flowing through the temperature sensor; and a measurement of the voltage across the temperature sensor. This allows the measurement of a resistance of approximately 100 Ω with an uncertainty of just a few mΩ.

The resistance of the wires connecting the sensor to the ADC must also be considered. Typically such wires have an electrical resistance of a few tenths of an ohm per metre. For a Pt100 sensor, an additional resistance of 0.39 Ω is equivalent to an error of 1 °C. And so for Pt100 sensors a four-wire measurement configuration must be used in which an additional pair of wires sense the voltage (Figure 2.6).

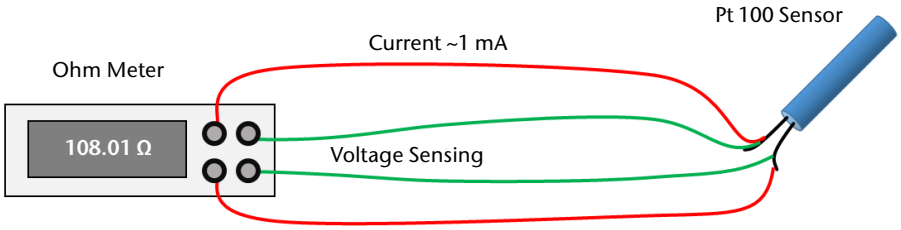



**Figure 2.6. A four-wire arrangement for reading a Pt100 sensor**

For a thermistor, the error caused by the connecting wires varies strongly with temperature, but tends to be much less significant than for Pt100 sensors. For the sensor with $R_0$ = 1 kΩ and $\beta$=3700 K illustrated in Figure 2.4, at -20 °C the sensor resistance is 9.08 kΩ and the sensitivity is -542 Ω °C $^{-1}$, a change of 6.0% °C $^{-1}$, and at 20 °C the sensor resistance is 1.24 kΩ and the sensitivity is -55 Ω °C $^{-1}$, a change of 4.4% °C $^{-1}$. Thus, at -20 °C an additional resistance of 0.39 Ω is equivalent to an error of 0.0007 °C, and at 20°C an error of 0.007 °C, which in many cases can be considered negligible.

To maintain the advantages of thermistors, such as rapid response and high heat transfer coefficient, but avoid the disadvantages of the high dynamic range and varying sensitivity, thermistors are often used in "linearizing" circuits. A large number of such circuits exist, but the simplest consists of a parallel constant resistor (White, 2015, 2017).

### 2.2.2.2 *Thermocouples*

Historically thermocouples were used in a wide variety of configurations that required the open ends of the thermocouple – the so-called "cold-junction" – to be immersed in melting ice (Figure 2.7(a)). The temperature of the hot junction was then deduced from standard tables for the pair of metals used in the thermocouple. In practice it is inconvenient to maintain an ice point and this is now only rarely done.

Instead, the measurements are referenced to the temperature of the terminals of the digital voltmeter. This technique – known as cold-junction compensation – requires a measurement of the temperature of the voltmeter terminals using a thermistor or PRT (Figure 2.7(b)). The additional thermocouple voltage that would have been expected if an ice point had been used is then calculated and added to the measured voltage. The sum is then used to determine the temperature using interpolation of standard tables. Where cold-junction compensation is used, special care must be taken close to voltmeter junctions where small temperature differences between the terminals can generate spurious voltages.

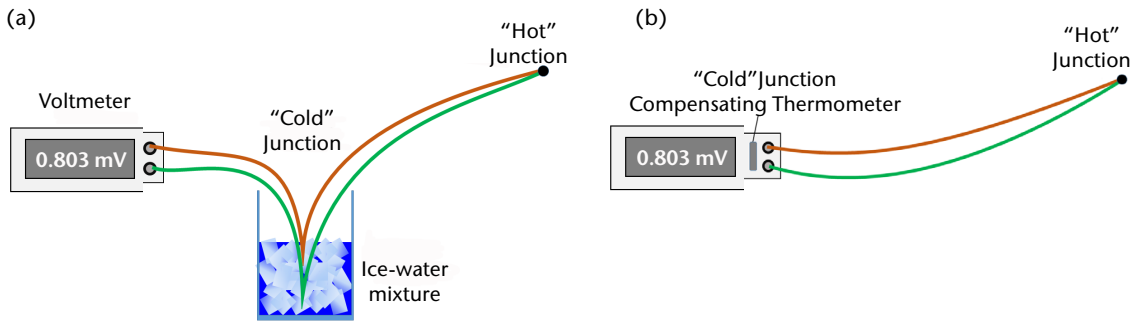



**Figure 2.7. Arrangements for reading a thermocouple: (a) one of several traditional arrangements in which the cold junction is immersed in melting ice; (b) a modern alternative in which a thermistor or Pt100 thermometer measures the temperature of the "cold junction".**

Typically a purchased thermocouple is not long enough to connect to a voltmeter in an environmentally isolated casing, and a so-called "extension cable" is required for this purpose. As noted above, the thermo-voltage is generated along the entire length of the thermocouple, including any extension cable. Since the temperature gradients in the cable are often largest close to the enclosure containing the data acquisition equipment, the thermo-voltages generated in the extension cable are as significant as those generated close to the hot junction of the thermocouple. For this reason thermocouples are generally not chosen for routine meteorological use.

In meteorology, thermocouples are used for thermometry for two special applications. The first application is when a thermometer with a low mass and very small time constant is required for special research tasks (see for example, Bugbee et al., 1996). The second application is for the measurement of small temperature differences; for this the thermocouple is wired as two thermocouples in opposition (Figure 2.8(a)). In this configuration the measured voltage is sensitive only to the difference in temperature between the two junctions. A modification of the differential thermocouple is the "thermo pile" (Figure 2.8(b)), which consists of a large number of differential thermocouples wired in series. The output voltage from a thermopile of $N$ junctions is just $N$ times the thermocouple output from a single thermocouple, and for 10 junctions this can approach 400 μV °C$^{-1}$. This allows high resolution detection of very small temperature differences such as those that occur in a pyranometer.

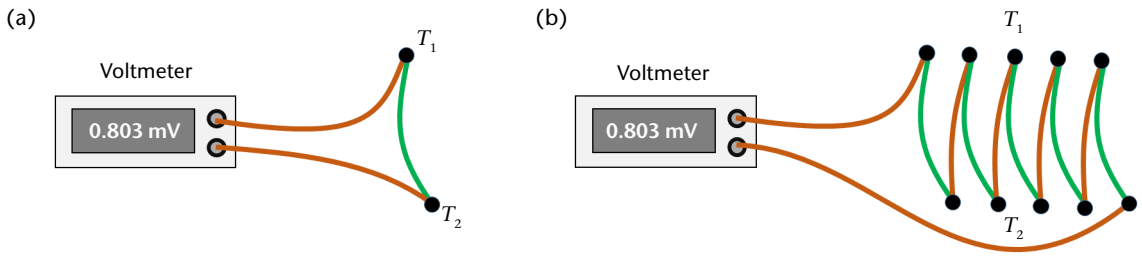



**Figure 2.8. Use of thermocouple in differential mode: (a) difference between the two junctions; (b) thermo pile**

### 2.2.3 Exposure and siting

The general requirements relating to the exposure and siting of thermometers are described in 2.1.4.2. Additional requirements include the following:

(a) The measurement of extreme values: Separate maximum and minimum thermometers may no longer be required if the electrical thermometer is connected to a continuously operating data recording system;

(b) The measurement of surface temperatures (bare soil or grass minimum thermometer): The radiative properties of electrical thermometers will be different from liquid-in-glass thermometers. Electrical thermometers exposed as grass minimum (or other surface) thermometers will, therefore, record different values compared to similarly exposed conventional thermometers. These differences may be minimized by placing the electrical thermometer within a glass sheath with the same diameter as the superseded thermometers;

(c) The measurement of soil temperatures: Electrical thermometers are deployed in brass plugs, inserted at the required depth into an undisturbed vertical soil face, the latter having been exposed by trenching. Electrical connections are brought out through plastic tubes via the trench, which is then refilled in such a way to restore, as far as possible, the original strata and drainage characteristics.

## 2.2.4 Sources of error

### 2.2.4.1 *Electrical resistance thermometers*

The main sources of error in a temperature measurement taken with electrical resistance thermometers are the following:

(a) Self-heating of the thermometer element;

(b) Inadequate compensation for lead resistance;

(c) Inadequate compensation for non-linearities in the sensor or processing instrument;

(d) Sudden changes in switch contact resistances.

Self-heating occurs because the passage of a current through the resistance element produces heat and, thus, the temperature of the thermometer element becomes higher than that of the surrounding medium. For a 1 mA (10 mA) current in a Pt100 sensor, the heating is approximately 0.1 mW (10 mW). For a sensor with a diameter of 6 mm, 30 mm long, in a wind speed of 1 m $s^{-1}$, the heat transfer coefficient will be approximately 40 $Wm^{-2}$ $K^{-1}$ and the resultant sensor heating will be between 0.004 K and 0.4 K.

The resistance of the connecting leads will introduce an error in the temperature reading. This will become more significant for long leads, for example, when the resistance thermometer is located at some distance from the measuring instrument; the reading errors will also vary as the temperature of the cables changes. To reduce errors, it is highly recommended to use four-wire measurements of Pt100 thermometers (see Figure 2.6).

Neither the electrical resistance thermometer nor the thermistor is linear over an extended temperature range. While for electrical resistance thermometers the output may be considered to be approximately linear for a limited range, appropriate provision must be made to compensate for such non-linearities with thermistors (White, 2016).

Sudden changes in switch contact resistance can occur as switches age. They may be variable and can go undetected unless regular system calibration checks are performed (see 2.2.5).

### 2.2.4.2 *Thermocouples*

The main uncertainty arising in the use of thermocouples arises from the distributed nature of the thermo-voltage generation. As shown in Figure 2.5, the measured voltage is generated along the entire length of the thermocouple along with its extension wires. This requires extreme uniformity in the alloy composition of thin wires. Additionally, the thermocouple must then be calibrated with the temperature gradients that the thermocouple will experience operationally.

Additionally, the secondary measurement of temperature used for the cold-junction compensation introduces an unknown error based on the environment of the ADC within the voltmeter or data acquisition system.

For meteorological deployments, proper calibration is not practical and the effectiveness of the cold-junction compensation cannot be assessed without additional knowledge. For these reasons, thermocouples are not recommended for standard meteorological deployment.

### 2.2.5 Comparison and calibration

#### 2.2.5.1 *Electrical resistance thermometers*

Laboratory calibrations of thermometers should be carried out regularly by calibration laboratories with ISO/IEC 17025 accreditation. Thermometers should be compared against standard thermometers usually in a stirred liquid bath, climatic chamber or a dry-block calibrator in the temperature range of interest. More details can be found in 2.6.

Since the measurement instrument is an integral part of the electrical thermometer, its calibration should be checked by substituting the resistance thermometer by an accurate, calibrated resistance reference and by applying resistances equivalent to fixed temperature increments (for example, 10 K) over the operational temperature range. The error at any point should not exceed 0.1 K. This work would normally be performed by a servicing technician.

#### 2.2.5.2 *Thermocouples*

The calibration and checking of thermocouples require the hot and cold junctions to be maintained at accurately known temperatures and the gradient between these temperatures to be varied to assess non-uniformity of the Seebeck coefficient. The techniques and instrumentation necessary to undertake this work are very specialized and will not be described here (Bentley, 1998; Nicholas and White, 1993; ASTM, 1993).

### 2.2.6 Corrections

When initially issued, electrical thermometers should be provided with either:

(a) A dated certificate confirming compliance with the appropriate standard;

(b) A dated calibration certificate giving the actual resistance or temperature (using the IEC standard Callendar–van Dusen parameters) at fixed points in the temperature range. These resistances/temperatures should be used when checking the uncertainty of the measuring instrument or system interface before and during operation. The magnitude of the resistance difference from the nominal value should not, in general, be greater than an equivalent temperature error of 0.1 or 0.2 K.

After each calibration, a Pt100 sensor will have a table of values of resistance, $R_i$, at a set temperatures $T_i$. These values may be used to generate a table of corrections (either $\Delta R_i$ or $\Delta T_i$) to be used with the thermometer. Based on this calibration data, conformance to the specified standard (for example, IEC 60751), class or tolerance band can be checked. However, to properly assess conformance within a tolerance band, users should additionally consider the effect of measurement uncertainty, $u_T$, associated with the calibration. There are three cases to consider:

– In the first case, the correction $\pm u_T$ falls entirely within the conformance band. In this case, the thermometer can be judged as being compliant with the specification. If this is the case, the thermometer can be returned to use and its temperature inferred from the standard IEC 60751 curve specified by the standard Callendar–van Dusen coefficients. For the example in Figure 2.9, this would be the case for an uncertainty of $u_T = 0.05$ °C.

– In the second case, the correction $\pm u_T$ falls entirely outside the conformance band. The thermometer can be judged as being non-compliant with the specification. In this case, the thermometer cannot be returned to use and the sensor would typically be discarded.

– In the third case, the correction $\pm u_T$ overlaps the conformance band so that there is a significant possibility that the sensor is non-compliant. In this case, the action taken is a matter of judgement depending on the degree of overlap. If the likelihood of non-conformance is judged to be sufficiently small, the thermometer might be returned

to use and its temperature inferred from the standard IEC 60751 curve specified by the standard Callendar–van Dusen coefficients. For the example in Figure 2.9, this would be the case for an uncertainty of $u_T = 0.15$ °C.

Note that conformance or non-conformance may depend on the coverage factor ascribed to the uncertainty.

In the simplest scheme that applies corrections, the corrections at a particular temperature are presumed to apply to all temperatures that are closer to that calibration point than any other calibration point. The temperature is thus inferred from the resistance using a standard curve, and then the correction is added. This scheme (Figure 2.9(a)) has the disadvantage of generating a discontinuity in the temperature versus resistance curve midway between the calibration points.

An improvement on the simple correction scheme is a linear interpolation (Figure 2.9(b)). The correction that applies to a particular measurement is calculated by linearly interpolating between the corrections from the calibration points above and below the particular temperature chosen. This has the advantage of generating a continuous temperature versus resistance curve.

A more sophisticated treatment of the data would be to use the data to generate custom Callendar–van Dusen parameters associated with that particular thermometer. This procedure is described in (Nicholas and White, 1993).

### 2.2.7 **Maintenance**

Regular field checks should identify any changes in system calibration. These may occur as a result of long-term changes in the electrical characteristics of the thermometer, degradation of the electrical cables or their connections, changes in the contact resistance of switches or changes in the electrical characteristics of the measuring equipment. Identification of the exact source and correction of such errors requires specialized equipment and training and should be undertaken only by a maintenance technician.

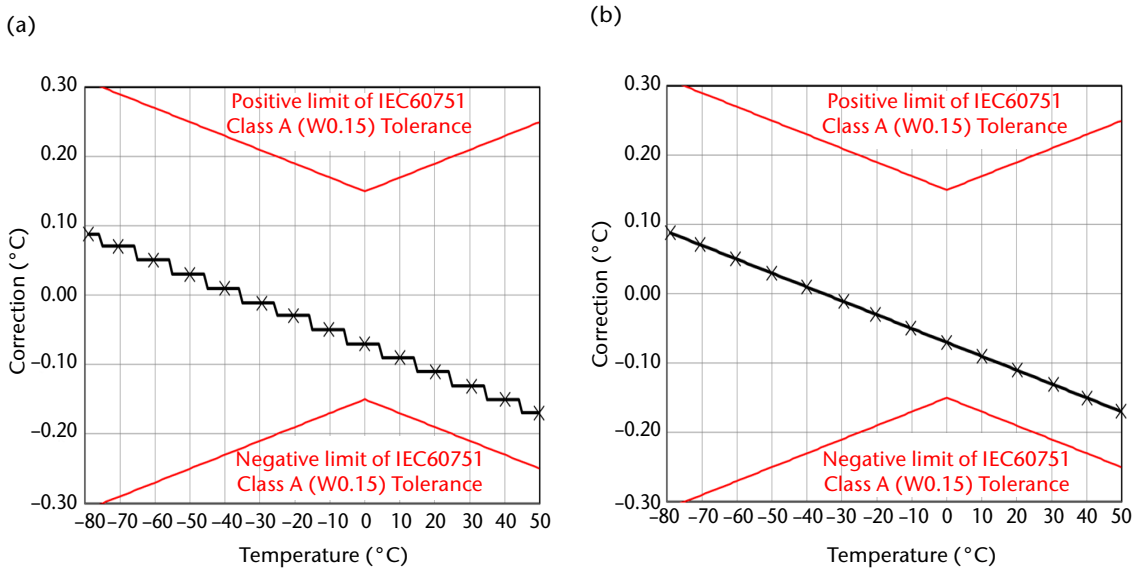



**Figure 2.9. Schemes for applying corrections derived from the calibration data: (a) stepwise; (b) linear**

## 2.3 LIQUID-IN-GLASS THERMOMETERS

Mercury-in-glass thermometers have been in widespread use, but as a result of the Minamata Convention on Mercury (see 2.1.4.5) are no longer recommended. NMHSs are encouraged to take appropriate measures to replace mercury-in-glass thermometers with modern alternatives (for example, electrical resistance thermometers). Considering the historical development of thermometry and the residual use of mercury-in-glass thermometers, the following text includes also mercury-in-glass thermometers.

### 2.3.1 General description

For routine observations of air temperature, including maximum, minimum and wet-bulb temperatures, liquid-in-glass thermometers are still commonly used. Such thermometers make use of the differential expansion of a pure liquid with respect to its glass container to indicate the temperature. The stem is a tube which has a fine bore attached to the main bulb; the volume of liquid in the thermometer is such that the bulb is filled completely but the stem is only partially filled at all temperatures to be measured. The change in volume of the liquid with respect to its container are indicated by change in the liquid column; by calibration with respect to a standard thermometer, a scale of temperature can be marked on the stem, or on a separate scale tightly attached to the stem.

The liquid used depends on the required temperature range; mercury has been used for temperatures above its freezing point (–38.9 °C), while ethyl alcohol or other pure organic liquids are used for lower temperatures. The glass should be one of the normal or borosilicate glasses approved for use in thermometers. The glass bulb is made as thin as practical, while maintaining reasonable strength, to facilitate the conduction of heat to and from the bulb and its contents. A narrower bore provides greater movement of liquid in the stem for a given temperature change, but reduces the useful temperature range of the thermometer for a given stem length. The thermometer should be suitably annealed before it is graduated in order to minimize the slow changes that occur in the glass with ageing.

There are four main types of construction for meteorological thermometers, as follows:

(a) The sheathed type with the scale engraved on the thermometer stem;

(b) The sheathed type with the scale engraved on an opal glass strip attached to the thermometer tube inside the sheath;

(c) The unsheathed type with the graduation marks on the stem and mounted on a metal, porcelain or wooden back carrying the scale numbers;

(d) The unsheathed type with the scale engraved on the stem.

The stems of some thermometers are lens-fronted to provide a magnified image of the liquid thread.

Types (a) and (b) have the advantage over types (c) and (d) that their scale markings are protected from wear. For types (c) and (d), the markings may have to be reblackened from time to time; on the other hand, such thermometers are easier to make than types (a) and (b). Types (a) and (d) have the advantage of being less susceptible to parallax errors (see 2.3.4). An overview of thermometers, designed for use in meteorological practices is given by Her Majesty's Stationary Office/Meteorological Office (1980).

Whichever type is adopted, the sheath or mounting should not be unduly bulky as this would keep the heat capacity high. At the same time, the sheath or mounting should be sufficiently robust to withstand the normal risks associated with handling and transit.

For mercury-in-glass thermometers, especially maximum thermometers, it is important that the vacuum above the mercury column be nearly perfect. All thermometers should be graduated

for total immersion, with the exception of thermometers for measuring soil temperature. The special requirements of thermometers for various purposes are dealt with hereafter under the appropriate headings.

#### 2.3.1.1 *Ordinary (station) thermometers*

Historically a very accurate mercury-in-glass-type thermometer has been used. Its scale markings have an increment of 0.2 K or 0.5 K, and the scale is longer than that of the other meteorological thermometers.

The ordinary thermometer is mounted in a thermometer screen to avoid radiation errors. A support keeps it in a vertical position with the bulb at the lower end. The form of the bulb is that of a cylinder or a sphere.

A pair of ordinary thermometers can be used as a psychrometer if one of them is fitted with a wet-bulb[2] sleeve (see the present volume, Chapter 4, 4.3).

#### 2.3.1.2 *Maximum thermometers*

The recommended type for maximum thermometers has been a mercury-in-glass thermometer with a constriction in the bore between the bulb and the beginning of the scale. This constriction prevents the mercury column from receding with falling temperatures. However, observers can reset by holding it firmly, bulb-end downwards, and swinging their arm until the mercury column is reunited. A maximum thermometer should be mounted at an angle of about 2° from the horizontal position, with the bulb at the lower end to ensure that the mercury column rests against the constriction without gravity forcing it to pass. It is desirable to have a widening of the bore at the top of the stem to enable parts of the column which have become separated to be easily united. As the only liquid suitable for liquid-in-glass maximum thermometers is mercury, electrical alternatives should be used to measure maximum temperature (see 2.2).

#### 2.3.1.3 *Minimum thermometers*

As regards minimum thermometers, the most common instrument is a spirit thermometer with a dark glass index, about 2 cm long, immersed in the spirit. Since some air is left in the tube of a spirit thermometer, a safety chamber should be provided at the upper end which should be large enough to allow the instrument to withstand a temperature of 50 °C or greater without being damaged. Minimum thermometers should be supported in a similar manner to maximum thermometers, in a near-horizontal position. Various liquids can be used in minimum thermometers, such as ethyl alcohol, pentane and toluol. It is important that the liquid should be as pure as possible since the presence of certain impurities increases the tendency of the liquid to polymerize with exposure to light and after the passage of time; such polymerization causes a change in calibration. In the case of ethyl alcohol, for example, the alcohol should be completely free of acetone.

Minimum thermometers are also exposed to obtain grass minimum temperature (see 2.1.4.2.3).

#### 2.3.1.4 *Soil thermometers*

For measuring soil temperatures at depths of 20 cm or less, mercury-in-glass thermometers, with their stems bent at right angles, or any other suitable angle, below the lowest graduation, have been in common use. The thermometer bulb is sunk into the ground to the required depth, and the scale is read with the thermometer in situ. These thermometers are graduated for immersion up to the measuring depth. Since the remainder of the thermometer is kept at air temperature, a safety chamber should be provided at the end of the stem for the expansion of the mercury.

---

[2] Wet-bulb temperatures are explained in the present volume, Chapter 4.

For measuring temperature at depths of over 20 cm, mercury-in-glass thermometers have been used mounted on wooden, glass or plastic tubes, with their bulbs embedded in wax or metallic paint. The thermometer–tube assemblies are then suspended or slipped in thin-walled metal or plastic tubes sunk into the ground to the required depth. In cold climates, the tops of the outer tubes should extend above the ground to a height greater than the expected depth of snow cover.

The technique of using vertical steel tubes is unsuitable for measuring the diurnal variation of soil temperature, particularly in dry soil, and calculations of soil thermal properties based on such measurements could be significantly in error because they will conduct heat from the surface layer.

The large time constant due to the increased heat capacity enables the thermometers to be removed from the outer tubes and read before their temperature has had time to change appreciably from the soil temperature.

When the ground is covered by snow, and in order that the observer may approach the line of thermometers without disturbing the snow cover, it is recommended that a lightweight bridge be constructed parallel to the line of thermometers. The bridge should be designed so that the deck can be removed between readings without affecting the snow cover.

## 2.3.2 Measurement procedures

### 2.3.2.1 *Reading ordinary thermometers*

Thermometers should be read as rapidly as possible in order to avoid changes of temperature caused by the observer's presence. Since the liquid meniscus, or index, and the thermometer scale are not on the same plane, care must be taken to avoid parallax errors. These will occur unless the observer ensures that the straight line from his/her eye to the meniscus, or index, is at a right angle to the thermometer stem. Since thermometer scales are not normally subdivided to less than one fifth of a degree, readings to the nearest tenth of a degree, which are essential in psychrometry, must be made by estimation. Corrections for scale errors, if any, should be applied to the readings. Maximum and minimum thermometers should be read and set at least twice daily. Their readings should be compared frequently with those of an ordinary thermometer in order to ensure that no serious errors develop.

### 2.3.2.2 *Measuring grass minimum temperatures*

The temperature is measured with a minimum thermometer such as that described in 2.3.1.3. The thermometer should be mounted on suitable supports so that it is inclined at an angle of about 2° from the horizontal position, with the bulb lower than the stem, 50 mm above the ground.

Normally, the thermometer is exposed at the last observation hour before sunset, and the reading is taken the next morning. The instrument is kept within a screen or indoors during the day. However, at stations where an observer is not available near sunset, it may be necessary to leave the thermometer exposed throughout the day. In strong sunshine, exposing the thermometer in this way can cause the spirit to distil and collect in the top of the bore. This effect can be minimized by fitting a cotton sock on a black metal shield over the safety chamber end of the thermometer; this shield absorbs more radiation and consequently reaches a higher temperature than the rest of the thermometer. Thus, any vapour will condense lower down the bore at the top of the spirit column.

### 2.3.3 Thermometer siting and exposure

Both ordinary thermometers and maximum and minimum thermometers are always exposed in a thermometer screen as described in 2.2.3. Extreme thermometers are mounted on suitable supports so that they are inclined at an angle of about 2° from the horizontal position, with the bulb being lower than the stem.

The siting and exposure of grass minimum thermometers is as prescribed in 2.1.4.2.3 and 2.3.2.2.

### 2.3.4 Sources of error in liquid-in-glass thermometers

The main sources of error common to all liquid-in-glass thermometers are the following:

(a) Elastic errors;

(b) Errors caused by the emergent stem;

(c) Parallax and gross reading errors;

(d) Changes in the volume of the bulb produced by exterior or interior pressure;

(e) Capillarity;

(f) Errors in scale division and calibration;

(g) Inequalities in the expansion of the liquid and glass over the range considered.

The last three errors can be minimized by the manufacturer and included in the corrections to be applied to the observed values. Some consideration needs to be given to the first three errors. Error (d) does not usually arise when the thermometers are used for meteorological purposes.

#### 2.3.4.1 *Elastic errors*

There are two kinds of elastic errors, namely reversible and irreversible errors. The first is of importance only when a thermometer is exposed to a large temperature range in a short period of time. Thus, if a thermometer is checked at the steam point and shortly afterwards at the ice point, it will read slightly too low at first and then the indicated temperature will rise slowly to the correct value. This error depends on the quality of the glass employed in the thermometer, and may be as much as 1 K (with glass of the highest quality it should be only 0.03 K) and would be proportionately less for smaller ranges of temperature. The effect is of no importance in meteorological measurements, apart from the possibility of error in the original calibration.

The irreversible changes may be more significant. The thermometer bulb tends to contract slowly over a period of years and, thus, causes the zero to rise. The greatest change will take place in the first year, after which the rate of change will gradually decrease. This alteration can be reduced by subjecting the bulb to heat treatment and by using the most suitable glass. Even with glass of the highest quality, the change may be about 0.01 K per year at first. For accurate work, and especially with inspector or check thermometers, the zero should be redetermined at the recommended intervals and the necessary corrections applied.

#### 2.3.4.2 *Errors caused by the emergent stem*

A thermometer used to measure air temperature is usually completely surrounded by air at an approximately uniform temperature, and is calibrated by immersing the thermometer either completely or only to the top of the liquid column (namely, calibrated by complete or partial

immersion). When such a thermometer is used to determine the temperature of a medium which does not surround the stem, so that the effective temperature of the stem is different from that of the bulb, an error will result.

For meteorological applications, the most likely circumstance where this might be encountered is when checking the calibration of an ordinary thermometer in a vessel containing another liquid at a temperature significantly different from ambient temperature and only the bulb or lower part of the stem is immersed.

#### 2.3.4.3 *Parallax and gross reading errors*

If the thermometer is not viewed on the plane that is perpendicular to the stem of the thermometer, parallax errors will arise. The error increases with the thickness of the thermometer stem and the angle between the actual and the correct line of sight. This error can be avoided only by taking great care when making an observation. With mercury-in-glass thermometers suspended vertically, as in an ordinary screen, the thermometer must be viewed at the horizontal level of the top of the mercury column.

Errors can also occur because observers usually disturb the surroundings in some way when they approach to read the thermometer. It is, therefore, necessary for observers to take the readings to the nearest tenth of a degree as soon as possible. Gross reading errors are usually 1°, 5° or 10° in magnitude. Such errors will be avoided if observers recheck the tens and units figure after taking their initial reading.

#### 2.3.4.4 *Errors due to differential expansion*

The coefficient of cubical expansion of mercury is $1.82 \cdot 10^{-4}$ $K^{-1}$, and that of most glass lies between $1.0 \cdot 10^{-5}$ and $3.0 \cdot 10^{-5}$ $K^{-1}$. The expansion coefficient of the glass is, thus, an important fraction of that of mercury and cannot be neglected. As neither the coefficients of cubical expansion of mercury and glass nor the cross-sectional area of the bore of the stem are strictly constant over the range of temperature and length of the stem being used, the scale value of unit length of the stem varies along the stem, and the thermometer has to be calibrated by the manufacturer against a standard thermometer before it can be used.

#### 2.3.4.5 *Errors associated with spirit thermometers*

The expansion coefficients of the liquids used in spirit thermometers are very much larger than those of mercury, and their freezing points are much lower (ethyl alcohol freezes at –115 °C). Spirit is used in minimum thermometers because it is colourless and because its larger expansion coefficient enables a larger bore to be used. Spirit thermometers are less accurate than mercury thermometers of similar cost and quality. In addition to having the general disadvantages of liquid-in-glass thermometers, spirit thermometers have some peculiarities to themselves:

(a) Adhesion of the spirit to the glass: Unlike mercury, organic liquids generally wet the glass. Therefore, when the temperature falls rapidly, a certain amount of the liquid may remain on the walls of the bore, causing the thermometer to read low. The liquid gradually drains down the bore if the thermometer is suspended vertically;

(b) Breaking of the liquid column: Drops of the liquid often form in the upper part of the thermometer stem by a process of evaporation and condensation. These can be reunited with the main column, but errors may be caused at the beginning of the process before it is noticed. The column is also often broken during transport. This error is reduced during manufacture by sealing off the thermometer at its lowest temperature so that it contains the maximum amount of air in the stem;

(c) Slow changes in the liquid: The organic liquids used tend to polymerize with age and exposure to light, with a consequent gradual diminution in liquid volume. This effect is

speeded up by the presence of impurities; in particular, the presence of acetone in ethyl alcohol has been shown to be very deleterious. Great care has therefore to be taken over the preparation of the liquid for the thermometers. This effect may also be increased if dyes are used to colour the liquid to make it more visible.

The reduction of errors caused by breakage in the liquid column and the general care of spirit thermometers are dealt with later in this chapter.

### 2.3.5 Comparison and calibration in the field and laboratory

#### 2.3.5.1 *Laboratory calibration*

Laboratory calibrations of thermometers should be carried out by ISO/IEC 17025-accredited calibration laboratories. For liquid-in-glass thermometers, a liquid bath should be employed, within which it should be possible to maintain the temperature at any desired values within the required range. The rate of temperature change within the liquid should not exceed the recommended limits, and the calibration apparatus should be provided with a means of stirring the liquid. The reference standard thermometers and thermometers being calibrated should be suspended independently of the container and fully immersed, and should not touch the sides.

Sufficient measurements should be taken to ensure that the corrections to be applied represent the performance of the thermometer under normal conditions, with errors due to interpolation at any intermediate point not exceeding the non-systematic errors (see Volume V, Chapter 4 of the present Guide).

#### 2.3.5.2 *Field checks*

All liquid-in-glass thermometers experience gradual changes of zero. For this reason, it is desirable to check them at regular intervals, usually about once every two years. The thermometers should be stored in an upright position at room temperature for at least 24 h before the checking process begins.

The ice point may be checked by a Dewar flask filled with crushed ice made from distilled water and moistened with more distilled water. The space between the ice pieces as well as the bottom of the vessel should be free from air. The water should remain 2 cm beneath the ice surface. An ordinary thermos flask will accommodate the total immersion of most thermometers up to their ice point. The thermometers should be inserted so that as little of the mercury or spirit column as possible emerges from the ice. An interval of at least 15 min should elapse to allow the thermometer to take up the temperature of the melting ice before a reading of the indicated temperature is taken. Each thermometer should be moved backwards and forwards through the mixture and immediately read to a tenth part of the scale interval. Further readings at 5 min intervals should be taken and a mean value computed.

Other points in the range can be covered by reference to a travelling standard or inspection thermometer. Comparison should be made by immersing the reference thermometer and the thermometer, or thermometers, to be checked in a deep vessel of water. It is generally better to work indoors, especially if the sun is shining, and the best results will be obtained if the water is at, or close to, ambient temperature.

Each thermometer is compared with the reference thermometer; thermometers of the same type can be compared with each other. For each comparison, the thermometers are held with their bulbs close together, moved backwards and forwards through the water for about 1 min, and then read. It must be possible to read both thermometers without changing the depth of immersion; subject to this, the bulbs should be as deep in the water as possible. Most meteorological thermometers are calibrated in the laboratory for total immersion; provided that the difference between the water and air temperature is not more than 5 K, the emergent stem

correction should be negligible. Often, with the bulbs at the same depth, the tops of the columns of mercury (or other liquid) in the reference thermometer and the thermometer being checked will not be very close together. Particular care should therefore be taken to avoid parallax errors.

These comparisons should be made at least three times for each pair of thermometers. For each set of comparisons, the mean of the differences between readings should not exceed the specified uncertainties given in the present volume, Chapter 1, Annex 1.A.

Soil thermometers may be checked in this manner, but should be left in the water for at least 30 min to allow the wax in which the bulbs are embedded to take up the temperature of the water. The large time constant of the soil thermometer makes it difficult to conduct a satisfactory check unless the temperature of the water can be kept very steady. If the check is carefully carried out in water whose temperature does not change by more than 1 K in 30 min, the difference from the corrected reading of the reference thermometer should not exceed 0.25 K.

### 2.3.6 Corrections

When initially issued, thermometers identified by a serial number should be provided with either a dated certificate confirming compliance with the uncertainty requirement, or a dated calibration certificate giving the corrections that should be applied to the readings to achieve the required uncertainty.

In general, if the errors at selected points in the range of a thermometer (for example, 0 °C, 10 °C, 20 °C) are all within 0.05 K, no corrections will be necessary and the thermometers can be used directly as ordinary thermometers in naturally ventilated screens and as maximum, minimum, soil or grass minimum thermometers. If the errors at these selected points are greater than 0.05 K, a table of corrections should be available to the observer at the place of reading, together with unambiguous instructions on how these corrections should be applied.

Thermometers for which certificates would normally be issued are those:

(a) For use in ventilated psychrometers;

(b) For use as travelling standards;

(c) For laboratory calibration references;

(d) For special purposes for which the application of corrections is justified.

For psychrometric use, two identical thermometers should be selected.

### 2.3.7 Maintenance

#### 2.3.7.1 *Breakage in the liquid column*

The most common fault encountered is the breaking of the liquid column, especially during transportation. This is most likely to occur in spirit (minimum) thermometers. Other problems associated with these thermometers are adhesion of the spirit to the glass and the formation by distillation of drops of spirit in the support part of the bore.

A broken liquid column can usually be reunited by holding the thermometer bulb-end downward and tapping the thermometer lightly and rapidly against the fingers or something else which is elastic and not too hard. The tapping should be continued for some time (5 min if necessary), and afterwards the thermometer should be hung, or stood, upright in a suitable container, bulb downward, for at least 1 h to allow any spirit adhering to the glass to drain down to the main column. If such treatment is not successful, a more drastic method is to cool the bulb in a freezing mixture of ice and salt, while keeping the upper part of the stem warm; the liquid will slowly distil back to the main column. Alternatively, the thermometer may be held upright

with its bulb in a vessel of warm water, while the stem is tapped or shaken from the water as soon as the top of the spirit column reaches the safety chamber at the top of the stem. Great care must be taken when using this method as there is a risk of bursting the thermometer if the spirit expands into the safety chamber.

#### 2.3.7.2 *Scale illegibility*

Another shortcoming of unsheathed liquid-in-glass thermometers is that with time their scale can become illegible. This can be corrected at the station by rubbing the scale with a dark crayon or black lead pencil.

### 2.3.8 Safety

Mercury, which has been the most commonly used liquid in liquid-in-glass thermometers, is poisonous if swallowed or if its vapour is inhaled. If a thermometer is broken and the droplets of mercury are not removed there is some danger to health, especially in confined spaces. More information on safety precautions for the use of mercury is given in the present volume, Chapter 3, Annex 3.A. There are also restrictions on the carriage of mercury-in-glass thermometers on aircraft, or special precautions that must be taken to prevent the escape of mercury in the event of a breakage. The advice of the appropriate authority or carrier should be sought.

## 2.4 MECHANICAL THERMOGRAPHS

### 2.4.1 General description

The types of mechanical thermographs still commonly used are supplied with bimetallic or Bourdon-tube sensors since these are relatively inexpensive, reliable and portable. However, they are not readily adapted for remote or electronic recording. Such thermographs incorporate a rotating chart mechanism common to the family of classic recording instruments. In general, thermographs should be capable of operating over a range of about 60 K or even 80 K if they are to be used in continental climates. A scale value is needed such that the temperature can be read to 0.2 K without difficulty on a reasonably sized chart. To achieve this, provisions should be made for altering the zero setting of the instrument according to the season. The maximum error of a thermograph should not exceed 1 K.

#### 2.4.1.1 *Bimetallic thermograph*

In bimetallic thermographs, the movement of the recording pen is controlled by the change in curvature of a bimetallic strip or helix, one end of which is rigidly fixed to an arm attached to the frame. A means of finely adjusting this arm should be provided so that the zero of the instrument can be altered when necessary. In addition, the instrument should be provided with a means of altering the scale value by adjusting the length of the lever that transfers the movement of the bimetal to the pen; this adjustment is best left to authorized personnel. The bimetallic element should be adequately protected from corrosion; this is best done by heavy copper, nickel or chromium plating, although a coat of lacquer may be adequate in some climates. A typical time constant of about 25 s is obtained at an air speed of 5 m $s^{-1}$.

#### 2.4.1.2 *Bourdon-tube thermograph*

The general arrangement is similar to that of the bimetallic type but its temperature-sensitive element is in the form of a curved metal tube of flat, elliptical section, filled with alcohol. The

Bourdon tube is less sensitive than the bimetallic element and usually requires a multiplying level mechanism to give sufficient scale value. A typical time constant is about 6 s at an air speed of 5 m $s^{-1}$.

### 2.4.2 Measurement procedures

In order to improve the resolution of the reading, thermographs will often be set, in different seasons, to one of two different ranges with corresponding charts. The exact date for changing from one set of charts to the other will vary according to the locality. However, when the change is made the instrument will need to be adjusted. This should be done either in the screen on a cloudy, windy day at a time when the temperature is practically constant or in a room where the temperature is constant. The adjustment is made by loosening the screw holding the pen arm to the pen spindle, moving the pen arm to the correct position and retightening, the screws. The instrument should then be left as is before rechecking, and any further adjustments made as necessary.

### 2.4.3 Exposure and siting

These instruments should be exposed in a large thermometer screen (for example, Stevenson screen with an indoor measurement chamber of 450 x 700 x 400 mm).

### 2.4.4 Sources of error

In the thermograph mechanism itself, friction is the main source of error. One cause of this is bad alignment of the helix with respect to the spindle. Unless accurately placed, the helix acts as a powerful spring and, if rigidly anchored, pushes the main spindle against one side of the bearings. With modern instruments this should not be a serious problem. Friction between the pen and the chart can be kept to a minimum by suitably adjusting the gate suspension.

### 2.4.5 Comparison and calibration

#### 2.4.5.1 *Laboratory calibration*

There are two basic methods for the laboratory calibration of bimetallic thermographs. They may be checked by fixing them in a position with the bimetallic element in a bath of water. Alternatively, the thermograph may be placed in a commercial calibration chamber equipped with an air temperature control mechanism, a fan and a reference thermometer.

Comparisons should be made at two temperatures; from these, any necessary changes in the zero and magnification can be found. Scale adjustments should be performed by authorized personnel, and only after reference to the appropriate manufacturer's instrument handbook.

#### 2.4.5.2 *Field comparison*

The time constant of the instrument may be as low as one half that of the ordinary mercury thermometer, so that routine comparisons of the readings of the dry bulb and the thermograph at fixed hours will, in general, not produce exact agreement even if the instrument is working perfectly. A better procedure is to check the reading of the instrument on a suitable day at a time when the temperature is almost constant (usually a cloudy, windy day) or, alternatively, to compare the minimum readings of the thermograph trace with the reading of the minimum thermometer exposed in the same screen. Any necessary adjustment can then be made by means of the setting screw.

### 2.4.6 **Corrections**

Thermographs would not normally be issued with correction certificates. If station checks show an instrument to have excessive errors, and if these cannot be adjusted locally, the instrument should be returned to an appropriate calibration laboratory for repair and recalibration.

### 2.4.7 **Maintenance**

Routine maintenance will involve an inspection of the general external condition, the play in the bearings, the inclination of the recording arm, the set of the pen, and the angle between the magnification arm and recording arm, and a check of the chart-drum clock timing. Such examinations should be performed in accordance with the recommendations of the manufacturer. In general, the helix should be handled carefully to avoid mechanical damage and should be kept clean. The bearings of the spindle should also be kept clean and oiled at intervals using a small amount of clock oil. The instrument is mechanically very simple and, provided that precautions are taken to keep the friction to a minimum and prevent corrosion, it should give good service.

## 2.5 **RADIATION SHIELDS**

A radiation shield or screen should be designed to provide an enclosure with an internal temperature that is both uniform and the same as that of the outside air. It should completely surround the thermometers and exclude radiant heat, precipitation and other phenomena that might influence the measurement.

Screens with forced ventilation, in which air is drawn over the thermometer element by a fan, may help to reduce biases when the microclimate inside the screen deviates from the surrounding air mass. Such a deviation is most significant when the natural wind speed is very low ($< 1$ m $s^{-1}$). When such artificial ventilation is used, care should be taken to prevent the deposition of aerosols and rain droplets on the sensor which decrease its temperature towards the wet-bulb temperature. Artificially ventilated radiation shields should provide a clear indication of the fan status directly on the screen or on the control unit or data logger to allow maintenance staff to check whether the fan is functioning properly by visual inspection. Additionally, the fan status and preferably the fan speed should be provided in the data output for automatic monitoring purposes.

As a shield material, highly polished, non-oxidizable metal is favourable because of its high reflectivity and low heat absorption. Nevertheless, plastic-based material with low thermal conductivity is widely used because of its simple maintenance requirements. Material with low thermal conductivity must be used if the system relies on natural ventilation as well.

The performance of a screen (response behaviour and microclimate effects introducing unwanted biases) depends predominantly on its design, in which care must be taken to ensure both radiation protection and sufficient ventilation. Since the start of meteorological temperature measurements, very diverse types of screens have been designed. Following the introduction of temperature measurements taken in AWSs, the variety of these designs has increased significantly (see WMO, 1998*a*). Because of differences in specific applications, the degree of automation and climatology, it is difficult to recommend one specific type of design suitable for worldwide measurements. Nevertheless, many investigations and intercomparisons on designs and their performance have been carried out. A clear overview of screen designs is given by WMO (1972). Results of thermometer screen intercomparisons are reported by Andersson and Mattison (1991), Sparks (2001), WMO (1998*b*, 1998*c*, 1998*d*, 2000*a*, 2000*b*, 2002*b*, 2002*c*, 2002*d*, 2011) and Zanghi (1987).

An international standard (ISO/DIS 17714) defines most relevant screen types and describes the methods to determine or compare screen performances (ISO, 2007).

As the radiation shield can contribute greatly to the uncertainty budget of temperature measurements, the effect of different meteorological situations should be evaluated and calculated (for example, rising sun after clear night, frost pattern or snow inside and outside, condensation inside and outside, and effect of liquid precipitation).

### 2.5.1 **Louvred screens**

Most of the numerous varieties of louvred screen rely on natural ventilation. The walls of such a screen should be double-louvred and the floor should be made of staggered boards, but other types of construction may be found to meet the above requirements. The roof should be double-layered, with provisions for ventilation of the space between the two layers. In cold climates, owing to the high reflectivity of snow (up to 88%), the screen should also have a double floor. At the same time, however, the floor should easily drop or tilt so that any snow entering the screen during a storm can be removed.

The size and construction of the screen should be such that it keeps the heat capacity as low as practicable and allows ample space between the instruments and the walls. The latter feature excludes all possibility of direct contact between the thermometer sensing elements and the walls, and is particularly important in the tropics where insolation may heat the sides to the extent that an appreciable temperature gradient is caused in the screen. Direct contact between the sensing elements and the thermometer mounting should also be avoided. The screen should be painted both inside and outside with white, non-hygroscopic paint.

When double walls are provided, the layer of air between them serves to reduce the amount of heat that would otherwise be conducted from the outer wall to the inner enclosure, especially in strong sunshine. When the wind is appreciable, the air between the walls is changed continually so that the conduction of heat inwards from the outer walls is further decreased.

The free circulation of air throughout the screen helps the temperature of the inner wall adapt to ambient air changes. In this way, the influence of the inner wall upon the temperature of the thermometer is reduced. Also, the free circulation of air within the screen enables the thermometer to follow the ambient air changes more quickly than if radiative exchanges alone were operative. However, the air circulating through the screen spends a finite time in contact with the outer walls and may have its temperature altered thereby. This effect becomes appreciable when the wind is light and the temperature of the outer wall is markedly different from the air temperature. Thus, the temperature of the air in a screen can be expected to be higher than the true air temperature on a day of strong sunshine and calm wind, and slightly lower on a clear, calm night, with errors perhaps reaching 2.5 and –0.5 K, respectively, in extreme cases. Additional errors may be introduced by cooling due to evaporation from a wet screen after rain. All these errors also have a direct influence on the readings of other instruments inside the screen, such as hygrometers, evaporimeters, and the like.

Errors due to variations in natural ventilation can be reduced if the screen is fitted with a suitably designed forced ventilation system that maintains a constant and known ventilation rate, at least at low wind speeds. Care should be taken in the design of such systems to ensure that heat from the fan or an electrical motor does not affect the screen temperature.

In general, only one door is needed, with the screen being placed so that the sun does not shine on the thermometers when the door is open at the times of observation. In the tropics, two doors are necessary for use during different periods of the year. Likewise, in polar regions (where the sun is at a low angle) precautions should be taken to protect the inside of the screen from the direct rays of the sun either by a form of shading or by using a screen which is mounted so that it can be turned to an appropriate angle while the door is open for readings.

Although most screens are still made of wood, some recent designs using plastic materials offer greater protection against radiation effects because of an improved louvre design that provides a better airflow. In any case, the screen and stand should be constructed of sturdy materials and should be firmly installed so that errors in maximum and minimum thermometer readings

caused by wind vibration are kept to a minimum. In some areas where wind vibration cannot be entirely damped, elastic mounting brackets are recommended. The ground cover beneath the screen should be grass or, in places where grass does not grow, the natural surface of the area.

The screen should be kept clean and repainted regularly; in many places, repainting the screen once every two years is sufficient, but in areas subject to atmospheric pollution it may be necessary to repaint it at least once a year.

### 2.5.2 Other artificially ventilated shields

The main alternative to exposure in a louvred screen, which is either naturally or artificially ventilated, is to shield the thermometer bulb from direct radiation by placing it on the axis of two concentric cylindrical shields and drawing a current of air (with a speed between 2.5 and 10 m $s^{-1}$) between the shields and past the thermometer bulb. This type of exposure is normal in aspirated psychrometers (see the present volume, Chapter 4). In principle, the shields should be made of a thermally insulating material, although in the Assmann psychrometer the shields are made of highly polished metal to reduce the absorption of solar radiation. The inner shield is kept in contact with a moving stream of air on both sides so that its temperature, and consequently that of the thermometer, can approximate very closely to that of the air. Such shields are usually mounted with their axes in a vertical position. The amount of direct radiation from the ground entering through the base of such shields is small and can be reduced by extending the base of the shields appreciably below the thermometer bulb. When the artificial ventilation is provided by an electrically driven fan, care should be taken to prevent any heat from the motor and fan from reaching the thermometers.

## 2.6 TRACEABILITTY ASSURANCE AND CALIBRATION

A national meteorological or other accredited calibration laboratory should have, as a working standard, a high-quality PRT, traceable to the national and international standards (WMO, 2010). The high-quality PRT may be an SPRT or PRT. SPRTs should be traceable to national and international level by external calibration in selected fixed points (see annex table). As SPRTs are state-of-art thermometers with lowest uncertainty available, laboratory procedures require additional laboratory equipment (measurement bridge, standard resistors, and so forth) and techniques for best utilization of the instrument's capabilities. The behaviour of SPRTs may be checked periodically in a water triple-point cell. The triple point of water can be reproduced in a triple-point cell with an uncertainty of $1 \cdot 10^{-4}$ K. PRTs should be traceable to national and international level by external comparison calibration in the meteorological range of interest. SPRTs or PRTs are used in calibration laboratories for value dissemination to working standards and/or instruments under calibration usually by comparison calibration. All laboratory equipment involved in the calibration process contributes to measurement uncertainty and must be traceable to SI in accordance with the traceability strategy (see the present volume, Chapter 1, Annex 1.B).

Comparison calibration is typically performed by measurements of the reference standard and the resistance or voltage of the instrument under calibration while exposed to a stable temperature over the whole temperature range of interest. Fundamentally, four types of instruments are required:

– Reference standard;

– Data acquisition system for the reference standard;

– Data acquisition system for the instrument under calibration;

– Source of a stable temperature.

The reference standard should be checked at the ice or water triple point before use to ensure that the resistance has not significantly changed since the previous calibration of the instrument. External calibration of the reference standard should be carried out at intervals depending upon the frequency and temperature range of use. Internal procedures for QA must be applied (redundant stability checks).

When calibrating the resistance thermometer against a reference PRT or SPRT, the technical requirements for the readout devices are the same for the instruments under calibration and the reference thermometer. If a multiplexing system is available, one readout device can usually be used for both. This is the case if the readout device is designed for temperature calibration (not just temperature measurement) and has variable settings (current, timing, and so forth). However, if the readout device is not designed for temperature calibration and/or a switching system is not available, then two or more readout devices are required. Best results will be obtained with readout devices designed specifically for thermometer calibration. There are two important points to consider with regard to PRT and SPRT:

– Ensure that the readout device has a resistance range appropriate for the reference thermometer and instruments under calibration for which it is intended. Many modern thermometer readout devices are designed to cover this span on a single range;

– Ensure that the readout device is using the proper source current. Incorrect source current will result in excessive self-heating and incorrect calibration.

During the calibration, the thermometers are placed into a heat transfer medium in the temperature source. The heat transfer medium might be a stirred fluid, a metal block or air. The heat transfer medium maintains a constant and uniform temperature environment that allows the reading of the thermometer under test to be compared to a more accurate thermometer. A calibration bath or chamber cannot be considered as completely stable in time and homogeneous throughout its volume, especially when temperature calibrations by comparison are performed at the lowest uncertainties. This typically represents a major contribution to the total uncertainty of a calibration procedure. To decrease this contribution to uncertainty, equalizing blocks can be used in calibration baths. The dimension of the block depends on the bath dimension.

The measurement uncertainty in the calibration of a thermometer depends on the calibration method used, the contribution to uncertainty of the standards, the characteristics of the measuring equipment used and the characteristics of the device under calibration.

In general, the intervals between calibrations depend upon the conditions of use. Since different temperature-measuring devices may be used under a wide variety of conditions, precise calibration intervals cannot necessarily be specified. In such cases, evidence (for example, from regular “between-calibration” checks) should be available to demonstrate that calibration intervals have been selected so that calibration takes place before any significant changes in calibration corrections occur.

# ANNEX. DEFINING THE FIXED POINTS OF THE INTERNATIONAL TEMPERATURE SCALE OF 1990

The fixed points of the ITS-90 of interest to meteorological measurements are contained in the table below.

The standard method of interpolating between the fixed points uses formulae to establish the relation between indications of the standard instruments and the values of the ITS-90 (BIPM, 1990). The standard instrument used from –259.34 °C to 961.78 °C is a PRT.

An alternative practical method for ITS-90 approximation in PRT calibration (determination of $R_0$, $A$, $B$ and $C$, see equation below) is to obtain resistance-temperature data by making a comparison with a calibrated SPRT at numerous temperatures in the range of interest and then fit a polynomial to the data by a least-squares technique.

The relationship between the resistance of the PRT under calibration and the temperature measured with a reference thermometer is described with an interpolation equation. The Callendar–Van Dusen equation is generally accepted as the interpolation equation for industrial PRTs (defined in the IEC 60751 (2008)) rather than for SPRTs:

$$R = R_0\left(1 + At + Bt^2 + C\left(t - 100\right)t^3\right)$$

where $R$ is the resistance at temperature $t$ of a platinum wire, $R_0$ is its resistance at 0 °C (ice point) and $A$, $B$ and $C$ ($C = 0$ for $t > 0$ °C) are constants which are found using the least-squares method on the data acquired during the calibration.

**Defining fixed points on the ITS-90 in the meteorological range**

| *Equilibrium state* | *Assigned value of ITS* | |
|---|---|---|
| | *K* | *°C* |
| Equilibrium between the solid, liquid and vapour phases of argon (triple point of argon) | 83.8058 | –189.3442 |
| Equilibrium between the solid, liquid and vapour phases of mercury (triple point of mercury) | 234.3156 | –38.8344 |
| Equilibrium between the solid, liquid and vapour phases of water (triple point of water) | 273.1600 | 0.01 |
| Equilibrium between the solid and liquid phases of gallium (melting point of gallium) | 302.9146 | 29.7646 |
| Equilibrium between the solid and liquid phases of indium (freezing point of indium) | 429.7485 | 156.5985 |

## REFERENCES AND FURTHER READING


Andersson, T. and I. Mattison, 1991: *A Field Test of Thermometer Screens*. SMHI Report No. RMK 62, Norrköping.

ASTM, 1993: *ASTM Manual on The Use of Thermocouples in Temperature Measurement*. Philadelphia, ASTM.

Bentley, R.E. (Ed.), 1998: *Temperature and Humidity Measurement*. Singapore, Springer-Verlag.

Bugbee, B., O. Monje and B. Tanner, 1996: Quantifying energy and mass transfer in crop canopies. *Advances in Space Research*, 18:149–156.

Bureau International des Poids et Mesures, 1989: *Procès-Verbaux du Comité International des Poids et Mesures*, 78th meeting, 1989, Paris (available from https://www.bipm.org/documents/20126/41791796/ITS-90.pdf/).

Bureau International des Poids et Mesures/Comité Consultatif de Thermométrie, 1990: The International Temperature Scale of 1990 (ITS-90) (H. Preston-Thomas). Metrologia, 27:3–10 (amended version) (available from https://doi.org/10.1088/0026-1394/27/1/002).

Çengal, Y.A. and A.J. Ghajar, 2014: *Heat and Mass Transfer: Fundamentals and Application.* Fifth edition. New York, McGraw-Hill Education.

Diamond, H. J., T.R. Karl, M.A. Palecki, C.B. Baker, J.E. Bell, R.D. Leeper, D.R. Easterling, J.H. Lawrimore, T.P. Meyers, M.R. Helfert, G. Goodge and P.W. Thorne, 2013: U.S. Climate Reference Network after one decade of operations: status and assessment. *Bulletin of the American Meteorological Society*, 94:489–498, doi: 10.1175/BAMS-D-12-00170.1.

Erell, E., V. Leal and E. Maldonaldo, 2005: Measurement of air temperature in the presence of a large radiant flux: an assessment of passively ventilated thermometer screens. *Boundary Layer Meteorology*, 114:205–231.

Harrison, R.G., 2010: Natural ventilation effects on temperatures within Stevenson screens. *Quarterly Journal of the Royal Meteorological Society*, 136(646)A:253–259, DOI: 10.1002/qj.537.

———, 2015: *Meteorological Measurements and Instrumentation.* Chichester, Wiley.

Harrison R.G. and M.A. Pedder, 2001: Fine wire thermometer for air measurement. *Review of Scientific Instruments*, 72(2):1539–1541.

Harrison, R.G. and G.W Rogers, 2006: Fine wire thermometer amplifier for atmospheric measurements. *Review of Scientific Instruments*, 77(11):116112.

Harvey, A.H., M.O. McLinden and W.L. Tew, 2013: Thermodynamic analysis and experimental study of the effect of atmospheric pressure on the ice point. *AIP Conference Proceedings.* 1552:221, doi: 10.1063/1.4819543.

Her Majesty's Stationery Office/Meteorological Office, 1980: *Handbook of Meteorological Instruments*, Volume 2: Measurement of temperature. London.

Incropera, F.P. and D.P. de Witt, 2011: *Fundamentals of Heat and Mass Transfer.* Chichester, Wiley.

International Electrotechnical Commission, 2008: *Industrial Platinum Resistance Thermometers and Platinum Temperature Sensors*, IEC 60751:2008. Geneva.

International Organization for Standardization, 2007: *Meteorology – Air Temperature Measurements – Test Methods for Comparing the Performance of Thermometer Shields/Screens and Defining Important Characteristics*, ISO/DIS 17714:2007. Geneva.

Jones, E.B., 1992: *Jones' Instrument Technology*. Volume 2: Measurement of temperature and chemical composition, Butterworths-Heinemann, Oxford.

Middleton, W.E.K. and A.F. Spilhaus, 1960: *Meteorological Instruments*. University of Toronto Press.

Ney, E.P., R.W. Maas and W.F. Huch, 1960: The measurement of atmospheric temperature. *Journal of Meteorology*, 18:60–80.

Nicholas, J.V. and D.R. White, 1993: *Traceable Temperatures*. Second edition. Chichester, Wiley.

Quinn, T.J., 1990: *Temperature*. Second edition. San Diego, Academic Press.

Richiardone, R., M. Manfrin, S. Ferrarese, C. Francone, V. Fernicola, R. M. Gavioso and L. Mortarini, 2012: Influence of the Sonic Anemometer Calibration on Turbulent Heat-Flux Measurements. *Boundary-Layer Meteorology*, 142(3):425–442.

Schotanus, P., F.T.M. Nieuwstadt and H.A.R e Bruin, 1983: Temperature measurement with a sonic anemometer and its application to heat and moisture fluxes. *Boundary-Layer Meteorol.* 26:81–93.

Sparks, W.R., 1970: Current concepts of temperature measurement applicable to synoptic networks. *Meteorological Monographs*, 11(33):247–251.

———, 2001: Field trial of Metspec screens. *Technical Report TR19*, Met Office/OD, Wokingham, United Kingdom of Great Britain and Northern Ireland.

Underwood, R., M. de Podesta, G. Sutton, L. Stanger, R. Rusby, P Harris, P. Morantz and G. Machin, 2017: Further estimates of ($T - T_{90}$) close to the triple point of water. *International Journal of Thermophysics*, 38:44.

Underwood, R., T. Gardiner, A. Finlayson, S. Bell and M. de Podesta, 2017: An improved non-contact thermometer and hygrometer with rapid response. *Metrologia*, 54(1):S9.

Underwood, R., T. Gardiner, A. Finlayson, J. Few, J. Wilkinson, S. Bell, J. Merrison, J.J. Iverson and M. de Podesta, 2015: A combined non-contact acoustic thermometer and infrared hygrometer for atmospheric measurements. *Meteorological Applications*, 22:830–835.

White, D.R., 2015: Temperature errors in linearizing resistance networks for thermistors. *International Journal of Thermophysics*, 36:3404–3420, DOI 10.1007/s10765-015-1968-2.

———, 2017: Interpolation errors in thermistor calibration equations. *International Journal of Thermophysics*, 38(4):59, DOI 10.1007/s10765-017-2194-x.

World Meteorological Organization, 1972: *The Effect of Thermometer Screen Design on the Observed Temperature* (W.R. Sparks). (WMO-No. 315). Geneva.

———, 1992: *Measurement of Temperature and Humidity: Specification, Construction, Properties and Use of the WMO Reference Psychrometer* (R.G. Wylie and T. Lalas). Technical Note No. 194 (WMO-No. 759). Geneva.

———, 1998*a*: *Recent Changes in Thermometer Screen Design and their Impact* (A. Barnett, D.B. Hatton and D.W. Jones). Instruments and Observing Methods Report No. 66 (WMO/TD-No. 871). Geneva.

———, 1998*b*: An investigation of temperature screens and their impact on temperature measurements (J. Warne). Paper presented at the WMO Technical Conference on Meteorological and Environmental Instruments and Methods of Observation (TECO-98). Instruments and Observing Methods Report No. 70 (WMO/TD-No. 877). Geneva.

———, 1998*c*: A thermometer screen intercomparison (J.P. van der Meulen). Paper presented at the WMO Technical Conference on Meteorological and Environmental Instruments and Methods of Observation (TECO-98). Instruments and Observing Methods Report No. 70 (WMO/TD-No. 877). Geneva.

———, 1998*d*: Comparison of meteorological screens for temperature measurement (G. Lefebvre). Paper presented at the WMO Technical Conference on Meteorological and Environmental Instruments and Methods of Observation (TECO-98). Instruments and Observing Methods Report No. 70 (WMO/TD-No. 877). Geneva.

———, 2000*a*: A comparison of air temperature radiation screens by field experiments and computational fluid dynamics (CFD) simulations (A. Spetalen, C. Lofseik and P. Ø. Nordli). Paper presented at the WMO Technical Conference on Meteorological and Environmental Instruments and Methods of Observation (TECO-2000). Instruments and Observing Methods Report No. 74 (WMO/TD-No. 1028). Geneva.

———, 2000*b*: Temperature measurements: Some considerations for the intercomparison of radiation screens (J.P. van der Meulen). Paper presented at the WMO Technical Conference on Meteorological and Environmental Instruments and Methods of Observation (TECO-2000). Instruments and Observing Methods Report No. 74 (WMO/TD-No. 1028). Geneva.

———, 2002*a*: Measurement of temperature with wind sensors during severe winter conditions (M. Musa, S. Suter, R. Hyvönen, M. Leroy, J. Rast and B. Tammelin). Paper presented at the WMO Technical Conference on Meteorological and Environmental Instruments and Methods of Observation (TECO-2002). Instruments and Observing Methods Report No. 75 (WMO/TD-No. 1123). Geneva.

———, 2002*b*: Norwegian national thermometer screen intercomparison (M.H. Larre and K. Hegg). Paper presented at the WMO Technical Conference on Meteorological and Environmental Instruments and Methods of Observation (TECO-2002). Instruments and Observing Methods Report No. 75 (WMO/TD-No. 1123). Geneva.

———, 2002*c*: Results of an intercomparison of wooden and plastic thermometer screens (D.B. Hatton). Paper presented at the WMO Technical Conference on Meteorological and Environmental Instruments and Methods of Observation (TECO-2002). Instruments and Observing Methods Report No. 75 (WMO/TD-No. 1123). Geneva.

———, 2002*d*: Temperature and humidity measurements during icing conditions (M. Leroy, B. Tammelin, R. Hyvönen, J. Rast and M. Musa). Paper presented at the WMO Technical Conference on Meteorological and Environmental Instruments and Methods of Observation (TECO-2002). Instruments and Observing Methods Report No. 75 (WMO/TD-No. 1123). Geneva.

———, 2010: *Guidance on Instrumentation for Calibration Laboratories, Including Regional Instrument Centres* (D. Groselj) (WMO/TD-No. 1543). Instruments and Observing Methods Report No. 101. Geneva.

———, 2011: *WMO Field Intercomparison of Thermometer Screens/Shields and Humidity Measuring Instruments* (M. Lacombe, D. Bousri, M. Leroy and M. Mezred). Instruments and Observing Methods Report No. 106 (WMO/TD-No. 1579). Geneva.

Zanghi, F., 1987: *Comparaison des Abris Météorologiques*. Technical Memorandum No. 11, Météo-France/SETIM, Trappes.

# CHAPTER 3. MEASUREMENT OF ATMOSPHERIC PRESSURE

## 3.1 GENERAL

### 3.1.1 Definition

The atmospheric pressure on a given surface is the force per unit area exerted by virtue of the weight of the atmosphere above. The pressure is thus equal to the weight of a vertical column of air above a horizontal projection of the surface, extending to the outer limit of the atmosphere.

Apart from the actual pressure, pressure trend or tendency has to be determined as well. Pressure tendency is the character and amount of atmospheric pressure change for a three-hour or other specified period ending at the time of observation. Pressure tendency is composed of two parts, namely the pressure change and the pressure characteristic. The pressure change is the net difference between pressure readings at the beginning and end of a specified interval of time. The pressure characteristic is an indication of how the pressure has changed during that period of time, for example, decreasing then increasing, or increasing and then increasing more rapidly.

### 3.1.2 Units and scales

The basic unit for atmospheric pressure measurements is the pascal (Pa) (or newton per square metre, $Nm^{-2}$). It is accepted practice to add the prefix “hecto” to this unit when reporting pressure for meteorological purposes, making the hectopascal (hPa), equal to 100 Pa, the preferred terminology. This is largely because one hectopascal equals one millibar (mbar), the formerly used unit. Further details on the mandatory use of SI units are explained in the present volume, Chapter 1. Note that units used for barometer readings such as "mm Hg", "in Hg" or "mbar" are not defined within SI and may not be used for the international exchange of data when reporting atmospheric pressure (see also Annex 3.A of this chapter).

In this chapter only the unit hPa is used.

### 3.1.3 Meteorological requirements

Analysed pressure fields are a fundamental requirement of the science of meteorology. It is imperative that these pressure fields be accurately defined as they form the basis for all subsequent predictions of the state of the atmosphere. Pressure measurements must be as accurate as technology allows, within realistic financial constraints, and there must be uniformity in the measurement and calibration procedures across national boundaries.

The level of accuracy needed for pressure measurements to satisfy the requirements of various meteorological applications has been identified by the respective WMO commissions and is outlined in the present volume, Chapter 1, Annex 1.A, which is the primary reference for measurement specifications in the present Guide.

These requirements should be considered achievable for new barometers in a strictly controlled environment, such as those available in a properly equipped laboratory. They provide an appropriate target uncertainty for barometers to meet before their installation in an operational environment.

For barometers installed in an operational environment, practical constraints will require well-designed equipment for an NMHS to maintain this target uncertainty. Not only the barometer itself, but the exposure also requires special attention. Nevertheless, the performance of the operational network station barometer should not be below the stated criteria.

## 3.1.4 Methods of measurement and observation

### 3.1.4.1 *General measurement principles*

For meteorological purposes, atmospheric pressure is generally measured with electronic barometers, aneroid barometers or hypsometers. The latter class of instruments, which depend on the relationship between the boiling point (temperature) of a liquid and the atmospheric pressure, has so far seen only limited application and will not be discussed in depth in this publication.

Mercury barometers are still in use, but no longer recommended, taking into account the Minamata Convention on Mercury (see the present volume, Chapter 1, 1.4.2). NMHSs are encouraged to urgently take appropriate measures to replace mercury barometers with modern alternatives (see 3.1.4.5). Information on observation practices with mercury barometers is maintained in Annex 3.A only to inform the reader on this obsolete practice.

Most barometers with recent designs make use of transducers which transform the sensor response into pressure-related quantities. These are subsequently processed by using appropriate electrical integration circuits or data-acquisition systems with appropriate smoothing algorithms. A time constant of about 10 s (and definitely no greater than 20 s) is desirable for most synoptic barometer applications.

There are several general methods for measuring atmospheric pressure and these are outlined in the following paragraphs.

A membrane of elastic substance, held at the edges, is deformed if the pressure on one side is greater than on the other. In practice, this is achieved by using a completely or partially evacuated closed metal capsule containing a strong metal spring to prevent the capsule from collapsing due to external atmospheric pressure. Mechanical or electrical means are used to measure the deformation caused by the pressure differential between the inside and outside of the capsule. This is the principle of the well-known aneroid barometer.

Pressure sensor elements comprising thin-walled nickel alloy cylinders, surrounded by a vacuum, have been developed. The natural resonant frequency of these cylinders varies as a function of the difference in pressure between the inside of the cylinder, which is at ambient atmospheric pressure, and the outside of the cylinder, which is maintained as a vacuum. In fact, these instruments measure the pressure by sensing the density of the gas (air) inside.

Absolute pressure transducers, which use a crystalline quartz element, are also commonly used. Pressure exerted via flexible bellows on the crystal face causes a compressive force on the crystal. On account of the crystal's piezoresistive properties, the application of pressure alters the balance of an active Wheatstone bridge. Balancing the bridge enables accurate determination of the pressure. These types of pressure transducers are virtually free of hysteresis effects.

### 3.1.4.2 *General exposure requirements*

It is important that the location of barometers at observation stations be selected with great care. The main requirements of the place of exposure are good light to read out (in case of manual readings), a draught-free environment, a solid, non-vibrating mounting, and protection against rough handling.

Special effort in positioning is required to prevent any artificial wind impact. Such impact is typical for indoor measurement due to the build-up of pressure outside the building and generating errors which are sometime larger than 1 hPa. For further details, see 3.1.4.3.2.

### 3.1.4.3 *Sources of error: general comments*

Errors in the measurement of pressure may be caused by an inappropriate placement of the instrument. The instrument must be placed in an environment where external effects will not lead to measurement errors. These effects include wind, radiation and temperature, shocks and vibrations, fluctuations in the electrical power supply, and pressure shocks. It is important that every meteorological observer or technical staff should fully understand these effects and be able to assess whether any of them are affecting the accuracy of the readings of the barometer in use.

In case of manual readings, the instrument (or its display) should be easy to read. Instruments must be designed so that the resolution of their readings is better than the required measurement uncertainty, that is, rounding error does not increase significantly the uncertainty of the measurement results.

#### 3.1.4.3.1 **The effects of temperature**

Instrument readings should not be affected by temperature variations. Instruments are suitable only if at least one of the following conditions is met:

(a) The instrument is designed to be temperature independent or compensated for the whole temperature range, to be proven by adequate calibration and tests;

(b) Procedures for correcting the readings for temperature effects are developed and implemented to ensure the required uncertainty;

(c) The pressure sensing element is placed in an environment where the temperature is stabilized so that the required uncertainty is met.

Most instruments measure the temperature of the pressure sensor to compensate for temperature effects. It is necessary to control and calibrate these temperature-compensating functions as part of the standard calibration activity.

#### 3.1.4.3.2 **The effects of wind**

It should be noted that the effects of wind apply to all types of barometers. More information on wind effects is found in Liu and Darkow (1989).

A barometer will not give a true reading of the static pressure if it is influenced by gusty wind. Its reading will fluctuate with the wind speed and direction and with the magnitude and sign of the fluctuations, depending also on the nature of the room's openings and their position in relation to the direction of the wind. At sea, error is always present due to the ship's motion. A similar problem will arise if the barometer is installed in an air-conditioned room.

Wind can often cause dynamic changes of pressure in the room where the barometer is placed. These fluctuations are superimposed on the static pressure and, with strong and gusty wind, may amount to up to 2 or 3 hPa. It is usually impractical to correct for such fluctuations because the "pumping" effect is dependent on both the direction and the force of the wind, as well as on the local circumstances of the barometer's location. Thus, the "mean value" does not represent the true static pressure. When comparing barometers in different buildings, the possibility of a difference in readings due to the wind effect should be borne in mind.

It is possible to overcome this effect to a very large extent by using a static head between the exterior atmosphere and the inlet port of the barometer. Details concerning the operating principles of static heads can be found in several publications (Miksad, 1976; United States Weather Bureau, 1963). Aneroid and electronic barometers usually have simple connections to allow for the use of a static head, which should be located in an open environment not

affected by the proximity of buildings. The design of such a head requires careful attention. Static pressure heads are commercially available, but there is limited published literature on intercomparisons to demonstrate their performance (WMO, 2012).

#### 3.1.4.3.3 **The effects of air conditioning**

Air conditioning may create a significant pressure differential between the inside and outside of a room. Therefore, if a barometer is to be installed in an air-conditioned room, it is advisable to use a static head with the barometer which will couple it to the air outside the building.

#### 3.1.4.3.4 **The effects of hysteresis**

Some barometers (in particular aneroid barometers) are affected by hysteresis, with an impact larger than 0.1 hPa. To demonstrate that any hysteresis is within the required measurement uncertainty, calibrations must be performed in both ascending and descending pressure steps.

#### 3.1.4.3.5 **Transport and use in a non-stabilized environment**

Barometers may be sensitive to vibrations and shocks affecting the adjustment of the equipment. Special care must be taken to avoid any shock impact during transport and the instruments should be placed in a vibration-free environment.

### 3.1.4.4 ***Maintenance: general comments***

The following maintenance procedures should be considered:

(a) The instruments and especially the pressure inlet should be kept clean and free from obstruction;

(b) The installation height of the sensing instrument and the mounting should be checked regularly;

(c) The instruments must be calibrated (and adjusted if appropriate) regularly; the interval between two calibrations must be short enough to ensure that the total absolute measurement error will meet the uncertainty requirements;

(d) Any variations in the uncertainty (long term and short term) must be much smaller than those outlined in the present volume, Chapter 1, Annex 1.A. If some instruments have a history of drift in calibration, they will be suitable operationally only if the period between calibrations is short enough to ensure the required measurement uncertainty at all times;

(e) If the instrument has to be calibrated away from its operational location, the method of transportation employed must not affect the stability or accuracy of the instrument; effects that may alter the calibration of the instrument include mechanical shocks and vibrations, displacement from the vertical position, and large pressure variations that may be encountered during transportation by air.

### 3.1.4.5 ***Implications of the Minamata Convention for pressure measurement***

The UNEP Minamata Convention on Mercury came into force globally in August 2017 and bans all production, import and export of mercury barometers (see the present volume, Chapter 1, 1.4.2). Therefore, mercury barometers are no longer recommended and it is strongly encouraged to take appropriate measures to replace such barometers with modern alternatives. Electronic

barometers provide an economical, accurate and reliable alternative to these dangerous, mercury-based instruments and offer significant advantages in terms of data storage and real-time data display.

## 3.2 ELECTRONIC BAROMETERS

Most barometers with recent designs make use of transducers that transform the sensor response into a pressure-related electrical quantity in the form of either analogue signals (for example, voltage (DC or AC with a frequency related to the actual pressure)), or digital signals (for example, pulse frequency or with standard data communication protocols such as RS232, RS422, RS485 or IEEE488). Analogue signals can be displayed on a variety of electronic meters. Monitors and data-acquisition systems, such as those used in AWSs, are frequently used to display digital outputs or digitized analogue outputs.

Current digital barometer technology employs various levels of redundancy to improve the long-term stability and accuracy of the measurements. One technique is to use three independently operating sensors under centralized microprocessor control. Even higher stability and reliability can be achieved by using three completely independent barometers, incorporating three sets of pressure transducers and microprocessors. Each configuration has automatic temperature compensation from internally mounted temperature sensors. Triple redundancy ensures excellent long-term stability and measurement accuracy, even in the most demanding applications. These approaches allow for continuous monitoring and verification of the individual sensor performances.

### 3.2.1 Integrated-circuit-based variable capacitive sensors

Capacitive pressure sensors use the electrical property of capacitance to measure the displacement of a diaphragm. The diaphragm is an elastic pressure sensor displaced in proportion to changes in pressure. It acts as one plate of a capacitor that detects strain due to applied pressure to become a variable capacitor. The change in value of the capacitance causes this electrical signal to vary. This is then conditioned and displayed on a device calibrated in terms of pressure. Common technologies use metal, ceramic and silicon diaphragms. Because this measurement is temperature dependent, sensor temperature is also measured for compensation to meet the accuracy requirements.

Silicon-diaphragm sensors are popular in integrated circuit technology today (with a size of about 1 µm). For this technique the absolute pressure is measured using a vacuum-based chamber (pressure smaller than $10^{-3}$ hPa).

### 3.2.2 Digital piezoresistive barometers

Measurements of atmospheric pressure have become possible by utilizing the piezoelectric (piezoresistive) effect. A common configuration features four measuring resistors placed onto the flexible surface of a monolithic silicon substratum interconnected to form a Wheatstone bridge circuit.

Axially loaded crystalline quartz elements are used in digital piezoresistive barometers and are a type of absolute pressure transducer. Crystalline quartz has been chosen because of its piezoelectric properties, stable frequency characteristics, small temperature effects and precisely reproducible frequency characteristics. Pressure applied to an inlet port causes an upward axial force by means of flexible bellows, thus resulting in a compressive force on the quartz crystal element. Since the crystal element is a substantially rigid membrane, the entire mechanical structure is constrained to minute deflections, thereby virtually eliminating mechanical hysteresis.

The fully active Wheatstone bridge mentioned above may consist either of semiconductor strain gauges or piezoresistive gauges. The strain gauges are either bonded to a thin circular diaphragm, which is clamped along its circumference, or atomically diffused into a silicon diaphragm configuration. In the case of diffused devices, the silicon integrated chip itself is the diaphragm. Applied pressure presents a distributed load to the diaphragm which, in turn, provides bending stress and resultant strains to which the strain gauges react. This stress creates a strain that is proportional to the applied pressure and which results in a bridge imbalance. The bridge output is then proportional to the net difference in pressure acting upon the diaphragm.

This mode of operation is based on the fact that the atmospheric pressure acts on the sensor element covering a small evacuated cell, through which the resistors are submitted to compressive and tensile stresses. By the piezoelectric effect, the values of resistance change proportionally with atmospheric pressure. To eliminate temperature errors, the instrument often incorporates a built-in thermostat.

The output from the Wheatstone bridge, which is fed from a direct-current source, is transduced into a standard signal by an appropriate amplifier. A light-emitting diode (LED) or liquid crystal display usually presents the measured pressure values.

In a modern version of the pressure transducer using a piezoelectric transducer, two resonance frequencies of the piezoelectric element are determined. By calculating a linear function of these frequencies and with an appropriate set of variables obtained after calibration, a pressure is calculated by a microprocessor which is independent of the temperature of the sensor.

### 3.2.3 Cylindrical resonator barometers

Cylindrical resonator barometers use a sensing element which is a thin-walled cylinder of nickel alloy. This is electromagnetically maintained in a "hoop" mode of vibration. The input pressure is sensed by the variation it produces in the natural resonant frequency of the vibrating mechanical system. Cylinder wall movement is sensed by a pick-up coil whose signal is amplified and fed back to a drive coil. The air pressure to be measured is admitted to the inside of the cylinder, with a vacuum reference maintained on the outside. The natural resonant frequency of vibration then varies precisely with the stress set up in the wall due to the pressure difference across it. An increase in pressure gives rise to an increase in frequency.

The thin cylinder has sufficient rigidity and mass to cater for the pressure ranges over which it is designed to operate, and is mounted on a solid base. The cylinder is placed in a vacuum chamber and its inlet is connected to the free atmosphere for meteorological applications. Since there is a unique relationship between the natural resonant frequency of the cylinder and the pressure, the atmospheric pressure can be calculated from the measured resonant frequency. However, this relationship, determined during calibration, depends on the temperature and the density of the gas. Temperature compensation is therefore required and the air should be dried before it enters the inlet.

### 3.2.4 Aneroid displacement transducers

Contact-free measurement of the displacement of the aneroid capsule is a virtual necessity for precision pressure-measuring instruments for meteorological applications. A wide variety of such transducers are in use, including capacitive displacement detectors, potentiometric displacement detectors, strain gauges placed at strategic points on the sensor, and force-balanced servo-systems which keep the sensor dimensions constant regardless of pressure.

All sensitive components must be encased in a die-cast housing. Unless designed with an adequate temperature compensation, this housing must be kept at a constant temperature by an electronically controlled heater. Condensation of water vapour must be completely prevented. An effective technique is to put a hygroscopic agent, such as silica gel crystals, into the die-cast

housing and to prevent water vapour diffusion into the housing by connecting a long plastic tube (approximately 25 m) with a bore of 2 mm or less, between the pressure port and a static head (see 3.1.4.3.2).

The pressure-sensor housing must be airtight, allowing external connection to the compartment where the pressure is to be measured.

### 3.2.5 Exposure of electronic barometers

Details on general exposure requirements are provide in 3.1.4.2. Electronic barometers should be mounted away from electromagnetic sources; where this is not possible, the wires and casing should be shielded.

### 3.2.6 Reading electronic barometers

An electronic barometer measures the atmospheric pressure of the surrounding space or any space that is connected to it via a tube. In general, the barometer should be set to read the pressure at the level of the instrument. On board a ship or at low-level land stations, however, the instrument may be set to indicate the pressure at MSL, provided that the difference between the station pressure and the sea-level pressure can be regarded as constant.

Electronic barometers give accurate readings on a digital read-out, normally scaled in hPa, but readily adaptable to other units if required. Provision can usually be made for digital recording. Trend in pressure changes can be presented if the unit is microprocessor-controlled.

Circuits may be attached to primary transducers which correct the primary output for sensor non-linearities and temperature effects and which convert output to standard units. Standard modern barometer versions comprise the barometer sensor, the microcomputer unit (including the display) and an interface circuit to communicate with any data logger or AWS.

Electronic barometers which have more than one transducer or sensing element generally calculate a weighted mean of the outputs from each of the sensors and establish the resultant pressure with a resolution of at least 0.1 hPa. During calibration, each of the sensing elements can be checked with a resolution of at least 0.01 hPa.

### 3.2.7 Sources of error

The accuracy of electronic barometers depends on the uncertainty of the barometer's calibration, the effectiveness of the barometer's temperature compensation (residual air method, temperature measurement and correction, use of a thermostat) and the drift with time.

#### 3.2.7.1 *Drift between calibrations*

Drift between calibrations is one of the key sources of error with barometers. It is often greater when the barometer is new and decreases with the passage of time. Step jumps in calibration may occur.

In order to maintain the acceptable performance of a barometer, the calibration corrections applied to the readings must be checked at relatively frequent intervals, for example, starting annually, for early detection and replacement of defective instruments.

The need to check frequently the calibration of electronic barometers imposes an additional burden on NMHSs, particularly on those with extensive barometer networks. The ongoing cost of calibration must be taken into consideration when planning to replace mercury barometers with electronic barometers.

#### 3.2.7.2 *Temperature*

Most electronic barometers are adequately compensated for temperature, which can be proven during calibration or testing. In the case that an electronic barometer is not sufficiently compensated for temperature, it must be kept at a constant temperature if the calibration is to be maintained. The temperature should be near the calibration temperature. Electronic barometers that are not temperature-controlled are usually prone to greater error. Most depend on accurate temperature measurement of the sensing element and electronic correction of the pressure. This assumes that there are no thermal gradients within the sensing element of the barometer. In situations where the temperature changes reasonably quickly, this can result in short-term hysteresis errors in the measured pressure.

The change in calibration may also be dependent on the thermal history of the barometer. Prolonged exposure to temperature changes may result in medium- to long-term calibration shifts.

The electronics of the barometer can also introduce errors if it is not held at the same temperature as the sensing element. Electronic barometers are very often used in extreme climatic conditions, especially in AWSs. In these situations, the barometer can be exposed to temperatures well in excess of its manufacturer's design and calibration specifications.

#### 3.2.7.3 *Electrical interference*

As with all sensitive electronic measurement devices, electronic barometers should be shielded and kept away from sources of strong magnetic fields, such as transformers, computers, radar, and so forth. Although this is not often a problem, it can cause an increase in noise, with a resultant decrease in the precision of the device.

#### 3.2.7.4 *Nature of operation*

Apparent changes in the calibration of an electronic barometer can be caused by differences in the way in which the barometer is operated during calibration, as compared with its operational use. A pressure read on a barometer that is run continuously and, therefore, warmed up will read differently from that read in a pulsed fashion every few seconds.

## 3.3 ANEROID BAROMETERS

### 3.3.1 Construction requirements

The principal components are a closed metal chamber, completely or partly evacuated, and a strong spring system that prevents the chamber from collapsing under the external atmospheric pressure. At any given pressure, there will be an equilibrium between the force caused by the spring and that of the external pressure.

The aneroid chamber may be made of materials (steel or beryllium copper) that have elastic properties such that the chamber itself can act as a spring.

A means is required to detect and display the changes in deflection which occur. This may be a system of levers that amplify the deflections and drive a pointer over a scale graduated to indicate the pressure. Alternatively, a ray of light may be deviated over the scale. Instead of these mechanical analogue techniques, certain barometers are provided with a manually operated micrometer whose counter indicates the pressure directly in tenths of a hectopascal. A reading is taken when a luminous indicator signals that the micrometer has just made contact with the aneroid. This type of aneroid is portable and robust.

### 3.3.2 Achievable measurement uncertainty

The achievable measurement uncertainty of 0.3 hPa is possible for a well-designed and constructed aneroid barometer. To achieve this uncertainty, apart from a regular, frequent calibration to reduce calibration drift (as already mentioned for electronic barometers in 3.2.7.1) the following rules should be considered:

(a) It should be compensated for temperature so that the reading does not change by more than 0.3 hPa for a change in temperature of 30 K;

(b) The scale errors at any point should not exceed 0.3 hPa and should remain within this tolerance over periods of at least one year, when in normal use;

(c) The hysteresis should be sufficiently small to ensure that the difference in reading before a change in pressure of 50 hPa and after a return to the original value does not exceed 0.3 hPa;

(d) It should be capable of withstanding ordinary transit risks without introducing inaccuracies beyond the limits specified above.

### 3.3.3 Exposure of aneroid barometers

Details on general exposure requirements are provide in 3.1.4.2. The place selected for mounting the device should preferably have a fairly uniform temperature throughout the day. Therefore, a location is required where the barometer is shielded from the direct rays of the sun and from other sources of either heat or cold, which can cause abrupt and marked changes in its temperature.

### 3.3.4 Reading aneroid barometers

#### 3.3.4.1 *Accuracy of readings*

An aneroid barometer should always be read in the same orientation (vertical or horizontal) as during calibration. It should be tapped lightly before being read. As far as possible, it should be read to the nearest 0.1 hPa. Optical and digital devices are available to reduce the errors caused by mechanical levers. The readings should be corrected for instrumental errors, but the instrument is usually assumed to be sufficiently compensated for temperature, and it needs no correction for gravity.

#### 3.3.4.2 *Reductions applied to barometers*

In general, aneroid barometers should be set to read the pressure at the level of the instrument. On board a ship or at low-lying land stations, however, the instrument may be set to indicate the pressure at MSL, provided that the difference between the station pressure and the sea-level pressure can be regarded as constant.

### 3.3.5 Sources of error

#### 3.3.5.1 *Incomplete compensation for temperature*

In an aneroid barometer, if the spring is weakened by an increase in temperature, the pressure indicated by the instrument will be too high. This effect is generally compensated for in one of the following ways:

(a) By means of a bimetallic link in the lever system;

(b) By leaving a certain amount of gas inside the aneroid chamber.

In most ordinary aneroid barometers, the compensation obtained by these methods is complete only at one particular compensation pressure. It is desirable that all aneroid barometers and barographs used at meteorological stations should be properly compensated for temperatures over the full range of pressure. In digital read-out systems suitable for automation, such complete corrections can be applied as part of the electronic system.

#### 3.3.5.2 *Elasticity errors*

An aneroid barometer may be subjected to a large and rapid change in pressure. For example, a strong gust of wind would cause an aneroid barometer to experience a rapid increase in pressure followed by a more gradual return to the original value. In such circumstances, the instrument will, owing to hysteresis, indicate a slightly different reading from the true pressure; a considerable time may elapse before this difference becomes negligible. However, since aneroids and barographs at surface stations are not usually directly exposed to such pressure changes, their hysteresis errors are not excessive.

There is also a secular error caused by slow changes in the metal of the aneroid capsule. This effect can be allowed for only by comparison at regular intervals, for example, annually, with a standard barometer. A good aneroid barometer should retain an accuracy of 0.1 hPa over a period of one year or more. In order to detect departures from this accuracy by individual barometers, a regular inspection procedure with calibration and adjustment as necessary should be instituted.

## 3.4 BAROGRAPHS

### 3.4.1 General requirements

Of the various types of barographs, only aneroid barographs are dealt with in detail here. For synoptic purposes, it is recommended that charts for barographs:

(a) Be graduated in hPa;

(b) Be readable to 0.1 hPa;

(c) Have a scale factor of 10 hPa to 1.5 cm on the chart.

In addition, the following requirements are desirable:

(a) The barograph should employ a high quality aneroid unit (see 3.4.2);

(b) The barograph should be compensated for temperature, so that the reading does not change by more than 1 hPa for a 20 K change in temperature;

(c) Scale errors should not exceed 1.5 hPa at any point;

(d) Hysteresis should be sufficiently small to ensure that the difference in reading before a change in pressure of 50 hPa and after a return to the original value does not exceed 1 hPa;

(e) There should be a time-marking arrangement that allows the marks to be made without lifting the cover;

(f) The pen arm should be pivoted in a “gate”, the axis of which should be inclined in such a way that the pen rests on the chart through the effects of gravity. A means of adjustment should be provided for setting the position of the pen.

Marine barographs are subject to special requirements, which are considered in Volume III, Chapter 4 of the present Guide.

### 3.4.2 Construction of barographs

The principle of the aneroid barograph is similar to that of the aneroid barometer, except that a recording pen is used instead of a pointer. This involves some change in the design of the capsule stack, and usually means a decrease in the overall magnification and an increase in the number and size of the capsules used.

The "control" of the barograph may be expressed as the force required to move the pointer over one unit of the scale (1 hPa) and is, thus, equal to the force required to prevent the pen from moving when the pressure changes by 1 hPa. It is a measure of the effect that friction is likely to have on the details of the record.

The force required to overcome the movement of the capsule when the pressure changes by 1 hPa is 100 A newtons, where A is the effective cross-sectional area of the capsule in square metres. If the magnification is X, the force necessary to keep the pen from moving is 100 A/X newtons and varies as A/X. For a given type of capsule and scale value, the value of X will be largely independent of A, so that the control of a barograph pen may be considered to vary approximately with the effective cross-sectional area of the capsule.

### 3.4.3 Exposure of barographs

Details on general exposure requirements are provide in 3.1.4.2. The barograph should be placed at a location where it is unlikely to be tampered with by unauthorized persons. Mounting the barograph on a sponge rubber cushion is a convenient means of reducing the effects of vibration. The site selected should be clean and dry. The air should also be relatively free of substances which would cause corrosion and fouling of the mechanism.

It is important to place the instrument so that its face will be at a convenient height to be read at eye-level under normal operating conditions with a view to minimizing the effects of parallax. The exposure ought to be such that the barometer is uniformly illuminated, with artificial lighting being provided if necessary.

### 3.4.4 Sources of error

In addition to the sources of error mentioned for the aneroid (see 3.3.5), the friction between the pen and the paper is important. The control of the pen depends largely on the effective cross-section of the aneroid. In a well-made barograph, the friction of the pen is appreciably greater than the total friction at all the pivots and bearings of the instrument; special attention should, therefore, be given to reduce such errors, for example, by having a sufficiently large aneroid capsule.

A high quality barograph should be capable of an uncertainty of about 0.2 hPa after corrections have been applied and should not alter for a period of one or two months. The barometric change read from such a barograph should usually be obtained within the same limits.

### 3.4.5 Reading a barograph

The barograph should be read without touching the instrument. The time mark and any inspection of the instrument involving lifting the cover, and so on, should always be made after the reading is completed.

#### 3.4.5.1 *Accuracy of readings*

The chart should be read to the nearest 0.1 hPa. The barometric change should be obtained within the same resolution limits.

#### 3.4.5.2 *Corrections to be applied to barograph readings*

The temperature compensation of each individual instrument should be tested before the instrument is used, and the scale factor should be adjusted by testing in a vacuum chamber. If the barograph is used only to find the barometric change, the corrections are not usually applied to the readings. In this case, the accurate setting of the pen position is not important. When absolute pressure values are required from the barograph, the record should be compared with the reading of an electronic barometer or a good aneroid barometer at least once every 24 h and the desired values found by interpolation.

### 3.4.5 Transport

If a barograph has to be transported by air or transported at a high altitude, the pen arm should be disconnected and precautions should be taken to ensure that the mechanism is able to withstand the overload caused by exceeding the normal measuring range of the instrument.

## 3.5 BAROMETRIC CHANGE AND PRESSURE TENDENCY

### 3.5.1 Pressure tendency and pressure tendency characteristics

At surface synoptic observing stations, pressure tendency and the pressure tendency characteristic should be derived from pressure observations from the last 3 h (over 24 h in tropical regions). Typically, the pressure tendency characteristic can be expressed by the shape of the curve recorded during the 3 h period preceding an observation. In the case of hourly observations, the amount and characteristic can be based on only four observations, and misinterpretations may result. Therefore, it is recommended that the characteristic should be determined on a higher frequency of observations, for example with 10-min intervals (WMO, 1985). Nine types of pressure tendency characteristics are defined (see WMO, 2011).

### 3.5.2 Measurement of a barometric change

Several methods are available to stations making observations at least every 3 h, as follows:

(a) Digital electronic barometers usually display the pressure tendency together with the actual pressure;

(b) The change can be read directly from a barograph;

(c) The change can be obtained from appropriate readings of the barometer, corrected to station level.

The error of a single barometric reading is mainly random, assuming that the barometer functions perfectly. Therefore, when two independent readings are subtracted to find the amount of change, the errors may be cumulative. Errors are partly systematic in nature, so that during the relatively short period of 3 h, the errors are likely to have the same sign and would therefore be diminished by subtraction.

## 3.6 TRACEABILITY ASSURANCE AND CALIBRATION

### 3.6.1 General comments

In view of the importance of accurate pressure observations, especially for aeronautical and synoptic purposes, and of the various possible errors to which barometers are subject, traceability assurance and regular calibration of barometers has a very high importance. Starting

in the 1960s, a concept of barometer comparison, including designated regional standard barometers in each WMO regional association, had been used to ensure traceability of pressure measurements. This concept was discontinued by Decision 36 (EC-69) made by the WMO Executive Council at its sixty-ninth session in 2017. Currently, the traceability of atmospheric pressure measurements to SI units can be provided more efficiently and economically through an unbroken traceability chain and a new "strategy for traceability assurance" is implemented instead (see the present volume, Chapter I, Annex 1.B).

Some guidance is given in the following sections regarding the equipment to be used for laboratory or mobile calibration and for field checks. Definitions and general comments on calibration can be found in Volume V, Chapter 4 of the present Guide; while guidance on the computation of calibration uncertainties can be found in WMO (2015).

### 3.6.2 Laboratory calibration

Laboratory calibration of barometers should be carried out regularly by calibration laboratories with ISO/IEC 17025 accreditation or by an NMI service covered by a CIPM MRA. If a suitable laboratory is not available, traceability to SI should be assured according to the strategy for traceability assurance as described in the present volume, Chapter 1, Annex 1.B.

In general, calibrations can be performed at different locations. To achieve lower uncertainties the calibration should be performed at a permanent calibration laboratory situated at a fixed location. Under such circumstances more sensitive primary standards can be used, the environmental conditions (for example, temperature and humidity) can be controlled very well and a vibration-proof set-up can be realized.

If the instruments to be calibrated cannot be moved to a permanent calibration laboratory regularly, the calibrations can be performed with mobile calibration equipment on-site in a building at the observation site or in a specially equipped vehicle. As the environmental conditions cannot be controlled so precisely as in a permanent calibration laboratory, the achievable uncertainties are usually larger.

#### 3.6.2.1 *General equipment set-up*

In most cases calibration equipment includes a pressure controller in combination with the reference barometer that is traceable to SI. Pressure controllers regulate the pressure in a hose with the connected instrument to be calibrated. A vacuum pump and pressure supply are connected to the pressure controller. It is highly recommended to use a pressurized gas cylinder with dry, clean air with very high purity as the pressure source. The container must be equipped with a pressure-reducing valve. A micro-filter has to be attached between the pressure-reducing valve and the hose to the pressure controller. Data from the reference barometer are used as the reference data, not the data from the controller. Purified nitrogen may also be used for some barometers. However, for barometers using a technology based on the measurement on air density (such as cylindrical resonator barometers) nitrogen may not be used because the density of air differs from the density of nitrogen.

The following aspects based on European Association of National Metrology Institutes (EURAMET) guidelines (EURAMET, 2017) should also be taken into account:

(a) The whole equipment must be protected from direct sunlight and any source of heat.

(b) The instruments to be calibrated should be placed as close as possible to the reference instrument and at the same height.

(c) The pressure reference levels of both instruments should be as close as possible. If there are differences they have to be taken in account for corrections and uncertainties.

(d) The equipment needs time for warming and acclimatization to reach thermal equilibrium in the whole system.

(e) All barometers measure pressure using techniques that are sensitive to temperature. Therefore, these instruments are temperature compensated (mechanically or by appropriate software). When barometers are used within a wider temperature range than at normal indoor temperatures, the barometers must be calibrated or tested at a number of temperatures to be representative for that specific range.

(f) The calibration should be performed at an ambient temperature stable to within ±1 °C. This temperature should be representative for the range used in operational conditions, typically lying between 18 °C and 28 °C. Temperature should be recorded.

(g) Normally the calibration of meteorological pressure instruments is performed in absolute pressure mode so the air density has no effect. If the air density has an effect on the calibration result, not only the ambient temperature, but also the atmospheric pressure and the relative humidity are to be recorded.

(h) The workplace should be kept clean and well organized.

#### 3.6.2.2 ***Laboratory standards***

The reference instrument must be traceable to national or international standards and the uncertainty should be better than that of the instrument to be calibrated. The ratio of the uncertainty of the instrument to be calibrated to that of the reference should be, if practicable, at least two.

##### 3.6.2.2.1 **Pressure controller with internal reference**

Pressure controllers can be used as working standards, but only if the measurement uncertainty is within the required limits and traceable to SI (WMO, 2010).These controllers work in absolute pressure mode. The preselected pressure is generated by gas supply, vacuum pump and valves. The internal pressure gauge is used as reference and for regulation of the pressure. The devices under test are connected directly or via pressure hose. A slight drift may occur so the pressure controller must be recalibrated in regular intervals. Either the whole pressure controller should be sent to the calibration laboratory or only the internal pressure reference, which can be uninstalled. An uncertainty better than 0.1 hPa is possible.

##### 3.6.2.2.2 **Pressure controller with an external reference**

In this case the internal pressure controller has a reduced precision or cannot be calibrated to be traceable to SI. An external precision pressure gauge is used as working standard. It is connected in parallel to the device under test. Maintenance and calibration of the external reference is easier than with an internal reference. An uncertainty better than 0.05 hPa can be achieved.

Examples of such external references, with high stability (less than 0.1 hPa in 10 years), excellent temperature compensation (better than 0.001 hPa $K^{-1}$) and without hysteresis are typically high precision electrical digital barometers that use the technology explained in 3.2. These types of reference barometers are highly efficient because they can be used in an automatic calibration environment requiring limited human resources. Despite high stability, it is recommended to calibrate this reference with SI-traceable equipment every year.

#### 3.6.2.2.3 **Piston gauges**

A piston gauge is a primary standard and offers the lowest possible uncertainties and the highest stability. Due to its ultra-low drift, a recalibration interval of five years is recommended. The uncertainty is about 0.05 hPa or less. Although they are primary standards, they are often used also as working standards.

There are two principles based on a piston–cylinder system made of tungsten carbide. The effective area of the piston has been determined by an accredited calibration laboratory or an NMI. The temperature is measured with a PRT and the change of the effective area due to the change of temperature is calculated permanently by the piston gauge controller.

The piston rotates in a cylinder driven by a motor. The surface of the piston and the cylinder is ultra-smooth, cleaned and there is no lubrication except the molecules of the used gas.

An additional pressure controller is needed in any case, so the investment is by far the highest.

In absolute pressure mode built-in vacuum gauges are needed for both systems. Due to the relatively complicated calibration of these vacuum gauges, external vacuum gauges are recommended. In most cases vacuum-gauges suffer from the problem of drift so the calibration intervals are shorter than the calibration interval of the piston gauge itself. The uncertainty of the vacuum-gauge must be taken into account.

**Piston gauges with a dynamometer gauge**

The preselected pressure is generated by the pressure controller. The piston gauge and the devices under test are connected in parallel via a pressure hose. The generated pressure acts on the piston that is connected to a dynamometer which measures the force. The area around the dynamometer is evacuated so there is only a very low force due to the residual gas.

With known temperature-corrected effective area and the measured force, the pressure is calculated. The vacuum is measured with a vacuum gauge. The residual pressure must be taken into account by the piston gauge controller.

Regular adjustments of the dynamometer zero point and the gradient are performed with precision weights that are calibrated by an accredited calibration laboratory or an NMI.

**Piston gauges with loaded piston**

This kind of primary standard does not measure the pressure. Its piston is loaded with weights that are calibrated by an accredited calibration laboratory or an NMI. Due to the absence of a dynamometer, this kind of pressure gauge is a fundamental gauge with the lowest possible uncertainty. It is directly traceable to SI units of mass, length, temperature and time.

The pressure is generated by, and its value derived from, the known mass of the piston and the weights, the local gravity and the temperature-corrected effective area (A in Figure 3.1). To determine the measurement uncertainty, among other contributions to the uncertainty budget, the uncertainty of these three components must be known. Special attention must be given to the local gravity and its uncertainty. It is necessary that this local gravity (at the location of the standard) is determined by qualified personnel or accredited services. Note that the building in which the standard operates will affect the local gravity. See also Annex 3.B on the use of gravimeters.

A pressure controller is needed to raise the weights. At a certain height the piston is accelerated by a temporarily connected belt which is driven by a motor. At a certain rotation speed the belt is disconnected and the motor stops. Due to the extremely low friction of the nitrogen molecules the rotation speed will decelerate very slow. Depending on the amount of weights the rotation can persist up to a half an hour.

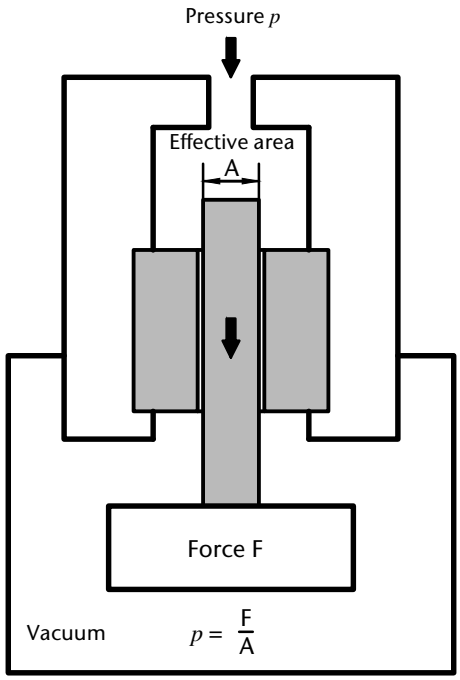



**Figure 3.1. Piston gauge with dynamometer**

If the piston rotates, the height of the piston vary slightly. To bring the piston back to a specific height, the pressure controller regulates the pressure below the piston area. Then, the pressure controller becomes inactive and its valves close. The pressure in the area below the piston and the connected pressure hose is generated by the rotating and very slowly sinking piston (Figure 3.2).

The area above the piston–cylinder system is covered with a glass bell. The bell is evacuated using a strong vacuum pump. The vacuum is measured with a vacuum gauge. The residual pressure has to be taken into account by the piston gauge controller.

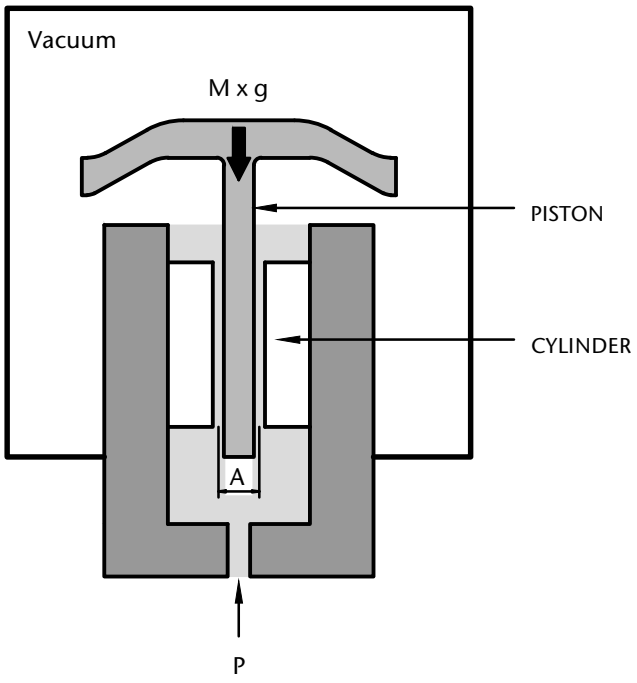



**Figure 3.2. Loaded piston gauge**

A disadvantage of piston gauges is the exchange of the weights. The evacuated area must be pressurized and the glass bell must be removed to change the weights. After reinstalling the glass bell the area must be evacuated again. The work with piston gauges is very time-consuming, but an automatic mass handling system is available for some types of piston gauges. Note that this technique requires well-trained personnel.

### 3.6.2.3 *Method of calibration*

To achieve the required expanded measurement uncertainty, a comprehensive calibration procedure should be performed. Several guidelines are available. The following describes a proven procedure that is commonly used by accredited laboratories. It allows the evaluation of linearity, repeatability and reversibility.

The pressure range for calibration can be chosen either from 0% to 100% of the full scale of the instrument, or the interval can be reduced based on a client's requirements (for example, the range to be expected in operational use, such as 850–1050 hPa). Figure 3.3 shows the general calibration process.

The calibration process starts with generating maximum and minimum calibration points, sequentially, three times. The preloading time at the highest value and the time between two preloadings should be at least 30 seconds. The change of the pressure should be realized in 30 seconds and at least 120 seconds of holding time is needed.

The calibration should then be carried out at calibration points uniformly distributed over the calibration range. A cycle of measurements, each consisting of a series of increasing pressure and a series of decreasing pressure, must be taken. The number of points a series consists of should not be less than nine. The time between two successive load steps should be the same and not shorter than 30 seconds. At each calibration point, the waiting time, during which steady-state conditions are achieved, should be at least 120 seconds.

The mounting and connections should stay unchanged during the whole process.

The determination of the zero point deviation is usually omitted in the case of absolute pressure gauges, such as barometers, and consequently a zero-point adjustment is not performed.

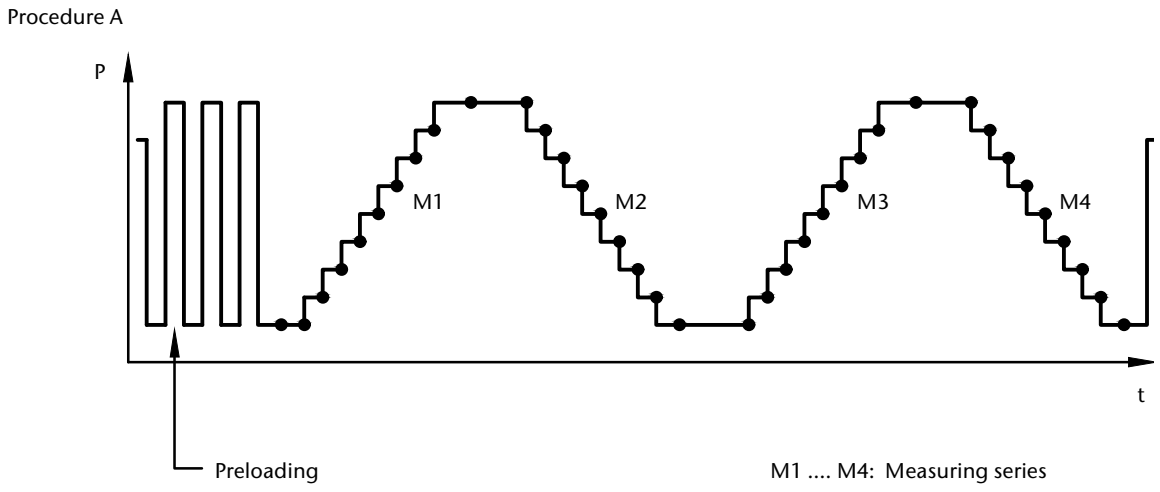



**Figure 3.3. Calibration procedure**

#### 3.6.2.3.1 Calculation of repeatability

The repeatability is calculated from the difference between the deviations measured in the corresponding measurement series. The index *j* represents the nominal pressure point:

$$b_{up,j} = \left|\Delta p_{3,j} - \Delta p_{1,j}\right|$$

$$b_{down,j} = \left|\Delta p_{4,j} - \Delta p_{2,j}\right|$$

$$b_{mean,j} = max\left\{b_{up,j}, b_{down,j}\right\}$$

The repeatability must be considered for the calculation of the uncertainty.

Example:

| *Reference (hPa)* | *Series 1 Δp (hPa)* | *Series 2 Δp (hPa)* | *Series 3 Δp (hPa)* | *Series 4 Δp (hPa)* |
|---|---|---|---|---|
| 996.371 | -0.002 | 0.008 | 0.001 | 0.007 |

$$b_{up,j} = \left|0.001\,hPa - \left(-0.002\,hPa\right)\right| = 0.003\,hPa$$

$$b_{down,j} = \left|0.007\,hPa - 0.008\,hPa\right| = 0.001\,hPa$$

$$b_{mean,j} = \max\left\{0.003\,hPa, 0.001\,hPa\right\} = 0.003\,hPa$$

#### 3.6.2.3.2 Calculation of reversibility (hysteresis)

The reversibility (hysteresis) is calculated from the differences between the corresponding deviations of the output values measured at increasing and decreasing pressure:

$$h_{mean,j} = \frac{1}{4}\left\{\left|\Delta p_{2,j} - \Delta p_{1,j}\right| + \left|\Delta p_{4,j} - \Delta p_{3,j}\right|\right\}$$

The reversibility must be considered for the calculation of the uncertainty.

Example:

| *Reference (hPa)* | *Series 1 Δp (hPa)* | *Series 2 Δp (hPa)* | *Series 3 Δp (hPa)* | *Series 4 Δp (hPa)* |
|---|---|---|---|---|
| 996.371 | -0.002 | 0.008 | 0.001 | 0.007 |

$$h_{mean,j} = \frac{1}{4}\left\{\left|0.008\,hPa - \left(-0.002\,hPa\right)\right| + \left|0.007\,hPa - 0.001\,hPa\right|\right\} = 0.004\,hPa$$

### 3.6.3 Field inspections

During field inspection, a comparison with a travelling standard should be carried out. This comparison is not a calibration, as in most cases just a one-point comparison at actual atmospheric pressure is performed. These checks can therefore only indicate the plausibility of the readings of the instrument on-site.

For field inspections, a mobile electronic pressure gauge, preferably with more than one pressure transducer, should be used as a travelling standard (see 3.2). With an appropriate temperature compensation, an uncertainty of 0.1 hPa or less can be achieved. Instruments with rechargeable batteries are available and the values from the internal transducers can be displayed separately or as a mean value. Before comparison, the instrument should always be acclimated to ambient conditions.

Field inspections should be performed in low gradient weather conditions with stable atmospheric pressure and low wind speeds.

Field inspection equipment should be calibrated by an accredited calibration laboratory, preferably before and after field use, or at appropriate calibration intervals, depending on the drift of the equipment.

## 3.7 ADJUSTMENT OF BAROMETER READINGS TO STANDARD AND OTHER LEVELS

To compare barometer readings taken at stations at different altitudes, it is necessary to reduce them to the same level. Whereas various methods are in use for carrying out this reduction, WMO has recommended a standard method described in the following paragraphs.

The recommended method is described in more detail in WMO (1954, 1964,1968). WMO (1966) contains a comprehensive set of formulae that may be used for calculations involving pressure.

### 3.7.1 Standard levels

The observed atmospheric pressure should be reduced to MSL (see the present volume, Chapter 1) for all stations where this can be done with reasonable accuracy. Where this is not possible, a station should, by regional agreement, report either the geopotential of an agreed "constant pressure level" or the pressure reduced to an agreed datum for the station. The level chosen for each station should be reported to the WMO Secretariat for promulgation (that is, the WMO Observing Systems Capability Analysis and Review Tool (OSCAR)/Surface, https://oscar.wmo.int/surface/#/).

### 3.7.2 General reduction formula

Reduction formula for sea-level pressure feasible for stations below 750 m (from WMO, 1964, p. 22, equation 2):

$$\log_{10}\frac{p_0}{p_s} = \frac{K_p \cdot H_p}{T_{mv}} = \frac{K_p \cdot H_p}{T_s + \frac{a \cdot H_p}{2} + e_s \cdot C_h} \tag{3.1}$$

where $p_0$ is the pressure reduced to sea level in hPa; $p_S$ is the station pressure in hPa; $K_p$ is the constant = 0.0148275 K gpm$^{-1}$; $H_p$ is the station elevation in gpm; $T_{mv}$ is the mean virtual temperature of the fictitious air column below station level in K, ($T_{mv} = T_s + (a \cdot H_p)/2 + e_S \cdot C_h$); $T_S$ is the station temperature in K, $T_S = 273.15 + t$; $t$ is the station temperature in °C; $a$ is the assumed lapse-rate in the fictitious air column extending from sea level to the station elevation level = 0.0065 K gpm$^{-1}$; $e_S$ is the vapour pressure at the station in hPa; and $C_h$ is the coefficient = 0.12 K hPa$^{-1}$.

The same formula is often used in the exponential form:

$$p_0 = p_s \cdot \exp\left(\frac{\frac{g_n}{R} \cdot H_p}{T_s + \frac{a \cdot H_p}{2} + e_s \cdot C_h}\right) \tag{3.2}$$

where $g_n$ is the standard acceleration of gravity = 9.80665 m s$^{-2}$ and $R$ is the gas constant of dry air = 287.05 J kg$^{-1}$ K$^{-1}$.

### 3.7.3 **Reduction formula for low-level stations**

At low-level stations (namely, those at a height of less than 50 m above MSL), pressure readings should be reduced to MSL by adding to the station pressure a reduction constant $C$ given by the following expression:

$$C = p \cdot H_p / (29.27\, T_v) \tag{3.3}$$

where $p$ is the observed station pressure in hectopascals; $H_p$ is the station elevation in metres; and $T_v$ is the mean annual normal value of virtual temperature at the station in K.

Note: The virtual temperature of damp air is the temperature at which dry air of the same pressure would have the same density as the damp air. WMO (1966) contains virtual temperature increments of saturated moist air for various pressures and temperatures.

This procedure should be employed only at stations of such low elevation that when the absolute extreme values of virtual temperature are substituted for $T_v$ in the equation, the deviation of the result due to the other approximations of the equation (used for height rather than standard geopotential, and with $C$ to be small compared with $p$) is negligible in comparison.

# ANNEX 3.A. METHODS OF MEASUREMENT WITH MERCURY BAROMETERS

As outlined in 3.1.4.5, the use of mercury barometers is not recommended anymore. The reasons to move away from their use are: mercury vapour is highly toxic; free mercury is corrosive to the aluminium alloys used in air; special lead glass is required for the tube; the barometer is very delicate and difficult to transport; it is difficult to maintain the instrument and to clean the mercury; the instrument must be read and corrections applied manually; and other barometers of equivalent accuracy and stability with electronic read-out are now commonly available.

This annex is kept for information only.

## 1. UNITS AND SCALES

Some barometers are graduated in "millimetres or inches of mercury under standard conditions", $(\text{mm Hg})_n$ and $(\text{in Hg})_n$, respectively. When it is clear from the context that standard conditions are implied, the briefer terms "millimetre of mercury" or "inch of mercury" may be used. Under these standard conditions, a column of mercury having a true scale height of 760 $(\text{mm Hg})_n$ exerts a pressure of 1 013.250 hPa.

The following conversion factors will then apply:

$1 \text{ hPa} = 0.750062 \ (\text{mm Hg})_n$
$1 \ (\text{mm Hg})_n = 1.333224 \text{ hPa}$

In the case where the conventional engineering relationship between the inch and the millimetre is assumed, namely 1 in = 25.4 mm, the following conversion factors are obtained:

$1 \text{ hPa} = 0.029530 \ (\text{in Hg})_n$
$1 \ (\text{in Hg})_n = 33.8639 \text{ hPa}$
$1 \ (\text{mm Hg})_n = 0.03937008 \ (\text{in Hg})_n$

Scales on mercury barometers for meteorological purposes should be so graduated that they yield true pressure readings directly in standard units when the entire instrument is maintained at a standard temperature of 0 °C and the standard value of gravity is 9.80665 m $s^{-2}$.

Barometers may have more than one scale engraved on them, for example, hPa and mm Hg, or hPa and in Hg, provided that the barometer is correctly calibrated, adjusted and compensated for use under standard conditions.

## 2. REQUIREMENTS FOR MERCURY BAROMETERS

### 2.1 Construction requirements

The basic principle of a mercury barometer is that the pressure of the atmosphere is balanced against the weight of a column of mercury. In some barometers, the mercury column is weighed on a balance, but, for normal meteorological purposes, the length of the mercury column is measured against a scale graduated in units of pressure.

There are several types of mercury barometers in use at meteorological stations, with the fixed cistern and the Fortin types being the most common. The length to be measured is the distance between the top of the mercury column and the upper surface of the mercury in the cistern. Any change in the length of the mercury column is, of course, accompanied by a change in the level of the mercury in the cistern. In the Fortin barometer, the level of the mercury in the cistern can

be adjusted to bring it into contact with an ivory pointer, the tip of which is at the zero of the barometer scale. In the fixed-cistern barometer, often called the Kew-pattern barometer, the mercury in the cistern does not need to be adjusted as the scale engraved on the barometer is constructed to allow for changes in the level of the mercury in the cistern.

## 2.2 General requirements

The main requirements of a good mercury station barometer include the following:

(a) Its accuracy should not vary over long periods. In particular, its hysteresis effects should remain small;

(b) It should be quick and easy to read, and readings should be corrected for all known effects. The observers employing these corrections must understand their significance to ensure that the corrections applied are correct and not, in fact, causing a deterioration in the accuracy of the readings;

(c) It should be transportable without a loss of accuracy;

(d) The bore of the tube should not be less than 7 mm and should preferably be 9 mm;

(e) The tube should be prepared and filled under vacuum. The purity of the mercury is of considerable significance. It should be double-distilled, degreased, repeatedly washed, and filtered;

(f) The actual temperature, for which the scale is assumed to give correct readings, at standard gravity, should be engraved upon the barometer. The scale should preferably be calibrated to give correct readings at 0 °C;

(g) The meniscus should not be flat unless the bore of the tube is large (greater than 20 mm);

(h) For a marine barometer, the error at any point should not exceed 0.5 hPa.

The response time for mercury barometers at land stations is usually very small compared with that of marine barometers and instruments for measuring temperature, humidity and wind.

## 2.3 Exposure of mercury barometers

The general exposure requirements of mercury barometers have been outlined in the preceding sections. Mercury barometers have additional exposure requirements above those already mentioned. It is always preferable to hang the mercury barometer on an inside wall. For very accurate work, the best position would be in an unheated basement room with no windows and with a small electric fan to prevent any stratification of temperature.

In order to obtain uniform lighting conditions for reading the barometer, it is advisable to use artificial lighting for all observations. For this purpose, some sort of illuminator – which can provide a white and slightly luminous background for the mercury meniscus and, if necessary, for the fiducial point – may be provided. If no illuminator is used, care should be taken to provide the meniscus and the fiducial point with a light background, by such means as pieces of milk glass, white celluloid, or a sheet of white paper. Artificial light should also be provided for reading the barometer scale and the attached thermometer. Care should, however, be taken to guard against heating the barometer with artificial light during a barometer reading.

The barometer should be mounted in a place where it is not subject to vibration, preferably on a solid wall. The instrument must be mounted with the mercury column in a vertical position. Errors due to departure from verticality are more critical for asymmetric barometers.

Such barometers should be mounted with their longest axis vertical in order that a true setting of the mercury surface to the fiducial point remains correct even when the instruments are tilted from the vertical.

To protect the barometer from rough handling, dust and air currents, it is recommended that the instrument be placed in a box furnished with a hinged door with provisions for sufficient ventilation to prevent stratification of the air inside.

Great care should be taken when transporting a mercury barometer. The safest method is to carry the barometer upside down in a wooden case furnished with a sling. If the barometer cannot be accompanied by a responsible person, it ought to be transported in a suitable sprung crate with the cistern uppermost. The barometer should not be subject to violent movements and must always be turned over very slowly. Special precautions must be taken for some individual types of barometers before the instrument is turned over.

## 3. MEASUREMENTS USING MERCURY BAROMETERS

### 3.1 Standard conditions

Given that the length of the mercury column of a barometer depends on other factors, especially on temperature and gravity, in addition to the atmospheric pressure, it is necessary to specify the standard conditions under which the barometer should theoretically yield true pressure readings. The following standards are laid down in the international barometer conventions.

#### 3.1.1 *Standard temperature and density of mercury*

The standard temperature to which mercury barometer readings are reduced to remove errors associated with the temperature-induced change in the density of mercury is 0 °C.

The standard density of mercury at 0 °C is taken to be $1.35951 \cdot 10^4$ kg $m^{-3}$ and, for the purpose of calculating absolute pressure using the hydrostatic equation, the mercury in the column of a barometer is treated as an incompressible fluid.

The density of impure mercury is different from that of pure mercury. Hence, a barometer containing impure mercury will produce reading errors as the indicated pressure is proportional to the density of mercury.

#### 3.1.2 *Standard gravity*

Barometric readings have to be reduced from the local acceleration of gravity to standard (normal) gravity. The value of standard gravity ($g_n$) is regarded as a conventional constant, $g_n = 9.80665$ m $s^{-2}$.

Note: The need to adopt an arbitrary reference value for the acceleration of gravity is explained in WMO (1966). This value cannot be precisely related to the measured or theoretical value of the acceleration of gravity in specified conditions, for example, sea level at latitude 45°, because such values are likely to change as new experimental data become available.

### 3.2 Reading mercury barometers

When making an observation with a mercury barometer, the attached thermometer should be read first. This reading should be taken as quickly as possible, as the temperature of the thermometer may rise owing to the presence of the observer. The barometer should be tapped a few times with the finger in two places, one adjacent to the meniscus and the other near the cistern, so as to stabilize the mercury surfaces. If the barometer is not of a fixed-cistern type,

the necessary adjustment should be made to bring the mercury in the cistern into contact with the fiducial pointer. Lastly, the vernier should be set to the meniscus and the reading taken. The vernier is correctly adjusted when its horizontal lower edge appears to be touching the highest part of the meniscus; with a magnifying glass it should be possible to see an exceedingly narrow strip of light between the vernier and the top of the mercury surface. Under no circumstances should the vernier "cut off" the top of the meniscus. The observer's eye should be in such a position that both front and back lower edges of the vernier are in the line of vision.

### 3.2.1 *Accuracy of readings*

The reading should be taken to the nearest 0.1 hPa. Usually it is not possible to read the vernier to any greater accuracy.

Optical and digital systems have been developed to improve the reading of mercury barometers. Although they normally ease the observations, such systems may also introduce new sources of error, unless they have been carefully designed and calibrated.

### 3.2.2 *Changes in index correction*

Any change in the index correction shown during an inspection should be considered on its merits, keeping in mind the following:

(a) The history of the barometer;

(b) The experience of the inspector in comparison work;

(c) The magnitude of the observed change;

(d) The standard deviation of the differences;

(e) The availability of a spare barometer at the station, the correction of which is known with accuracy;

(f) The behaviour of travelling standards during the tour;

(g) The agreement, or otherwise, of the pressure readings of the station with those of neighbouring stations on the daily synoptic chart if the change is accepted;

(h) Whether or not the instrument was cleaned before comparison.

Changes in index errors of station barometers, referred to as drift, are caused by:

(a) Variations in the capillary depression of the mercury surfaces due to contamination of the mercury. In areas of severe atmospheric pollution from industrial sources, mercury contamination may constitute a serious problem and may require relatively frequent cleaning of the mercury and the barometer cistern;

(b) The rise of air bubbles through the mercury column to the space above.

These changes may be erratic, or consistently positive or negative, depending on the cause.

Changes in index correction are also caused by:

(a) Observer error resulting from failure to tap the barometer before taking the reading and improper setting of the vernier and fiducial point;

(b) Lack of temperature equilibrium in either the station barometer or the travelling standard;

(c) Non-simultaneity of readings when the pressure is changing rapidly.

Such changes can be caused by accidental displacement of the adjustable scale and the shrinkage or loosening of fiducial points in Fortin-type barometers.

### 3.2.3 *Permissible changes in index correction*

Changes in index correction should be treated as follows:

(a) A change in correction within 0.1 hPa may be neglected unless persistent;

(b) A change in correction exceeding 0.1 hPa but not exceeding 0.3 hPa may be provisionally accepted unless confirmed by at least one subsequent inspection;

(c) A change in correction exceeding 0.3 hPa may be accepted provisionally only if the barometer is cleaned and a spare barometer with known correction is not available. This barometer should be replaced as soon as a correctly calibrated barometer becomes available.

Barometers with changes in index correction identified in (b) and (c) above warrant close attention. They should be recalibrated or replaced as soon as practicable.

The same criteria apply to changes in the index corrections of the travelling standards as those applied as to station barometers. A change in correction of less than 0.1 hPa may be neglected unless persistent. A larger change in correction should be confirmed and accepted only after repeated comparisons. The “before” and “after” tour index corrections of the travelling standard should not differ by more than 0.1 hPa. Only barometers with a long history of consistent corrections should, therefore, be used as travelling standards.

## 3.3 Correction of barometer readings to standard conditions

In order to transform barometer readings taken at different times and different places into usable atmospheric pressure values, the following corrections should be made:

(a) Correction for index error;

(b) Correction for gravity;

(c) Correction for temperature.

For a large number of operational meteorological applications, it is possible to obtain acceptable results by following the barometer manufacturer’s instructions, provided that it is clear that these procedures give pressure readings of the required uncertainty. However, if these results are not satisfactory or if higher precision is required, detailed procedures should be followed to correct for the above factors; these procedures are described in Annex 3.B.

## 3.4 Errors and faults with mercury barometers

### 3.4.1 *Uncertainties as to the temperature of the instrument*

The temperature indicated by the attached thermometer will not usually be identical to the mean temperature of the mercury, the scale and the cistern. The resultant error can be reduced by favourable exposure and by using a suitable observation procedure. Attention is drawn to the frequent existence of a large, stable vertical temperature gradient in a room, which may cause a considerable difference between the temperature of the upper and lower parts of the barometer. An electric fan can prevent such a temperature distribution but may cause local pressure variations and should be switched off before an observation is made. Under normal conditions, the error associated with the temperature reduction will not exceed 0.1 hPa if such precautions are taken.

### 3.4.2 *Defective vacuum space*

It is usually assumed that there is a perfect vacuum, or only a negligible amount of gas, above the mercury column when the instrument is calibrated. Any change in this respect will cause an error in pressure readings. A rough test for the presence of gas in the barometer tube can be made by tilting the tube and listening for the click when the mercury reaches the top, or by examining the closed end for the presence of a bubble, which should not exceed 1.5 mm in diameter when the barometer is inclined. The existence of water vapour cannot be detected in this way, as it is condensed when the volume decreases. According to Boyle's Law, the error caused by air and unsaturated water vapour in the space will be inversely proportional to the volume above the mercury. The only satisfactory way to overcome this error is by conducting a recalibration over the entire scale; if the error is large, the barometer tube should be refilled or replaced.

### 3.4.3 *The capillary depression of the mercury surfaces*

The height of the meniscus and the capillary depression[1], for a given tube, may change with the ageing of the glass tube, mercury contamination, pressure tendency, and the position of the mercury in the tube. As far as is practicable, the mean height of the meniscus should be observed during the original calibration and noted on the barometer certificate. No corrections should be made for departures from the original meniscus height, and the information should be used only as an indication of the need, or otherwise, to overhaul or recalibrate the barometer. A 1 mm change in the height of the meniscus (from 1.8 to 0.8 mm) for an 8 mm tube may cause an error of about 0.5 hPa in the pressure readings.

It should be noted that large variations in the angle of contact between the mercury and the wall of the cistern in a fixed-cistern barometer may cause small but appreciable errors in the observed pressure.

### 3.4.4 *Lack of verticality*

If the bottom of a symmetrical barometer of normal length (about 90 cm), which hangs freely, is displaced by about 6 mm from the vertical position, the indicated pressure will be about 0.02 hPa too high. Such barometers generally hang more truly vertical than this.

In the case of an asymmetrical barometer, however, this source of error is more critical.
For example, if the fiducial pointer in the cistern is about 12 mm from the axis, the cistern needs to be displaced by only about 1 mm from the vertical to cause an error of 0.02 hPa.

[1] Capillary depression is a reduction in height of the meniscus of a liquid contained in a tube where the liquid (such as mercury) does not wet the walls of the tube. The meniscus is shaped convex upward.

### 3.4.5 *General accuracy of the corrected pressure readings*

The standard deviation of a single, corrected barometer reading at an ordinary meteorological station should be within 0.1 hPa. This error will mainly be the result of the unavoidable uncertainty in the instrument correction, the uncertainty concerning the temperature of the instrument, and the error caused by the pumping effect of wind gusts on the mercury surface.

## 4. SAFETY PRECAUTIONS FOR THE USE OF MERCURY

Mercury is used in relatively large quantities in barometers and, because it is poisonous, must be handled with care. Elemental mercury is a liquid at temperatures and pressures experienced at the Earth's surface. Mercury vapour forms in the air whenever liquid mercury is present. Mercury can be absorbed through the skin in both liquid and gaseous states and can be inhaled as a vapour. The properties of mercury are described by Sax (1975). In many countries, precautions for its use are prescribed by regulations governing the handling of hazardous goods. The UNEP Minamata Convention on Mercury entered into force in August 2017 and has a significant impact on the use of mercury for meteorological applications.

A large dose of mercury may cause acute poisoning. It can also accumulate in the body's hard and soft tissues and prolonged exposure to even a low dose can cause long-term damage to organs, or even death. Mercury mainly affects the central nervous system, and the mouth and gums, with symptoms that include pain, loosening of teeth, allergic reactions, tremors and psychological disturbance.

For barometric applications, the main risks occur in laboratories where barometers are frequently emptied or filled. There may also be problems in meteorological stations if quantities of mercury, for example from a broken barometer, are allowed to remain in places where it may continuously vaporize into an enclosed room where people work.

A danger exists even if the mercury is properly contained and if it is cleaned up after an accident. The following points must be considered when using mercury:

(a) Vessels containing mercury must be well sealed and not likely to leak or easily break, and must be regularly inspected;

(b) The floor of a room where mercury is stored or used in large quantities should have a sealed, impervious and crack-free floor covering, such as PVC. Small cracks in the floor, such as those between floor tiles, will trap mercury droplets. It is preferable to have the flooring material curving up the walls by approximately 10 cm, leaving no joint between the floor and the walls at floor level;

(c) Mercury must not be stored in a metal container as it reacts with almost all metals, except iron, forming an amalgam which may also be hazardous. Mercury should not come into contact with any other metallic object;

(d) Mercury must not be stored with other chemicals, especially amines, ammonia or acetylene;

(e) Large quantities of mercury should always be stored and handled in a well-ventilated room. The raw material should be handled in a good-quality fume cupboard;

(f) Mercury should never be stored near a heat source of any kind as it has a relatively low boiling point (357 °C) and may produce hazardous concentrations of toxic vapour, especially during a fire;

(g) If mercury is handled, the room where it is used and the personnel using it should be regularly tested to determine if hazardous quantities of mercury are being encountered.

Under the Minamata Convention, imports and exports of mercury will no longer be allowed. In this context, the production, import and export of mercury-added products such as thermometers will be stopped by 2020. The Convention states that "[e]ach party shall not allow, by taking appropriate measures, the manufacture, import or export of mercury-added products listed in Part I of Annex A [of the Convention] after the phase-out date specified for those products" (UNEP, 2013). More specifically, this list includes:

> The following non-electronic measuring devices except non-electronic measuring devices installed in large-scale equipment or those used for high precision measurement, where no suitable mercury-free alternative is available:
>
> (a) barometers;
>
> (b) hygrometers;
>
> (c) manometers;
>
> (d) thermometers;
>
> (e) sphygmomanometers.

## 4.1 Spillages and disposal

The two common methods of cleaning up mercury spillages are either with a suitable aspirated pick-up system, as outlined below, or by adsorption/amalgamation of the mercury onto a powder.

Mercury should be cleaned up immediately. The operator should wear PVC gloves or gauntlets, safety goggles and, for significant spills, a respirator fitted with a mercury vapour cartridge. Depending upon how large the spillage is, the mercury will be picked up by using a vacuum system; an adsorption kit should then be used to clean up the small droplets. The use of an adsorption kit is imperative because, during a spillage, dozens of small droplets of less than 0.02 mm in diameter will adhere to surfaces and cannot be efficiently removed with a vacuum system.

In an aspirated pick-up system, the mercury is drawn through a small-diameter plastic tube into a glass flask with approximately 3 cm of water in the bottom, with the tube opening being below the water line in the flask. One end of a larger diameter plastic tube is connected to the air space above the water in the flask, and the other end is connected to a vacuum cleaner or vacuum pump. The water prevents the mercury vapour or droplets from being drawn into the vacuum cleaner or pump. The slurry is then placed in a clearly labelled plastic container for disposal.

By using adsorption material, a variety of compounds can be used to adsorb or amalgamate mercury. These include zinc powder, sulphur flour or activated carbon. Commercial kits are available for cleaning up mercury spills. The powder is sprinkled on the spill and allowed to adsorb or amalgamate the mercury. The resulting powder is swept up and placed in a clearly labelled plastic container for disposal.

The collected mercury can be either disposed of or recovered. Details on how to dispose of mercury can be obtained from local authorities and/or the supplier. The supplier can also advise on recovery and purification.

## 4.2 Fire

Mercury will not burn but does give off significant concentrations of toxic fumes. After a fire, the mercury vapour will condense on the nearest cool surfaces, contaminating large areas and being adsorbed onto open surfaces, such as carbonized timber. During a fire, evacuate the area and remain upwind of any fumes. Advise the fire authorities of the location and quantity of mercury involved.

## 4.3 Transportation

The transportation by air of mercury or instruments containing mercury is regulated by the International Air Transport Association. Airlines will provide the specific conditions for such transport upon request. Transportation by rail or road is usually governed by the hazardous material regulations in each country.

In general, metallic mercury must be packed in glass or plastic containers. The containers should be packed with sufficient cushioning to prevent breakage and should be clearly labelled. Mercury-containing instruments should be packed in a strong cushioned case which is leak-proof and impervious to mercury.

# ANNEX 3.B. CORRECTION OF MERCURY BAROMETER READINGS TO STANDARD CONDITIONS

### Correction for index error

The residual errors in the graduation of the scale of a barometer should be determined by comparison with a standard instrument. They may include errors due to inaccurate positioning or subdividing of the scale, capillarity and imperfect vacuum. Certificates of comparison with the standard should state the corrections to be applied for index error at no fewer than four points of the scale, for example, at every 50 hPa. In a good barometer, these corrections should not exceed a few tenths of a hectopascal.

### Corrections for gravity

The reading of a mercury barometer at a given pressure and temperature depends upon the value of gravity, which in turn varies with latitude and altitude. Barometers for meteorological applications are calibrated to yield true pressure readings at the standard gravity of 9.80665 m $s^{-2}$ and their readings at any other value of gravity must be corrected. The following method is recommended for reducing such barometer readings to standard gravity. Let $B$ be the observed reading of the mercury barometer, $B_t$ the barometer reading reduced to standard temperature but not to standard gravity, and corrected for instrumental errors, $B_n$ be the barometer reading reduced to standard gravity and standard temperature, and corrected for instrumental errors, $B_{ca}$ be the climatological average of $B_t$ at the station, $g_{\varphi H}$ the local acceleration of gravity (in m $s^{-2}$) at a station at latitude $\varphi$ and elevation $H$ above sea level, and $g_n$ the standard acceleration of gravity, 9.80665 m $s^{-2}$.

The following relations are appropriate:

$$B_n = B_t \left( g_{\varphi H} / g_n \right) \tag{3.A.1}$$

or:

$$B_n = B_t + B_t \left[ \left( g_{\varphi H} / g_n \right) - 1 \right] \tag{3.A.2}$$

The approximate equation 3.A.3 may be used, provided that the results obtained do not differ by more than 0.1 hPa from the results that would be obtained with the aid of equation 3.A.2:

$$B_n = B_t + B_{ca} \left[ \left( g_{\varphi H} / g_n \right) - 1 \right] \tag{3.A.3}$$

The local acceleration of gravity $g_{\varphi H}$ should be determined by the procedure outlined in the following section. The values so derived should be referred to as being on the International Gravity Standardization Net 1971 (IGSN71).

### Determining local acceleration of gravity

In order to determine the local value of the acceleration of gravity at a station to a satisfactory degree of precision, one of two techniques should be used. These techniques involve, in the first case, the use of a gravimeter (an instrument for measuring the difference between the values of the acceleration of gravity at two points) and, in the second case, the use of the so-called Bouguer anomalies. Preference should be given to the gravimeter method. If neither of these methods can be applied, the local acceleration of gravity may be calculated using a simple model of the Earth.

**Use of a gravimeter**

Suppose $g_1$ represents the known local acceleration of gravity at a certain point $O$, usually a gravity base station established by a geodetic organization, where $g_1$ is on the IGSN71, and suppose further that $g$ represents the unknown local acceleration of gravity on the meteorological gravity system at some other point $X$ for which the value $g$ is desired. Let $\Delta g$ denote the difference in gravity acceleration at the two places, as observed by means of a gravimeter. That is, $\Delta g$ is the value at point $X$ minus the value at point $O$ on a consistent system. Then, $g$ is given by equation 3.A.4:

$$g = g_1 + \Delta g \tag{3.A.4}$$

**Use of Bouguer anomalies**

If a gravimeter is not available, interpolated Bouguer anomalies ($A_B$) may be used to obtain $g$ at a given point. It is necessary that a contour chart of these anomalies be available from a geodetic organization or from a network of gravity stations spaced at a density of at least one station per 10 000 km$^2$ (no more than a 100 km distance between stations) in the vicinity of the point.

Gravity networks of somewhat less density can be used as a basis provided that a geodetic organization considers that this method is expected to yield more reliable results than those that could be obtained by using a gravimeter.

The definition of the Bouguer anomaly ($A_B$) is derivable from equation 3.A.5:

$$g_s = \left(g_{\varphi,0}\right)s - C \cdot H + A_B \tag{3.A.5}$$

where $(g_{\varphi,0})s$ is the theoretical value of the acceleration of gravity at latitude $\varphi$ at sea level, as given by the formula actually used in computing the Bouguer anomaly. This formula expresses the value as a function of latitude in some systems. $H$ is the elevation of the station (in metres) above sea level at which $g_s$ is measured, $g_s$ is the observed value of the acceleration of gravity (in m s$^{-2}$); $A_B$ is the Bouguer anomaly (in m s$^{-2}$); and $C$ is the elevation correction factor used in computing the Bouguer anomaly (for example, using a crustal specific gravity of 2.67, this factor is 0.000001968 m s$^{-2}$).

When $g$ is desired for a given station and has not been measured, the value of $g_s$ should be computed by means of equation 3.A.5, provided that the appropriate value of $A_B$ for the locality of the station can be interpolated from the aforementioned contour charts or from data representing the Bouguer anomalies supplied by a suitable network of gravity stations, as defined.

**Calculating local acceleration of gravity**

If neither of the preceding methods can be applied, the local value may be calculated less accurately according to a simple model. According to the Geodetic Reference System 1980, the theoretical value ($g_{\varphi,0}$) of the acceleration of gravity at MSL at geographic latitude, $\varphi$, is computed by means of equation 3.A.6:

$$g_{\varphi,0} = 9.806\,20\left(1 - 0.002\,644\,2\cos 2\varphi + 0.000\,005\,8\cos^2 2\varphi\right) \tag{3.A.6}$$

The local value of the acceleration of gravity at a given point on the surface of the ground at a land station is computed by means of equation 3.A.7:

$$g = g_{\varphi,0} - 0.000\,003\,086\,H + 0.000\,001\,118\left(H - H'\right) \tag{3.A.7}$$

where $g$ is the calculated local value of the acceleration of gravity, in m s$^{-2}$, at a given point; $g_{\varphi,0}$ is the theoretical value of the acceleration of gravity in m s$^{-2}$ at MSL at geographic latitude $\varphi$, computed according to equation 3.A.6 above; $H$ is the actual elevation of the given point, in metres above MSL; and $H'$ is the absolute value in metres of the difference between the height of the given point and the mean height of the actual surface of the terrain included within a circle whose radius is about 150 km, centred at the given point.

The local value of the acceleration of gravity at a given point within height $H$ above MSL of not more than about 10 km, and where that point lies over the sea water surface, is computed by means of equation 3.A.8:

$$g = g_{\varphi,0} - 0.000\,003\,086\ H - 0.000\,006\,88\left(D - D'\right) \tag{3.A.8}$$

where $D$ is the depth of water in metres below the given point; and $D'$ is the mean depth of water, in metres, included within a circle whose radius is about 150 km centred at the given point.

At stations or points on or near the coast, the local value of acceleration of gravity should be calculated, so far as practicable, through the use of equations 3.A.7 and 3.A.8 on a pro rata basis, weighting the last term of equation 3.A.7 according to the relative area of land included within the specified circle, and weighting the last term of equation 3.A.8 according to the relative area of the sea included within the circle. The values thus obtained are then combined algebraically to obtain a correction which is applied to the final term in the right-hand side of both equations, as shown in equation 3.A.9:

$$\begin{aligned} g = g_{\varphi,0} &- 0.000\,003\,086\ H + 0.000\,001\,118\ \alpha \\ &\left(H - H'\right) - 0.000\,006\,88\left(1 - \alpha\right)\left(D - D'\right) \end{aligned} \tag{3.A.9}$$

where $\alpha$ is the fraction of land area in the specified area, and $H'$ and $D'$ refer to the actual land and water areas, respectively.

**Corrections for temperature**

Barometer readings must be corrected to the values that would have been obtained if the mercury and the scale had been at their standard temperatures. The standard temperature for mercury barometers is 0 °C. With reference to scales, some barometers have scales which read accurately at this same temperature, but some read accurately at 20 °C.

The temperature correction necessary for adjustable cistern barometers (Fortin-type barometers) is different from that required for fixed-cistern barometers, though the principle reasons leading to the necessity for temperature corrections are the same for both types, namely, the fact that the coefficient of cubic thermal expansion of mercury is different from the coefficient of linear thermal expansion of the scale. Thus, a certain correction term is required for both types of mercury barometer.

A fixed-cistern barometer requires an additional correction. The reason for this is that an increase in temperature of the instrument causes an increase both in the volume of the mercury and in the cross-sectional areas of the (iron) cistern and the (glass) tube. Owing to these area changes, the apparent rise of the mercury resulting from a temperature increase is less than would be the case if the areas remained constant. This is because some of the mercury from the barometer goes to occupy the capacity increment produced by the expansion of the cistern and tube.

The scale of a fixed-cistern barometer must, for a variety of reasons, undergo a calibration check against a primary standard barometer of the adjustable-cistern type. Some manufacturers decrease the volume of mercury by such an amount that the readings of the test barometer agree with the readings of the standard barometer at 20 °C. Correction tables can be generated for fixed-cistern barometers using the readings from a primary standard barometer whose scales are accurate when 20 °C is used as the reference temperature.

**Temperature corrections for mercury barometers**

Researchers have conducted exhaustive studies for temperature corrections for mercury barometers, the results of which are summarized below:

| | | | |
|---|---|---|---|
| 1 | (a) Scale correct at 0 °C and additionally | $C_t$ | $= -B(\alpha - \beta) \cdot t$ |
| | (b) Hg volume correct at 0 ° | $C_{t,V}$ | $= -B(\alpha - \beta) \cdot t - (\alpha - 3\eta) \cdot t \cdot 4V/3A$ |
| 2 | Scale correct at 0 °C and Hg volume correct at 20 °C | $C_{t,V}$ | $= -B(\alpha - \beta) \cdot t - (\alpha - 3\eta) \cdot (t - 20) \cdot 4V/3A$ |
| 3 | (a) Scale correct at 20 °C | $C_t$ | $= -B[\alpha \cdot t - \beta \cdot (t - 20)]$ |
| | (b) Hg volume correct at 0 °C | $C_{t,V}$ | $= -B[\alpha \cdot t - \beta \cdot (t - 20)] - (\alpha - 3\eta) \cdot t \cdot (4V/3A)$ |
| | (c) Hg volume decreasing by an amount equivalent to 0.36 hPa | $C_{t,V}$ | $= -B(\alpha - \beta) \cdot t - (\alpha - 3\eta) \cdot t \cdot (4V/3A)$ |
| 4 | Scale correct at 20 °C and | | |
| | (a) Hg volume correct at 20 °C | $C_{t,V}$ | $= -B[\alpha \cdot t - \beta (t - 20)] - (\alpha - 3\eta) \cdot (t - 20) \cdot (4V/3A)$ |
| | (b) Hg volume decreasing by an amount equivalent to 0.36 hPa | $C_{t,V}$ | $= -B(\alpha - \beta) \cdot t - (\alpha - 3\eta) \cdot (t - 20) \cdot (4V/3A)$ |

where:

$C_t$ = temperature correction;

$C_{t,V}$ = additional correction for fixed-cistern barometers;

$B$ = observed barometer reading;

$V$ = total volume of mercury in the fixed-cistern barometer;

$A$ = effective cross-sectional area of the cistern;

$t$ = temperature;

$\alpha$ = cubic thermal expansion of mercury;

$\beta$ = coefficient of linear thermal expansion of the scale;

$\eta$ = coefficient of linear thermal expansion of the cistern.

## REFERENCES AND FURTHER READING


Brock, F.V. and S.J. Richardson, 2001: *Meteorological Measurement Systems*. New York, Oxford University Press.

European Association of National Metrology Institutes, 2017: *Guidelines on the Calibration of Electromechanical and Mechanical Manometers*. Calibration Guide No. 17 (Version 3.0). Braunschweig, Germany, EURAMET.

Liu, H. and G. Darkow, 1989: Wind effect on measured atmospheric pressure. *Journal of Atmospheric and Oceanic Technology*,6(1):5–12.

Miksad, R., 1976: An omni-directional static pressure probe. *Journal of Applied Meteorology*,15:1215–1225.

Sax, N.I., 1975: *Dangerous Properties of Industrial Materials*. Van Nostrand Reinhold Co., New York.

United Nations Environment Programme, 2013: *Minamata Convention on Mercury*. Geneva, United Nations.

United States Weather Bureau, 1963: *Manual of Barometry* (WBAN). 1, US Government Printing Office, Washington DC.

World Meteorological Organization, 1954: *Reduction of Atmospheric Pressure: Preliminary Report on Problems Involved*. Technical Note No. 7 (WMO-No. 36,TP. 12). Geneva.

———, 1964: *Note on the Standardization of Pressure Reduction Methods in the International Network of Synoptic Stations: Report of a Working Group of the Commission for Synoptic Meteorology*. Technical Note No. 61 (WMO-No. 154,TP. 74). Geneva.

———, 1966: *International Meteorological Tables* (S. Letestu, ed.) (1973 amendment).(WMO-No. 188, TP. 94). Geneva.

———, 1968: *Methods in Use for the Reduction of Atmospheric Pressure*. Technical Note No. 91 (WMO-No. 226,TP. 120). Geneva.

———, 1985: "Pressure tendency" and "discontinuity in wind" – discussion of two algorithms used in Swedish automatic weather stations (L. Bergman, T. Hovberg and H. Wibeck). Paper presented at the Third WMO Technical Conference on Instruments and Methods of Observation (TECIMO-III). Instruments and Observing Methods Report No. 22 (WMO/TD-No. 50). Geneva.

———, 1992: *The WMO Automatic Digital Barometer Intercomparison* (J.P. van der Meulen). Instruments and Observing Methods Report No. 46 (WMO/TD-No. 474). Geneva.

———, 2010: *Guidance on Instrumentation for Calibration Laboratories, Including Regional Instrument Centres* (D. Groselj) (WMO/TD-No. 1543). Instruments and Observing Methods Report No. 101. Geneva.

———, 2011(updated in 2018): *Manual on Codes*. (WMO-No. 306). Volume I.1. Geneva.

———, 2012: *A Laboratory Intercomparison of Static Pressure Heads* (E. Lanzinger and K. Schubotz). In: Papers and Posters presented at the WMO Technical Conference on Instruments and Methods of Observation (TECO 2012), Brussels, 16–18 October, poster P1(15). Instruments and Observing Methods Report No. 109. Geneva

———, 2014: *Guide to Meteorological Observing and Information Distribution Systems for Aviation Weather Services* (WMO-No. 731). Geneva.

———, 2015: *Guidance on the Computation of Calibration Uncertainties* (J. Duvernoy). Instruments and Observing Methods Report No. 119. Geneva.

# CHAPTER 4. MEASUREMENT OF HUMIDITY

## 4.1 GENERAL

The measurement of atmospheric humidity, and often its continuous recording, is an important requirement in most areas of meteorological activity. This chapter deals with the measurement of humidity at or near the Earth's surface. There are many different methods in use, and there is extensive literature on the subject. Accounts of techniques are given in Burt (2012), Harrison (2014) and Sonntag (1994). An older but still useful wide-ranging account of many measurement principles is given in Wexler (1965).

### 4.1.1 Definitions

Definitions of the most frequently used quantities in humidity measurements are as follows. Further definitions are found in Annex 4.A.

**Mixing ratio** $r$**.** Ratio between the mass of water vapour and the mass of dry air;

**Specific humidity** $q$**.** Ratio between the mass of water vapour and the mass of moist air;

**Dew-point temperature or dew point** $t_d$**.** The temperature at which moist air saturated with respect to water at a given pressure has a saturation mixing ratio equal to the given mixing ratio; or more simply, the temperature at which moist air is saturated with water vapour;

**Relative humidity** $U$**.** Ratio in per cent of the observed vapour pressure to the saturation vapour pressure with respect to water at the same temperature and pressure; the term "relative humidity" is often abbreviated to RH;

**Vapour pressure** $e'$**.** The partial pressure of water vapour in air;

**Saturation vapour pressures** $e'_w$ **and** $e'_i$**.** Vapour pressures in air in equilibrium with the surface of water and ice, respectively.

Annex 4.B provides the formulae for the computation of various measures of humidity. These versions of the formulae and coefficients were adopted by WMO in 1990.[1] They are convenient for computation and sufficiently accurate for all normal meteorological applications, strictly within temperature limitation with T > -45 °C for liquid water and T > -65 °C for ice (WMO, 1989*a*). More accurate, extended in range and detailed formulations of these and other quantities may be found in Sonntag (1990, 1994). Other detailed formulations[2] are presented in WMO (1966, introductions to tables 4.8–10).

### 4.1.2 Units and scales

The following units and symbols are normally used for expressing the most commonly used quantities associated with water vapour in the atmosphere:

(a) Mixing ratio $r$ and specific humidity $q$ (dimensionless quotient of masses, in kilogrammes per kilogramme, kg kg$^{-1}$);

(b) Vapour pressure in air $e'$, $e'_w$, $e'_i$ and pressure $p$ (in units of pressure, such as hPa);[3]

---

[1] Adopted by the Executive Council at its forty-second session through Resolution 6 (EC-XLII).
[2] Adopted by the Fourth Congress through Resolution 19 (Cg-IV).
[3] 1 hPa = 1 mbar.

(c) Temperature $t$, wet-bulb temperature $t_w$, dew-point temperature $t_d$, and frost-point temperature $t_f$ (in degrees Celsius, °C);

(d) Temperature $T$, wet-bulb temperature $T_w$, dew-point temperature $T_d$, and frost-point temperature $T_f$ (in K, as used for certain humidity calculations, and for expressing differences, rather than for general expression of humidity values);

(e) Relative humidity $U$ (in per cent; the alternative symbol, %RH, is also often used to avoid confusion with other percentages; it is used throughout this chapter).

### 4.1.3 Meteorological requirements

Humidity measurements at the Earth's surface are required for meteorological analysis and forecasting, for climate studies, and for many special applications in hydrology, agriculture, aeronautical services and environmental studies, in general. They are particularly important because of their relevance to the changes of state of water in the atmosphere.

General requirements for the range, resolution and accuracy of humidity measurements are given in the present volume, Chapter 1, Annex 1.A. The uncertainties listed in the table are requirements, not performances of any particular instruments. In practice, these uncertainties are not easy to achieve, even using good quality instruments that are well operated and maintained. In particular, the psychrometer in a thermometer shelter without forced ventilation, still in use, may have significantly worse performance. Even modern electronic humidity instruments can suffer drift that is significant relative to the requirements.

For most purposes, time constants of the order of 1 min are appropriate for humidity measurements. The response times readily available with operational instruments are discussed in 4.8.1.

### 4.1.4 Methods of measurement and observation

General overviews of humidity instruments for meteorology, and their usage, are given by Burt (2012), Harrison (2014) and Sonntag (1994). Wexler (1965) gives somewhat dated, but still useful, details of many hygrometer principles.

#### 4.1.4.1 *Overview of general measurement principles*

Any instrument for measuring humidity is known as a hygrometer. The physical principles most widely used for humidity measurement in meteorology are given in the following subsections. Reports of WMO international comparisons of various hygrometers are given in WMO (2011*a*, 1989*b*).

The main methods and types of instruments used in meteorology for measuring relative humidity are reviewed here in 4.1.4. Some outdated or no longer used methods and instruments are shortly described in Annex 4.C.

##### 4.1.4.1.1 Electronic sensing

Electronic relative humidity instruments exploit the change in electrical properties of a material on taking up a variable amount water vapour from the air. For relative humidity measurement, the material is commonly a specialized polymer film coated with electrodes. The measured change in electrical impedance (capacitance or resistance) is scaled to indicate relative humidity. Usually, a compact temperature sensor is also incorporated in the same probe housing.

Relative humidity sensor-based hygrometers are increasingly the preferred method for remote-reading applications, particularly where a direct reading of relative humidity is required and where data are to be automatically logged.

It is essential to have temperature information alongside humidity observations because relative humidity is strongly affected by temperature, and because temperature values are needed to calculate other humidity quantities (such as dew point) from relative humidity. Meteorological observations do not commonly use the integral temperature sensor in an electronic relative humidity instrument; it is normal to use a separate temperature measurement.

Capacitive polymer hygrometers are the most convenient and leading technology for meteorological applications, as they are easier to produce, maintain and calibrate. More detail about electrical capacitance hygrometers is given in 4.2.

Electrical resistance hygrometers, while not commonly in use in meteorology, are nevertheless described in Annex 4.C.4.

#### 4.1.4.1.2 **Psychrometric method**

A psychrometer measures evaporative cooling of a wet surface. The steady-state cooling can be related to the partial pressure of water vapour, and to the relative humidity.

A psychrometer consists essentially of two thermometers exposed side by side, with the surface of the sensing element of one being covered with a sleeve maintaining a thin film of water or ice and termed the wet or ice bulb, as appropriate. The sensing element of the second thermometer is simply exposed to the air and is termed the dry bulb. The measurement is either aspirated or under natural ventilation.

Owing to evaporation of water from the wet bulb, the temperature measured by the wet-bulb thermometer is generally lower than that measured by the dry bulb. The difference in the temperatures measured by the pair of thermometers is a measure of the humidity of the air; the lower the ambient humidity, the greater the rate of evaporation and, consequently, the greater the depression of the wet-bulb temperature below the dry-bulb temperature. The size of the wet-bulb depression is related to the ambient humidity by a psychrometer formula.

Psychrometers remain in use for observational purposes, although they are increasingly being replaced by electronic sensor based hygrometers. Psychrometers are also sometimes used as working standards.

More detail about this instrument type is given in 4.3.

#### 4.1.4.1.3 **Condensation method**

The temperature of condensation of water vapour (dew point or frost point) is related to the partial pressure of water and can be measured using a chilled-mirror hygrometer (condensation hygrometer).

When moist air is cooled, it eventually reaches its saturation point with respect to water (or to ice) and condensation can form as dew or frost. The temperature of this saturation point is the dew point or frost point.

A typical chilled-mirror hygrometer uses a small mirrored surface, cooled using a Peltier-effect device, to obtain a film of water or ice. Usually, optical detection of the condensed film is used in a feedback loop to control the temperature at the threshold of constant condensation. This temperature is measured using an embedded temperature sensor. Air to be measured is typically sampled through tubing and flowed through the instrument.

Condensation hygrometers are not widely used for meteorological observations but are commonly used as laboratory reference instruments.

More detail about this instrument type is given in 4.4.

#### 4.1.4.1.4 Water vapour spectrometers

The water molecule absorbs EMR in a range of wavebands and discrete wavelengths; this property can be exploited to obtain a measure of the molecular concentration of water vapour in a gas. This principle is used in a variety of instruments, using absorption lines of different strengths for different ranges of measurement (stronger absorption for lower concentrations).

In simplest form, an instrument measures the transmission (or absorption) of narrowband IR radiation from a fixed-intensity source to a calibrated detector, sometimes compared to a reference wavelength. Certain instruments based on this principle can measure ranges of humidity observed at ground level.

For the trace water vapour range, absorption spectrometers measure the absorption of IR light in multiple reflections through the gas within the measurement cell, giving a long optical path length to extend the range downwards. A particular instrument type is the tunable diode laser spectrometer. The amplitude of light absorption is related to the concentration of water vapour.

Cavity ring-down spectroscopy also uses IR absorption through a long path for measuring trace concentrations. A pulse of light is multiply reflected through the gas in a measurement cell. The time taken for the light intensity to decay is measured and is related to the concentration of water vapour.

Lyman alpha hygrometers operate in the ultraviolet (UV) range. UV light from an instrument source is absorbed by water molecules in proportion to the concentration of water vapour. The so-called “Lyman alpha line” corresponds to radiation emitted or absorbed during an energy transition of atomic hydrogen.

Absorption spectrometers and Lyman alpha instrument are used for some aircraft-borne observations, including measurement of trace levels of water at high flight altitudes. These applications benefit from the relatively fast response time of these instruments.

More detail about this instrument type is given in 4.5.

#### 4.1.4.1.5 Mechanical methods

Historically, hygrometers have used the dimensional change of organic materials to indicate relative humidity. Water sorption processes of materials are related to relative humidity because the driving force is chemical potential. Sensing elements have included hair and, more recently, synthetic fibres. The change in length with humidity of the sensing element is amplified using a lever system, moving a pointer to indicate relative humidity on a scale, a chart (as a record for the hygrograph), or less commonly via a transducer to an electrical output.

Only the hair hygrograph is still in use in meteorology, though phasing out. More detail about this instrument is given in 4.6.

#### 4.1.4.2 *Exposure: general comments*

The general requirements for the exposure of humidity instruments are similar to those for temperature sensors, and a suitably positioned thermometer screen can be used for the purpose. Particular requirements include:

(a) Protection from direct solar radiation, atmospheric contaminants, rain and wind;

(b) Avoidance of the creation of a local microclimate within the instrument housing structure or sampling device. Note that wood and many synthetic materials will adsorb or desorb water vapour according to the atmospheric humidity.

Exposures appropriate to particular instruments are described in 4.2 to 4.6.

The siting classification for surface observing stations on land (see the present volume, Chapter 1, Annex 1.D) provides additional guidance on the selection of a site and the location of a hygrometer within a site to optimize representativeness.

#### 4.1.4.3 *Sources of error: general comments*

Errors in the measurement of humidity can be caused by any of the following:

(a) Modification of the air sample: for example, by a heat or water-vapour source or sink;

(b) Contamination of the sensor: for example, by dirt, sea spray, chemical exposure or other pollution;

(c) Calibration error, including pressure correction, temperature coefficient of sensor, and electrical interface;

(d) Inappropriate treatment of water/ice phase;

(e) Intrinsic design weaknesses of instruments: for example, stem heat conduction in the wet-bulb thermometer;

(f) Slow response time of instrument, or failure to achieve stable equilibrium in operation;

(g) Inappropriate sampling and/or averaging intervals;

(h) Hysteresis: Many humidity-measuring instruments indicate differently depending on whether they approach the condition after having previously been wetter, or dryer;

(i) Long-term drift between calibrations, particularly for electronic humidity measuring instruments in high relative humidity environments;

(j) Radiant heating of the humidity sensor to above the air temperature: for example, due to heating from a radiation screen that is itself warmed by solar radiation;

(k) Error of any kind in temperature measurement, if the temperature value is used in calculating other humidity quantities (for example, calculating dew point from relative humidity).

The time constant of the sensor (see 4.8.1), the time averaging of the output and the data requirement should be consistent.

The different types of humidity-measuring instruments vary in their susceptibility to, and the significance of, each of the above; further discussion will be found in the appropriate sections of this Chapter.

#### 4.1.4.4 *Maintenance: general comments*

The vast majority of commercially available hygrometers have operating manuals freely available online. These are generally a good source of guidance for maintenance of instruments, and manufacturers are generally willing and able to advise about particular questions.

The following maintenance procedures should be considered:

(a) Cleanliness: Instruments and housings should be kept clean. Some humidity-measuring instruments, for example, chilled-mirror and hair hygrometers, may be cleaned with distilled water and this should be carried out regularly. Others, notably those having some form of electrolyte coating, but also some with a polymeric substrate, should never be cleaned. The provision of clear instructions for observers and maintenance staff is vital.

(b) Calibration of field instruments: Regular calibration is required for all humidity-measuring instruments installed in the field. A calibration identifies any errors in readings by comparison against a reference. Such errors are ideally addressed by applying corrections (for example by adjustment, for an electronic hygrometer). Any uncorrected errors need to be considered as part of the uncertainty of the measurement. Calibrations should be made using a reference with metrological traceability (JCGM, 2012) to a national standard wherever possible (see the present volume, Chapter 1, Annex 1.B).

(c) Checking of field instruments is useful in between calibrations. A check against another instrument can be used to assess consistent operation. Results of checks are usually assessed according to a tolerance or criterion based on the uncertainties of the two instruments being compared.

Field hygrometers can be checked conveniently using a calibrated electronic hygrometer. An instrument used for such checks should be equilibrated to the local ambient temperature, and should have a response time well within the period allowed for the check.

Saturated salt solution systems are commercially available to be used for either checking or calibration. However, they must be equilibrated to the ambient temperature, and the salt mixture itself may need additional equilibration time to generate the correct humidity. It is difficult to be confident about their use in the field, unless used together with a transfer standard (calibrated hygrometer).

The use of a standard type of aspirated psychrometer, such as the Assmann, as a field reference has the advantage that some degree of self-checking can be made by comparing the dry- and (unsheathed) wet-bulb thermometers, and that adequate aspiration may be expected from a healthy sounding fan. However, psychrometers emit water vapour in operation, and this can affect the humidity conditions in the surrounding atmosphere, possibly limiting the accuracy of the check if it is close to the instrument being compared.

For any calibration or check, the reference instrument should itself be calibrated at intervals that are appropriate to its type.

It is important to check the calibration of electrical interfaces regularly and throughout their operational range. A simulator may be used in place of the sensor for this purpose. However, it will still be necessary to calibrate the ensemble at selected points, since the combination of calibration errors for sensor and interface that are individually within specification may be outside the specification for the ensemble.

Detailed maintenance requirements specific to each class of hygrometer described in this chapter are included in the appropriate section below.

### 4.1.5 Implications of the Minamata Convention for humidity measurement

The UNEP Minamata Convention on Mercury came into force globally in August 2017 and bans all production, import and export of mercury thermometers (see the present volume, Chapter 1, 1.4.2). Therefore, humidity instruments based on mercury thermometers are no longer recommended and it is strongly encouraged to take appropriate measures to replace them with modern alternatives as soon as possible.

## 4.2 ELECTRICAL CAPACITANCE HYGROMETERS

### 4.2.1 General considerations

Electronic relative humidity instruments exploit the change in electrical properties of a material on taking up a variable amount water vapour from the air. Water sorption processes of materials are related to relative humidity because the driving force is chemical potential. For relative humidity measurement, the material is commonly a specialized polymer film, coated with electrodes. The measured change in electrical impedance is scaled to indicate relative humidity. Usually, a compact temperature sensor is also incorporated in the same probe housing.

The humidity sensor is typically housed in a probe, and this usually incorporates a compact temperature sensor. The sensor region is normally protected by a cage or a filter. In addition, the humidity sensor itself is often directly encased in a protective porous material.

The instruments typically incorporate linearizing electronics, with temperature compensation if needed, to optimize accurate response to relative humidity. Manufacturers variously supply display, data-processing, or data-logging systems. In some cases this is integral to the instrument; in others a cable connects to the supporting electronics unit.

Hygrometers using electrical relative humidity sensors are increasingly used for remote-reading applications, particularly where a direct display of relative humidity is required.

### 4.2.2 Electrical capacitance hygrometer

The method is based upon the variation of the dielectric properties of a solid, hygroscopic material in relation to the ambient relative humidity. Sensing dielectric materials are chosen or deliberately developed for humidity sensor purposes. Polymers are most widely used for their stability, selectivity and water sorption, but also because adequate capacitor properties are achieved with such materials. The water bound in the polymer alters its dielectric properties owing to the large dipole moment of the water molecule.

Typically, the humidity sensor is built on ceramic or glass substrate. It is a parallel thin film stack with layer thicknesses from a few nanometers to one micrometer. The active part of the humidity sensor consists of a polymer film sandwiched between two electrodes to form a capacitor. The upper electrode is permeable for water molecules and the polymer absorbs water proportional to the relative humidity. The upper electrode may also be covered with a protective layer to improve stability in harsh environments.

The capacitance provides a measure of relative humidity. The nominal value of capacitance may be only a few hundred picofarads, depending upon the size of the electrodes and the thickness of the dielectric. This will, in turn, influence the range of excitation frequency used to measure the impedance of the device, which is normally at least several kilohertz and, thus, requires that short connections be made between the sensor and the signal processing electronics to minimize the effect of stray capacitance. Therefore, capacitance sensors often have the signal processing built into the instrument. Typical sensitivity for a 200 pF device is 0.5 pF per %RH.

To prevent condensation when the condition approaches 100%RH, instrument manufacturers provide different heating options. The sensor may be heated by an integrated heater or the

whole probe itself is warmed. The heating is controlled using either temperature difference between ambient temperature and internal temperature or a relative humidity threshold. For good measurement results, it is crucial to measure both the temperature of the humidity sensor and the temperature of the ambient air accurately. By using the relative humidity measured by the sensor, the sensor temperature and the temperature of the air, it is possible to calculate the relative humidity of the air. Even without the known air temperature, heated measurement can be used to determine dew-point temperature. Chemical exposure-related drift can be reduced by using an integrated heater to heat the humidity sensor, at repeatable intervals, during a short time at high temperature. A drawback is the dead time during heating.

### 4.2.3 Observation procedure

Hygrometers using electronic relative humidity sensors are frequently used in AWSs, and wherever unattended or data-logged humidity measurements are needed.

Temperature observations are essential alongside humidity observations, since temperature values are used to calculate other humidity quantities (such as dew point) from relative humidity. This normally involves a separate thermometer, not the integral temperature sensor in an electronic relative humidity instrument.

### 4.2.4 Exposure and siting

Hygrometer probes should be mounted inside a thermometer screen. The manufacturer's advice regarding the mounting of the actual instrument should be followed. The use of a protective filter is essential to minimize contamination which can cause progressive error. Instruments using hygroscopic electrolyte as a sensing element will be damaged by direct contact with liquid. Capacitive sensors that have been wetted can often recover at least partially after drying. However, exposure to high or condensing humidity is associated with long-term drift of some capacitive sensors.

### 4.2.5 Sources of error

Measurements using relative humidity sensors can be particularly affected by any of the following causes of error:

– Calibration error can be present, such that the initial adjustment of the instrument leaves residual uncorrected errors. This error can have the character of non-linearity, or some other form. This can also appear to be temperature dependent, since it is typically not possible to calibrate at multiple temperatures, or to implement temperature-dependent calibrations.

– Sensors can suffer contamination; for example, by dirt, sea spray, chemical exposure or other pollution. This type of error can take the form of reduced sensitivity across the whole range, with over-reading at low humidity and under-reading at high humidity, or it can follow some other pattern.

– Hysteresis can affect electronic humidity instruments, so that they read differently depending on whether they approach the condition after having previously been wetter, or dryer. Response time can also differ for rising and falling changes in condition.

– Long-term drift between calibrations can be significant, particularly for instruments exposed to high or condensing relative humidity (dew, fog or other wetting). Such drift is most typically upwards at high humidity although it can be downwards, and varies greatly (Burt, 2012; Bell et al., 2017). Upwards drift leads to over-reading at high humidity values, for example indicating 100%RH at a condition of 95%RH. Heated sensors are potentially less prone to such drift.

– Radiant heating of the humidity sensor to above air temperature can mean that the sensor is warmer than the air. This can happen even within a screen if the screen itself is warmed by solar radiation. This can potentially give a falsely low reading of relative humidity.

Error in the measurement of temperature of any kind is significant with relative humidity if both values are used in calculating other humidity quantities (for example, calculating dew point from relative humidity). In such calculations, an error of 0.1 °C near 20 °C has the same magnitude of effect as an error of 0.6%RH. WMO (2011*a*) details this effect at other temperatures.

### 4.2.6 Calibration and field inspection

A calibration identifies any errors in readings by comparison against a reference. Calibration of relative humidity instruments is normally a laboratory process that involves comparison against reference for relative humidity, often in a climatic chamber. Calibrations should be made using a reference with metrological traceability to a national standard wherever possible (see the present volume, Chapter 1, Annex 1.B). Further details are given in 4.7 and Volume V, Chapter 4 of the present Guide.

Calibrations are ideally implemented by applying corrections (commonly, for an electronic hygrometer, by applying instrument adjustments). For some electronic hygrometers, adjustments can be applied using manufacturer software at the time of calibration. In other cases, adjustments can be made by adjusting potentiometers corresponding to the "range" and "zero" of the hygrometer indication. While calibration corrections can be applied arithmetically, this is more useful in a laboratory application than in meteorology settings. Any uncorrected calibration errors need to be considered as part of the uncertainty of the measurement.

Field inspections of electronic relative humidity instruments involve viewing the condition and functioning of the instruments. In particular, the condition of the sensor filter is inspected, and this is cleaned or replaced if it is dirty.

Field checks of hygrometers can conveniently be made using another calibrated electronic hygrometer. An instrument used for such checks should be equilibrated to the local ambient temperature. It should either be calibrated at the temperature of use, or allowance should be made for the different temperatures of operation. The hygrometer used for any field check should have a response time well within the time period allowed for the check. A check will normally have a defined criterion for acceptance.

In principle, field checks of relative humidity instruments can be made using salt-based systems, which are supplied by some instrument manufacturers. These are only reliable after they are fully equilibrated to the local ambient temperature. Therefore it is difficult to be confident about their use in the field. In principle, a field humidity generator can be used for checking on site, but these are not widely available. Further details are given at 4.7.6.3.

The use of a standard type of aspirated psychrometer, such as the Assmann, as a field reference has been advocated. However, psychrometers emit water vapour in operation, and this can affect the surrounding conditions of humidity, possibly affecting the accuracy of the check if it is close to the instrument being compared.

For any calibration or check, the reference instrument should itself be calibrated at intervals that are appropriate to its type.

Where relevant, a check of an electronic hygrometer should include checking the data-logging interfaces. A simulator can possibly be used in place of the sensor for this purpose. Depending on the configuration of the system, whole-system checks (hygrometer plus interface) may be needed. For example, on older systems the combination of calibration errors for sensor and interface that are individually within specification could be outside the specification for the ensemble.

### 4.2.7 Maintenance

Observers should be encouraged to keep the hygrometer clean (see 4.1.4.4). If it is fitted with an interchangeable protective filter-cap, this should be visually inspected for evidence of contamination and replaced if necessary. The body of a hygrometer can be cleaned if necessary using a damp cloth, taking care not to wet the sensor. Electronic elements must not be cleaned in the field, as this would alter their calibration.

Time intervals for field servicing and calibration of relative humidity instruments will generally depend on the level of long-term stability expected and required, on the location, and on the availability of facilities and personnel. The lifetime before failure, for electronic relative humidity instruments in service in weather stations in damp climates, is commonly between six months and two or more years. There is often significant sensor drift on shorter timescales. The cause of failure (especially early failures) is commonly the sensor element. Usually, this can be replaced, and the hygrometer recalibrated before being used again.

In some cases, field servicing of an electronic hygrometer will mean the replacement of a failed instrument. In other cases, field hygrometers are replaced (perhaps annually) with a newly calibrated instrument, and the one taken out of use is sent for servicing, recalibration and (if satisfactory) re-deployment. If a hygrometer has failed, often this can be remedied by the replacement of just the sensor element, followed by recalibration.

In order to address the tendency of sensors to drift, a more intensive management approach can be adopted where resources allow. Sensor drift can be evaluated on return from the field, by comparison against a reference in a calibration facility. Those instruments showing minor drift can be adjusted and then recalibrated for redeployment. However, these can be expected to have worse ongoing reliability than new instruments. Those instruments that are found to have more extreme in-field drift can be refurbished (by buying a new sensing element, changing it in the laboratory and calibrating the renewed instrument). However, after a number of deployments, performance can be expected to worsen, and a policy of routinely replacing these hygrometers after a defined period can lead to improved overall reliability of the observations.

The vast majority of commercially available hygrometers have operating manuals freely available online. These are generally a good source of guidance for maintenance of instruments, and manufacturers are generally willing and able to advise about particular questions.

## 4.3 THE PSYCHROMETER

### 4.3.1 General considerations

#### 4.3.1.1 *Psychrometric formulae*

The usual practice is to derive the vapour pressure $e'$ under the conditions of observation from the following semi-empirical psychrometric formulae:

$$e' = e'_w\left(p, t_w\right) - Ap\left(t - t_w\right) \tag{4.1}$$

and:

$$e' = e'_i\left(p, t_i\right) - Ap\left(t - t_i\right) \tag{4.2}$$

where $e'_w$ is the saturation vapour pressure with respect to water at temperature $t_w$ and pressure $p$ of the wet bulb; $e'_i$ is the saturation vapour pressure with respect to ice at temperature $t_i$ and pressure $p$ of the ice bulb; $p$ is the pressure of the air; $t$ is the temperature of the dry bulb; and $A$ is the psychrometer coefficient (the latter is preferred to the term "psychrometer constant", which is a misnomer).

The formulae and coefficients appropriate for the various forms of psychrometer are discussed in the following sections.

#### 4.3.1.2 *The specification of a psychrometer*

The equipment used for psychrometric observations should, as far as practicable, conform to the following recommendations:

(a) At sea level, and in the case where the thermometers are of the types ordinarily used at meteorological stations, air should be drawn past the thermometer bulbs at a rate of no less than 2.2 m $s^{-1}$ and no greater than 10 m $s^{-1}$. For appreciably different altitudes, these air speed limits should be adjusted in inverse proportion to the density of the atmosphere;

(b) The wet and dry bulbs must be protected from radiation, preferably by a minimum of two shields. In a psychrometer with forced ventilation, such as the Assmann, the shields may be of polished, unpainted metal, separated from the rest of the apparatus by insulating material. Thermally insulating material is preferable in principle and must be used in psychrometers which rely on natural ventilation;

(c) If the psychrometer is exposed in a louvred screen with forced ventilation, separate ventilation ducts should be provided for the two thermometers. The entrance to the ducts should be located so as to yield a measurement of the true ambient temperature, and the air should be exhausted above the screen in such a way as to prevent recirculation;

(d) The greatest care should be taken to prevent the transfer of significant amounts of heat from an aspirating motor to the thermometers;

(e) The water reservoir and wick should be arranged in such a way that the water will reach the bulb with sensibly the wet-bulb temperature, so as not to affect the temperature of the dry bulb.

#### 4.3.1.3 *The wet-bulb sleeve*

The wet bulb usually has a cotton wick, or similar fabric, fitting closely around the sensing element in order to maintain an even covering of water, which is either applied directly or by some form of capillary feed from a reservoir. The wick commonly takes the form of a sleeve that has a good fit around the bulb and extends at least 2 cm up the stem of the thermometer to give extended cooling, to reduce stem conduction. Distilled water should be used for the wet bulb.

The fabric used to cover the wet bulb should be thin and closely woven. Where the supplier offers a wick designed for the size of the thermometers, this should be used. Before installation, it should be washed thoroughly in an aqueous solution of sodium bicarbonate ($NaHCO_3$) at a dilution of 5 g per litre, and rinsed several times in distilled water. Alternatively, boiling in a dilute solution of pure detergent in water may be performed, followed by boiling in distilled water. Great care should be exercised in handling the clean sleeve or wick to prevent contamination from hands, for example by using tweezers that have been cleaned, or clean plastic residue-free gloves.

The proper management of the wet bulb is particularly important. Any visible contamination of the wick or the wet-bulb sleeve should be considered an absolute indication of the necessity for its immediate replacement. Otherwise, observers should be encouraged to change the wet-bulb sleeve and wick at least once a week for all psychrometers that are continuously exposed. At places near the sea and industrialized districts it may be necessary to replace these items more frequently. The water supply should be checked frequently and replaced or replenished as required.

Under hot, dry conditions, it can be an advantage to wet the covering with water from a porous vessel. This will cause the water to be pre-cooled by evaporation from the porous surface. The vessel should be kept in the shade, but not in the immediate vicinity of the psychrometer.

#### 4.3.1.4 *Operation of the wet bulb below freezing*

The psychrometer is difficult to operate at temperatures below freezing, but it is still used in climates where such temperatures occur. A wick cannot be used to convey water from a reservoir to the wet-bulb sleeve by capillary action when the wick is frozen. Under these conditions, care should be taken to allow the formation of only a thin layer of ice on the sleeve. It is an absolute necessity that the thermometers be artificially ventilated; if they are not, the management of the wet bulb will be extremely difficult.

The wet bulb of the aspirated and sling psychrometers should be moistened immediately before use. The water should, as far as possible, have a temperature close to freezing point. If a button of ice forms at the lowest part of the bulb, it should be immersed in water long enough to melt the ice.

The time required for the wet bulb to reach a steady reading after the sleeve is wetted depends on the ventilation rate and the actual wet-bulb temperature. An unventilated thermometer usually requires from 15 to 45 min, while an aspirated thermometer will require a much shorter period. It is essential that the formation of a new ice film on the bulb be made at an appropriate time. If hourly observations are being made with a simple psychrometer, it will usually be preferable to form a new coating of ice just after each observation. If the observations are made at longer intervals, the observer should visit the screen sufficiently in advance of each observation to form a new ice film on the bulb.

The evaporation of an ice film between readings can be prevented or slowed by enclosing the wet bulb in a small glass tube, or by stopping the ventilation inlet of the wet bulb between periods of measurement. If this is done the wet-bulb temperature will not be accurate during these interventions. (Note that the latter course should not be taken if the circumstances are such that the ventilating fan would overheat.)

The effect of supercooled water on the wet bulb may be dealt with in two ways:

(a) By using different formulae or tables when the wet bulb is coated with ice and with supercooled water, respectively. To find out which table should be used, the wet bulb should be touched with a snow crystal, a pencil, needle, or other object, just after each observation is completed. The degree of gloss on the surface of the wet-bulb is also useful to check if the wet bulb is frozen. If the temperature rises towards 0 °C, and then commences to fall again, it can be assumed that the water on the wet bulb was supercooled at the time of the observation;

(b) By using a formula or table appropriate for an ice-covered wet bulb, and inducing the freezing of supercooled water in the same way as for method (a). In order to save time and to ensure that the wet bulb is ice-covered, the observer should make a point of initiating the freezing of the water at each observation as soon as possible after moistening the bulb. From the behaviour of the wetted thermometer at the freezing point it may usually be determined whether the bulb is covered by ice or by supercooled water. The recommended procedure, however, is to initiate the freezing of the water at each observation when the wet-bulb temperature is assumed to be below 0 °C, regardless of whether the behaviour of the thermometer after moistening has been observed or not.

Although the first method is usually the quickest, it requires two tables and this may cause some confusion.

#### 4.3.1.5 *General procedure for making observations*

The procedures outlined in the present volume, Chapter 2, for the measurement of temperature should be followed, in addition to the following procedures:

(a) If the wet-bulb sleeve, wick or water has to be changed, this should be done sufficiently in advance of the observation. The period required for the correct wet-bulb temperature to be attained will depend upon the type of psychrometer;

(b) The thermometers should be read to the nearest 0.1 degree;

(c) When making an observation, the readings of the two thermometers should, as far as possible, be taken simultaneously (reading first the dry thermometer, then the wet one, and finally the dry one again is a reasonable solution) and it should be ascertained that the wet bulb is receiving a sufficient water supply.

#### 4.3.1.6 *Use of electrical resistance thermometers*

Precision platinum electrical resistance thermometers are widely used in place of liquid-in-glass thermometers, in particular where remote reading and continuous measurements are required. It is necessary to ensure that the devices, and the related electronics, meet the performance requirements. These are detailed in the present volume, Chapter 2. Particular care should always be taken with regard to self-heating effects in electrical thermometers.

The psychrometric formulae in Annex 4.B used for Assmann aspiration psychrometers are also valid if PRTs are used in place of the mercury-in-glass instruments, with different configurations of elements and thermometers. The formula for water on the wet bulb is also valid for some transversely ventilated psychrometers (WMO, 1989*a*).

#### 4.3.1.7 *Psychrometric formulae and tables*

The following paragraphs summarize some existing principles and practice in drawing up psychrometric tables.

The wet-bulb thermometer temperature $T_w$ for most instruments is not identical to the theoretical thermodynamic wet-bulb temperature, defined in Annex 4.A, which depends only upon $p$, $T$ and $r$ (the humidity mixing ratio). The temperature measured by a practical wet-bulb thermometer depends also upon a number of variables that are influenced by the dynamics of heat transfer across a liquid/gas interface (in which the gas must be characterized in terms of its component laminar and turbulent layers). The description of a satisfactory thermodynamic model is beyond the scope of this publication. The inequality of the thermodynamic and measured wet-bulb temperatures is resolved in practice through the empirical determination of the psychrometer coefficient $A$ (WMO, 1992).

In general, coefficient $A$ depends upon the design of the psychrometer (in particular the wet-bulb system), the diameter of the thermometers, the rate of airflow past the wet bulb (termed the ventilation rate), and the air temperature and its humidity. At low rates of ventilation, $A$ depends markedly upon the ventilation rate. However, at ventilation rates of 3 to 5 m $s^{-1}$ (for thermometers of conventional dimensions) or higher, the value of $A$ becomes substantially independent of the ventilation rate and is practically the same for all well-designed psychrometers. The value of $A$ does not, then, depend very much on temperature or humidity and its dependence on these variables is usually ignored. $A$ is smaller when the wet bulb is coated with ice than when it is covered with water.

#### 4.3.1.8 *Sources of error in psychrometry*

The following main sources of error must be considered:

(a) Errors of the thermometers: It is very important in psychrometric measurements that the errors of the thermometers be known over the actual temperature range and that corrections for these errors be applied to the readings before the humidity formulae tables are used. In general, thermometers should be pre-selected to have minimum errors.

Any other errors in the wet-bulb or ice-bulb temperature caused by other influences will appear in the same way as thermometer errors.

Table 4.1 shows the error in relative humidity $\varepsilon$ ($U$), derived from wet- and ice-bulb measurements having errors $\varepsilon$ ($t_x$), where $x$ is water for $t > 0$ °C and ice for $t < 0$ °C, respectively of 0.5 and 0.1 K, for a relative humidity $U$ of 50%RH and a range of true air temperatures (where the dry-bulb reading is assumed to give the true air temperature).

(b) Thermometer response-time coefficients (sometimes called lag coefficients): To obtain the highest accuracy with a psychrometer it is desirable to arrange for the wet and dry bulbs to have approximately the same response-time coefficient; with thermometers having the same bulb size, the wet bulb has an appreciably smaller response time than the dry bulb.

(c) Errors relating to ventilation: Errors due to insufficient ventilation can lead to overestimation of humidity.

(d) Errors due to the use of inappropriate humidity formulae or tables (see sections covering individual psychrometer types). Other errors can be magnified though inappropriate evaluations.

(e) Errors due to excessive covering of ice on the wet bulb: Since a thick coating of ice will increase the response time of the thermometer, it should be removed immediately by dipping the bulb into distilled water.

(f) Errors due to contamination of the wet-bulb sleeve or to impure water: Large errors can be caused by the presence of substances that alter the vapour pressure of water. The wet bulb with its covering sleeve should be washed at regular intervals in distilled water to remove soluble impurities. This procedure is more frequently necessary in some regions than others, for example, at or near the sea or in areas subject to air pollution.

**Table 4.1. Error in derived relative humidity resulting from wet- and ice-bulb index errors $\varepsilon$ ($t_x$) for $U$ = 50%RH**

| *Air temperature in °C* | *Error in relative humidity, $\varepsilon$ (U) in % due to an error in wet- or ice-bulb temperature* | |
|---|---|---|
| | *$\varepsilon$ ($t_x$) = 0.5 K* | *$\varepsilon$ ($t_x$) = 0.1 K* |
| –30 | 60 | 12 |
| –20 | 27 | 5 |
| –10 | 14 | 3 |
| 0 | 8 | 2 |
| 10 | 5 | 1 |
| 20 | 4 | 0.5 |
| 30 | 3 | 0.5 |
| 40 | 2 | 0.5 |
| 50 | 2 | 0 |

(g) Errors due to heat conduction from the thermometer stem to the wet-bulb system: The conduction of heat from the thermometer stem to the wet bulb will reduce the wet-bulb depression and lead to determinations of humidity that are too high. The effect is most pronounced at low relative humidity but can be effectively reduced or eliminated by extending the wet-bulb sleeve at least 2 cm beyond the bulb, up the stem of the thermometer.

(h) Errors due to radiative effects: The wet-bulb temperature will always be colder that the surroundings and radiation shields will not always protect completely against radiative heating of all parts of the assembly.

It should be noted that psychrometers are generally less accurate at low relative humidities (large wet-bulb depressions).

### 4.3.2 Assmann and other aspirated psychrometers

An alternative instrument to the traditional (mercury-in-glass) Assmann psychrometer is an electrically aspirated psychrometer using two PRTs, instead of two mercury-in-glass thermometers. Newer designs of aspirated psychrometers do not follow the exact pattern of Assmann instruments, and commonly incorporate a reservoir supplying water to the wick over an extended period. Overall, any alternative designs will still require precautions in operation similar to the Assmann types.

This change of instrumentation should be recorded meticulously and "side-by-side" comparisons made for a period of two or more years in line with WMO recommendations. (WMO, 2011*b*, 2015).

#### 4.3.2.1 *Description*

Two thermometers, mounted vertically side by side in a chromium- or nickel-plated polished metal frame, are connected by ducts to an aspirator (fan). The aspirator may be driven by a spring or an electric motor. In the traditional Assmann design, mercury-in-glass thermometers were used, but updated designs could in principle use suitably characterized alternatives (resistance thermometers, or other liquid-in-glass types) of suitable diameter and measuring range. One thermometer has a well-fitting muslin wick which, before use, is moistened with distilled water. The wick covers the sensing part of the thermometer (for a liquid-in-glass thermometer, this is the bulb) and a defined additional length of the thermometer stem. Where a resistance thermometer is used for the wet-bulb, it is important that the wick covers and extends beyond the region of the sensing element; this region is not usually obvious by inspection of a thermometer but will be based on knowledge of its internal structure.

Each thermometer is located inside a pair of coaxial metal tubes, highly polished inside and out, which screen the bulbs from external thermal radiation. The tubes are all thermally insulated from each other.

A WMO international intercomparison of Assmann-type psychrometers from 10 countries (WMO, 1989*a*) showed that there is good agreement between dry- and wet-bulb temperatures of psychrometers with the dimensional specifications close to the original specification, and with aspiration rates above 2.2 m $s^{-1}$. Not all commercially available instruments fully comply. A more detailed discussion is found in WMO (1989*a*). It has been suggested that the performance of the Assmann psychrometer in the field may be as good as the achievable accuracy stated in the present volume, Chapter 1, Annex 1.A, but this level of accuracy will not reliably be achieved due to possible errors of airflow, contamination and radiant heat transfer, among others. As for all types of psychrometer, calibration of the instrument, as in 4.3.2.4 below, is the best way to ensure accuracy. This will be especially important for any emerging designs where alternatives are used in place of mercury-in-glass thermometers.

Annex 4.B lists standard formulae for the computation of measures of humidity using an Assmann psychrometer,[4] and these formulae are also used for some of the other artificially ventilated psychrometers, in the absence of well-established alternatives.

#### 4.3.2.2 *Observation procedure*

The wick, which must be free of grease, is moistened with distilled water. Dirty or crusty wicks should be replaced. Care should be taken not to introduce a water bridge between the wick and the radiation shield.

The instrument is normally operated with the thermometers held vertically, ideally by mounting it on a stand. The thermometer stems should be protected from solar radiation by turning the instrument so that the lateral shields are in line with the sun. If the instrument is handheld, it should be tilted so that the inlet ducts open into the wind, but care should be taken so that solar radiation does not fall on the thermometer bulbs. A wind screen is necessary in very windy conditions when the rotation of the aspirator is otherwise affected.

The psychrometer should be in thermal equilibrium with the surrounding air. At air temperatures above 0 °C, at least three measurements at 1 min intervals should be taken following an aspiration period. Below 0 °C it is necessary to wait until the freezing process has finished, and to observe whether there is water or ice on the wick. During the freezing and thawing processes the wet-bulb temperature remains constant at 0 °C. In the case of outdoor measurements, several measurements should be taken and the average taken. Thermometer readings should be made with a resolution of 0.1 K or better.

A summary of the observation procedure is as follows:

(a) Moisten the wet bulb;

(b) Wind the clockwork motor (or start the electric motor);

(c) Wait 2 or 3 min or until the wet-bulb reading has become steady;

(d) Read the dry bulb;

(e) Read the wet bulb;

(f) Check the reading of the dry bulb.

#### 4.3.2.3 *Exposure and siting*

Observations should be made in an open area. The instrument is either suspended from a clamp or attached using a bracket to a thin post, or held with one hand at arm's length with the inlets slightly inclined into the wind. The inlets should be at a height of 1.25 to 2 m above ground for normal measurements of air temperature and humidity.

Great care should be taken to prevent the presence of the observer or any other nearby sources of heat and water vapour, such as the exhaust pipe of a motor vehicle, from having an influence on the readings.

#### 4.3.2.4 *Calibration*

Calibration of a psychrometer has two aspects: calibration of the thermometers, and calibration of the whole instrument functioning as a hygrometer. Maintenance steps (particularly for wick and fan) should be performed before an instrument is calibrated.

[4] Recommended by CIMO at its tenth session (1989).

Calibration of the thermometers is recommended at regular intervals according to the thermometer type and quality, and the degree of handling or other stresses on the thermometers. For further information, see the present volume, Chapter 2.

For resistance thermometers, calibration corrections can be applied by applying different coefficients in the formula for converting resistance to temperature. If calibration-specific coefficients are not applied, then the calibration process is used to confirm accuracy of the thermometers to within a given tolerance. If thermometers do not meet the tolerance, they should be replaced.

For liquid-in-glass thermometers, calibration corrections can in principle be applied arithmetically; otherwise, again, the calibration process is used to confirm accuracy of the thermometers to within a given tolerance. If thermometers do not meet the tolerance, they can be replaced.

After temperature calibration is applied, the whole psychrometer is calibrated as a hygrometer, usually against a reference in terms of relative humidity. This reference may be a reference dew-point hygrometer or one or more reference thermometers. The calibration may be undertaken in ambient air - or in a humidity- and temperature-controlled chamber for remote-reading (PRT) psychrometers. The possibility of calibration in a chamber at multiple temperatures and humidities is a strongly advised for psychrometers using electrical thermometers.

Ideally, where a psychrometer calibration can be carried out at a range of temperature and humidity conditions, it is possible to use the results to evaluate a psychrometer coefficient, or a corresponding function, specific to the psychrometer. The function is typically a constant plus a second term representing a slight temperature dependence. The coefficient or function derived from calibration can replace the value of $A$ in the psychrometer equation, if this can be implemented (for example, in software). This approach to implementing calibration provides better accuracy than using the generalized default psychrometer coefficient.

If temperature calibration is neglected before humidity calibration, the uncorrected temperature values will usually cause larger errors in humidity values than if temperature corrections are applied (or tolerances met).

Pressure is normally reported for calibration of psychrometers, since evaluation of the psychrometer equation uses pressure, and the psychrometric effect has some pressure dependence.

#### 4.3.2.5 ***Maintenance***

The calibration of the thermometers should be checked regularly. The two may be compared together, with both thermometers measuring the dry-bulb temperature. The ventilation system should be checked, at least once per month, or before use if that is a longer interval. Checks of thermometers by comparison against a reference thermometer are useful at intervals, for example annually.

Mercury instruments should no longer be used. But as long as any remain, the mercury columns of the thermometers should be inspected for breaks, which, if they exist, should be rejoined or the instrument(s) replaced.

Between uses, the instrument should be stored in an unheated room or be otherwise protected from precipitation and strong insolation. When not in use, the instrument should be stored indoors in a sturdy packing case such as that supplied by the manufacturer.

### 4.3.3 Screen psychrometer

Traditionally, mercury-in-glass thermometers have been used as screen psychrometers. Alternative instruments are psychrometers using two PRTs with appropriate instrumentation, or two liquid-in-glass thermometers of other type, instead of two mercury-in-glass thermometers.

This change of instrumentation should be recorded meticulously and "side-by-side" comparisons made for a period of two or more years in line with WMO recommendations. (WMO, 2011*b*, 2015)

#### 4.3.3.1 *Description*

Two thermometers are mounted vertically in a thermometer screen. One thermometer sensing element (for a liquid-in-glass thermometer, this is the bulb) is fitted with a cotton or muslin wick sleeve generally known as the "wet-bulb sleeve", which should fit closely, covering and extending past the sensing part of the thermometer. Where a resistance thermometer is used for the wet-bulb, it is important that the wick covers and extends beyond the region of the sensing element; this region is not usually obvious by inspection of a thermometer but will be based on knowledge of its internal structure. If a wick and water reservoir are used to keep the wet-bulb sleeve in a moist condition, the reservoir should preferably be placed to the side of the thermometer and with the mouth at the same level as, or slightly lower than, the top of the sensing element. The wick should be kept as straight as possible and its length should be such that water reaches the sensing element at a temperature that is approximately the same as the wet-bulb temperature and in sufficient (but not excessive) quantity. If no wick is used, the wet bulb should be protected from dirt by enclosing it in a small glass tube between readings.

The performance of a screen psychrometer can be expected to be much worse than that shown in the present volume, Chapter 1, Annex 1.A, especially in light winds if the screen is not artificially ventilated.

It is therefore desirable that screen psychrometers be artificially aspirated where possible. Both thermometers should be aspirated at an air speed of about 3 m $s^{-1}$. The air should be drawn in horizontally across the bulbs, rather than vertically, and expelled in such a way as to avoid recirculation.

The psychrometric formulae given in 4.3.1.1 apply to screen psychrometers, but the coefficients are quite uncertain, and the following summary indicates varied practices going back many years. If there is artificial ventilation at 3 m $s^{-1}$ or more across the wet bulb, the formulae may be applied, using a psychrometer coefficient of $6.53 \cdot 10^{-4}$ $K^{-1}$ for water. However, values from 6.50 to $6.78 \cdot 10^{-4}$ $K^{-1}$ have been used for wet bulbs above 0 °C, and 5.70 to $6.53 \cdot 10^{-4}$ $K^{-1}$ for below 0 °C. For a naturally ventilated screen psychrometer, coefficients in the range from 7.7 to $8.0 \cdot 10^{-4}$ $K^{-1}$ above freezing and 6.8 to $7.2 \cdot 10^{-4}$ $K^{-1}$ for below freezing have been used when there is some air movement in the screen, which is probably nearly always the case. However, coefficients up to $12 \cdot 10^{-4}$ $K^{-1}$for water and $10.6 \cdot 10^{-4}$ $K^{-1}$ for ice have been advocated for when there is no air movement. As for all types of psychrometer, calibration of the instrument, as in 4.3.2.4 above, would be the best way to determine the choice of psychrometer coefficient or function, although for screen psychrometers this is less straightforward than for other psychrometer types.

#### 4.3.3.2 *Observation procedure*

The procedures described in 4.3.1.5 apply to the screen psychrometer.

In the case of a naturally aspirated wet bulb, provided that the water reservoir has about the same temperature as the air, a stable wet-bulb temperature will be attained approximately 15 minutes after fitting a new sleeve; if the water temperature differs substantially from that of the air, it may be necessary to wait for 30 minutes.

#### 4.3.3.3 *Exposure and siting*

The exposure and siting of the screen are described in the present volume, Chapter 2.

#### 4.3.3.4 *Calibration*

Calibration principles for a screen psychrometer are in principle similar to those for an Assmann or other aspirated psychrometer. However, removal of a screen psychrometer to a climatic chamber or other laboratory setting is unlikely to be representative of normal operation, while calibration in situ will probably not provide a range of temperature and humidity conditions.

The psychrometer coefficient appropriate for a particular configuration of screen, shape of wet bulb and degree of ventilation can be determined by comparison with a suitable working or reference standard, as described for Assmann psychrometers in 4.3.2.4. However, a large dataset (ideally in a humidity- and temperature-controlled chamber) would be necessary, and wide scatter in the data might be expected. This evaluation is not commonly performed for this basic type of instrument, and there would be little justification for departing from established national practices.

#### 4.3.3.5 *Maintenance*

The calibration of the thermometers should be checked regularly. The two may be compared together, with both thermometers measuring the dry-bulb temperature. Checks of thermometers by comparison against a reference thermometer are useful at intervals, for example annually.

The liquid-in-glass columns of the thermometers should be inspected for breaks, which, if they exist, should be rejoined. Otherwise, the instrument(s) should be replaced.

### 4.3.4 Sling or whirling psychrometers

These instruments are still in use, mainly on board ships.

#### 4.3.4.1 *Description*

A small portable type of whirling or sling psychrometer consists of two liquid-in-glass thermometers mounted on a sturdy frame, which is provided with a handle and spindle located at the furthest end from the thermometer bulbs, by means of which the frame and thermometers may be rotated rapidly about a horizontal axis.

The wet-bulb arrangement varies according to individual design. Some designs shield the thermometer bulbs from direct insolation, and these are to be preferred for meteorological measurements.

The psychrometric formulae in Annex 4.B may be used. However, these hygrometers suffer the same sources of error as other psychrometers, while being difficult to calibrate against a humidity reference. In addition, the need to cease aspiration in order to take a reading is a particular source of error, leading to probable overestimations of the wet-bulb temperature. For these reasons, measurements using whirling or sling psychrometers tend to have significant uncertainty.

#### 4.3.4.2 *Observation procedure*

The following guidelines should be applied:

(a) All instructions with regard to the handling of Assmann aspirated psychrometers apply also to sling psychrometers;

(b) Sling psychrometers lacking radiation shields for the thermometer bulbs should be shielded from direct insolation in some other way;

(c) Thermometers should be read at once after aspiration ceases because the wet-bulb temperature will begin to rise immediately, and the thermometers are likely to be subject to insolation effects.

## 4.4 THE CHILLED-MIRROR DEW-POINT HYGROMETER

### 4.4.1 General considerations

#### 4.4.1.1 *Theory*

The dew-point (or frost-point) hygrometer is used to measure the temperature at which moist air, when cooled, reaches saturation and a deposit of dew (or ice) can be detected on a solid surface, which usually is a mirror. The deposit is normally detected optically. The principle of the measurement is described in 4.1.4.1.3 and below.

The thermodynamic dew point is defined for a plane surface of pure water. In practice, water droplets have curved surfaces, over which the saturation vapour pressure is higher than for the plane surface (known as the Kelvin effect). Hydrophobic contaminants will exaggerate the effect, while soluble ones will have the opposite effect and lower the saturation vapour pressure (the Raoult effect). The Kelvin and Raoult effects (which, respectively, raise and lower the apparent dew point) are minimized if the critical droplet size adopted is large rather than small; this reduces the curvature effect directly and reduces the Raoult effect by lowering the concentration of a soluble contaminant. Contaminants are minimized by suitable care in operation (see 4.4.3), and general influences of Raoult and Kelvin effects are taken into account by calibration (see 4.4.5).

#### 4.4.1.2 *Principles*

When moist air at temperature $T$, pressure $p$ and mixing ratio $r_w$ (or $r_i$) is cooled, it eventually reaches its saturation point with respect to a free water surface (or to a free ice surface) and a deposit of dew (or frost) can be formed on a non-hygroscopic surface. The temperature of this saturation point is called the dew-point temperature $T_d$ (or the frost-point temperature $T_f$). The corresponding saturation vapour pressure with respect to water $e'_w$ (or ice $e'_i$) is a function of $T_d$ (or $T_f$), as shown in the following equations:

$$e'_w\left(p, T_d\right) = f\left(p\right) \cdot e_w\left(T_d\right) = \frac{r \cdot p}{0.62198 + r} \tag{4.3}$$

$$e'_i\left(p, T_f\right) = f\left(p\right) \cdot e_i\left(T_f\right) = \frac{r \cdot p}{0.62198 + r} \tag{4.4}$$

The hygrometer measures $T_d$ or $T_f$. Despite the great dynamic range of moisture in the troposphere, this instrument is capable of detecting both very high and very low concentrations.

It is important to determine whether the deposit is supercooled liquid or ice when the surface temperature is at or below freezing point. For a given condensation temperature, the vapour pressure over supercooled water is higher than over ice.

The chilled-mirror hygrometer is used occasionally for meteorological measurements and as a reference instrument both in the field and in the laboratory.

### 4.4.2 Description

#### 4.4.2.1 *Sensor assembly*

The most widely used systems employ a small polished-metal reflecting surface, cooled electrically using a Peltier-effect device. The sensor consists of a thin metallic mirror of small (approximately 5 mm to 10 mm) diameter that is thermally regulated using a cooling assembly (and usually a heater), with a temperature sensor (usually a miniature PRT) embedded on the underside of the mirror. The mirror should have a high thermal conductance, optical reflectivity and corrosion resistance combined with a low permeability to water vapour. Materials used include gold, rhodium-plated silver, chromium-plated copper and stainless steel.

The mirror may be equipped with an optical detection assembly part to automatically detect contaminants that may increase or decrease the apparent dew point (see 4.4.2.2), so that they may be removed.

#### 4.4.2.2 *Optical detection assembly*

An electro-optical system is usually employed to detect the formation of condensate and to provide the input to the servo-control system to regulate the temperature of the mirror. A narrow beam of light is directed at the mirror at an angle of incidence of about 55°. The light source may be incandescent or an LED. In simple systems, the intensity of the directly reflected light is detected by a photodetector that regulates the cooling and heating assembly through a servo-control. The specular reflectivity of the surface decreases as the thickness of the deposit increases; cooling should reduce while the deposit is thin, with a reduction in reflectance in the range of 5% to 40%. More elaborate systems use an auxiliary photodetector which additionally detects the light scattered by the deposit; the two detectors are capable of very precise control. A second, uncooled, mirror may be used to improve the control system.

Greatest precision is obtained by controlling the mirror to a temperature at which condensate neither accumulates nor dissipates; however, in practice, the servo-system will oscillate around this temperature. The response time of the mirror to heating and cooling is critical in respect of the amplitude of the oscillation, and should be of the order of 1 to 2 s. Airflow rate needs to be reasonably stable and sudden changes should be avoided to maintain a stable deposit on the mirror. It is possible to determine the temperature at which condensation occurs with a resolution of 1 mK in some cases, and an overall uncertainty of 0.1 K (at coverage probability of 95%, coverage factor $k = 2$), or more, depending on the calibration uncertainty as well as other factors.

Historical types of dew-point hygrometer with manual control of temperature are largely obsolete.

#### 4.4.2.3 *Thermal control assembly*

A Peltier-effect thermo-junction device provides a simple reversible heat pump; the polarity of direct current energization determines whether heat is pumped to, or from, the mirror. The device is bonded to, and in good thermal contact with, the underside of the mirror. Commonly, a multistage Peltier device is used, with the greatest cooling requiring the most stages. When measuring relatively dry gases, initial cooling is needed to several degrees below the condensation temperature to form a detectable film of droplets or ice particles.

Thermal control is achieved by using an electrical servo-system that takes as input the signal from the optical detector subsystem. Modern systems operate under microprocessor control.

Integral supplementary cooling is commonly provided to control overall temperature at the instrument head and to extract heat generated by the Peltier element. This can take the form of forced air cooling, or a closed-cycle refrigerant system. Alternatively, some instrument types use a sterling engine for supplementary temperature control. In older instruments, a low-boiling-point fluid, such as ethanol, is used with external refrigeration to provide supplementary cooling, but this is becoming less common. In addition, supplementary heating (and in some regimes a heated sampling tube) is used to protect against unwanted condensation.

#### 4.4.2.4 *Temperature display system*

The mirror temperature, as measured by the electrical thermometer embedded beneath the mirror surface, is output as the dew point of the air sample. Commercial instruments normally include an electrical interface for the mirror thermometer and a digital display, but may also provide digital and analogue electrical outputs for use with data-logging equipment. A chart recorder can be used for continuous monitoring of an analogue output of the mirror thermometer signal, but this is becoming less common. Some hygrometers provide a separate PRT output, distinct from the PRT that is used for temperature control, of the mirror.

#### 4.4.2.5 *Instrument format*

Commonly, laboratory dew-point hygrometers are bench-top or rack-mounted instruments used with tubing to sample air from a chosen location. The sample tubing is heated if used in a range where there is a risk of condensation

An alternative format has a remote sensor head containing the Peltier, mirror, optics and temperature sensing systems. In some cases the remote head is designed to measure in free air, without forced ventilation.

#### 4.4.2.6 *Auxiliary systems*

A microscope may be incorporated to provide a visual method to discriminate between supercooled water droplets and ice crystals for mirror temperatures below 0 °C. Some instruments have a detector mounted on the mirror surface to provide an automatic procedure for this purpose, while others employ a method based on reflectance.

A microprocessor-based system may incorporate algorithms to calculate and display relative humidity. In this case, it is important that the instrument should discriminate correctly between a water and an ice deposit. In addition, the calibration and placement of the external thermometer will be critical for obtaining correct and representative relative humidity values. If other humidity quantities are calculated, such as volume fraction or ratio, the result also depends on pressure, which is either measured, or based on a set value.

Many instruments provide an automatic procedure for minimizing the effects of contamination. This may be a regular heating cycle in which volatile contaminants are evaporated and removed in the air stream. During such a heating cycle, the instrument will either give elevated readings, or will output a fixed recent value until normal readings resume. Systems with a wiper to automatically clean the mirror are also in use. Visual inspection, where possible, can confirm the quality of the water or ice film as an indication of cleanliness.

For meteorological measurements, and in most laboratory applications, a small pump is required to draw the sampled air through the measuring chamber. A regulating device is also required to set the flow at a rate that is consistent with the stable operation of the mirror temperature servo-control system and at an acceptable rate of response to changes in humidity. This can

usually be achieved by using a needle valve between the hygrometer outlet and the pump. In some instruments an internal pump is provided. The optimum flow rate is dependent upon the moisture content of the air sample and is normally within the range of 0.25 to 1 L $min^{-1}$.

### 4.4.3 Observation procedure

The correct operation of a dew-point hygrometer requires an appropriate volume airflow rate through the measuring chamber, although the exact flowrate is not usually critical. The setting of a needle valve for this purpose, usually located downstream of the measuring chamber, is likely to require adjustment to accommodate diurnal variations in air temperature. Sudden adjustment of the airflow can momentarily disturb the operation of the hygrometer. Any adjustment should be made with sufficient time in order for a stable operation to be achieved before a reading is taken. The amount of time required will depend upon the control cycle of the individual instrument. The manufacturer's instructions should be consulted to provide appropriate guidance on the airflow rate to be set and on details of the instrument's control cycle.

The condition of the mirror should be checked frequently; the mirror should be cleaned as necessary. The stable operation of the instrument does not necessarily imply that the mirror is clean. It should be washed with distilled water and dried carefully by wiping it with a soft cloth or cotton bud to remove any soluble contaminant. Alternatively, instead of wiping dry, a generous drop of water on the mirror can be pulled away using the cotton bud. It is a sign of a clean mirror if the drop pulls away cleanly. If the mirror is not visually clean and free from tide-marks, then cleaning should be repeated. Care must be taken not to scratch the surface of the mirror, most particularly where the surface has a thin plating to protect the substrate or where an ice/liquid detector is incorporated. However, an isolated surface scratch will not typically prevent the instrument from operating. If an air filter is not in use, cleaning should be performed at least daily. If an air filter is in use, its condition should be inspected at each observation. The observer should take care not to stand next to the air inlet or to allow the outlet to become blocked.

For readings at, or below, 0 °C the observer should determine whether the mirror condensate is supercooled water or ice. If no automatic indication is given, the mirror must be observed. From time to time the operation of any automatic system should be verified.

An uncertainty of ±0.1 K over a wide dew-point range (–60 °C to 50 °C) is specified for the best instruments. The uncertainty in use will depend on the uncertainty of calibration, and on other factors.

### 4.4.4 Exposure and siting

The criteria for the siting of the sensor unit are similar to those for any aspirated hygrometer. They tend to be less stringent than for either a psychrometer or a relative humidity sensor. This is because the dew or frost point of an air sample is unaffected by changes to the ambient temperature provided that it remains above the dew point at all times. For this reason, a temperature screen is not required. The sensor should be exposed in an open space and may be mounted on a post, within a protective housing structure, with an air inlet at the required level.

For hygrometers requiring a flow of gas through the instrument, an air-sampling system is required. This is normally a small pump that must draw air from the outlet port of the measuring chamber and eject it away from the inlet duct. In some cases, the pump is integral to the hygrometer. Recirculation of the airflow should be avoided as this represents a poor sampling technique, although under stable operation the water-vapour content at the outlet should be effectively identical to that at the inlet. Recirculation may be avoided by fixing the outlet above the inlet, although this may not be effective under radiative atmospheric conditions when a negative air temperature lapse rate exists.

An air filter should be provided for continuous outdoor operations. It must be capable of allowing an adequate throughflow of air without a large blocking factor, as this may result in

a significant drop in air pressure and affect the condensation temperature in the measuring chamber. A sintered metal filter may be used in this application to capture all but the smallest aerosol particles. A metal filter has the advantage that it may be heated easily by an electrical element in order to keep it dry under all conditions. It is more robust than the membrane-type filter and more suited to passing the relatively high airflow rates required by the chilled-mirror method as compared with the sorption method. On the other hand, a metallic filter may be more susceptible to corrosion by atmospheric pollutants than some membrane filters.

Instruments requiring an air sampling system need to pay attention to possible pressure changes during the air sampling. Where a filter or lengthy sample tubing causes a pressure drop, this can lead to an underestimate of dew point. If the air pressure in the sensing volume above the mirror is significantly different from the ambient pressure, this needs to be measured and the change in dew-point temperature must be properly considered.

### 4.4.5 Calibration and field inspection

#### 4.4.5.1 *Calibration*

A dew-point hygrometer should be calibrated in terms of dew-point temperature against a dew-point reference, usually in a laboratory. A calibration can be made directly against a primary dew-point generator, or by comparison against a traceably calibrated dew-point hygrometer, using as a transfer medium any stable source of humid gas sampled by both of them simultaneously. To apply the calibration, in some cases the dew-point hygrometer readings can be adjusted (for example, in software). In other cases, an adjustment to electronics can partly or fully implement the calibration. Alternatively, corrections may be applied arithmetically, particularly in laboratory usage. To whatever extent calibration corrections or functions are applied, any residual error needs to be taken into account as a component of uncertainty in using the instrument.

If any associated air temperature sensor is used, it too needs to be calibrated. General guidance on calibration of thermometers is given in the present volume, Chapter 2. For use in air, either the thermometer is calibrated in air or, if calibrated in a liquid bath, suitable additional uncertainty is allowed for applying this calibration to measurements in air. This would include components due to the different self-heating in air, the different thermal exchange with air, and radiative effects.

If a hygrometer derives relative humidity from measured dew point and temperature, calibration of the relative humidity output is also relevant. Although, in principle, this output can be calibrated directly in terms of relative humidity, this will normally be temperature-dependent and will therefore require an extensive matrix of calibration values. A better approach is to ensure that the relative humidity is evaluated from dew-point and temperature values whose calibration corrections have already been applied – whether this is done wholly arithmetically, or in corrections applied within the instrument.

#### 4.4.5.2 *Field inspection*

Regular comparisons should be made against a reference instrument, such as an Assmann psychrometer or another chilled-mirror hygrometer, or even a relative humidity instrument, as the operation of a field chilled mirror is subject to a number of influences which may degrade its performance. An instrument operating continuously in the field should be the subject of weekly check measurements. As the opportunity arises, its operation at both dew and frost points should be verified. When the mirror temperature is below 0 °C the deposit should be inspected visually, if this is possible, to determine whether it is of supercooled water or ice.

A possible check is to compare the mirror temperature measurement with the air temperature while the thermal control system of the hygrometer is inactive. The check is best done with the mirror as openly exposed as possible to ambient air, by removing any head cover. Checking is best performed under stable, non-condensing conditions. In bright sunshine, the sensor and

duct should be shaded and allowed to come to equilibrium. For the check to be meaningful, it is essential that the mirror and its housing reach ambient temperature. This can take considerable time after switching off normal operation.

An independent field check of the mirror thermometer interface can be performed by simulating the thermometer signal. In the case of a PRT, a standard platinum resistance simulation box, or a decade resistance box and a set of appropriate tables, may be used. A special simulator interface for the hygrometer control unit may also be required.

## 4.5 HYGROMETERS USING ABSORPTION OF ELECTROMAGNETIC RADIATION

The water molecule absorbs EMR in a range of wavebands and discrete wavelengths; this property can be exploited to obtain a measure of the molecular concentration of water vapour in a gas. The most useful regions of the electromagnetic spectrum for this purpose lie in the UV and IR. Therefore, the techniques are often classified as optical hygrometry or, more correctly, EMR absorption hygrometry.

The method makes use of measurements of the attenuation of radiation in a waveband specific to water-vapour absorption, along the path between a source of the radiation and a detector. There are two principal methods for determining the degree of attenuation of the radiation as follows:

(a) Transmission of radiation at two wavelengths, one of which is strongly absorbed by water vapour and the other being either not absorbed or only very weakly absorbed: if a single source is used to generate the radiation at both wavelengths, the ratio of their emitted intensities may be accurately known, so that the attenuation at the absorbed wavelength can be determined by measuring the ratio of their intensities at the receiver. The most widely used source for this technique is a tungsten lamp, filtered to isolate a pair of wavelengths in the IR region. The measuring path is normally greater than 1 m.

(b) Transmission of narrowband radiation at a fixed intensity to a calibrated detector: the most commonly used source of radiation is hydrogen gas; the emission spectrum of hydrogen includes the Lyman-Alpha line at 121.6 nm, which coincides with a water-vapour absorption band in the UV region where there is little absorption by other common atmospheric gases. The measuring path is typically a few centimetres in length.

Both types of EMR absorption hygrometers require frequent calibration and are more suitable for measuring changes in vapour concentration than absolute levels. The most widespread application of the EMR absorption hygrometer is to monitor very high-frequency variations in humidity since the method does not require the detector to achieve vapour-pressure equilibrium with the sample. The time constant of an optical hygrometer is typically just a few milliseconds. The use of optical hygrometers remains restricted to research activities.

## 4.6 THE HAIR HYGROGRAPH

### 4.6.1 General considerations

The change in the length of hair has been found to be a function primarily of the change in relative humidity with respect to liquid water (both above and below an air temperature of 0 °C), with an increase of about 2% to 2.5% when the humidity changes from 0%RH to 100%RH. By rolling the hairs to produce an elliptical cross-section and by dissolving out the fatty substances with alcohol, the ratio of the surface area to the enclosed volume increases and yields a decreased lag coefficient which is particularly relevant for use at low air temperatures. This procedure also results in a more linear response function, although the tensile strength is reduced. For accurate measurements, a single hair element is to be preferred, but a bundle of hairs is commonly used to provide a degree of ruggedness. Chemical treatment with barium (BaS) or sodium sulphide ($Na_2S$) yields further linearity of response.

The hair hygrograph is considered to be a satisfactory though not very precise instrument for use in situations or during periods where extreme and very low humidities are seldom or never found. The mechanism of the instrument should be as simple as possible, even if this makes it necessary to have a non-linear scale. This is especially important in industrial regions, since air pollutants may act on the surface of the moving parts of the mechanism and increase friction between them.

The rate of response of the hair hygrograph is very dependent on air temperature. At –10 °C the lag of the instrument is approximately three times greater than the lag at 10 °C. For air temperatures between 0 °C and 30 °C and relative humidities between 20%RH and 80%RH, a good hygrograph should indicate 90% of a sudden change in humidity within about 3 min.

A good hygrograph in perfect condition should be capable of recording relative humidity at moderate temperatures with an uncertainty of ±3%RH. At low temperatures, the uncertainty will be greater.

Using hair pre-treated by rolling (as described above) is a requirement if useful information is to be obtained at low temperatures.

### 4.6.2 **Description**

The detailed mechanism of hair hygrographs varies according to the manufacturer. Some instruments incorporate a transducer to provide an electrical signal, and these may also provide a linearizing function so that the overall response of the instrument is linear with respect to changes in relative humidity.

The hair hygrograph uses a bundle of hairs held under slight tension by a small spring and connected to a pen arm in such a way as to magnify a change in the length of the bundle. A pen at the end of the pen arm is in contact with a paper chart fitted around a metal cylinder and registers the angular displacement of the arm. The cylinder rotates about its axis at a constant rate determined by a mechanical clock movement. The rate of rotation is usually one revolution either per week or per day. The chart has a scaled time axis that extends round the circumference of the cylinder and a scaled humidity axis parallel to the axis of the cylinder. The cylinder normally stands vertically.

The mechanism connecting the pen arm to the hair bundle may incorporate specially designed cams that translate the non-linear extension of the hair in response to humidity changes into a linear angular displacement of the arm.

The hair used in hair hygrographs may be of synthetic fibre. Where human hair is used, it is normally first treated as described in 4.6.1 to improve both the linearity of its response and the response lag, although this does result in lower tensile strength.

The pen arm and clock assembly are normally housed in a box with glass panels which allow the registered humidity to be observed without disturbing the instrument, and with one end open to allow the hair element to be exposed in free space outside the limits of the box. The sides of the box are separate from the solid base, but the end opposite the hair element is attached to it by a hinge. This arrangement allows free access to the clock cylinder and hair element. The element may be protected by an open mesh cage.

### 4.6.3 **Observation procedure**

The hair hygrograph should always be tapped lightly before being read in order to free any tension in the mechanical system. The hygrograph should, as far as possible, not be touched between changes of the charts except in order to make time marks.

The hair hygrograph can normally be read to the nearest 1%RH. Attention is drawn to the fact that the instrument measures relative humidity with respect to saturation over liquid water even at air temperatures below 0 °C.

The humidity of the air may change very rapidly and, therefore, accurate setting of time marks on a hygrograph is very important. In making the marks, the pen arm should be moved only in the direction of decreasing humidity on the chart. This is done so that the hairs are slackened by the displacement and, to bring the pen back to its correct position, the restoring force is applied by the tensioning spring. However, the effect of hysteresis may be evidenced in the failure of the pen to return to its original position.

### 4.6.4 Exposure and siting

The hygrograph should be exposed in a thermometer screen. Ammonia is very destructive to natural hair. Exposure in the immediate vicinity of stables and industrial plants using ammonia should be avoided.

### 4.6.5 Sources of error

#### 4.6.5.1 *Changes in zero offset*

For various reasons which are poorly understood, the hygrograph is liable to change its zero. The most likely cause is that excess tension has been induced in the hairs. For instance, the hairs may be stretched if time marks are made in the direction of increasing humidity on the chart or if the hygrograph mechanism sticks during decreasing humidity. The zero may also change if the hygrograph is kept in very dry air for a long time, but the change may be reversed by placing the instrument in a saturated atmosphere for a sufficient length of time.

#### 4.6.5.2 *Errors due to contamination of the hair*

Most kinds of dust will cause appreciable errors in observations (perhaps as much as 15%RH). In most cases this may be eliminated, or at least reduced, by cleaning and washing the hairs. However, the harmful substances found in dust may also be destructive to hair (see 4.6.4).

#### 4.6.5.3 *Hysteresis*

Hysteresis is exhibited both in the response of the hair element and in the recording mechanism of the hair hygrometer. Hysteresis in the recording mechanism is reduced through the use of a hair bundle, which allows a greater loading force to overcome friction. It should be remembered that the displacement magnification of the pen arm lever applies also to the frictional force between the pen and paper, and to overcome this force it requires a proportionately higher tension in the hair. The correct setting of the tensioning spring is also required to minimize hysteresis, as is the correct operation of all parts of the transducing linkage. The main fulcrum and any linearizing mechanism in the linkage introduce much of the total friction.

Hysteresis in the hair element is normally a short-term effect related to the absorption–desorption processes and is not a large source of error once vapour pressure equilibrium is established (see 4.6.5.1 in respect of prolonged exposure at low humidity).

### 4.6.6 Calibration and field inspection

The readings of a hygrograph should be checked as frequently as is practical. In the case where wet- and dry-bulb thermometers are housed in the same thermometer screen, these may be used to provide a comparison whenever suitable steady conditions prevail, but otherwise field comparisons have limited value due to the difference in response rate of the instruments.

Accurate calibration can only be obtained through the use of an environmental chamber and by comparison with reference instruments.

The 100%RH point may be checked, preferably indoors with a steady air temperature, by surrounding the instrument with a saturated cloth (though the correct reading will not be obtained if a significant mass of liquid water droplets forms on the hairs).

The ambient indoor humidity may provide a low relative humidity checkpoint for comparison against a reference aspirated psychrometer. A series of readings should be obtained.

Long-term stability and bias may be appraised by presenting comparisons with a reference aspirated psychrometer in terms of a correlation function.

### 4.6.7 Maintenance

Observers should be encouraged to keep the hair hygrograph clean.

The hair should be washed at frequent intervals using distilled water on a soft brush to remove accumulated dust or soluble contaminants. At no time should the hair be touched by fingers. The bearings of the mechanism should be kept clean and a small amount of clock oil should be applied occasionally. The bearing surfaces of any linearizing mechanism will contribute largely to the total friction in the linkage, which may be minimized by polishing the surfaces with graphite. This procedure may be carried out by using a piece of blotting paper rubbed with a lead pencil.

With proper care, the hairs may last for several years in a temperate climate and when not subject to severe atmospheric pollution. Recalibration and adjustment will be required when hairs are replaced.

## 4.7 TRACEABILITY ASSURANCE AND CALIBRATION

### 4.7.1 Principles involved in the calibration of hygrometers

Precision in the calibration of humidity-measuring instruments entails special problems, to a great extent owing to the relatively small quantity of water vapour which can exist in an air sample at normal temperatures, but also due to the general difficulty of isolating and containing gases and, more particularly, vapour. An ordered hierarchy of international traceability in humidity standards is only now emerging.

Table 4.2 shows a summary of humidity standard instruments and their performances.

### 4.7.2 Primary standards

#### 4.7.2.1 *Gravimetric hygrometry*

This instrument type is only rarely used in a small number of NMIs, but the description below is given for information.

The gravimetric method yields an absolute measure of the water-vapour content of an air sample in terms of the proportion of water vapour to air – either as a ratio of the two components (mixing ratio) or as a fraction of the total. This is expressed in terms of masses of water and air, or sometimes as volume fraction (or rarely as amount fraction, in moles, if the composition of air can be known). This is obtained by first removing the water vapour from the sample using a known mass of a drying agent, such as anhydrous phosphorous pentoxide ($P_2O_5$) or magnesium perchlorate ($Mg(ClO_4)_2$). The mass of the water vapour is determined by weighing the drying

**Table 4.2. Standard instruments for the measurement of humidity**

| *Standard instrument* | *Dew-point temperature* | | *Relative humidity (%RH)* | |
|---|---|---|---|---|
| | *Range (°C)* | *Uncertainty (K)* | *Range* | *Uncertainty* |
| *Primary standard* | | | | |
| Requirement | –60 to –15<br>–15 to 40 | 0.3<br>0.1 | 5 to 100<br>5 to 100 | 0.2<br>0.2 |
| Gravimetric hygrometer | –60 to –35<br>–35 to 35<br>35 to 60 | 0.25<br>0.03<br>0.25 | | |
| Standard two-temperature humidity generator | –75 to –15<br>–15 to 30<br>30 to 80 | 0.25<br>0.1<br>0.2 | | |
| Standard two-pressure humidity generator | –75 to 30 | 0.2 | | |
| *Secondary standard* | | | | |
| Requirement | –80 to –15<br>–15 to 40 | 0.75<br>0.25 | 5 to 100 | 0.5 |
| Chilled-mirror hygrometer | –60 to 40 | 0.15 | | |
| Reference psychrometer | | | 5 to 100 | 0.6 |
| *Reference standard* | | | | |
| Requirement | –80 to –15<br>–15 to 40 | 1.0<br>0.3 | 5 to 100 | 1.5 |
| Reference psychrometer | | | 5 to 100 | 0.6 |
| Chilled-mirror hygrometer | –60 to 40 | 0.3 | | |
| *Working standard* | | | | |
| Requirement | –15 to 40 | 0.5 | 5 to 100 | 2 |
| Assmann psychrometer | –10 to 25 | | 40 to 90 | 1 |
| Chilled-mirror hygrometer | –10 to 30 | 0.5 | | |
| Electrical capacitive hygrometer (*for regularly calibrated and carefully maintained high performance instruments*) | –20 to 40<br>15 to 30 | | 5 to 95<br>5 to 95 | 2<br>1 |

agent before and after absorbing the vapour. The mass of the dry sample is determined either by weighing (after liquefaction to render the volume of the sample manageable) or by measuring its volume (and having knowledge of its density).

The complexity of the apparatus required to accurately carry out the procedure described limits the application of this method to the laboratory environment. In addition, a substantial volume sample of air is required for accurate measurements to be taken and a practical apparatus requires a steady flow of the humid gas for a number of hours, depending upon the humidity, in order to remove a sufficient mass of water vapour for an accurate weighing measurement. As a consequence, the method is restricted to providing an absolute calibration reference standard. Such an apparatus is found mostly in NMIs.

#### 4.7.2.2 *Dynamic two-pressure standard humidity generator*

This laboratory apparatus serves to provide a source of humid gas whose relative humidity is determined on an absolute basis. A stream of the carrier gas is passed through a saturating chamber at pressure $P_1$ and allowed to expand isothermally in a second chamber at a lower pressure $P_2$. Both chambers are maintained at the same temperature in an oil bath. The relative humidity of the water vapour-gas mixture is straightforwardly related to the total pressures in each of the two chambers through Dalton's law of partial pressures. The partial pressure $e'$ of the vapour in the low-pressure chamber will have the same relation to the saturation vapour pressure $e'_w$ as the total pressure in the high-pressure saturator has to the total pressure in the low-pressure chamber. Thus, the relative humidity $U_w$ is given by:

$$U_w = 100 \cdot e'/e'_w = 100 \cdot P_1/P_2 \tag{4.5}$$

The relation also holds for the solid phase if the gas is saturated with respect to ice at pressure $P_1$:

$$U_i = 100 \cdot e'/e'_i = 100 \cdot P_1/P_2 \tag{4.6}$$

#### 4.7.2.3 *Dynamic two-temperature standard humidity generator*

This laboratory apparatus provides a stream of humid gas at temperature $T_1$ having a dew- or frost-point temperature $T_2$. Two temperature-controlled baths, each equipped with heat exchangers and one with a saturator containing either water or ice, are used first to saturate the air-stream at temperature $T_1$ and then to heat it isobarically to temperature $T_2$. In practical designs, the air-stream is continuously circulated to ensure saturation. Test instruments draw off air at temperature $T_2$ and a flow rate that is small in proportion to the main circulation.

### 4.7.3 Secondary standards

A secondary standard instrument should be carefully maintained and removed from the calibration laboratory only for calibration with a primary standard or for intercomparison with other secondary standards. Secondary standards may be used as transfer standards from the primary standards.

A chilled-mirror hygrometer may be used as a secondary standard instrument under controlled conditions of air temperature, humidity and pressure. For this purpose, it should be calibrated from a recognized accredited laboratory, giving uncertainty limits throughout the operational range of the instrument. This calibration must be directly traceable to a primary standard and should be renewed at an appropriate interval (usually once every 12 to 24 months).

General considerations for chilled-mirror hygrometers are discussed in 4.4. This method presents a fundamental technique for determining atmospheric humidity and any change of the air pressure resulting from the sampling technique must be taken into account by using the equations given in 4.4.1.2.

High-performance capacitive hygrometers can also be used as secondary standards. They must be traceable and regularly calibrated against a primary standard in a laboratory, typically every 12 months.

### 4.7.4 Working standards (and field reference instruments)

A chilled-mirror hygrometer or an Assmann psychrometer may be used as a working standard for comparisons under ambient conditions in the field or the laboratory. For this purpose, it is necessary to have performed comparisons at least at the reference standard level. The comparisons should be performed at least once every 12 months under stable room conditions. The working standard will require a suitable aspiration device to sample the air.

High-performance capacitive hygrometers can also be used as working standards or field reference instruments. They must be traceable and regularly calibrated against a traceable standard in a laboratory, typically every 12 months. For additional caution, they may be checked quarterly or monthly against other standards.

### 4.7.5 Salt solutions

A salt solution creates characteristic values of the relative humidity in the air above it. The values of relative humidity are dependent on the chemical structure of the salt, the salt concentration and the temperature. Two types of salt solutions are available:

(a) An unsaturated salt solution, which comes in the form of ampoules of the solution, generates an atmosphere with a certain relative humidity. These ampoules are generally used to soak a pad in a housing designed for exposing a sensor to the humidity produced.

(b) A saturated salt solution, in which some salt remains in the solid phase, maintains a stable concentration of relative humidity. In this case, the vapour pressure depends only on temperature.

Vessels containing saturated solutions of appropriate salts may be used to calibrate relative humidity measuring instruments. Commonly used salts and their saturation relative humidities at 25 °C are as follows:

| | |
|---|---|
| Potassium sulphate ($K_2SO_4$): | 97.0%RH |
| Barium chloride ($BaCl_2$): | 90.3%RH |
| Sodium chloride (NaCl): | 75.3%RH |
| Magnesium nitrate ($Mg(NO_3)_2$): | 52.9%RH |
| Magnesium chloride (MgCl): | 33.0%RH |
| Calcium chloride ($CaCl_2$): | 29.0%RH |
| Lithium chloride (LiCl): | 11.1%RH |

Potassium sulphate and lithium chloride are convenient saturated salt solutions and provide easy and extended ranges of relative humidity environments at 11%RH and 97%RH.

It is important that the surface area of the solution is large compared to that of the sensor element and the enclosed volume of air so that equilibrium may be achieved quickly; an airtight access port is required for the test sensor. The temperature of the vessel should be measured and maintained at a constant level as the saturation humidity for most salts has a significant temperature coefficient. The homogeneity of the relative humidity above the solutions is improved by mixing the air with a fan in the airtight volume.

Care should be taken when using saturated salt solutions. The degree of toxicity and corrosiveness of the solutions should be known to the personnel dealing with them. The salts listed above may all be used quite safely, but it is nevertheless important to avoid contact with the skin, and to avoid ingestion and splashing into the eyes. The salts should always be kept in secure and clearly labelled containers which detail any hazards involved. Care should be taken when dissolving calcium chloride crystals in water, as much heat is evolved. Chemical hazards are described in 4.8.3 in greater detail.

Saturated salt solutions provide a practical method for adjusting a certain type of hygrometer (capacitive). But for calibration purposes, a traceable relative humidity reference instrument should also be used in the airtight volume above the saturated salt solutions.

### 4.7.6 Calibration methods

#### 4.7.6.1 *General comments*

Humidity calibrations are normally carried out by comparing the instrument against a calibrated humidity reference, in a suitable humidity environment.

Environments for humidity calibration are most commonly provided using a humidity generator or a humidity-controlled (and temperature-controlled) chamber.

A humidity generator, a precision chilled mirror hygrometer, a carefully designed psychrometer or a high-performance capacitive hygrometer is used as a standard in NMHS laboratories.

#### 4.7.6.2 *Laboratory calibration*

Laboratory calibration is essential for maintaining accuracy in the following ways:

(a) Calibration method: The method for calibrating an hygrometer uses as a standard either a humidity generator or a hygrometer:

  (i) Using a humidity generator as a standard: The hygrometer to be calibrated is placed in the chamber of the humidity generator, or alternatively, the moist air generated by the humidity generator is led to the hygrometer to be calibrated. The humidity value indicated by the humidity generator is then compared with the indication value of the hygrometer to be calibrated;

  (ii) Using a hygrometer as a standard: The humidity value indicated by the hygrometer to be calibrated is compared with the standard hygrometer, while both hygrometers are placed in a chamber of humidity generator, or alternatively while the moist air generated by the humidity generator is led to both hygrometers.

(b) Humidity generation method: The main methods of humidity generation are as follows:

  (i) Two-pressure generator;

  (ii) Two-temperature generator;

  (iii) Two-pressure and two-temperature generator;

  (iv) Mixed-flow generator;

  (v) Salt solution;

  (vi) Humidity chamber;

(c) Reference and standard instruments: Laboratory calibration of reference and standard instruments requires a precision humidity generator and a suitable transfer standard hygrometer. Two-pressure and two-temperature humidity generators can deliver a suitably controlled flow of air at a predetermined temperature and dew point. The calibration should be performed at least every 12 months and over the full range of the reference application for the instrument. The calibration of the mirror thermometer and the temperature display system could be performed independently at least once every 12 months;

(d) Field and working standard instruments: Laboratory calibration of field and working standard instruments should be carried out on the same regular basis as for other operational thermometers. For this purpose, the chilled-mirror sensor device may be considered separately from the control unit. The mirror thermometer should be calibrated independently and the control unit could be calibrated on the same regular basis as other

items of precision electronic equipment. The calibration of a field instrument in a humidity generator is not strictly necessary if the components have been calibrated separately, as described previously.

The correct operation of an instrument may be verified under stable room conditions by comparison with a reference instrument, such as a standard chilled-mirror hygrometer or an Assmann psychrometer. If the field instrument incorporates an ice detector, the correct operation of this system should be verified.

#### 4.7.6.3 *Field calibration*

Regular calibration is required for all humidity instruments installed in the field. Depending on the instruments, calibration is done in the field only, in the laboratory only, or, alternatively, in both the laboratory and field.

For psychrometers and dew-point hygrometers that use a temperature detector, calibration can be checked whenever a regular maintenance routine is performed. Comparison with a working standard, such as an Assmann psychrometer, should be performed very regularly.

The use of a standard type of aspirated psychrometer, such as the Assmann, as a working standard has the advantage that its integrity can be verified by comparing the dry- and wet-bulb thermometers, and that adequate aspiration may be expected from a healthy sounding fan. The reference instrument should itself be calibrated at an interval appropriate to its type.

A practical field inspection is most frequently achieved using well-designed aspirated psychrometers and dew-point measuring instruments or capacitive hygrometers as working standards. These specific types of standards must be traceable to the higher levels of standards by careful calibrations. Any instrument used as a standard must be individually calibrated for all variables involved in calculating humidity (air temperature, wet-bulb temperature, dew-point temperature, and so forth). Other factors affecting performance, such as airflow, must also be checked.

Saturated salt solutions can be applied with humidity-measuring instruments that require only a small-volume sample. A very stable ambient temperature is required and it is difficult to be confident about their use in the field. This limitation can be overcome by careful comparison with a working standard above the saturated salt solutions. This method can also be applied in the laboratory for humidity-measuring instruments used in the field.

When using salt solutions for control purposes, it should be borne in mind that the nominal humidity value given for the salt solution itself is not traceable to any primary standard.

Another option is to generate some points of specific humidity using a portable humidity generator at a field and calibrate with a working standard hygrometer.

## 4.8 TIME CONSTANTS, PROTECTIVE FILTERS AND SAFETY

### 4.8.1 Time constants of humidity sensors

The specification of the time constant for a humidity sensor implies that the response of the sensor to a step change in humidity is consistent with a known function. In general usage, the term refers to the time taken for the sensor to indicate 63.2% ($1/e$) of a step change in the measurand (in this case humidity), and assumes that the sensor has a first-order response to changes in the measurand (namely, the rate of change of the measurement is proportional to the difference between the measurement and the measurand). It is then possible to predict that 99.3% of the change will take place after a period of five time constants in duration.

Table 4.3 gives $1/e$ time-constant values typical for various types of humidity sensor.

**Table 4.3. Time constants for humidity sensors**

| *85% relative humidity* | *1/e time constant (s)* | | |
|---|---|---|---|
| *Sensor type* | *20 °C* | *0 °C* | *–20 °C* |
| Ordinary human hair | 32 | 75 | 440 |
| Rolled hair | 10 | 10 | 12 |
| Electrical capacitance | 1–10 | 1–10 | 1–10 |
| Electrical resistance | 1–10 | — | — |
| Assmann psychrometer | | | |
| Condensation hygrometers | 30–50 | 30–50 | 30–50 |
| Electrolytic hygrometers | | | |
| Optical hygrometer | < 0.01 | < 0.01 | < 0.01 |

Note: The first-order relation does not hold particularly well for sorption sensors since the forcing agent for vapour equilibrium, the local gradient of vapour pressure, is dependent upon the local migration of water vapour molecules within the body of a solid humidity element. In general, a first-order response will be most closely exhibited by those sensors having a thin active element.

### 4.8.2 **Protective filters**

A protective filter is commonly used to protect a humidity sensor from contaminants that may adversely affect its performance. Where a sensor is not artificially aspirated, the use of a filter tends to slow the response rate of the sensor by preventing the bulk movement of air and by relying upon molecular diffusion through the filter material. Although the diffusion of water vapour through some materials, such as some cellulose products, is theoretically more rapid than for still air, porous hydrophobic membranes achieve better diffusion rates in practice. The pore size should be sufficiently small to trap harmful aerosol particles (in a maritime environment sea-salt particles may be present in significant quantity down to a diameter of 0.1 μm) and the porosity should be sufficient to allow an adequate diffusion rate.

The size of the filter as well as its porosity affects the overall diffusion rate. Diffusion is enhanced by aspiration, but it must be remembered that this technique relies upon maintaining low air pressure on the sensing side of the filter, and that this can have a significant effect on the measurement.

Non-aspirated sensors should, in general, be protected using a hydrophobic, inert material. High-porosity polymer membranes made from an expanded form of polytetrafluoroethylene have been used successfully for this purpose in a variety of situations and are fairly robust.

Sintered metal filters may be used, but they should be heated to avoid problems with condensation within the material. This is not normally appropriate for a relative humidity sensor, but is quite acceptable for a dew-point sensor. Sintered metal filters are robust and well suited for aspirated applications, which allow the use of a filter having a large surface area and, consequently, an acceptably small pressure differential.

Where diffusion is not enhanced by artificial aspiration, the relation of the surface area of the filter to the volume of the air being sampled by the sensor must be considered. In the case of a typical sorption sensor composed of a flat substrate, a flat membrane positioned close to the sensor surface will provide the optimum configuration. In the case of a cylindrical sensing surface, a cylindrical filter is appropriate.

### 4.8.3 **Safety**

Chemical agents are widely used in the measurement of humidity. The properties of such agents should always be made known to the personnel handling them. All chemicals should be kept in secure and clearly labelled containers and stored in an appropriate environment. Instructions concerning the use of toxic materials may be prescribed by local authorities.

The safety data sheet, also called the material safety data sheet, should be carefully read and understood before handling chemicals. This compulsory document provided by the manufacturer for each chemical or salt details all relevant information on the composition, properties, potential danger, safety measures, handling and storage of the said chemical.

Saturated salt solutions are widely used in the measurement of humidity. The notes that follow give some guidance for the safe use of some commonly used salts:

(a) Barium chloride ($BaCl_2$): Colourless crystals; very soluble in water; stable, but may emit toxic fumes in a fire; no hazardous reaction with water, acids, bases, oxidizers or with combustible materials; ingestion causes nausea, vomiting, stomach pains and diarrhoea; harmful if inhaled as dust and if it comes into contact with the skin; irritating to eyes; treat with copious amounts of water and obtain medical attention if ingested;

(b) Calcium chloride ($CaCl_2$): Colourless crystals; deliquescent; very soluble in water, dissolves with increase in heat; will initiate exothermic polymerization of methyl vinyl ether; can react with zinc to liberate hydrogen; no hazardous reactions with acids, bases, oxidizers or combustibles; irritating to the skin, eyes and respiratory system; ingestion causes gastric irritation; ingestion of large amounts can lead to hypercalcaemia, dehydration and renal damage; treat with copious amounts of water and obtain medical attention;

(c) Lithium chloride (LiCl): Colourless crystals; stable if kept dry; very soluble in water; may emit toxic fumes in a fire; ingestion may affect ionic balance of blood leading to anorexia, diarrhoea, vomiting, dizziness and central nervous system disturbances; kidney damage may result if sodium intake is low (provide plenty of drinking water and obtain medical attention); no hazardous reactions with water, acids, bases, oxidizers or combustibles;

(d) Magnesium nitrate ($Mg(NO_3)_2$): Colourless crystals; deliquescent; very soluble in water; may ignite combustible material; can react vigorously with deoxidizers, can decompose spontaneously in dimethylformamide; may emit toxic fumes in a fire (fight the fire with a water spray); ingestion of large quantities can have fatal effects (provide plenty of drinking water and obtain medical attention); may irritate the skin and eyes (wash with water);

(e) Potassium nitrate ($KNO_3$): White crystals or crystalline powder; very soluble in water; stable but may emit toxic fumes in a fire (fight the fire with a water spray); ingestion of large quantities causes vomiting, but it is rapidly excreted in urine (provide plenty of drinking water); may irritate eyes (wash with water); no hazardous reaction with water, acids, bases, oxidizers or combustibles;

(f) Sodium chloride (NaCl): Colourless crystals or white powder; very soluble in water; stable; no hazardous reaction with water, acids, bases, oxidizers or combustibles; ingestion of large amounts may cause diarrhoea, nausea, vomiting, deep and rapid breathing and convulsions (in severe cases obtain medical attention).

Advice concerning the safe use of mercury is given in the present volume, Chapter 3, Annex 3.A, 4.

# ANNEX 4.A. DEFINITIONS AND SPECIFICATIONS OF WATER VAPOUR IN THE ATMOSPHERE

(1) ***The mixing ratio r*** of moist air is the ratio of the mass $m_v$ of water vapour to the mass $m_a$ of dry air with which the water vapour is associated:

$$r = \frac{m_v}{m_a} \tag{4.A.1}$$

(2) ***The specific humidity, mass concentration*** or ***moisture content q*** of moist air is the ratio of the mass $m_v$ of water vapour to the mass $m_v + m_a$ of moist air in which the mass of water vapour $m_v$ is contained:

$$q = \frac{m_v}{m_v + m_a} \tag{4.A.2}$$

(3) ***Vapour concentration (density of water vapour in a mixture)*** or ***absolute humidity***: For a mixture of water vapour and dry air the vapour concentration $\rho_v$ is defined as the ratio of the mass of vapour $m_v$ to the volume $V$ occupied by the mixture:

$$\rho_v = \frac{m_v}{V} \tag{4.A.3}$$

(4) ***Mole fraction of the water vapour of a sample of moist air***: The mole fraction $x_v$ of the water vapour of a sample of moist air, composed of a mass $m_a$ of dry air and a mass $m_v$ of water vapour, is defined by the ratio of the number of moles of water vapour ($n_v = m_v/M_v$) to the total number of moles of the sample $n_v + n_a$, where $n_a$ indicates the number of moles of dry air ($n_a = m_a/M_a$) of the sample concerned. This gives:

$$x_v = \frac{n_v}{n_a + n_v} \tag{4.A.4}$$

or:

$$x_v = \frac{r}{0.621\,98 + r} \tag{4.A.5}$$

where $r$ is merely the mixing ratio ($r = m_v/m_a$) of the water vapour of the sample of moist air.

(5) ***The vapour pressure e'*** of water vapour in moist air at total pressure $p$ and with mixing ratio $r$ is defined by:

$$e' = \frac{r}{0.621\,98 + r}\, p = x_v \cdot p \tag{4.A.6}$$

(6) ***Saturation***: Moist air at a given temperature and pressure is said to be saturated if its mixing ratio is such that the moist air can coexist in neutral equilibrium with an associated condensed phase (liquid or solid) at the same temperature and pressure, the surface of separation being plane.

(7) ***Saturation mixing ratio***: The symbol $r_w$ denotes the saturation mixing ratio of moist air with respect to a plane surface of the associated liquid phase. The symbol $r_i$ denotes the saturation mixing ratio of moist air with respect to a plane surface of the associated solid phase. The associated liquid and solid phases referred to consist of almost pure water and almost pure ice, respectively, there being some dissolved air in each.

(8) ***Saturation vapour pressure in the pure phase***: The saturation vapour pressure $e_w$ of pure aqueous vapour with respect to water, is the pressure of the vapour when in a state of neutral equilibrium with a plane surface of pure water at the same temperature and pressure; similarly for $e_i$ with respect to ice; $e_w$ and $e_i$ are temperature-dependent functions only, namely:

$$e_w = e_w(T) \tag{4.A.7}$$

$$e_i = e_i(T) \tag{4.A.8}$$

(9) ***Mole fraction of water vapour in moist air saturated with respect to water***: The mole fraction of water vapour in moist air saturated with respect to water, at pressure $p$ and temperature $T$, is the mole fraction $x_{vw}$ of the water vapour of a sample of moist air, at the same pressure $p$ and the same temperature $T$, that is in stable equilibrium in the presence of a plane surface of water containing the amount of dissolved air corresponding to equilibrium. Similarly, $x_{vi}$ will be used to indicate the saturation mole fraction with respect to a plane surface of ice containing the amount of dissolved air corresponding to equilibrium.

(10) ***Saturation vapour pressure of moist air***: The saturation vapour pressure with respect to water $e'_w$ of moist air at pressure $p$ and temperature $T$ is defined by:

$$e'_w = \frac{r_w}{0.621\,98 + r_w} p = x_{vw} \cdot p \tag{4.A.9}$$

Similarly, the saturation vapour pressure with respect to ice $e'_i$ of moist air at pressure $p$ and temperature $T$ is defined by:

$$e'_i = \frac{r_i}{0.621\,98 + r_i} p = x_{vi} \cdot p \tag{4.A.10}$$

(11) ***Relations between saturation vapour pressures of the pure phase and of moist air***: In the meteorological range of pressure and temperature the following relations hold with an error of 0.5% or less:

$$e'_w = e_w \tag{4.A.11}$$
$$e'_i = e_i \tag{4.A.12}$$

(12) ***The thermodynamic dew-point temperature*** $T_d$ of moist air at pressure $p$ and with mixing ratio $r$ is the temperature at which moist air, saturated with respect to water at the given pressure, has a saturation mixing ratio $r_w$ equal to the given mixing ratio $r$.

(13) ***The thermodynamic frost-point temperature*** $T_f$ of moist air at pressure $p$ and mixing ratio $r$ is the temperature at which moist air, saturated with respect to ice at the given pressure, has a saturation mixing ratio $r_i$ equal to the given ratio $r$.

(14) ***The dew-point and frost-point temperatures*** so defined are related to the mixing ratio $r$ and pressure $p$ by the respective equations:

$$e'_w(p, T_d) = f(p) \cdot e_w(T_d) = x_v \cdot p = \frac{r \cdot p}{0.621\,98 + r} \tag{4.A.13}$$

$$e'_i(p, T_f) = f(p) \cdot e_i(T_f) = x_v \cdot p = \frac{r \cdot p}{0.621\,98 + r} \tag{4.A.14}$$

(15)[1] ***The relative humidity*** $U_w$ ***with respect to water of moist air*** at pressure $p$ and temperature $T$ is the ratio in % of the vapour mole fraction $x_v$ to the vapour mole fraction $x_{vw}$ which the air would have if it were saturated with respect to water at the same pressure $p$ and temperature $T$. Accordingly:

$$U_w = 100\left(\frac{x_v}{x_{vw}}\right)_{p,T} = 100\left(\frac{px_v}{px_{vw}}\right)_{p,T} = 100\left(\frac{e'}{e'_w}\right)_{p,T} \tag{4.A.15}$$

where subscripts $p$, $T$ indicate that each term is subject to identical conditions of pressure and temperature. The last expression is formally similar to the classic definition based on the assumption of Dalton's law of partial pressures.

$U_w$ is also related to the mixing ratio $r$ by:

$$U_w = 100\frac{r}{r_w} \cdot \frac{0.621\,98 + r_w}{0.621\,98 + r} \tag{4.A.16}$$

where $r_w$ is the saturation mixing ratio at the pressure and temperature of the moist air.

(16)[1] ***The relative humidity $U_i$ with respect to ice of moist air*** at pressure $p$ and temperature $T$ is the ratio in % of the vapour mole fraction $x_v$ to the vapour mole fraction $x_{vi}$ which the air would have if it were saturated with respect to ice at the same pressure $p$ and temperature $T$. Corresponding to the defining equation in paragraph 15:

$$U_i = 100\left(\frac{x_v}{x_{vi}}\right)_{p,T} = 100\left(\frac{px_v}{px_{vi}}\right)_{p,T} = 100\left(\frac{e'}{e'_i}\right)_{p,T} \qquad (4.A.17)$$

(17) ***Relative humidity at temperatures less than 0 °C*** is to be evaluated with respect to water. The advantages of this procedure are as follows:

(a) Most hygrometers which are essentially responsive to the relative humidity indicate relative humidity with respect to water at all temperatures;

(b) The majority of clouds at temperatures below 0 °C consist of water, or mainly of water;

(c) Relative humidities greater than 100%RH would in general not be observed. This is of particular importance in synoptic weather messages, since the atmosphere is often supersaturated with respect to ice at temperatures below 0 °C;

(d) The majority of existing records of relative humidity at temperatures below 0 °C are expressed on a basis of saturation with respect to water.

(18) ***The thermodynamic wet-bulb temperature of moist air*** at pressure $p$, temperature $T$ and mixing ratio $r$ is the temperature $T_w$ attained by the moist air when brought adiabatically to saturation at pressure $p$ by the evaporation into the moist air of liquid water at pressure $p$ and temperature $T_w$ and containing the amount of dissolved air corresponding to equilibrium with saturated air of the same pressure and temperature. $T_w$ is defined by the equation:

$$h\left(p,T,r\right)+\left[r_w\left(p,T_w\right)-r\right]h_w\left(p,T_w\right)=h\left(p,T_w,r_w\left(p,T_w\right)\right) \qquad (4.A.18)$$

where $r_w(p,T_w)$ is the mixing ratio of saturated moist air at pressure $p$ and temperature $T_w$; $h_w(p,T_w)$ is the enthalpy[2] of 1 gram of pure water at pressure $p$ and temperature $T_w$; $h(p,T,r)$ is the enthalpy of $1 + r_w$ grams of moist air, composed of 1 gram of dry air and $r$ grams of water vapour, at pressure $p$ and temperature $T$; and $h(p,T_w,r_w\,(p,T_w))$ is the enthalpy of $1 + r_w$ grams of saturated air, composed of 1 gram of dry air and $r_w$ grams of water vapour, at pressure $p$ and temperature $T_w$. (This is a function of $p$ and $T_w$ only and may appropriately be denoted by $h_{sw}(p,T_w)$.)

If air and water vapour are regarded as ideal gases with constant specific heats, the above equation becomes:

$$T-T_w=\frac{\left[r_w\left(p,T_w\right)-r\right]L_v\left(T_w\right)}{c_{pa}+rc_{pv}} \qquad (4.A.19)$$

where $L_v(T_w)$ is the heat of vaporization of water at temperature $T_w$, $c_{pa}$ is the specific heat of dry air at constant pressure; and $c_{pv}$ is the specific heat of water vapour at constant pressure.

Note: Thermodynamic wet-bulb temperature as here defined has for some time been called "temperature of adiabatic saturation" by air-conditioning engineers.

---

[1] Equations 4.A.15 and 4.A.17 do not apply to moist air when pressure $p$ is less than the saturation vapour pressure of pure water and ice, respectively, at temperature $T$.

[2] The enthalpy of a system in equilibrium at pressure $p$ and temperature $T$ is defined as $E + pV$, where $E$ is the internal energy of the system and $V$ is its volume. The sum of the enthalpies of the phases of a closed system is conserved in adiabatic isobaric processes.

(19) ***The thermodynamic ice-bulb temperature of moist air*** at pressure $p$, temperature $T$ and mixing ratio $r$ is the temperature $T_i$ at which pure ice at pressure $p$ must be evaporated into the moist air in order to saturate it adiabatically at pressure $p$ and temperature $T_i$. The saturation is with respect to ice. $T_i$ is defined by the equation:

$$h\left(p,T,r\right)+\left[r_i\left(p,T_i\right)-r\right]h_i\left(p,T_i\right)=h\left(p,T_i,r_i\left(p,T_i\right)\right) \tag{4.A.20}$$

where $r_i(p,T_i)$ is the mixing ratio of saturated moist air at pressure $p$ and temperature $T_i$; $h_i(p,T_i)$ is the enthalpy of 1 gram of pure ice at pressure $p$ and temperature $T_i$; $h(p,T,r)$ is the enthalpy of $1 + r$ grams of moist air, composed of 1 gram of dry air and $r$ grams of water vapour, at pressure $p$ and temperature $T$; and $h(p,T_i,r_i\ (p,T_i))$ is the enthalpy of $1 + r_i$ grams of saturated air, composed of 1 gram of dry air and $r_i$ grams of water vapour, at pressure $p$ and temperature $T_i$. (This is a function of $p$ and $T_i$ only, and may appropriately be denoted by $h_{si}(p,T_i)$.)

If air and water vapour are regarded as ideal gases with constant specific heats, the above equation becomes:

$$T-T_i=\frac{\left[r_i\left(p,T_i\right)-r\right]L_s\left(T_i\right)}{c_p+rc_{pv}} \tag{4.A.21}$$

where $L_s(T_i)$ is the heat of sublimation of ice at temperature $T_i$.

The relationship between $T_w$ and $T_i$ as defined and the wet-bulb or ice-bulb temperature as indicated by a particular psychrometer is a matter to be determined by carefully controlled experiment, taking into account the various variables concerned, for example, ventilation, size of thermometer bulb and radiation.

# ANNEX 4.B. FORMULAE FOR THE COMPUTATION OF MEASURES OF HUMIDITY

These formulae are convenient for computation and sufficiently accurate for all normal meteorological applications, limited to temperature T > -45 °C for liquid water and T > -65 °C for ice. These formulae are not suitable at all below the stated temperature thresholds.

More accurate, extended in range and detailed formulations of these and other quantities may be found in Sonntag (1990, 1994). With respect to their limits, they are adequate for normal meteorological applications with a lower temperature range extension, and are specifically relevant for radiosonde purposes.

***Saturation vapour pressure:***

$e_w(t) = 6.112 \exp [17.62\, t/(243.12 + t)]$ (4.B.1) Water (–45 °C to 60 °C) (pure phase)

$e'_w(p,t) = f(p) \cdot e_w(t)$ (4.B.2) Moist air

$e_i(t) = 6.112 \exp [22.46\, t/(272.62 + t)]$ (4.B.3) Ice (–65 °C to 0 °C) (pure phase)

$e'_i(p,t) = f(p) \cdot e_i(t)$ (4.B.4) Moist air

$f(p) = 1.0016 + 3.15 \cdot 10^{-6}\, p - 0.074\, p^{-1}$ (4.B.5) [see note]

***Dew point and frost point:***

$$t_d = \frac{243.12 \cdot \ln\left[e' / 6.112 f(p)\right]}{17.62 - \ln\left[e' / 6.112 f(p)\right]}$$ (4.B.6) Water (–45 °C to 60 °C)

$$t_f = \frac{272.62 \cdot \ln\left[e' / 6.112 f(p)\right]}{22.46 - \ln\left[e' / 6.112 f(p)\right]}$$ (4.B.7) Ice (–65 °C to 0 °C)

***Psychrometric formulae for the Assmann psychrometer:***

$e' = e'_w(p,t_w) - 6.53 \cdot 10^{-4} \cdot (1 + 0.000944\, t_w) \cdot p \cdot (t - t_w)$ (4.B.8) Water

$e' = e'_i(p,t_i) - 5.75 \cdot 10^{-4} \cdot p \cdot (t - t_i)$ (4.B.9) Ice

***Relative humidity:***

$U = 100\, e'/e'_w(p,t)$ %RH (4.B.10)

$U = 100\, e'_w(p,t_d)/e'_w(p,t)$ %RH (4.B.11)

Symbols applied:

| | |
|---|---|
| $t$ | *air temperature (dry-bulb temperature);* |
| $t_w$ | wet-bulb temperature; |
| $t_i$ | ice-bulb temperature; |
| $t_d$ | dew-point temperature; |
| $t_f$ | frost-point temperature; |
| $p$ | *pressure of moist air;* |
| $e_w(t)$ | saturation vapour pressure in the pure phase with regard to water at the dry-bulb temperature; |
| $e_w(t_w)$ | saturation vapour pressure in the pure phase with regard to water at the wet-bulb temperature; |
| $e_i(t)$ | saturation vapour pressure in the pure phase with regard to ice at the dry-bulb temperature; |
| $e_i(t_i)$ | saturation vapour pressure in the pure phase with regard to ice at the ice-bulb temperature; |
| $e'_w(t)$ | saturation vapour pressure of moist air with regard to water at the dry-bulb temperature; |
| $e'_w(t_w)$ | saturation vapour pressure of moist air with regard to water at the wet-bulb temperature; |
| $e'_i(t)$ | saturation vapour pressure of moist air with regard to ice at the dry-bulb temperature; |
| $e'_i(t_i)$ | saturation vapour pressure of moist air with regard to ice at the ice-bulb temperature; |
| $U$ | *relative humidity.* |

Note: In fact, $f$ is a function of both pressure and temperature, that is, $f = f(p, t)$, as explained in WMO (1966) in the introduction to Table 4.10. In practice, the temperature dependency (±0.1%) is much lower with respect to pressure (0% to +0.6%). Therefore, the temperature dependency may be omitted in the formula above (see also WMO (1989*a*), Chapter 10). This formula, however, should be used only for pressure around 1 000 hPa (that is, surface measurements) and not for upper-air measurements, for which WMO (1966), Table 4.10 should be used.

# ANNEX 4.C. INSTRUMENTS AND METHODS IN LIMITED USE, OR NO LONGER USED

## 1 MECHANICAL INSTRUMENTS USING ORGANIC MATERIALS

### 1.1 The hair hygrometer

The change in the length of hair due to changes in the air relative humidity has been used to measure humidity in hygrometers. All types of hair hygrometers have fallen out of use in meteorology except for the hair hygrograph described in 4.6, which is progressively being phased out.

### 1.2 Other mechanical methods

Mechanical methods using dimensional change of organic materials to indicate relative humidity have in earlier times used sensing elements made of animal tissue, such as Goldbeater's skin (an organic membrane obtained from the gut of domestic animals). These sensing elements are no longer used.

## 2 THE LITHIUM CHLORIDE HEATED CONDENSATION HYGROMETER (DEW CELL)

### 2.1 General considerations

#### 2.1.1 *Principles*

The equilibrium vapour pressure at the surface of a saturated lithium chloride solution is exceptionally low. As a consequence, a solution of lithium chloride is extremely hygroscopic under typical conditions of surface atmospheric humidity; if the ambient vapour pressure exceeds the equilibrium vapour pressure of the solution, water vapour will condense over it (for example, at 0 °C water vapour condenses over a plane surface of a saturated solution of lithium chloride to only 15%RH).

A thermodynamically self-regulating device may be achieved if the solution is heated directly by passing an electrical current through it from a constant-voltage device. An alternating current should be used to prevent polarization of the solution. As the electrical conductivity decreases, so will the heating current, and an equilibrium point will be reached whereby a constant temperature is maintained; any cooling of the solution will result in the condensation of water vapour, thus causing an increase in conductivity and an increase in heating current, which will reverse the cooling trend. Heating beyond the balance point will evaporate water vapour until the consequent fall in conductivity reduces the electrical heating to the point where it is exceeded by heat losses, and cooling ensues.

It follows from the above that there is a lower limit to the ambient vapour pressure that may be measured in this way at any given temperature. Below this value, the salt solution would have to be cooled in order for water vapour to condense. This would be equivalent to the chilled-mirror method except that, in the latter case, condensation takes place at a lower temperature when saturation is achieved with respect to a pure water surface, namely, at the ambient dew point.

A degree of uncertainty is inherent in the method due to the existence of four different hydrates of lithium chloride. At certain critical temperatures, two of the hydrates may be in equilibrium with the aqueous phase, and the equilibrium temperature achieved by heating is affected according to the hydrate transition that follows. The most serious ambiguity for meteorological

purposes occurs for ambient dew-point temperatures below –12 °C. For an ambient dew point of –23 °C, the potential difference in equilibrium temperature, according to which one of the two hydrate-solution transitions takes place, results in an uncertainty of ±3.5 K in the derived dew-point value.

### 2.1.2 *Description*

The dew-cell hygrometer measures the temperature at which the equilibrium vapour pressure for a saturated solution of lithium chloride is equal to the ambient water-vapour pressure. Empirical transformation equations, based on saturation vapour pressure data for lithium chloride solution and for pure water, provide for the derivation of the ambient water vapour and dew point with respect to a plane surface of pure water. The dew-point temperature range of –12 °C to 25 °C results in dew-cell temperatures in the range of 17 °C to 71 °C.

### 2.1.3 *Sensors with direct heating*

The sensor consists of a tube, or bobbin, with a resistance thermometer fitted axially within. The external surface of the tube is covered with a glass fibre material (usually tape wound around and along the tube) that is soaked with an aqueous solution of lithium chloride, sometimes combined with potassium chloride. Bifilar silver or gold wire is wound over the covering of the bobbin, with equal spacing between the turns. An alternating electrical current source is connected to the two ends of the bifilar winding; this is commonly derived from the normal electrical supply (50 or 60 Hz). The lithium chloride solution is electrically conductive to a degree determined by the concentration of solute. A current passes between adjacent bifilar windings, which act as electrodes, and through the solution. The current heats the solution, which increases in temperature.

Except under conditions of extremely low humidity, the ambient vapour pressure will be higher than the equilibrium vapour pressure over the solution of lithium chloride at ambient air temperature, and water vapour will condense onto the solution. As the solution is heated by the electrical current, a temperature will eventually be reached above which the equilibrium vapour pressure exceeds the ambient vapour pressure, evaporation will begin, and the concentration of the solution will increase.

An operational equilibrium temperature exists for the instrument, depending upon the ambient water-vapour pressure. Above the equilibrium temperature, evaporation will increase the concentration of the solution, and the electrical current and the heating will decrease and allow heat losses to cause the temperature of the solution to fall. Below the equilibrium temperature, condensation will decrease the concentration of the solution, and the electrical current and the heating will increase and cause the temperature of the solution to rise. At the equilibrium temperature, neither evaporation nor condensation occurs because the equilibrium vapour pressure and the ambient vapour pressure are equal.

In practice, the equilibrium temperature measured is influenced by individual characteristics of sensor construction and has a tendency to be higher than that predicted from equilibrium vapour-pressure data for a saturated solution of lithium chloride. However, reproducibility is sufficiently good to allow the use of a standard transfer function for all sensors constructed to a given specification.

Strong ventilation affects the heat transfer characteristics of the sensor, and fluctuations in ventilation lead to unstable operation.

In order to minimize the risk of excessive current when switching on the hygrometer (as the resistance of the solution at ambient temperature is rather low), a current-limiting device, in the form of a small lamp, is normally connected to the heater element. The lamp is chosen so that, at normal bobbin-operating currents, the filament resistance will be low enough for the

hygrometer to function properly, while the operating current for the incandescent lamp (even allowing for a bobbin offering no electrical resistance) is below a value that might damage the heating element.

The equilibrium vapour pressure for saturated lithium chloride depends upon the hydrate being in equilibrium with the aqueous solution. In the range of solution temperatures corresponding to dew points of –12 °C to 41 °C monohydrate normally predominates. Below –12 °C, dihydrate forms, and above 41 °C, anhydrous lithium chloride forms. Close to the transition points, the operation of the hygrometer is unstable and the readings ambiguous. However, the –12 °C lower dew-point limit may be extended to –30 °C by the addition of a small amount of potassium chloride (KCl).

#### 2.1.4 *Sensors with indirect heating*

Improved accuracy may be obtained when a solution of lithium chloride is heated indirectly. The conductance of the solution is measured between two platinum electrodes and provides control of a heating coil.

### 2.2 Operational procedure

Readings of the equilibrium temperature of the bobbin are taken and a transfer function applied to obtain the dew-point temperature.

Disturbing the sensor should be avoided as the equilibrium temperature is sensitive to changes in heat losses at the bobbin surface.

The instrument should be energized continuously. If allowed to cool below the equilibrium temperature for any length of time, condensation will occur and the electrolyte will drip off.

Verification measurements with a working reference hygrometer must be taken at regular intervals and the instrument must be cleaned and retreated with a lithium chloride solution, as necessary.

A current-limiting device should be installed if not provided by the manufacturer, otherwise the high current may damage the sensor when the instrument is powered-up.

### 2.3 Exposure and siting

The hygrometer should be located in an open area in a housing structure which protects it from the effects of wind and rain. A system for providing a steady aspiration rate is required.

The heat from the hygrometer may affect other instruments; this should be taken into account when choosing its location.

The operation of the instrument will be affected by atmospheric pollutants, particularly substances which dissociate in solutions and produce a significant ion concentration.

### 2.4 Sources of error

An electrical resistance thermometer is required for measuring the equilibrium temperature; the usual sources of error for thermometry are present.

The equilibrium temperature achieved is determined by the properties of the solute, and significant amounts of contaminant will have an unpredictable effect.

Variations in aspiration affect the heat exchange mechanisms and, thus, the stability of operation of the instrument. A steady aspiration rate is required for a stable operation.

### 2.5 Calibration and field inspection

A field inspection should be performed at least once a month by means of comparison with a working standard instrument.

Calibration of the bobbin thermometer and temperature display should be performed regularly, as for other operational thermometers and display systems.

### 2.6 Maintenance

The lithium chloride should be renewed regularly. This may be required once a month, but will depend upon the level of atmospheric pollution. When renewing the solution, the bobbin should be washed with distilled water and fresh solution subsequently applied. The housing structure should be cleaned at the same time.

Fresh solution may be prepared by mixing five parts by weight of anhydrous lithium chloride with 100 parts by weight of distilled water. This is equivalent to 1 g of anhydrous lithium chloride to 20 ml of water.

The temperature-sensing apparatus should be maintained in accordance with the recommendations for electrical instruments used for making air temperature measurements, but bearing in mind the difference in the range of temperatures measured.

## 3 HEATED PSYCHROMETER

This instrument type is not used for observations, but the description below is given for information.

The principle of the heated psychrometer is that the water-vapour content of an air mass does not change if it is heated. This property may be exploited to the advantage of the psychrometer by avoiding the need to maintain an ice bulb under freezing conditions.

### 3.1 Description

Air is drawn into a duct where it passes over an electrical heating element and then into a measuring chamber containing both dry- and wet-bulb thermometers and a water reservoir. The heating element control circuit ensures that the air temperature does not fall below a certain level, which might typically be 10 °C. The temperature of the water reservoir is maintained in a similar way. Thus, neither the water in the reservoir nor the water at the wick should freeze, provided that the wet-bulb depression is less than 10 K, and that the continuous operation of the psychrometer is secured even if the air temperature is below 0 °C. At temperatures above 10 °C the heater may be automatically switched off, when the instrument reverts to normal psychrometric operation.

Electrical thermometers are used so that they may be entirely enclosed within the measuring chamber and without the need for visual readings.

A second dry-bulb thermometer is located at the inlet of the duct to provide a measurement of the ambient air temperature. Thus, the ambient relative humidity may be determined.

The psychrometric thermometer bulbs are axially aspirated at an air velocity in the region of 3 m $s^{-1}$.

### 3.2 Observation procedure

A heated psychrometer could be suitable for AWSs.

### 3.3 Exposure and siting

The instrument itself should be mounted outside a thermometer screen. The air inlet, where ambient air temperature is measured, should be inside the screen.

## 4 ELECTRICAL RESISTANCE HYGROMETERS

Most of Chapter 4, 4.2 on electrical capacitance hygrometers (with the exception of 4.2.2) is also relevant to electrical resistance hygrometers.

Resistive humidity instruments feature chemically treated plastic material having an electrically conductive surface layer on the non-conductive substrate. The surface resistivity varies according to the uptake of water vapour that is dependent on the ambient relative humidity. The process of adsorption, rather than absorption, is dominant because the humidity-sensitive part of such a sensor is restricted to the surface layer. As a result, this type of sensor is capable of responding rapidly to a change in ambient humidity.

This class of sensor includes various electrolytic types in which the availability of conductive ions in a hygroscopic electrolyte is a function of the amount of adsorbed water vapour. The electrolyte may take various physical forms, such as liquid or gel solutions, or an ion-exchange resin. The change in impedance to an alternating current, rather than to a direct current, is measured to avoid polarization of the electrolyte. Low-frequency supply can be used, given that the DC resistance is to be measured, and therefore it is possible to employ quite long leads between the sensor and its electrical interface.

## REFERENCES AND FURTHER READING


Anderson, P.S., 1995: Mechanism for the behavior of hydroactive materials used in humidity sensors. *Journal of Atmospheric Oceanic Technology,* 12:662–667.

Bell, S.A., P.A. Carroll, S.L. Beardmore, C. England and N. Mander, 2017: A methodology for study of in-service drift of meteorological humidity sensors. *Metrologia*, 54(3):S63.

Bindon, H.H., 1965: A critical review of tables and charts used in psychrometry. In: *Humidity and Moisture* (A. Wexler, ed.). New York, Reinhold, 1:3–15.

British Standard, 2002: *Humidity terms definitions and formulae.* BS 1339 – Part 1.

British Standard, 2004: *Guide to the measurement of humidity.* BS 1339 – Part 3.

Burt, S., 2012: *The Weather Observer's Handbook*. Cambridge University Press.

Harrison, R.G., 2014: *Meteorological Measurements and Instrumentation*. John Wiley & Sons.

Ingleby, B., D. Moore, C. Sloan and R. Dunn, 2013: Evolution and accuracy of surface humidity reports. *Journal of Atmospheric Oceanic Technology*, 30(9):2025–2043.

Institute of Measurement and Control and National Physical Laboratory, 1996: *A Guide to the Measurement of Humidity*. London, Institute of Measurement and Control.

Joint Committee for Guides in Metrology, 2012: *International Vocabulary of Metrology – Basic and General Concepts and Associated Terms (VIM)*. Third edition. JCGM 200:2012.

Sonntag, D., 1990: Important new values of the physical constants of 1986, vapour pressure formulations based on the ITS-90 and psychrometer formulae. *Zeitschrift für Meteorologie*, 40(5):340–344.

———, 1994: Advancements in the field of hygrometry. *Meteorologische Zeitschrift*, 3(2):51–66.

Wexler, A. (ed.), 1965: *Humidity and Moisture*. Volumes 1–3. New York, Reinhold.

World Meteorological Organization, 1966: *International Meteorological Tables* (S. Letestu, ed.) (WMO-No. 188, TP. 94). 1973 amendment. Geneva.

———, 1989*a*: *WMO Assmann Aspiration Psychrometer Intercomparison* (D. Sonntag) (WMO/TD-No. 289). Instruments and Observing Methods Report No. 34. Geneva.

———, 1989*b*: *WMO International Hygrometer Intercomparison* (J. Skaar, K. Hegg, T. Moe and K. Smedstud) (WMO/TD-No. 316). Instruments and Observing Methods Report No. 38. Geneva.

———, 1992: *Measurement of Temperature and Humidity: Specification, Construction, Properties and Use of the WMO Reference Psychrometer* (R.G. Wylie and T. Lalas) (WMO-No. 759). Technical Note No. 194. Geneva.

———, 2011*a*: *WMO Field Intercomparison of Thermometer Screens/Shields and Humidity Measuring Instruments: Ghardaia, Algeria, November 2008–October 2009* (M. Lacombe, D. Bousri, M. Leroy and M. Mezred) (WMO/TD-No. 1579). WMO Instruments and Observing Methods Report No. 106. Geneva.

———, 2011*b*: *Guide to Climatological Practices* (WMO-No. 100). Geneva.

———, 2015 (updated in 2017): *Manual on the WMO Integrated Global Observing System* (WMO-No. 1160). Geneva.

# CHAPTER 5. MEASUREMENT OF SURFACE WIND

## 5.1 GENERAL

### 5.1.1 Definitions

The following definitions are used in this chapter (see Mazzarella, 1972, for more details).

**Wind velocity.** A three-dimensional vector quantity with small-scale random fluctuations in space and time superimposed upon a larger-scale organized flow. It is considered in this form in relation to, for example, airborne pollution and the landing of aircraft. For the purpose of the present Guide, however, surface wind will be considered mainly as a two-dimensional vector quantity specified by two numbers representing direction and speed. The extent to which wind is characterized by rapid fluctuations is referred to as gustiness, and single fluctuations are called gusts.

Most users of wind data require the averaged horizontal wind, usually expressed in polar coordinates as speed and direction. More and more applications also require information on the variability or gustiness of the wind. For this purpose, three quantities are used, namely the peak gust and the standard deviations of wind speed and direction.

**Averaged quantities.** Quantities (for example, horizontal wind speed) that are averaged over a period of 2 to 60 min. This chapter deals mainly with averages over 10 min intervals, as used for forecasting purposes. Climatological statistics usually require averages over each entire hour, day and night. Aeronautical applications often use shorter averaging intervals (see Volume III, Chapter 2 of the present Guide). Averaging periods shorter than a few minutes do not sufficiently smooth the usually occurring natural turbulent fluctuations of wind; therefore, 1 min "averages" should be described as long gusts.

**Peak gust.** The maximum observed wind speed over a specified time interval. With hourly weather reports, the peak gust refers to the wind extreme in the last full hour.

**Gust duration.** A measure of the duration of the observed peak gust. The duration is determined by the response of the measuring system. Slowly responding systems smear out the extremes and measure long smooth gusts; fast response systems may indicate sharp wave-front gusts with a short duration.

For the definition of gust duration an ideal measuring chain is used, namely a single filter that takes a running average over $t_0$ seconds of the incoming wind signal. Extremes detected behind such a filter are defined as peak gusts with duration $t_0$. Other measuring systems with various filtering elements are said to measure gusts with duration $t_0$ when a running average filter with integration time $t_0$ would have produced an extreme with the same height (see Beljaars, 1987; WMO, 1987 for further discussion).

**Standard deviation.**

$$s_u = \sqrt{\overline{(u_i - U)^2}} = \sqrt{\left(\left(\sum u_i^2\right) - \left(\sum u_i\right)^2 / n\right) / n} \qquad (5.1)$$

where $u$ is a time-dependent signal (for example, horizontal wind speed) with average $U$ and an overbar indicates time-averaging over $n$ samples $u_i$. The standard deviation is used to characterize the magnitude of the fluctuations in a particular signal.

**Time constant (of a first-order system).** The time required for a device to detect and indicate about 63% of a step-function change.

**Response length.** Approximately, the passage of wind (in metres) required for the output of a wind-speed sensor to indicate about 63% of a step-function change of the input speed.

**Critical damping (of a sensor such as a wind vane, having a response best described by a second-order differential equation).** The value of damping which gives the most rapid transient response to a step change without overshoot.

**Damping ratio.** The ratio of the actual damping to the critical damping.

**Undamped natural wavelength.** The passage of wind that would be required by a vane to go through one period of an oscillation if there were no damping. It is less than the actual "damped" wavelength by a factor $\sqrt{(1-D^2)}$ if D is the damping ratio.

**Variable wind with no mean wind direction.** This is wind where the total variation from the mean wind direction during the previous 10 minutes is 60° or more, and less than 180°, and the wind speed is less than 1.5 m $s^{-1}$ (3 kt), or when the total variation is 180° or more.

### 5.1.2 Units and scales

Wind speed and direction for synoptic reports should represent an average over 10 min. Averages over a shorter period are necessary for certain aeronautical purposes (see Volume III, Chapter 2 of the present Guide).

Wind direction is defined as the direction from which the wind blows, and is measured clockwise from geographical north, namely, true north (based on WGS-84 and its EGM96).

"Calm" should be reported when the average wind speed is less than or equal to 0.2 m $s^{-1}$ (< 1 kt). The direction in this case is coded as 00.

Wind direction at stations within 1° of the North Pole or 1° of the South Pole should be measured so that the azimuth ring should be aligned with its zero coinciding with the Greenwich 0° meridian.

### 5.1.3 Meteorological requirements

Wind observations or measurements are required for weather monitoring and forecasting, for wind-load climatology, for probability of wind damage and estimation of wind energy, and as part of the estimation of surface fluxes, for example, evaporation for air pollution dispersion and agricultural applications. Performance requirements are given in the present volume, Chapter 1, Annex 1.A. A required measurement uncertainty for horizontal speed of 0.5 m $s^{-1}$ below 5 m $s^{-1}$ and better than 10% above 5 m $s^{-1}$ is usually sufficient. Wind direction should be measured with an uncertainty of 5°. Apart from mean wind speed and direction, many applications require standard deviations and extremes (see 5.8.2). The required uncertainty is easily obtained with modern instrumentation. The most difficult aspect of wind measurement is the exposure of the anemometer. Since it is nearly impossible to find a location where the wind speed is representative of a large area, it is recommended that estimates of exposure errors be made (requirements on siting and exposure are provided in 5.9 and in the present volume, Chapter 1, Annex 1.D).

Many applications require information about the gustiness of the wind. Such applications provide "nowcasts" for aircraft take-off and landing, wind-load climatology, air pollution dispersion problems and exposure correction. Two variables are suitable for routine reading, namely the standard deviation of wind speed and direction and the 3 s peak gust (see Recommendations 3 and 4 (CIMO-X) (WMO, 1990)).

### 5.1.4 Methods of measurement and observation

Surface wind can be measured by a wind vane and cup or propeller anemometer. When the instrumentation is temporarily out of operation or when it is not provided, the direction and force of the wind may be estimated subjectively (Tables 5.1 and 5.2 provide wind speed equivalents in common use for estimations).

The instruments and techniques specifically discussed here are only a few of the more convenient ones available and do not comprise a complete list. The references and further reading at the end of this chapter provide a good literature on this subject.

The sensors briefly described below are cup-rotor and propeller anemometers, and direction vanes. Cup and vane, propeller and vane, and propellers alone are common combinations. Other classic sensors, such as the pitot tube, are less used now for routine measurements but can perform satisfactorily, while new types being developed or currently in use as research tools may become practical for routine measurement with advanced technology.

**Table 5.1. Wind speed equivalents**

| *Beaufort scale number and description* | | *Wind speed equivalent at a standard height of 10 m above open flat ground* | | | | *Specifications for estimating speed over land* |
|---|---|---|---|---|---|---|
| | | *(kt)* | *(m $s^{-1}$)* | *(km $h^{-1}$)* | *(mi $h^{-1}$)* | |
| 0 | Calm | < 1 | 0 – 0.2 | < 1 | < 1 | Calm; smoke rises vertically |
| 1 | Light air | 1 – 3 | 0.3 – 1.5 | 1 – 5 | 1 – 3 | Direction of wind shown by smoke-drift but not by wind vanes |
| 2 | Light breeze | 4 – 6 | 1.6 – 3.3 | 6 – 11 | 4 – 7 | Wind felt on face; leaves rustle; ordinary vanes moved by wind |
| 3 | Gentle breeze | 7 – 10 | 3.4 – 5.4 | 12 – 19 | 8 – 12 | Leaves and small twigs in constant motion; wind extends light flag |
| 4 | Moderate breeze | 11 – 16 | 5.5 – 7.9 | 20 – 28 | 13 – 18 | Raises dust and loose paper; small branches are moved |
| 5 | Fresh breeze | 17 – 21 | 8.0 – 10.7 | 29 – 38 | 19 – 24 | Small trees in leaf begin to sway, crested wavelets form on inland waters |
| 6 | Strong breeze | 22 – 27 | 10.8 – 13.8 | 39 – 49 | 25 – 31 | Large branches in motion; whistling heard in telegraph wires; umbrellas used with difficulty |
| 7 | Near gale | 28 – 33 | 13.9 – 17.1 | 50 – 61 | 32 – 38 | Whole trees in motion; inconvenience felt when walking against the wind |
| 8 | Gale | 34 – 40 | 17.2 – 20.7 | 62 – 74 | 39 – 46 | Breaks twigs off trees; generally impedes progress |
| 9 | Strong gale | 41 – 47 | 20.8 – 24.4 | 75 – 88 | 47 – 54 | Slight structural damage occurs (chimney-pots and slates removed) |
| 10 | Storm | 48 – 55 | 24.5 – 28.4 | 89 – 102 | 55 – 63 | Seldom experienced inland; trees uprooted; considerable structural damage occurs |
| 11 | Violent storm | 56 – 63 | 28.5 – 32.6 | 103 – 117 | 64 – 72 | Very rarely experienced; accompanied by widespread damage |
| 12 | Hurricane | 64 and over | 32.7 and over | 118 and over | 73 and over | |

**Table 5.2. Wind speed equivalents for arctic areas and areas where there is no vegetation**

| *Beaufort scale number and description* | | *Wind speed equivalent at a standard height of 10 m above open flat ground* | | | | *Specifications for estimating speed for arctic areas and areas where there is no vegetation* |
|---|---|---|---|---|---|---|
| | | *(kt)* | *(m $s^{-1}$)* | *(km $h^{-1}$)* | *(mi $h^{-1}$)* | |
| 0 | Calm | < 1 | 0 – 0.2 | < 1 | < 1 | |
| 1 | Light air | 1 – 3 | 0.3 – 1.5 | 1 – 5 | 1 – 3 | No noticeable wind; smoke rises nearly vertically |
| 2 | Light breeze | 4 – 6 | 1.6 – 3.3 | 6 – 11 | 4 – 7 | Wind felt on face, leaves rustle |
| 3 | Gentle breeze | 7 – 10 | 3.4 – 5.4 | 12 – 19 | 8 – 12 | Hair is disturbed, clothing flaps |
| 4 | Moderate breeze | 11 – 16 | 5.5 – 7.9 | 20 – 28 | 13 – 18 | Dust and loose paper raised, hair disarranged |
| 5 | Fresh breeze | 17 – 21 | 8.0 – 10.7 | 29 – 38 | 19 – 24 | Force of wind felt on body; limit of agreeable wind on land |
| 6 | Strong breeze | 22 – 27 | 10.8 – 13.8 | 39 – 49 | 25 – 31 | Some inconvenience in walking |
| 7 | Near gale | 28 – 33 | 13.9 – 17.1 | 50 – 61 | 32 – 38 | Difficulty when walking against wind |
| 8 | Gale | 34 – 40 | 17.2 – 20.7 | 62 – 74 | 39 – 46 | Difficulty with balance in walking |
| 9 | Strong gale | 41 – 47 | 20.8 – 24.4 | 75 – 88 | 47 – 54 | Danger in being blown over |
| 10 | Storm | 48 – 55 | 24.5 – 28.4 | 89 – 102 | 55 – 63 | Trees uprooted, considerable structural damage |
| 11 | Violent storm | 56 – 63 | 28.5 – 32.6 | 103 – 117 | 64 – 72 | |
| 12 | Hurricane | 64 and over | 32.7 and over | 118 and over | 73 and over | |

For nearly all applications, it is necessary to measure the averages of wind speed and direction. Many applications also need gustiness data. A wind-measuring system, therefore, consists not only of a sensor, but also of a processing and recording system. The processing takes care of the averaging and the computation of the standard deviations and extremes. In its simplest form, the processing can be done by writing the wind signal with a pen recorder and estimating the mean and extreme by reading the record.

## 5.2 ESTIMATION OF WIND

In the absence of equipment for measuring wind, the observations must be made by estimation. The errors in observations made in this way may be large, but, provided that the observations are used with caution, the method may be justified as providing data that would otherwise not be available in any way. If either temporarily or permanently the wind data of some stations are obtained by estimation instead of measurement, this fact should be documented in station records made accessible to data users.

### 5.2.1 Wind speed

Estimates are based on the effect of the wind on movable objects. Almost anything which is supported so that it is free to move under the influence of the wind can be used, but the descriptive specifications given in the Beaufort scale of wind force, as reproduced in the tables 5.1 and 5.2, will be found especially useful.

In order to make the estimates, the observer (and the wind-susceptible object) must stand on open flat terrain as far as possible from obstructions. It must always be remembered that even small obstructions cause serious changes in wind speed and deviations in wind direction, especially at their lee side.

### 5.2.2 Wind direction

In the case of an absence of instruments, or when the instrumental equipment is unserviceable, the direction should be estimated by observing the drift of smoke from an elevated chimney, the movement of leaves, and so on, in an open situation, or a streamer or pennant fixed to a tall flagstaff. In addition, the wind drogue at an airport may be used when the wind speed is sufficient to move such a device.

Whichever of these aids is used, errors due to perspective are liable to be made unless the observer stands vertically below the indicator. Care should be taken to guard against mistaking local eddies caused by buildings, and the like, for the general drift of the wind.

In an open location, the surface wind direction can be estimated rather accurately by facing the wind. The direction of the movement of clouds, however low, should not be taken into account.

### 5.2.3 Wind fluctuations

No attempt should be made to estimate peak gusts or standard deviations without proper instruments and recording devices.

## 5.3 SIMPLE INSTRUMENTAL METHODS

At stations where orthodox anemometers cannot be installed it may be possible to provide some very low-cost, simple instruments that help the observer take measurements that are somewhat more reliable than those obtained by unaided estimation.

### 5.3.1 Wind speed

Simple handheld anemometers, if they are used, should be set up and read in accordance with the maker's instructions. The measurement should be taken from a point well exposed to the wind, and not in the lee of obstructions such as buildings, trees and hillocks. If this is not possible, the measurement point should be a good distance from obstructions, namely at least 10 times the obstruction height and upwind or sideways by at least twice the obstruction height.

### 5.3.2 Wind direction

Direction may be estimated from a vane (or banner) mounted on a pole that has pointers indicating the principal points of the compass. The vane is observed from below, and wind direction may be estimated to the nearest of the 16 points of the compass. If the vane oscillates in the wind, the wind direction must be estimated as the average direction about which the oscillations occur.

## 5.4 CUP AND PROPELLER SENSORS

Cup and propeller anemometers are used to determine wind speed and consist of two sub-assemblies: the rotor and the signal generator. In well-designed systems, the angular velocity of the cup or propeller rotor is directly proportional to the wind speed, or, more

precisely, in the case of the propeller rotor, to the component of the wind speed parallel to the axis of rotation. Also, in well-designed anemometers, the calibration linearity is independent of air density, has good zero and range stability, and is easily reproduced in a manufacturing process. Near the starting threshold, or for wind speeds of less than 4 m $s^{-1}$, the calibration of cup anemometers can deviate substantially from linearity, if the arm connecting the cup to the rotation axis is much longer than the diameter of the cup (Patterson, 1926).

The nature of the response of the cup and propeller-type wind-speed sensors to changes in wind speed can be characterized by a response length, the magnitude of which is directly proportional to the moment of inertia of the rotor and, in addition, depends on a number of geometric factors (Busch and Kristensen, 1976; Coppin, 1982).

For almost all cup and propeller-type wind sensors, the response is faster for acceleration than for deceleration, so that the average speed of these rotors overestimates the actual average wind speed. Moreover, vertical velocity fluctuations can cause overspeeding of cup anemometers as a result of reduced cup interference in oblique flow (MacCready, 1966). The total overspeeding can be as much as 10% for some designs and turbulent wind conditions (cup anemometers at 10 m height with a response length of 5 m over very rough terrain; Coppin, 1982). This effect can be minimized by choosing fast-response anemometers, either cup anemometers of a design verified as having a good cosine response or propeller vanes that have virtually no vertical component of overspeeding. In case that performance cannot be investigated in a wind tunnel, operational anemometers can be compared in the field with a calibrated anemometer (Albers et al., 2000).

Since both cup and propeller rotors turn with an angular velocity that is directly proportional to speed or to the axial component, they are particularly convenient for driving a wide variety of signal generators. Alternating and direct current generators, optical and magnetic pulse generators, and turn-counting dials and registers have been used (WMO, 2001). The choice of signal generator or transducer depends largely on the type of data processor and read-out to be used. Care should be taken to ensure that the bearings and signal generator have low starting and running frictional torques, and that the moment of inertia of the signal generator does not reduce the response too much. In cases of long-distance transmission, voltage signals decrease due to cable resistance losses and are therefore inferior to pulse frequency signals, which are not so affected during transmission.

The required and achievable characteristics for wind-speed sensors are included in the present volume, Chapter 1, Annex 1.A.

## 5.5 WIND-DIRECTION VANES

For the purpose of obtaining a satisfactory measurement, a wind vane can be suitable if it is well balanced so as not to have a preferred position in case the axis is not vertical. Multiple vane fins should preferably be parallel to the vane axis, because a vane with two fins at angles > 10° to its axis has two equilibrium positions which each differ significantly from the real wind direction (Wieringa and van Lindert, 1971).

The response of the usual underdamped wind vane to a sudden change in wind direction is normally characterized by overshoot and oscillation about its true position, with the amplitude decreasing approximately exponentially. Two variables are used to define this response: the "undamped natural frequency" or "wavelength" and the "damping ratio", the ratio of the actual damping to the critical damping (MacCready, 1966; Mazzarella, 1972). A damping ratio between 0.3 and 0.7 is considered to be good and as having not too much overshoot, and a reasonably fast response (Wieringa, 1967). Where a relatively long period average is to be computed from data captured at short intervals, it is self-evident that lower damping ratios may be acceptable.

The signal generator is essentially a shaft-angle transducer, and many varieties have been employed. Potentiometers, alternating and direct current synchros, digital angle-encoder discs, direct reading dials and rotary switches have been used to advantage. The choice of signal generator is largely a matter of the type of data processor and read-out used. Care should be

taken to ensure that the bearings and signal generator have low starting and running frictional torques. The simplest recording method is to have a sheet mounted around a cylinder rotating with the vane axis, on which a writing instrument slowly travels downward.

The absolute accuracy of direction measurement also depends on the care with which the instrument has been aligned to true north. The required and achievable characteristics for wind-direction vanes are included in the present volume, Chapter 1, Annex 1.A.

## 5.6 OTHER WIND SENSORS

Many physical principles can be used to measure wind speed and direction, all of which have their own merits and problems. Some systems have been developed for specific purposes, such as small-scale fluctuations and air pollution studies (see for example, Smith (1980)). The following are other types of sensors:

(a) Pitot tube anemometers, which measure the overpressure in a tube that is kept aligned with the wind vector by means of a direction vane (see Gold (1936) and WMO (1984*a*) for a description of the Dines anemometer). The Dines linearizing recording system deals with the speed averaging problem caused by the quadratic relation between wind speed and pressure, and it also provides useful gustiness records without requiring electrical power;

(b) Sonic anemometers, which measure the time between emission and reception of an ultrasonic pulse travelling over a fixed distance (Kaimal, 1980). Because sonic anemometers have no moving parts owing to their principle, they have high durability and little accuracy deterioration;

(c) Hot-disc anemometers are solid-state instruments that measure the temperature gradient across a chip arrangement. This provides both wind speed and direction at uncertainties within the specification of the present volume, Chapter 1, Annex 1.A (van Oudheusden and Huijsing, 1991; Makinwa et al., 2001). They are sturdy and steady in calibration, but operational experience is limited so far;

(d) Hot-wire anemometers measure the cooling of thin heated wires. Operationally they are rather unreliable, both because of excessive fragility and because their calibration changes rather quickly in unclean or wet surroundings. They are not recommended for use in precipitation;

(e) Antique swinging-plate vanes are a little better than no instrument at all;

(f) Remote wind-sensing techniques with sound (sodar), light (light detection and ranging (lidar)) or electromagnetic waves (radar) are less common in routine meteorological networks. Details are provided in Volume III, Chapter 5 of the present Guide, and Lenschow (1986).

## 5.7 SENSORS AND SENSOR COMBINATIONS FOR COMPONENT RESOLUTION

Propellers which respond only to the wind speed component that is parallel to the axis of rotation of the rotor can be mounted orthogonally to produce two read-outs which are directly proportional to the components in the axis directions. Other sensors, such as twin-axis sonic anemometers, perform the same function at the expense of more sophisticated electronic adjuncts. Orthogonal propellers have the disadvantage that exact cosine response (namely, pure component sensitivity) is difficult to attain. A cup anemometer/vane combination or a propeller vane can also be used as a component device when the velocity components are computed from the measured wind speed and direction.

## 5.8 DATA-PROCESSING METHODS

Signals from anemometer/vane combinations can be processed and averaged in many different ways. Before considering the aspects of the entire wind-measuring chain (exposure, sensing, transmission, filtering, recording and processing), it is useful to discuss the problem of averaging. This chapter deals with the following outputs: averaged horizontal wind (components or speed/direction), standard deviations and peak gust.

### 5.8.1 Averaging

The averaging of wind vectors or their components is straightforward in principle, but there are a few problems associated with it. The first is that the mean vector speed in the average wind direction $U$ is less than the average of all instantaneous wind speeds by a small amount, generally a few per cent (MacCready, 1966; Wieringa, 1980*a*). If necessary, this may be corrected if the standard deviation of wind direction $s_d$ is measured; for the ratio of $U$, and the averaged instantaneous wind speeds is (Frenkiel, 1951):

$$U \Big/ \overline{\sqrt{\left(u_i^2 + v_i^2\right)}} = 1 - s_d^2 / 2 \qquad (5.2)$$

This effect of crosswind turbulence is often confused with the overestimation (overspeeding), causing distortion in the standard deviation $s_u$ (see 5.4).

The second problem is the discontinuity of the wind direction between 0° and 360°. This problem can be solved either by recording on a cylinder or by extending the recorder range (for example to 540° with an automatic device switching the range from 0 to 360 and from 540 to 180), or by a computer algorithm that makes successive samples continuous by adding or subtracting 360° when necessary. The fact that the first-order response of a cup anemometer and the second-order response of a vane cannot be fully matched is a problem of minor importance, because the response differences are reflected only in the high-frequency part of the fluctuations.

From the fundamental point of view, component averaging is preferable over the independent averaging of speed and direction. However, the differences are very small and, for most applications, component averages can easily be derived from average speed and direction. This also applies to the corresponding standard deviations. From the technical point of view, the independent treatment of speed and direction is preferable for a number of reasons. First, the processing of the signal for speed and direction is independent, which implies that the operation of one instrument can continue even when the other drops out. Second, this data reduction is simpler than in those cases where components have to be computed. Lastly, the independent treatment of speed and direction is compatible with common usage (including SYNOP and SHIP coding).

The averages of horizontal wind speed can be obtained with a number of both mechanical and electrical devices. Perhaps the simplest example is a mechanical rotation-counting register on a cup anemometer commonly used to measure the passage of wind during a chosen averaging time interval. At the other end of the complexity spectrum, electrical pulse generators drive special-purpose digital processors, which can easily calculate averages, peak gusts and standard deviations.

If wind speed and direction are recorded as continuous graphs, an observer can estimate 10 min averages fairly accurately from a pen recording. The recorded wind trace can also be used to read peak gusts. The reading of dials or meters gives a feel for the wind speed and its variability, but is subject to large errors when averages are needed. Instantaneous read-outs are, therefore, less suitable to obtain 10 min averages for standard weather reports.

### 5.8.2 Peak gusts and standard deviations

The computation or recording of wind fluctuations is extremely sensitive to the dynamic response of all the elements of the measuring chain, including response length and damping ratio of the sensors. Additionally, the dynamic response of the system as a whole determines the duration of peak gusts, as defined in 5.1.1. Slowly responding systems spread out the extremes and indicate wide gusts with small amplitude, whereas fast-response systems record high and narrow peaks (gusts of short duration). It is clear that the dynamic response of wind systems has to be carefully designed to obtain gusts or standard deviations that are accurate, reliable and compatible between stations.

Before specifying the appropriate response characteristics of wind-measuring systems, it is necessary to define the gust duration as required by the application. Wind extremes are mainly used for warning purposes and for the climatology of extreme loads on buildings, constructions and aircraft. It is important to realize that the shortest gusts have neither the time nor the horizontal extent to exert their full damaging effect on large constructions. WMO (1987) concludes that a gust duration of about 3 s accommodates most potential users. Gusts that persist for about 3 s correspond to a "wind run" (duration multiplied by the average wind speed) of the order of 50 to 100 m in strong wind conditions. This is sufficient to engulf structures of ordinary suburban/urban size and to expose them to the full load of a potentially damaging gust.

The standard deviation of wind direction and wind speed can easily be computed with microprocessor-based equipment by taking samples of the signals at intervals of about 1 s. Sampling frequencies should not be too great, because the sensor itself provides smoothing over a multiple of its response distance (Wieringa, 1980*b*). A sampling frequency of 0.25 Hz is suitable in most cases, but depends on the response distance of the sensor and the wind speed. Volume V, Chapter 2 of the present Guide includes a detailed discussion of the theory of sampling sensor signals.

Simultaneous computation of the standard deviation of the horizontal wind speed over 10 min together with the detection of gusts with a duration of a few seconds gives interesting requirements for electronic filters. The gusts are most critical with regard to filtering, so in practice the system is optimized for them. Any low-pass filter used for the detection of peak gusts measured by fast anemometers, smoothing over a few seconds, may reduce the standard deviation by up to 10%. This can be corrected if the filtering variables in the measuring chain are well documented. Often, in practice, the reduction is less because the standard deviation increases if the average wind speed shows a positive or negative trend. Alternatively, the unfiltered signal can be recorded separately for the purpose of measuring an unbiased standard deviation. In the next section, recommendations are made for wind-measuring systems with exact values for the filter variables.

In order to determine peak gusts accurately, it is desirable to sample the filtered wind signal every 0.25 s (frequency 4 Hz). Lower sampling frequencies can be used, but it should be realized that the estimate of the extreme will generally be lower as the extreme in the filtered signal may occur between samples.

Apart from the wind vane inertial damping, any further filtering should be avoided for wind direction. This means that the standard deviation of wind direction can be determined within 2% with most wind vanes.

Accurate computation of the standard deviation of wind direction requires a minimum resolution of the digitization process, which is often done on the shaft of the vane by means of a digital encoder. A 7 bit resolution is quite sufficient here because then a 5° unit for the standard deviation can still be measured with an uncertainty of 1% (WMO, 1987).

### 5.8.3 Recommendations for the design of wind-measuring systems[1]

Wind-measuring systems can be designed in many different ways; it is impossible to cover all design options in this chapter. Two common examples are given here, one with mainly analogue signal treatment and the other with digital signal processing (WMO, 1987).

The first system consists of an anemometer with a response length of 5 m, a pulse generator that generates pulses at a frequency proportional to the rotation rate of the anemometer (preferably several pulses per rotation), a counting device that counts the pulses at intervals of 0.25 s, and a microprocessor that computes averages and standard deviation over 10 min intervals on the basis of 0.25 s samples. The extreme has to be determined from 3 s averages, namely, by averaging over the last 12 samples. This averaging has to be done every 0.25 s (namely, overlapping 3 s averages every 0.25 s). The wind direction is measured with a vane that has an undamped wavelength of 5 m, a damping ratio of 0.3, and a 7 bit digital encoder that is sampled every second. Averages and standard deviations are computed over 10 min intervals, where successive samples are checked for continuity. If two successive samples differ by more than 180°, the difference is decreased by adding or subtracting 360° from the second sample. With response lengths of 5 m for the anemometer and the wind vane (damping ratio 0.3, undamped wavelength 10 m), the standard deviations of wind speed and wind direction are reduced by about 7% and 2%, respectively. The gust duration corresponding to the entire measuring chain (as defined in 5.1.1) is about 3 s.

The second system consists of an anemometer with a response length of 5 m, a voltage generator producing a voltage proportional to the rotation rate of the anemometer, analogue-to-digital conversion every second, and the digital processing of samples. The wind-direction part consists of a vane with an undamped wavelength of 5 m and a damping ratio of 0.3, followed by analogue-to-digital conversion every second and digital computation of averages and standard deviations. To determine peak gusts the voltage is filtered with a first-order filter with a time constant of 1 s and analogue-to-digital conversion every 0.25 s. With regard to filtering, this system is slightly different from the first one in that standard deviations of wind speed and direction are filtered by 12% and 2%, respectively, while again the gust duration is about 3 s. This system can also be operated with a pen recorder connected to the analogue output instead of the ADC. Only averages and extremes can be read now, and the gust duration is about 3 s, unless the pen recorder responds more slowly than the first-order filter.

The signal-processing procedure, as described above, is in accordance with Recommendation 3 (CIMO-X) (WMO, 1990) and guarantees optimal accuracy. The procedure, however, is fairly complicated and demanding as it involves overlapping averages and a relatively high sampling frequency. For many applications, it is quite acceptable to reduce the sampling rate down to one sample every 3 s, provided that the wind signal has been averaged over 3 s intervals (namely, non-overlapping averaging intervals). The resulting gust duration is about 5 s and the reduction in standard deviation is 12% (Beljaars, 1987; WMO, 1987).

## 5.9 EXPOSURE OF WIND INSTRUMENTS

### 5.9.1 General problems

Wind speed increases considerably with height, particularly over rough terrain. For this reason, a standard height of 10 m above open terrain is specified for the exposure of wind instruments. For wind direction, the corresponding shift over such a height interval is relatively small and can be ignored in surface wind measurements. An optimum wind observation location is one where the observed wind is representative of the wind over an area of at least a few kilometres, or can easily be corrected to make it representative.

For terrain that is uneven, contains obstacles, or is non-homogeneous in surface cover, both wind speed and direction can be affected considerably. Corrections are often possible, and the tools

[1] Recommended by CIMO at its tenth session (1989).

to compute such corrections are becoming available. To improve the applicability of wind data, essential information to perform such corrections should be transmitted to the users in addition to the direct measurements.

### 5.9.2 Anemometers over land

The standard exposure of wind instruments over open, level terrain is 10 m above the ground. Open terrain is defined as an area where the distance between the anemometer and any obstruction is at least 10 times the height of the obstruction. Wind measurements that are taken in the direct wake of tree rows, buildings or any other obstacle are of little value and contain little information about the unperturbed wind. Since wakes can easily extend downwind to 12 or 15 times the obstacle height, the requirement of 10 obstruction heights is an absolute minimum. In practice, it is often difficult to find a good or even acceptable location for a wind station. The importance of optimizing the location can hardly be overstressed; nonetheless, it is difficult to give universal guidelines. In some cases, however, the data can be largely corrected for obstructions, as follows:

(a) Obstacles at a distance of more than 30 times their height: no correction needs to be applied;

(b) Obstacles at a distance of more than 20 times their height: correction can be applied;

(c) Obstacles at a distance of more than 10 times their height: correction may be applied in some situations, taking special care.

It should be noted that when the distance is less than 20 times the height of the obstacle, the measured value before correction can be erroneous by up to 25%; when the distance is about 10 times the height of the obstacle, the measured value can in some cases even indicate the opposite direction.

Detailed information on the exposure correction is provided in 5.9.4.

In Table 5.3, the classification of wind observing sites based on siting and exposure is summarized. Full details on the siting classification for surface observing stations on land, which provides additional guidance on the selection of a site and the location of a wind sensor within a site to optimize representativeness, can be found in the present volume, Chapter 1, Annex 1.D.

**Table 5.3. Classification of wind observing sites based on siting and exposure**

| *Class* | *Distance of mast to surrounding obstacles[a] (with height h)* | *Distance of sensors to thin obstacles[b] (with height > 8 m, width w)* | *Roughness class index[c]* | *Ignore single obstacles below x m* |
|---|---|---|---|---|
| 1 | ≥ 30 $h$ | ≥ 15 $w$ | 2 – 4 (roughness length ≤ 0.1 m) | $x = 4$ |
| 2 | ≥ 10 $h$ | ≥ 15 $w$ | 2 – 5 (roughness length ≤ 0.25 m) | $x = 4$ |
| 3 | ≥ 5 $h$ | ≥ 10 $w$ | | $x = 5$ |
| 4 | ≥ 2.5 $h$ | No obstacle with angular width > 60° and height > 10 m within 40 m distance | | $x = 6$, if measurement at ≥ 10 m |
| 5 | Not meeting requirements of any other class | | | |

Notes:
a An obstacle is defined as an object having an angular width > 10°.
b A thin obstacle is for instance a mast, thin tree or lamp post.
c Roughness is defined in the annex of this chapter.

Two aspects are very important. First, the sensors should be kept away from local obstructions as much as possible. When wind measurements are taken on the side of masts or towers rather than at their top, the instruments should be placed on booms with a length of at least three mast or tower widths (Gill et al., 1967). When wind instruments are placed on top of a building, they should be raised at least one building width above the top. Second, the local situation should be well documented (Wieringa, 1983). There should at least be a map of the station surroundings within a radius of 2 km, documenting obstacle and vegetation locations and height, terrain elevation changes, and so forth. Changes in the surroundings, such as the construction of buildings or growth of trees nearby, should be explicitly recorded in station logbooks. Station instrumentation should be specified in detail.

Where standard exposure is unobtainable, the anemometer may be installed at such a height that its indications should not be too much affected by local obstructions and represent as far as possible how the wind at 10 m would be if there were no obstructions in the vicinity. If the terrain varies little with azimuth, this may be effected by placing the anemometer at a height exceeding 10 m by an amount depending on the effective surface roughness length $z_0$ of the surroundings (see the annex): about 13 m if $z_0 = 0.1$ m, and about 19 m if $z_0 = 0.5$ m. Wieringa (1980*b*) shows that the strategy of anemometer height increase does not work well if local sheltering varies strongly with azimuth. Simple calculation procedures now exist to determine the effect of local topography (Walmsley et al., 1990), and the climatology of the gustiness records can be used to determine exposure corrections in inhomogeneous surroundings (Verkaik, 2000). Evans and Lee (1981) and Grimmond et al. (1998) discuss the problem in urban areas (see also Volume III, Chapter 9 of the present Guide).

In freezing weather, special precautions must be taken to keep the wind sensors free from sleet and ice accumulations. In some localities it may be desirable to provide some form of artificial heating for the exposed parts such as a thermostatically controlled IR radiator. Sleet and ice shields have been designed for particular types of wind equipment (see Curran et al., 1977).

### 5.9.3 Anemometers at sea

There is an increasing requirement for instrumental measurements of wind over the sea, especially by means of automatic unattended systems (see also Volume III, Chapter 4 of the present Guide). This task presents special problems since the standard exposure height of 10 m specified for land use cannot always be achieved in a marine environment owing to the state of the sea and/or tidal height variation. The obvious extrapolation of the exposure criteria for land sites leads to the idea that, on moored buoys, the anemometer should be mounted 10 m above the waterline of the buoy. However, other sources of error are often more significant than those arising from different exposure heights (for a review, see WMO, 1981). On fixed platforms and ships, it is of the utmost importance that wind sensors be exposed sufficiently high above the platform and its superstructure to avoid the often extensive influence of the platform on the local wind structure. In general, it is never safe to assume that a wind sensor is unaffected by the platform structure, even if it is exposed at least 10 m above the height of the tallest obstruction on the platform, unless the platform is relatively small. WMO (1981) concludes that, at sea, good exposure should have higher priority in obtaining accurate and useful measurements than standardization of the measurements at 10 m (WMO, 1989). Despite careful siting, it is often impossible in practice to avoid exposure errors. In order to allow height and flow distortion corrections to be made, it is very important to keep a record and detailed information about anemometer location and platform or ship type (shape, dimension). If wind speed is measured at a height significantly greater than 10 m (namely, when the appropriate reduction factor would be > 1.2), a reduction to the 10 m level should be performed according to the procedures recommended in the following paragraph, and using the constant for “open sea” in the table of the annex.

### 5.9.4 Exposure correction

Surface wind measurements without exposure problems hardly exist. The requirement of open level terrain is difficult to meet, and most wind stations over land are perturbed by topographic effects or surface cover, or by both (WMO, 1987; Wieringa, 1996).

It is clear that exposure errors pose problems to users of wind data and often make the data useless. This problem is particularly serious in numerical forecast models where there is a tendency to analyse the wind and pressure fields separately. Surface winds, however, can be used for initialization only if they are representative of a large area. This means that errors due to local exposure and/or non-standard measurement height must be removed.

The correction of wind readings for local exposure can be performed only with measurements of reasonable quality at locations that are not too rough ($z_0 \leq 0.5$ m) and reasonably level. No attempt should be made to correct measurements that have hardly any relation to a regional average. For example, a wind station in a deep valley, where the flow is dominated by katabatic effects, may be important for local forecasts, but cannot be used as a regionally representative wind.

If $U$ is the wind speed measured at height $z$, the corrected wind speed $U_c$ which would be indicated locally at 10 m above terrain with roughness $z_0$ follows from:

$$U_c = U \cdot C_F \cdot C_T \cdot \frac{\ln(10 / z_{0u})}{\ln(z / z_{0u})} \cdot \frac{\ln(60 / z_{0u})\ln(10 / z_0)}{\ln(10 / z_{0u})\ln(60 / z_0)} \tag{5.3}$$

where $C_F$ is the flow distortion correction; $C_T$ is the correction factor due to topographic effects; $z_{0u}$ is the effective roughness length of the terrain upstream of the measurement station, and $z_0$ is roughness length in the application (for example, a grid box value in a numerical forecast model). In this expression, $z$, $z_0$ and $z_{0u}$ are specified in metres. The different correction terms represent the following:

(a) Flow distortion: The correction factor $C_F$ accounts for flow distortion by nearby big objects. This is particularly important for anemometers on buildings, ships, and platforms at sea. The best way of finding $C_F$ as a function of wind direction is by means of model simulation in a wind tunnel (Mollo-Christensen and Seesholtz, 1967). Estimates based on potential flow around simple configurations can also be applied (Wyngaard, 1981; WMO, 1984*b*). For measurements on top of a free-standing mast, flow distortion is negligible ($C_F = 1$).

(b) Topographic correction: This correction accounts for terrain height effects around the wind station. $C_T$ is the ratio of the regionally averaged wind speed (averaged over ridges and valleys at 10 m above local terrain) and the wind speed measured at the wind station. In the example of an isolated hill with a station at the top of the hill, $C_T$ should be less than 1 to correct for the speed-up induced by the hill, to make the result representative of the area rather than of the hill top only. $C_T$ equals 1 for flat terrain. For isolated hills and ridges, estimates of $C_T$ can be made with the help of simple guidelines (Taylor and Lee, 1984). In more complicated topography, model computations are needed on the basis of detailed height contour maps of the terrain surrounding the wind stations (Walmsley et al., 1990). Such computations are fairly complicated but need to be done only once for a single station and lead to a semi-permanent table of $C_T$ as a function of wind direction.

(c) Non-standard measurement height: This effect is simply included in the $U_c$ formula by assuming a logarithmic profile combined with the roughness length $z_{0u}$ of the upstream terrain. For stations over sea, this reduction to standard height can be important, but stability corrections are relatively small there, justifying the logarithmic form of the reduction.

(d) Roughness effects: Upstream roughness effects as well as the effects of surface obstacles can be corrected by extrapolating the wind speed logarithmic profile to a height of 60 m with the station specific effective roughness length $z_{0u}$ and by interpolating back to 10 m

with the roughness length $z_0$ necessary for the application. The roughness length $z_{0u}$ should be representative of a 2 km fetch upwind of the wind station; the value usually depends on wind direction. The annex discusses how to estimate $z_{0u}$.

If flow distortion and topography problems are negligible or have been corrected, apply the (c) to (d) exposure correction using formula 5.3 with $z$ = 10 m and $z_0$ = 0.03 m. Corrected wind speeds then will be equivalent to those which would have been measured at a local hypothetical wind station conforming fully with WMO requirements (10 m over open terrain). Wind speeds corrected in this way are called potential wind speeds (WMO, 2001). Two comments are appropriate here. First, the extrapolation height of 60 m should not be seen as a very firm value. Heights between 40 and 80 m would have been acceptable; 60 m is about the correct magnitude in relation to the 2 km fetch for which $z_{0u}$ is representative and has proved to give satisfactory results (Wieringa, 1986). Second, stability-related changes in the wind profile cannot be neglected over the height range from 10 to 60 m, but the effect of stability is relatively small in the present formulation because the stability corrections in the transformations upwards and downwards cancel out. A practical example of the application of wind measurement correction in an operational context is given in WMO (2000) and WMO (2001). Although most of the exposure correction can be directly applied to the measurements, both unadjusted (Level I) data and adjusted (Level II) data are to be disseminated.

## 5.10 CALIBRATION AND MAINTENANCE

A fully reliable calibration of cup, propeller and vane anemometers is possible only in a wind tunnel; the performance of such instruments is now well known and the manufacturer's calibration can be relied upon for most purposes, when the instrument is in good condition. Wind-tunnel tests are useful for special projects or for type-testing new models. For more information, see ISO standards ISO 16622:2002 and ISO 17713-1:2007).

In the field, anemometers are prone to deterioration and regular inspections are advisable. A change in sensor characteristics leading to a deterioration in wind data quality may occur as a result of physical damage, an increase in bearing friction from the ingress of dust, corrosion, or degradation of the transduction process (for example, a reduction in the output of a cup or propeller generator as a result of brush wear).

The inspection of analogue traces will show faults as indicated by incorrect zero, stepped traces due to friction, noise (which may be evident at low wind speeds), low sensitivity (at low speeds), and irregular or reduced variability of recorded wind.

Instruments should be inspected for physical damage, by checking the zero of the anemometer system by holding the cups or propeller, and by checking vane orientation by holding it fixed in a predetermined position or positions. Repairs to the sensors are usually only practicable in a workshop.

System checks should regularly be carried out on the electrical and electronic components of electrical recording or telemetering instruments. Zero and range checks should be made on both the speed and direction systems.

# ANNEX. THE EFFECTIVE ROUGHNESS LENGTH

For the purpose of exposure correction, a roughness length $z_{0u}$ that represents the terrain over 2 km of upstream fetch is needed as a function of wind direction. The quality of the roughness correction is very much dependent on the accuracy of this roughness length.

Assuming a uniform fetch over sea, the calculation of roughness correction is relatively simple because the so-called Charnock relation can be applied. It expresses the sea surface roughness as a function of the friction velocity $u^*$ and the acceleration due to gravity $g$ by means of $z_{0u} = \alpha u^{*2}/g$, where $\alpha$ is an empirical constant approximately equal to 0.014. The friction velocity relates to the neutral wind profile by means of $U(z) = (u^*/\kappa)\ \ln\ (z/z_{0u})$, where $\kappa$ is the Von Karman constant (0.4) and $z$ is the measurement height. These two equations have to be solved iteratively, which can be done by starting with $z_{0u} = 0.0001$, computing $u^*$ from the log-profile, evaluating $z_{0u}$ again, and repeating this a few times.

The surface roughness length over land depends on the surface cover and land use and is often difficult to estimate. A subjective way of determining $z_{0u}$ is by a visual survey of the terrain around the wind station with the help of the table below, the validity of which has been recently corroborated (Davenport et al., 2000). Choosing wind direction sectors of 30° up to a distance of 2 km is most convenient. With very non-homogeneous fetch conditions, an effective roughness should be determined by averaging ln ($z_{0u}$) rather than $z_{0u}$ itself.

The best way of determining $z_{0u}$ is with the help of about one year of measurements of the standard deviations. The standard deviations of wind speed and wind direction are related to the upstream roughness over a few kilometres and can be used for an objective estimate of $z_{0u}$. Both the standard deviation of wind speed $s_u$ and the standard deviation of wind direction $s_d$ (in radians) can be employed by means of the following formulae:

$$s_u/U = c_u\kappa\left[\ln\left(z/z_{0u}\right)\right]^{-1} \qquad 5.A.1$$

$$s_d/U = c_v\kappa\left[\ln\left(z/z_{0u}\right)\right]^{-1} \qquad 5.A.2$$

where $c_u = 2.2$ and $c_v = 1.9$ and $\kappa = 0.4$ for unfiltered measurements of $s_u$ and $s_d$. For the measuring systems described in 5.8.3, the standard deviation of wind speed is filtered by about 12%, and that of wind direction by about 2%, which implies that $c_u$ and $c_v$ reduce to 1.94 and 1.86,

**Terrain classification from Davenport (1960) adapted by Wieringa (1980*b*) in terms of aerodynamic roughness length $z_0$**

| *Class index* | *Short terrain description* | $z_0$ *(m)* |
|---|---|---|
| 1 | Open sea, fetch at least 5 km | 0.0002 |
| 2 | Mud flats, snow; no vegetation, no obstacles | 0.005 |
| 3 | Open flat terrain; grass, few isolated obstacles | 0.03 |
| 4 | Low crops; occasional large obstacles, $x/H > 20$ | 0.10 |
| 5 | High crops; scattered obstacles, $15 < x/H < 20$ | 0.25 |
| 6 | Parkland, bushes; numerous obstacles, $x/H \approx 10$ | 0.5 |
| 7 | Regular large obstacle coverage (suburb, forest) | 1.0 |
| 8 | City centre with high- and low-rise buildings | ≥ 2 |

Note: Here $x$ is a typical upwind obstacle distance and $H$ is the height of the corresponding major obstacles. For more detailed and updated terrain class descriptions see Davenport et al. (2000) (see also Volume III, Chapter 9, Table 9.2 of the present Guide).

respectively. In order to apply the above equations, it is necessary to select strong wind cases ($U$ > 4 m s$^{-1}$) and to average $s_u/U$ and/or $s_d$ over all available data per wind sector class (30° wide) and per season (surface roughness depends, for example, on tree foliage). The values of $z_{0u}$ can now be determined with the above equations, where comparison of the results from $s_u$ and $s_d$ give some idea of the accuracy obtained.

In cases where no standard deviation information is available, but the maximum gust is determined per wind speed averaging period (either 10 min or 1 h), the ratios of these maximum gusts to the averages in the same period (gust factors) can also be used to determine $z_{0u}$ (Verkaik, 2000). Knowledge of system dynamics, namely, the response length of the sensor and the response time of the recording chain, is required for this approach.

## REFERENCES AND FURTHER READING


Ackermann, G.R., 1983: Means and standard deviations of horizontal wind components. *Journal of Climate and Applied Meteorology*, 22:959–961.

Albers, A., H. Klug and D. Westermann, 2000: Outdoor comparison of cup anemometers. *DEWI Magazin*, No. 17.

Beljaars, A.C.M., 1987: The influence of sampling and filtering on measured wind gusts. *Journal of Atmospheric and Oceanic Technology*, 4:613–626.

Busch, N.E. and L. Kristensen, 1976: Cup anemometer overspeeding. *Journal of Applied Meteorology*, 15:1328–1332.

Coppin, P.A., 1982: An examination of cup anemometer overspeeding. *Meteorologische Rundschau*, 35:1–11.

Curran, J.C., G.E. Peckham, D. Smith, A.S. Thom, J.S.G. McCulloch and I.C. Strangeways, 1977: Cairngorm summit automatic weather station. *Weather*, 32:60–63.

Davenport, A.G., 1960: Rationale for determining design wind velocities. *Journal of the Structural Division*, American Society of Civil Engineers, 86:39–68.

Davenport, A.G., C.S.B. Grimmond, T.R. Oke and J. Wieringa, 2000: Estimating the roughness of cities and sheltered country. *Preprints of the Twelfth American Meteorological Society Conference on Applied Climatology* (Asheville, NC, United States), pp. 96–99.

Evans, R.A. and B.E. Lee, 1981: The problems of anemometer exposure in urban areas: a wind-tunnel study. *Meteorological Magazine*, 110:188–189.

Frenkiel, F.N., 1951: Frequency distributions of velocities in turbulent flow. *Journal of Meteorology*, 8:316–320.

Gill, G.C., L.E. Olsson, J. Sela and M. Suda, 1967: Accuracy of wind measurements on towers or stacks. *Bulletin of the American Meteorological Society*, 48:665–674.

Gold, E., 1936: Wind in Britain: The Dines anemometer and some notable records during the last 40 years. *Quarterly Journal of the Royal Meteorological Society*, 62:167–206.

Grimmond, C.S.B., T.S. King, M. Roth and T.R. Oke, 1998: Aerodynamic roughness of urban areas derived from wind observations. *Boundary-Layer Meteorology*, 89:1–24.

International Organization for Standardization, 2002: *Meteorology – Sonic Anemometers/Thermometers – Acceptance Test Methods for Mean Wind Measurements*, ISO 16622:2002. Geneva.

———, 2007: *Meteorology – Wind Measurements – Part I: Wind Tunnel Test Methods for Rotating Anemometer Performance*, ISO 17713-1:2007. Geneva.

Kaimal, J.C., 1980: Sonic anemometers. In: *Air-sea Interaction: Instruments and Methods* (F. Dobson, L. Hasse and R. Davis, eds.). Plenum Press, New York, pp. 81–96.

Lenschow, D.H. (ed.), 1986: *Probing the Atmospheric Boundary Layer*. American Meteorological Society, Boston.

MacCready, P.B., 1966: Mean wind speed measurements in turbulence. *Journal of Applied Meteorology*, 5:219–225.

MacCready, P.B. and H.R. Jex, 1964: Response characteristics and meteorological utilization of propeller and vane wind sensors. *Journal of Applied Meteorology*, 3:182–193.

Makinwa, K.A.A., J.H. Huijsing and A. Hagedoorn, 2001: Industrial design of a solid-state wind sensor. *Proceedings of the First ISA/IEEE Conference* (Houston, November 2001), pp. 68–71.

Mazzarella, D.A., 1972: An inventory of specifications for wind-measuring instruments. *Bulletin of the American Meteorological Society*, 53:860–871.

Mollo-Christensen, E. and J.R. Seesholtz, 1967: Wind tunnel measurements of the wind disturbance field of a model of the Buzzards Bay Entrance Light Tower. *Journal of Geophysical Research*, 72:3549–3556.

Patterson, J., 1926: The cup anemometer. *Transactions of the Royal Society of Canada*, 20(III):1–54.

Smith, S.D., 1980: Dynamic anemometers. In: *Air-sea Interaction: Instruments and Methods* (F. Dobson, L. Hasse and R. Davis, eds.). Plenum Press, New York, pp. 65–80.

Taylor, P.A. and R.J. Lee, 1984: Simple guidelines for estimating wind speed variations due to small scale topographic features. *Climatological Bulletin*, Canadian Meteorological and Oceanographic Society, 18:3–22.

van Oudheusden, B.W. and J.H. Huijsing, 1991: Microelectronic thermal anemometer for the measurement of surface wind. *Journal of Atmospheric and Oceanic Technology*, 8:374–384.

Verkaik, J.W., 2000: Evaluation of two gustiness models for exposure correction calculations. *Journal of Applied Meteorology*, 39:1613–1626.

Walmsley, J.L., I.B. Troen, D.P. Lalas and P.J. Mason, 1990: Surface-layer flow in complex terrain: Comparison of models and full-scale observations. *Boundary-Layer Meteorology*, 52:259–281.

Wieringa, J., 1967: Evaluation and design of wind vanes. *Journal of Applied Meteorology*, 6:1114–1122.

———, 1980*a*: A revaluation of the Kansas mast influence on measurements of stress and cup anemometer overspeeding. *Boundary-Layer Meteorology*, 18:411–430.

———, 1980*b*: Representativeness of wind observations at airports. *Bulletin of the American Meteorological Society*, 61:962–971.

———, 1983: Description requirements for assessment of non-ideal wind stations, for example Aachen. *Journal of Wind Engineering and Industrial Aerodynamics*,11:121–131.

———, 1986: Roughness-dependent geographical interpolation of surface wind speed averages. *Quarterly Journal of the Royal Meteorological Society*, 112:867–889.

———, 1996: Does representative wind information exist? *Journal of Wind Engineering and Industrial Aerodynamics*, 65:1–12.

Wieringa, J. and F.X.C.M. van Lindert, 1971: Application limits of double-pin and coupled wind vanes. *Journal of Applied Meteorology*, 10:137–145.

World Meteorological Organization, 1981: *Review of Reference Height for and Averaging Time of Surface Wind Measurements at Sea* (F.W. Dobson). Marine Meteorology and Related Oceanographic Activities Report No. 3. Geneva.

———, 1984*a*: *Compendium of Lecture Notes for Training Class IV Meteorological Personnel* (B.J. Retallack). (WMO-No. 266), Volume II. Geneva.

———, 1984*b*: Distortion of the wind field by the Cabauw Meteorological Tower (H.R.A. Wessels). Paper presented at the WMO Technical Conference on Instruments and Cost-effective Meteorological Observations (TECEMO). Instruments and Observing Methods Report No. 15. Geneva.

———, 1987: *The Measurement of Gustiness at Routine Wind Stations: A Review* (A.C.M. Beljaars). Instruments and Observing Methods Report No. 31. Geneva.

———, 1989: *Wind Measurements Reduction to a Standard Level* (R.J. Shearman and A.A. Zelenko). Marine Meteorology and Related Oceanographic Activities Report No. 22 (WMO/TD-No. 311). Geneva.

———, 1990: *Abridged Final Report of the Tenth Session of the Commission for Instruments and Methods of Observation* (WMO-No. 727). Geneva.

———, 1991: *Guidance on the Establishment of Algorithms for Use in Synoptic Automatic Weather Stations: Processing of Surface Wind Data* (D. Painting). Report of the CIMO Working Group on Surface Measurements, Instruments and Observing Methods Report No. 47 (WMO/TD-No. 452). Geneva.

———, 2000: Wind measurements: Potential wind speed derived from wind speed fluctuations measurements, and the representativity of wind stations (J.P. van der Meulen). Paper presented at the WMO Technical Conference on Meteorological and Environmental Instruments and Methods of Observation (TECO-2000). Instruments and Observing Methods Report No. 74 (WMO/TD-No. 1028). Geneva.

———, 2001: *Lecture Notes for Training Agricultural Meteorological Personnel* (J. Wieringa and J. Lomas) (WMO-No. 551). Geneva.

———, 2011 (updated in 2017): *Manual on Codes* (WMO-No. 306), Volume I.1. Geneva.

Wyngaard, J.C., 1981: The effects of probe-induced flow distortion on atmospheric turbulence measurements. *Journal of Applied Meteorology*, 20:784–794.

# CHAPTER 6. MEASUREMENT OF PRECIPITATION

*This chapter was authored by:*

***Samuel Buisán**, State Meteorological Agency (AEMET) (Spain);*
***Craig Smith**, Climate Research Division, Environment and Climate Change Canada (Canada);*
***Yves-Alain Roulet**, Federal Office of Meteorology and Climatology MeteoSwiss (Switzerland);*
***Michael Earle**, Meteorological Service of Canada, Environment and Climate Change Canada (Canada);*
***Mareile Astrid Wolff**, Norwegian University of Life Sciences (Norway) and Norwegian Meteorological Institute (Norway).*

## 6.1 GENERAL

This chapter describes established methods of measuring precipitation at ground stations, including both traditional methods of measurement and newer technologies being used in operational networks. It has been updated primarily with respect to measurements of solid precipitation based on the final report of the WMO Solid Precipitation Intercomparison Experiment (WMO-SPICE) (Nitu et al., 2018) and related publications. Recommendations and best practices relating to the measurement of snow on the ground can be found in Volume II, Chapter 2 of the present Guide.

This chapter is divided into sections, beginning with the classification of measurements by technology (type of instrument), including a description of the technology, sources of error and recommendations on calibration and maintenance. Subsequently, the challenges of measuring liquid and solid precipitation are discussed, and recommendations are provided. The final sections discuss the importance of, and recommendations for, reference configurations for instrument intercomparison and transfer functions to adj1ust instrument observations to better match the "true" precipitation amount.

The extent to which a measurement is representative is a particularly critical issue for precipitation. Precipitation measurements are extremely sensitive to exposure, wind and topography. Metadata and ancillary data, such as temperature, describing the conditions of the measurements, are therefore crucial for data users. The following sections offer recommendations on how to perform reliable measurements taking into account environmental factors that can have a significant impact on measurement uncertainty and quality.

The manner in which this chapter is organized necessitates a certain amount of repetition with respect to the content because the same sources of error, recommendations, and suggestions for maximizing measurement quality apply to multiple instruments and situations. It is expected that this repetition will benefit those readers who may only refer to the particular sections that are of interest to them. Numerous tables and images are also included to summarize information and provide quick references for readers.

### 6.1.1 Definitions

Precipitation is defined as the liquid or solid products of the condensation of water vapour falling from clouds in the form of rain, drizzle, snow, snow grains, snow pellets, hail and ice pellets, or falling from clear air in the form of diamond dust, that are large enough to fall as a result of gravity.

Solid precipitation in the form of snow is less dense than liquid precipitation and more variable in terms of structure (for example, different ice crystal shapes, or habits) and related aerodynamics.

Solid precipitation in the form of hail and ice pellets is denser than snow, and the related aerodynamics are closer to those affecting liquid precipitation.

Moisture can also be transferred to the ground through dew, rime, hoar frost, or fog, but these forms of deposited water vapour and particles are not included in the definition of precipitation. Nevertheless, they are described in 6.8.

The total amount of precipitation that reaches the ground in a stated period is expressed in terms of the vertical depth of water (or water equivalent in the case of solid forms) that would cover a horizontal projection of the Earth's surface.

Precipitation intensity is defined as the amount of precipitation collected per unit of time, usually per minute or per hour.

### 6.1.2 Units, scales, resolution, integration periods and observation times

The unit of precipitation is linear depth, usually in millimetres (volume/area), or kg $m^{-2}$ (mass/area) for liquid precipitation.

For manual measurements, daily amounts of precipitation should be read to the nearest 0.2 mm and, if feasible, to the nearest 0.1 mm; weekly or monthly amounts should be read to the nearest 1 mm (at least). Daily measurements of precipitation should be taken at fixed times common to the entire network or networks of interest. Amounts less than 0.1 mm are generally referred to as a trace amounts.

Precipitation intensity is usually measured in millimetres per hour (mm $h^{-1}$); however, other time intervals may also be used (for example, 10- or 30-minute periods) depending on the purpose of the measurement (official certificates for insurance in case of damages, and so forth).

New technologies can measure precipitation amounts (even those less than 0.01 mm) with very high resolution and can achieve temporal resolutions on the order of seconds. However, it is recommended that one-minute intervals be used as the minimum integration time to derive precipitation intensity because of the high variability of intensity from minute to minute. Chapter 1, Annex 1.A of the present volume provides a comprehensive overview of the requirements for uncertainty, range, and resolution for precipitation measurements.

The common observation times for synoptic, climatological and hydrological purposes are hourly, three-hourly and daily. However, some applications, such as the design and management of urban drainage systems, the forecasting and mitigation of flash floods, transport safety measures, and most real-time applications, require a much greater time resolution to measure very high precipitation rates over very short periods (typically 1 min for precipitation intensity). Applications requiring measurements over extended periods of time may use storage gauges with observation intervals of weeks or months, or even one year in mountains and deserts. In some cases, for aviation purposes, it may be necessary to measure solid precipitation in the form of snow at intervals of less than one minute.

### 6.1.3 Methods of measurement

Precipitation gauges are the most common instruments used to measure precipitation. Generally, an open receptacle with vertical sides is used, usually in the form of a right cylinder, with a funnel if its main purpose is to measure rain. Since various gauge heights and sizes and shapes of orifices are used in different countries, measurements are not strictly comparable (Sevruk and Klemm, 1989). The volume or weight of the catch is measured, the latter in particular for solid precipitation. The gauge orifice may be at one of many specified heights above the ground or at the same level as the surrounding ground. The orifice must be placed above the maximum expected depth of snow cover and above the height of significant potential in-splashing from the ground. The most commonly used elevation height in more than 100 countries varies between 0.5 and 1.5 m (Sevruk and Klemm, 1989).

Precipitation gauges have evolved from manual and storage gauges requiring human intervention, to float gauges using chart recorders or digital transducers, to modern

tipping-bucket and weighing gauges. Tipping-bucket precipitation gauges collect precipitation in a funnel, from which it falls into a calibrated bucket that tips when it is full, empties, and records the tip. Weighing gauges determine the precipitation amount based on the accumulated weight of water collected over time. Hybrid technologies using a combination of tipping-bucket and weighing technologies are also available.

New technologies that measure precipitation without capturing hydrometeors in a container ("non-catchment"-type instruments) are increasingly being used operationally. The measurements performed by these instruments are based on the principles of light scattering, microwave backscatter, and mass and heat transfer.

Point measurements of precipitation serve as the primary source of data for areal and numerical weather prediction (NWP) analysis products. However, even the best measurement of precipitation at one point is only representative of a limited area, the size of which is a function of the length of the accumulation period, the physiographic homogeneity of the region, local topography and the precipitation-producing process. Radar and satellites are used to define and quantify the spatial distribution of precipitation. In principle, a suitable integration of all sources of precipitation data (automatic gauges, radar, and satellites) into national precipitation networks can be expected to provide more representative precipitation estimates on an operational basis for a wide range of precipitation data users than data from a single source.

Instruments that detect and identify precipitation, as opposed to measuring the amount of precipitation, may be used as present weather sensors; they are discussed in Chapter 14 of the present volume.

## 6.2 TYPES OF INSTRUMENTS

### 6.2.1 Non-recording (manual) precipitation gauges

The conventional manual precipitation gauge for rainfall consists of a collector placed above a funnel leading into a container where the accumulated water is usually stored in a bucket between observation times (see Figure 6.1). Different gauge shapes are in use worldwide (see Figure 6.2). Where solid precipitation is common and substantial, a number of special modifications are used to improve the accuracy of measurements. Such modifications include the removal of the funnel (see Figure 6.3) at the beginning of the snow season or the provision of a specialized snow fence or shield to improve collection efficiency under windy conditions (this will be discussed in 6.3).

The stored liquid water is poured from the container into a measuring cylinder, or its level in the container is measured directly with a scale of appropriate accuracy and resolution. As another option, the container can be weighed with a balance of appropriate accuracy and resolution.

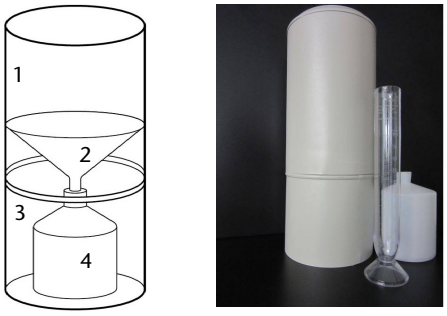



**Figure 6.1. (Left) diagram of a manual rainfall precipitation gauge (1) collector (2) funnel (3) container (4) bucket (Right) measuring cylinder and bucket (Hellman type)**

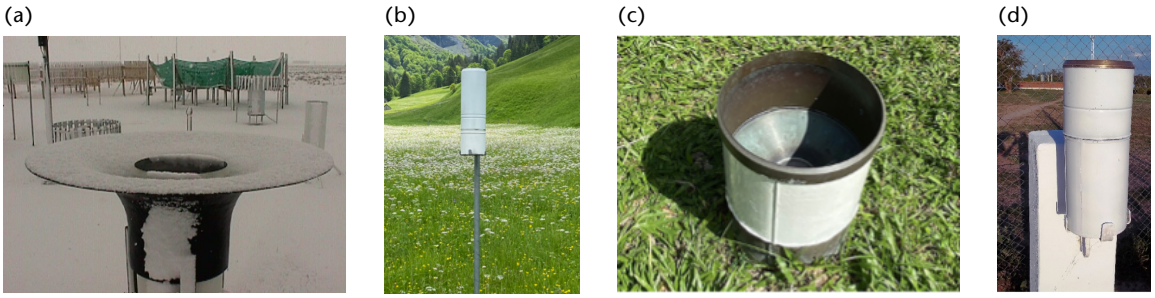



**Figure 6.2. Examples of different manual gauges used worldwide: (a) Nipher gauge (Canada), used for solid precipitation; (b) gauge used by MeteoSwiss (Switzerland); (c) gauge used by the Hong Kong Observatory (Hong Kong, China); (d) gauge used by the National Meteorological Service of Argentina (Argentina)**

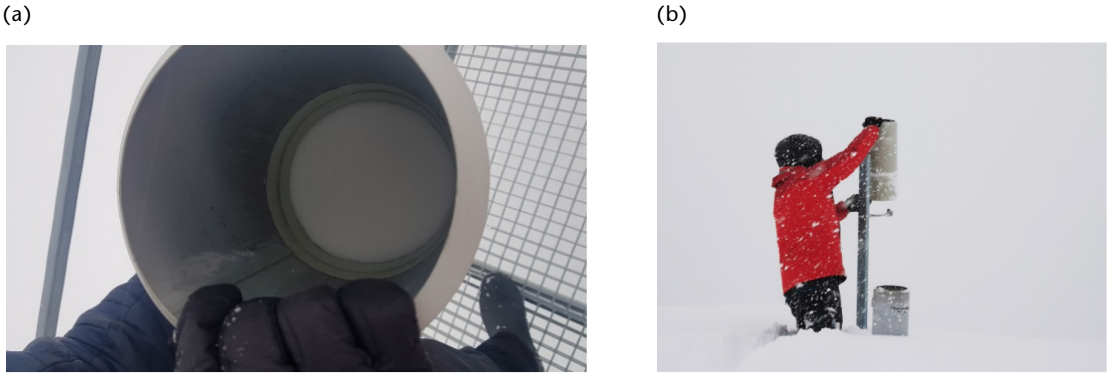



**Figure 6.3. (a) Modified precipitation gauge (funnel removed) for collecting and melting snow; (b) replacement of gauges to minimize the loss of precipitation**

Overall, gauges with a large collector orifice (or opening) should have a lower statistical error in the measurements. However, gauges with larger collector openings also collect more water and therefore may not be usable in regions which often receive high amounts of precipitation since the water collected may exceed the storage capacity of the gauge. On the other hand, gauges with small collector areas collect less water but can be more difficult to read, increasing the potential for error. Smaller collector openings are also more likely to become blocked with debris, which negatively impacts measurements. The size of the collector orifice is less critical for liquid precipitation, but an area of at least 200 $cm^2$ is required if significant amounts of solid precipitation are expected. Gauges with collecting areas of 200 $cm^2$ to 500 $cm^2$ are the most common, but users need to balance application requirements, budget and other operational considerations.

The most important requirements for a manual precipitation gauge are as follows:

(a) The rim of the collector should have a sharp edge and should fall away vertically on the inside and be steeply bevelled on the outside;

(b) The area of the orifice should be known to the nearest 0.5%, and the construction should be such that this area remains constant while the gauge is in normal use;

(c) The collector should be designed to prevent rain from splashing in and out. This can be achieved if the vertical wall is sufficiently deep and the slope of the funnel is sufficiently steep (at least 45°);

(d) The construction should be such as to minimize wetting errors. This can be achieved by choosing the proper material and minimizing the total inner surface of the collector;

(e) The container should have a narrow entrance and be sufficiently protected from radiation to minimize the loss of water by evaporation; it should use a funnel when collecting rainfall. Precipitation gauges used in locations where only weekly or monthly readings are practicable should be similar in design to the type used for daily measurements, but with a container of larger capacity and stronger construction. The collector needs to have sufficient capacity to hold the highest expected amount of precipitation between observations.

Different kinds of errors, such as wetting, splashing and evaporation, will be discussed in 6.2.1.2.

The measuring cylinder should be made of clear glass or plastic that has a suitable coefficient of thermal expansion and should be clearly marked to show the size or type of gauge with which it is to be used. Its diameter should be less than 33% of that of the rim of the gauge; the smaller the relative diameter, the greater the precision of measurement. The graduations should be finely engraved; in general, there should be marks at 0.2 mm intervals and clearly visible lines at each whole millimetre. It is also desirable that the line corresponding to 0.1 mm be marked. The maximum error of the graduations should not exceed ±0.05 mm at or above the 2 mm graduation mark and ±0.02 mm below this mark. Measurements of less than 0.1 mm can be considered as trace.

To measure small liquid precipitation amounts, the inside diameter of the measuring cylinder should taper off at its base. In all measurements, the bottom of the water meniscus should define the water level, and the cylinder should be kept vertical when reading to avoid parallax errors. Repetition of the main graduation lines on the back of the measure is also helpful for reducing such errors.

The following two methods are broadly used to measure solid precipitation in the form of snow:

(a) Snow is collected in a container and the snow plus the container are weighed with a scale of appropriate accuracy and resolution (and the known weight of the container is subtracted);

(b) Snow is melted after each observation, and the volume of the collected water is measured using a standard graduated measuring cylinder. The use of strong heating sources to melt the snow is not recommended because this could lead to sublimation and/or evaporation. It is preferable to melt the snow slowly or to mix the snow with a known quantity of warm water (which will be subtracted from the total) to facilitate a controlled and efficient melting of the snow.

It is recommended to exchange gauge collectors between each observation (see Figure 6.3) to ensure a more continuous measurement and to remove any water adhering to the collector so that it is not included in the next measurement.

Storage gauges are a specific type of manual precipitation gauge used to measure long-term (monthly to seasonal) precipitation in remote and sparsely inhabited areas. Such gauges consist of a collector above a funnel leading to a container that is large enough to store the yearly, seasonal, or monthly catch (depending on the desired time resolution).

A layer of no less than 5 mm of a suitable oil or other evaporation suppressant should be placed in the container to reduce evaporation (Sevruk, 1972). This layer should allow the free passage of precipitation into the solution below it. In locations where solid precipitation occurs and temperatures fall below 0 °C, an antifreeze solution should be placed in the container to convert any snow that falls into the gauge into a liquid state and to prevent the gauge contents from freezing. In this case, oil is also needed to prevent the evaporation of both water and antifreeze (see 6.3.1).

The precipitation catch is determined by weighing or measuring the volume of the contents of the container (as with ordinary gauges; see 6.3.1). The amount of oil and antifreeze solution placed in the container at the beginning of the season and any expansion/contraction of the storage vessel, if the measurement is volumetric, must be carefully taken into account.

The operation and maintenance of storage gauges in remote areas pose several problems, such as the capping of the gauge by snow (see 6.3.1) and the difficulty in accessing the gauge for measurement recording. Particular attention should be paid to assessing the quality of data from such gauges.

Dip-rods can be used to check the level of liquid in the container. They should be made of cedar wood or another suitable material that does not absorb water appreciably and possesses only a small capillary effect. Wooden dip-rods are unsuitable if oil has been added to the collector to suppress evaporation. When this is the case, rods made of metal or other materials from which oil can be readily cleaned must be used. Non-metallic rods should be provided with a brass foot to avoid wear and be graduated according to the relative areas of cross-section of the gauge orifice and the collector; graduations should be marked at least every 10 mm and include an allowance for the displacement caused by the rod itself. The maximum error in the dip-rod graduation should not exceed ±0.5 mm at any point. A dip-rod measurement should be checked using a volumetric measure wherever possible.

#### 6.2.1.1 *Calibration, field verification and maintenance*

The graduation of the measuring cylinder or dip-rod (for storage gauges) must be consistent with the chosen size of the collector. The calibration of the gauge, therefore, includes checking the diameter of the gauge orifice and ensuring that it is within allowable tolerances. It also includes volumetric checks of the measuring cylinder or stick. For measurements based on weight, regular calibration of the weighing balance is required.

Routine maintenance should at all times include keeping the gauge level to prevent it from becoming out of level (see Rinehart, 1983; Sevruk, 1984). The outer container of the gauge and the graduate should be regularly cleaned both inside and outside using a long-handled brush, soapy water and a clean water rinse. Worn, damaged or broken parts should be replaced, as required. Ground vegetation around the gauge should be kept trimmed to 5 cm (where applicable). The exposure should be checked and recorded.

#### 6.2.1.2 *Sources of error and corrections*

The true amount of precipitation may be estimated by correcting for some or all of the various error terms listed below:

(a) Error due to systematic wind field deformation above the gauge orifice: typically 2% to 10% for rain and 10% to 50% or more for snow (this will be discussed further in 6.5);

(b) Error due to wetting loss on the internal walls of the collector;

(c) Error due to wetting loss in the container when it is emptied;

(d) Error due to evaporation from the container;

(e) Error due to blowing and drifting snow;

(f) Error due to the in- and out-splashing of water (1% to 2%);

(g) Random observational and instrumental errors, including incorrect gauge reading times.

Wetting loss (Sevruk, 1974a) is a cumulative systematic loss from manual gauges that varies with precipitation and gauge type. Its magnitude is also a function of the number of times the gauge

is emptied. Wetting losses typically account for 2% to 15% of measured values in summer and 1% to 8% in winter, and the average wetting loss can be up to 0.2 mm per observation. At synoptic stations where precipitation is measured every 6 h, this can become a very significant loss. In some countries, wetting loss has been calculated to be 15% to 20% of the measured winter precipitation.

Correcting for wetting loss at the time of observation is a feasible alternative. Wetting loss can be kept low in a well-designed gauge. The methodology to determine the wetting loss of manual gauges outlined by Goodison et al. (1998) in the *WMO Solid Precipitation Measurement Intercomparison* (WMO/TD-No. 872) final report is an excellent reference. It is recommended that the wetting loss for manual gauges be re-examined periodically (for example, every five years) as it tends to change with the age of the collector. The internal surfaces should be of a material that can be kept smooth and clean; paint, for example, is unsuitable, but baked enamel is satisfactory. Seams in the construction should be kept to a minimum.

Evaporation losses (Sevruk, 1974b) vary by gauge type, climatic zone and time of year (the seasons mentioned below correspond to the northern hemisphere). Evaporation loss is a problem with gauges that do not have a funnel device in the bucket, especially in late spring at mid-latitudes. Losses of over 0.8 mm per day have been reported. Losses during winter, which range from 0.1 mm to 0.2 mm per day, are much less than those during summer; these losses, however, are cumulative. In a well-designed gauge, only a small water surface is exposed, its ventilation is minimized, and the water temperature is kept low by a reflective outer surface.

### 6.2.2 Weighing (automated) gauges

The most significant difference between a conventional manual precipitation gauge and a weighing gauge is that a weighing gauge generally accumulates falling precipitation in a collector and measures the interval precipitation amount as the difference in bucket weight between the start and the end of the interval. Often referred to as “recording” or “automated” gauges, weighing gauges necessarily require a means to record the bucket weights at the beginning and end of the measurement interval. The recording mechanism can be an analogue strip chart rotating on a timing device and marked with the changing bucket weight, or the bucket weight (or differential bucket weight) or can be transmitted and recorded in digital format via an electronic data logger. While recording gauges with strip charts can be simple mechanical devices, electronic recording gauges are technically more complex and often include on-board processing to filter signal noise and output interval precipitation amounts, precipitation intensity, and other diagnostic information. Most weighing gauges have a finite storage capacity requiring periodic servicing to empty the collecting bucket.

Many of the considerations for weighing gauges are similar to those discussed for manual gauges in 6.2.1, including the area and accuracy of the collector orifice and the design and shape of the collector to prevent splashing. The capacity of the bucket is an important factor and is dependent on both the collection area of the orifice and the expected precipitation between servicing. Users need to keep in mind that the use of oil to supress bucket evaporation and the use of antifreeze required for operation below freezing both decrease total bucket capacity.

#### 6.2.2.1 *Description of technology*

The measurement principles and technology for weighing gauges vary in both technique and complexity. Early weighing gauges used spring mechanisms to transfer the change in bucket weight to a strip chart. These mechanical gauges were then adapted to convert bucket weight to analogue voltage (via a potentiometer). Changes in voltage are calibrated to changes in bucket weight, and hence precipitation amount (as a differential), and recorded at specific time intervals by a data logger. Modern weighing precipitation gauges now use more complex weighing methods, such as vibrating wire strain gauges or load cells (Figure 6.4), to measure the weight of the bucket. Some tipping-bucket gauges (discussed further in 6.2.3) now employ

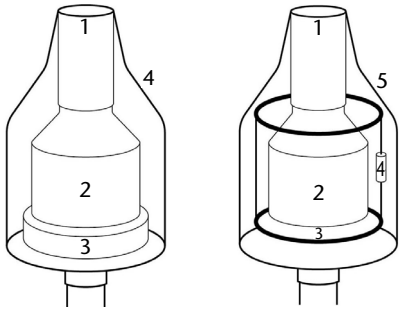



**Figure 6.4. Diagram of a weighing gauge**
**Left: Load cell type gauge with (1) collector orifice; (2) bucket; (3) load cell; (4) gauge casing;**
**Right: Vibrating wire strain gauge with (1) collector orifice; (2) bucket; (3) suspended frame; (4) vibrating wire transducer; (5) gauge casing**

a hybrid strategy by weighing the small reservoir of the tipping bucket before the bucket tips and empties. Each measurement principle has both advantages and disadvantages, and the choice often depends on user preference.

The three types of weighing gauges are described below.

(a) **Load cell gauges** (Figure 6.4, left) use a fast response transducer that converts weight into an electrical output. The bucket sits on top of the load cell so that the transducer can calculate the weight change of the bucket between measurement intervals. The output from load cell transducers is typically temperature compensated and noise filtered via built-in algorithms and transferred to the data logger via a digital message or converted to an analogue pulse (switch closure) to replicate a tipping bucket. Advantages of this type of gauge include a pre-filtered (clean) estimate of interval precipitation available to the user (no post-processing required by the user) and the capability of the gauge to output derived products such as precipitation intensity as well as sensor diagnostic information. The disadvantages include the unavailability of unprocessed data (for example, raw bucket weights) due to the often-proprietary, built-in, firmware-dependent algorithms;

(b) **Vibrating wire strain gauges** (Figure 6.4, right) operate by supporting the weight of the bucket (via one or more magnetically "plucked" vibrating wires) so that increasing the weight of the bucket puts additional strain on the vibrating wire, hence increasing the frequency of the vibration. A calibration equation converts the vibrating wire frequency to bucket weight. Advantages of this type of gauge include the capability to carry analogue frequency over longer conductor distances and the capability of logging raw frequency. Raw frequency can be used to re-calculate bucket weight in the event of a calibration issue. Disadvantages include the potential interference in the signal via either electrical or mechanical (vibration) noise and potential impacts of ambient temperature change on the vibration frequency causing apparent diurnal cycles in measured bucket weight. This often necessitates post-processing by the user to calculate interval precipitation;

(c) **Weighing tipping-bucket gauges** (not shown, but similar to Figure 6.5) use a hybrid measurement technique in that precipitation is funnelled into the "bucket" where it is collected and weighed via a load cell transducer before the bucket is tipped and emptied. The realized advantages and disadvantages of this type of gauge are similar to those for any load cell gauge. This type of gauge requires heating of the collector surface, the funnel, and the discharge area to melt solid precipitation for measurement and drainage, but the advantage over conventional weighing gauges is that these gauges are not limited by a finite bucket capacity. Some types of weighing tipping buckets revert to counting tips at higher rainfall intensities.

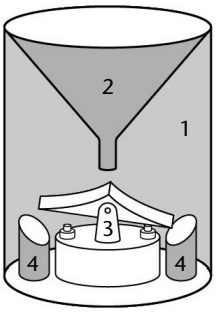



**Figure 6.5. Diagram of a tipping bucket**
**The shaded areas are the recommended heated parts: (1) collector; (2) funnel; (3) tipping bucket; (4) discharge outlets.**

### 6.2.2.2 *Calibration, field verification and maintenance*

Precipitation gauges should be calibrated at intervals suggested by the manufacturer, but those intervals may be revised based on the operational experience of the user in order to reduce operational costs but still meet user requirements for data quality. For weighing gauges, the accuracy of the measurement of the total bucket weight is less important than the measurement of the bucket weight increment over a specific period. Simple field verification can be achieved by adding increments of a known weight of water (or dry weights with known masses if appropriate) to the gauge and observing the difference between the calculated precipitation amount (using Equation 6.1) and the instrument observed amount (bucket weight after the addition of verification water minus bucket weight before the addition of verification water):

$$C = \frac{W_f - W_e}{A} \times 10 \qquad (6.1)$$

where $C$ is the calculated calibration amount of precipitation in mm, $W_f$ is the weight of a full bottle of water in grams, $W_e$ is the weight of the empty bottle of water in grams (this is the tare weight but should be weighed after the bottle is emptied so that any water left in the bottle is included in the tare), and $A$ is the area of the collector in cm$^2$.

The verification water should be carefully poured into the gauge bucket without splashing or excessive disturbance of the gauge (such as shaking), which could impact gauge performance.

The amount of water used for a field verification will depend on the resolution and capacity of the gauge; for example, a 500 ml bottle of water poured into a gauge with a 200 cm$^2$ collection area should elicit a response of 25 mm of precipitation. If possible, the field verification should be performed over the entire capacity range of the gauge to test response linearity. Site conditions need to be considered when interpreting the verification test since excessive wind or large swings in temperature may impact the ability of the gauge to accurately measure the increment. Also, the gauge should be given sufficient time to produce a measurement. If possible, calibration should be done in a laboratory where conditions can be more controlled; however, field verification may better characterize gauge behaviour in natural operating conditions. Verification water may be replaced with known verification weights if the weights can be properly balanced on the weighing mechanism. The advantage of using water is that water is self-levelling; however, this may not be practical in all situations. Ideally, a field verification procedure should be repeated many times to obtain statistics on gauge behaviour, but usually this is not practical for an in situ gauge. Calibration techniques using peristaltic pumps increase the accuracy and precision of a calibration but generally can only be used in a laboratory setting.

Another consideration for field verification is the data logging device for recording gauges, especially if the gauge measurement is analogue. Data-logger calibration, usually performed by a qualified technician, can help ensure correct observation of the gauge measurement.

The manufacturer usually prescribes necessary routine gauge maintenance. In addition, periodically check the in situ gauge (the orifice and the bucket) for level and for damage to the orifice, which may change the collecting area. Routinely check electronic cables for damage (especially where rodents are present), and replace damaged cables if necessary. Gauges that use funnels to decrease evaporation can be prone to plugging by debris and should be inspected and cleaned often. On mechanical weighing gauges, all moving parts and springs should be routinely inspected for damage and repaired if necessary. Weighing gauges intended for use below freezing temperatures require additional maintenance. See 6.3.1 for recommendations on the use of oil and antifreeze for operation at temperatures below freezing.

A procedure for calibrating weighing-recording gauges when dealing with precipitation intensity measurements is given in Annex 6.A. This calibration, referred to as a dynamic calibration in steady-state conditions of the reference flow rates, is performed to evaluate the measurement errors of the weighing gauge. The procedure can also be used to assess the dynamic response of the weighing gauge by performing the classic step response test, that is, by providing the instrument with a reference flow rate showing a single abrupt change from zero to a given equivalent rainfall rate. Moreover, by repeating the dynamic calibration in unsteady conditions (using time-varying reference flow rates as a simulation of real-world events), weighing gauges can be more finely calibrated (especially for systematic delays due to the instrument's response time). This may lead to improved dynamic performance and accuracy in real-world events (Colli et al., 2013b).

For rainfall intensity gauges, a recommended procedure by means of a portable device for reference flow rates is given in Annex 6.B. Other simplified procedures are also explained in 6.2.3.3.

#### 6.2.2.3 *Sources of error and corrections*

The increased complexity of weighing gauges vs. manual gauges also adds complexity to the potential errors and error corrections. Section 6.2.1.2 lists seven errors associated with manual gauges. Errors (a), (b), (d), and (e) also apply to weighing gauges. Error (c) does not apply to most weighing gauges because the container is not emptied for a measurement (although this error does apply to weighing tipping buckets). Wetting loss, error (b), can occur in gauges that have a long chimney leading to the collector bucket, providing an opportunity for precipitation to evaporate from the chimney walls before it falls into the bucket for measurement. Generally, this error is relatively small except in the case of very light precipitation events. Error (d) is usually minimized through the use of oil to supress evaporation from the bucket but also becomes less significant with shorter measurement intervals. Error (f) is typically resolved by the design of weighing gauges but may not be eliminated completely. Error (a), the systematic error due to wind, is discussed further in 6.6. Error (g), random observational and instrumental errors in weighing gauges, requires further discussion.

Random and instrumental errors can include:

(a) Errors due to signal noise caused by either mechanical or electrical interference. This interference prevents the precise measurement of the bucket weight and therefore increases the uncertainty of the interval precipitation amount. These errors are difficult to correct but can be minimized by ensuring proper electrical grounding, adequate integration/averaging periods during the measurement, and solid installation. Manufacturers will often make recommendations on how to minimize signal noise.

(b) Errors due to calibration. These errors will result in the incorrect calculation of bucket weight or precipitation. In an analogue gauge, the signal originating from the gauge may be incorrectly converted to a precipitation amount by the data logger. In digital gauges, the built-in algorithms may incorrectly estimate interval precipitation. Generally, if the gauge response is linear, calibration errors may cancel out when an interval precipitation amount is calculated from the differential bucket weight; this is not the case when the response to precipitation is not linear. These errors can be minimized by ensuring

that correct calibration coefficients are used and tested through calibration checks. Often, calibration errors can be corrected post-measurement if the raw bucket weights are logged along with the interval precipitation amount; this is recommended where possible.

(c) Errors due to a damaged orifice or due to the gauge being out of level. A damaged orifice (such as a dented or bent rim) may change the effective collection area of the gauge and create a negative bias error. Similarly, a gauge with an orifice that is not horizontally level will impact the catch, although this bias may be positive or negative depending on wind direction and hydrometeor fall angle.

### 6.2.3 Tipping buckets

Tipping-bucket gauges are used broadly in operational networks to measure precipitation (Nitu and Wong, 2010), mainly rainfall. The addition of heaters extends their application to colder environments and the measurement of solid and mixed-phase precipitation.

Tipping-bucket precipitation gauges are used for measuring accumulated totals and the rate of precipitation.

Suitable intensity-dependent corrections should be applied to improve the accuracy of the intensity measurements and to overcome the underestimation of intensity for high rainfall rates and the overestimation of intensity for low rainfall rates, both of which are typical in non-corrected tipping-bucket gauges.

#### 6.2.3.1 *Description of technology*

The principle behind the operation of this instrument is simple. A tipping-bucket uses a metallic or plastic twin bucket balance to measure the incoming water in portions of equal weight. When one bucket is full, its centre of mass is outside the pivot, and the balance tips, dumping the collected water and bringing the other bucket into position to collect. The bucket compartments are shaped in such a way that the water is emptied from the lower one (Figure 6.5). The water mass content $M$ in g of the bucket is constant. Therefore, by using the density of water $\rho$ = 1 g cm$^{-3}$, the corresponding volume $V$ in cm$^3$ is derived from the weight of the water and, consequently, the corresponding accumulation height $h$ in mm is retrieved by using the area of the collector $S$ in cm$^2$ (see Equation 6.2):

$$V = \frac{M}{\rho} = h \cdot S \tag{6.2}$$

Thus, by using the density of water, $h$ is calculated, where 1 mm corresponds to 1 g of water over an area of 10 cm$^2$. To have detailed records of precipitation, the amount of water should not exceed 0.2 mm. For a gauge area of 1 000 cm$^2$, this corresponds to a bucket content of 20 g of water.

Tipping-bucket gauges usually employ a contact closure (reed switch or relay contact), such that each tip produces an electrical impulse as a signal output.

This output must be recorded by a data logger or an analogue to digital converter (ADC) (data acquisition system equipped with reed switch reading ports). This mechanism provides continuous measurement without manual interaction.

The precipitation intensity of non-corrected tipping-bucket gauges is calculated based on the number of tips in a periodic sampling rate and averaged over a chosen time interval (for example, 1 min). In this way, an intensity value is available every minute and represents the intensity of the past minute or minutes. This sampling scheme reduces the uncertainty of the average. In addition, the precipitation intensity resolution depends on the size of the bucket and the chosen time interval. For example, a tip equivalent to 0.2 mm leads to a 1 min precipitation intensity resolution of 12 mm h$^{-1}$ which is constant over the measurement range of the gauge if no intensity-dependent corrections are applied.

The pulse generated by a contact closure can be monitored by a data logger, preferably including the time the tips occurred, to calculate a corrected precipitation intensity, which can then be used to retrieve the precipitation amount over selected periods. It may also be used with a chart recorder.

Although the main purpose of tipping buckets is to measure rainfall, if the gauge is equipped with sufficient heating for melting the solid precipitation in the funnel, this instrument, taking into account some limitations that will be discussed in 6.3.1, can be used for measuring all types of precipitation. The primary function of heaters for tipping-bucket gauges is to melt solid precipitation collected by the gauge so that it can pass into the bucket assembly and be measured. In addition to funnel heating for the purpose of melting, the bucket assembly and/or outlet ports are typically heated to prevent re-freezing of precipitation and potential gauge blockage.

Heating can be thermostatically and automatically controlled using a sensor which detects when the temperature drops below a certain value. To save power, this can be combined with the detection of precipitation in the catch area. If an external system monitors ambient temperature and precipitation, it can control the tipping-bucket heaters directly

An international survey (Nitu and Wong, 2010) showed that for tipping buckets used operationally, the amount of precipitation required to tip the bucket ranged from 0.1 mm to 0.5 mm, and the size of the collecting area ranged from 200 $cm^2$ to 1 000 $cm^2$, respectively.

### 6.2.3.2 *Sources of error and corrections*

Some sources of error typical of tipping-bucket gauges include the following:

(a) The loss of water during the tipping action in heavy rain. The bucket takes a small but finite time to tip and, during the first half of its motion, additional precipitation may enter the compartment that already contains the calculated amount of rainfall. The water losses during the tipping movement indicate a systematic mechanical error that is rather a function of the intensity itself and can be appreciable during heavy rainfall (> 100 mm $h^{-1}$). This can be reduced considerably by conducting a dynamic calibration (see Annex 6.A) and applying an intensity-dependent correction;

(b) With the usual bucket design, the exposed water surface is large in relation to its volume, meaning that appreciable evaporation losses can occur, especially in hot regions. This error may be significant in light rain;

(c) The discontinuous nature of the record may not provide satisfactory data during light drizzle or very light rain. In particular, the time of onset and cessation of precipitation cannot be accurately determined;

(d) Water may adhere to both the walls and the lip of the bucket, resulting in precipitation residue in the bucket and additional weight to be overcome by the tipping action. Tests on waxed buckets produced a 4% reduction in the volume required to tip the balance compared with non-waxed buckets. Volumetric calibration can change, without adjustment of the calibration screws, by variation of bucket wettability through surface oxidation or contamination by impurities and variations in surface tension;

(e) The stream of water falling from the funnel onto the exposed bucket may cause over-reading depending on the size, shape and position of the nozzle;

(f) The instrument is particularly prone to bearing friction and to having an improperly balanced bucket when the gauge is not level;

(g) The limited repeatability at various precipitation intensities of the inter-tip time interval due to the low stability of the mechanics of the buckets (that is, bucket movement) degrades

the measurements; this systematic mechanical effect can be investigated by means of specific tests recording a series of inter-tip time intervals that make it possible to estimate the mechanical precision of the bucket (see Colli et al., 2013b); such errors may be reduced by improving the construction quality of the gauges;

(h) Under light precipitation regimes, the tipping-bucket mechanism can be delayed in assigning the collected amount of water to the corresponding time interval (Habib et al., 2001); different calculation techniques exist for reducing the impact of sampling errors and providing rainfall intensity measurements at a higher resolution than the tipping-bucket gauges' sensitivity would allow (see Colli et al., 2013a; Stagnaro et al., 2016);

(i) For solid precipitation events measured on operational tipping buckets that are not heated, the data should be removed or accumulated (after a detailed analysis) over a period of time (usually daily totals) once the solid precipitation has naturally melted;

(j) The evaporation effect may cause water to be lost if heating is not properly controlled and the temperature of the critical parts is not consistently slightly above the melting point of water. Lower heating power could be advantageous in terms of reducing evaporative losses from the funnel relative to heating with higher power. The specific gauge and heating configuration should be selected with consideration given to the availability of site resources (for example, power) and to the characteristic site conditions;

(k) The time required to melt precipitation in the funnel can further delay the tipping-bucket response and can be exacerbated by the specific heating mechanism. This can result not only in delays, but also in the potential to report false accumulation due to the reduction of the timeliness in reporting the precipitation. This delay can be particularly high when the intensity is low as it takes longer to fill the tipping bucket and for the bucket to tip and register the precipitation amount (depending on the sensitivity of the tipping mechanism);

(l) Melting delays give rise to another potential loss mechanism: wind blowing snow out of the funnel. Low and/or insufficient heating power may further extend melt times, providing more opportunity for losses due to wind or to the funnel filling to capacity and being unable to collect more snow;

(m) Under strong winds, if the instrument is not well fixed to the ground, false precipitation can be recorded due to pulses generated by internal movement of the tipping bucket producing contact closures;

(n) Damaged cables connected to the instrument in moist environments or during precipitation events and due to water conductivity can generate contact closures similar to those of the tipping buckets, producing false records of precipitation;

(o) Tipping-bucket gauges may malfunction when the instantaneous rainfall intensity is extremely high, exceeding the upper limit of tipping-bucket measurement capacity. Instruments should be selected considering the highest intensity of rainfall in the area where the measurements will be made.

#### 6.2.3.3 *Calibration, field verification and maintenance*

Calibration can provide corrections for some of the systematic parts of these errors. Effective corrections for improving the measurement of precipitation intensity (Vuerich et al., 2009), and consequently, the corresponding accumulated amount, consist in performing a dynamic calibration and applying correction curves, for example, by applying a software correction or an algorithm in the data acquisition system. Alternatively, they can involve conducting a linearization procedure in the instrument's electronics circuit (generating an intensity-dependent emission of extra pulses) or through a mechanism (for example, small deflectors that induce a dynamic pressure which increases with intensity, allowing the tip to occur before the bucket is full). In Vuerich et al. (2009), it is shown that linearization by extra electronic pulses is well suited for measuring precipitation amount but less so for measuring

intensity. On the other hand, mechanical linearization compensates for the loss of water during the movement of the balance and greatly minimizes the intensity underestimation during high-rate events. The software correction (correction curve or algorithm) was the most effective method for correcting systematic mechanical errors. The field performances in a tropical environment of three different types of tipping-bucket gauges, without correction, with software correction and with extra pulse correction, can be found in Chan et al. (2015).

Proper calibration of the tipping bucket is usually accomplished by passing a known amount of water through the tipping mechanism at various rates and by adjusting the mechanism to the known volume. This procedure should be followed under laboratory conditions. The recommended calibration procedure for these gauges is described in Annex 6.A.

A recommended field verification procedure, including a detailed method for amount verification, especially to control the response of the instrument at high intensities, is given in Annex 6.B. This procedure can be conducted by means of a portable device for reference flow rates.

A simplified procedure solely for testing the performance of the instrument, which can be also applied in the field, involves using water containers with air intakes to maintain constant pressure and different flow nozzles. The water containers are filled with known amounts of water to test the instrument's relative error in total precipitation measurement at different intensities and to verify the performance of its intensity correction, if available.

Proper field verification should also be conducted on a regular basis as part of the routine maintenance and verification and should take into account site and operational constraints. Routine maintenance should include cleaning the accumulated dirt and debris from the funnel and buckets, as well as ensuring that the gauge is level. It is highly recommended that the tipping mechanism be checked during the maintenance and replaced with a newly calibrated unit if needed.

Routine maintenance in the field should also include verifying the power supply for heating, testing the continuity of the electrical circuit, and verifying that the heating mechanisms are triggered properly. To simulate solid precipitation and diagnose any failure in the temperature sensors on the gauge, a source of material providing a temperature environment below 0 °C is necessary. If available, it is recommended that snow on the ground be used; during the warm season, or in absence of snow or ice, it is recommended that freeze spray be used.

### 6.2.4 Float gauge

In this type of instrument, used increasingly less frequently in meteorological services, the precipitation (in liquid form) passes into a float chamber containing a light float. As the level of the water within the chamber rises, the vertical movement of the float is transmitted by a suitable mechanism to the movement of a pen on a chart or a digital transducer. By making the appropriate adjustments to the dimensions of the collector orifice, the float and the float chamber, any desired chart scale can be used. Heating devices can be installed to melt solid precipitation. In addition, the reservoir is often filled with an antifreeze mixture to keep the contents and float from freezing and to melt any solid precipitation falling into the solution.

In order to provide a record over a useful period (at least 24 h are normally required), either the float chamber has to be very large (in which case, a compressed scale on the chart or other recording medium is obtained), or a mechanism must be provided to empty the float chamber automatically and quickly whenever it becomes full so that the chart pen or other indicator returns to zero. Usually, a siphoning arrangement is used. The actual siphoning process should begin precisely at the predetermined level, with no tendency for the water to dribble over at either the beginning or the end of the siphoning period, which should not be longer than 15 s. In some instruments, the float chamber assembly is mounted on knife edges so that the full chamber overbalances; the surge of the water assists the siphoning process, and, when the chamber is empty, it returns to its original position. Other rain recorders have a forced siphon which operates in less than 5 s. One type of forced siphon has a small chamber that is separate

from the main chamber and accommodates the rain that falls during siphoning. This chamber empties into the main chamber when siphoning ceases, thus ensuring a correct record of total rainfall.

A heating device (preferably controlled by a thermostat) should be installed inside the gauge if there is a possibility that water might freeze in the float chamber during the winter. This will prevent damage to the float and float chamber and will enable rain to be recorded during that period. A small heating element or electric lamp is suitable where a mains supply of electricity is available; otherwise, other sources of power may be employed. One convenient method uses a short heating strip wound around the collecting chamber and connected to a large-capacity battery. The amount of heat supplied should be kept to the minimum necessary in order to prevent freezing because the heat may reduce the accuracy of the observations by stimulating vertical air movements above the gauge and increasing evaporation losses.

Calibration can be performed using the procedure presented for the laboratory in Annex 6.A, and field verification can be performed using the procedure available in Annex 6.B.

### 6.2.5 Non-catching technologies

New technologies that measure precipitation without capturing and collecting hydrometeors (so-called "non-catchment" type instruments) are increasingly being used in operational networks. Lanza et al. (2021) published a detailed review of the main existing non-catching technologies and their calibration procedures. One of the main advantages of these instruments is their ability to detect, with high temporal accuracy, the start and end of precipitation events, which can be very useful for some applications.

#### 6.2.5.1 *Optical instruments*

These non-catching instruments, also called optical disdrometers, are classified into three categories:

(a) Optical transmission instruments (Figure 6.6), which are based on the magnitude and duration of the attenuation in the intensity of a laser beam due to hydrometeors crossing the optical beam into a known volume;

(b) Optical scattering instruments, which are based on the scatter of the intensity of light in various directions when encountering a hydrometeor. This scatter is different depending on the wavelength of the emitted light and the size of the particle;

(c) Optical imaging instruments, which are based on multiple images in the visible frequency band crossing the sensing volume.

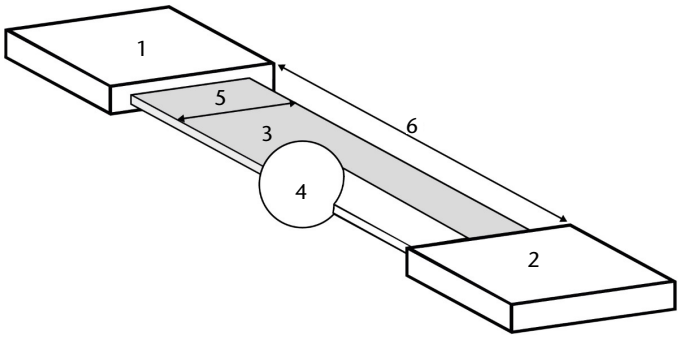



**Figure 6.6. Diagram of an optical disdrometer (1) Transmitter; (2) receiver; (3) laser beam; (4) precipitation particle; (5) width of laser beam; (6) distance between transmitter and receiver**

With the information gathered by the sensor and through the use of internal algorithms, a particle size and velocity distribution is calculated, allowing for the output of different precipitation-related products, such as precipitation phase and total accumulation.
The maintenance of these instruments is usually minimal as compared to conventional instruments and usually only includes cleaning the lens. However, they usually have high power consumption, which limits their use in isolated environments where alternating current (AC) power is not available.

#### 6.2.5.2 *Impact instruments*

These instruments can be classified into three main categories:

(a) **Electro-acoustic instruments**, which are based on falling precipitation particles (raindrops or graupel) impacting a target or sensor cover made of metal or plastic. Impact information from the particle hitting the sensor allows for the calculation of the mass and the terminal velocity, which are used to derive the rainfall rate and the accumulated precipitation.

(b) **Displacement instruments**, which are based on the displacement of a sensor cover when impacted by a falling precipitation particle that moves a magnet, which then produces an electrical signal, the amplitude of which depends on the impact energy. That information, in turn, is used to calculate precipitation rate and accumulation.

(c) **Hot plate instruments**, which are based on the provision of energy to maintain a fixed temperature of a metallic plate during precipitation, use the power consumption required to evaporate precipitation to proportionally determine the precipitation rate and amount (Rasmussen et al, 2011).

#### 6.2.5.3 *Radar instruments*

These instruments operate by emitting vertical microwave signals and measuring the power of the backscattered signal and its Doppler shift to estimate the size of hydrometeors (Figure 6.7). They usually have low power consumption, are easy to install and have very low maintenance requirements.

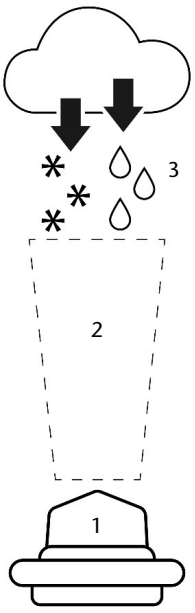



**Figure 6.7. Diagram of a Doppler radar precipitation instrument (1) Transmitter; (2) microwave signal; (3) precipitation particles**

#### 6.2.5.4 *Field verification*

Overall, verification and adjustment of non-catching instruments in the field can be performed using the instructions and kits provided by the manufacturers. However, the complexity of these instruments is a limiting factor for proper field verification, which, generally, can only be done in a controlled laboratory environment. Additionally, each manufacturer has its own field verification system, which either simulates falling drops with metallic or glass spheres (or other materials) or uses simplified raindrop generators.

#### 6.2.5.5 *Other operational considerations*

It has been demonstrated that the use of some non-catchment instruments for reporting accumulated precipitation amounts can significantly overestimate or underestimate solid precipitation amounts relative to the Double Fence Automatic Reference (DFAR) (Reverdin et al., 2016; Nitu et al., 2018; Beguería et al., 2018). Additionally, other intercomparison studies have shown that disdrometers tend to underestimate rainfall (Johannsen et al., 2020; Angulo-Martínez et al., 2018). More work is needed to determine the causes of these discrepancies and make the necessary adjustments. As with traditional gauge measurements, meteorological conditions can significantly impact measurements using non-catchment instruments. For example, wind direction was found to affect the performance of some instruments due to their design configuration and their orientation relative to the wind (anisotropic effects). Temperature can also impact the internal calculations of the instruments, especially during the transition phase from solid to liquid precipitation, resulting in illogical precipitation values (Monforte et al., 2022). In addition, the absence of heating can lead to ice and snow accumulations on the sensors, significantly altering measurement capabilities.

The assumptions used in the often proprietary data processing algorithms of non-catchment instruments (for example, assumed hydrometeor shape, density of solid precipitation, and so forth) can have an important impact on the calculation of precipitation rate, type, and amount. Changes in firmware over time introduce another source of uncertainty for consistency in long-term monitoring since different versions of the instrument, or even the same version of the instrument using different firmware, can impact measurement results.

One key consideration to keep in mind before installing non-catchment instruments in operational networks is the availability of a detailed intercomparison with traditional instruments historically used in the network to avoid data inhomogeneity and inconsistency with respect to the spatial distribution of precipitation. This, in turn, impacts climate and hydrologic monitoring, model verification and nowcasting.

## 6.3 CHALLENGES OF MEASURING PRECIPITATION

### 6.3.1 Solid precipitation

#### 6.3.1.1 *Undercatch*

It is well understood that a precipitation gauge installed above the surface of the ground represents a barrier to the flow of air around the gauge. As air flows around the gauge, it is deformed by the gauge surfaces, resulting in trajectory deflection of hydrometeors such that precipitation that would normally fall into the gauge is deflected past the gauge orifice (and therefore not measured). The severity of the deformation of the wind field is related to the shape of the gauge. This is illustrated in the conceptual diagram shown in Figure 6.8 and has more recently been illustrated and quantified by computational fluid dynamics modelling (see, for example, Baghapour and Sullivan, 2017). In the case of solid precipitation, wind plays a dominant role in reducing gauge collection efficiency as compared to its efficiency with respect to liquid precipitation, resulting a wind-induced undercatch. Wind bias can be reduced using a windshield. The relative effectiveness of different types of windshields is described by Rassmusen et al. (2012) and Kochendorfer et al. (2022), among others.

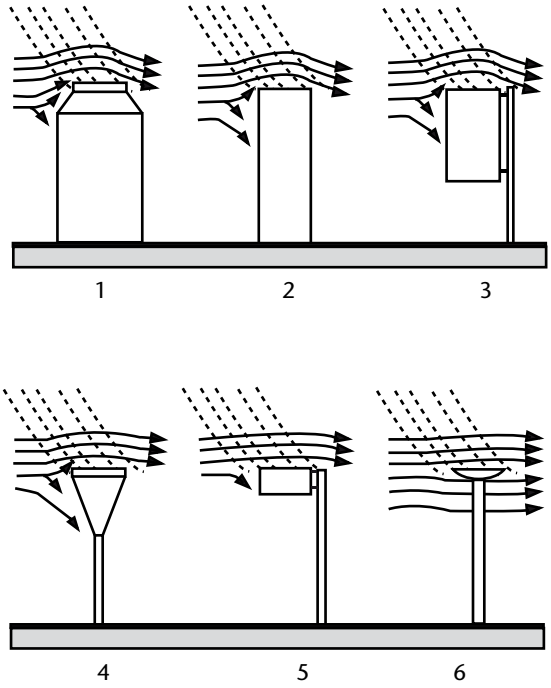



**Figure 6.8. Conceptual diagram showing the impact of airflow (solid lines) on hydrometeor trajectories (dashed lines) as the airflow is deformed around various precipitation gauge shapes and configurations**

*Source:* Sevruk and Nespor, 1994

### 6.3.1.2 ***Capping***

#### 6.3.1.2.1 **Description of capping**

Snow capping is the process of partially or fully blocking the orifice of a precipitation gauge with snowfall accumulation, thus inducing precipitation measurement errors (Figure 6.9). Partial capping could block a portion of the orifice during a precipitation event but still allow some precipitation to fall through and be measured. Partial blocking results in undercatch or delays in recording the event. It will not be detected by a quality check since the instrument continues to accumulate and report precipitation. A full blockage will prevent any precipitation from being measured until the blockage clears. A full or partial blockage of a gauge may eventually clear without intervention (for example, due to wind and/or evaporation), but the blocked snow falling into the gauge will result in quantitative errors.

Gauge capping is a problem that usually occurs in sheltered (low wind) areas and in locations with heavy and wet snow. In climates that experience these weather conditions, capping could be one of the most significant sources of error in the measurement of solid precipitation. Errors caused by capping can have significant impacts on nowcasting, climatology and hydrology. Table 6.1 summarizes the relevant factors that influence capping.

Accretion of snow occurs not only on the gauge itself but also on the shield blades, affecting their performance.

#### 6.3.1.2.2 **Detecting capping**

Capping can be very difficult to detect from the data alone without an on-site observer or the help of other instruments, such as precipitation detectors or snow depth sensors, or camera pictures, which can be used to verify the occurrence of precipitation even if the gauge is capped and observing nothing. Such auxiliary observations can help to determine when a capping event begins and when some or all of the snow blocking the orifice falls into the bucket.



**Figure 6.9. Left: partial capping on a heated tipping-bucket gauge; centre: full capping on a weighing gauge; right: accretion of snow on blades and (probably) on the inner gauge**

**Table 6.1. Summary of all relevant factors for capping issues**

| *Capping* | *No capping* | |
|---|---|---|
| | **Weather conditions** | |
| Wind | Calm conditions | Windy conditions |
| Precipitation rate | Heavy snowfalls | Light precipitation |
| Precipitation phase | Fast transition from mixed snow to snow or wet snow | Dry snow |
| Temperature | Near 0 °C condition | Extremely cold |
| | **Location** | |
| Sunlight | Low radiation | High radiation (melting) |
| Exposure | Sheltered (for example, forest clearings) | Open |
| | **Installation** | |
| Power supply for heating | Not available | Available |
| Windshield and configuration | Double Fence Intercomparison Reference (DFIR) and DFAR | Unshielded or shields with moving parts |
| | **Gauge design** | |
| Heaters | Not available | |
| Shoulders | Existing and low inclination | |

*Source:* Nitu et al., 2018

Following the falling of snow after a capping event, ancillary observations can assist in the adjustment of data errors associated with the measured amount and the precipitation timelines for the event, as neither of these will likely be accurate without intervention.

Special algorithms and quality control procedures should be implemented to detect episodes of capping.

For weighing gauges, one procedure is to identify baseline shifts on the accumulation plot (in this case, caused by large amounts of snow dumping into the gauge); if the difference between each data record is more than a predetermined threshold for a realistic accumulation for that data record, it can be flagged as suspect. If the difference is greater than an erroneous

threshold, it can be flagged as erroneous. The suspect and erroneous thresholds will be highly dependent on site and in situ climatology of solid precipitation events (see 6.7). It should be noted that some weighing gauges use proprietary algorithms to filter (or smooth) erroneous accumulations, including dumping events, from the reported observations, thus preventing the data user from detecting these episodes. It is therefore recommended that raw data be used to detect capping and dumping events.

Tipping buckets are generally not susceptible to large baseline shifts due to capping and dumping in the same way that weighing gauges are. Rather, tipping buckets will experience a smoother and delayed accumulation as the snow melts following the event. The result will be a lower-than-expected precipitation rate during the snowfall event and a higher-than-expected precipitation rate following the event as the snow in the gauge melts. In the absence of other instruments for comparison, the detection of these events is difficult.

It is also recommended that transfer function adjustments not be applied to data with suspicious capping events to avoid potentially exacerbating associated errors.

#### 6.3.1.2.3 **Preventing capping**

The most effective way to avoid capping is to heat the areas of the instrument that collect snow to prevent the snow from accumulating in the first place. However, the occurrence of capping is generally not dependent on a single factor but rather on a combination of several weather phenomena and gauge configuration issues. For example, some gauges are designed to minimize snow accumulation on the gauge casing by reducing the flatter area of the gauge surfaces where snow tends to accumulate (an ideal gauge shape being cylindrical with no shoulders). The combination of factors that increases the risk of snow build-up includes a smaller heating surface, low winds and pronounced shoulders on the gauge housing. The increased risk of snow build-up, in turn, increases the risk of capping and related measurement impacts (Figure 6.10).

For weighing gauges, heating must be applied to the gauge rim or orifice to keep the collector free of snow so that the falling precipitation can continue to enter the gauge uninhibited for measurement. It is also recommended that heating be installed between the orifice and the shoulder of the gauge on the exterior of the gauge, and on the outside of the chimney cylinder, inside the gauge cover (Figure 6.11). Heaters should be maintained at a fixed temperature, typically between 2 °C and 4 °C when the ambient temperature drops below 2 °C. In the case of a limited power supply, other strategies could be used, such as periodic (for example, once daily) heating activation via the data logger or limiting heating to when precipitation is detected.

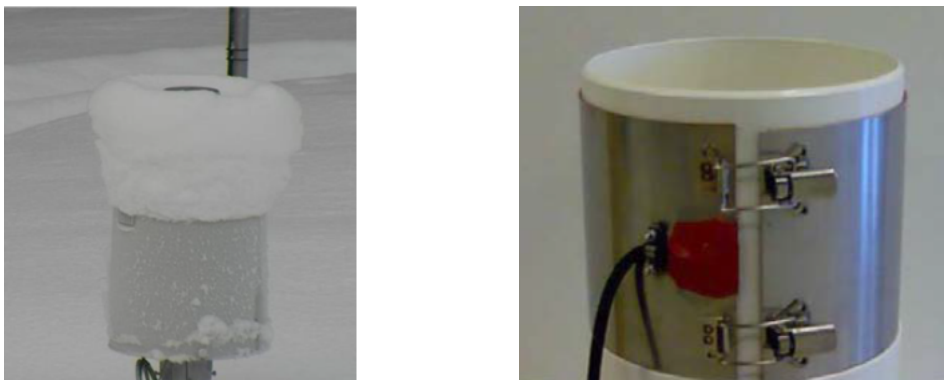


**Figure 6.10. Left: build-up of snow on the shoulders of a weighing gauge; right: external heater installed on a weighing gauge to prevent snow build-up and rim capping**

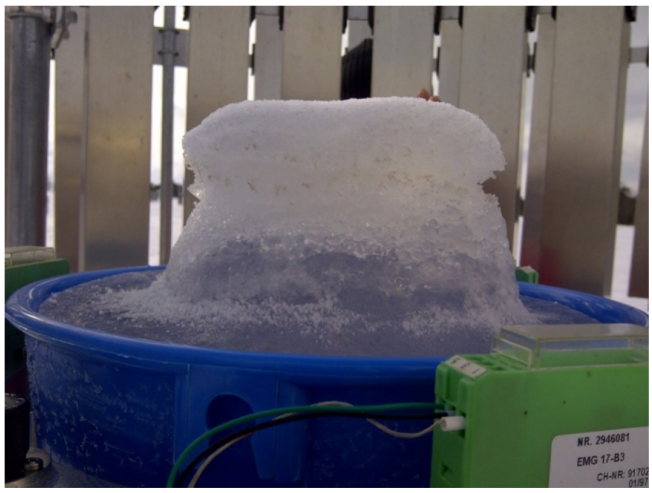



**Figure 6.11. Frozen contents in a precipitation gauge bucket resulting from operating the gauge below 0 °C without a sufficient antifreeze solution**

For tipping-bucket gauges, the primary function of heaters is to melt solid precipitation collected by the gauge so that it can pass into the tipping-bucket assembly in liquid form and be measured. In addition to heating the funnel to melt the snow, the bucket assembly and/or outlet ports are typically heated to prevent re-freezing of the precipitation inside the gauge mechanisms, resulting in gauge blockages. Heating power and configuration vary by gauge type and manufacturer, with varying degrees of user configurability. The selection of a heated tipping-bucket gauge for a given site must consider the power available to operate the heaters and the typical operating conditions at the site. Usually, more power is required to operate heated tipping-bucket gauges than to heat weighing gauges.

Although heating is recommended to mitigate the influence of capping, excessive heating may induce a "chimney effect", where a heat plume deflects lighter particles from entering the collector. For tipping buckets, heating may also cause the evaporation or sublimation of hydrometeors from the inner wall/funnel of the gauge before they can be measured by the instrument.

Heating of non-catchment-type instruments is used primarily to prevent icing or snow accumulation on the measuring components of the instruments. The heated surfaces and the power required can vary depending on the type of instrument.

Unfortunately, even if heating is available, episodes of capping can still occur.

#### 6.3.1.3 *Use of antifreeze and oil*

The measurement of solid precipitation requires instrument operation at temperatures below freezing. The operation of accumulating precipitation gauges (either automatic weighing or manual storage gauges) at temperatures below 0 °C requires the use of an antifreeze mixture in the collecting bucket to melt the precipitation as it falls and to prevent the bucket contents from freezing (Figure 6.11). Freezing of the bucket contents can damage to the bucket/gauge and lead to measurement errors.

Antifreeze solution placed inside the collecting bucket prior to winter operation will melt any solid precipitation falling into the bucket and will prevent the entire contents from freezing. The concentration and volume of antifreeze required will depend on the capacity of the bucket and the expected maximum dilution of the antifreeze due to precipitation at the minimum expected temperature between service intervals. Different products and concentrations have different freezing points, and local experimentation may be required to determine appropriate

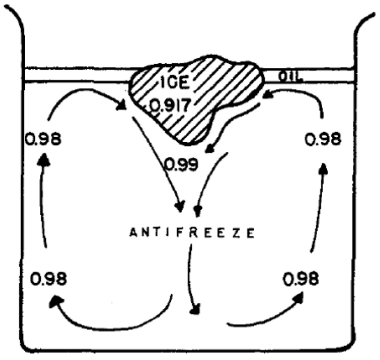



**Figure 6.12. Conceptual diagram of bucket self-mixing following the addition of snow The numbers illustrate the solution density in kg $L^{-1}$ as mixing occurs in a solution of 40% glycol and 60% methanol at –2 °C.**

*Source:* Mayo (1972)

concentrations and volumes. Common antifreeze solutions include calcium chloride (such as a mixture of 37.5% commercial grade $CaCl_2$ by weight with 62.5% water), methanol and propylene glycol solutions, and saturated propylene glycol and water mixtures. Caution is required to avoid solutions with a higher density than water as they may lead to stratification in the bucket following precipitation, resulting in slush formation and freezing of the top layer of undiluted water. According to Mayo (1972), the antifreeze density must be lower than that of water in order to be "self-mixing" (Figure 6.12). When added to a self-mixing solution, solid precipitation will melt and sink through the antifreeze, promoting mixing of the bucket contents. To prevent stratification when using propylene glycol, a mixture of 60% methanol and 40% propylene glycol can be used. However, caution is required when mixing methanol as it is flammable, and an oil layer is necessary to prevent the methanol from rapidly evaporating from the antifreeze mixture. Although ethylene glycol can also be used as an antifreeze solution, it is a moderately toxic material and therefore should be avoided if possible.

It should also be noted that propylene glycol is hygroscopic and should be saturated with water to prevent the absorption of water from the air. The hygroscopic properties of unsaturated glycol can lead to a false increase in bucket weight not related to precipitation and possibly a false report of precipitation of several mm per day. Typically, a propylene glycol to water ratio of 4:1 should saturate the propylene glycol. The water and propylene glycol should be well mixed.

The practice of using a layer of oil in the bucket of an accumulating gauge to prevent evaporation and splashing of the bucket contents is common for either liquid or solid precipitation measurement. Some manufacturers suggest that using oil to prevent evaporation is not necessary as internal gauge processing can remove the impacts of evaporation from the data. In this case, the internal gauge processing must account for evaporation of the bucket contents in addition to gauge uncertainties from environmental sources (for example, wind and temperature). However, any gauge that relies on a self-mixing antifreeze solution to prevent the bucket contents from freezing will require oil to supress evaporation of that solution. This is especially necessary when methanol is used, as it will evaporate from the bucket relatively quickly without suppression, diminishing the self-mixing quality of the solution.

When using oil for evaporation suppression in an accumulating precipitation gauge, the oil must fulfil the following requirements (Hoover et al., 2014a):

(a) It must float on top of the contents of the bucket without mixing;

(b) It must allow precipitation, including light snow, to penetrate even at cold temperatures;

(c) It must provide very low evaporation rates;

(d) It must not induce a chemical reaction with the other contents of the bucket or the bucket itself;

(e) It should exhibit low toxicity to animals and humans;

(f) It should not attract insects or animals.

Viscosity at the lowest expected operating temperature is an important consideration for winter operation to ensure that snow collecting in the bucket will transit through the oil to be melted in the antifreeze solution. If it does not pass through the oil, the snow can accumulate on the surface (Figure 6.13), potentially contributing to the sublimation and evaporation of precipitation above the oil layer, inhomogeneities in the bucket contents, and, in extreme cases, the premature filling of the gauge with snow. The specifications and performance of some oils are discussed by Hoover et al. (2014b) and Nitu et al. (2018).

The amount of oil used in the bucket needs to be sufficient to entirely cover the surface of the bucket contents but not too thick as to prevent precipitation (including snow) from penetrating the oil and transiting to the liquid contents underneath. The requirements may vary depending on the type of oil used and the conditions in which it is used, but a 0.5 cm to 1 cm layer of oil on top of the bucket contents is generally recommended (Figure 6.14). The volume (or even the type) of oil can be varied with the season, with more oil and higher viscosity oils used during warm periods when evaporation and liquid precipitation are more prevalent, and less oil and lower viscosity oils used during cold (snow) periods to hasten the transit of precipitation through the oil. Some local experimentation may be required to assess these practices.

When using oil and antifreeze in accumulating precipitation gauges, waste material must be handled and disposed of in accordance with local regulations.



**Figure 6.13. Unmelted snow sitting on top of a viscous oil layer in a precipitation gauge bucket inside a –20 °C freezer.**



**Figure 6.14. Visible oil layer of several centimetres, marked in red, floating on top of the bucket contents in an accumulating precipitation gauge bucket**

### 6.3.2 Liquid precipitation

The challenges related to accurately measuring liquid precipitation are fewer than those for solid precipitation. However, because the absolute amounts of measured liquid precipitation are typically greater than those of solid precipitation, the corresponding absolute errors are also greater. These challenges, therefore, need to be carefully considered. The WMO laboratory intercomparison and field intercomparison of rainfall intensity gauges (Lanza et al., 2006; Vuerich et al., 2009) provide assessments of quantification errors in rainfall intensity measurements, and, by proxy, errors in total rainfall measurements.

#### 6.3.2.1 *Undercatch due to wind*

It has been shown that the undercatch of rainfall measured with a standard rain gauge can be as high as 10% when compared to rainfall caught in a pit reference gauge (Duchon and Essenberg, 2001; Sieck et al., 2007). Although the relative undercatch of liquid precipitation due to wind is less than that for solid precipitation, it should still be considered. However, transfer functions for the wind adjustment of rainfall are difficult to develop and apply due to the large scatter in the relationship between catch efficiency and wind speed, with scatter shown to be related to rainfall intensity and drop size distribution (Chvíla et al., 2005). Gauge shielding may have some impact on reducing wind bias, but because the impact is not as obvious as it is for solid precipitation measurements, the effectiveness needs to be balanced with increased infrastructure costs. Decisions to use shielding may also be based on the need to use the same gauge and/or infrastructure to measure solid precipitation where required.

#### 6.3.2.2 *Evaporation and wetting loss*

Unmitigated evaporation from rain gauges can be a significant measurement error but varies by gauge type, climatic zone and time of year (Sevruk, 1974b). Evaporation loss is a problem with gauges that do not have a funnel device in the bucket, especially in late spring at mid-latitudes, where losses of over 0.8 mm per day have been reported. Losses during winter are much less than those during the summer months, ranging from 0.1 mm to 0.2 mm per day. These losses, however, are cumulative. In a well-designed gauge, only a small water surface area is exposed, its ventilation is minimized, and the water temperature is kept low by a reflective outer surface (bare aluminium or painted white). In storage and accumulating weighing gauges, errors associated with evaporation can be virtually eliminated through the use of oil in the collector. Note that gauges that use a funnel and that are also used for measuring solid precipitation will require the funnel to be removed before the winter season, and the type of oil needs to be appropriate for colder temperatures (see 6.3.1.3). Some more modern automated weighing gauges use built-in (usually proprietary) algorithms to remove the impacts of evaporation of the contents of the collector from the determination of interval precipitation amount.

Wetting loss (Sevruk, 1974a) is another cumulative systematic loss from manual rain gauges which varies with gauge type; its magnitude is a function of the number of times the gauge is emptied. The average wetting loss can be up to 0.2 mm per observation. At synoptic stations where precipitation is measured every six hours, this loss can become very significant. In some countries, wetting loss has been calculated to be as high as 15% to 20% of the measured precipitation. Correcting for wetting loss at the time of observation is a feasible alternative. Wetting loss can be kept low in a well-designed gauge. The methodology for determining the wetting loss of manual gauges described by Goodison et al. (1998) is adequate for this purpose. It is recommended that the wetting loss for manual gauges be re-examined periodically (for example, every five years) as it tends to change with the age of the collector. The internal surfaces should be made of a material which can be kept smooth and clean; paint, for example, is unsuitable, but baked enamel is satisfactory. Seams in the construction should be kept to a minimum. Wetting loss is not an issue for automated weighing gauges.

Because both evaporation and wetting loss are dependent on many environmental and infrastructure-based factors, it is challenging to be able to estimate either with any known uncertainty. Therefore, the best course of action is mitigation.

#### 6.3.2.3 *Clogging*

Higher precipitation amounts often necessitate a smaller collector area. The use of a funnel is often required to prevent evaporation. Both of these measures can increase the propensity for a gauge measuring liquid precipitation to partially or fully clog with debris. Clogging, in a worst case scenario, will prevent any precipitation from being measured. The partial clogging of automated gauges (such as a tipping bucket) may not be noticed immediately since precipitation may still be recorded during events. In this scenario, the timing of precipitation may be incorrectly recorded and precipitation may be under-reported if the collector overflows before the precipitation is measured. Correcting this error is usually not possible. Clogging can be prevented or minimized by positioning instruments away from possible falling debris (such as tree leaves or needles) and through routine inspection and maintenance of automated instruments.

#### 6.3.2.4 *Splashing*

Splashing can be an issue for either a manual or an automated rain gauge. If the gauge is improperly located too close to obstacles or other infrastructure (see siting guidelines in 6.6) or too close to the ground where water can pool, high-intensity precipitation may splash or blow into the collector and bias the measurement. Improperly installed shielding could also result in splashing errors. Some gauge wind shielding, such as the Canadian Nipher shield (see Figure 6.2), is designed to reduce the undercatch of solid precipitation due to wind but should not be used for high-intensity rainfall due to the tendency for rain to splash off the shield and into the collector.

For tipping-bucket rain gauges, the loss of water during the tipping action in heavy rain can be a gauge-dependent issue and cause the under-reporting of precipitation by up to 20% in some gauges; this can be considerably reduced by conducting a dynamic calibration (see Annex 6.A) and applying an intensity-dependent correction. In Vuerich et al. (2009), it is shown that linearization by extra electronic pulses is well suited for measuring precipitation amounts but less so for measuring precipitation intensity. On the other hand, mechanical linearization (generating an intensity-dependent emission of extra pulses) compensates for the loss of water during the movement of the balance and greatly minimizes intensity underestimation during high-rate events. The software correction (correction curve or algorithm) method is the most effective method for correcting systematic mechanical errors. Chan et al. (2015) describe field performances without correction, with software correction and with extra pulse correction for three different types of tipping-bucket rain gauges in a tropical environment.

The improper design of accumulating gauges, whether manual or automated, could result in precipitation splashing out of the collector during high-intensity events and in the under-reporting of total precipitation. This could occur if the fluid level in the collecting bucket approaches the top of the collector and raindrops hitting the surface are able to splash out of the collector. Such a situation could be mitigated by the design of the gauge (that is, by including in the design a chimney that directs falling rain into the collector, which is suitably lower than the gauge orifice) or by the use of a funnel.

## 6.4 REFERENCE CONFIGURATIONS

The measurement of precipitation cannot be traced directly to absolute references given the difficulty in defining the "true" amount of precipitation; however, sensor measurements can be compared to accepted reference measurements.

Accepted reference configurations must be robust, produce the same value under the same conditions, be easy to install following standard designs and specifications, and have error sources that are clearly understood.

It is recommended that reference precipitation sites be established and maintained in order to characterize the measurement biases and uncertainties of national network gauges. The use of international references ensures proper intercomparison and the appropriate exchange of information among WMO members, facilitating more global and homogeneous precipitation records.

The physical differences between the characteristics of falling solid and liquid precipitation imply that reference configurations must be different for each type of precipitation.

### 6.4.1 Solid precipitation

For solid precipitation, the main objective of the reference is to reduce as much as possible the wind-induced undercatch, generally collecting the most solid precipitation relative to other test configurations on a given site, particularly in strong wind.

The manual Double Fence Intercomparison Reference (DFIR) configuration, was established as the primary field reference for the previous WMO intercomparison of solid precipitation manual measurements (Goodison et al., 1998).

The DFIR configuration consists of an octagonal vertical double fence set within circles 12 m and 4 m in diameter, with the outer fence 3.5 m high and the inner fence 3.0 m high surrounding a Tretyakov precipitation gauge mounted at a height of 3.0 m. Equally spaced wooden slats are mounted vertically to reduce the flow of wind through the fences. The slats create a porosity of 50%. There is a gap of 2.0 m between the ground and the bottom of the outer fence, and there is a gap of 1.5 m between the ground and the bottom of the inner fence (Figure 6.15).

The DFIR configuration was adopted to establish the WMO Solid Precipitation Intercomparison Experiment (SPICE) primary reference for automated measurements. It incorporates an automated weighing gauge installed within a single-Alter shield and using a precipitation detector (Figure 6.16 and Figure 6.17). This configuration was named the Double Fence Automatic Reference (DFAR) by Nitu et al. (2018).

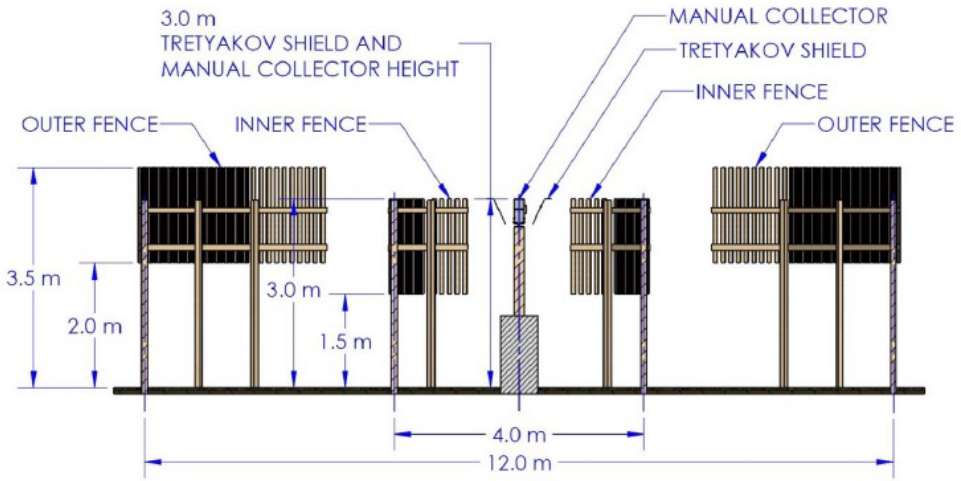



**Figure 6.15. Cross-section of WMO DFIR**

*Source:* J. Hoover, Environment and Climate Change Canada

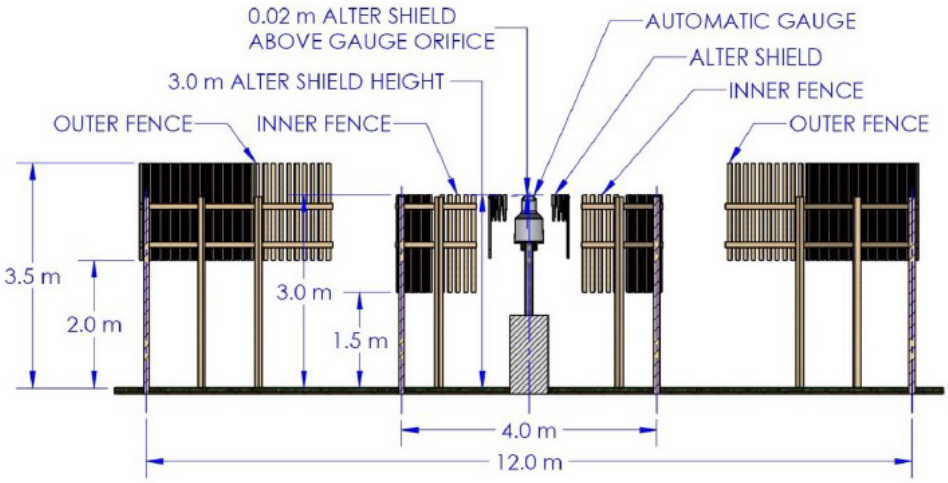



**Figure 6.16. DFAR cross-section**

*Source:* J. Hoover, Environment and Climate Change Canada



**Figure 6.17. Interior view of a DFAR during a snowfall event**
**The weighing gauge is in the centre, and the precipitation detector is on the right (red arrow).**

*Source:* Formigal site, Spain

### 6.4.2 Liquid precipitation

Reference rain gauges should be installed in a well-drained pit according to the design and specifications reported in European Standard EN 13798:2010 to minimize environmental interference on measured rainfall intensities and to protect against in-splash by a metal or plastic grating.

It is expected that a buried or sunken gauge (Sieck et al., 2007) will show a higher rainfall reading than a gauge above ground; the difference may be 10% or more when both instruments are working perfectly and accurately. Pits are preferably sited at ground level to avoid possible surface runoff (see ground-level configuration in Figure 6.18).

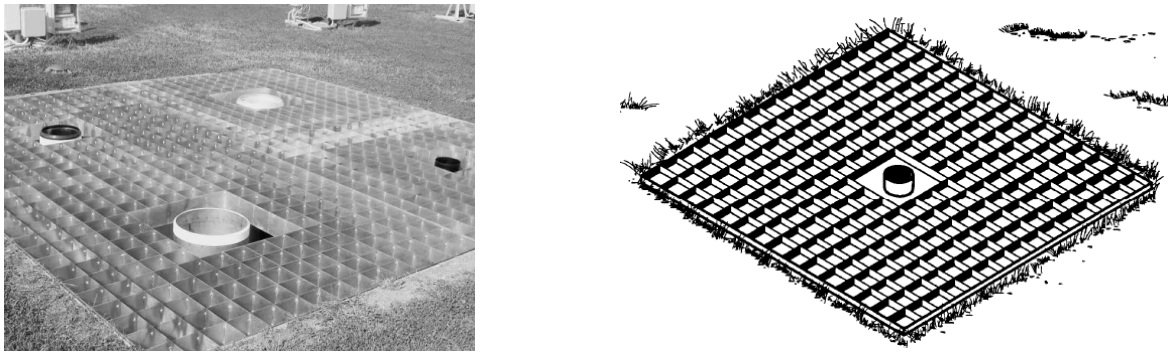


**Figure 6.18. Rain gauge pit and its grating (ground-level configuration) and diagram of the reference gauge pit at Vigna di Valle, Italy (2007)**

*Source:* Vuerich et al., 2009

The pit should be deep enough to accommodate the rain gauge and to centre and level the collector with the top of the grating (at ground level). The design of the pit should take into account the dimensions of the rain gauge and its method of installation. The base of the pit should have a recess (extra pit) to allow water to be drained. The square space of the grating should also be adapted according to the diameter of the rain gauge collector in order to satisfy the standard requirements reported in EN 13798:2010.

The sides of the pit should be formed of bricks and concrete and should be supported to prevent collapse. Supporting walls should be built around the edges and a grating of approximately 1 875 mm x 1 875 mm x 120 mm (L x W x H) should be installed on the pit walls and should be able to be lifted to give access to the rain gauge for checks and maintenance operations. The grating distance should be approximately 120–125 mm. The grating should be strong enough to walk on and should be able to maintain its shape without distortion. To prevent in-splash from the top surface of the grating, the strips of the grating should be at least 2 mm thick, and the distance between the edge of the central square and the ground should be greater than 600 mm (for further details see EN 13798:2010). Figure 6.18 shows a reference rain gauge pit with four standard rain gauges.

### 6.4.3 Intercomparison sites

One recommendation of the WMO-SPICE project (Nitu et al., 2018) was for national observation programmes to operate at least one intercomparison site to evaluate national gauges. Intercomparisons within national observation programmes should provide guidance on national observation standards and should be used to assess the impacts of changes in methods and instrument configurations on the homogeneity of observation time series. Intercomparison sites should:

(a) Operate according to the WMO recommended reference configurations (reference figures above) following the recommended installation and operation specifications. Note that a DFIR/DFAR is not required where only rain is observed. Should it not be possible to follow the installation and operation specifications of the WMO reference configurations, the site should operate according to a configuration that is traceable to previous intercomparisons with the WMO reference;

(b) Operate past, current, and new types of operational gauges (or other methods of observation) according to standard operating procedures (SOPs) to evaluate accuracy and performance against the WMO reference(s);

(c) Collect ancillary meteorological measurements to adequately characterize precipitation events. These should include, but are not limited to, air temperature, humidity, wind speed

and direction (at 10 m and at the height of the instruments under test), verification of the occurrence of precipitation, and precipitation type (where precipitation can occur in more than one phase);

(d) Provide intercomparison data in the same or a similar climate regime as that which exists where the operational instruments are used.

The size and physical set up of an intercomparison site will depend on the available space and user requirements. Ideally, the site will be situated in a flat, accessible area. If possible, AC grid power should be used along with off-grid (for example, battery) backup to maximize continuous operation. A good communication infrastructure is crucial for transmitting data and enhancing monitoring, which will ultimately maximize data quality, especially at unmanned sites. When designing an intercomparison site, considerations should include the potential for future expansion of the infrastructure, adequate and maintained documentation (metadata, site diagrams), data storage and backup, and instrument maintenance and calibration schedules. An example of a recommended reference site is shown in Figure 6.19.

Instrument spacing for precipitation observations should follow WMO guidelines (summarized in 6.6) designed to prevent infrastructure (such as buildings and other instruments) from having an impact on measurements. All instruments under test should have the same exposure. Instruments for ancillary meteorological measurements (for example, wind speed, wind direction, temperature) need to be carefully positioned within the intercomparison site to ensure that the data they gather are representative of conditions at or near the instrument being tested. At large sites or sites with substantial obstacles, more than one location may be required for representative ancillary measurements.

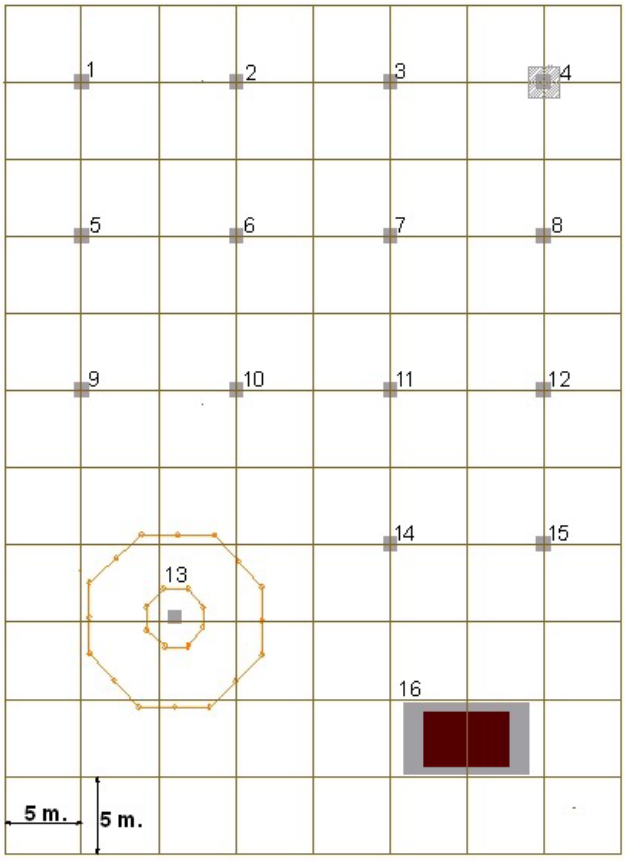



**Figure 6.19. Scale diagram of a recommended reference site.**
**1–12: Instruments under test; 4: liquid reference, 13: solid reference;**
**14–15: cameras, antennas; 16: infrastructure cabin**

Besides the ancillary observations noted above, a very useful tool at intercomparison sites, especially if they are unmanned, is time-lapse photography. Hourly photographs of the intercomparison site and individual instruments can provide valuable information about site and instrument conditions and potential insight into instrument behaviour, including malfunctions and other events that may assist in data quality control. The observation frequency for precipitation and ancillary data at intercomparison sites depends chiefly on the instruments under test, observation and data logging capabilities, and user requirements. For the intercomparison of automated instruments, the collection of 1-minute data is most desirable. Even if phenomena are not discernible at 1-minute resolutions, higher frequency data can be statistically aggregated to lower frequencies (for example, 15 min, hourly, daily, etc.). Higher frequency observations (for example, 5 s to 30 s) may be desirable for assessing events such as signal noise phenomena, but they are generally not necessary for assessing gauge performance. For manual instruments, the maximum observation interval should be daily, while sub-daily observations (1 to 6 hours) may be necessary to meet some user requirements.

## 6.5 TRANSFER FUNCTIONS

Transfer functions are the means to adjust the measurements made by a gauge such that the adjusted measurement is a closer representation of the true precipitation amount. Generally, transfer functions are derived by comparing precipitation observations made by a gauge configuration under test to a reference configuration that has a known uncertainty or traceability.

The development and application of transfer functions require measurements of ancillary meteorological conditions at the site during precipitation: typically, wind speed, either at a standard (10 m) height or at gauge height, and standard air temperature (2 m). More recent transfer functions, such as those developed during WMO-SPICE (Nitu et al., 2018), have models fitted with data from both wind speed measurement heights, and the recommendation is to utilize the best available wind data for the site, regardless of whether it is measured at gauge height or at the standard height of 10 m. However, if wind speed at gauge height is required but only measured at 10 m, it can be derived by using a mean wind speed reduction procedure after estimating both the roughness length and displacement height for the site. Kochendorfer et al. (2017) suggest using generic values of 0.01 m and 0.4 m for roughness length and displacement height, respectively. The wind speed $U_z$ at height $z$ can then be estimated as:

$$U_z = ln\left(\frac{(z-d)}{z_0}\right) \tag{6.3}$$

where $z_0$ is the estimated roughness length and $d$ is the estimated displacement height. More complex methods to determine roughness parameters for wind speed reductions can be found in the literature, including Thom (1975).

The adjusted precipitation over a measured interval $I$, $P_{ai}$, using an appropriate transfer function to calculate catch efficiency, $C_E$, is estimated as:

$$P_{ai} = P_{ui}\frac{1}{C_E} \tag{6.4}$$

where $P_{ui}$ is the measured unadjusted precipitation. Data archives should maintain both $P_{ai}$ and $P_{ui}$ and document the method of adjustment such that $P_{ui}$ can be recalculated if the transfer functions for estimating $C_E$ are revised.

Shielded gauges catch more precipitation than their unshielded counterparts, especially for solid precipitation. Therefore, gauges should be shielded either naturally (for example, forest clearing) or artificially (for example, Alter shield, Canadian Nipher type shield, Tretyakov windshield) to minimize the adverse effect of wind speed on measurements of solid precipitation (for some information on shield design, refer to Goodison et al., 1998; Nitu et al., 2018). The type of windshield configuration, as well as the gauge type, will alter the relationship between wind speed and catch efficiency, and thereby the transfer function, and have implications on data homogeneity.

### 6.5.1 Liquid precipitation: rain

It is less critical to use transfer functions to adjust liquid precipitation measurements than solid precipitation measurements due to the fact that larger and faster-falling rain droplets are less prone to undercatch. However, intercomparisons with known references suggest that both accumulating and tipping-bucket gauges measuring rainfall are impacted by wind. It is important to be aware of the uncertainty in not adjusting rainfall measurements because, although the relative bias due to rainfall undercatch is lower than for solid precipitation, the potential for large absolute errors is higher since generally rainfall accumulations are higher than snowfall accumulations.

### 6.5.2 Solid precipitation: snow

The systematic bias in measuring solid (or mixed) precipitation using precipitation gauges is typically 30% or higher, depending on gauge exposure, wind speed at gauge height $H_g$, and the crystal structure of the hydrometeor (which impacts its fall speed). Since the mass of solid precipitation (snow) hydrometeors is considerably less than that of liquid hydrometeors (rain), the former are more susceptible than the latter to deflection by wind-induced turbulence around the orifice of the collector. This results in a significantly lower gauge catch efficiency for snow than for rain. Although the absolute bias in solid precipitation measurements is lower than in rainfall (because total accumulations are generally less), the relative bias is much larger. This bias can be reduced, although generally not eliminated, by the use of shielding. The WMO recommendation, therefore, is to employ gauge shielding where wind-induced undercatch is anticipated to be significant and to perform a bias adjustment of solid precipitation measurements using an available transfer function (Nitu et al., 2018). The need for transfer functions is greater at stations where a significant amount of annual precipitation falls as snow.

#### 6.5.2.1 *Weighing gauges*

Most weighing-type gauges are also accumulating gauges. In these gauges, falling precipitation is collected in a bucket that is then weighed, and the precipitation falling during a given period is calculated as the differential bucket weight. The collection of precipitation in a bucket for weighing necessitates a gauge shape that allows for the bucket reservoir to be housed inside the gauge. This results in a gauge profile that is wider around the bottom where the bucket is housed, tapering towards the orifice at the top of the gauge. Aerodynamically (Figure 6.8), this causes air flowing across the gauge to be deflected over the taper or shoulder of the gauge and creates flow over and around the orifice, which deflects some lighter hydrometeors from entering the gauge, resulting in undercatch.

The WMO-SPICE project (Nitu et al., 2018) introduced a methodology to develop transfer functions for high frequency measurements of accumulated precipitation (that is, intervals of 30 or 60 minutes) by combining data from gauges with common shielding at multiple sites. The results were transfer function models and coefficient sets that could be used anywhere solid precipitation is measured, with some limitations (for example, complex terrain around the gauge can generate vortices and stronger vertical wind components). The most commonly used functions and coefficients, those for single Alter-shielded and unshielded gauges, are published in Kochendorfer et al. (2017). Two models are shown in this publication: one that is continuous with temperature (Equation 6.5) and one that requires the user to specify the precipitation phase (Equation 6.6):

$$C_E = e^{-a(U)\left(1-\tan^{-1}\left(b(T_{air})\right)+c\right)} \tag{6.5}$$

and

$$C_e = (a)\, e^{-b(U)} + c \tag{6.6}$$

where $C_E$ is the catch efficiency represented by the ratio of the catch of the test gauge to the catch of the reference (the DFAR) during the measurement interval $I$, $T_{air}$ is the mean near-surface air temperature in degrees Celsius, and $U$ is the mean wind speed in meters per second during $I$.

Either 10-m or gauge height wind measurements can be used, selecting Equation 6.5 or Equation 6.6, respectively, and coefficients based on measurement height. Kochendorfer et al. (2017) recommend using an upper wind speed threshold of 7.2 m $s^{-1}$ and 9.0 m $s^{-1}$ for gauge height and 10-m wind speed measurements, respectively. The upper threshold is based on the limited data availability at higher wind speeds for transfer function development, prevents potentially large over-adjustment errors at high wind speeds and ensures that adjustments are not made for blowing snow events. The coefficients for Equations 6.5 and 6.6, as well as the wind speed thresholds, are given in Table 6.2 and Table 6.3.

For illustrative purposes, Figure 6.20 shows the WMO-SPICE transfer functions as a function of wind speed at $H_g$, with Equation 6.5 (red) calculated at $T_{air}$ of –5 °C and Equation 6.6 (blue) shown for snow. The solid and dashed lines are the transfer functions for single Alter-shielded and unshielded gauges, respectively. The grey vertical line represents the maximum wind speed threshold at gauge height $H_g$.

Below are some additional points regarding the application of the SPICE multiple site transfer functions:

(a) The performance of the SPICE transfer functions will vary by site, generally over-adjusting for solid precipitation at sites with gauge height wind speeds during precipitation less than ~3 m $s^{-1}$ and under-adjusting for solid precipitation at sites with wind speeds during precipitation greater than ~3 m $s^{-1}$ (Smith et al., 2020). Given this, the recommendation is to use the SPICE transfer functions with caution.

**Table 6.2. WMO-SPICE transfer function coefficients for single Alter-shielded (SA) and unshielded (UN) gauges for Equation 6.5 for wind speed measured at gauge height $H_g$ and at 10 m. $U_{thresh}$ is the maximum wind speed threshold.**

| *Shield* | *Wind height* | *a* | *b* | *c* | $U_{thresh}$ m $s^{-1}$ |
|---|---|---|---|---|---|
| SA | $H_g$ | 0.0348 | 1.3660 | 0.7790 | 7.2 |
| UN | $H_g$ | 0.0785 | 0.7290 | 0.4070 | 7.2 |
| SA | 10 m | 0.0281 | 1.6280 | 0.8370 | 9.0 |
| UN | 10 m | 0.0623 | 0.7760 | 0.4310 | 9.0 |

*Source:* Kochendorfer et al., 2017

**Table 6.3. WMO-SPICE transfer function coefficients for single Alter-shielded (SA) and unshielded (UN) gauges for Equation 6.6 for wind speed measured at gauge height $H_g$ and at 10 m. $U_{thresh}$ is the maximum wind speed threshold. Equation 6.6 requires pre-determination of the dominant precipitation phase during the adjustment period.**

| *Precipitation phase* | *Shield* | *Wind height* | *a* | *b* | *c* | $U_{thresh}$ m $s^{-1}$ |
|---|---|---|---|---|---|---|
| Snow | SA | $H_g$ | 0.7280 | 0.2300 | 0.3360 | 7.2 |
| Snow | UN | $H_g$ | 0.8601 | 0.3709 | 0.2294 | 7.2 |
| Snow | SA | 10 m | 0.7420 | 0.1810 | 0.3220 | 9.0 |
| Snow | UN | 10 m | 0.8650 | 0.2980 | 0.2250 | 9.0 |
| Mixed | SA | $H_g$ | 0.6680 | 0.1320 | 0.3390 | 7.2 |
| Mixed | UN | $H_g$ | 0.6410 | 0.2360 | 0.3560 | 7.2 |
| Mixed | SA | 10 m | 0.8210 | 0.0770 | 0.1750 | 9.0 |
| Mixed | UN | 10 m | 0.6240 | 0.1850 | 0.8364 | 9.0 |

*Source:* Kochendorfer et al., 2017

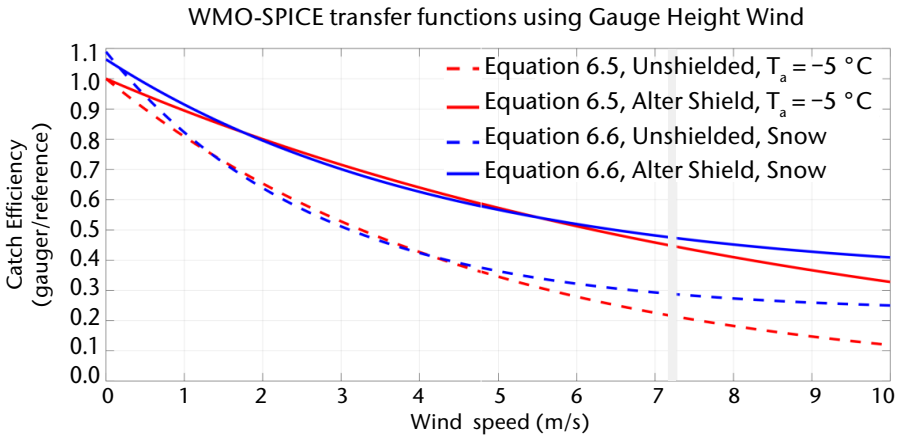



**Figure 6.20. WMO-SPICE transfer functions from Kochendorfer et al. (2017). Equation 6.5 (red) and Equation 6.6 (blue) are plotted for unshielded (dashed), and single Alter-shielded (solid) gauges. Equation 6.5 is plotted using an air temperature of –5 °C, and Equation 6.6 is plotted for snow. Both transfer functions are plotted for gauge height wind speed, with the maximum wind speed threshold $U_{thresh}$ shown at 7.2 m s$^{-1}$.**

(b) The coefficients for single Alter-shielded and unshielded gauges (Table 6.2. and Table 6.3) should not be used with other shield configurations (double Alter, Tretyakov, and so forth).

(c) The coefficients for single Alter-shielded and unshielded gauges (Table 6.2. and Table 6.3) are intended to be used with high frequency data (intervals of 30 minutes to 60 minutes) but can be applied to longer accumulation periods (intervals of 12 hours to 24 hours), with the recognition that applying them to longer accumulation intervals could increase the uncertainty in the adjustment (Kochendorfer et al., 2017).

(d) The data fit to Equation 6.5 allow the catch efficiency to exceed 1, but the catch efficiency should be set to 1 when this occurs.

(e) Since Equation 6.5 is continuous with temperature, it allows for adjustments at all temperatures. However, the transfer function is only intended to adjust snow and mixed precipitation – not rain; the adjustment should be capped at an upper temperature threshold where only rainfall is expected (for example, 5 °C).

(f) Transfer functions such as Equation 6.5 or Equation 6.6 can be used to determine whether shielding is required at a given site by using the anticipated meteorological conditions during precipitation (wind speed, temperature, dominant precipitation phase).

Alternative transfer functions can be found in the literature. Some include solid precipitation intensity in the equations (Colli et al., 2018); others are more climate specific (Wolff et al., 2015) or are based on the type of shielding (Kochendorfer et al., 2017).

As is the case with weighing gauges, the catch efficiency of solid precipitation for manual gauges is also impacted by wind speed. The major differences in transfer function adjustment are the following:

(a) Manual observations are made less frequently, typically at 12- to 24-hour intervals;

(b) Manual gauges often incur other errors, such as wetting loss and evaporation, which need to be corrected before applying a transfer function for wind undercatch. Non-wind corrections are described in 6.2.1. Since, unlike automated weighing gauges, most manual gauges do not need to house large collection reservoirs (storage gauges being the exception), their shape is often (but not always) less conducive to large wind undercatch potential.

**Table 6.4. Regression equations for catch ratio versus wind and temperature for Nipher, Tretyakov, US NWS8" and Hellmann gauges. $C_E$ is the calculated catch efficiency during the observation period, *i*, where i is usually 6, 12, or 24 hours, $W_s$ is the mean gauge height wind in m s$^{-1}$ during *i*, and $T_{max}$ and $T_{min}$ and $T_{mean}$ are the maximum, minimum and mean near-surface air temperatures during *i*.**

| *Gauge configuration* | *Catch efficiency equation* |
|---|---|
| **Snow** | |
| Nipher | $C_E = 1.0 - 0.0044W_s^2 - 0.0198W_s$ |
| Tretyakov | $C_E = 1.0311 - 0.0867W_s + 0.003T_{max}$ |
| US NWS 8" Alter Shield | $C_E = \exp(0.0461 - 0.0004\ W_s^{1.75})$ |
| US NWS 8" Unshielded | $C_E = \exp(0.0461 - 0.0016\ W_s^{1.28})$ |
| Hellmann | $C_E = 1.0 + 0.013W_s^2 - 0.1945W_s$ |
| **Mixed** | |
| Nipher | $C_E = 0.9729 - 0.0318W_s + 0.0058\ T_{max} - 0.0067T_{min}$ |
| Tretyakov | $C_E = 0.9699 - 0.0446W_s + 0.0088\ T_{max} - 0.0022T_{min}$ |
| US NWS 8" shielded | $C_E = 1.0104 - 0.0562W_s$ |
| US NWS 8" unshielded | $C_E = 1.0077 - 0.0834W_s$ |
| Hellmann | $C_E = 0.9663 - 0.041W_s^2 - 0.0984W_s + 0.0595T_{mean}$ |

Historical transfer functions for manual gauges (Table 6.4) are reported in the literature and are summarized by Goodison et al. (1998), who describe the intercomparison of many common manual precipitation gauge configurations during the first WMO Solid Precipitation Measurement Intercomparison. Manual observations of precipitation are made at substantially lower frequencies than those employed by automated weighing gauges (for example, 6, 12, or 24 hours), and the transfer functions shown in Table 6.4 are applied at these lower frequencies.

Below are some additional points regarding the application of transfer functions to manual gauges:

(a) Wind speed measured at a height other than that of the gauge orifice needs to be reduced to the height of the gauge;

(b) All non-wind-related errors in the measurement (for example, wetting loss, evaporation) should be corrected before applying the wind adjustment (if possible);

(c) A calculated $C_E$ greater than 1 should always be reduced to 1.

#### 6.5.2.2 ***Heated tipping buckets***

Tipping-bucket gauges also suffer from wind-induced undercatch, and, as with manual gauges, their shape and size often (but not always) influence wind undercatch potential. However, heated tipping-bucket gauges are also significantly affected by other factors, such as evaporation from heated surfaces and response delays due to snowmelt time, which may impact their ability to accurately identify the start and end times of solid precipitation events, making transfer function derivation more difficult than for weighing gauges.

Since unshielded heated tipping-bucket precipitation gauges are widely used in national observation networks, it is important to have methodologies available to derive estimates of true accumulation. For that purpose, the transfer functions derived by Kochendorfer et al. (2020) to adjust solid precipitation measurements from unshielded heated tipping-bucket gauges at SPICE intercomparison sites can be used. This methodology also provides calculated resultant uncertainties. Based on the results of these studies, the minimum accumulation period for adjustment should be one hour to minimize the effects of delayed instrument response due to the melting of collected snow.

According to Kochendorfer et al. (2020), the recommended multi-gauge optimized transfer function has the form given in Equation 6.7:

$$C_E = (a)e^{-b(U)} \tag{6.7}$$

where $U$ is the wind speed, and a and b are coefficients. This equation was fit separately to mixed and solid precipitation, with solid precipitation defined as occurring when $T_{air} < -2$ °C, and mixed precipitation defined as occurring when 2 °C ≥ $T_{air}$ ≥ –2 °C. The coefficients for both mixed and solid (snowfall) events are provided in Table 6.5.

**Table 6.5. Coefficients (*a*, *b*) for gauge height ($H_g$) and 10-m height wind speeds for mixed and solid precipitation, where $U_{thresh}$ indicates the maximum average wind speed (threshold) to which the transfer function can be applied**

| *Wind height* | *Mixed* | | *Solid* | | $U_{thresh}$ m s$^{-1}$ |
|---|---|---|---|---|---|
| | *a* | *b* | *a* | *b* | |
| $H_g$ | 0.726 | 0.0495 | 0.701 | 0.227 | 6.1 |
| 10 m | 0.722 | 0.0354 | 0.7116 | 0.1925 | 8.0 |

The literature also lists alternative tipping-bucket gauge-specific transfer functions that are continuous with temperature (Buisán et al., 2017)

Similar recommendations on the application of transfer functions for weighing gauges also apply to heated tipping-bucket transfer functions, but users must also consider the unique problems heated tipping buckets experience with the measurement of solid precipitation. These can limit the application of transfer functions.

Intercomparisons with shielded tipping buckets, which is a configuration not usually used in operational networks, showed some interesting results. When shielded, the gauges tend to respond faster (shorter delays) than unshielded gauges because shielded gauges catch more precipitation, increasing the possibility to trigger a tip. Regarding total accumulation and when compared with DFAR, single Alter-shielded tipping buckets showed similar values to those of single Alter-shielded weighing gauges but showed more spread, which may result from the influence of response delays (partial melting). Also, using double Alter-shielded tipping buckets during snowfall events close to 0 °C and with wind speeds below 5–6 m s$^{-1}$ resulted in precipitation amounts similar to those measured by a DFAR (Buisán et al., 2018, 2022).

## 6.6 SITING AND EXPOSURE

All methods for measuring precipitation should aim to obtain a sample that is representative of the true amount falling over the area which the measurement is intended to represent, whether on the synoptic scale, mesoscale or microscale.

The immediate surroundings of the gauge location may affect this representativeness in different ways:

(a) Obstacles (that is, buildings, trees) very close to the gauge can directly obstruct the collection or registration of precipitation, thus leading to an underestimation of the true precipitation amount;

(b) All surrounding obstacles, as well as the topography or vegetation of a location, affect the wind field around a precipitation gauge, by, for example, channelling or creating additional turbulence or general inhomogeneity in the wind field, potentially giving rise to local excesses and deficiencies in precipitation;

(c) Moderate and high wind speeds around the orifice of a collection gauge (a tipping-bucket or an accumulating gauge) will cause systematic underestimation of precipitation. The lighter the particles, the larger the underestimation. Optical instruments,

which measure the terminal velocity of the precipitation particles to determine the precipitation type, and based on this, derive the precipitation amount, are affected by higher wind speeds in a more unpredictable way.

Impact severity will vary strongly with precipitation type, and to a lesser extent, with precipitation intensity. In most cases, light particles such as snow and mixed precipitation or drizzle will be more affected than heavy precipitation particles.

For a further discussion of the effects of site exposure on precipitation measurement, see Sevruk and Zahlavova (1994). A classification of the exposure of a measurement site has been developed to indicate the representativeness of a measurement with respect to its environment. See the present volume, Chapter 1, Annex 1.D. Siting classifications for surface observing stations on land, which gives advice on how to document and classify the influence of the surrounding environment on precipitation measurements (and other parameters).

In general, objects which can cause obstruction should not be closer to the gauge than a distance equivalent to twice their height above the gauge orifice (equal to an elevation angle smaller than 26° from the height of the precipitation gauge collector). For each site, environmental exposure should be estimated based on the siting classifications for precipitation defined in the present volume, Chapter 1, Annex 1.D.

Further, a rather homogeneous environment should be chosen, minimizing turbulence and channelling affects. Sites on a slope or the roof of a building should be avoided.

At locations where a large amount of the annual precipitation falls as snow, placing the precipitation gauge in a wind-sheltered area is preferable in order to minimize wind-induced loss (see 6.5). The best sites are often in clearings within forests or orchards, among trees, in scrub or shrub forests, or where other objects act as effective wind-breaks from all directions; the impact of objects in close proximity to the gauge and the impacts of extra turbulence or the creation of wake effects must also be taken into consideration. An ideal natural shelter would be one with low obstacles of uniform height surrounding the gauge, with subtending elevation angles between 14° and 26° (obstacles at a distance from the gauge between two and four times their height). Semi-permeable shelters such as trees, hedges or fences are preferable to solid shelters, such as buildings or walls, because they result in a more even wind flow. Note that these kinds of sheltered locations may be non-optimal for the measurement of other meteorological parameters, such as temperature, humidity and wind, as they affect the radiation balance and the wind field of the site (see the siting classification criteria for each variable in Chapter 1, Annex 1.D of the present volume). Separate locations for the different parameters may be advisable where feasible (taking into consideration the cost, technical limitations, and so forth).

Where the co-location of several measured parameters is required, or when sheltered but unobstructed siting is unavailable or impractical, the following siting recommendations (listed in order of decreasing effectiveness) can minimize exposure-related measurement issues:

(a) In areas where solid precipitation is rare, a ground-level gauge is ideal;

(b) In areas with homogeneous dense vegetation, the height of such vegetation should be kept at the same level as the gauge orifice by regular clipping;

(c) In other areas, simulate the effect described in (b) through the use of appropriate fence structures, such as that used for the DFIR or DFAR;

(d) Use other windshields around the gauge (see the WMO-SPICE final report for examples and their effectiveness (Nitu et al., 2018)). In general, more significant shielding (that is, double shields instead of single shields) is more effective at increasing gauge catch efficiency.

When precipitation measurements are made close to the surface (as recommended above), rather than mounting gauges over hard, flat surfaces, such as concrete, the surface surrounding the precipitation gauge can be covered with short grass, gravel or shingle to prevent excessive splashing that may enter the gauge and bias the measurement.

The location of precipitation stations within the area of interest is important because the number and locations of the gauge sites determine how well the measurements represent the actual amount of precipitation falling in the area. Areal representativeness is discussed at length in Sevruk (1992) for rain and snow. The *Guide to Hydrological Practices* (WMO-No. 168), Volume I gives an introduction to the literature on the calculation of areal precipitation and corrections for topography. Since the surrounding environment of a gauge will evolve in time (growing trees, new buildings, and so forth), it is necessary to re-evaluate the impact of close obstacles regularly (for example, every two years) and to take the necessary actions to guarantee a constant level of quality over a long period. This is mandatory in order to allow for long-term data series and trend assessment.

## 6.7 PRECIPITATION DATA QUALITY CONTROL (AUTOMATED GAUGES)

Precipitation accumulation, observed as the depth of liquid water, is not measured directly by automated gauges; rather, these gauges measure an instrument response to an accumulated weight or volume of precipitation, from which an equivalent depth of liquid amount is determined. For weighing gauges, accumulation values are derived from the weight of the contents of a collector (for example, a bucket) reported by a load cell or via the frequency of a vibrating wire transducer and a calibration equation. For tipping-bucket gauges, precipitation is determined from the number of bucket tips over a specified time period, where the bucket holds a known weight or volume of liquid precipitation.

Environmental influences on an automated gauge and its contents can impact how the instrument responds to accumulation (the measurement) and contaminate the reported output, reducing the quality of the precipitation data. By understanding how the environment impacts an instrument and its data, it is possible to install and configure instruments in a way that reduces the likelihood and severity of data quality issues. These approaches can be categorized as impact mitigation by prevention and target the first stage in the data chain, between the instrument and its data output. Some instruments have built-in functionality to mitigate environmental influences at this stage.

Post-processing approaches target the next stage in the data chain, between data output and application. These approaches can be informed by an understanding of the instrument (for example, minimum instrument detection limits and how the instrument reacts to the causes of signal noise), as well as the characteristics of precipitation in the operating environment (for example, the maximum expected change in accumulation within a given time). These processes can also be informed by approaches used to improve signal quality in other domains (for example, signal processing, filtering).

### 6.7.1 Environmental factors impacting precipitation data quality and mitigation approaches

Environmental factors impacting precipitation data quality and some mitigating approaches are presented in Table 6.6. These factors include interference by humans and other fauna, and the effects of wind and temperature on the instrument's capabilities to measure precipitation. While specific factors have different impacts, in general, the outcome is a precipitation dataset that possibly contains errors, which increases the difficulty in identifying and isolating actual precipitation. It is also possible for multiple environmental factors to impact precipitation gauges and their data at the same time or within a specified time period.

The key to mitigating the environmental sources of data quality issues is to carefully consider the gauge configuration and siting. This can prevent or minimize quality issues from occurring at the first stage in the data chain, increasing the quality of the "raw" precipitation accumulation data and reducing the requirements for further quality control via post-processing.

**Table 6.6. Environmental factors impacting precipitation data quality and mitigation approaches related to instrument or site configuration and practices**

| *Factor* | *Impact(s) on data* | *Mitigation approach(es)* |
|---|---|---|
| Human interference | – Potential for erroneous or missing data | – Site security (e.g. fences), site and data monitoring<br>– Detailed site logs with times of site visits recorded |
| Fauna (insects, wildlife) | – Potential for erroneous or missing data | – Site and data monitoring, fencing, protection of instrument wiring and electronics |
| Wind | – High frequency noise due to vibration<br>– Missed or false precipitation data | – Installation of windshields<br>– Separation of windshields from instrument and mounting infrastructure to minimize vibration<br>– Secure instrument base (e.g. concrete) |
| Temperature fluctuations | – Low frequency noise, often diurnal<br>– Missed or false precipitation data | – Thermal isolation of sensing elements from environment |
| Freezing of gauge components or contents | – Erroneous reports due to impaired instrument functioning and/or performance | – Heating of components, use of antifreeze to prevent bucket contents from freezing |
| Capping of gauge orifice | – Missed precipitation due to full or partial blockage; delayed or erroneous precipitation data | – Heating of orifice and/or gauge housing<br>– Site and data monitoring |

### 6.7.2 Post-processing approaches for precipitation accumulation data

Not all quality issues impacting precipitation accumulation data can be prevented; indeed, the capabilities and specifications of a precipitation gauge and the range of environmental conditions experienced in the field can present additional quality issues that need to be addressed via post-processing. A two-stage approach to post-processing is recommended. In the first stage, information from site logs, instrument specifications, and instrument diagnostics (if available) are leveraged to identify suspect or erroneous data. In the second stage, targeted approaches are applied to address specific environmental impacts (for example, wind noise or gauge capping), as well as any apparent issues not resolved in the first stage of post-processing. The second stage tends to be more subjective than the first stage.

Recommended approaches in the first and second post-processing stages are outlined in Table 6.7 and Table 6.8, respectively. For each approach, recommended steps are presented for implementation. The approaches are presented at a high level for broad guidance. More detailed descriptions of Stage 2 approaches with specific thresholds and example cases are available elsewhere (Nitu et al., 2018; Ross et al., 2020).

## 6.8 MEASUREMENT OF DEW, ICE ACCUMULATION AND FOG PRECIPITATION

### 6.8.1 Measurement of dew and leaf wetness

The deposition of dew is essentially a nocturnal phenomenon. Although relatively small in amount and locally variable, dew is of significant interest in arid zones, and in very arid regions, it may be comparable in amount to rainfall. The exposure of plant leaves to liquid moisture from dew, fog and precipitation also plays an important role in plant disease, insect activity, and the harvesting and curing of crops.

**Table 6.7. Post-processing approaches (Stage 1): incorporating site logs, instrument specifications and diagnostic parameters (if available)**

| *Instrument specification or parameter* | *Data issue to address* | *Recommended action* |
|---|---|---|
| Minimum and maximum instrument reporting range | Outlying or erroneous reports | Flag and remove values outside of instrument range |
| Range of operating conditions (e.g. temperature) | Outlying or erroneous reports | Flag and remove values when conditions exceed range of operating conditions |
| Use of diagnostic parameters (e.g. reports of gauge malfunction, heater issues) | Variable | Parameter-dependent<br>In general, flag suspect values; flag and remove erroneous values |

**Table 6.8. Post-processing approaches (Stage 2): addressing remaining quality issues**

| *Apparent data issue* | *Recommended approach* | *Implementation notes* |
|---|---|---|
| Outlying reports | Range checks | – May be addressed in Stage 1<br>– Maximum accumulation values can be informed by site climatology |
| Spurious data jumps | Jump filter | – Threshold values provided by manufacturer specifications in some cases<br>– Threshold selection can be informed by anticipated rates of change of accumulation based on site climatology (i.e. maximum hourly precipitation rates) |
| Baseline shifts (due to gauge capping, drain and recharge of weighing gauges) | Baseline shift filter | – Apply a threshold of consecutive jumps to identify baseline shifts<br>– In suspected capping scenarios (baseline shift to higher accumulation when the cap falls into the gauge), independent observations are valuable in identifying start/end of capping period for flagging and removal |
| Noise | Noise filter | – Different approaches available (moving average, Gaussian, noise aggregation)<br>– Specific filter parameters vary depending on dataset, informed by instrument specifications (e.g. minimum resolution) and noise characteristics (frequency and amplitude) |
| False precipitation | Independent observations | – In some cases, gauges may report erroneous accumulation based on responses to specific conditions<br>– Independent observations from different technologies (e.g. precipitation detector, disdrometer) can be used to identify and flag potential false reports |
| Undercatch | Adjustment functions | – Approach dependent on ancillary instrumentation available (wind and temperature, disdrometer). See 6.5.2.1. |

In order to assess the hydrological contribution of dew, it is necessary to distinguish between dew formed:

(a) As a result of the downward transport of atmospheric moisture condensed on cooled surfaces, known as “dew-fall”;

(b) By water vapour evaporated from the soil and plants and condensed on cooled surfaces, known as “distillation dew”;

(c) As water exuded by leaves, known as “guttation”.

All three forms of dew may contribute simultaneously to the observed dew, although only the first provides additional water to the surface, and the latter usually results in a net loss. A further source of moisture results from fog or cloud droplets being collected by leaves and twigs and reaching the ground by dripping or by stem flow.

The amount of dew deposited on a given surface in a stated period is usually expressed in units of kg $m^{-2}$ or in millimetres depth of dew. Whenever possible, the amount should be measured to the nearest tenth of a millimetre.

Leaf wetness may be described as light, moderate or heavy, but its most important measurements are time of onset and duration.

A review of the instruments designed for measuring dew and the duration of leaf wetness, as well as a bibliography, are given in Getz (1992).

The amount of dew depends critically on the properties of the surface, such as its radiative properties, size and aspect (horizontal or vertical). Dew may be measured by exposing a plate or surface, whether natural or artificial, with known or standardized properties, and then assessing the amount of dew by weighing it, visually observing it, or using another method such as measuring electrical conductivity. The challenge lies in selecting the appropriate surface as the results obtained instrumentally may not necessarily be representative of the dew deposit on the surrounding objects. Empirical relationships between instrumental measurements and dew deposition on a natural surface should therefore be established for each specific set of surface and exposure conditions. Empirical relationships should also be established to distinguish between the processes of dew formation if that is important for the particular application.

A number of instruments are currently being used to directly measure the occurrence, amount and duration of leaf wetness and dew. Dew-duration recorders use either elements that change to indicate or record the wetness period, or electrical sensors in which the electrical conductivity of the surface of natural or artificial leaves changes in the presence of water resulting from rain, snow, wet fog or dew. In dew balances, the amount of moisture deposited in the form of precipitation or dew is weighed and recorded. In most instruments providing a continuous trace, it is possible to distinguish between moisture deposits caused by fog, dew or rain by considering the type of trace. The only certain method of measuring net dew-fall by itself is through the use of a very sensitive lysimeter (see the present volume, Chapter 10).

Getz advocates for the development as reference instruments of two particular electronic instruments for measuring leaf wetness and proposes various leaf-wetting simulation models. Some use an energy balance approach (the inverse of evaporation models), while others use correlations. Many of the models require micrometeorological measurements; however, unfortunately, there is no recognized standard method of measurement by which they can be verified.

### 6.8.2 Measurement of ice accumulation

#### 6.8.2.1 *Measurement methods*

At meteorological stations, the observation of ice accumulation is generally more qualitative than quantitative, primarily due to the lack of a suitable sensor. Ice accretion indicators, usually made of anodized aluminium, are used to observe and report the occurrence of freezing precipitation, frost or rime icing.

Observations of ice accumulation can include both the measurement of the dimensions and the weight of the ice deposit, as well as a visual description of its appearance. These observations are particularly important in mountainous areas where such accumulation on the windward side of a mountain may exceed normal precipitation. A system consisting of rods and stakes with two pairs of parallel wires (one pair oriented north–south and the other east–west) can be used to accumulate ice. The wires may be suspended at any level, and the upper wire of each pair should be removable. At the time of observation, both upper wires are removed, placed in a special container, and taken indoors for melting and weighing of the deposit. The cross-section of the deposit is measured on the permanently fixed lower wires.

Recording instruments are used in some countries for the continuous registration of rime. A vertical or horizontal rod, ring or plate is used as the sensor, and the increase in the amount of rime with time is recorded on a chart. A simple device called an ice-scope is used to determine the appearance and presence of rime and hoar frost on a snow surface. The ice-scope consists of a round plywood disc, 30 cm in diameter, which can be moved up or down and set at any height on a vertical rod fixed in the ground. Normally, the disc is set flush with the snow surface to collect the rime and hoar frost. Rime is also collected on a 20 cm diameter ring fixed on the rod, 20 cm from its upper end. A wire or thread 0.2 mm to 0.3 mm in diameter, stretched between the ring and the top end of the rod, is used for the observation of rime deposits. If necessary, each sensor can be removed and weighed.

In international standard ISO 12494:2017, which applies to ice accretion on all kinds of structures except electrical overhead line conductors, a standard ice-measuring device is described as follows:

(a) A smooth cylinder with a diameter of 30 mm is placed vertically and rotates around its axis. The cylinder length should be a minimum of 0.5 m, but, if heavy ice accretion is expected, the length should be 1 m;

(b) The cylinder is placed 10 m above terrain;

(c) Ice weight recordings may be performed automatically.

Fikke et al. (2007) identify several types of ice detectors, some of which are used to determine the start and end of icing periods, while others are able to quantify the ice accretion rate (usually expressed in kg $m^{-2}$ $h^{-1}$). Many sensors are designed to measure the ice mass on a vertical tube used as a target for icing. An optical sensor (infrared (IR) beam) detects the change in reflecting properties of a target tube when covered with ice. Another sensor, widely used for freezing rain, consists of a vibrating probe. Ice accreted on this probe changes the vibrating frequency, which allows both the detection of icing conditions and an estimate of the ice accretion rate. An internal probe heater is applied to melt the ice and keep the sensor within its operational limits.

#### 6.8.2.2 *Ice on pavements*

Sensors have been developed and are in operation to detect and describe ice on roads and runways and to support warning and maintenance programmes. Volume III, Chapter 10 of the present Guide provides more specific information on this subject.

With a combination of measurements, it is possible to detect dry and wet snow and various forms of ice. One sensor, using two electrodes embedded in the road flush with the surface,

measures the electrical conductivity of the surface and readily distinguishes between dry and wet surfaces. A second measurement, of ionic polarizability, determines the ability of the surface to hold an electrical charge; a small charge is passed between a pair of electrodes for a short time, and the same electrodes measure the residual charge, which is higher when there is an electrolyte with free ions, such as salty water. The polarizability and conductivity measurements together can distinguish between dry, moist and wet surfaces, frost, snow, white ice and some de-icing chemicals. However, because the polarizability of the non-crystalline black ice is indistinguishable from water under some conditions, the dangerous black ice state can still not be detected with the two sensors. In at least one system, this problem has been solved by adding a third specialized capacitive measurement which detects the unique structure of black ice.

The above method is a passive technique. There is an active in situ technique that uses either a heating element, or both heating and cooling elements, to melt or freeze any ice or liquid present on the surface. Simultaneous measurements of temperature and of the heat energy involved in the thaw-freeze cycle are used to determine the presence of ice and to estimate the freezing point of the mixture on the surface.

Most in situ systems include a thermometer to measure the road surface temperature. The quality of the measurement depends critically on the mounting (especially the materials) and exposure, and care must be taken to avoid radiation errors.

There are two remote-sensing methods under development which lend themselves to car-mounted systems. The first method is based on the reflection of IR and microwave radiation at several frequencies (about 3 000 nm and 3 GHz, respectively). The microwave reflections can determine the thickness of the water layer (and hence the risk of aquaplaning), but not the ice condition. Two IR frequencies can be used to distinguish between dry, wet and icy conditions. It has also been demonstrated that the magnitude of reflected power at wavelengths around 2 000 nm depends on the thickness of the ice layer.

The second method applies pattern recognition techniques to the reflection of laser light from the pavement to distinguish between dry and wet surfaces and black ice.

### 6.8.3 Measurement of fog precipitation

Fog consists of minute water droplets suspended in the atmosphere to form a cloud at the Earth's surface. Fog droplets have diameters from about 1 $\mu$m to 40 $\mu$m and fall velocities from less than 1 cm $s^{-1}$ to approximately 5 cm $s^{-1}$. In fact, the fall speed of fog droplets is so low that, even in light winds, the drops travel almost horizontally. When fog is present, horizontal visibility is less than 1 km; it is rarely observed when the temperature and dewpoint differ by more than 2 °C.

Meteorologists are generally more concerned with fog as an obstruction to vision than as a form of precipitation. However, from a hydrological standpoint, some forested high-elevation areas experience frequent episodes of fog as a result of the advection of clouds over the surface of the mountain, where the consideration of precipitation alone may seriously underestimate the water input to the watershed (Stadtmuller and Agudelo, 1990). More recently, the recognition of fog as a water supply source in upland areas (Schemenauer and Cereceda, 1994a) and as a wet deposition pathway (Schemenauer and Cereceda, 1991; Vong et al., 1991) has led to the requirement for standardizing methods and units of measurement.

Although there have been a great number of measurements for the collection of fog by trees and various types of collectors over the last century, it is difficult to compare the collection rates quantitatively. The most widely used fog-measuring instrument consists of a vertical wire mesh cylinder centrally fixed on the top of a rain gauge in such a way that it is fully exposed to the free flow of the air. The cylinder is 10 cm in diameter and 22 cm in height, and the mesh is 0.2 cm by 0.2 cm (Grunow, 1960). The droplets from the moisture-laden air are deposited on the mesh and drop down into the gauge collector where they are measured or registered in the same way as rainfall. Some problems with this instrument are its small size, the lack of representativeness with respect to vegetation, the storage of water in the small openings

in the mesh, and the ability of precipitation to enter directly into the rain gauge portion, which confounds the measurement of fog deposition. In addition, the calculation of fog precipitation by simply subtracting the amount of rain in a standard rain gauge (Grunow, 1964) from that in the fog collector leads to erroneous results whenever wind is present.

An inexpensive, 1 $m^2$ standard fog collector and standard unit of measurement is proposed by Schemenauer and Cereceda (1994b) to quantify the importance of fog deposition to forested high-elevation areas and to measure the potential collection rates in denuded or desert mountain ranges. The collector consists of a flat panel made of a durable polypropylene mesh and mounted with its base 2 m above the ground. The collector is coupled to a tipping-bucket rain gauge to determine deposition rates. When wind speed measurements are taken in conjunction with the fog collector, reasonable estimates of the proportions of fog and rain being deposited on the vertical mesh panel can be taken. The output of this collector results in litres of water. Since the surface area is 1 $m^2$, the water collected is measured in kg $m^{-2}s$

# ANNEX 6.A. STANDARDIZED PROCEDURE FOR LABORATORY CALIBRATION OF CATCHMENT-TYPE RAINFALL INTENSITY GAUGES

## 1. PRINCIPLES

The calibration laboratory should be well prepared to perform calibrations of instruments to be used for operational practices. Apart from a well-designed reference system, the calibration procedures should be documented in full detail, the equipment should be set up and the relevant staff should be well prepared before starting any calibration activity (see the International Organization for Standardization (ISO)/International Electrotechnical Commission (IEC) standard ISO/IEC 17025 for details). The result of any calibration will be a calibration certificate presenting the results of the calibration (including corrections to be applied), allowing compliance with the relevant WMO recommendations to be verified.

This certificate should also contain the measurement uncertainty for rainfall intensity. It should document the traceability of the rainfall intensity reference, the environmental conditions, such as temperature, and the applied time-averaging method.

Rainfall intensity gauges should be calibrated using a calibration system that:

(a) Is capable of generating a constant water flow at various flow rates corresponding to the entire operational range of measurement specified by each manufacturer;

(b) Is able to measure the flow by weighing the amount of water over a given period of time;

(c) Is able to measure the output of the calibrated instrument at regular intervals or when a pulse occurs, which is typical for the majority of tipping-bucket rain gauges.

## 2. REQUIREMENTS

(a) The calibration system should be designed to obtain uncertainties of less than 1% for the generated rainfall intensity, and such performances should be reported and detailed;

(b) In the case of tipping-bucket rain gauges, correct and suitable balancing of the buckets should be verified in order to guarantee a minimal variance of the tipping duration during the measurement process;

(c) At least five reference intensities suitably spaced to cover the whole operating range of the instrument should be used;

(d) The number of rainfall intensity reference setting points should be large enough to be able to determine a fitting curve by interpolation. The reference setting should be selected and well spaced so that the calibration curve can be established by interpolation such that the uncertainty of the fitting curve is less than the required measurement uncertainty for the full range;

(e) The calculation of the flow rate should be based on the measurements of mass and time;

(f) The mass should be measured to an accuracy of greater than 0.1%;

(g) The duration of any test should be long enough to guarantee an uncertainty of less than 1% on the generated intensity;

(h) The maximum time resolution for the measurement of rainfall intensities should be 1 s;

(i) The following considerations must be taken into account in any related laboratory activity in order to address potential error sources:

  (i) The water quality/purity used for calibration should be well defined;

  (ii) The reproducibility of the calibration conditions should be a priority;

  (iii) Suitable control and recording equipment should be used (such as PC-controlled equipment);

  (iv) All acquisition systems must comply with electromagnetic compatibility standards to avoid parasitic pulses;

(j) Precipitation is generally measured in height, expressed in millimetres, although weighing gauges measure mass. Since the density of rain depends on ambient temperature, the relationship between mass and the equivalent height of rainfall introduces an inaccuracy that must be taken into account during calibration and uncertainty calculation;

(k) The environmental conditions during each calibration must be noted and recorded:

  (i) Date and hour (start/end);

  (ii) Air temperature (°C);

  (iii) Water temperature (°C);

  (iv) Atmospheric pressure (hPa);

  (v) Ambient relative humidity (%);

  (vi) Any special condition that may be relevant to calibration (for example, vibrations);

  (vii) An estimate of evaporation losses (mm);

(l) The number of tests performed for each instrument, their description in terms of time units and/or number of tips, must be documented.

## 3. PROCEDURE FROM DATA INTERPRETATION

(a) The results should be presented in the form of a graph where the relative error is plotted against the reference intensity. The relative error is evaluated for each reference flow rate as:

$$e = \frac{I_m - I_r}{I_r} \cdot 100\% \qquad (6.A.1)$$

where $I_m$ is the intensity measured by the instrument and $I_r$ is the actual reference intensity provided to the instrument;

(b) Ideally five tests, but a minimum of three, should be performed for each set of reference intensities, so that five error figures are associated with each instrument. The average error and the average values of $I_r$ and $I_m$ are obtained by discarding the minimum and maximum values of $e$ obtained for each reference flow rate, then evaluating the arithmetic mean of the three remaining errors and reference intensity values. For each reference intensity, an error bar encompassing the five error values used to obtain the average figures should be reported;

(c) In addition, $I_r$ versus $I_m$ can be plotted, where $I_m$ and $I_r$ are average values, calculated as indicated above; all data are fitted with an interpolating curve, obtained as the best fit (linear, power law or second order polynomial are acceptable);

(d) In the graphs presenting the results, the ±5% limits must be drawn to allow easy comparison of the results with WMO recommendations;

(e) If water storage occurs at an intensity below the maximum declared level, the point at which storage begins should be documented in the calibration certificate, and intensities above this limit should not be considered;

(f) In addition to measurements based on constant flow rates, the step response of each non-tipping-bucket rain gauge instrument should be determined. The step response should be measured by switching between two different constant flows, namely from 0 mm $h^{-1}$ to the reference intensity and back to 0 mm $h^{-1}$. The constant flow should be applied until the output signal of the instrument is stabilized, that is, when the further changes or fluctuation in the established rainfall intensity can be neglected with respect to the stated measurement uncertainty of the reference system. The sampling rate must be at least one per minute for those instruments that allow it. The time before stabilization is assumed to be a measure of the delay of the instrument in measuring the reference rainfall intensity. A delay of less than one minute is required for accurate rainfall intensity measurements. The response time should always be documented in the calibration certificate.

## 4. UNCERTAINTY CALCULATION

The following sources of measurement uncertainty should be considered and quantified:

(a) Flow generator: Uncertainty regarding flow steadiness, deriving from possible variations in the constant flow generation mechanism, including pressure difference inside the water content and in the distribution pipes;

(b) Flow measuring devices (both reference and device under calibration): Uncertainties pertaining to the weighing apparatus, to time measurement and delays in acquisition and data processing, and to the variation of experimental and ambient conditions such as temperature and relative humidity.

These two sources of uncertainty are independent of each other; therefore a separate analysis can be performed for each, and the results can then be combined into the uncertainty budget.

# ANNEX 6.B. DETAILED FIELD VERIFICATION PROCEDURE FOR CATCHMENT-TYPE RAINFALL INTENSITY GAUGES

Field verifications are part of routine field maintenance and should be performed on a regular basis. Their main purpose is to verify the operational status of precipitation gauges: to detect malfunctions, output anomalies and calibration drifts over time or between two laboratory calibrations. Field verifications also provide valuable insight for data analysis and interpretation. The field verification procedure is based on the same principles as the laboratory calibration procedure (see Annex 6.A) and is performed using the generation of constant intensity (stationary reference flow) within the gauge's range of operational use.

A field verification instrument is typically composed of a cylindrical water tank of suitable capacity, a combination of air intakes and output nozzles for different rainfall intensities, and an electronic system to calculate the emptying time (see Figure 6.B.1 below). A suitable combination of air intakes and nozzles must be selected based on the precipitation gauge collector size and the intensity value chosen for the verification. By opening the top tap and bottom nozzle, a constant flow is conveyed to the funnel of the gauge and, by measuring the emptying time and using the conversion table (volume–time–intensity), it is possible to retrieve the reference intensity. Air intakes provide pressure compensation, thus maintaining a constant push.

From an operational viewpoint, the portable field verification instrument permits rapid tests due to its very simple operation. It does not contain any sophisticated components and is therefore cost-effective to use.

The repeatability of the field verification instrument (and its uncertainty) should be rigorously assessed in a laboratory before operational use. The assessment should reference the following three metrology units: mass, capacity and time. The field verification instrument should be traceable with known uncertainty. The uncertainty should preferably be expressed as relative expanded uncertainty in relation to the statistical coverage interval (95% confidence level, $k = 2$) and should be lower than 2%.

A statistical analysis of relative errors with respect to the field reference flow of the field verification instrument should be conducted for each field-verified precipitation gauge. At least 25–30 data points (normally 1 min intensity values in mm $h^{-1}$) should be recorded for each reference intensity (selected by the field verification instrument). This makes it possible to assume a normal distribution of the data around the mean value and to better estimate the average and improve the accuracy of the results (central limit theorem). All tests must be performed in environmental conditions without precipitation or fog and with low wind flows (to avoid

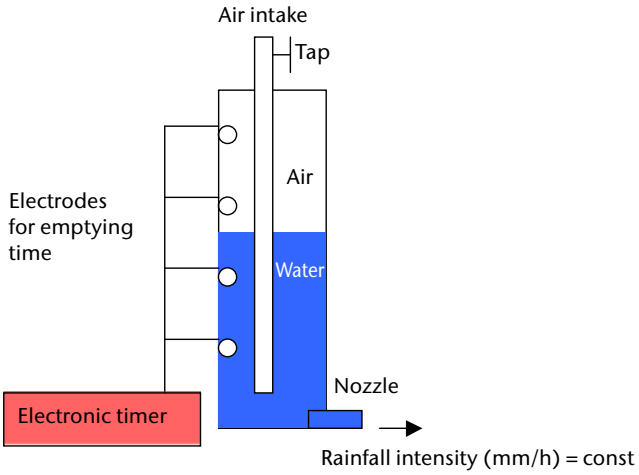



**Figure 6.B.1. A simplified scheme of a portable field calibrator**

dynamic pressure perturbations to air intakes). The reference intensity should always be started at the beginning of a minute synchronized with the instrument clock or data-logger timer (official/station time-stamp).

The minimum statistical parameters and metadata to be reported after each field verification are the following:

(a) Date and time;

(b) Reference intensity in mm $h^{-1}$ ($I_{ref}$): constant intensity generated by the field calibrator;

(c) Average (avg$I$) of intensity values ($I_{1\,min}$) in mm $h^{-1}$ of the precipitation gauge during the calibration, calculated as follows:

$$\text{avg}I = \frac{1}{N}\sum_{j=1}^{N}\left(I_{1\text{min}}^{j}\right) \tag{6.B.1}$$

(d) Extremes (namely $I_{+CL95\%}$, $I_{-CL95\%}$) of an interval

[avg$I$ – $\delta$(95%); avg$I$ + $\delta$(95%)] = [$I_{+CL95\%}$; $I_{-CL95\%}$]

corresponding to the 95% confidence level. The amplitude $\delta$(95%) is the half-width of the confidence interval calculated according to a normal or Student's $t$ probability distribution of samples (it includes a calculation of the standard deviation);

(e) Relative error in percentage of the average intensity, calculated as follows:

$$RE_{avgI} = 100 \cdot \left(\frac{\text{avg}I - I_{\text{ref}}}{I_{\text{ref}}}\right) \tag{6.B.2}$$

(f) Relative errors in percentage of $I_{+CL95\%}$ and $I_{-CL95\%}$, calculated as follows:

$$RE_{+CL95\%} = 100 \cdot \left(\frac{I_{+CL95\%} - I_{\text{ref}}}{I_{\text{ref}}}\right) \tag{6.B.3}$$

$$RE_{-CL95\%} = 100 \cdot \left(\frac{I_{-CL95\%} - I_{\text{ref}}}{I_{\text{ref}}}\right) \tag{6.B.4}$$

The last three statistical parameters are used to calculate the gauge's relative errors with regard to intensity with an uncertainty interval at the 95% confidence level for each reference intensity used during the field verification. The regular repetition of the field verification and the comparison of results makes it possible to evaluate the stability of the field verification status and possible anomalies.

# REFERENCES


Angulo-Martínez, M.; Beguería, S.; Latorre, B. et al. Comparison of Precipitation Measurements by OTT Parsivel2 and Thies LPM Optical Disdrometers. *Hydrology and Earth System Sciences* **2018**, *22* (5), 2811–2837. https://doi.org/10.5194/hess-22-2811-2018.

Baghapour, B.; Sullivan, P. E. A CFD Study of the Influence of Turbulence on Undercatch of Precipitation Gauges. **2017**. https://doi.org/10.1016/j.atmosres.2017.07.008.

Beguería, S.; Buisán, S. T.; Collado, J. L. et al. Impact of Wind and Temperature on Snowfall Measurements by Thies LPM and OTT Parsivel2 Optical Disdrometers compared with DFAR (Double Fence Automated Reference) Measurements at WMO.SPICE Formigal-Sarrios site [Poster]. Presented at the *WMO Technical Conference on Meteorological and Environmental Instruments and Methods of Observation (CIMO TECO-2018)*, Amsterdam, Netherlands (Kingdom of the), 8–11 October 2018. https://community.wmo.int/publications-and-iom-reports/teco-2018-presentations.

Buisán, S. T.; Earle, M. E.; Collado, J. L. et al. Assessment of Snowfall Accumulation Underestimation by Tipping Bucket Gauges in the Spanish Operational Network. *Atmospheric Measurement Techniques* **2017**, *10* (3), 1079–1091. https://doi.org/10.5194/amt-10-1079-2017.

Buisán, S. T.; Earle. M. E; Monteagudo Lerma, L. et al. An Assessment of the Impact of a Single-Alter Windshield on Snowfall Accumulation Reported by a Heated Tipping Bucket Gauge [Poster]. Presented at the *WMO Technical Conference on Meteorological and Environmental Instruments and Methods of Observation (CIMO TECO-2018)*, Amsterdam, Netherlands (Kingdom of the), 8–11 October 2018. https://community.wmo.int/publications-and-iom-reports/teco-2018-presentations.

Buisán, S. T.; Collado, J. L.; Alastrue, J. Cost/benefit Decisions for Choosing the Right Gauge Configuration under Wet Snow Conditions [Poster]. Presented at the *WMO Technical Conference on Meteorological and Environmental Instruments and Methods of Observation (TECO-2022)*, Paris, France, 10–13 October 2022. https://community.wmo.int/en/activity-areas/imop/publications-and-iom-reports/teco-2022-presentations.

Chan, Y. W.; Yu, C. L.; Tam, K. H. Inter-comparison of Raingauges on Rainfall Amount and Intensity Measurements in a Tropical Environment. *Journal of Geodesy and Geomatics Engineering* **2015**, *2* (1). https://www.davidpublisher.com/index.php/Home/Article/index?id=6857.html.

Chvíla, B.; Sevruk, B.; Ondrás, M. The Wind-Induced Loss of Thunderstorm Precipitation Measurements. *Atmospheric Research* **2005**, *77* (1), 29–38. https://doi.org/10.1016/j.atmosres.2004.11.032.

Colli, M.; Lanza, L. G.; Chan, P. W. Co-Located Tipping-Bucket and Optical Drop Counter RI Measurements and a Simulated Correction Algorithm. *Atmospheric Research* **2013a**, *119*, 3–12. https://doi.org/10.1016/j.atmosres.2011.07.018.

Colli, M.; Lanza, L. G.; La Barbera, P. Performance of a Weighing Rain Gauge under Laboratory Simulated Time-varying Reference Rainfall Rates. *Atmospheric Research* **2013b**, *131*, 3–12. https://doi.org/10.1016/j.atmosres.2013.04.006.

Colli, M.; Stagnaro, M.; Lanza, L. et al. Using Snowfall Intensity to Improve the Correction of Wind-induced Undercatch in Solid Precipitation Measurements. *Hydrology and Earth System Sciences Discussions* **2018** [preprint], 1–24. https://doi.org/10.5194/hess-2018-447.

Duchon, C. E.; Essenberg, G. R. Comparative Rainfall Observations from Pit and Aboveground Rain Gauges with and without Wind Shields. *Water Resources Research* **2001**, *37* (12), 3253–3263. https://doi.org/10.1029/2001WR000541.

European Committee for Standardization (CEN). *Hydrometry – Specification for a Reference Raingauge Pit*; EN 13798:2010, 2010. https://standards.iteh.ai/catalog/standards/sist/d51efdb7-0299-4196-8682-aba95721c868/sist-en-13798-2010.

Fikke, S.; Ronsten, G.; Heimo, A. et al. *COST-727: Atmospheric Icing on Structures; Measurements and data collection on icing: State of the Art*; MeteoSwiss Publication No. 75, 2007.

Getz, R. R. *Report on the Measurement of Leaf Wetness* (WMO/TD-No. 478). Commission for Agricultural Meteorology (CAgM) Report No. 38; World Meteorological Organization (WMO): Geneva, 1992.

Goodison, B. E.; Louie, P. Y. T.; Yang, D. *WMO Solid Precipitation Measurement Intercomparison* (WMO/TD-No. 872). Final report. Instruments and Observing Methods (IOM) Report No. 67; World Meteorological Organization (WMO): Geneva, 1998.

Grunow, J. The Productiveness of Fog Precipitation in Relation to the Cloud Droplet Spectrum. In: *Physics of Precipitation: Proceedings of the Cloud Physics Conference, Woods Hole, Massachusetts, June 3–5, 1959, Volume 5*); Weickmann, H., Ed.; American Geophysical Union, Geophysical Monograph Series, 1960, 110–117.

Grunow, J. *Weltweite Messungen des Nebelniederschlags nach der Hohenpeissenberger Methode.* International Association of Scientific Hydrology Publication No. 65, 1964, 324–342.

Habib, E.; Krajewski, W. F.; Kruger, A. Sampling Errors of Tipping-Bucket Rain Gauge Measurements. *Journal of Hydrologic Engineering* **2001**, *6* (2), 159–166. https://doi.org/10.1061/(ASCE)1084-0699(2001)6:2(159).

Hoover, J.; Mouradian, H.; Earle, M. et al. Oil Comparison for Weighing Precipitation Gauges as Used in Environment Canada. Presented at the *WMO Technical Conference on Meteorological and Environmental Instruments and Methods of Observation, (TECO-2014)*, Saint Petersburg, Russian Federation, 9 July 2014a. https://library.wmo.int/idurl/4/53114.

Hoover, J.; Watson, S.; Morin, S. Annex VIII – Overview of Antifreeze and Oil Assessment. In *Project Team and (Reduced) International Organizing Committee for the WMO Solid Precipitation Intercomparison Experiment – Fifth Session*, Sodankylä, Finland, 19–23 May 2014; World Meteorological Organization (WMO), 2014b.

Johannsen, L. L.; Zambon, N.; Strauss, P. et al. Comparison of Three Types of Laser Optical Disdrometers under Natural Rainfall Conditions. *Hydrological Sciences Journal* **2020**, *65* (4), 524–535. https://doi.org/10.1080/02626667.2019.1709641.

International Organization for Standardization (ISO), *Atmospheric Icing of Structures*, ISO 12494:2017. Geneva, 2017.

International Organization for Standardization (ISO)/International Electrotechnical Commission (IEC), *General Requirements for the Competence of Testing and Calibration Laboratories*, ISO/IEC 17025:2017. Geneva, 2017.

Kochendorfer, J.; Nitu, R.; Wolff, M. et al. Analysis of Single-Alter-shielded and Unshielded Measurements of Mixed and Solid Precipitation from WMO-SPICE. *Hydrology and Earth System Sciences* **2017**, *21* (7), 3525–3542. https://doi.org/10.5194/hess-21-3525-2017.

Kochendorfer, J.; Earle, M. E.; Hodyss, D. et al. Undercatch Adjustments for Tipping-bucket Gauge Measurements of Solid Precipitation. *Journal of Hydrometeorology* **2020**, *21* (6), 1193–1205. https://doi.org/10.1175/JHM-D-19-0256.1.

Kochendorfer, J.; Earle, M.; Rasmussen, R. et al. How Well Are We Measuring Snow Post-SPICE? *Bulletin of the American Meteorological Society* **2022**, *103* (2), E370–E388. https://doi.org/10.1175/BAMS-D-20-0228.1.

Lanza, L. G.; Leroy, M.; Alexandropoulos, C. et al. *WMO Laboratory Intercomparison of Rainfall Intensity Gauges* (WMO/TD-No. 1304). Instruments and Observing Methods (IOM) Report No. 84; World Meteorological Organization (WMO): Geneva, 2006.

Lanza, L. G.; Merlone, A.; Cauteruccio, A. et al. Calibration of Non-catching Precipitation Measurement Instruments: A Review. *Meteorological Applications* **2021**, *28* (3), e2002. https://doi.org/10.1002/met.2002.

Mayo, L. R. Self-Mixing Antifreeze Solution for Precipitation Gages. *Journal of Applied Meteorology and Climatology* **1972**, *11* (2), 400–404. https://doi.org/10.1175/1520-0450(1972)011<0400:SMASFP>2.0.CO;2.

McSaveney, M. J. An Effective Antifreeze for Storage Raingauges. *Journal of Hydrology New Zealand* **1979**, *18* (1), 52–54. https://www.hydrologynz.org.nz/journal/journal-18.

Monforte, J., Buisán, S. T., Collado, J. L.,et al. Radar Precipitation Technology Compared with the WMO Precipitation Reference [Poster]. Presented at the *WMO Technical Conference on Meteorological and Environmental Instruments and Methods of Observation (TECO-2022)*, Paris, France, 10–13 October 2022. https://community.wmo.int/en/activity-areas/imop/publications-and-iom-reports/teco-2022-presentations.

Nitu, R.; Wong, K. *CIMO Survey on National Summaries of Methods and Instruments for Solid Precipitation Measurement at Automatic Weather Stations.* (WMO/TD-No. 1544). Instruments and Observing Methods (IOM) Report No. 102; World Meteorological Organization (WMO), Geneva, 2010.

Nitu, R.; Roulet, Y.-A.; Wolff, M. et al. *WMO Solid Precipitation Intercomparison Experiment (SPICE) (2012–2015).* Instruments and Observing Methods (IOM) Report No. 131; World Meteorological Organization (WMO), Geneva, 2018.

Rasmussen, R. M.; Hallett, J.; Purcell, R. et al. The Hotplate Precipitation Gauge. *Journal of Atmospheric and Oceanic Technology* **2011**, *28* (2), 148–164. https://doi.org/10.1175/2010JTECHA1375.1.

Rasmussen, R.; Baker, B.; Kochendorfer, J. et al. How Well Are We Measuring Snow: The NOAA/FAA/NCAR Winter Precipitation Test Bed. *Bulletin of the American Meteorological Society* **2012**, *93* (6), 811–829. https://doi.org/10.1175/BAMS-D-11-00052.1.

Reverdin, A.; Buisán, S; Roulet, Y. A. et al. Intercomparison of Snowfall Measurements Using Disdrometers in Two Mountainous Environments: Weissfluhjoch (Switzerland) and Formigal-Sarrios (Spain)

[Poster]. Presented at the *WMO Technical Conference on Meteorological and Environmental Instruments and Methods of Observation (TECO-2016)*, Madrid, Spain, 27–30 September 2016. https://community.wmo.int/en/teco-2016session3.

Rinehart, R. E. Out-of-level Instruments: Errors in Hydrometeor Spectra and Precipitation Measurements. *Journal of Applied Meteorology and Climatology* **1983**, *22* (8), 1404–1410. https://doi.org/10.1175/1520-0450(1983)022<1404:OOLIEI>2.0.CO;2.

Ross, A.; Smith, C. D.; Barr, A. An Improved Post-Processing Technique for Automatic Precipitation Gauge Time Series. *Atmospheric Measurement Techniques* **2020**, *13* (6), 2979–2994. https://doi.org/10.5194/amt-13-2979-2020.

Schemenauer, R. S.; Cereceda, P. Fog-Water Collection in Arid Coastal Locations. *Ambio* **1991**, *20* (7), 303–308. http://www.jstor.org/stable/4313850.

Schemenauer, R. S.; Cereceda, P. Fog Collection's Role in Water Planning for Developing Countries. *Natural Resources Forum*, **1994a**, *18* (2), 91–100. https://doi.org/10.1111/j.1477-8947.1994.tb00879.x.

Schemenauer, R. S.; Cereceda, P. A Proposed Standard Fog Collector for Use in High-Elevation Regions. *Journal of Applied Meteorology and Climatology* **1994b**, *33* (11), 1313–1322. https://doi.org/10.1175/1520-0450(1994)033<1313:APSFCF>2.0.CO;2.

Sevruk, B. Evaporation Losses from Storage Gauges. *Presented at the Geilo Symposium*, Norway, 31 July–5 August 1972. In *Distribution of Precipitation in Mountainous Areas* (WMO-No. 326), Volume II; World Meteorological Organization (WMO): Geneva, 1972.

Sevruk, B. Correction for the Wetting Loss of a Hellmann Precipitation Gauge. *Hydrological Sciences Bulletin* **1974*a***, *19* (4), 549–559.

Sevruk, B. Evaporation Losses from Containers of Hellmann Precipitation Gauges. *Hydrological Sciences Bulletin* **1974*b***, *19* (2), 231–236. https://doi.org/10.1080/02626667409493902.

Sevruk, B. Comments on "Out-of-level Instruments: Errors in Hydrometeor Spectra and Precipitation Measurements". *Journal of Climate and Applied Meteorology* **1984**, *23* (6), 988–989. https://doi.org/10.1175/1520-0450(1984)023%3C0988:COOLIE%3E2.0.CO;2.

Sevruk, B. *Methods of Correction for Systematic Error in Point Precipitation Measurement for Operational Use* (WMO-No. 589). Operational Hydrology Report No. 21; World Meteorological Organization (WMO): Geneva, 1982.

Sevruk, B. *Papers Presented at the Workshop on the Correction of Precipitation Measurements* (WMO/TD-No. 104). Instruments and Observing Methods (IOM) Report No. 25; World Meteorological Organization (WMO): Geneva, 1985.

Sevruk, B.; Klemm, S. *Catalogue of National Standard Precipitation Gauges* (WMO/TD-No. 313). Instruments and Observing Methods (IOM) Report No. 39; World Meteorological Organization (WMO): Geneva, 1989.

Sevruk, B. *Snow Cover Measurements and Areal Assessment of Precipitation and Soil Moisture* (WMO-No. 749). Operational Hydrology Report No. 35; World Meteorological Organization (WMO): Geneva, 1992.

Sevruk, B.; Nespor, V. The Effect of Dimensions and Shape of Precipitation Gauges on the Wind-Induced Error. In *Global Precipitations and Climate Change*; Desbois, M., Désalmand, F., Eds.; Springer: Berlin, Heidelberg, 1994; 231–246. https://doi.org/10.1007/978-3-642-79268-7_14.

Sevruk, B.; Zahlavova, L. Classification System of Precipitation Gauge Site Exposure: Evaluation and Application. *International Journal of Climatology* **1994**, *14* (6), 681–689. https://doi.org/10.1002/joc.3370140607.

Sieck, L. C.; Burges, S. J.; Steiner, M. Challenges in Obtaining Reliable Measurements of Point Rainfall. *Water Resources Research* **2007**, *43* (1). https://doi.org/10.1029/2005WR004519.

Smith, C. D.; Ross, A.; Kochendorfer, J. et al. Evaluation of the WMO Solid Precipitation Intercomparison Experiment (SPICE) Transfer Functions for Adjusting the Wind Bias in Solid Precipitation Measurements. *Hydrology and Earth System Sciences* **2020**, *24* (8), 4025–4043. https://doi.org/10.5194/hess-24-4025-2020.

Stadtmuller, T.; Agudelo, N. Amount and Variability of Cloud Moisture Input in a Tropical Cloud Forest. In *Proceedings of the Lausanne Symposia*, Wallingford, August/November 1990; International Association of Hydrological Sciences (IAHS) Publication No. 193.

Stagnaro, M.; Colli, M.; Lanza, L. G. et al. Performance of Post-Processing Algorithms for Rainfall Intensity Using Measurements from Tipping-Bucket Rain Gauges. *Atmospheric Measurement Techniques* **2016**, *9* (12), 5699–5706. https://doi.org/10.5194/amt-9-5699-2016.

Thom, A. S. Momentum, Mass and Heat Exchange of Plant Communities, Volume 1; Academic Press, 1975.

Vong, R. J.; Sigmon, J. T.; Mueller, S. F. Cloud Water Deposition to Appalachian Forests. *Environmental Science and Technology* **1991**, *25* (6), 1014–1021. https://doi.org/10.1021/es00018a002.

Vuerich, E.; Monesi, C.; Lanza, L. G. et al. *WMO Field Intercomparison of Rainfall Intensity Gauges* (WMO/TD-No. 1504). Instruments and Observing Methods (IOM) Report No. 99; World Meteorological Organization (WMO): Geneva, 2009.

Wolff, M. A.; Isaksen, K.; Petersen-Øverleir, A. et al. Derivation of a New Continuous Adjustment Function for Correcting Wind-induced Loss of Solid Precipitation: Results of a Norwegian Field Study. *Hydrology and Earth System Sciences* **2015**, *19* (2), 951–967. https://doi.org/10.5194/hess-19-951-2015.

World Meteorological Organization (WMO). *Guide to Hydrological Practices* (WMO-No. 168), Volume I. Geneva, 2008, updated in 2020.

# CHAPTER 7. MEASUREMENT OF RADIATION

## 7.1 GENERAL

The various fluxes of radiation to and from the Earth's surface are among the most important variables in the heat economy of the Earth as a whole and at any individual place at the Earth's surface or in the atmosphere. Radiation measurements are used for the following purposes:

(a) To study the transformation of energy within the Earth–atmosphere system and its variation in time and space;

(b) To analyse the properties and distribution of the atmosphere with regard to its constituents, such as aerosols, water vapour, ozone, and so on;

(c) To study the distribution and variations of incoming, outgoing and net radiation;

(d) To satisfy the needs of biological, medical, agricultural, architectural and industrial activities with respect to radiation;

(e) To verify satellite radiation measurements and algorithms.

Such applications require a widely distributed regular series of records of solar and terrestrial surface radiation components and the derivation of representative measures of the net radiation. In addition to the publication of serial values for individual observing stations, an essential objective must be the production of comprehensive radiation climatologies, whereby the daily and seasonal variations of the various radiation constituents of the general thermal budget may be more precisely evaluated and their relationships with other meteorological elements better understood.

A very useful account of the operation and design of networks of radiation stations is contained in the *Revised Instruction Manual on Radiation Instruments and Measurements* (WMO/TD-No. 149). Volume V of the present Guide describes the scientific principles of the measurements and gives advice on QA, which is of vital importance for radiation measurements. The *Baseline Surface Radiation Network (BSRN) Operations Manual* (McArthur, 2005) gives an overview of the latest state of radiation measurements.

Other useful documents are:

ISO/TR 9901:2021 Solar Energy – Pyranometers – Recommended Practice for Use;

ISO 9060:2018 Solar Energy – Specification and Classification of Instruments for Measuring Hemispherical Solar and Direct Solar Radiation;

ISO 9846:1993 Solar Energy – Calibration of a Pyranometer Using a Pyrheliometer;

ISO 9847:2023 Solar energy – Calibration of Pyranometers by Comparison to a Reference Pyranometer.

Following normal practice in this field, errors and uncertainties are expressed in this chapter as a 66% confidence interval of the difference from the true quantity, which is similar to one standard deviation of the population of values. Where needed, specific uncertainty confidence intervals are indicated, and uncertainties are estimated using the ISO method (ISO/IEC, 2008 (JCGM, 2008)). For example, 95% uncertainty implies that the stated uncertainty is for a confidence interval of 95%.

### 7.1.1 Definitions

Annex 7.A contains the nomenclature of radiometric and photometric quantities. It is based on definitions recommended by the International Radiation Commission of the International Association of Meteorology and Atmospheric Sciences and by the International Commission on Illumination (CIE). Annex 7.B gives the meteorological radiation quantities, symbols and definitions.

**Radiation quantities.** These may be classified into two groups according to their origin, namely, solar and terrestrial radiation. In the context of this chapter, "radiation" can imply a process or apply to multiple quantities. For example, "solar radiation" could mean solar energy, solar exposure or solar irradiance (see Annex 7.B).

**Solar energy.** This is the electromagnetic energy emitted by the Sun. The solar radiation incident on the top of the terrestrial atmosphere is called extraterrestrial solar radiation. Most of its energy (97%) is confined to the spectral range 290 to 3 000 nm. Radiation in this range is sometimes referred to as short-wave radiation and is usually associated with, or considered equivalent to, solar radiation. Part of the extraterrestrial solar radiation penetrates through the atmosphere to the Earth's surface, while part of it is scattered and/or absorbed by the gas molecules, aerosol particles, cloud droplets and cloud crystals in the atmosphere.

**Terrestrial radiation.** This is the long-wave electromagnetic energy emitted by the Earth's surface and by the gases, aerosols and clouds of the atmosphere; it is also partly absorbed within the atmosphere. For a temperature of 300 K, 99.99% of the power of the terrestrial radiation has a wavelength longer than 3 000 nm, and about 99% has a wavelength longer than 5 000 nm. For lower temperatures, the spectrum is shifted to longer wavelengths.

Since the spectral distributions of solar and terrestrial radiation overlap very little, they can very often be treated separately in measurements and computations. In meteorology, the sum of both types is called total radiation.

**Light.** This is the radiation visible to the human eye. The spectral range of visible radiation is defined by the spectral luminous efficiency for the standard observer. The lower limit is taken to be between 360 and 400 nm, and the upper limit between 760 and 830 nm (CIE 069-1987). The radiation of wavelengths shorter than about 400 nm is called ultraviolet (UV) and longer than about 800 nm is called infrared (IR). The UV range is sometimes divided into three sub-ranges (IEC, 2020):

UV-A: 315–400 nm;
UV-B: 280–315 nm;
UV-C: 100–280 nm.

### 7.1.2 Units and/or scales

#### 7.1.2.1 *Units*

The International System of Units (SI) is preferred for meteorological radiation variables. A general list of the units is given in Annex 7.A and 7.B.

#### 7.1.2.2 *Standardization of solar radiation measurements*

The responsibility for the calibration of radiometric instruments rests with the World, Regional and National Radiation Centres, the specifications for which are given in Annex 7.C. Furthermore, the World Radiation Centre (WRC), at Davos, Switzerland, is responsible for maintaining the basic reference, the World Standard Group (WSG) of instruments, which is used to establish the World Radiometric Reference (WRR). During international comparisons, organized every five years, the standards of the regional centres are compared with the WSG, and their calibration factors are adjusted to the WRR. These standards are, in turn, periodically used to transmit

the WRR to the national centres, which calibrate their network instruments using their own standards. Annex 7.D gives guidelines for radiometer comparisons, especially with respect to the traceability propagation of radiation references.

### Definition of the World Radiometric Reference

In the past, several radiation references or scales were used in meteorology, namely the Ångström scale of 1905, the Smithsonian scale of 1913, and the international pyrheliometric scale of 1956 (IPS 1956). The developments in absolute radiometry in recent years have very much reduced the uncertainty of radiation measurements. With the results of many comparisons of 15 individual absolute pyrheliometers of 10 different types, a WRR has been defined. The old scales can be transferred into the WRR using the following factors:

$$\frac{\text{WRR}}{\text{Angstrom scale 1905}} = 1.026$$

$$\frac{\text{WRR}}{\text{Smithsonian scale 1913}} = 0.977$$

$$\frac{\text{WRR}}{\text{IPS 1956}} = 1.022$$

The WRR is accepted as representing the physical units of total irradiance within 0.3%.

### Realization of the World Radiometric Reference: World Standard Group

To guarantee the long-term stability of the new reference, a group of at least four absolute pyrheliometers of different design is used as the WSG. Upon incorporation into this group, the instruments are given a reduction factor to correct their readings to the WRR. To be included in the group, a radiometer must fulfil the following specifications:

(a) Its stability must be better than 0.2% of the measured value over timescales of decades;

(b) The 95% uncertainty of the series of measurements with the instrument must fall within the limits of the uncertainty of the WRR;

(c) The instrument must have a different design from the other WSG instruments.

To meet the stability criteria, the WSG instruments are the subjects of an intercomparison at least once a year, and, for this reason, the WSG is kept at the WRC in Davos.

### Computation of World Radiometric Reference values

To calibrate radiometric instruments, the reading of a WSG instrument, or an instrument that is directly traceable to the WSG, should be used. During international pyrheliometer comparisons (IPCs), the WRR value is calculated from the mean of at least three participating instruments of the WSG. To yield WRR values, the readings of the WSG instruments are always corrected with the individual reduction factor, which is determined at the time of their incorporation into the WSG. The calculation of the mean value of the WSG, serving as the reference, may be jeopardized by the failure of one or more radiometers. To address this issue CIMO resolved[1] that at each IPC, an ad hoc group should be established, comprising the Rapporteur on Meteorological Radiation Instruments (or designate) and at least five members, including the chair. This group assesses the stability of the WSG instruments and selects instruments to be used in the calculation of the WRR. The director of the comparison must participate in the group's meetings as an expert. The group should discuss the preliminary results of the comparison based on criteria defined by the WRC, evaluate the reference and recommend updating the calibration factors.

[1] Recommended by CIMO at its eleventh session (1994).

### 7.1.2.3 *Standardization of terrestrial radiation measurements*

In response to the requirement to standardize terrestrial radiation measurements, WMO established the Infrared Radiometry Section (WRC-IRS) at the Physikalisch Meteorologisches Observatorium Davos (PMOD), and WRC-IRS established an interim WMO Pyrgeometer Infrared Reference, the World Infrared Standard Group (WISG), in 2004. WRC-IRS should serve as a centre for the international calibration of meteorological instruments measuring infrared radiation and maintaining WISG, and the calibration results should be disseminated, in a hierarchical manner, through Regional Radiation Centres to National Radiation Centres and then to other government laboratories and private sector laboratories following the guidelines in *Commission for Instruments and Methods of Observation – Thirteenth Session: Abridged Final Report with Resolutions and Recommendations* (WMO-No. 947).

The WISG provides internal consistency for terrestrial radiation measurements, and its traceability to the SI is necessary to integrate terrestrial radiation measurements from ground-based networks with solar radiation fluxes. This integration is essential in order to establish a coherent global radiation budget estimate.

#### Realization of the interim WMO Pyrgeometer Infrared Reference: World Infrared Standard Group (WISG)

The WISG consists of four state-of-the-art pyrgeometers of two different types. Two of these pyrgeometers were calibrated against the Absolute Sky-Scanning Radiometer (ASR) (Philipona, 2001) during the International Pyrgeometer and Absolute Sky-scanning Radiometer comparison (IPASRC-I) in 1999 (Philipona et al., 2001), while the other two were calibrated relative to this initial set.

The WISG is operated continuously on the PMOD/WRC roof platform. Its stability is monitored by internal consistency checks of the four pyrgeometers, as well as annual characterizations in the blackbody BB2007 (Gröbner, 2008, Feierabend et al., 2023). Measurements have shown that the WISG has been stable to within ±1 $Wm^{-2}$ since 2004 (Gröbner and Wacker, 2013), which is significantly lower than its associated uncertainty of ±4 $Wm^{-2}$. This confirms its suitability as a long-term reference for terrestrial radiation measurements.

#### Governance framework for the WISG

To review the status and stability of the WISG governance framework, an advisory group of experts in atmospheric longwave radiation measurements was appointed by the president of the Commission for Observation, Infrastructure and Information Systems (INFCOM) as per Resolution 1 (CIMO-17) – Governance and traceability of atmospheric longwave irradiance (*Commission for Instruments and Methods of Observation: Abridged Final Report of the Seventeenth Session* (WMO-No. 1227) and its annex (see Annex 7.E. to the present chapter).

According to this governance framework, the WRC-IRS reported the status and stability of the WISG to the advisory group established for the third WMO International Pyrgeometer Intercomparison (IPgC-III), held in 2021. At the advisory group meeting, the stability of the WISG since its establishment in 2004 was reported. An update of the WISG instrument coefficients was proposed based on evidence that the WISG instrument coefficients in operational use since its inception have changed, as determined by the annual characterization in the reference blackbody (Gröbner and Thomann, 2023). The advisory group confirmed the stablity of WISG, approved the update of the WISG instruments coefficients, and recommended that INFCOM (formerly CIMO) approve the update of the WISG coefficients. The new WISG coefficients have been used operationally since 1 January 2022.

### 7.1.3 Meteorological requirements

#### 7.1.3.1 *Data to be reported*

Irradiance and radiant exposure are the quantities most commonly recorded and archived, with averages and totals of over 1 h. There are also many requirements for data over shorter periods, down to 1 min or even tens of seconds (for some energy applications). Daily totals of radiant exposure are frequently used, but these are expressed as a mean daily irradiance. Measurements of atmospheric extinction must be made with very short response times to reduce the uncertainties arising from variations in the airmass.

For radiation measurements, it is particularly important to record and make available information about the circumstances of the observations. This includes the type and traceability of the instrument, its calibration history, and its location in space and time, spatial exposure and maintenance record.

#### 7.1.3.2 *Uncertainty*

There are no formally agreed statements of required uncertainty for most radiation quantities, but uncertainty is discussed in the sections of this chapter dealing with the various types of measurements, and best practice uncertainties are stated for the Global Climate Observing System's (GCOS) Baseline Surface Radiation Network (see McArthur, 2005). In general, good quality measurements are difficult to achieve in practice, and for routine operations, they can be achieved only with modern equipment and redundant measurements. Some systems still in use fall short of best practice as the lesser performance has been acceptable for many applications. However, data of the highest quality are increasingly in demand.

Statements of uncertainty for net radiation and radiant exposure are given in the present volume, Chapter 1, Annex 1.A. The required 95% uncertainty for radiant exposure for a day, stated by WMO for international exchange, is 0.4 MJ $m^{-2}$ for ≤ 8 MJ $m^{-2}$ and 5% for > 8 MJ $m^{-2}$.

#### 7.1.3.3 *Sampling and recording*

The uncertainty requirements can best be satisfied by making observations at a sampling period less than the $1/e$ time constant of the instrument, even when the data to be finally recorded are integrated totals for periods of up to 1 h, or more. The data points may be integrated totals or an average flux calculated from individual samples. Digital data systems are greatly to be preferred. Chart recorders and other types of integrators are much less convenient, and the resultant quantities are difficult to maintain at adequate levels of uncertainty.

#### 7.1.3.4 *Observation times*

In a worldwide network of radiation measurements, it is important that the data be homogeneous not only for calibration, but also for observation times. Therefore, all radiation measurements should be referred to what is known in some countries as local apparent time, and in others as true solar time. Standard or universal time (UT) is attractive for automatic systems because it is easier to use, but it is acceptable only if a reduction of the data to true solar time does not introduce a significant loss of information (that is to say, if the sampling and storage rates are high enough, as indicated in 7.1.3.3 above). See Annex 7.F for useful formulae for the conversion from standard to solar time.

### 7.1.4 *Methods of measurement*

Meteorological radiation instruments are classified using various criteria, namely the type of variable to be measured, the field of view, the spectral response, the main use, and the like. The most important types of classifications are listed in Table 7.1.

**Table 7.1. Meteorological radiation instruments**

| *Instrument classification* | *Parameter to be measured* | *Main use* | *Viewing angle (sr) (see Figure 7.1)* |
|---|---|---|---|
| Absolute pyrheliometer | Direct solar radiation | Primary standard | $6 \times 10^{-3}$ (approx. 2.5° half-angle) |
| Pyrheliometer | Direct solar radiation | (a) Secondary standard for calibrations<br>(b) Network | $6 \times 10^{-3}$ to $2.4 \times 10^{-2}$ |
| Spectral pyrheliometer | Direct solar radiation in broad spectral bands (e.g. with OG 530, RG 630, etc. filters) | Network | $6 \times 10^{-3}$ to $2.4 \times 10^{-2}$ |
| Sunphotometer | Direct solar radiation in narrow spectral bands (e.g. at 500 ±2.5 nm, 368 ± 2.5 nm) | (a) Standard<br>(b) Network | $1 \times 10^{-3}$ to $1 \times 10^{-2}$<br>(approx. 2.3° full angle) |
| Pyranometer | (a) Global (solar) radiation<br>(b) Diffuse sky (solar) radiation<br>(c) Reflected solar radiation | (a) Working standard<br>(b) Network | $2\pi$ |
| Spectral pyranometer | Global (solar) radiation in broadband spectral ranges (e.g. with OG 530, RG 630, etc. filters) | Network | $2\pi$ |
| Net pyranometer | Net global (solar) radiation | (a) Working standard<br>(b) Network | $4\pi$ |
| Pyrgeometer | (a) Upward long-wave radiation (downward-looking)<br>(b) Downward long-wave radiation (upward-looking) | Network | $2\pi$ |
| Pyrradiometer | Total radiation | Working standard | $2\pi$ |
| Net pyrradiometer | Net total radiation | Network | $4\pi$ |

The quality of the instruments is characterized by items (a) to (h) below. The instruments and their operation are described in 7.2 to 7.6 below. The *Revised Instruction Manual on Radiation Instruments and Measurements* (WMO/TD-No. 149) provides a detailed account of instruments and the principles according to which they operate.

Absolute radiometers are self-calibrating, meaning that the irradiance falling on the sensor is replaced by electrical power, which can be accurately measured. The substitution, however, cannot be perfect; the deviation from the ideal case determines the uncertainty of the radiation measurement.

Most radiation sensors, however, are not absolute and must be calibrated against an absolute instrument. The uncertainty of the measured value, therefore, depends on the following factors, all of which should be known for a well-characterized instrument:

(a) Resolution, namely, the smallest change in the radiation quantity which can be detected by the instrument;

(b) Drifts of sensitivity (the ratio of electrical output signal to the irradiance applied) over time;

(c) Changes in sensitivity owing to changes of environmental variables, such as temperature, humidity, pressure and wind;

(d) Non-linearity of response, namely, changes in sensitivity associated with variations in irradiance;

(e) Deviation of the spectral response from that postulated, namely the blackness of the receiving surface, the effect of the aperture window, and so on;

(f) Deviation of the directional response from that postulated, namely cosine response and azimuth response;

(g) Time constant of the instrument or the measuring system;

(h) Uncertainties in the auxiliary equipment.

Instruments should be selected according to their end use and the required uncertainty of the derived quantity. Certain instruments perform better for particular climates, irradiances and solar positions.

## 7.2 MEASUREMENT OF DIRECT SOLAR RADIATION

Direct solar radiation is measured using pyrheliometers, the receiving surfaces of which are arranged to be normal to the solar direction. Using apertures, only the radiation from the Sun and a narrow annulus of the sky is measured; the latter radiation component is sometimes referred to as circumsolar radiation or aureole radiation. In modern instruments, the measurement extends out to a half-angle of about 2.5° on some models, and to about 5° from the Sun's centre (corresponding, respectively, to $6 \cdot 10^{-3}$ and $2.4 \cdot 10^{-2}$ sr). The pyrheliometer mount must allow for the rapid and smooth adjustment of the azimuth and elevation angles. A sighting device is usually included, with a small spot of light or solar image falling upon a mark in the centre of the target when the receiving surface is exactly normal to the direct solar beam. For continuous recording, it is advisable to use automatic Sun-following equipment (Sun tracker).

For all new designs of direct solar radiation instruments, it is recommended that the opening half-angle be 2.5° ($6 \cdot 10^{-3}$ sr) and the slope angle 1°. For the definition of these angles, refer to Figure 7.1.

During the comparison of instruments with different view-limiting geometries, the aureole radiation influences the readings more significantly for larger slope and aperture angles.

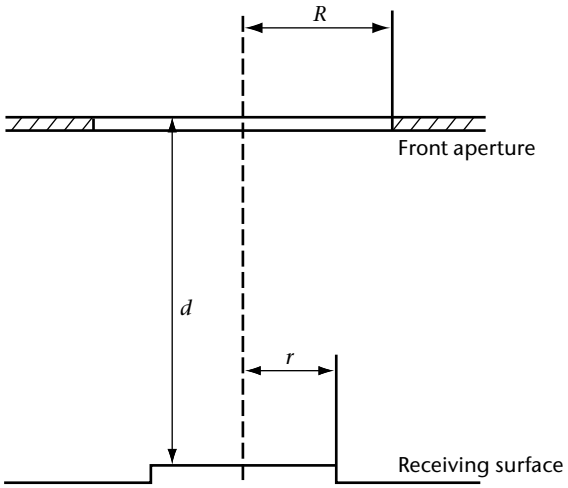



**Figure 7.1. View-limiting geometry: The opening half-angle is arctan $R/d$; the slope angle is arctan $(R–r)/d$.**

The difference can be as great as 2% between the two apertures mentioned above for an airmass of 1.0. In order to enable climatological comparison of direct solar radiation data during different seasons, it may be necessary to reduce all data to a mean Sun–Earth distance:

$$E_N = E / R^2 \quad (7.1)$$

where $E_N$ is the solar radiation, normalized to the mean Sun–Earth distance, which is defined to be one astronomical unit (AU) (see Annex 7.F); $E$ is the measured direct solar radiation; and $R$ is the Sun–Earth distance in AUs.

### 7.2.1 Direct solar radiation

Some of the characteristics of operational pyrheliometers (other than primary standards) are given in Table 7.2 (adapted from ISO 9060:2018), with indicative estimates of the uncertainties of measurements made with them if they are used with appropriate expertise and QC. Cheaper pyrheliometers are available (see ISO 9060:2018), but without efforts to characterize their response, the resulting uncertainties reduce the quality of the data, and, given that a Sun tracker is required, in most cases the incremental cost for a good pyrheliometer is minor. The estimated uncertainties are based on the following assumptions:

(a) Instruments are well-maintained, calibrated, correctly aligned and cleaned regularly in accordance with 7.2.2;

(b) 1 min and 1 h figures are for clear-sky irradiances at solar noon;

(c) Daily exposure values are for clear-sky days at mid-latitudes.

#### 7.2.1.1 *Primary standard pyrheliometers*

An absolute pyrheliometer can define the scale of total irradiance without resorting to reference sources or radiators. The limits of uncertainty of the definition must be known; the quality of this knowledge determines the reliability of an absolute pyrheliometer. Only specialized laboratories should operate and maintain primary standards. Details of their construction and operation are given in the *Revised Instruction Manual on Radiation Instruments and Measurements* (WMO/TD-No. 149). However, for the sake of completeness, a brief account is given here.

**Table 7.2. Characteristics of operational pyrheliometers**

| *Characteristic* | | *High quality*[a] | *Good quality*[b] |
|---|---|---|---|
| Response time (95% response) | | < 10 s | < 15 s |
| Zero offset A (response to 5 K $h^{-1}$ change in ambient temperature)<br>Zero offset B (complete zero offset including offset A and other sources) | | 1 W $m^{-2}$<br>2 W $m^{-2}$ | 3 W $m^{-2}$<br>4 W $m^{-2}$ |
| Resolution (smallest detectable change in W $m^{-2}$) | | 0.5 | 1 |
| Stability (percentage change in responsivity per year) | | 0.5 | 1 |
| Temperature response (percentage deviation due to change in ambient temperature within the interval from –10 °C to 40 °C relative to the signal at 20 ˚C) | | 0.5 | 1 |
| Non-linearity (percentage deviation from the responsivity at 500 W $m^{-2}$ due to the change in irradiance within 100 W $m^{-2}$ to 1 000 W $m^{-2}$) | | 0.2 | 0.5 |
| Spectral sensitivity (percentage deviation of the product of spectral absorptance and spectral transmittance from the corresponding mean within the range 300 to 3 000 nm)<br>Clear-sky direct normal incidence spectral error (maximum spectral error observed for a set of direct normal irradiance clear-sky spectra defined in the ISO 9060 standard) | | 0.5<br>0.2 | 1.0<br>1 |
| Tilt response (percentage deviation from the responsivity at 0° tilt (horizontal) due to change in tilt from 0° to 90° at 1 000 W $m^{-2}$ irradiance) | | 0.2 | 0.5 |
| Achievable uncertainty, 95% confidence level (see above) | | | |
| 1 min totals | %<br>kJ $m^{-2}$ | 0.9<br>0.56 | 1.8<br>1 |
| 1 h totals | %<br>kJ $m^{-2}$ | 0.7<br>21 | 1.5<br>54 |
| Daily totals | %<br>kJ $m^{-2}$ | 0.5<br>200 | 1.0<br>400 |

a Near state of the art; suitable for use as a working standard; maintainable only at stations with special facilities and staff.
b Acceptable for network operations.

All absolute pyrheliometers of modern design use cavities as receivers and electrically calibrated, differential heat-flux meters as sensors. At present, this combination has proved to yield the lowest uncertainty possible for the radiation levels encountered in solar radiation measurements (namely, up to 1.5 kW $m^{-2}$).

Normally, the electrical calibration is performed by replacing the radiative power with electrical power, which is dissipated in a heater winding as close as possible to where the absorption of solar radiation takes place.

The uncertainties of such an instrument's measurements are determined by a close examination of the physical properties of the instrument and by performing laboratory measurements and/or model calculations to determine the deviations from ideal behaviour, that is, how perfectly the electrical substitution can be achieved. This procedure is called characterization of the instrument.

The following specification should be met by an absolute pyrheliometer (an individual instrument, not a type) to be designated and used as a primary standard:

(a) At least one instrument out of a series of manufactured radiometers has to be fully characterized. The 95% uncertainty of this characterization should be less than 2 W $m^{-2}$

under the clear-sky conditions suitable for calibration (see ISO 9060:2018). The 95% uncertainty (for all components of the uncertainty) for a series of measurements should not exceed 4 W $m^{-2}$ for any measured value;

(b) Each individual instrument of the series must be compared with the one which has been characterized, and no individual instrument should deviate from this instrument by more than the characterization uncertainty as determined in (a) above;

(c) A detailed description of the results of such comparisons and of the characterization of the instrument should be made available upon request;

(d) Traceability to the WRR by comparison with the WSG or some carefully established reference with traceability to the WSG is needed in order to prove that the design is within the state of the art. The latter is fulfilled if the 95% uncertainty for a series of measurements traceable to the WRR is less than 1 W $m^{-2}$.

#### 7.2.1.2 *Secondary standard pyrheliometers*

An absolute pyrheliometer which does not meet the specification for a primary standard or which is not fully characterized can be used as a secondary standard if it is calibrated by comparison with the WSG with a 95% uncertainty for a series of measurements less than 1 W $m^{-2}$.

Other types of instruments with measurement uncertainties similar or approaching those for primary standards may be used as secondary standards.

The Ångström compensation pyrheliometer has been, and still is, used as a convenient secondary standard instrument for the calibration of pyranometers and other pyrheliometers. It was designed by K. Ångström as an absolute instrument, and the Ångström scale of 1905 was based on it; now it is used as a secondary standard and must be calibrated against a standard instrument.

The sensor consists of two platinized manganin strips, each of which is about 18 mm long, 2 mm wide and 0.02 mm thick. The strips are blackened with a coating of candle soot or with an optical matt black paint. A thermo-junction of copper-constantan is attached to the back of each strip so that the temperature difference between the strips can be indicated by a sensitive galvanometer or an electrical microvoltmeter. The dimensions of the strip and front diaphragm yield opening half-angles and slope angles as listed in Table 7.3.

**Table 7.3. View-limiting geometry of Ångström pyrheliometers**

| *Angle* | *Vertical* | *Horizontal* |
|---|---|---|
| Opening half-angle | 5° – 8° | ~2° |
| Slope angle | 0.7° – 1.0° | 1.2° – 1.6° |

The measurement set consists of three or more cycles, during which the left- or right-hand strip is alternately shaded from or exposed to the direct solar beam. The shaded strip is heated by an electric current, which is adjusted in such a way that the thermal electromagnetic force of the thermocouple and, hence, the temperature difference between the two strips, approximate zero. Before and after a measuring sequence, the zero is checked either by shading or by exposing both strips simultaneously. Depending on which of these methods is used and on the operating instructions of the manufacturer, the irradiance calculation differs slightly. The method adopted for the IPCs uses the following formula:

$$E = K \cdot i_{\mathrm{L}} \cdot i_{\mathrm{R}} \tag{7.2}$$

where $E$ is the irradiance in W $m^{-2}$; $K$ is the calibration constant determined by comparison with a primary standard (W $m^{-2}$ $A^{-2}$); and $i_{\mathrm{L}}$ $i_{\mathrm{R}}$ is the current in amperes measured with the left- or right-hand strip exposed to the direct solar beam, respectively.

Before and after each series of measurements, the zero of the system is adjusted electrically by using either of the foregoing methods, the zeros being called "cold" (shaded) or "hot" (exposed), as appropriate. Normally, the first reading, say $i_R$, is excluded and only the following $i_L - i_R$ pairs are used to calculate the irradiance. When comparing such a pyrheliometer with other instruments, the irradiance derived from the currents corresponds to the geometric mean of the solar irradiances at the times of the readings of $i_L$ and $i_R$.

The auxiliary instrumentation consists of a power supply, a current-regulating device, a nullmeter and a current monitor.

The sensitivity of the nullmeter should be about $0.05 \cdot 10^{-6}$ A per scale division for a low-input impedance (< 10 Ω), or about 0.5 $\mu$V with a high-input impedance (> 10 kΩ). Under these conditions, a temperature difference of about 0.05 K between the junction of the copper-constantan thermocouple causes a deflection of one scale division, which indicates that one of the strips is receiving an excess heat supply amounting to about 0.3%.

The uncertainty of the derived direct solar irradiance is highly dependent on the qualities of the current-measuring device, whether a moving-coil milliammeter or a digital multimeter which measures the voltage across a standard resistor and on the operator's skill. The fractional error in the output value of irradiance is twice as large as the fractional error in the reading of the electric current. The heating current is directed to either strip by means of a switch and is normally controlled by separate rheostats in each circuit. The switch can also cut the current off so that the zero can be determined. The resolution of the rheostats should be sufficient to allow the nullmeter to be adjusted to within one half of a scale division.

#### 7.2.1.3 *Field and network pyrheliometers*

These pyrheliometers generally make use of a thermopile as the detector. They have similar view-limiting geometry to that of standard pyrheliometers. Older models tend to have larger fields of view and slope angles. These design features were primarily designed to reduce the need for accurate Sun tracking. However, the larger the slope (and opening) angle, the larger the amount of aureole radiation sensed by the detector; this amount may reach several per cent for high optical depths and large limiting angles. With new designs of Sun trackers, including computer-assisted trackers in both passive and active (Sun-seeking) configurations, the need for larger slope angles is unnecessary. However, a slope angle of 1° is still required to ensure that the energy from the direct solar beam is distributed evenly on the detector and allows for minor Sun tracker pointing errors of the order of 0.1°.

The intended use of the pyrheliometer may dictate the selection of a particular type of instrument. Some manually oriented models are used mainly for spot measurements, while others, installed on a Sun tracker, are designed specifically for the long-term monitoring of direct irradiance. Before deploying an instrument, the user must consider the significant differences found among operational pyrheliometers:

(a) The field of view of the instrument;

(b) Whether the instrument measures both the long-wave and short-wave portion of the spectrum (namely, whether the aperture is open or covered with a glass or quartz window);

(c) The temperature compensation or correction methods;

(d) The magnitude and variation of the zero irradiance signal;

(e) Whether the instrument can be installed on an automated tracking system for long-term monitoring;

(f) Whether, for the calibration of other operational pyrheliometers, differences (a) to (c) above are the same, and whether the pyrheliometer is of the quality required to calibrate other network instruments.

#### 7.2.1.4 *Calibration of pyrheliometers*

All pyrheliometers, other than absolute pyrheliometers, must be calibrated by comparison using the Sun as the source with a pyrheliometer that has traceability to the WSG and a likely uncertainty of calibration equal to or better than the pyrheliometer being calibrated.

As all solar radiation data must be referred to the WRR, absolute pyrheliometers also use a factor determined by comparison with the WSG and not their individually determined one. After such a comparison (for example, during the periodically organized IPCs), such a pyrheliometer can be used as a standard to calibrate, again by comparison with the Sun as a source or a suitable Sun simulator employing a lamp as a source, secondary standards and field pyrheliometers. Secondary standards can also be used to calibrate field instruments, but with increased uncertainty.

The quality of Sun-source calibrations may depend on the aureole influence if instruments with different view-limiting geometries are compared. Also, the quality of the results will depend on the variability of the solar irradiance if the time constants and zero irradiance signals of the pyrheliometers are significantly different. Lastly, environmental conditions, such as temperature, pressure, wind and net long-wave irradiance, can influence the results. If a very high quality of calibration is required, only data taken during very clear and stable days should be used.

The procedures for the outdoor calibration of field pyrheliometers using the Sun as a source are given in an ISO standard (ISO 9059:1990). Indoor Sun simulators may be the same as those used for pyranometers (see paragraph 7.3.1.5). They may be used under the restriction that the calibration reference has the same spectral response as the instrument that is calibrated.

From recent experience at IPCs, a period of five years between traceable calibrations to the WSG should suffice for primary and secondary standards. Field pyrheliometers should be calibrated every one to two years; the more prolonged the use and the more rigorous the conditions, the more often they should be calibrated.

### 7.2.2 Exposure

For continuous recording and reduced uncertainties, an accurate Sun tracker that is not influenced by environmental conditions is essential. Sun tracking to within 0.2° is required, and the instruments should be inspected at least once a day, or more frequently if weather conditions so demand (with protection against adverse conditions).

The principal exposure requirement for monitoring direct solar radiation is freedom from obstructions to the solar beam at all times and seasons of the year. Furthermore, the site should be chosen so that the incidence of fog, smoke and airborne pollution is as typical as possible of the surrounding area.

For continuous observations, typically a window is used to protect the sensor and optical elements against rain, snow, and so forth. Care must be taken to ensure that such a window is kept clean and that condensation does not appear on the inside. Window cleaning is regularly required when instruments are inspected.

## 7.3 MEASUREMENT OF GLOBAL AND DIFFUSE SKY RADIATION

The solar radiation received from a solid angle of $2\pi$ sr on a horizontal surface is referred to as global radiation. This includes radiation received directly from the solid angle of the Sun's disc, as well as diffuse sky radiation that has been scattered in traversing the atmosphere.

The instrument needed for measuring solar radiation from a solid angle of $2\pi$ sr into a plane surface and a spectral range from 300 to 3 000 nm is the pyranometer. The pyranometer is sometimes inclined to measure solar radiation on inclined surfaces and sometimes placed

in an inverted position to measure reflected global radiation. When measuring the diffuse sky component of solar radiation, the direct solar component is screened from the pyranometer by a shading device (see 7.3.3.3).

Pyranometers normally use thermo-electric, photoelectric, pyro-electric or bimetallic elements as sensors. Since pyranometers are exposed continually in all weather conditions, they must be robust in design and resist the corrosive effects of humid air (especially near the sea). The receiver should be hermetically sealed inside its casing, or the casing must be easy to take off so that any condensed moisture can be removed. Where the receiver is not permanently sealed, a desiccator is usually fitted in the base of the instrument. The properties of pyranometers which are of concern when evaluating the uncertainty and quality of radiation measurements are: sensitivity, stability, response time, directional response, linearity, temperature response, thermal offset, zero irradiance signal and spectral response. Further advice on the use of pyranometers is given in ISO/TR 9901:2021 and McArthur, 2005.

Table 7.4 (adapted from ISO: 9060:2018) describes the characteristics of pyranometers of various levels of performance, with the uncertainties that may be achieved with appropriate facilities, well-trained staff and good QC under the sky conditions outlined in 7.2.1.

### 7.3.1 Calibration of pyranometers

The calibration of a pyranometer consists of the determination of one or more calibration factors and the dependence of these on environmental conditions, such as:

(a) Angular distribution of irradiance, the solar zenith angle;

(b) Calibration methods;

(c) Directional response of the instrument;

(d) Inclination/tilt angle of the instrument;

(e) Irradiance level;

(f) Net long-wave irradiance for zero offset A;

(g) Spectral distribution of irradiance;

(h) Temperature;

(i) Temporal variation.

The users of pyranometers must recognize that the uncertainty of observations will increase when the sensor exposure conditions deviate from the conditions in which the pyranometer was calibrated.

Normally, it is necessary to specify the test environmental conditions, which can be quite different for different applications. The method and conditions must also be given in some detail in the calibration certificate.

There are a variety of methods for calibrating pyranometers using the Sun or laboratory sources. These include the following:

(a) By comparison with a standard pyrheliometer for the direct solar irradiance and a calibrated shaded pyranometer for the diffuse sky irradiance;

(b) By comparison with a standard pyrheliometer using the Sun as a source, with a removable shading disc for the pyranometer;

**Table 7.4. Characteristics of operational pyranometers**

| *Characteristic* | *High quality*[a, d] | *Good quality*[b] | *Moderate quality*[c] |
|---|---|---|---|
| Response time (95% response) | < 10 s | < 20 s | < 30 s |
| Zero offset:<br>(a) Response to 200 W $m^{-2}$ net thermal radiation (ventilated)<br>(b) Response to 5 K $h^{-1}$ change in ambient temperature<br>(c) Total zero offset, including the effects of (a) and (b) and other sources | <br>≤ 7 W $m^{-2}$<br><br>≤ 2 W $m^{-2}$<br><br>≤ 10 W $m^{-2}$ | <br>≤ 15 W $m^{-2}$<br><br>≤ 4 W $m^{-2}$<br><br>≤ 21 W $m^{-2}$ | <br>≤ 30 W $m^{-2}$<br><br>≤ 8 W $m^{-2}$<br><br>≤ 41 W $m^{-2}$ |
| Resolution (smallest detectable change) | 1 W $m^{-2}$ | 5 W $m^{-2}$ | 10 W $m^{-2}$ |
| Stability (percentage change in responsivity per year) | 0.8 | 1.5 | 3 |
| Directional response for beam radiation (the range of errors caused by assuming that the normal incidence responsivity is valid for all directions when measuring, from any direction, a beam radiation whose normal incidence irradiance is 1 000 W $m^{-2}$) | 10 W $m^{-2}$ | 20 W $m^{-2}$ | 30 W $m^{-2}$ |
| Temperature response (percentage deviation due to change in ambient temperature within the interval from –10 °C to 40 °C relative to the signal at 20 ˚C) | 1 | 2 | 4 |
| Non-linearity (percentage deviation from the responsivity at 500 W $m^{-2}$ due to any change in irradiance within the range 100 to 1 000 W $m^{-2}$) | 0.5 | 1 | 3 |
| Spectral sensitivity (percentage deviation of the product of spectral absorptance and spectral transmittance from the corresponding mean within the range 300 to 3 000 nm)<br><br>Clear-sky global horizontal irradiance spectral error (maximum spectral error observed for a set of global horizontal irradiance clear-sky spectra defined in ISO 9060:2018) | 2<br><br>0.5 | 5<br><br>1 | 10<br><br>5 |
| Tilt response (percentage deviation from the responsivity at 0˚ tilt (horizontal) due to change in tilt from 0˚ to 180˚ at 1 000 W $m^{-2}$ irradiance) | 0.5 | 2 | 5 |
| Achievable uncertainty (95% confidence level):<br>Hourly totals<br>Daily totals | <br>3%<br>2% | <br>8%<br>5% | <br>20%<br>10% |

a Near state of the art; suitable for use as a working standard; maintainable only at stations with special facilities and staff.
b Acceptable for network operations.
c Suitable for low-cost networks where moderate to low performance is acceptable.
d For conditions of measurement and maintenance requirements for the high quality category, see 7.2.1.

(c) With a standard pyrheliometer using the Sun as a source and two pyranometers to be calibrated alternately measuring global and diffuse irradiance;

(d) By comparison with a standard pyranometer using the Sun as a source, under other natural conditions of exposure (for example, a uniform cloudy sky and direct solar irradiance not statistically different from zero);

(e) In the laboratory, on an optical bench with an artificial source, either normal incidence or at some specified azimuth and elevation, by comparison with a similar pyranometer previously calibrated outdoors;

(f) In the laboratory, with the aid of an integrating chamber simulating diffuse sky radiation, by comparison with a similar type of pyranometer previously calibrated outdoors.

These are not the only methods; however, (a), (b), (c), and (d) are commonly used. It is essential that, except for (b), either the zero irradiance signals for all instruments are known, or pairs of identical model pyranometers in identical configurations are used. Ignoring these offsets and differences can bias the results significantly.

Method (c) is considered to give very good results without the need for a calibrated pyranometer.

It is difficult to determine a specific number of measurements on which to base the calculation of the pyranometer calibration factor. However, the standard error of the mean can be calculated and should be less than the desired limit when sufficient readings have been taken under the desired conditions. The principal variations (apart from fluctuations due to atmospheric conditions and observing limitations) in the derived calibration factor are due to the following:

(a) Departures from the zenith response following the Lambert cosine law response, particularly at solar elevations of less than 10° (for this reason it is better to restrict calibration work to occasions when the solar elevation exceeds 30°);

(b) The ambient temperature;

(c) Imperfect levelling of the receiver surface;

(d) Non-linearity of instrument response;

(e) The net long-wave irradiance between the detector and the sky.

The pyranometer should be calibrated only in the position of use.

When using the Sun as the source, the apparent solar elevation should be measured or computed (to the nearest 0.01°) for this period from solar time (see Annex 7.F). The mean instrument or ambient temperature should also be noted.

#### 7.3.1.1 *By reference to a standard pyrheliometer and a shaded reference pyranometer*

In this method, described in ISO 9846:1993, the pyranometer's response to global irradiance is calibrated against the sum of separate measurements of the direct and diffuse components. Periods with clear skies and steady radiation (as judged from the record) should be selected. The vertical component of the direct solar irradiance is determined from the pyrheliometer output, and the diffuse sky irradiance is measured with a second pyranometer that is continuously shaded from the Sun. The direct component is eliminated from the diffuse sky pyranometer by shading the whole outer dome of the instrument with a disc of sufficient size mounted on a slender rod and held some distance away. The diameter of the disc and its distance from the receiver surface should be chosen in such a way that the screened angle approximately equals the aperture angles of the pyrheliometer. Rather than using the radius of the pyranometer sensor,

the radius of the outer dome should be used to calculate the slope angle of the shading disc and pyranometer combination. This shading arrangement occludes a close approximation of both the direct solar beam and the circumsolar sky irradiance as sensed by the pyrheliometer.

On a clear day, the diffuse sky irradiance is less than 15% of the global irradiance; hence, the calibration factor of the reference pyranometer does not need to be known very accurately. However, care must be taken to ensure that the zero irradiance signals from both pyranometers are accounted for, given that for some pyranometers under clear-sky conditions, the zero irradiance signal can be as high as 15% of the diffuse sky irradiance.

The calibration factor is then calculated according to:

$$E \cdot \sin h + V_s k_s = V \cdot k \tag{7.3}$$

or:

$$k = (E \sin h + V_s k_s) / V \tag{7.4}$$

where $E$ is the direct solar irradiance measured with the pyrheliometer (W m$^{-2}$), $V$ is the global irradiance output of the pyranometer to be calibrated ($\mu$V), $V_s$ is the diffuse sky irradiance output of the shaded reference pyranometer ($\mu$V), $h$ is the apparent solar elevation at the time of reading, $k$ is the calibration factor of the pyranometer to be calibrated (W m$^{-2}$ $\mu$V$^{-1}$), and $k_s$ is the calibration factor of the shaded reference pyranometer (W m$^{-2}$ $\mu$V$^{-1}$), and all the signal measurements are taken simultaneously.

The direct, diffuse and global components will change during the comparison, and care must be taken with the appropriate sampling and averaging to ensure that representative values are used.

#### 7.3.1.2 *By reference to a standard pyrheliometer*

This method, described in ISO 9846:1993, is similar to the method of the preceding paragraph, except that the diffuse sky irradiance signal is measured by the same pyranometer. The direct component is eliminated temporarily from the pyranometer by shading the whole outer dome of the instrument as described in 7.3.1.1. The period required for occulting depends on the steadiness of the radiation flux and the response time of the pyranometer, including the time interval needed to bring the temperature and long-wave emission of the glass dome to equilibrium; 10 times the thermopile 1/$e$ time constant of the pyranometer should generally be sufficient.

The difference between the representative shaded and unshaded outputs from the pyranometer is due to the vertical component of direct solar irradiance $E$ measured by the pyrheliometer. Thus:

$$E \cdot \sin h = (V_{un} - V_s) \cdot k \tag{7.5}$$

or:

$$k = (E \cdot \sin h) / (V_{un} - V_s) \tag{7.6}$$

where $E$ is the representative direct solar irradiance at normal incidence measured by the pyrheliometer (W m$^{-2}$), $V_{un}$ is the representative output signal of the pyranometer ($\mu$V) when in unshaded (or global) irradiance mode, $V_s$ is the representative output signal of the pyranometer ($\mu$V) when in shaded (or diffuse sky) irradiance mode, $h$ is the apparent solar elevation, and $k$ is the calibration factor (W m$^{-2}$ $\mu$V$^{-1}$), which is the inverse of the sensitivity ($\mu$V W$^{-1}$ m$^2$).

Both the direct and diffuse components will change during the comparison, and care must be taken with the appropriate sampling and averaging to ensure that representative values of the shaded and unshaded outputs are used for the calculation. To reduce uncertainties associated with representative signals, a continuous series of shade and un-shade cycles should be performed and time-interpolated values used to reduce temporal changes in global and diffuse sky irradiance. Since the same pyranometer is being used in differential mode, and the difference in zero irradiance signals for global and diffuse sky irradiance is negligible, there is no need to account for zero irradiances in equation 7.6.

### 7.3.1.3 *Alternate calibration using a pyrheliometer*

This method uses the same instrumental set-up as the method described in 7.3.1.1 but only requires the pyrheliometer to provide calibrated irradiance data ($E$), and the two pyranometers are assumed to be un-calibrated (Forgan, 1996). The method calibrates both pyranometers by solving a pair of simultaneous equations analogous to equation 7.3. Irradiance signal data are initially collected with the pyrheliometer. One pyranometer (pyranometer A) measures global irradiance signals ($V_{gA}$), and the other pyranometer (pyranometer B) measures diffuse irradiance signals ($V_{dB}$) over a range of solar zenith angles in clear-sky conditions. After sufficient data have been collected in the initial configuration, the pyranometers are exchanged so that pyranometer A, which initially measured the global irradiance signal, now measures the diffuse irradiance signal ($V_{dA}$), and vice versa with regard to pyranometer B. The assumption is that for each pyranometer, the diffuse ($k_d$) and global ($k_g$) calibration coefficients are equal, and the calibration coefficient for pyranometer A is given by:

$$k_A = k_{gA} = k_{dA} \tag{7.7}$$

with an identical assumption for pyranometer B coefficients. For a time $t_0$ in the initial period, a modified version of equation 7.3 is:

$$E(t_0)\sin(h(t_0)) = k_A V_{gA}(t_0) - k_B V_{dB}(t_0) \tag{7.8}$$

For time $t_1$ in the alternate period when the pyranometers are exchanged:

$$E(t_1)\sin(h(t_1)) = k_B V_{gB}(t_1) - k_A V_{dA}(t_1) \tag{7.9}$$

As the only unknowns in equations 7.8 and 7.9 are $k_A$ and $k_B$, these can be solved for any pair of times ($t_0$, $t_1$). Pairs covering a range of solar elevations provide an indication of the directional response. The resultant calibration information for both pyranometers is representative of the global calibration coefficients and produces almost identical information to method 7.3.1.1, but without the need for a calibrated pyranometer.

As with method 7.3.1.1, to produce coefficients with minimum uncertainty, this alternate method requires that the irradiance signals from the pyranometers be adjusted to remove any estimated zero irradiance offset. To reduce uncertainties due to changing directional response, it is recommended to use a pair of pyranometers of the same model and observation pairs when $\sin h\,(t_0) \sim \sin h\,(t_1)$.

The method is ideally suited to automatic field monitoring situations where three solar irradiance components (direct, diffuse and global) are monitored continuously. Experience suggests that the data collection necessary for the application of this method may be conducted during as little as one day, with the exchange of instruments taking place around solar noon. However, at a field site, the extended periods and days either side of the instrument change may be used for data selection, provided that the pyrheliometer has a valid calibration.

### 7.3.1.4 *By comparison with a reference pyranometer*

As described in ISO 9847:2023, this method entails the simultaneous operation of two pyranometers mounted horizontally, side by side, outdoors, for a sufficiently long period to acquire representative results. If the instruments are of the same model and monitoring configuration, only one or two days of comparison should be sufficient. The more pronounced the difference between the types of pyranometer configurations, the longer the period of comparison required. A long period, however, could be replaced by several shorter periods covering typical conditions (clear, cloudy, overcast, rainfall, snowfall, and so on). The derivation of the instrument factor is straightforward, but, in the case of different pyranometer models, the resultant uncertainty is more likely to be a reflection of the difference in models, rather than the stability of the instrument being calibrated. Data selection should be carried out when irradiances are relatively high and varying slowly. Each mean value of the ratio $R$ of the response of the test instrument to that of the reference instrument may be used to calculate $k = R \cdot k_r$, where $k_r$ is the calibration factor of the reference, and $k$ is the calibration factor

being derived. During a sampling period, provided that the time between measurements is less than the 1/*e* time constant of the pyranometers, data collection can occur during times of fluctuating irradiance.

The mean temperature of the instruments or the ambient temperature should be recorded during all outdoor calibration work to allow for any temperature effects.

#### 7.3.1.5 ***By comparison in the laboratory***

There are two methods which involve laboratory-maintained artificial light sources providing either direct or diffuse irradiance. In both cases, the test pyranometer and a reference standard pyranometer are exposed under the same conditions.

In one method, the pyranometers are exposed to a stabilized tungsten-filament lamp installed at the end of an optical bench. A practical source for this type of work is a 0.5 to 1.0 kW halogen lamp mounted in a water-cooled housing with forced ventilation and with its emission limited to the solar spectrum by a quartz window. This kind of lamp can be used if the standard and the instrument to be calibrated have the same spectral response. For general calibrations, a high-pressure xenon lamp with filters to give an approximate solar spectrum should be used. When calibrating pyranometers in this way, reflection effects should be excluded from the instruments by using black screens. The usual procedure is to install the reference instrument and measure the radiant flux. The reference is then removed and the measurement repeated using the test instrument. The reference is then replaced and another determination is made. Repeated alternation with the reference should produce a set of measurement data of good precision (about 0.5%).

In the other method, the calibration procedure uses an integrating light system, such as a sphere or hemisphere illuminated by tungsten lamps, with the inner surface coated with highly reflective diffuse-white paint. This offers the advantage of simultaneous exposure of the reference pyranometer and the instrument to be calibrated. Since the sphere or hemisphere simulates a sky with an approximately uniform radiance, the angle errors of the instrument at 45° dominate. As the cosine error at these angles is normally low, the repeatability of integrating-sphere measurements is generally within 0.5%. As for the source used to illuminate the sphere, the same considerations apply as for the first method.

#### 7.3.1.6 ***Routine checks on calibration factors***

There are several methods for checking the constancy of pyranometer calibration, depending upon the equipment available at a particular station. Every opportunity to check the performance of pyranometers in the field must be seized.

At field stations where carefully preserved standards (either pyrheliometers or pyranometers) are available, the basic calibration procedures described above may be employed. Where standards are not available, other techniques can be used. If there is a simultaneous record of direct solar radiation, the two records can be examined for consistency by the method used for direct standardization, as explained in 7.3.1.2. This simple check should be applied frequently.

If there are simultaneous records of global and diffuse sky radiation, the two records should frequently be examined for consistency. In periods of total cloud, the global and diffuse sky radiation should be identical, and these periods can be used when a shading disc is used for monitoring diffuse sky radiation. When using shading bands, it is recommended that the band be removed so that the diffuse sky pyranometer measures global radiation, and its data can be compared to simultaneous data from the global pyranometer.

The record may be verified with the aid of a travelling working standard sent from the central station of the network or from a nearby station. Lastly, if calibrations are not performed at the site, the pyranometer can be exchanged for a similar one sent from the calibration facility.

Either of the last two methods should be used at least once a year. Pyranometers used for measuring reflected solar radiation should be moved into an upright position and checked using the methods described above.

### 7.3.2 Performance of pyranometers

Considerable care and attention to details are required to attain the desirable standard of uncertainty. A number of properties of pyranometers and measurement systems should be evaluated so that the uncertainty of the resultant data can be estimated. For example, it has been demonstrated that, for a continuous record of global radiation without ancillary measurements of diffuse sky and direct radiation, an uncertainty better than 5% in daily totals represents the result of good and careful work. Similarly, when a protocol similar to that proposed by McArthur (2005) is used, uncertainties for daily totals can be of the order of 2%.

#### 7.3.2.1 *Sensor levelling*

For accurate global radiation measurements with a pyranometer, it is essential that the spirit level indicate when the plane of the thermopile is horizontal. This can be tested in the laboratory on an optical levelling table using a collimated lamp beam at about a 20° elevation. The levelling screws of the instrument are adjusted until the response is as constant as possible during rotation of the sensor in the azimuth. The spirit level is then readjusted, if necessary, to indicate the horizontal plane. This is called radiometric levelling and should be the same as physical levelling of the thermopile. However, this may not be true if the quality of the thermopile surface is not uniform.

#### 7.3.2.2 *Change of sensitivity due to ambient temperature variation*

Thermopile instruments exhibit changes in sensitivity with variations in instrument temperature. Some instruments are equipped with integrated temperature compensation circuits in an effort to maintain a constant response over a large range of temperatures. The temperature coefficient of sensitivity may be measured in a temperature-controlled chamber. The temperature in the chamber is varied over a suitable range in 10 °C steps and held steady at each step until the response of the pyranometers has stabilized. The data are then fitted with a smooth curve. If the maximum percentage difference due to temperature response over the operational ambient range is 2% or more, a correction should be applied on the basis of the fit of the data.

If no temperature chamber is available, the standardization method with pyrheliometers (see 7.3.1.1, 7.3.1.2 or 7.3.1.3) can be used at different ambient temperatures. Attention should be paid to the fact that not only the temperature, but also, for example, the cosine response (namely, the effect of solar elevation) and non-linearity (namely, variations of solar irradiance) can change the sensitivity.

#### 7.3.2.3 *Variation of response with orientation*

The calibration factor of a pyranometer may very well be different when the instrument is used in an orientation other than that in which it was calibrated. Inclination testing of pyranometers can be conducted in the laboratory or with the standardization method described in 7.3.1.1 or 7.3.1.2. It is recommended that the pyranometer be calibrated in the orientation in which it will be used. A correction for tilting is not recommended unless the instrument's response has been characterized for a variety of conditions.

#### 7.3.2.4 *Variation of response with angle of incidence*

The dependence of the response of the sensor upon solar elevation and azimuth is usually known as the directional response. Ideally, the solar irradiance response of the receiver should

be proportional to the cosine of the zenith angle of the solar beam, and constant for all azimuth angles. For pyranometers, it is recommended that the cosine or directional error (or percentage difference from ideal cosine response) be specified for at least two solar elevation angles, preferably 30° and 10°. A better way of prescribing the directional response is given in Table 7.4, which specifies the permissible error for all angles.

Only lamp sources should be used to determine the variation of the response of the sensor with the angle of incidence because the spectral distribution of the Sun changes with the angle of elevation. Using the Sun as a source, spectral anisotropy with solar elevation can induce an apparent variation of response with the solar elevation angle that is not due to the non-ideal directional response of the sensor.

#### 7.3.2.5 *Uncertainties in hourly and daily totals*

As most pyranometers in a network are used to determine hourly or daily exposures (or exposures expressed as mean irradiances), it is evident that the uncertainties in these values are important.

Table 7.4 lists the expected maximum deviation from the true value, excluding calibration errors. The types of pyranometers in the third column of Table 7.4 (namely, those of moderate quality) are not suitable for hourly or daily totals, although they may be suitable for monthly and yearly totals.

### 7.3.3 Installation and maintenance of pyranometers

The site selected to expose a pyranometer should be free from any obstruction above the plane of the sensing element and, at the same time, should be readily accessible. If it is impracticable to obtain such exposure, the site must be as free as possible of obstructions that may shadow it at any time in the year. The pyranometer should not be close to light-coloured walls or other objects likely to reflect solar energy onto it, nor should it be exposed to artificial radiation sources.

In most places, a flat roof provides a good location for mounting the radiometer stand. If such a site cannot be secured, a stand placed some distance from buildings or other obstructions should be used. If practicable, the site should be chosen so that no obstruction, in particular within the azimuth range of sunrise and sunset over the year, should have an elevation exceeding 5°. Other obstructions should not reduce the total solar angle by more than 0.5 sr. At stations where this is not possible, complete details of the horizon and the solid angle subtended should be included in the description of the station.

A site survey should be carried out before the initial installation of a pyranometer whenever its location is changed or if a significant change occurs with regard to any surrounding obstructions. An excellent method of doing this is to use a survey camera that provides azimuthal and elevation grid lines on the negative. A series of exposures should be made to identify the angular elevation above the plane of the receiving surface of the pyranometer and the angular range in azimuth of all obstructions throughout the full 360° around the pyranometer. If a survey camera is not available, the angular outline of obscuring objects may be mapped out by means of a theodolite or a compass and clinometer combination.

The description of the station should include the altitude of the pyranometer above sea level (that is, the altitude of the station plus the height of pyranometer above the ground), together with its geographical longitude and latitude. It is also most useful to have a site plan, drawn to scale, showing the position of the recorder, the pyranometer, and all connecting cables.

The accessibility of instrumentation for frequent inspection is probably the most important single consideration when choosing a site. It is most desirable that pyranometers and recorders be inspected at least daily, and preferably more often.

The foregoing remarks apply equally to the exposure of pyranometers on ships, towers and buoys. The exposure of pyranometers on these platforms is a very difficult and sometimes hazardous undertaking. Seldom can an instrument be mounted where it is not affected by at least one significant obstruction (for example, a tower). Because of platform motion, pyranometers are subject to wave motion and vibration. Precautions should be taken, therefore, to ensure that the plane of the sensor is kept horizontal and that severe vibration is minimized. This usually requires the pyranometer to be mounted on suitably designed gimbals.

#### 7.3.3.1 *Correction for obstructions to a free horizon*

If the direct solar beam is obstructed (which is readily detected on cloudless days), the record should be corrected wherever possible to reduce uncertainty.

Only when there are separate records of global and diffuse sky radiation can the diffuse sky component of the record be corrected for obstructions. The procedure requires first that the diffuse sky record be corrected and subsequently that the global record be adjusted. The fraction of the sky which is obscured should not be computed; rather, the fraction of the irradiance coming from that part of the sky which is obscured should be calculated. Since the diffuse sky radiation from elevations below 5° contributes less than 1% to the overall diffuse sky radiation, it can normally be neglected. Attention should be concentrated on objects subtending angles of 10° or more, as well as those which might intercept the solar beam at any time. In addition, it must be borne in mind that light-coloured objects can reflect solar radiation onto the receiver.

Strictly speaking, when determining corrections for the loss of diffuse sky radiation due to obstacles, the variance in sky radiance over the hemisphere should be taken into account. However, the only practical procedure is to assume that the radiance is isotropic, that is, the same from all parts of the sky. In order to determine the relative reduction in diffuse sky irradiance for obscuring objects of finite size, the following expression may be used:

$$\Delta E_{\text{sky}} = \pi^{-1} \int_{\phi} \int_{\Theta} \sin\theta \, \cos\theta \, d\theta \, d\varphi \tag{7.10}$$

where $\theta$ is the angle of elevation; $\phi$ is the azimuth angle, $\Theta$ is the extent in elevation of the object; and $\varphi$ is the extent in azimuth of the object.

The expression is valid only for obstructions with a black surface facing the pyranometer. For other objects, the correction has to be multiplied by a reduction factor depending on the reflectivity of the object. Snow glare from a low Sun may even lead to an opposite sign for the correction.

#### 7.3.3.2 *Installation of pyranometers for measuring global radiation*

A pyranometer should be securely attached to whatever mounting stand is available, using the holes provided in the tripod legs or in the baseplate. Precautions should always be taken to avoid subjecting the instrument to mechanical shocks or vibration during installation. This operation is best effected as follows. First, the pyranometer should be oriented so that the emerging leads or the connector is located poleward of the receiving surface. This minimizes heating of the electrical connections by the Sun. Instruments with Moll-Gorcynski thermopiles should be oriented so that the line of thermo-junctions (the long side of the rectangular thermopile) points east-west. This constraint sometimes conflicts with the first, depending on the type of instrument, and should have priority since the connector could be shaded, if necessary. When towers are nearby, the instrument should be situated on the side of the tower towards the Equator, and as far away from the tower as practical.

Radiation reflected from the ground or the base should not be allowed to irradiate the instrument body from underneath. A cylindrical shading device can be used, but care should be taken to ensure that natural ventilation still occurs and is sufficient to maintain the instrument body at ambient temperature.

The pyranometer should then be secured lightly with screws or bolts and levelled with the aid of the levelling screws and spirit level provided. After this, the retaining screws should be tightened, taking care that the setting is not disturbed so that, when properly exposed, the receiving surface is horizontal, as indicated by the spirit level.

The stand or platform should be sufficiently rigid so that the instrument is protected from severe shocks and the horizontal position of the receiver surface is not changed, especially during periods of high winds and strong solar energy.

The cable connecting the pyranometer to its recorder should have twin conductors and be waterproof. The cable should be firmly secured to the mounting stand to minimize rupture or intermittent disconnection in windy weather. Wherever possible, the cable should be properly buried and protected underground if the recorder is located at a distance. The use of a shielded cable is recommended, the pyranometer, cable and recorder being connected by a very low resistance conductor to a common ground. As with other types of thermo-electric devices, care must be exercised to obtain a permanent copper-to-copper junction between all connections prior to soldering. All exposed junctions must be weatherproof and protected from physical damage. After identification of the circuit polarity, the other extremity of the cable may be connected to the data-collection system in accordance with the relevant instructions.

#### 7.3.3.3 *Installation of pyranometers for measuring diffuse sky radiation*

For measuring or recording separate diffuse sky radiation, the direct solar radiation must be screened from the sensor by a shading device. Where continuous records are required, the pyranometer is usually shaded either by a small metal disc held in the Sun's beam by a Sun tracker, or by a shadow band mounted on a polar axis.

The first method entails the rotation of a slender arm synchronized with the Sun's apparent motion. If tracking is based on Sun-synchronous motors or solar almanacs, frequent inspection is essential to ensure proper operation and adjustment, since spurious records are otherwise difficult to detect. Sun trackers with Sun-seeking systems minimize the likelihood of such problems. The second method involves frequent personal attention at the site and significant corrections to the record on account of the appreciable screening of diffuse sky radiation by the shading arrangement. Assumptions about the sky radiance distribution and band dimensions are required to correct for the band and increase the uncertainty of the derived diffuse sky radiation compared to the uncertainty obtained using a Sun-seeking disc system. Annex 7.G provides details on the construction of a shading ring and the necessary corrections to be applied.

A significant error source for diffuse sky radiation data is the zero irradiance signal. In clear-sky conditions, the zero irradiance signal is the equivalent of 5 to 10 W $m^{-2}$, depending on the pyranometer model, and could approach 15% of the diffuse sky irradiance. The *Baseline Surface Radiation Network (BSRN) Operations Manual* (McArthur, 2005) provides methods to minimize the influence of the zero irradiance signal.

The installation of a diffuse sky pyranometer is similar to that of a pyranometer which measures global radiation. However, there is the complication of an equatorial mount or shadow-band stand. The distance to a neighbouring pyranometer should be sufficient to guarantee that the shading ring or disc never shadows it. This may be more important at high latitudes where the Sun angle can be very low.

Since the diffuse sky radiation from a cloudless sky may be less than one tenth of the global radiation, careful attention should be given to the sensitivity of the recording system.

#### 7.3.3.4 *Installation of pyranometers for measuring reflected radiation*

The height above the surface should be 1 to 2 m. In the summer, the ground should be covered with grass that is kept short. For regions with snow in the winter, a mechanism should be available to adjust the height of the pyranometer in order to maintain a constant separation

between the snow and the instrument. Although the mounting device is within the field of view of the instrument, it should be designed to cause less than a 2% error in the measurement. Access to the pyranometer for levelling should be possible without disturbing the surface beneath, especially if it is snow.

#### 7.3.3.5 *Maintenance of pyranometers*

Pyranometers in continuous operation should be inspected at least once a day and perhaps more frequently, for example when meteorological observations are being made. During these inspections, the glass dome of the instrument should be wiped clean and dry (care should be taken not to disturb routine measurements during the daytime). If frozen snow, glazed frost, hoar frost or rime is present, an attempt should be made to remove the deposit very gently (at least temporarily), with the sparing use of a de-icing fluid, before wiping the glass clean. A daily check should also ensure that the instrument is level, that there is no condensation inside the dome, and that the sensing surfaces are still black.

In some networks, the exposed dome of the pyranometer is continuously ventilated by a blower and simultaneously heated to avoid or minimize dew and frost deposition in cold weather and to minimize the zero offsets caused by the temperature difference between the dome and the case. The temperature difference between the ventilating air and the ambient air should not be more than about 1 K. Ventilation systems require regular inspection and cleaning of the ventilator and air filters. Ventilation does not reduce the risk of fouling of pyranometer domes by pollution, dust or sand, and the same regular cleaning recommended above is applicable. If local pollution or dust forms a deposit on the dome, it should be wiped very gently, preferably after blowing off most of the loose material or after wetting it a little, in order to prevent the surface from being scratched. Such abrasive action can appreciably alter the original transmission properties of the material. Desiccators should be kept charged with active material (usually a colour-indicating silica gel).

#### 7.3.3.6 *Installation and maintenance of pyranometers on special platforms*

Very special care should be taken when installing equipment on such diverse platforms as ships, buoys, towers and aircraft. Radiation sensors mounted on ships should be provided with gimbals because of the substantial motion of the platform.

If a tower is employed exclusively for radiation equipment, it may be capped by a rigid platform on which the sensors can be mounted. Obstructions to the horizon should be kept to the side of the platform farthest from the Equator, and booms for holding pyranometers measuring the upward radiation flux should extend towards the Equator.

Radiation sensors should be mounted as high as is practicable above the water surface on ships, buoys and towers, in order to keep the effects of water spray to a minimum.

Radiation measurements have been taken successfully from aircraft for a number of years. Care must be exercised, however, in selecting the correct pyranometer and proper exposure.

Particular attention must be paid during installation, especially for systems that are difficult to access, to ensure the reliability of the observations. It may be desirable, therefore, to provide a certain amount of redundancy by installing duplicate measuring systems at certain critical sites.

## 7.4 MEASUREMENT OF TOTAL AND LONG-WAVE RADIATION

The measurement of total radiation includes both short wavelengths of solar origin (300 to 3 000 nm) and longer wavelengths of terrestrial and atmospheric origin (3 000 to 100 000 nm). The instruments used for this purpose are pyrradiometers. They may be used for measuring either upward or downward radiation flux components, and a pair

of them may be used to measure the differences between the two, which is the net radiation. Single-sensor pyrradiometers, with an active surface on both sides, are also used for measuring net radiation. Pyrradiometer sensors must have a constant sensitivity across the whole wavelength range from 300 to 100 000 nm.

The measurement of long-wave radiation can be accomplished either directly using pyrgeometers, or indirectly by subtracting the measured global radiation from the total radiation measured. Most pyrgeometers eliminate the short wavelengths by means of filters which have approximately constant transparency to long wavelengths while being almost opaque to the shorter wavelengths (300 to 3 000 nm). Some pyrgeometers – either without filters or with filters that do not eliminate radiation below 3 000 nm – can be used only during the night. Often, the combination of a pyranometer and a pyrgeometer is used as a pyrradiometer. Net radiation may be measured with net radiometers or alternatively, with instruments composed of two pyranometers and two pyrgeometers; these are called "four-component net radiometers".

The instruments used for longwave measurement are predominantly pyrgeometers. For the measurement of total radiation and net radiation, a combination of pyranometers and pyrgeometers is used. The use of pyrradiometers, typically equipped with plastic domes, is less common, mainly due to their high vulnerability. The use of non-protected instruments is not recommended because of their high sensitivity to wind.

The long-wave flux $L^{-}$ measured by a pyrgeometer or a pyrradiometer using the thermopile sensor has two components, the blackbody flux from the surface temperature of the sensing element and the net radiative flux measured by the receiver:

$$L^{-} = L^{*} + \sigma T_b^4 \tag{7.11}$$

$\sigma$ is the Stefan-Boltzmann constant (5.6704 · $10^{-8}$ W $m^{-2}$ $K^{-1}$); $T_b$ is the body temperature of the instrument (K); $L^{-}$ is the irradiance measured either by a reference pyrgeometer or calculated from the temperature of the blackbody cavity capping the upper receiver (W $m^{-2}$); $L^{*}$ is the net radiative flux at the receiver (W $m^{-2}$). The procedure for measuring the short-wave component with a pyrradiometer follows the description in 7.3.

### 7.4.1 Instruments for the measurement of long-wave radiation

Significant advances have been made in the measurement of terrestrial radiation by pyrgeometers, particularly with the advent of the silicon-domed pyrgeometer, and as a result, pyrgeometers provide the highest accuracy measurements of terrestrial radiation. Nevertheless, the measurement of terrestrial radiation is still more difficult and less understood than the measurement of solar irradiance. Table 7.5 provides an analysis of the sources of errors.

Pyrgeometers have been developed in two forms. In the first form, the thermopile receiving surface is covered with a hemispheric dome, inside which an interference filter is deposited. In the second form, the thermopile is covered with a flat plate, on which the interference filter is deposited. In both cases, the surface on which the interference filter is deposited is made of silicon. The first style of instrument provides a full hemispheric field of view, while for the second, a 150° field of view is typical, and the hemispheric flux is modelled using the manufacturer's procedures. The arguments used for the latter method are that the longwave radiation exchange between the instrument and the atmosphere in the lowest 30° is negligible and that it leads to cost reduction. Both types of instruments are operated on the principle that the measured output signal is the difference between the irradiance emitted from the source and the blackbody radiative temperature of the instrument. In general, pyrgeometer-derived terrestrial radiation can be approximated by a modification to equation 7.11:

$$L^{-} = L^{*} + k_2 \sigma T_b^4 + k_3 \sigma \left( T_d^4 - T_b^4 \right) \tag{7.12}$$

where $k_2$ takes into account the emission properties of the thermopile and uncertainties of the temperature measurement of the cold surface of the thermopile, $k_3$ is the instrument dome sensitivity to IR irradiance ($\mu$V/(W $m^{-2}$)), and $T_d$ is the dome temperature (K).

**Table 7.5. Sources of error in pyrgeometer and pyrradiometer measurements**

| *Elements influencing the measurements* | *Nature of influence on pyrgeometers and pyrradiometers* | | *Effects on the precision of measurements* | *Methods for determining these characteristics* |
|---|---|---|---|---|
| | *With domes* | *Without domes* | | |
| Screening properties | Spectral characteristics of transmission | None | (a) Spectral variations in the calibration coefficient<br>(b) The effect of reduced incident radiation on the detector due to short-wave diffusion in the domes (depends on thickness)<br>(c) Ageing and other variations in the sensors | (a) Spectrally determine the extinction in the screen<br>(b) Measure the effect of diffuse sky radiation or measure the effect with a varying angle of incidence<br>(c) Spectral analysis: compare with a new dome; determine the extinction of the dome |
| Convection effects | Changes due to non-radiative energy exchanges: sensor-dome environment (thermal resistance) | Changes due to non-radiative energy exchanges: sensor-air (variation in areal exchange coefficient) | Uncontrolled changes due to wind gusts are critical in computing the radiative flux divergence in the lowest layer of the atmosphere | Study the dynamic behaviour of the instrument as a function of temperature and speed in a wind tunnel |
| Effects of hydrometeors (rain, snow, fog, dew, frost) and dust | Variation of the spectral transmission plus the non-radiative heat exchange by conduction and change | Variation of the spectral character of the sensor and of the dissipation of heat by evaporation | Changes due to variations in the spectral characteristics of the sensor and to non-radiative energy transfers | Study the influence of forced ventilation on the effects |
| Properties of the sensor surface (emissivity) | Depends on the spectral absorption of the blackening substance on the sensor | | Changes in calibration coefficient<br>(a) As a function of spectral response<br>(b) As a function of intensity and azimuth of incident radiation<br>(c) As a function of temperature effects | (a) Spectrophotometric analysis of the calibration of the absorbing surfaces<br>(b) Measure the sensor's sensitivity variability with the angle of incidence |
| Temperature effects | Non-linearity of the sensor as a function of temperature | | A temperature coefficient is required | Study the influence of forced ventilation on these effects |
| Asymmetry effects (only for pyrradiometers) | (a) Differences between the thermal capacities and resistance of the upward- and downward-facing sensors<br>(b) Differences in ventilation of the upward- and downward-facing sensors<br>(c) Control and regulation of sensor levelling | | (a) Influence on the time constant of the instrument<br>(b) Error in the determination of the calibration factors for the two sensors | (a) Control the thermal capacity of the two sensor surfaces<br>(b) Control the time constant over a narrow temperature range |

The net radiative flux measured by the receiver, $L^*$, is defined as:

$$L^* = \frac{U}{C}\left(1 + k_1 \sigma T_b^3\right) \tag{7.13}$$

where $C$ is the sensitivity of the receiver ($\mu$V/(W m$^{-2}$)), and $k_1$ is a residual temperature coefficient of the receiver. While state-of-the-art pyrgeometers have a temperature correction circuitry implemented in their receiver to bring $k_1$ very close to zero (as described in 7.3.2.2), it is still recommended to determine $k_1$ by a laboratory characterization as described in 7.4.3.

Several recent comparisons have been made using instruments of similar manufacture in a variety of measurement configurations. These studies have indicated that, following careful calibration, fluxes measured at night agree to within ±1 W m$^{-2}$, but in periods of high solar energy, the difference between unshaded instruments can be significant. The reason for the differences is that the silicon dome and the associated interference filter may transmit solar radiation and is not a perfect reflector of solar energy. Thus, a solar contribution may reach the sensor, and solar heating of the dome occurs. By shading the instrument in a manner similar to that used for diffuse solar measurements, ventilating it as recommended by ISO 9060:2018, and measuring the temperature of the dome and the instrument case, this discrepancy can be reduced to ±2 W m$^{-2}$. For pyrgeometers, it is particularly important to avoid dew and frost deposition; water absorbs and therefore blocks longwave radiation. Water deposition during clear-sky nights causes large measurement errors on the order of 100 Wm$^{-2}$. Water deposition may be prevented by heating, or ventilating and simultaneously heating the instrument. For some instrument models, ventilation reduces solar contributions to the signal by promoting the equilibrium between the dome and the sensor body. Based upon these and other comparisons, the following recommendations should be followed for the measurement of long-wave radiation:

(a) When using pyrgeometers that have a built-in battery circuit to emulate the blackbody condition of the instrument, extreme care must be taken to ensure that the battery is well-maintained. Even a small change in the battery voltage will significantly increase the measurement error. If at all possible, the battery should be removed from the instrument, and the case and dome temperatures of the instrument should be measured according to the manufacturer's instructions;

(b) Where possible, both the case and dome temperatures of the instrument should be measured and used in the determination of irradiance;

(c) The instrument should be heated to avoid dew and frost deposition, or alternatively heated and ventilated;

(d) For best results, the instrument should be shaded from direct solar irradiance by a small Sun-tracking disc, as used for diffuse sky radiation measurement.

These instruments should be calibrated at National or Regional Calibration Centres by using reference pyrgeometers traceable to the WISG of Pyrgeometers of the WRC Davos that is governed under the framework described in Annex 7.E.

### 7.4.2 Instruments for the measurement of total radiation

One problem with instruments for measuring total radiation is that there are no absorbers which have a completely constant sensitivity over the extended range of wavelengths concerned. Similarly, it is difficult to find suitable filters that have constant transmission between 300 and 100 000 nm. Therefore, the recommended practice for measuring total radiation is to perform simultaneous separate measurements of short- and long-wave radiation using a pyranometer and a pyrgeometer, respectively.

The use of thermally sensitive sensors requires a good knowledge of the heat budget of the sensor. Otherwise, it is necessary to reduce sensor convective heat losses to near zero by protecting the sensor from the direct influence of the wind. The technical difficulties linked with such heat losses are largely responsible for the fact that net radiative fluxes are determined less precisely than global radiation fluxes. In fact, different laboratories have developed their own

pyrradiometers on technical bases which they consider to be the most effective for reducing the convective heat transfer in the sensor. Pyrradiometers which, although not perfect, embody good measurement principles have been built during the last few decades. Thus, there is a great variety of pyrradiometers employing different methods for eliminating, or allowing for, wind effects, as follows:

(a) No protection, in which case, empirical formulae are used to correct for wind effects;

(b) Determination of wind effects by the use of electrical heating;

(c) Stabilization of wind effects through artificial ventilation;

(d) Elimination of wind effects by protecting the sensor from the wind.

The long-wave component of a pyrradiometer is described in equation 7.11.

Table 7.5 provides an analysis of the sources of error arising in pyrradiometric measurements and proposes methods for determining these errors.

It is difficult to determine the uncertainty likely to be obtained in practice. In situ comparisons at different sites between different designs of pyrradiometer yield results manifesting differences of up to 5% to 10% under the best conditions. In order to improve such results, an exhaustive laboratory study should precede the in situ comparison to determine the different effects separately.

Deriving total radiation by independently measuring the short-wave and long-wave components achieves the highest accuracies and is recommended over pyrradiometer measurements. Short-wave radiation can be measured using the methods outlined in 7.2 and 7.3, while long-wave radiation can be measured with pyrgeometers.

Table 7.6 lists the characteristics of pyrradiometers of various levels of performance and the uncertainties to be expected in the measurements obtained from them.

**Table 7.6. Characteristics of operational pyrradiometers**

| *Characteristic* | *High quality*[a] | *Good quality*[b] | *Moderate quality*[c] |
|---|---|---|---|
| Resolution (W $m^{-2}$) | 1 | 5 | 10 |
| Stability (annual change; % of full scale) | 2% | 5% | 10% |
| Cosine response error at 10° elevation | 3% | 7% | 15% |
| Azimuth error at 10° elevation (additional to cosine error) (deviation from mean) | 3% | 5% | 10% |
| Temperature dependence (–20 °C to 40 °C) (deviation from mean) | 1% | 2% | 5% |
| Non-linearity (deviation from mean) | 0.5% | 2% | 5% |
| Variation in spectral sensitivity integrated over 200 nm intervals from 300 to 75 000 nm | 2% | 5% | 10% |

a Near state of the art; maintainable only at stations with special facilities and specialist staff.
b Acceptable for network operations.
c Suitable for low-cost networks where moderate to low performance is acceptable.

### 7.4.3 Calibration of pyrgeometers

Longwave radiation measured by the pyrgeometer is calculated by the following formula from (7.12) and (7.13):

$$L^{-} = \frac{U}{C}\left(1 + k_1\sigma T_b^3\right) + k_2\sigma T_b^4 + k_3\sigma\left(T_d^4 - T_b^4\right) \quad (7.14)$$

where $L^{-}$ is the longwave radiation in watts per square metre ($Wm^{-2}$); $U$ is the measured voltage of the pyrgeometer thermopile in volts; $C$ is the pyrgeometer sensitivity in $VW^{-1}m^2$; $\sigma$ is the Stefan-Boltzmann constant ($5.6704 \times 10^{-8}$ $Wm^{-2}K^{-4}$); $T_b$ and $T_d$ are, respectively, the measured body and dome temperatures of the pyrgeometer in Kelvin; and the $k_i$ values are the instrument constants. Recent state-of-the-art pyrgeometers have been improved in temperature effects, and the dome temperature is considered to be very close to the body temperature, so such pyrgeometers have no dome temperature sensor, and the third term in equation 7.14 is neglected.

As all longwave radiation data must be traceable to the WISG, the standard pyrgeometers at National or Regional Radiation Centres need to be calibrated according to the standard pyrgeometer calibration procedure summarized in WMO Instrument and Observing Methods (IOM) Report No. 120 (Gröbner and Wacker, 2015). In the procedure, $k_i$ are determined in the laboratory using a reference blackbody, while $C$ is retrieved relative to the WISG average from outdoor night-time measurements during clear-sky conditions. The operational pyrgeometer used in the field network also should be calibrated according to the standard procedure using their standard pyrgeometer so that the measured longwave radiation data are traceable to the WISG.

The instrument sensitivities should be checked periodically in situ by a careful selection of well-described environmental conditions with slowly varying fluxes. Pyrgeometers should also be checked periodically to ensure that the transmission of short-wave radiation has not changed.

The symmetry of net pyrradiometers requires regular checking. This is done by inverting the instrument, or the pair of instruments, in situ and noting any difference in output. Differences of greater than 2% of the likely full scale between the two directions demand instrument recalibration because either the ventilation rates or the absorption factors have become significantly different for the two sensors. Such tests should also be carried out during calibration or installation.

### 7.4.4 Installation of pyrradiometers and pyrgeometers

Pyrradiometers and pyrgeometers are generally installed at a site which is free from obstructions, or at least has no obstruction with an angular size greater than 5° in any direction, and which has a low Sun angle at all times during the year.

A daily check of the instruments should ensure that:

(a) The instrument is level;

(b) Each sensor and its protection devices are kept clean and free from dew, frost, snow and rain;

(c) The domes do not retain water (any internal condensation should be dried up);

(d) The black receiver surfaces have emissivities very close to 1.

Since it is not generally possible to directly measure the reflected solar radiation and the upward long-wave radiation exactly at the surface level, it is necessary to place the pyrradiometers, or pyranometers and pyrgeometers at a suitable distance from the ground to measure these upward components. Such measurements integrate the radiation emitted by the surface beneath the sensor. For those instruments which have an angle of view of $2\pi$ sr and are installed 2 m

above the surface, 90% of all the radiation measured is emitted by a circular surface underneath with a diameter of 12 m (this figure is 95% for a diameter of 17.5 m and 99% for a diameter of 39.8 m), assuming that the sensor uses a cosine detector.

This characteristic of integrating the input over a relatively large circular surface is advantageous when the terrain has large local variations in emittance, provided that the net pyrradiometer can be installed far enough from the surface to achieve a field of view which is representative of the local terrain. The output of a sensor located too close to the surface will show large effects caused by its own shadow in addition to the observation of an unrepresentative portion of the terrain. On the other hand, the readings from a net pyrradiometer located too far from the surface can be rendered unrepresentative of the fluxes near that surface because of the existence of undetected radiative flux divergences. Usually, a height of 2 m above short homogeneous vegetation is adopted, while in the case of tall vegetation, such as a forest, the height should be sufficient to eliminate local surface heterogeneities adequately.

### 7.4.5 Recording and data reduction

In general, the text in 7.1.3 applies to pyrradiometers and pyrgeometers. The following effects can specifically influence the readings of these radiometers, and they should be recorded:

(a) The effect of hydrometeors (rain, snow, dew, frost) on non-protected and non-ventilated instruments;

(b) The effect of wind and air temperature;

(c) The drift of zero of the data system. This is much more important for pyrradiometers, which can yield negative values, than for pyranometers, where the zero irradiance signal is itself a property of the net irradiance at the sensor surface.

Special attention should be paid to the position of instruments if the derived long-wave radiation requires subtraction of the solar irradiance component measured by a pyranometer; the pyrradiometer and pyranometer should be positioned within 5 m of each other and in such a way that they are essentially influenced in the same way by their environment.

## 7.5 MEASUREMENT OF SPECIAL RADIATION QUANTITIES

### 7.5.1 Measurement of daylight

Illuminance is the incident flux of radiant energy that emanates from a source with wavelengths between 380 and 780 nm and is weighted by the response of the human eye to energy in this wavelength region. The CIE has defined the response of the human eye to photons with a peak responsivity at 555 nm. Figure 7.2 and Table 7.7 provide the relative response of the human eye normalized to this frequency. Luminous efficacy is defined as the relationship between radiant emittance (W m$^{-2}$) and luminous emittance (lm). It is a function of the relative luminous sensitivity $V(\lambda)$ of the human eye and a normalizing factor $K_m$ (683) describing the number of lumens emitted per watt of electromagnetic radiation (EMR) from a monochromatic source of 555.19 nm (the freezing point of platinum), as follows:

$$\Phi_v = K_m \int_{380}^{780} \Phi(\lambda) V(\lambda) d\lambda \qquad (7.15)$$

where $\Phi_v$ is the luminous flux (lm m$^{-2}$ or lx), $\Phi(\lambda)$ is the spectral radiant flux (W m$^{-2}$ nm$^{-1}$), $V(\lambda)$ is the sensitivity of the human eye, and $K_m$ is the normalizing constant relating luminous to radiation quantities. Thus, 99% of the visible radiation lies between 400 and 730 nm.

Quantities and units for luminous variables are given in Annex 7.A.

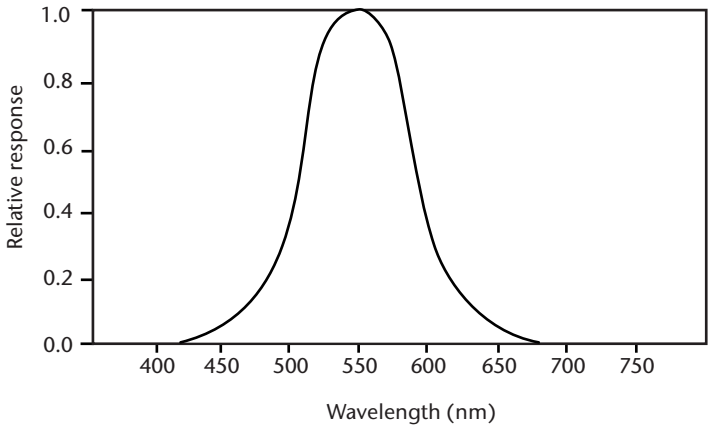



**Figure 7.2. Relative luminous sensitivity $V(\lambda)$ of the human eye for photopic vision**

**Table 7.7. Photopic spectral luminous efficiency values (unity at wavelength of maximum efficacy)**

| *Wavelength (nm)* | *Photopic V(λ)* | *Wavelength (nm) (continued)* | *Photopic V(λ) (continued)* |
|---|---|---|---|
| 380 | 0.00004 | 590 | 0.757 |
| 390 | 0.00012 | 600 | 0.631 |
| 400 | 0.0004 | 610 | 0.503 |
| 410 | 0.0012 | 620 | 0.381 |
| 420 | 0.0040 | 630 | 0.265 |
| 430 | 0.0116 | 640 | 0.175 |
| 440 | 0.023 | 650 | 0.107 |
| 450 | 0.038 | 660 | 0.061 |
| 460 | 0.060 | 670 | 0.032 |
| 470 | 0.091 | 680 | 0.017 |
| 480 | 0.139 | 690 | 0.0082 |
| 490 | 0.208 | 700 | 0.0041 |
| 500 | 0.323 | 710 | 0.0021 |
| 510 | 0.503 | 720 | 0.00105 |
| 520 | 0.710 | 730 | 0.00052 |
| 530 | 0.862 | 740 | 0.00025 |
| 540 | 0.954 | 750 | 0.00012 |
| 550 | 0.995 | 760 | 0.00006 |
| 560 | 0.995 | 770 | 0.00003 |
| 570 | 0.952 | 780 | 0.000015 |
| 580 | 0.870 | | |

#### 7.5.1.1 *Instruments*

Illuminance meters comprise a photovoltaic detector, one or more filters to yield sensitivity according to the $V(\lambda)$ curve, and often a temperature control circuit to maintain signal stability. The CIE has developed a detailed guide to the measurement of daylight (CIE 108-1994), which describes expected practices in the installation of equipment, instrument characterization, data-acquisition procedures and initial QC.

The measurement of global illuminance parallels the measurement of global irradiance. However, the standard illuminance meter must be temperature controlled or corrected from at least –10 °C to 40 °C. Furthermore, it must be ventilated to prevent condensation and/or frost from coating the outer surface of the sensing element. Illuminance meters should normally be able to measure fluxes over the range 1 to 20 000 lx. Within this range, uncertainties should remain within the limits of Table 7.8. These values are based upon CIE recommendations (CIE 069-1987), but only for uncertainties associated with high-quality illuminance meters specifically intended for external daylight measurements.

Diffuse sky illuminance can be measured following the same principles as those used for the measurement of diffuse sky irradiance. Direct illuminance measurements should be taken with instruments that have a field of view whose open half-angle is no greater than 2.85° and whose slope angle is less than 1.76°.

#### 7.5.1.2 *Calibration*

Calibrations should be traceable to a Standard Illuminant A following the procedures outlined in CIE 069-1987. Such equipment is normally available only at national standards laboratories. The calibration and specification tests should be performed yearly. These should also include tests to determine ageing, zero setting drift, mechanical stability and climatic stability. It is also recommended that a field standard be used to check calibrations at each measurement site between laboratory calibrations.

**Table 7.8. Specification of illuminance meters**

| *Specification* | *Uncertainty percentage* |
|---|---|
| $V(\lambda)$ match | 2.5 |
| UV response | 0.2 |
| IR response | 0.2 |
| Cosine response | 1.5 |
| Fatigue at 10 klx | 0.1 |
| Temperature coefficient | 0.1 $K^{-1}$ |
| Linearity | 0.2 |
| Settling time | 0.1 s |

#### 7.5.1.3 *Recording and data reduction*

The CIE has recommended that the following climatological variables be recorded:

(a) Global and diffuse sky daylight illuminance on horizontal and vertical surfaces;

(b) Illuminance of the direct solar beam;

(c) Sky luminance for 0.08 sr intervals (about 10° · 10°) all over the hemisphere;

(d) Photopic albedo of characteristic surfaces such as grass, earth and snow.

Hourly or daily integrated values are usually needed. The hourly values should be referenced to true solar time. For the presentation of sky luminance data, stereographic maps depicting isolines of equal luminance are most useful.

## 7.6 MEASUREMENT OF ULTRAVIOLET RADIATION

Measurements of solar UV radiation are in demand because of its effects on the environment and human health, and because of the enhancement of radiation at the Earth's surface as a result of ozone depletion (Kerr and McElroy, 1993) and changes in other parameters, such as clouds and aerosols. The UV spectrum is conventionally divided into three parts, as follows:

(a) UV-A is the band with wavelengths of 315 to 400 nm, namely, just outside the visible spectrum. It is usually[1] less biologically active, and its intensity at the Earth's surface does not vary significantly with atmospheric ozone content;

(b) UV-B is defined as radiation in the 280 to 315 nm band. It is biologically active and its intensity at the Earth's surface depends on the atmospheric ozone column, depending on wavelength. A frequently used expression of its biological activity is its erythemal effect, which is the extent to which it causes the reddening of human skin;

(c) UV-C, in wavelengths of 100 to 280 nm, is completely absorbed in the atmosphere and does not occur naturally at the Earth's surface.

UV-B is the band on which most interest is centred for measurements of UV radiation. An alternative but now non-standard definition of the boundary between UV-A and UV-B is 320 nm rather than 315 nm.

Measuring UV radiation is difficult because of the small amount of energy reaching the Earth's surface, the variability due to changes in stratospheric ozone levels, and the rapid increase in the magnitude of the flux with increasing wavelength. Figure 7.3 illustrates changes in the spectral irradiance between 290 and 325 nm at the top of the atmosphere and at the surface in W $m^{-2}$ $nm^{-1}$. Global UV irradiance is strongly affected by atmospheric phenomena such as clouds, and to a lesser extent, by atmospheric aerosols in addition to the ozone concentration in the atmosphere.

The influence of surrounding surfaces is also significant because of multiple scattering. This is especially the case in snow-covered areas.

Difficulties in the standardization of UV radiation measurement stem from the variety of uses to which the measurements are put (Webb et al., 2003; Fioletov et al., 2011). Unlike most meteorological measurements, standards based upon global needs have not yet been reached. In many countries, measurements of UV radiation are not taken by Meteorological Services, but by health or environmental protection authorities. This leads to further difficulties

[1] The phytoplankton photosynthesis action spectrum, for example, has an important component in the UV-A.

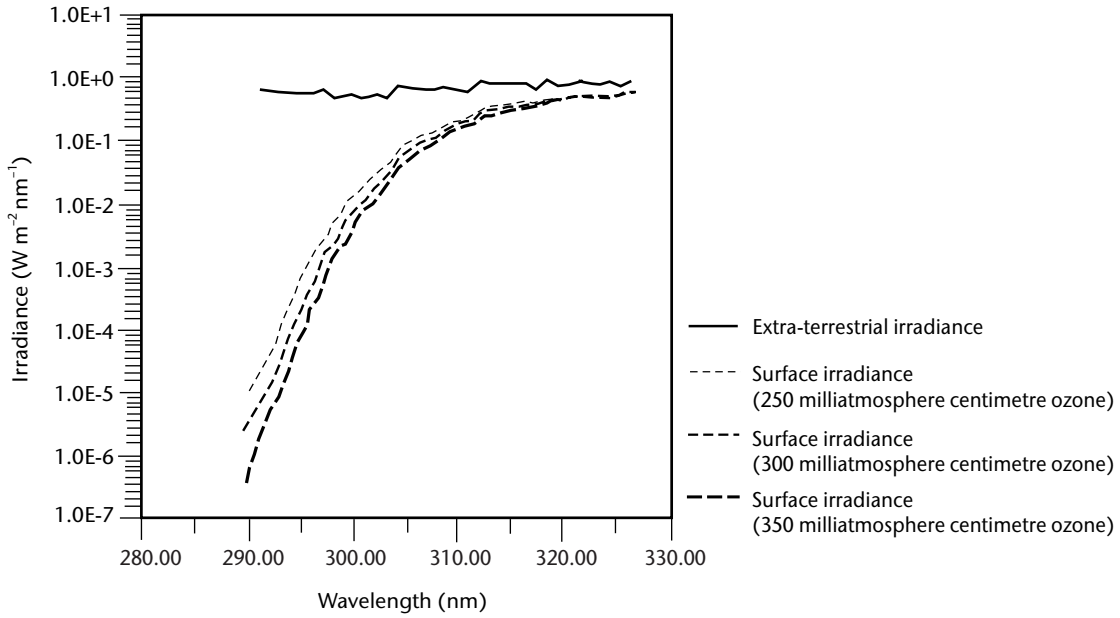



**Figure 7.3. Model results illustrating the effect of increasing ozone levels on the transmission of UV-B radiation through the atmosphere**

in the standardization of instruments and methods of observation. Standards are necessary for compatible observations, QA and QC of measurements, data archiving, and connecting measurements with user communities (Webb et al., 2003).

Guidelines and standard procedures have been developed on how to characterize and calibrate UV broadband instruments, spectroradiometers and filter radiometers used to measure solar UV irradiance (see *WMO-UMAP Workshop on Broad-Band UV Radiometers* (WMO/TD-No. 894); Webb et al., 1998; Bais et al., 2000; Seckmeyer et al., 1999; Seckmeyer et al., 2008; Seckmeyer et al., 2010a). Although not available commercially yet, guides and standard procedures have also been developed for array spectroradiometers (Seckmeyer et al., 2010b). The application of the recommended procedures for data QA performed at sites operating instruments for solar UV radiation measurements will ensure a valuable UV radiation database. This is needed to derive a climatology of solar UV irradiance in space and time for studies of the Earth's climate. Recommendations for measuring sites and instrument specifications are also provided in these documents. Requirements for UV-B measurements were put forward in the WMO Global Atmosphere Watch (GAW) Programme (*Report of the Second Meeting of the Ozone Research Managers of the Parties to the Vienna Convention for the Protection of the Ozone Layer* (WMO Global Ozone Research and Monitoring Project Report No. 32); Seckmeyer et al., 1999; *Commission for Instruments and Methods of Observation – Thirteenth Session: Abridged Final Report with Resolutions and Recommendations* (WMO-No. 947); Seckmeyer et al., 2010a; Seckmeyer et al., 2010b; Fioletov et al., 2011; Janjai et al., 2014). For UV-B global spectral irradiance, the requirements depend on the objective. Specifications for less demanding objectives are reproduced in Table 7.9 (Seckmeyer et al., 1999).

The following instrument descriptions are provided for general information and for assistance in selecting appropriate instrumentation.

### 7.6.1 Instruments

Three general types of instruments are available commercially for the measurement of UV radiation. The first class of instruments uses broadband filters. These instruments integrate over either the UV-B or UV-A spectrum or the entire broadband UV region responsible for affecting human health. The second class of instruments uses one or more interference filters to integrate

**Table 7.9. GAW Programme requirements for UV-B global spectral irradiance measurements**

| *Characteristic* | *Requirements* |
|---|---|
| Cosine error[a] | (a) < ±10% for incidence angles < 60°<br>(b) < ±10% for integrated isotropic radiance |
| Minimum spectral range | 290–325 nm[b] |
| Bandwidth (full width half maximum (FWHM)) | < 1 nm |
| Wavelength precision | < ±0.05 nm |
| Wavelength uncertainty | < ±0.1 nm |
| Slit function | < $10^{-3}$ of maximum at 2.5 FWHM away from centre |
| Sampling wavelength interval | < FWHM |
| Maximum irradiance | > 1 W $m^{-2}$ $nm^{-1}$ at 325 nm and, if applicable,<br>2 W $m^{-2}$ $nm^{-1}$ at 400 nm (noon maximum) |
| Detection threshold | < $5 \cdot 10^{-5}$ W $m^{-2}$ $nm^{-1}$ (for signal-to-noise ratio (SNR) = 1 at 1 nm FWHM) |
| Stray light | < $5 \cdot 10^{-4}$ W $m^{-2}$ $nm^{-1}$ when the instrument is exposed to the Sun at minimum solar zenith angle |
| Instrument temperature | Monitored and sufficiently stable to maintain overall instrument stability |
| Scanning duration | < 10 min per spectrum, e.g. for ease of comparison with models |
| Overall calibration uncertainty[c] | < ±10% (unless limited by detection threshold) |
| Scan date and time | Recorded with each spectrum such that timing is known to within 10 s at each wavelength |
| Ancillary measurements required | – Direct normal spectral irradiance or diffuse spectral irradiance<br>– Total ozone column, e.g. derived from measurements of direct normal spectral irradiance<br>– Erythemally weighted irradiance, measured with a broadband radiometer<br>– Atmospheric pressure<br>– Cloud amount<br>– Illuminance, measured with a luxmeter<br>– Direct irradiance at normal incidence measured with a pyrheliometer<br>– Visibility |
| Data frequency | At least one scan per hour, and additionally a scan at local solar noon |

a Smaller cosine errors would be desirable but are unrealistic for the majority of the instruments that are currently in use.

b An extension to longer wavelengths is desirable for the establishment of a UV climatology with respect to biological applications. See Seckmeyer et al. (1999, 2010b).

c The overall calibration uncertainty is expressed at 95% confidence level and includes all uncertainties associated with the irradiance calibration (for example, uncertainty of the standard lamps, transfer uncertainties, alignment errors during calibration, and drift of the instrument between calibrations). For more details, see Bernhard and Seckmeyer (1999), Cordero et al. (2008), and Cordero et al. (2013).

over discrete portions of the UV-A and/or UV-B spectrum. The third class of instruments is spectroradiometers that measure across a pre-defined portion of the spectrum sequentially, or simultaneously, using a fixed passband.

### 7.6.1.1 *Broadband sensors*

Most, but not all, broadband sensors are designed to measure a UV spectrum that is weighted by the erythemal function proposed by McKinlay and Diffey (1987) and reproduced in Figure 7.4. Another action spectrum found in some instruments is that of Parrish et al. (1982). Two methods (and their variations) are used to accomplish this hardware weighting.

One of the means of obtaining erythemal weighting is to first filter out nearly all visible wavelength light using UV-transmitting, black-glass blocking filters. The remaining radiation then strikes a UV-sensitive phosphor. In turn, the green light emitted by the phosphor is filtered again by using coloured glass to remove any non-green visible light before impinging on a gallium arsenic or a gallium arsenic phosphorus photodiode. The quality of the instrument is dependent on such items as the quality of the outside protective quartz dome, the cosine response of the instrument, the temperature stability, and the ability of the manufacturer to match the erythemal curve with a combination of glass and diode characteristics. Instrument temperature stability is crucial, with respect to both the electronics and the response of the phosphor to incident UV radiation. Phosphor efficiency decreases by approximately 0.5% $K^{-1}$, and its wavelength response curve shifts by approximately 1 nm towards longer wavelengths every 10 K. This latter effect is particularly important because of the steepness of the radiation curve at these wavelengths.

More recently, instruments have been developed to measure erythemally weighted UV irradiance using thin film metal interference filter technology and specially developed silicon photodiodes. These overcome many problems associated with phosphor technology but must contend with very low photodiode signal levels and filter stability.

Other broadband instruments use one of the two measurement technologies to measure the complete spectra by using either a combination of glass filters or interference filters. The bandpass is as narrow as 20 nm FWHM to as wide as 80 nm FWHM for instruments

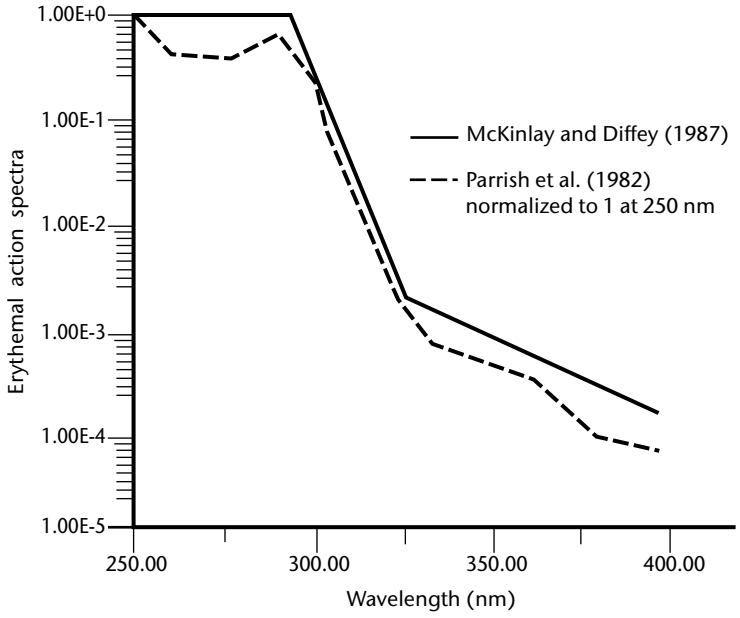



**Figure 7.4. Erythemal curves**

*Source:* Parrish et al. (1982) and McKinlay and Diffey (1987)

measuring a combination of UV-A and UV-B radiation. Some manufacturers of these instruments provide simple algorithms to approximate erythemal dosage from the unweighted measurements.

The basic maintenance of these instruments consists of ensuring that the domes are cleaned, the instrument is levelled, the desiccant (if provided) is active, and the heating/cooling system is working correctly, if so equipped. QC and QA, as well as detailed maintenance, should be done by well-experienced staff.

#### 7.6.1.2 ***Narrowband sensors***

The definition of narrowband for this classification of instrument is vague. The widest bandwidth for instruments in this category is 10 nm FWHM. The narrowest bandwidth at present for commercial instruments is of the order of 2 nm FWHM (Seckmeyer et al., 2010a).

These sensors use one or more interference filters to obtain information about a portion of the UV spectra. The simplest instruments consist of a single filter, usually at a wavelength that can be measured by a good-quality, UV-enhanced photodiode, although more than one filter is desirable. Specifications required for this type of instrument (Seckmeyer et al., 2010a) are given in Table 7.10. Wavelengths near 305 nm are typical for such instruments. The out-of-band rejection of such filters should be equal to, or greater than, $10^{-6}$ throughout the sensitive region of the detector. Higher quality instruments of this type use either Peltier cooling to maintain a constant temperature near 20 °C or heaters to increase the instrument filter and diode temperatures to above normal ambient temperatures, usually 40 °C. However, the latter alternative markedly reduces the life of interference filters. A modification of this type of instrument uses a photomultiplier tube instead of the photodiode. This allows the accurate measurement of energy from shorter wavelengths and lower intensities at all measured wavelengths.

**Table 7.10. Requirements for UV-B global narrowband irradiance measurements**

| *Characteristic* | *Requirements* |
|---|---|
| Stray light including sensitivity to visible and IR radiation | < 1% contribution to the signal of wavelengths outside 2.5 FWHM for a solar zenith angle less than 70° |
| Stability over time on timescales up to a year | Signal change:<br>Currently in use: better than 5%<br>Desired: 2% |
| Minimum number of channels | At least one channel with centre wavelength < 310 nm and at least one with centre wavelength > 330 nm |
| Maximum irradiance | Signal of the instruments must not saturate at radiation levels encountered on the Earth's surface |
| Detection threshold | SNR = 3 for irradiance at solar zenith angle of 80° and total ozone column of 300 Dobson units |
| Instrument temperature | Monitored and sufficiently stable to maintain overall instrument stability |
| Response time | < 1 s |
| Multiplexing time | < 1 s |
| Accuracy of time | Better than ±10 s |
| Sampling frequency | ≤ 1 min |
| Levelling | < 0.2° |
| Calibration uncertainty | < 10% (unless limited by detection threshold) |

Manufacturers of instruments that use more than a single filter often provide a means of reconstructing the complete UV spectrum and determining biologically effective doses for a variety of action spectra, the total column ozone amount and cloud attenuation, through modelled relationships developed around the measured wavelengths (Seckmeyer et al., 2010a). Single wavelength instruments are used similarly to supplement the temporal and spatial resolution of more sophisticated spectrometer networks or for long-term accurate monitoring of specific bands to detect trends in the radiation environment.

The construction of the instruments must be such that the radiation passes through the filter close to normal incidence so that wavelength shifting to shorter wavelengths is avoided. For example, a 10° departure from normal incidence may cause a wavelength shift of 1.5 nm, depending on the refractive index of the filter. The effect of temperature can also be significant in altering the central wavelength by about 0.012 nm $K^{-1}$ on very narrow filters (< 1 nm).

Maintenance for simple one-filter instruments is similar to that of broadband instruments. For instruments that have multiple filters in a moving wheel assembly, maintenance includes determining whether or not the filter wheel is properly aligned. Regular testing of the high-voltage power supply for photomultiplier-equipped instruments and checking the quality of the filters are also recommended.

#### 7.6.1.3 ***Spectroradiometers***

The most sophisticated commercial instruments are those that use either ruled or holographic gratings to disperse the incident energy into a spectrum. The low energy of the UV radiation compared with that in the visible spectrum necessitates a strong out-of-band rejection. This is achieved by using a double monochromator or by blocking filters, which transmit only UV radiation, in conjunction with a single monochromator. A photomultiplier tube is most commonly used to measure the output from the monochromator (Seckmeyer et al., 1999). Some less expensive instruments use photodiode or charge-coupled detector arrays (Seckmeyer et al., 2010b), enabling the measurement of an entire spectral region of interest at the same time. These instruments are unable to measure energy in the shortest wavelengths of the UV-B radiation and generally have more problems associated with stray light.

Monitoring instruments are now available with several self-checking features. Electronic tests include checking the operation of the photomultiplier and the analogue-to-digital conversion. Tests to determine whether the optics of the instrument are functioning properly include testing the instrument by using internal mercury lamps and standard quartz halogen lamps. While these do not give absolute calibration data, they provide the operator with information on the stability of the instrument with respect to both spectral alignment and intensity.

Commercially available instruments are constructed to provide measurement capabilities from approximately 290 nm to the mid-visible wavelengths, depending upon the type of construction and configuration. The bandwidth of the measurements is usually between 0.5 and 2.0 nm. The time required to complete a full scan across the grating depends upon both the wavelength resolution and the total spectrum to be measured. Scan times to perform a spectral scan across the UV region and part of the visible region (290 to 450 nm) with small wavelength steps range from less than 1 min per scan with modern fast scanning spectroradiometers to about 10 min per scan for some types of conventional high-quality spectroradiometers.

For routine monitoring of UV radiation, it is recommended that the instrument be either environmentally protected or developed in such a manner that the energy incident on a receiver is transmitted to a spectrometer housed in a controlled climate. In both cases, care must be taken in the development of optics so that uniform responsivity is maintained down to low solar elevations.

The maintenance of spectroradiometers designed for monitoring UV-B radiation requires well-trained on-site operators who will care for the instruments. It is crucial to follow the manufacturer's maintenance instructions because of the complexity of this instrument.

### *7.6.2* **Calibration**

The calibration of all sensors in the UV-B band is both very important and difficult. Guidelines on the calibration of UV spectroradiometers and UV filter radiometers are given in Bais et al., 2000, Seckmeyer et al., 1999; Seckmeyer et al., 2008; Seckmeyer et al., 2010a, Seckmeyer et al., 2010b; Webb, et al., 1998; *WMO-UMAP Workshop on Broad-Band UV Radiometers* (WMO/TD-No. 894) and in the relevant scientific literature. Spectroradiometers must be calibrated against standard lamps, which have to be traceable to national standards laboratories. Many countries do not have laboratories capable of characterizing lamps in the UV range. In these countries, lamps are usually traceable to the National Institute of Standards and Technology (NIST) in the United States of America or to the Physikalisch-Technische Bundesanstalt in Germany.

It is estimated that a 5% uncertainty in spot measurements at 300 nm can be achieved only under the most rigorous conditions at the present time. The uncertainty of measurements of daily totals is about the same using best practices. Fast changes in cloud cover and/or cloud optical depths at the measuring site require fast spectral scans and small sampling time steps between subsequent spectral scans in order to obtain representative daily totals of spectral UV irradiance. Measurements of erythemal irradiance typically have uncertainties in the range 5% to 20%, depending on a number of factors, including the quality of the procedures and the equipment. The sources of error are discussed in the following paragraphs and include:

(a) Uncertainties associated with standard lamps;

(b) The stability of instruments, including the stability of the spectral filter and, in older instruments, temperature coefficients;

(c) Cosine error effects;

(d) The fact that the calibration of an instrument varies with wavelength, and that:

  (i) The spectrum of a standard lamp is not the same as the spectrum being measured;

  (ii) The spectrum of the UV-B irradiance being measured varies greatly with the solar zenith angle.

The use of standard lamps as calibration sources leads to large uncertainties at the shortest wavelengths, even if the transfer of the calibration is perfect. For example, at 350 nm, the uncertainty associated with the standard irradiance is of the order of 1.3%; when transferred to a standard lamp, another 0.7% uncertainty is added. Uncertainties in calibration decrease with increasing wavelength. Consideration must also be given to the set-up and handling of standard lamps. Even variations as small as 1% in the current, for example, can lead to errors in the UV flux of 10% or more at the shortest wavelengths. Inaccurate distance measurements between the lamp and the instrument being calibrated can also lead to errors of the order of 1% as the inverse square law applies to the calibration. Webb et al. (1994) discuss various aspects of uncertainty as related to the use of standard lamps in the calibration of UV or visible spectroradiometers.

The problems associated with broadband instruments stem from: (a) the complex set of filters used to integrate the incoming radiation into the erythemal signal; and (b) the fact that the spectral nature of the atmosphere changes with airmass and ozone amount. Even if the characterization of the instrument by using calibrated lamp sources is perfect, the difference between the measured solar spectrum and the lamp spectrum affects the uncertainty of the final measurements. The use of high-output deuterium lamps, a double monochromator and careful filter selection will help in the characterization of these instruments, but the number of laboratories capable of calibrating these devices is extremely limited. Different calibration methods for broadband instruments are described in Seckmeyer et al. (2008).

Trap detectors could potentially be used effectively for narrowband sensors, but they have been used only in research projects to date. In recalibrating these instruments, whether they have

a single filter or multiple filters, care must be taken to ensure that the spectral characteristics of the filters have not shifted over time. Different methods for calibrating narrowband sensors, as well as their advantages and disadvantages, are described in Seckmeyer et al. (2010a).

Spectroradiometers should be calibrated in the same position as that in which the measurements are to be taken, as many spectroradiometers are adversely affected by changes in orientation. The calibration of a spectroradiometer should also include testing the accuracy of the wavelength positioning of the monochromator, checking for any changes in internal optical alignment and cleanliness, and an overall test of the electronics. The out-of-band rejection needs to be characterized, possibly by scanning a helium cadmium laser ($\lambda$ = 325 nm), only once, as it usually does not change with time.

Most filter instrument manufacturers indicate a calibration frequency of once a year. Spectroradiometers should be calibrated at least twice a year, and more frequently if they do not have the ability to perform self-checks on the photomultiplier output or the wavelength selection. In all cases, absolute calibrations of the instruments should be performed by qualified technicians at the sites on a regular schedule. The sources used for calibration must guarantee that the calibration can be traced back to absolute radiation standards kept at National Metrological Institutes (NMIs). If the results of QA routines applied at the sites indicate a significant change in an instrument's performance or changes of its calibration level over time, an additional calibration may be needed in between two regular calibrations. All calibrations should be based on the expertise and documentation available at the site and on the guidelines and procedures such as those published in Bais, et al. (2000); Seckmeyer et al. (1999, 2008, 2010a, 2010b); Webb, et al. (1998); *WMO-UMAP Workshop on Broad-Band UV Radiometers* (WMO/TD-No. 894). In addition to absolute calibrations of instruments, intercomparisons between the sources used for calibration, for example, calibration lamps, and the measuring instruments are useful to detect and remove inconsistencies or systematic differences between station instruments at different sites.

# ANNEX 7.A. NOMENCLATURE OF RADIOMETRIC AND PHOTOMETRIC QUANTITIES

### (1) Radiometric quantities

| *Name* | *Symbol* | *Unit* | *Relation* | *Remarks* |
|---|---|---|---|---|
| Radiant energy | $Q$, *(W)* | J = W s | – | – |
| Radiant flux | $\Phi$, *(P)* | W | $\Phi = \frac{dQ}{dt}$ | Power |
| Radiant flux density | *(M), (E)* | W m$^{-2}$ | $\frac{d\Phi}{dA} = \frac{d^2Q}{dA \cdot dt}$ | Radiant flux of any origin crossing an area element |
| Radiant exitance | $M$ | W m$^{-2}$ | $M = \frac{d\Phi}{dA}$ | Radiant flux of any origin emerging from an area element |
| Irradiance | $E$ | W m$^{-2}$ | $E = \frac{d\Phi}{dA}$ | Radiant flux of any origin incident onto an area element |
| Radiance | $L$ | W m$^{-2}$ sr$^{-1}$ | $L = \frac{d^2\Phi}{d\Omega \cdot dA \cdot \cos\theta}$ | The radiance is a conservative quantity in an optical system |
| Radiant exposure | $H$ | J m$^{-2}$ | $H = \frac{dQ}{dA} = \int_{t_1}^{t_2} E dt$ | May be used for daily sums of global radiation, etc. |
| Radiant intensity | $I$ | W sr$^{-1}$ | $I = \frac{d\Phi}{d\Omega}$ | May be used only for radiation outgoing from "point sources" |

### (2) Photometric quantities

| *Name* | *Symbol* | *Unit* |
|---|---|---|
| Quantity of light | $Q_v$ | lm · s |
| Luminous flux | $\Phi_v$ | Lm |
| Luminous exitance | $M_v$ | lm m$^{-2}$ |
| Illuminance | $E_v$ | lm m$^{-2}$ = lx |
| Light exposure | $H_v$ | lm m$^{-2}$ s = lx · s |
| Luminous intensity | $I_v$ | lm sr$^{-1}$ = cd |
| Luminance | $L_v$ | lm m$^{-2}$ sr$^{-1}$ = cdm$^{-2}$ |
| Luminous flux density | ($M_v$ ; $E_v$) | lm m$^{-2}$ |

### (3) Optical characteristics

| *Characteristic* | *Symbol* | *Definition* | *Remarks* |
|---|---|---|---|
| Emissivity | $\varepsilon$ | $\varepsilon = \frac{M_\varepsilon}{M_{\varepsilon=1}}$ | $\varepsilon = 1$ for a blackbody |
| Absorptance | $\alpha$ | $\alpha = \frac{\Phi_a}{\Phi_i}$ | $\Phi_a$ and $\Phi_i$ are the absorbed and incident radiant flux, respectively |
| Reflectance | $\rho$ | $\rho = \frac{\Phi_r}{\Phi_i}$ | $\Phi_r$ is the reflected radiant flux |
| Transmittance | $\tau$ | $\tau = \frac{\Phi_t}{\Phi_i}$ | $\Phi_t$ is the radiant flux transmitted through a layer or a surface |
| Optical depth | $\delta$ | $\tau = e^{-\delta}$ | In the atmosphere, $\delta$ is defined in the vertical. Optical thickness equals $\delta/\cos\theta$, where $\theta$ is the apparent zenith angle |

# ANNEX 7.B. METEOROLOGICAL RADIATION QUANTITIES, SYMBOLS AND DEFINITIONS

| *Quantity* | *Symbol* | *Relation* | *Definitions and remarks* | *Units* |
|---|---|---|---|---|
| Downward radiation | $\Phi\downarrow$[a] | $\Phi\downarrow = \Phi_g\downarrow + \Phi_l\downarrow$ | Downward radiant flux | W |
| | $Q\downarrow$ | $Q\downarrow = Q_g\downarrow + Q_l\downarrow$ | " radiant energy | J (W s) |
| | $M\downarrow$ | $M\downarrow = M_g\downarrow + M_l\downarrow$ | " radiant exitance[b] | W m$^{-2}$ |
| | $E\downarrow$ | $E\downarrow = E_g\downarrow + E_l\downarrow$ | " irradiance | W m$^{-2}$ |
| | $L\downarrow$ | $L\downarrow = L_g\downarrow + L_l\downarrow$ | " radiance | W m$^{-2}$ sr$^{-1}$ |
| | $H\downarrow$ | $H\downarrow = H_g\downarrow + H_l\downarrow$ ($g$ = global) ($l$ = long wave) | " radiant exposure for a specified time interval | J m$^{-2}$ over a specified time interval |
| Upward radiation | $\Phi\uparrow$[a] | $\Phi\uparrow = \Phi_r\uparrow + \Phi_l\uparrow$ | Upward radiant flux | W |
| | $Q\uparrow$ | $Q\uparrow = Q_r\uparrow + Q_l\uparrow$ | " radiant energy | J (W s) |
| | $M\uparrow$ | $M\uparrow = M_r\uparrow + M_l\uparrow$ | " radiant exitance | W m$^{-2}$ |
| | $E\uparrow$ | $E\uparrow = E_r\uparrow + E_l\uparrow$ | " irradiance | W m$^{-2}$ |
| | $L\uparrow$ | $L\uparrow = L_r\uparrow + L_l\uparrow$ | " radiance | W m$^{-2}$ sr$^{-1}$ |
| | $H\uparrow$ | $H\uparrow = H_r\uparrow + H_l\uparrow$ | " radiant energy per unit area for a specified time interval | J m$^{-2}$ over a specified time interval |
| Global radiation | $E_g\downarrow$ | $E_g\downarrow = E\cos\theta_\odot + E_d\downarrow$ | Hemispherical irradiance on a horizontal surface ($\theta_\odot$ = *apparent solar zenith angle*)[c] | W m$^{-2}$ |
| Sky radiation: downward diffuse solar radiation | $\Phi_d\downarrow$<br>$Q_d\downarrow$<br>$M_d\downarrow$<br>$E_d\downarrow$<br>$L_d\downarrow$<br>$H_d\downarrow$ | | Subscript $d$ = diffuse | As for downward radiation |
| Upward/downward long-wave radiation | $\Phi_l\uparrow$, $\Phi_l\downarrow$<br>$Q_l\uparrow$, $Q_l\downarrow$<br>$M_l\uparrow$, $M_l\downarrow$<br>$E_l\uparrow$, $E_l\downarrow$<br>$H_l\uparrow$, $H_l\downarrow$ | | Subscript $l$ = long wave. If only atmospheric radiation is considered, the subscript $a$ may be added, e.g. $\Phi_{l,a}\uparrow$ | As for downward radiation |

| *Quantity* | *Symbol* | *Relation* | *Definitions and remarks* | *Units* |
|---|---|---|---|---|
| Reflected solar radiation | $\Phi_r\uparrow$<br>$Q_r\uparrow$<br>$M_r\uparrow$<br>$E_r\uparrow$<br>$L_r\uparrow$<br>$H_r\uparrow$ | | Subscript $r$ = reflected (the subscript $s$ (specular) and $d$ (diffuse) may be used, if a distinction is to be made between these two components) | As for downward radiation |
| Net radiation | $\Phi^*$<br>$Q^*$<br>$M^*$<br>$E^*$<br>$L^*$<br>$H^*$ | $\Phi^* = \Phi\downarrow - \Phi\uparrow$<br>$Q^* = Q\downarrow - Q\uparrow$<br>$M^* = M\downarrow - M\uparrow$<br>$E^* = E\downarrow - E\uparrow$<br>$L^* = L\downarrow - L\uparrow$<br>$H^* = H\downarrow - H\uparrow$ | The subscript $g$ or $l$ is to be added to each of the symbols if only short-wave or long-wave net radiation quantities are considered | As for downward radiation |
| Direct solar radiation | $E$ | $E = E_0\tau$<br>$\tau = e^{-\delta/\cos\theta_\odot}$ | $\tau$ = atmospheric transmittance<br>$\delta$ = optical depth (vertical) | W m$^{-2}$ |
| Solar constant | $E_0$ | | Solar irradiance, normalized to mean Sun–Earth distance | W m$^{-2}$ |

a The symbols – or + could be used instead of ↓ or ↑ (e.g. $\Phi^+ = \Phi\uparrow$).

b Exitance is radiant flux emerging from the unit area; irradiance is radiant flux received per unit area. For flux density in general, the symbol $M$ *or the symbol* $E$ can be used. Although not specifically recommended, the symbol $F$, defined as $\Phi$/area, may also be introduced.

c In the case of inclined surfaces, $\theta_\odot$ is the angle between the normal to the surface and the direction to the Sun.

# ANNEX 7.C. SPECIFICATIONS FOR WORLD, REGIONAL AND NATIONAL RADIATION CENTRES

**World Radiation Centres**

World Radiation Centres were designated by the Executive Committee at its thirtieth session in 1978 through Resolution 11 (EC-XXX) to serve as centres for the international calibration of meteorological radiation standards within the global network and to maintain the standard instruments for this purpose.

A World Radiation Centre shall fulfil the following requirements. Either:

(a) It shall possess and maintain a group of at least three stable absolute pyrheliometers with a traceable 95% uncertainty of less than 1 W $m^{-2}$ to the WRR, and in stable, clear Sun conditions with direct irradiances above 700 W $m^{-2}$, 95% of any single measurements of direct solar irradiance are expected to be within 4 W $m^{-2}$ of the irradiance. The World Radiation Centre Davos is requested to maintain the WSG for the realization of the WRR;

(b) It shall undertake to train specialists in radiation;

(c) The staff of the centre should provide for continuity and include qualified scientists with wide experience in radiation;

(d) It shall take all steps necessary to ensure, at all times, the highest possible quality of its standards and testing equipment;

(e) It shall serve as a centre for the transfer of the WRR to the regional centres;

(f) It shall have the necessary laboratory and outdoor facilities for the simultaneous comparison of large numbers of instruments and for data reduction;

(g) It shall follow closely or initiate developments leading to improved standards and/or methods in meteorological radiometry;

(h) It shall be assessed by an international agency or by CIMO experts, at least every five years, to verify traceability of the direct solar radiation measurements;

or:

(a) It shall provide and maintain an archive for solar radiation data from all the Member States of WMO;

(b) The staff of the centre should provide for continuity and include qualified scientists with wide experience in radiation;

(c) It shall take all steps necessary to ensure, at all times, the highest possible quality of, and access to, its database;

(d) It shall be assessed by an international agency or by CIMO experts, at least every five years.

**Regional Radiation Centres**

A Regional Radiation Centre is a centre designated by a regional association to serve as a centre for intraregional comparisons of radiation instruments within the region and to maintain the standard instrument necessary for this purpose.

A Regional Radiation Centre shall satisfy the following conditions before it is designated as such and shall continue to fulfil them after being designated:

(a) It shall possess and maintain a standard group of at least three stable pyrheliometers with a traceable 95% uncertainty of less than 1 W $m^{-2}$ to the WSG, and in stable, clear Sun conditions with direct irradiances above 700 W $m^{-2}$, 95% of any single measurements of direct solar irradiance are expected to be within 6 W $m^{-2}$ of the irradiance;

(b) One of the radiometers shall be compared through a WMO/CIMO sanctioned comparison, or calibrated, at least once every five years against the WSG;

(c) Standard radiometers shall be intercompared at least once a year to check the stability of the individual instruments. If the mean ratio, based on at least 100 measurements, and with a 95% uncertainty less than 0.1%, has changed by more than 0.2%, and if the erroneous instrument cannot be identified, a recalibration at one of the WRCs must be performed prior to its further use as a standard;

(d) It shall have, or have access to, the necessary facilities and laboratory equipment for checking and maintaining the accuracy of the auxiliary measuring equipment;

(e) It shall provide the necessary outdoor facilities for the simultaneous comparison of national standard radiometers from the region;

(f) The staff of the centre should provide for continuity and include a qualified scientist with wide experience in radiation;

(g) It shall be assessed by a national or international agency or by CIMO experts, at least every five years, to verify traceability of the direct solar radiation measurements.

**National Radiation Centres**

A National Radiation Centre is a centre designated at the national level to serve as a centre for the calibration, standardization and checking of the instruments used in the national network of radiation stations and for maintaining the national standard instrument necessary for this purpose.

A National Radiation Centre shall satisfy the following requirements:

(a) It shall possess and maintain at least two pyrheliometers for use as a national reference for the calibration of radiation instruments in the national network of radiation stations with a traceable 95% uncertainty of less than 4 W $m^{-2}$ to the regional representation of the WRR, and in stable, clear Sun conditions with direct irradiances above 700 W $m^{-2}$, 95% of any single measurements of direct solar irradiance are expected to be within 20 W $m^{-2}$ of the irradiance;

(b) One of the national standard radiometers shall be compared with a regional standard at least once every five years;

(c) National standard radiometers shall be intercompared at least once a year to check the stability of the individual instruments. If the mean ratio, based on at least 100 measurements, and with a 95% uncertainty less than 0.2%, has changed by more than 0.6% and if the erroneous instrument cannot be identified, a recalibration at one of the Regional Radiation Centres must be performed prior to its further use as a standard;

(d) It shall have, or have access to, the necessary facilities and equipment for checking the performance of the instruments used in the national network;

(e) The staff of the centre should provide for continuity and include a qualified scientist with experience in radiation.

**List of World and Regional Radiation Centres**

***World Radiation Centres***

| | |
|---|---|
| Davos | (Switzerland) |
| Saint Petersburg (see note) | (Russian Federation) |

***Regional Radiation Centres***

*Region I (Africa):*

| | |
|---|---|
| Cairo | (Egypt) |
| Khartoum | (Sudan) |
| Kinshasa | (Democratic Republic of the Congo) |
| Lagos | (Nigeria) |
| Tamanrasset | (Algeria) |
| Tunis | (Tunisia) |

*Region II (Asia):*

| | |
|---|---|
| Pune | (India) |
| Tokyo | (Japan) |

*Region III (South America):*

| | |
|---|---|
| Buenos Aires | (Argentina) |
| Santiago | (Chile) |
| Huayao | (Peru) |

*Region IV (North America, Central America and the Caribbean):*

| | |
|---|---|
| Toronto | (Canada) |
| Boulder | (United States) |
| Mexico City/Colima | (Mexico) |

*Region V (South-West Pacific):*

| | |
|---|---|
| Melbourne | (Australia) |

*Region VI (Europe):*

| | |
|---|---|
| Budapest | (Hungary) |
| Davos | (Switzerland) |
| Saint Petersburg | (Russian Federation) |
| Norrköping | (Sweden) |
| Toulouse/Carpentras | (France) |
| Uccle | (Belgium) |
| Lindenberg | (Germany) |

Note: The Centre in Saint Petersburg is mainly operated as a World Radiation Data Centre.

National Radiation Centres shall be responsible for preparing and keeping up to date all necessary technical information for the operation and maintenance of the national network of radiation stations.

Arrangements should be made for the collection of the results of all radiation measurements taken in the national network of radiation stations and for the regular scrutiny of these results with a view to ensuring their accuracy and reliability. If this work is done by some other body, the National Radiation Centre shall maintain close liaison with the body in question.

# ANNEX 7.D. GUIDELINES FOR RADIOMETER COMPARISONS

## 1. INTRODUCTION

1.1. These guidelines define a conceptual framework for enabling comparisons of surface radiometer measurements and improving their analysis, especially for comparisons that allow the traceability propagation of radiation references. They aim to facilitate different analyses (potentially using different methods) to be performed and compared. They also help to define clear criteria to be applied during the analyses.

1.2. This conceptual framework allows for some flexibility so that it can be used for different types of radiometer comparisons. However, when a WMO global or regional radiometer comparison is organized, these guidelines should be carefully considered and are complementary to the general procedures of WMO global and regional intercomparisons of meteorological instruments (in particular, the guidelines of Volume V, Chapter 4, Annexes 4B and 4C).

1.3. The implementation of the guidelines and criteria will depend on the purpose of the comparison and often the location (typical environmental conditions at the location). The recommendations herein are not formulated as strict limits but should serve as guidelines for criteria to be considered by the organizers in advance of the comparison campaigns.

1.4. It should be noted that these guidelines were developed to ensure that comparisons, including those involving reference instruments, and potentially new reference instruments, are properly documented to ensure the long-term traceability of radiation measurements and to allow for the recalculation of the results if needed. However, they also present good practices that should be considered in organizing other types of radiometer comparisons.

1.5. The following recommendations draw on the procedures implemented by the World Radiation Centre described in Finsterle (2023), Gröbner and Thomann (2023) and Gröbner and Wacker (2015).

## 2. GENERAL RECOMMENDATIONS

2.1. Radiometer comparisons should be performed over periods of sufficient duration – usually several weeks – to allow for the collection of a sizable dataset, enabling statistically significant analyses even when selecting data measured under the environmental conditions described in the following section.

2.2. Data should be collected with a uniform time reference (with the synchronicity of clocks used by different data acquisition systems to be verified frequently enough to ensure that deviations are about one second or less).

2.3. Data sampling should allow time aggregation (for example, time averages, or other statistical indicators, such as standard deviation) to enable meaningful comparisons between instruments, taking into account the different time constants of the instruments being compared.

2.4. Radiometers have time constants that vary widely, from milliseconds to several seconds. When comparing measurements of such different instruments, proper sampling rates and time averaging should be used so that the compared quantities represent irradiances averaged over the same periods. The difficulty is exacerbated when the irradiance varies significantly within periods corresponding to the time constants of the slowest instruments. It is therefore recommended to use data corresponding to periods when the irradiance varies slowly

for the analysis, although continuous data recording is also recommended, with data selection applied only during the analysis. The data not fulfilling the selection criteria should be flagged so that it can be easily excluded from analysis, *but it should not be deleted*.

## 3. ENVIRONMENTAL CONDITIONS

### 3.1. Solar radiation instrument comparisons

Solar radiation instrument comparisons often exploit direct normal irradiance (DNI) as a source. The criteria relating to the environmental conditions listed below are specified to ensure optimal comparisons of DNI measured by different radiometers. Using a parameter other than DNI, for instance, global irradiance for pyranometer comparisons, would result in different criteria for the environmental conditions.

(a) Fair weather daytime conditions with no clouds close to the Sun. This criterion reduces the variability of the irradiance during periods corresponding to the longest radiometer time constants. Organizers should anticipate the need for a method for determining the presence of clouds in the proximity of the Sun in advance. (For example, the analysis of the Thirteenth International Pyrheliometer Comparison (IPC-XIII) excluded times when clouds were present within 8° of the Sun; this required a cloud detection system, in this case, an IR camera.)

(b) A strong DNI signal (or global irradiance signal for pyranometer comparisons) should be selected for analysis. The *relative* uncertainty is smaller for large signals, which improves the precision of the comparisons. It is not possible to recommend a fixed lower irradiance limit since the range of irradiances depends on the location, typically because of solar zenith angle limitations at high latitudes or prevailing significant aerosol optical depth in some regions (for example, deserts). The lower limit should therefore be determined depending on the local conditions. (For example, IPC-XIII required DNI as measured by a reference instrument to be larger than 700 $Wm^{-2}$; however, at locations with prevailing significant aerosol optical depth, the comparison organizers are permitted to lower this limit, taking into consideration typical values for high DNI at the site.)

(c) Limits should be considered on aerosol optical depth (AOD). High AOD conditions lower the irradiance and usually increase its variability. They also increase the circumsolar radiation and add uncertainty when comparing instruments with different fields of view. Low AOD conditions are thus more favourable, and setting a higher AOD limit above which data are excluded from the analysis is recommended. However, as mentioned above, some regions (for example, deserts) experience high aerosol loads and such a criterion may be too stringent; if this is the case, it can be replaced by criteria on AOD stability. It is recommended that AOD be monitored during the comparison. (As an example, IPC-XIII excluded times when AOD at 500 nm was greater than 0.120.)

(d) Rainy conditions should be excluded, as many solar radiation reference instruments are windowless and can be altered or damaged by water. It is often necessary to consult weather forecasts when deciding when to set up instruments for comparisons.

(e) The integrated water vapour column (IWV) or humidity should be recorded and considered in the analysis. Solar radiation comparisons may involve both windowless instruments and instruments with windows or domes that exclude part of the near-IR end of the solar spectrum. In addition, windowed or domed instruments may have different cut-off limits. Because the near-IR end of the solar spectrum is influenced by IWV, it may affect the comparisons.

(f) Wind should be recorded and considered in the analysis. The operating principle of many radiometers is based on a temperature effect induced by solar irradiance. Windy conditions can create temperature gradients in radiometers, increasing the uncertainty, especially in windowless instruments.

## 3.2. **Terrestrial radiation instrument comparisons**[1]

3.2.1. Terrestrial radiation instrument comparisons usually focus on the performance of radiometers in measuring the downward longwave infrared radiation emitted by the atmosphere. This is determined by combining the net (thermal) infrared radiation (netIR) measured by the radiometer sensor and the radiation emitted upward towards the atmosphere by the sensor, the latter requiring the determination of the sensor temperature. Comparisons aimed at determining the uncertainty of pyrgeometer sensitivities therefore require significant netIR signals.

3.2.2. The criteria on environmental conditions listed below are specified to ensure optimal comparisons of this parameter when measured by different instruments. Testing a parameter other than netIR – for instance the ability to determine the irradiance emitted upward towards the atmosphere by the sensor – would result in different criteria for environmental conditions. In addition, comparisons or characterizations of instruments measuring terrestrial radiation can be conducted indoors using near-ambient temperature blackbody cavities under well-controlled conditions.

3.2.3. The environmental conditions mentioned below apply to outdoor comparisons. For indoor comparisons using blackbody cavities, it is only necessary to specify the type of data to be collected; the organizers will determine and set the conditions suitable for the experiments.

(a) Cloud-free night-time conditions should be selected for assessing pyrgeometer responsivities since such conditions favour large netIR signals (in absolute value) and slow varying radiation levels. As with solar irradiance comparisons, it is not possible to recommend a fixed netIR limit as the netIR range depends on the local conditions, in particular, the typical relative humidity at the site. (For example, the analysis of the Third International Pyrgeometer Comparison (IPgC-3) defined night-time as a solar zenith angle greater than 95° and required that netIR < –70 $Wm^{-2}$.)

(b) Rainy conditions should be excluded. In case windowless terrestrial radiation reference instruments are used, even minor rain must be excluded since these instruments can be altered or damaged by water. It is often necessary to consult weather forecasts when deciding when to set up instruments for comparisons. (IPgC-3 excluded nights with rain.)

(c) Relative humidity and temperature should be recorded. This is necessary because these parameters allow the in situ atmospheric water vapour content to be determined, which helps to avoid high water vapour content conditions that may induce condensation in or on the instruments. It is recommended to set a limit on in situ atmospheric water content in such cases.

(d) IWV must be recorded and considered in the analysis. Humidity may be used to estimate IWV, although such estimations involve significant uncertainty. Some pyrgeometers are known to exhibit different behaviour when compared to reference instruments when IWV is low, typically when IWV < 10 mm (Gröbner and Wacker, 2015); such conditions may be excluded. When pyrgeometers are used in conditions with very low IWV, the uncertainty is increased.

(e) Wind must be recorded and considered in the analysis in case absolute cavity pyrgeometers (ACPs) are used in the comparison. A subsection at the end of this annex addresses comparisons including ACPs and lists specific recommendations for reducing the uncertainty linked to convection effects, which are pertinent to such comparisons.

[1] Establishing the traceability of common pyrgeometers presents challenges when they are used to monitor terrestrial irradiance emitted by the atmosphere towards the surface because the spectrum of this irradiance differs from that of a blackbody emitter, and the domes or windows of the pyrgeometers do not have uniform spectral transmittance. When pyrgeometers are used to monitor the terrestrial irradiance emitted by the ground surface, the irradiance spectrum is more similar to that of a blackbody, and a blackbody calibration may be more pertinent than one using night comparisons to a reference under a clear-sky atmosphere.

## 4. MANAGEMENT OF COMPARISON DATA

4.1. WMO promotes the FAIR (Findable, Accessible, Interoperable and Reusable) data principles. However, these principles involve strict criteria on metadata that may be too difficult to implement for comparison campaigns. For radiometer comparisons, the data should at least be findable and accessible in the long term, possibly on request rather than being generally accessible, and preferably reusable.

4.2. The comparison organizers should define the data format and extent of the metadata required for the datasets in advance for easy data exchange. The environmental condition section above has highlighted auxiliary parameters to be recorded and available to all participants so that selection criteria can be applied during the analysis. The data that do not fulfil the chosen selection criteria should be *flagged* as not satisfying the criteria, *but they should not be deleted and should remain available for potential alternate analyses*. For consistency, the auxiliary parameters are also listed below as data to be collected.

### 4.3. Data to be collected for solar radiation instrument comparisons

(a) Solar DNI[2] or global irradiance for pyranometer comparisons;

(b) Continuous raw data sampling (typically, voltage, current or resistance, and, if available, instrument temperature) at the recommended sampling rate depending on the instrument type;

(c) AOD, humidity or IWV, and wind.[3]

### 4.4. Data to be collected for terrestrial radiation instrument comparisons

#### 4.4.1. *Outdoor comparisons*

(a) Terrestrial irradiance[4] and netIR;

(b) Continuous raw data sampling (typically voltage and instrument temperature) at the usual sampling rate;[5] however, additional sampling rate recommendations for evaluating terrestrial radiation stability for comparisons including ACPs are listed in the subsection at the end of this annex addressing comparisons including ACPs;

(c) Temperature, humidity, IWV column and wind.[6]

#### 4.4.2. *Indoor characterizations of thermal infrared radiometers*

Indoor characterizations of thermal infrared radiometers, especially those using blackbody cavities, rely on the precise determination of radiation and temperature changes affecting the instrument. Typically, an attempt is made to determine the spatial temperature distribution

---

[2] Solar DNI is the main parameter to be analysed. It should be recorded as a time aggregate, for example, an average, to ensure comparability when instruments with different time constants are compared.

[3] Auxiliary parameters, such as AOD, humidity or IWV, and wind are most likely to be used for data selection criteria. IWV influences the solar spectrum, especially in the near infrared, possibly leading to significant uncertainties when windowed pyrheliometers are compared to windowless absolute cavity radiometers.

[4] Terrestrial irradiance is the main parameter to be analysed. It should be recorded as a time aggregate, for example, a one-minute average, that is comparable when instruments with different time constants are compared.

[5] For radiation reference comparisons, the raw data at the original sampling rate must be available to allow the recalculation of irradiance using different calibration methods. The metadata should enable the original irradiance to be recalculated.

[6] Auxiliary meteorological parameters, such as temperature, humidity and wind are most likely to be used as criteria for data selection.

and its evolution, and multiple sensors are used to determine temperature (of the controlled environment and instrument). Knowledge of the humidity is also important. The data to be collected are the following:

(a) Ambient temperature and humidity of the controlled environment in which the experiment takes place (laboratory and/or blackbody cavity; for blackbody cavities, data from the different blackbody temperature sensors must be recorded);

(b) Instrument signal (for example, thermopile signal);

(c) Instrument temperature (or temperatures for instruments featuring multiple temperature sensors).

## 5. SPECIFIC RECOMMENDATIONS FOR COMPARISONS INCLUDING ABSOLUTE CAVITY PYRGEOMETERS

If ACPs are used in radiation reference comparisons, convection in the ACP concentrator is suspected to be a significant source of variability. Windy conditions can lead to increased convection in the ACP concentrator and thus, increased variability. This is an ongoing area of research, but the following recommendations are issued to help advance such research and reduce the uncertainty linked to convection. These recommendations may change pending new analysis results:

(a) There should be a requirement that the terrestrial irradiance must be stable to within less than 1 $Wm^{-2}$ during the ACP calibration cycle when using the rate of change in the thermopile voltage signal as a predictand helps to reduce uncertainty due to the convection effect. However, a reliable method for estimating terrestrial irradiance variability must be available, including an estimation of the variability within time aggregation periods (typically one minute). Thus, one instrument should provide reference stability measurements of terrestrial irradiance at a sub-minute sampling rate (about 10 or more measurements per minute).

(b) ACP raw data should also be acquired during least squares regression (LSQ) calibration heating and cooling periods if LSQ calibrations are performed. This applies to both outdoor comparisons and indoor characterizations. Such data have proven to be valuable in reducing the uncertainty of the LSQ calibration procedure.

(c) Since wind most likely influences ACP convection, wind monitoring should be performed during outdoor comparisons including ACPs. Wind data should facilitate the analysis. In addition, a limit on wind speed may be chosen, but a specific value for such a limit cannot yet be recommended.

(d) While there are empirical models of the convection coefficient developed from ACP measurements and comparisons to SI reference radiometers, a model developed independent of reference irradiance and using the design of the concentrator and subsequently confirmed in indoor or outdoor measurements has yet to be developed. Temperature and humidity should be monitored during comparisons including ACPs. It should be noted that infrared integrating sphere (IRIS) radiometers are insensitive to convection, and comparisons between IRIS radiometers and ACPs can potentially help resolve this issue.

# ANNEX 7.E. GOVERNANCE AND TRACEABILITY OF ATMOSPHERIC LONGWAVE IRRADIANCE

**Comprising the Annex to Resolution 1 (CIMO-17)**

According to its terms of reference, in response to the requirement for standardization of atmospheric longwave radiation measurements, the Commission for Instruments and Methods of Observation (CIMO) decides to establish a governance framework for the World Infrared Standard Group (WISG).

The governance framework comprises an advisory group of at least five experts in atmospheric longwave radiation measurements, appointed by the president of CIMO for each International Pyrgeometer Comparison, preferably from among the participants in the comparison.

The comparison's leader, appointed by the Physikalisch Meteorologisches Observatorium Davos (PMOD), will be invited to participate in the advisory group's meeting.

The tasks of the advisory group are, but are not limited to:

(a) To review the status and stability of WISG, and evaluate its role as operational reference standard for providing a stable longwave reference, based on the analysis provided by the PMOD WRC;

(b) To recommend the updating of the calibration factors and changes to WISG, if necessary;

(c) To ensure the supervision of the International Pyrgeometer Comparison, scheduled to take place every five years in conjunction with the International Pyrheliometer Comparison;

(d) To review progress in and provide advice on maintaining and improving traceability to the SI through the International Pyrgeometer Comparison;

(e) To report its findings and recommendations to the CIMO Management Group.

# ANNEX 7.F. USEFUL FORMULAE

## General

All astronomical data can be derived from tables in the nautical almanacs or ephemeris tables. However, approximate formulae are presented for practical use. Michalsky (1988a, 1988b) compared several sets of approximate formulae and found that the best are the equations presented as convenient approximations in the *Astronomical Almanac* (United States Naval Observatory, 1993). They are reproduced here for convenience.

## The position of the Sun

To determine the actual location of the Sun, the following input values are required:

(a) Year;

(b) Day of year (for example, 1 February is day 32);

(c) Fractional hour in UT (for example, hours + minutes/60 + number of hours from Greenwich);

(d) Latitude in degrees (north positive);

(e) Longitude in degrees (east positive).

To determine the Julian date (JD), the *Astronomical Almanac* determines the present JD from a prime JD set at noon 1 January 2000 UT. This JD is 2 451 545.0. The JD to be determined can be found from:

$$\mathrm{JD} = 2\,432\,917.5 + \mathrm{delta} \cdot 365 + \mathrm{leap} + \mathrm{day} + \mathrm{hour}/24$$

where:

delta = year – 1949
leap = integer portion of (delta/4)

The constant 2 432 917.5 is the JD for 0000 1 January 1949 and is simply used for convenience.

Using the above time, the ecliptic coordinates can be calculated according to the following steps ($L$, $g$ and $l$ are in degrees):

(a) $n$ = JD – 2 451 545;

(b) $L$ (mean longitude) = 280.460 + 0.9856474 · $n$ ($0 \le L < 360°$);

(c) $g$ (mean anomaly) = 357.528 + 0.9856003 · $n$ ($0 \le g < 360°$);

(d) $l$ (ecliptic longitude) = $L$ + 1.915 · sin ($g$) + 0.020 · sin ($2g$) ($0 \le l < 360°$);

(e) $ep$ (obliquity of the ecliptic) = 23.439 – 0.0000004 · $n$ (degrees).

It should be noted that the specifications indicate that all multiples of 360° should be added or subtracted until the final value falls within the specified range.

From the above equations, the celestial coordinates can be calculated – the right ascension (*ra*) and the declination (*dec*) – by:

$$\tan(ra) = \cos(ep) \cdot \sin(l) / \cos(l)$$
$$\sin(dec) = \sin(ep) \cdot \sin(l)$$

To convert from celestial coordinates to local coordinates, that is, right ascension and declination to azimuth ($A$) and altitude ($a$), it is convenient to use the local hour angle ($h$). This is calculated by first determining the Greenwich mean sidereal time (GMST, in hours) and the local mean sidereal time (LMST, in hours):

$$\mathrm{GMST} = 6.697\ 375 + 0.065\ 709\ 824\ 2 \cdot n + \mathrm{hour}(\mathrm{UT})$$

where: 0 ≤ GMST < 24 h

$$\mathrm{LMST} = \mathrm{GMST} + (\text{east longitude}) / (15^\circ\,\mathrm{h}^{-1})$$

From the LMST, the hour angle (*ha*) is calculated as (*ha* and *ra* are in degrees):

$$ha = 15 \cdot \mathrm{LMST} - ra \quad (-12 \le ha < 12\mathrm{h})$$

Before the Sun reaches the meridian, the hour angle is negative. Caution should be observed when using this term, because it is opposite to what some solar researchers use.

The calculations of the solar elevation (*el*) and the solar azimuth (***az***) follow (*az* and *el* are in degrees):

$$\sin(el) = \sin(dec) \cdot \sin(\mathrm{lat}) + \cos(dec) \cdot \cos(\mathrm{lat}) \cdot \cos(ha)$$

and:

$$\sin(az) = -\cos(dec) \cdot \sin(ha) / \cos(el)$$
$$\cos(az) = (\sin(dec) - \sin(el) \cdot \sin(\mathrm{lat})) / (\cos(el) \cdot \cos(\mathrm{lat}))$$

where the azimuth is from 0° north, positive through east.

To take into account atmospheric refraction and to derive the apparent solar elevation ($h$) or the apparent solar zenith angle, the *Astronomical Almanac* proposes the following equations:

(a) A simple expression for refraction $r$ for zenith angles less than 75°:

$$r = 0^\circ.004\ 52\, P \tan z / (273 + T)$$

where $z$ is the zenith distance in degrees, $P$ is the pressure in hectopascals, and $T$ is the temperature in °C.

(b) For zenith angles greater than 75° and altitudes below 15°, the following approximate formula is recommended:

$$r = \frac{P(0.159\ 4 + 0.019\ 6a + 0.000\ 02a^2)}{\left[(273 + T)(1 + 0.505a + 0.084\ 5a^2)\right]}$$

where $a$ is the elevation (90° – $z$) where $h = el + r$ and the apparent solar zenith angle $z_0 = z + r$.

### Sun–Earth distance

The present-day eccentricity of the orbit of the Earth around the Sun is small but significant to the extent that the square of the Sun–Earth distance $R$ and, therefore, the solar irradiance at the Earth, varies by 3.3% from the mean. In AU, to an uncertainty of $10^{-4}$:

$$R = 1.000\,14 - 0.016\,71 \cdot \cos(g) - 0.000\,14 \cdot \cos(2g)$$

where $g$ is the mean anomaly and is defined above. The solar eccentricity is defined as the mean Sun–Earth distance (1 AU, $R_0$) divided by the actual Sun–Earth distance squared:

$$E_0 = (R_0/R)^2$$

### Airmass

In calculations of extinction, the path length through the atmosphere, which is called the absolute optical airmass, must be known. The relative airmass for an arbitrary atmospheric constituent, $m$, is the ratio of the airmass along the slant path to the airmass in the vertical direction; hence, it is a normalizing factor. In a plane parallel, non-refracting atmosphere $m$ is equal to 1/sin $h_0$ or 1/cos $z_0$.

### Local apparent time

The mean solar time, on which our civil time is based, is derived from the motion of an imaginary body called the mean Sun, which is considered as moving at uniform speed in the celestial equator at a rate equal to the average rate of movement of the true Sun. The difference between this fixed time reference and the variable local apparent time is called the equation of time, $E_q$, which may be positive or negative depending on the relative position of the true mean Sun. Thus:

$$LAT = LMT + E_q = CT + LC + E_q$$

where $LAT$ is the local apparent time (also known as $TST$, true solar time), $LMT$ is the local mean time; $CT$ is the civil time (referred to a standard meridian, thus also called standard time); and $LC$ is the longitude correction (4 min for every degree). $LC$ is positive if the local meridian is east of the standard and vice versa.

For the computation of $E_q$, in minutes, the following approximation may be used:

$$E_q = 0.017\,2 + 0.428\,1 \cos \Theta_0 - 7.351\,5 \sin \Theta_0 - 3.349\,5 \cos 2\Theta_0 - 9.361\,9 \sin 2\Theta_0$$

where $\Theta_0 = 2\,\pi d_n/365$ in radians or $\Theta_0 = 360\,d_n/365$ in degrees, and where $d_n$ is the day number ranging from 0 on 1 January to 364 on 31 December for a normal year or to 365 on 31 December for a leap year. The maximum error of this approximation is 35 s (which is excessive for some purposes, such as airmass determination).

## ANNEX 7.G. DIFFUSE SKY RADIATION – CORRECTION FOR A SHADING RING

The shading ring is mounted on two rails oriented parallel to the Earth's axis in such a way that the centre of the ring coincides with the pyranometer during the equinox. The diameter of the ring ranges from 0.5 to 1.5 m, and the ratio of the width to the radius $b/r$ ranges from 0.09 to 0.35. The adjustment of the ring to the solar declination is made by sliding the ring along the rails. The length of the shading band and the height of the mounting of the rails relative to the pyranometer are determined from the solar position during the summer solstice; the higher the latitude, the longer the shadow band and the lower the rails.

Several authors, for example, Drummond (1956), Dehne (1980) and Le Baron et al. (1980), have proposed formulae for operational corrections to the sky radiation accounting for the part not measured due to the shadow band. For a ring with $b/r < 0.2$, the radiation $D_v$ lost during a day can be expressed as:

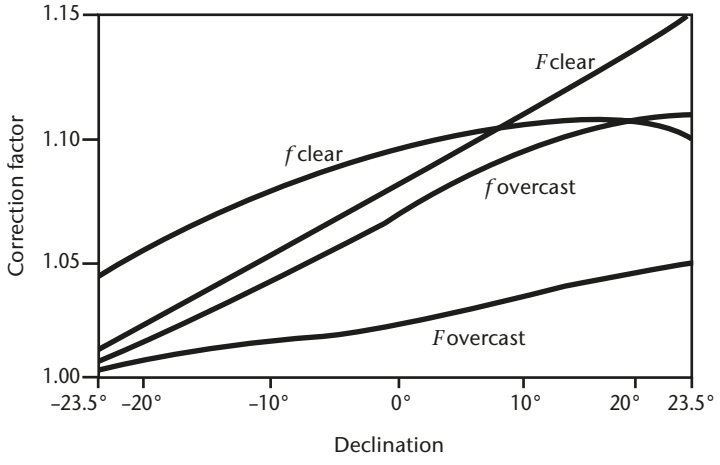
$$D_v \approx \frac{b}{r} \cos^3\delta \int_{t_{rise}}^{t_{set}} L(t) \cdot \sin h_\odot(t)\, dt$$

where $\delta$ is the declination of the Sun; $t$ is the hour angle of the Sun; $t_{rise}$ and $t_{set}$ are the hour angle at sunrise and sunset, respectively, for a mathematical horizon ($\Phi$ being the geographic latitude, $t_{rise} = -t_{set}$ and $\cos t_{rise} = -\tan\Phi \cdot \tan\delta$); $L(t)$ is the sky radiance during the day; and $h_\odot$ is the solar elevation.

With this expression and some assumptions on the sky radiance, a correction factor $f$ can be determined:

$$f = \frac{1}{1 - \frac{D_v}{D}}$$

$D$ being the unobscured sky radiation. In the figure below, an example of this correction factor is given for both a clear and an overcast sky, compared with the corresponding empirical curves.




**Comparison of calculated and empirically determined correction factors for a shading ring, with $b/r$ = 0.169; $f$ indicates calculated curves and $F$ indicates empirical ones. Note that this curve is valid for a specific latitude only; in this case, the latitude is close to the polar circle, where in mid-winter (declination –23 degrees), the Sun stays close to the horizon, and the correction factor is close to 1.**

*Source:* Dehne (1980)

It is evident that the deviations from the theoretical curves depend on the climatological factors of the station and should be determined experimentally by comparing the instrument equipped with a shading ring with an instrument shaded by a continuously traced disc. If no experimental data are available for the station, data computed for the overcast case with the corresponding $b/r$ should be used. Thus:

$$\frac{D_{\mathrm{v}}}{D_{\mathrm{overcast}}} = \frac{b}{r}\cos^3\delta\left(t_{\mathrm{set}} - t_{\mathrm{rise}}\right)\cdot\sin\Phi\cdot\sin\delta + \cos\Phi\cdot\cos\delta\cdot\left(\sin t_{\mathrm{set}} - \sin t_{\mathrm{rise}}\right)$$

where $\delta$ is the declination of the Sun, $\Phi$ is the geographic latitude, and $t_{\mathrm{rise}}$ and $t_{\mathrm{set}}$ are the solar hour angle for set and rise, respectively (for details, see above).

## REFERENCES AND FURTHER READING


Bais, A.; Topaloglou, C. Kazadtzis, S. et al. *Report of the LAP/COST/WMO Intercomparison of Erythemal Radiometers* (WMO/TD-No. 1051). Global Atmosphere Watch (GAW) Report No. 141; World Meteorological Organization (WMO): Geneva, 2000.

Bass, A. M. and Paur, R. J. The Ultraviolet Cross-sections of Ozone: I. The Measurements. In Atmospheric Ozone, Proceedings of the Quadrennial Ozone Symposium held in Halkidiki, Greece 3–7 September 1984; Zerefos, C. S.; Ghazi, A., Eds.; Reidel: Dordrecht, Netherlands, 1985, 606–610. https://doi.org/10.1007/978-94-009-5313-0_120.

Bernhard, G.; Seckmeyer, G. Uncertainty of Measurements of Spectral Solar UV Irradiance. Journal of Geophysical Research: Atmospheres **1999**, *104* (D12), 14321–14345. https://doi.org/10.1029/1999JD900180.

Bodhaine, B. A.; Wood, N. B.: Dutton, E. G. et al. On Rayleigh Optical Depth Calculations. Journal of Atmospheric and Oceanic Technology **1999,** *16* (11), 1854–1861. https://doi.org/10.1175/1520-0426(1999)016<1854:ORODC>2.0.CO;2.

Cordero R. R., Seckmeyer, G.; Pissulla, D. et al. Uncertainty Evaluation of Spectral UV Irradiance Measurements. Measurement Science and Technology **2008**, *19* (4), 1–15. https://dx.doi.org/10.1088/0957-0233/19/4/045104.

Cordero R. R.; Seckmeyer, G.; Damiani, A. et al. Monte Carlo-based Uncertainties of Surface UV Estimates from Models and from Spectroradiometers. Metrologia **2013**, *50* (5), L1–L5. https://dx.doi.org/10.1088/0026-1394/50/5/L1.

Dehne, K. Vorschlag zur standardisierten Reduktion der Daten verschiedener nationaler Himmelsstrahlungs-Messnetze. Annalen der Meteorologie (Neue Folge) **1980**, *16, 57–59.* https://www.dwd.de/EN/ourservices/pbfb_verlag_annalen/pdf_einzelbaende/16_pdf.pdf?__blob=publicationFile&v=3.

Drummond, A. J. On the Measurement of Sky Radiation. Archiv für Meteorologie, Geophysik und Bioklimatologie Serie B **1956**, *7*, 413–436. https://doi.org/10.1007/BF02242969.

Feierabend, M.; Gröbner, J.; Müller, I. et al. Bilateral Comparison of Irradiance Scales between PMOD/WRC and PTB for Longwave Downward Radiation Measurements. Metrologia **2023** *60* (2), 025010. . https://doi.org/10.1088/1681-7575/acbd51.

Finsterle, W. *Report on the WMO International Pyrheliometer Comparison (IPC-XIII)* (Instruments and Observing Methods (IOM) report No. 140); World Meteorological Organization (WMO): Geneva, 2023.

Fioletov, V.; Janjai, S.; Koide, T. et al. *Data Quality Objectives (DQO) for Solar Ultraviolet Radiation Measurements – Part I: Scanning Spectral and Broadband Instruments. Addendum to Global Atmosphere Watch (GAW) Report No. 146 – Quality Assurance in Monitoring Solar Ultraviolet Radiation: State of the Art* (GAW Report No. 198); World Meteorological Organization (WMO): Geneva, 2011.

Forgan, B. W. A New Method for Calibrating Reference and Field Pyranometers. Journal of Atmospheric and Oceanic Technology **1996**, *13* (3),638–645. https://doi.org/10.1175/1520-0426(1996)013%3C0638:ANMFCR%3E2.0.CO;2.

Frouin, R.; Deschamps, P.-Y.; Lecomte, P. Determination from Space of Atmospheric Total Water Vapour Amounts by Differential Absorption near 940 nm: Theory and Airborne Verification. Journal of Applied Meteorology **1990**, *29* (6), 448–460. https://www.jstor.org/stable/26185098.

Gröbner, J. Operation and Investigation of a Tilted Bottom Cavity for Pyrgeometer Characterizations. Appl. Opt., AO **2008**, *47* (24), 4441–4447. https://doi.org/10.1364/AO.47.004441.

Gröbner, J.; Wacker, S. Longwave Irradiance Measurements Using IRIS Radiometers at the PMOD/WRC-IRS. In AIP Conference Procedings, 2013; *1531*, 488, https://doi.org/10.1063/1.4804813.

Gröbner, J.; Wacker, S. *Pyrgeometer Calibration Procedure at the PMOD/WRC-IRS*, (Instruments and Observing Methods (IOM) Report No. 120); World Meteorological Organization (WMO): Geneva, 2015.

Gröbner, J.; Thomann, C. *Report on the 3rd WMO International Pyrgeometer Intercomparison (IPgC-III)* (Instruments and Observing Methods (IOM) Report No. 141); World Meteorological Organization (WMO): Geneva, 2023.

International Commission on Illumination (CIE). Methods of Characterizing Illuminance Meters and Luminance Meters: Performance, Characteristics and Specifications, CIE 069-1987. Vienna, 1987.*

[*Replaced by

International Organization for Standardization (ISO)/International Commission on Illumination (CIE). *Characterization of the Performance of Illuminance Meters and Luminance Meters, ISO/CIE 19476:2014*. Vienna, 2014.]

International Commission on Illumination (CIE). *Guide to Recommended Practice of Daylight Measurement*, CIE 108-1994. Vienna, 1994.

International Electrotechnical Commission (IEC). *International Electrotechnical Vocabulary*, Part 845: Lighting, IEC 60050-845. Geneva, 2020.

International Organization for Standardization (ISO). *Solar Energy – Calibration of Field Pyrheliometers by Comparison to a Reference Pyrheliometer*, ISO 9059:1990. Geneva, 1990. https://www.iso.org/standard/16628.html.

International Organization for Standardization (ISO). *Solar Energy – Calibration of a Pyranometer Using a Pyrheliometer*; ISO 9846:1993; Geneva, 1993. https://www.iso.org/standard/17724.html.

International Organization for Standardization (ISO). *Solar Energy – Specification and Classification of Instruments for Measuring Hemispherical Solar and Direct Solar Radiation*; ISO 9060:2018; Geneva, 2018, https://www.iso.org/standard/67464.html.

International Organization for Standardization (ISO). *Solar Energy – Pyranometers – Recommended Practice for Use*; ISO/TR 9901:2021; Geneva, 2021. https://www.iso.org/standard/81937.html.

International Organization for Standardization (ISO). *Solar Energy – Calibration of Field Pyranometers by Comparison to a Reference Pyranometer*; ISO 9847:2023 (Cor. 2023-11); Geneva, 2023. https://www.iso.org/standard/78800.html.

International Organization for Standardization (ISO)/International Electrotechnical Commission (IEC). Uncertainty of Measurement – Part 3: Guide to the Expression of Uncertainty in Measurement; ISO/IEC Guide 98-3:2008, Incl. Suppl. 1:2008/Cor 1:2009, Suppl. 1:2008, Suppl. 2:2011. Geneva, 2008. https://www.iso.org/standard/50461.html.(equivalent to: Joint Committee for Guides in Metrology (JCGM) *Evaluation of Measurement Data – Guide to the Expression of Uncertainty in Measurement*; JCGM 100:2008; 2008, Corrected in 2010. https://www.bipm.org/documents/20126/2071204/JCGM_100_2008_E.pdf/cb0ef43f-baa5-11cf-3f85-4dcd86f77bd6.)

Janjai, S.; Webb, A.; Seckmeyer, G. et al. *Standard Operating Procedures (SOPs) for Spectral Instruments Measuring Spectral Solar Ultraviolet Irradiance* (Global Atmosphere Watch (GAW) Report No. 212). Geneva, 2014.

Kerr, J. B.; McElroy, C. T. Evidence for Large Upward Trends of Ultraviolet-B Radiation Linked to Ozone Depletion. Science **1993**, *262* (5136), 1032–1034 https://doi.org/10.1126/science.262.5136.1032.

Le Baron, B. A.; Peterson, W. A.;. Dirmhirn, I. Corrections for Diffuse Irradiance Measured with Shadowbands. Solar Energy **1980**, *25* (1),1–13. https://doi.org/10.1016/0038-092X(80)90401-6.

McArthur, L. J. B. *Baseline Surface Radiation Network (BSRN) Operations Manual* (WMO/TD-No. 1274), Version 2.1. World Climate Research Programme (WCRP)-121; World Meteorological Organization (WMO): Geneva, 2005.

McKinlay, A. F; Diffey, B. L. A Reference Action Spectrum for Ultraviolet Induced Erythema in Human Skin. In: *Human Exposure to Ultraviolet Radiation: Risks and Regulations*, Passchier, W. F.; Bosnjakovic, B. F. M., Eds.; Elsevier: Amsterdam, 1987; 83–87.

Michalsky, J. J. The Astronomical Almanac's Algorithm for Approximate Solar Position (1950–2050). Solar Energy **1988a**, *40* (3), 227–235. https://doi.org/10.1016/0038-092X(88)90045-X.

Michalsky, J. J. Errata. The Astronomical Almanac's Algorithm for Approximate Solar Position (1950–2050). Solar Energy **1988b**, *41* (1):113. https://doi.org/10.1016/0038-092X(88)90122-3.

Parrish, J. A.; Jaenicke, K. F.; Anderson, R. R. Erythema and Melanogenesis Action Spectra of Normal Human Skin. Photochemistry and Photobiology **1982**, *36* (2), 187–191. https://doi.org/10.1111/j.1751-1097.1982.tb04362.x.

Philipona, R. Sky-scanning radiometer for absolute measurements of atmospheric long-wave radiation. Applied Optics **2001**, *40* (15), 2376–2383. https://doi.org/10.1364/AO.40.002376.

Philipona, R.; Dutton, E. G.; Stoffel, T. et al. Atmospheric Longwave Irradiance Uncertainty: Pyrgeometers Compared to an Absolute Sky-scanning Radiometer, Atmospheric Emitted Radiance Interferometer, and Radiative Transfer Model Calculations. Journal of Geophysical Research: Atmospheres **2001**, *106* (D22), 28129–28141. https://doi.org/10.1029/2000JD000196.

Rüedi, I., Ed. International Pyrheliometer Comparison IPC-IX, 25 September – 13 October 2000, Davos, Switzerland, Results and Symposium. MeteoSwiss Working Report No. 197, Swiss Meteorological Institute: Davos and Zurich, 2001; PMOD/WRC Internal Report. https://doi.org/10.3929/ethz-a-004371547.

Schneider, W.; Moortgat, G. K.; Tyndall, G. S. et al. Absorption Cross-Sections of $NO_2$ in the UV and Visible Region (200 – 700 Nm) at 298 K. Journal of Photochemistry and Photobiology A: Chemistry **1987**, *40* (2), 195–217. https://doi.org/10.1016/1010-6030(87)85001-3.

Seckmeyer, G.; Bais, A.; Bernhard, G. et al. *Instruments to Measure Solar Ultraviolet Radiation – Part 1: Spectral Instruments* (WMO/TD-No. 1066). Global Atmosphere Watch (GAW) Report No. 125; World Meteorological Organization (WMO): Geneva, 1999.

Seckmeyer, G.; Bais, A.; Bernhard, G. et al. *Instruments to Measure Solar Ultraviolet Radiation – Part 2: Broadband Instruments Measuring Erythemally Weighted Solar Irradiance*. (WMO/TD-No. 1289), Global Atmosphere Watch (GAW) Report No. 164; World Meteorological Organization (WMO): Geneva, 2008.

Seckmeyer, G.; Bais, A.; Bernhard, G. et al. *Instruments to Measure Solar Ultraviolet Radiation – Part 3: Multi-channel Filter Instruments* (WMO/TD-No. 1537), Global Atmosphere Watch Report (GAW) No. 190; World Meteorological Organization (WMO): Geneva, 2010a.

Seckmeyer, G.; Bais, A.; Bernhard, G. et al. *Instruments to Measure Solar Ultraviolet Radiation – Part 4: Array Spectroradiometers* (WMO/TD-No. 1538), Global Atmosphere Watch Report No. 191; World Meteorological Organization (WMO): Geneva, 2010b.

United States Naval Observatory. *The Astronomical Almanac*; Nautical Almanac Office: Washington, 1993.

Vigroux, E. Contribution à l'étude expérimentale de l'absorption de l'ozone. Annales de Physique **1953**, *12* (8),709–762. https://doi.org/10.1051/anphys/195312080709.

Webb, A. R.; Gardiner, B. G.; Blumthaler, M. et al. A Laboratory Investigation of Two Ultraviolet Spectroradiometers. Photochemistry and Photobiology **1994**, *60* (1), 84–90. https://doi.org/10.1111/j.1751-1097.1994.tb03947.x.

Webb, A.; Gardiner, B. G.; Martin, T. J. et al. *Guidelines for Site Quality Control of UV Monitoring* (WMO/TD-No. 884), Global Atmosphere Watch (GAW) Report No. 126; World Meteorological Organization (WMO): Geneva, 1998.

Webb, A.; Gardiner, B. G.; Leszczynski, K. et al. *Quality Assurance in Monitoring Solar Ultraviolet Radiation: the State of the Art* (WMO/TD-No. 1180). Global Atmosphere Watch (GAW) Report No. 146; World Meteorological Organization (WMO): Geneva, 2003.

World Meteorological Organization (WMO). *Revised Instruction Manual on Radiation Instruments and Measurements* (WMO/TD-No. 149). World Climate Research Programme (WCRP) Publications Series No. 7. Geneva, 1986.

World Meteorological Organization (WMO). *Report of the Second Meeting of the Ozone Research Managers of the Parties to the Vienna Convention for the Protection of the Ozone Layer* (WMO Global Ozone Research and Monitoring Project Report No. 32). Geneva, 1993.

World Meteorological Organization (WMO). *WMO-UMAP Workshop on Broad-Band UV Radiometers* (WMO/TD-No. 894). Global Atmosphere Watch (GAW) Report No. 120. Geneva, 1997.

World Meteorological Organization (WMO). *Commission for Instruments and Methods of Observation – Thirteenth Session: Abridged Final Report with Resolutions and Recommendations* (WMO-No. 947). Geneva, 2003.

World Meteorological Organization (WMO). *WMO/GAW Experts Workshop on a Global Surface-based Network for Long Term Observations of Column Aerosol Optical Properties* (WMO/TD-No. 1287), Global Atmosphere Watch (GAW) Report No. 162; World Meteorological Organization (WMO): Geneva, 2005.

World Meteorological Organization (WMO). *Commission for Instruments and Methods of Observation – Abridged Final Report of the Seventeenth Session* (WMO-No. 1227). Geneva, 2018.

# CHAPTER 8. MEASUREMENT OF SUNSHINE DURATION

## 8.1 GENERAL

The term "sunshine" is associated with the brightness of the solar disc exceeding the background of diffuse sky light, or, as is better observed by the human eye, with the appearance of shadows behind illuminated objects. As such, the term is related more to visual radiation than to energy radiated at other wavelengths, although both aspects are inseparable. In practice, however, the first definition was established directly by the relatively simple Campbell-Stokes sunshine recorder (see 8.2.3), which detects sunshine if the beam of solar energy concentrated by a special lens is able to burn a special dark paper card. This recorder was already introduced in meteorological stations in 1880 and is still used in many networks. Since no international regulations on the dimensions and quality of the special parts were established, applying different laws of the principle gave different sunshine duration values.

In order to homogenize the data of the worldwide network for sunshine duration, a special design of the Campbell-Stokes sunshine recorder, the so-called interim reference sunshine recorder (IRSR), was recommended as the reference (WMO, 1962). The improvement made by this "hardware definition" was effective only during the interim period needed for finding a precise physical definition allowing for both designing automatic sunshine recorders and approximating the "scale" represented by the IRSR as near as possible. With regard to the latter, the settlement of a direct solar threshold irradiance corresponding to the burning threshold of the Campbell-Stokes recorders was strongly advised. Investigations at different stations showed that the threshold irradiance for burning the card varied between 70 and 280 W $m^{-2}$ (Bider, 1958; Baumgartner, 1979). However, further investigations, especially performed with the IRSR in France, resulted in a mean value of 120 W $m^{-2}$, which was finally proposed as the threshold of direct solar irradiance to distinguish bright sunshine.[1] With regard to the spread of test results, a threshold accuracy of 20% in instrument specifications is accepted. A pyrheliometer was recommended as the reference sensor for the detection of the threshold irradiance. For future refinement of the reference, the settlement of the field-of-view angle of the pyrheliometer seems to be necessary (see the present volume, Chapter 7, 7.2 and 7.2.1.3).

### 8.1.1 Definition

According to WMO (2010),[2] sunshine duration during a given period is defined as the sum of the time for which the direct solar irradiance exceeds 120 W $m^{-2}$.

### 8.1.2 Units and scales

The physical quantity of sunshine duration ($SD$) is, evidently, time. The units used are seconds or hours. For climatological purposes, derived terms such as "hours per day" or "daily sunshine hours" are used, as well as percentage quantities, such as "relative daily sunshine duration", where $SD$ may be related to the extra-terrestrial possible, or to the maximum possible, sunshine duration ($SD_0$ and $SD_{max}$, respectively). The measurement period (day, decade, month, year, and so on) is an important addendum to the unit.

### 8.1.3 Meteorological requirements

Performance requirements are given in the present volume, Chapter 1. Hours of sunshine should be measured with an uncertainty of ±0.1 h and a resolution of 0.1 h.

---

1 Recommended by CIMO at its eighth session (1981) through Recommendation 10 (CIMO-VIII).
2 Recommended by CIMO at its tenth session (1989) through Recommendation 16 (CIMO-X).

Since the number and steepness of the threshold transitions of direct solar radiation determine the possible uncertainty of sunshine duration, the meteorological requirements on sunshine recorders are essentially correlated with the climatological cloudiness conditions (WMO, 1985).

In the case of a cloudless sky, only the hourly values at sunrise or sunset can (depending on the amount of dust) be erroneous because of an imperfectly adjusted threshold or spectral dependencies.

In the case of scattered clouds (cumulus, stratocumulus), the steepness of the transition is high and the irradiance measured from the cloudy sky with a pyrheliometer is generally lower than 80 W $m^{-2}$; that means low requirements on the threshold adjustment. But the field-of-view angle of the recorder can influence the result if bright cloud clusters are near the sun.

The highest precision is required if high cloud layers (cirrus, altostratus) with small variations of the optical thickness attenuate the direct solar irradiance around the level of about 120 W $m^{-2}$. The field-of-view angle is effective as well as the precision of the threshold adjustment.

The requirements on sunshine recorders vary, depending on site and season, according to the dominant cloud formation. The latter can be roughly described by three ranges of relative daily sunshine duration $SD/SD_0$ (see 8.1.2), namely "cloudy sky" by ($0 \le SD/SD_0 < 0.3$), "scattered clouds" by ($0.3 \le SD/SD_0 < 0.7$) and "fair weather" by ($0.7 \le SD/SD_0 \le 1.0$). The results for dominant clouded sky generally show the highest percentage of deviations from the reference.

### 8.1.3.1 *Application of sunshine duration data*

One of the first applications of $SD$ data was to characterize the climate of sites, especially of health resorts. This also takes into account the psychological effect of strong solar light on human well-being. It is still used by some local authorities to promote tourist destinations.

The description of past weather conditions, for instance of a month, usually contains the course of daily $SD$ data.

For these fields of application, an uncertainty of about 10% of mean $SD$ values seemed to be acceptable over many decades.

### 8.1.3.2 *Correlations to other meteorological variables*

The most important correlation between sunshine duration and global solar radiation $G$ is described by the so-called Ångström formula:

$$G/G_0 = a + b \cdot (SD/SD_0) \tag{8.1}$$

where $G/G_0$ is the so-called clearness index (related to the extra-terrestrial global irradiation), $SD/SD_0$ is the corresponding sunshine duration (related to the extra-terrestrial possible $SD$ value), and $a$ and $b$ are constants which have to be determined monthly. The uncertainty of the monthly means of daily global irradiation derived in this way from Campbell-Stokes data was found to be lower than 10% in summer, and rose up to 30% in winter, as reported for German stations (Golchert, 1981).

The Ångström formula implies the inverse correlation between cloud amount and sunshine duration. This relationship is not fulfilled for high and thin cloudiness and obviously not for cloud fields which do not cover the sun, so that the degree of inverse correlation depends first of all on the magnitude of the statistical data collected (Stanghellini, 1981; Angell, 1990). The improvement of the accuracy of $SD$ data should reduce the scattering of the statistical results, but even perfect data can generate sufficient results only on a statistical basis.

#### 8.1.3.3 *Requirement of automated records*

Since electrical power is available in an increasing number of places, the advantage of the Campbell-Stokes recorder of being self-sufficient is of decreasing importance. Furthermore, the required daily maintenance requirement of replacing the burn card makes the use of Campbell-Stokes recorders problematic at either AWSs or stations with reduced numbers of personnel. Another essential reason to replace Campbell-Stokes recorders by new automated measurement procedures is to avoid the expense of visual evaluations and to obtain more precise results on data carriers permitting direct computerized data processing.

### 8.1.4 Measurement methods

The principles used for measuring sunshine duration and the pertinent types of instruments are briefly listed in the following methods:

(a) Pyrheliometric method: Pyrheliometric detection of the transition of direct solar irradiance through the 120 W $m^{-2}$ threshold (according to Recommendation 10 (CIMO-VIII)). Duration values are readable from time counters triggered by the appropriate upward and downward transitions.

Type of instrument: Pyrheliometer combined with an electronic or computerized threshold discriminator and a time-counting device.

(b) Pyranometric method:

(i) Pyranometric measurement of global ($G$) and diffuse ($D$) solar irradiance to derive the direct solar irradiance as the WMO threshold discriminator value and further as in (a) above.

Type of instrument: Radiometer systems of two fitted pyranometers and one sunshade device combined with an electronic or computerized threshold discriminator and a time-counting device.

(ii) Pyranometric measurement of global ($G$) solar irradiance to estimate sunshine duration.

Type of instrument: A pyranometer combined with an electronic or computerized device which is able to deliver 10 min means as well as minimum and maximum global ($G$) solar irradiance within those 10 min, or alternatively to deliver 1 min means of global ($G$) solar irradiance.

(c) Burn method: Threshold effect of burning paper caused by focused direct solar radiation (heat effect of absorbed solar energy). The duration is read from the total burn length.

Type of instrument: Campbell-Stokes sunshine recorders, especially the recommended version, namely the IRSR (see 8.2).

(d) Contrast method: Discrimination of the insolation contrasts between some sensors in different positions to the sun with the aid of a specific difference of the sensor output signals which corresponds to an equivalent of the WMO recommended threshold (determined by comparisons with reference $SD$ values) and further as in (b) above.

Type of instrument: Specially designed multi-sensor detectors (mostly equipped with photovoltaic cells) combined with an electronic discriminator and a time counter.

(e) Scanning method: Discrimination of the irradiance received from continuously scanned, small sky sectors with regard to an equivalent of the WMO recommended irradiance threshold (determined by comparisons with reference $SD$ values).

Type of instrument: One-sensor receivers equipped with a special scanning device (rotating diaphragm or mirror, for instance) and combined with an electronic discriminator and a time-counting device.

The sunshine duration measurement methods described in the following paragraphs are examples of ways to achieve the above-mentioned principles. Instruments using these methods, with the exception of the Foster switch recorder, participated in the WMO Automatic Sunshine Duration Measurement Comparison in Hamburg from 1988 to 1989 and in the comparison of pyranometers and electronic sunshine duration recorders of Regional Association VI in Budapest in 1984 (WMO, 1986).

The description of the Campbell-Stokes sunshine recorder in 8.2.3 is relatively detailed since this instrument is still widely used in national networks, and the specifications and evaluation rules recommended by WMO should be considered (however, note that this method is no longer recommended,[3] since the duration of bright sunshine is not recorded with sufficient consistency).

A historical review of sunshine recorders is given in Coulson (1975), Hameed and Pittalwala (1989) and Sonntag and Behrens (1992).

## 8.2 INSTRUMENTS AND SENSORS

### 8.2.1 Pyrheliometric method

#### 8.2.1.1 *General*

This method, which represents a direct consequence of the WMO definition of sunshine (see 8.1.1) and is, therefore, recommended to obtain reference values of sunshine duration, requires a weatherproof pyrheliometer and a reliable solar tracker to point the radiometer automatically or at least semi-automatically to the position of the sun. The method can be modified by the choice of pyrheliometer, the field-of-view angle of which influences the irradiance measured when clouds surround the sun.

The sunshine threshold can be monitored by the continuous comparison of the pyrheliometer output with the threshold equivalent voltage $V_{th} = 120\ \mathrm{W\ m^{-2}} \cdot R\ \mu\mathrm{V\ W^{-1}\ m^2}$, which is calculable from the responsivity $R$ of the pyrheliometer. A threshold transition is detected if $\Delta V = V - V_{th}$ changes its sign. The connected time counter is running when $\Delta V > 0$.

#### 8.2.1.2 *Sources of error*

The field-of-view angle is not yet settled by agreed definitions (see the present volume, Chapter 7, 7.2 and 7.2.1.3). Greater differences between the results of two pyrheliometers with different field-of-view angles are possible, especially if the sun is surrounded by clouds. Furthermore, typical errors of pyrheliometers, namely tilt effect, temperature dependence, non-linearity and zero-offset, depend on the class of the pyrheliometer. Larger errors appear if the alignment to the sun is not precise or if the entrance window is covered by rain or snow.

[3] See Recommendation 10 (CIMO-VIII).

### 8.2.2 Pyranometric method

#### 8.2.2.1 *General*

The pyranometric method to derive sunshine duration data is based on the fundamental relationship between the direct solar radiation ($I$) and the global ($G$) and diffuse ($D$) solar radiation:

$$I \cdot \cos\zeta = G - D \tag{8.2}$$

where $\zeta$ is the solar zenith angle and $I \cdot \cos\zeta$ is the horizontal component of $I$. To fulfil equation 8.2 exactly, the shaded field-of-view angle of the pyranometer for measuring $D$ must be equal to the field-of-view angle of the pyrheliometer (see the present volume, Chapter 7). Furthermore, the spectral ranges, as well as the time constants of the pyrheliometers and pyranometers, should be as similar as possible.

In the absence of a sun-tracking pyrheliometer, but where computer-assisted pyranometric measurements of $G$ and $D$ are available, the WMO sunshine criterion can be expressed according to equation 8.2 by:

$$(G - D)/\cos\zeta > 120 \text{ W m}^{-2} \tag{8.3}$$

which is applicable to instantaneous readings.

The modifications of this method in different stations concern first of all:

(a) The choice of pyranometer;

(b) The shading device applied (shade ring or shade disc with solar tracker) and its shade geometry (shade angle);

(c) The correction of shade-ring losses.

As a special modification, the replacement of the criterion in equation 8.3 by a statistically derived parameterization formula (to avoid the determination of the solar zenith angle) for applications in more simple data-acquisition systems should be mentioned (Sonntag and Behrens, 1992).

Different algorithms, based on different assumptions, can be used to estimate sunshine duration from the measurement of only one pyranometer.

The Slob and Monna method (Slob and Monna, 1991) is based on two assumptions on the relation between irradiance and cloudiness, as follows:

(a) A rather accurate calculation of the potential global irradiance at the Earth's surface based on the calculated value of the extra-terrestrial irradiation ($G_0$) by taking into account extinction in the atmosphere. The attenuation factor depends on the solar elevation $h$ and the turbidity $T$ of the atmosphere. The ratio between the measured global irradiance and this calculated value of the clear sky global irradiance is a good measure for the presence of clouds;

(b) An evident difference between the minimum and maximum value of the global irradiance, measured during a 10 min interval, presumes a temporary eclipse of the sun by clouds. On the other hand, in the case of no such difference, there is no sunshine or continuous sunshine during the 10 min interval (namely, $SD = 0$ or $SD = 10$ min).

Based on these assumptions, an algorithm can be used (Slob and Monna, 1991) to calculate the daily $SD$ from the sum of 10 min $SD$. Within this algorithm, $SD$ is determined for succeeding 10 min intervals (namely, $SD_{10'} = f \cdot 10$ min, where $f$ is the fraction of the interval with sunshine, $0 \le f \le 1$). The attenuation factor largely depends on the optical path of the sunlight travelling through the atmosphere. Because this path is related to the elevation of the sun, $h = 90° - z$, the algorithm discriminates between three time zones. Although usually $f = 0$ or $f = 1$, special

attention is given to $0 < f < 1$. This algorithm is given in Annex 8.A. The uncertainty is about 0.6 h for daily sums, though recent work (Hinssen and Knap, 2007; WMO, 2012) showed that the expanded uncertainty ($k = 2$) on daily totals can exceed 1 h.

The Carpentras method assumes the possibility of parameterizing and calculating over 1 min intervals an irradiance threshold ($G_{thr}$) of $G$ as a function of the most frequent in situ conditions of atmospheric turbidity and solar elevation ($h$). The corresponding algorithm of this method is given in Annex 8.B. The achievable expanded uncertainty ($k = 2$) for daily totals is about 0.7 h (WMO, 2012).

The application of the Carpentras method can be optimized by using 1 min average global and direct irradiances (used as reference) for a few consecutive years (at least four), which makes it possible to determine the coefficients for the parameterization of the 1 min $G_{thr}$ for the specific location. This minimizes the total relative error of daily $SD$ calculated by the Carpentras method over a long period of time (years) by using the $SD$ cumulative differences, and also provides an evaluation of the achievable uncertainty of the Carpentras method (Morel et al., 2012).

#### 8.2.2.2 *Sources of error*

According to equation 8.3, the measuring errors in global and diffuse solar irradiance are propagated by the calculation of direct solar irradiance and are strongly amplified with increasing solar zenith angles. Therefore, the accuracy of corrections for losses of diffuse solar energy by the use of shade rings (WMO, 1984*a*) and the choice of pyranometer quality is of importance to reduce the uncertainty level of the results.

### 8.2.3 The Campbell-Stokes sunshine recorder (burn method)

The Campbell-Stokes sunshine recorder consists essentially of a glass sphere mounted concentrically in a section of a spherical bowl, the diameter of which is such that the sun's rays are focused sharply on a card held in grooves in the bowl. The method of supporting the sphere differs according to whether the instrument is operated in polar, temperate or tropical latitudes. To obtain useful results, both the spherical segment and the sphere should be made with great precision, the mounting being so designed that the sphere can be accurately centred therein. Three overlapping pairs of grooves are provided in the spherical segment so that the cards can be suitable for different seasons of the year (one pair for both equinoxes), their length and shape being selected to suit the geometrical optics of the system. It should be noted that the aforementioned problem of burns obtained under variable cloud conditions indicates that this instrument, and indeed any instrument using this method, does not provide accurate data of sunshine duration.

The table below summarizes the main specifications and requirements for a Campbell-Stokes sunshine recorder of the IRSR grade.

#### 8.2.3.1 *Adjustments*

In installing the recorder, the following adjustments are necessary:

(a) The base must be levelled;

(b) The spherical segment should be adjusted so that the centre line of the equinoctial card lies in the celestial equator (the scale of latitude marked on the bowl support facilitates this task);

(c) The vertical plan through the centre of the sphere and the noon mark on the spherical segment must be in the plane of the geographic meridian (north-south adjustment).

**Campbell-Stokes recorder (IRSR grade) specifications**

| *Glass sphere* | *Spherical segment* | *Record cards* |
|---|---|---|
| Shape: Uniform | Material: Gunmetal or equivalent durability | Material: Good quality pasteboard not affected appreciably by moisture |
| Diameter: 10 cm | Radius: 73 mm | Width: Accurate to within 0.3 mm |
| Colour: Very pale or colourless | Additional specifications: | Thickness: 0.4 ± 0.05 mm |
| Refractive index: 1.52 ± 0.02 | (a) Central noon line engraved transversely across inner surface | Moisture effect: Within 2% |
| Focal length: 75 mm for sodium "D" light | (b) Adjustment for inclination of segment to horizontal according to latitude | Colour: Dark, homogeneous, no difference detected in diffuse daylight |
| | (c) Double base with provision for levelling and azimuth setting | Graduations: Hour-lines printed in black |

A recorder is best tested for (c) above by observing the image of the sun at the local apparent noon; if the instrument is correctly adjusted, the image should fall on the noon mark of the spherical segment or card.

### 8.2.3.2 ***Evaluation***

To obtain uniform results from Campbell-Stokes recorders, it is especially important to conform closely to the following directions for measuring the IRSR records. The daily total duration of bright sunshine should be determined by marking off on the edge of a card of the same curvature the lengths corresponding to each mark and by measuring the total length obtained along the card at the level of the recording to the nearest tenth of an hour. The evaluation of the record should be made as follows:

(a) In the case of a clear burn with round ends, the length should be reduced at each end by an amount equal to half the radius of curvature of the end of the burn; this will normally correspond to a reduction of the overall length of each burn by 0.1 h;

(b) In the case of circular burns, the length measured should be equal to half the diameter of the burn. If more than one circular burn occurs on the daily record, it is sufficient to consider two or three burns as equivalent to 0.1 h of sunshine; four, five, six burns as equivalent to 0.2 h of sunshine; and so on in steps of 0.1 h;

(c) Where the mark is only a narrow line, the whole length of this mark should be measured, even when the card is only slightly discoloured;

(d) Where a clear burn is temporarily reduced in width by at least a third, an amount of 0.1 h should be subtracted from the total length for each such reduction in width, but the maximum subtracted should not exceed one half of the total length of the burn.

In order to assess the random and systematic errors made while evaluating the records and to ensure the objectivity of the results of the comparison, it is recommended that the evaluations corresponding to each one of the instruments compared be made successively and independently by two or more persons trained in this type of work.

#### 8.2.3.3 *Special versions*

Since the standard Campbell-Stokes sunshine recorder does not record all the sunshine received during the summer months at stations with latitudes higher than about 65°, some countries use modified versions.

One possibility is to use two Campbell-Stokes recorders operated back to back, one of them being installed in the standard manner, while the other should be installed facing north.

In many climates, it may be necessary to heat the device to prevent the deposition of frost and dew. Comparisons in climates like that of northern Europe between heated and normally operated instruments have shown that the amount of sunshine not measured by a normal version, but recorded by a heated device, is about 1% of the monthly mean in summer and about 5% to 10% of the monthly mean in winter.

#### 8.2.3.4 *Sources of error*

The errors of this recorder are mainly generated by the dependence on the temperature and humidity of the burn card as well as by the overburning effect, especially in the case of scattered clouds (Ikeda et al., 1986).

The morning values are frequently affected by dew or frost at middle and high latitudes.

### 8.2.4 Contrast-evaluating devices

The Foster sunshine switch is an optical device that was introduced operationally in the network of the United States in 1953 (Foster and Foskett, 1953). It consists of a pair of selenium photocells, one of which is shielded from direct sunshine by a shade ring. The cells are corrected so that in the absence of the direct solar beam no signal is produced. The switch is activated when the direct solar irradiance exceeds about 85 W $m^{-2}$ (Hameed and Pittalwala, 1989). The position of the shade ring requires adjustments only four times a year to allow for seasonal changes in the sun's apparent path across the sky.

### 8.2.5 Contrast-evaluating and scanning devices

#### 8.2.5.1 *General*

A number of different opto-electronic sensors, namely contrast-evaluating and scanning devices (see, for example, WMO, 1984*b*), were compared during the WMO Automatic Sunshine Duration Measurement Comparison at the Regional Radiation Centre of Regional Association VI in Hamburg (Germany) from 1988 to 1989. The report of this comparison contains detailed descriptions of all the instruments and sensors that participated in this event.

#### 8.2.5.2 *Sources of error*

The distribution of cloudiness over the sky or solar radiation reflected by the surroundings can influence the results because of the different procedures to evaluate the contrast and the relatively large field-of-view angles of the cells in the arrays used. Silicon photovoltaic cells without filters typically have the maximum responsivity in the near-IR, and the results, therefore, depend on the spectrum of the direct solar radiation.

Since the relatively small, slit-shaped, rectangular field-of-view angles of this device differ considerably from the circular-symmetrical one of the reference pyrheliometer, the cloud distribution around the sun can cause deviations from the reference values.

Because of the small field of view, an imperfect glass dome may be a specific source of uncertainty. The spectral responsivity of the sensor should also be considered in addition to solar elevation error. At present, only one of the commercial recorders using a pyroelectric detector is thought to be free of spectral effects.

## 8.3 EXPOSURE OF SUNSHINE DETECTORS

The three essential aspects for the correct exposure of sunshine detectors are as follows:

(a) The detectors should be firmly fixed to a rigid support. This is not required for the SONI (WMO, 1984*b*) sensors that are designed also for use on buoys;

(b) The detector should provide an uninterrupted view of the sun at all times of the year throughout the whole period when the sun is more than 3° above the horizon. This recommendation can be modified in the following cases:

  (i) Small antennas or other obstructions of small angular width (≤2°) are acceptable if no alternative site is available. In this case, the position, elevation and angular width of obstructions should be well documented and the potential loss of sunshine hours during particular hours and days should be estimated by the astronomical calculation of the apparent solar path;

  (ii) In mountainous regions (valleys, for instance), natural obstructions are acceptable as a factor of the local climate and should be well documented, as mentioned above;

(c) The site should be free of surrounding surfaces that could reflect a significant amount of direct solar radiation to the detector. Reflected radiation can influence mainly the results of the contrast-measuring devices. To overcome this interference, white or gloss paint should be avoided and nearby surfaces should either be kept free of snow or screened.

The adjustment of the detector axis is mentioned above. For some detectors, the manufacturers recommend tilting the axis, depending on the season.

The siting classification for surface observing stations on land (see the present volume, Chapter 1, Annex 1.D) provides additional guidance on the selection of a site and the location of a sunshine detector within a site in order to optimize representativeness.

## 8.4 GENERAL SOURCES OF ERROR

The uncertainty of sunshine duration recorded using different types of instrument and methods was demonstrated as deviations from reference values in WMO for the weather conditions of Hamburg (Germany) in 1988–1989.

The reference values are also somewhat uncertain because of the uncertainty of the calibration factor of the pyrheliometer used and the dimensions of its field-of-view angle (dependency on the aureole). For single values, the time constant should also be considered.

General sources of uncertainty are as follows:

(a) The calibration of the recorder (adjustment of the irradiance threshold equivalent (see 8.5));

(b) The typical variation of the recorder response due to meteorological conditions (for example, temperature, cloudiness, dust) and the position of the sun (for example, errors of direction, solar spectrum);

(c) The poor adjustment and instability of important parts of the instrument;

(d) The simplified or erroneous evaluation of the values measured;

(e) Erroneous time-counting procedures;

(f) Dirt and moisture on optical and sensing surfaces;

(g) Poor quality of maintenance.

## 8.5 CALIBRATION

The following general remarks should be made before the various calibration methods are described:

(a) No standardized method to calibrate $SD$ detectors is available;

(b) For outdoor calibrations, the pyrheliometric method has to be used to obtain reference data;

(c) Because of the differences between the design of the $SD$ detectors and the reference instrument, as well as with regard to the natural variability of the measuring conditions, calibration results must be determined by long-term comparisons (some months);

(d) Generally the calibration of $SD$ detectors requires a specific procedure to adjust their threshold value (electronically for opto-electric devices, by software for pyranometric systems);

(e) For opto-electric devices with an analogue output, the duration of the calibration period should be relatively short;

(f) The indoor method (using a lamp) is recommended primarily for regular testing of the stability of field instruments.

### 8.5.1 Outdoor methods

#### 8.5.1.1 *Comparison of sunshine duration data*

Reference values $SD_{ref}$ have to be measured simultaneously with the sunshine duration values $SD_{cal}$ of the detector to be calibrated. The reference instrument used should be a pyrheliometer on a solar tracker combined with an irradiance threshold discriminator (see 8.1.4). Alternatively, a regularly recalibrated sunshine recorder of selected precision may be used. Since the accuracy requirement of the sunshine threshold of a detector varies with the meteorological conditions (see 8.1.3), the comparison results must be derived statistically from datasets covering long periods.

If the method is applied to the total dataset of a period (with typical cloudiness conditions), the first calibration result is the ratio $q_{tot} = \Sigma_{tot}\, SD_{ref} / \Sigma_{tot}\, SD_{cal}$.

For $q > 1$ or $q < 1$, the threshold equivalent voltage has to be adjusted to lower and higher values, respectively. Since the amount of the required adjustment is not strongly correlated to $q_{tot}$, further comparison periods are necessary to validate iteratively the approach to the ideal threshold by approximation of $q_{tot} = 1$. The duration of a total calibration period may be three to six months at European mid-latitudes. Therefore, the facilities to calibrate network detectors should permit the calibration of several detectors simultaneously. (The use of $q_{tot}$ as a correction factor for the $\Sigma\, SD$ values gives reliable results only if the periods to be evaluated have the same cloud formation as during the calibration period. Therefore, this method is not recommended.)

If the method is applied to datasets which are selected according to specific measurement conditions (for example, cloudiness, solar elevation angle, relative sunshine duration, daytime), it may be possible, for instance, to find factors $q_{sel} = \Sigma_{sel}\, SD_{ref} / \Sigma_{sel}\, SD_{cal}$ statistically for different types of cloudiness. The factors could also be used to correct datasets for which the cloudiness is clearly specified.

On the other hand, an adjustment of the threshold equivalent voltage is recommended, especially if $q_{sel}$ values for worse cloudiness conditions (such as cirrus and altostratus) are considered. An iterative procedure to validate the adjustment is also necessary; depending on the weather, some weeks or months of comparison may be needed.

#### 8.5.1.2 *Comparison of analogue signals*

This method is restricted to $SD$ detectors which have an analogue output that responds linearly to the received direct solar irradiance, at least in the range <500 W m$^{-2}$. The comparison between the reference irradiance measured by a pyrheliometer and the simultaneously measured analogue output should be performed at cloudless hours or other intervals with slowly variable direct solar irradiance below 500 W m$^{-2}$.

The linear regression analysis of such a dataset generates a best-fit line from which the threshold equivalent voltage at 120 W m$^{-2}$ can be derived. If this calibration result deviates from the certified voltage by more than ±20%, the threshold of the detector should be adjusted to the new value.

For detectors with a pronounced spectral response, the measured data at low solar elevation angles around 120 W m$^{-2}$ should be eliminated because of the stronger non-linearity caused by the spectrum, unless the threshold voltage at sunrise and sunset is of special interest. The threshold equivalent voltage has to be extrapolated from higher irradiance values.

#### 8.5.1.3 *Mean effective irradiance threshold method*

The so-called mean effective irradiance threshold (MEIT) method is based on the determination of an hourly MEIT, $I_m$, for the detector to be calibrated.

As a first step of this method, $SD$ values $SD_{ref}(h_k, I(n))$ have to be determined from computer-controlled pyrheliometric measurements for hours $h_k$ and fictitious threshold irradiances $I(n)$ between 60 and 240 W m$^{-2}$ (this means that $I(n) = (60 + n)$ W m$^{-2}$ with $n = 0, 1, 2, \ldots 180$). As a second step, the hourly $SD$ value $SD(h_k)$ of the detector must be compared with the $SD_{ref}(h_k, I(n))$ to find the $n = n_k$ for which $SD(h_k)$ equals $SD_{ref}(h_k, I(n_k))$. $I(n_k)$ represents the MEIT value of the hour $h_k$: $I_m(h_k) = (60 + n_k)$ W m$^{-2}$. If $n_k$ is not found directly, it has to be interpolated from adjacent values.

The third step is the adjustment of the threshold equivalent voltage of the recorder if the relative deviation between a MEIT value $I_m$ and the ideal threshold 120 W m$^{-2}$ is larger than ±20%. The mean value should be a monthly average, for instance, because of the large spread of the deviations of hourly MEIT values.

The method is not applicable to hours with dominant fast threshold transitions; the average gradient of an hour should be lower than 5 W m$^{-2}$ s$^{-1}$. The MEIT values are not representative of the total dataset of the calibration period.

### 8.5.2 **Indoor method**

Since the simulation of the distribution of direct and diffuse solar fluxes is difficult indoors, only a "spare calibration" can be recommended which is applicable for $SD$ detectors with an adjustable threshold equivalent voltage. The laboratory test equipment consists of a stabilized

radiation source (preferably with an approximated solar spectrum) and a stand for a precise local adjustment of the *SD* detector as well as of an *SD* detector (carefully calibrated outdoors) which is used as reference. Reference and test detectors should be of the same model.

At the beginning of the test procedure, the reference detector is positioned precisely in the beam of the lamp so that 120 W $m^{-2}$ is indicated by an analogue output or by the usual "sunshine switch". Afterwards, the reference device is replaced precisely by the test device, whose threshold voltage must be adjusted to activate the switch, or to get a 120 W $m^{-2}$ equivalent. The repeatability of the results should be tested by further exchanges of the instruments.

## 8.6 MAINTENANCE

The required maintenance routine for technicians consists of the following:

(a) Cleaning: The daily cleaning of the respective entrance windows is necessary for all detectors, especially for scanning devices with small field-of-view angles. Instruments without equipment to prevent dew and frost should be cleared more than once on certain days;

(b) Checking: The rotation of special (scanning) parts as well as the data-acquisition system should be checked daily;

(c) Exchange of record: In Campbell-Stokes sunshine recorders, the burn card must be exchanged daily; in other devices, the appropriate data carriers have to be replaced regularly;

(d) Adjustments: Adjustments are required if a seasonal change of the tilt of the detector is recommended by the manufacturer, or possibly after severe storms.

Special parts of the detectors and of the data-acquisition systems used should undergo maintenance by trained technicians or engineers according to the appropriate instruction manuals.

# ANNEX 8.A. ALGORITHM TO ESTIMATE SUNSHINE DURATION FROM DIRECT GLOBAL IRRADIANCE MEASUREMENTS

*(See Slob and Monna, 1991)*

The estimation of the daily $SD$ is based on the sum of the fractions $f$ of 10 min intervals, namely, $SD = \Sigma\, SD_{10'}$, where $SD_{10} = f \leq 10$ min. In practice $f = 0$ (no sunshine at all, overcast) or 1 (only sunshine, no clouds), but special attention is given to $0 < f < 1$ (partly sunshine, part clouded). Because the correlation between $SD$ and the global irradiation, measured horizontally, depends on the elevation of the sun ($h$), discrimination is made in the first place in terms of sin ($h$).

The following variables are applicable:

$h$ Elevation angle of the sun in degrees
$G$ Global irradiance on a horizontal surface in W m$^{-2}$
$I$ Direct irradiance on a surface perpendicular to the direction of the sun in W m$^{-2}$
$D$ Diffuse radiation on a horizontal surface in W m$^{-2}$
$T_L$ "Linke" – turbidity (dimensionless)

For the measured values of $G$ it holds that:

$G$ represents a 10 min average of the measured global irradiance
$G_{min}$ represents the minimum value of the global irradiance, measured during the 10 min interval
$G_{max}$ represents the maximum value of the global irradiance, measured during the 10 min interval ($G_{min} \leq G \leq G_{max}$)

Equations used:

$G_0$ = $I_0 \sin(h)$, $I_0$ = 1 367 W m$^{-2}$ (for extra-terrestrial irradiance)
$I$ = $I_0 \exp(-T_L/(0.9 + 9.4 \sin(h)))$, $I_0$ = 1 367 W m$^{-2}$
$c$ = $(G - D)/(I \sin(h))$, where
$T_L = 4$ and
$D = 1.2\, G_{min}$ if $(1.2\, G_{min} < 0.4)$ else
$D = 0.4$

<table>
<tr><td>Sun elevation</td><td>sin ($h$) < 0.1, $h$ < 5.7°</td><td colspan="2">0.1 ≤ sin ($h$) ≤ 0.3, 5.7° ≤ $h$ ≤ 17.5°</td><td colspan="6">sin ($h$) ≥ 0.3, $h$ ≥ 17.5°</td></tr>
<tr><td rowspan="6">Other criteria</td><td rowspan="6">No further decision criteria</td><td colspan="2" rowspan="2">Is $G/G_0 \leq \{0.2 + \sin(h)/3 + \exp(-T_L/(0.9 + 9.4 \sin(h)))\}$ with $T_L = 6$?</td><td colspan="6">Is $G_{max}/G_0 < 0.4$?</td></tr>
<tr><td rowspan="5">If "yes"</td><td colspan="5">If "no"</td></tr>
<tr><td rowspan="2"></td><td rowspan="2"></td><td colspan="5">Is $G_{min}/G_0 > \{0.3 + \exp(-T_L/(0.9 + 9.4 \sin(h)))\}$ with $T_L = 10$?</td></tr>
<tr><td>If "yes"</td><td rowspan="3">If "yes"</td><td colspan="4">If "no"</td></tr>
<tr><td>If "yes"</td><td colspan="4">Is $G_{max}/G_0 > \{0.3 + \exp(-T_L/(0.9 + 9.4 \sin(h)))\}$ and $G_{max} - G_{min} < 0.1\, G_0$ with $T_L = 10$?</td></tr>
<tr><td>If "yes"</td><td colspan="3">If "no"</td></tr>
<tr><td>Result</td><td>$f = 0$</td><td>$f = 0$</td><td>$f = 1$</td><td>$f = 0$</td><td>$f = 1$</td><td>$f = 1$</td><td>$f = 0$</td><td>$f = c$</td><td>$f = 1$</td></tr>
<tr><td></td><td></td><td></td><td></td><td></td><td></td><td></td><td>$c < 0$</td><td>$0 \leq c \leq 1$</td><td>$c > 1$</td></tr>
</table>

# ANNEX 8.B. ALGORITHM TO ESTIMATE SUNSHINE DURATION FROM 1 MIN GLOBAL IRRADIANCE MEASUREMENTS

*(Carpentras method; see WMO, 1998, 2012)*

This method, developed at the WMO Regional Radiation Centre of Carpentras (France) and described by Oliviéri (WMO, 1998), consists of an algorithm that calculates the $SD$ every minute through the measurement of 1 min means of global irradiance ($G$) compared with a threshold value ($G_{thr}$) that is parameterized by two coefficients ($A$, $B$) and the solar elevation $h$ (specifically sin ($h$)).

The following variables are applicable:

$h$ Elevation angle of the sun in degrees (see the present volume, Chapter 7, Annex 7.D)
$G$ Global irradiance on a horizontal surface in W m$^{-2}$ (1 s sampled, 1 min averaged)

Equations used:

$G_{thr} = F_c$ x Mod
Mod = 1 080 (sin ($h$))$^{1.25}$
$F_c = A + B \cos(2\pi d/365)$

where Mod represents the global irradiance obtained from a cloudless day model (clear sky and mean value of turbidity); $F_c$ represents a factor, the empirical value of which is close to 0.7; and $d$ is the day number of the annual sequence.

The $F_c$ factor, generally varying between 0.5 and 0.8, depends on the climatic conditions of the location, and the $A$, $B$ coefficients can be empirically calculated by long-term comparison between $SD$ and pyrheliometer measurements (Morel et al., 2012). Alternatively, the presence of near or, even better, co-located instruments for atmospheric turbidity permits an improved determination of the $F_c$ factor. A variability of the $A$ and $B$ coefficients has been observed in relation to latitude ($B$ tends towards negative values for the southern hemisphere, while $A$ decreases with latitude).

The algorithm is run every minute and can be expressed as follows:

| *Sun elevation* | $h < 3°$ | $h \geq 3°$ | |
|---|---|---|---|
| *Criteria* | No decision | Is $G \geq G_{thr}$? | |
| | | If "yes" | If "no" |
| *Result* | $SD$ = 0 min | $SD$ = 1 min | $SD$ = 0 min |

The solar elevation must be calculated every minute contemporarily to the sun hour angle, right ascension and geocentric declination according to the astronomical formulae reported in the present volume, Chapter 7, Annex 7.D.

The data filtering ($h \geq 3°$) is applied before the execution of the main test and permits the filtering of errors due to the imperfection of the model, the height of the sun (low heights) and the atmospheric refraction. A tolerance of 3° above the horizon is accepted for the requirement that the $SD$ detectors have an uninterrupted view of the sun at all times of the year. The errors introduced by the data filtering on $h$ produce a small underestimation that, due to their systematic nature, can be corrected after a long period of measurements. A comparison of this method with other methods and with reference $SD$ data is reported in WMO (2012).

## REFERENCES AND FURTHER READING


Angell, J.K., 1990: Variation in United States cloudiness and sunshine duration between 1950 and the drought year of 1988. *Journal of Climate*, 3:296–308.

Baumgartner, T., 1979: Die Schwellenintensität des Sonnenscheinautographen Campbell-Stokes an wolkenlosen Tagen. *Arbeitsberichte der Schweizerischen Meteorologischen Zentralanstalt*, No. 84, Zürich.

Bider, M., 1958: Über die Genauigkeit der Registrierungen des Sonnenscheinautographen Campbell-Stokes. *Archiv für Meteorologie, Geophysik und Bioklimatologie*, Serie B, 9(2):199-230.

Coulson, K.L., 1975: *Solar and Terrestrial Radiation. Methods and Measurements*. Academic Press, New York, pp. 215–233.

Dyson, P., 2003: *Investigation of the Uncertainty of Sunshine Duration in the Solar and Terrestrial Radiation Network*. Instrument Test Report 674, Commonwealth Bureau of Meteorology.

Foster, N.B. and L.W. Foskett, 1953: A photoelectric sunshine recorder. *Bulletin of the American Meteorological Society*, 34:212–215.

Golchert, H.J., 1981: Mittlere Monatliche Global-strahlungsverteilungen in der Bundesrepublik Deutschland. *Meteorologische Rundschau*, 34:143–151.

Hameed, S. and I. Pittalwala, 1989: An investigation of the instrumental effects on the historical sunshine record of the United States. *Journal of Climate*, 2:101–104.

Hinssen, Y.B.L. and W.H. Knap, 2007: Comparison of pyranometric and pyrheliometric methods for the determination of sunshine duration. *Journal of Atmospheric and Oceanic Technology*, 24(5):835–846.

Ikeda, K., T. Aoshima and Y. Miyake, 1986: Development of a new sunshine-duration meter. *Journal of the Meteorological Society of Japan*, 64(6):987–993.

Jaenicke, R. and F. Kasten, 1978: Estimation of atmospheric turbidity from the burned traces of the Campbell-Stokes sunshine recorder. *Applied Optics*, 17:2617–2621.

Morel, J.P., E. Vuerich, J. Oliviéri and S. Mevel, 2012: Sunshine duration measurements using the Carpentras method. Baseline Surface Radiation Network meeting, Postdam, Germany, 1–3 August 2012.

Painter, H.E., 1981: The performance of a Campbell-Stokes sunshine recorder compared with a simultaneous record of normal incidence irradiance. *The Meteorological Magazine*, 110:102–109.

Slob, W.H. and W.A.A. Monna, 1991*: Bepaling van een directe en diffuse straling en van zonneschijnduur uit 10-minuutwaarden van de globale straling*. KNMI TR136, de Bilt.

Sonntag, D. and K. Behrens, 1992: Ermittlung der Sonnenscheindauer aus pyranometrisch gemessenen Bestrahlungsstärken der Global-und Himmelsstrahlung. *Berichte des Deutschen Wetterdienstes*, No. 181.

Stanghellini, C., 1981: A simple method for evaluating sunshine duration by cloudiness observations. *Journal of Applied Meteorology*, 20:320–323.

World Meteorological Organization, 1962: *Abridged Final Report of the Third Session of the Commission for Instruments and Methods of Observation* (WMO-No. 116, R.P. 48). Geneva.

———, 1982: *Abridged Final Report of the Eighth Session of the Commission for Instruments and Methods of Observation* (WMO-No. 590). Geneva.

———, 1984*a*: Diffuse solar radiation measured by the shade ring method improved by a new correction formula (K. Dehne). Paper presented at the WMO Technical Conference on Instruments and Cost-effective Meteorological Observations (TECEMO). Instruments and Observing Methods Report No. 15. Geneva.

———, 1984*b*: A new sunshine duration sensor (P. Lindner). Paper presented at the WMO Technical Conference on Instruments and Cost-effective Meteorological Observations (TECEMO). Instruments and Observing Methods Report No. 15. Geneva.

———, 1985: Dependence on threshold solar irradiance of measured sunshine duration (K. Dehne). Paper presented at the Third WMO Technical Conference on Instruments and Methods of Observation (TECIMO-III). Instruments and Observing Methods Report No. 22 (WMO/TD-No. 50). Geneva.

———, 1986: *Radiation and Sunshine Duration Measurements: Comparison of Pyranometers and Electronic Sunshine Duration Recorders of RA VI* (G. Major). Instruments and Observing Methods Report No. 16 (WMO/TD-No. 146). Geneva.

———, 1990: *Abridged Final Report of the Tenth Session of the Commission for Instruments and Methods of Observation* (WMO-No. 727). Geneva.

———, 1998: Sunshine duration measurement using a pyranometer (J.C. Oliviéri). Paper presented at the WMO Technical Conference on Meteorological and Environmental Instruments and Methods of Observation (TECO-98). Instruments and Observing Methods Report No. 70 (WMO/TD-No. 877). Geneva.

———, 2012: Updating and development of methods for worldwide accurate measurements of sunshine duration (E. Vuerich, J.P. Morel, S. Mevel, J. Oliviéri). Paper presented at the WMO Technical Conference on Meteorological and Environmental Instruments and Methods of Observation (TECO-2012). Instruments and Observing Methods Report No. 109. Geneva.

———, 2015 (updated in 2017): *Manual on the Global Observing System* (WMO-No. 544), Volume I. Geneva.

# CHAPTER 9. MEASUREMENT OF VISIBILITY

## 9.1 GENERAL

### 9.1.1 Definitions

Visibility has traditionally been defined for meteorological purposes as a quantity to be estimated by a human observer, and observations made in that way are widely used. However, the estimation of visibility is affected by many subjective and physical factors. The essential meteorological quantity, which is the transparency of the atmosphere, can be measured objectively and is represented by the MOR.

**Meteorological optical range.** The length of path in the atmosphere required to reduce the luminous flux in a collimated beam from an incandescent lamp, at a colour temperature of 2 700 K, to 5% of its original value. The luminous flux is evaluated by means of the photometric luminosity function of CIE, which describes the average spectral sensitivity of human visual perception of brightness (see 9.1.4).

**Visibility, meteorological visibility (by day) and meteorological visibility at night.**[1] Defined as the greatest distance at which a black object of suitable dimensions (located on the ground) can be seen and recognized when observed against the horizon sky during daylight or could be seen and recognized during the night if the general illumination were raised to the normal daylight level (WMO, 1992*a*).

**Visual range (meteorological).** The distance at which the contrast of a given object with respect to its background is just equal to the contrast threshold of an observer (WMO, 1992*a*).

**Airlight.** Light from the sun and the sky that is scattered into the eyes of an observer by atmospheric suspensoids (and, to a slight extent, by air molecules) lying in the observer's cone of vision. That is, airlight reaches the eye in the same manner as diffuse sky radiation reaches the Earth's surface. Airlight is the fundamental factor limiting the daytime horizontal visibility for black objects, because its contributions, integrated along the cone of vision from eye to object, raise the apparent luminance of a sufficiently remote black object to a level which is indistinguishable from that of the background sky. Contrary to subjective estimates, most of the airlight entering observers' eyes originates in portions of their cone of vision lying rather close to them.

The following four photometric qualities are defined in detail in various standards, such as by IEC (IEC, 1987):

(a) *Luminous flux* (symbol: $F$ (or $\Phi$); unit: lumen): A quantity derived from radiant flux by evaluating the radiation according to its action upon the CIE standard photometric observer;

(b) *Luminous intensity* (symbol: $I$; unit: candela or lm $sr^{-1}$): Luminous flux per unit solid angle;

(c) *Luminance* (symbol: $L$; unit: cd $m^{-2}$): Luminous intensity per unit area;

(d) *Illuminance* (symbol: $E$; unit: lux or lm $m^{-2}$): Luminous flux per unit area.

---

[1] To avoid confusion, visibility at night should not be defined in general as "the greatest distance at which lights of specified moderate intensity can be seen and identified" (see the *Abridged Final Report of the Eleventh Session of the Commission for Instruments and Methods of Observation* (WMO-No. 807)). If visibility should be reported based on the assessment of light sources, it is recommended that a visual range should be defined by specifying precisely the appropriate light intensity and its application, like runway visual range. Nevertheless, at its eleventh session CIMO agreed that further investigations were necessary in order to resolve the practical difficulties of the application of this definition.

**The extinction coefficient (symbol $\sigma$).** This gives the extent to which the luminous flux of a collimated beam, emitted by an incandescent source at a colour temperature of 2 700 K, is reduced while travelling the length of a unit distance in the atmosphere. The coefficient is a measure of the attenuation due to both absorption and scattering.

**The luminance contrast (symbol C).** The ratio of the difference between the luminance of an object and its background and the luminance of the background.

**The contrast threshold (symbol $\varepsilon$).** The minimum value of the luminance contrast that the human eye can detect, namely, the value which allows an object to be distinguished from its background. The contrast threshold varies with the individual.

**The illuminance threshold (symbol $E_t$).** The smallest illuminance, required by the eye, for the detection of point sources of light against a background of specified luminance. The value of Et, therefore, varies according to lighting conditions.

**The transmission factor (symbol $T$).** This is defined, for a collimated beam from an incandescent source at a colour temperature of 2 700 K, as the fraction of luminous flux which remains in the beam after traversing an optical path of a given length in the atmosphere. The transmission factor is also called the transmission coefficient. The terms transmittance or transmissive power of the atmosphere are also used when the path is defined, that is, of a specific length (for example, in the case of a transmissometer). In the latter case, $T$ is often multiplied by 100 and expressed in %.

**An aerodrome.** A defined area on land or water (including any buildings, installations and equipment) intended to be used either wholly or in part for the arrival, departure and surface movement of aircraft (ICAO, 2016).

### 9.1.2 Units and scales

The meteorological visibility or MOR is expressed in metres or kilometres. The measurement range varies according to the application. While for synoptic meteorological requirements, the scale of MOR readings extends from below 100 m to more than 70 km, the measurement range may be more restricted for other applications. This is the case for civil aviation, where the upper limit may be 10 km. This range may be further reduced when applied to the measurement of runway visual range representing landing and take-off conditions in reduced visibility. Runway visual range is required from 50 m or below to 2 000 m or above and is calculated from MOR using, amongst other variables, the runway light intensity and the background luminance (see Volume III, Chapter 2 of the present Guide). For other applications, such as road or sea traffic, different limits may be applied according to both the requirements and the locations where the measurements are taken.

The errors of visibility measurements increase in proportion to the visibility, and measurement scales take this into account. This fact is reflected in the code used for synoptic reports by the use of three linear segments with decreasing resolution, namely, 100 to 5 000 m in steps of 100 m, 6 to 30 km in steps of 1 km, and 35 to 70 km in steps of 5 km. This scale allows visibility to be reported with a better resolution than the accuracy of the measurement, except when visibility is less than about 1 000 m.

### 9.1.3 Meteorological requirements

The concept of visibility is used extensively in meteorology in two distinct ways. First, it is one of the elements identifying air-mass characteristics, especially for the needs of synoptic meteorology and climatology. Here, visibility must be representative of the optical state of the atmosphere. Second, it is an operational variable which corresponds to specific criteria or special applications. For this purpose, it is expressed directly in terms of the distance at which specific markers or lights can be seen.

One of the most important special applications is meteorological services to aviation (see Volume III, Chapter 2 of the present Guide).

The measure of visibility used in meteorology should be free from the influence of extra-meteorological conditions; it must be simply related to intuitive concepts of visibility and to the distance at which common objects can be seen under normal conditions. MOR has been defined to meet these requirements, as it is convenient for the use of instrumental methods by day and night, and as the relations between MOR and other measures of visibility are well understood. MOR has been formally adopted by WMO as the measure of visibility for both general and aeronautical uses (WMO, 2014). It is also recognized by IEC (IEC, 1987) for application in atmospheric optics and visual signalling.

MOR is related to the intuitive concept of visibility through the contrast threshold. In 1924, Koschmieder, followed by Helmholtz, proposed a value of 0.02 for $\varepsilon$. Other values have been proposed by other authors. They vary from 0.0077 to 0.06, or even 0.2. The smaller value yields a larger estimate of the visibility for given atmospheric conditions. For aeronautical requirements, it is accepted that $\varepsilon$ is higher than 0.02, and it is taken as 0.05 since, for a pilot, the contrast of an object (runway markings) with respect to the surrounding terrain is much lower than that of an object against the horizon. It is assumed that, when an observer can just see and recognize a black object against the horizon, the apparent contrast of the object is 0.05, and, as explained below, this leads to the choice of 0.05 as the transmission factor adopted in the definition of MOR.

Accuracy requirements for MOR, runway visual range and background luminance are given in the present volume, Chapter 1.

### 9.1.4 Measurement methods

Visibility is a complex psycho-physical phenomenon, governed mainly by the atmospheric extinction coefficient associated with solid and liquid particles held in suspension in the atmosphere; the extinction is caused primarily by scattering rather than by absorption of the light. Its estimation is subject to variations in individual perception and interpretative ability, as well as the light source characteristics and the transmission factor. Thus, any visual estimate of visibility is subjective.

When visibility is estimated by a human observer it depends not only on the photometric and dimensional characteristics of the object which is, or should be, perceived, but also on the observer's contrast threshold. At night, it depends on the intensity of the light sources, the background illuminance and, if estimated by an observer, the adaptation of the observer's eyes to darkness and the observer's illuminance threshold. The estimation of visibility at night is particularly problematic. The first definition of visibility at night in 9.1.1 is given in terms of equivalent daytime visibility in order to ensure that no artificial changes occur in estimating the visibility at dawn and twilight. The second definition has practical applications especially for aeronautical requirements, but it is not the same as the first and usually gives different results. Both are evidently imprecise.

Instrumental methods measure the extinction coefficient from which the MOR may be calculated. The visibility may then be calculated from knowledge of the contrast and illuminance thresholds, or by assigning agreed values to them. It has been pointed out by Sheppard (1983) that "…strict adherence to the definition (of MOR) would require mounting a transmitter and receiver of appropriate spectral characteristics on two platforms which could be separated, for example along a railroad, until the transmittance was 5%. Any other approach gives only an estimate of MOR.".

However, fixed instruments are used on the assumption that the extinction coefficient is independent of distance. Some instruments measure attenuation directly and others measure the scattering of light to derive the extinction coefficient. These are described in 9.3. The brief

analysis of the physics of visibility in this chapter may be useful for understanding the relations between the various measures of the extinction coefficient, and for considering the instruments used to measure it.

### Visual perception – photopic and scotopic vision

The conditions of visual perception are based on the measurement of the photopic efficiency of the human eye with respect to monochromatic radiation in the visible light spectrum. The terms “photopic vision" and “scotopic vision” refer to daytime and night-time conditions, respectively.

The adjective “photopic” refers to the state of accommodation of the eye for daytime conditions of ambient luminance. More precisely, the photopic state is defined as the visual response of an observer with normal sight to the stimulus of light incident on the retinal fovea (the most sensitive central part of the retina). The fovea permits fine details and colours to be distinguished under such conditions of adaptation.

In the case of photopic vision (vision by means of the fovea), the relative luminous efficiency of the eye varies with the wavelength of the incident light. The luminous efficiency of the eye in photopic vision is at a maximum for a wavelength of 555 nm. The response curve for the relative efficiency of the eye at the various wavelengths of the visible spectrum may be established by taking the efficiency at a wavelength of 555 nm as a reference value. The curve in Figure 9.1, adopted by CIE for an average normal observer, is therefore obtained.

Night-time vision is said to be scotopic (vision involving the rods of the retina instead of the fovea). The rods, the peripheral part of the retina, have no sensitivity to colour or fine details, but are particularly sensitive to low light intensities. In scotopic vision, maximum luminous efficiency corresponds to a wavelength of 507 nm.

Scotopic vision requires a long period of accommodation, up to 30 min, whereas photopic vision requires only 2 min.

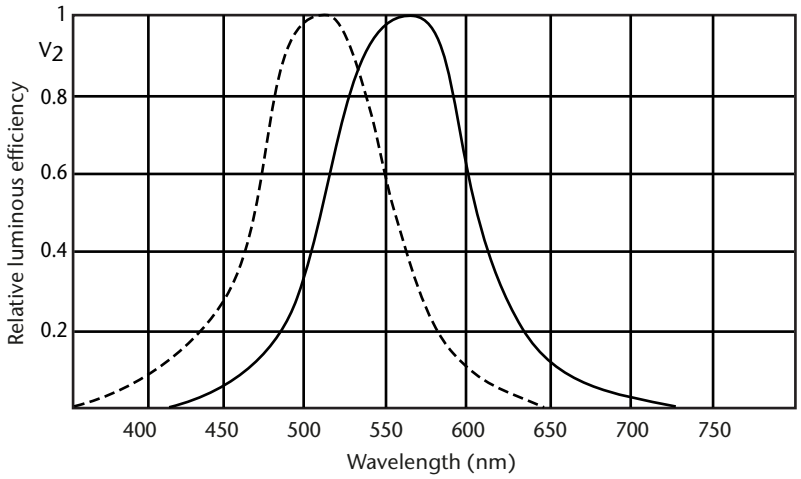



**Figure 9.1. Relative luminous efficiency of the human eye for monochromatic radiation. The continuous line indicates daytime vision, while the broken line indicates night-time vision.**

### Basic equations

The basic equation for visibility measurements is the Bouguer-Lambert law:

$$F = F_0 e^{-\sigma x} \tag{9.1}$$

where $F$ is the luminous flux received after a length of path $x$ in the atmosphere, $F_0$ is the flux for $x = 0$ and $\sigma$ is the extinction coefficient per unit length. Differentiating, we obtain:

$$\sigma = \frac{-dF}{F} \cdot \frac{1}{dx} \tag{9.2}$$

Note that this law is valid only for monochromatic light, but may be applied to a spectral flux to a good approximation. The transmission factor is:

$$T = F/F_0 \tag{9.3}$$

Mathematical relationships between MOR and the different variables representing the optical state of the atmosphere may be deduced from the Bouguer-Lambert law. The relationship between the transmission factor and MOR is valid for fog droplets, but when visibility is reduced by other hydrometeors (such as rain or snow) or lithometeors (such as blowing sand), MOR values should be treated with more care.

From equations 9.1 and 9.3 we may write:

$$T = F \,/\, F_0 = e^{-\sigma x} \tag{9.4}$$

If this law is applied to the MOR definition $T = 0.05$, and setting $x = P$, where $P$ denotes MOR, then the following may be written:

$$T = 0.05 = e^{-\sigma P} \tag{9.5}$$

Hence, the mathematical relation of MOR to the extinction coefficient is:

$$P = (1/\sigma) \cdot \ln(1/0.05) \approx 3/\sigma \tag{9.6}$$

where ln is the log to base $e$ or the natural logarithm. When combining equation 9.4, after being deduced from the Bouguer-Lambert law, and equation 9.6, the following equation is obtained:

$$P = x \cdot \ln(0.05)/\ln(T) \tag{9.7}$$

This equation is used as a basis for measuring MOR with transmissometers where $x$ is, in this case, equal to the transmissometer baseline $a$ in equation 9.14.

### Meteorological visibility in daylight

The contrast of luminance is:

$$C = \frac{L_b - L_h}{L_h} \tag{9.8}$$

where $L_h$ is the luminance of the horizon, and $L_b$ is the luminance of the object.

The luminance of the horizon arises from the airlight scattered from the atmosphere along the observer's line of sight.

It should be noted that, if the object is darker than the horizon, $C$ is negative, and that, if the object is black ($L_b = 0$), $C = -1$.

In 1924, Koschmieder established a relationship, which later became known as Koschmieder's law, between the apparent contrast ($C_x$) of an object, seen against the horizon sky by a distant observer, and its inherent contrast ($C_0$), namely, the contrast that the object would have against the horizon when seen from very short range. Koschmieder's relationship can be written as:

$$C_x = C_0 e^{-\sigma x} \tag{9.9}$$

This relationship is valid provided that the scatter coefficient is independent of the azimuth angle and that there is uniform illumination along the whole path between the observer, the object and the horizon.

If a black object is viewed against the horizon ($C_0 = -1$) and the apparent contrast is –0.05, equation 9.9 reduces to:

$$0.05 = e^{-\sigma x} \tag{9.10}$$

Comparing this result with equation 9.5 shows that when the magnitude of the apparent contrast of a black object, seen against the horizon, is 0.05, that object is at MOR ($P$).

**Meteorological visibility at night**

The distance at which a light (a night visibility marker) can be seen at night is not simply related to MOR. It depends not only on MOR and the intensity of the light, but also on the illuminance at the observer's eye from all other light sources.

In 1876, Allard proposed the law of attenuation of light from a point source of known intensity ($I$) as a function of distance ($x$) and extinction coefficient ($\sigma$). The illuminance ($E$) of a point light source is given by:

$$E = I \cdot x^{-2} \cdot e^{-\sigma x} \tag{9.11}$$

When the light is just visible, $E = E_t$ and the following may be written:

$$\sigma = (1/x) \cdot \ln\left\{I \Big/ \left(E_t \cdot x^2\right)\right\} \tag{9.12}$$

Noting that $P = (1/\sigma) \cdot \ln(1/0.05)$ in equation 9.6, we may write:

$$P = x \cdot \ln(1/0.05) \Big/ \ln\left(I \Big/ \left(E_t \cdot x^2\right)\right) \tag{9.13}$$

The relationship between MOR and the distance at which lights can be seen is described in 9.2.3, while the application of this equation to visual observations is described in 9.2.

## 9.2 VISUAL ESTIMATION OF METEOROLOGICAL OPTICAL RANGE

### 9.2.1 General

A meteorological observer can make a visual estimation of MOR using natural or man-made objects (groups of trees, rocks, towers, masts, churches, lights, and so forth).

Each station should prepare a plan of the objects used for observation, showing their distances and bearings from the observer. The plan should include objects suitable for daytime observations and objects suitable for night-time observations. The observer must also pay special attention to significant directional variations of MOR during the assessment of visibility.

Observations should be made by observers who have "normal" vision and have received suitable training. The observations should normally be made without any additional optical devices (binoculars, telescope, theodolite, and the like) and, preferably, not through a window, especially when objects or lights are observed at night. The eye of the observer should be at a normal height above the ground (about 1.5 m); observations should, thus, not be made from the upper storeys of control towers or other high buildings. This is particularly important when visibility is poor.

When visibility varies in different directions, the value recorded or reported may depend on the coding practises of the report. In synoptic messages, the lower value should be reported, but in reports for aviation the guidance in WMO (2014) should be followed.

### 9.2.2 Estimation of meteorological optical range by day

For daytime observations, the visual estimation of visibility gives a good approximation of the true value of MOR.

Provided that they meet the following requirements, objects at as many different distances as possible should be selected for observation during the day. Only black, or nearly black, objects which stand out on the horizon against the sky should be chosen. Light-coloured objects or objects located close to a terrestrial background should be avoided as far as possible. This is particularly important when the sun is shining on the object. Provided that the albedo of the object does not exceed about 25%, no error larger than 3% will be caused if the sky is overcast, but it may be much larger if the sun is shining. Thus, a white house would be unsuitable, but a group of dark trees would be satisfactory, except when brightly illuminated by sunlight. If an object against a terrestrial background has to be used, it should stand well in front of the background, namely, at a distance at least half that of the object from the point of observation. A tree at the edge of a wood, for example, would not be suitable for visibility observations.

For observations to be representative, they should be made using objects subtending an angle of no less than 0.5° at the observer's eye. An object subtending an angle less than this becomes invisible at a shorter distance than would large objects in the same circumstances. It may be useful to note that a hole of 7.5 mm in diameter, punched in a card and held at arm's length, subtends this angle approximately; a visibility object viewed through such an aperture should, therefore, completely fill it. At the same time, however, such an object should not subtend an angle of more than 5°.

### 9.2.3 Estimation of meteorological optical range at night

Methods which may be used to estimate MOR at night from visual observations of the distance of perception of light sources are described below.

Any source of light may be used as a visibility object, provided that the intensity in the direction of observation is well defined and known. However, it is generally desirable to use lights which can be regarded as point sources, and whose intensity is not greater in any one more favoured direction than in another and not confined to a solid angle which is too small. Care must be taken to ensure the mechanical and optical stability of the light source.

A distinction should be made between sources known as point sources, in the vicinity of which there is no other source or area of light, and clusters of lights, even though separated from each other. In the latter case, such an arrangement may affect the visibility of each source considered separately. For measurements of visibility at night, only the use of suitably distributed point sources is recommended.

It should be noted that observations at night, using illuminated objects, may be affected appreciably by the illumination of the surroundings, by the physiological effects of dazzling, and by other lights, even when these are outside the field of vision and, more especially, if the observation is made through a window. Thus, an accurate and reliable observation can be made only from a dark and suitably chosen location.

Furthermore, the importance of physiological factors cannot be overlooked, since these are an important source of measurement dispersion. It is essential that only qualified observers with normal vision take such measurements. In addition, it is necessary to allow a period of adaptation (usually from 5 to 15 min) during which the eyes become accustomed to the darkness.

For practical purposes, the relationship between the distance of perception of a light source at night and the value of MOR can be expressed in two different ways, as follows:

(a) For each value of MOR, by giving the value of luminous intensity of the light, so that there is a direct correspondence between the distance where it is barely visible and the value of MOR;

(b) For a light of a given luminous intensity, by giving the correspondence between the distance of perception of the light and the value of MOR.

The second relationship is easier and also more practical to use since it would not be an easy matter to install light sources of differing intensities at different distances. The method involves using light sources which either exist or are installed around the station and replacing $I$, $x$ and $E_t$ in equation 9.13 by the corresponding values of the available light sources. In this way, the Meteorological Services can draw up tables giving values of MOR as a function of background luminance and the light sources of known intensity. The values to be assigned to the illuminance threshold $E_t$ vary considerably in accordance with the ambient luminance. The following values, considered as average observer values, should be used:

(a) $10^{-6.0}$ lux at twilight and at dawn, or when there is appreciable light from artificial sources;

(b) $10^{-6.7}$ lux in moonlight, or when it is not yet quite dark;

(c) $10^{-7.5}$ lux in complete darkness, or with no light other than starlight.

Tables 9.1 and 9.2 give the relations between MOR and the distance of perception of light sources for each of the above methods for different observation conditions. They have been compiled to guide Meteorological Services in the selection or installation of lights for night visibility observations and in the preparation of instructions for their observers for the computation of MOR values.

An ordinary 100 W incandescent bulb provides a light source of approximately 100 cd.

In view of the substantial differences caused by relatively small variations in the values of the visual illuminance threshold and by different conditions of general illumination, it is clear that Table 9.2 is not intended to provide an absolute criterion of visibility, but indicates the need for calibrating the lights used for night-time estimation of MOR so as to ensure as far as possible that night observations made in different locations and by different Services are comparable.

**Table 9.1. Relation between MOR and intensity of a just-visible point source for three values of $E_t$**

| *MOR* | *Luminous intensity (candela) of lamps only just visible at distances given in column P* | | |
|---|---|---|---|
| *P (m)* | *Twilight ($E_t = 10^{-6.0}$)* | *Moonlight ($E_t = 10^{-6.7}$)* | *Complete darkness ($E_t = 10^{-7.5}$)* |
| 100 | 0.2 | 0.04 | 0.006 |
| 200 | 0.8 | 0.16 | 0.025 |
| 500 | 5 | 1 | 0.16 |
| 1 000 | 20 | 4 | 0.63 |
| 2 000 | 80 | 16 | 2.5 |
| 5 000 | 500 | 100 | 16 |
| 10 000 | 2 000 | 400 | 63 |
| 20 000 | 8 000 | 1 600 | 253 |
| 50 000 | 50 000 | 10 000 | 1 580 |

**Table 9.2. Relation between MOR and the distance at which a 100 cd point source is just visible for three values of $E_t$**

| *MOR* | *Distance of perception (metres) of a lamp of 100 cd as a function of MOR value* | | |
|---|---|---|---|
| *P (m)* | *Twilight ($E_t = 10^{-6.0}$)* | *Moonlight ($E_t = 10^{-6.7}$)* | *Complete darkness ($E_t = 10^{-7.5}$)* |
| 100 | 250 | 290 | 345 |
| 200 | 420 | 500 | 605 |
| 500 | 830 | 1 030 | 1 270 |
| 1 000 | 1 340 | 1 720 | 2 170 |
| 2 000 | 2 090 | 2 780 | 3 650 |
| 5 000 | 3 500 | 5 000 | 6 970 |
| 10 000 | 4 850 | 7 400 | 10 900 |
| 20 000 | 6 260 | 10 300 | 16 400 |
| 50 000 | 7 900 | 14 500 | 25 900 |

### 9.2.4 Estimation of meteorological optical range in the absence of distant objects

At certain locations (open plains, ships, and so forth), or when the horizon is restricted (valley or cirque), or in the absence of suitable visibility objects, it is impossible to make direct estimations, except for relatively low visibilities. In such cases, unless instrumental methods are available, values of MOR higher than those for which visibility points are available have to be estimated from the general transparency of the atmosphere. This can be done by noting the degree of clarity with which the most distant visibility objects stand out. Distinct outlines and features, with little or no fuzziness of colours, are an indication that MOR is greater than the distance between the visibility object and the observer. On the other hand, indistinct visibility objects are an indication of the presence of haze or of other phenomena reducing MOR.

### 9.2.5 Accuracy of visual observations

#### General

Observations of objects should be made by observers who have been suitably trained and have what is usually referred to as normal vision. This human factor has considerable significance in the estimation of visibility under given atmospheric conditions, since the perception and visual interpretation capacity vary from one individual to another.

#### Accuracy of daytime visual estimates of meteorological optical range

Observations show that estimates of MOR based on instrumental measurements are in reasonable agreement with daytime estimates of visibility. Visibility and MOR should be equal if the observer's contrast threshold is 0.05 (using the criterion of recognition) and the extinction coefficient is the same in the vicinity of the instrument, and between the observer and the objects.

Middleton (1952) found, from 1 000 measurements, that the mean contrast ratio threshold for a group of 10 young airmen trained as meteorological observers was 0.033 with a range, for individual observations, from less than 0.01 to more than 0.2. Sheppard (1983) has pointed out that when the Middleton data are plotted on a logarithmic scale they show good agreement with a Gaussian distribution. If the Middleton data represent normal observing conditions,

we must expect daylight estimates of visibility to average about 14% higher than MOR with a standard deviation of 20% of MOR. These calculations are in excellent agreement with the results from the First WMO Intercomparison of Visibility Measurements (WMO, 1990), where it was found that, during daylight, the observers' estimates of visibility were about 15% higher than instrumental measurements of MOR. The interquartile range of differences between the observer and the instruments was about 30% of the measured MOR. This corresponds to a standard deviation of about 22%, if the distribution is Gaussian.

**Accuracy of night-time visual estimates of meteorological optical range**

From Table 9.2 in 9.2.3, it is easy to see how misleading the values of MOR can be if based simply on the distance at which an ordinary light is visible, without making due allowance for the intensity of the light and the viewing conditions. This emphasizes the importance of giving precise, explicit instructions to observers and of providing training for visibility observations.

Note that, in practice, the use of the methods and tables described above for preparing plans of luminous objects is not always easy. The light sources used as objects are not necessarily well located or of stable, known intensity, and are not always point sources. With respect to this last point, the lights may be wide- or narrow-beam, grouped, or even of different colours to which the eye has different sensitivity. Great caution must be exercised in the use of such lights.

The estimation of the visual range of lights can produce reliable estimates of visibility at night only when lights and their background are carefully chosen; when the viewing conditions of the observer are carefully controlled; and when considerable time can be devoted to the observation to ensure that the observer's eyes are fully accommodated to the viewing conditions. Results from the First WMO Intercomparison of Visibility Measurements (WMO, 1990) show that, during the hours of darkness, the observer's estimates of visibility were about 30% higher than instrumental measurements of MOR. The interquartile range of differences between the observer and the instruments was only slightly greater than that found during daylight (about 35% to 40% of the measured MOR).

### 9.2.6 Usage of cameras

Camera systems are sometimes used as an aid for an observer to assess the visibility for an area that is blocked from view by buildings or to make visibility observations for a remote location. Automated determination of the presence of fog and the estimation of visibility from camera images is under development. This is not surprising given that the availability and quality of (web)cameras has increased, the costs of these systems decreased and the images can easily be made available on the Internet. Furthermore, image processing techniques are evolving and are now readily available. Various techniques have been implemented, such as determining whether objects at known distances are visible by evaluating the presence of edges or contrast reduction. Other techniques use statistical parameters of an image, such as gradients or Fourier analysis, and relate these to visibility, or use the results of image enhancement methods such as dehazing. These techniques can be applied to either individual images, or two images of the same scene obtained with two cameras at different distances, or one image relative to a (set of) reference image(s) under specific atmospheric conditions. Often the techniques are limited to daytime and implementation needs to be tuned to the images/scenes for a specific site (see for example, WMO, 2016).

## 9.3 INSTRUMENTAL MEASUREMENT OF THE METEOROLOGICAL OPTICAL RANGE

### 9.3.1 General

The adoption of certain assumptions allows the conversion of instrumental measurements into MOR. It is not always advantageous to use an instrument for daytime measurements if a number

of suitable visibility objects can be used for direct observations. However, a visibility-measuring instrument is often useful for night observations or when no visibility objects are available, or for automatic observing systems. Instruments for the measurement of MOR may be classified into one of the following two categories:

(a) Those measuring the extinction coefficient or transmission factor of a horizontal cylinder of air: Attenuation of the light is due to both scattering and absorption by particles in the air along the path of the light beam;

(b) Those measuring the intensity of light scattered in specific directions by a small volume of air from which the scatter coefficient is derived: in natural fog, absorption is often negligible and the scatter coefficient may be considered as being the same as the extinction coefficient.

Both of the above categories include instruments using a light source and photodetector to detect the scattered and attenuated light beam.

The main characteristics of these two categories of MOR-measuring instruments are described below.

### 9.3.2 Instruments measuring the extinction coefficient

#### Telephotometric instruments

A number of telephotometers have been designed for daytime measurement of the extinction coefficient by comparing the apparent luminance of a distant object with that of the sky background, but they are not normally used for routine measurements since, as stated above, it is preferable to use direct visual observations. These instruments may, however, be useful for extrapolating MOR beyond the most distant object.

#### Visual extinction meters

A very simple instrument for use with a distant light at night takes the form of a graduated neutral filter, which reduces the light in a known proportion and can be adjusted until the light is only just visible. The meter reading gives a measure of the transparency of the air between the light and the observer, and, from this, the extinction coefficient can be calculated. The overall accuracy depends mainly on variations in the sensitivity of the eye and on fluctuations in the radiant intensity of the light source. The error increases in proportion to MOR.

The advantage of this instrument is that it enables MOR values over a range from 100 m to 5 km to be measured with reasonable accuracy, using only three well-spaced lights, whereas without it a more elaborate series of lights would be essential if the same degree of accuracy were to be achieved. However, the method of using such an instrument (determining the point at which a light appears or disappears) considerably affects the accuracy and homogeneity of the measurements.

#### Transmissometers

The use of a transmissometer is the method most commonly used for measuring the mean extinction coefficient in a horizontal cylinder of air between a transmitter, which provides a modulated flux light source of constant mean power, and a receiver incorporating a photodetector (generally a photodiode at the focal point of a parabolic mirror or a lens). The most frequently used light source is a halogen lamp or xenon pulse discharge tube. Modulation of the light source prevents disturbance from sunlight. The transmission factor is determined from the photodetector output and this allows the extinction coefficient and the MOR to be calculated.

Since transmissometer estimates of MOR are based on the loss of light from a collimated beam, which depends on scatter and absorption, they are closely related to the definition of MOR. A good, well-maintained transmissometer working within its range of highest accuracy provides a very good approximation to the true MOR.

There are two types of transmissometer:

(a) Those with a transmitter and a receiver in different units and at a known distance from each other, as illustrated in Figure 9.2;

(b) Those with a transmitter and a receiver in the same unit, with the emitted light being reflected by a remote mirror or retroreflector at a known distance that is half the baseline (since the light beam travels to the reflector and back), as illustrated in Figure 9.3.

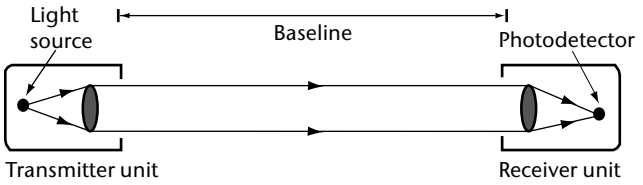



**Figure 9.2. Double-ended transmissometer**

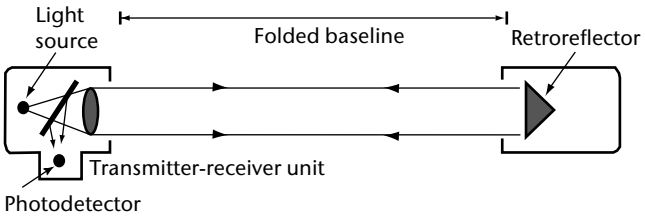



**Figure 9.3. Single-ended transmissometer**

The distance covered by the light beam between the transmitter and the receiver is commonly referred to as the baseline and may range from a few metres to 150 m (or even 300 m) depending on the range of MOR values to be measured and the applications for which these measurements are to be used.

As seen in the expression for MOR in equation 9.7, the relation:

$$P = a \cdot \ln(0.05) / \ln(T) \tag{9.14}$$

where $a$ is the transmissometer baseline, is the basic formula for transmissometer measurements. Its validity depends on the assumptions that the application of the Koschmieder and Bouguer-Lambert laws is acceptable and that the extinction coefficient along the transmissometer baseline is the same as that in the path between an observer and an object at MOR.

If the measurements are to remain acceptable over a long period, the luminous flux must remain constant during this same period. When halogen light is used, the problem of lamp filament ageing is less critical and the flux remains more constant. However, some transmissometers use feedback systems (by sensing and measuring a small portion of the emitted flux) giving greater homogeneity of the luminous flux with time or compensation for any change.

As will be seen in the section dealing with the accuracy of MOR measurements, the value adopted for the transmissometer baseline determines the MOR measurement range. It is

generally accepted that this range is between about 1 and 25 times the baseline length. Modern opto-electronics, however, may provide more accurate results with an extended range (see 9.3.6 and WMO, 1992*b*).

A further refinement of the transmissometer measurement principle is to use two receivers or retroreflectors at different distances to extend both the lower limit (short baseline) and the upper limit (long baseline) of the MOR measurement range. These instruments are referred to as "double baseline" instruments.

Many state-of-the-art transmissometers use LEDs as light sources. It is generally recommended that polychromatic light in the visible spectrum be used to obtain a representative extinction coefficient.

**Visibility lidars**

The lidar technique as described for the laser ceilometer in the present volume, Chapter 15, may be used to obtain visibility when the beam is directed horizontally. The range-resolved profile of the backscattered signal $S$ depends on the output signal $S_{0,}$ the distance $x$, the backscatter coefficient $\beta$, and transmission factor $T$, such that:

$$S(x) \sim S_0 \cdot 1/x^2 \cdot \beta(x) \cdot T^2 \text{ where } T = \int -\sigma(x)\, dx \tag{9.15}$$

Under the condition of horizontal homogeneity of the atmosphere, $\beta$ and $\sigma$ are constant and the extinction coefficient $\sigma$ is determined from only two points of the profile:

$$\ln\left(S(x) \cdot x^2/S_0\right) \sim \ln\beta - 2\,\sigma\, x \tag{9.16}$$

In an inhomogeneous atmosphere the range-dependent quantities of $\beta(x)$ and $\sigma(x)$ may be separated with the Klett Algorithm (Klett, 1985).

As MOR approaches 2 000 m, the accuracy of the lidar method becomes poor.

More information on the requirements for performing visual-range lidar measurements to determine the direction-dependent meteorological optical range can be found in the ISO standard, ISO 28902-1:2012 (ISO, 2012).

### 9.3.3 Instruments estimating the scatter coefficient

The attenuation of light in the atmosphere is due to both scattering and absorption. The presence of pollutants in the vicinity of industrial zones, ice crystals (freezing fog) or dust may make the absorption term significant. However, in general, the absorption factor is negligible and the scatter phenomena due to reflection, refraction, or diffraction on water droplets constitute the main factor reducing visibility. The extinction coefficient may then be considered as equal to the scatter coefficient, and an instrument for determining the latter can, therefore, be used to estimate MOR.

Measurements are most conveniently taken by concentrating a beam of light on a small volume of air and by determining, through photometric means, the proportion of light scattered in a sufficiently large solid angle in directions where scattering provides the best estimate of the scatter coefficient in all conditions. Provided that it is completely screened from interference from other sources of light, or that the light source is modulated, an instrument of this type can be used during both the day and night. The scatter coefficient $b$ is a function that may be written in the following form:

$$b = \frac{2\pi}{\Phi_v}\int_0^{\pi} I(\phi)\sin(\phi)\, d\phi \tag{9.17}$$

where $\Phi_v$ is the flux entering the volume of air $V$ and $I(\phi)$ is the intensity of the light scattered in direction $\phi$ with respect to the incident beam.

Note that the accurate determination of *b* requires the measurement and integration of light scattered out of the beam over all angles. Practical instruments measure the scattered light over a limited angle and rely on a high correlation between the limited integral and the full integral in all conditions.

Three measurement methods are used in these instruments: backscatter, forward scatter, and scatter integrated over a wide angle.

(a) *Backscatter*: In these instruments (Figure 9.4), a light beam is concentrated on a small volume of air in front of the transmitter, the receiver being located in the same housing as the light source where it receives the light backscattered by the volume of air sampled. Several researchers have tried to find a relationship between visibility and the coefficient of backscatter, but it is generally accepted that that correlation is not satisfactory.

(b) *Forward scatter*: The amount of light scattered by small particles (aerosols, small droplets) is angular dependent. Moreover, the angular dependency is determined by the chemical composition (for example, salt concentration), type of nucleus (sand, dust) and size and shape of the particles. As a consequence, a scattering angle should be chosen so that the angular dependence is minimal and representative for the scatter coefficient. Several authors have shown that the best angle is between 20° and 50° (Van de Hulst, 1957; Barteneva, 1960; Kneizys et al., 1983; Jia and Lü, 2014). The instruments, therefore, comprise a transmitter and a receiver, the angle between the beams being 20° to 50°. Another arrangement involves placing either a single diaphragm half-way between a transmitter and a receiver or two diaphragms each a short distance from either a transmitter or a receiver. Figure 9.5 illustrates the two configurations that are used. Instruments determining MOR based on the forward-scatter principle are generally called forward-scatter instruments or forward-scatter meters.

(c) *Scatter over a wide angle*: Such an instrument, illustrated in Figure 9.6, which is usually known as an integrating nephelometer, is based on the principle of measuring scatter over as wide an angle as possible, ideally 0° to 180°, but in practice about 0° to 120°. The receiver is positioned perpendicularly to the axis of the light source which provides light over a wide angle. Although, in theory, such an instrument should give a better estimate of the scatter coefficient than an instrument measuring over a small range of scattering angles, in practice it is more difficult to prevent the presence of the instrument from modifying the extinction coefficient in the air sampled. Integrating nephelometers are not widely used for measuring MOR, but this type of instrument is often used for measuring pollutants.

In all the above instruments, as for most transmissometers, the receivers comprise photodetector cells or photodiodes. The light used is pulsed (for example, high-intensity discharge into xenon).

These types of instruments require only limited space (1 to 2 m in general). They are, therefore, useful when no visibility objects or light sources are available (on board ships, by roadsides, and so forth). Since the measurement relates only to a very small volume of air, the representativeness of measurements for the general state of the atmosphere at the site may be open to question.

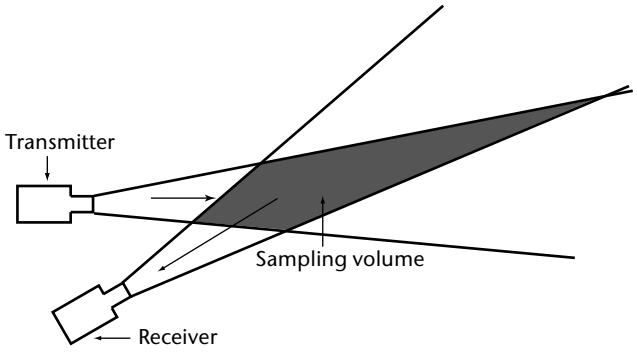



**Figure 9.4. Visibility meter measuring backscatter**

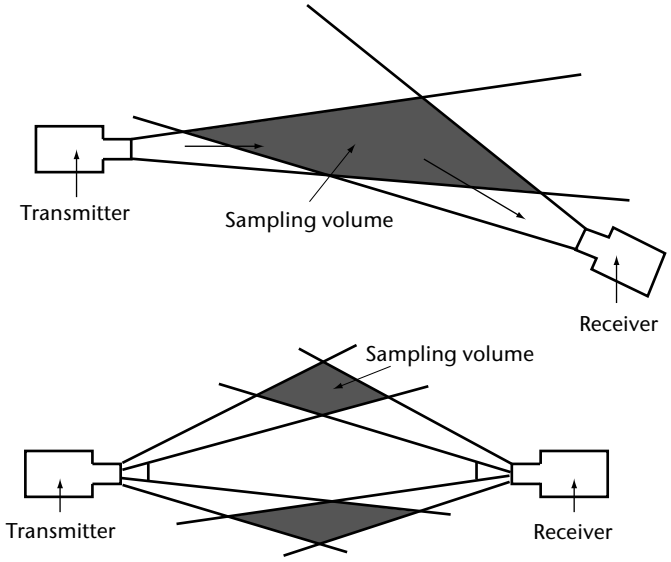



**Figure 9.5. Two configurations of visibility meters measuring forward scatter**

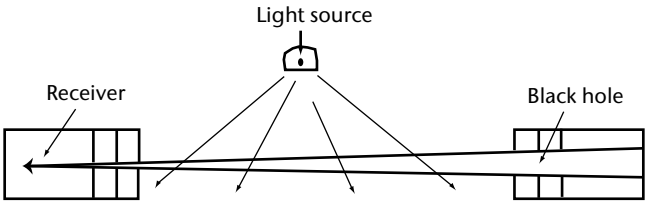



**Figure 9.6. Visibility meter measuring scattered light over a wide angle**

However, this representativeness can be improved by averaging a number of samples or measurements. In addition, smoothing of the results is sometimes achieved by eliminating extreme values.

The use of these types of instruments has often been limited to specific applications (for example, highway visibility measurements, or to determine whether fog is present) or when less precise MOR measurements are adequate. These instruments are now being used in increasing numbers in automatic meteorological observation systems because of their ability to measure MOR over a wide range and their relatively low susceptibility to contamination of optical surfaces compared with transmissometers.

### 9.3.4 Instrument exposure and siting

Measuring instruments should be located in positions which ensure that the measurements are representative for the intended purpose. Thus, for general synoptic purposes, the instruments should be installed at locations free from local atmospheric pollution, for example, smoke, industrial pollution, dusty roads.

The volume of air in which the extinction coefficient or scatter coefficient is measured should normally be at the eye level of an observer, about 1.5 m above the ground.

It should be borne in mind that transmissometers and forward-scatter meters should be installed in such a way that the sun is not in the optical field of view of the receiver at any time of the day. This is normally achieved either by mounting with a north-south optical axis (to ±45°) with the

receiver horizontal and pointing away from the equator for latitudes up to 50°, or by using a system of screens or baffles. Forward-scatter meters should also be aligned such that reflecting objects in the optical field of view of the receiver are avoided.

For aeronautical purposes, measurements are to be representative of conditions at the aerodrome or along the runway. These conditions, which relate more specifically to aerodrome operations, are described in Volume III, Chapter 2 of the present Guide.

The instruments should be installed in accordance with the directions given by the manufacturers. Particular attention should be paid to the correct alignment of transmissometer transmitters and receivers and to the correct adjustment of the light beam. The poles on which the transmitter/receivers are mounted should be mechanically firm (while remaining frangible when installed at aerodromes) to avoid any misalignment due to ground movement during freezing and, particularly, during thawing. In addition, the mountings must not distort under the thermal stresses to which they are exposed. Some modern transmissometers can automatically adjust their alignment to compensate for this.

### 9.3.5 Calibration and maintenance

In order to obtain satisfactory and reliable observations, instruments for the measurement of MOR should be operated and maintained under the conditions prescribed by the manufacturers, and should be kept continuously in good working order. Regular checks and calibration in accordance with the manufacturer's recommendations should ensure optimum performance.

#### 9.3.5.1 *Maintenance*

Most transmissometers require their optical surfaces to be cleaned regularly; therefore frequent servicing must be planned, particularly at aerodromes. The instruments should be cleaned during and/or after major atmospheric disturbances, since rain or violent showers together with strong wind may cover the optical systems with a large number of water droplets and solid particles resulting in major MOR measurement errors. The same is true for snowfall, which could block the optical systems. Heating systems are often placed at the front of the optical systems and in the hood to improve instrument performance under such conditions. Air-blowing systems are sometimes used to reduce the above problems and the need for frequent cleaning. However, it must be pointed out that these blowing and heating systems may generate air currents warmer than the surrounding air and may adversely affect the measurement of the extinction coefficient of the air mass. In arid zones, sandstorms or blowing sand may block the optical system and even damage it. Modern transmissometers and forward-scatter meters monitor the contamination on the optical lens or window and produce warnings and errors when the contamination reaches a threshold. Some instruments make a correction for the window contamination.

The MOR measurement of a forward-scatter meter is affected by cobwebs or even individual spider silk in the measurement volume. Flying insects, which typically swarm around dusk in calm weather conditions can contribute to the scattered signal. Both cause the forward-scatter meter to report artificially low MOR values. The reduction of the MOR of a forward-scatter meter by cobwebs and flying insects can be very large, whereas these hardly affect the MOR obtained by a transmissometer. Some forward-scatter meters filter the raw signal for spikes induced by flying insects (WMO, 2012). However, care must be taken that spikes resulting from particles or droplets are not filtered out, as this filtering leads to higher MOR values which may lead to safety issues.

The main sources of error and recommended actions are summarized in Table 9.3 for transmissometers and in Table 9.4 for forward-scatter meters.

#### 9.3.5.2 ***Calibration***

The calibration should be verified regularly (this is normally performed in very good visibility, that is, over 10 to 15 km) and the instrument should be calibrated and adjusted if necessary. Atmospheric conditions resulting in erroneous calibration must be avoided. When, for example, there are strong updraughts, or after heavy rain, considerable variations in the extinction coefficient are encountered in the layer of air close to the ground; if several transmissometers are in use on the site (in the case of aerodromes), dispersion is observed in their measurements. Calibration should not be attempted under such conditions.

A transmissometer can be calibrated by direct comparison with the distance at which specified objects and lights of known intensity can be seen by an observer. The observation should be as close as possible to MOR, as it is MOR that is used for conversion to obtain transmittance. The calibration can also be performed by directly using traceable optical neutral density filters.

**Table 9.3. Transmissometers: sources of error, and actions**

| *Error source* | *Action* |
|---|---|
| Atmospheric pollutants deposited on optical surfaces | 1. Instrument self-diagnostic features: contamination measurement and contamination compensation algorithms in instrument software<br>2. Preventative maintenance: regular cleaning in accordance with manufacturer's instructions<br>3. Reactive maintenance: cleaning at need |
| Instability of system electronics | Regular calibration check, using a graduated set of attenuation filters under stable, high-visibility conditions. Adjust instrument settings, if required, in accordance with manufacturer's instructions |
| Snow or ice build-up on surfaces near to the optical measurement path | Preventative measure: install instrument head heaters and hood heaters |
| Aging of transmitter light source or incorrect centring of lamps | 1. Instrument self-diagnostic features: lamp intensity measurement and aging warning messages<br>2. Preventative/reactive maintenance: replacement of transmitter light source, if required<br>3. Use automatic alignment assistant, where available |
| Insufficient rigidity and stability of transmitter and receiver mounts and effects of freezing or thawing of the ground and thermal stress | Regular calibration check, using a graduated set of attenuation filters under stable, high visibility conditions. Adjust instrument settings, if required, in accordance with manufacturer's instructions |
| Remote transmission of the extinction coefficient as a low current signal may be subject to interference from electromagnetic fields (a particular problem at aerodromes) | Digital signal formats are less prone to interference than analogue signals |
| Calibration error due to calibration/adjustment being carried out when visibility is low, or unstable atmospheric conditions that affect the extinction coefficient | Calibration and adjustment should be carried out in accordance with manufacturer's instructions |
| Incorrect alignment of transmitters and receivers | Use automatic alignment assistant, where available |
| Disturbance when sun is near horizon, or due to reflections from adjacent surfaces | Installation and orientation should be carried out in accordance with manufacturer's instructions |

**Table 9.4. Forward-scatter meters: sources of error, and actions**

| *Error Source* | *Action* |
|---|---|
| Atmospheric pollutants deposited on optical surfaces and/or incorrect compensation for this contamination | 1. Instrument self-diagnostic features: contamination measurement and contamination compensation algorithms in instrument software<br>2. Design features: look-down geometry and hoods over instrument heads provide better protection to optics and enable longer intervals between maintenance<br>3. Preventative maintenance: regular cleaning in accordance with manufacturer's instructions<br>4. Reactive maintenance: cleaning at need |
| Instability of system electronics | Regular calibration check, using scatter plates (also known as scatter meter calibration units – SCU) that emulate defined fog conditions. Adjust instrument settings, if required, in accordance with manufacturer's instructions |
| Snow or ice build-up on surfaces near to the optical measurement path | Preventative measure: install instrument head heaters and hood heaters |
| Aging of transmitter light source | 1. Instrument self-diagnostic features: light source intensity measurement and aging warning messages<br>2. Preventative/reactive maintenance: replacement of transmitter light source, if required |
| Light source not at visible wavelengths | Design feature taken into account during verification of calibration against transmissometer |
| Atmospheric conditions (for example, rain, snow, ice crystals, sand, local atmospheric pollutants) giving a scatter coefficient that differs from the extinction coefficient | 1. Design feature: optimized scattering angle<br>2. Discrimination and correction for atmospheric conditions |
| Extra absorption by sand, dust and smoke that affects visibility and its measurement | Discrimination and correction for absorption or application of calibration factor obtained for these conditions |
| Calibration error due to calibration/adjustment being carried out when visibility is low, or unstable atmospheric conditions that affect the extinction coefficient | Calibration and adjustment should be carried out in accordance with manufacturer's instructions |
| Incorrect procedures for calibration/adjustment, or use of incorrect or damaged scatter plates | Calibration and adjustment should be carried out in accordance with manufacturer's instructions |
| Disturbance when sun is near horizon, or due to reflections from adjacent surfaces | Installation and orientation should be carried out in accordance with manufacturer's instructions |
| Disturbance by cobwebs, or even individual spider silk, and flying insects in the measurement volume | 1. Preventative maintenance: regular cleaning in accordance with manufacturer's instructions<br>2. Reactive maintenance: cleaning at need<br>3. Discrimination and correction for spikes in scattered signal due to flying insects |

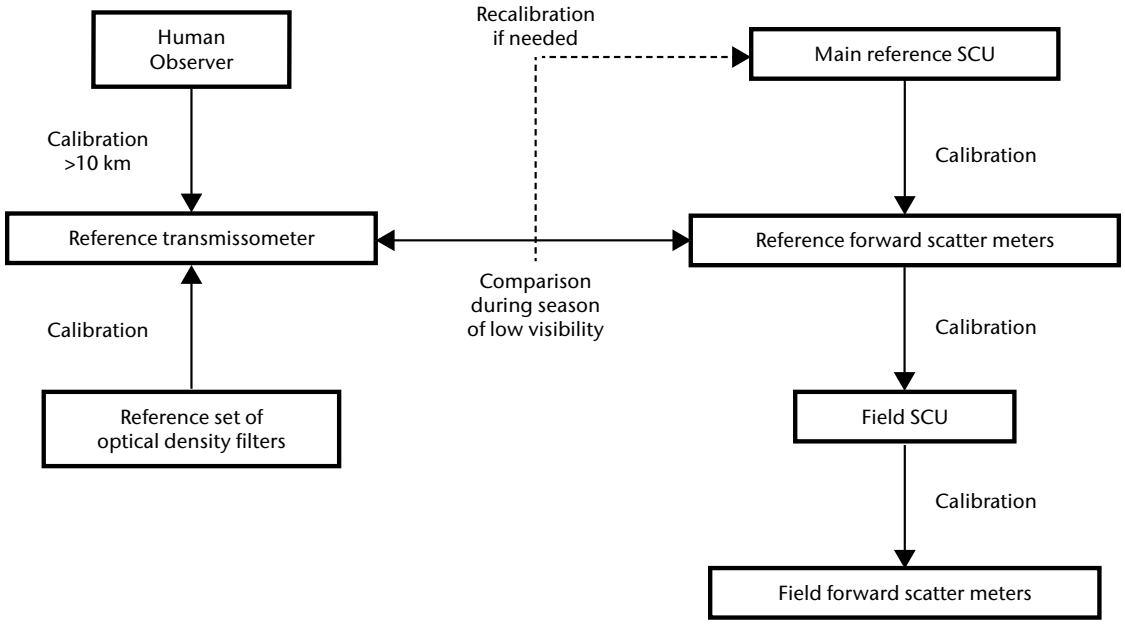



**Figure 9.7. Visibility calibration chain for scatter meters**

Calibration of instruments based on measurement of the scattering coefficient, also known as scatter meters, cannot be carried out directly. The calibration of a forward-scatter meter has to be traceable and verifiable to a transmissometer standard, the accuracy of which has been verified over the intended operational range (ICAO, 2016). The calibration of a scatter meter involves the insertion of optical plates (SCU) into the measurement volume, at a fixed position, which simulates a defined value of MOR. These SCU are specific and provided by the instrument manufacturer. Generally only SCU corresponding to a low MOR value are provided that in combination with blocking the receiver (high MOR value) can be used to perform a two-point calibration.

SCU are susceptible to changes over a period of use due to contamination and ageing and should be initially and then regularly checked and calibrated. This should be done by returning the plates to a suitable testing facility equipped with adequate visibility references and a traceable calibration chain. For some instruments, the manufacturer may offer an equivalent calibration service for SCU supplied by themselves.

According to the ICAO (2005), section 9.4.3 on references for visibility: an “ideal” reference is a set of instruments of at least two transmissometers (ideally using two different baselines) and two forward-scatter meters exhibiting median values with a bias less than 5% when compared to the transmissometers.

At the visibility calibration facility, the SCU should be checked on a known reference forward-scatter meter, and if necessary recalibrated with a new coefficient.

There, the known reference forward-scatter meters are themselves regularly calibrated with a reference SCU and they are systematically checked against the reference transmissometers during low visibility episodes. In case of a bias over a defined threshold (5% for ICAO), the reference SCU is recalibrated with a new coefficient. The reference transmissometers must also be regularly calibrated. This can be done against human observations or by using a set of optical neutral density filters. The traceability of the MOR measurements to a known standard should be established. A visibility reference and calibration chain is described in, for example, WMO (2006). The resulting chain of calibration is described in Figure 9.7.

The comparison of forward-scatter meters and transmissometers should be carefully conducted with validated data. Comparison of scatter meters and transmissometers should be carried out

during periods of low visibility, as a SCU generally simulates these conditions. Additionally, the accuracy of the reference transmissometers is very good at lower visibility and low visibility values are critical for aviation purposes.

Data from fog-only episodes should be kept and episodes including precipitations (rain, snow) must be excluded. The reason was noted in 9.1.4: the relationship between the transmission factor and MOR is valid for fog droplets, but when visibility is reduced by other hydrometeors (such as rain or snow) or lithometeors (such as blowing sand), MOR values should be treated with more care.

Finally, as explained in ICAO (2005), when comparing instruments, it is necessary to check the homogeneity of fog. Non-homogeneous fogs may strongly disturb the MOR distribution ratio of an instrument. Therefore, such periods must be identified and excluded from the data analysis.

Note that higher visibility values may also be considered in the comparison of forward-scatter meters and transmissometers as long as the transmissometer can serve as a reference. This extension of the MOR range also serves as a check of the linearity and the two-point calibration of the forward-scatter meters over a larger visibility range.

### 9.3.6 Accuracy estimates for the measurement of meteorological optical range

#### 9.3.6.1 *General*

All practical operational instruments for the measurement of MOR sample a relatively small region of the atmosphere compared with that scanned by a human observer. Instruments can provide an accurate measurement of MOR only when the volume of air that they sample is representative of the atmosphere around the point of observation out to a radius equal to MOR. It is easy to imagine a situation, with patchy fog or a local rain or snow storm, in which the instrument reading is misleading. However, experience has shown that such situations are not frequent and that the continuous monitoring of MOR using an instrument will often lead to the detection of changes in MOR before they are recognized by an unaided observer. Nevertheless, instrumental measurements of MOR must be interpreted with caution.

Another factor that must be taken into account when discussing representativeness of measurements is the homogeneity of the atmosphere itself. At all MOR values, the extinction coefficient of a small volume of the atmosphere normally fluctuates rapidly and irregularly, and individual measurements of MOR from forward-scatter meters and short baseline transmissometers, which have no in-built smoothing or averaging system, show considerable dispersion. It is, therefore, necessary to take many samples and to smooth or average them to obtain a representative value of MOR. The analysis of the results from the First WMO Intercomparison of Visibility Measurements (WMO, 1990) indicates that, for most instruments, no benefit is gained by averaging over more than 1 min, but for the "noisiest" instruments an averaging time of 2 min is preferable.

#### 9.3.6.2 *Accuracy of transmissometers*

The principal sources of error in transmissometer measurements are listed in Table 9.3 in 9.3.5.1.

The use of a transmissometer that has been properly calibrated and well maintained should give good representative MOR measurements if the extinction coefficient in the optical path of the instrument is representative of the extinction coefficient everywhere within the MOR. However, a transmissometer has only a limited range over which it can provide accurate measurements of MOR. A relative error curve for MOR may be plotted by differentiating the basic transmissometer formula (see equation 9.7). Figure 9.8 shows how the relative error varies with transmission, assuming that the measurement accuracy of the transmission factor $T$ is 1%.

This 1% value of transmission error, which may be considered as correct for many older instruments, does not include instrument drift, dirt on optical components, or the scatter of

measurements due to the phenomenon itself. If the accuracy drops to around 2% to 3% (taking the other factors into account), the relative error values given on the vertical axis of the graph must be multiplied by the same factor of 2 or 3. Note also that the relative MOR measurement error increases exponentially at each end of the curve, thereby setting both upper and lower limits to the MOR measurement range. The example shown by the curve indicates the limit of the measuring range if an error of 5%, 10% or 20% is accepted at each end of the range measured, with a baseline of 75 m. It may also be deduced that, for MOR measurements between the limits of 1.25 and 10.7 times the baseline length, the relative MOR error should be low and of the order of 5%, assuming that the error of *T* is 1%. The relative error of MOR exceeds 10% when MOR is less than 0.87 times the baseline length or more than 27 times this length. When the measurement range is extended further, the error increases rapidly and becomes unacceptable. However, since contemporary transmissometers produce transmission errors that are clearly lower than the exemplary 1%, the usable measurement range may be extended accordingly.

Already results from the First WMO Intercomparison of Visibility Measurements (WMO, 1990) show that the best transmissometers, when properly calibrated and maintained, can provide measurements of MOR with a standard error of about 10% when MOR is up to 60 times their baseline.

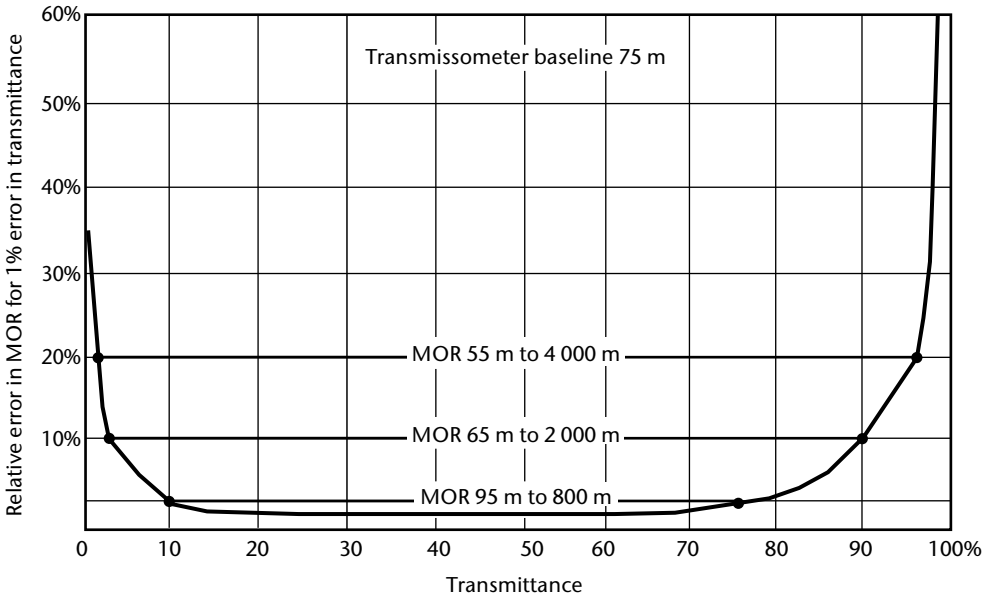



**Figure 9.8. Error in measurements of meteorological optical range as a function of a 1% error in transmittance**

#### 9.3.6.3 *Accuracy of forward-scatter meters*

The principal sources of error in measurements of MOR taken with forward-scatter meters are listed in Table 9.4 in 9.3.5.1.

Results from the First WMO Intercomparison of Visibility Measurements (WMO, 1990) show that forward-scatter meters are generally less accurate than transmissometers at low values of MOR, and forward-scatter meters show greater variability in their readings. There was also evidence that forward-scatter meters, as a class, were more affected by precipitation than transmissometers. However, the best forward-scatter meters showed little or no susceptibility to precipitation and provided estimates of MOR with standard deviation of about 10% over a range of MOR from about 100 m to 50 km. Almost all the forward-scatter meters in the intercomparison exhibited significant systematic error over part of their measurement range. Forward-scatter meters showed very low susceptibility to contamination of their optical systems.

An overview of the differences between forward-scatter meters and transmissometers is given by WMO (1992*b*).

#### 9.3.6.4 *Accuracy of telephotometers and visual extinction meters*

Visual measurements based on the extinction coefficient are difficult to take. The main source of error is the variability and uncertainty of the performance of the human eye. These errors have been described in the sections dealing with the methods of visual estimation of MOR.

## REFERENCES AND FURTHER READING


Barteneva, O.D., 1960: Scattering functions of light in the atmospheric boundary layer. *Izv. Akad. Nauk SSR, Ser. Geofiz. [Bull. Acad. Sci. USSR, Geophysics Series]*, 12:1237–1244.

International Civil Aviation Organization, 2005: *Manual of Runway Visual Range Observing and Reporting Practices*. Doc 9328, AN/908. Third edition. Montreal, ICAO.

———, 2016: *Annex 3 to the Convention on International Civil Aviation – Meteorological Service for International Air Navigation*. Nineteenth edition. Montreal, ICAO.

International Electrotechnical Commission, 1987: *International Electrotechnical Vocabulary*, Chapter 845: Lighting, IEC 60050-845. Geneva.

International Organization for Standardization, 2012: *Air Quality – Environmental Meteorology – Part 1: Ground-based Remote Sensing of Visual Range by Lidar*. ISO 28902-1:2012. Geneva.

Jia S-J. and D-R. Lü, 2014: Optimal forward-scattering angles of atmospheric aerosols in North China. *Atmospheric and Oceanic Science Letters*, 7(3):236–242.

Klett, J.D., 1985: Lidar inversion with variable backscatter/extinction ratios. *Applied Optics*, 24(11):1638–1643.

Kneizys, F.X., E.P. Shettle, W.O. Gallery, J.H. Chetwynd, L.W. Abreu, J.E.A. Selby, S.A. Clough and R.W. Fenn, 1983: Atmospheric Transmittance/Radiance: Computer Code LOWTRAN 6, Appendix D. AFGL-TR-83-0187, Environmental Research Papers No. 846. Air Force Geophysics Laboratory, Massachusetts.

Middleton, W.E.K., 1952: *Vision Through the Atmosphere*. Toronto, University of Toronto Press.

Sheppard, B.E., 1983: Adaptation to MOR. Preprints of the Fifth Symposium on Meteorological Observations and Instrumentation (Toronto, 11–15 April 1983), pp. 226–269.

Van de Hulst, H.C., 1957: *Light Scattering by Small Particles*. New York, Wiley & Sons (repr. Dover Books on Physics, 1981).

World Meteorological Organization, 1990: *The First WMO Intercomparison of Visibility Measurements: Final Report* (D.J. Griggs, D.W. Jones, M. Ouldridge and W.R. Sparks). Instruments and Observing Methods Report No. 41 (WMO/TD-No. 401). Geneva.

———, 1992*a*: *International Meteorological Vocabulary* (WMO-No. 182). Geneva.

———, 1992*b*: *Visibility Measuring Instruments: Differences between Scatterometers and Transmissometers* (J.P. van der Meulen) (WMO/TD-No. 462). Paper Presented at the WMO Technical Conference on Instruments and Methods of Observation (TECO-92) (Vienna, Austria, 11–15 May 1992). Instruments and Observing Methods Report No. 49. Geneva.

———, 2006: *KNMI Visibility Standard for Calibration of Scatterometers* (H. Bloemink) (WMO/TD-No. 1354). Paper presented at the WMO Technical Conference on Instruments and Methods of Observation (TECO-2006) (Geneva, Switzerland, 4–6 December 2006). Instruments and Observing Methods Report No. 94. Geneva.

———, 2012: Filtering of insect reduced MOR measurements by a forward scatter sensor (W. Wauben). Paper presented at the WMO Technical Conference on Meteorological and Environmental Instruments and Methods of Observation (TECO-2012) (Brussels 16–18 October 2012). Instruments and Observing Methods Report No. 109. Geneva.

———, 2014: *Guide to Meteorological Observing and Information Distribution Systems for Aviation Weather Services* (WMO-No. 731). Geneva.

———, 2016: Exploration of fog detection and visibility estimation from camera images (W. Wauben and M. Roth). Paper presented at the WMO Technical Conference on Meteorological and Environmental Instruments and Methods of Observation (TECO-2016) (Madrid, 27-30 September 2016). Instruments and Observing Methods Report No. 125. Geneva.


———————

# CHAPTER 10. MEASUREMENT OF EVAPORATION

## 10.1 GENERAL

### 10.1.1 Definitions

The *International Glossary of Hydrology* (WMO/United Nations Educational, Scientific and Cultural Organization, 2012) and the *International Meteorological Vocabulary* (WMO, 1992) present the following definitions (but note some differences):

**(Actual) evaporation.** Quantity of water evaporated from an open water surface or from the ground.

**Transpiration.** Process by which water from vegetation is transferred into the atmosphere in the form of vapour.

**(Actual) evapotranspiration (or effective evapotranspiration).** Quantity of water vapour evaporated from the soil and plants when the ground is at its natural moisture content.

**Potential evaporation (or evaporativity).** Quantity of water vapour which could be emitted by a surface of pure water, per unit surface area and unit time, under existing atmospheric conditions.

**Potential evapotranspiration.** Maximum quantity of water capable of being evaporated in a given climate from a continuous expanse of vegetation covering the whole ground and well supplied with water. It includes evaporation from the soil and transpiration from the vegetation from a specific region in a specific time interval, expressed as depth of water.

If the term *potential evapotranspiration* is used, the types of evaporation and transpiration occurring must be clearly indicated. For more details on these terms refer to WMO (2008), Volume I.

### 10.1.2 Units and scales

The rate of evaporation is defined as the amount of water evaporated from a unit surface area per unit of time. It can be expressed as the mass or volume of liquid water evaporated per area in unit of time, usually as the equivalent depth of liquid water evaporated per unit of time from the whole area. The unit of time is normally a day. The amount of evaporation should be read in millimetres (WMO, 2015). Depending on the type of instrument, the usual measuring accuracy is 0.1 to 0.01 mm.

### 10.1.3 Meteorological requirements

Estimates both of evaporation from free water surfaces and from the ground and of evapotranspiration from vegetation-covered surfaces are of great importance to hydrological modelling and in hydrometeorological and agricultural studies, for example, for the design and operation of reservoirs and irrigation and drainage systems.

Performance requirements are given in the present volume, Chapter 1. For daily totals, an extreme outer range is 0 to 100 mm, with a resolution of 0.1 mm. The uncertainty, at the 95% confidence level, should be ±0.1 mm for amounts of less than 5 mm, and ±2% for larger amounts. A figure of 1 mm has been proposed as an achievable accuracy. In principle, the usual instruments could meet these accuracy requirements, but difficulties with exposure and practical operation cause much larger errors (WMO, 1976).

Factors affecting the rate of evaporation from any body or surface can be broadly divided into two groups, meteorological factors and surface factors, either of which may be rate-limiting. The meteorological factors may, in turn, be subdivided into energy and aerodynamic variables. Energy is needed to change water from the liquid to the vapour phase; in nature, this is largely supplied by solar and terrestrial radiation. Aerodynamic variables, such as wind speed at the surface and vapour pressure difference between the surface and the lower atmosphere, control the rate of transfer of the evaporated water vapour.

It is useful to distinguish between situations where free water is present on the surface and those where it is not. Factors of importance include the amount and state of the water and also those surface characteristics which affect the transfer process to the air or through the body surface. Resistance to moisture transfer to the atmosphere depends, for example, on surface roughness; in arid and semi-arid areas, the size and shape of the evaporating surface is also extremely important. Transpiration from vegetation, in addition to the meteorological and surface factors already noted, is largely determined by plant characteristics and responses. These include, for example, the number and size of stomata (openings in the leaves), and whether these are open or closed. Stomatal resistance to moisture transfer shows a diurnal response but is also considerably dependent upon the availability of soil moisture to the rooting system.

The availability of soil moisture for the roots and for the evaporation from bare soil depends on the capillary supply, namely, on the texture and composition of the soil. Evaporation from lakes and reservoirs is influenced by the heat storage of the water body.

Methods for estimating evaporation and evapotranspiration are generally indirect; either by point measurements by an instrument or gauge, or by calculation using other measured meteorological variables (WMO, 1997).

### 10.1.4 **Measurement methods**

Direct measurements of evaporation or evapotranspiration from extended natural water or land surfaces are not practicable at present. However, several indirect methods derived from point measurements or other calculations have been developed which provide reasonable results.

The water loss from a standard saturated surface is measured with evaporimeters, which may be classified as atmometers and pan or tank evaporimeters. These instruments do not directly measure either evaporation from natural water surfaces, actual evapotranspiration or potential evapotranspiration. The values obtained cannot, therefore, be used without adjustment to arrive at reliable estimates of lake evaporation or of actual and potential evapotranspiration from natural surfaces.

An evapotranspirometer (lysimeter) is a vessel or container placed below the ground surface and filled with soil, on which vegetation can be cultivated. It is a multi-purpose instrument for the study of several phases of the hydrological cycle under natural conditions. Estimates of evapotranspiration (or evaporation in the case of bare soil) can be made by measuring and balancing all the other water budget components of the container, namely, precipitation, underground water drainage, and change in water storage of the block of soil. Usually, surface runoff is eliminated. Evapotranspirometers can also be used for the estimation of the potential evaporation of the soil or of the potential evapotranspiration of plant-covered soil, if the soil moisture is kept at field capacity.

For reservoirs or lakes, and for plots or small catchments, estimates may be made by water budget, energy budget, aerodynamic and complementarity approaches. The latter techniques are discussed in 10.5.

It should also be emphasized that different evaporimeters or lysimeters represent physically different measurements. The adjustment factors required for them to represent lake or actual or

potential evaporation and evapotranspiration are necessarily different. Such instruments and their exposure should, therefore, always be described very carefully and precisely, in order to understand the measuring conditions as fully as possible.

More details on all methods are found in WMO (2008), Volumes I and II.

## 10.2 ATMOMETERS

### 10.2.1 Instrument types

An atmometer is an instrument that measures the loss of water from a wetted, porous surface. The wetted surfaces are either porous ceramic spheres, cylinders, plates, or exposed filter-paper discs saturated with water. The evaporating element of the livingstone atmometer is a ceramic sphere of about 5 cm in diameter, connected to a water reservoir bottle by a glass or metal tube. The atmospheric pressure on the surface of the water in the reservoir keeps the sphere saturated with water. The Bellani atmometer consists of a ceramic disc fixed in the top of a glazed ceramic funnel, into which water is conducted from a burette that acts as a reservoir and measuring device. The evaporating element of the Piche evaporimeter is a disc of filter paper attached to the underside of an inverted graduated cylindrical tube, closed at one end, which supplies water to the disc. Successive measurements of the volume of water remaining in the graduated tube will give the amount lost by evaporation in any given time.

### 10.2.2 Measurement taken by atmometers

Although atmometers are frequently considered to give a relative measure of evaporation from plant surfaces, their measurements do not, in fact, bear any simple relation to evaporation from natural surfaces.

Readings from Piche evaporimeters with carefully standardized shaded exposures have been used with some success to derive the aerodynamic term, a multiplication of a wind function and the saturation vapour pressure deficit, required for evaporation estimation by, for example, Penman's combination method after local correlations between them were obtained.

While it may be possible to relate the loss from atmometers to that from a natural surface empirically, a different relation may be expected for each type of surface and for differing climates. Atmometers are likely to remain useful in small-scale surveys. Their great advantages are their small size, low cost and small water requirements. Dense networks of atmometers can be installed over a small area for micrometeorological studies. The use of atmometers is not recommended for water resource surveys if other data are available.

### 10.2.3 Sources of error in atmometers

One of the major problems in the operation of atmometers is keeping the evaporating surfaces clean. Dirty surfaces will affect significantly the rate of evaporation, in a way comparable to the wet bulb in psychrometry.

Furthermore, the effect of differences in their exposure on evaporation measurements is often remarkable. This applies particularly to the exposure to air movement around the evaporating surface when the instrument is shaded.

## 10.3 EVAPORATION PANS AND TANKS

Evaporation pans or tanks have been made in a variety of shapes and sizes and there are different modes of exposing them. Among the various types of pans in use, the United States Class A pan, the Russian GGI-3000 pan and the Russian 20 $m^2$ tank are described in the following subsections. These instruments are now widely used as standard network evaporimeters and their performance has been studied under different climatic conditions over fairly wide ranges of latitude and elevation. The pan data from these instruments possess stable, albeit complicated and climate-zone-dependent, relationships with the meteorological elements determining evaporation, when standard construction and exposure instructions have been carefully followed.

The adoption of the Russian 20 $m^2$ tank as the international reference evaporimeter has been recommended.

### 10.3.1 United States Class A pan

The United States Class A pan is of cylindrical design, 25.4 cm deep and 120.7 cm in diameter. The bottom of the pan is supported 3 to 5 cm above the ground level on an open-frame wooden platform, which enables air to circulate under the pan, keeps the bottom of the pan above the level of water on the ground during rainy weather, and enables the base of the pan to be inspected without difficulty. The pan itself is constructed of 0.8 mm thick galvanized iron, copper or Monel metal, and is normally left unpainted. The pan is filled to 5 cm below the rim (which is known as the reference level).

The water level is measured by means of either a hookgauge or a fixed-point gauge. The hookgauge consists of a movable scale and vernier fitted with a hook, the point of which touches the water surface when the gauge is correctly set. A stilling well, about 10 cm across and about 30 cm deep, with a small hole at the bottom, breaks any ripples that may be present in the tank, and serves as a support for the hookgauge during an observation. The pan is refilled whenever the water level, as indicated by the gauge, drops by more than 2.5 cm from the reference level.

### 10.3.2 Russian GGI-3000 pan

The Russian GGI-3000 pan is of cylindrical design, with a surface area of 3 000 $cm^2$ and a depth of 60 cm. The bottom of the pan is cone-shaped. The pan is set in the soil with its rim 7.5 cm above the ground. In the centre of the tank is a metal index tube upon which a volumetric burette is set when evaporation observations are made. The burette has a valve, which is opened to allow its water level to equalize that in the pan. The valve is then closed and the volume of water in the burette is accurately measured. The height of the water level above the metal index tube is determined from the volume of water in, and the dimensions of, the burette. A needle attached to the metal index tube indicates the height to which the water level in the pan should be adjusted. The water level should be maintained so that it does not fall more than 5 mm or rise more than 10 mm above the needle point. A GGI-3000 raingauge with a collector that has an area of 3 000 $cm^2$ is usually installed next to the GGI-3000 pan.

### 10.3.3 Russian 20 $m^2$ tank

This tank has a surface of 20 $m^2$ and a diameter of about 5 m; it is cylindrical with a flat bottom and is 2 m deep. It is made of 4 to 5 mm thick welded iron sheets and is installed in the soil with its rim 7.5 cm above the ground. The inner and exposed outer surfaces of the tank are painted white. The tank is provided with a replenishing vessel and a stilling well with an index pipe upon which the volumetric burette is set when the water level in the tank is measured. Inside the stilling well, near the index pipe, a small rod terminating in a needle point indicates the height to which the water level is to be adjusted. The water level should always be maintained

so that it does not fall more than 5 mm below or rise more than 10 mm above the needle point. A graduated glass tube attached laterally to the replenishing tank indicates the amount of water added to the tank and provides a rough check of the burette measurement.

### 10.3.4 Measurements taken by evaporation pans and tanks

The rate of evaporation from a pan or tank evaporimeter is measured by the change in level of its free water surface. This may be done by such devices as described above for Class A pans and GGI-3000 pans.

Several types of automatic evaporation pans are in use. The water level in such a pan is kept constant by releasing water into the pan from a storage tank or by removing water from the pan when precipitation occurs. The amount of water added to, or removed from, the pan is recorded. In some tanks or pans, the level of the water is also recorded continuously by means of a float in the stilling well. The float operates a recorder.

Measurements of pan evaporation are the basis of several techniques for estimating evaporation and evapotranspiration from natural surfaces whose water loss is of interest. Measurements taken by evaporation pans are advantageous because they are, in any case, the result of the impact of the total meteorological variables, and because pan data are available immediately and for any period required. Pans are, therefore, frequently used to obtain information about evaporation on a routine basis within a network.

### 10.3.5 Exposure of evaporation pans and tanks

Three types of exposures are mainly used for pans and tanks as follows:

(a) Sunken, where the main body of the tank is below ground level, the evaporating surface being at or near the level of the surrounding surface;

(b) Above ground, where the whole of the pan and the evaporation surface are at some small height above the ground;

(c) Mounted on moored floating platforms on lakes or other water bodies.

Evaporation stations should be located at sites that are fairly level and free from obstructions such as trees, buildings, shrubs or instrument shelters. Such single obstructions, when small, should not be closer than 5 times their height above the pan; for clustered obstructions, this becomes 10 times. Plots should be sufficiently large to ensure that readings are not influenced by spray drift or by upwind edge effects from a cropped or otherwise different area. Such effects may extend to more than 100 m. The plot should be fenced off to protect the instruments and to prevent animals from interfering with the water level; however, the fence should be constructed in such a way that it does not affect the wind structure over the pan.

The ground cover at the evaporation station should be maintained as similar as possible to the natural cover common to the area. Grass, weeds, and the like should be cut frequently to keep them below the level of the pan rim with regard to sunken pans (7.5 cm). Preferably this same grass height of below 7.5 cm applies also to Class A pans. Under no circumstance should the instrument be placed on a concrete slab or asphalt, or on a layer of crushed rock. This type of evaporimeter should not be shaded from the sun.

### 10.3.6 Sources of error in evaporation pans and tanks

The mode of pan exposure leads both to various advantages and to sources of measurement errors.

Pans installed above the ground are inexpensive and easy to install and maintain. They stay cleaner than sunken tanks as dirt does not, to any large extent, splash or blow into the water from the surroundings. Any leakage that develops after installation is relatively easy to detect and rectify. However, the amount of water evaporated is greater than that from sunken pans, mainly because of the additional radiant energy intercepted by the sides. Adverse side-wall effects can be largely eliminated by using an insulated pan, but this adds to the cost, would violate standard construction instructions and would change the "stable" relations mentioned in 10.3.

Sinking the pan into the ground tends to reduce objectionable boundary effects, such as radiation on the side walls and heat exchange between the atmosphere and the pan itself. But the disadvantages are as follows:

(a) More unwanted material collects in the pan, with the result that it is difficult to clean;

(b) Leaks cannot easily be detected and rectified;

(c) The height of the vegetation adjacent to the pan is somewhat more critical. Moreover, appreciable heat exchange takes place between the pan and the soil, and this depends on many factors, including soil type, water content and vegetation cover.

A floating pan approximates more closely evaporation from the lake than from an onshore pan exposed either above or at ground level, even though the heat-storage properties of the floating pan are different from those of the lake. It is, however, influenced by the particular lake in which it floats and it is not necessarily a good indicator of evaporation from the lake. Observational difficulties are considerable and, in particular, splashing frequently renders the data unreliable. Such pans are also costly to install and operate.

In all modes of exposure it is most important that the tank should be made of non-corrosive material and that all joints be made in such a way as to minimize the risk of the tank developing leaks.

Heavy rain and very high winds are likely to cause splash-out from pans and may invalidate the measurements.

The level of the water surface in the evaporimeter is important. If the evaporimeter is too full, as much as 10% (or more) of any rain falling may splash out, leading to an overestimate of evaporation. Too low a water level will lead to a reduced evaporation rate (of about 2.5% for each centimetre below the reference level of 5 cm, in temperate regions) due to excessive shading and sheltering by the rim. If the water depth is allowed to become very shallow, the rate of evaporation rises due to increased heating of the water surface.

It is advisable to restrict the permitted water-level range either by automatic methods, by adjusting the level at each reading, or by taking action to remove water when the level reaches an upper-limit mark, and to add water when it reaches a lower-limit mark.

### 10.3.7 Maintenance of evaporation pans and tanks

An inspection should be carried out at least once a month, with particular attention being paid to the detection of leaks. The pan should be cleaned out as often as necessary to keep it free from litter, sediment, scum and oil films. It is recommended that a small amount of copper sulphate, or of some other suitable algacide, be added to the water to restrain the growth of algae.

If the water freezes, all the ice should be broken away from the sides of the tank and the measurement of the water level should be taken while the ice is floating. Provided that this is

done, the fact that some of the water is frozen will not significantly affect the water level. If the ice is too thick to be broken the measurement should be postponed until it can be broken, the evaporation should then be determined for the extended period.

It is often necessary to protect the pan from birds and other small animals, particularly in arid and tropical regions. This may be achieved by the use of the following:

(a) Chemical repellents: In all cases where such protection is used, care must be taken not to change significantly the physical characteristics of the water in the evaporimeter;

(b) A wire-mesh screen supported over the pan: Standard screens of this type are in routine use in a number of areas. They prevent water loss caused by birds and animals, but also reduce the evaporation loss by partly shielding the water from solar radiation and by reducing wind movement over the water surface. In order to obtain an estimate of the error introduced by the effect of the wire-mesh screen on the wind field and the thermal characteristics of the pan, it is advisable to compare readings from the protected pan with those of a standard pan at locations where interference does not occur. Tests with a protective cylinder made of 25 mm hexagonal-mesh steel wire netting supported by an 8 mm steel-bar framework showed a consistent reduction of 10% in the evaporation rate at three different sites over a two-year period.

## 10.4 EVAPOTRANSPIROMETERS (LYSIMETERS)

Several types of lysimeters have been described in the technical literature. Details of the design of some instruments used in various countries are described in WMO (1966, 2008 (Volume I)).

In general, a lysimeter consists of the soil-filled inner container and retaining walls or an outer container, as well as special devices for measuring percolation and changes in the soil-moisture content.

There is no universal international standard lysimeter for measuring evapotranspiration. The surface area of lysimeters in use varies from 0.05 to some 100 $m^2$ and their depth varies from 0.1 to 5 m. According to their method of operation, lysimeters can be classified into non-weighable and weighable instruments. Each of these devices has its special merits and drawbacks, and the choice of any type of lysimeter depends on the problem to be studied.

Non-weighable (percolation-type) lysimeters can be used only for long-term measurements, unless the soil-moisture content can be measured by some independent and reliable technique. Large-area percolation-type lysimeters are used for water budget and evapotranspiration studies of tall, deep-rooting vegetation cover, such as mature trees. Small, simple types of lysimeters in areas with bare soil or grass and crop cover could provide useful results for practical purposes under humid conditions. This type of lysimeter can easily be installed and maintained at a low cost and is, therefore, suitable for network operations.

Weighable lysimeters, unless of a simple microlysimeter-type for soil evaporation, are much more expensive, but their advantage is that they secure reliable and precise estimates of short-term values of evapotranspiration, provided that the necessary design, operation and siting precautions have been taken.

Several weighing techniques using mechanical or hydraulic principles have been developed. The simpler, small lysimeters are usually lifted out of their sockets and transferred to mechanical scales by means of mobile cranes. The container of a lysimeter can be mounted on a permanently installed mechanical scale for continuous recording. The design of the weighing and recording system can be considerably simplified by using load cells with strain gauges of variable electrical resistance. The hydraulic weighing systems use the principle of fluid displacement resulting from the changing buoyancy of a floating container (so-called floating lysimeter), or the principle of fluid pressure changes in hydraulic load cells.

The large weighable and recording lysimeters are recommended for precision measurements in research centres and for standardization and parameterization of other methods of evapotranspiration measurement and the modelling of evapotranspiration. Small weighable types of lysimeters are quite useful and suitable for network operation. Microlysimeters for soil evaporation are a relatively new phenomenon.

### 10.4.1 Measurements taken by lysimeters

The rate of evapotranspiration may be estimated from the general equation of the water budget for the lysimeter containers. Evapotranspiration equals precipitation/irrigation minus percolation minus change in water storage.

Hence, the observational programme on lysimeter plots includes precipitation/irrigation, percolation and change in soil water storage. It is useful to complete this programme through observations of plant growth and development.

Precipitation – and irrigation, if any – is preferably measured at ground level by standard methods. Percolation is collected in a tank and its volume may be measured at regular intervals or recorded. For precision measurements of the change in water storage, the careful gravimetric techniques described above are used. When weighing, the lysimeter should be sheltered to avoid wind-loading effects.

The application of the volumetric method is quite satisfactory for estimating long-term values of evapotranspiration. With this method, measurements are taken of the amount of precipitation and percolation. It is assumed that a change in water storage tends to zero over the period of observation. Changes in the soil moisture content may be determined by bringing the moisture in the soil up to field capacity at the beginning and at the end of the period.

### 10.4.2 Exposure of evapotranspirometers

Observations of evapotranspiration should be representative of the plant cover and moisture conditions of the general surroundings of the station (WMO, 2015). In order to simulate representative evapotranspiration rates, the soil and plant cover of the lysimeter should correspond to the soil and vegetation of the surrounding area, and disturbances caused by the existence of the instrument should be minimized. The most important requirements for the exposure of lysimeters are given below.

In order to maintain the same hydromechanical properties of the soil, it is recommended that the lysimeter be placed into the container as an undisturbed block (monolith). In the case of light, rather homogenous soils and a large container, it is sufficient to fill the container layer by layer in the same sequence and with the same density as in the natural profile.

In order to simulate the natural drainage process in the container, restricted drainage at the bottom must be prevented. Depending on the soil texture, it may be necessary to maintain the suction at the bottom artificially by means of a vacuum supply.

Apart from microlysimeters for soil evaporation, a lysimeter should be sufficiently large and deep, and its rim as low as practicable, to make it possible to have a representative, free-growing vegetation cover, without restriction to plant development.

In general, the siting of lysimeters is subject to fetch requirements, such as that of evaporation pans, namely, the plot should be located beyond the zone of influence of buildings, even single trees, meteorological instruments, and so on. In order to minimize the effects of advection, lysimeter plots should be located at a sufficient distance from the upwind edge of the surrounding area, that is, not less than 100 to 150 m. The prevention of advection effects is of special importance for measurements taken at irrigated land surfaces.

### 10.4.3 Sources of error in lysimeter measurements

Lysimeter measurements are subject to several sources of error caused by the disturbance of the natural conditions by the instrument itself. Some of the major effects are as follows:

(a) Restricted growth of the rooting system;

(b) Change of eddy diffusion by discontinuity between the canopy inside the lysimeter and in the surrounding area. Any discontinuity may be caused by the annulus formed by the containing and retaining walls and by discrepancies in the canopy itself;

(c) Insufficient thermal equivalence of the lysimeter to the surrounding area caused by:

  (i) Thermal isolation from the subsoil;

  (ii) Thermal effects of the air rising or descending between the container and the retaining walls;

  (iii) Alteration of the thermal properties of the soil through alteration of its texture and its moisture conditions;

(d) Insufficient equivalence of the water budget to that of the surrounding area caused by:

  (i) Disturbance of soil structure;

  (ii) Restricted drainage;

  (iii) Vertical seepage at walls;

  (iv) Prevention of surface runoff and lateral movement of soil water.

Some suitable arrangements exist to minimize lysimeter measurement errors, for example, regulation of the temperature below the container, reduction of vertical seepage at the walls by flange rings, and so forth. In addition to the careful design of the lysimeter equipment, sufficient representativeness of the plant community and the soil type of the area under study is of great importance. Moreover, the siting of the lysimeter plot must be fully representative of the natural field conditions.

### 10.4.4 Lysimeters maintenance

Several arrangements are necessary to maintain the representativeness of the plant cover inside the lysimeter. All agricultural and other operations (sowing, fertilizing, mowing, and the like) in the container and surrounding area should be carried out in the same way and at the same time. In order to avoid errors due to rainfall catch, the plants near and inside the container should be kept vertical, and broken leaves and stems should not extend over the surface of the lysimeter.

The maintenance of the technical devices is peculiar to each type of instrument and cannot be described here.

It is advisable to test the evapotranspirometer for leaks at least once a year by covering its surface to prevent evapotranspiration and by observing whether, over a period of days, the volume of drainage equals the amount of water added to its surface.

## 10.5 ESTIMATION OF EVAPORATION FROM NATURAL SURFACES

Consideration of the factors which affect evaporation, as outlined in 10.1.3, indicates that the rate of evaporation from a natural surface will necessarily differ from that of an evaporimeter exposed to the same atmospheric conditions, because the physical characteristics of the two evaporating surfaces are not identical.

In practice, evaporation or evapotranspiration rates from natural surfaces are of interest, for example, reservoir or lake evaporation, crop evaporation, as well as areal amounts from extended land surfaces such as catchment areas.

In particular, accurate areal estimates of evapotranspiration from regions with varied surface characteristics and land-use patterns are very difficult to obtain (WMO, 1966, 1997).

Suitable methods for the estimation of lake or reservoir evaporation are the water budget, energy budget and aerodynamic approaches, the combination method of aerodynamic and energy-balance equations, and the use of a complementarity relationship between actual and potential evaporation. Furthermore, pan evaporation techniques exist which use pan evaporation for the establishment of a lake-to-pan relation. Such relations are specific to each pan type and mode of exposure. They also depend on the climatic conditions (see WMO, 1985, 2008 (Volume I, Chapter 4)).

The water non-limiting point or areal values of evapotranspiration from vegetation-covered land surfaces may be obtained by determining such potential (or reference crop) evapotranspiration with the same methods as those indicated above for lake applications, but adapted to vegetative conditions. Some methods use additional growth stage-dependent coefficients for each type of vegetation, such as crops, and/or an integrated crop stomatal resistance value for the vegetation as a whole.

The Royal Netherlands Meteorological Institute employs the following procedure established by G.F. Makkink (Hooghart, 1971) for calculating the daily (24 h) reference vegetation evaporation from the averaged daily air temperature and the daily amount of global radiation as follows:

Saturation vapour pressure at air temperature $T$:

$$e_s(T) = 6.107 \cdot 10^{7.5 \cdot \frac{T}{237.3+T}} \quad \text{hPa}$$

Slope of the curve of saturation water vapour pressure versus temperature at $T$:

$$\Delta(T) = \frac{7.5 \cdot 237.3}{(237.3+T)^2} \cdot \ln(10) \cdot e_s(T) \quad \text{hPa/°C}$$

Psychrometric constant:

$$\Delta(T) = 0.646 + 0.0006T \quad \text{hPa/°C}$$

Specific heat of evaporation of water:

$$\lambda(T) = 1\,000 \cdot (2\,501 - 2.38 \cdot T) \quad \text{J/kg}$$

Density of water:

$$\rho = 1\,000 \quad \text{kg/m}^3$$

Global radiation (24 h amount):

$$Q \quad \text{J/m}^2$$

Air temperature (24 h average):

$$T \quad \text{°C}$$

Daily reference vegetation evaporation:[1]

$$E_r = \frac{1000 \cdot 0.65 \cdot \delta(T)}{\{\delta(T) + \gamma(T)\} \cdot \rho \cdot \lambda(T)} \cdot Q \quad \text{mm}$$

By relating the measured rate of actual evapotranspiration to estimates of the water non-limiting potential evapotranspiration and subsequently relating this normalized value to the soil water content, soil water deficits, or the water potential in the root zone, it is possible to devise coefficients with which the actual evapotranspiration rate can be calculated for a given soil water status.

Point values of actual evapotranspiration from land surfaces can be estimated more directly from observations of the changes in soil water content measured by sampling soil moisture on a regular basis. Evapotranspiration can be measured even more accurately using a weighing lysimeter. Further methods make use of turbulence measurements (for example, eddy-correlation method) and profile measurements (for example, in boundary-layer data methods and, at two heights, in the Bowen-ratio energy-balance method). They are much more expensive and require special instruments and sensors for humidity, wind speed and temperature. Such estimates, valid for the type of soil and canopy under study, may be used as reliable independent reference values in the development of empirical relations for evapotranspiration modelling.

The difficulty in determining basin evapotranspiration arises from the discontinuities in surface characteristics which cause variable evapotranspiration rates within the area under consideration. When considering short-term values, it is necessary to estimate evapotranspiration by using empirical relationships. Over a long period (in order to minimize storage effects) the water-budget approach can be used to estimate basin evapotranspiration (see WMO, 1971). One approach, suitable for estimates from extended areas, refers to the atmospheric water balance and derives areal evapotranspiration from radiosonde data. WMO (2008, Volume I, Chapter 4) describes the above-mentioned methods, their advantages and their application limits.

The measurement of evaporation from a snow surface is difficult and probably no more accurate than the computation of evaporation from water.

Evaporimeters made of polyethylene or colourless plastic are used in many countries for the measurement of evaporation from snow-pack surfaces; observations are made only when there is no snowfall.

Estimates of evaporation from snow cover can be made from observations of air humidity and wind speed at one or two levels above the snow surface and at the snow-pack surface, using the turbulent diffusion equation. The estimates are most reliable when evaporation values are computed for periods of five days or more.

---

[1] The constant 1 000 is for conversion from metres to millimetres; the constant 0.65 is a typical empirical constant.

## REFERENCES AND FURTHER READING


Hooghart, J.C. (ed.), 1971: *Evaporation and Weather*. TNO Committee of Hydrological Research, Technical Meeting 44, Proceedings and Information No. 39, TNO, The Hague.

World Meteorological Organization, 1966: *Measurement and Estimation of Evaporation and Evapotranspiration*. Technical Note No. 83 (WMO-No. 201, TP. 105). Geneva.

———, 1971: *Problems of Evaporation Assessment in the Water Balance* (C.E. Hounam). WMO/IHD Report No. 13 (WMO-No. 285). Geneva.

———, 1973: *Atmospheric Vapour Flux Computations for Hydrological Purposes* (J.P. Peixoto). WMO/IHD Report No. 20 (WMO-No. 357). Geneva.

———, 1976: *The CIMO International Evaporimeter Comparisons* (WMO-No. 449). Geneva.

———, 1977: *Hydrological Application of Atmospheric Vapour-Flux Analyses* (E.M. Rasmusson). Operational Hydrology Report No. 11 (WMO-No. 476). Geneva.

———, 1985: *Casebook on Operational Assessment of Areal Evaporation*. Operational Hydrology Report No. 22 (WMO-No. 635). Geneva.

———, 1992: *International Meteorological Vocabulary* (WMO-No. 182). Geneva.

———, 1997: *Estimation of Areal Evapotranspiration.* Technical Reports in Hydrology and Water Resources No. 56 (WMO/TD-No. 785). Geneva.

———, 2008: *Guide to Hydrological Practices* (WMO-No. 168), Volumes I and II. Geneva.

———, 2015 (updated in 2017): *Manual on the Global Observing System* (WMO-No. 544), Volume I. Geneva.

World Meteorological Organization/United Nations Educational, Scientific and Cultural Organization, 2012: *International Glossary of Hydrology* (WMO-No. 385). Geneva.

# CHAPTER 11. MEASUREMENT OF SOIL MOISTURE

## 11.1 GENERAL

Soil moisture is an important component in the atmospheric water cycle, both on a small agricultural scale and in large-scale modelling of land/atmosphere interaction. Vegetation and crops always depend more on the moisture available at root level than on precipitation occurrence. Water budgeting for irrigation planning, as well as the actual scheduling of irrigation action, requires local soil moisture information. Knowledge of the degree of soil wetness helps to understand the initiation of convective events and to forecast the risk of flash floods or the occurrence of fog.

Nevertheless, soil moisture has been seldom observed routinely at meteorological stations. Documentation of soil wetness was usually restricted to the description of the "state of the ground" by means of WMO Code Tables 0901 and 0975, and its measurement was left to hydrologists, agriculturalists and other actively interested parties. Around 1990, the interest of meteorologists in soil moisture measurement increased. This was partly because, after the pioneering work by Deardorff (1978), numerical atmosphere models at various scales became more adept at handling fluxes of sensible and latent heat in soil surface layers. Moreover, newly developed soil moisture measurement techniques are more feasible for meteorological stations than most of the classic methods.

To satisfy the increasing need for determining soil moisture status, the most commonly used methods and instruments will be discussed, including their advantages and disadvantages. Some less common observation techniques are also mentioned. This chapter discusses both in situ and remote-sensing soil moisture measurements. Space-based remote-sensing is also included, complemented by information in Volume IV of the present Guide.

### 11.1.1 Definitions

Soil moisture determinations measure either the soil water content or the soil water potential.

**Soil water content.** An expression of the mass or volume of water in the soil, while the soil water potential is an expression of the soil water energy status. The relation between content and potential is not universal and depends on the characteristics of the local soil, such as soil density and soil texture.

Soil water content on the basis of mass is expressed in the gravimetric soil moisture content, $\theta_g$, defined by:

$$\theta_g = M_{water}/M_{soil} \tag{11.1}$$

where $M_{water}$ is the mass of the water in the soil sample and $M_{soil}$ is the mass of dry soil that is contained in the sample. Values of $\theta_g$ in meteorology are usually expressed in %.

Because precipitation, evapotranspiration and solute transport variables are commonly expressed in terms of flux, volumetric expressions for water content are often more useful. The volumetric soil moisture content of a soil sample, $\theta_v$, is defined as:

$$\theta_v = V_{water}/V_{sample} \tag{11.2}$$

where $V_{water}$ is the volume of water in the soil sample and $V_{sample}$ is the total volume of dry soil + air + water in the sample. Again, the ratio is usually expressed in %, although many research

communities are now adopting volumetric water content ($m^3/m^3$) as the standard for expressing soil moisture. The relationship between gravimetric and volumetric moisture contents is:

$$\theta_v = \theta_g \left( \rho_b / \rho_w \right) \tag{11.3}$$

where $\rho_b$ is the dry soil bulk density and $\rho_w$ is the soil water density.

The basic technique for measuring soil water content is the gravimetric method, described in 11.2. Because this method is based on direct measurements, it is the standard with which all other methods are compared. Unfortunately, gravimetric sampling is destructive, rendering repeat measurements on the same soil sample impossible. Because of the difficulties of accurately measuring dry soil and water volumes, volumetric water contents are not usually determined directly.

**Soil water potential.** This describes the energy status of the soil water and is an important parameter for water transport analysis, water storage estimates and soil-plant-water relationships. A difference in water potential between two soil locations indicates a tendency for water flow, from high to low potential. When the soil is drying, the water potential becomes more negative and the work that must be done to extract water from the soil increases. This makes water uptake by plants more difficult, so the water potential in the plant drops, resulting in plant stress and, eventually, severe wilting.

Formally, the water potential is a measure of the ability of soil water to perform work, or, in the case of negative potential, the work required to remove the water from the soil. The total water potential $\psi_t$, the combined effect of all force fields, is given by:

$$\psi_t = \psi_z + \psi_m + \psi_o + \psi_p \tag{11.4}$$

where $\psi_z$ is the gravitational potential based on elevation above the MSL; $\psi_m$ is the matric potential, suction due to attraction of water by the soil matrix; $\psi_o$ is the osmotic potential, due to energy effects of solutes in water; and $\psi_p$ is the pressure potential, the hydrostatic pressure below a water surface.

The potentials which are not related to the composition of water or soil are together called hydraulic potential, $\psi_h$. In saturated soil, this is expressed as $\psi_h = \psi_z + \psi_p$, while in unsaturated soil, it is expressed as $\psi_h = \psi_z + \psi_m$. When the phrase "water potential" is used in studies, sometimes with the notation $\psi_w$, it is advisable to check the author's definition because this term has been used for $\psi_m + \psi_z$ as well as for $\psi_m + \psi_o$.

The gradients of the separate potentials will not always be significantly effective in inducing flow. For example, $\psi_o$ requires a semi-permeable membrane to induce flow, and $\psi_p$ will exist in saturated or ponded conditions, but most practical applications are in unsaturated soil.

### 11.1.2 Units

In solving the mass balance or continuity equations for water, it must be remembered that the components of water content parameters are not dimensionless. Gravimetric water content is the weight of soil water contained in a unit weight of soil (kg water/kg dry soil). Likewise, volumetric water content is a volume fraction ($m^3$ water/$m^3$ soil).

The basic unit for expressing water potential is energy (in joules = kg $m^2$ $s^{-2}$) per unit mass, J $kg^{-1}$. Alternatively, energy per unit volume (J $m^{-3}$) is equivalent to pressure, expressed in pascals (Pa = kg $m^{-1}$ $s^{-2}$). Units encountered in older literature are bar (= 100 kPa),

atmosphere (= 101.32 kPa), or pounds per square inch (= 6.895 kPa). A third class of units are those of pressure head in (centi)metres of water or mercury, energy per unit weight. The relation of the three potential unit classes is:

$$\psi\left(\mathrm{J\ kg^{-1}}\right) = \gamma \cdot \psi\left(\mathrm{Pa}\right) = \left[\psi\left(\mathrm{m}\right)\right]/\mathrm{g} \tag{11.5}$$

where $\gamma = 10^3$ kg m$^{-3}$ (density of water) and g = 9.81 m s$^{-2}$ (gravity acceleration). Because the soil water potential has a large range, it is often expressed logarithmically, usually in pressure head of water. A common unit for this is called pF, and is equal to the base 10 logarithm of the absolute value of the head of water expressed in centimetres.

### 11.1.3 Meteorological requirements

Soil consists of individual particles and aggregates of mineral and organic materials, separated by spaces or pores which are occupied by water and air. The relative amount of pore space decreases with increasing soil grain size (intuitively one would expect the opposite). The movement of liquid water through soil depends upon the size, shape and generally the geometry of the pore spaces.

If a large quantity of water is added to a block of otherwise "dry" soil, some of it will drain away rapidly by the effects of gravity through any relatively large cracks and channels. The remainder will tend to displace some of the air in the spaces between particles, the larger pore spaces first. Broadly speaking, a well-defined "wetting front" will move downwards into the soil, leaving an increasingly thick layer retaining all the moisture it can hold against gravity. That soil layer is then said to be at "field capacity", a state that for most soils occurs about $\psi_m \approx -33$ J/kg, with a range of values from –1 J/kg for organic soils to –100 J/kg for heavy clay soils. A value of –10 J/kg (pF ≈ 2) can be assigned for a loamy sand soil. This state must not be confused with the undesirable situation of "saturated" soil, where all the pore spaces are occupied by water. After a saturation event, such as heavy rain, the soil usually needs at least 24 h to reach field capacity. When moisture content falls below field capacity, the subsequent limited movement of water in the soil is partly liquid, partly in the vapour phase by distillation (related to temperature gradients in the soil), and sometimes by transport in plant roots.

Plant roots within the block will extract liquid water from the water films around the soil particles with which they are in contact. The rate at which this extraction is possible depends on the soil moisture potential. A point is reached at which the forces holding moisture films to soil particles cannot be overcome by root suction, and plants are starved of water and lose turgidity: soil moisture has reached the "wilting point", which in most cases occurs at a soil water potential of –1.5 MPa (pF = 4.2). In agriculture, the soil water available to plants is commonly taken to be the quantity between field capacity and the wilting point, and this varies highly between soils: in sandy soils it may be less than 10 volume per cent, while in soils with much organic matter it can be over 40 volume per cent.

Usually it is desirable to know the soil moisture content and potential as a function of depth. Evapotranspiration models concern mostly a shallow depth (tens of centimetres); agricultural applications need moisture information at root depth (order of a metre); and atmospheric general circulation models incorporate a number of layers down to a few metres. For hydrological and water-balance needs – such as catchment-scale runoff models, as well as for effects upon soil properties such as soil mechanical strength, thermal conductivity and diffusivity – information on deep soil water content is needed. The accuracy needed in water content determinations and the spatial and temporal resolution required vary by application. An often-occurring problem is the inhomogeneity of many soils, meaning that a single observation location cannot provide absolute knowledge of the regional soil moisture, but only relative knowledge of its change.

### 11.1.4 Measurement methods

The methods and instruments available to evaluate soil water status may be classified in three ways. First, a distinction is made between the determination of water content and the

determination of water potential. Second, a so-called direct method requires the availability of sizeable representative terrain from which large numbers of soil samples can be taken for destructive evaluation in the laboratory. Indirect methods use an instrument placed in the soil to measure some soil property related to soil moisture. Third, methods can be ranged according to operational applicability, taking into account the regular labour involved, the degree of dependence on laboratory availability, the complexity of the operation and the reliability of the result. Moreover, the preliminary costs of acquiring instrumentation must be compared with the subsequent costs of local routine observation and data processing.

Reviews such as WMO (1968, 1989, 2001) and Schmugge et al. (1980) are very useful for learning about practical problems, but dielectric measurement methods were only developed well after 1980, so too-early reviews should not be relied on much when choosing an operational method.

There are five operational alternatives for the determination of soil water content. First, there is classic gravimetric moisture determination, which is a simple direct method. Second, there is lysimetry, a non-destructive variant of gravimetric measurement. A container filled with soil is weighed either occasionally or continuously to indicate changes in total mass in the container, which may in part or totally be due to changes in soil moisture (lysimeters are discussed in more detail in the present volume, Chapter 10). Third, water content may be determined indirectly by various radiological techniques, such as neutron scattering and gamma absorption. Fourth, water content can be derived from the dielectric properties of soil, for example, by using time-domain reflectometry. Lastly, soil moisture can be inferred on a global scale from remotely sensed measurements of the Earth's thermal or reflective properties.

Soil water potential measurement can be performed by several indirect methods, in particular using tensiometers, resistance blocks and soil psychrometers. None of these instruments is effective at this time over the full range of possible water potential values. For extended study of all methods of various soil moisture measurements, up-to-date handbooks are provided by Klute (1986), Dirksen (1999), Gardner et al. (2001) and Mullins (2001).

## 11.2 GRAVIMETRIC DIRECT MEASUREMENT OF SOIL WATER CONTENT

The gravimetric soil moisture content $\theta_g$ is typically determined directly. Soil samples of about 50 g are removed from the field with the best available tools (shovels, spiral hand augers, bucket augers, perhaps power-driven coring tubes), disturbing the sample soil structure as little as possible (Dirksen, 1999). The soil sample should be placed immediately in a leak-proof, seamless, pre-weighed and identified container. As the samples will be placed in an oven, the container should be able to withstand high temperatures without melting or losing significant mass. The most common soil containers are aluminium cans, but non-metallic containers should be used if the samples are to be dried in microwave ovens in the laboratory. If soil samples are to be transported for a considerable distance, tape should be used to seal the container to avoid moisture loss by evaporation.

The samples and container are weighed in the laboratory both before and after drying, the difference being the mass of water originally in the sample. The drying procedure consists in placing the open container in an electrically heated oven at 105 °C until the mass stabilizes at a constant value. The drying times required usually vary between 16 and 24 h. Note that drying at 105 ± 5 °C is part of the usually accepted definition of "soil water content", originating from the aim to measure only the content of "free" water which is not bound to the soil matrix (Gardner et al., 2001).

If the soil samples contain considerable amounts of organic matter, excessive oxidation may occur at 105 °C and some organic matter will be lost from the sample. Although the specific temperature at which excessive oxidation occurs is difficult to specify, lowering the oven temperature from 105 °C to 70 °C seems to be sufficient to avoid significant loss of organic matter, but this can lead to water content values that are too low. Oven temperatures and drying times should be checked and reported.

Microwave oven drying for the determination of gravimetric water contents may also be used effectively (Gee and Dodson, 1981). In this method, soil water temperature is quickly raised to boiling point, then remains constant for a period due to the consumption of heat in vaporizing water. However, the temperature rapidly rises as soon as the energy absorbed by the soil water exceeds the energy needed for vaporizing the water. Caution should be used with this method, as temperatures can become high enough to melt plastic containers if stones are present in the soil sample.

Gravimetric soil water contents of air-dry (25 °C) mineral soil are often less than 2%, but, as the soil approaches saturation, the water content may increase to values between 25% and 60%, depending on soil type. Volumetric soil water content, $\theta_v$, may range from less than 10% for air-dry soil to between 40% and 50% for mineral soils approaching saturation. Soil $\theta_v$ determination requires measurement of soil density, for example, by coating a soil clod with paraffin and weighing it in air and water, or some other method (Campbell and Henshall, 2001).

Water contents for stony or gravelly soils can be grossly misleading. When rocks occupy an appreciable volume of the soil, they modify direct measurement of soil mass, without making a similar contribution to the soil porosity. For example, gravimetric water content may be 10% for a soil sample with a bulk density of 2 000 kg $m^{-3}$; however, the water content of the same sample based on finer soil material (stones and gravel excluded) would be 20% if the bulk density of fine soil material was 1 620 kg $m^{-3}$.

Although the gravimetric water content for the finer soil fraction, $\theta_{g,fines}$, is the value usually used for spatial and temporal comparison, there may also be a need to determine the volumetric water content for a gravelly soil. The latter value may be important in calculating the volume of water in a root zone. The relationship between the gravimetric water content of the fine soil material and the bulk volumetric water content is given by:

$$\theta_{v,stony} = \theta_{g,fines}\left(\rho_b/\rho_w\right)\left(1 + M_{stones}/M_{fines}\right) \quad (11.6)$$

where $\theta_{v,stony}$ is the bulk volumetric water content of soil containing stones or gravel and $M_{stones}$ and $M_{fines}$ are the masses of the stone and fine soil fractions (Klute, 1986).

## 11.3 SOIL WATER CONTENT: INDIRECT METHODS

The capacity of soil to retain water is a function of soil texture and structure. When removing a soil sample, the soil being evaluated is disturbed, so its water-holding capacity is altered. Indirect methods of measuring soil water are helpful as they allow information to be collected at the same location for many observations without disturbing the soil water system. Moreover, most indirect methods determine the volumetric soil water content without any need for soil density determination.

### 11.3.1 Radiological methods

Two different radiological methods are available for measuring soil water content. One is the widely used neutron scatter method, which is based on the interaction of high-energy (fast) neutrons and the nuclei of hydrogen atoms in the soil. The other method measures the attenuation of gamma rays as they pass through soil. Both methods use portable equipment for multiple measurements at permanent observation sites and require careful calibration, preferably with the soil in which the equipment is to be used.

When using any radiation-emitting device, some precautions are necessary. The manufacturer will provide a shield that must be used at all times. The only time the probe leaves the shield is when it is lowered into the soil access tube. When the guidelines and regulations regarding radiation hazards stipulated by the manufacturers and health authorities are followed, there is no need to fear exposure to excessive radiation levels, regardless of the frequency of use.

Nevertheless, whatever the type of radiation-emitting device used, the operator should wear some type of film badge that will enable personal exposure levels to be evaluated and recorded on a monthly basis.

#### 11.3.1.1 *Neutron scattering method*

In neutron soil moisture detection (Visvalingam and Tandy, 1972; Greacen, 1981), a probe containing a radioactive source emitting high-energy (fast) neutrons and a counter of slow neutrons is lowered into the ground. The hydrogen nuclei, having about the same mass as neutrons, are at least 10 times as effective for slowing down neutrons upon collision as most other nuclei in the soil. Because in any soil most hydrogen is in water molecules, the density of slow "thermalized" neutrons in the vicinity of the neutron probe is nearly proportional to the volumetric soil water content.

Some fraction of the slowed neutrons, after a number of collisions, will again reach the probe and its counter. When the soil water content is large, not many neutrons are able to travel far before being thermalized and ineffective, and then 95% of the counted returning neutrons come from a relatively small soil volume. In wet soil, the "radius of influence" may be only 15 cm, while in dry soil that radius may increase to 50 cm. Therefore, the measured soil volume varies with water content, and thin layers cannot be resolved. This method is hence less suitable to localize water-content discontinuities, and it cannot be used effectively in the top 20 cm of soil on account of the soil air discontinuity.

Several source and detector arrangements are possible in a neutron probe, but it is best to have a probe with a double detector and a central source, typically in a cylindrical container. Such an arrangement allows for a nearly spherical zone of influence and leads to a more linear relation of neutron count to soil water content.

A cable is used to attach a neutron probe to the main instrument electronics, so that the probe can be lowered into a previously installed access tube. The access tube should be seamless and thick enough (at least 1.25 mm) to be rigid, but not so thick that the access tube itself slows neutrons down significantly. The access tube must be made of non-corrosive material, such as stainless steel, aluminium or plastic, although polyvinylchloride should be avoided as it absorbs slow neutrons. Usually, a straight tube with a diameter of 5 cm is sufficient for the probe to be lowered into the tube without a risk of jamming. Care should be taken in installing the access tube to ensure that no air voids exist between the tube and the soil matrix. At least 10 cm of the tube should extend above the soil surface, in order to allow the box containing the electronics to be mounted on top of the access tube. All access tubes should be fitted with a removable cap to keep rainwater from entering the tubes.

In order to enhance experimental reproducibility, the soil water content is not derived directly from the number of slow neutrons detected, but rather from a count ratio (CR), given by:

$$\mathrm{CR} = C_{\mathrm{soil}} / C_{\mathrm{background}} \tag{11.7}$$

where $C_{\mathrm{soil}}$ is the count of thermalized neutrons detected in the soil and $C_{\mathrm{background}}$ is the count of thermalized neutrons in a reference medium. All neutron probe instruments now come with a reference standard for these background calibrations, usually against water. The standard in which the probe is placed should be at least 0.5 m in diameter so as to represent an "infinite" medium. Calibration to determine $C_{\mathrm{background}}$ can be done by a series of ten 1 min readings, to be averaged, or by a single 1 h reading. $C_{\mathrm{soil}}$ is determined from averaging several soil readings at a particular depth/location. For calibration purposes, it is best to take three samples around the access tube and to average the water contents corresponding to the average CR calculated for that depth. A minimum of five different water contents should be evaluated for each depth. Although some calibration curves may be similar, a separate calibration for each depth should be conducted. The lifetime of most probes is more than 10 years.

#### 11.3.1.2 *Gamma-ray attenuation*

Whereas the neutron method measures the volumetric water content in a large sphere, gamma-ray absorption scans a thin layer. The dual-probe gamma device is nowadays mainly used in the laboratory since dielectric methods became operational for field use. Another reason for this is that gamma rays are more dangerous to work with than neutron scattering devices, as well as the fact that the operational costs for the gamma rays are relatively high.

Changes in gamma attenuation for a given mass absorption coefficient can be related to changes in total soil density. As the attenuation of gamma rays is due to mass, it is not possible to determine water content unless the attenuation of gamma rays due to the local dry soil density is known and remains unchanged with changing water content. Determining accurately the soil water content from the difference between the total and dry density attenuation values is therefore not simple.

Compared to neutron scattering, gamma-ray attenuation has the advantage of allowing accurate measurements at a few centimetres below the air-surface interface. Although the method has a high degree of resolution, the small soil volume evaluated will exhibit more spatial variation due to soil heterogeneities (Gardner and Calissendorff, 1967).

### 11.3.2 **Soil water dielectrics**

When a medium is placed in the electric field of a capacitor or waveguide, its influence on the electric forces in that field is expressed as the ratio between the forces in the medium and the forces which would exist in vacuum. This ratio, called permittivity or "dielectric constant", is for liquid water about 20 times larger than that of average dry soil, because water molecules are permanent dipoles. The dielectric properties of ice, and of water bound to the soil matrix, are comparable to those of dry soil. Therefore, the volumetric content of free soil water can be determined from the dielectric characteristics of wet soil by reliable, fast, non-destructive measurement methods, without the potential hazards associated with radioactive devices. Moreover, such dielectric methods can be fully automated for data acquisition. At present, two methods which evaluate soil water dielectrics are commercially available and used extensively, namely time-domain reflectometry and frequency-domain measurement.

#### 11.3.2.1 *Time-domain reflectometry*

Time-domain reflectometry is a method which determines the dielectric constant of the soil by monitoring the travel of an electromagnetic pulse, which is launched along a waveguide formed by a pair of parallel rods embedded in the soil. The pulse is reflected at the end of the waveguide and its propagation velocity, which is inversely proportional to the square root of the dielectric constant, can be measured well by actual electronics.

The most widely used relation between soil dielectrics and soil water content was experimentally summarized by Topp et al. (1980) as follows:

$$\theta_v = -0.053 + 0.029\,\varepsilon - 5.5 \cdot 10^{-4}\varepsilon^2 + 4.3 \cdot 10^{-6}\varepsilon^3 \qquad (11.8)$$

where $\varepsilon$ is the dielectric constant of the soil water system. This empirical relationship has proved to be applicable in many soils, roughly independent of texture and gravel content (Drungil et al., 1989). However, soil-specific calibration is desirable for soils with low density or with a high organic content. For complex soil mixtures, the De Loor equation has proved useful (Dirksen and Dasberg, 1993).

Generally, the parallel probes are separated by 5 cm and vary in length from 10 to 50 cm; the rods of the probe can be of any metallic substance. The sampling volume is essentially a cylinder of a few centimetres in radius around the parallel probes (Knight, 1992). The coaxial cable from the probe to the signal-processing unit should not be longer than about 30 m. Soil water profiles can be obtained from a buried set of probes, each placed horizontally at a different depth, linked to a field data logger by a multiplexer.

#### 11.3.2.2 *Frequency-domain measurement*

While time-domain reflectometry uses microwave frequencies in the gigahertz range, frequency-domain sensors measure the dielectric constant at a single microwave megahertz frequency. The microwave dielectric probe utilizes an open-ended coaxial cable and a single reflectometer at the probe tip to measure amplitude and phase at a particular frequency. Soil measurements are referenced to air, and are typically calibrated with dielectric blocks and/or liquids of known dielectric properties. One advantage of using liquids for calibration is that a perfect electrical contact between the probe tip and the material can be maintained (Jackson, 1990).

As a single, small probe tip is used, only a small volume of soil is ever evaluated, and soil contact is therefore critical. As a result, this method is excellent for laboratory or point measurements, but is likely to be subject to spatial variability problems if used on a field scale (Dirksen, 1999).

## 11.4 SOIL WATER POTENTIAL INSTRUMENTATION

The basic instruments capable of measuring matric potential are sufficiently inexpensive and reliable to be used in field-scale monitoring programmes. However, each instrument has a limited accessible water potential range. For example, tensiometers work well only in wet soil, while resistance blocks do better in moderately dry soil.

### 11.4.1 Tensiometers

The most widely used and least expensive water potential measuring device is the tensiometer. Tensiometers are simple instruments, usually consisting of a porous ceramic cup and a sealed plastic cylindrical tube connecting the porous cup to some pressure-recording device at the top of the cylinder. They measure the matric potential, because solutes can move freely through the porous cup.

The tensiometer establishes a quasi-equilibrium condition with the soil water system. The porous ceramic cup acts as a membrane through which water flows, and therefore must remain saturated if it is to function properly. Consequently, all the pores in the ceramic cup and the cylindrical tube are initially filled with de-aerated water. Once in place, the tensiometer will be subject to negative soil water potentials, causing water to move from the tensiometer into the surrounding soil matrix. The water movement from the tensiometer will create a negative potential or suction in the tensiometer cylinder which will register on the recording device. For recording, a simple U-tube filled with water and/or mercury, a Bourdon-type vacuum gauge or a pressure transducer (Marthaler et al., 1983) is suitable.

If the soil water potential increases, water moves from the soil back into the tensiometer, resulting in a less negative water potential reading. This exchange of water between the soil and the tensiometer, as well as the tensiometer's exposure to negative potentials, will cause dissolved gases to be released by the solution, forming air bubbles. The formation of air bubbles will alter the pressure readings in the tensiometer cylinder and will result in faulty readings. Another limitation is that the tensiometer has a practical working limit of $\psi \approx -85$ kPa. Beyond –100 kPa ($\approx$ 1 atm), water will boil at ambient temperature, forming water vapour bubbles which destroy the vacuum inside the tensiometer cylinder. Consequently, the cylinders occasionally need to be de-aired with a handheld vacuum pump and then refilled.

Under drought conditions, appreciable amounts of water can move from the tensiometer to the soil. Thus, tensiometers can alter the very condition they were designed to measure. Additional proof of this process is that excavated tensiometers often have accumulated large numbers of roots in the proximity of the ceramic cups. Typically, when the tensiometer acts as an "irrigator", so much water is lost through the ceramic cups that a vacuum in the cylinder cannot be maintained, and the tensiometer gauge will be inoperative.

Before installation, but after the tensiometer has been filled with water and degassed, the ceramic cup must remain wet. Wrapping the ceramic cup in wet rags or inserting it into a container of water will keep the cup wet during transport from the laboratory to the field. In the field, a hole of the appropriate size and depth is prepared. The hole should be large enough to create a snug fit on all sides, and long enough so that the tensiometer extends sufficiently above the soil surface for de-airing and refilling access. Since the ceramic cup must remain in contact with the soil, it may be beneficial in stony soil to prepare a thin slurry of mud from the excavated site and to pour it into the hole before inserting the tensiometer. Care should also be taken to ensure that the hole is backfilled properly, thus eliminating any depressions that may lead to ponded conditions adjacent to the tensiometer. The latter precaution will minimize any water movement down the cylinder walls, which would produce unrepresentative soil water conditions.

Only a small portion of the tensiometer is exposed to ambient conditions, but its interception of solar radiation may induce thermal expansion of the upper tensiometer cylinder. Similarly, temperature gradients from the soil surface to the ceramic cup may result in thermal expansion or contraction of the lower cylinder. To minimize the risk of temperature-induced false water potential readings, the tensiometer cylinder should be shaded and constructed of non-conducting materials, and readings should be taken at the same time every day, preferably in the early morning.

A new development is the osmotic tensiometer, where the tube of the meter is filled with a polymer solution in order to function better in dry soil. For more information on tensiometers see Dirksen (1999) and Mullins (2001).

### 11.4.2 **Resistance blocks**

Electrical resistance blocks, although insensitive to water potentials in the wet range, are excellent companions to the tensiometer. They consist of electrodes encased in some type of porous material that within about two days will reach a quasi-equilibrium state with the soil. The most common block materials are nylon fabric, fibreglass and gypsum, with a working range of about –50 kPa (for nylon) or –100 kPa (for gypsum) up to –1 500 kPa. Typical block sizes are 4 cm × 4 cm × 1 cm. Gypsum blocks last a few years, but less in very wet or saline soil (Perrier and Marsh, 1958).

This method determines water potential as a function of electrical resistance, measured with an alternating current bridge (usually ≈ 1 000 Hz) because direct current gives polarization effects. However, resistance decreases if soil is saline, falsely indicating a wetter soil. Gypsum blocks are less sensitive to soil saltiness effects because the electrodes are consistently exposed to a saturated solution of calcium sulphate. The output of gypsum blocks must be corrected for temperature (Aggelides and Londra, 1998).

Because resistance blocks do not protrude above the ground, they are excellent for semi-permanent agricultural networks of water potential profiles, if installation is careful and systematic (WMO, 2001). When installing the resistance blocks it is best to dig a small trench for the lead wires before preparing the hole for the blocks, in order to minimize water movement along the wires to the blocks. A possible field problem is that shrinking and swelling soil may break contact with the blocks. On the other hand, resistance blocks do not affect the distribution of plant roots.

Resistance blocks are relatively inexpensive. However, they need to be calibrated individually. This is generally accomplished by saturating the blocks in distilled water and then subjecting them to a predetermined pressure in a pressure-plate apparatus (Wellings et al., 1985), at least at five different pressures before field installation. Unfortunately, the resistance is less on a drying curve than on a wetting curve, thus generating hysteresis errors in the field because resistance blocks are slow to equilibrate with varying soil wetness (Tanner and Hanks, 1952). As resistance-block calibration curves change with time, they need to be calibrated before installation and to be checked regularly afterwards, either in the laboratory or in the field.

### 11.4.3 **Psychrometers**

Psychrometers are used in laboratory research on soil samples as a standard for other techniques (Mullins, 2001), but a field version is also available, called the Spanner psychrometer (Rawlins and Campbell, 1986). This consists of a miniature thermocouple placed within a small chamber with a porous wall. The thermocouple is cooled by the Peltier effect, condensing water on a wire junction. As water evaporates from the junction, its temperature decreases and a current is produced which is measured by a meter. Such measurements are quick to respond to changes in soil water potential, but are very sensitive to temperature and salinity (Merrill and Rawlins, 1972).

The lowest water potential typically associated with active plant water uptake corresponds to a relative humidity of between 98% and 100%. This implies that, if the water potential in the soil is to be measured accurately to within 10 kPa, the temperature would have to be controlled to better than 0.001 K. This means that the use of field psychrometers is most appropriate for low matric potentials, of less than –300 kPa. In addition, the instrument components differ in heat capacities, so diurnal soil temperature fluctuations can induce temperature gradients in the psychrometer (Brunini and Thurtell, 1982). Therefore, Spanner psychrometers should not be used at depths of less than 0.3 m, and readings should be taken at the same time each day, preferably in the early morning. In summary, soil psychrometry is a difficult and demanding method, even for specialists.

## 11.5 **SITE SELECTION AND SAMPLE SIZE**

There is no standard depth or measurement interval at which soil moisture observations are taken, since this strongly depends on the research objectives for which the sensors are installed. The International Soil Moisture Network (ISMN; Dorigo et al., 2011) provides an extensive database with harmonized in situ soil moisture time series of networks all over the world. Here the data are harmonized to a half-hourly measurement interval whenever possible. Most networks and stations in the ISMN measure soil moisture at several depths, from 0.05 m up to 0.50 m or 1 m. As a result, the behaviour of soil moisture at different depths can be compared and used to validate measurements. Measurements of other meteorological parameters are very valuable for determining soil moisture. For example, precipitation data at the measurement site can help validate the soil moisture data.

The representativeness of any soil moisture observation point is limited because there are likely to be significant variations, both horizontally and vertically, in the soil structure (porosity, density, chemical composition), land cover and relief. It is pivotal that soil moisture and its variability be captured on the scale necessary for conducting studies on hydrological processes and for satellite validation. Gravimetric water content determinations or indirect measurements of soil moisture are only reliable at the point of measurement, making it necessary to collect a large number of samples to adequately describe the site's soil moisture status. In order to estimate the number of samples $n$ needed at a local site to determine soil water content at an observed level of accuracy ($L$), the following equation can be used:

$$n = 4\left(\sigma^2 / L^2\right) \tag{11.9}$$

where $\sigma^2$ is the sample variance generated from a preliminary sampling experiment. For example, suppose that a preliminary sample yielded a (typical) $\sigma^2$ of 25% and the accuracy level needed to be within 3%, 12 samples would be required from the site (if it can be assumed that water content is normally distributed across the site). A study by Brocca et al. (2007) showed that the minimum number of point samples needed for an area in central Italy with an extent of about 9 to 8 800 m$^2$ varied between 15 and 35. The higher number of samples was needed for sites with more significant relief. Famiglietti et al. (2008) found that 30 samples are sufficient for a footprint of 50 km, assuming that the data are independent and spatially uncorrelated.

Upscaling the point measurements obtained by gravimetric water content determination or indirect measurements with in situ sensors has been the subject of many studies. Upscaling methods vary from relatively straightforward interpolation and time/rank stability techniques to more complicated techniques such as statistical transformations and land surface modelling.

The widely used time/rank stability analysis developed by Vachaud et al. (1985) assesses whether a single soil moisture sensor location can be used to estimate the average over the site. A new method was presented by Friesen et al. (2008) and applied by Bircher et al. (2011), where soil moisture sampling was based on landscape units with internally consistent hydrological behaviour. This method ensures statistically reliable validation via the reduction of the footprint variance and reduces the chance of sampling bias.

## 11.6 REMOTE-SENSING OF SOIL MOISTURE

As mentioned earlier in this chapter, a single observation location cannot provide absolute knowledge of regional soil moisture. Soil moisture is highly variable in both space and time, rendering it difficult to measure on the continental or global scale needed by researchers (Seneviratne et al., 2010). Space-based remote-sensing of soil moisture accommodates these needs by providing surface soil moisture observations on a global scale every one to two days under a variety of conditions.

In general, remote-sensing aims to measure properties of the Earth's surface by analysing the interactions between the ground and EMR. This can be done by recording the naturally emitted radiation (passive systems) or by illuminating the ground and recording the reflecting signal (active systems). Soil moisture is usually assessed through its effects on the soil's electric or thermal properties. While microwave remote-sensing observations are sensitive to the soil's dielectric constant, IR remote-sensing systems are sensitive to its thermal conditions. Information about space-based observations can be found in Volume IV, Chapter 5, 5.6.2 and 5.6.3 of the present Guide, where the basic principles of soil moisture observation are included within the context of many observed geophysical variables. In the section here, additional detail and practical information is provided.

Over the last decades, many soil moisture datasets have been developed from various space-borne instruments using different retrieval algorithms (Owe et al., 2001; Njoku et al., 2003; Naeimi et al., 2009). Recently, several of these datasets from both active and passive microwave remote-sensing observations have been combined (Liu et al., 2011), generating a global soil moisture dataset covering the last 30 years (Liu et al., 2012).

Although remote-sensing has proven to be a valuable tool to measure soil moisture on a global scale, in situ measurements are imperative for the calibration and validation of satellite-based soil moisture retrievals. ISMN, a global in situ soil moisture database, was mainly developed for the validation of satellite products. Many validation efforts have been undertaken to assess the quality of remote-sensing products using in situ measurements (Albergel et al., 2012; Matgen et al., 2012; Pathe et al., 2009; Su et al., 2013; Wagner et al., 2008). In addition, many studies have focused on error characterization of the different soil moisture products (Dorigo et al., 2010; Draper et al., 2013). These studies show that most soil moisture products from remote-sensing are capable of depicting seasonal and short-term soil moisture changes quite well. However, biases in the absolute value and dynamic range may be large when compared to in situ and modelled soil moisture data.

The following paragraphs will give an overview of the theoretical background behind the different remote-sensing techniques, space-borne instruments and algorithms in use.

### 11.6.1 Microwave remote-sensing

#### 11.6.1.1 *Introduction*

Microwave remote-sensing uses electromagnetic waves with wavelengths of 1 m to 1 cm, which corresponds to frequencies of 0.3 to 300 GHz. An important quality of these microwaves is that they can travel through the Earth’s atmosphere undisturbed and thus allow observations to be made independent from cloud coverage. Furthermore, since they are not bound to illumination by the sun, microwave measurements are operable all day long.

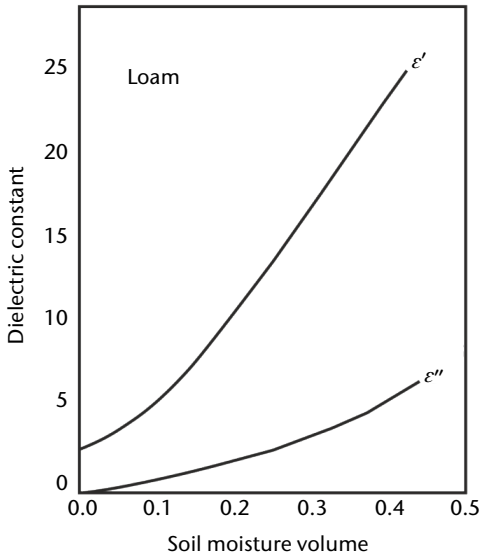



**Figure 11.1. The relationship between the complex dielectric constant ($\varepsilon'$ and $\varepsilon''$ are magnitudes of the real and imaginary parts, respectively) and volumetric soil moisture for a loamy soil at a frequency of 5 GHz (after Hallikainen et al., 1985)**

When applied to remote-sensing of the Earth's surface, Kirchhoff's radiation law states that the emission of a body is equal to one minus its reflectivity. This means that emission and reflection are complementary, and thus that surfaces that are good scatters are weak emitters and vice versa. As a result, active and passive microwave systems are influenced inversely by the same physical phenomena on the ground. Fresnel's reflection law describes the relationship between the dielectric constant and reflectivity (and thus emissivity), where a higher dielectric constant yields a higher rate of reflection (and smaller emissivity). At microwave lengths, the dielectric constant of water is of an order of magnitude larger than that of dry soils. Therefore, the dielectric constant of soils rises with increasing soil moisture (see Figure 11.1). With these physical relations, it is possible to retrieve soil moisture of the Earth's surface from passive as well as from active microwave remote-sensing systems.

Microwave beams are able to interact to some extent with the volumes of targets since their waves are longer and are not reflected immediately at the surface. Thus, information about the inner conditions of vegetation or soils, for example, can be gained. As a rule of thumb, the longer the wavelength, the deeper the radiation penetrates into volumes. In contrast, optical waves only interact with surfaces and tell us about the visible colour and brightness.

When observed from above the canopy, vegetation affects the microwave emission in two ways: first, vegetation absorbs or scatters the radiation emitted from the soil; second, the vegetation also emits its own radiation. Under a sufficiently dense canopy, the emitted soil radiation will become totally masked and the observed radiation will be mostly due to vegetation. Generally, all frequency bands used in microwave remote-sensing of soil moisture are sensitive to vegetation and require some correction in the data for this. Higher-frequency bands are more vulnerable to vegetation influences.

#### 11.6.1.2 *Multi-frequency radiometers*

Passive systems like radiometers record the brightness temperature of the Earth's surface. Brightness temperatures are related to the amount of emissivity (and thus reflection) described by the Rayleigh-Jeans approximation of Planck's law. This law states that brightness temperatures are a function of the physical temperature and emissivity. The amount of emission depends on the dielectric constant of the emitting body as described by Fresnel's reflection law.

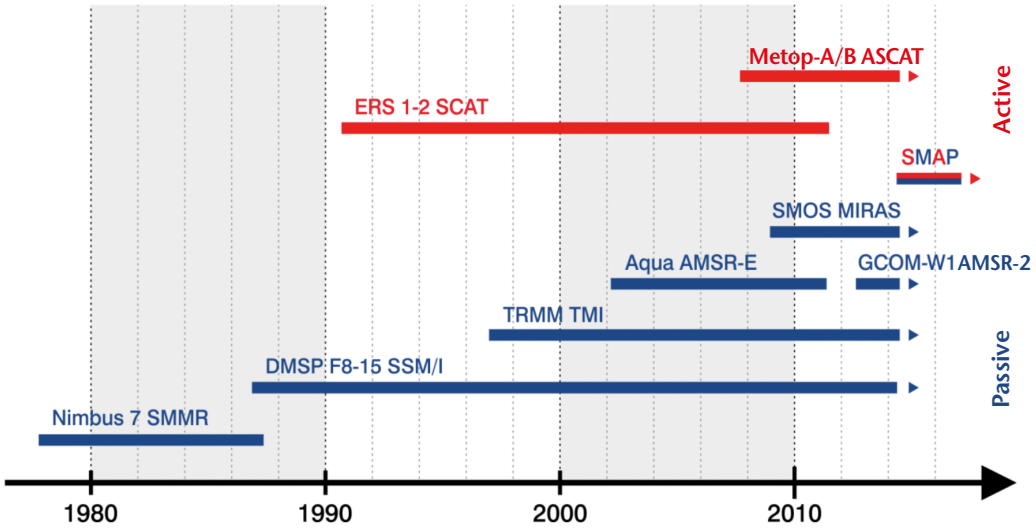



**Figure 11.2. Active and passive microwave sensors used for soil moisture retrieval**

Since 1978, instruments have been providing global passive data over land and oceans (Figure 11.2), beginning with the Scanning Multichannel Microwave Radiometer (1978–1987), the Special Sensor Microwave – Imager (since 1987), the Tropical Rainfall Measuring Mission (since 1997) and, more recently, the Advanced Microwave Scanning Radiometers (AMSR-E, 2002–2011 and AMSR-2 since 2012), the Coriolis WindSat (since 2003) and the Chinese satellites FengYun-3 (since 2010). Initially these instruments were not designed for soil moisture observations but for precipitation, evaporation, sea-surface temperatures and cryospheric parameters. However, in the 1970s studies already showed the potential of retrieving soil moisture from brightness temperatures at these frequencies (Schmugge, 1976). The big advantage of radiometers is that data are available from multiple multi-frequency microwave radiometers since 1978, providing a long-term dataset to investigate trends and anomalies.

The instruments used for soil moisture remote-sensing have frequencies varying from 6.6 to 10.7 GHz. It has to be taken into account that a higher microwave frequency leads to less accurate estimates of soil moisture since attenuation due to vegetation increases and penetration ability decreases. Therefore, retrievals from the Scanning Multichannel Microwave Radiometer (6.6 GHz), AMSR-E (6.9 GHz), WindSat (6.8 GHz) and AMSR-2 (6.9 GHz) tend to be more accurate. Another advantage of these sensors is that spatial resolution and radiometric accuracy are much improved. The spatial resolution of AMSR-E is 56 km where the soil moisture products are provided at a spatial resolution of 0.25°.

### 11.6.1.3 *Scatterometers*

A scatterometer is an active microwave instrument (AMI) that continuously transmits short directional pulses of energy towards the Earth's surface and detects the returned energy. The amount of energy returned to the instrument depends upon geometric and dielectric properties of the surface and is often referred to as normalized radar cross-section or backscatter (sigma nought, $\sigma^0$). Sacrificing range and spatial resolution, scatterometers surpass other types of radars in accuracy and stability for measuring the radar cross-section of a target. Space-borne scatterometers were initially developed and designed to derive wind speed and direction over the oceans. Nevertheless, a number of studies acknowledge the capacity of scatterometers for land applications such as soil moisture monitoring (Magagi and Kerr, 1997; Pulliainen et al., 1998; Wagner et al., 1999). Since European scatterometers operate in longer wavelengths (5.3 GHz) than those of the United States (14 GHz), they are more suitable for soil moisture retrieval.

The unique instrument design of the European scatterometers on board the European Remote-sensing (ERS) satellites and the Meteorological Operational (MetOp) satellites enables soil moisture retrieval on a global scale with almost daily coverage. Both scatterometers, the AMI in wind mode on board ERS (Attema, 1991) and the Advanced Scatterometer (ASCAT) on board MetOp (Figa-Saldaña et al., 2002), operate in C-band (5.3 GHz) with a wavelength of approximately 5.6 cm. The major differences between these two scatterometers are the number of sideways-looking antennas and the range of the incidence angles observed. The spatial resolution of the AMI is approximately 50 km while the ASCAT product is provided at spatial resolutions of 25 km and 50 km.

#### 11.6.1.4 *Synthetic aperture radars*

Space or airborne synthetic aperture radars (SAR) are active microwave sensor systems that offer a higher spatial resolution than scatterometers due to advanced signal processing. As side-looking imaging radars, they operate similarly to scatterometers and use the same frequency domain. Besides hydrological applications, SAR systems can be used for the accurate retrieval of three-dimensional geometries, as they enable interferometry.

As a side-looking imaging radar moves along its path on the ground, it accumulates data. The spatial resolution of radars is dependent on the (limited) physical size of its antenna, the aperture. Taking advantage of the along-track motion of the carrier, an SAR system simulates a bigger synthetic aperture as it records amplitude and phase of the ground targets continuously while they are visible to the SAR. These multiple measurements of each target are then summed up coherently. Smaller objects are subsequently resolved on the ground. However, higher energy consumption and a smaller footprint result in a longer revisit time on individual locations and thus the temporal resolution of SARs is inferior to other microwave systems these days.

The higher complexity of soil and surface properties at the scale below 10 km introduces additional error and uncertainty sources. As a consequence, SAR systems are not yet employed in operational soil moisture services but instead are used for pre-operational services and scientific products (Doubkova et al., 2009; Pathe et al., 2009). Nonetheless, upcoming SAR satellite missions such as the European Space Agency (ESA) Sentinel-1 programme (Attema et al., 2007) promise improved temporal and radiometric resolution and a suggestion has been made to use SARs for operational soil moisture services on a local scale (Hornacek et al., 2012).

#### 11.6.1.5 *Dedicated L-band missions*

As stated before, lower frequencies tend to be less sensitive to vegetation interactions and are therefore thought to be more suitable for soil moisture retrieval. Hence, the first two space-borne missions specifically designed for soil moisture retrieval operate in the L-band channel (1.4 GHz). The aim of the Soil Moisture and Ocean Salinity (SMOS) and the Soil Moisture Active Passive (SMAP) missions is to provide absolute soil moisture with a maximum root mean square (RMS) error of 0.04 $m^3/m^3$.

The SMOS mission of ESA was launched successfully on 2 November 2009. The instrument on board the SMOS satellite has a unique design to provide the spatial resolution needed for measuring soil moisture. The so-called Microwave Imaging Radiometer using Aperture Synthesis (MIRAS) is a 2D interferometric radiometer, on which the size of the antenna needed for measuring at the required spatial resolution is simulated through 69 small antennas. MIRAS provides brightness temperatures with a spatial resolution varying between 30 and 50 km. Global coverage is achieved every 2–3 days.

The SMAP mission, run by the United States National Aeronautics and Space Administration (NASA), was launched on 31 January 2015. Like SMOS, the passive microwave instrument operates in L-band to enhance the sensitivity to soil moisture. However, the instrument design for SMAP is very different from SMOS. SMAP uses a real aperture antenna in the shape of a large (6 m) parabolic reflector that rotates. Measurements are made with a spatial resolution of 40 km.

In addition to the passive measurements, SMAP also carries a radar that makes concurrent measurements at a spatial resolution of 1–3 km. By combining active and passive measurements, SMAP provides a soil moisture product with a spatial resolution of 10 km.

#### 11.6.1.6 *Soil moisture retrieval*

For retrieving soil moisture it is necessary to have models that are capable of accounting for vegetation and surface roughness effects on the microwave signal and then to convert accordingly the received intensity to soil moisture values. Again, it should be noted that a shorter wavelength leads to inferior performance due to vegetation scattering and less penetration depth. Soil moisture retrieval is not possible over densely vegetated areas such as tropical rainforests due to the lack of penetration of the L-band and C-band waves through the vegetation canopy. Additionally, retrieved estimates of soil moisture are only reasonable over snow-free and non-frozen soils.

Passive systems measure the microwave brightness temperature and derive indirectly the emissivity, which is then ingested into a radiative transfer model. Data on soil temperature, roughness, texture and other parameters of the observed area are necessary ancillary information. Data from passive microwave observations are available from AMSR-E using either the Vrije Universiteit Amsterdam (VUA)–NASA retrieval algorithm developed by VUA and NASA and based on the land parameter retrieval model as described by Owe et al. (2001), the official NASA AMSR-E product (Njoku et al., 2003; Njoku, 2004) or the retrieval algorithm from the University of Montana (Jones et al., 2009; Jones and Kimball, 2010). All of these retrieval algorithms are based on radiative transfer equations. However, the retrieval algorithms vary significantly and generate quite different soil moisture values. The VUA–NASA retrieval algorithm solves for vegetation optical depth and the soil dielectric constant simultaneously. Soil moisture is calculated using the Wang–Schmugge mixing model (Wang and Schmugge, 1980).

The SMOS instrument provides an operational soil moisture product (Kerr et al., 2012). The SMOS retrieval algorithm uses an iterative approach to minimize the cost function between modelled brightness temperatures and the direct measurements. In this way the best set of parameters is found, including the soil moisture and vegetation. SMOS Level 2 soil moisture data can be downloaded via ESA Earthnet Online (https://earth.esa.int/eogateway/missions/smos/data).

Active instruments measure the backscattered intensity, which is a function of roughness, incidence angle and dielectric properties of the surface. Again, vegetation and other influences contribute to the signal, which is used to determine the backscatter coefficient. Soil moisture retrieval provided as an operational product from the ASCAT instrument and as a scientific product from the AMI in wind mode relies on a semi-empirical change-detection method. This method, the TU Wien change detection algorithm, is tailored to the unique instrument design. Assuming a linear relationship between radar backscatter and soil moisture, in the decibel domain, a relative measure of moisture in the first few centimetres of soil can be obtained, representing the degree of saturation (0%–100%). In very dry regions, particularly over sand deserts, the retrieval approach fails, seemingly due to a complex mechanism of surface, volume and sub-surface scattering. Soil moisture data from the TU Wien change detection algorithm are freely available on the website of the European Organization for the Exploitation of Meteorological Satellites (EUMETSAT; https://navigator.eumetsat.int/product/EO:EUM:DAT:METOP:SOMO25).

An overview of operational soil moisture products is given in the table below.

**Operational soil moisture products and their characteristics**

| *Product reference* | *SMOS* | *AMSR-E* | *ASCAT* |
|---|---|---|---|
| ***Satellite*** | | | |
| Name | SMOS | Aqua | MetOp-A/B |
| Agencies | ESA/CNES[a]/CDTI[b] | NASA | EUMETSAT/ESA |
| Lifetime | Since 2.11.09 | 4.5.02 – 4.10.11 | Since 19.10.06 |
| Orbit | Polar | Polar | Polar |
| Altitude | 758 km | 705 km | 837 km |
| Period | 100 min | 99 min | 100 min |
| Equator crossing time | 6 a.m. (ascending)<br>6 p.m. (descending) | 1.30 p.m. (ascending)<br>1.30 a.m. (descending) | 9.30 p.m. (ascending)<br>9.30 a.m. (descending) |
| Type | Research satellite | Research satellite | Operational (3 satellites) |
| ***Sensor*** | | | |
| Name | MIRAS | AMSR-E | ASCAT |
| Type | Synthetic aperture radiometer | Multi-frequency real aperture radiometer | Real aperture scatterometer |
| Swath | 1 000 km | 1 450 km | 2 x 550 km |
| Scanning principle | Forward looking 2D interferometer | Rotating parabolic reflector | 6 side-looking fan beam antennas |
| Incidence angle range | 0°– 55° | 55° | 25°– 53° (mid beam);<br>34°– 64° (fore and aft beams) |
| Frequency | 1.4 GHz | 6.9, 10.7, 18.7, 23.8, 36.5, and 89 GHz | 5.3 GHz |
| Polarization | H and V (polarimetric mode optional) | H and V | VV |
| Spatial resolution | 30–50 km | 75 x 43 km at 6.9 GHz | 25/50 km |
| Daily global coverage | ~82% | ~90% | ~82% |
| ***Retrieval*** | | | |
| Model name | L-MEB | Land parameter retrieval model | WARP |
| Forward model | Radiative transfer model | Radiative transfer model | Semi-empirical change-detection |
| Model complexity | High | Medium | Low |
| Inversion approach | Iterative least-square matching | Iterative least-square matching | Direct inversion |
| Concurrent retrievals | Soil temperature, vegetation optical depth, roughness | Soil temperature, vegetation optical depth | None |
| Model calibration | None | None | Based on long-term time series |

| *Product reference* | *SMOS* | *AMSR-E* | *ASCAT* |
|---|---|---|---|
| Need for auxiliary data | High | Medium | Low |
| Error propagation estimates | Not available | Available | Available |
| ***Product*** | | | |
| Target quantity | Volumetric soil moisture | Volumetric soil moisture | Degree of saturation |
| Units | $m^3\,m^{-3}$ | $m^3\,m^{-3}$ | 0–1 or % |
| Grid | Fixed ISEA4-9 Discrete Global Grid | Regular grid | Swath geometry |
| Pixel spacing | 15 km | 0.25° | 12.5 km |
| Data latency | Within a few days after sensing | Irregular updates | Within 130 min after sensing |

Notes:
a National Centre for Space Studies (France)
b Centro para el Desarrollo Tecnológico Industrial (Spain)

### 11.6.2 Thermal infrared remote-sensing

All bodies with a temperature above absolute zero emit electromagnetic energy in the thermal IR domain. By detecting the thermal properties of the Earth's surface, soil moisture can be derived based on the distinct differences in thermal properties of soil and water (Idso et al., 1975; Van de Griend et al., 1985). Thermal IR remote-sensing has been used in an increasing number of studies for the derivation of soil moisture. The advantage of thermal IR remote-sensing is that it can provide soil moisture information on a spatial resolution down to a few metres. Furthermore, it can provide soil moisture information over dense vegetation, which is one of the limitations of microwave remote-sensing. The disadvantages of thermal IR remote-sensing are that it is unable to measure soil moisture when cloud cover is present and it is considerably affected by atmospheric phenomena. Therefore, complex noise-removal mechanisms are needed in most cases. Thermal IR remote-sensing of soil moisture is not as straightforward as microwave remote-sensing since there is no direct link between temperature data and soil moisture. Nevertheless, several approaches exist to indirectly retrieve soil moisture data using thermal IR observations from the geostationary operational environmental satellite (GOES), advanced very high resolution radiometer (AVHRR), moderate resolution imaging spectroradiometer, Landsat and others.

The first approach is called the triangle approach and is based on the empirical relationship between soil moisture, soil temperature and fractional vegetation cover. This relationship was demonstrated by Price (1990) and resulted in a triangular scatterplot of surface temperatures and the remotely sensed normalized difference vegetation index. The triangle approach was later used in several studies to estimate soil moisture, namely by Sandholt et al. (2002) and Carlson et al. (1994) among others.

The second approach makes use of the differences in thermal properties between water and soils. Water differs from many other matters in its relatively large heat capacity and thermal inertia. Thermal inertia is defined as the resistance of an object against its heating for 1 K. The thermal inertia of water is relatively high, which indicates a high resistance to temperature changes. It has been shown that the behaviour of land surface temperature in the morning strongly depends on soil moisture in the soil, since the water will heat up more slowly. One of the approaches that

uses this behaviour is the calculation of the apparent thermal inertia (ATI), which can be done when measuring the difference between maximum and minimum temperatures over one day. It is described as:

$$\mathrm{ATI} = (1 - A) / \Delta T \tag{11.10}$$

where $A$ is the albedo of the pixel in the visible band and $\Delta T$ the difference between the minimum and maximum temperature. Many studies have already assessed the potential of ATI to describe soil moisture and its spatial and temporal variability (for example, Verstraeten et al., 2006; Van doninck et al., 2011).

Another method to retrieve soil moisture using thermal IR remote-sensing is by integrating the data into land surface models. Soil moisture controls latent heat fluxes by way of both evaporation and transpiration, where wet soil conditions lead to increased evaporation and transpiration. The atmosphere–land exchange inversion model (ALEXI) uses the relationship between evaporation, transpiration and soil moisture to derive soil moisture data. All major components, including the latent heat flux, of the energy budget are estimated from net radiation and vegetation parameters retrieved from AVHRR and GOES. Accordingly, soil moisture can be derived from latent heat fluxes by using a soil water stress function (Anderson et al., 1997; Anderson et al., 2007; Hain et al., 2011). An intercomparison of soil moisture retrieved from microwave remote-sensing and ALEXI showed that the two datasets are complementary: ALEXI is better at estimating soil moisture over dense vegetation and microwave remote-sensing shows more reliable results over low to moderate vegetation (Hain et al., 2011).

## REFERENCES AND FURTHER READING


Aggelides, S.M. and P.A. Londra, 1998: Comparison of empirical equations for temperature correction of gypsum sensors. *Agronomy Journal*, 90:441–443.

Albergel, C., P. de Rosnay, C. Gruhier, J. Muñoz-Sabater, S. Hasenauer, L. Isaksen, Y. Kerr and W. Wagner, 2012: Evaluation of remotely sensed and modelled soil moisture products using global ground-based in situ observations. *Remote Sensing of Environment*, 118:215–226.

Anderson, M.C., J.M. Norman, G.R. Diak, W.P. Kustas and J.R. Mecikalski, 1997: A two-source time-integrated model for estimating surface fluxes using thermal infrared remote sensing. *Remote Sensing of Environment*, 60:195–216.

Anderson, M.C., J.M. Norman, J.R. Mecikalski, J.A. Otkin and W.P. Kustas, 2007: A climatological study of evapotranspiration and moisture stress across the continental United States based on thermal remote sensing: 1. Model formulation. *Journal of Geophysical Research: Atmospheres*, 112(D10117).

Attema, E.P.W., 1991: The Active Microwave Instrument on-board the ERS-1 satellite. *Proceedings of the IEEE*, 79(6):791–799.

Attema, E., P. Bargellini, P. Edwards, G. Levrini, S. Lokas, L. Moeller, B. Rosich-Tell, P. Secchi, R. Torres, M. Davidson and P. Snoeij, 2007: Sentinel-1: The radar mission for GMES operational land and sea services. *ESA Bulletin*, 131:10–17.

Bircher, S., N. Skou, K.H. Jensen, J.P. Walker and L. Rasmussen, 2011: A soil moisture and temperature network for SMOS validation in Western Denmark. *Hydrol. Earth Syst. Sci. Discuss.*, 8:9961–10006.

Brocca, L., R. Morbidelli, F. Melone and T. Moramarco, 2007: Soil moisture spatial variability in experimental areas of central Italy. *Journal of Hydrology*, 333(2–4):356–373.

Brunini, O. and G.W. Thurtell, 1982: An improved thermocouple hygrometer for in situ measurements of soil water potential. *Soil Science Society of America Journal*, 46:900–904.

Campbell, D.J. and J.K. Henshall, 2001: Bulk density. In: *Soil and Environmental Analysis: Physical Methods* (K.A. Smith and C.E. Mullins, eds.), Marcel Dekker, New York, pp. 315–348.

Carlson, T.N., R.R. Gillies and E.M. Perry, 1994: A method to make use of thermal infrared temperature and NDVI measurements to infer surface soil water content and fractional vegetation cover. *Remote Sensing Reviews*, 9:161–173.

Deardorff, J.W., 1978: Efficient prediction of ground surface temperature and moisture, with inclusion of a layer of vegetation. *Journal of Geophysical Research*, 83:1889–1904.

De Jeu, R.A.M., 2003: Retrieval of land surface parameters using passive microwave remote sensing. PhD Thesis, VU Amsterdam.

Dirksen, C., 1999: *Soil Physics Measurements*. Catena Verlag, Reiskirchen, Germany.

Dirksen, C. and S. Dasberg, 1993: Improved calibration of time domain reflectometry soil water content measurements. *Soil Science Society of America Journal*, 57:660–667.

Dorigo, W.A., K. Scipal, R.M. Parinussa, Y.Y. Liu, W. Wagner, R.A.M. de Jeu and V. Naeimi, 2010: Error characterisation of global active and passive microwave soil moisture datasets. *Hydrology and Earth System Sciences*, 14:2605–2616.

Dorigo, W.A., W. Wagner, R. Hohensinn, S. Hahn, C. Paulik, A. Xaver, A. Gruber, M. Drusch, S. Mecklenburg, P. van Oevelen, A. Robock and T. Jackson, 2011: The International Soil Moisture Network: a data hosting facility for global in situ soil moisture measurements. *Hydrology and Earth System Sciences*, 15:1675–1698.

Doubkova, M., A. Bartsch, C. Pathe, D. Sabel and W. Wagner, 2009: The medium resolution soil moisture dataset: Overview of the SHARE ESA DUE TIGER project. *2009 IEEE International Geoscience and Remote Sensing Symposium: Proceedings*, I:116–119.

Draper, C., R. Reichle, R. de Jeu, V. Naeimi, R. Parinussa and W. Wagner, 2013: Estimating root mean square errors in remotely sensed soil moisture over continental scale domains. *Remote Sensing of Environment*, 137:288–298.

Drungil, C.E.C., K. Abt and T.J. Gish, 1989: Soil moisture determination in gravelly soils with time domain reflectometry. *Transactions of the American Society of Agricultural Engineering*, 32:177–180.

Famiglietti, J.S., D. Ryu, A.A. Berg, M. Rodell and T.J. Jackson, 2008: Field observations of soil moisture variability across scales. *Water Resources Research*, 44(1).

Figa-Saldaña, J., J.J.W. Wilson, E. Attema, R. Gelsthorpe, M.R. Drinkwater and A. Stoffelen, 2002: The advanced scatterometer (ASCAT) on the meteorological operational (MetOp) platform: A follow on for European wind scatterometers. *Canadian Journal of Remote Sensing*, 28(3):404–412.

Friesen, J., C. Rodgers, P.G. Oguntunde, J.M.H. Hendrickx and N. Van de Giesen, 2008: Hydrotope-based protocol to determine average soil moisture over large areas for satellite calibration and validation – with results from an observation campaign in the Volta Basin, West Africa. *IEEE Transactions on Geoscience and Remote Sensing*, 46(7):1995–2004.

Gardner, C.M.K., D.A. Robinson, K. Blyth and J.D. Cooper, 2001: Soil water content. In: *Soil and Environmental Analysis: Physical Methods* (K.A. Smith and C.E. Mullins, eds.), Marcel Dekker, New York, pp. 1–64.

Gardner, W.H. and C. Calissendorff, 1967: Gamma-ray and neutron attenuation measurement of soil bulk density and water content. *Proceedings of the Symposium on the Use of Isotope and Radiation Techniques in Soil Physics and Irrigation Studies* (Istanbul, 12–16 June 1967). International Atomic Energy Agency, Vienna, pp. 101–112.

Gee, G.W. and M.E. Dodson, 1981: Soil water content by microwave drying: A routine procedure. *Soil Science Society of America Journal*, 45:1234–1237.

Greacen, E.L., 1981: *Soil Water Assessment by the Neutron Method*. CSIRO, Australia.

Hain, C.R., W.T. Crow, J.R. Mecikalski, M.C. Anderson and T. Holmes, 2011: An intercomparison of available soil moisture estimates from thermal infrared and passive microwave remote sensing and land surface modeling. *Journal of Geophysical Research: Atmospheres*, 116(D15107).

Hallikainen, M., F. Ulaby, M. Dobson, M. El-Rayes and L.K. Wu, 1985: Microwave dielectric behavior of wet soil – Part 1: Empirical models and experimental observations. *IEEE Transactions on Geoscience and Remote Sensing*, 23:25–34.

Hasenauer, S., W. Wagner, K. Scipal, V. Naeimi and Z. Bartalis, 2006: Implementation of near real-time soil moisture products in the SAF network based on MetOp ASCAT data. *EUMETSAT Meteorological Satellite Conference*, 12–16 June 2006, Helsinki.

Hornacek, M., W. Wagner, D. Sabel, H.-L. Truong, P. Snoeij, T. Hahmann, E. Diedrich and M. Doubkova, 2012: Potential for high resolution systematic global surface soil moisture retrieval via change detection using Sentinel-1. *IEEE Journal of Selected Topics in Applied Earth Observation and Remote Sensing*, 5(4):1303–1311.

Idso, S.B., R.D. Jackson, R.J. Reginato and T.J. Schmugge, 1975: The utility of surface temperature measurements for the remote sensing of sun for soil water status. *Journal of Geophysical Research*, 80:3044–3049.

Jackson, T.J., 1990: Laboratory evaluation of a field-portable dielectric/soil moisture probe. *IEEE Transactions on Geoscience and Remote Sensing*, 28:241–245.

Jackson, T.J. and T.J. Schmugge, 1989: Passive microwave remote sensing system for soil moisture: Some supporting research. *IEEE Transactions on Geoscience and Remote Sensing*, 27:225–235.

Jones, L.A. and J.S. Kimball, 2010: *Daily Global Land Surface Parameters Derived from AMSR-E*. Boulder, Colorado: NASA National Snow and Ice Data Center Distributed Active Archive Center (available from https://nsidc.org/data/nsidc-0451/versions/3).

Jones, L.A., J.S. Kimball, E. Podest, K.C. McDonald, S.K. Chan and E.G. Njoku, 2009: A method for deriving land surface moisture, vegetation optical depth, and open water fraction from AMSR-E. *2009 IEEE International Geoscience and Remote Sensing Symposium: Proceedings*, III:916–919.

Kerr, Y.H., P. Waldteufel, P. Richaume, J.P. Wigneron, P. Ferrazzoli, A. Mahmoodi, A. Al Bitar, F. Cabot, C. Gruhier, S.E. Juglea, D. Leroux, A. Mialon and S. Delwart, 2012: The SMOS soil moisture retrieval algorithm. *IEEE Transactions on Geoscience and Remote Sensing*, 50(5):1384–1403.

Klute, A. (ed.), 1986: *Methods of Soil Analysis, Part 1: Physical and Mineralogical Methods*. American Society of Agronomy, Madison, Wisconsin, United States.

Knight, J.H., 1992: Sensitivity of time domain reflectometry measurements to lateral variations in soil water content. *Water Resources Research*, 28:2345–2352.

Liu, Y.Y., W.A. Dorigo, R.M. Parinussa, R.A.M. De Jeu, W. Wagner, M.F. McCabe, J.P. Evans and A.I.J.M van Dijk, 2012: Trend-preserving blending of passive and active microwave soil moisture retrievals. *Remote Sensing of Environment*, 123:280–297.

Liu, Y.Y., R.M. Parinussa, W.A. Dorigo, R.A.M. De Jeu, W. Wagner, A.I.J.M van Dijk, M.F. McCabe and J.P. Evans, 2011: Developing an improved soil moisture dataset by blending passive and active microwave satellite-based retrievals. *Hydrology and Earth System Sciences*, 15:425–436.

Magagi, R.D. and Y.H. Kerr, 1997: Retrieval of soil moisture and vegetation characteristics by use of ERS-1 wind scatterometer over arid and semi-arid areas. *Journal of Hydrology*, 188–189:361–384.

Marthaler, H.P., W. Vogelsanger, F. Richard and J.P. Wierenga, 1983: A pressure transducer for field tensiometers. *Soil Science Society of America Journal*, 47:624–627.

Matgen, P., S. Heitz, S. Hasenauer, C. Hissler, L. Brocca, L. Hoffmann, W. Wagner and H.H.G. Savenije, 2012: On the potential of MetOp ASCAT-derived soil wetness indices as a new aperture for hydrological monitoring and prediction: a field evaluation over Luxembourg. *Hydrological Processes*, 26(15):2346–2359.

Merrill, S.D. and S.L. Rawlins, 1972: Field measurement of soil water potential with thermocouple psychrometers. *Soil Science*, 113:102–109.

Mullins, C.E., 2001: Matric potential. In: *Soil and Environmental Analysis: Physical Methods* (K.A. Smith and C.E. Mullins, eds.), Marcel Dekker, New York, pp. 65–93.

Naeimi, V., K. Scipal, Z. Bartalis, S. Hasenauer and W. Wagner, 2009: An improved soil moisture retrieval algorithm for ERS and MetOp scatterometer observations. *IEEE Transactions on Geoscience and Remote Sensing*, 47(7):1999–2013.

Njoku, E.G., 2004: *AMSR-E/Aqua L2B Surface Soil Moisture, Ancillary Parms, & QC EASE-Grids, Version 2*. Boulder, Colorado: NASA National Snow and Ice Data Center Distributed Active Archive Center (available from https://doi.org/10.5067/AMSR-E/AE_LAND.002).

Njoku, E.G., T.J. Jackson, V. Lakshmi, T.K. Chan and S.V. Nghiem, 2003: Soil moisture retrieval from AMSR-E. *IEEE Transactions on Geoscience and Remote Sensing*, 41(2):215–229.

Owe, M., R. de Jeu and T. Holmes, 2008: Multisensor historical climatology of satellite-derived global land surface moisture. *Journal of Geophysical Research*, 113(F01002).

Owe, M., R. de Jeu and J. Walker, 2001: A methodology for surface soil moisture and vegetation optical depth retrieval using the microwave polarization difference index. *IEEE Transactions on Geoscience and Remote Sensing*, 39(8):1643–1654.

Pathe, C., W. Wagner, D. Sabel, M. Doubkova and J. B. Basara, 2009: Using ENVISAT ASAR global mode data for surface soil moisture retrieval over Oklahoma, USA. *IEEE Transactions on Geoscience and Remote Sensing*, 47(2):468–480.

Perrier, E.R. and A.W. Marsh, 1958: Performance characteristics of various electrical resistance units and gypsum materials. *Soil Science*, 86:140–147.

Price, J.C., 1990: Using spatial context in satellite data to infer regional scale evapotranspiration. *IEEE Transactions on Geoscience and Remote Sensing*, 28(5):940–948.

Pulliainen, J.T., T. Manninen and M.T. Hallikainen, 1998: Application of ERS-1 wind scatterometer data to soil frost and soil moisture monitoring in boreal forest zone. *IEEE Transactions on Geoscience and Remote Sensing*, 36(3):849–863.

Rawlins, S.L. and G.S. Campbell, 1986: Water potential: Thermocouple psychrometry. In: *Methods of Soil Analysis – Part 1: Physical and Mineralogical Methods* (A. Klute, ed.), American Society of Agronomy, Madison, Wisconsin, United States, pp. 597–618.

Sandholt, I., K. Rasmussen and J. Andersen, 2002: A simple interpretation of the surface temperature/ vegetation index space for assessment of surface moisture status. *Remote Sensing of Environment*, 79(2–3):213–224.

Schmugge, T.J., 1976: *Remote Sensing of Soil Moisture*. Doc. X-913-76-118, NASA Goddard Space Flight Center, Greenbelt, Maryland.

Schmugge, T.J., T.J. Jackson and H.L. McKim, 1980: Survey of methods for soil moisture determination. *Water Resources Research*, 16:961–979.

Seneviratne, S.I., T. Corti, E.L. Davin, M. Hirschi, E.B. Jaeger, I. Lehner, B. Orlowsky and A.J. Teuling, 2010: Investigating soil moisture–climate interactions in a changing climate: A review. *Earth-Science Reviews*, 99(3–4):125–161.

Su, C.-H., D. Ryu, R.I. Young, A.W. Western and W. Wagner, 2013: Inter-comparison of microwave satellite soil moisture retrievals over the Murrumbidgee Basin, southeast Australia. *Remote Sensing of Environment*, 134:1–11.

Tanner, C.B. and R.J. Hanks, 1952: Moisture hysteresis in gypsum moisture blocks. *Soil Science Society of America Proceedings*, 16:48–51.

Topp, G.C., J.L. Davis and A.P. Annan, 1980: Electromagnetic determination of soil water content: Measurement in coaxial transmission lines. *Water Resources Research*, 16:574–582.

Ulaby, F.T., R.K. Moore and A.K. Fung, 1986: *Microwave Remote Sensing: Active and Passive*, Volume III. Artech House, Norwood, Massachusetts.

Vachaud, G., A. Passerat De Silans, P. Balabanis and M. Vauclin, 1985: Temporal stability of spatially measured soil water probability density function. *Soil Science Society of America Journal*, 49(4):822–828.

Van de Griend, A.A., P.J. Camillo and R.J. Gurney, 1985: Discrimination of soil physical parameters, thermal inertia and soil moisture from diurnal surface temperature fluctuations. *Water Resources Research*, 21:997–1009.

Van doninck, J., J. Peters, B. De Baets, E. De Clercq, E. Ducheyne and N. Verhoest, 2011: The potential of multitemporal Aqua and Terra MODIS apparent thermal inertia as a soil moisture indicator. *International Journal of Applied Earth Observation and Geoinformation*, 13(6):934–941.

Verstraeten, W.W., F. Veroustraete, C.J. van der Sande, I. Grootaers and J. Feyen, 2006: Soil moisture retrieval using thermal inertia, determined with visible and thermal spaceborne data, validated for European forests. *Remote Sensing of Environment*, 101(3):299–314.

Visvalingam, M. and J.D. Tandy, 1972: The neutron method for measuring soil moisture content: A review. *European Journal of Soil Science*, 23:499–511.

Wagner, W., G. Lemoine and H. Rott, 1999: A method for estimating soil moisture from ERS scatterometer and soil data. *Remote Sensing of Environment*, 70(2):191–207.

Wagner, W., C. Pathe, M. Doubkova, D. Sabel, A. Bartsch, S. Hasenauer, G. Blöschl, K. Scipal, J. Martínez-Fernández and A. Löw, 2008: Temporal stability of soil moisture and radar backscatter observed by the Advanced Synthetic Aperture Radar (ASAR). *Sensors*, 8(2):1174–1197.

Wang, J.R. and T.J. Schmugge, 1980: An empirical model for the complex dielectric permittivity of soils as a function of water content. *IEEE Transactions on Geoscience and Remote Sensing*, GE-18(4): 288–295.

Wellings, S.R., J.P. Bell and R.J. Raynor, 1985: *The Use of Gypsum Resistance Blocks for Measuring Soil Water Potential in the Field*. Report No. 92, Institute of Hydrology, Wallingford, United Kingdom.

World Meteorological Organization, 1968: *Practical Soil Moisture Problems in Agriculture*. Technical Note No. 97 (WMO-No. 235, TP.128). Geneva.

———, 1989: *Land Management in Arid and Semi-arid Areas*. Technical Note No. 186 (WMO-No. 662). Geneva.

———, 2001: *Lecture Notes for Training Agricultural Meteorological Personnel* (J. Wieringa and J. Lomas) (WMO-No. 551). Geneva.

# CHAPTER 12. MEASUREMENT OF UPPER-AIR PRESSURE, TEMPERATURE AND HUMIDITY

## 12.1 GENERAL

### 12.1.1 Definitions

The following definitions based on the *International Meteorological Vocabulary* (WMO-No. 182) and the *Manual on the WMO Integrated Global Observing System* (WMO-No. 1160) are relevant to upper-air measurements using a radiosonde:

**Radiosonde.** Instrument intended to be carried by a balloon through the atmosphere, equipped with devices to measure one or several meteorological variables (such as pressure, temperature, humidity), and provided with a radio transmitter for sending this information to the observing station.

**Radiosonde observation.** An observation of meteorological variables in the upper air, usually atmospheric pressure, temperature, humidity, and horizontal wind speed and direction, by means of a radiosonde.

Note: The radiosonde may be attached to a balloon (or another slow-moving uncrewed aircraft), or the design adjusted to be dropped (as a dropsonde) from an aircraft or rocket.

**Radiosonde station.** A station at which observations of atmospheric pressure, temperature, humidity and usually horizontal wind in the upper air are made by electronic means.

**Upper-air observation.** A meteorological observation made in the free atmosphere, either directly or indirectly.

**Upper-air station, upper-air synoptic station, aerological station.** A surface location from which upper-air observations are made.

**Sounding.** Determination of one or several upper-air meteorological variables by means of instruments carried aloft by balloon, aircraft, kite, glider, rocket, and so on.

This chapter deals with radiosonde systems. Measurements using special platforms, specialized equipment, and aircraft, or made indirectly by remote-sensing instruments such as microwave radiometers and Raman water vapour lidars in the boundary layer and troposphere, are discussed in other chapters of Volume III of the present Guide. Radiosonde systems are normally used to measure pressure, temperature and relative humidity. At most operational sites, the radiosonde system is also used for upper-air wind determination (see the present volume, Chapter 13). In addition, some radiosondes are flown with sensing systems for atmospheric constituents, such as ozone concentration or radioactivity. These additional measurements are not discussed in any detail in this chapter.

### 12.1.2 Units used in upper-air measurements

The units of measurement for the meteorological variables of radiosonde observations are hectopascals for pressure, degrees Celsius or Kelvin for temperature, and per cent for relative humidity. Relative humidity is reported relative to saturated vapour pressure over a water surface, even at temperatures less than 0 °C.

The unit of geopotential height used in upper-air observations is the standard geopotential metre (gpm), defined as 0.980665 dynamic metres. The relationship between geopotential height and geometric height is shown in 12.5.5.2. Differences in the lower troposphere are not very large but get larger as the height increases.

The values of the physical functions and constants adopted by the *Technical Regulations* (WMO-No. 49), Volume I, Appendix A should be used in radiosonde computations.

## 12.1.3 Meteorological requirements

### 12.1.3.1 *Radiosonde data for meteorological operations*

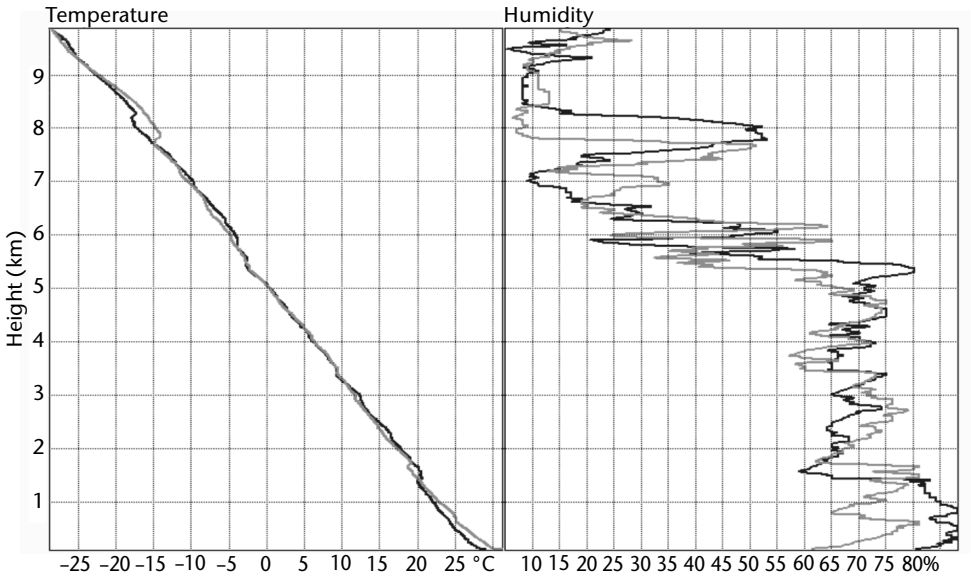
Upper-air measurements of temperature, wind and relative humidity are three of the basic measurements used in the initialization of the analyses of numerical weather prediction (NWP) models for operational weather forecasting. Radiosondes provide most of the in situ temperature and relative humidity measurements over land, while radiosondes launched from remote islands or ships can provide limited but important coverage over the oceans. Temperatures with resolution in the vertical similar to radiosondes can be observed by aircraft either during ascent, descent, or at cruise levels. Aircraft observations during ascent and descent are used to supplement radiosonde observations over land and in some cases may be used to replace the radiosondes at a given site. Aircraft observations give measurements over both land and oceans at cruise level. Nadir-viewing satellite observations of temperature and water vapour distribution have lower vertical resolution than radiosonde or aircraft measurements. Satellite observations have a large impact on NWP analyses over the oceans and other areas of the globe where radiosonde and aircraft observations are sparse or unavailable.

Accurate measurements of the vertical structure of temperature, wind and water vapour fields in the troposphere are extremely important for all types of forecasting. Atmospheric temperature profiles have discontinuities in the vertical, and the changes in relative humidity associated with the temperature discontinuities are usually quite pronounced (see Figure 12.1). The measurements indicate the typical structure of cloud or fog layers in the vertical. This vertical structure of temperature and water vapour determines the stability of the atmosphere and, subsequently, the amount and type of cloud that will be forecast. Radiosonde measurements of the vertical structure can usually be provided with sufficient accuracy to meet most user requirements.

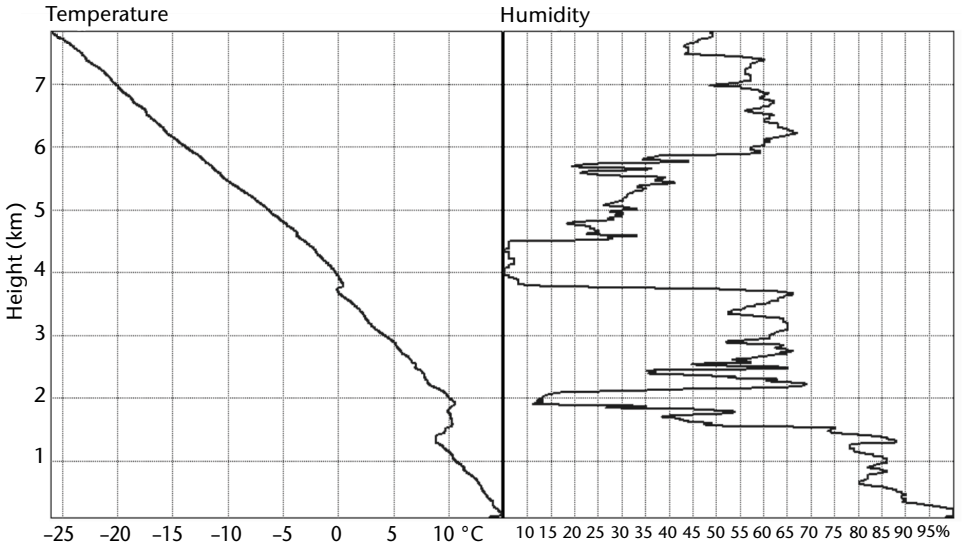
High-resolution measurements of the vertical structure of temperature and relative humidity are important for environmental pollution studies (for instance, identifying the depth of the atmospheric boundary layer). This high vertical resolution is also necessary for computing the effects of atmospheric refraction on the propagation of electromagnetic radiation (EMR) or sound waves. The time resolution should be as high as possible, for instance 1 s, but not more than 5 s. Besides that, information on the time and position of the radiosonde at each level is required to obtain the correct description of the atmosphere.

Civil aviation, artillery and other ballistic applications, such as space vehicle launches, have operational requirements for detailed measurements of the density of air at given pressures (derived from radiosonde temperature and relative humidity measurements).

Radiosonde observations are also important for studies of upper-air climate change. Hence, it is necessary to keep adequate records of the systems, including the software version and corrections, and consumables used for measurements, as well as the methods of observation (for example, suspension length from the balloon) used with the systems. Climatologists would prefer that raw data be archived in addition to processed data and made available for subsequent climatological studies. It is essential to record any changes in the methods of observation introduced over time. In this context, it has proved essential to establish the changes in radiosonde instruments and practices that have taken place since radiosondes were used on a regular basis (see, for instance, Gaffen, 1993). Climate change studies based on radiosonde measurements require extremely high stability in the systematic errors of the radiosonde measurements. However, the errors in early radiosonde measurements of some




(a) Example of daytime temperature and humidity profiles from the WMO Intercomparison of High Quality Radiosonde Systems, Yangjiang, China (22°N). The grey sounding was made 8 h after the black. Relatively small shifts in the rate of temperature change in the vertical were associated with rapid drops in relative humidity (near 0.7, 1.6, 3.5, 5.5 and 8 km).




(b) Example of temperature and relative humidity in summer at 0600 UTC in the United Kingdom (50°N), showing a shallow layer of 100% relative humidity in fog near the ground and very rapid drops in relative humidity in the temperature inversion layers between 1.5 and 2 km and at 3.8 km.

**Figure 12.1. Examples of temperature and relative humidity profiles in the lower and middle troposphere**

meteorological variables, particularly relative humidity and pressure, were too high and complex to generate meaningful corrections at all the heights required for climate change studies. Thus, improvements and changes in radiosonde design were necessary. Furthermore, expenditure limitations on meteorological operations require that radiosonde consumables remain cheap if widespread radiosonde use is to continue.

When new radiosonde designs are introduced, it is essential that enough testing be conducted of the performance of the new radiosonde relative to the old, so that time series of observations at a station can be harmonized based on comparison data. This harmonization should not result in the degradation of good measurements generated by the improved radiosonde in order to

make them compatible with the poorer measurements of an earlier design. It should also be recognized that in some cases the errors in the earlier measurements were too large for use in climatological studies.

Certain compromises in system measurement accuracy have to be accepted by users, taking into account that radiosonde manufacturers are producing systems that need to operate over an extremely wide range of meteorological conditions:

- 1 050 hPa to 5 hPa for pressure
- 50 °C to –95 °C for temperature
- 100% to 1% for relative humidity
- 30 hPa at the surface to $10^{-4}$ hPa at the tropopause for water vapour pressure in the tropics

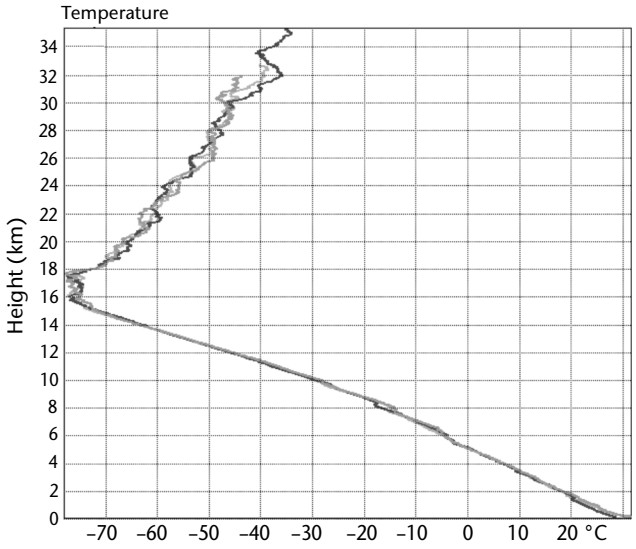
Systems also need to be able to sustain continuous reliable operation when operating in heavy rain, in the vicinity of thunderstorms, and in severe icing conditions.

The coldest temperatures are most often encountered near the tropical and subtropical tropopause, although in winter very cold temperatures can also be observed at higher levels in the stratospheric polar vortex. Figure 12.2 shows examples of profiles from the subtropics: example (a) in Yangjiang, China (22°N) in summer, and example (b) at 50°N in summer and winter in the United Kingdom. The colder temperatures near the tropopause in the tropics pose a major challenge for operational relative humidity sensors, because few currently respond very rapidly at temperatures below –70 °C (Nash, 2015). Thus, radiosondes that can perform well throughout the troposphere at mid-latitudes may have less reliable relative humidity measurements in the upper troposphere in the tropics.

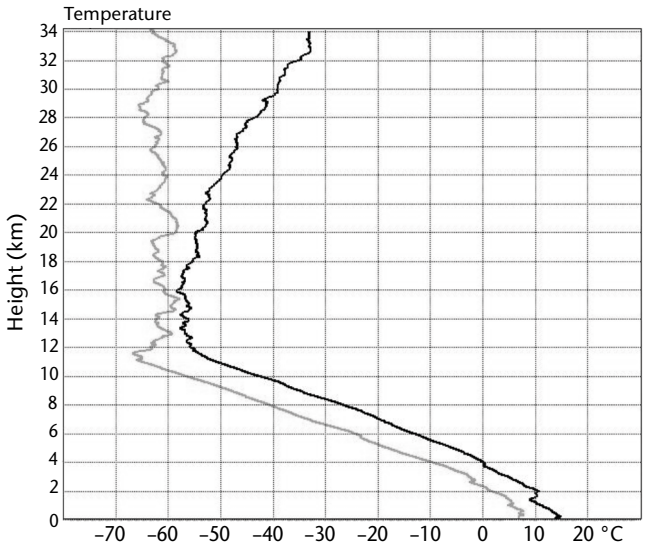
A radiosonde measurement is close to an instant sample of a given layer of the atmosphere (a radiosonde usually ascends 300 m in 1 min). When short-term fluctuations in atmospheric temperature from gravity waves and turbulence are small, the radiosonde measurement can represent the situation above a location very effectively for many hours. On the other hand, when the atmosphere is very variable (for example, a convective atmospheric boundary layer), the instant sample may not be valid for longer than a minute and may not represent a good average value above the location, even for an hour. In Figure 12.2(a), radiosonde temperatures in the troposphere were more reproducible with time than in the stratosphere because of the larger influence of gravity waves in the stratosphere. These larger differences at upper levels were not the result of instrument uncertainty. Similarly, the variation of temperatures in the vertical in the stratosphere in Figure 12.2(b) was not the result of instrument uncertainty, as the same structure was measured by two different radiosonde types on the test flights.

#### 12.1.3.2 *Relationships between satellite and radiosonde upper-air measurements*

A recent review of satellite measurements and their use in NWP was undertaken by Eyre et al. (2022). Nadir-viewing satellite observing systems do not measure vertical structure with the same accuracy or degree of confidence as radiosonde or aircraft systems. The current satellite temperature and water vapour sounding systems either observe upwelling radiances from carbon dioxide or water vapour emissions in the IR, or alternatively oxygen or water vapour emissions at microwave frequencies (see Chapter 3 of Volume IV of the present Guide). Both IR and microwave sounding measurements are essential for current operational NWP. The radiance observed by a satellite channel is composed of atmospheric emissions from a range of heights in the atmosphere. This range is determined by the distribution of emitting gases in the vertical and the atmospheric absorption at the channel frequencies. Most radiances from a single satellite temperature channel approximate the mean layer temperature of a layer at least 10 km thick. However, finer vertical resolution is achieved by Fourier-transform interferometers operating in the IR, using information from a much larger number of channels with slightly different absorption characteristics. The height distribution (weighting function) of the observed temperature channel radiance will vary with geographical location to some extent. This is because the radiative transfer properties of the atmosphere have a small dependence on temperature. The concentrations of the emitting gas may vary to a small extent with location and cloud; aerosol and volcanic dust may also modify the radiative heat exchange. IR and microwave




(a) July, Yangjiang, China (3 ascents in 8 h)




(b) United Kingdom, summer (black) and winter (grey)

**Figure 12.2. Examples of complete individual temperature profiles made with large balloons suitable for climate observations**

soundings are difficult to use in the lower troposphere, over snow or ice surfaces. Hence, basic satellite temperature sounding observations provide good horizontal resolution and spatial coverage worldwide for relatively thick layers in the vertical, but the precise distribution in the vertical of the atmospheric emission observed may be more difficult to specify at any given location.

Most radiances observed by nadir-viewing satellite water vapour channels in the troposphere originate from layers of the atmosphere about 4 to 5 km thick. The pressures of the atmospheric layers contributing to the radiances observed by a water vapour channel vary with location to a much larger extent than for the temperature channels. This is because the thickness and central pressure of the layer observed depend heavily on the distribution of water vapour in the vertical. For instance, the layers observed in a given water vapour channel will be lowest when the upper troposphere is very dry. The water vapour channel radiances observed depend on the temperature of the water vapour. Therefore, water vapour distribution in the vertical can be derived only once suitable measurements of vertical temperature structure are available.

Limb-viewing satellite systems can provide measurements of atmospheric structure with higher vertical resolution than nadir-viewing systems; an example of this type of system is refractivity measurements derived from global positioning system (GPS) radio occultation. This provides temperature information at upper levels and some humidity information at low levels. In this technique, vertical structure is measured along paths in the horizontal of at least 200 km (Ruston et al., 2022). The technique is now in widespread use as it provides improved measurements of vertical temperature structure, particularly in the stratosphere. Unlike the nadir soundings, the radio occultation measurements do not need bias correction.

Bias correction is an important aspect of the use of satellite sounding information in NWP systems. As pointed out by Eyre (2016), the effect of model bias on background and analysis biases will increase as more observations are bias-corrected and a smaller proportion are used as 'anchor' observations. For atmospheric temperatures, the main anchor observations are radio occultation and radiosonde observations. Currently, aircraft temperatures need bias correction, but it might be possible to improve the on-board processing so that this is unnecessary. Traditionally satellite calibration/validation involved collocated radiosonde observations – but only a tiny proportion of satellite data points could be used in this process. There is a trend towards using NWP fields for satellite calibration/validation (involving all satellite data points) and using other observations, including radiosondes, to calibrate the NWP fields (Newman et al., 2020).

Hence, radiosonde and satellite sounding systems, together with aircraft, are complementary observing systems and provide a more reliable global observation system when used together. Radiosonde and aircraft observations improve NWP, even given the much larger volume of satellite measurements available.

#### 12.1.3.3 *Maximum height of radiosonde observations*

Radiosonde observations are used regularly for measurements up to heights of about 35 km (see an example in Figure 12.2). However, many observations worldwide will not be made to heights greater than about 25 km, because of the higher cost of the balloons and gas necessary to lift the equipment to the lowest pressures. Temperature errors tend to increase with height, but modern radiosondes are capable of providing useful measurements up to 35 km, particularly at night. Use of large balloons at some stations/times will be necessary to fulfil the Global Basic Observing Network (GBON) requirements (*Manual on the WMO Integrated Global Observing System* (WMO-No. 1160)).

The problems associated with the contamination of sensors during flight and very long time constants of sensor response at low temperatures and pressures currently limit the usefulness of quality radiosonde relative humidity measurements in the stratosphere.

There are various factors that may limit the usefulness of quality radiosonde relative humidity measurements in the stratosphere. In some cases, problems associated with the moisture contamination of sensors during the ascent can generate bias and additional noise in the relative humidity results. In general, very long time constants of sensor response at low temperatures may limit the accuracy, especially during the phase of rapidly decreasing humidity typically found above the tropopause. At altitudes higher up in the stratosphere, the basic accuracy of the measurement may face its limits. As the relative humidity levels typically decrease gradually towards levels below 1%RH, at some point, the relative humidity level to be measured reaches the measurement uncertainty of the sensor.

### 12.1.4 Uncertainty requirements

This section summarizes the requirements for uncertainty (usually stated in terms of $k = 2$, which implies 95% confidence level; see the present volume, Chapter 1) of the meteorological variables measured by radiosondes and compares them with typical operational performance. A more detailed discussion of performance and sources of errors is given in detail in the later sections

dealing with the individual meteorological variable (see 12.3.7, 12.4.6, 12.5.4 and 12.5.6, for temperature, relative humidity, pressure and height, respectively). The definition of uncertainty, systematic error, bias and so on can be found in the present volume, Chapter 1.

Estimates of achievable optimum uncertainty for radiosonde observations, as of 2012, are included in Annex 12.A. This annex was generated following the WMO Intercomparison of High-quality Radiosonde Systems in Yangjiang, China (Nash et al., 2011). It describes the optimum performance that can currently be obtained from operational radiosondes.

A summary of requirements for uncertainty and vertical resolution limits for radiosonde observations extracted from WMO documents is presented in Annex 12.B. These tables include information from the WMO observing requirements database (OSCAR/Requirements; see https://space.oscar.wmo.int/observingrequirements), the observation requirement targets published by WMO (2009) for the GCOS Reference Upper-air Network (GRUAN), and limited information from atmospheric variability studies in *Performance Requirements of Aerological Instruments* (WMO-No. 267). Dirksen et al. (2014) provide a detailed description of the uncertainties associated with the first GRUAN data product.

The WMO observing requirements database includes three limits for most meteorological variables:

(a) The goal: an ideal requirement;

(b) The threshold: the minimum requirement to be met to ensure that data are useful;

(c) A breakthrough: an intermediate level between threshold and goal which, if achieved, would result in a significant improvement for the target application.

Tables 12.B.1, 12.B.2 and 12.B.3 in Annex 12.B are based mainly on the requirements of the high-resolution NWP application area, although information on goals derived from atmospheric variability studies are also shown when the goals differ from those established in the WMO observing requirements database. Climate requirements are based on the GRUAN requirements and those in the section of the observing requirements database for Atmospheric Observation Panel of GCOS or Stratospheric Processes and their Role in Climate activities. Again, when there are significant differences between the goals from the two databases, these are indicated in the tables. Requirements for geopotential height in Table 12.B.4 were derived as described in Annex 12.B.

A radiosonde meeting the less stringent breakthrough requirements, as summarized in Annex 12.A, should provide measurements that give good value for money in terms of national targeted use. However, the less stringent accuracy requirements will not meet the expectations of some users, for instance for primary sites used to detect climate change. Thus, an operational decision has to be made as to the quality of the observation required by the national network, taking into account that the use of such data in forecasts will improve forecast quality across the country if the observation meets the breakthrough targets.

The requirements for spacing between observations in the horizontal from the WMO observing requirements database (https://space.oscar.wmo.int/observingrequirements) have not been shown here, but these clearly show that radiosonde observations on their own cannot meet the minimum requirements of WIGOS, and must be supplemented by temperature, relative humidity and wind measurements from other observing systems.

#### 12.1.4.1 *Geopotential height: requirements and performance*

Modern radiosonde systems can have systematic pressure error a little larger than 1 hPa near the surface, but systematic errors as large as this at pressures lower than 100 hPa are now rare (see Table 12.10). The radiosondes still using the best pressure sensors can measure heights near 10 hPa with an uncertainty ($k = 2$) between 300 and 400 m, that is, with an uncertainty in pressure of about 0.6 hPa.

Thus, the uncertainty goal for height measurements for NWP can be met by most radiosondes using a pressure sensor up to 100 hPa. However, it requires a radiosonde measuring height with GPS technology to measure up to 30 km with an uncertainty of only 20 m, which is equivalent to an uncertainty less than or equal to 0.05 hPa in pressure, depending on the uncertainty of the radiosonde temperature measurements.

Ozone concentrations in the stratosphere have pronounced gradients in the vertical, and height assignment errors from even relatively small pressure sensor errors introduce significant inaccuracies into the ozonesonde profile reports at all latitudes. This has proved to be one of the limiting factors in these measurements when using the older type of radiosonde with larger pressure measurement uncertainties in the stratosphere.

#### 12.1.4.2 *Temperature: requirements and performance*

Most modern radiosonde systems (introduced since 2000) measure temperature in the troposphere and stratosphere up to a height of about 31 km with an uncertainty ($k = 2$) between 0.4 and 1 K. This is usually close to the optimum performance for NWP suggested in Table 12.B.2 of Annex 12.B. However, uncertainty well in excess of 2 K can still be found in some national radiosonde networks in tropical regions. If used, measurements with such large errors damage NWP forecasts.

In the stratosphere, radiosonde temperature uncertainties can be close to the goal for NWP, but require some improvement in daytime conditions to be optimized for climate requirements.

As the goals for climate temperatures are more demanding than for NWP, the GRUAN Lead Centre continues to work with manufacturers and operators to reduce the uncertainty of the current operational measurements in the troposphere and stratosphere. In this case, it is extremely important that systematic errors be as near constant with time as possible, requiring tighter limits on the methods of observation than at standard operational sites. To obtain the most useful performance, operators must take care to prepare and operate the radiosondes according to the instructions, whether from the present Guide, the manufacturer or at GRUAN stations, according to the procedures agreed with the GRUAN Lead Centre. In the case of GRUAN, the details of the radiosonde preparation must be noted and archived as part of the metadata associated with the measurement (Dirksen et al., 2014; von Rohden et al., 2022).

#### 12.1.4.3 *Relative humidity: requirements and performance*

The uncertainties in modern relative humidity sensor measurements at temperatures higher than –50 °C fall mostly within the range of 5% to 14% relative humidity. Thus, the measurements mostly meet the breakthrough limit for NWP, but many need improvement to meet the breakthrough limit for climate measurements (see Annex 12.B, Table 12.B.3).

At temperatures lower than –50 °C, the uncertainties increase, with the best operational radiosonde sensors having an uncertainty of about 16% relative humidity at –70 °C, i.e. close to the breakthrough for NWP and not meeting the breakthrough for climate requirements. However, most modern sensors have uncertainties of about 24% relative humidity at the lowest temperatures. Several problems were identified in the WMO Intercomparison of High-quality Radiosonde Systems in Yangjiang, China (Nash et al., 2011). It is expected that the uncertainties in upper troposphere relative humidity will improve with time as these are rectified.

### 12.1.5 Methods of measurement

This section discusses radiosonde methods in general terms. Details of instrumentation and procedures are given in other sections.

#### 12.1.5.1 *Constraints on radiosonde design*

Certain compromises are necessary when designing a radiosonde:

(a) Temperature measurements are found to be most reliable when sensors are exposed unprotected above the top of the radiosonde, but this also leads to direct exposure to solar radiation. In most modern radiosondes, coatings are applied to the temperature sensor to minimize solar heating and heat exchange in the IR. The radiation corrections work most reliably if the temperature sensor and its supports are designed so that the solar heating does not vary significantly as the radiosonde rotates in flight relative to the sun. Software corrections for the residual solar heating are then applied during data processing.

(b) To protect from rain, some relative humidity sensors used a cover or duct, but this reduces the ventilation of the sensor and hence the speed of response of the sensing system. The cover or duct also provides a source of contamination after passing through cloud. One of the alternatives is to have two sensors which alternate: one is heated to drive off contamination while the other reports the relative humidity; then the second sensor is heated while the first reports the relative humidity, and so on. Best results are now achieved by having one humidity sensor with modest heating (about 5 K above the ambient temperature), combined with a direct measurement of the humidity sensor's temperature.

(c) Pressure sensors are usually mounted internally to minimize the temperature changes in the sensor during flight and to avoid conflicts with the exposure of the temperature and relative humidity sensors.

(d) In many modern radiosondes a pressure sensor is not used, and geometric height is measured using GPS technology and then converted into geopotential height based on knowledge of the gravitational fields at the location.

Other important features required in radiosonde design are reliability, robustness, and light weight and small dimensions to facilitate the launch. With modern electronic multiplexing readily available, it is also important to sample the radiosonde sensors at a high rate. If possible, this rate should be about once per second, corresponding to a minimum sample separation of about 5 m in the vertical. Since radiosondes are generally used only once, or not more than a few times, they must be designed for mass production at low cost. Ease and stability of calibration is very important, since radiosondes must often be stored for long periods (more than a year) prior to use. Some of the most important GCOS stations, for example, in Antarctica, are on sites where radiosondes cannot be delivered more than once per year.

A radiosonde should be capable of transmitting an intelligible signal to the ground receiver over a slant range of at least 200 km. The voltage of the radiosonde battery varies with both time and temperature. Therefore, the radiosonde must be designed to accept battery variations without a loss of measurement accuracy or an unacceptable drift in the transmitted radio frequency.

#### 12.1.5.2 *Radio frequency used by radiosondes*

The radio frequency spectrum bands currently used for most radiosonde transmissions are shown in Table 12.1. These correspond to the meteorological aids allocations specified by the International Telecommunication Union Radiocommunication Sector radio regulations.

The radio frequency actually chosen for radiosonde operations in a given location will depend on various factors. At sites where strong upper winds are common, slant ranges to the radiosonde are usually large and balloon elevations are often very low. Under these circumstances, the 400-MHz band will normally be chosen for use since a good communication link from the radiosonde to the ground system is more readily achieved at 400 MHz than at 1 680 MHz. When upper winds are not so strong, the choice of frequency will, on average, be usually determined by the method of upper-wind measurement used (see the present volume, Chapter 13).

**Table 12.1. Primary frequencies used by radiosondes in the meteorological aids bands**

| *Radio frequency band (MHz)* | *Status* | *International Telecommunication Union Regions* |
|---|---|---|
| 400.15 – 406 | Primary | All |
| 1 668.4 – 1 700 | Primary | All |

Note: Some secondary radar systems manufactured and deployed in the Russian Federation may still operate in a radio frequency band centred at 1 780 MHz.

The frequency band of 400 MHz is usually used when navigational aid windfinding is chosen, and 1 680 MHz when radiotheodolites or a tracking antenna are to be used with the radiosonde system.

The radio frequencies listed in Table 12.1 are allocated on a shared basis with other services. In some countries, the national radiocommunication authority has allocated part of the bands to other users, and the whole of the band is not available for radiosonde operations. In other countries, where large numbers of radiosonde systems are deployed in a dense network, there are stringent specifications on radio frequency drift and bandwidth occupied by an individual flight.

Any organization proposing to fly radiosondes should check that suitable radio frequencies are available for their use and should also check that they will not interfere with the radiosonde operations of the NMHS.

There are now strong requirements from governments to improve the efficiency of radio frequency use. Therefore, radiosonde operations will have to share with a greater range of users in the future. Wideband radiosonde systems occupying most of the available spectrum of the meteorological aids bands will become impracticable in many countries. Therefore, preparations for the future in most countries should be based on the principle that radiosonde transmitters and receivers will have to work with bandwidths of much less than 1 MHz in order to avoid interfering signals. Transmitter stability will have to be better than ±5 kHz in countries with dense radiosonde networks, and not worse than about ±200 kHz in most of the remaining countries.

NMHSs need to maintain contact with national radiocommunication authorities in order to keep adequate radio frequency allocations and to ensure that their operations are protected from interference. Radiosonde operations will also need to avoid interference with, or from, data collection platforms transmitting to meteorological satellites between 401 and 403 MHz, with the downlinks from meteorological satellites between 1 690 and 1 700 MHz and with the command and data acquisition operations for meteorological satellites at a limited number of sites between 1 670 and 1 690 MHz.

### 12.1.6 Radiosonde errors: general considerations

#### 12.1.6.1 *Types of error*

This section contains a detailed discussion of the errors encountered with radiosonde sensors.

Measurement errors by radiosondes may be classified into three types (Hooper, 1975):

(a) Systematic errors characteristic of the type of radiosonde in general;

(b) Sonde error, representing the variation in errors that persist through thick layers in the vertical for a particular type of radiosonde from one flight to the next;

(c) Random errors (now called uncertainties) in individual observations, producing the scatter superimposed on the sonde error through a given ascent.

However, for many users it is also helpful to take note of the magnitude of the representativeness errors that are associated with a measurement (see Kitchen (1989) and the present volume, Chapter 1). For instance, radiosonde temperature observations are assigned an uncertainty in data assimilation schemes, and this has more to do with a representativeness error than the small instrumentation uncertainties identified in 12.3.7. These errors differ depending on the atmospheric situation and also on the use made of the measurement. For example, as the scales of motion represented in a NWP model increase, the radiosonde representativeness errors ought to decrease because the model represents more of what the radiosonde measures. On the other hand, a climatologist wants measurements that are close to a longer-term average, representing a significant area around the launch site. The structure introduced by localized small-scale fluctuations in the radiosonde measurement is undesirable for this purpose.

#### 12.1.6.2 ***Potential references***

High-precision tracking radar measurements or Global Navigation Satellite System (GNSS) height measurements can allow systematic errors in geopotential height measurements to be quantified. These results can then be used to identify systematic errors in radiosonde pressure sensor measurements, given that uncertainties in temperature measurements are known to be relatively small.

Most newly developed radiosondes measure temperatures at night which fall within a range of ±0.2 K at a height of 30 km (Nash et al., 2006, 2011). Thus, at night, it is possible to identify systematic errors that bias radiosonde measurements away from this consensus.

However, interpreting daytime temperature comparisons with similar uncertainty is still not feasible. For instance, average temperature uncertainties in the same tests fall within about ±0.5 K at a height of 30 km. Dirksen et al. (2014) clearly show the uncertainties from solar radiation at upper levels. One issue is that radiation corrections assume average cloud conditions: more/less reflected solar radiation than average will make the correction suboptimal. The radiation error also varies with the sensor orientation, which changes as the radiosonde swings and rotates.

Relative humidity measurements can be checked at high humidity when the radiosondes pass through clouds. Here, laser ceilometer and cloud radars can provide better evidence on the cloud observed by the radiosonde during its ascent. The vertical structure in relative humidity reported by radiosondes, including the presence of very dry layers, can be validated by comparison with Raman lidar measurements. For GRUAN stations, Dirksen et al. (2014) recommend the use of a standard humidity chamber (at 100%RH) as a pre-launch check (this is better than using a desiccant to give ~0%RH).

In most radiosonde comparison tests, the results from one radiosonde design are compared with those of another to provide an estimate of their systematic differences. The most extensive series of comparison tests performed since 1984 have been those of the WMO international radiosonde comparisons (Nash and Schmidlin, 1987; Ivanov et al., 1991; Yagi et al., 1996; Balagurov et al., 2006) and the tests performed in Brazil (da Silveira et al., 2006), Mauritius (Nash et al., 2006) and Yangjiang, China (Nash et al., 2011). Results from these and other tests using the same standards in the United Kingdom (see results from the Camborne Met Office (Smees et al., 2010)), the United States and Switzerland will sometimes be quoted in the subsequent sections.

There are several national facilities in which the performance of radiosonde sensors can be tested at different pressures and temperatures in the laboratory. The WMO Radiosonde Humidity Sensor Intercomparison (Balagurov et al., 2006) contains results from laboratory comparisons with humidity standards in the Russian Federation. These results can be helpful in identifying some, but not all, of the problems identified when flying in the atmosphere.

#### 12.1.6.3 *Sources of additional error during radiosonde operations*

Modern radiosondes have reduced or automated pre-flight checks. Where they are still performed manually it is extremely important to perform pre-flight radiosonde checks very carefully, since mistakes in measuring values for control data used to adjust calibrations can produce significant errors in measurement during the ascent. Observation errors in the surface data obtained from a standard screen and then included in the radiosonde message must also be avoided. An error in surface pressure will affect all the computed geopotential heights. For the same reason, it is important that the surface pressure observation should correspond to the official station height.

Uncertainties in modern radiosonde measurements are now generally small. This is the result of improved radiosonde electronics and multiplexing, providing more reliable data telemetry links between the ground station, and reliable automated data processing in the ground station. Thus, the uncertainties are usually less significant than systematic radiosonde errors and flight-to-flight variation in sensor performance and calibration (sonde error). However, uncertainties may become large if there is a partial radiosonde failure in flight, if interference is caused by another radiosonde using a similar transmission frequency, or if the radiosondes are at long slant ranges and low elevations that are incompatible with the specifications of the ground system receiver and aerials.

Thus, errors in radiosonde measurements may be caused not only by the radiosonde sensor design and problems with calibration in the factory during manufacture, but also by problems in the reception of the radiosonde signal at the ground and the effect on subsequent data processing. When signal reception is poor, data-processing software will often interpolate values between the occasional measurements judged to be valid. Under this circumstance, it is vital that the operator is aware of the amount of data interpolation occurring. Data quality may be so poor that the flight should be terminated and a replacement radiosonde launched.

## 12.2 RADIOSONDE ELECTRONICS

### 12.2.1 General features

A basic radiosonde design usually comprises three main parts as follows:

(a) The sensors plus references;

(b) An electronic transducer, converting the output of the sensors and references into electrical signals;

(c) The radio transmitter.

In rawinsonde systems (see the present volume, Chapter 13), there are also electronics associated with the reception and retransmission of radionavigation signals, or transponder system electronics for use with secondary radars.

Radiosondes are usually required to measure more than one meteorological variable. Reference signals are used to compensate for instability in the conversion between sensor output and transmitted telemetry. Thus, a method of switching between various sensors and references in a predetermined cycle is required. Most modern radiosondes use electronic switches operating at high speed with one measurement cycle lasting typically between 1 and 2 s. This rate of sampling allows the meteorological variables to be sampled at height intervals of between 5 and 10 m at normal rates of ascent.

### 12.2.2 Power supply for radiosondes

Radiosonde batteries should be of sufficient capacity to power the radiosonde for the required flight time in all atmospheric conditions. For radiosonde ascents to 5 hPa, radiosonde batteries should be of sufficient capacity to supply the required currents for up to three hours, given that the radiosonde launch may often be delayed and that flight times may be as long as two hours. Three hours of operation would be required if descent data from the radiosonde were to be used. Batteries should be as light as practicable and should have a long storage life. They should also be environmentally safe following use. Many modern radiosondes can tolerate significant changes in output voltage during flight. Two types of batteries were in common use, the dry-cell type and water-activated batteries. The use of dry-cell batteries increased rapidly as these have the advantages of being widely available at very low cost because of the high volume of production worldwide and of posing less risk in terms of occupational health and safety (and environmental impact). Use of water-activated batteries appears to have ceased.

Care must be taken to ensure that batteries do not constitute an environmental hazard once the radiosonde falls to the ground after the balloon has burst. See 12.7.5 and Annex 12.C for a more detailed discussion on environmental issues.

### 12.2.3 Methods of data transmission

#### 12.2.3.1 *Radio transmitter*

A wide variety of transmitter designs are in use. Solid-state circuitry is mainly used up to 400 MHz and valve (cavity) oscillators may be used at 1 680 MHz. Modern transmitter designs are usually crystal-controlled to ensure a good frequency stability during the sounding. Good frequency stability during handling on the ground prior to launch and during flight are important. At 400 MHz, widely used radiosonde types are expected to have a transmitter power output lower than 250 mW. At 1 680 MHz the most widely used radiosonde type has a power output of about 330 mW. The modulation of the transmitter varies with radiosonde type. It would be preferable in the future if radiosonde manufacturers could agree on a standard method and format for transmission of data from the radiosonde to the ground station, which would allow user interoperability between radiosonde types without the need to modify the ground reception hardware and software each time. In any case, the radiocommunication authorities in many regions of the world will require that radiosonde transmitters meet certain specifications in the future, so that the occupation of the radio-frequency spectrum is minimized and other users can share the nominated meteorological aids radio-frequency bands (see 12.1.5.2).

## 12.3 TEMPERATURE SENSORS

### 12.3.1 General requirements

The best modern temperature sensors have a speed of response to changes of temperature which is fast enough to ensure that systematic error from thermal lag during an ascent, the typical rate of ascent being 5 to 6 m $s^{-1}$, remains less than 0.1 K through any layer of depth of 1 km in the troposphere and less than 0.2 K through any layer of similar depth in the stratosphere. This is achieved in most locations using a sensor with a time constant of response faster than 1 s in the early part of the ascent. In addition, the temperature sensors should be designed to be as free as possible from radiation errors introduced by direct or backscattered solar radiation. There must be as small a variation as possible in the area of cross-section for solar heating as the sensor rotates relative to the sun during ascent. Heat exchange in the IR needs to be avoided by using sensor coatings that have low emissivity in the IR.

Temperature sensors also need to be sufficiently robust to withstand buffeting during launch and sufficiently stable to retain accurate calibration over several years. The main types of temperature sensors in routine use are resistive sensors (for example, thermistors made of ceramic resistive semiconductors or metal resistors), capacitive sensors and thermocouples.

The rate of response of the sensor is usually measured in terms of the time constant of response, $\tau$. This is defined (as in the present volume, Chapter 1, 1.6.3) by:

$$dT_e/dt = -1/\tau \cdot (T_e - T) \tag{12.1}$$

where $T_e$ is the temperature of the sensor and $T$ is the true air temperature.

Thus, the time constant is defined as the time required to respond by 63% to a sudden change of temperature. The time constant of the temperature sensor is proportional to thermal capacity and inversely proportional to the rate of heat transfer by convection/diffusion from the sensor. Thermal capacity depends on the volume and composition of the sensor, whereas the heat transfer from the sensor depends on the sensor surface area, the heat transfer coefficient and the rate of the air mass flow over the sensor. The heat transfer coefficient has a weak dependence on the diameter of the sensor. Thus, the time constants of response of temperature sensors made from a given material are approximately proportional to the ratio of the sensor volume to its surface area. Consequently, thin sensors of large surface area are the most effective for obtaining a fast response. The variation of the time constant of response with the mass rate of airflow can be expressed as:

$$\tau = \tau_0 \cdot (\rho \cdot v)^{-n} \tag{12.2}$$

where $\rho$ is the air density, $v$ the air speed over the sensor, and $n$ a constant.

The value of $n$ varies between 0.4 and 0.8, depending on the shape of the sensor and on the nature of the airflow (laminar or turbulent). A selection of the time constants of response of both older and modern types of temperature sensors is shown in Table 12.2. These are for pressures of 1 000, 100 and 10 hPa, with a rate of ascent of 5 m $s^{-1}$. The values were derived from a combination of laboratory testing and comparisons with very fast response sensors during ascent in radiosonde comparison tests.

Modern bead thermistors, wire thermocapacitors and thermocouples have a very fast response, so the systematic errors from thermal lag are expected to be less than 0.05 K in the upper troposphere for the better sensors, and less than 0.1 K in the upper stratosphere.

Nash et al. (2011) show examples in which the response speeds of most of the bead thermistors used by radiosondes in the test were similar or slightly faster than those of the chip thermistor included in Table 12.2.

**Table 12.2. Typical time constants of response of radiosonde temperature sensors**

| *Temperature sensor* | *Operational use* | *τ (1 000 hPa)* | *τ (100 hPa)* | *τ (10 hPa)* |
|---|---|---|---|---|
| Chip thermistor,[a] 0.4 x 0.8 x 0.8 mm | 2003– | ≤ 1 | ≤ 3 | ≤ 10 |
| Wire thermocapacitor,[a] diameter 0.1 mm | 2002– | 0.4 | 1.1 | 3 |
| Copper-constantan thermocouple,[a] diameter 0.06 mm | 1991– | < 0.3 | < 0.8 | 2 |
| Other modern bead thermistors[a] | 2005– | ≤ 1 | ≤ 4 | 5 – 12 |

Note:

a The time constants of response at 10 hPa of the chip thermistors in Yangjiang, China, were larger than those of the Copper-constantan thermocouple by about 4 s. The other small bead thermistors had time constants of response between 3 and 10 s larger than the Copper-constantan thermocouple. The wire thermocapacitor showed time constants of response of at least 4 s, a little larger than the results from the laboratory test cited above. This may be because the diameter of the wire thermocapacitor in the Vaisala RS92 radiosondes had been increased in 2007 by incorporating a quartz support fibre, and may also be a consequence of the software used with the sensor in Yangjiang.

### 12.3.2 Thermistors

Across the entire meteorological temperature range the electrical resistance of most pure metals is an almost linear function of temperature. Although many pure metals could be used for thermometry, platinum metal is most widely used for electrical resistance thermometers because of its exceptional resistance to corrosion. The linear response of platinum resistance thermometers (PRTs) enables highly accurate calibration over the wide temperature range needed in atmospheric profiling. The good stability properties of PRTs are very beneficial in operational soundings that involve storing the radiosondes for long periods. PRTs are also the most common type of temperature sensor for metrological reference measurements.

Some thermistors are made of a ceramic material whose resistance changes with temperature. The sensors have a high resistance that decreases with absolute temperature. The relationship between resistance, $R$, and temperature, $T$, can be expressed approximately as:

$$R = A \cdot \exp\left(B/T\right) \tag{12.3}$$

where $A$ and $B$ are constants. Sensitivity to temperature changes is very high, but the response to temperature changes is far from linear since the sensitivity decreases roughly with the square of the absolute temperature. As thermistor resistance is very high, typically tens of thousands of ohms, self-heating from the voltage applied to the sensor is negligible. It is possible to manufacture very small thermistors and, thus, fast rates of response can be obtained. Solar heating of a modern chip thermistor is about 1 K at 10 hPa.

### 12.3.3 Thermocapacitors

Thermocapacitors are usually made of a ceramic material whose permittivity varies with temperature. The ceramic used is usually barium-strontium titanate. This ferro-electric material has a temperature coefficient of permittivity of the order of $10^{-2}$ per K. The temperature coefficient is positive at temperatures below the Curie point and negative at temperatures above the Curie point. Sensors can now have a diameter of about 0.1 mm. The wire thermocapacitor measures the change in capacitance between two fine platinum wires separated by a glass ceramic (see Turtiainen et al., 1995). This sensor gives improved speed of response, and solar heating errors are less than 1 K at 10 hPa.

### 12.3.4 Thermocouples

Copper-constantan thermocouple junctions were used as a temperature sensor in one national radiosonde used in the 2010 intercomparison (Nash et al., 2011) but have been discontinued since. Wires of 0.05 mm in diameter are used to form the external thermocouple junction and these provide a sensor with a very fast response. The relationship between the thermal electromotive force and the temperature difference between the sensor and its reference is an established physical relationship. The thermocouple reference is mounted internally within the radiosonde in a relatively stable temperature environment. A copper resistor is used to measure this reference temperature. In order to obtain accurate temperatures, stray electromotive force introduced at additional junctions between the sensor and the internal references must also be compensated.

### 12.3.5 Scientific sounding instruments

Two specialized scientific temperature sounding sensors were deployed during the WMO Intercomparison of High-quality Radiosonde Systems in Yangjiang, China (Nash et al., 2011):

(a) The MTR temperature sensor uses an ultrathin tungsten wire as a sensor. The wire is 0.01 mm in diameter, 44 cm long and wound into a helical coil with a diameter of 0.2 mm and a pitch of 0.1 mm. The wire is coated with aluminium to improve reflectivity and thus reduce solar heating (see Shimizu and Hasebe, 2010). This sensor has smaller time constants of response than the Copper-constantan thermocouple;

(b) The multithermistor radiosonde in Yangjiang was an independent instrument based on the NASA Accurate Temperature Measuring (ATM) Multithermistor Radiosonde (see Schmidlin, 2006; Schmidlin et al., 1995). The system made measurements with three aluminized thermistors and one white and one black thermistor. In Yangjiang, the time constants of response were similar to those of the modern bead thermistors. With the measurements from the five sensors and an exact knowledge of the optical properties of the different sensor coatings, a reference temperature is derived as well as estimates of the solar and IR radiation environments. This estimated temperature does not depend on any assumption about the backscattering from the surface and clouds, unlike other radiosonde temperature correction schemes.

The reliability of the absolute calibration and daytime corrections of these scientific systems did not prove to be better than those of the good operational radiosondes in the Yangjiang test.

### 12.3.6 **Exposure**

Radiosonde temperature sensors are best exposed in a position above the main body of the radiosonde (but below the body of a dropsonde). Thus, air heated or cooled by contact with the radiosonde body or sensor supports cannot subsequently flow over the sensor. This is usually achieved by mounting the sensor on an arm or outrigger that holds the sensor in the required position during flight. For long-term stability of operation, this position needs to be reproducible and must not vary from flight to flight. For good exposure at low pressures, the supports and electrical connections to the sensor should be thin enough so that heating or cooling errors from thermal conduction along the connections are negligible.

With this method of exposure, the radiosonde temperature sensors are exposed directly to solar radiation and to the IR environment in the atmosphere. The sensors receive solar radiation during daytime soundings and will exchange long-wave radiation with the ground and the sky at all times. The magnitude of radiation errors is only weakly dependent on the size and shape of the sensors, since convective heat transfer coefficients are only weakly dependent on sensor size. Thus, small radiation errors may be obtained with small sensors, but only when the sensor coating is chosen to provide low absorption for both solar and long-wave radiation. The required coating can be achieved by the deposition of a suitable thin metallic layer.

An additional consequence of exposing the temperature sensor above the radiosonde body is that, when ascending during precipitation or through cloud, the sensor may become coated with water or ice unless protected by a hydrophobic coating. It is extremely important that the sensor design sheds water and ice efficiently. Evaporation of water or ice from the sensor when emerging from a cloud into drier layers will cool the sensor below true ambient temperature. The absorptivity in the IR of a temperature sensor that remains coated with ice throughout a flight differs from usual. Thus, an abnormal systematic error from IR heat exchange will be introduced into the iced sensor measurements, particularly at low pressures.

### 12.3.7 **Temperature errors**

Errors in older radiosonde types widely used in the period 1980–2000 are discussed in more detail in Nash (2015).

#### 12.3.7.1 ***Calibration***

Temperature errors related to calibration during an ascent may result from:

(a) Errors in factory calibration. This can occur from time to time and is one of the reasons the radiosonde measurements should be checked on the ground before launch;

(b) Small changes in the sensor, such as the stray capacitance associated with a capacitive sensor or in the electrical connections to the sensor;

(c) Instabilities in the radiosonde transducer system and references. This is possible during storage or during the ascent. Sensor or transducer drift during storage can usually be partially corrected during data processing, using adjustments based on pre-flight ground checks.

Table 12.3 summarizes the relative performance of temperature sensors at night for different temperature sensors in operation in 2013. The results represent the typical performance averaged over a minimum of at least 15 test flights. The absolute uncertainty of the reference at night was probably better than 0.3 K, with NASA and Sippican multithermistor radiosondes agreeing as well as can be expected from the error analysis.

Where a range of systematic errors has been attributed to a radiosonde type, the range represents the spread in systematic difference found in a number of tests and also takes into account the range of likely performance up to 30 hPa estimated from radiosonde monitoring (Elms, 2003). As modern sensors have aluminized coatings, IR errors are very small, and any spread in the performance is mainly down to the long-term consistency of factory calibration, small instabilities in the sensors, perhaps depending on the atmospheric structure and internal temperature of the radiosonde electronics, and so on. It is difficult to differentiate between the best systems in Table 12.3 as similar errors have been attributed to the sensors. The reproducibility of the temperature measurements can be measured relatively easily, but it is not currently possible to ascertain the bias better than the limits shown in the table. Large-scale tests in the tropics have not given the same results for bias as those in Europe, so the values shown are an average between the two conditions with the range of values necessary to encompass both sets of results.

**Table 12.3. Systematic error, sonde error and uncertainty ($k = 2$) at night from the WMO international radiosonde comparisons and other associated tests (using the NASA-ATM multithermistor reference as an arbitrary reference for systematic offsets where available)**

| *Temperature sensor* | *System error (K)* | | | | *Sonde error* | | *Uncertainty (k = 2)* | | |
|---|---|---|---|---|---|---|---|---|---|
| *Pressure (hPa)* | *300* | *100* | *30* | *10* | *30* | *10* | *100* | *30* | *10* |
| Rod thermistor, white paint, MRZ (Russian Federation) | 0.2±0.5 | 0.2±0.5 | –0.3±0.7 | –0.8±0.7 | 1 | 1 | 1–1.7 | 1–2 | 1.1–2.5 |
| Copper-constantan thermocouple, Meteolabor (Switzerland) | 0.1±0.1 | 0±0.1 | –0.1±0.2 | –0.1±0.2 | 0.3 | 0.4 | 0.3–0.4 | 0.3–0.6 | 0.4–0.7 |
| Wire thermos-capacitor, Vaisala RS92 (Finland) | 0.05±0.1 | 0.05±0.1 | 0.07±0.2 | 0.07±0.2 | 0.2 | 0.3 | 0.2–0.4 | 0.2–0.5 | 0.3–0.6 |
| Chip thermistor, Lockheed Martin Sippican (United States) | 0±0.1 | –0.05±0.2 | –0.07±0.2 | –0.07±0.2 | 0.2 | 0.3 | 0.2–0.4 | 0.2–0.5 | 0.3–0.6 |
| Bead thermistor, aluminized | 0±0.2 | 0.1±0.2 | 0.1±0.2 | 0.2±0.2 | 0.2 | 0.4 | 0.2–0.5 | 0.2–0.5 | 0.4–0.8 |
| NASA-ATM multi-thermistors, used by F. Schmidlin | Bias assumed to be within ±0.1 K | | | | 0.2 | 0.2 | 0.2–0.3 | 0.2–0.3 | 0.2–0.3 |

Sonde errors are only quoted for pressures of 30 hPa and 10 hPa in Table 12.3 since, for most modern temperature sensors, sonde errors show little variation between the surface and 30 hPa, although some systems had problems near the tropopause (Nash et al., 2011). Ho et al. (2017) compare radiosonde temperatures with results from satellite radio occultation data.

#### 12.3.7.2 *Thermal lag*

Most modern radiosonde temperature sensors are fast enough to not require significant correction for thermal lag errors in the troposphere and lower stratosphere.

#### 12.3.7.3 *Radiative heat exchange in the infrared*

Most white paints used on radiosonde sensors have relatively high emissivity in the IR (> 0.8). Heat exchange with the IR background is then capable of producing significant errors in temperature measurements. For a given vertical temperature structure, the IR fluxes will also vary significantly from flight to flight depending on the cloud present in the vicinity of the ascent. Luers and Eskridge (1998) provide a good example of users who tried to model the solar and IR radiation errors on radiosondes in use in the 1990s.

Infrared errors affect both day and night observations. The effects of IR heat exchange errors at night can be seen in the measurements of the rod thermistors (used on the Russian radiosonde) in Table 12.3. At high pressures, these sensors give temperatures close to the reference, but at low pressures the temperatures reported are much colder than the reference. At pressures lower than 30 hPa, the radiative equilibrium temperature at night was usually significantly lower than the actual atmospheric temperatures. Therefore, the IR radiation emitted by the temperature sensor exceeded the IR radiation absorbed by the sensor from the atmospheric environment, and the sensor cooled to a temperature lower than truth. Additional information on the effects of IR errors in the past can be found in Nash (2015).

The use of white paint on the temperature sensor should be discontinued as soon as possible so that variation in systematic temperature error from IR errors will then be negligible across the radiosonde network.

#### 12.3.7.4 *Heating by solar radiation*

All radiosonde temperature sensors will have heating errors in daytime caused by incident solar radiation, including backscattered radiation from clouds and the surface. Table 12.4 shows the day–night differences associated with the temperature measurements of the radiosondes considered in Table 12.3. These values were derived mostly from the software corrections used for daytime temperatures by each system for solar elevations between 30° and 80°. Temperature sensors of the Russian radiosonde had relatively poor thermal isolation from supporting structures, which could often be heated more than the sensor itself, and so the Russian radiosondes also had large day–night differences at upper levels.

In all modern operational radiosonde systems, software corrections are applied during data processing to compensate for the solar heating (see Table 12.4). These correction schemes are usually derived from special investigations of day–night differences in temperature (taking into account real diurnal variation in temperature caused by atmospheric tides) coupled with solar heating models, and possibly laboratory testing. The correction is then expressed as a function of solar elevation during the ascent. The correction may also take into account the actual rates of ascent, since ventilation and heating errors will change if the rate of ascent differs from the standard test conditions. At low solar elevations (less than 10°) the heating errors are extremely sensitive to changes in solar elevation. Thus, if the correction software does not update solar elevation during flight, significant errors will be generated when correcting sunrise or sunset flights. A simple correction scheme will work effectively only for certain cloud and surface conditions and cannot provide adequate correction for all flight conditions that might be encountered. For instance, in many ascents from coastal sites the radiosonde proceeds out

**Table 12.4. Day–night differences for selected temperature sensors from the WMO international radiosonde comparisons and other associated tests**

| *Temperature sensor* | *Systematic error (K)* | | | |
|---|---|---|---|---|
| *Pressure (hPa)* | *300* | *100* | *30* | *10* |
| Rod thermistor, white paint, MRZ (Russian Federation) | 1 | 1.8 | 3.3 | 5.1 |
| Copper-constantan thermocouple, Meteolabor (Switzerland) | 0.5[a]<br>0.3[b] | 0.75[a]<br>0.5[b] | 1.1[a]<br>0.75[b] | 1.8[a]<br>1[b] |
| Chip thermistor, Lockheed Martin Sippican (USA) | 0.3 | 0.5 | 0.8 | 0.95 |
| Wire thermocapacitor, Vaisala (Finland) | 0.15 | 0.3 | 0.5 | 0.8 |
| Bead thermistor,[c] aluminized | 0.2 – 0.5 | 0.3 – 1.1 | 0.4 – 1.5 | 0.6 – 2.3 |

Notes:
a As used in Nash et al. (2011)
b As revised in subsequent tests (Philipona et al., 2013)
c Summary of the range of results from other radiosonde systems using bead thermistors in the Yangjiang comparison (Nash et al., 2011). See Nash (2015) for details of the individual radiosonde types at Yangjiang.

to sea. In clear sky conditions, the low surface albedo of the sea will reduce backscattered solar radiation by a factor of two or three compared with average atmospheric conditions during flight. In such circumstances, software corrections based on average conditions will be up to 30% too large. On the other hand, in ascents over thick upper cloud with very high albedo or over desert conditions, backscattering may be much larger than usual and the software correction will underestimate the required correction.

Table 12.5 contains a review of the systematic and sonde errors in modern radiosonde types. In the systematic errors derived from the test in Yangjiang, China (Nash et al., 2011), it was assumed that zero systematic error in Yangjiang was halfway between Vaisala/MODEM and LMS/multithermistor at 30 and 10 hPa. This is because subsequent testing in the United States has not shown significant errors in the multithermistor system used in Yangjiang, that is to say, there was some real atmospheric diurnal variation in temperature between 30 and 10 hPa in Yangjiang, with a probable amplitude of about 0.15 K. In the estimates of the range of systematic error in Table 12.5, it has been assumed that the standardized software correction schemes produce a range of possible bias of ±30%. During a particular radiosonde test, the radiative conditions (cloud, surface albedo) do not usually change much, so the illusion is given that the bias is accurately defined. However, a test performed at another location can give systematic errors that differ by much more than the sonde error found in the individual test.

The sonde errors for all radiosondes are larger in daytime than in night-time conditions (see Tables 12.3 and 12.5). During ascent, radiosondes swing and rotate like a pendulum suspended from the balloon, so the absorption cross-sections of the sensor change as the sensor rotates. Also, air heated by contact with either the sensor supports or the radiosonde body may flow over the external sensor from time to time. If these possibilities have not been prevented in the design (for example, if the temperature sensor is mounted close to the radiosonde body, perhaps halfway between the top and the bottom), much larger sonde errors will result in daytime. Backscattered radiation varies from flight to flight with changing cloud cover and also contributes to the increase in daytime sonde errors. The systematic errors in daytime measurements should be smallest for the radiosonde systems with the smallest day–night differences (Table 12.4).

When a support frame surrounds the temperature sensor, air heated by contact with the frame passes over the sensor in part of the pendulum cycle, producing positive pulses in the reported temperature as the radiosonde moves around in flight. These pulses can be as large as 1 K at 10 hPa. The heating pulses can be readily recognized when flying radiosondes on the rigs used in WMO radiosonde comparisons since the radiosondes rotate in a very regular fashion during

**Table 12.5. Systematic error, sonde error and uncertainty ($k$ = 2) for selected temperature sensors in the day from WMO international radiosonde comparisons and other associated tests, and from operational monitoring as in Elms (2003)**

| *Temperature sensor* | *Systematic error (K)* | | | *Sonde error* | | | *Uncertainty (k = 2)* | | |
|---|---|---|---|---|---|---|---|---|---|
| *Pressure (hPa)* | *100* | *30* | *10* | *100* | *30* | *10* | *100* | *30* | *10* |
| Rod thermistor, white paint, MRZ (Russian Federation) | 0.7±0.5 | 0.5±1 | –0.7±1.3 | 1 | 1.2 | 1.5 | 1.2–2.2 | 1.2–2.7 | 1.5–3.5 |
| Copper-constantan thermos-couple, Meteolabor (Switzerland) | –0.2[a]<br>–0.05[b] | –0.5[a]<br>–0.2[b] | –0.8[a]<br>0[b] | 0.4 | 0.4 | 0.8 | 0.6 | 0.9 | 1.5 |
| Wire thermos-capacitor, Vaisala (Finland) | 0±0.2 | –0.2±0.2 | –0.3±0.3 | 0.4 | 0.4 | 0.4 | 0.4–0.7 | 0.4–0.9 | 0.4–0.9 |
| Chip thermistor, Lockheed Martin Sippican (USA) | –0.1±0.2 | 0.2±0.2 | 0.3±0.3 | 0.3 | 0.3 | 0.4 | 0.3–0.6 | 0.3–0.8 | 0.4–1.0 |
| Bead thermistor,[c] aluminized | 0.1±0.2 | 0±0.3 | 0±0.5 | 0.4–0.8 | 0.4–1.3 | 0.4–1.7 | 0.5–1.0 | 0.8–1.6 | 0.4–2.3 |
| Multi-thermistor | ±0.2 | ±0.2 | ±0.3 | 0.3 | 0.3 | 0.4 | 0.3–0.5 | 0.4–0.6 | 0.4–0.7 |

Notes:
a As used in Nash et al. (2011)
b As revised in subsequent tests (Philipona et al., 2013)
c Summary of the range of results from other radiosonde systems using bead thermistors in the Yangjiang comparison (Nash et al., 2011). See Nash (2015) for details of the individual radiosonde types at Yangjiang.

the flight. In this situation, suitable raw data filtering can remove the positive pulses to some extent. Thus, the filtering applied to the basic observations of several systems must also be taken into account when investigating daytime radiosonde temperature errors.

The WMO intercomparison tests were performed with the radiosondes suspended at least 30 m and most commonly 40 m under the balloon. However, many national networks, such as China, Japan and the Russian Federation, have used much shorter suspensions which will produce additional daytime bias and increased sonde errors compared to those quoted in Tables 12.4 and 12.5, especially at pressures lower than 30 hPa.

One of the most practical ways to obtain the correction for the heating of the sensor by solar radiation is to test sensors using ground-based facilities that are capable of simulating the environments from the ground to the stratosphere. Two independent laboratory studies, undertaken by GRUAN (von Rohden et al., 2022) and the Korea Research Institute of Standards and Science (KRISS) (Lee et al., 2022a), showed that the correction of sensors for radiation was proportional to the radiation flux but negatively correlated with air pressure and ventilation speed. The properties of air surely play a dominant role in the convective cooling of sensors in such a way that the heat transfer from the sensor to the air is increasingly facilitated as the air

pressure and ventilation speed are increased. In addition, the radiation correction is dependent on the temperature of air mainly due to the positive correlation between the temperature and the thermal conductivity of air. The upper-air simulator at KRISS revealed that the radiation corrections for both a rod-shaped temperature sensor and a bead-type thermistor needed to be increased by about 20% at –70 °C with respect to those at 20 °C at a constant air pressure of 5 hPa (Lee et al., 2022*a*, 2022*b*). These observations suggest that radiation corrections for radiosonde temperature sensors can be made more accurate as laboratory setups faithfully simulate the environments that can be encountered by radiosondes.

#### 12.3.7.5 *Deposition of ice or water on the sensor*

Another source of temperature error is the deposition of water or ice on the temperature sensor. This will lead to psychrometric cooling (from the wet-bulb effect) of the temperature sensor, once atmospheric relative humidity drops to less than 100% later in the ascent. If the sensor tends to collect water or ice, rather than rapidly shed the precipitation, large parts of the temperature measurements during the ascent may be corrupted. At night, a coating of ice will cause an aluminized sensor to act like a black sensor in the IR, leading to large cooling at low pressures in commonly encountered conditions.

Furthermore, if water deposited on the sensor freezes as the sensor moves into colder air, the latent heat released will raise the temperature towards 0 °C. If a sensor becomes coated with ice and then moves into a warmer layer, the temperature will not rise above 0 °C until the ice has melted. Thus, isothermal layers reported close to 0 °C in wet conditions should be treated with some caution.

#### 12.3.7.6 *Representativeness issues*

Representativeness issues are discussed in Nash (2015).

## 12.4 RELATIVE HUMIDITY SENSORS

### 12.4.1 General aspects

Operational relative humidity measurements worldwide have a wide range of performance (from good to poor). All the sensor types listed in Table 12.7 were still in use in some national networks in 2013, but some have since been retired. The most widely used sensor was the heated twin thin-film capacitor. Its successor is a single, heated thin-film capacitor with an integrated temperature sensor (Jensen et al., 2016). This sensor is mounted externally, without a cover, on a boom which holds it above the top of the radiosonde body. The other modern thin-film capacitors are usually deployed externally on a boom with an aluminized cover to protect against contamination from precipitation and minimize solar heating of the humidity sensor. Carbon hygristors and goldbeater's skin did not meet modern user requirements and their operational use has been phased out.

A good modern radiosonde relative humidity sensor should be able to measure relative humidity to a useful accuracy at all temperatures from 40 °C down to about –70 °C. Temperatures are lower than this near the tropical and subtropical tropopause, and radiosonde sensors can make useful measurements at these temperatures provided that certain corrections are applied (see below). However, the most reliable practical method of measuring water vapour at these lowest temperatures is with a frost-point hygrometer (see Vömel et al. (2007) and the results from the WMO Intercomparison of High-quality Radiosonde Systems (Nash et al., 2011)). Table 12.6 shows the range of saturated water vapour pressures with respect to a water surface that must be resolved to provide relative humidity measurements at all levels. At temperatures below 0 °C, relative humidity sensors should be calibrated to report relative humidity with respect to a water surface.

The saturation with respect to water cannot be measured much below –50 °C, so manufacturers should use one of the following expressions for calculating saturation vapour pressure relative to water at the lowest temperatures – Wexler (1976, 1977), Hyland and Wexler (1983) or Sonntag (1994) – and not the Goff–Gratch equation recommended in earlier WMO publications. Saturation vapour pressure in ice clouds at the lowest temperatures in the tropical upper troposphere will be about 50% of the saturation vapour pressure with respect to a water surface in Table 12.6.

Satisfactory relative humidity sensor operation becomes extremely difficult at very low temperatures and pressures. The free exchange of water molecules between the sensor and the atmosphere becomes more difficult as the temperature falls. Also, contamination of the sensor from high water vapour concentrations earlier in the ascent may cause substantial systematic errors in sensor measurements at the lowest temperatures. For instance, if a positive bias of 5% relative humidity is caused by contamination at –60 °C, this would become a positive bias of 40% relative humidity at –75 °C unless the contamination is ventilated away.

In the lower stratosphere and upper troposphere, water vapour measurements should be evaluated in terms of mixing ratio as well as relative humidity. Figure 12.3 shows the variation of temperature, relative humidity and mixing ratio with height, measured by four different radiosonde sensors in the WMO Intercomparison of High-quality Radiosonde Systems (Nash et al., 2011). Just under the tropopause, relative humidity was slightly higher than saturation, but the water vapour mixing ratio was close to the minimum, having dropped rapidly with temperature, as would be expected from Table 12.6. Where the temperature rises above the tropopause, the two relative humidity sensors with slower response (grey) show much higher water vapour mixing ratio than is realistic. The corrected sensor and the chilled-mirror hygrometer (black) show a short-lived maximum in water vapour mixing ratio immediately above the tropopause. This is unlikely to be real and suggests that the relative humidity reported by the black sensors in this layer between minutes 48.4 and 50 are too high by up to a factor of 2.5. This is probably the result of contamination of the payload or the radiosonde sensing area, and not a calibration issue. Contamination could have occurred earlier in the flight between minutes 33 and 38 after passing through a thick layer of cirrus cloud detected by the cloud radar (not shown in Figure 12.3).

**Table 12.6. Variation of saturation vapour pressure over a water surface as a function of temperature after Sonntag (1994)**

| *Temperature (°C)* | *Saturation vapour pressure (hPa)* |
|---|---|
| 40 | 73.9 |
| 30 | 42.5 |
| 15 | 17.1 |
| 0 | 6.1 |
| –15 | 1.92 |
| –30 | 0.51 |
| –45 | 0.112 |
| –60 | 0.0195 |
| –75 | 0.0025 |
| –90 | 0.00023 |
| –100 | 0.000036 |

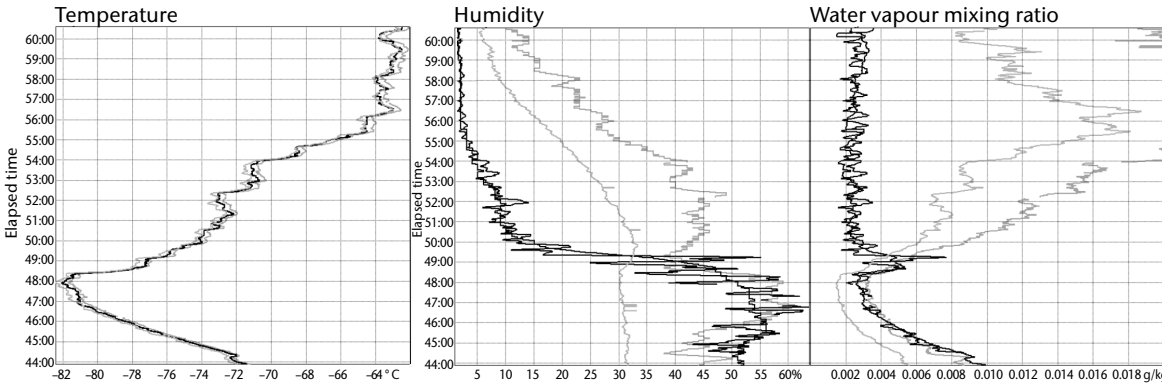



**Figure 12.3. Temperature, relative humidity and water vapour mixing ratio presented as a function of time into flight, from flight 56 of the WMO Intercomparison of High-quality Radiosonde Systems. The grey measurements are from radiosondes with capacitive sensors, uncorrected for slow response time. The black measurements are from a heated twin capacitor sensor (corrected for time constant of response) and a frost-point hygrometer. (The frost-point hygrometer shows more variation with time in relative humidity and mixing ratio than the heated twin capacitor.)**

The rate of response of the relative humidity sensors can be defined as:

$$dU_e/dt = -1/\tau \cdot (U_e - U) \tag{12.4}$$

where $U_e$ is the relative humidity reported by the sensor, $U$ is the actual relative humidity and $\tau$ is the time constant of response.

A further complication is that the relative humidity sensor reports relative humidity for the temperature of the sensor itself. If this differs from the true atmospheric temperature, then an additional error is introduced because of the thermal lag of the humidity sensor relative to the air temperature. Modern humidity sensors have become much smaller than in the older radiosonde types to minimize this problem, and the temperature of the sensor is in any case measured directly in many, but not all, widely used modern radiosondes.

The time constant of response of a relative humidity sensor increases much more rapidly during a radiosonde ascent than the time constant of response of a temperature sensor. This can be seen in Table 12.7, where approximate values of the time constant of response of two older and three modern sensor types are shown. In the case of the goldbeater's skin, the time constant of response quoted is for changes between about 70% and 30% relative humidity. The time constants of response of the goldbeater's skin sensors are much larger at a given temperature if measuring high or low relative humidity. The values for the twin thin-film capacitor (Vaisala RS92) in this table differ from those in Miloshevich et al. (2004) and were taken from updated information supplied by the manufacturer.

Two profiles of radiosonde temperature and relative humidity are shown in Figures 12.4. and 12.5. Figure 12.4 is an example of a radiosonde ascent in the United Kingdom, where the measurements from two different sensors were combined. Sudden changes in relative humidity with height occur on many flights and were observed here by both radiosonde types. The very dry layers in particular are associated with temperature inversions. The existence of these very dry layers is accepted as correct, but in the past they were considered erroneous because the earlier sensors could not measure them well. In this case, the rate of change of relative humidity with height above the lowest inversion was 6% relative humidity per second. Thus, modern sensors offer advantages to those who need a detailed knowledge of the variation of atmospheric refractive index with height, which is significant for radio propagation. At mid-levels, rates of change of 3% relative humidity per second are often found.

**Table 12.7. Time constants of response $\tau$ (in seconds) of relative humidity sensors**

| *Humidity sensor* | *In use* | *$\tau$ at 20 °C* | *$\tau$ at 0 °C* | *$\tau$ at –20 °C* | *$\tau$ at –40 °C* | *$\tau$ at –70 °C* |
|---|---|---|---|---|---|---|
| Heated twin thin-film capacitor, no cap | 2004 | < 0.15 | 0.4 | 2 | 10 | 80 |
| Other single thin-film capacitors covered with cap | 2000– | 0.1 – 0.6 | 0.6 – 0.9 | 4 – 6 | 15 – 20 | 150 – 300[a] |
| Carbon hygristor | 1960– | 0.3 | 1.5 | 9 | 20 | Not reliable |
| Goldbeater's skin | 1950– | 6 | 20 | 100 | > 300 | Not usable |
| Frost-point hygrometer, CFH | 2003– for science | | < 2[b] | < 4[b] | | < 25 |
| Chilled-mirror hygrometer, Snow White at night | 1996– for science | | < 2[b] | < 4[b] | | < 25 |

Notes:
a Values derived from a comparison with hygrometers, from the WMO Intercomparison of High-quality Radiosonde Systems (Nash et al., 2011); may include problems with the ventilation of the caps covering the sensor.
b Value estimated from an in-flight comparison with best quality radiosonde relative humidity sensors, from Nash et al. (2011).

Miloshevich et al. (2004) proposed a method for correcting the slow time constant of response in humidity measurements based on the equation:

$$U = U_e(t_2) - U_e(t_1) \cdot X/(1 - X) \tag{12.5}$$

where $U$ is the true ambient relative humidity, $U_e$ is the reported relative humidity for times $t_1$ and $t_2$, $U$ is assumed not to change significantly between $t_1$ and $t_2$ (limiting the size of the time step used), and $X = e^{-(t_2 - t_1)/\tau}$, where $\tau$ is the time constant of response of the relative humidity sensor.

For the algorithm to give satisfactory results, the data used must be as free as possible of anomalous data, noise and so on. Therefore, some form of QC has to be applied to the basic observations and to other corrections (such as for solar heating of the humidity sensor) before the time constant of response correction is attempted. This correction cannot retrieve exact detail of the vertical profile of relative humidity at a much higher temporal resolution than the time constant of response of the sensor. It generates a smoothed vertical profile, with higher rates of change of relative humidity than in the original measurements, but any detail in the profile at time steps much smaller than the time constant of response should be treated with caution. As seen in Miloshevich et al. (2004), for a given original measurement there are quite a few possible answers, consistent with the known time constants of response. The type of smoothing applied to the original data influences the retrieved profile, so the smoothing used needs to be well documented and the assumptions made in the use of the algorithm need to be explained to the users.

From the examples seen in Yangjiang (Nash et al., 2011, Annex D), it was concluded that to report the relative humidity structure near the tropical tropopause, the humidity sensing system should have a time constant of response of 3 min or better, so that the adjustments for a slow time constant of response are not too large and are not merely amplifying errors from noise in the measurements or from water/ice contamination.

Figure 12.5 illustrates the magnitude of the adjustments in a relative humidity profile for a sensor with a time constant of response of about 80 s at –70 °C and which was observing in the tropical upper troposphere during the WMO Intercomparison of High-quality Radiosonde Systems in Yangjiang, China (Nash et al., 2011). The corrected profile in Figure 12.5 is clearly much smoother than the relative humidity profiles measured in the upper troposphere by the chilled-mirror

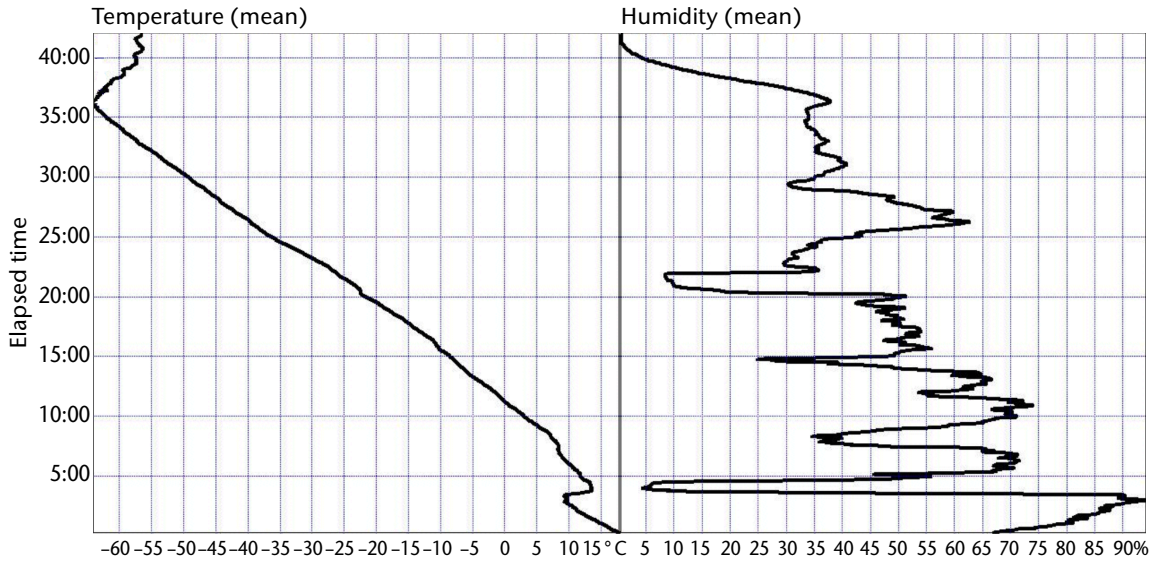



**Figure 12.4. Average of simultaneous measurements at first intervals by two radiosondes suspended together under one balloon, with measurements made at night**

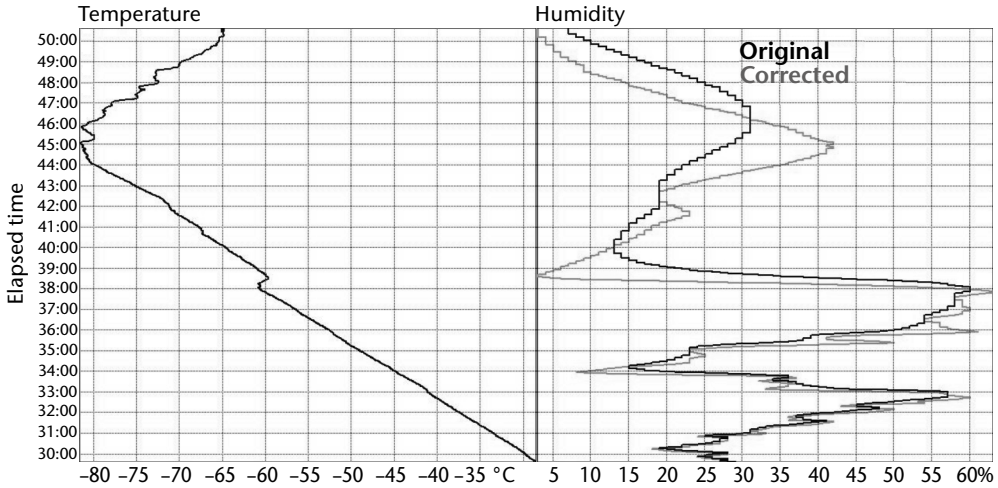



**Figure 12.5. Twin thin-film capacitor measurement in the upper troposphere at night in Yangjiang, China, presented as a function of time into flight, showing the humidity profile measured directly by the sensor (black) and then corrected for time constant of response errors (grey)**

hygrometers in Figure 12.4. In Yangjiang, where corrections for slow response were applied, the result looked reasonable in about 65% of the cases and quite wrong the rest of the time. Further testing of this type of adjustment and the type of smoothing applied seems to be justified at this time.

During the Yangjiang test, the highest rates of change observed in the troposphere/stratosphere transition were about 30% relative humidity over about 30 seconds. Thus, at the moment even the fastest operational radiosonde relative humidity sensor cannot define the true height of the rapid drop in humidity at the tropical tropopause without correction. Corrections to the height of the top of the humid layer in Yangjiang were found to be in the range of 200 to 500 m. However, the two scientific sounding instruments in Yangjiang had faster response and could resolve this height better when the instruments were functioning correctly (see Table 12.7).

### 12.4.2 Thin-film capacitors

Capacitive thin-film sensors are now used in nearly all modern radiosonde designs, and they often have an integrated temperature sensor (which alleviates the radiation dry bias seen in previous generations of sensors). Some systems heat the humidity sensor to prevent ice forming on it. These sensors rely on the variation of the dielectric constant of a polymer film with ambient water vapour pressure. The dielectric constant is proportional to the number of water molecules captured at binding sites in the polymer structure. The lower electrode of the capacitor is usually formed by etching a metal-coated glass plate, with dimensions of either 5 by 3 mm or 4 by 1.5 mm and a thickness of 0.55 or 0.2 mm. There is often a trade-off in thickness, with a thinner film having a faster time constant of response at low temperatures but perhaps less stability in performance over time. The upper electrode is vacuum-evaporated onto the polymer surface and is permeable to water vapour. Sensor capacitance is usually a nearly linear function of relative humidity, and the temperature dependence of calibration is not large. These sensors are always mounted on a supporting boom which should expose the sensor above the top of the radiosonde or a long way away from the radiosonde body to the side.

The calibration of these relative humidity sensors is temperature dependent. The correction for this dependence must be applied during data processing by the ground system if the accuracy claimed for the sensor at room temperatures in the laboratory is to be obtained throughout most of the troposphere.

Contamination from rain, water drops in clouds or ice accretion has to be driven off if no protective cap is used with the sensor. This can be achieved by heating the sensor above ambient temperature. The Vaisala RS92 used twin sensors, with one sensor measuring while the other is heated and then cooled back to normal operation (Paukkunen, 1995). The twin sensors are mounted about 1 cm apart. These particular sensors also have a thin hydrophobic coating to minimize contamination from liquid water. As the sun shines directly on the sensors and their supports, the humidity sensors warm up relative to the correct temperature, particularly in the upper troposphere. This warming effect needs to be compensated in order to achieve accurate humidity measurements. One method is to directly measure the temperature of the humidity sensor and use this information for the compensation. In early versions of this sensor system, the surrounding printed circuit board was not coated with a highly reflective surface, and the humidity sensor was warming too much in the upper troposphere in daytime. So, all the support surfaces were then aluminized, and this was first tested in Mauritius (Nash et al., 2006) and then as an operational product in Yangjiang, China (Nash et al., 2011). Initially, the manufacturer advised users to use this sensor with correction software for slow time constants of response at low temperatures and a correction for solar heating of the sensor in the daytime. However, the most recent version of the manufacturer's system software applies these corrections automatically by default.

Four radiosondes in the WMO Intercomparison of High-quality Radiosonde Systems (Nash et al., 2011) used another sensor, manufactured by E+E Elektronik. This sensor was always deployed with a protective cap to minimize contamination. This cap usually has a highly reflective coating, so the sensor does not warm up too much in the daytime in the upper troposphere. Also, the sensor supports and the cap must not be hygroscopic, otherwise outgassing from these surfaces will cause significant errors. Some of the manufacturers apply corrections for slow time constants. With this sensor, the errors from a slow time constant are larger than with the twin sensor. Most of the radiosondes using this sensor used an additional thermistor to measure the temperature of the humidity sensor directly, rather than assuming the humidity sensor was at the same temperature as the corrected temperature sensor.

### 12.4.3 Carbon hygristors and goldbeater's skin

Both types of sensors were used until about 2013 but were phased out shortly afterwards. They were susceptible to cloud contamination and poor/slow performance at low or high relative humidity. More details can be found in previous versions of this chapter or in Nash (2015).

### 12.4.4 Scientific sounding instruments

Two specialized scientific water vapour sounding instruments were successfully deployed during the WMO Intercomparison of High-quality Radiosonde Systems in Yangjiang, China (Nash et al., 2011). These systems were not as inherently reliable as the operational radiosondes, but when they worked correctly they were extremely useful in identifying the limitations of the operational radiosondes.

(a) The Cryogenic Frost-point Hygrometer (CFH) (Vömel et al., 2007) is a chilled-mirror hygrometer. The CFH uses a feedback loop that actively regulates the temperature of a small mirror, which is coated with ice (or dew in the lower troposphere). In the feedback loop, an optical detector senses the amount of ice covering the mirror, and the feedback controller regulates the temperature of the mirror such that the amount of ice remains constant.

When the feedback controller is operating correctly, the mirror temperature is equal to the frost-point temperature, and if there is no internal ice/water contamination, then the frost-point temperature of the atmosphere. The inlet tubes to the CFH are stainless steel and 17 cm long with a diameter of 2.5 cm, mounted directly above and below the hygrometer. This is intended to ensure that contamination from the air passing through the hygrometer is minimal, and the test results in Yangjiang confirmed that the CFH contamination was lower than experienced by the Snow White chilled-mirror hygrometer in the upper troposphere and lower stratosphere.

Time constants of response vary from a few seconds in the lower troposphere and increase with height up to about 20 to 30 s in the stratosphere. Thus, in the lower troposphere, the CFH time constant of response is not distinguishable from the best operational radiosondes. However, in the upper troposphere and lower stratosphere, it is faster in response than the best operational radiosondes. The main measurement uncertainty in CFH measurements is the stability and drift of the feedback controller. Thus, the total measurement uncertainty is estimated to be about 0.5 K in dewpoint or frost-point temperature, corresponding approximately to about 9% relative humidity at the tropical tropopause and 4% relative humidity in the lower troposphere.

The CFH uses a cold liquid at temperatures below –100 °C to cool the mirror during flight. Preparation and handling of this coolant before flight requires training and special handling procedures to avoid personal injury.

Correction schemes (solar heating, time constant) applied to the operational radiosonde relative humidity in the upper troposphere have benefited from comparisons with CFH measurements, for example the unpublished comparisons of the Lapland Atmosphere–Biosphere Facility Upper Troposphere Lower Stratosphere Water Vapour Validation Project in Sodankyla, Finland (2004), and the Lindenberg Upper-air Methods Intercomparison in Lindenberg, Germany (2008).

(b) The Snow White hygrometer also uses the chilled-mirror principle for sensing water vapour (see Fujiwara et al., 2003). However, this uses a Peltier cooler to cool its mirror. There are two versions of the sensing system. The daytime mirror hygrometer was mounted in an internal duct in the sensing system. This configuration did not prevent contamination, thus affecting the accuracy of the measurements below temperatures of about –50 °C, and was only used on a few flights in Yangjiang. In the night-time version, the mirror hygrometer was mounted above the radiosonde body. Thus, the night-time mirror hygrometer had little direct protection against contamination, but a very good exposure to ambient conditions. In Yangjiang, the Snow White night-time system was able to measure dewpoint temperatures down to below –75 °C on 70% of the night-time flights. Two daytime flights suffered bad contamination near thunderstorms in the afternoon, but night-time Snow White sensing systems were not significantly contaminated in upper cloud because on this occasion ascent conditions were favourable to the Snow White operation. However, contamination around the hygrometer structure limited the use of Snow White to heights

less than 18 km, just above the tropical tropopause in Yangjiang. Snow White has the same advantage as CFH in terms of the time constants of response that are much smaller than the operational humidity sensors in the upper troposphere.

It is necessary to have a skilled operator who can recognize when the mirror film changes phase from water to ice (Snow White must also be flown with a good operational humidity sensor). The operator must also be able to detect possible failure modes (such as the mirror losing its ice film) in the middle and upper troposphere. Identifying when contamination has corrupted the hygrometer measurements is a skill required for both Snow White and CFH.

The two chilled-mirror hygrometers have the advantage over operational relative humidity sensors of being sensitive in the upper troposphere and lower stratosphere down to the lowest temperatures, provided that contaminated measurements are recognized and excluded. Their measurements also do not have significant day–night differences in performance. Therefore, as working references, their measurements have proved to be the best method of identifying these differences. Comparison with the chilled-mirror measurements has allowed the development of correction procedures or changes in operational procedures to produce better-quality operational measurements in the middle and upper troposphere.

Sensors in ducts do not provide the best method of observing relative humidity structure through rain and low cloud, so it is unwise to treat the chilled mirrors as more reliable than the best operational radiosonde sensors in the lower troposphere.

### 12.4.5 **Exposure**

Rapid changes in relative humidity greater than 25% are common during radiosonde ascents. Accurate measurements of these changes are significant for some users. Accurate measurements require that the humidity sensor is well ventilated, but the sensor also needs to be protected as far as possible from the deposition of water or ice onto the surface of the sensor or its supports, and also from solar heating.

Thus, the smaller relative humidity sensors, such as thin-film capacitors, are mounted on an external outrigger. The sensor may be covered by a small protective cap, or the sensors may be heated to drive off contamination from water or ice in cloud or fog. The design of the protective cap may be critical, and it is essential to ensure that the cap design is such that the humidity sensor is well ventilated during the radiosonde ascent.

Protective covers or duct coatings should not be hygroscopic. For examples, see the stainless steel inlet pipes used by CFH or the aluminized sensor mounts of some operational radiosondes.

### 12.4.6 **Relative humidity errors**

#### 12.4.6.1 ***General considerations***

Operational relative humidity sensors have improved greatly compared to the sensors in use before the 1980s, especially at low temperatures in the middle and upper troposphere. Relative humidity observations at temperatures lower than –40 °C were not reported in most of the early radiosonde systems, and relative humidity reports at such temperatures were not in significant use until about 2000.

When testing radiosondes, it should not be assumed that the uncertainty in the measurements is the same for all relative humidity bands. Non-uniform performance across the relative humidity range was still found for many systems in the WMO Intercomparison of High-quality Radiosonde Systems (Nash et al., 2011). However, the better systems are now much closer to uniformity at all relative humidity than what was found at the start of the WMO radiosonde comparison series in 1984. During manufacture, calibrations on individual sensors are often

performed only at a few (less than three) pre-set relative humidity points, and possibly only at one temperature (see, for example, Wade, 1995). In many cases, the temperature dependence of the sensor calibration is not checked individually, or in batches, but is again assumed to follow curves determined in a limited number of tests. Sensor calibrations have often varied by several per cent in relative humidity from batch to batch, as can be seen from measurements in low-level cloud (Nash et al., 1995). This may be a consequence of faulty calibration procedures during manufacture. For instance, actual sensor performance in a given batch may differ from the standardized calibration curves fitted to the pre-set humidity checks. On the other hand, it could be the result of batch variation in the stability of the sensors during storage. In addition, the thickness of the film in some thin-film capacitors is not always the same, so the thicker sensors are sometimes quite unresponsive to humidity changes at low temperatures, while the majority of the sensors of the same type respond well in the same conditions. Comparisons of radiosonde humidity with satellite data and NWP fields are reported by Moradi et al. (2013), Sun et al. (2021) and Ingleby (2017).

Night-time humidity measurements may be less reliable than those in the daytime because, in many cases, there seems to be a greater chance of contamination around the sensor at night if its ventilation is poor, while solar heating of the sensor surroundings drives off more of the contamination in the day. At upper levels, the instrument response is slow; this may be compensated using a time-lag correction (Miloshevich et al., 2004 and 12.4.1 above). There was a daytime radiation dry bias in various capacitive sensors (see Vömel et al., 2007; Wang et al., 2013; Dirksen et al., 2014); this has mostly been addressed now by adding a separate temperature sensor to the humidity sensor.

Systematic errors in relative humidity measurements may occur because of changes in calibration during storage. This may simply be due to sensor ageing or the build-up of chemical contamination, where contamination occupies sites that normally would be open for water vapour molecules. The rate of contamination may depend on the chemicals used in manufacturing the radiosonde body or the packaging, and cannot be assumed to be the same when the manufacturing of the radiosonde body or printed circuit boards changes with time. The manufacturer's instructions regarding the storage of the sensors and preparations for use must be applied carefully. In some cases the ground check process drives off any build-up of chemical contamination that would cause bias in the ascent.

Since 2005 and even more since 2014, the majority of the modern humidity sensors have shown improved stability and protection against water contamination in cloud (contamination effects normally being short lived and not resulting in permanent offsets during the ascent), and improved reproducibility from batch to batch. Thus, the results from dry and wet conditions can now be combined, apart from in very heavy rain when no system performs reliably. Thus, for the better sensor types, uncertainties ($k = 2$) in the range of 5% to 10% seem achievable across the whole relative humidity range. Nash (2015) provides details of humidity sensor performance around the year 2010 and earlier.

Most thin-film humidity sensors show a temperature dependency because their measurement principle is based on the adsorption of water vapour. The adsorption capacity of thin films for water vapour is negatively correlated with the temperature, whereas the amount of water vapour in the air is generally positively correlated with the temperature. These two parameters play opposite roles in the adsorption of water vapour in sensors especially when the temperature significantly deviates from that of the sensor calibration. A laboratory experiment showed that the relative humidity measurement at –40 °C was about 10% lower than the reference by a saturator-based humidity generator when the calibration curve obtained at 20 °C is applied (Lee et al., 2019). The deviation grew bigger as the temperature was further lowered. These observations indicate that the effect of the decrease of the water vapour at cold temperatures dominates over that of the increase of the adsorption capacity for water vapour. Therefore, it is highly recommended that thin-film humidity sensors should be calibrated at many different temperatures and compensated for a potential temperature dependency.

#### 12.4.6.2 *Wetting or icing in cloud*

Humidity sensors can get contaminated when passing through cloud. Heated sensors on some systems prevent or reduce this, while unheated sensors may have a positive bias (humidity too close to saturation) until the contamination ventilates away. Icing in cloud can occur at temperatures much lower than –40 °C; this may not ventilate away as quickly as the contamination in the lower troposphere.

#### 12.4.6.3 *Representativeness issues*

Representativeness issues are discussed in Nash (2015).

## 12.5 PRESSURE SENSORS (INCLUDING HEIGHT MEASUREMENTS)

### 12.5.1 General aspects

Radiosonde pressure sensors must sustain accuracy over a very large dynamic range from 1080 to 3 hPa, with a resolution of 0.1 hPa over most of the range and a resolution of 0.01 hPa for pressures less than 100 hPa. Changes in pressure are usually identified by a small electrical or mechanical change. For instance, the typical maximum deflection of an aneroid capsule is about 5 mm, so that the transducer used with the sensor has to resolve a displacement of about 0.5 μm. Changes in calibration caused by sensor temperature changes during the ascent must also be compensated. These temperature changes may be as large as several tens of degrees, unless the pressure sensor is mounted in a stabilized environment.

Thus, pressure sensors are usually mounted internally within the radiosonde body to minimize the temperature changes that occur. If a pressure sensor has an actively controlled temperature environment, the sensor assembly should be mounted in a position on the radiosonde where heat contamination from the pressure sensor assembly cannot interfere with the temperature or relative humidity measurements.

The pressure sensor and its transducer are usually designed so that sensitivity increases as pressure decreases. The time constant of response of radiosonde pressure sensors is generally very small, and uncertainties from sensor lag are not significant.

Historically, when reliable pressure sensors for low pressure were being manufactured, sensors with poor performance were replaced by pressure measurements deduced from radar heights, as in the United Kingdom before 1978. In the Russian Federation and some adjacent countries, secondary radars are used to measure geometric heights instead of using a pressure sensor on the radiosonde.

Today, many modern radiosonde systems use GNSS navigation signals to locate the position of the radiosonde and have dispensed with the use of a pressure sensor on the radiosonde (to save on consumable costs). As a result, geometric height, and hence geopotential height, is measured directly (see 12.5.5), with the pressure changes in flight computed from the radiosonde temperature and humidity measurements.

### 12.5.2 Silicon sensors

Following rapid developments in the use of silicon, reliable pressure sensors can now be made with this material. A small cavity is formed from a hole in a thick semiconductor layer. This hole is covered with a very thin layer of silicon, with the cavity held at a very low pressure. The cavity will then perform as a pressure sensor, with atmospheric pressure sensed from the deflection of the thin silicon cover.

A method of detecting the deflection of the silicon is to use a capacitive sensor. In this case, the thin silicon layer across the cavity is coated with a thin metallic layer, and a second metallic layer is used as a reference plate. The deflection of the silicon cover is measured by using the variation in the capacitance between these two layers. This type of sensor has a much lower temperature dependence than the strain gauge sensor and is now in widespread use. Because the sensor is very small, it is possible to avoid the calibration errors of the larger capacitive aneroid sensors introduced by changes in temperature gradients across the aneroid sensor and associated electronics during an ascent.

### 12.5.3 **Aneroid capsule (capacitive)**

Many modern radiosonde designs use aneroid capsules of smaller diameter (30 mm or less in diameter) with the deflection of the capsule directly measured by an internal capacitor. A parallel plate capacitor used for this purpose is formed by two plates each fixed directly to one side of the capsule. The capacitance, $C$, is then:

$$C = \in \cdot S/e \tag{12.6}$$

where $S$ is the surface area of each plate, $e$ is the distance between the plates and $\epsilon$ is the dielectric constant. As $e$ is a direct function of the deflection of the capsule, the capacitance $C$ is a direct electrical measurement of the deflection. In many radiosonde sensors, each capacitor plate is fixed to the opposite side of the capsule by mounts passing through holes in the other plate. With this configuration, $e$ decreases when the pressure lowers. The sensitivity of the capacitive sensor is:

$$- \in \cdot S/e^2 \cdot de/dp \tag{12.7}$$

This will be greatest when $e$ is small and the pressure is smallest. The capacitive sensor described is more complicated to manufacture but is best suited for upper-air measurements, as the sensitivity can be 10 times greater at 10 hPa than at 1 000 hPa. The value of the capacitance is usually close to 6 pF.

Capacitive aneroid capsules are usually connected to a resistance-capacitance electronic oscillator with associated reference capacitors. This arrangement needs to measure very small variations of capacity (for example, 0.1% change in a maximum of 6 pF) without any significant perturbation of the oscillator from changes in temperature, power supply or ageing. Such high stability in an oscillator is difficult to achieve at a low price. However, one solution is to multiplex the input to the oscillator between the pressure sensor and two reference capacitors. A reference capacitor $C_1$ is connected alone to the oscillator, then in parallel with $C_p$, the pressure sensor capacitor, and then in parallel with a second reference $C_2$ to provide a full-scale reference.

The calibration of an aneroid capacitive sensor will usually have significant temperature dependence. This can be compensated either by referencing to an external capacitor which has a temperature coefficient of similar magnitude or during data processing in the ground system using calibration coefficients from factory calibrations. The correction applied during processing will depend on the internal temperature measured close to the pressure sensor. In practice, both of these compensation techniques may be necessary to achieve the required accuracy.

### 12.5.4 **Pressure sensor errors**

Systematic errors and the radiosonde errors (flight-to-flight variation at $k = 2$) have been estimated from the WMO international radiosonde comparisons for selected radiosonde types. The results are shown in Table 12.8. The range of values of systematic error usually represents the spread of results from several tests.

Aneroid capsules were liable to change calibration unless they had been well seasoned through many pressure cycles over their working range before use. Software corrections applied during data processing, but based on ground control readings before launch, went some way toward

**Table 12.8. Range of systematic error and radiosonde error (flight to flight, $k = 2$) and overall uncertainty in pressure from the WMO international radiosonde comparisons and associated tests**

| *Radiosonde type* | *Systematic error* | | | *Sonde error* | | | *Uncertainty* | | |
|---|---|---|---|---|---|---|---|---|---|
| *Pressure level (hPa)* | *850* | *100* | *10* | *850* | *100* | *10* | *850* | *100* | *10* |
| MRZ[a] (Russian Federation) | –1.5 to –0.5 | –1.2 to –0.8 | 0 – 0.2 | 7 | 3.5 | 0.5 | 8 | 4 | 0.7 |
| Meisei RS2-91 | 0.2 – 1 | –0.1 – 0.5 | –0.2 – 0.2 | 1 | 0.6 | 0.6 | 2 | 1.1 | 0.8 |
| VIZ MKII | 0 – 1 | 0.7 – 1.1 | 0.3 – 0.7 | 1.6 | 0.6 | 0.4 | 2.5 | 1.6 | 1 |
| Vaisala RS92, silicon sensor | < 0.5 | < 0.3 | < 0.2 | 0.8 | 0.4 | 0.2 | 1 | 0.6 | 0.4 |
| MODEM M2K2[a] | –0.8 to –0.4 | < 0.1 | < 0.05 | 1.2 | 0.4 | 0.03 | 1.6 | 0.4 | 0.05 |
| Vaisala RS92[a] | < 0.5 | < 0.1 | < 0.05 | 1.2 | 0.4 | 0.03 | 1.6 | 0.4 | 0.05 |
| Lockheed Martin Sippican (LMS),[a] LMG-6 | < 0.5 | < 0.1 | < 0.05 | 1.2 | 0.4 | 0.03 | 1.2 | 0.4 | 0.05 |

Note:
a Does not use a pressure sensor but computes pressure from geopotential height measurements; see 12.5.5.

reducing these errors. Nevertheless, corrections based on ground checks relied on a fixed error correction pattern across the working range. In practice, the change in pressure sensor calibration was more variable over the working range.

The consequences of the pressure errors in Table 12.8 on reported temperatures would be as follows: a 1 hPa pressure error will produce a temperature error, on average, of –0.1 K at 900 hPa, –0.3 K in the upper troposphere (at 200 hPa in the tropics), ±0.5 K at 30 hPa (varying between summer and winter conditions at about 55°N) and up to at least 1 K for most situations at 10 hPa.

#### 12.5.4.1 *Relationship of geopotential height errors to pressure errors*

The error, $\varepsilon_z(t_1)$, in the geopotential height at a given time into flight is given by:

$$\varepsilon_z(t_1) = \frac{R}{g}\int_{p_0}^{p_1}\left[\varepsilon_T(p) - \frac{\delta T}{\delta p}\varepsilon_p(p)\right]\frac{dp}{p} + \frac{R}{g}\int_{p_1}^{p_1+\varepsilon_p(p_1)}\left[T_v(p) + \varepsilon_T(p) - \frac{\delta T}{\delta p}\varepsilon_p(p)\right]\frac{dp}{p} \qquad (12.8)$$

where $p_0$ is the surface pressure; $p_1$ is the true pressure at time $t_1$; $p_1 + \varepsilon_p(p_1)$ is the actual pressure indicated by the radiosonde at time $t_1$; $\varepsilon_T(p)$ and $\varepsilon_p(p)$ are the errors in the radiosonde temperature and pressure measurements, respectively, as a function of pressure; $T_v(p)$ is the virtual temperature at pressure $p$; and $R$ and $g$ are the gas and gravitational constants as specified in the WMO *Technical Regulations* (WMO-No. 49), Volume I, Appendix A.

For a specified standard pressure level, $p_s$, the second term in equation 12.8 disappears because there is no error in $p_s$, and so the error in the standard pressure level geopotential height is smaller:

$$\varepsilon_z(p_s) = \frac{R}{g}\int_{p_0}^{p_s}\left[\varepsilon_T(p) - \frac{\delta T}{\delta p}\varepsilon_p(p)\right]\frac{dp}{p} \qquad (12.9)$$

And for radiosondes without a pressure sensor using a radar:

$$\varepsilon_z\left(p_s\right) = T_v\left(p_s\right) \int_{z_0}^{z_{ps}} g \,/\, T^2 \left[\varepsilon_T\left(z\right) + \varepsilon_z\left(Range, \theta\right) \cdot dT_v \,/\, dz\right] \tag{12.10}$$

where $Z_{ps}$ is the geopotential height of the specified pressure level $p_s$, and the error in geopotential height for a radar is a function of slant range and elevation angle ($\theta$), and will vary from flight to flight according to the wind conditions.

Table 12.9 shows the errors in geopotential height that are caused by radiosonde sensor errors for typical atmospheres. The geopotentials of given pressure levels have small errors, whether caused by a radiosonde temperature or pressure error. The pressure error has a slightly different effect at different latitudes because the typical temperature profile structure varies with latitude. However, the same pressure sensor errors produce much larger errors at the heights of specific structures, such as temperature inversions, including at the tropopause, and cloud tops and bases.

The importance of equations 12.9 and 12.10 is that the errors in standard pressure level geopotentials are primarily related to the temperature errors, and so if geopotential heights are compared against collocated NWP first-guess forecast fields, the height anomalies give an indication of the relative temperature performance at the two sites (see Elms, 2003).

### 12.5.5 Use of geometric height observations instead of pressure sensor observations

#### 12.5.5.1 *General*

Geometric height observations can now be provided by GNSS radiosondes that decode global positioning satellite signals, as opposed to the early GPS radiosondes that did not decode the signals. The geometric height observations have small enough uncertainty (between 10 and 20 m) to be used to compute pressure at a given time into flight, using surface pressure and temperature and relative humidity observations (see equations 12.17 and 12.18). Internally, GNSS systems use an ellipsoid as the height reference and an adjustment must be made for the

**Table 12.9. Systematic errors in geopotential height (gpm) from given pressure and temperature errors**

| | $\varepsilon_T$, $T$ error (K) | $\varepsilon_p$, $P$ error (hPa) | *Latitude* | *300 hPa* | *100 hPa* | *30 hPa* | *10 hPa* |
|---|---|---|---|---|---|---|---|
| Standard pressure height, $T$ error | 0.25 | 0 | All | 9 | 17 | 26 | 34 |
| Standard pressure height, $p$ error | 0 | –1 | 25°N | 3 | 12 | –2 | –24 |
| Standard pressure height, $p$ error | 0 | –1 | 50°N summer | 3 | 5 | 1 | –20 |
| Standard pressure height, $p$ error | 0 | –1 | 50°N winter | 3 | 5 | 6 | –4 |
| Significant level height, $p$ error | 0 | –1 | 25°N | 27 | 72 | 211 | 650 |
| Significant level height, $p$ error | 0 | –1 | 50°N summer | 26 | 72 | 223 | 680 |
| Significant level height, $p$ error | 0 | –1 | 50°N winter | 26 | 70 | 213 | 625 |

difference between the geoid (MSL) and the ellipsoid; this is known as the undulation of the geoid. In the stratosphere, the computed pressures are found to have smaller uncertainty than measurements provided by the best radiosonde pressure sensors (see Table 12.8).

The elimination of the pressure sensor from GPS radiosondes provides a considerable saving in terms of the cost of some radiosondes, but it is also necessary to check user requirements for the non-hydrostatic NWP models that are being introduced, since direct measurements of pressure and geopotential height in the troposphere may be of some advantage when hydrostatic balance does not represent atmospheric conditions.

### 12.5.5.2 *Method of calculation*

The conversion from geometric height measured with a GPS radiosonde to geopotential height is purely a function of the gravitational field at a given location and does not depend on the temperature and humidity profile at the location. The gravitational potential energy ($\Phi_1$) of a unit mass of anything is the integral of the normal gravity from MSL ($z = 0$) to the height of the radiosonde ($z = z_1$), as given by equation 12.11:

$$\Phi_1 = \int_0^{z_1} \gamma\left(z, \varphi\right) \cdot dz \tag{12.11}$$

where $\gamma(z, \varphi)$ is the normal gravity above the geoid. This is a function of geometric altitude, $z$, and the geodetic latitude $\varphi$.

This geopotential is divided by the normal gravity at 45° latitude to give the geopotential height used by WMO, as:

$$Z_1 = \Phi_1 / \gamma_{45^\circ} \tag{12.12}$$

where $\gamma_{45^\circ}$ was taken in the definition as 9.80665 m s$^{-2}$. Note that surface gravity is greatest at the poles (9.83218 m s$^{-2}$) and least at the Equator (9.78033 m s$^{-2}$).

The variation of gravity with height must take into account the ellipsoidal shape of the Earth and the Earth's rotation. However, when the variation of $\gamma$ with height was taken into account, the geopotential height, $Z_1$, at geometric height, $z_1$, was approximated using the Smithsonian meteorological tables (List, 1968) as:

$$Z_1\left(z_1, \varphi\right) = \left(\gamma_{\mathrm{SMT}}\left(\varphi\right)/\gamma_{45^\circ}\right) \cdot \left(\left(R_{\mathrm{SMT}}\left(\varphi\right) \cdot z_1\right)/\left(R_{\mathrm{SMT}}\left(\varphi\right) + z_1\right)\right) \tag{12.13}$$

where $R_{\mathrm{SMT}}(\varphi)$ is an effective radius of the Earth for latitude ($\varphi$) and is the value in the Smithsonian tables which was chosen to take account of the actual changes with geometric height in the combined gravitational and centrifugal forces. It is not the actual radius of the Earth at the given latitude. This is shown in Figure 12.6, where the Smithsonian radius increases from the Equator to high latitudes, but the actual radius of the Earth's ellipsoid is largest at the Equator and smallest at the poles.

As the values for $R_{\mathrm{SMT}}(\varphi)$ in the Smithsonian tables were obtained around 1949, the International Ellipsoid 1935 was used in the computations rather than the WGS-84 currently used with GPS receivers. Also, the Smithsonian tables used a value for $\gamma_{\mathrm{SMT}}(\varphi)$ of:

$$\gamma_{\mathrm{SMT}}\left(\varphi\right) = 9.806\,16 \cdot \left(1 - 0.002\,637\,3 \cdot \cos\left(2\varphi\right) + 0.000\,005\,9 \cdot \cos\left(2\varphi\right)^2\right) \text{ [m s}^{-2}\text{]} \tag{12.14}$$

This formula was not explicitly derived in the published scientific literature, although it was recommended for meteorological use by the International Association of Geodesy in 1949.

An alternative expression for the relationship in equation 12.13 has been proposed by Mahoney (personal communication), based on the WGS-84 geoid. Then, geopotential height for geometric height, $z_1$, becomes:

$$Z_1(z_1, \varphi) = \left(\gamma_s(\varphi)/\gamma_{45^\circ}\right) \cdot \left(\left(R(\varphi) \cdot z_1\right)/\left(R(\varphi) + z_1\right)\right) \quad (12.15)$$

where $\gamma_s(\varphi)$ is the normal gravity on the surface of an ellipsoid of revolution, and where:

$$\gamma_s(\varphi) = 9.780\ 325 \cdot \left(\left(1 + 0.001\ 931\ 85 \cdot \sin(\varphi)^2\right)/\left(1 - 0.006\ 694\ 35 \cdot \sin(\varphi)^2\right)^{0.5}\right) \quad (12.16)$$

with the radius $R(\varphi) = 6\ 378.137/(1.006803 - 0.006706 \cdot \sin(\varphi)^2)$, giving results for $R$ similar to the values in the Smithsonian tables.

If the geopotential height for a geometric height of 30 km is computed, it ranges from 29.7785 km at the Equator to 29.932 km at 80°N, whether equations 12.13 and 12.14 or 12.15 and 12.16 are used. Differences between the geopotential height values obtained by the two methods are less than 1 m, and as such are not critical for meteorologists.

The difference between geometric height and geopotential height increases with height above the Earth's surface. An example of typical differences taken from measurements in the WMO Intercomparison of High-quality Radiosonde Systems in Yangjiang, China, at 22°N is shown in Table 12.10.

**Table 12.10. Differences between geopotential and geometric height measured at the WMO Radiosonde Intercomparison in Yangjiang, China, at 22°N**

| *Geopotential height* | *Geopotential – geometric height* |
|---|---|
| 8 000 | -25 |
| 16 000 | -70 |
| 24 000 | -135 |
| 32 000 | -220 |

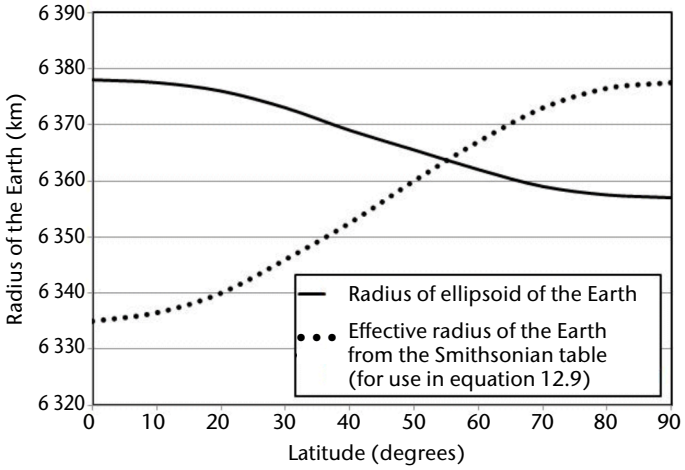



**Figure 12.6. Variation of the Earth's radius with latitude compared to the variation of the Smithsonian table radius used in equation 12.13**

Once the variation of the geopotential heights with respect to temperature and relative humidity has been established, the pressures can be computed integrating upwards from the measured surface pressure, using the hypsometric relationship, in a discrete form:

$$ln\left(p_{i+1}/p_i\right) = -9.806\ 65 \cdot dZ/R^* \cdot T_v \tag{12.17}$$

where $ln()$ is the natural logarithm; $p$ is the pressure in hPa; $R^*$ is the gas constant for dry air; $T_v$ is the mean virtual temperature for the layer in K; $dZ$ is the layer thickness in geopotential height; and $I$ refers to the lower boundary of this layer.

The virtual temperature $T_v$ is computed from:

$$T_v = T/\left(1 - \left(U/100\right) \cdot \left(e_s\left(T\right)/p\right) \cdot \left(1 - \varepsilon_a\right)\right) \tag{12.18}$$

where $U$ is the relative humidity of the air, $e_s$ is the saturation vapour pressure for water vapour and $\varepsilon_a$ the ratio of the molecular weight of wet and dry air, with $\varepsilon_a = 0.622$.

It has to be emphasized again that the radiosonde temperature and relative humidity are used only in the computation of the pressures with systems using GNSS geometric height measurements, as the geopotential values come purely from the geometric heights and the Earth's gravitational fields.

The algorithms for computing geometric height from windfinding radar observations of slant range and elevation and for the conversion of geometric heights to geopotential heights are included in Hooper (1986). The actual algorithm used with secondary radar systems in the Russian Federation can be found in Ivanov et al. (1991). If radar height observations are used as a replacement for pressure sensor observations, the heights need to be corrected for the effects of the Earth's curvature and radio-wave refraction before pressure is computed. Corrections for refraction can be made using seasonal averages of atmospheric profiles, but better pressure accuracy might require height corrections for the conditions encountered in individual flights.

### 12.5.6 Sources of error in direct height measurements

#### 12.5.6.1 *In GNSS geometric height measurements*

As long as there is no local interference at GNSS navigation signal frequencies, most modern radiosonde systems are able to generate heights with good accuracy relative to the height where GNSS lock occurs in flight. However, the software has to be able to interpolate reliably back to the surface (taking into account changes in the balloon rate of ascent just after launch) in order to ensure best performance of GNSS measurements. In the WMO Intercomparison of High-quality Radiosondes in Yangjiang, China (Nash et al., 2011), some of these interpolation software modules worked better than others, and systematic errors larger than 10 m resulted in the worst cases, persisting throughout the flight of a given radiosonde type.

It is essential to check the height of the local GPS antenna relative to the surface pressure sensor and ensure that this is used correctly in the radiosonde system software computations. Remember that a mismatch (or pressure error) of 1 hPa in the pressure at the antenna relative to the surface pressure sensor at the radiosonde station will result in a 10 m height bias throughout the flight.

In-flight processing must be able to cope with significant variations (positive and negative) in the rates of ascent of the balloons lifting the radiosonde. Errors in temperature and relative humidity will only affect the pressure computation from the geopotential heights (see equations 12.17 and 12.18). The effect of temperature errors on pressure computations can be judged from the values of height errors in Table 12.9 resulting from a 0.25 K temperature error throughout the profile. This temperature error would lead to pressure errors of 0.4, 0.3, 0.13 and 0.05 hPa at nominal pressures of 300, 100, 30 and 10 hPa, respectively.

Thus, in the stratosphere, GNSS geometric measurement is able to deliver much more reliable height measurements than any other operational height measuring system. Near the surface,

GNSS height measurements must be performed with care to be of similar quality to those of the best pressure sensors. The breakthrough requirements for pressure in Annex 12.A can be achieved with GNSS radiosondes at all pressures. However, it is not obvious that all GNSS radiosonde systems can achieve the optimum pressure sensor requirements at low levels, while at pressures lower than 100 hPa, optimum requirements could be achieved as long as temperature uncertainties are low.

#### 12.5.6.2 *In radar height measurements*

The effect of radar observational errors upon windfinding is considered in the present volume, Chapter 13. However, for radar heights (random and systematic) errors in elevation are much more significant than for winds. Systematic error in slant range is also more critical for height than for wind measurements. Therefore, radars providing satisfactory wind measurements often have errors in elevation and slant range that prevent best quality height (and hence pressure) measurements. The errors are largest at low radar elevation angles – usually at long range in the stratosphere.

Small but significant systematic errors in elevation may arise from a variety of sources as follows:

(a) Misalignment of the axes of rotation of azimuth and elevation of the radar during manufacture. If this is to be avoided, the procurement specification must clearly state the accuracy required;

(b) Errors in levelling the radar during installation and in establishing the zero elevation datum in the horizontal;

(c) Differences between the electrical and mechanical axes of the tracking aerials, possibly introduced when electrical components of the radar are repaired or replaced.

Errors may arise from errors introduced by the transducer system measuring the radar elevation angle from the mechanical position of the tracking aerial.

Systematic errors in slant range may arise from the following:

(a) A delay in triggering the range-timing circuit or incorrect compensation for signal delay in the radar detection electronics;

(b) Error in the frequency of the range calibrator.

Thus, radiosonde systems operating without pressure sensors and relying solely on radar height measurements require frequent checks and adjustments of the radars as part of routine station maintenance. These systems are not suitable for use in countries where technical support facilities are limited.

## 12.6 GROUND STATION EQUIPMENT

### 12.6.1 General features

The detailed design of the ground equipment of a radiosonde station will depend on the type of radiosonde that is used. However, the ground station will always include the following:

(a) An aerial and radio receiver for receiving the signals from the radiosonde;

(b) Equipment to decode the radiosonde signals and to convert the signals to meteorological units;

(c) Equipment to present the meteorological measurements to the operator so that the necessary messages can be transmitted to users, as required.

Other equipment may be added to provide wind measurements when required (for example, radar interface or GNSS trackers).

The output of the decoder should usually be input to a computer for archiving and subsequent data processing and correction.

Modern ground station systems can be either purchased as an integrated system from a given manufacturer, or may be built up from individual modules supplied from a variety of sources. If maintenance support will mainly be provided by the manufacturer or its agents, and not by the operators, an integrated system may be the preferred choice. A system composed of individual modules may be more readily adapted to different types of radiosonde. This could be achieved by adding relevant decoders, without the extra cost of purchasing the remainder of the integrated ground system offered by each manufacturer. A modular type of system may be the preferred option for operators with their own technical and software support capability, independent of a given radiosonde manufacturer. Systems built from modules have encountered problems in the last 10 years because of the complexity of testing such systems and the problems introduced when adapting manufacturers' standard correction software to non-standard use by another processing system.

Note: The rate of development in modern electronics is such that it will prove difficult for manufacturers to provide in-depth support to particular integrated systems for longer than 10 to 15 years. Thus replacement cycles for integrated ground systems should be taken as about 10 years when planning long-term expenditure.

### 12.6.2 Software for data processing

Satisfactory software for a radiosonde ground system is much more complicated than that needed merely to evaluate, for example, standard level geopotential heights from accurate data. Poor quality measurements need to be rejected and interpolation procedures developed to cope with small amounts of missing data. There is a serious risk that programmers not thoroughly versed in radiosonde work will make apparently valid simplifications that introduce very significant uncertainties under some circumstances. For instance, if reception from the radiosonde is poor, it is counterproductive to allow too much interpolation of data using mathematical techniques that will be quite stable when data quality is generally good, but will become unstable when data quality is generally poor. A good example of an algorithm that can become unstable when signal quality is poor is the time constant of response correction used by some manufacturers for temperature.

In the past, certain problems with signal reception and pressure errors near the launch were sometimes compensated by adjusting the time associated with incoming data. This may not cause significant uncertainties in reported measurements, but can make it almost impossible to check radiosonde sensor performance in radiosonde comparison tests.

Thus, it is essential to use the services of a radiosonde specialist or consultant to provide overall control of the software design.[1] The specialist skills of a professional programmer will usually be necessary to provide efficient software. This software will include the display and interactive facilities for the operator which are required for operational use. The software must be robust and not easily crashed by inexpert operators. In the last decade, most software for commercial radiosonde ground systems has required at least two or three years of development in collaboration with testing by NMHSs. This testing was performed by highly skilled operators and test staff, until the software had become thoroughly reliable in operation. The ground system software was then suitable for use by operators without any significant specialized computing skills.

[1] As recommended by CIMO at its twelfth session (1998), through Recommendation 2 (CIMO-XII).

The software in the ground system should be well documented and should include clear descriptions of the algorithms in use.[2] The overall system should be designed to allow sounding simulations for testing and comparison purposes. It is proposed that sets of a suitable range of raw pressure, temperature and humidity data records should be used to check the reliability of newly developed software. Software errors are often the limiting factors in the accuracy of data reports from the better radiosonde types.

## 12.7 RADIOSONDE OPERATIONS

### 12.7.1 Control corrections immediately before use

It is recommended that radiosonde measurement accuracy should always be checked in a controlled environment before the radiosonde is launched. These control checks should be made when the radiosonde is ready for flight, and should take place a few minutes before release. The aim is to prevent the launch of faulty radiosondes. A further aim is to improve calibration accuracy by adjusting for small changes in calibration that may have occurred when the radiosonde was transported to the launch site and during storage.

These control checks are usually performed indoors. They can be conducted in a ventilated chamber with a reference temperature and relative humidity sensors of suitable accuracy to meet user specifications. Relative humidity can then be checked at ambient humidity and lower and higher humidity, if necessary. If no reference psychrometer is available, known humidity levels can be generated by saturated saline solutions or silica gel.

The differences between the radiosonde measurements and the control readings can be used to adjust the calibration curves of the sensors prior to flight. The sensors used for controlling the radiosonde must be checked regularly in order to avoid long-term drifts in calibration. A suitable software adjustment of radiosonde calibration normally improves the reproducibility of the radiosonde measurements in flight to some extent. The type of adjustment required will depend on the reasons for calibration shift following the initial calibration during manufacture and will vary with radiosonde type.

If there are large discrepancies relative to the control measurements, the radiosonde may have to be rejected as falling outside the manufacturer's specification and returned for replacement. Maximum tolerable differences in ground checks need to be agreed upon with the manufacturer when purchasing the radiosondes.

It is also wise to monitor the performance of the radiosonde when it is taken to the launch area. The reports from the radiosonde should be checked for compatibility with the surface observations at the station immediately before launch.

In modern radiosonde systems pre-launch checks have been partially or completely automated. For a previous generation of radiosondes CIMO recommended that:[3]

(a) The performance of the radiosonde pressure, temperature and relative humidity sensors should be checked in a controlled environment, such as a calibration cabinet or baseline check facility prior to launch;

(b) The baseline check should be automated as far as possible to eliminate the possibility of operator error;

[2] See Recommendation 2 (CIMO-XII).

[3] As recommended by CIMO at its eleventh session, held in 1994, through Recommendation 9 (CIMO-XI).

(c) The temperature and relative humidity observations should also be checked against the standard surface temperature and relative humidity observations at the station immediately before the launch;

(d) The sensors used as the reference should be at least as accurate as the radiosonde sensors and be calibrated regularly according to the manufacturer's instructions.

### 12.7.2 Deployment methods

Radiosondes are usually carried by balloons rising with a rate of ascent of between 5 and 7 m $s^{-1}$, depending on the specifications and characteristics of the balloon in use (see Chapter 8 of Volume III of the present Guide). These rates of ascent allow the measurements to be completed in a timely fashion – i.e. about 40 min to reach 16 km and about 90 min to reach heights above 30 km – so that the information can be relayed quickly to the forecast centres. The designs and positioning of the temperature and relative humidity sensors on the radiosonde are usually intended to provide adequate ventilation at an ascent rate of about 6 m $s^{-1}$. Corrections applied to temperature for solar heating errors will usually only be valid for the specified rates of ascent.

A radiosonde transmits information to a ground station that is usually at a fixed location. However, advances in modern technology mean that fully automated radiosonde ground systems are now very small. Therefore, the ground systems are easily deployed as mobile systems on ships or in small vans or trailers on land. Radiosondes keep transmitting after balloon burst but the data have usually been discarded. Since about 2020, some stations have processed and provided the descent profiles and some NWP systems have used subsets of the data. At upper levels the radiosonde can fall very fast, even with a parachute, and this is linked to a temperature bias at those levels (Ingleby et al., 2021). Preliminary results suggest that the quality of descent data varies strongly with radiosonde type.

Dropsondes deployed from research aircraft use parachutes to slow the rate of descent. Temperature sensors are mounted at the bottom of the dropsonde. Rates of descent are often about 12 m $s^{-1}$ to allow the dropsonde measurement to be completed in about 15 min. The high descent rate allows one aircraft to deploy sufficient dropsondes at a suitable spacing in the horizontal for mesoscale research (less than 50 km). The dropsonde transmissions are received and processed on the aircraft. For about 15 years the dropsonde described by Hock and Franklin (1999) was the main one in use. Remotely piloted vehicles have also been used to deploy dropsondes. Dropsondes are used for field experiments and for high-impact weather events, particularly tropical cyclones.

### 12.7.3 Radiosonde launch procedures

Once a radiosonde is prepared for launch, the meteorological measurements should be checked against surface measurements either in an internal calibration chamber or externally against surface observations in a ventilated screen. This is necessary since the radiosonde may have been damaged during shipment from the factory, manufacture may have been faulty, or sensor calibrations may have drifted during storage. Radiosondes producing measurements with errors larger than the limits specified in the procurement contract should be returned to the manufacturer for replacement.

Radiosondes are often launched by hand or using a launch aid from a shed or shelter. The complexity of the shed and the launch procedures will depend on the gas used to fill the balloon (see Chapter 8 of Volume III of the present Guide) and on the strength and direction of the surface winds at the site. At times there have been fatal accidents in the global radiosonde network through careless use of hydrogen gas. Managers of radiosonde stations using hydrogen gas must be aware of the dangers of an explosion and must ensure that all staff are properly informed and trained in the use of hydrogen. It is essential that equipment for generating and storing hydrogen is well maintained. Faulty equipment shall not be used. The balloon filling equipment must be grounded to earth to prevent static discharge.

In strong winds the launching procedure is aided by the use of unwinders that allow the suspension cord for the radiosonde to deploy slowly following the launch. Very strong surface winds require unwinders that deploy the suspension cord at rates as low as 0.5 to 1 m $s^{-1}$.

Automatic launch systems for radiosondes are commercially available and becoming more common. These may offer cost advantages at radiosonde stations where staff are used solely for radiosonde operations. These systems may not be suitable for operations in very exposed conditions where very strong surface winds are common.

If users require accurate vertical structure in the atmospheric boundary layer, the surface observations incorporated in the upper-air report should be obtained from a location close to the radiosonde launch site. The launch site should also be representative of the boundary layer conditions relevant to the surface synoptic network in the area. It is preferable that the operator (or automated system) should make the surface observation immediately after the balloon release rather than prior to the release. The operator should be aware of inserting surface observations into the ground system prior to launch, as meteorological conditions may change before the launch actually takes place when a significant delay in the launch procedure occurs (for instance, a balloon burst prior to launch, or air traffic control delay). It is particularly important to ensure that the surface pressure measurement inserted into the ground system is accurate if the radiosonde system's pressure measurements are GNSS-based.

The speed of response of the radiosonde sensors is such that conditioning the radiosonde before launch is less critical than in the past. However, when it is raining, it will be necessary to provide some protection for the radiosonde sensors prior to launch.

### 12.7.4 Radiosonde suspension during flight

The radiosonde must not be suspended too close to the balloon when in flight. This is because the balloon is a source of contamination for the temperature and relative humidity measurements. A wake of air, heated from contact with the balloon surface during the day, and cooled to some extent during the night, is left behind the balloon as it ascends. The balloon wake may also be contaminated with water vapour from the balloon surface after ascent through clouds. The length of suspension needed to prevent the radiosonde measurements from suffering significant contamination from the balloon wake varies with the maximum height of observation. This is because the balloon wake is heated or cooled more strongly at the lowest pressures. A suspension length of 20 m may be sufficient to prevent significant error for balloons ascending only to 20 km. However, for balloons ascending to 30 km or higher, a suspension length of about 40 m is more appropriate (see, for instance, Elms et al., 1994).

Note: When investigating the influence of the balloon wake on radiosonde measurements, it is vital to ensure that the sensors on the radiosonde used for the investigation are correctly exposed. The sensors must be mounted so that it is impossible for air that has had contact with other surfaces on the radiosonde to flow over the radiosonde sensor during ascent. Possible sources of heat or water vapour contamination from the radiosondes are the internal surfaces of protective ducts, the mounts used for the sensor, or the external surfaces of the radiosonde body.

### 12.7.5 Public safety

The radiosonde design must fall well within existing air traffic safety regulations as to size, weight and density. These should ensure that the radiosonde should not cause significant damage if it collides with an aircraft or if ingested by the aircraft engine. In many countries, the national air traffic authority issues regulations governing the use of free flight balloons. Balloon launch sites must often be registered officially with the air traffic control authorities. Balloon launches may be forbidden or possible only with specific authorization from the air traffic controllers in certain locations. The situation with respect to flight authorization must be checked before new balloon launch locations are established.

In some countries, safety regulations require that a parachute or other means of reducing the rate of descent after a balloon burst must also be attached to the radiosonde suspension.

This is to protect the general public from injury. The parachute must reduce the rate of descent near the surface to less than about 6 m $s^{-1}$. The remains of the balloon following a burst usually limit the rate of descent at lower levels. However, on occasion, most of the balloon will be detached from the flight rig following a burst and the rates of descent will be too high unless a parachute is used.

It is important that radiosondes should be environmentally safe after returning to Earth or after falling in the sea, whether picked up by the public or by an animal, or left to decay. Further considerations on environmentally friendly radiosondes are detailed in Annex 12.C.

## 12.8 COMPARISON, CALIBRATION AND MAINTENANCE

### 12.8.1 Comparisons

The overall quality of operational measurements of geopotential height by radiosonde (and hence temperature measurements averaged through thick layers) is monitored at particular forecast centres by comparison to geopotential heights at standard pressures with short-term (6 or 12 h) forecasts from global NWP models for the same location. The statistics are summarized into monthly averages that are used to identify both substandard measurement quality and significant systematic changes in radiosonde performance (see 12.8.1.1).

Statistics of the performance of the relative humidity sensors are also generated by the NWP centres, and are also compared with satellite observations.

The performance of radiosondes or radiosonde sensors can be investigated in the laboratory with suitably equipped test chambers, where temperature and pressure can be controlled to simulate radiosonde flight conditions.

Detailed investigations of temperature, pressure and relative humidity sensor performance in flight are best performed using radiosonde comparison tests, where several radiosonde types are flown together on the same balloon ascent. These may be performed by NMHSs as part of a procurement process, testing one or two new radiosonde types against a more established system (unfortunately the results are usually commercial in confidence). WMO coordinates radiosonde intercomparisons with a larger variety of operational systems. Annex 12.D gives guidelines for organizing radiosonde intercomparisons and for the establishment of test sites. The error characteristics of the other radiosondes should have been established in earlier tests. An ideal comparison test site would have an independent method of measuring the heights of the radiosondes during flight. This can now be achieved by using measurements taken from two different well-tested GNSS radiosondes.

#### 12.8.1.1 *Quality evaluation using short-term forecasts*

For the better global NWP models, the uncertainty in short-term (6 or 12 h) forecasts of 100 hPa geopotential heights is between 10 and 20 m in most areas of the world. These uncertainties correspond to a mean layer temperature error from the surface to 100 hPa of between 0.15 and 0.3 K. Thus, the comparison with the forecast fields provides good sensitivity in detecting sonde errors in temperature, if sonde errors are greater than about 0.3 K. Forecast fields, rather than analysis fields, are used as the reference in this comparison. Forecast fields provide a reference that is less influenced by the systematic errors in geopotential heights of the radiosonde measurements in the area than the meteorological analysis fields. However, 6 or 12 h forecast fields will have small systematic errors and should not be considered as an absolute reference. Uncertainty in the systematic error of the forecast field is at least 10 m at 100 hPa. The systematic differences of forecasts from the measurements of a given radiosonde station vary between forecast centres by at least this amount. In addition, systematic errors in forecast fields may also change with time by similar amounts, when forecast models and data assimilation techniques are improved. Nonetheless, comparisons with the forecast fields at the lead centres for operational monitoring give clear indications of those radiosonde stations and radiosonde

types where there are large systematic errors in the radiosonde reports. Elms (2003) provided a review of radiosonde errors in the global network for heights up to 30 hPa, and subsequent monitoring statistics up to 2017 can be found on the WMO website at https://community.wmo.int/activity-areas/imop/upper-air-monitoring-statistics. This has now been replaced by the WIGOS Data Quality Monitoring System: https://wdqms.wmo.int/.

#### 12.8.1.2 *Comparison of water vapour measurements with remote-sensing*

Given that many radiosonde stations now have collocated GNSS water vapour sensors and some scientific sites have collocated microwave radiometers, it is practical to use the integrated water vapour measurements from these two systems to check the quality of the radiosonde water vapour measurements, primarily at low levels. Comparison with GPS measurements was performed during the last two WMO radiosonde comparisons (Nash et al., 2006, 2011), where the GPS measurements were used to quantify day–night differences in the radiosonde relative humidity measurements. A more extensive global study was performed by Wang and Zhang (2008). The use of microwave radiometers to check day–night differences is illustrated in Turner et al. (2003).

Although identification of day–night differences with integrated water vapour measurements seems relatively reliable, this does not mean that all the differences seen between radiosonde and remotely sensed water vapour are due to errors in the radiosonde water vapour, since both the GNSS water vapour and microwave radiometer measurements have errors that are not necessarily constant with time.

#### 12.8.1.3 *Radiosonde comparison tests*

Radiosonde comparison tests allow the performance of the pressure, temperature and relative humidity sensors of the radiosondes to be compared independently as a function of time. However, it is important to design the support rig for the radiosondes so that the motion of the radiosondes under the supports is not too dissimilar from the motion on an individual balloon, and to ensure that in daylight the support rig (including the balloon) does not shed warmer air onto some of the sensors from time to time.

Laboratory tests should be performed in facilities similar to those required for the detailed calibration of the radiosondes by the manufacturer. These tests can be used to check the adequacy of radiosonde calibration, for example, the dependence of calibration on sensor temperature. In the laboratory, it is difficult to simulate real atmospheric conditions such as wetting or icing of sensors, but progress has been made with radiative errors (von Rohden et al., 2022). A combination of laboratory studies and comparisons made during actual ascents offers the best way forward.

In order to compare measurements taken during actual ascents, the timing of the samples for the different systems must be synchronized as accurately as possible, ideally to better than ±1 s. In recent years, software packages have been developed to support WMO radiosonde comparison tests. These allow all the radiosonde samples to be stored in a comparison database and to be compared by the project scientists immediately following a test flight. It is important that comparison samples are reviewed very quickly during a test. Any problem with the samples caused by test procedures (for example, interference between radiosondes) or faults in the radiosondes can then be identified very quickly and suitable additional investigations initiated. The software also allows the final radiosonde comparison statistics to be generated in a form that is suitable for publication.

As the reproducibility of the measurements of most modern radiosondes has improved, it has become possible to obtain useful measurements of bias in temperature and pressure from about 10 to 15 flights for one given flight condition (i.e., one time of day). Since it is unwise to assume that daytime flights at all solar elevations will have the same bias, it is preferable to organize tests that produce at least 10 to 15 comparison flights at a similar solar elevation. The measurements of temperature sensor performance are best linked to other test results by comparisons performed

at night. The link should be based on measurements from radiosondes with wire or aluminized sensors and not from sensors with significant IR heat exchange errors. If a continuous series of comparison flights (alternating between day and night) can be sustained, it is possible to use the atmospheric time-series technique to estimate the magnitude of day–night differences in temperature measurements.

As noted earlier, the most extensive series of comparison tests performed in recent years were those of the WMO International Radiosonde Comparison. Initial results have been published in Nash and Schmidlin (1987), Ivanov et al. (1991), Yagi et al. (1996), Nash et al. (2006, 2011), Balagurov et al. (2006) and da Silveira et al. (2006). The results from these tests were the basis of the information provided in Tables 12.3, 12.4, 12.5 and 12.8.

The first international comparison of radiosondes was held at Payerne (Switzerland) in 1950. Average systematic differences between radiosonde pressures and temperatures (at pressures higher than 100 hPa) were 4 hPa and 0.7 K, with uncertainties (two standard deviations) of 14 hPa and 2 K. These values should be compared with the results for modern systems shown in Tables 12.3, 12.4, 12.5 and 12.8. The results from a second comparison carried out at the same site in 1956 showed that accuracy needed to be improved by the application of radiation corrections to the temperature readings. The errors in pressure and temperature at the 50-hPa level were quite large for most radiosondes and increased rapidly at higher levels, especially during daylight. In 1973, a regional comparison was held in Trappes (France). This identified significant calibration errors in some radiosondes, with one bimetallic temperature sensor having a radiation error as large as 10 K.

### 12.8.2 **Calibration**

The calibration methods used by manufacturers should be identified before purchasing radiosondes in large numbers. The QC procedures used to ensure that measurement accuracy will be sustained in mass production must also be checked for adequacy. Purchasers should bear in mind that certain specified levels of error and product failure may have to be tolerated if the cost of the radiosonde is to remain acceptable. However, the in-flight failure rate of radiosondes from reliable manufacturers should not be higher than 1% or 2%.

Unless radiosonde sensors can be produced in large batches to give the reproducibility and uncertainty, with the associated confidence level, required by users, it is necessary to calibrate the instruments and sensors individually. Even if the sensors can be produced in large batches to meet an agreed set of standardized performance checks, it is necessary for representative samples, selected at random, to be checked in more detail. The calibration process should, as far as possible, simulate flight conditions of pressure and temperature. Calibrations should normally be performed with falling pressure and temperature. Relative humidity will probably be checked in a separate facility. The reference sensors used during calibration should be traceable to national standards and checked at suitable intervals in standards laboratories. The references should be capable of performing over the full temperature range required for radiosonde measurements.

The design of the calibration apparatus depends largely on whether the complete radiosonde must be calibrated as a unit or on whether the meteorological units can be tested while separated from the radiosonde transmitter. In the latter case, although a much smaller apparatus can be used, the temperature effect on the performance of the electronics board should be independently investigated and corrected if there is any. The calibration facility should be able to cover the range of pressures and temperatures likely to be encountered in actual soundings. In addition, considering the typical ascent speed of radiosondes, an investigation of the effect of the air ventilation on the sensor calibration is recommended in the range of 5 to 6 m $s^{-1}$. It should be possible to maintain the conditions in the calibration chamber stable at any desired value better than ±0.2 hPa $min^{-1}$ for pressure, ±0.25 K $min^{-1}$ for temperature and 1% relative humidity per minute. PRTs with an uncertainty better than 0.05 K are recommended as reference thermometers. The conditions in the calibration chamber should be measured with systematic errors less than ±0.2 hPa for pressure, ±0.1 K for temperature and ±1% relative humidity. Multiple, calibrated reference PRTs should be positioned in the calibration chamber in order to identify

the range of temperatures in the space occupied by the sensors under calibration. The maximum temperature deviation among reference thermometers should not exceed 0.3 K. Sufficient measurements should be taken to ensure that the calibration curves represent the performance of the sensors. The uncertainty of the sensor calibration should be presented to be compared with the uncertainty required by the users. Typical uncertainty factors are the reference thermometer calibration, the spatial temperature deviation of the chamber, the stability of temperature sensors under calibration and fitting the residuals of the calibration curves. Pressure sensors which are not fully compensated for temperature variations must be calibrated at more than one temperature. Thus, it may be an advantage if the temperature calibration chamber is capable of changing the air pressure and also air ventilation speed simultaneously.

Humidity calibration is usually carried out in a separate apparatus. The calibration chamber should be able to generate a wide range of relative humidity at varied temperatures likely to be encountered in actual soundings. The calibration chamber itself can change the relative humidity as in the case of commercial climate chambers. A separate humidity generating system such as salt solutions and water vapour saturators can be connected to the calibration chamber. An additional dry-gas generating system will be helpful to control the humidity by mixing with wet gas. The reference relative humidity used for the calibration should be determined by either a calibrated dew-point hygrometer or a humidity generating system traceable to the international humidity standard. The standard deviation of the variation in relative humidity should not exceed 1% in the space occupied by the units under calibration. The uncertainty of the reference dew-point temperature in the calibration chamber should be better than 0.3 K. The stability of the reference temperature should be within ±0.15 K $min^{-1}$. The uncertainty of the humidity sensor calibration should be presented with the valid temperature range. Typical uncertainty factors are the reference PRT calibration, the spatial temperature deviation inside the chamber, the stability of humidity sensors under calibration, the dew-point hygrometers or humidity generators and fitting the residuals of the calibration curves.

An alternative arrangement for humidity calibration is a duct or chamber ventilated with a mixture of air from two vessels, one of which is kept saturated with water while the other is dried by silica gel, with the relative humidity of the mixture being manually controlled by a valve which regulates the relative amounts passing into the duct.

Because of the importance of the type or batch calibration of radiosondes, WMO urges Members to test, nationally or regionally, selected samples of radiosondes under laboratory conditions in order to ensure that the calibrations supplied by the manufacturer are valid.[4]

### 12.8.3 Maintenance

Failure rates in the ground system should be low for radiosonde systems based on modern electronics, as long as adequate protection is provided against lightning strikes close to the aerials. The manufacturer should be able to advise on a suitable set of spares for the system. A faulty module in the ground system would normally be replaced by a spare module while it is returned to the manufacturer for repair.

The maintenance requirements for radiosonde systems relying on radar height measurements to replace radiosonde pressure measurements are quite different. In this case, local maintenance should be readily available throughout the network from staff with good technical capabilities (both mechanical and electrical). This will be essential if accurate tracking capability is to be retained and if long-term drifts in systematic height errors are to be avoided.

## 12.9 COMPUTATIONS AND REPORTING

There are no prescribed standardized procedures for the computation of radiosonde observations. The main issue is the selection of levels or the provision of measurements

[4] As recommended by CIMO at its eleventh session held in 1994, through Recommendation 9 (CIMO-XI).

in sufficient detail to reproduce accurately and efficiently the temperature and humidity profile (such as the heights of temperature inversions) against geopotential from the radiosonde data. Guidance was given in Hooper (1986) and in the coding procedures agreed by WMO in the *Manual on Codes* (WMO-No. 306), Volume I.1 (Code FM 35–XI Ext. TEMP). This reporting method was suitable for the performance and use of radiosondes in 1970s, but not for today. To meet the GBON requirements (*Manual on the WMO Integrated Global Observing System* (WMO-No. 1160)), it is essential that the radiosonde information be reported at high vertical resolution using relevant BUFR codes (*Manual on Codes* (WMO-No. 306), Volume I.1).

### 12.9.1 Radiosonde computations and reporting procedures

According to the GBON requirements, high vertical resolution (100 m) should be reported. This makes the selection of significant levels redundant. Some users still find standard pressure levels useful. Sometimes standard level geopotential height is reported outside the measurement profile (that is, below launch or above balloon burst). Such extrapolation should be minimized or ceased entirely.

In Code FM 35–XI Ext. TEMP, temperatures were reported to a precision of 0.2 °C. In BUFR temperatures are reported in Kelvin to two decimal places. Comparing the two, Ingleby (2017) found that different radiosonde systems were using different rounding methods for TEMP reporting. One radiosonde system was rounding values in two decimal places towards 0 °C giving biases of 0.05 K but different sign above and below 0 °C. One decoding system had an offset of 0.1 K.

In modern radiosonde ground systems, the use of cheap but powerful computing systems means that much higher sampling rates can be used for archiving and processing the radiosonde measurements than is possible with manual computations. The manual processing of radiosonde measurements nearly always introduces unnecessary errors in upper-air computations and should be eliminated. From 2023 GBON requires reporting of high vertical resolution (using BUFR format), so manual or algorithmic selection of 'significant' levels becomes obsolete. High resolution reporting maximizes the usefulness of radiosonde profiles and makes sense given the large amount of money spent each year on radiosonde consumables.

### 12.9.2 Corrections

It should be clear from earlier sections that the variation in radiosonde sensor performance caused by the large range of conditions encountered during a radiosonde ascent is too large to be represented by a simple calibration obtained at a given temperature. Modern data processing allows more complex calibration algorithms to be used. These have provided measurements of smaller uncertainty than that achieved with manual systems. It is vital that these algorithms are adequately documented. Users should be informed of any significant improvements or modifications to the algorithms. Records archived in radiosonde stations should include the model numbers of radiosondes in use and an adequate reference to the critical algorithms used for data processing. The radiosonde serial number and software version can and should be reported in the BUFR messages.

All radiosonde temperature measurements have radiation errors. Therefore, it is recommended that a radiation correction (based on expected sensor performance in usual conditions) should always be applied during data processing, if known. The details of this radiation correction should be recorded and kept with the station archive, along with an adequate archive of the original raw radiosonde observations, if required by national practice. Dirksen et al. (2014) present a comprehensive attempt to quantify and correct radiation and other radiosonde errors.

Errors from IR heat exchange pose a particular problem for correction, since these errors are not independent of atmospheric temperature. Thus, it is preferable to eliminate as soon as possible the use of white paint with high emissivity in the IR as a sensor coating, rather than to develop very complex correction schemes for IR heat exchange errors.

Similarly, it is unwise to attempt to correct abnormally high solar radiation heating errors using software, rather than to eliminate the additional sources of heating by positioning the sensor correctly with respect to its supports, connecting leads and radiosonde body.

Relative humidity measurements may have corrections applied for slow time constants of response and for daytime heating of the humidity sensor system. As with temperature, the records of corrections and changes to the correction procedures need to be known by the user and retained in the station archive of observations, preferably along with a raw data archive. The details of these algorithms need to be clear to those purchasing new systems.

Considering the importance of the ways in which corrections are applied, WMO[5] urges Members:

(a) To correct and make available the corrected upper-air data from the various Global Observing System upper-air stations;

(b) To make users of the data aware of changes in the methodology used to correct reports, so that they may be adjusted, if desired;

(c) To archive both the corrected and uncorrected upper-air observations and produce records for climatological applications of the correction applied. The method used should be determined nationally;

(d) To inform WMO of the method of correction applied.

## 12.10 PROCUREMENT ISSUES

### 12.10.1 Use and update of the results from the WMO Intercomparison of High-quality Radiosonde Systems

The results of the WMO Intercomparison of High-quality Radiosonde Systems (Nash et al., 2011) were published to provide a snapshot in 2010 of the relative performance of the different systems in tropical conditions. The report includes an assessment of the operational performance of the radiosonde systems (see Nash et al., 2011, Table 12.1). While many of the systems performed well, some radiosondes had limitations in their measurements, mostly in daytime temperature but also in night-time relative humidity measurements at temperatures higher than –40 °C and in daytime relative humidity measurements in the upper troposphere at temperatures lower than –40 °C. Another WMO Upper-Air Instrument Intercomparison takes place in 2022.

Nash (2015) contains individual radiosonde values for Tables 12.2 to 12.10 from the test in Yangjiang, China, and these can also be used as a guide to the systems with low bias and fast enough time constants of response leading to small sonde error in relative humidity. Low and stable bias is very desirable for radiosonde measurements for climate records.

### 12.10.2 Some issues to be considered in procurement

The first stage in the procurement process should be to determine what quality of radiosonde is necessary for use in a given network. Here, it is recommended that any radiosonde used should be capable of meeting the breakthrough requirements indicated in Annex 12.A in the climate of that country. If the radiosonde station is considered important for climate records, then a radiosonde performing closer to the optimum requirement should be considered. Ideally the procurement should be competitive. This may mean cooperating with other countries in a similar region to procure larger numbers together and to try and set up a system where the radiosondes are procured on a regular basis, for instance each year or every two years. It should

[5] As recommended by CIMO at its eleventh session, held in 1994, through Recommendation 8 (CIMO-XI).

be remembered that systems that differ only slightly in their performance would probably come out in a different order if the tests were repeated. Thus, only marked differences in performance should be treated as significant and not small differences in the relative marking.

Experience from consultations in regional training workshops suggests that there are some issues which need to be considered when procuring equipment:

(a) Equipment must be sustainable over the long term. In other words, in addition to purchasing the hardware and software, arrangements must be made for the long-term support of the system, either by the manufacturer or the local staff, or a mixture of both.

(b) Make sure that the ground antenna is sufficiently sensitive to receive signals under all conditions at the site, whether upper winds are very weak or very strong. Do not try to save money by buying a cheap antenna which is inadequate in some conditions.

(c) Decide whether local staff can maintain a secondary radar, or whether a fully automated GNSS radiosonde system is more suitable. Note that the use of radar-derived measurements will result in increased uncertainty in wind and height measurements than those obtained by GNSS radiosondes. Therefore, one must also decide whether the increased measurement uncertainty is tolerable if opting for non-GNSS radiosondes.

(d) If a GNSS radiosonde system is to be procured, check whether there is any source of local radio-frequency interference likely to cause problems.

(e) Decide what altitude performance is required and determine which sondes and balloon size will suit (if the radiosondes are not to be used at pressures lower than 30 hPa, then there is a wider range of suitable radiosondes available; see Tables 12.2 to 12.5).

(f) Decide what relative humidity sensor performance is required (for example, a GRUAN or GCOS Upper-air Network station has a higher standard required than a routine GCOS station) basing the requirement on Table 12.1 of Nash et al. (2011) and Tables in Annex 12.A and Annex 12.B.

(g) If conditions are often wet and cloudy, specify that radiosonde sensors need to have some protection against wetting and contamination, and ask for evidence on how this works.

(h) Ask for a compensation agreement if too many radiosondes fail in flight.

(i) Ask for evidence that the manufacturer has reliably supplied radiosondes to other users on the scale that will be used at the station.

(j) Make sure that the ground equipment can produce messages which allow high resolution data to be reported. This message must be suitable for the communications available from the site and meet user requirements for data with good vertical resolution.

(k) Ensure that the ground equipment computers are compatible with the local telecommunication system (including internet links, if required).

# ANNEX 12.A. CURRENT BREAKTHROUGH AND OPTIMUM UNCERTAINTY REQUIREMENTS FOR RADIOSONDE MEASUREMENTS

Note: The requirements are based on current technological capability as assessed in the eighth WMO international radiosonde intercomparison, in Yangjiang, China (Nash et al., 2011). They apply to radiosonde measurements in synoptic and climate meteorology.

| *Variable* | *Height (km) (temperature (°C) in the case of humidity)* | *Breakthrough uncertainty requirement*[a,b] | *Optimum uncertainty requirement*[b] |
|---|---|---|---|
| ***Pressure*** | 1 | 3 hPa | 2 hPa |
| | 10 | 3 hPa | 1 hPa |
| | 16 | 2 hPa | 0.6 hPa |
| | 24 | 1 hPa | 0.2 hPa |
| | 32 | 0.4 hPa | 0.1 hPa |
| ***Temperature*** | 0 to 16 | 1 K | 0.4 K |
| | Above 16 | 2 K | 0.8 K |
| ***Relative humidity*** | 0 to 12 (40 °C to –50 °C)[c] | 15%RH | 6%RH |
| (Troposphere only) | 12 to 17 (–50 °C to –90 °C)[c] | 30%RH | 10%RH |
| ***Mixing ratio***, lower stratosphere (specialized systems) | 12 to 25 | 20% ppmv[d] | 4% ppmv |
| ***Wind direction*** | 0 to 16 | 10°, speed < 10 m $s^{-1}$<br>4° at higher speeds | 5°, speed < 10 m $s^{-1}$<br>2° at higher speeds |
| | Above 16 | 20°, speed < 10 m $s^{-1}$<br>8° at higher speeds | 5°, speed < 10 m $s^{-1}$<br>2° at higher speeds |
| ***Wind speed*** | 0 to 16 | 2 m $s^{-1}$ | 1 m $s^{-1}$ |
| | Above 16 | 4 m $s^{-1}$ | 1 m $s^{-1}$ |
| ***Wind components*** | 0 to 16 | 2 m $s^{-1}$ | 1 m $s^{-1}$ |
| | Above 16 | 3 m $s^{-1}$ | 1 m $s^{-1}$ |
| ***Geopotential height of significant level*** | 1 | 30 gpm | 20 gpm |
| | 5 | 40 gpm | 20 gpm |
| | 10 | 60 gpm | 20 gpm |
| | 16 | 120 gpm | 40 gpm |
| | 20 | 200 gpm | 40 gpm |
| | 32 | 240 gpm | 60 gpm |

Notes:
a Values derived for the main targeted applications for radiosondes.
b Expressed as expanded uncertainties ($k = 2$), which encompass approximately 95% of the variation of results in sounding conditions including all significant sources of uncertainty (e.g. dynamic and radiative conditions).
c Change in expected relative humidity sensor performance corresponds better with temperature than with altitude in the troposphere.
d ppmv = parts per million by volume

# ANNEX 12.B. ESTIMATES OF GOAL, BREAKTHROUGH AND THRESHOLD LIMITS FOR UPPER WIND, UPPER-AIR TEMPERATURE, RELATIVE HUMIDITY AND GEOPOTENTIAL HEIGHT (DERIVED FROM THE WMO ROLLING REVIEW OF REQUIREMENTS FOR UPPER-AIR OBSERVATIONS)

(a) The *goal* is an ideal requirement above which further improvements are not necessary.

(b) The *breakthrough* is an intermediate level between *threshold* and *goal* which, if achieved, would result in a significant improvement for the targeted application. The breakthrough level may be considered as an optimum, from a cost-benefit point of view, when planning or designing observing systems.

(c) The *threshold* is the minimum requirement to be met to ensure that data are useful.

It is recommended that expenditure on radiosondes be considered as justified when the uncertainty and vertical resolution obtained is equal to or better than the threshold and as close to the goal as is affordable.

The information in these tables is taken primarily from the OSCAR/Requirements (see https://space.oscar.wmo.int/observingrequirements) for global and high-resolution NWP and climate. These are 1 $\sigma$ ($k$=1) uncertainties. In turn, the climate requirement comes from GCOS (GCOS-200). Planetary boundary layer is abbreviated to PBL below, and upper troposphere/lower stratosphere to UTLS.

**Table 12.B.1. Summary of WMO/GCOS limits for uncertainty (RMS vector error, $k$=1) and vertical resolution for upper wind measurements**

| *Layer* | | *Goal for NWP* | *Goal for climate* | *Breakthrough for NWP* | *Threshold for NWP* |
|---|---|---|---|---|---|
| PBL | Uncertainty | 1 m $s^{-1}$ | 2 m $s^{-1}$ | 3 m $s^{-1}$ | 5 m $s^{-1}$ |
| PBL | Vertical resolution | 100–200 m | 500 m | 250 m | 400 m |
| Free troposphere | Uncertainty | 1 m $s^{-1}$ | 2 m $s^{-1}$ | 3 m $s^{-1}$ | 5 m $s^{-1}$ |
| Free troposphere | Vertical resolution | 500 m | 500 m | 700 m | 1 km |
| UTLS | Uncertainty | 1 m $s^{-1}$ | 2 m $s^{-1}$ | 3 m $s^{-1}$ | 5 m $s^{-1}$ |
| UTLS | Vertical resolution | 500 m | 500 m | 1 km | 3 km |
| Upper stratosphere | Uncertainty | 1 m $s^{-1}$ | 2 m $s^{-1}$ | 5 m $s^{-1}$ | 10 m $s^{-1}$ |
| Upper stratosphere | Vertical resolution | 1 km | 500 m | 2 km | 3 km |
| Long-term stability | | | 0.1 m $s^{-1}$ in 10 years | | |

**Table 12.B.2. Summary of WMO/GCOS uncertainty ($k$=1) and vertical resolution limits for upper-air temperature measurements (Note: These limits are for temperatures at a given height and may be different to those when temperatures are integrated over relatively deep layers, for example see Table 12.B.4 for breakthrough limits derived from requirements for 100 hPa geopotential height.)**

| *Layer* | | *Goal for NWP* | *Goal for climate* | *Breakthrough for NWP* | *Threshold for NWP* |
|---|---|---|---|---|---|
| PBL | Uncertainty | 0.5 K | 0.5 K | 1 K | 3 K |
| PBL | Vertical resolution | 100–300 m | 1 km | 250 m | 1 km |
| Free troposphere | Uncertainty | 0.5 K | 0.5 K | 1 K | 3 K |
| Free troposphere | Vertical resolution | 300 m | 1 km | 500 m | 1 km |
| UTLS | Uncertainty | 0.5 K | 0.5 K | 1 K | 3 K |
| UTLS | Vertical resolution | 300 m | 2 km | 1 km | 3 km |
| Upper stratosphere | Uncertainty | 0.5 K | 0.2 K | 3 K | 5 K |
| Upper stratosphere | Vertical resolution | 1 km | 5 km | 1 km | 3 km |
| Long-term stability | | | 0.05 K in 10 years | | |

**Table 12.B.3. Summary of WMO/GCOS performance limits ($k$=1) for aerological instruments measuring humidity**

| *Layer* | | *Goal for NWP* | *Goal for climate* | *Breakthrough for NWP* | *Threshold for NWP* |
|---|---|---|---|---|---|
| Lower troposphere | Uncertainty | 2%RH | 5%RH | 5%RH | 10%RH |
| Lower troposphere | Vertical resolution | 100–300 m | 2 km | 200 m | 1 km |
| Upper troposphere | Uncertainty | 2%RH | 5%RH | 5%RH | 10%RH |
| Upper troposphere | Vertical resolution | 300 m | 2 km | 500 m | 1 km |
| UTLS | Uncertainty | Not stated | 5%RH | Not stated | Not stated |
| UTLS | Vertical resolution | Not stated | 2 km | Not stated | Not stated |
| Long-term stability | | | 0.3% in 10 years | | |

Note: The OSCAR/Requirement and GCOS requirement refer to specific humidity, but this leads to far too stringent limits on uncertainty in layers where relative humidity is very low in the lower and middle troposphere. So values are shown as approximately equivalent relative humidity, and mixing ratio should be used at very low temperatures or in the stratosphere.

**Table 12.B.4. Summary of uncertainty (*k*=2) and vertical resolution limits for geopotential heights of 100 hPa and significant levels, consistent with WMO/GCOS limits for upper-air temperature**

| *Layer* | | *Goal for NWP* | *Goal for climate* | *Breakthrough for NWP* |
|---|---|---|---|---|
| Surface to 100 hPa | Uncertainty | 24 gpm (= to 0.4 K temperature layer) | 12 gpm (= to 0.2 K temperature layer) | 50 gpm (= to 0.8 K temperature layer) |
| Lower troposphere | Uncertainty for temperature[a] | 40 gpm | 16 gpm on average | 120 gpm |
| Lower troposphere | Uncertainty for cloud base[b] | 30 gpm | | |
| Upper troposphere | Uncertainty for temperature[a] | 40 gpm | 14 gpm on average | 120 gpm |
| Lower stratosphere equatorial | Uncertainty for temperature[a] | 70 gpm | 48 gpm | 200 gpm |
| Lower stratosphere extratropical | Uncertainty for temperature[a] | 100 gpm | 68 gpm | 300 gpm |
| Upper stratosphere | Uncertainty for temperature[a] | 80 gpm | 60 gpm | 240 gpm |
| Long-term stability | | | 4 – 8 gpm in 10 years | |

Notes:
a Limit for height error produces a typical temperature error of half the magnitude specified for the limits for temperature in Table 12.B.2.
b Limit derived to be compatible with measurements from operational laser ceilometers in the lower troposphere.

## ANNEX 12.C. ENVIRONMENTALLY FRIENDLY RADIOSONDES

About 620 000 radiosondes are launched worldwide annually. After launch the radiosonde ascends through the atmosphere until the balloon bursts and the radiosonde falls to the earth. All radiosondes with balloon segments and flight train fall to the ground or in the ocean, and thus create environmental pollution.

Balloon-borne waste has the ability to reach very remote areas and is often the only source of human-made waste in inland wilderness areas, wildlife sanctuaries and other environmentally sensitive areas.

Flight trains pose a particular environmental issue. They often cause the radiosonde payload to get caught in trees, power lines and towers, or to float in the oceans, possibly remaining for years. Flight trains present a long-term entanglement threat to wildlife on land and in the oceans.

The main difficulty in producing environmentally friendly radiosondes is identifying materials that both meet the functional requirements and are biodegradable. Most current radiosonde parts are made from non-biodegradable materials. There are biodegradable plastics, but currently only one radiosonde manufacturer has showcased a radiosonde housing made from such materials. Other manufacturers are encouraged to use biodegradable plastics or other suitable materials for radiosondes.

Radiosondes vary in size and weight. As the larger, heavier radiosondes descend they pose a threat to people and animals. Current technologies allow the manufacture of smaller and lighter radiosondes – about 100 g. The balloon, perhaps 350 g or 600 g, is heavier. All manufacturers are encouraged to reduce the size and weight of their radiosondes while maintaining functionality. An advantage of lighter radiosondes is that a smaller balloon can be employed, therefore requiring less gas. The reduced size of the balloon also means less polluting materials.

Flight trains are often made of non-biodegradable cord, such as nylon, which can persist in the environment for decades. Switching flight train material to a biodegradable cordage, such as cotton twine, or polypropylene without UV protection, is recommended. This will reduce the entanglement risk to wildlife in the oceans and on land, and will result in the more rapid release of radiosonde payloads caught in trees, powerlines and other structures.

Synthetic latex balloons have a much slower rate of decomposition than natural rubber latex ones, therefore usage of the latter is preferred.

Radiosonde batteries of all types, for example alkaline, lithium and water-activated batteries, contain toxic and corrosive chemicals. There are currently no environmentally friendly batteries, however lithium batteries present lower impacts. As manufacturers reduce the power consumption of radiosondes this will allow for smaller batteries and a further reduction in the overall waste.

Operators and manufacturers of radiosondes should encourage the collection and return, or the disposal of radiosondes according to the local regulations for the treatment of electronic and chemical waste. The balloon and flight train should be disposed of as normal waste. Local treatment minimizes any additional environmental footprint related to transport of the used radiosondes. Used lithium batteries require special handling and are not allowed in air cargo.

# ANNEX 12.D. GUIDELINES FOR ORGANIZING RADIOSONDE INTERCOMPARISONS AND FOR THE ESTABLISHMENT OF TEST SITES

Note: Based on *Commission for Instruments and Methods of Observation Twelfth Session: Abridged Final Report with Resolutions and Recommendations* (WMO-No. 881), Annex II, and updated thereafter.

## PART I – GUIDELINES FOR ORGANIZING RADIOSONDE INTERCOMPARISONS

### 1. Introduction

1.1 These guidelines assume that procedures that may be established by various test facilities are consistent with procedures established by other national and international organizations. They also assume that an Organizing Committee will be formed of participants (Members) interested in comparing radiosondes and that at least one non-participant will be included with ability to provide guidance for conducting the intercomparison. The involvement of an independent non-participant is important in order to avoid bias during the planning of the intercomparison. Consideration must also be given to whether radiosonde manufacturers' personnel should actively participate or whether independent operational personnel of the host should prepare and launch such radiosondes.

1.2 All intercomparisons differ from each other to some extent; therefore, these guidelines are to be construed only as a generalized checklist of tasks needing to be accomplished. Modifications should be made by the Organizing Committee, as required, but the validity of the results and scientific evaluation should not be compromised.

1.3 Final reports of previous intercomparisons and organizational meeting reports of other Organizing Committees may serve as an example of the methods that can be adopted for the intercomparison. These previous reports should be maintained and made available by the WMO Secretariat.

### 2. Objectives of intercomparisons

2.1 The intercomparison objectives must be clear, must list what is expected from the intercomparisons and identify how results will be disseminated. The Organizing Committee is tasked to examine the achievements to be expected from the radiosonde intercomparison and to identify and anticipate any potential problem. The Organizing Committee's role is to provide guidance, but it must also prepare clear and detailed statements of the main objectives and agree on the criteria to be used in evaluating the results. The Organizing Committee should also determine how best to guarantee the success of the intercomparison by drawing on background knowledge and accumulated experience from previous intercomparisons.

### 3. Place, date and duration of intercomparison

3.1 The host facility should provide to the Organizing Committee and the participants a description of the proposed intercomparison site and facilities (the locations and other details), environmental and climatological conditions, and site topography. The host facility should also name a Project Leader or Project Manager who will be responsible for the day-to-day operation and act as the facility point of contact.

3.2 The Organizing Committee should visit the proposed site to determine the suitability of its facilities and to propose changes, as necessary. After the Organizing Committee agrees that the site and facilities are adequate, a site and environmental description should be prepared by the Project Leader for distribution to the participants. The Project Leader, who is familiar with his facility's schedule, must decide the date for the start of the intercomparison, as well as its duration. A copy of this schedule shall be delivered to the Organizing Committee.

3.3 In addition to the starting date of the intercomparisons, the Project Leader should propose a date when his facility will be available for the installation of the participant's equipment and arrange for connections to the data acquisition system. Time should be allowed for all of the participants to check and test equipment prior to starting the intercomparison and to allow additional time to familiarize the operators with the procedures of the host facility.

## 4. Participation

4.1 As required, the Project Leader and/or Organizing Committee should invite, through the Secretary-General of WMO, participation of Members. However, once participants are identified, the Project Leader should handle all further contacts.

4.2 The Project Leader should draft a detailed questionnaire to be sent by the Secretary-General to each participant in order to obtain information on each instrument type proposed to be intercompared. Participants are expected to provide information on their space, communication, unique hardware connection requirements, and software characteristics. They also should provide adequate documentation describing their ground and balloon-borne instrumentation.

4.3 It is important that participants provide information about their radiosonde calibration procedures against recognized standards. Although it is expected that operational radiosondes will be intercompared, this may not always be the case; new or research-type radiosondes may be considered for participation with the agreement of all of the participants, the Project Leader, and the Organizing Committee.

## 5. Responsibilities

### 5.1 *Participants*

5.1.1 The participants shall be responsible for the transportation of their own equipment and costs associated with this transportation.

5.1.2 The participants should install and remove their own equipment with the cognizance of the Project Leader. The host facility shall assist with unpacking and packing, as appropriate.

5.1.3 The participants shall provide all necessary accessories, mounting hardware for ground equipment, signal and power cables, spare parts and expendables unique to their system. The participants shall have available (in the event that assistance from the host facility should become necessary) detailed instructions and manuals needed for equipment installation, operation, maintenance and, if applicable, calibration.

5.1.4 The participants should sign the data protocol agreement of the intercomparison.

### 5.2 *Host facility*

5.2.1 The host facility should assist participants in the unpacking and installation of equipment as necessary, and provide storage capability to house items such as expendables, spare parts and manuals.

5.2.2 The host facility should provide auxiliary equipment as necessary, if available.

5.2.3 The host facility should assist the participants with connections to the host facility's data acquisition equipment, as necessary.

5.2.4 The host shall insure that all legal obligations relating to upper-air measurements (for example, the host country's aviation regulations and frequency utilization) are properly met.

5.2.5 The host facility may provide information on items such as accommodation, local transportation and daily logistics support, but is not obligated to subsidize costs associated with personnel accommodation.

## 6. Rules during the intercomparison

6.1 The Project Leader shall exercise control of all tests and will keep a record of each balloon launch, together with all the relevant information on the radiosondes used in the flight and the weather conditions.

6.2 Changes in equipment or software will be permitted with the cognizance and concurrence of the Project Leader. Notification to the other participants is necessary. The Project Leader shall maintain a log containing a record of all the equipment participating in the comparison and any changes that occur.

6.3 Minor repairs (for example, fuse replacement, and the like) not affecting instrumentation performance are allowed. The Project Leader should be made aware of these minor repairs and also submit the information to the record log.

6.4 Calibration checks and equipment servicing by participants requiring a specialist or specific equipment will be permitted after notification to the Project Leader.

6.5 Any problem that compromises the intercomparison results or the performance of any equipment shall be addressed by the Project Leader.

## 7. Data acquisition

7.1 The Organizing Committee should agree on appropriate data acquisition procedures such as measurement frequency, sampling intervals, data averaging, data reduction (this may be limited to an individual participant's capability), data formats, real-time QC, post-analysis QC and data reports.

7.2 The initial international Organizing Committee shall decide on the data acquisition hardware and software for the test. This should be well tested before commencement of the intercomparison.

7.3 The time delay between observation and delivery of data to the Project Leader shall be established by the Project Leader and agreed by the participants. One hour after the end of the observation (balloon burst) should be considered adequate.

7.4 The responsibility for checking data prior to analysis, the QC steps to follow, and delivery of the final data rests with the Project Leader.

7.5 Data storage media shall be the Project Leader's decision after taking into consideration the capability of the host facility, but the media used to return final test data to participants may vary in accordance with each of the participant's computer ability. The Project Leader should be cognizant of these requirements.

7.6 The Project Leader has responsibility for providing final data to all participants and, therefore, the host facility must be able to receive all individual data files from each participant.

## 8. Data processing and analysis

### 8.1 *Data analysis*

8.1.1 A framework for data analysis should be encouraged and decided upon even prior to beginning the actual intercomparison. This framework should be included as part of the experimental plan.

8.1.2 There must be agreement among the participants as to methods of data conversion, calibration and correction algorithms, terms and abbreviations, constants, and a comprehensive description of proposed statistical analysis methods. It is essential that the data processing be performed by experienced experts, nominated by WMO.

8.1.3 The Organizing Committee should verify the appropriateness of the analysis procedures selected.

8.1.4 The results of the intercomparisons should be reviewed by the Organizing Committee, who should consider the contents and recommendations given in the final report.

### 8.2 *Data processing and database availability*

8.2.1 All essential meteorological and environmental data shall be stored in a database for further use and analysis by the participants. The Project Leader shall exercise control of these data.

8.2.2 After completion of the intercomparison, the Project Leader shall provide a complete set of all of the participants' data to each participant.

## 9. Final report of the intercomparison

9.1 The Project Leader shall prepare the draft final report which shall be submitted to the Organizing Committee and to the participating members for their comments and amendments. A time limit for reply should be specified.

9.2 Comments and amendments should be returned to the Project Leader with copies also going to the Organizing Committee.

9.3 When the amended draft final report is ready, it should be submitted to the Organizing Committee, who may wish to meet for discussions, if necessary, or who may agree to the final document.

9.4 After the Organizing Committee approves the final document for publication, it should be sent to the Secretariat for publication and distribution by WMO.

9.5 Reproduction for commercial purposes of any plots or tables from the final report should not be allowed without specific permission from WMO.

## 10. Final comments

10.1 The Organizing Committee may agree that intermediate results may be presented only by the Project Leader, and that participants may present limited data at technical conferences, except that their own test data may be used without limitation. Once the WMO Secretariat has scheduled the final report for publication, WMO shall make the data available to all Members who request them. The Members are then free to analyse the data and present the results at meetings and in publications.

## PART II – GUIDELINES FOR THE ESTABLISHMENT OF TEST SITES

### 1. Introduction

1.1 In order to support the long-term stability of the global upper-air observing system, it is essential to retain the capability of performing quantitative radiosonde comparisons. Current and new operational radiosonde systems must be checked against references during flight on a regular basis. Members must ensure that a minimum number of test sites with the necessary infrastructure for performing radiosonde comparison tests are retained.

1.2 Experience with the series of WMO Radiosonde Intercomparisons since 1984 has shown that it is necessary to have a range of sites in order to compare the radiosondes over a variety of flight conditions.

1.3 Relative humidity sensor performance is particularly dependent on the conditions during a test, for example, the amount of cloud and rain encountered during ascents, or whether surface humidity is high or low.

1.4 Daytime temperature errors depend on the solar albedo, and hence the surface albedo and cloud cover. Thus, temperature errors found at coastal sites may differ significantly from continental sites. Infrared errors on temperature sensors will not only depend on surface conditions and cloud distribution, but also on atmospheric temperature. Thus, IR temperature errors in the tropics (for instance near the tropopause) will be quite different from those at mid-latitudes.

1.5 The errors of many upper-wind observing systems depend on the distance the balloon travels from the launch site (and also the elevation of the balloon from the launch site). Thus, comparison tests must cover situations with weak upper winds and also strong upper winds.

### 2. Facilities required at locations

2.1 Locations suitable for testing should have enough buildings/office space to provide work areas to support the operations of at least four different systems.

2.2 The site should have good quality surface measurements of temperature, relative humidity, pressure and wind, measured near the radiosonde launch sites. Additional reference quality measurements of temperature, pressure and relative humidity would be beneficial.

2.3 The test site should have a method of providing absolute measurements of geopotential height during test flights (probably using a GPS radiosonde capable of producing accurate heights).

2.4 The test site should have a well-established surface-based GPS sensor for measuring integrated water vapour, or ground-based radiometers and interferometers.

2.5 Cloud observing systems at the test site, such as laser ceilometers and cloud radars, are desirable.

2.6 Aerosol lidars and relative humidity lidars may also prove useful at the test site.

2.7 The site must be cleared by the national air traffic control authorities for launching larger balloons (3 000 g) with payloads of up to 5 kg. Balloon sheds must be able to cope with launching these large balloons.

### 3. Suggested geographical locations

3.1 In order to facilitate testing by the main manufacturers, it is suggested that test sites should be retained or established in mid-latitudes in North America, Europe and Asia. Ideally, each of these regions would have a minimum of two sites, one representing coastal (marine) conditions, and another representing conditions in a mid-continent location.

3.2 In addition, it is suggested that a minimum of two test locations should be identified in tropical locations, particularly for tests of relative humidity sensors.

3.3 If the main test sites noted above do not provide adequate samples of extreme conditions for relative humidity sensors (for example, very dry low-level conditions), it may be necessary to identify further test sites in an arid area, or where surface temperatures are very cold (below –30 °C in winter). It is possible that some of these could be selected from established GRUAN sites.

## PART III – GUIDELINES FOR PROTOTYPE TESTING

### 1. Introduction

1.1 The major WMO radiosonde comparisons are organized about every 5 to 6 years, when a large group of manufacturers can benefit from a large-scale test, with systems that have already been through prototype testing. For new designs or for those manufacturers rectifying problems identified in the WMO radiosonde comparisons, there is a need to perform smaller, less expensive tests.

1.2 It is probably best for manufacturers trying to demonstrate that a problem has been resolved to have the tests done at one of the designated WMO test sites.

### 2. Recommended procedures

2.1 Testing to prove that problems have been rectified needs to be done to similar standards and methods used in the WMO radiosonde comparisons. This requires that the test site must have staff who are fully conversant with the procedures and techniques of the WMO radiosonde comparisons, and also requires the use of two radiosonde types of known good quality as working references/link radiosondes to the WMO radiosonde comparison results.

2.2 With prototype testing it is essential to compare measurements with radiosondes flown together under one balloon. Ideally the radiosondes should be suspended in such a way that they are free to rotate in flight, as this is what happens on individual ascents. The radio-frequency performance of the new radiosonde needs to be good enough to ensure that the frequency does not drift and cause interference to the radiosonde with which it is being compared. Comparison of results should be performed as a function of time into flight, since it is unwise to assume that height/pressure assignments to temperature and relative humidity measurements have negligible errors. The number of initial test flights may be quite small since some initial errors are often large and can be quickly identified.

2.3 If the aim is to improve the new radiosonde design so that its measurement quality comes close to that of the high-quality radiosondes tested in the WMO Intercomparison of High-quality Radiosonde Systems, then it will be necessary to use one of the better quality radiosondes as a test reference. Always follow the manufacturer's instructions when preparing the radiosondes for the test flights. Testing must be performed both day and night, since the sonde errors for daytime temperatures need to be identified and at night the errors in relative humidity are often worse than in daytime.

2.4 Final prototype tests need to be performed at a time of year when the variation of relative humidity in the vertical and with time is high at all levels in the troposphere.

## 3. Archiving of results

3.1 Results of tests at CIMO test centres need to be forwarded to the relevant CIMO expert team for checking and display on the CIMO websites.

3.2 Once a new national development becomes mature, it would also be helpful for the future to forward comparison test results to the relevant CIMO expert team.

## REFERENCES AND FURTHER READING


Balagurov, A.; Kats, A.; Krestyannikova, N. et al. *WMO Radiosonde Humidity Sensor Intercomparison* (WMO/TD-No. 1305). Instruments and Observing Methods (IOM) Report No. 85; World Meteorological Organization (WMO): Geneva, 2006.

da Silveira, R. B.; Fisch, G. F.; Machado, L. A. T. et al. *WMO Intercomparison of GPS Radiosondes – Alcântara (Brazil), 20 May–10 June 2001* (WMO/TD-No. 1314). Instruments and Observing Methods (IOM) Report No. 90. World Meteorological Organization (WMO): Geneva, 2006.

Dirksen, R. J.; Sommer, M.; Immler, F. J. et al. Reference Quality Upper-air Measurements: GRUAN Data Processing for the Vaisala RS92 Radiosonde. *Atmos Meas Tech* **2014**, *7*, 4463–4490. https://doi.org/10.5194/amt-7-4463-2014.

Elms, J. *WMO Catalogue of Radiosondes and Upper-air Wind Systems in Use by Members in 2002 and Compatibility of Radiosonde Geopotential Measurements for Period from 1998 to 2001* (WMO/TD-No. 1197). Instruments and Observing Methods (IOM) Report No. 80; World Meteorological Organization (WMO): Geneva, 2003.

Elms, J. B.; Nash, J.; Williams, G. The Difference in Observed Temperatures from Radiosondes Suspended 10 m and 40 m Beneath a 1400 g Balloon. Presented at the *WMO Technical Conference on Instruments and Methods of Observation (TECO-94)*, Geneva, 28 February–2 March 1994. In *Papers Presented at the WMO Technical Conference on Instruments and Methods of Observation (TECO-94)* (WMO/TD-No. 588). Instruments and Observing Methods (IOM) Report No. 57; World Meteorological Organization (WMO): Geneva, 1994.

Eyre, J. R. Observation Bias Correction Schemes in Data Assimilation Systems: A Theoretical Study of Some of Their Properties. *Q J R Meteorol Soc* **2016**, *142*, 2284–2291. https://doi.org/10.1002/qj.2819.

Eyre, J. R.; Bell, W.; Cotton, J. et al. Assimilation of Satellite Data in Numerical Weather Prediction. Part II: Recent Years. *Q J R Meteorol Soc* **2022**, *148*, 521–556. https://doi.org/10.1002/qj.4228.

Fujiwara, M.; Shiotani, M.; Hasebe, F. et al. Performance of the Meteolabor "Snow White" Chilled-mirror Hygrometer in the Tropical Troposphere: Comparisons with the Vaisala RS80 A/H-Humicap Sensors. *Journal of Atmospheric and Oceanic Technology* **2003**, *20*, 1534–1542. https://doi.org/10.1175/1520-0426(2003)020<1534:POTMSW>2.0.CO;2.

Gaffen, D. J. *Historical Changes in Radiosonde Instruments and Practices* (WMO/TD-No. 541). Instruments and Observing Methods (IOM) Report No. 50; World Meteorological Organization (WMO): Geneva, 1993.

Global Climate Observing System (GCOS). *The Global Observing System for Climate: Implementation Needs*. (GCOS-200); World Meteorological Organization (WMO): Geneva, 2016.

Hawson, C. L. *Performance Requirements of Aerological Instruments: An Assessment Based on Atmospheric Variability* (WMO-No. 267). Technical Note No. 112; World Meteorological Organization (WMO): Geneva, 1970.

Ho, S.-P.; Peng, L.; Vömel, H. Characterization of the Long-term Radiosonde Temperature Biases in the Upper Troposphere and Lower Stratosphere Using COSMIC and Metop-A/GRAS Data from 2006 to 2014. *Atmospheric Chemistry and Physics* **2017**, 17, 4493–4511. https://doi.org/10.5194/acp-17-4493-2017.

Hock, T. F.; Franklin, J. L. The NCAR GPS Dropwindsonde. *Bull Amer Meteor Soc* **2017**, *80*, 407–420. https://doi.org/10.1175/1520-0477(1999)080<0407:TNGD>2.0.CO;2.

Hooper, A. H. *Upper-air Sounding Studies* (WMO-No. 394), Volume I. Technical Note No. 140; World Meteorological Organization (WMO): Geneva, 1975.

Hooper, A. H. *Algorithms for Automatic Aerological Soundings* (WMO/TD-No. 175). Instruments and Observing Methods (IOM) Report No. 21; World Meteorological Organization (WMO): Geneva, 1986.

Hyland, R. W.; Wexler, A. Formulations for the Thermodynamic Properties of the Saturated Phases of $H_2O$ from 173.15 K to 473.15 K. *ASHRAE Transactions* **1983**, *89*(2A) 500–519.

Ingleby, B. *An Assessment of Different Radiosonde Types 2015/2016*. Unpublished ECMWF Technical Memorandum (ECMWF Technical Memorandum No. 807), 2017.

Ingleby, B.; Motl, M.; Marlton, G. et al. On the Quality of RS41 Radiosonde Descent Data, *Atmos Meas Tech Discuss* **2021** [preprint]. https://doi.org/10.5194/amt-2021-183.

Ivanov, A.; Kats, A.; Kurnosenko, S. et al. *WMO International Radiosonde Comparison – Phase III, Dzhambul (USSR), 1989: Final Report* (WMO/TD-No. 451). Instruments and Observing Methods (IOM) Report No. 40; World Meteorological Organization (WMO): Geneva, 1991.

Jensen, M. P.; Holdridge, D. J.; Survo, P. et al. Comparison of Vaisala Radiosondes RS41 and RS92 at the ARM Southern Great Plains Site, *Atmos Meas Tech* **2016**, *9*, 3115–3129. https://doi.org/10.5194/amt-9-3115-2016.

Kitchen, M. Representativeness Errors for Radiosonde Observations. *Q J R Meteorol Soc* **1989**, *115*, 673–700. https://doi.org/10.1002/qj.49711548713.

Lee, S.-W.; Choi, B. I.; Woo S.-B. et al. Calibration of a Radiosonde Humidity Sensor at Low Temperature and Low Pressure. *Metrologia* **2019**, 56:055008. https://doi.org/10.1088/1681-7575/ab336f.

Lee, S.-W.; Kim, S.; Lee, Y.-S. et al. Radiation Correction and Uncertainty Evaluation of RS41 Temperature Sensors by Using an Upper-air Simulator. *Atmos Meas Tech* **2022a**, *15*, 1107–1121. https://doi.org/10.5194/amt-15-1107-2022.

Lee, S.-W.; Kim, S.; Lee, Y.-S. et al. Laboratory Characterisations and Intercomparison Sounding Test of Dual Thermistor Radiosondes for Radiation Correction. *Atmos Meas Tech Discuss* **2022b** [preprint]. https://doi.org/10.5194/amt-2021-343.

List, R. J. *Smithsonian Meteorological Tables*; Washington, DC: Smithsonian Institution Press, 1968.

Luers, J. K.; Eskridge, R. E. Use of Radiosonde Temperature Data in Climate Studies. *Journal of Climate* **1998**, *11*, 1002–1019. https://www.jstor.org/stable/26242973.

Miloshevich, L. M.; Paukkunen, A.; Vömel H. et al. Development and Validation of a Time-lag Correction for Vaisala Radiosonde Humidity Measurements. *Journal of Atmospheric and Oceanic Technology* **2004**, *21*, 1305–1327. https://doi.org/10.1175/1520-0426(2004)021<1305:DAVOAT>2.0.CO;2.

Moradi, I.; Soden, B.; Ferraro, R. et al. Assessing the Quality of Humidity Measurements from Global Operational Radiosonde Sensors, *J Geophys Res Atmos* **2013**, 118, 8040–8053. https://doi.org/10.1002/jgrd.50589.

Nash, J. *Measurement of Upper-air Pressure, Temperature and Humidity*. Instruments and Observing Methods (IOM) Report No. 121. World Meteorological Organization (WMO): Geneva, 2015.

Nash, J.; Elms, J. B.; Oakley, T. J. Relative Humidity Sensor Performance Observed in Recent International Radiosonde Comparisons. In *Proceedings of the Ninth Symposium on Meteorological Observations and Instrumentation*, Charlotte, North Carolina, 27–31 March 1995, 43–48.

Nash, J.; Oakley, T.; Vömel, H. et al. *WMO Intercomparison of High Quality Radiosonde Systems – Yangjiang, China, 12 July–3 August 2010* (WMO/TD-No. 1580). Instruments and Observing Methods (IOM) Report No. 107; World Meteorological Organization (WMO): Geneva, 2011.

Nash, J.; Schmidlin, F. J. *WMO International Radiosonde Comparison (UK 1984, USA 1985): Final Report* (WMO/TD-No. 195). Instruments and Observing Methods (IOM) Report No. 30; World Meteorological Organization (WMO): Geneva, 1987.

Nash, J.; Smout, R.; Oakley, T. et al. *WMO Intercomparison of Radiosonde Systems – Vacoas, Mauritius, 2–25 February 2005* (WMO/TD-No. 1303). Instruments and Observing Methods (IOM) Report No. 83; World Meteorological Organization (WMO): Geneva, 2005.

Newman, S.; Carminati, F.; Lawrence, H. et al. Assessment of New Satellite Missions within the Framework of Numerical Weather Prediction. *Remote Sensing* **2020**, *12*, 1580. https://doi.org/10.3390/rs12101580.

Paukkunen, A. Sensor Heating to Enhance Reliability of Radiosonde Humidity Measurement. In *Proceedings of the Ninth Symposium on Meteorological Observations and Instrumentation*, Charlotte, North Carolina, 27–31 March 1995, 65–69.

Philipona, R.; Kräuchi, A.; Romanens, G. et al. Solar and Thermal Radiation Errors on Upper-air Radiosonde Temperature Measurements. *Journal of Atmospheric and Oceanic Technology* **2013**, *30*, 2382–2393. https://doi.org/10.1175/JTECH-D-13-00047.1.

Ruston, B.; Bowler, N.; Healy S. et al. GNSS-RO Sounding in the Troposphere and Stratosphere. In *Data Assimilation for Atmospheric, Oceanic and Hydrologic Applications, Volume IV*; Park, S. K.; Xu, L., Eds. Springer, 2022; 373–395. https://link.springer.com/book/10.1007/978-3-030-77722-7.

Schmidlin, F. Recent Application of the Accurate Temperature Measuring (ATM) Radiosonde. Presented at the *WMO Technical Conference on Meteorological and Environmental Instruments and Methods of Observation (TECO-2006)*, Geneva, 4–6 December 2006. In *Papers Presented at the WMO Technical Conference on Meteorological and Environmental Instruments and Methods of Observation (TECO-2006)* (WMO/TD-No. 1354). Instruments and Observing Methods (IOM) Report No. 94; World Meteorological Organization (WMO): Geneva, 2006.

Schmidlin, F. J.; Sang Lee, H.; Ranganayakamma, B. Deriving the Accuracy of Different Radiosonde Types Using the Three-thermistor Radiosonde Technique. In *Proceedings of the Ninth Symposium on Meteorological Observations and Instrumentation*, Charlotte, North Carolina, 27–31 March 1995, 27–31.

Shimizu, K.; Hasebe, F. Fast-response High-resolution Temperature Sonde Aimed at Contamination-free Profile Observations. *Atmospheric Measurement Techniques* **2010**, *3*, 1673–1681. https://doi.org/10.5194/amt-3-1673-2010.

Smees, M; Nash, J. et al. A New Operational Radiosonde for the UK: Procurement Testing at Camborne Met Office, September–October 2009 [Poster]. Presented at the *WMO Technical Conference on Meteorological and Environmental Instruments and Methods of Observation (TECO-2010)*, Helsinki, 30 August–1 September 2010. In *Papers Presented at the WMO Technical Conference on Meteorological and Environmental Instruments and Methods of Observation (TECO-2010)* (WMO/TD-No. 1546). Instruments and Observing Methods (IOM) Report No. 104; World Meteorological Organization (WMO): Geneva, 2010.

Sonntag, D. Advancements in the Field of Hygrometry. *Meteorologische Zeitschrift* **1994**, *3*(2), 51–66. https://doi.org/10.1127/metz/3/1994/51.

Sun B.; Calbet, X.; Reale, A. et al. Accuracy of Vaisala RS41 and RS92 Upper Tropospheric Humidity Compared to Satellite Hyperspectral Infrared Measurements. *Remote Sensing* **2021** *13*(2), 173. https://doi.org/10.3390/rs13020173.

Turner, D. D.; Lesht, B. M.; Clough, S. A. et al. Dry Bias and Variability in Vaisala RS80-H Radiosondes: The ARM Experience. *Journal of Atmospheric and Oceanic Technology* **2003**, *20*, 117–132. https://doi.org/10.1175/1520-0426(2003)020<0117:DBAVIV>2.0.CO;2.

Turtiainen, H.; Tammela, S.; Stuns, I. A New Radiosonde Temperature Sensor with Fast Response Time and Small Radiation Error. In *Proceedings of the Ninth Symposium on Meteorological Observations and Instrumentation*, Charlotte, North Carolina, 27–31 March 1995, 60–64.

Vömel, H.; David D. E.; Smith, K. Accuracy of Tropospheric and Stratospheric Water Vapor Measurements by the Cryogenic Frost Point Hygrometer: Instrumental Details and Observations. *Journal of Geophysical Research* **2007**, *112*, D08305. https://doi.org/10.1029/2006JD007224.

von Rohden, C.; Sommer, M.; Naebert, T. et al. Laboratory Characterisation of the Radiation Temperature Error of Radiosondes and its Application to the GRUAN Data Processing for the Vaisala RS41, *Atmos Meas Tech* **2022**, *15*, 383–405. https://doi.org/10.5194/amt-15-383-2022.

Wade, C. G. Calibration and Data Reduction Problems Affecting National Weather Service Radiosonde Humidity Measurements. In *Proceedings of the Ninth Symposium on Meteorological Observations and Instrumentation*, Charlotte, North Carolina, 27–31 March 1995, 37–42.

Wang, J.; Zhang, L. Systematic Errors in Global Radiosonde Precipitable Water Data from Comparisons with Ground-based GPS Measurements. *Journal of Climate* **2008**, *21*, 2218–2238. https://doi.org/10.1175/2007JCLI1944.1.

Wang, J.; Zhang, L.; Dai, A. et al. Radiation Dry Bias Correction of Vaisala RS92 Humidity Data and its Impacts on Historical Radiosonde Data. *Journal of Atmospheric and Oceanic Technology* **2013**, *30*, 197–214. https://doi.org/10.1175/JTECH-D-12-00113.1.

Wexler, A. Vapor Pressure Formulation for Water in Range 0 to 100 °C. A Revision. *Journal of Research of the National Bureau of Standards – A. Physics and Chemistry* **1976**, *80A(5 and 6)*, 775–785. https://doi.org/10.6028%2Fjres.080A.071.

Wexler, A. Vapor Pressure Formulation for Ice. *Journal of Research of the National Bureau of Standards – A. Physics and Chemistry* **1977**, *81A(1)*, 5–20. https://doi.org/10.6028%2Fjres.081A.003.

World Meteorological Organization (WMO). *International Meteorological Vocabulary* (WMO-No. 182). Geneva, 1992.

World Meteorological Organization (WMO). *GRUAN Implementation Plan 2009–2013* (WMO/TD-No. 1506). GCOS-134. Geneva, 2009.

World Meteorological Organization (WMO). *Manual on Codes* (WMO-No. 306), Volume I.1. Geneva, 2019.

World Meteorological Organization (WMO). *Technical Regulations* (WMO-No. 49), Volume I. Geneva, 2019.

World Meteorological Organization (WMO). *Manual on the WMO Integrated Global Observing System* (WMO-No. 1160). Geneva, 2021.

Yagi, S.; Mita, A.; Inoue, N. *WMO International Radiosonde Comparison – Phase IV, Tsukuba, Japan, 15 February–12 March 1993: Final Report* (WMO/TD-No. 742). Instruments and Observing Methods (IOM) Report No. 59; World Meteorological Organization (WMO): Geneva, 1996.

# CHAPTER 13. MEASUREMENT OF UPPER WIND

## 13.1 GENERAL

### 13.1.1 Definitions

For background and some definitions see the *Manual on the WMO Integrated Global Observing System* (WMO-No. 1160).

**Pilot-balloon observation.** A determination of upper winds by tracking of a free balloon. (Often "pilot" is used to mean any wind-only balloon report.)

**Radiowind observation.** A determination of upper winds by tracking of a free balloon by electronic means.

**Upper-air observation.** A meteorological observation made in the free atmosphere either directly or indirectly.

**Upper-wind observation.** An observation at a given height or the result of a complete sounding of wind direction and speed in the atmosphere.

This chapter will deal primarily with radiowind and pilot-balloon observations. Balloon techniques, and measurements using special platforms, specialized equipment, or made indirectly by remote-sensing methods are discussed in various chapters of Volume III of the present Guide. Large numbers of observations are now received from commercial aircraft and also from wind profiler and weather radars. Data from balloons are mainly acquired by using rawinsonde techniques, although pilot-balloon and radiowind observations may be used when additional upper wind data are required without the expense of launching a radiosonde.

Before about 2010, radiosonde profiles were reported as if they were vertical, that is, only the launch position was provided. However, there can be substantial horizontal drift during a balloon ascent (up to about 300 km) and reporting of the position at each level is now possible and strongly recommended. Position and wind determination are closely linked.

### 13.1.2 Units of measurement of upper wind

The speed of upper winds is usually reported in metres per second or knots, but kilometres per hour are also used. The direction from which the airflow arrives is reported in degrees from north: 90° represents a wind arriving from the east, 180° from the south, 270° from the west and 0/360° from the north. In TEMP reports, the wind direction is rounded to the nearest 5°. Reporting to this resolution degrades the accuracy achievable by the best modern windfinding systems, particularly when upper winds are strong. Data from these systems encoded in BUFR provide more accurate information on the direction and speed of upper wind.

Particular care is needed in reporting wind direction near to the North or South Pole, especially with the reporting of position at each level. A radiosonde crossing the North Pole must be in a southerly airflow just before crossing the pole and in a northerly airflow just afterwards. BUFR reports should give wind direction relative to the longitude at each level. (The older alphanumeric codes used a special coordinate system for stations within 1° latitude of the pole.)

The height used in reporting radiowind/rawinsonde measurements is geopotential height so that the wind measurements are at the same heights as the radiosonde measurements of temperature and relative humidity (see the present volume, Chapter 12, 12.3.6). The conversion from geometric height, as measured with a GPS radiosonde or radar, to geopotential height is purely a function of the gravitational field at a given location and does not depend on the temperature

and humidity profile at the location. The gravitational potential energy ($\Phi$) of a unit mass of anything is the integral of the normal gravity from MSL ($z_{geometric} = 0$) to the height of the mass ($z_{geometric} = Z$), as given by equation 13.1:

$$\Phi = \int_0^z \gamma(z_{geometric}, \varphi) dz_{geometric} \tag{13.1}$$

where $\gamma(z_{geometric}, \varphi)$ is the normal gravity above the geoid. This is a function of geometric altitude, $z_{geometric}$, and the geodetic latitude $\varphi$.

This geopotential is divided by the normal gravity at 45° latitude to give the geopotential height used by WMO, as:

$$z\left(z_{geometric}, \varphi\right) = \Phi\left(z_{geometric}, \varphi\right) / \gamma_{45^\circ} = \left(\int_0^z \gamma\left(z_{geometric}, \varphi\right) dz_{geometric}\right) / \gamma_{45^\circ} \tag{13.2}$$

where $\gamma_{45^\circ}$ was taken in the definition as 9.80665 m s$^{-2}$.

Thus, the unit of height is the standard geopotential metre. In the troposphere, the value of geopotential height is a close approximation to the geometric height expressed in metres (see, for example, the present volume, Chapter 12, Table 12.4). The geopotential heights used in upper-wind reports are reckoned from the geoid (sea level), although in many systems the computations of geopotential height will initially be performed in terms of height above the station level.

The conversion of geometric height to geopotential height is derived in fuller detail in the present volume, Chapter 12, with suitable expressions given for the dependence of the gravitational field on height and latitude.

## 13.1.3 Meteorological requirements

### 13.1.3.1 *Uses in meteorological operations*

Observations of upper winds are essential for operational weather forecasting on all scales globally, and are often most effective when used in conjunction with simultaneous measurements of mass field (temperature and relative humidity). For global forecasting, winds are particularly important at the jet level and in the tropics.

(a) In the boundary layer, upper winds providing reliable measurements of vertical wind shear are essential for environmental pollution forecasting;

(b) They are vital to the safety and economy of aircraft operations;

(c) Accurate upper wind and vertical wind shear measurements are critical for the launching of space vehicles and other types of rockets; uncertainties in upper winds limit the accuracy of modern artillery, and reliable wind measurements are therefore important for safety in military operations;

(d) Upper winds are one of the essential climate variables;

(e) In situ upper winds are used in verification of NWP forecasts and validation of satellite winds.

### 13.1.3.2 *Improvements in reporting procedures*

In modern radiowind systems, computers have the capability of readily providing all the detailed structure (often 1 second, ~5 m in the vertical) relevant to meteorological operations and scientific research. The upper-wind reports should contain enough information to define the vertical wind shear across the boundaries between the various layers in the mass fields.

For instance, wind shear across temperature inversions or significant wind shear associated with large changes in relative humidity in the vertical should be reported whenever possible. As agreed, as part of the Global Basic Observing Network (GBON) (*Manual on the WMO Integrated Global Observing System* (WMO-No. 1160)) values should be reported at least every 100 m in the vertical (if possible); from January 2023 this supersedes the resolution requirements in the present volume, Chapter 12, Annex 12.B. Some users still find it useful to have reports at standard pressure levels in addition. Profiles should be provided as high-resolution BUFR reports. The BUFR reports should be generated from the full profiles – attempts to convert TEMP to BUFR reports have several problems and do not provide high resolution or the position at each level, see Ingleby et al. (2016).

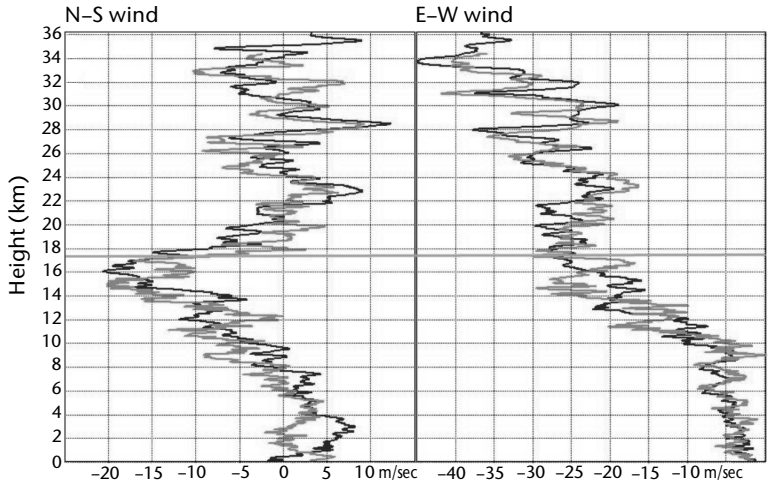
There is still some use of the obsolescent alphanumeric codes FM 35–XI Ext. TEMP and FM 32–XI Ext. PILOT. According to the *Manual on Codes* (WMO-No. 306), Volume I.1, wind speeds are allowed to deviate by as much as 5 m $s^{-1}$ from the linear interpolation between significant levels. The use of automated algorithms with this fitting limit can produce errors in reported messages which are much larger than the observational uncertainties. On occasion, the coding procedure may also degrade the reported resolution beyond the uncertainty requirements outlined in the present volume, Chapter 12. Better results are achieved using a fitting limit for a wind speed of 3 m $s^{-1}$ instead of 5 m $s^{-1}$, which can be implemented as a national practice for TEMP and PILOT messages. In earlier years, upper winds were generally processed manually or with a small calculator, and it was impractical to produce detailed reports of the vertical wind structure – hence the use of significant levels and the relatively crude fitting limits, which are not appropriate for the quality of observation produced by modern rawinsonde systems. With high vertical resolution reporting there is no need for "significant" (turning point) levels.

#### 13.1.3.3 ***Uncertainty requirements***

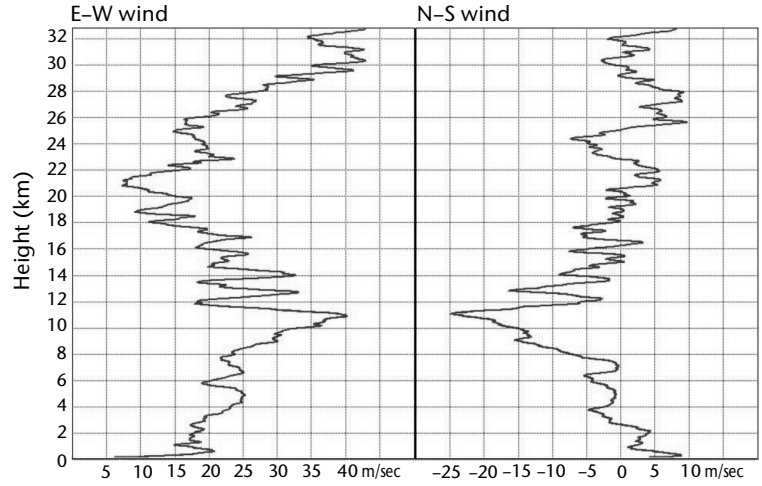
Uncertainty requirements for upper-wind measurements are presented in terms of wind speed and direction and also orthogonal wind components in the present volume, Chapter 12, Annex 12.A and Annex 12.B. Most upper-wind systems should be capable of measuring winds over a range from 0 to 100 m $s^{-1}$. If systems are designed to provide winds at low levels, they may not need to cope with such a large range. Systematic errors in wind direction must be kept as small as possible and certainly much less than 5°, especially at locations where upper winds are usually strong. In the 1990s, most well-maintained operational windfinding systems provided upper winds with a standard vector uncertainty ($2\sigma$) that was better than or equal to 3 m $s^{-1}$ in the lower troposphere and 5 to 6 m $s^{-1}$ in the upper troposphere and stratosphere (Nash, 1994). Widely used Global Navigation Satellite System (GNSS) windfinding systems means that many modern systems are capable of even better performance than this, with a standard vector uncertainty ($k = 2$) less than 1 m $s^{-1}$ with little degradation of the measurement quality in the vertical (see the results of the WMO Intercomparison of High-quality Radiosonde Systems in Yangjiang, China (Nash et al., 2011)).

Examples of vertical profiles of horizontal wind from Yangjiang, China, and the United Kingdom are shown in Figure 13.1. These measurements were made with a vertical resolution better than 150 m. Figure 13.1(a) shows two measurements from Yangjiang spaced six hours apart. The fine structure in the vertical is not the result of noise, but is the real structure in the atmosphere also measured by the other rawinsonde systems on the respective flights. During this test, there were very strong easterly winds at upper levels in the stratosphere (associated with the easterly phase of the quasi-biennial oscillation). The stronger northerly winds associated with the jet at about 16 km extend up to about 21 km and thus through the tropopause at 17.5 km. The detailed wind structure in the stratosphere between 22 and 34 km mostly persists over seven hours, illustrating that much of the detailed structure is not transient and thus merits archiving and reporting.

Figure 13.1(b) is from early winter in the United Kingdom, with the tropopause much lower at about 11 km, but again the stronger winds associated with the upper troposphere jet extend up to at least 16 km. The large perturbations in wind caused by the gravity waves immediately above the tropopause would not be resolved at 1 km vertical resolution. On this occasion,




(a) Flight 1 at 0800 hours (black) and flight 3 at 1448 hours (grey) on 14 July 2010, from the WMO Intercomparison of High Quality Radiosonde Systems in Yangjiang, China




(b) November measurement made at Camborne, United Kingdom; data from two different radiosonde types are superimposed. (Note: In this frame, the zonal and meridional wind components are reversed, i.e. the zonal component is displayed on the left.)

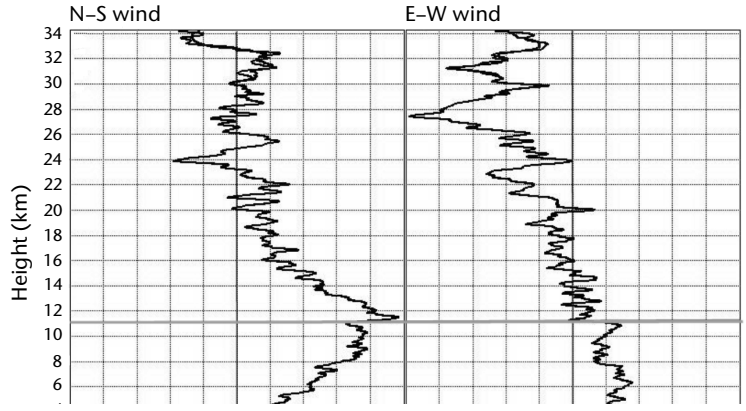



**Figure 13.1. Examples of vertical profiles of horizontal wind measured at about 150 m vertical resolution in Yangjiang, China, and in early winter and summer in the United Kingdom; horizontal grey line shows tropopause height.**

there is another jet associated with circulation around the polar vortex at heights above 30 km. Figure 13.1(c) is from United Kingdom summertime conditions. In this case there is significant wind shear across the tropopause. Easterly winds predominate in the stratosphere above about 16 km, and these are not as strong as the westerly winds in the winter. However, between 20 and 32 km, there are again significant perturbations in the winds in summertime.

A vertical resolution of 50 to 150 m can prove beneficial for general meteorological operations in the atmospheric boundary layer (up to 2 km above the surface). However, the tracking system used must be able to sustain acceptable wind measurement uncertainty at the higher vertical resolution if the increased resolution is to be useful.

Very low-uncertainty upper-wind measurements are often specified for range operations such as rocket launches. In this case, special balloons with sculptured surfaces which follow the winds more closely than standard meteorological balloons must be used. The observing schedules required to meet a low-uncertainty specification need careful planning since the observations must be located close to the required site and within a given time frame. The following characteristic of atmospheric variability should be noted. The RMS vector differences between two error-free upper-wind observations at the same height (sampled at the 300 m vertical resolution) will usually be less than 1.5 m $s^{-1}$ if the measurements are simultaneous and separated by less than about 5 km in the horizontal. This will also be the case if the measurements are at the same location, but separated by an interval of less than about 10 min (derived from similar, smaller-scale studies to the representativeness studies of Kitchen (1989)).

#### 13.1.3.4 *Maximum height requirements*

Upper winds measured from balloon-borne equipment, as considered in this chapter, can be required at heights up to and above 35 km at some sites, especially those designated as part of GCOS. The balloons necessary to reach these heights are more expensive than the smaller balloons that will lift the rawinsonde systems to heights between 20 and 25 km. From January 2023, GBON (*Manual on the WMO Integrated Global Observing System* (WMO-No. 1160)) specifies the required spacing and frequency of reports reaching 30 and 10 hPa.

An ideal upper-wind observing network must adequately sample all scales of motion, from planetary scale to mesoscale, in the troposphere and lower stratosphere. The observing network will also identify significant small-scale wind structures using high temporal resolution remote-sensing systems. However, in the middle and upper stratosphere, the predominant scales of motion observed for meteorological operations are larger, primarily the planetary scale and larger synoptic scales. Thus, all the upper-air observing sites in a national network with network spacing being optimized for tropospheric observations may not need to measure to heights above 25 km. Overall operating costs may be less if a mix of the observing systems described in this chapter with the sensing systems described in Volume III of the present Guide is used. If this is the case, national technical infrastructure must be able to provide adequate maintenance for the variety of systems deployed.

### 13.1.4 Methods of measurement

Data on upper winds from balloon-borne systems are mainly acquired by using rawinsonde techniques, although pilot-balloon and radiowind observations may be used when additional upper wind data are required without the expense of launching a radiosonde. Observations from the upper-air stations in the Global Observing System are supplemented over land by measurements from aircraft, wind profilers and Doppler weather radars. In areas with high levels of aircraft operations, the information available from aircraft and radars dominates that available from radiosondes up to heights of about 12 km. Over the sea, data on upper winds are mainly produced by civilian aircraft at aircraft cruise levels. These are supplemented with vertical profiles from rawinsondes launched from ships or remote islands, and also by tracking clouds or water vapour structures observed from meteorological satellites. In 2020 some NWP systems started using line-of-sight wind measurements from a satellite-borne lidar; the largest impact was in the

tropics at upper levels. Sodars (sound detection and ranging), lidars and kite anemometers are also used to provide high temporal resolution winds for specific applications. Low-cost pilotless aircraft technology is being developed for meteorological applications.

Rawinsonde methods for measuring the speed and direction of the wind in the upper air generally depend upon the observation of either the movement of a free balloon ascending at a more or less uniform rate or an object falling under gravity, such as a dropsonde on a parachute. Given that the horizontal motion of the air is to be measured, the target being tracked should not have any significant horizontal motion relative to the air under observation. The essential information required from direct tracking systems includes the height of the target and the measurements of its plan position or, alternatively, its horizontal velocity at known time intervals. The uncertainty requirements in the present volume, Chapter 12, Annex 12.A include the effect of errors in the height or pressure assigned to the wind measurement. It is unlikely that the usual operational uncertainty requirements can be met for levels above the atmospheric boundary layer with any tracking method that needs to assume a rate of ascent for the balloon, rather than using a measurement of height from the tracking system or from the radiosonde attached to the target.

Remote-sensing systems measure the motion of the atmosphere by scattering EMR or sound from one or more of the following targets: hydrometeors, dust, aerosol, or inhomogeneities in the refractive index caused by small-scale atmospheric turbulence or the air molecules themselves.

The direct windfinding methods considered in this chapter use targets whose position can be tracked continuously. While the targets can be tracked by a large number of methods, only two widely used types of methods will be considered here.

#### 13.1.4.1 *Tracking using radionavigation signals*

A radiosonde with the capability of receiving signals from a system of navigational radio transmitters is attached to a target (either an ascending balloon or dropsonde parachute). The most widely used system is to use signals from navigation satellites. In practice, this usually means using the NAVSTAR GPS signals, although other, more recently introduced satellite radionavigation services may also be used. The signals from the satellites are received by a dedicated antenna on the radiosonde. The system will also have a GPS antenna on the ground to receive signals for reference. A GPS engine, either on the ground or in the radiosonde, will decode the signals or allow computation of the radiosonde position in three dimensions as a function of time.

Tracking using radionavigation signals was first achieved on a large scale with the surface-based Omega navigation chain, but once this service was closed most of these radiosonde operators changed to GPS windfinding. Surface-based long-range navigation signals were also used from the LORAN system, described in Lange (1985). By 2016 most LORAN transmitter stations had closed, and most radiosonde users changed to GPS some years earlier.

The use of GPS navaid tracking has increased in routine meteorological operations because of the high degree of automation that can be achieved with this type of windfinding system. The level of maintenance required by navaid ground equipment is also very low. Height measurements from the GPS radiosonde provide the best method for assigning heights for accurate stratospheric temperatures in climate studies.

Most GNSS radiosondes use the meteorological aids (MetAids) frequency band centred at 403 MHz for transmitting data to the ground, but there are a few countries where large-scale civilian radiosonde operation in this band is not feasible, and GNSS radiosondes using the higher frequency MetAids band centred at 1 680 MHz have also been developed.

#### 13.1.4.2 *Tracking using a directional aerial*

In some large national networks the higher cost of GPS radiosonde consumables has meant that non-GPS radiosondes continue to be used with a ground system that tracks the target with a directional aerial measuring azimuth, plus any two of the following parameters: elevation angle, slant range, and height. Measurements are mostly achieved using a radiotheodolite (see 13.2.3) or secondary radar (see 13.2.2.2) to track a radiosonde carried by a balloon. In some cases, an optical theodolite is used to track the balloon. A primary radar (see 13.2.2.1) can also track a reflecting target carried by the balloon, but although this system was quite widely used in the past, it is not in common use now. The difference between primary and secondary radars is that the primary radar detects pulses reflected from its target, while the secondary radar only transmits pulses and does not look for reflections. With a secondary radar, the radiosonde/transponder attached to the balloon receives the radar pulses and then transmits information on the time of receipt back to the radar ground station. Radar and radiotheodolite systems usually have a tracking uncertainty for elevation and azimuth of about 0.1°, while for radar systems, the range uncertainty should normally be less than 30 m.

Modern radiotheodolite systems with antenna dimensions of less than 2 m are best suited for upper-wind measurements when balloon elevations stay above 10° to 15°. Secondary radar systems continue to be used in national networks where sufficient radio-frequency spectrum in the meteorological aids bands is available. Successful directional antennas are operated mostly in the 1 680 MHz band, as the antenna size required for directional tracking at 403 MHz is too large for most modern operational practice.

The choice between using a radiotheodolite or GPS radiosonde for upper-wind measurements will be partly influenced by the maximum slant range expected at the observation site. The GPS windfinding system will provide good measurement uncertainty at very long ranges. The maximum range varies considerably with latitude, with 70 km being adequate in equatorial and polar regions, but with ranges of up to at least 200 km being possible in some mid-latitude temperate zones. Table 13.1 shows the proportion of occasions when certain slant ranges were exceeded for a balloon at 30 km. The data are for stations located in Europe between 50° N and 60° N. The proportions are given for a whole year, but it should be noted that the soundings which exceeded the limits were centred in the winter season.

**Table 13.1. Proportion of occasions when certain slant ranges were exceeded (balloon at 30 km altitude)**

| Slant range exceeded (km) | 140 | 160 | 175 | 190 |
|---|---|---|---|---|
| Proportion of occasions (%) | 5 | 2 | 1 | 0.5 |

## 13.2 UPPER-WIND SENSORS AND INSTRUMENTS

Radiowind systems were originally introduced to allow measurements of upper wind in the presence of clouds. The systems were also capable of low measurement uncertainty at long ranges when balloons were tracked up to heights of 30 km. The use of these systems is now essential to satisfy the majority of modern upper-wind uncertainty requirements. The high degree of automation possible with most modern rawinsonde systems has eliminated the need for operator intervention in most of the measurement cycle. This has major advantages in reducing costs for meteorological operations. For theodolite and radar tracking systems it is important that the system orientation (to true north) is set correctly to avoid bias in the wind direction.

### 13.2.1 Navaid tracking systems

In navaid tracking systems, the radiosonde incorporates an aerial system which receives the signals from a radionavigation system. This radionavigation system will be operated by agencies independent of the national weather Services. The navaid systems currently used operationally for windfinding are the satellite-based GPS giving global coverage, supplemented by other GNSSs in some cases.

One of the main advantages of navaid systems is the simplicity of the ground system, which does not consist of moving parts and does not need very accurate alignment of tracking aerials. This makes the systems suitable for deployment from aircraft and ships, as well as from land-based sites.

In order to keep the costs of the radiosonde to a minimum, the majority of the processing to produce wind measurements is performed after the radiosonde has relayed the navaid signals back to the ground system. Thus, good reception from the radiosonde is essential for this windfinding system; the siting of the ground system aerials must provide a good line of sight to the radiosondes in all directions. As the cost of GPS engines which process the GPS signals reduces, it is possible to perform much of the processing of the GPS signals on the radiosonde, although some processing on the ground is required to incorporate the information from the GPS reference signals received by a local ground-based antenna. In normal operation, the uncertainty of GPS radiosonde position measurements does not reduce significantly with range from the ground stations (see Nash et al., 2011).

The main operational problems with modern operational GPS radiosondes have been when there are radio transmitters in the vicinity at frequencies which cause interference to the reception of GPS signals by the radiosonde.

Height is assigned to upper-wind measurements using the radiosonde geopotential height measurements. It is vital that time stamping of the processed navaid wind data by the ground system is accurately aligned with the time stamping of the radiosonde height measurements.

#### 13.2.1.1 *Availability of navaid signals*

International navigational operations have mainly moved to navigation using signals from the array of GPS navigational satellites orbiting the Earth. These satellite signals have now replaced reliance on signals from fixed terrestrial transmitters. The other global satellite navigation services in operation are GLONASS (Russian Federation), BeiDou (COMPASS, China) and Galileo (Europe). In the past some radiosondes used signals from LORAN terrestrial transmitters – see previous editions of this chapter for more details.

Although the computation of winds using GPS navigation is complex because the satellites move continuously relative to the radiosondes, the development of the GPS radiosonde systems is now mature, and 11 commercial systems were thus able to be tested in Yangjiang, China (see Nash et al., 2011). Very few designs had any significant problems, with most having adequate signal reception (signals from between five and eight satellites received at a given time) and suitable processing algorithms relating the GPS signals received by the radiosonde to the signals received by a reference antenna at the ground station.

#### 13.2.1.2 *Global positioning system*

GNSS radiosondes are now used at about 65% of the active global radiosonde network stations.

NAVSTAR GPS is a low-uncertainty radionavigation system based on radio signals transmitted from a constellation of 25 satellites orbiting the Earth in six planes. Each of the orbital planes intersects the Equator at a spacing of 60°, with the orbit planes inclined at 55° to the polar axis. An individual satellite orbits during a period of about 11 h and 58 min. The constellation

of satellites is configured so that in any location worldwide a minimum of four satellites appear above the horizon at all times, but, in some situations, up to eight satellites may be visible from the ground.

The signals transmitted from the satellites are controlled by atomic frequency standards intended to provide a frequency stability of better than $1 \cdot 10^{-13}$. Each satellite transmits two unique pseudo-random digital ranging codes, along with other information including constellation almanac, ephemeris, UTC and satellite performance. The ranging codes and system data are transmitted using biphase digital spread spectrum technology. The power level of the ranging code signals is –130 dBm, well below thermal background noise.

The following codes are taken into consideration:

(a) The coarse acquisition code is transmitted on a carrier at 1 575.42 MHz. This is modulated by a satellite-specific pseudo-random noise code with a chipping rate of 1.023 MHz. This modulation effectively spreads the coarse acquisition spectrum width to 2 MHz;

(b) The precision code may be replaced by a military controlled Y-code during periods when anti-spoofing is active. The precision code and system data are transmitted coherently on carriers L1 (1 575 MHz) and L2 (1 228 MHz).

The small aerial used for receiving the GPS signals is positioned at the top of the radiosonde body and should be free of obstructions in all directions towards the horizon. The small size provides some protection from the damaging effects of atmospheric electricity. Although the siting of the GPS aerial could cause a conflict with siting of the temperature sensor on the radiosonde, this has now been overcome in the designs available. Usually, GNSS windfinding is combined with temperature and humidity measurements, but there are systems that just provide wind profiles.

The GPS signals need to be pre-processed on the radiosonde to reduce the GPS information to signals that can be transmitted to the ground station on the radiosonde carrier frequency (either as analogue information or as a digital data stream). The pre-processing can be carried out by a variety of techniques. Modern GPS radiosondes use the precision code in a differential mode. This requires simultaneous reception of the GPS signals by a receiver at the ground station as well as the receiver on the radiosonde. Accurate wind computations require signals from a minimum of four satellites (there are occasional gaps in wind profiles because of insufficient good signals). In a differential mode, the phase of the signals received at the radiosonde is referenced to those received at the ground station. This is especially beneficial when the radiosonde is near the ground station, since location errors introduced by propagation delays from the spacecraft to the receivers or by anti-spoofing are similar in both receivers and can be eliminated to a large extent.

GPS tracking systems are able to track accurately at a very high sample rate (rates of a few seconds). Thus, it is possible to measure the modulation of apparent horizontal velocity when the radiosonde swings as a pendulum under the balloon during a period of about 10 to 15 s. Most of the small differences found between GPS radiosonde wind measurements in Yangjiang, China, resulted from the use of different algorithms to filter out the balloon motion, with the algorithm often tuned to suit a particular configuration of radiosonde suspension and not that used in the radiosonde comparison test (Nash et al., 2011). The winds can be derived from a series of positions or from the instantaneous Doppler shift of the signals, or a combination of the two.

One of the practical considerations with GPS radiosondes is the time taken for the GPS tracker on the radiosonde to synchronize with the signals being received from the satellite. It is unwise to launch the radiosonde before this synchronization has been achieved. This may require placing the radiosonde outside for several minutes before launch or, alternatively, a method for transmitting GPS signals to the radiosonde at the location where it is being prepared.

### 13.2.2 Radar

#### 13.2.2.1 *Primary radars*

The essential feature of the radar-tracking technique compared to the radiotheodolite method is that slant range is measured directly together with azimuth and elevation. A primary radar relies on the detection of pulses of ultra-short radio waves reflected from a suitable target carried by the balloon. With a reliable primary radar, the uncertainty requirements for upper winds outlined in the present volume, Chapter 12, can be met in almost all circumstances. Very low-uncertainty specifications for upper winds can be met with high-precision tracking radars, but in practice these are very expensive to use. For measurement uncertainty better than about 1 m $s^{-1}$ it is essential to use balloons with sculptured surfaces (which are also very expensive) rather than standard meteorological balloons.

A radiosonde does not have to be used in order to determine winds with a primary radar, a suitable reflector is enough. Substantial savings from minimizing expenditure on radiosondes might be possible as long as there is a technical support structure to maintain the radar and staff costs are very low. However, the use of primary radar as a windfinding tool to provide cheap operational measurements has not been successful in developing countries, with equipment rarely being maintained; in most countries, GPS radiosondes or radiotheodolites are now used.

#### 13.2.2.2 *Secondary radars*

In secondary radar systems, pulses of energy transmitted from the ground station are received by a responder system carried by the balloon. This can either be a separate transponder package or a feature that is incorporated in the basic radiosonde design. The frequency of the return signal does not necessarily have to be the same as that of the outgoing signal. The time taken between the transmission of the pulse and the response from the responder allows the slant range to be measured directly. This type of system is still in widespread use in large national networks.

The advantage of this technique over a primary radar is that tracking can be sustained to longer ranges for a given power output from the ground transmitter. This is because the energy transmitted by the responder is independent and usually larger than the energy received from the ground transmitter. Thus, the energy received at the ground receiver is inversely proportional to the square of the slant range of the target. The energy received is inversely proportional to the fourth power of the slant range in the case of a primary radar.

The complexity of the system and the maintenance requirements of a secondary radar system usually fall between that of radiotheodolites and primary radars. The network managers must be able to ensure that the systems are well maintained. For instance, in the Russian Federation some older systems (see Table 13.5) with good tracking performance, which are in widespread use but difficult to maintain, are now being replaced by improved ground tracking systems, which are relatively easy to maintain (see Ivanov and Tseitlin, 2005).

### 13.2.3 Radiotheodolite

Radiotheodolite windfinding is best suited to situations where the balloon elevations from the ground station remain high throughout the flight. If the balloon elevations remain above about 16°, most of the upper-wind uncertainty requirements in the present volume, Chapter 12, can be met with relatively small tracking aerials. At low balloon elevations, the measurement errors with radiotheodolites increase rapidly with decreasing elevation, even with larger tracking aerials (see 13.5.3). It is extremely difficult to satisfy the uncertainty requirements detailed in the present volume, Chapter 12, with a radiotheodolite if upper winds are consistently very strong, unless a transponder is used to provide a measurement of the slant range (see 13.2.2.2).

A radiotheodolite is usually used to track the emissions from a radiosonde suspended beneath a weather balloon. A directional aerial coupled to a radio receiver is rotated around the vertical and horizontal axes to determine maximum signal strength using suitable servo-mechanisms.

The radio frequency employed is usually 1 680 MHz. A good aerial design with a diameter of about 2 m should have low sensitivity in its side lobes relative to the main beam; with this size, angular tracking of 0.1° uncertainty can be achieved. If this is the case, the radiotheodolite should be able to track at elevations as low as 6° to 10° without interference between signals received directly from the radiosondes and those received by reflection from adjacent surfaces. Interference between direct and reflected signals is termed multipath interference and is usually the limiting factor in radiotheodolite tracking capability at low elevations. The amount of multipath interference depends very critically on the positioning of the antenna relative to adjacent reflecting surfaces, whether the radiotheodolite is positioned on a roof or on the ground.

Detailed descriptions of the radiotheodolite aerial performance, detection system, servo-controls, and data-processing algorithms should be obtained from the manufacturer prior to purchase. Modern portable radiotheodolites with aerial dimensions of less than 2 m can encounter multipath interference problems at elevations as high as 16°. When multipath interference occurs, the maximum signal will not usually be found in the direction of the balloon. The elevation error varies with time as the multi-path interference conditions change as the radiosonde moves; this can lead to large systematic errors in wind data (greater than 10 m $s^{-1}$).

While the radiotheodolite is tracking the radiosonde, the observed azimuth and elevation angles are transmitted from the radiotheodolite to the ground system computer. The incoming radiosonde measurements give, with time, the variation of geopotential height corresponding to the observed directions. The rates for the change in the position of the balloon can then be derived. The computer should display the upper-wind measurements in tabular or graphical form. The continuity of winds in the vertical will allow the operator to check for faulty tracking. Once the operator is satisfied that tracking is adequate, a suitable upper-wind report can be issued to users.

Balloons will sometimes reverse direction shortly after launch because of marked wind shear just above the surface. The balloon will fly back over the radiotheodolite even though it is launched so that it should move away from the radiotheodolite. If the radiotheodolite is to sustain accurate automated tracking when this happens, it must be capable of very high scan rates in azimuth and elevation. This leads to a more demanding mechanical specification than is necessary for the majority of the flights when the balloon is at longer ranges. In order to reduce the mechanical specification needed for accurate tracking, several modern radiotheodolite designs incorporate interferometric tracking. In these systems, the interferometer compares the phase of the signals arriving at different sections of its tracking aerial in order to determine the position of the transmitting source relative to the aerial orientation. In practice, the phase data are sampled at a high rate using microprocessors, while a simple servo-mechanism orientates the aerial approximately in the direction of the radiosonde. The approximate orientation of the aerial is necessary to provide a good SNR for the interferometer and to minimize the reflections received from the ground. The elevation and azimuth are then derived from a combination of aerial positions, while the direction to the source is deduced by the interferometer from the phase measurements. The measurement uncertainty achieved is similar to that of the better standard radiotheodolites. The interferometric radiotheodolite systems are often more reliable and cheaper to maintain.

### 13.2.4 **Optical theodolite**

Optical theodolites may be used for tracking balloons when the expense of radiowind measurements cannot be met, for example at intermediate times between main ascents or at other locations in a country to fill gaps in the network at lower levels (see Douglas et al., 2008). Operators need significant training and skill if upper-wind measurement errors are not to increase rapidly as the balloon ascends above the boundary layer, but useful periods of observation have been achieved in parts of South America and Africa.

The optical system of the pilot balloon theodolite should be such that the axis of the eyepiece remains horizontal irrespective of the direction in which the telescope is pointed. A pentagonal prism is preferable to a right-angled prism since a slight displacement of the former does not affect the perpendicularity of the two parts of the optical axis.

The focusing eyepiece of the telescope should be fitted with cross-wires or a graticule and should have a magnification of between 20 and 25 times and a field of view of no less than 2°. The mounting of the theodolite should be of robust construction. It should be possible to turn the theodolite rapidly by hand or slowly by friction or worm gearing on the azimuth and elevation circles. These circles should be subdivided into sections no larger than 1° and should be provided with verniers or micrometer hand wheels allowing the angles to be read to 0.05°, with estimation possible to 0.01°. The scales should be arranged and illuminated so that readings can be taken by day and night. Backlash in the gearing of the circles should not exceed 0.025°. Uncertainties in horizontal and vertical collimation should not exceed 0.1°.

The theodolite should be fitted with open sights to facilitate the tracking of a rapidly moving balloon. A secondary telescope with a wide field of view of no less than 8° is also useful for this purpose.

The base of the theodolite should be designed to fit into a standard tripod or other support and should incorporate some means of adjustment to allow accurate levelling. It should be possible to adjust the supports to suit the height of the observer. The theodolite should be of robust construction and should be protected against corrosion.

The system should be used with a suitable computer programme for inputting and checking the observational data for uncertainties.

## 13.3 MEASUREMENT METHODS

### 13.3.1 General considerations concerning data processing

Modern tracking sensors can take readings much more frequently than at the 1 min intervals commonly used with earlier manual systems. The processing of the winds will normally be fully automated using an associated ground system computer. The upper winds will be archived and sometimes displayed by the operator for checking before the information is issued to users.

Thus, the sampling of tracking data is optimal at intervals of 10 s or less. Sampling should be at the highest rate considered useful from the tracking system. High sampling rates make it easier to control the quality of the data with automated algorithms. After editing, the tracking data can then be smoothed by statistical means and used to determine the variation in position with time, if required. The smoothing applied will determine the thickness of the atmospheric layer to which the upper-wind measurement applies. The smoothing will often be changed for different parts of the flight to account for the differing user requirements at different heights and the tracking limitations of the upper-wind system used. If measurement uncertainty is too high at higher levels, the vertical resolution of the measurement may have to be reduced below the optimum requirement to keep the wind measurement uncertainties within acceptable limits. It is also possible to use the Doppler shift of the GNSS signals to give the velocity directly.

Effective algorithms for editing and smoothing may use low-order polynomials (Acheson, 1970), or cubic splines (de Boor, 1978). Algorithms for computing winds from radar and radiotheodolite observations can be found in Hooper (1986a). In general, winds may either be derived from differentiating positions derived from the tracking data, or from the rates of change of the smoothed engineering variables from the tracking system (see Passi, 1978). Many modern systems use this latter technique, but the algorithms must then be able to cope with some singularities in the engineering variables, for instance when a balloon transits back over the tracking site at high elevation.

When the winds computed from the tracking data are displayed for checking, it is important to indicate those regions of the flight where tracking data were missing or judged too noisy for use. Some of the algorithms used for interpolation may not be very stable when there are gaps in the tracking data. It is important to differentiate between reliable measurements of vertical wind shear and shears that are artefacts of the automated data processing when tracking data are absent. Tracking data are often of poor quality early in a balloon ascent. If the upper-wind system is unable to produce a valid wind measurement shortly after launch, it is preferable to leave a gap in the reported winds until valid tracking data are obtained. This is because interpolation between the surface and the first levels of valid data often requires interpolation across layers of marked wind shear in the vertical. The automated algorithms rarely function adequately in these circumstances.

### 13.3.2 Observations using radionavigation systems

The development of observations using GPS winds was first reported by Call (1994) and Kaisti (1995). These systems did not decode the GPS signals received, but they have now been superseded by GPS radiosondes that do decode the signals.

The geometry for using satellite navigation signals is such that GPS windfinding algorithms seem to work most reliably when signals are received from at least five satellites during the ascent. The GPS almanac can be used to identify times when satellite geometry is weak for windfinding. In practice, this rarely occurs with the current satellite configuration and the good satellite reception antenna used with modern radiosondes.

When making upper-wind measurements with navaid tracking systems, the ground system navaid tracker should be accurately synchronized to the navaid transmissions prior to launch. Synchronization is usually achieved by using signals received by a local aerial connected to the ground system receiver. This aerial should be capable of receiving adequate signals for synchronization in all the weather conditions experienced at the site. The ground system should provide clear indications to the operator of the navaid signals available for windfinding prior to launch and also during the radiosonde flight. Where the GPS radiosonde is being used to make height measurements for the operational ascent, it is essential that the height of the local GPS antenna relative to the surface is accurately determined and entered into the ground station processing software.

Once launched, the navaid windfinding systems are highly automated. However, estimates of the expected measurement errors and uncertainties based on the configuration and quality of the navaid signals received would be helpful to the operators. During flight, the operator must be able to identify faulty radiosondes with poor receiver or transmitter characteristics which are clearly providing below-standard observations. These observations need to be suppressed and a re-flight attempted, where necessary.

### 13.3.3 Observations using a directional aerial

Windfinding systems that track using directional aerials require very careful installation and maintenance procedures. Every effort must be made to ensure the accuracy of elevation and azimuth measurements. This requires accurate levelling of the installation and careful maintenance to ensure that the orientation of the electrical axis of the aerial remains close to the mechanical axis. This may be checked by various methods, including tracking the position of local transmitters or targets of known position. Poor alignment of the azimuth has caused additional errors in wind measurement at many upper-air stations in recent years.

The calibration of the slant range of a primary radar may be checked against known stationary targets, if suitable targets exist. The tracking of the radar in general may be checked by comparing radar geopotential heights with simultaneous radiosonde measurements. The corrections to the radar height measurements for tracking errors introduced by atmospheric refraction are discussed in 13.7.

The comparison of radar height measurements with GPS radiosonde geopotential heights may be used to identify radar tracking which fails to meet the standards. Furthermore, if the radar slant range measurements are known to be reliable, it is possible to identify small systematic biases in elevation by comparing radar heights with radiosonde heights as a function of the cotangent of elevation. The typical uncertainties in GPS radiosonde geopotential heights were established for the most widely used radiosondes by Nash et al. (2011).

Both radar and radiotheodolite systems can encounter difficulties when attempting to follow a target at close ranges. This is because the signal strength received by a side lobe of the aerial may be strong enough to sustain automated tracking at short ranges; however, when tracking on a side lobe, the signal strength received will then drop rapidly after a few minutes and the target will apparently be lost. Following target loss, it may be difficult to recover tracking with some systems when low cloud, rain or fog is present at the launch site. Thus, it is necessary to have a method to check that the target is centred in the main beam early in flight. This check could be performed by the operator using a bore-sight, telescope or video camera aligned with the axis of the aerial. The tracking alignment is more difficult to check with an interferometric radiotheodolite, where the mechanical tracking of the radiotheodolite will not necessarily coincide exactly with the observed direction of travel of the balloon.

### 13.3.4 Pilot-balloon observations

The accurate levelling and orientation of the optical theodolite with respect to the true north are an essential preliminary to observing the azimuth and elevation of the moving balloon. Readings of azimuth and elevation should be taken at intervals of no less than 1 min. Azimuth angles should be read to the nearest tenth of a degree. In a pilot-balloon ascent, the elevation angles should be read to the nearest tenth of a degree whenever the angles are 15° or greater. It is necessary to measure elevation to the nearest 0.05° whenever the angles are less than 15°.

If a radiosonde ascent is being followed by optical theodolite, a lower upper-wind measurement uncertainty can be achieved at lower elevations. Thus, the elevation angles should be read to the nearest tenth of a degree whenever the angles are greater than 20°, to the nearest 0.05° whenever the angles are 20° or less, but greater than 15°, and to the nearest 0.01° whenever the angles are 15° or less. Timing may be accomplished by either using a stop-watch or a single alarm clock which rings at the desired intervals.

In single-theodolite ascents, the evaluation of wind speed and direction involves the trigonometric computation of the minute-to-minute changes in the plane position of the balloon. This is best achieved by using suitable computer software.

If lower uncertainty is required, the double-theodolite technique should be used. The baseline between the instruments should be at least 2 km long, preferably in a direction nearly at right angles to that of the wind prevailing at the time. Computations are simplified if the two tracking sites are at the same level. Communication between the two sites by radio or land-line should help to synchronize the observations from the two sites. Synchronization is essential if good measurement accuracy is to be achieved. Recording theodolites, with the readings logged electronically, will be helpful in improving the measurement uncertainty achieved.

For multiple-theodolite tracking, alternative evaluation procedures can be used. The redundancy provided by all the tracking data allows improved measurement uncertainty, but the calculations must be performed on a personal computer (see Lange, 1988; Passi, 1978).

## 13.4 EXPOSURE OF GROUND EQUIPMENT

The tracking system should be provided with a firm foundation on which the equipment can be mounted. Good reception of signals by a local navaid aerial and by the ground system aerial

for the radiosonde is essential if the navaid measurements are to be successful. These aerials should be mounted in positions on the upper-air site where there is a good horizon for reception in all directions.

An appropriate site for a radiotheodolite or radar is on high ground, with the horizon being as free from obstructions as possible. There should be no extensive obstructions subtending an angle exceeding 6° at the observation point. An ideal site would be a symmetrical hill with a downward slope of about 6° for a distance of 400 m, in a hollow surrounded by hills rising to a 1° or 2° elevation.

Upper-wind measurements are usually reported in association with surface-wind measurements. It is preferable that surface wind be obtained from a site close to the balloon launch site. The launch site should be chosen to provide winds that are appropriate to the purpose of the upper-wind measurement. For example, if the upper-wind measurement is required to detect a localized effect influencing an airfield, the optimum location might differ from a site needed to observe mesoscale and synoptic scale motions over a larger area.

## 13.5 SOURCES OF UNCERTAINTY

### 13.5.1 General

Uncertainties in upper-wind measurements are a combination of the errors resulting from imperfect tracking of the horizontal motion of the target, the uncertainties in the height assigned to the target, and the differences between the movement of the target and the actual atmospheric motion.

#### 13.5.1.1 *Target tracking uncertainties*

The relationship between wind errors and tracking errors differs according to the method of observation. For some systems, such as radiotheodolites, the wind errors vary markedly with range, azimuth and elevation, even when the errors of these tracking parameters remain constant with time. On the other hand, wind errors from systems using navaid tracking do not usually vary much with range or height.

The uncertainties caused by the manual computation of wind were evaluated in Vockeroth (1975). It was concluded that the risks of introducing significant uncertainties by using manual methods for wind computations (such as plotting tables, slide rules, and so forth) were too great, and that upper-wind computations should be automated as far as possible.

The measurement uncertainty of all upper-wind systems varies from time to time. This variation may occur for short periods during a given target flight, when tracking temporarily degrades, or during an entire flight, for instance if the transmitted signals from a navaid radiosonde are faulty. At some locations, the accuracy of upper-wind tracking may gradually degrade with time over several months because of either instability in the tracking capability or the set-up of the ground system. In all cases, it would be helpful if estimates of wind measurement uncertainties were derived by the upper-wind systems in real time to supplement the reported upper-wind measurements. The reported errors would allow poorer quality measurements to be identified and less weight would be given in numerical analyses. The reporting of uncertainties could be achieved in practice by using the appropriate BUFR tables (*Manual on Codes* (WMO-No. 306), Volume I.1).

When uncertainties in target tracking start to introduce unacceptable wind uncertainties at a given vertical resolution, the situation is usually compensated by computing the winds at a lower vertical resolution.

The practice of reducing the vertical resolution of upper-wind measurements in steps through the upper troposphere and lower stratosphere was mainly adopted to overcome the tracking

limitations of radiotheodolites. This practice is not justified by the actual vertical structure observed in the atmosphere. Many of the larger vertical wind shears are found in the upper levels of jet streams at heights between 10 and 18 km (see, for instance, the detailed vertical wind profiles presented in Nash, 1994).

#### 13.5.1.2 *Height assignment uncertainties*

Height assignment errors for rawinsonde winds in the troposphere and lower stratosphere will be the same as those discussed for height measurements in the present volume, Chapter 12. These errors will be highest for radiosondes using pressure sensors in the upper stratosphere, and would be most significant for NWP or climate studies if there were significant wind shear in the vertical, such as in the polar-night vortex (see Figure 13.1(b)).

For pilot balloons tracked with a single theodolite, height is derived from time into flight, and the rate of ascent for the balloon is assumed. In practice, it is difficult to launch balloons with a precisely determined rate of ascent. Thus, where there is significant vertical shear in the vertical at low levels, possibly associated with significant differences in vertical velocity from thermals, pilot-balloon measurements could be adversely affected by the height assignment uncertainties.

There should be no discrepancies between the times assigned to wind observations and those assigned to the associated radiosonde measurements. In some cases, the wind timing is not initiated at the same time as that of the radiosonde, in others synchronization is lost during flight for a variety of reasons. Times assigned to the reported winds are not always those corresponding to the data sample used to compute the wind, but rather to the time at the beginning or end of the sample, resulting in an offset or bias. All types of timing error could produce large uncertainties in the heights assigned to wind measurements and need to be eliminated during prototype testing if reliable operations are to be achieved.

#### 13.5.1.3 *Target motion relative to the atmosphere*

The motion of the target relative to the air matters most for systems with the highest tracking accuracy and highest vertical resolution. For instance, the swinging of the GPS radiosonde under a balloon is clearly visible in the GPS tracking measurements and must be filtered out as far as possible. The filtering methods are generally proprietary and unpublished. The amplitude of pendulum oscillations in the raw data has probably increased over time with the use of longer suspensions to reduce wake effects on stratospheric temperature measurements.

The balloon motion relative to the atmosphere, introduced by the shedding of vortices by the balloon wake, may result in uncertainties as large as 1 to 2 m $s^{-1}$ ($2\sigma$ level or 95% confidence) when tracking small pilot balloons (50 g weight) at vertical resolutions of 50 m. Balloon motion uncertainties are less significant in routine operational measurements (vertical resolutions of about 300 m) where measurements are obtained by tracking larger balloons (weight exceeding 350 g) (MacCready, 1965).

The horizontal slip of the dropsonde parachutes relative to the atmosphere may also be the limiting factor in the uncertainty of GPS dropsonde measurements. The descent rates used in dropsonde deployments are usually about twice the ascent rate of operational radiosonde balloons.

### 13.5.2 Uncertainties in the global positioning system windfinding systems

In theory, GPS windfinding systems using coarse acquisition ranging codes in a differential mode should be capable of measuring winds to an uncertainty of 0.2 m $s^{-1}$. The estimates of uncertainty in Table 13.2 were made on the basis of recent WMO tests of GPS radiosondes. The main difference between systems comes from the filtering applied to the winds to remove the motion of the radiosonde relative to the balloon. This motion is partly a regular pendulum of the

**Table 13.2. Random vector uncertainty ($k$ = 2) and systematic bias for good quality GPS navaid windfinding systems during the WMO Intercomparison of High-quality Radiosonde Systems in Yangjiang, China**

| *Height range* | *Systematic bias ($m\ s^{-1}$)* | *RMS vector uncertainty at 2 km vertical resolution ($m\ s^{-1}$)* | *RMS vector uncertainty at 300 m vertical resolution ($m\ s^{-1}$)* | *RMS vector uncertainty at 100 m vertical resolution ($m\ s^{-1}$)* |
|---|---|---|---|---|
| Lower troposphere 0–8 km | Up to ±0.05 | 0.06 – 0.15 | 0.12 – 0.50 | 0.3 – 0.7 |
| Upper troposphere 8–17 km | Up to ±0.10 | 0.1 – 0.4[a] | 0.3 – 0.9[a] | 0.4 – 1.4[a] |
| Stratosphere 17–34 km | Up to ±0.15 | 0.15 – 0.40[b] | 0.3 – 0.8[b] | 0.4 – 1.1[b] |

Notes:
a Poorest performance found at heights near 16 km
b Poorest performance found at heights greater than 28 km

radiosondes under the balloon, and partly some additional irregular rotation and displacement in reaction to differences between the winds experienced by the balloon and the radiosonde as the balloon ascent progresses.

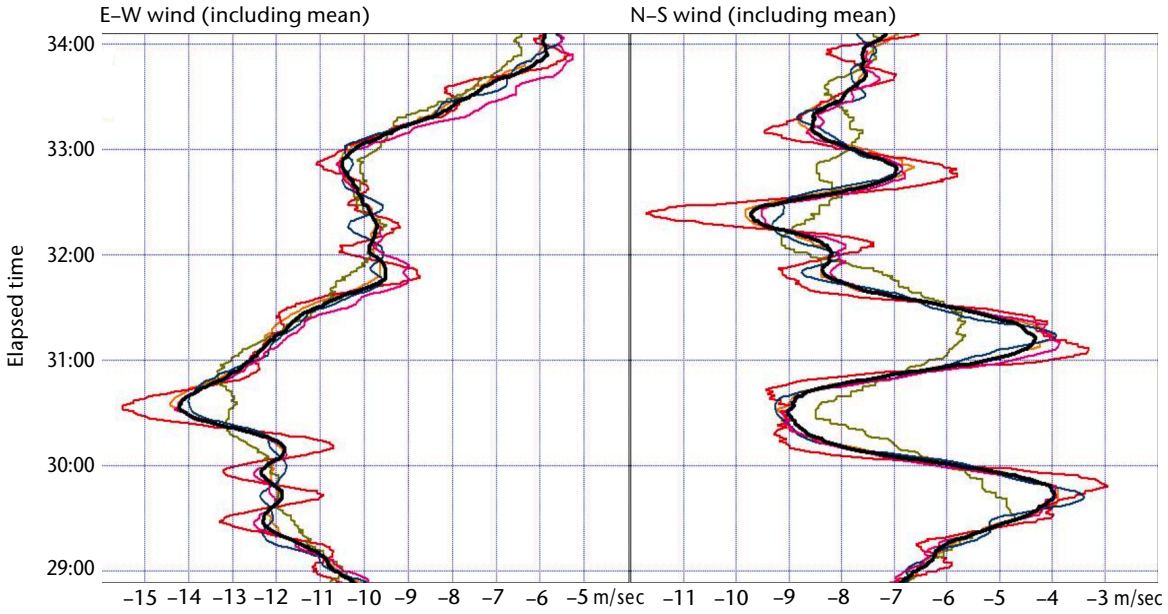
Examples of simultaneous observations of winds obtained in the upper troposphere from the GPS radiosondes in the WMO Intercomparison of High-quality Radiosonde Systems are shown in Figure 13.2. Only excerpts from the flights are shown because it is only when looking at a short sample of data from the flights that the differences can be seen, as the general agreement is much better than what the standard has been for earlier operational wind measurements.

The extracts in Figure 13.2 show that nearly all the systems agree well in resolving vertical structure with peaks in the wave structures separated by about 90 s, but not to the same extent for fluctuations where the peaks were separated by 40 s or less. Thus, the vertical wavelengths that generally resolved without any ambiguity were 600 m, but those where there was considerable ambiguity corresponded to 200 m or less. One system in Figure 13.2(a) was over-smoothed compared to the others, while one system in Figure 13.2(b) attempted to fit straight lines to the GPS measurements; both behaviours lead to outliers from the correct values on occasion.

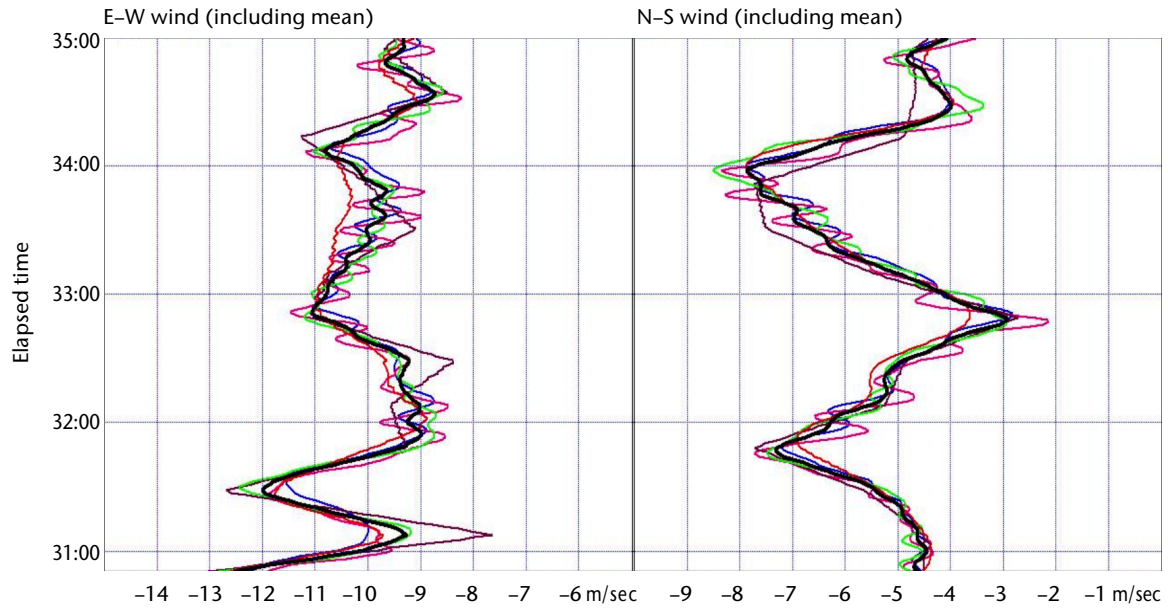
These extracts, representing neither the best nor the worst, suggest that the processing of GPS wind measurements is relatively mature and that a large number of manufacturers have achieved satisfactory results. This was confirmed when the statistics from the 60 flights performed with operational GPS radiosondes in Yangjiang were generated (see Table 13.2). In this table, the wind differences (obtained from about 30 comparison flights) were averaged over either 2 min, 30 s or 10 s, and the best performance was attributed to the two systems with the lowest RMS vector differences. The uncertainties found in Table 13.2 are good enough to meet the optimum user requirement for winds stated in the present volume, Chapter 12, Annex 12.A.

In time, the differences in the filtering of the GPS position measurements to minimize the effects of the radiosonde measurements relative to the balloon will probably reduce compared to the ranges indicated in Table 13.2. However, the irregular movements (as opposed to the relatively smooth pendulum motion) of the radiosonde relative to the balloon will limit the agreement that can be obtained between two radiosondes in a test flight. For the same reason, the error in an individual radiosonde measurement can be expected to be larger than might be computed given the expected uncertainty of radiosonde position that can be obtained with the satellite radionavigation systems.

The external balloon of the double balloons used in China often burst near 16 km, and the resulting perturbations on the stability of the radiosonde motion may have led to the largest RMS vector uncertainties near 16 km in Table 13.2. In United Kingdom tests (60 flights), conducted over several seasons in 2009/2010 on GPS radiosondes from two different manufacturers present in Yangjiang, results in the lower troposphere and the stratosphere were similar to those




(a) Flight 33: Jinyang, InterMet, Lockheed Martin Sippican, MODEM and Vaisala




(b) Flight 34: Changfeng, Graw, Huayun, Meisei and Meteolabor

**Figure 13.2. Extracts from intercomparison flights of GPS winds made at Yangjiang, China, during the WMO Intercomparison of High-quality Radiosonde Systems (Nash et al., 2011)**

in Table 13.2. However, RMS vector wind uncertainties in the upper troposphere were in the range 0.3 to 0.6 m $s^{-1}$ at a vertical resolution of 100 m, and 0.2 to 0.5 m $s^{-1}$ at a vertical resolution of 300 m. Thus, for these two systems the fine structure in the wind measurements in the United Kingdom in the upper troposphere agreed more closely than for the systems in Yangjiang.

On occasion, a GPS radiosonde malfunctions and does not report winds throughout a flight when reporting temperature and humidity until the balloon bursts. On some occasions, radio-frequency interference from an external source causes problems, and winds may have larger errors. The processing software needs to be able to inform the operator when problems like these are present, as it is difficult to distinguish between real atmospheric structure and measurements with large random uncertainties (for example, see the wind profile in Figure 13.3).

### 13.5.3 Uncertainties of systems using a directional aerial

The relationship between vector wind errors and the errors of the actual tracking measurements can be expressed as an approximate function of height and mean wind (or ratio of the latter to the mean rate of ascent of the balloon). The relationships for random errors in primary radar and radiotheodolite wind measurements are as follows:

(a) Primary or secondary radar measuring slant range, azimuth and elevation:

$$\varepsilon_{\mathrm{v}}{}^2 = 2 \cdot \left[ \varepsilon_{\mathrm{r}}{}^2 \cdot Q^2 \Big/ \left( Q^2 + 1 \right) + \varepsilon_{\theta}{}^2 \cdot h^2 + \varepsilon_{\varphi}{}^2 \cdot h^2 \cdot Q^2 \right] \Big/ \tau^2 \qquad (13.3)$$

(b) Optical theodolite or radiotheodolite and radiosonde measuring azimuth, elevation angle and height:

$$\varepsilon_{\mathrm{v}}{}^2 = 2 \cdot \left[ \varepsilon_{h}{}^2 \cdot Q^2 + \varepsilon_{\theta}{}^2 \cdot h^2 \cdot \left( Q^2 + 1 \right)^2 + \varepsilon_{\varphi}{}^2 \cdot h^2 \cdot Q^2 \right] \Big/ \tau^2 \qquad (13.4)$$

where $\varepsilon_{\mathrm{v}}$ is the vector uncertainty in computed wind; $\varepsilon_{r}$ is the random uncertainty in the measurement of slant range; $\varepsilon_{\theta}$ is the random uncertainty in the measurement of elevation angle; $\varepsilon_{\varphi}$ is the random uncertainty in the measurement of azimuth; $\varepsilon_{h}$ is the random uncertainty in height (derived from pressure measurement); $Q$ is the magnitude of mean vector wind up to height $h$ divided by the mean rate of ascent of the balloon up to height $h$; and $\tau$ is the time interval between samples.

Table 13.3 illustrates the differences in vector wind uncertainty obtained with these two methods of upper-wind measurement. The mean rate of ascent used in upper-wind measurements will usually be in the range of 5 to 8 m $s^{-1}$. The vector wind uncertainty values are derived from equations 13.3 and 13.4 for various heights and values of $Q$, for a system tracking with the following characteristics: $\varepsilon_{r}$ 20 m; $\varepsilon_{\theta}$ 0.1°; $\varepsilon_{\varphi}$ 0.1°; $\varepsilon_{h}$ height uncertainty equivalent to a pressure uncertainty of 1 hPa; $\tau$ 1 min.

Table 13.3 demonstrates that measurements with a radio (or optical) theodolite clearly produce higher uncertainty winds for a given tracking accuracy than primary or secondary radars.

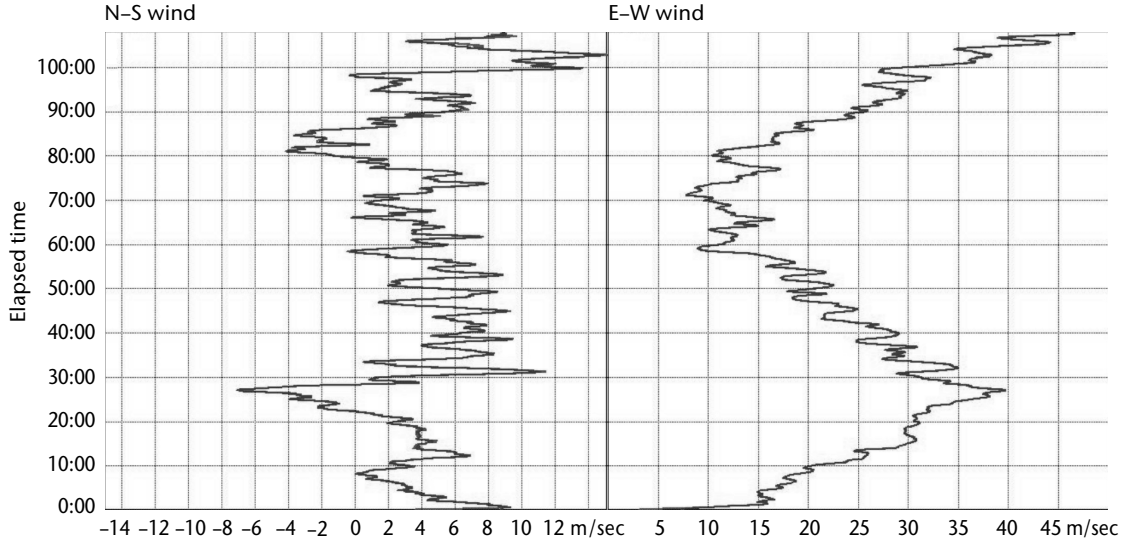



**Figure 13.3. Example of a vertical wind profile measured independently by GPS radiosondes from two different manufacturers at Camborne, United Kingdom, and showing the small-scale structure which is present in many correct measurements. The radiosonde processing software needs to indicate which parts of a flight are less reliable when the reception of GPS signals is clearly not as reliable as usual.**

In the expressions for vector error in the computed winds in equations 13.3 and 13.4, the first two terms within the square brackets represent the radial error and the error in the winds observed with the same azimuth as the tracking aerial. The third term in the square brackets represents the tangential error, the error in winds observed at right angles to the azimuth of the tracking aerial. With these types of upper-wind systems, the error distribution is not independent of the directions and cannot be adequately represented by a single parameter. Thus, the values in Table 13.3 indicate the size of the uncertainties but not the direction in which they act.

When the tangential and radial uncertainties are very different in size, the error distribution is highly elliptic and the combined uncertainties tend to concentrate either parallel to the axis of the tracking antenna or perpendicular to the axis. Table 13.4 shows the ratio of some of the tangential and radial uncertainties that are combined to give the vector uncertainties in Table 13.3. Values above 3 in Table 13.4 indicate situations where the tangential error component dominates. Thus, in radar windfinding, the tangential errors dominate at longer ranges (high mean winds and hence high $Q$ values, plus largest heights). With radiotheodolite windfinding, the radial errors dominate at longer ranges and the ratios become very much smaller than 1. Errors in elevation angle produce the major contribution to the radiotheodolite radial uncertainties. However, random uncertainties in the radiosonde height make the most significant contribution at high altitudes when values of $Q$ are low.

The results in Tables 13.3 and 13.4 are based on a theoretical evaluation of the uncertainties from the different types of systems. However, it is assumed that winds are computed from a simple difference between two discrete samples of tracking data. The computations take no account of the probable improvements in uncertainty from deriving rates of change of position from large samples of tracking information obtained at high temporal resolution. Table 13.5 contains estimates of the actual measurement uncertainty achieved by a variety of radars and radiotheodolites in the four phases of the WMO International Radiosonde Comparison (see 13.6.1.2 for references to the tests).

Of the three radiotheodolites tested in the WMO International Radiosonde Comparison, the Japanese system coped best with high $Q$ situations, but this system applied a large amount of smoothing to elevation measurements and did not measure vertical wind very accurately in the upper layers of the jet streams. The smaller portable radiotheodolite deployed by the United States in Japan had the largest wind errors at high $Q$ because of problems with multipath interference.

**Table 13.3. 90% vector uncertainty (m s$^{-1}$) as a function of height and ratio $Q$ of mean wind to rate of ascent**

| | *Radar* | | | | | | *Radiotheodolite* | | | | | |
|---|---|---|---|---|---|---|---|---|---|---|---|---|
| $Q$ | $\varepsilon_v$ *5 km* | $\varepsilon_v$ *10 km* | $\varepsilon_v$ *15 km* | $\varepsilon_v$ *20 km* | $\varepsilon_v$ *25 km* | $\varepsilon_v$ *30 km* | $\varepsilon_v$ *5 km* | $\varepsilon_v$ *10 km* | $\varepsilon_v$ *15 km* | $\varepsilon_v$ *20 km* | $\varepsilon_v$ *25 km* | $\varepsilon_v$ *30 km* |
| 1 | 1 | 1 | 1.5 | 1.5 | 2.5 | 2.5 | 1 | 1.5 | 3 | 5.5 | 9 | 25 |
| 2 | 1 | 1.5 | 2.5 | 3 | 4 | 4 | 5 | 4 | 6.5 | 11 | 19 | 49 |
| 3 | 1.5 | 2.5 | 3 | 4 | 5 | 6 | 4 | 7 | 11 | 19 | 30 | 76 |
| 5 | 1.5 | 3 | 5 | 6 | 8 | 10 | 9 | 18 | 27 | 42 | 59 | 131 |
| 7 | 2.5 | 5 | 7 | 9 | 11 | 13 | 18 | 34 | 51 | 72 | 100 | 194 |
| 10 | 3 | 6.5 | 10 | 13 | 16 | 19 | 34 | 67 | 100 | 139 | 182 | 310 |

Notes:

a This table does not include the additional uncertainties introduced by multipath interference on radiotheodolite observations. Additional uncertainties can be expected from these effects for values of $Q$ between 7 and 10.

b In practice, radiotheodolite wind observations are smoothed over thicker layers than indicated in these calculations at all heights apart from 5 km. Thus, at heights of 15 km and above, the radiotheodolite uncertainties should be divided by at least a factor of four to correspond to operational practice.

**Table 13.4. Ratio of upper-wind error components ($\alpha_{\varepsilon v}$ = tangential error/radial error $\alpha$)**

| | *Radar* | | | | | | *Radiotheodolite* | | | | | |
|---|---|---|---|---|---|---|---|---|---|---|---|---|
| $Q$ | $\alpha_{\varepsilon v}$ *5 km* | $\alpha_{\varepsilon v}$ *10 km* | $\alpha_{\varepsilon v}$ *15 km* | $\alpha_{\varepsilon v}$ *20 km* | $\alpha_{\varepsilon v}$ *25 km* | $\alpha_{\varepsilon v}$ *30 km* | $\alpha_{\varepsilon v}$ *5 km* | $\alpha_{\varepsilon v}$ *10 km* | $\alpha_{\varepsilon v}$ *15 km* | $\alpha_{\varepsilon v}$ *20 km* | $\alpha_{\varepsilon v}$ *25 km* | $\alpha_{\varepsilon v}$ *30 km* |
| 1 | 1/2 | 1 | 1 | 1 | 1 | 1 | 1/3 | 1/2 | 1/3 | 1/4 | 1/5 | 1/13 |
| 2 | 1 | 1 | 2 | 2 | 2 | 2 | 1/3 | 1/3 | 1/3 | 1/4 | 1/6 | 1/13 |
| 3 | 1 | 2 | 2 | 3 | 3 | 3 | 1/4 | 1/4 | 1/4 | 1/5 | 1/6 | 1/13 |
| 5 | 1 | 3 | 4 | 4 | 5 | 5 | 1/5 | 1/5 | 1/6 | 1/6 | 1/7 | 1/14 |
| 7 | 3 | 5 | 5 | 6 | 6 | 7 | 1/7 | 1/7 | 1/7 | 1/7 | 1/9 | 1/14 |
| 10 | 4 | 7 | 8 | 9 | 9 | 9 | 1/10 | 1/10 | 1/10 | 1/11 | 1/11 | 1/16 |

**Table 13.5. Estimates of the typical random vector uncertainties (2$s$ level, unit: m s$^{-1}$) in upper-wind measurements obtained during the WMO International Radiosonde Comparison (estimates of typical values of $Q$ and $\alpha_{\varepsilon v}$ for each of the four phases are included)**

| *System* | $\varepsilon_v$ *3 km* | $\alpha_{\varepsilon v}$ *3 km* | $Q$ *3 km* | $\varepsilon_v$ *18 km* | $\alpha_{\varepsilon v}$ *18 km* | $Q$ *18 km* | $\varepsilon_v$ *28 km* | $\alpha_{\varepsilon v}$ *28 km* | $Q$ *28 km* | *Test site* |
|---|---|---|---|---|---|---|---|---|---|---|
| Primary radar (United Kingdom) | 1.1 | 1 | 3.5 | 2.1 | 1.3 | 5 | 2.7 | 1.6 | 5 | United Kingdom[a] |
| Radiotheodolite (United States) | 2.1 | ≈ 1 | 1.5 | 4.8 | ≈ 1 | 2.5 | 5.2 | ≈ 1 | 1 | United Kingdom |
| Radiotheodolite (United States) | 2.8 | ≈ 1 | 2.5 | 10.4 | 0.4 | 6 | 9 | 0.33 | 4 | United States |
| Radiotheodolite portable | 1.5 | ≈ 1 | < 1 | 4.8 | ≈ 1 | 3 | 5.8 | ≈ 1 | 1.5 | Kazakhstan |
| Radiotheodolite portable | 2.2 | ≈ 1 | 1.5 | 12 | 0.31 | 5.5 | 9 | 0.23 | 4 | Japan |
| Radiotheodolite (Japan) | 1.7 | ≈ 1 | 1.5 | 6.4 | 0.48 | 5.5 | 4.7 | 0.48 | 4 | Japan |
| Secondary radar (AVK, Russian Federation) | 1.5 | ≈ 1 | < 1 | 2.6 | ≈ 1 | 3 | 2.6 | ≈ 1 | 1.5 | Kazakhstan |
| Secondary radar (China) | 1.5 | ≈ 1 | <1 | 3.8 | ≈ 1 | 3 | 3.4 | ≈ 1 | 1.5 | Kazakhstan |

Note:
a Data obtained in the United Kingdom test following Phase I of the WMO International Radiosonde Comparison (See Edge et al., 1986).

The ellipticity of the error distributions for radar and radiotheodolite observations showed the tendencies predicted at high values of $Q$. However, the ellipticity in the uncertainties was not as high as that shown in Table 13.4, probably because the random uncertainties in the rates of change of the azimuth and elevation were, in practice, smaller than those taken for Table 13.4.

In the WMO Intercomparison of High-quality Radiosonde Systems in Yangjiang, China (Nash et al., 2011), China used a modern secondary radar operating at 1 680 MHz with the Daqiao radiosonde system. When winds were strong in the lower troposphere, values of $Q$ at a height of about 4 km were between 2 and 3, range was about 15 km, and the RMS vector uncertainties

($k = 2$) in the winds were about 1 to 1.2 m s$^{-1}$ with an ellipticity between 1 and 1.3. Towards the ends of the flights in the stratosphere, $Q$ was again about 2.5 on average, but at the longer ranges of 70 to 100 km, $\varepsilon_v$ for $k = 2$ was about 2.7 m s$^{-1}$ and the ellipticity was 2. The reference winds in Yangjiang were GPS winds at a high vertical resolution, better than 150 m, whereas the vertical resolution of the working reference in Kazakhstan was 300 m at the best. Thus, the modern Chinese secondary radar was working well and is an improvement on the previous 403 MHz system.

### 13.5.4 Uncertainties in pilot-balloon observations

The instrumental errors of a good optical theodolite are not likely to exceed ±0.05°. The errors may vary slowly with azimuth or elevation but are small compared with the errors introduced by the observer. Errors of reading scales should not exceed 0.1°. These errors become increasingly important at long ranges and when working at low elevations.

In single-theodolite ascents, the largest source of uncertainty is the balloon rate of ascent. This uncertainty arises from variations in filling the balloon with gas, in the shape of the balloon, and in the vertical velocity of the atmosphere through which the balloon ascends. A given proportional error in the rate of ascent results in a proportional error in the height of the balloon and, hence, as modified by elevation angle, a proportional error in wind speed.

In double-theodolite ascents, the effect of system errors depends upon the method of evaluation adopted. Uncertainty analyses have been provided by Schaefer and Doswell (1978).

### 13.5.5 Representativeness uncertainties

Most modern radiowind measurements observe small-scale variations in wind in the atmosphere which are not represented in current NWP models. Thus, for instance, when GPS wind component profiles are compared directly with numerical model output from global models, the standard deviation of observation/numerical model output ($k = 2$) in mid-latitudes is usually between 4 and 6 m s$^{-1}$ in the lower troposphere, and between 4 and 9 m s$^{-1}$ in the upper troposphere, that is, it is always much larger than the instrumental vector uncertainties quoted in Table 13.2 for a vertical resolution of 300 m. Some of this discrepancy will result from the high uncertainty of the reported winds as noted earlier in 13.1.3.2. One cause of large discrepancies for individual profiles can be gravity waves – partially represented in current NWP models.

Root-mean-square vector differences between radiosonde upper-wind measurements 2, 6, 18 and 54 h apart have been computed from the time series of measurements produced in the WMO Intercomparison of High-quality Radiosonde Systems in Yangjiang, China (Nash et al., 2011), applying the technique used by Kitchen (1989). The results are shown as a function of height in Figure 13.4.

The RMS vector uncertainty in wind can then be expected to relate to time separation using the relationship, after Kitchen (1989):

$$\left(\tau_v\left(\Delta t\right)\right)^2 = \left(b_v \Delta t^{\gamma}\right)^2 + \left(\tau_{v(\text{small scale})}\left(\Delta t\right)\right)^2 \qquad (13.5)$$

where $\tau_V(\Delta t)$ is the RMS vector difference between wind measurements separated by the time separation $\Delta t$; and $b_V \Delta t^{\gamma}$ is the structure function representing the RMS deviation due to synoptic scale and mesoscale changes with time, with $b_V$ a constant and $\gamma$ a constant. In Yangjiang, $\gamma$ had a value of between 0.5 and 0.6 for wind measurements in the troposphere at time separations between 6 and 54 h. Finally, $\tau_{V(\text{small scale})}$ $(\Delta t)$ is the RMS vector difference in upper wind from small-scale structures, such as quasi-inertial gravity waves, turbulent layers or cloud-scale structure.

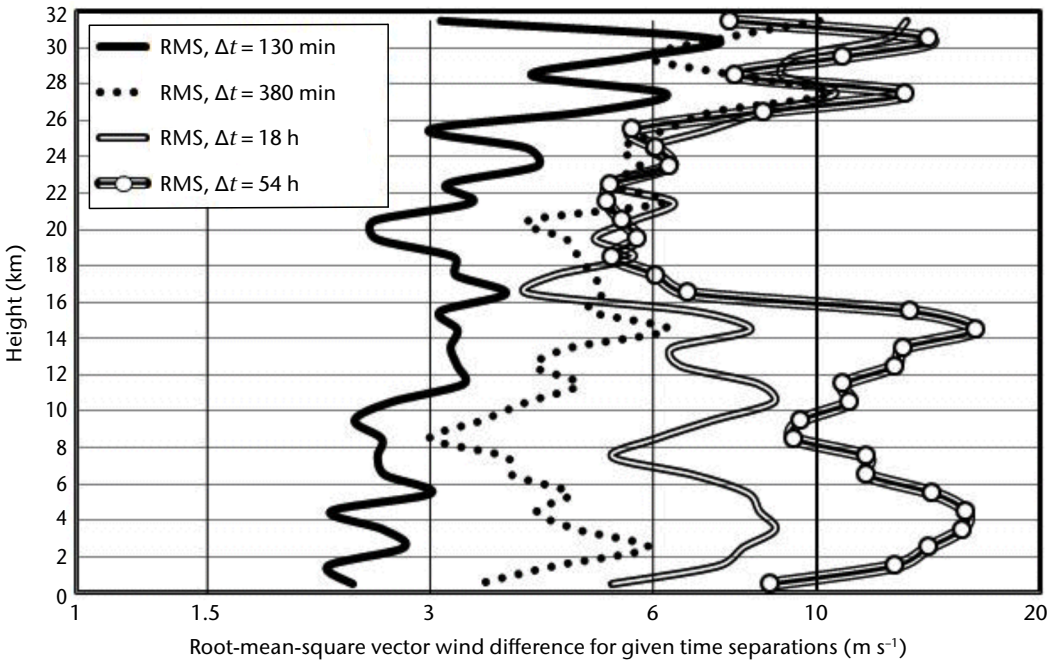



**Figure 13.4. RMS vector wind differences ($k$ = 1) for time separations of 2, 6, 18 and 54 h for 11 pairs of observations, with vertical resolution of 1 km, from the WMO Intercomparison of High-quality Radiosonde Systems in Yangjiang, China, in July 2010. The contributions from instrumental error have been removed from the differences.**

In the troposphere in Yangjiang, the small-scale structure RMS vector difference was about 2 m $s^{-1}$ ± 0.5 m $s^{-1}$, while the synoptic and mesoscale RMS vector difference was between 2 and 3 m $s^{-1}$ at a time separation of 2 h, increasing to about 7 m $s^{-1}$ at a time separation of 18 h. These values are of similar magnitude to the values found by Kitchen (1989) in the lower and middle troposphere in the United Kingdom. The RMS vector differences were higher in the upper troposphere in the United Kingdom because of the synoptic scale variations associated with mid-latitude jet streams. Whereas the synoptic and mesoscale vector difference might be expected to fall to lower than 1 m $s^{-1}$ at a time separation of 40 min in Yangjiang, there is no information on the time separations necessary to reduce the small-scale RMS vector difference to a value less than 1 m $s^{-1}$. This is why, to get close agreement between wind measurements, or for the measurement to represent the conditions in the atmosphere at a given time with low uncertainty, the measurement needs to be performed at a time separation much lower than 20 min, as stated in 13.1.3.3.

In Yangjiang, the small-scale fluctuations associated with quasi-inertial gravity waves dominate the variation of RMS vector difference with time, and it is not possible to fit a structure function for synoptic and mesoscale variation with time, as was also found in the United Kingdom in summertime conditions by Kitchen. The RMS vector differences at 18-hour time separation in Yangjiang were in the range 5 to 9 m $s^{-1}$, values of similar magnitude to those found in the United Kingdom.

Thus, representativeness errors in the winds will normally be most influenced by the small-scale variations, with synoptic and mesoscale variations most likely to be significant in association with the structures found with jet streams in the upper troposphere and lower stratosphere. As a result, there will be variation between different sites, and the values discussed here are only a snapshot of one type of location and synoptic condition, which did include measurements with typhoons approaching and leaving the area.

## 13.6 COMPARISON, CALIBRATION AND MAINTENANCE

### 13.6.1 Comparison

Radiotheodolite and radar upper-wind systems are usually complex, with a number of different failure modes. It is not uncommon for the systems to suffer a partial failure, while still producing a vertical wind structure that appears plausible to the operators. Many of the systems need careful alignment and maintenance to maintain tracking accuracy. GNSS-based systems are usually more reliable and easier to use.

The wind measurement uncertainty of operational systems can be checked by reference to observation monitoring statistics produced by NWP centres. The monitoring statistics consist of summaries of the differences between the upper-wind measurements from each site and the short-term forecast (background) fields for the same location. With current data assimilation and analysis techniques, observation errors influence the meteorological analysis fields to some extent. Thus, it has been shown that observation errors are detected reliably by using a short-term forecast from an analysis performed 6 or 12 h before the observation time. The root-mean-square fit in the stratosphere can be improved by 5%–10% by using the actual radiosonde time and location rather than treating the ascent as instantaneous and vertical (Ingleby et al., 2018).

The performance of upper-wind systems can also be compared with other systems of known measurement quality in special tests. These tests can allow tracking errors to be evaluated independently of height assignment errors.

Both types of comparisons may be interpreted using the statistical methods proposed in Lange (1989).

#### 13.6.1.1 *Operational monitoring by comparison with forecast fields*

The statistics for daily comparisons between operational wind measurements and short-term forecast fields of NWP models are available through the WIGOS Data Quality Monitoring System (https://wdqms.wmo.int/).

Interpretation of the monitoring statistics for upper winds is not straightforward. The random uncertainties in the forecast fields are of similar magnitude to those in the upper-wind system if it is functioning correctly. The forecast errors vary with geographical location, and guidance for their interpretation from the NWP centre may be necessary. However, it is relatively easy to identify upper-wind systems where the uncertainties are much larger than normal. In recent years, about 1% or 2% of the upper-wind systems in the global network have been identified as faulty. The system types associated with faulty performance have mainly been radiotheodolites and secondary radar systems.

Summaries of systematic biases between observations and forecast fields over several months or for a whole year are also helpful in identifying systematic biases in wind speed and wind direction for a given system. Small misalignments of the tracking aerials of radiotheodolites or radars are a relatively common fault.

#### 13.6.1.2 *Comparison with other windfinding systems*

Special comparison tests between upper-wind systems have provided a large amount of information on the actual performance of the various upper-wind systems in use worldwide. In these tests, a variety of targets are suspended from a single balloon and tracked simultaneously by a variety of ground systems. The timing of the wind reports from the various ground stations is synchronized to better than 1 s. The wind measurements can then be compared as a function of time into flight, and the heights assigned to the winds can also be

compared independently. The interpretation of the comparison results will be more reliable if at least one of the upper-wind systems produces low-uncertainty wind measurements with established error characteristics.

A comprehensive series of comparison tests was performed between 1984 and 1993 as part of the WMO International Radiosonde Comparison. Phases I and II of the tests were performed in the United Kingdom and United States, respectively (Nash and Schmidlin, 1987). Phase III was performed by the Russian Federation at a site in Kazakhstan (Ivanov et al., 1991), and Phase IV was performed in Japan (Yagi et al., 1996). Further tests in Brazil in 2001 (da Silveira et al., 2006) were performed specifically to identify problems in GPS windfinding in the tropics, and this led to improved GPS radiosonde systems which were also tested in Mauritius in 2005 (Nash et al., 2006) and most comprehensively in Yangjiang, China in 2010 (Nash et al., 2011).

The information in Tables 13.2 and 13.5 was primarily based on results from the WMO International Radiosonde Comparison and additional tests performed to the same standard as the WMO tests.

Now that the development of GPS windfinding systems is mature, most of these systems can be used as reliable travelling standards for upper-wind comparison tests in more remote areas of the world.

### 13.6.2 Calibration

The calibration of slant range should be checked for radars using signal returns from a distant object whose location is accurately known. Azimuth should also be checked in a similar fashion.

The orientation of the tracking aerials of radiotheodolites or radars should be checked regularly by comparing the readings taken with an optical theodolite. If the mean differences between the theodolite and radar observations of elevation exceed 0.1°, the adjustment of the tracking aerial should be checked. When checking azimuth using a compass, the conversion from geomagnetic north to geographical north must be performed accurately.

With navaid systems, it is important to check that the ground system location is accurately recorded in the ground system computer. The navaid tracking system needs to be configured correctly according to the manufacturer's instructions and should be in stable operation prior to the radiosonde launch.

### 13.6.3 Maintenance

Radiotheodolites and radars are relatively complex and usually require maintenance by an experienced technician. The technician will need to cope with both electrical and mechanical maintenance and repair tasks. The level of skill and frequency of maintenance required will vary with the system design. Some modern radiotheodolites have been engineered to improve mechanical reliability compared with the earlier types in use. The cost and feasibility of maintenance support must be considered important factors when choosing the type of upper-wind system to be used.

Electrical faults in most modern navaid tracking systems are repaired by the replacement of faulty modules. Such modules would include, for instance, the radiosonde receivers or navaid tracker systems. There are usually no moving parts in the navaid ground system and mechanical maintenance is negligible, though antenna systems, cables and connectors should be regularly inspected for corrosion and other weathering effects. Provided that sufficient spare modules are purchased with the system, maintenance costs can be minimal.

## 13.7 CORRECTIONS

When radiowind observations are produced by a radar system, the radar tracking information is used to compute the height assigned to the wind measurements. These radar heights need to be corrected for the curvature of the Earth using the following:

$$\Delta z_{\text{curvature}} = 0.5\left(r_{\text{s}} \cdot \cos\theta\right)^2 \Big/ \left(R_{\text{c}} + r_{\text{s}} \sin\theta\right) \tag{13.6}$$

where $r_{\text{s}}$ is the slant range to the target; $\Theta$ is the elevation angle to the target; and $R_{\text{c}}$ is the radius of the Earth curvature at the ground station.

In addition, the direction of propagation of the radar beam changes since the refractive index of air decreases on average with height, as temperature and water vapour also decrease with height. The changes in refractive index cause the radar wave to curve back towards the Earth. Thus, atmospheric refraction usually causes the elevation angle observed at the radar to be larger than the true geometric elevation of the target.

Typical magnitudes of refraction corrections, $\Delta z_{\text{refraction}}$, are shown in Table 13.6. These were computed by Hooper (1986b). With recent increases in available processing power for ground system computers, algorithms for computing refractive index corrections are more readily available for applications with high-precision tracking radars. The corrections in Table 13.6 were computed from five-year climatological averages of temperature and water vapour for a variety of locations. On days when refraction errors are largest, the correction required could be larger than the climatological averages in Table 13.6 by up to 30% at some locations.

**Table 13.6. Examples of corrections to radar height observations for Earth curvature and typical refraction**

| *Plan range (km)* | *Altitude (km)* | $\Delta z_{curvature}$ | $\Delta z_{refraction}$ *60°N 01°W* | $\Delta z_{refraction}$ *36°N 14°E* | $\Delta z_{refraction}$ *1°S 73°E* |
|---|---|---|---|---|---|
| 25 | 10 | 49 | –9 | –10 | –12 |
| 50 | 15 | 196 | –31 | –34 | –39 |
| 100 | 20 | 783 | –106 | –117 | –133 |
| 150 | 25 | 1 760 | –211 | –231 | –262 |
| 200 | 30 | 3 126 | –334 | –363 | –427 |

## REFERENCES AND FURTHER READING


Acheson, D. T. *LORAN-C Windfinding Capabilities: Wallops Island Experiments*; ESSA Technical Memorandum WBTM EDL 111970; United States Department of Commerce, Weather Bureau: Silver Spring, MD, 1970.

Call, D. B. A New GPS Rawinsonde System. Presented at the *WMO Technical Conference on Instruments and Methods of Observation (TECO-94)*, Geneva, 28 February–2 March 1994. In *Papers Presented at the WMO Technical Conference on Instruments and Methods of Observation (TECO-94)* (WMO/TD-No. 588). Instruments and Observing Methods (IOM) Report No. 57; World Meteorological Organization (WMO): Geneva, 1994.

da Silveira, R. B.; Fisch, G. F.; Machado, L. A. T. et al. *WMO Intercomparison of GPS Radiosondes – Alcântara (Brazil), 20 May–10 June 2001* (WMO/TD-No. 1314). Instruments and Observing Methods (IOM) Report No. 90. World Meteorological Organization (WMO): Geneva, 2006.

de Boor, C. *A Practical Guide to Splines*. Springer Verlag: New York, 1978.

Douglas, M.; Mejia, J.; Orozco R. et al. Suggestions for Upgrading the Pilot Balloon Network in West Africa and Elsewhere in the Tropics. Presented at the *WMO Technical Conference on Meteorological and Environmental Instruments and Methods of Observation (TECO-2008)*, St. Petersburg, 27–29 November 2008. In *Papers Presented at the WMO Technical Conference on Meteorological and Environmental Instruments and Methods of Observation (TECO-2008)* (WMO/TD-No. 1462). Instruments and Observing Methods (IOM) Report No. 96. World Meteorological Organization (WMO): Geneva, 2008.

Edge, P.; Kitchen, M.; Harding, J. et al. *The Reproducibility of RS3 Radiosonde and Cossor WF Mk IV Radar Measurements*; OSM No. 351986; Meteorological Office, Bracknell.

Hooper, A. H. *Algorithms for Automatic Aerological Soundings* (WMO/TD-No. 175). Instruments and Observing Methods (IOM) Report No. 21; World Meteorological Organization (WMO): Geneva, 1986a.

Hooper, A. H. *The Calculation of Radio-wave Refraction, with Special Reference to Data Height-finding Radars*; OSM No. 17; Meteorological Office: Bracknell, 1986b.

Ingleby, B.; Isaksen, L.; Kral, T. et al. Improved Use of Atmospheric In Situ Data. *ECMWF Newsletter* **2018**, *155*, 20–25.

Ingleby, B.; Pauley, P.; Kats, A. et al. Progress toward High-Resolution, Real-Time Radiosonde Reports. *Bull Amer Meteor Soc* **2016**, *97*, 2149–2161. https://doi.org/10.1175/BAMS-D-15-00169.1.

Ivanov, A.; Kats, A.; Kurnosenko, S. et al. *WMO International Radiosonde Comparison – Phase III, Dzhambul (USSR), 1989: Final Report* (WMO/TD-No. 451). Instruments and Observing Methods (IOM) Report No. 40; World Meteorological Organization (WMO): Geneva, 1991.

Ivanov, A.; Tseitlin, V. Studying the Accuracy of AFAR-based Radar Sounding System. Presented at the *WMO Technical Conference on Meteorological and Environmental Instruments and Methods of Observation (TECO-2005)*, Bucharest, 4–7 May 2005. In *Papers Presented at the WMO Technical Conference on Meteorological and Environmental Instruments and Methods of Observation* (WMO/TD-No. 1265). Instruments and Observing Methods (IOM) Report No. 82; World Meteorological Organization (WMO): Geneva, 2005.

Kaisti, K. New Low-cost GPS Solution for Upper-air Windfinding. In *Proceedings of the Ninth Symposium on Meteorological Observations and Instrumentation*, Charlotte, North Carolina, 27–31 March 1995, 16–20.

Kitchen, M. Representativeness Errors for Radiosonde Observations. *Quarterly Journal of the Royal Meteorological Society* **1989**, *115*, 673–700. https://doi.org/10.1002/qj.49711548713.

Lange, A. A. *Meteorological Observations Using Navaid Methods* (WMO-No. 641). Technical Note No. 185; Geneva, 1985.

Lange, A. A. A High-pass Filter for Optimum Calibration of Observing Systems with Applications. In *Simulation and Optimization of Large Systems*; Osiadacz, A. J., Ed.; Clarendon Press: Oxford, 1988; 311–327.

Lange, A. A. An Algorithmic Approach for Improving and Controlling the Quality of Upper-air Data. Paper presented at the *Fourth WMO Technical Conference on Instruments and Methods of Observation (TECIMO-IV)* (WMO/TD-No. 303). Instruments and Observing Methods (IOM) Report No. 35; World Meteorological Organization (WMO): Geneva, 1989.

MacCready P. B. Jr. Comparison of Some Balloon Techniques. *J Appl Meteor* **1965**, *4*, 504–508. https://doi.org/10.1175/1520-0450(1965)004<0504:COSBT>2.0.CO;2.

Nash, J. Upper Wind Observing Systems Used for Meteorological Operations. *Annales Geophysicae* **1994**, *12*, 691–710. https://doi.org/10.1007/s00585-994-0691-2.

Nash, J.; Oakley, T.; Vömel, H. et al. *WMO Intercomparison of High Quality Radiosonde Systems – Yangjiang, China, 12 July–3 August 2010* (WMO/TD-No. 1580). Instruments and Observing Methods (IOM) Report No. 107; World Meteorological Organization (WMO): Geneva, 2011.

Nash, J.; Schmidlin, F. J. *WMO International Radiosonde Comparison (UK 1984, USA 1985): Final Report* (WMO/TD-No. 195). Instruments and Observing Methods (IOM) Report No. 30; World Meteorological Organization (WMO): Geneva, 1987.

Nash, J.; Smout, R.; Oakley, T. et al. *WMO Intercomparison of Radiosonde Systems – Vacoas, Mauritius, 2–25 February 2005* (WMO/TD-No. 1303). Instruments and Observing Methods (IOM) Report No. 83; World Meteorological Organization (WMO): Geneva, 2006.

Passi, R. M. Overdetermined Windfinding Systems. *Atmospheric Technology* **1978**, *10*, 65–75.

Schaefer, J. T.; Doswell, C. A. The Inherent Position Errors in Double-theodolite Pibal Measurements. *Journal of Applied Meteorology* **1978**, *17*, 911–915. https://doi.org/10.1175/1520-0450(1978)017<0911:TIPEID>2.0.CO;2.

Vockeroth, R. E. World Meteorological Organization (WMO). *Upper-air Sounding Studies* (WMO-No. 394), Volume II. Technical Note No. 140; Geneva, 1975.

World Meteorological Organization (WMO). *Manual on Codes* (WMO-No. 306), Volume I.1. Geneva, 2019.

World Meteorological Organization (WMO). *Manual on the WMO Integrated Global Observing System* (WMO-No. 1160). Geneva, 2021.

Yagi, S.; Mita, A.; Inoue, N. *WMO International Radiosonde Comparison – Phase IV, Tsukuba, Japan, 15 February–12 March 1993: Final Report* (WMO/TD-No. 742). Instruments and Observing Methods (IOM) Report No. 59; World Meteorological Organization (WMO): Geneva, 1996.

# CHAPTER 14. OBSERVATION OF PRESENT AND PAST WEATHER; STATE OF THE GROUND

## 14.1 GENERAL

### 14.1.1 Definitions

In observational practice the term "weather" is regarded as covering those observations of the state of the atmosphere, and of phenomena associated with it, which were initially not intended to be measured quantitatively. These observations are qualitative descriptions of phenomena observed in the atmosphere or on the Earth's surface, such as precipitation (hydrometeors falling through the atmosphere), suspended or blowing particles (hydrometeors and lithometeors), or other specially designated optical phenomena (photometeors) or electrical manifestations (electrometeors). Detailed descriptions can be found in the *International Cloud Atlas* (WMO-No. 407).

**Hydrometeors.** These consist of liquid or solid water particles. They may be suspended in the atmosphere, fall through the atmosphere, be blown by the wind from the Earth's surface or be deposited on other objects.

**Lithometeors.** These consist of an ensemble of particles, most of which are solid and non-aqueous. The particles are either suspended in the air or lifted by the wind from the ground.

**Photometeor.** An optical phenomenon produced by the reflection, refraction, diffraction or interference of light from the Sun or the Moon.

**Electrometeor.** A visible or audible manifestation of atmospheric electricity.

A special class of weather phenomena are localized weather events. Definitions of such events can be found in the *International Meteorological Vocabulary* (WMO-No. 182). Specific events such as dust whirls and funnel clouds are defined and described in 14.2.3.

In meteorological observations, weather is reported in two forms. *Present weather* is a description of the weather phenomena present at the time of observation. Past weather is used to describe significant weather events occurring during the previous hour, but not occurring at the time of observation.

This chapter also describes the methods of observing a related item, namely the *state of the ground*. State of the ground refers to the condition of the Earth's surface resulting from the recent climate and weather events, in terms of the amount of moisture or description of any layers of solid, or aqueous or non-aqueous particles covering the normal surface.

### 14.1.2 Units and scales

At staffed stations, the observations identified as present weather, past weather and state of the ground are reported together with quantitative data. Such observations have been standardized on scales that enable the observer to select an appropriate term from a large number of descriptions derived from the perceptions of human observers and laid down in the *Manual on Codes* (WMO-No. 306), Volume I.1.

Since 1990, the introduction of Automatic Weather Stations (AWSs) has created the need to quantify the functions previously performed by observers. In order to accommodate the varying levels of sophistication and effectiveness of automated meteorological stations in observing present and past weather, specific coding directives have been included in the *Manual on Codes*

(WMO-No. 306), Volume I.1. Because of the complexity of reporting data on present and past weather determined by sophisticated present weather systems, such data should be reported as quantities in binary code format given that the alphanumeric code format suffers from many restrictions in comprehensive reporting.[1]

### 14.1.3 Meteorological requirements

Present and past weather, as well as the state of the ground, are primarily meant to serve as a qualitative description of weather events. They are required basically because of their impact on human activities and transport safety, as well as for their significance for understanding and forecasting synoptic weather systems. Several other chapters in the present Guide deal with related topics. The quantitative measurement of precipitation amounts and cloud observations are described in the present volume, Chapter 6 and Chapter 15, respectively. Volume III of the present guide includes topics that are specific to aeronautical and marine observations, automated systems, radar and atmospherics.

In this chapter, weather observations of interest in the determination of present and past weather are categorized into three types, namely precipitation (falling hydrometeors), atmospheric obscurity and suspensoids (lithometeors and suspended or blowing hydrometeors), and other weather events (such as funnel clouds, squalls and lightning). Liquid precipitation or fog which leave frozen deposits on surfaces are included in the appropriate precipitation and suspended hydrometeor category.

Other phenomena, such as those of an optical nature (photometeors) or electrometeors other than lightning, are indicators of particular atmospheric conditions and may be included in the running record maintained at each station of the weather sequence experienced. However, they are of no significance in the determination of present and past weather when coding standard meteorological observations, and are included here only for completeness.

### 14.1.4 Observation methods

The only current capability for observing all of the different forms of weather are the visual and auditory observations of a trained human observer. However, given the high cost of maintaining a significant staff of trained observers, a number of Meteorological Services are increasing their use of automated observing systems in primary observing networks, as well as continuing their use for supplementing staffed networks with automated observations from remote areas.

Basic research (Bespalov et al., 1983) has confirmed the possibility that weather phenomena may be determined by the logical analysis of a group of data variables. No single sensor is currently available which classifies all present weather; rather, data from a variety of sensors are used (such as visibility, temperature, dewpoint, wind speed and the differentiation of rain versus snow) to make such determinations. Automated observing systems have the capability to perform this logical analysis, but they vary in their ability to observe the required weather phenomenon, based on the instrumentation included in the system and the sophistication of the algorithms. While automated systems cannot observe all types of weather event, those of significance can be observed, making such systems cost-effective alternatives to the fully trained human observer.

## 14.2 OBSERVATION OF PRESENT AND PAST WEATHER

The observations to be recorded under the present weather and past weather headings include the phenomena of precipitation (rain, drizzle, snow, ice pellets, snow grains, diamond dust and hail), atmospheric obscurity and suspensoids (haze, dust, smoke, mist, fog, drifting and blowing snow, dust or sandstorms, dust devils), funnel clouds, squalls and lightning.

[1] Recommendation 3 (CBS-XII) refers to the requirement "to report observed quantities rather than qualitative parameters for present weather in observation from automatic stations in FM 94 BUFR and FM 95 CREX".

When observing present weather, it is necessary to note the various phenomena occurring at the station or in sight of the station at the time of observation. In synoptic reports, if there is no precipitation at the time of observation, account is taken of the conditions during the last hour in selecting the code figure.

## 14.2.1 Precipitation

### 14.2.1.1 *Objects of observation*

The character of precipitation can be distinguished in three forms, namely showers, intermittent precipitation and continuous precipitation. Showers are the precipitation events associated with physically separated convective clouds. Observers (or instruments replacing humans) also have to classify precipitation into the three intensity categories, namely slight, moderate and heavy, according to the rates of precipitation fall or other related factors (such as visibility).

The type of precipitation (for example, rain, drizzle, snow, hail) is the third major observable of precipitation. Observations of rain or drizzle at low temperatures should distinguish whether or not the precipitation is freezing. By definition, frozen rain or drizzle causes glazed frost by freezing on coming into contact with solid objects. Solid precipitation can occur in the form of diamond dust, snow grains, isolated star-like snow crystals, ice pellets and hail, full descriptions of which are given in the *International Cloud Atlas* (WMO-No. 407).

The precipitation character (intermittent, continuous, showery) and type (rain, drizzle, snow, hail) affect the definition of scales of precipitation intensity. Several joint meetings of the expert teams of the Commission for Instruments and Methods of Observation and the Commission for Basic Systems have developed tables to obtain a more universal relation between the qualitative and subjective interpretation by an observer and the measured quantities obtained by a present weather system. For an example of these tables and other relations see the annex.

### 14.2.1.2 *Instruments and measuring devices: precipitation type*

One major area of instrumentation involves the identification of the type of precipitation. Systems which are currently under evaluation, or in operational use, generally involve optical methods or radar (van der Meulen, 2003). Field tests (Leroy et al., 1998) have shown that all of these systems are capable of detecting major precipitation types – except for the very lightest snow or drizzle – in over 90% of occurrences compared to a trained observer. The percentage of detection of very slight precipitation is usually much lower.[2] Sophisticated algorithms are required to differentiate between several of the precipitation types. For example, wet or melting snow is difficult to distinguish from rain. The information of the sensor reporting precipitation type is often post-processed to optimize the results (see for example McRobbie et al., 2002; de Haij and Wauben, 2010; Bloemink, 2004). Currently, sensors reporting precipitation type do not provide information on the quality or uncertainty of the report. Where there are several possible outputs they should all be provided in the form of a probability distribution as this information would be very valuable, particularly during post-processing. Measurement principles commonly applied in sensors detecting precipitation type are listed below. Results of field evaluations of several of these sensors are reported in, for example, de Haij (2007), Lyth (2008), de Haij and Wauben (2010), and Wauben et al., (2016, 2018). Note that while sensors and automated systems are often capable of reporting a large number of different precipitation types, it is especially important to report the different classes (liquid, freezing, mixed, solid) correctly. A common way of analyzing the performance of automated observations is to compare the known local precipitation type distribution and the measured type distribution.

[2] The threshold for the detection of rain intensity is 0.02 mm $h^{-1}$ (see the present volume, Chapter 1, Annex 1.A).

### Forward-scatter/backscatter present weather sensor

A variety of scatter sensors are used to report present weather, in particular precipitation type. In general, scatter of a light source by the precipitation particles is observed under a fixed angle. This gives information on the size of the particles. Additional measurements (such as forward-/backscatter ratio, water content of the particles, fall speed, temperature) help determine the nature of the particles. For example, large particles with small water content will be classified as snow. Some sensors report unidentified precipitation when the precipitation type cannot be properly determined by the system. This mainly occurs at low precipitation intensities and during the start and cessation of precipitation events. Apart from precipitation type, these sensors may (depending on the sensor type) also provide precipitation intensity, precipitation duration (thus able to indicate intermittent precipitation) and visibility. Common sources of uncertainty associated with forward-scatter/backscatter sensors and their impact on the identification of precipitation type are described in Heyn et al. (2018).

These sensors are widely in use and generally give acceptable results for common precipitation types (rain, snow), with 70%–90% detection rates (van der Meulen, 1994; Leroy et al., 1998; Wauben, 2002), depending on the exact test set up and the specific instrument. Other precipitation types are not so well observed, particularly mixed precipitation (rain and snow) and hail. Thresholds for slight precipitation may vary.

### Optical disdrometer

Optical disdrometers are also used to determine precipitation type. These instruments use the extinction of a horizontal infrared (IR)/red light sheet to detect hydrometeors. When a particle falls through the light sheet, the receiver intensity is reduced. The amplitude of this reduction correlates with the particle size, and the duration correlates with the particle fall speed. The type of precipitation is determined by comparing the particle fall speed distribution of a series of detected particles against known relationships for different types of liquid, mixed and solid precipitation (for example, see Gunn and Kinzer, 1949). To derive precipitation type and intensity from raw particle data, several assumptions have to be made that also regard particle shape and density.

These sensors also generally give acceptable results for common precipitation types. Detection rates compared to human observers are similar to those found for scatter sensors (Bloemink and Lanzinger, 2005; de Haij and Wauben 2010). Again, mixed precipitation types and hail are difficult to detect. Issues in the retrieval of precipitation type mainly occur as a result of splashing, margin fallers and undercatch due to masking in strong wind conditions, but may also be caused by spiders obstructing the measurement volume (Upton and Brawn, 2008; Fehlmann et al., 2020).

A new measurement technique related to disdrometers are the so-called 2D and 3D video disdrometers that also capture projected images of the hydrometeors. These instruments are currently under development or used for research purposes. Examples are the 2D video disdrometer (Schönhuber et al., 2007), the video precipitation sensor (Liu et al., 2014) and the multi-angle snowflake camera (Praz et al., 2017).

### Doppler radar

Specific Doppler radars can also be used to determine precipitation type. The (vertically) emitted beam from the radar is backscattered by the falling hydrometeors. From the Doppler shift of the backscattered signal, the particle fall speeds can be determined. Near the ground, these are terminal fall velocities and correspond with the particle sizes. Some instruments have a measuring volume above the sensor; others determine the fall speeds at different altitudes above the sensor to determine precipitation type. Additional measurements (for example, surface temperature) are also used.

Different types of Doppler radar are available for detection of precipitation type. They tend to be insensitive to small particles, like all radar-based detection techniques. Some types show similar results compared with forward-scatter/backscatter sensors and disdrometers, that is, they produce decent results for rain and for snow, but not for mixtures. Hail and grey sleet are not observed.

### Impact detector

This type of sensor consists of a piezoelectric material which is capable of detecting the impact of the individual hydrometeors. The difference between the impact of hail and rain differs sufficiently to distinguish these two precipitation types. Other precipitation types are not reported (Salmi and Ikonen, 2005).

Since only rain and hail can be reported, this sensor is not a fully operational present-weather sensor. The hail detection part may, however, be helpful to some users, since this is generally a weak point of other present weather sensors. New sensors are under development that use a detection surface composed of parallel metal strings instead of a closed surface. Only relatively large hail stones have enough momentum to move the strings. These movements are picked up by a contactless transducer, and the output signal allows a distinction between large and small hail. A first prototype was developed around 2010 at Deutscher Wetterdienst (DWD). Further development took place in partnership with a German company in 2017. Field operation began at Hamburg Airport in March 2022. The measuring principle was patented by DWD. However, DWD has not yet published anything about the sensor operation and the measuring principle due to time constraints.

### Acoustic detector

The acoustic detector senses the sound of the falling hydrometeors. This is related to the precipitation type. The sensor was developed to supplement a forward-scatter/backscatter present weather sensor, in particular to improve the detection of hail and ice pellets.

### Other methods

Cameras can also be used to monitor precipitation type. An observer/operator can then monitor the various cameras from a central facility. A proper background needs to be selected in order to observe the precipitation. Since this type of measurement requires an observer/operator, it is not an automatic measurement of present/past weather.

A sensor specifically designed to detect freezing rain or glaze is in operational use (Starr and van Cauwenberghe, 1991). It senses the amount of ice accumulation on a probe. The probe vibrates at a frequency that is proportional to the mass of the probe. When ice freezes on the probe, its mass changes and the vibration frequency decreases. A heater is built into the sensor to de-ice the probe when required. The sensor has also been found effective for identifying wet snow.

A sensor that uses the differences in scintillation patterns when particles pass through a coherent light beam is able to differentiate between rain and snow (United States National Oceanic and Atmospheric Administration (US NOAA), 1998). Icing detectors may be used to identify freezing precipitation. Various methods exist. For instance, the weight of ice on a pole can be measured. Another method uses a probe that vibrates ultrasonically and the frequency of this probe changes when ice is formed on it. An extensive test has recently been performed (Fikke et al., 2007). Results from present weather sensors improve by including data from icing detectors, particularly freezing rain (Sheppard and Joe, 2000). Automated Weather Observing Systems use this technique.

Hail and other precipitation type products can also be obtained from weather radar measurements (see Chapter 7 of Volume III of the present Guide).

#### 14.2.1.3 *Instruments and measuring devices: precipitation intensity and character*

Present weather reports include an indication for the intensity of precipitation and thus of the precipitation character (that is, showers, intermittent precipitation or continuous precipitation). In many cases, these parameters are measured by the same sensor that determines the precipitation type. But it is also possible to employ a different sensor for this purpose. Measuring intensity also allows for the determination of intermittent precipitation (for example, snow showers). A laboratory and field intercomparison for precipitation intensity measurements has recently been completed (Lanza et al., 2006; Vuerich et al., 2009). This intercomparison included many different instruments using a variety of measurement techniques for collecting precipitation. Automatic measurement methods to provide an indication of precipitation intensity are listed below.

**Forward-scatter/backscatter present weather sensor**

The sensor is described in 14.2.1.2. By combining the particle size distribution, number of particles and precipitation type, the intensity of the precipitation is calculated. The precipitation intensity determined in this manner is usually less accurate than using conventional methods (for example, weighing raingauges, tipping-bucket raingauges). Calibration of the precipitation intensity is also a problem. For a coarse indication of precipitation intensity (slight, heavy, and the like), this method is usable. Manufacturers are working on refining the precipitation intensity output.

**Optical disdrometer**

This sensor type is also described in 14.2.1.2. By combining the particle size distribution, number of particles and precipitation type, the intensity of the precipitation is calculated. Work is being done to refine the precipitation intensity output (see, for example, Lanzinger et al., 2006).

**Doppler radar**

The sensor is described in 14.2.1.2. By combining the particle size distribution, number of particles and precipitation type, the intensity of the precipitation is calculated. Precipitation intensity results have shown decent correlations ($\rho = 0.9$) with conventional raingauges when 30 min intervals are considered (see Peters et al., 2002).

**Raingauge**

There are many different types of "conventional" raingauges. These are based on several different measurement methods and described in the present volume, Chapter 6. They are generally designed to measure precipitation amount, although some (smaller) instruments are also specifically designed to give (an indication of) precipitation intensity. Those raingauges designed for precipitation amount tend to be less accurate in reporting precipitation intensity. However, an indication of precipitation intensity, which is required for the present weather reporting, is generally satisfactory. Also, many manufacturers are improving these instruments with respect to the precipitation intensity (Lanza et al., 2006; Vuerich et al., 2009).

#### 14.2.1.4 *Instruments and measuring devices: multi-sensor approach*

To determine present weather characteristics and quantities of precipitation, observing systems use a variety of sensors in combination with algorithms. This multi-sensor approach creates a constraint on the techniques involved. Typical observations also involved are the measurement of precipitation, visibility, air temperature, dewpoint and cloud base. The algorithms are

characterized by filtering (for example, liquid precipitation only if the air temperature is above 6 °C). Combining numerous sensors to determine present weather is also used in road-weather systems (see also 14.3).

## 14.2.2 Atmospheric obscurity and suspensoids

### 14.2.2.1 *Objects of observation*

In reports taking into account the atmospheric conditions during the last hour, haze should be distinguished from mist or water fog. With haze, the air is relatively dry, whereas with mist or water fog there is usually evidence of high humidity in the form of, for example, water droplets or rime on grass and leaves. If the station is equipped with measuring instruments, it is fairly safe to assume that the obscurity is haze if the relative humidity is less than a certain percentage, for example 80%, and if the visibility is within certain limit values, for example, greater than 1 km in the horizontal, and greater than 2 km in the vertical. Mist is to be reported at high humidity values and at a visibility of 1 km or more. In synoptic reporting, fog is regarded as applying to water or ice fogs, generally reducing the horizontal visibility at the Earth's surface to less than 1 km. Wherever the term "fog" occurs in present weather and past weather codes, it should be read in this sense. In climatological summaries, however, all occasions of visibility of less than 1 km are regarded as fog.

Rime deposit is caused by the solidification into ice of water droplets in fog on coming into contact with solid objects at a temperature below freezing point. The present and past weather codes do not distinguish between different types of rime.

Drifting or blowing snow is snow blown off the ground into the air after it has already fallen. In the present weather code, drifting and blowing snow are distinguished separately, the former referring to snow not raised above the observer's eye level.

Other meteorological phenomena to be identified include widespread dust in suspension in the air, dust or sand raised by wind, a duststorm and sandstorm caused by turbulent winds raising large quantities of dust or sand into the air and reducing visibility severely, dust whirls or sand whirls and, occasionally, funnel clouds.

The *International Cloud Atlas* (WMO-No. 407) should be at the observer's disposal as an auxiliary means.

### 14.2.2.2 *Instruments and measuring devices for obscurity and suspensoid characteristics*

A possible approach for the identification of obscurity and suspensoid characteristics is the complex processing of measured values which can act as predictors. This approach requires researching the meteorological quantities that accompany the formation, intensification and disappearance of the phenomenon, as well as determining the limiting conditions. The problem of identifying fog, mist, haze, snowstorms and duststorms is reported in Goskomgidromet (1984) and Mezösi et al. (1985). The meteorological visual range serves as the most important indicating element. Of the remaining variables, wind velocity, humidity, temperature and dewpoint have proved to be important identifying criteria.

Instruments measuring visibility can be used to determine the meteorological visual range, as described in the present volume, Chapter 9, particularly 9.3. Note that for the determination of fog, mist and haze, however, the range of these instruments can be limited to a few kilometres. Three types of visibility instruments used in the determination of fog, haze and mist are described below. Dedicated automated systems exist for detection of blowing and drifting snow, both based on a direct measurement (impact of particles on a tube) or a combination of meteorological instruments such as snow particle counters, precipitation detectors and wind sensors combined with an algorithm. Examples can be found in Parry et al. (1999), Bellot et al. (2011) and Trouvilliez et al. (2015).

#### Transmissometer

Transmissometers measure the extinction of a light source over a known distance. Usually, the light of a flash lamp is detected at a distance of between 10 and 200 m. The visibility is calculated from the extinction of this light. In order to increase the range of detection, two detectors at different distances can be used (a so-called double-baseline transmissometer). Transmissometers are well suited to measure visibility, and are widely in use, particularly at airports. For larger visibilities, the uncertainty in the measurement increases with an increase in visibility (for further details, see the present volume, Chapter 9, 9.3). They are relatively expensive to install and to maintain, as they require regular cleaning. Some transmissometers are capable of maintaining their operational accuracy significantly longer due to automatic calibration and automatic compensation of contamination effects.

#### Forward-scatter sensor

This sensor is described in 14.2.1.2. Apart from precipitation type, visibility can also be measured using this instrument (see the present volume, Chapter 9, 9.3). The amount of scatter is related to the optical extinction. This is determined empirically in the calibration process by comparing the output with a transmissometer. Forward-scatter sensors are also well suited for measuring visibility and are being used increasingly. Compared to the transmissometer, the forward-scatter sensor can be generally used for a larger visibility range. One drawback is that its calibration is not trivial and needs attention. The instrument is relatively inexpensive to install and to maintain, as it does not require cleaning as often as transmissometers. Certain sensors can further extend the cleaning interval by automatic compensation of the optical impact of contamination.

#### Lidar

A relatively small lidar system can also be used to determine the visibility used in the determination of fog. A diode laser emits light pulses, and the light reflected back by the fog/haze particles (if present) is measured. The visibility is determined from the intensity of the reflected light and its time-of-flight. The visibility range measured by a lidar is limited, but for the determination of fog and haze and similar phenomena, a large visibility range is not required.

### 14.2.3 Other weather events

#### 14.2.3.1 *Objects of observation*

One event of critical importance in the protection of life and property is the recognition and observation of spouts (landspouts, cold air funnels, tornados, or waterspouts; see the *International Cloud Atlas* (WMO- No. 407).

**Spout.** A phenomenon consisting of an often violent whirlwind, revealed by the presence of a cloud column or inverted cloud cone (funnel cloud) protruding from the base of a cumulonimbus or cumulus cloud and of a "bush" composed of water droplets raised from the surface of the sea or of dust, sand or litter raised from the ground. The diameter can vary from a few metres to some hundreds of metres. A funnel cloud is considered well developed if the violent rotating column of air touches the ground or water surface. A well-developed funnel cloud is considered a tornado when over ground, and a waterspout when over water. The most violent tornadoes can have associated wind speeds of up to 150 m $s^{-1}$.

**Dust/sand whirls (dust devils).** An ensemble of particles of dust or sand, sometimes accompanied by small litter, raised from the ground in the form of a whirling column of varying height with a small diameter and an approximately vertical axis. Dust or sand whirls are a few metres in diameter. Normally, in the vertical they extend no higher than 60 to 90 m (dust devils). Well-developed dust or sand whirls in very hot desert regions may reach 600 m.

**Squall.** A strong wind that rises suddenly, lasts for a few minutes, then passes away. Squalls are frequently associated with the passage of cold fronts. In such circumstances, they occur in a line and are typically accompanied by a sharp fall in temperature, veering wind (northern hemisphere) or backing wind (southern hemisphere), a rise in relative humidity, and a roll-shaped cloud with a horizontal axis (line squall).

The definition of a thunderstorm (see *International Meteorological Vocabulary* (WMO-No. 182)) is an example of deriving the description exclusively from the perception of human observers. The event should be considered as a thunderstorm when thunder is heard (even if lightning is not observed).

#### 14.2.3.2 *Instruments and measuring devices*

The presence of funnel clouds, or tornadoes, can often be determined with the use of weather radar (see Chapter 7 of Volume III of the present Guide). Modern Doppler weather radars have become quite effective in the recognition of mesocyclones, thus providing more detailed and advanced information about this severe weather phenomenon than visual observation alone.

Squalls can be determined from the discrete succession of measured values of wind velocity. If the output of a wind velocity measuring device is combined with that of a wind direction sensor, a thermometer or a humidity sensor, the identification of a line squall seems to be possible.

Thunderstorms are mainly detected through the use of lightning counters. On the basis of the instructions provided to observers and issued by different Services, a certain number of lightning strokes per interval of time must be selected which can be used in combination with precipitation rates or wind speeds to define slight, moderate and heavy thunderstorms (see Chapter 6 of Volume III of the present Guide).

### 14.2.4 State of the sky

#### 14.2.4.1 *Objects of observation*

The specifications of the state of the sky are used to describe the progressive changes that have occurred in the sky during a given time. Changes in the total amount of clouds, in the height of the cloud base and in the type of cloud are to be considered likewise.

#### 14.2.4.2 *Instruments and measuring devices*

Cloud amount characteristics (total cloud cover in oktas, height of cloud base, and total cloud cover in various cloud layers) can be approximated from the variation of cloud-base height measured by a cloud-base optical measuring system by the application of statistical methods (see also the present volume, Chapter 15). Obviously, this is limited to cloud layers within the vertical range of the cloud-base measuring system (Persin, 1987; US NOAA, 1988; ZAMG, 1999).

## 14.3 OBSERVATION OF STATE OF THE GROUND

### 14.3.1 Objects of observation

State of the ground refers to the condition of the surface resulting from recent weather events in terms of amount of moisture or a description of solid, aqueous or non-aqueous particles covering the natural surface. Observations of the state of the ground (symbolic letters E and E') should be made in accordance with the specifications given in the *Manual on Codes* (WMO-No. 306).

Reporting state of the ground is also a part of present weather reporting, which, until recently, was carried out solely by human observers. Automatic measurement of state of the ground is still relatively new (for example, see Stacheder et al., 2008) and not widely in use.

### 14.3.2 Instruments and measuring devices

Research has shown that it is possible to discriminate main states of soil by means of reflecting and scattering phenomena (dry, humid, wet, snow-covered, rimed or iced) (Gaumet et al., 1991). Methods in use are briefly described below.

**Scatter sensor.** These sensors have an optical design that uses the reflecting and scattering properties of the surface. Various light sources may be used. For example, flux from a white light source reflected from a reference tile will depend on the state of this surface. Other (road-) sensors analyse reflection of an IR light source on a road surface. Here the wavelength of the reflected light depends on the state of the surface. Not all these sensors are suited for meteorological purposes, as they may be designed for surfaces other than natural surfaces. Sensors are currently being improved.

**Capacitive sensor.** A new, capacitive sensor is currently being developed and tested. A grid mat with conductive strips is placed on the (natural) surface. It is basically a capacitor with the natural ground as the dielectric. The dielectric constant for dry and wet earth differs considerably. The capacitance thus depends on the humidity of surface and, by measuring the absolute values and phase of the emitted signals at two frequencies, the state of the ground can be determined.

**Combination of sensors.** Particularly for road surfaces, a combination of sensors may be used to determine the surface state. For example, optical detection may determine the surface coverage; a conductivity measurement may determine the presence of chemical substances, surface temperature and ground temperature, and so forth. All these measurements, combined with atmospheric data, can be used in determining road condition. However, state of the ground is defined as the state on the natural surface present; this method thus determines not the exact state of the ground, but a related property.

**Cameras (and observer).** Cameras are also used to determine state of the ground. They can be pointed at various surfaces and an observer/operator determines the state of the ground. As this method is basically a manual method of observation, it is not analysed here.

## 14.4 OBSERVATION OF SPECIAL PHENOMENA

### 14.4.1 Electrical phenomena

Electrometeors either correspond to discontinuous electrical discharges (lightning, thunder) or occur as more or less continuous phenomena (Saint Elmo's fire, polar aurora). Full descriptions of electrometeors are given in the *International Cloud Atlas* (WMO-No. 407).

Special records of lightning should include information regarding its type and intensity, the frequency of flashes and the range of azimuth over which discharges are observed; the lapse of time between lightning and the corresponding thunder should be noted. Care should be taken to distinguish between the actual lightning flash and its possible reflection on clouds or haze. Automatic detection systems for lightning location are in operational use in many countries. Chapter 6 of Volume III of the present Guide contains more information on this topic.

Exceptional polar aurora should be described in detail. Light filters, where available, may be used as a means of increasing the sensitivity of the observations, and theodolites or clinometers (alidades) may be used to increase the accuracy of the angular measurements.

### 14.4.2 **Optical phenomena**

A photometeor is a luminous phenomenon produced by the reflection, refraction, diffraction or interference of light from the sun or moon. Photometeors may be observed in more or less clear air (mirage, shimmer, scintillation, green flash, twilight colours), on or inside clouds (halo phenomena, corona, irisation, glory) and on or inside certain hydrometeors or lithometeors (glory, rainbow, fog bow, Bishop's ring, crepuscular rays).

Observers should take careful note of any optical phenomena that occur. A written description should be accompanied by drawings and photographs, if possible. Full descriptions of these phenomena are given in the *International Cloud Atlas* (WMO-No. 407). Concise instructions for observing the more common phenomena are given in some observers' handbooks, for example, the United Kingdom Meteorological Office (1982).

A theodolite is a very suitable instrument for precise measurements. However, when one is not available, a graduated stick held at arm's length is useful; with the occurrence of a mock sun, the position may be determined by noting its relation to fixed landmarks. The diameter of a corona may be estimated by taking the angular diameter of the sun or moon as approximately half a degree.

# ANNEX. CRITERIA FOR SLIGHT, MODERATE AND HEAVY PRECIPITATION INTENSITY

Note: Recommended by the WMO Expert Meeting on Automation of Visual and Subjective Observations (Trappes/Paris, France, 14–16 May 1997) and the Working Group on Surface Measurements (Geneva, 27–31 August 2001).

(Slight, moderate and heavy precipitation defined with respect to the type of precipitation and to intensity, $i$)[a]

| *Variable* | *Range* | *Intensity* |
|---|---|---|
| Drizzle | $i < 0.1$ mm $h^{-1}$ | Slight |
| | $0.1 \leq i < 0.5$ mm $h^{-1}$ | Moderate |
| | $i \geq 0.5$ mm $h^{-1}$ | Heavy |
| Rain (also showers) | $i < 2.5$ mm $h^{-1}$ | Slight |
| | $2.5 \leq i < 10.0$ mm $h^{-1}$ | Moderate |
| | $10.0 \leq i < 50.0$ mm $h^{-1}$ | Heavy |
| | $i \geq 50.0$ mm $h^{-1}$ | Violent[b] |
| Snow (also showers) | $i < 1.0$ mm $h^{-1}$ (water equivalent) | Slight |
| | $1.0 \leq i < 5.0$ mm $h^{-1}$ (water equivalent) | Moderate |
| | $i \geq 5.0$ mm $h^{-1}$ (water equivalent) | Heavy |

Notes:
a Intensity values based on a 3 min measurement period.
b The term "violent", as it pertains to precipitation rate, is inconsistent with the other categories and is confusing. A term such as "intense" or "extreme" may be more appropriate.

### Criteria for other precipitation types

Mixed precipitation of rain and snow: The same as for snow (since the rain/snow ratio is not subject to any measurement, a simple choice should be made).

Hail: The same as for rain.

Ice pellets and snow pellets: The same as for snow.

Freezing phenomena: The same as for the non-freezing phenomena.

### Guide for approximating the intensity of snow

Slight: Snowflakes small and sparse; in the absence of other obscuring phenomena, snow at this intensity generally reduces visibility, but to no less than 1 000 m.

Moderate: Larger, more numerous flakes generally reducing visibility to between 400 and 1 000 m.

Heavy: Numerous flakes of all sizes generally reducing visibility to below 400 m.

**Showers or intermittent precipitation**

Automated systems should report showers or intermittent precipitation. Intermittent can be defined as no precipitation within 10 min of two consecutive precipitation events; that is, if there is a period of 10 min of no precipitation in a running 10-min average of precipitation within the last hour, it should be reported as intermittent.

**Representativeness of present weather events**

A present weather event may be well defined by a 3-min observing period. The highest running 3-min average in the 10-min period should be reported for present weather.

## REFERENCES AND FURTHER READING


Bellot, H.; Trouvilliez, A.; Naaim-Bouvet, F.; et al. Present Weather-Sensor Tests for Measuring Drifting Snow. *Annals of Glaciology* **2011**, *52* (58), 176–184. https://doi.org/10.3189/172756411797252356.

Bespalov, S. M. et al. Osnovnyje voprosy razrabotki setevoj avtomaticeskoj gidrometeorologiceskoj stancii [Main Aspects of Designing a Network of Automatic Hydrometeorological Stations]. *Trudy GGO* **1983**, *473*, 3–12.

Bloemink, H. I. *Precipitation Type Detection – Present Weather Sensor: Final Report*; KNMI TR-259; De Bilt, 2004. https://cdn.knmi.nl/knmi/pdf/bibliotheek/knmipubTR/TR259.pdf.

Bloemink, H. I.; Lanzinger, E. Precipitation Type from the Thies Disdrometer. Presented at the *WMO Technical Conference on Meteorological and Environmental Instruments and Methods of Observation (TECO-2005)*, Bucharest, 4–7 May 2005. In *Papers Presented at the WMO Technical Conference on Meteorological and Environmental Instruments and Methods of Observation* (WMO/TD-No. 1265). Instruments and Observing Methods (IOM) Report No. 82; World Meteorological Organization (WMO): Geneva, 2005.

de Haij, M. J. *Automated Discrimination of Precipitation Type Using the FD12P Present Weather Sensor: Evaluation and Opportunities*; KNMI TR-297; De Bilt, 2007. https://www.knmi.nl/kennis-en-datacentrum/publicatie/automated-discrimination-of-precipitation-type-using-the-fd12p-present-weather-sensor-evaluation-and-opportunities.

de Haij M.; Wauben, W. Investigations into the Improvement of Automated Precipitation Type Observations at KNMI. Presented at the *WMO Technical Conference on Meteorological and Environmental Instruments and Methods of Observation (TECO-2010)*, Helsinki, 30 August–1 September 2010. In *Papers Presented at the WMO Technical Conference on Meteorological and Environmental Instruments and Methods of Observation (TECO-2010)* (WMO/TD-No. 1546). Instruments and Observing Methods (IOM) Report No. 104; World Meteorological Organization (WMO): Geneva, 2010.

Fehlmann, M.; Rohrer, M.; von Lerber, A.; et al. Automated Precipitation Monitoring with the Thies Disdrometer: Biases and Ways for Improvement. *Atmospheric Measurement Techniques* **2020**, *13* (9), 4683–4698. https://doi.org/10.5194/amt-13-4683-2020.

Fikke, S.; Ronsten, G.; Heimo, A. et al. COST-727: Atmospheric Icing on Structures – Measurements and Data Collection on Icing: State of the Art; MeteoSwiss No. 752007; MeteoSwiss, 2007.

Gaumet, J. L.; Salomon P.; Paillisse, R. Automatic Observations of the State of the Soil for Meteorological Applications. In *Preprints of the Seventh Symposium on Meteorological Observations and Instrumentation: Special Sessions on Laser Atmospheric Studies*, New Orleans, 13–18 January 1991, American Meteorological Society: 1991; J191–J193.

Goskomgidromet. Opredelenije atmosfernych javlenij po dannym avtomaticeskich stancij, soveqanije gruppy ekspertov GMS/MS socialisticeskich stran po teme 9.1. KR GMS/MS [Identification of Atmospheric Phenomena from the Data from Automatic Weather Stations: Meeting of the Panel of Socialist Countries HMS/MS on Theme 9.1.], Obninsk, 24–28 August 1984; Moscow, 1984.

Gunn, R.; Kinzer, G. D. The Terminal Velocity of Fall for Water Droplets in Stagnant Air, *J Meteorol* **1949**, *6*, 243–248.

Heyn, K.; Lönnqvist, J.; Linna, T. Uncertainty Sources that Limit the Precipitation Identification / Quantification and Extinction Coefficient Determination Capabilities of Optical Present Weather and Visibility Sensors. Presented at the *WMO Technical Conference on Meteorological and Environmental Instruments and Methods of Observation (TECO-2018), Amsterdam, 8–11 October 2018*. In *The 2018 WMO/CIMO Technical Conference on Meteorological and Environmental Instruments and Methods of Observation (CIMO TECO-2018)*. Instruments and Observing Methods (IOM) Report No. 132; World Meteorological Organization (WMO): Geneva, 2018.

Lanza, L. G.; Leroy, M.; Alexandropoulos, C. et al. *WMO Laboratory Intercomparison of Rainfall Intensity Gauges: Trappes (France) – Genoa (Italy) – De Bilt (Netherlands) September 2004–September 2005* (WMO/TD-No. 1304). Instruments and Observing Methods (IOM) Report No. 84; World Meteorological Organization (WMO): Geneva, 2006.

Lanzinger, E.; Theel, M.; Windolph, H. Rainfall Amount and Intensity Measured by the Thies Laser Precipitation Monitor. Presented at the *WMO Technical Conference on Meteorological and Environmental Instruments and Methods of Observation (TECO-2006)*, Geneva, 4–6 December 2006. In *Papers Presented at the WMO Technical Conference on Meteorological and Environmental Instruments and Methods of Observation (TECO-2006)* (WMO/TD-No. 1354). Instruments and Observing Methods (IOM) Report No. 94; World Meteorological Organization (WMO): Geneva, 2006.

Leroy, M.; Bellevaux, C; Jacob, J. P. *WMO Intercomparison of Present Weather Sensors/Systems – Canada and France, 1993–1995: Final Report* (WMO/TD-No. 887). Instruments and Observing Methods (IOM) Report No. 73; World Meteorological Organization (WMO): Geneva, 1998.

Liu, X. C.; Gao, T. C.; Liu, L. A Video Precipitation Sensor for Imaging and Velocimetry of Hydrometeors. *Atmospheric Measurement Techniques* **2014**, *7*, 2037–2046. https://doi.org/10.5194/amt-7-2037-2014.

Loeffler-Mang, M. HARE – A New Intelligent Hail Recorder for Networks and Field Campaigns. In *Proceedings of the Fifth European Conference on Severe Storms*, Landshut, Germany, 12–16 October 2009. http://www.essl.org/ECSS/2009/preprints/P09-06-loefflermang.pdf.

Lyth, D. Results from UK Met Office Investigations into New Technology Present Weather Sensors. Presented at the *WMO Technical Conference on Meteorological and Environmental Instruments and Methods of Observation (TECO-2008)*, St. Petersburg, 27–29 November 2008. In *Papers Presented at the WMO Technical Conference on Meteorological and Environmental Instruments and Methods of Observation (TECO-2008)* (WMO/TD-No. 1462). Instruments and Observing Methods (IOM) Report No. 96; World Meteorological Organization (WMO): Geneva, 2008.

McRobbie, S. G.; Molyneux, M. J.; Shearn, P. D. Improvements to Automated Present Weather Reporting in the Met Office. Presented at the *WMO Technical Conference on Meteorological and Environmental Instruments and Methods of Observation (TECO-2002)*, Bratislava, 23–25 September 2002. In *Papers Presented at the WMO Technical Conference on Meteorological and Environmental Instruments and Methods of Observation (TECO-2002)* (WMO/TD-No. 1123). Instruments and Observing Methods (IOM) Report No. 75; World Meteorological Organization (WMO): Geneva, 2002.

Mezösi, M.; Simon, A.; Hanák, P. et al. Algorithms for Automatic Coding of the Present and Past Weather by Unmanned Meteorological Stations. Presented at *the Third WMO Technical Conference on Instruments and Methods of Observation (TECIMO-III)*, Ottawa, 8–12 July 1985. In *Papers Presented at the Third WMO Technical Conference on Instruments and Methods of Observation (TECIMO-III)* (WMO/TD-No. 50). Instruments and Observing Methods (IOM) Report No. 22; World Meteorological Organization: Geneva, 1985.

Parry, R. N.; Gifford, M. D. ASOS Blowing Snow Algorithm. In *Proceedings of the Second International Conference on Experiences with Automatic Weather Stations – ICEAWS-1999*, Vienna, 27–29 September 1999.

Persin, S. M. Izmerrenije vysoty niznej granicy oblakov i charakteristika oblacnosti kak zadaca paspoznavanija obrazov [Measuring Cloud Ceiling and Characterizing Cloudiness as a Task of Image Identification]. *Trudy GGO* **1987**, *512*, 49–91.

Peters, G.; Fischer B.; Andersson, T. Rain Observations with a Vertically Looking Micro Rain Radar (MRR). *Boreal Environment Research* **2002**, *7*, 353–362.

Praz, C.; Roulet, Y.-A.; Berne, A. Solid Hydrometeor Classification and Riming Degree Estimation from Pictures Collected with a Multi-angle Snowflake Camera. *Atmospheric Measurement Techniques* **2017**, *10*, 1335–1357. http://doi.org/10.5194/amt-10-1335-2017.

Salmi, A.; Ikonen, J. Piezoelectric Precipitation Sensor from Vaisala. Presented at the *WMO Technical Conference on Meteorological and Environmental Instruments and Methods of Observation (TECO-2005)*, Bucharest, 4–7 May 2005. In *Papers Presented at the WMO Technical Conference on Meteorological and Environmental Instruments and Methods of Observation* (WMO/TD-No. 1265). Instruments and Observing Methods (IOM) Report No. 82; World Meteorological Organization (WMO): Geneva, 2005.

Schönhuber, M.; Lammer, G.; Randeu W. L. One Decade of Imaging Precipitation Measurement by 2D-Video-distrometer. *Advances in Geosciences* **2007**, *10*, 85–90. https://doi.org/10.5194/adgeo-10-85-2007.

Sheppard, B. E.; Joe, P. I. Automated Precipitation Detection and Typing in Winter: A Two-year Study. *Journal of Atmospheric and Oceanic Technology* **2000**, *17*(11), 1493–1507. https://doi.org/10.1175/1520-0426(2000)017<1493:APDATI>2.0.CO;2.

Stacheder, M.; Koeniger, F.; Schuhmann, R. et al. New Sensor for the Automatic Detection of the State of Ground. *Near Surface Geophysics* **2008**, *6* (1), 61–70. https://doi.org/10.3997/1873-0604.2007032.

Starr, K. M.; van Cauwenberghe R. The Development of a Freezing Rain Sensor for Automated Surface Observing Systems. In *Preprints of the Seventh Symposium on Meteorological Observations and Instrumentation: Special Sessions on Laser Atmospheric Studies*, New Orleans, 13–18 January 1991, American Meteorological Society: 1991; 338–343.

Trouvilliez, A.; Naaim-Bouvet, F.; Bellot, H. et al. Evaluation of the FlowCapt Acoustic Sensor for the Aeolian Transport of Snow. *Journal of Atmospheric and Oceanic Technology* **2015**, *32* (9), 1630–1641. https://doi.org/10.1175/JTECH-D-14-00104.1.

United Kingdom Meteorological Office. *Observer's Handbook*. Her Majesty's Stationery Office: London, 1982.

United States National Oceanic and Atmospheric Administration (US NOAA). *Federal Standard Algorithms for Automated Weather Observing Systems Used for Aviation Purposes*; FCM-S5-1988; Office of the Federal Coordinator for Meteorological Services and Supporting Research, United States Department of Commerce: Washington, DC, 1988.

United States National Oceanic and Atmospheric Administration (US NOAA). *Automated Surface Observing System (ASOS) User's Guide*. Department of Defense, Federal Aviation Administration, United States Navy: 1998. https://www.weather.gov/media/asos/aum-toc.pdf.

Upton, G.; Brawn, D. An Investigation of Factors Affecting the Accuracy of Thies Disdrometers. Presented at the *WMO Technical Conference on Meteorological and Environmental Instruments and Methods of Observation (TECO-2008)*, St. Petersburg, 27–29 November 2008. In *Papers Presented at the WMO Technical Conference on Meteorological and Environmental Instruments and Methods of Observation (TECO-2008)* (WMO/TD-No. 1462). Instruments and Observing Methods (IOM) Report No. 96; World Meteorological Organization (WMO): Geneva, 2008.

van der Meulen, J. P. A Comparison of Two Present Weather Systems with Human Observations. Presented at the *WMO Technical Conference on Instruments and Methods of Observation (TECO-94)*, Geneva, 28 February–2 March 1994. In *Papers Presented at the WMO Technical Conference on Instruments and Methods of Observation (TECO-94)* (WMO/TD-No. 588). Instruments and Observing Methods (IOM) Report No. 57; World Meteorological Organization (WMO): Geneva, 1994.

van der Meulen, J. P., Present Weather – Science: Exploratory Actions on Automatic Present Weather Observations. Final Report; E-PWS-SCI; Royal Netherlands Meteorological Institute: de Bilt, 2003.

Vuerich, E.; Monesi, C.; Lanza, L. G. et al. *WMO Field Intercomparison of Rainfall Intensity Gauges (Vigna di Valle, Italy), October 2007–April 2009* (WMO/TD-No. 1504). Instruments and Observing Methods (IOM) Report No. 99. World Meteorological Organization (WMO): Geneva, 2009.

Wade, C. G. Detecting Ice Pellets, Snow Pellets and Hail on ASOS Using an Acoustic Sensor. In the *Proceedings of the Twelfth AMS Symposium on Meteorological Observations and Instrumentation*, Long Beach, CA, 8–13 February 2003.

Wauben, W. Automation of Visual Observations at KNMI; (I) Comparison of Present Weather. In *Proceedings of the Symposium on Observations, Data Assimilation, and Probabilistic Prediction*, Orlando, FL, 13–17 January 2002; American Meteorological Society, 2002.

Wauben, W.; Mathijssen, T.; Oudshoorn, C. Field Evaluation of Sensors for Precipitation Type Discrimination. Presented at the *WMO Technical Conference on Meteorological and Environmental Instruments and Methods of Observation (TECO-2016), Madrid, 27–30 September 2016*. In *WMO Technical Conference on Meteorological and Environmental Instruments and Methods of Observation (CIMO TECO-2016)*. Instruments and Observing Methods (IOM) Report No. 125; World Meteorological Organization (WMO): Geneva, 2016.

Wauben, W.; Tukker, K.; Knoop, S. et al. Specification and Evaluation of Present Weather Sensors. Presented at the *WMO Technical Conference on Meteorological and Environmental Instruments and Methods of Observation (TECO-2018), Amsterdam, 8–11 October 2018*. In *The 2018 WMO/CIMO Technical Conference on Meteorological and Environmental Instruments and Methods of Observation (CIMO TECO-2018)*. Instruments and Observing Methods (IOM) Report No. 132; World Meteorological Organization (WMO): Geneva, 2018.

World Meteorological Organization (WMO). *International Meteorological Vocabulary* (WMO-No. 182). Geneva, 1992.

World Meteorological Organization (WMO). *International Cloud Atlas* (WMO-No. 407). Geneva, 2017.
World Meteorological Organization (WMO). *Manual on Codes* (WMO-No. 306), Volume I.1. Geneva, 2019.
Zentralanstalt für Meteorologie und Geodynamik (ZAMG). Present Weather Sensors and Manual Observations. In *Proceedings of the Second International Conference on Experiences with Automatic Weather Stations – ICEAWS-1999*, Vienna, 27–29 September 1999; *Österreichische Beiträge zu Meteorologie und Geophysik* **1999**, *20*.

# CHAPTER 15. OBSERVATION AND MEASUREMENT OF CLOUDS

## 15.1 GENERAL

The observation or measurement of clouds and the height of their bases above the Earth's surface are important for many purposes, especially for aviation and other operational applications of meteorology. An important application for the observation or measurement of cloudiness during daytime is the solar power forecasting for photovoltaic systems. This chapter describes the methods in widespread use. Further important information is to be found in the *International Cloud Atlas* (WMO, 2017), which contains scientific descriptions of clouds and illustrations to aid in the identification of cloud types. Information on the practices specific to aeronautical meteorology is given in *Guide to Meteorological Observing and Information Distribution Systems for Aviation Weather Services* (WMO, 2014).

### 15.1.1 Definitions

**Cloud.** An aggregate of very small water droplets, ice crystals, or a mixture of both, with its base above the Earth's surface, which is perceivable from the observation location. The limiting liquid particle diameter is of the order of 200 μm; drops larger than this comprise drizzle or rain.

With the exception of certain rare types (for example, nacreous and noctilucent) and the occasional occurrence of cirrus in the lower stratosphere, clouds are confined to the troposphere. They are formed mainly as the result of condensation of water vapour on condensation nuclei in the atmosphere. Cloud formation takes place in the vertical motion of air, in convection, in forced ascent over high ground, or in the large-scale vertical motion associated with depressions and fronts. Clouds may result, in suitable lapse-rate and moisture conditions, from low-level turbulence and from other minor causes. Human activity, such as aviation or industry, can also result in cloud formation, by adding condensation nuclei to the atmosphere.

At temperatures below 0 °C, cloud particles frequently consist entirely of water droplets supercooled down to about –10 °C in the case of layer clouds and to about –25 °C in the case of convective clouds. At temperatures below these very approximate limits and above about –40 °C, many clouds are "mixed", with ice crystals predominating in the lower part of the temperature range.

**Cloud amount.** The amount of sky estimated to be covered by a specified cloud type (partial cloud amount), or by all cloud types (total cloud amount). In either case, the estimate is made to the nearest okta (eighth) and is reported on a scale which is essentially one of the nearest eighth, except that figures 0 and 8 on the scale signify a completely clear and cloudy sky, respectively, with consequent adjustment to the adjacent 1 and 7 okta intervals (see 15.1.4.1).

**Cloud base.** The lowest zone in which the obscuration corresponding to a change from clear air or haze to water droplets or ice crystals causes significant changes in the profiles of the backscatter and extinction coefficients. In the air below the cloud, the particles causing obscuration show some spectral selectivity, while in the cloud itself, there is virtually no selectivity; the difference is due to the different droplet sizes involved. The height of the cloud base is defined as the height above ground level. For an aeronautical meteorological station, the ground (surface) level is defined as the official aerodrome elevation.

**Cloud type (classification).** Various methods of cloud classification are used, as follows:

(a) In WMO (2017), division is made into cloud genera with 10 basic characteristic forms, with further subdivision, as required, into:

(i) Cloud species (cloud shape and structure);

(ii) Cloud varieties (cloud arrangement and transparency);

(iii) Supplementary features and accessory clouds (for example, incus, mamma, virga, praecipitatio, arcus, tuba, pileus, velum and pannus);

(iv) Growth of a new cloud genus from a mother-cloud, indicated by the addition of "genitus" to the new cloud and mother-cloud genera – in that order, if a minor part of the mother-cloud is affected – and of "mutatus" if much or all of the mother-cloud is affected, for example, stratocumulus cumulogenitus, or stratus stratocumulomutatus;

(v) Special clouds that form or grow as a consequence of certain, often localized, generating factors. These may be either natural, or the result of human activity (for example, flammagenitus, cataractagenitus and aircraft condensation trails);

(b) A classification is made in terms of the level – high, middle or low – at which the various cloud genera are usually encountered. In temperate regions, the approximate limits are: high, 6–12 km (20 000–40 000 ft); middle, surface–6 km (0–20 000 ft); and low, surface–1.5 km (0–5 000 ft). The high clouds are cirrus, cirrocumulus and cirrostratus; the middle clouds are altocumulus and altostratus (the latter often extending higher) and nimbostratus (usually extending both higher and lower); and the low clouds are stratocumulus, stratus, cumulus and cumulonimbus (the last two often also reaching middle and high levels);

For synoptic purposes, a nine-fold cloud classification is made in each of these three latter divisions of cloud genera, the corresponding codes being designated $C_H$, $C_M$ and $C_L$, respectively. The purpose is to report characteristic states of the sky rather than individual cloud types;

(c) Less formal classifications are made as follows:

(i) In terms of the physical processes of cloud formation, notably into heap clouds and layer clouds (or "sheet clouds");

(ii) In terms of cloud composition, namely ice-crystal clouds, water-droplet clouds and mixed clouds.

Most of these forms of cloud are illustrated with photographs in WMO (2017).

**Vertical visibility.** The maximum distance at which an observer can see and identify an object on the same vertical as him/herself, above or below. Vertical visibility can be calculated from the measured extinction profile, $\sigma(h)$. The relationship, however, is less simple than for horizontal visibility, because $\sigma$ may not be regarded as a constant value. Nevertheless, the $I(h = VV)/I_0 = 5\%$ rule can be applied. Taking into account this assumption, the vertical visibility can be expressed in a relation with $\sigma(h)$, in which $VV$ is represented intrinsically, that is:

$$\int_{h=0}^{h=VV} \sigma(h)\, dh = -\ln(5\%) \approx 3 \qquad (15.1)$$

See also Volume III, Chapter 2, equations 2.6 and 2.7 of the present Guide.

### 15.1.2 Units and scales

The unit of measurement of cloud height is the metre or, for some aeronautical applications, the foot. The unit of cloud amount is the okta, which is an eighth of the sky dome covered by cloud. In BUFR FM 94 code (WMO, 2011) total cloud cover is given in percentage (113 indicating sky obscured by fog and/or other meteorological phenomena).

### 15.1.3 Meteorological requirements

For meteorological purposes, observations are required for cloud amount, cloud type and height of cloud base. For synoptic observations, specific coding requirements are stated in WMO (2011), which is designed to give an optimum description of the cloud conditions from the surface to high levels. From space, observations are made of cloud amount and temperature (from which the height of the cloud top is inferred). Measurements from space can also be used to follow cloud and weather development.

Uncertainty requirements are stated in the present volume, Chapter 1, Annex 1.A.

### 15.1.4 Observation and measurement methods

#### 15.1.4.1 *Cloud amount*

Traditionally, measurements of cloud amount were made by visual observation. Instrumental methods are now widely accepted and are used operationally in many applications for determination of cloud amount and height. The cloud amount in each identified layer and the total cloud amount in view of the observation point are determined.

The total cloud amount, or total cloud cover, is the fraction of the celestial dome covered by all clouds visible. The assessment of the total amount of cloud, therefore, consists in estimating how much of the total apparent area of the sky is covered with clouds.

The partial cloud amount is the amount of sky covered by each type or layer of clouds as if it were the only cloud type in the sky. The sum of the partial cloud amounts may exceed both the total cloud amount and eight oktas.

The scale for recording the amount of cloud is that given in Code table 2700 in WMO (2011), which is reproduced below:

| *Code figure* | *Meaning* | |
|---|---|---|
| 0 | 0 | 0 |
| 1 | 1 okta or less, but not zero | 1/10 or less, but not zero |
| 2 | 2 oktas | 2/10–3/10 |
| 3 | 3 oktas | 4/10 |
| 4 | 4 oktas | 5/10 |
| 5 | 5 oktas | 6/10 |
| 6 | 6 oktas | 7/10–8/10 |
| 7 | 7 oktas or more, but not 8 oktas | 9/10 or more, but not 10/10 |
| 8 | 8 oktas | 10/10 |
| 9 | Sky obscured by fog and/or other meteorological phenomena | |
| / | Cloud cover is indiscernible for reasons other than fog or other meteorological phenomena, or observation is not made | |

#### 15.1.4.2 *Cloud-base height*

The height of the cloud base lends itself to instrumental measurement, which is now widely used at places where cloud height is operationally important. However, the estimation of cloud-base height by human observer is still widespread.

Several types of instruments are in routine operational use, as described in this chapter. An international comparison of several types of instruments was conducted by WMO in 1986, and is reported in WMO (1988). The report contains a useful account of the accuracy of the measurements and the performance of the instruments.

Recent studies (WMO, 2016*a* and 2016*b*) show the enhanced performance of modern ceilometers concerning the detection of the cloud-base height of very low clouds, very high clouds and during precipitation. However the studies revealed systematic differences of 30 to 50 metres in the cloud-base heights reported by ceilometers from different manufacturers. As the shapes of the profiles and the location of the gradients and maxima in the measured backscatter are quite similar, the cloud detection algorithms implemented by the manufacturers appear to be the source of these differences. The algorithm may place the cloud base either at the altitude where the backscatter starts to increase significantly, or higher up allowing for a penetration depth into the cloud, or at the maximum of the backscattered signal. The different approaches cannot be verified at this time because the lack of an established and quantifiable definition for cloud base, and the lack of a suitable reference. Comparison of ceilometer cloud-base heights with visibility measurements at various altitudes up a mast, and the height up a tower that can be discerned from a camera image, are both currently under investigation to ensure the correct operation of a ceilometer.

Instrumental measurement of cloud-base height is common and important for aeronautical meteorological services. This is discussed further in Volume III, Chapter 2 of the present Guide.

#### 15.1.4.3 *Cloud type*

At present, the only method for observing most cloud types is visual. Pictorial guides and coding information are available from many sources, such as WMO (2011, 2017), as well as from publications of NMHSs.

The extraction of cloud type from camera images is still under development (see, for example, Heinle et al., 2010; Liu et al., 2011).

Some meteorological offices use lightning, weather radar and satellite information to identify cumulonimbus and towering cumulus for inclusion in automated aeronautical weather reports when appropriate.

## 15.2 ESTIMATION AND OBSERVATION OF CLOUD AMOUNT, CLOUD-BASE HEIGHT AND CLOUD TYPE BY HUMAN OBSERVER

### 15.2.1 Making effective estimations

The site used when estimating cloud variables should be one which commands the widest possible view of the sky, and it should not be affected by fixed lighting which would interfere with observations at night. In making observations at night, it is very important that the observer should allow sufficient time for the eyes to adjust to the darkness.

There are, of course, occasions when it is very difficult to estimate cloud amount, especially at night. The previous observation of cloud development and general knowledge of cloud structure will help the observer to achieve the best possible result. Access to reports from aircraft, if available, can also be of assistance.

### 15.2.2 Estimation of cloud amount

The observer should give equal emphasis to the areas overhead and those at the lower angular elevations. On occasions when the clouds are very irregularly distributed, it is useful to consider the sky in separate quadrants divided by diameters at right angles to each other. The sum of the estimates for each quadrant is then taken as the total for the whole sky.

Code figure 9 is reported when the sky is invisible owing to fog, falling snow, and the like, or when the observer cannot estimate cloud amount owing to darkness or extraneous lighting. During moonless nights, it should usually be possible to estimate the total amount by reference to the proportion of the sky in which the stars are dimmed or completely hidden by clouds, although haze alone may blot out stars near the horizon.

The observer must also estimate the partial cloud amount. There are times, for example, when a higher layer of cloud is partially obscured by lower clouds. In these cases, an estimate of the extent of the upper cloud can be made with comparative assurance in daylight by watching the sky for a short time. Movement of the lower cloud relative to the higher cloud should reveal whether the higher layer is completely covering the sky or has breaks in it.

It should be noted that the estimation of the amount of each different type of cloud is made independently of the estimate of total cloud amount. The sum of separate estimates of partial cloud amounts often exceeds both the total cloud amount, as well as eight oktas.

### 15.2.3 Estimation of cloud-base height

At stations not provided with measuring equipment, the values of cloud-base height can only be estimated. In mountainous areas, the height of any cloud base which is lower than the tops of the hills of the mountains around the station can be estimated by comparison with the heights of well-marked topographical features as given in a contour map of the district. It is useful to have, for permanent display, a diagram detailing the heights and bearings of hills and the landmarks which might be useful in estimating cloud height. Owing to perspective, the cloud may appear to be resting on distant hills, and the observer must not necessarily assume that this reflects the height of the cloud over the observation site. In all circumstances, the observer must use good judgment, taking into consideration the form and general appearance of the cloud.

The range of cloud-base heights above ground level which are applicable to various genera of clouds in temperate regions is given in the table below and refers to a station level of not more than 150 m (500 ft) above MSL. For observing sites at substantially greater heights, or for stations on mountains, the height of the base of the low cloud above the stations will often be less than indicated in the table below.

In other climatic zones, and especially under dry tropical conditions, cloud-base heights may depart substantially from the given ranges. The differences may introduce problems of cloud classification and increase the difficulty of estimating the height. For instance, when reports on tropical cumulus clouds of an obviously convective origin, with a base well above 2 400 m (8 000 ft) or even as high as 3 600 m (12 000 ft), have been confirmed by aircraft observations. It is noteworthy that, in such cases, surface observers frequently underestimate cloud heights to a very serious degree. These low estimates may be due to two factors, namely either the observer expects the cumulus cloud to be a “low cloud” with its base below 2 000 m (6 500 ft) and usually below 1 500 m (5 000 ft), or the atmospheric conditions and the form of the cloud combine to produce an optical illusion.

When a direct estimate of cloud-base height is made at night, success depends greatly on the correct identification of the form of the cloud. General meteorological knowledge and close observation of the weather are very important in judging whether a cloud base has remained substantially unchanged or has risen or fallen. A most difficult case, calling for great care and skill, occurs when a sheet of altostratus covers the sky during the evening. Any gradual lowering of such a cloud sheet may be very difficult to detect, but, as it descends, the base is rarely quite uniform and small contrasts can often be discerned on all but the darkest nights.

**Cloud-base height genera above ground level in temperate regions**

| *Cloud genera* | *Usual range of height of base*[a] | | *Wider range of height of base sometimes observed, and other remarks* | |
|---|---|---|---|---|
| | (m) | (ft) | (m) | (ft) |
| **Low** | | | | |
| Stratus | Surface–600 | Surface–2 000 | Surface–1 200 | Surface–4 000 |
| Stratocumulus | 300–1 350 | 1 000–4 500 | 300–2 000 | 1 000–6 500 |
| Cumulus | 300–1 500 | 1 000–5 000 | 300–2 000 | 1 000–6 500 |
| Cumulonimbus | 600–1 500 | 2 000–5 000 | 300–2 000 | 1 000–6 500 |
| **Middle** | (km) | | | |
| Nimbostratus | Surface–3 | Surface–10 000 | Nimbostratus is considered a middle cloud for synoptic purposes, although it can extend to other levels | |
| Altostratus | 2–6 | 6 500–20 000 | Altostratus may thicken with progressive lowering of the base to become nimbostratus | |
| Altocumulus | | | | |
| **High** | | | | |
| Cirrus | | | Cirrus from dissipating cumulonimbus may occur well below 6 km (20 000 ft) in winter | |
| Cirrostratus | 6–12 | 20 000–40 000 | Cirrostratus may develop into altostratus | |
| Cirrocumulus | | | | |

Note:

a For stations over 150 m above sea level, the base of low-level clouds will often be less than indicated.

### 15.2.4 Observation of cloud type

Observation of cloud type is still widely performed by human observers. Pictorial guides and coding information are available from many sources, such as WMO (2017), as well as from publications of NMHSs.

## 15.3 INSTRUMENTAL MEASUREMENT OF CLOUD AMOUNT

Multiple types of ground-based operational sensors are available to measure total cloud amount. Measurements from space-borne radiometers in the visible band, supplemented by IR images, can be used to estimate cloud amounts over wide areas, even though difficulties are often experienced – for example, the inability to distinguish between low stratus and fog. Amounts of cloud within the range of a ceilometer can be estimated by measuring the proportion of elapsed time occupied by well-identified layers and assuming that these time-averaged results are representative of the spatial conditions around the observing site. This technique generally gives satisfactory results, but it can lead to significant differences with the cloud amount estimated visually due to the limited spatial representativeness of the sky sampled by the ceilometer. For AWSs in the United States, a "clustering" technique has been developed using data from ceilometers. Other countries, such as Sweden (Larsson and Esbjörn, 1995) and the Netherlands (Wauben, 2002), have introduced similar techniques in their operational observations. Automated cloud measurements using ceilometers are also used at airports by several meteorological offices. This technique has been used to obtain cloud information at small airports without an observer, and also at bigger ones where the automated system provides a cost-effective method to collect information.

Other instruments used to measure cloud amount include pyrometers, which may sample in multiple fixed directions and/or scan the sky, and sky cameras that are designed specifically for this purpose. By suitable processing such information can also be derived from commercial camera systems, and visible and IR webcams.

### 15.3.1 Measurement of cloud amount by laser ceilometer

Several meteorological services use time series of cloud base measurements from laser ceilometers (see 15.4.1) to determine cloud amount. This method has some advantages compared to manual observations. Using a ceilometer gives more consistent results. Also, output can be generated more frequently and there are no problems during night-time. However, there are also some drawbacks and large deviations can occur in situations with high, thin cirrus clouds when the performance of the ceilometer is reduced; when a moist layer is reported as a cloud base by the ceilometer; when a ceilometer detects no cloud base or at the wrong height during precipitation; and when the ceilometer reports a cloud base at the lowest elevation during shallow fog. This method also relies on the clouds to move over the field of view of the instrument. Clouds do not always move in that way. Even if clouds do move across the field of view of the ceilometer, these clouds may not be representative of the total sky. Thus, the time series of the cloud base may not always represent the total sky, on which the reporting of cloud cover should be based. Most differences can be attributed to the limited spatial representativeness of a ceilometer sampling only a small area directly overhead. Agreements (within 2 okta) between this method and manual observation of total cloud amounts are typically 85%–90%, as found for coastal stations at mid-latitudes (WMO, 2006*a*). These results are affected by the relatively large number of overcast situations (7 or 8 okta occurs about 55% of the time). The characteristic difference between estimations of total cloud amount obtained with a ceilometer and by observation is because the ceilometer, with a limited view of the sky, will report 8 okta much more often than 7 okta, whereas an observer can detect gaps anywhere in the cloud cover, resulting in nearly equal occurrences of 7 and 8 okta.

Some airports are equipped with several ceilometers and a multiple-ceilometer sky condition algorithm. However, evaluation at an airport has shown only small improvements when using three ceilometers compared to one (Wauben, 2002). This indicates that monitoring three points instead of one is still not sufficient to get a representative value for the entire sky.

As an example of cloud amount measurement with laser ceilometers, the United States National Weather Service Automated Surface Observing System (ASOS) method is described in the following paragraphs.

The cloud height indicator (laser ceilometer – see 15.4.1) compiles samples of backscatter return signals every 30 s and determines the height of valid cloud "hits". Every minute, the last 30 min of 30-s data are processed to give double weighting to the last 10 min in order to be more responsive to recent changes in sky condition. The data are then sorted into height "bins".

Each minute, if more than five height bin values have been recorded (during the last 30 min), the cloud heights are clustered into layers using a least-square statistical procedure until there are only five bins remaining (each bin may have many hits in it). These bins, or clusters, are then ordered from lowest to highest height. Following this clustering, the ASOS determines whether clusters can be combined and rounded, depending on height, into meteorologically significant height groups. The resulting bins now are called "layers" and the algorithm selects up to three of these layers to be reported in the METAR/SPECI in accordance with the national cloud layer reporting priority.

The amount of sky cover is determined by adding the total number of hits in each layer and computing the ratio of those hits to the total possible. If there is more than one layer, the hits in the first layer are added to the second (and third) to obtain overall coverage. For reporting purposes, the ASOS-measured cloud amount for each layer is then converted to a statistical function equivalent to a human observation.

The algorithm also tests for total sky obscuration based on criteria of low surface visibility and a high percentage of "unknown hits" at low levels.

A sky condition algorithm has also been developed for use where cloud formation (or advection) typically occurs in (or from) a known location and results in significant concurrent differences in sky conditions over an airport. This meteorological discontinuity algorithm uses input from two cloud-height indicator sensors. The primary sensor is sited near the touchdown zone of the primary instrument runway. The second sensor is typically sited 3 to 6 km (2 to 4 miles) from the primary sensor, upwind in the most likely direction of the advection, or closer to the fixed source of the unique sky condition. The second cloud-height indicator serves to detect operationally significant differences in sky conditions.

Further details on the ASOS sky condition algorithm and its verification are provided by US NOAA (1988) and the United States Government (1999).

### 15.3.2 Measurement of cloud amount by infrared detector

Pyrometers, or passive IR radiometers, are basically remote-sensing IR thermometers (8–14 μm). These can be used to observe elementary solid angles of the sky either by using multiple fixed sensors (for example, four fixed sensors used to sample the whole sky), by scanning the entire sky dome with a single sensor, or by a combination of the two methods (one manufacturer's design has 14 sensors across 180 degrees of elevation from one horizon to the opposite horizon, and a physical mechanism scans the azimuth). The downward thermal emission from the clouds and from the air column between clouds and the instrument is measured and the temperature of each sampled solid angle is derived from a combination of the Planck and the Stefan-Boltzmann laws. The IR temperature can then be used to provide an indication of cloud presence in each sampled solid angle. The total proportion of sky containing cloud can then be derived and reported as the cloud cover.

Scanning pyrometers avoid the problems of representativeness of the measurement that is present in other methods, depending on the number of points sampled. Also, nocturnal observations are possible. A disadvantage is that fractioned and/or transparent "pixels" are difficult to classify. For example, a scanning pyrometer, the so-called NubiScope, can be operated continuously for routine measurements of the total cloud amount (WMO, 2010). Every 10 minutes a scan of the sky is obtained with a resolution of 36 by 30 pixels. The pyrometer is located at the end of the tube making it quite insensitive to contamination. The cloud detection threshold is about -65 °C, but depends on the contamination of the lens, the contribution of water vapour to the measured brightness temperature and the optical depth of the cloud. The NubiScope detects clouds when the measured atmospheric brightness temperature is above the clear sky background value. The clear sky brightness temperature increases with larger zenith angles due to the increasing slant path through the atmosphere, and varies over time due the variations in atmospheric water vapour. The sensor adapts the clear sky reference dynamically during each scan when sufficient cloud-free scenes at various elevations are available. Boers et al. (2010) concluded that a hemispheric cloud observation method (such as the NubiScope) instead of a column method (such as a ceilometer) should be used to replace an observer to avoid discontinuities in the cloudiness distribution function of climate records.

Infrared sky camera systems using uncooled micro-bolometer detector arrays measure the downwelling atmospheric radiation in the 8-14 μm wavelength band. The so-called whole-sky infrared cloud measuring system (Liu et al., 2013) combines several IR images of the sky to get a whole-sky image every 15 minutes with a resolution of 650 by 650 pixels. The processing of the IR images for cloudiness is similar to that of a scanning pyrometer. The system uses real-time temperature, relative humidity profiles and horizontal visibility data to optimize the threshold for cloud base detection. In addition, the high spatial resolution allows derivation of the cloud type as for a visual camera.

Pyrgeometers measure the downward atmospheric long-wave radiation (4.5-100 μm). The level of long wave radiation and its variability can be used to estimate the total cloud amount (Dürr and Philipona, 2004).

### 15.3.3 Measurement of cloud amount by sky camera

Cameras specifically designed to measure cloud amount exist. They view the total sky using, for example, curved mirrors. The image from the sky is analysed by an algorithm that determines whether a cloud is present in each pixel using the measured colour. The sum of all pixels results in cloud amount. In the past specifically designed sky imagers were used during daytime only to estimate the total amount of cloud. Nowadays, DSP IP (digital signal processing Internet Protocol) cameras or webcams can be used for that purpose, whereas cameras with IR night vision also give useful results in low lighting conditions. Extensive developments have been achieved in the software that is used to analyse sky images to determine not only cloud amount but also type (see, for example, Wacker et al., 2015).

This method avoids the problems of representativeness of the measurement that can be present in some other methods. Some cameras use daylight and are thus not applicable at night. Cameras measuring in the IR do not have this disadvantage, but these have a smaller field-of-view and are more expensive. Sky cameras require frequent maintenance in the form of cleaning of the optical surfaces.

## 15.4 INSTRUMENTAL MEASUREMENT OF CLOUD-BASE HEIGHT

Several methods exist for measuring cloud-base height. They are: using a laser ceilometer, using a rotating-beam ceilometer, using a searchlight and using a balloon. The method currently most used is the laser ceilometer. This technique has great advantages over other technologies and should therefore be considered as the most appropriate. Other techniques such as cloud radars and radiosonde also give information on the cloud-base height, but these systems are not cost effective when used solely for this purpose.

Note that, in addition, information on the cloud-base height is obtained from the pyrometers and micro-bolometers mentioned above as they measure the sky or cloud-base temperature. The observed temperature is affected by humidity and aerosol and requires the temperature profile to obtain the cloud-base height. Therefore the cloud-base height information from IR detectors is rather poor, especially for low altitudes.

Sky imagers can give cloud-base height stereographically by viewing the same cloud with two imagers. It must be possible to identify the same specific cloud feature on both images for the technique to work correctly. The accuracy of the cloud-base height depends on the geometry that involves the distance between the imagers and the position (orientation) of the feature on both images.

### 15.4.1 Measurement of cloud-base height by laser ceilometer

#### 15.4.1.1 *Measurement method*

With the laser ceilometer, the height of the cloud base is determined by measuring the time taken for a pulse of coherent light to travel from a transmitter to the cloud base and to return to a receiver (principle: light detection and ranging, lidar). The output from a laser is directed vertically upwards to where, if there is cloud above the transmitter, the radiation is scattered by the hydrometeors forming the cloud. The major portion of the radiation is scattered upward but some is scattered downward and is focused in the receiver onto a photoelectric detector. The radiant flux backscattered to the receiver decreases with range according to an inverse-square law. The ceilometer (Figure 15.1) generally comprises two units, a transmitter-receiver assembly and a recording unit.

The transmitter and receiver are mounted in a single housing, together with signal detection and processing electronics. The light source is generally a semiconductor laser with a wavelength in the near IR. The optics of the transmitter are arranged to place the laser source and receiver detector at the focus of a conventional or Newtonian telescope system. The surfaces of the

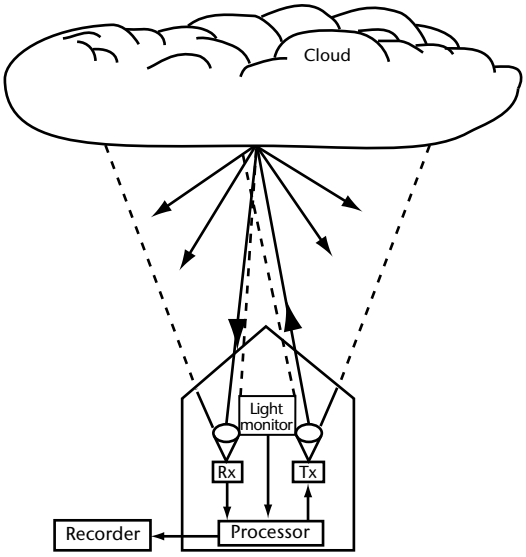



**Figure 15.1. Typical laser ceilometer**

lens are given a suitable quarter-wavelength coating to reduce reflection and to provide high transmission of light. The transmitter aperture is sealed by a glass window that is anti-reflection, coated on its inner surface and angled so that rain will run off it.

The receiver is of similar construction to the transmitter, except that the light source is replaced by a photodiode, and a narrowband optical filter is incorporated. The filter excludes most of the background diffuse solar radiation, thus improving the detection of the scattered laser radiation by day.

The transmitter and receiver can be mounted side-by-side so that the transmitter beam and the receiver field of view begin to overlap at about 80 m above the assembly and are fully overlapped at a few hundred metres (see, for example, WMO, 2016*c*). Cloud-base detection in the blind zone below the beginning of overlap relies on return signals from the emitted pulse that have been scattered at least twice. Some systems use the same lens for the transmitted and received radiation, so that this problem is avoided.

The housing is provided with heaters to prevent condensation from forming on the optical surfaces, and the humidity within the housing can be reduced by the use of a desiccator. The top of the housing is fitted with a cover hood incorporating optical baffles that exclude direct sunlight.

The output from the detector is separated into sequential "range gates", each range gate representing the minimum detectable height increment. A threshold is incorporated so that the probability of the instrument not "seeing" cloud, or "seeing" non-existent cloud, is remote.

#### 15.4.1.2 ***Exposure and installation***

Ceilometers should be installed following the recommendations of the manufacturer. The unit should be mounted on a firm base, with a clear view overhead within a cone of approximately 30° about the vertical. If necessary, a rooftop site can be used with suitable adjustment of reported heights to ground level. Although laser ceilometers in operational use are designed to be "eye safe", care should be taken to prevent the casual observer from looking directly into the transmitted beam. IEC has published a set of international standards on safety of laser products (IEC 60825:2018 SER) which also includes a classification scheme according to eye safety. Eye-safe laser ceilometers meeting the requirements of a class 1 or class 1M laser device as defined by this standard are commercially available.

Tilting of the instrument is necessary at some locations to prevent the sun from entering the field of view of the ceilometer. To reduce the impact of strongly reflecting raindrops, the beam with the telescope can be aligned about 5° from the vertical.

#### 15.4.1.3 *Sources of error*

There are five main sources of error:

(a) Ranging errors: These can occur if the main timing oscillator circuits develop faults, but, in normal operation, errors due to this source can be ignored;

(b) Verticality of the transmitted/received beams: Provided that the instrument is aligned with the beam at better than 5° from the vertical, errors from this source can be ignored;

(c) Errors due to the signal-processing system: Because a cloud base is generally diffuse and varies greatly in time and distance, complex algorithms have been developed to estimate a representative cloud-base height from the returned cloud signal. In conditions of fog (with or without cloud above) and during precipitation, serious errors can be generated. Thus, it is important to have an awareness of visibility and precipitation conditions to assess the value of ceilometer information. In conditions of well-defined stratiform cloud (for example, low stratocumulus), measurement errors are controlled solely by the cloud threshold algorithms and can be assumed to be consistent for a particular make of ceilometer;

(d) Measurement range: Due to the limited power available from the laser, reflected radiation from high altitudes may have such low intensity that it cannot be detected. Therefore, cloud-base height from cirrus clouds may not always be observed.

(e) Incorrect cloud base detections: These can be caused by instrument noise. Aerosol and moist atmospheric layers can also trigger incorrect cloud base detections. Overpassing airplanes and birds, overhanging vegetation, and snow caps on the ceilometer hood can generate faulty cloud base detections.

In operational use and conditions of uniform cloud base, laser ceilometer measurements can be compared with pilot balloon ascents, aircraft measurements, visibility measurements at various altitudes up a mast or the height up to which a tower can be discerned from a camera image, and at night with cloud searchlight measurements.

Intercomparisons of laser ceilometers of different manufacturers have been carried out extensively. During the WMO International Ceilometer Intercomparison (WMO, 1988), for example, several designs of ceilometer were intercompared and comparisons made with rotating-beam ceilometer and pilot-balloon observations. The international intercomparison revealed that, using current technology, laser ceilometers provided the most accurate, reliable and efficient means of measuring cloud-base height from the ground when compared with alternative equipment.

#### 15.4.1.4 *Calibration and maintenance*

Most laser ceilometers are provided with a built-in capability to monitor the transmitted output power and the sensitivity of the detector and guard against serious timing errors. Calibration checks are normally confined to checking both the master oscillator frequency and stability, using external high-quality frequency standards, and the output power of the transmitter. Calibration may also be performed by intercomparison (WMO, 1988). Some NMHSs perform a field acceptance test for each ceilometer during which the cloud base detection is verified against a trusted instrument. Pointing the ceilometer to a target at a known distance (for example, a tower) can be used to confirm the distance measurement of the instrument. Routine maintenance consists typically of cleaning the exposed optics and external covers and of replacing air filters when cooling blowers are provided. Note that ceilometers generally analyse the light pulse reflected by the window to monitor the window contamination. Warning and

alarm messages are generated that alert service staff when the instrument needs to be cleaned or when the sensitivity of the instrument over the entire range might be reduced due to window contamination.

Calibration checks and routine maintenance or troubleshooting should be carried out in accordance with the manufacturer's recommendations. Most laser ceilometers have built-in diagnostic capability to identify common faults. It is recommended that maintenance routines or troubleshooting should only be undertaken by suitably trained personnel, as hazardous voltages may be present and the laser may cause eye damage if viewed inappropriately. A ceilometer is generally designed such that precipitation runs off the window and in addition warm air is blown over the window at regular intervals to remove precipitation and leaves. Normally, little maintenance will be necessary beyond cleaning of optical surfaces and replacement of cooling fan dust filters. Snow caps on the ceilometer hood and objects or vegetation overhead of the instrument should also be removed during maintenance. During inspection it should be made sure that no snow or vegetation is or will grow overhead of the instrument, and that the ceilometer is not directly under the approach or take-off path of aircraft or exhaust plumes.

The range calibration may be checked in the field by comparison with cloud heights obtained using an alternative method. If cloud is not present, it is possible to point the instrument towards a solid target at a known distance. This may need to be located several hundred metres away, beyond the minimum range limit of the ceilometer. Extreme care must be taken to prevent accidental exposure to the laser beam by persons beyond the target. Some manufacturers provide a cloud simulator for verifying the operation of the ceilometer.

Modern ceilometers can make the backscatter profiles available from which the cloud base information is derived. This information is useful for verifying the correct operation of the instrument. Hence it is recommended to archive the backscatter data when possible. The data can also be used for troubleshooting, reprocessing results with optimized cloud detection algorithms, and generating additional products such as mixing-layer height and the detection of aerosol layers. In addition, the backscatter profile during cloud-free situations can be analysed to verify the overlap correction and instrument noise characteristics that might otherwise trigger faulty cloud base detections. Furthermore, two complementary calibration methods can be used in suitable conditions for ceilometer networks with access to backscatter data. These are: (a) the so-called Rayleigh method that is based on lidar returns from purely molecular layers, which is most suitable for ceilometers using photon-counting detection; (b) the so-called cloud method that is based on the full attenuation of the lidar signal in a liquid cloud, most suitable for ceilometers with analogue detection (see WMO, 2016*d*).

### 15.4.2 Measurement of cloud-base height by rotating-beam ceilometer

#### 15.4.2.1 *Measurement method*

The rotating-beam ceilometer involves the measurement of the angle of elevation of a light beam scanning in the vertical plane, at the instant at which a proportion of the light scattered by the base of the cloud is received by a photoelectric cell directed vertically upwards at a known distance from the light source (see Figure 15.2). The equipment comprises a transmitter, a receiver and a recording unit.

The transmitter emits a narrow light beam of a 2° divergence, with most of the emitted radiation on the near-IR wavelengths, that is, from 1 to 3 μm. Thus, the wavelength used is small in comparison with the size of the water droplets in clouds. The light beam is swept in a vertical arc extending typically from 8° to 85° and is modulated at approximately 1 kHz so that, through the use of phase-sensitive detection methods, the SNR in the receiver is improved.

The receiving unit comprises a photoelectric cell and an angle-of-view restrictor; the restrictor ensures that only light that falls vertically downwards can reach the photoelectric cell. A pen in the recording unit, moving simultaneously with the transmitter beam, records when a cloud signal is received.

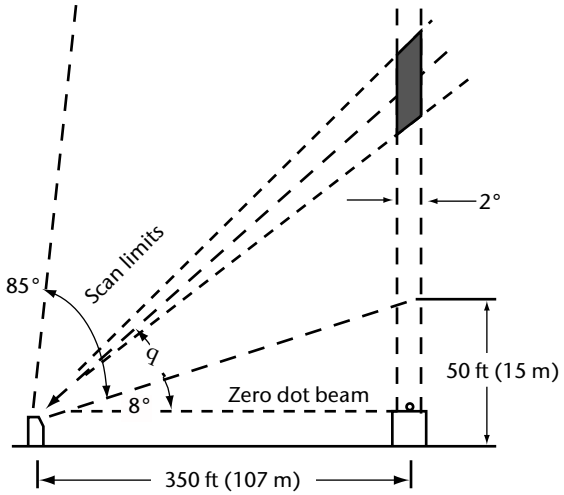



**Figure 15.2. A typical rotating-beam ceilometer**

15.4.2.2 ***Exposure and installation***

The transmitter and receiver should be sited on open, level ground separated by some 100 to 300 m and mounted on firm and stable plinths. It is extremely important that the transmitter scan in the same plane as the receiver. This is achieved by the accurate alignment of the optics and by checking the plane of the transmitter beam in suitable conditions at night.

15.4.2.3 ***Sources of error***

Errors in the measurement of cloud-base height using a rotating-beam ceilometer may be due to the following:

(a) Beamwidth;

(b) Optical misalignment;

(c) Mechanical tolerances in moving parts;

(d) Receiver response.

Since in most designs the volume of intersection of the transmitter and receiver cone is very significant with a cloud height above 500 m, beamwidth-induced errors are generally the most serious. The definition of cloud base given in 15.1.1 is not an adequate basis for the objective design of ceilometers, thus the algorithms in current use are based on experimental results and comparisons with other methods of estimation. Some rotating-beam ceilometers use a "threshold" technique to determine the presence of cloud, while others use a "peak" signal detection scheme. In either case, receiver sensitivity will affect reported cloud heights, giving rise to large errors in excess of stated operational requirements in some circumstances (Douglas and Offiler, 1978). These errors generally increase with indicated height.

Rotating-beam ceilometers are very sensitive to the presence of precipitation. In moderate or heavy precipitation, the instrument can either indicate low cloud erroneously or fail to detect clouds at all. In foggy conditions, the light beam may be dissipated at a low level and the ceilometer can fail to give any useful indication of clouds, even when a low cloud sheet is present.

Comparisons of rotating-beam ceilometers and laser ceilometers have been carried out and widely reported (WMO, 1988). These have shown good agreement between the two types of ceilometers at indicated heights up to some 500 m, but the detection efficiency of the rotating-beam ceilometer in precipitation is markedly inferior.

#### 15.4.2.4 *Calibration and maintenance*

The only maintenance normally undertaken by the user is that of cleaning the transmitter and receiver windows and changing the chart. The outside of the plastic windows of the transmitter and receiver should be cleaned at weekly intervals. A soft, dry cloth should be used and care should be taken not to scratch the window. If the transmitter lamp is replaced, the optical alignment must be checked. The transmitter and receiver levelling should be checked and adjusted, as necessary, at intervals of about one year.

### 15.4.3 Measurement of cloud-base height by searchlight

#### 15.4.3.1 *Measurement method*

Using this method, illustrated in Figure 15.3, the angle of elevation, $E$, of a patch of light formed on the base of the cloud by a vertically-directed searchlight beam is measured by an alidade from a distant point. If $L$ is the known horizontal distance in metres (feet) between the searchlight and the place of observation, the height, $h$, in metres (feet) of the cloud base above the point of observation is given as the following:

$$h = L \tan E \tag{15.2}$$

The optimum distance of separation between the searchlight and the place of observation is about 300 m (1 000 ft). If the distance is much greater than this, then the spot of light may be difficult to see; if it is much less, the accuracy of measuring a height above about 600 m (2 000 ft) suffers. A distance of 250–550 m (800–1 800 ft) is usually acceptable.

#### 15.4.3.2 *Exposure and installation*

It is desirable to have a clear line of sight between the searchlight and the alidade, both of which should be mounted on firm, stable stands. Where there is a difference in the height above the ground between the searchlight and the alidade, a correction must be incorporated in the calculated heights. If a clear line of sight is not possible, any obstruction between the searchlight beam and the alidade should not be higher than 100 feet.

#### 15.4.3.3 *Sources of error*

The largest source of error is due to uncertainty in the measured angle of elevation. Height errors due to small errors of verticality are insignificant.

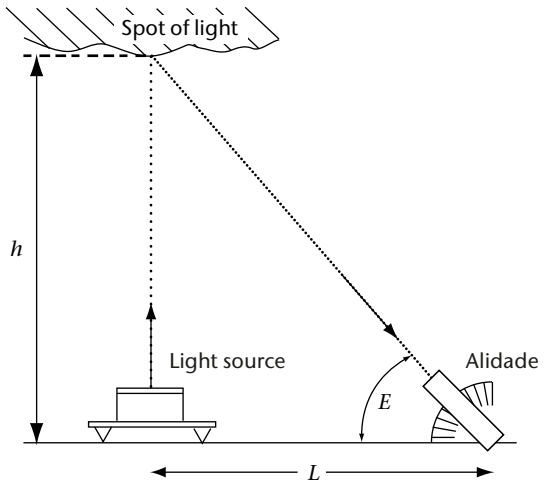



**Figure 15.3. Principle of the cloud searchlight method**

The absolute error $\Delta h$ in the derived cloud height due to an error $\Delta E$ in the measured elevation is given by the following ($L$ is assumed to be an accurately measured constant):

$$\Delta h = L \cdot \left(1/\cos^2 E\right) \cdot \Delta E = L \sec^2 E \cdot \Delta E \tag{15.3}$$

with $E$ in radians (1° = $\pi$/180 rad). Note that $\Delta h$ tends to infinity when $E \rightarrow 90°$. If $L$ = 1 000 ft (300 m) and $\Delta E$ = 1°, the value of $\Delta h$ is 17 ft (6 m) when $h$ = 1 000 ft (300 m), and $\Delta h$ is about 450 ft (140 m) when $h$ = 5 000 ft (1 500 m). The relative error in $h$ is given by:

$$\Delta h/h = 1/\left(\sin E \cdot \cos E\right) \cdot \Delta E \tag{15.4}$$

with $E$ in radians. $\Delta h/h$ is minimal when $E = 45°$ (or $h = L$).

### 15.4.3.4 *Calibration and maintenance*

The focusing and verticality of the beam, should, if possible, be checked about once a month because the lamp filament is liable to undergo slight changes in shape with time. When a lamp is replaced, the adjustment for lamp position should be carried out since not all lamps are identical.

The verticality of the beam should be checked during an overcast night with the aid of a theodolite. The check should be made from two positions, one near the alidade and the other at about the same distance away from the searchlight in a direction at right angles to the line joining the searchlight and the alidade (Figure 15.4). The azimuths of the searchlight and of the spot of light on the cloud should be measured as accurately as possible, together with the elevation of the spot of light. If the difference between the azimuth readings is $A$ and the angle of elevation is $E$, the deviation $\phi$ of the beam from the vertical is given by:

$$\phi = \arctan\left(\tan A/\tan E\right) \approx A/\tan E \quad \left(\text{for } A \approx 1° \text{ or less}\right) \tag{15.5}$$

If the value of $\phi$ is more than 1° when viewed from the alidade, or more than 0.5° in the other position, these adjustments should be repeated until the necessary accuracy is obtained.

Focusing can be checked and adjusted on an overcast night by observing the diameter of the light spot on the highest cloud above the instrument. If necessary, the focus should be adjusted to minimize the spot diameter.

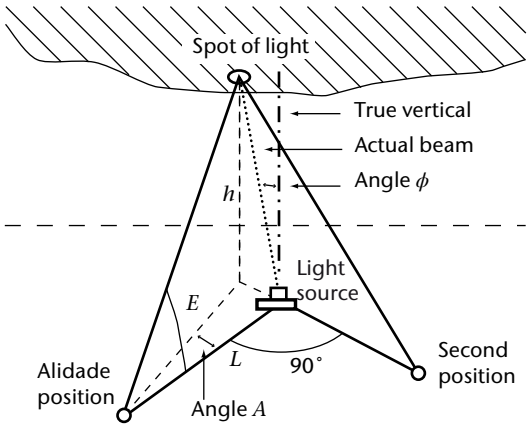



**Figure 15.4. Checking the verticality of the searchlight beam**

### 15.4.4 Balloon measurement of cloud-base height

#### 15.4.4.1 *Measurement method*

Cloud height may be measured in daylight by determining the time taken by a small rubber balloon, inflated with hydrogen or helium, to rise from ground level to the base of the cloud. The base of the cloud should be taken as the point at which the balloon appears to enter a misty layer before finally disappearing.

The rate of ascent of the balloon is determined mainly by the free lift of the balloon and can be adjusted by controlling the amount of hydrogen or helium in the balloon. The time of travel between the release of the balloon and its entry into the cloud is measured by means of a stop-watch. If the rate of ascent is $n$ metres per minute and the time of travel is $t$ minutes, the height of the cloud above ground is $n \cdot t$ metres, but this rule must not be strictly followed. Eddies near the launch site may prevent the balloon from rising until some time after it is released. Normally the stop-watch is started on the release of the balloon and, therefore, the elapsed time between when the balloon is released and the moment when it is observed to have left the eddies will need to be subtracted from the total time before determining the cloud height. Apart from eddy effects, the rate of ascent in the lowest 600 m (2 000 ft) or so is very variable.

Although the height of the base of a cloud at middle altitude is sometimes obtained as a by-product of upper wind measurements taken by pilot balloons, the balloon method is mainly applicable to low clouds. Where no optical assistance is available in the form of binoculars, telescope or theodolite, the measurement should not be attempted if the cloud base is judged to be higher than about 900 m (3 000 ft), unless the wind is very light. In strong winds, the balloon may pass beyond the range of unaided vision before it enters the cloud.

Precipitation reduces the rate of ascent of a balloon and measurements of cloud height taken by a pilot balloon should not be attempted in other than light precipitation.

This method can be used at night by attaching an electric light to the balloon. For safety reasons, the use of candle lanterns is strongly discouraged.

#### 15.4.4.2 *Sources of error*

Measurements of cloud base taken using a height balloon must be used with caution, since the mean rate of ascent of a balloon, especially in the first few hundred metres, may differ appreciably from the assumed rate of ascent (owing to the effects of vertical currents, the shape of the balloon, precipitation and turbulence).

## 15.5 INSTRUMENTAL MEASUREMENT OF CLOUD TYPE

Observation of cloud type is still generally performed by human observers. One automatic method to observe cloud type is used operationally, which is specifically for detecting cumulonimbus and towering cumulus for aeronautical applications. In this method, data from a precipitation radar and lightning detection network are used. The radar-reflectivity classes and the number of lightning discharges within a certain area are combined to give information on the presence of cumulonimbus and/or towering cumulus. This is a new method which is used by a few meteorological offices. The false alarm rate is relatively high (see WMO, 2006*b*). Some offices use satellite (VIS and IR channels) and model information to enhance the cumulonimbus and towering cumulus products.

The derivation of cloud type by considering several statistical spectral and textural features of the camera image is under development. The success rate is promising for homogenous cases (75%–88%), but lower in cases of mixed cloud types (see, for example, Heinle et al., 2010; Liu et al., 2011).

## 15.6 OTHER CLOUD-RELATED PROPERTIES

### 15.6.1 Vertical visibility

Vertical visibility is defined as the maximum distance at which an observer can see and identify an object on the same vertical as him/herself. It can be calculated from the extinction profile of the atmosphere. Ceilometers (see 15.4.1 and 15.4.2) may provide an estimate of vertical visibility based on the integrated extinction profile with range (see equation 15.1). WMO (1988) showed that this method frequently produces unreliable results. In practice, a vertical visibility report is often given by a ceilometer when the cloud-base requirements are not met, but when reflected light is received from a certain altitude.

## REFERENCES AND FURTHER READING


Boers, R., M.J. de Haij, W.M.F. Wauben, H.K. Baltink, L.H. van Ulft, M. Savenije and C.N. Long, 2010: Optimized fractional cloudiness determination from five ground-based remote sensing techniques. *Journal of Geophysical Research*, 115:D24116, doi:10.1029/2010JD014661.

Douglas, H.A. and D. Offiler, 1978: The Mk 3 cloud base recorder: A report on some of the potential accuracy limitations of this instrument. *Meteorological Magazine*, 107:23–32.

Dürr, B. and R. Philipona, 2004: Automatic cloud amount detection by surface longwave downward radiation measurements. *Journal of Geophysical Research*, 109:D5201, doi:10.1029/2003JD004182.

Heinle, A., A. Macke and A. Srivastav, 2010: Automatic cloud classification of whole sky images. *Atmospheric Measurement Techniques*, 3(3):557–567, doi:10.5194/amt-3-557-2010.

International Electrotechnical Commission, 2018: Safety of laser products – ALL PARTS. IEC 60825:2018 SER.

Larsson, B. and E. Esbjörn, 1995: *Cloud Cover Algorithm.* SMHI IO-BN 1995-01-11, SMHI, Norrköping, Sweden.

Liu, L., X.-J. Sun, F. Chen, S.-J. Zhao and T.-C. Gao, 2011: Cloud classification based on structure features of infrared images. *Journal of Atmospheric and Oceanic Technology*, 28:410–417, doi: 10.1175/2010JTECHA1385.1.

Liu, L., X.-J. Sun, T.-C. Gao and, S.-J. Zhao, 2013: Comparison of cloud properties from ground-based infrared cloud measurement and visual observations. *Journal of Atmospheric and Oceanic Technology,* 30:1171–1179, doi: 10.1175/JTECH-D-12-00157.1.

United States Government, 1999: *Automated Surface Observing System.* Air Force Operational Test and Evaluation Center: Final Assessment Report for the Federal Aviation Administration, California, United States.

United States National Oceanic and Atmospheric Administration (US NOAA), 1988: *Federal Standard Algorithms for Automated Weather Observing Systems Used for Aviation Purposes*. Office of the Federal Coordinator for Meteorological Services and Supporting Research, United States Department of Commerce, FCM-S5-1988, Silver Spring, MD, United States.

Wacker, S., J. Gröbner, C. Zysset, L. Diener, P. Tzoumanikas, A. Kazantzidis, L. Vuilleumier, R. Stöckli, S. Nyeki and N. Kämpfer, 2015: Cloud observations in Switzerland using hemispherical sky cameras. *Journal of Geophysical Research*, 120:A695–707, doi:10.1002/2014JD022643.

Wauben, W.M.F., 2002: Automation of visual observations at KNMI: (II) Comparison of automated cloud reports with routine visual observations. In: *Symposium on Observations, Data Assimilation and Probabilistic Prediction*. AMS Annual Meeting, 2002 Report, Orlando, FL, United States.

World Meteorological Organization, 1988: *WMO International Ceilometer Intercomparison* (D.W. Jones, M. Ouldridge and D.J. Painting). Instruments and Observing Methods Report No. 32 (WMO/TD-No. 217). Geneva.

———, 2006a: Status, evaluation and new developments of the automated cloud observations in the Netherlands (W. Wauben, H. Klein Baltink, M. de Haij, N. Maat and H. The). Paper presented at the WMO Technical Conference on Meteorological and Environmental Instruments and Methods of Observation (TECO-2006). Instruments and Observing Methods Report No. 94 (WMO/TD-No. 1354). Geneva.

———, 2006b: Status of the automatic observation on aerodrome and ongoing improvements in France (M. Leroy). Paper presented at the WMO Technical Conference on Meteorological and Environmental Instruments and Methods of Observation (TECO-2006). Instruments and Observing Methods Report No. 94 (WMO/TD-No. 1354). Geneva.

———, 2010: Laboratory and field evaluation of the NubiScope (W. Wauben, F. Bosveld and H. Klein Baltink). Paper presented at the WMO Technical Conference on Meteorological and Environmental Instruments and Methods of Observation (TECO-2010). Instruments and Observing Methods Report No. 104 (WMO/TD-No. 1546). Geneva.

———, 2011 (updated in 2017): *Manual on Codes* (WMO-No. 306), Volume I.1. Geneva.

———, 2014: *Guide to Meteorological Observing and Information Distribution Systems for Aviation Weather Services* (WMO-No. 731). Geneva.

———, 2016*a*: The ceilometer inter-comparison campaign CeiLinEx2015 - Cloud detection and cloud base height (U. Görsdorf, et al.). Paper presented at the WMO Technical Conference on Meteorological and Environmental Instruments and Methods of Observation (TECO-2016). Instruments and Observing Methods Report No. 125. Geneva.

———, 2016*b*: Transition towards a new ceilometer network in the Netherlands: challenges and experiences (M. de Haij, A. Apituley, W. Koetse and H. Bloemink). Paper presented at the WMO Technical Conference on Meteorological and Environmental Instruments and Methods of Observation (TECO-2016). Instruments and Observing Methods Report No. 125. Geneva.

———, 2016*c*: A new procedure to perform an absolute calibration of ceilometers (G. Martucci, A. Haefele, M. de Huu, M. Tschannen, A. Küng and V. Simeonov). Paper presented at the WMO Technical Conference on Meteorological and Environmental Instruments and Methods of Observation (TECO-2016). Instruments and Observing Methods Report No. 125. Geneva.

———, 2016*d*: The E-PROFILE network for the operational measurement of wind and aerosol profiles over Europe (A. Haefele, M. Hervo, M. Turp, J-L Lampin, M. Haefelin, V. Lehmann, the E-PROFILE team and the TOPROF team). Paper presented at the WMO Technical Conference on Meteorological and Environmental Instruments and Methods of Observation (TECO-2016). Instruments and Observing Methods Report No. 125. Geneva.

———, 2017: *International Cloud Atlas: Manual on the Observation of Clouds and Other Meteors* (WMO-No. 407). Geneva.

# CHAPTER 16. MEASUREMENT OF ATMOSPHERIC COMPOSITION

## 16.1 GENERAL

The main purpose of this chapter is to introduce readers (particularly those who are new to these types of measurements) to methods and specific techniques used for measuring various components of atmospheric composition and a number of related physical parameters. This is often accompanied by measurements of basic meteorological variables, as introduced in the preceding chapters. Within WMO, the GAW Programme was established in response to the growing concerns related to human impacts on atmospheric composition and the connection of atmospheric composition to weather and climate. GAW's mission is focused on the systematic global observations of the chemical composition and related physical characteristics of the atmosphere, integrated analysis of these observations and development of predictive capacity to forecast future atmospheric composition changes (WMO, 2017*a*).

Observations and analyses of the chemical composition of the atmosphere are needed to advance the scientific understanding of the effects of the increasing influence of human activity on it, as illustrated by pressing societal problems such as: changes in the weather and climate related to human influence on atmospheric composition, particularly on greenhouse gases (GHGs), ozone and aerosols; impacts of air pollution on human and ecosystem health and issues involving long-range transport and deposition of air pollution; changes in UV radiation as a consequence of changes in atmospheric ozone amounts and climate, and the subsequent impact of these changes on human health and ecosystems.

For further practical details on measurement activities, see the GAW reports and other references listed at the end of the chapter.

The GAW observations focus on six classes of variables:

(a) Ozone: column (total) ozone and ozone vertical profiles with a focus on the stratosphere and upper troposphere;

(b) GHGs: carbon dioxide ($CO_2$) (including $\Delta^{14}C$, $\delta^{13}C$ and $\delta^{18}O$ in $CO_2$, and oxygen/nitrogen ($O_2/N_2$) ratios), methane ($CH_4$) (including $\delta^{13}C$ and $\delta D$ in $CH_4$), nitrous oxide ($N_2O$) and halogenated compounds ($SF_6$);

(c) Reactive gases: surface and tropospheric ozone ($O_3$), carbon monoxide (CO), volatile organic compounds (VOCs), nitrogen oxides ($NO_x$), sulphur dioxide ($SO_2$), molecular hydrogen ($H_2$) and ammonia ($NH_3$);[1]

(d) Atmospheric total[2] deposition (focused largely on major ions in the wet deposition group);

(e) UV radiation;

(f) Aerosols (including near-surface in situ physical, optical and chemical properties, total integrated column properties and profiling).

---

[1] Ammonia was identified as one of the key substances required to address the nitrogen cycle but recommendations concerning measurement guidelines are not yet available.

[2] Measurement techniques for dry deposition have not been recommended yet.

A number of ancillary parameters are recommended for measurement at GAW stations:

(a) Solar radiation;

(b) Major meteorological parameters;

(c) Natural radioactivity including krypton-85, radon and some other radionuclides.

Atmospheric water vapour was tentatively included in GAW in 2015 at the decision of the Environmental Pollution and Atmospheric Chemistry Scientific Steering Committee (WMO, 2015*a*) but the infrastructure has yet to be defined.

Due to the low mixing ratios of atmospheric trace constituents, the instruments and methods used for the quantitative and qualitative determination of atmospheric constituents are complex and sometimes difficult to operate. Small errors, for example in spectral signatures or cross-sensitivities to other compounds, can easily confound the accuracy of atmospheric composition measurements. Therefore, besides correct operation, accurate and reliable measurements also require regular calibration of the equipment, participation in intercomparison exercises, station audits and personnel training. Obtaining reliable and high-quality results for most of the measurements described here is not feasible without the close involvement of specialist staff at a professional level. The main principles of the QA of atmospheric composition observations within GAW are described in 16.1.4.

The GAW Programme Implementation Plan builds around the concept of "science for services" and addresses multiple applications that utilize atmospheric chemical composition observations. The need to improve knowledge of air quality variations, for example, on an urban scale, along with current technical development, has brought new measurement techniques into the community, namely low-cost environmental sensors. Low-cost air pollution sensors have the potential to deliver new information, but they are also prone to a number of shortcomings. Long-term suitability of such sensors has yet to be proven, and an ongoing broader assessment of different sensor technologies and application-specific requirements for data quality and calibration is required. As this is a fast-changing field, continuous re-evaluation, including new developments and changes in performance, may be required. An expert group under the umbrella of the Commission for Atmospheric Sciences has developed a comprehensive statement on the use of low-cost sensor technology (WMO et al., 2018).

### 16.1.1 Definitions and descriptions

Depending on the measurement principle and instrument platform, two types of measurements are routinely performed and reported, namely:

**Point measurements.** This refers to the results of (continuous or discrete) measurements of a particular component's quantity in a specific place in space (either in an atmospheric layer of a few tens of metres above the surface at a particular location on the Earth's surface, or anywhere in the troposphere, the stratosphere or any other atmospheric layer). A series of point measurements at several altitudes above a given location constitute a vertical profile measurement (for example, measurements from an aircraft or balloons/sondes, rockets, and the like). The point measurements can also be performed along specific horizontal routes using mobile platforms (for example, ship, train, road vehicle). Results of point measurements are commonly given in units of partial pressure, concentration, mixing ratio or mole fraction, corrected for standard temperature and pressure (STP) conditions of 273.15 K and 101.325 kPa, respectively, when measurements are performed above sea-level. The use of units that are not part of SI is strongly discouraged.

**Integrated measurements.** This refers to the integrated or average amount of a particular substance contained in the atmosphere along the observational path. This can be a vertical total column extending from the Earth's surface to the upper edge of the atmosphere. Commonly used units of total ozone are (a) equivalent column thickness of a layer of pure ozone at STP (273.15 K and 101.325 kPa); (b) vertical column density (total number of

molecules per unit area in an atmospheric column). For the other atmospheric constituents, vertical column density or column-averaged abundances are used. It is also common to report the partial column content of a substance, for example the tropospheric column content of $NO_x$. Here, the vertical column that is integrated extends from the Earth's surface to the tropopause. The differential optical absorption spectroscopy (DOAS) instruments also allow for measurements of average amount of substance along horizontal pathways.

Observations of atmospheric composition include gaseous composition, aerosol and total atmospheric deposition. The characteristics of precipitation chemical composition (wet deposition) are given in 16.5. The variables describing aerosols (physical and chemical properties) are listed in 16.6.

### 16.1.2 Units and scales

The following units are used to express the results of atmospheric trace compound observations:

**Number of molecules per unit area.** This represents the column abundance of atmospheric trace compounds. Still widely used is the Dobson unit (DU), which corresponds to the number of molecules of ozone required to create a layer of pure ozone $10^{-5}$ m thick at STP conditions. Expressed another way, 1 DU represents a column of air containing about $2.6868 \cdot 10^{16}$ ozone molecules for every square centimetre of area at the base of the column.

**Mass concentration.** This represents the mass of the specific constituent in unit volume of the atmospheric air (for example, microgram per $m^3$).

**Milliatmosphere centimetre (m-atm-cm).** A measure of total ozone equal to a thickness of $10^{-3}$ cm of pure ozone at STP (1 m-atm-cm is equivalent to 1 DU).

Mole fractions of substances in dry air (dry air includes all gaseous species except water vapour ($H_2O$):

– μmol $mol^{-1}$ = $10^{-6}$ mole of trace substance per mole of dry air

– nmol $mol^{-1}$ = $10^{-9}$ mole of trace substance per mole of dry air

– pmol $mol^{-1}$ = $10^{-12}$ mole of trace substance per mole of dry air

Dry mole fraction requires either drying of air samples prior to measurement or correction of the measurement for water vapour abundance. When drying is impossible or the correction would add substantial uncertainty to the measurement, wet mole fractions can be reported instead. This must be clearly indicated in the metadata of the observational record.

The appropriate unit for expressing amount of substance is dry-air mole fraction, reported as parts per million (ppm, that is, μmol $mol^{-1}$), ppb (parts per billion, that is, nmol $mol^{-1}$) or ppt (parts per trillion, that is, pmol $mol^{-1}$). A "v" has often been appended to these units to indicate mixing ratio by volume. When reporting mole fractions as volume mixing ratios, one assumes the atmosphere to be an ideal gas. Deviations from the ideal under GAW conditions can be large (such as for $CO_2$), so the use of mole fraction is strongly preferred because it does not require an implicit assumption of ideality of the gases and, more importantly, because it is also applicable to condensed-phase species. In general, the use of SI units is highly recommended.

**Isotope or molecular ratio.** Atmospheric molecules can be present in different isotopic configurations.[3] Isotope ratio data are expressed as deviations from an agreed-upon reference standard using the delta notation:

$$\delta = \left(R_{\text{sample}} / R_{\text{reference}} - 1\right), \text{with } R = \left[\text{heavy isotope}\right] / \left[\text{light isotope}\right] \quad (16.1)$$

$\delta$-Values are expressed in multiples of 1 000 (‰ or per mil).

The international reference scale (that is, the primary scale) for $\delta^{13}C$ is Vienna Pee Dee Belemnite (VPDB). NBS 19 and LSVEC (Coplen et al., 2006) are the primary international reference materials defining the VPDB scale. For $\delta^{18}O$, multiple scales are in use (VPDB, Vienna Standard Mean Ocean Water, air-$O_2$ (de Laeter et al., 2003)).

The delta notation is also used to express relative abundance variations of $O_2/N_2$ (and argon/nitrogen ($Ar/N_2$)) ratios in air:

$$\delta\left(O_2/N_2\right) = \left(R_{\text{sample}} / R_{\text{standard}} - 1\right), \text{with } R = O_2/N_2 \quad (16.2)$$

The respective international air standard is not yet established. The Scripps Institution of Oceanography local $O_2/N_2$ scale, based on a set of cylinders filled at the Scripps Pier, is the most widely used scale.

$\delta(O_2/N_2)$ values are expressed in multiples of $10^6$ or "per meg".

Precipitation chemistry (wet deposition) observations include measurements of several parameters that are described in more detail in 16.5. The following units are used:

(a) pH measurements are expressed in units of acidity defined as: $pH = -\log_{10}[H^+]$, where $[H^+]$ is expressed in mole $L^{-1}$ ;

(b) Conductivity is expressed in µS $cm^{-1}$ (microsiemens per centimetre), a unit commonly used for measuring electric conductivity;

(c) Acidity/alkalinity is expressed in µmole $L^{-1}$ (micromole per litre);

(d) Major ions content is expressed in mg $L^{-1}$ (milligram per litre).

Aerosol observations of volumetric quantities, that is, the amount of substance in a volume of air, are reported for STP. These may refer to a particle number concentration ($cm^{-3}$), an area concentration ($m^2\ m^{-3}$, or $m^{-1}$) or a mass concentration (µg $m^{-3}$). Aerosol optical depth (AOD) is a dimensionless quantity. Absorption and scattering coefficients are expressed in $m^{-1}$.

### 16.1.3 Measurement principles and techniques

The existing techniques for atmospheric chemical composition measurements can be separated into three main groups: passive sampling, active sampling and remote-sensing techniques, which can themselves be both active (for example, lidar systems with their own light source) and passive (spectrometers using, for example, sunlight). Essentially, active sampling techniques draw the air sample through the detector or sampling device by a pump, whereas passive sampling techniques use the diffusion of air to the sampling device. In remote-sensing techniques, the analysed air volume and the detector are at different locations. Total or partial column measurements are possible only with remote-sensing techniques.

In the case of active sampling, measurements can either be made continuously (or at least quasi-continuously with short integration times)[4] or samples can be collected or specially prepared (in glass or stainless steel cylinders, on sorbent substrates or filters) and analysed offline in

[3] $CO_2$, for example, mostly consists of $^{12}C^{16}O^{16}O$, while the smaller abundance higher-mass isotopologues from mass 45 up to mass 49 ($^{13}C^{16}O^{16}O$, $^{14}C^{16}O^{16}O$, or $^{12}C^{18}O^{16}O$, the corresponding $^{17}O$ siblings and the mixed-isotope species) are also found in the atmosphere.

[4] This is, for example, common practice in GC measurements.

specialized laboratories. The collection of discrete samples entails the storage of these samples. During this time, flask properties may influence the composition of the sample due to chemical or surface effects or permeation through sealing polymers. This demands careful tests of the sampling containers.

The analytical techniques most commonly used (and recommended in the GAW Programme) for detecting and quantifying atmospheric trace constituents can be summarized as follows:

(a) *Spectroscopic methods* refer to the measurement of changes in radiation intensity due to absorption, emission, photoconductivity or Raman scattering by a molecule or aerosol particle as a function of wavelength. Spectral measurement devices are referred to as spectrometers, spectrophotometers, spectrographs or spectral analysers. Spectral measurements can be performed in different parts of a spectrum depending on the component to be measured, or at several individual wavelengths. As absorption lines are different for molecules with different isotopic composition, and line shapes depend on the bulk composition of the gas, care should be taken to ensure that reference gases have similar properties to the analysed atmospheric air.

(b) *Gas chromatography* (GC) is a physical method of separation that distributes components to be separated between two phases, one stationary (stationary phase), the other (the mobile phase) moving in a definite direction. There are numerous chromatographic techniques and corresponding instruments. To be suitable for GC analysis, a compound must have sufficient volatility and thermal stability. GC involves a sample being vapourized and injected onto the head of the chromatographic column. The sample is transported through the column by the flow of an inert, gaseous mobile phase. The column itself contains a liquid stationary phase which is adsorbed onto the surface of an inert solid. A chromatography detector is a device used to visualize components of the mixture being eluted off the chromatography column. There are two general types of detectors: destructive and non-destructive. The destructive detectors, such as a flame ionization detector (FID), perform continuous transformation of the column effluent (burning, evaporation or mixing with reagents) with subsequent measurement of some physical property of the resulting material (plasma, aerosol or reaction mixture). The non-destructive detectors, such as an electron capture detector (ECD), directly measure some property of the column effluent (for example, UV absorption) and thus allow for further analyte recovery.

(c) *Mass spectrometry* (MS) is an analytical technique that produces spectra of the masses of the molecules comprising a sample of material. The spectra are used to determine the elemental composition of a sample, the masses of particles and of molecules, and to elucidate the chemical structures of molecules. MS works by ionizing chemical compounds to generate charged molecules or molecule fragments and measuring their mass-to-charge ratios. In a number of instruments MS can be used as a detector method for GC.

Some other analytical techniques may be used at GAW stations where the amount of the analyte is defined through its chemical reaction with the reagent (for example, an electrochemical method or methods based on chemiluminescence).

Detection methods of gases and aerosols vary and are based on different physical phenomena. Details of the detection methods applicable to different gases and aerosol properties are summarized in the sections below.

The measurement techniques for the main compounds observed under the GAW Programme are briefly described in this chapter, while comprehensive measurement guidelines can be found in the specialized GAW reports, cited in individual sections. In the cases where GAW measurement guidelines or SOPs are not available, links are provided to the information necessary to carry out the respective measurements.

Satellite remote-sensing of the atmospheric species mentioned below is treated separately in Volume IV, Chapter 5 of the present Guide.

### 16.1.4 **Quality assurance**

The objectives of the GAW QA system are to ensure that data reported by station operators are consistent, of known and adequate quality, supported by comprehensive metadata, and regionally or globally representative with respect to spatial and temporal distribution.

The principles of the GAW QA system (WMO, 2017*a*) apply to each measured variable and include:

(a) Full support of the GCOS Climate Monitoring Principles;

(b) Network-wide use of only one reference standard or scale (primary standard). As a consequence, only one institution is responsible for this standard;

(c) Full traceability to the primary standard of all measurements made by global, regional and local GAW stations and network standards of contributing networks where such standards are established;

(d) The definition of data quality objectives;

(e) Establishment of guidelines on how to meet these quality targets, that is, harmonized measurement techniques published as measurement guidelines and SOPs and implemented at the stations;

(f) Use of detailed log books for each parameter containing comprehensive meta information related to the measurements, maintenance, and 'internal' calibrations;

(g) Regular independent assessments (system and performance audits);

(h) Timely submission of data and associated metadata to the responsible World Data Centre or a contributing network data centre as a means of permitting independent review of data by a wider community;

(i) Regular statistical and scientific analysis of data in the GAW data archives to ensure correctness, long-term consistency, and comparability of the archived measurement data.

Moreover, the GCOS monitoring principles (WMO, 2016*a*) also apply to the GAW observations. Among those, the most relevant principles for atmospheric composition measurements are:

(a) The impact of new systems or changes to existing systems should be assessed prior to implementation;

(b) A suitable period of overlap for new and old observing systems should be required;

(c) Operation of historically uninterrupted stations and observing systems should be maintained.

The GAW QA system further recommends the adoption and use of internationally accepted methods and vocabulary to describe uncertainty in measurements.

Five types of central facilities (see annex) dedicated to the six groups of measurement variables (see 16.1) are operated by WMO Members and form the basis of the QA and data archiving system. These include:

(a) Central Calibration Laboratories, which host primary standards and scales;

(b) World or Regional Calibration Centres, which coordinate intercomparison campaigns, help with instrument calibration and perform station/laboratory audits;

(c) QA/Science Activity Centres, which provide technical and scientific support and coordinate cooperation between the central facilities and GAW stations;

(d) World Data Centres, which mainly ensure dissemination and easy access of GAW data and secure the data through appropriate data archiving.

The nature of the data flow and the share of responsibilities for QA/QC implementation between the central facilities and the observation sites is specific to each variable. The work of the central facilities on the QA of the GAW observations is supported by respective scientific advisory groups, whose tasks include assisting in the development of measurement procedures and guidelines, data quality objectives and, when applicable, SOPs, reviewing new measurement techniques and making recommendations about their applicability for the GAW observations. See the GAW Implementation Plan 2016–2023 (WMO, 2017*a*) for more details and the terms of reference for the central facilities and the scientific advisory groups. An important issue is the recent establishment in Europe of atmospheric research infrastructures such as the Integrated Carbon Observing System (https://www.icos-ri.eu) and Aerosol, Cloud and Trace Gases Research Infrastructure (ACTRIS, https://www.actris.eu) that are implementing central facilities for QC and quality analysis in support of GAW QA/QC implementation strategies.

Given the variety in maturity of measurement and QC/QA systems within GAW it is particularly important all measurements be reported with an associated measurement uncertainty (ISO/IEC, 2008).

## 16.2 (STRATOSPHERIC) OZONE MEASUREMENTS

### 16.2.1 Ozone total column

Total ozone can only be measured using passive remote-sensing techniques. The most precise information on total ozone and its changes at individual sites can be obtained by measurements from the ground, for example by solar spectroscopy in the 300–340 nm wavelength region. Within the GAW Programme, Dobson (designed for manual operation) and Brewer (designed for automatic operation) spectrophotometers are used as the instruments of choice for routine total ozone observations, thus providing two independent networks.

Details of the total ozone measurements with the Dobson spectrophotometer and their QA are provided in WMO (2008*a*). Total ozone observations are made with this instrument by measuring the relative intensities of selected pairs of UV wavelengths, called the A, B*, C, C', and D wavelength pairs, emanating from the sun, moon or zenith sky. The A wavelength pair, for example, consists of the 3 055 Å (Ångström units, 1 Å = 0.1 nm) wavelength that is highly absorbed by ozone, and the more intense 3 254 Å wavelength that is relatively unaffected by ozone. Outside the Earth's atmosphere, the relative intensity of these two wavelengths remains essentially fixed. In passing through the atmosphere to the instrument, however, both wavelengths lose intensity because of scattering of the light by air molecules and dust particles; additionally, the 3 055 Å wavelength is strongly attenuated while passing through the ozone layer whereas the attenuation of the 3 254 Å wavelength is relatively weak. Therefore, the relative intensity of the A wavelength pair as seen by the instrument varies with the amount of ozone present in the atmosphere since, as the ozone amount increases, the observed intensity of the 3 055 Å wavelength decreases, whereas the intensity of the 3 254 Å wavelength remains practically unaltered. Thus, by measuring the relative intensities of suitably selected wavelength pairs with the Dobson instrument, it is possible to determine how much ozone is present in a vertical column of air extending from ground level to the top of the atmosphere in the neighbourhood of the instrument. The result is expressed in terms of thickness of an equivalent layer of pure ozone at STP.

The measurement principle of the Brewer spectrophotometer is similar to that of the Dobson instrument. The operating procedures are provided by the manufacturing company at http://www.kippzonen.com/?productgroup/26142/Brewer+Spectrophotometer.aspx.

The recommendations for the GAW network are available from the World Ozone and Ultraviolet Radiation Data Centre at http://woudc.org/archive/Documentation/SOP_Documents/brewerspectrophotometer_sop-june2008.pdf.

Results of comparisons of Brewer and Dobson instruments, as well as recommendations on the operation of the Brewer instruments, are provided in the reports of the biennial WMO consultations on Brewer ozone and UV spectrophotometer operation, calibration and data processing (for example, see WMO, 2008*b,* 2015*b,* 2015*c,* 2016*b*).

The world (primary) standard instruments of Brewer and Dobson networks are calibrated by the Langley plot method performed at the Mauna Loa Observatory in Hawaii (every 2–4 years); standards used by the Regional Calibration Centres to propagate traceability are calibrated against the primary standard every 2–3 years; and the station instruments are calibrated by side-by-side comparison with the standard instruments every 6 years for the Dobson and 2 years for the Brewer spectrophotometers. In addition, three successful Langley plot campaigns at the Izaña Atmospheric Observatory, on the island of Tenerife, with primary and regional standard Dobson instruments have proved the suitability of that location and facility for this absolute calibration method.

Complementary measurements of total ozone are provided by the DOAS-type UV/visible spectrometers that also allow detection of various minor trace gases (such as $NO_2$ and BrO). The French instrument is called Système d'Analyse par Observations Zénithales (SAOZ), but it is based on the same principle as DOAS. These instruments are part of the measurement suites within the Network for the Detection of Atmospheric Composition Change (NDACC) (https://ndacc.larc.nasa.gov/instruments). Compared to the more established Brewer/Dobson network, the measurement and analysis procedures for DOAS-type instruments are less standardized, but regular comparison campaigns have been carried out. Other instruments providing total ozone measurements from the ground (such as Russian filter instruments or those of the DOAS/SAOZ type) are not operated under the same data QA/QC programme as Dobson and Brewer instruments. They are not independently calibrated, but are tied to either Dobson or Brewer instruments. For example, the Russian filter instruments, M-124 field ozonometers, are recalibrated, on average, every two years by direct intercomparison with a D108 Dobson instrument at the A.I. Voeikov Main Geophysical Observatory (MGO) in St. Petersburg. The instruments at stations are replaced every two years by recently calibrated ozonometers and brought to the calibration site at MGO where they take simultaneous direct sun readings with the Dobson D108 spectrophotometer. Filter instrument calibration coefficients are determined as a function of solar zenith angle and total ozone by reference to the Dobson spectrophotometer measurements. The calibrated instruments are then returned to their respective field sites. In this way, the network of M-124 ozonometers is maintained in the calibration scale of the World Primary Dobson Spectrophotometer D083. Although the D108 is calibrated with about 1% precision every four years, the accuracy of the transfer of the calibration scale into the M-124 network is estimated to be about 3%.

Data quality of all individual total ozone series deposited at the World Ozone and Ultraviolet Radiation Data Centre needs to be documented for the users.

Determining ozone amounts by the DOAS technique relies on accurate knowledge of the absorption cross-section determined in the laboratory. However, the absorption cross-sections are both temperature and pressure dependent and so not a constant in the atmosphere. Care should be taken to select the appropriate version of the cross-sections and the most recent data should be used (WMO, 2015*d*).

### 16.2.2 **Ozone profile measurements**

Measurements of the vertical ozone distribution are possible by both active and remote-sensing methods.

#### 16.2.2.1 *Umkehr method*

Dobson and Brewer spectrophotometers can be used for the measurement of vertical ozone distribution utilizing the Umkehr method (WMO, 2008*c;* Jaroslawski, 2013). The reduction of the Umkehr measurement to an ozone profile requires a complex algorithm that includes knowledge of the radiative properties of the real atmosphere. As this knowledge changes, the algorithm will change. A standard Umkehr observation consists of a series of C-pair wavelength measurements made on a clear zenith sky during the morning or afternoon. The measurements are commenced a few minutes before sunrise and continued until the sun is at an elevation not lower than approximately 20 degrees, or commenced in the afternoon when the sun is at an elevation not lower than approximately 20 degrees and continued until shortly after sunset. The zenith sky must be free from clouds for a period of 30 min to 1 h near sunrise or sunset. This is especially true at low latitude stations where the sun rises or sets rapidly. At other times, it is desirable that the zenith sky be cloudless, but it is permissible that clouds cross it periodically when measurements are not being made. Umkehr observations cannot be made at a polar station or at high latitude stations during summertime when the sun does not sink below the horizon.

To be able to compute the vertical distribution of ozone, it is necessary to know the total amount of the compound present at the time of observation. Several total ozone measurements must, therefore, be made during the morning or afternoon, particularly if the ozone amount is changing fairly rapidly.

The resulting ozone profile derived from reduction of these measurements is quite dependent on the algorithm used. The Umkehr data analysis method was originally developed by Götz et al. (1934). Later the method was refined by Ramanathan and Dave (1957), Mateer and Dütsch (1964) and Mateer and DeLuisi (1992). The Umkehr algorithm is described by Petropavlovskikh et al. (2005) and updated information is available from https://gml.noaa.gov/ozwv/umkehr.

#### 16.2.2.2 *Ozonesonde measurements*

Ozone measurement from balloons (ozonesondes) is an active method for measuring ozone's vertical distribution in the atmosphere. Other active methods for ozone mole fraction measurements (used on aircraft platforms) are described in the section on reactive gases (see 16.4.1).

Ozonesondes are small, lightweight and compact balloon-borne instruments, developed for measuring the vertical distribution of atmospheric ozone up to an altitude of about 30–35 km. The sensing device is interfaced to a standard meteorological radiosonde for data transmission to the ground station. Two main types of ozonesondes – the Brewer–Mast sonde and the electrochemical concentration cell – are currently in use. Each sonde type has its own specific design.

The flight package typically weighs approximately 1 kg in total and can be flown on small weather balloons. Normally data are taken during ascent, at a vertical ascent rate of approximately 5 m $s^{-1}$, to a balloon burst altitude of 30–35 km. The inherent response time of the ozonesonde is 20–30 s such that the effective height resolution of the measured vertical ozone profile is typically 100–150 m.

The principles of ozonesonde operations and an overview of the different aspects of QA and QC for ozonesonde measurements in GAW are given in detail in WMO (2014).

#### 16.2.2.3 *Other measurement techniques*

Ozone profile measurements can also be obtained by other instruments operated under the umbrella of NDACC. Lidar and microwave measurements are part of the NDACC suite of measurements and are valuable for assessing ozone trends in the upper stratosphere and for validating satellite measurements in the upper atmosphere. The disadvantage of microwave

ozone measurements is the rather poor vertical resolution, but they have the potential to measure up to the mesopause region. The combination of sonde, Umkehr, lidar and microwave data from the ground is important for assessing the quality of the ozone profile measurements from space (van der A et al., 2010).

### 16.2.3 Aircraft and satellite observations

Ozone in the atmosphere is also measured by instruments located on board aircraft and space-borne satellites. The airborne observations are usually made by in-situ photometers sampling the air in the troposphere and lower stratosphere during a flight. The measurements are used mostly in research campaigns on atmospheric chemistry, but there have also been long-term projects using commercial aircraft, such as MOZAIC (measurement of ozone, water vapour, carbon monoxide and nitrogen oxides aboard airbus in-service aircraft), CARIBIC (Civil Aircraft for the Regular Investigation of the Atmosphere Based on an Instrument Container, http://www.caribic-atmospheric.com/), and IAGOS (In-service Aircraft for a Global Observing System, https://www.iagos.org/).

Large-scale monitoring of atmospheric ozone is performed by remote-sensing instruments from satellites. These programmes can be divided according to lifetime: the long-term operational monitoring systems that generate large (global) datasets used for trend analyses and for operational mapping of ozone, and the temporary experimental missions.

Satellite observations can be grouped according to the radiation-detection technology used for the instruments and the retrieval schemes applied for the derivation of ozone column density or concentration from the measured radiances. While nadir-viewing instruments are primarily used for column observations and coarse vertical profiling, limb sounding instruments are able to measure vertical profiles of ozone at high vertical resolution by solar, lunar or stellar occultation or by observing limb scatter and emission through the atmospheric limb (Tegtmeier et al., 2013; Sofieva et al., 2013).

## 16.3 GREENHOUSE GASES

All GHGs are reported in dry mole fraction on the most recent scales (https://www.esrl.noaa.gov/gmd/ccl/). The scales are reviewed every two years at the WMO/International Atomic Energy Agency (IAEA) Meetings on Carbon Dioxide, Other Greenhouse Gases and Related Measurement Techniques (WMO, 2016*c*). The primary reference for GHGs is a set of cylinders of natural air with known mole fractions of the studied gases. The primary scales are transferred to station working standards through secondary and tertiary gas standards in high-pressure cylinders.

### 16.3.1 Carbon dioxide (including $\Delta^{14}C$, $\delta^{13}C$ and $\delta^{18}O$ in $CO_2$, and $O_2/N_2$ ratios)

Carbon dioxide is usually measured by active methods in the atmospheric boundary layer.

Historically, most background atmospheric $CO_2$ measurements were made with non-dispersive IR (NDIR) gas analysers, but a few programmes used a GC method. NDIR instruments are based on the same principle that makes $CO_2$ a GHG: its ability to absorb IR radiation. They measure the intensity of IR radiation passing through a sample cell relative to radiation passing through a reference cell. It is not necessary to know the $CO_2$ mole fraction of the reference cell gas. Sample air is pumped from inlets mounted well away from the measurement building into the sample cell and for a fixed period of time measurements are taken. The sample is then flushed and replaced with reference or standard gas and further measurement gathered. The concentration of the $CO_2$ in the samples are determined by ratio comparison to the reference and/or standard gases. The GC method requires separation of $CO_2$ from other gases in the air sample by reduction of $CO_2$ to $CH_4$ over a catalyst with $H_2$. Detection of the $CO_2$-derived $CH_4$ is achieved using a FID.

Chromatographic peak responses from samples are compared to those from standards with known $CO_2$ mole fractions to calculate the $CO_2$ mole fraction in the sample. GC techniques are limited to a measurement frequency of one sample every few minutes.

Most of the newer methods for measurement of $CO_2$ use laser-based optical spectroscopic methods, such as Fourier transform IR (FTIR) absorption spectroscopy or high-finesse cavity absorption spectroscopy, which includes cavity ring-down spectroscopy (CRDS) and off-axis integrated cavity output spectroscopy (OA-ICOS). Among the advantages of these techniques are reduced calibration demands due to better linearity and stability.

Carbon dioxide abundances are reported in dry-air mole fraction, μmol $mol^{-1}$, often abbreviated as ppm, on the WMO $CO_2$ Mole Fraction Scale (WMO $CO_2$ X2007 scale, status as of 2018). Water vapour affects the measurement of $CO_2$ in two ways: (a) $H_2O$ also absorbs IR radiation and can interfere with the measurement of $CO_2$; (b) $H_2O$ occupies volume in the sample cell, while standards are dry. At warm, humid sites, 3% of the total volume of air can be water vapour. The impact of water vapour on the measurement of $CO_2$ must therefore be considered. Drying to a dewpoint of –50 °C is sufficient to eliminate interferences. The novel optical spectroscopic methods allow simultaneous determination of the water vapour content, making it possible to correct for dilution due to $H_2O$ and spectroscopic effects. Current best practice (see WMO, 2016*c*) recommends that water vapour must either be removed from the sample gas stream, or its influence on the mole fraction determination must be carefully quantified for each individual instrument.

An alternative method of $CO_2$ measurement that is generally applicable to many other trace gases is the collection of discrete air samples in vacuum-tight flasks. These flasks are returned to a central laboratory where the $CO_2$ mole fraction is determined by NDIR, GC or other techniques. This method is used where low-frequency sampling (for example, once a week) is adequate to define $CO_2$ spatial and temporal gradients, and for comparison with in-situ measurements as a QC step. This sampling strategy has the advantage that many species can be determined from the same sample.

Measurements of $O_2/N_2$ ratios and stable isotopes of $CO_2$ ($\delta^{13}C$ and $\delta^{18}O$) help to partition carbon sources and sinks between the ocean and biosphere. Isotopic measurements are often made from the same discrete samples used for $CO_2$ mole fraction measurements. No isotopic standards traceable to SI exist, but commonly agreed-upon reference material is maintained by IAEA. The measurements are performed as part of the GAW $CO_2$ network.

A measurement method for stable isotope determination is isotope ratio MS, a specialization of MS methods in which the relative abundances of isotopes in a given sample are measured. The measurement set-up is described by the GAW Central Calibration Laboratory for stable isotopes at the Max Planck Institute for Biogeochemistry in Jena, Germany (https://www.bgc-jena.mpg.de/en/servicegroups/isolab). In recent years, optical analysers that report mole fractions of individual isotopologues have become increasingly available and are now in routine use. Many of these instruments can provide isotopic ratios with a repeatability of about 0.05 ‰ for $\delta^{13}C$ of atmospheric $CO_2$ and are valuable for continuous measurements. Unlike MS, $\delta$ values obtained from such instruments are often calculated from the ratio of individual measured mole fractions using tabulated absorption line strengths, and not from direct measurements of a standard material. Some corrections applicable to MS methods, such as those for $^{17}O$ and $N_2O$, are not required, but other corrections, such as for interference from other atmospheric components and instrument fluctuations, may be required depending on the method used to calculate the isotopic $\delta$ values from individual mole fractions. It is important to know the compatibility between the techniques before measurement results are made public.

Measurements of the changes in atmospheric $O_2/N_2$ ratio are useful for identifying sources and sinks of $CO_2$ and testing land and ocean biogeochemical models. The relative variations in $O_2/N_2$ ratio are very small but can now be observed by at least six analytical techniques. These techniques can be grouped into two categories: (a) those that measure $O_2/N_2$ ratios directly (MS and GC), and (b) those that effectively measure the $O_2$ mole fraction in dry air (interferometric, paramagnetic, fuel cell, vacuum-UV photometric). A convention has emerged to convert the raw measurement signals, regardless of technique, into equivalent changes in $O_2$ to $N_2$ mole ratio. For

mole-fraction type measurements, this requires accounting for dilution due to variations in $CO_2$ and possibly other gases. If synthetic air is used as a reference material, corrections may also be needed for differences in $Ar/N_2$ ratio. There are currently about 10 laboratories measuring $O_2/N_2$ ratios worldwide. The $O_2/N_2$ reference is typically tied to natural air delivered from high-pressure gas cylinders. As there is no common source of reference material, each laboratory employs its own reference. There is currently no central calibration laboratory for $O_2/N_2$. Hence it has not been straightforward to report measurements on a common scale, but several laboratories report results on a local implementation of the Scripps scale. There are no named versions yet.

The practice of basing $O_2/N_2$ measurements on natural air stored in high-pressure cylinders appears to be acceptable for measuring changes in background air, provided the cylinders are handled according to certain best practices, including orienting cylinders horizontally in order to minimize thermal and gravitational fractionation. Nevertheless, improved understanding of the source of variability of measured $O_2/N_2$ ratios delivered from high-pressure cylinders is an important need of the community. An independent need is the development of absolute standards for $O_2/N_2$ calibration scales to the level of 5 per meg or better.

Atmospheric $^{14}CO_2$ measurements are usually reported in $\Delta^{14}C$ notation, the per mil deviation from the absolute radiocarbon reference standard, corrected for isotopic fractionation and for radioactive decay since the time of collection. For atmospheric measurements of $\Delta^{14}C$ in $CO_2$, two main sampling techniques are used: high-volume $CO_2$ absorption in basic solution or by molecular sieve, and whole-air flask sampling (typically 1.5–5 L flasks). Two methods of analysis are used: conventional radioactive counting and accelerator MS. The current level of measurement uncertainty for $\Delta^{14}C$ in $CO_2$ is 2‰–5‰, with a few laboratories at slightly better than 2‰. Recommendations on calibration are provided in (WMO, 2016*c*).

Recommendations on QA of $CO_2$ measurements (including $\Delta^{14}C$, $\delta^{13}C$ and $\delta^{18}O$ in $CO_2$, and $O_2/N_2$ ratios) are reviewed every two years at the WMO/IAEA Meeting on Carbon Dioxide, Other Greenhouse Gases and Related Measurement Techniques. The report (WMO, 2016*c*) can be used as the most recent reference regarding calibration and measurement QC.

### 16.3.2 **Methane**

Until recently, $CH_4$ measurements were made almost exclusively using the GC-FID technique, and recommendations regarding the use of these systems can be found in the WMO/GAW measurement guideline (WMO, 2009). In the meantime, commercially available instruments based on spectroscopic techniques such as CRDS, OA-ICOS and FTIR spectroscopy have become more widely available and affordable. Spectroscopic techniques have been shown to have a number of advantages over the GC-FID method that will lead to improved accuracy of atmospheric $CH_4$ measurements (Zellweger et al., 2016). However, these techniques also require calibration (WMO, 2016c), and current best practice recommends that water vapour must either be removed from the sample gas stream, or its influence on the mole fraction determination must be carefully quantified for each individual instrument (Rella et al., 2013).

An alternative method of $CH_4$ measurement is flask sampling followed by off-line analysis, very similar to the approach described in 16.3.1 for $CO_2$.

### 16.3.3 **Nitrous oxide**

Over the last few decades, measurements of atmospheric nitrous oxide ($N_2O$) have mainly been made using gas chromatographs with ECDs (GC-ECD). However, this technique is very challenging for the detection of the small variations of $N_2O$ in the troposphere. GC-ECDs are highly nonlinear and require a considerable amount of maintenance. Recommendations for $N_2O$ measurements using GC-ECD are provided in the WMO/GAW measurement guideline (WMO, 2009), and recommendations on calibration and QC are given in WMO (2016*c*).

Recently, spectroscopic analysers, including high-finesse cavity absorption spectrometers with near-IR laser sources, FTIR analysers and OA-ICOS analysers with mid-IR laser sources

became commercially available for $N_2O$ measurements. These techniques normally exceed the performance of GC-ECD systems, but reaching the data quality objectives (WMO, 2016c) remains challenging. A few field and laboratory studies (Lebegue et al., 2016; Vardag et al., 2014) show excellent performance and demonstrate the potential to replace the GC techniques. However, further studies are needed to assess their long-term applicability and to identify optimum calibration strategies.

Collecting discrete samples of ambient air in flasks is an alternative method of monitoring $N_2O$. Flasks should be returned to a central laboratory for off-line analysis. Typical sampling frequencies are weekly or bi-weekly.

### 16.3.4 Halocarbons and $SF_6$

Halocarbons and $SF_6$ are usually measured quasi-continuously or from discrete air samples by active methods. Measurement guidelines for these species are not yet formalized in the GAW Programme though some guidance on calibration is provided by the World Calibration Centre for $SF_6$ (WMO, 2018).

$SF_6$ is typically measured using GC-ECD techniques on the same channel as $N_2O$. Analytical methods are described in WMO (2015*e*).

Global measurements of halocarbons are currently performed by US NOAA and the Advanced Global Atmospheric Gases Experiment (AGAGE). The measurement histories for both US NOAA and AGAGE extend back to the late 1970s. Both groups measure halocarbons using GC-ECD and GC with MS (GC-MS) techniques. Halocarbons measured include chlorofluorocarbons (CFCs), hydrochlorofluorocarbons (HCFCs), chlorinated solvents such as $CCl_4$ and $CH_3CCl_3$, halons, hydrofluorocarbons (HFCs), methyl halides, $NF_3$ and $SF_6$. For many halocarbons, measurement of mole fractions in the background troposphere requires sample pre-concentration. The AGAGE group operates a network of in-situ systems, while the US NOAA group operates in-situ systems (for a limited number of gases) and a flask-based programme. For more information on instrumentation and sampling sites, see: http://agage.eas.gatech.edu, and http://www.esrl.noaa.gov/gmd/hats/. Reference gases are maintained by both AGAGE and US NOAA and the individual scales are regularly compared.

### 16.3.5 Remote-sensing of greenhouse gases

There are several techniques used for remote-sensing of GHGs. The Total Carbon Column Observing Network (https://tccon-wiki.caltech.edu/) is a network of surface-based Fourier transform spectrometers recording direct solar spectra in the near-IR spectral region. From these spectra, column-averaged abundances of $CO_2$, $CH_4$, $N_2O$, HF, CO, $H_2O$ and HDO are retrieved. Observations in the mid-IR (the NDACC network, https://www2.acom.ucar.edu/irwg) allow for accurate measurements of column-averaged abundances of $CH_4$, $N_2O$ and CO.

## 16.4 REACTIVE GASES

The reactive gases considered in the GAW Programme include tropospheric ozone, carbon monoxide, VOCs, oxidized nitrogen compounds and sulphur dioxide. All of these compounds play a major role in the chemistry of the atmosphere and, as such, are heavily involved in interrelations between atmospheric chemistry and climate, either through control of ozone and the oxidizing capacity of the atmosphere, or through the formation of aerosols. The global coverage in terms of observations is entirely unsatisfactory for most of them, the only exceptions being surface ozone and CO (Schultz et al., 2015).

Different reference standards and methods are used in the group of reactive gases. For more stable gases, the reference material can be prepared as a cylinder filled with air or another matrix with known gas mole fraction (for example, for CO, non-methane hydrocarbons and terpenes), while for others (such as ozone) only reference methods/instruments are possible.

### 16.4.1 Tropospheric (surface) ozone

Detailed measurement guidelines for measuring tropospheric ozone (surface ozone is a part of tropospheric ozone measured at the Earth's surface) are provided in WMO (2013).

The mole fraction most appropriate to the chemical and physical interpretation of ozone measurements is the mole fraction of ozone in dry air. However, ozone measurements are usually made without sample drying, because an efficient system for drying air and leaving the ozone content of the air unchanged has not been developed. It is recommended ozone measurements be accompanied by measurements of water vapour mole fraction of sufficient precision that the ozone measurements could be converted to mole fractions with respect to dry air without loss of precision.

A number of techniques are used for measurements of ozone in the background atmosphere. These include:

(a) UV absorption techniques;

(b) Chemiluminescence techniques;

(c) Electrochemical techniques;

(d) CRDS with NO titration;

(e) DOAS;

(f) Multi-axis DOAS (MAxDOAS);

(g) Tropospheric ozone lidar.

Because of its high accuracy and precision, low detection limit, long-term stability, sufficient time resolution and ease of operation (almost no consumables), the UV absorption technique is recommended for use for routine surface ozone measurements at all GAW stations.

A review of measurement techniques, along with information on their applicability for use at GAW stations, is provided in WMO (2013). Note that only techniques (a) to (d) (those conducted in situ) can be traceable via a chain of calibrations to the primary standard as recommended by GAW.

DOAS is a surface-based remote-sensing method suitable for observations of several trace substances. The instrument consists of a light source, a long ambient air open optical path generally between 100 m and several km, a retro-reflector and a spectrometer with a telescope, housed with the light source. The spectrometer observes the light source via the retro-reflector. The DOAS system uses Beer's law to determine the ozone concentration (averaged over the light path). In principle, DOAS should be a sensitive technique, but this is confounded by the inability of the system to regularly measure a definitive zero and determine the contribution of other UV-absorbing gases and aerosols to the observed signal. DOAS may be used as an experimental technique (Platt and Stutz, 2008).

MaxDOAS is a surface-based remote-sensing method for observations of several trace substances. While this method is suitable for stratospheric monitoring, it is also possible to apply it for trace gas profile measurements in the upper and lower troposphere. However, since the retrieval procedures, as well as possible tropospheric interferences, are more complicated in the lower troposphere, it needs highly experienced personnel for extracting and calculating the

mole fractions for the respective trace gases out of the various spectra. MaxDOAS measurements of ozone, nitrogen dioxide, formaldehyde, bromine monoxide (BrO) and other species are recommended especially for providing a link between surface-based and satellite measurements at selected GAW stations with extended research programmes (Hönninger et al., 2004).

Lidar is a surface-based remote-sensing method for observations of several trace substances. For tropospheric ozone measurements, a lidar typically uses two or more wavelengths between 266 nm and 295 nm (Kuang et al., 2013). The chosen wavelengths are shorter than the ones used for stratospheric ozone detection (typically between 308 and 353 nm). Compared to in the stratosphere, higher ozone absorption efficiency is necessary in the troposphere in order to get enough sensitivity because of the lower ozone mixing ratios in the troposphere. Too much absorption means that most light is extinguished at lower elevations, making it difficult to collect measurement signals from higher elevations. The extreme dynamic range of the backscattering signal over the troposphere (some decades over a few kilometres of height) is a major technical problem. Lidar tropospheric ozone measurements are recommended especially for providing a link between surface-based and satellite measurements at selected GAW stations with extended research programmes.

### 16.4.2 Carbon monoxide

Detailed measurement guidelines for CO measurements are provided in WMO (2010). The CO calibration scale is evaluated every two years together with the scales of the major GHGs (WMO, 2016*c*). The most recent calibration scale can be found on the web page of the Central Calibration Laboratory (https://www.esrl.noaa.gov/gmd/ccl/).

Measurements of CO are possible both in situ and by flask collection with subsequent analysis in the laboratory. In-situ continuous observations provide information about CO variability on a timescale ranging from seconds to one hour depending on the measurement technique. In contrast to flask sampling, continuous measurements allow for near-real-time data delivery.

In-situ observations can be made using a broad variety of analytical techniques. NDIR radiometry is based on spectral absorption at 4.7 µm. It is frequently used for air pollution monitoring and occasionally also for continuous measurements at remote locations; however, instrument drift, limited precision and long averaging times are factors limiting the achievable data quality. GC, when coupled with a number of different detectors (such as GC-FID, or hot mercuric oxide reduction/UV absorption (GC-HgO)) can provide high-precision and adequate detection limits. The HgO-reduction detector tends to have a non-linear response over the range of atmospheric CO, and requires careful, repeated multipoint characterization of the detector response. The GC-FID technique requires catalytic conversion of CO to $CH_4$. For confidence in the results, the catalytic conversion efficiency must be determined on a regular basis making the proper maintenance, instrument calibration and provision of accurate measurements challenging. GC measurements are quasi-continuous in nature and therefore may not detect fast changes of mole fractions that can be captured by high-frequency measurements.

In recent years, many alternative techniques have become available. These include resonance fluorescence of CO (induced by a high-frequency discharge) in the vacuum UV, spectroscopic techniques based on CRDS, quantum cascade laser (QCL) spectroscopy, and FTIR absorption spectroscopy. The CRDS technique operates using lasers in the near-IR and was previously mainly used for measurements of carbon dioxide, methane and ammonia. The QCL technique measures in the mid-IR, and commercial instruments are available that can determine both CO and $N_2O$ with a single laser. An overview of the performance of most analytical techniques can be found in Zellweger et al. (2009, 2012).

Remote-sensing of the CO column from the ground is undertaken by the Total Carbon Column Observing Network (http://www.tccon.caltech.edu/) using surface-based Fourier transform spectrometers in the near-IR spectral region (Wunch et al., 2010).

### 16.4.3 Volatile organic compounds

The measurement of VOCs is complex due to the many different molecules present in the atmosphere. While systematic surveying of many of these species is important for air quality purposes, the low concentrations of VOCs away from their sources imply that only a few molecules can be measured routinely in the background atmosphere. A core set of molecules recommended for measurement in the GAW Programme with suggested measurement methods is provided in Table 16.1.

The measurement guidelines for VOCs are currently under development in collaboration with ACTRIS. An SOP for taking air samples with stainless steel canisters is available in WMO (2012). General recommendations on VOC measurements can be found in WMO (2007). Regular GAW VOC workshops review the status of VOC measurements in the GAW Programme and provide further guidance on the development of measurement techniques, QA and gas standards.

**Table 16.1. List of the priority VOCs in the GAW Programme**

| | *Molecule* | *Lifetime (assuming OH concentration is $10^6$ $cm^{-3}$)* | *Importance to GAW* | *Steel flask*[a] | *Glass flask* | *Analysis method*[b] |
|---|---|---|---|---|---|---|
| 1. | Ethane | 1.5 months | – Tracer for fossil fuel emissions<br>– Natural sources<br>– Biomass burning<br>– Fossil fuel<br>– Trend in size of seasonal cycle<br>– Indicator of halogen chemistry | ✓ | ✓ | GC-FID |
| 2. | Propane | 11 days | – Tracer for fossil fuel emissions<br>– Biomass burning | ✓ | ✓ | GC-FID |
| 3. | Acetylene | 15 days | – Motor vehicle tracer<br>– Biomass burning tracer<br>– Ratios to the other hydrocarbons | ✓ | ✓ | GC-FID |
| 4. | Isoprene | 3 hours | – Biosphere product<br>– Sensitive to temperature/land<br>– Used for climate change<br>– $O_3$ precursor<br>– Oxidizing capacity<br>– Precursor to formaldehyde | ? | ? | GC-FID<br>PTR-MS |
| 5. | Formaldehyde | 1 day | – Indicator of isoprene oxidation<br>– Biomass burning<br>– Comparison with satellites– | – | – | DOAS |
| 6. | Terpenes | 1–5 hours | – Precursors to organic aerosols | – | – | GC-MS<br>PTR-MS |
| 7. | Acetonitrile | 0.5–1 year | – Biomass burning indicator<br>– Biofuel burning indicator | – | ? | GC-MS<br>PTR-MS |
| 8. | Methanol | 12 days | – Sources in the biosphere (methane oxidation)<br>– Abundant oxidation product | – | ? | GC-FID<br>PTR-MS |
| 9. | Ethanol | 4 days | – Tracer of alternative fuel usage | – | ? | GC-FID<br>PTR-MS |
| 10. | Acetone | 1.7 months | – Abundant oxidation product<br>– Free radical source in the upper troposphere | ? | ? | GC-FID<br>PTR-MS |

| | *Molecule* | *Lifetime (assuming OH concentration is $10^6$ $cm^{-3}$)* | | *Importance to GAW* | *Steel flask*[a] | *Glass flask* | *Analysis method*[b] |
|---|---|---|---|---|---|---|---|
| 11. | Dimethyl sulphide | 2 days | –<br>–<br>– | Major natural sulphur source<br>Sulphate aerosol precursor<br>Tracer of marine bioproductivity | ? | ? | GC-FID<br>PTR-MS |
| 12. | Benzene | 10 days | –<br>– | Tracer of combustion<br>Biomass burning indicator | ✓ | ? | GC-FID<br>GC-MS |
| 13. | Toluene | 2 days | –<br>– | Ratio to benzene used for airmass age<br>Precursor to particulates | – | ? | GC-FID<br>GC-MS |
| 14. | Iso/normal butane | 5 days | –<br>– | Chemical processing indicator<br>Lifetime/ozone production | ✓ | ✓ | GC-FID<br>GC-MS |
| 15. | Iso/normal pentane | 3 days | – | Ratio provides impact of $NO_3$ chemistry and oil and natural gas sources | ✓ | ✓ | GC-FID<br>GC-MS |

Notes:
a "✓" indicates state of current practice, "–" stands for not measured in flasks (only on-line measurements), while "?" means that stability in flasks is not well known
b GC-FID = gas chromatography flame ionization detection; GC-MS = gas chromatography mass spectrometry; DOAS = differential optical absorption spectroscopy; PTR-MS = proton transfer reaction mass spectrometry

Measurements of low molecular weight aliphatic and aromatic hydrocarbons (C2–C9) have been made successfully for many years, predominantly in short-term regional experiments. The preferred analytical method for these compounds, which include the molecules 1–4 and 12–15 of Table 16.1, is GC-FID. Air samples, from flasks or in situ, are normally pre-concentrated using cryogenic methods or solid adsorbents. An alternative technique is GC-MS. Although GC-MS is potentially the more sensitive method, it is typically subject to greater analytical uncertainties (changes in instrument response over time, detection of common, low-mass fragments). However, GC-MS may be valuable for the detection of certain hydrocarbons in very remote locations where ambient levels may be below the detection limit of a typical GC-FID.

The recommended analytical technique for monoterpenes is GC-MS. Although it is possible to measure some terpenes using a FID, the complexity of the chromatographic analysis (co-eluting peaks, particularly with aromatics) makes peak identification and quantification difficult. The GC-MS method gives better sensitivity.

Oxygenated hydrocarbons, including the target compounds 8–10 (Table 16.1), can also be measured using GC-FID or GC-MS. Particular care should be taken with sample preparation (including water removal), and inlet systems must be designed to minimize artefacts and component losses commonly encountered with oxygenate analysis. Acetone and methanol can also be measured using proton transfer reaction MS (PTR-MS). An advantage of PTR-MS is that it is an online method that does not require the pre-concentration of samples. However, it is less sensitive than GC methods, and there are potential interferences from isobaric compounds, such as $O_2H^+$ and methanol. As the stability of oxygenated VOCs in grab samples (stainless steel or glass flasks) remains highly uncertain, it is suggested that these species be measured primarily by online methods at a selection of surface-based measurement stations. The successful storage of acetone in certain flasks has been reported, so the possibility of analysing this compound in the glass or stainless steel flask network should be investigated.

Formaldehyde (HCHO) is not stable in flasks and has to be measured in situ. Methods of analysis include the Hantzsch fluorometric (wet chemical) method (Nash, 1953) or DOAS. Both are relatively complex and would require specialist training for potential operators. It is unlikely, therefore, to be able to make measurements at more than a few ground stations. Formaldehyde is routinely detected by satellites. Satellite retrievals yield total vertical column abundances, and an important objective of the GAW Programme would be to provide periodic surface-based measurements at selected sites for comparison/calibration purposes (ground truthing).

The feasibility of HCHO measurements with PTR-MS (Wisthaler et al., 2008; Warneke et al., 2011) and QCL (Herndon et al., 2007) was shown during limited measurement campaigns. Their applicability for long-term routine HCHO measurements has not yet been tested.

Acetonitrile is preferably measured with GC-MS, because this compound is relatively insensitive to FID detection. Measurements of acetonitrile have also been reported using various reduced gas and nitrogen-specific detectors. Many recently reported atmospheric measurements of acetonitrile have been made using PTR-MS or atmospheric pressure chemical ionization MS (AP-CIMS). The stability of acetonitrile in grab samples is highly uncertain, so grab sampling is not acceptable in the framework of GAW and measurements may be limited to a few selected comprehensive measurement sites.

Dimethyl sulphide (DMS) can be measured by GC-FID, GC using a flame photometric detector (GC-FPD), GC-MS and PTR-MS. However, as DMS concentrations can be measured routinely as part of a standard non-methane hydrocarbon analysis, GC-FID analysis of the whole air samples would be the simplest choice of measurement strategy. There is evidence in the literature that DMS is stable in some flasks, so its measurement as a component of a flask network is quite feasible. It is also desirable to make in situ measurements of DMS at least in the early stage of operation of the flask network to ensure method compatibility.

### 16.4.4 Nitrogen oxide

The sum of nitric oxide (NO) and nitrogen dioxide ($NO_2$) has traditionally been called $NO_x$. The sum of all nitrogen oxides with an oxidation number greater than 1 is called $NO_y$. Their measurement in the global atmosphere is very important since NO has a large influence on both ozone and the hydroxyl radical (OH). $NO_2$ is now being measured globally from satellites, and these measurements suggest that substantial concentrations of this gas are present over most of the continents. A large reservoir of fixed nitrogen is present in the atmosphere as $NO_y$. The influence of the deposition of this reservoir on the biosphere is not well known at present but could be substantial.

Nitrogen oxide (NO and $NO_2$) measurements can be done by passive, active and remote-sensing techniques. The active techniques can be divided into time-integrating and in-situ techniques: time-integrating techniques consist of a sampling step usually involving liquid-phase sample collection and offline analysis, whereas in-situ (continuous) measurements directly analyse the sample air. Passive methods are always time-integrating. Active time-integrating methods comprise the Saltzman method and related methods like the Griess or sodium iodide method. The latter is being used, for example, in the Cooperative Programme for Monitoring and Evaluation of the Long-range Transmission of Air Pollutants in Europe (EMEP, http://www.emep.int) network. Due to the high reactivity of $NO_x$, flask sampling is impossible.

Ozone-induced chemiluminescence detection is the most widely used among the in situ techniques. These instruments are typically very sensitive to NO; however, they cannot measure $NO_2$. Thus, $NO_2$ must be converted to NO before detection. The instrument makes measurements in a NO mode and then a NO + $NO_2$ mode. The difference, when conversion efficiency is determined carefully, gives the $NO_2$ mixing ratio. Thus, a high time resolution (< 10 min) is recommended to ensure sampling of the same airmass during subsequent NO and $NO_x$ measurements. The conversion of $NO_2$ to NO is achieved by photolysis of $NO_2$ at wavelengths $320 < \lambda < 420$ nm using a photolytic converter with an arc lamp or a blue-light converter with LEDs. Advantages of LEDs are the substantially longer lifetime and nearly constant conversion efficiencies, the mechanical simplicity and the simple on/off characteristic of the LED (no additional valves/dead volumes). Depending on the chosen LED, the conversion efficiency can be smaller or even larger than with a photolytic converter. However, the spectral range of the new LED-based converters and temperature effects need to be considered and characterized to prevent artifacts due to nitrous acid and peroxyacetyl nitrate. With careful selection, the use of UV-LED converters is recommended for GAW $NO_2$ measurements.

The use of molybdenum converters for $NO_2$ to NO conversion is strictly discouraged, as this conversion technique is not selective of $NO_2$ but also converts other oxidized nitrogen species in different quantities. Already-existing measurements with Mo converters should be marked as $NO_{2(Mo)}$ or $NO_{2+}$.

Detailed measurement guidelines for reactive nitrogen measurements are currently being developed in collaboration with ACTRIS. The focus there is mostly on NO and $NO_2$ point measurements because their measurements are presently more extensive and robust and allow for implementation of a complete QA system. Recommendations on NO and $NO_2$ measurements can be found in WMO (2017*b*).

The luminol-CLD method (Kelly et al., 1990) measures $NO_2$ directly and NO indirectly after oxidation. Since the sensitivity depends strongly on the quality of the luminol solution, which decreases during use due to ageing, frequent recalibration is needed.

In addition to these methods, optical absorption techniques for $NO_2$ detection have been developed, including tuneable diode laser absorption spectroscopy, DOAS, laser-induced fluorescence, FTIR absorption spectroscopy and CRDS. They all measure $NO_2$ directly. Recent developments in CRDS for the measurement of $NO_2$ and of NO as $NO_2$ after oxidation by ozone show some promise, but the measurements still suffer from uncertainties in the zero level.

Recently, the suitability of research-type QCL instrumentation for continuous and direct measurements of NO and $NO_2$ was shown (Tuzson et al., 2013). This technique may become an alternative standard method in the future.

Also recently, cavity attenuated phase shift monitors have become commercially available. A side-by-side intercomparison experiment at ACTRIS showed excellent results. However, a current lower detection limit of a few tens of ppts make this technique appropriate for either rural or anthropogenic-influenced sites (Ge et al., 2013) but not fully suitable for remote ones with typical $NO_2$ mole fractions below 50 ppt. Moreover, calibration of $NO_2$ specific detectors remains challenging as reference gases with ambient levels of $NO_2$ in high pressure cylinders are known to be susceptible to instabilities.

At present, there is no mature point measurement technique that can compete with the ozone-induced chemiluminescence detection of NO at remote locations. Passive and active time-integrating methods are not accepted in the GAW Programme due to their poor selectivity and time resolution.

More details on procedures for standard operations can be found at https://actris.nilu.no/Content/?pageid=68159644c2c04d648ce41536297f5b93.

Ground-based remote-sensing techniques for $NO_2$ are currently being developed towards more operational use and better defined uncertainties in the framework of ACTRIS. MaxDOAS instruments are increasingly used for vertical profile measurements, FTIR and zenith-sky UV/Vis measurements are also used for $NO_2$ vertical column information.

### 16.4.5 Sulphur dioxide

Measurement guidelines for $SO_2$ observations are so far not available in the GAW Programme. General recommendations are given in WMO (2001). However, the GAW Scientific Advisory Group for Reactive Gases is planning to establish the same QA system for $SO_2$ (including measurement guidelines and central facilities) as it is doing at present for nitrogen oxides after the latter is completed.

There are various measurement techniques for determining atmospheric $SO_2$. EMEP is using integrating techniques, such as an alkaline-impregnated filter (pack) or coated annular denuder, both followed by ion chromatography in a central laboratory. These methods yield potentially

more accurate results, but with a time resolution of usually one sample per day, as is typical for integrative techniques. Additionally, they require frequent attention, and personnel costs for filter analysis are high.

In the group of in-situ measurements, the TCM (photometry after reaction of $SO_2$ with tetrachloromercurate) and the pulsed fluorescence methods are widely used. TCM has a high accuracy but high lower detection limit, and the handling of mercury in the laboratory could be harmful. Even though the response of the pulsed-fluorescence sensor is slower, its ease of calibration, dependability, accuracy and $SO_2$ specificity make it preferable. More sensitive GC techniques are also available. However, they require significant technical expertise and regular attention. In order to enhance the sensitivity, some fluorescence analysers are equipped with more selective excitation filters. For example, two mirror assemblies are connected in series and specially selected PMTs are employed. Numerical corrections for interfering substances are possible; however, this is not necessary in rural or remote areas. The typical lower detection limit which can be reached with these provisions is some 50 ppt. A further enhancement of sensitivity may be possible by means of a second channel in which only $SO_2$ is removed, leading to a highly specific read-out after subtraction of both channels.

Since $SO_2$ has a short atmospheric lifetime, understanding the sulphur cycle requires knowledge of the source and sink terms. This is best accomplished with sampling frequencies of less than 1 h. Therefore, the best technique for long-term monitoring of $SO_2$ today is a combination of the pulsed-fluorescence analyser and filter sampling. Filter samples should be exposed at intervals, but often enough to act as a QC for the continuous analyser.

More detailed recommendations can be found in EMEP (2014), available at https://projects.nilu.no/ccc/manual/index.html.

### 16.4.6 Molecular hydrogen

Detailed measurement guidelines for molecular hydrogen are currently not available in the GAW Programme.

Molecular hydrogen is reported as dry mole fraction on the most recent scale (WMO, 2016c). Measurements of $H_2$ are possible both in situ and by flask collection with subsequent analysis in the laboratory. An example of the measurement system set up at the GAW global stations is given in (Grant et al., 2010).

Molecular hydrogen measurements are performed with GC followed by hot mercuric oxide reduction/UV absorption detection. An alternative GC set-up with pulsed-discharge detectors has a more linear detector response and provides better repeatability for molecular hydrogen measurements (Novelli et al., 2009).

Problems with instability of $H_2$ in reference gases have frequently been experienced (Jordan and Steinberg, 2011). Therefore, recommendations on calibration and QA of $H_2$ measurements available in WMO (2016*c*) should be consulted.

## 16.5 ATMOSPHERIC WET DEPOSITION

Atmospheric wet deposition refers to the gases and particles deposited by precipitation on the Earth's surface. These gases and particles have a wide variety of sources and compositions and generally are present in trace amounts in the atmosphere and in precipitation. These trace materials are captured by precipitation as it forms in the atmosphere and falls to the Earth. The deposited materials constitute an important contribution to the mass balance of pollutants associated with long-range transport. These materials not only affect the chemistry of precipitation but also can affect the chemistry of the terrestrial and aquatic surfaces on which they are deposited. The effects can be either harmful or beneficial, and they can be either direct or indirect. For example, acidic wet deposition is an environmental problem

that results from combustion of fossil fuels. It occurs when oxides of sulphur and nitrogen, emitted during combustion, are transformed in the atmosphere and become acidic sulphate and nitrate in precipitation. Other trace materials that occur in wet deposition include sea salt, nutrients, chemicals found in soil particles, toxic organic and inorganic chemicals, organic acids, and the like. Research has shown that some wet-deposited chemicals can stimulate marine biotic production, potentially linking atmospheric wet deposition to the carbon cycle and climate change.

Measuring the chemistry of precipitation tells us what trace materials are present in wet deposition and in what amounts. This information can be used to evaluate air quality and to identify and track changes in gaseous and particulate emissions to the atmosphere. In short, precipitation chemistry measurements provide information on the exchange of trace materials between the atmosphere and the land/oceans, and hence are important in furthering our understanding of the chemical cycles of these materials, especially those that can result in damage to terrestrial and aquatic systems or affect our climate.

Special care is required when planning precipitation chemistry measurements to ensure that they are representative. Though the measurements are made at a particular location, on average they should represent measurements in the surrounding region. In general, the sample collection site should be characteristic of the land use in the region. For example, the site in an area dominated by agricultural activities should have an agricultural setting. This quality of spatial representativeness should extend across seasons and even over years. Ideally, a site would be both spatially and temporally representative. Contamination of a localized nature from agricultural, industrial or other human activities must be avoided, as must the local impact of natural sources, such as oceanic shores, volcanoes or fumaroles. Sample collection should not be impacted by trees or other vegetation, and the on-site topography should be level and the exposure relatively unaffected by wind patterns that may result in an unrepresentative catch of rain and snow. Human contact with the sample or contact with anything that might change the sample chemistry must be avoided as well. Ensuring representative precipitation chemistry measurements entails strict adherence to requirements for site location, site conditions, equipment installation and site operational protocols and maintenance. These requirements are documented in WMO (2004*a*).

Precipitation chemistry monitoring can be divided into sample collection activities and chemical analysis activities.

### 16.5.1 **Sample collection**

The primary goal of the GAW Precipitation Chemistry Programme is to collect wet-only deposition samples. This means that the samplers are exposed only during precipitation and trace materials in the samples are deposited only by precipitation. The trace materials from dust or fine particles or gases deposited during dry weather are excluded. This makes it possible to study precipitation chemistry without contamination from dry deposition. More importantly, the equipment and methods for collecting a representative wet deposition sample are inappropriate for collecting a representative dry deposition sample. The physical and chemical processes affecting wet and dry deposition are distinctly different.

The best way to ensure collection of a wet-only sample is to employ an automated sampler that is open only during precipitation. A typical automated, wet-only deposition sampler has the following components: a precipitation sample container (funnel-and-bottle, bucket, and the like), a lid that opens and closes over the sample container orifice, a precipitation sensor, a motorized drive mechanism with associated electronic controls and a support structure to house the components. The containers should have sufficient volume to hold all precipitation collected during the sampling period. A system that can be activated manually for testing, cleaning and routine maintenance is recommended. A modular design that allows removal of individual components, such as the sensor, facilitates rapid repair with a minimum of tools and expertise. An alternative to using an automated sampler is to collect samples by manually exposing a

sample container at the very onset of precipitation and closing it as soon as precipitation ceases. This requires diligent round-the-clock observers alert to weather conditions; as a consequence, manual sample collection is very labour-intensive.

To complement the collection of wet-only deposition samples, the GAW Precipitation Chemistry Programme requires every site to measure precipitation depths using the standard precipitation gauge designated by NMHSs or its equivalent (see the present volume, Chapter 6). Manual gauges are preferred. Precipitation depths are used to calculate the mass of a chemical deposited by precipitation on an area of the Earth's surface (called the wet deposition flux or loading). Standard precipitation gauges are designed to be the most accurate and representative means of measuring precipitation depths. Thus, each site must operate a precipitation gauge in parallel with its precipitation chemistry sampler. Precipitation chemistry sampler volumes are used to calculate wet deposition fluxes only when the standard gauge fails or is temporarily out of service. The data record should document such cases.

The highest priority of the GAW Precipitation Chemistry Programme is to collect a wet-only sample on a daily (24 h) basis with sample removal set at a fixed time each day, preferably 0900 local time. Should the resources be inadequate to collect and analyse daily samples, multi-day sampling periods up to one week is the next highest priority. Alternative sampling protocols are described in WMO (2004*a*). Collecting samples daily reduces the potential for the degradation of labile chemical species and for other physical and chemical changes in the sample while it is held in the field sampler. Not only is the sample integrity less likely to be compromised by a daily sampling protocol but the data have greater value as well. Storm trajectory analyses and source-receptor models are much less complicated when precipitation is more likely to have come from a single event or storm. Multi-day and one-week samples are much more likely to contain precipitation from several storms, each occurring under different meteorological settings. Further, daily data can be integrated mathematically to determine weekly or longer-term averages, but weekly data cannot be differentiated into daily components without making substantial assumptions.

Containers used to collect, store and ship samples should be unbreakable and sealable against leakage of liquids or gases. High-density polyethylene containers are recommended. All sample containers must be cleaned with deionized water of known and assured quality. The report (WMO, 2004*a*) contains detailed descriptions of the procedures for cleaning containers and ensuring that cleanliness standards are maintained throughout the collection, storage and shipment of samples.

### 16.5.2 **Chemical analysis**

The following chemical parameters are recommended for analysis in GAW precipitation samples: pH, conductivity, sulphate, nitrate, chloride, ammonium, sodium, potassium, magnesium and calcium. Analyses for formate and acetate are recommended for areas suspected of having high organic acid concentrations. Nitrite, phosphate and fluoride concentrations also may be important in certain areas, although their analyses are not required by GAW at this time. Preferred analytical methods are given in Table 16.2.

Past experience from regional networks and laboratory intercomparisons has shown that measuring pH in precipitation is difficult due mainly to the low ionic strength of the samples. Samples may also degrade due to biological activities and should therefore be kept refrigerated until the time of analysis, when they are brought to room temperature. The pH measurements should be carried out within one day of sample arrival in the laboratory.

Commercial pH meters are available with different specifications and options. A pH meter should have both an intercept and slope adjustment and should be capable of measuring to within ±0.01 pH unit. Combination electrodes containing both measuring and reference functions are often preferred since they require smaller amounts of a sample, but a set of two electrodes may also be used with the pH meter. The measuring glass electrode is sensitive to hydrogen ions and the reference electrode can be calomel, or silver/silver chloride. Low ionic strength electrodes are now available commercially. Other reference electrodes can also be used as long as they

**Table 16.2. Chemical parameters required for analysis in the GAW Precipitation Chemistry Programme with recommended analytical methods**

| *Analyte* | *Status* | *Preferred methods*[a] |
|---|---|---|
| pH | Required | Glass electrode |
| Conductivity | Required | Conductivity cell |
| Alkalinity | Optional | Titration |
| $Cl^-$, $NO_3^-$, $SO_4^{2-}$ | Required | IC |
| $NH_4^+$ | Required | IC, AC |
| $Na^+$, $K^+$, $Ca^{2+}$, $Mg^{2+}$ | Required | IC, ICP, AAS/AES |
| Organic acids[b] | Optional | IExC, IC |
| $NO_2^-$, $F^-$ | Optional | IC |
| $PO_4^{3-}$ | Optional | IC, AC |

Notes:
a IC = ion chromatography; AC = automated colorimetry; ICP = inductively coupled plasma spectrometry; IExC = ion exclusion chromatography; AAS = atomic absorption spectrometry; AES = atomic emission spectrometry
b For areas with high organic acid concentrations, formate and acetate analyses are recommended.

have a constant potential. When selecting any electrode, confirm its ability to measure low ionic strength solutions by measuring a certified reference material. Response time should be less than 1 min and the addition of potassium chloride (KCl) should not be needed.

The conductivity of a solution is the reciprocal value of its specific resistance and can be directly measured using a conductivity bridge with a measuring cell. Conductivity varies with the temperature of the solution and is proportional to the concentration and the species of free ions present in the solution. Since the conductivity also depends on the electrode area and its spacing, the measuring apparatus has to be calibrated to obtain the cell constant or to adjust the meter. A KCl solution of known concentration and conductivity is used for calibration. Conductivity is measured and expressed in units of microsiemens per centimetre (µS $cm^{-1}$), corrected to 25 °C. The conductivity range of precipitation samples is 5 to 1 000 µS $cm^{-1}$. In case of small sample volumes, the aliquot that is used for conductivity measurement can be used for pH determination. If this is done, the conductivity should be measured first to avoid any possible error due to salt contamination from the pH electrode.

The apparatus for conductivity measurements consists of:

(a) A conductivity meter (with operating range of 0.1 to 1 000 µS $cm^{-1}$; or, better, 0.01 to 1 000 µS $cm^{-1}$). Precision has to be within 0.5% of the range and accuracy at 1% of the range;

(b) A conductivity cell (if the values in precipitation samples are expected to be mainly very low (<20 µS $cm^{-1}$), use special conductivity cells, with a low cell constant);

(c) A thermometer (0 °C to 40 °C / 0.1 °C);

(d) A water bath at 25 °C;

(e) A polyethylene or glass vessel corresponding to the diameter of the cell used.

Ion chromatography has been widely used in recent years to analyse major anions and cations in precipitation, mainly in combination with electrochemical detection.

Sulphate, nitrate, chloride as well as other anions in precipitation are separated on an ion exchange column because of their different affinities for the exchange material. The material commonly used for anion separation is a polymer coated with quaternary ammonium active sites. After separation, the anions pass through a suppressor that exchanges all cations for $H^+$ ions. Instead of strong acid cation exchange columns, today micro membrane and self-regenerating suppressors with chemical or electrochemical regeneration are used. As a result of the suppression reaction, corresponding acids of the eluent ions and of chloride, nitrate and sulphate will reach the conductivity detector. A decreased basic conductivity and higher analytical signals now allow the detection of anions in the lower $\mu g\ L^{-1}$ range.

There are several anion exchangers with different properties available on the market. The time for one analysis and the quality of separation of single signals are dependent on the type of column and eluent, and on the concentration and flow rate of the eluent.

Any anions with a retention time similar to that of the main anions in the solution can cause interference. For example, when $NO_2^-$ is present, it elutes just after $Cl^-$, which can cause the peak to be asymmetric. In rare cases, when the concentration of $Cl^-$ is very high compared with that of $NO_3^-$, it can also influence the determination of $NO_3^-$. The manual should be consulted to see how different integration programmes handle this problem.

With care, up to several thousand analyses can be performed with the same anion separator column. The most effective method of protecting the separator column is to use a pre-column in front of it. Details are provided by the manufacturers in the manuals for the columns.

The principle of cation measurements is the same as that of anion determination except that different column materials are used and the suppressor column is often omitted. The material commonly used for cation separation is a cation exchange resin with active surface groups. Sodium, ammonium, potassium, calcium and magnesium ions are detected by a conductivity detector, without changing the eluent when certain columns are used. In other columns, monovalent cations ($Na^+$, $NH_4^+$, $K^+$) are determined using one eluent and divalent cations ($Mg^{2+}$ and $Ca^{2+}$) with another eluent (because of their higher affinity to the resin).

Any cation with a retention time similar to that of the main cations may cause interference. For example, in samples with high concentrations of $Na^+$, the peak of $NH_4^+$ becomes asymmetrical and often causes significant error. In this case, measurement using more dilute eluent could improve the separation of peaks.

Sodium, potassium, magnesium and calcium in precipitation are often analysed by atomic spectroscopic methods. Both flame (atomic absorption spectrometry (AAS) and atomic emission spectrometry (AES)) and plasma (inductively coupled plasma atomic emission spectrometry and inductively coupled plasma MS (ICP-MS)) based methods can be used. For these ions, ion chromatography has no special advantage in terms of sensitivity, precision and accuracy over the spectroscopic methods, although analysis of all ions in one sample run is not possible with flame AAS or AES (single element methods).

The ions in the sample solution are transformed to neutral atoms in an air/acetylene flame. Light from a hollow cathode or an electrodeless discharge lamp is passed through the flame. In the AAS mode, light absorption of the atoms in the flame is measured by a detector following a monochromator set at the appropriate wavelength. Light absorption is proportional to the ion concentration in the sample. In the AES mode, the light emitted from the atoms excited in the flame is measured. Most commercial instruments can be run in both modes. AES is the preferred mode for sodium measurements.

In AAS, both ionization and chemical interferences may occur. These interferences are caused by other ions in the sample, which reduce the number of neutral atoms in the flame. Ionization interference is avoided by adding a relatively high amount of an easily ionized element to the samples and calibration solutions. For the determination of sodium and potassium, caesium is added. For the elimination of chemical interferences from aluminium and phosphate, lanthanum can be added to the samples and calibration solutions for calcium and magnesium.

Formic and acetic acids (HCOOH and $CH_3COOH$, respectively) are major chemical constituents of precipitation in both continental and marine regions. Available evidence suggests that these compounds originate primarily from natural biogenic sources; both direct emissions (over continents) and emissions of precursor compounds appear to be important. Biomass and fossil fuel combustion also result in the emission of carboxylic acids and/or their precursors to the atmosphere.

Carboxylic acids in precipitation are very unstable and rapidly disappear from unpreserved samples. To generate reliable data, precipitation must be sampled on a daily or event basis and immediately preserved with the addition of a biocide such as chloroform ($CHCl_3$). Typically, 250 ml aliquots of sample (or less for low volume events) are treated with 0.5 ml of $CHCl_3$. Samples are then tightly sealed and refrigerated until analysis.

Carboxylic species can be analysed by both ion (using a dilute eluent) and ion exclusion chromatography. However, acetate and propionate typically co-elute when analysed by ion chromatography and are thus impossible to resolve quantitatively. The ion exclusion chromatography method exhibits fewer interferences associated with co-eluting species and is thus preferred for analysis of precipitation samples.

For analysis by ion exclusion chromatography, samples are added to a hydrochloric acid (HCl) eluent which then flows through a separator column, a suppressor column and a detector. Resin in the separator column partitions anions using the principle of Donnan exclusion; anions are retained and sequentially separated based on their respective $pK_a$s and van der Waals interactions with the resin. Anions of stronger acids with lower $pK_a$s, such as $H_2SO_4$, $HNO_3$ and HCl, are effectively excluded and co-elute early in the chromatogram; those of weaker acids with higher $pK_a$s, such as HCOOH and $CH_3COOH$, elute later in the chromatogram. The suppressor column incorporates a cation exchange resin with silver added to the exchange sites; $H^+$ exchanges with the silver; the released silver subsequently reacts with $Cl^-$ in the eluent to form silver chloride (AgCl), which precipitates within the column. Acid analytes exit the suppressor in a stream of deionized water. Detection is by conductivity.

## 16.6 AEROSOLS

Atmospheric aerosols are important for a diverse range of issues including global climate change, acidification, regional and local-scale air quality, and human health. The climate impact of aerosols is a result of direct radiative effects and indirect effects on cloud properties. Regional problems include potential impacts on human health and mortality and environmental impacts such as visibility impairment. Major sources of aerosols include urban/industrial emissions, smoke from biomass burning, secondary formation from gaseous aerosol precursors, sea salt and dust. Outstanding problems include determining the natural sources of aerosols and the organic fraction.

Table 16.3 provides a list of aerosol parameters recommended for measurement in the GAW Programme. Comprehensive measurement guidelines for aerosol measurements are provided in WMO (2016*d*) and WMO (2011).

### 16.6.1 Aerosol chemical measurements

At present, filter collection of ambient aerosols, followed by laboratory analyses, still remains the most commonly used and cost-efficient method available for the determination of aerosol chemical composition despite well-documented artefacts. Artefacts are very often linked to the presence of semi-volatile species that can either condense upon sampling (positive artefact) or evaporate from the filter media after sampling (negative artefact). A number of methods have been proposed to account for these artefacts (Cavalli et al., 2010).

The optimal set-up for the characterization of chemical properties of aerosol would be composed of a series of denuders to remove condensable species present in the gas phase (limiting positive

**Table 16.3. List of comprehensive aerosol variables recommended for long-term measurements in the global network**

| *Variable* | *Frequency of observation* |
|---|---|
| Multiwavelength AOD | Continuous |
| Mass concentration in two size fractions (fine, coarse) | Continuous |
| Mass concentration of major chemical components in two size fractions | Continuous |
| Light absorption coefficient at various wavelengths | Continuous |
| Light scattering and hemispheric backscattering coefficient at various wavelengths | Continuous |
| Aerosol number concentration | Continuous |
| Aerosol number size distribution | Continuous |
| Cloud condensation nuclei (CCN) number concentration at various supersaturations | Continuous |
| Vertical distribution of aerosol backscattering and extinction | Continuous |
| Detailed size fractionated chemical composition | Intermittent |
| Dependence of aerosol variables on relative humidity, especially aerosol number size distribution and light scattering coefficient | Intermittent |

*Source*: WMO (2016*d*)

artefacts) and a filter pack collecting both particles and condensable species re-emitted from the first filter (accounting for negative artefacts). Filter packs have been developed, consisting of a sandwich of filters and collection media of various types in series, to collect aerosols and selectively trap gases and aerosol volatilization products. Ideally, sampling for inorganic and carbonaceous species is performed with two different sampling lines since different kinds of denuders and filter media are required for analyses of elemental and organic carbon (EC/OC), and inorganic species. A third line could be implemented for sampling and analysis of elemental aerosol composition. The optimal set-up for OC/EC sampling is described in EN-16909 (CEN, 2017) and in (Cavalli et al., 2010).

Clearly, methods for artefact limitation add complexities with respect to plain filter measurements. For GAW purposes, considering remoteness and the availability of resources at a number of sites, the use of denuders is recommended for EC/OC measurements only and not a requirement for other chemical species. This means, however, that sampling artefacts do exist for a number of inorganic semi-volatile species, in particular when temperatures in the sampling system exceed 20 °C. This should be accounted for when reporting data to the World Data Centre for Aerosols.

High- and low-volume sampling lines are accepted in the context of GAW. For simplicity, it is suggested that a differencing technique be utilized to separate the coarse fraction from the fine fraction. Specifically, one filter should be run behind the 10 µm aerodynamic diameter cut inlet. A parallel filter should be run behind the inlet suitable for the fine fraction (that is, 2.5 µm aerodynamic diameter at ambient relative humidity). While the second filter will yield the fine fraction, the difference between the two filters will yield the coarse fraction. For high-volume sampling, use of dichotomous samplers is an interesting alternative to differentiate fine and coarse aerosol fractions.

Low-volume samplers are less expensive than high-volume samplers. For the routine long-term aerosol measurements at GAW stations, it is recommended that up to three sets of 47 mm diameter filters be collected in parallel by low-volume samplers. If financial constraints are a limiting factor, the priorities for filter sampling are: (a) Teflon filters for gravimetric and ionic

analyses; (b) quartz-fibre filters for carbonaceous aerosol analyses with lines equipped with carbon denuders; (c) Teflon filters for elemental analyses. Each set would consist, ideally, of two filters, one for total mass below 10 µm diameter and one for the fine fraction. The separation would be achieved by running the filters behind the size-selective inlets. High-volume samplers are usually more expensive, and running more than one set of samplers in parallel is often impractical. For that reason, it is recommended that high-volume samplers be operated with quartz fibre filters for both inorganic and EC/OC analyses. It should be noted that denuders for high-volume samplers have only recently become commercially available.

There is no recommendation for determining sampling time as this will be highly site-dependent. In general, short sampling time (24 to 48 h) provides information that is more easily used in models and should be preferred over week-long sampling, even if discontinuous. Filters should be removed from the sampling unit shortly after collection and stored between 0 °C and 5 °C if analyses cannot be performed immediately. Regular blank samples should be taken in order to control for contamination. Ideally, such blanks are prepared by mounting filters into the sampling unit with the pump switched off. It is recommend that one blank be performed for every 10 samples.

For each GAW aerosol station, a list of core aerosol chemical measurements is strongly recommended: (a) mass; (b) major ionic species; (c) carbonaceous components; (d) dust aerosols.

The mass concentration of atmospheric aerosols is clearly a fundamental parameter in the GAW measurement programme. It is recommended that this be measured gravimetrically on Teflon filters. It is expressed in units of µg $m^{-3}$, where the volume is related to STP. Updated measurement guidelines on mass concentration measurements using gravimetric analysis of Teflon filters are provided in WMO (2011).

The tapered element oscillating microbalance (TEOM) has been widely used for aerosol mass measurements. The instrument provides continuous measurements and can produce high time resolution data. It is recommended that TEOM is used with Filter Dynamics Measurement System corrections to account for the loss of semi-volatile components of aerosols, and humidity.

A different type of instrument for continuous mass measurements, the β-meter, has also been commercialized. It operates on the principle of β-ray attenuation by a layer of aerosol. The β-ray source is usually $^{14}C$ or $^{85}Kr$ decay, and the attenuation can be calibrated with a known mass. Sampling can be performed with individual filters or filter tapes, and the β-ray that passes through the filter is continuously monitored. The β-meters have the same inherent difficulties concerning volatilization as the TEOM. However, comparison with gravimetric methods usually produces reasonable agreement. Updated guidelines on the mass concentration measurements with beta attenuation (with the Met One Instruments model BAM-1020) are provided in WMO (2011).

The concentration of major inorganic species is one of the core pieces of information recommended for the GAW stations. Major ionic species include sulphate, nitrate, chloride, sodium, ammonium, potassium, magnesium and calcium. This selection is based on the fact that analytical procedures for these species have become well established. More importantly, under most atmospheric conditions, this set of ions is expected to account for a major part of the aerosol mass, and the measurements here are an important step towards mass closure of the aerosols. As mentioned above, quantitative measurements of nitrate with a filter technique remain problematic and are associated with high uncertainties.

In the GAW Programme, it is recommended that analyses be performed using ion chromatography for the most cost-effective approach. The ion chromatography technique has the advantage of chemical speciation and relatively low cost per analysis, and has matured to the degree that the sensitivities for each ionic species, the cost and the maintenance are all reasonably well known. If ion chromatography is set up properly, all the recommended ionic species can be analysed in one single sample injection. Alternative analytical techniques exist but their use may introduce systematic differences among GAW stations. It is part of each laboratory's responsibility to document the equivalence of these alternative techniques,

such as AAS or ICP-MS, with ion chromatography whenever they are used. Calibration of ion chromatography instruments is an integral part of every laboratory's SOPs, and each laboratory must implement QC procedures that guarantee the accuracy of calibrations. Recommendations for GAW are similar to those reported in WMO (2004*a*) for precipitation chemistry. In addition, protocols for filter extraction should be well documented.

Instruments are becoming available that can accomplish continuous and semi-continuous measurement of sulphate, nitrate, and OC in aerosols. In particular, progress in aerosol MS (AMS) has led to the development of instruments that can be used for monitoring purposes, providing quantitative measurements of the total mass and size distribution of non-refractory chemical composition in the submicron-size range. Simpler versions of AMS now exist commercially that can provide chemically speciated mass loadings and aerosol mass spectra with one-hour time resolution. No SOPs endorsed by GAW/WMO exist yet although ACTRIS is operating a central facility targeting AMS that provides recommendations for long-term monitoring operations.

The concentration of carbonaceous species (with both elemental and organic fractions) is also one of the core pieces of information recommended at GAW stations. Carbonaceous species are still the least understood and most difficult to characterize of all aerosol chemical components. Total aerosol carbon mass can be divided into three fractions: inorganic carbonates, OC, and a third fraction ambiguously called elemental carbon (EC), black carbon (BC), soot or refractory carbon in the scientific literature with no clear definition of the terms. Recommendations for proper use of terminology for BC-related species have been proposed by Petzold et al. (2013) to clarify the terms used in atmospheric research; they recommend that the term "black carbon" be used only in a qualitative sense, and that terms related to the measurement technique be used when reporting quantitative results. According to this terminology, thermo-optical methods can be used to derive total carbon (TC) and OC/EC fraction in atmospheric aerosol filters. When using optical methods, the light-absorbing component is called equivalent black carbon (EBC), even though the optical method is not specific for carbon.

It is recommended that TC, OC and EC be measured in the GAW Programme, leaving out the relatively minor and difficult inorganic carbon component and the more complicated issue of OC speciation. Sampling of aerosol carbonaceous materials is recommended using quartz filters, pre-fired at 350 to 400 °C for 2 h, and deployed at the same sampling frequency as the Teflon filters. The quartz filter can be analysed for TC using the thermal evolution technique. The mass concentration of TC is obtained by thermal oxidation of the carbon, usually at 750 °C in the presence of a catalyst, to measurable carbon dioxide. Detection of the evolved carbon dioxide is done in one of two ways: either by reduction to methane in the presence of a catalyst, and then FID, or by direct detection by NDIR detectors.

The measurement of the TC components (OC and EC) is more difficult than the measurement of TC (Schmid et al., 2001). The distinction between the fractions is made by temperature-controlled volatilization/pyrolysis. This is followed by catalysed oxidation to $CO_2$ and detection by NDIR, or in some instruments, further catalysed reduction of the $CO_2$ to $CH_4$ and final detection by FID. There are different temperature-control programmes in use. At present, GAW recommends the use of one of three thermo-optical techniques: the Interagency Monitoring of Protected Visual Environments (IMPROVE) protocol (Chow et al., 1993; Chow et al., 2005); National Institute for Occupational Safety and Health (NIOSH) protocol (Birch and Cary, 1996); and European Supersites for Atmospheric Aerosol Research (EUSAAR-2) protocol (Cavalli et al., 2010). Relatively good agreement is obtained between the IMPROVE, NIOSH and EUSAAR-2 protocols for TC determination, while they strongly differ for EC determination (Chow et al., 2001). Because EC represents a relatively small fraction of TC, OC determination by the three protocols is also comparable. It is accepted that the IMPROVE and EUSAAR-2 protocols are best suited for non-urban background sites, while the NIOSH is applied to samples from urban sites by the US Environmental Protection Agency. The use of IMPROVE (Watson et al., 2009) or EUSAAR-2 may therefore be preferred over NIOSH for global remote GAW stations. Use of the EUSAAR-2 and IMPROVE protocols for EC determination may lead to different results but should be preferred over any alternative techniques. Whenever an alternative approach is used for OC measurements, it is recommended that a periodic determination of OC using one of the thermo-optical methods be conducted so that results can be compared.

The use of optical methods for estimating EBC involves measuring the change in optical transmission of a deposit of particles on a filter (absorption) and applying a site-specific and instrument type-specific mass absorption efficiency to derive EBC. Two key assumptions are required to derive the equivalent BC mass concentration from light absorption measurements: (a) BC is the only species responsible for the aerosol light absorption, and (b) the sampled BC has the same mass absorption efficiency as the standards used in laboratory calibrations of the absorption instrument. These assumptions can be evaluated by experimentally determining the mass absorption efficiency by simultaneously making light absorption measurements and EC measurements as described above. At sites where EC concentrations are not routinely determined on quartz-fibre filters, less frequent filter collections can be used to derive site- and season-specific values of the mass absorption efficiency. Thus, for GAW measurements of EBC, experimentally derived values of the mass absorption efficiency at a site are essential when estimating BC mass concentration from light absorption measurements.

The use of incandescent methods, such as single-particle soot photometers, or volatility techniques, such as volatility scanning mobility particle sizer, can provide information on refractory material present in aerosol, but their use in monitoring activities at GAW stations remains problematic given the lack of standardized protocols and of consistent intercomparison with thermo-optical techniques.

Dust aerosols can be sampled relatively easily without the problems posed by more semi-volatile aerosol components such as organics and ammonium nitrate. For GAW stations, it is recommended that a multi-elemental analysis approach be used to determine the mineral dust component. Teflon filters should be analysed for at least four of the major crustal elements, aluminium (Al), silicon (Si), iron (Fe), titanium (Ti) and scandium (Sc), and the related elements, sodium (Na), magnesium (Mg), potassium (K) and calcium (Ca). No specific analytical technique is recommended as there is a good selection available, including proton-induced X-ray emission, instrumental neutron activation analysis, X-ray fluorescence, AAS and ICP-MS. These techniques usually have high sensitivities for the crustal elements. Not all techniques can provide all the required elements, and depending on availability, a combination of two or more techniques may be necessary.

### 16.6.2 In situ measurements of aerosol radiative properties

The following aerosol radiative properties are needed for climate studies, all at multiple wavelengths across the visible spectrum:

(a) Aerosol light extinction coefficient ($\sigma_{ep}$) and its two components (scattering and absorption);

(b) AOD ($\delta$, see 16.6.5), defined as the integral over the vertical column of the aerosol light extinction coefficient;

(c) Aerosol single-scattering albedo ($\omega_o$), defined as $\sigma_{sp}/(\sigma_{ap} + \sigma_{sp})$, which describes the relative contributions of scattering and absorption to the total light extinction; purely scattering aerosols (such as sulphuric acid) have values of 1, while very strong absorbers (such as BC) have values of about 0.3;

(d) Radiative transfer models commonly require one of two integral properties of the angular distribution of scattered light (phase function): the asymmetry factor ($g$) or the upscatter fraction ($\beta$); the asymmetry factor is the cosine-weighted average of the phase function, ranging from a value of –1 for entirely backscattered light to +1 for entirely forward-scattered light; the upscatter fraction gives the fraction of sunlight scattered in the upwards direction (back to space), which depends on the solar zenith angle as well as the size distribution and chemical composition of the particles; it can be estimated from the hemispheric backscatter fraction ($b$);

(e) Mass scattering efficiency for species $i$, ($\alpha_{si}$), used in chemical transport models to evaluate the radiative effects of each chemical species forecast by the model; it is often calculated

as the slope of the linear regression line relating the aerosol light scattering coefficient ($\sigma_{sp}$) and the mass concentration of the chemical species (though multiple linear regression is preferred, to deal with covariance of some chemical species); this parameter has units of $m^2\ g^{-1}$;

(f) Mass absorption efficiency for species *i*, ($\alpha_{ai}$), used in chemical transport models to evaluate the radiative effects of each chemical species forecast by the model; it is often calculated as the slope of the linear regression line relating the aerosol light absorption coefficient ($\sigma_{ap}$) and the mass concentration of the chemical species (though multiple linear regression is preferred, to deal with covariance of some chemical species); this parameter has units of $m^2\ g^{-1}$;

(g) The functional dependence of components of the aerosol light extinction coefficient ($\sigma_{ep}$, $\sigma_{sp}$, $\sigma_{ap}$) on relative humidity, f(RH), expressed as a multiple of the value at a low reference relative humidity (typically < 40%).

The aerosol light scattering coefficient is measured with an integrating nephelometer. Integrating nephelometers have been operated at baseline monitoring stations since the deployment of a four-wavelength instrument at the US NOAA Mauna Loa Observatory in 1974. At present, there are about four dozen sites monitoring $\sigma_{sp}$ routinely around the globe as part of the GAW global network. A few of these are operating single-wavelength units, but most are measuring $\sigma_{sp}$ at three wavelengths. The multiwavelength integrating nephelometer TSI model 3563 operates at wavelengths of 450, 550 and 700 nm, and has the added feature of being able to measure $\sigma_{sp}$ over two angular ranges: total scattering (7–170°) and hemispheric backscattering (90–170°, denoted as $\sigma_{bsp}$). The Aurora 3000 integrating nephelometer, manufactured by Ecotech, makes comparable measurements. While instruments do not exist for direct determination of $g$ or $\beta$, the ratio $b = \sigma_{bsp}/\sigma_{sp}$ can be used to estimate either of these parameters (updated measurement guidelines are available in WMO (2011)). Simpler, less expensive and less sensitive one-wavelength instruments are also commercially available. These instruments can provide useful information on the aerosol light scattering coefficient at regional sites where aerosol loadings allow the use of a less sensitive instrument.

Instruments capable of high time-resolution determination of the aerosol light absorption coefficient are commercially available. They are based on the rate of change of transmission through a fibre filter as particles are deposited on the filter. Calibration of these filter-based methods is difficult but required because the relationship between the change in light transmission and aerosol absorption optical depth on the filter depends on many factors, including the particular filter medium and the light-scattering nature of the particles.

One instrument in common use is the aethalometer. Originally, this instrument was calibrated in terms of an equivalent mass of BC rather than the fundamental property that provides the instrumental response: aerosol light absorption. Early models of the aethalometer have a very broad wavelength response, while newer versions offer narrowband measurements at multiple wavelengths.

Another commercial, filter-based instrument for determining $\sigma_{ap}$ is the particle soot absorption photometer (PSAP) that measures laboratory aerosols with different single-scattering albedos, using a calibration standard based on the difference between $\sigma_{ep}$, measured with a long-path extinction cell, and $\sigma_{sp}$, measured with an integrating nephelometer. Updated measurement guidelines for particle soot absorption photometer instruments are provided in WMO (2011).

Yet another filter-based instrument is the multi-angle absorption photometer. This instrument uses a different optical configuration than the aethalometer and the particle soot absorption photometer, with measurements of the filter reflectivity at two different angles in addition to the filter transmission measurement. The two reflectivity measurements allow correction for multiple scattering processes involving the deposited particles and the filter matrix. This approach eliminates the need for a correction scheme based on independent measurements of the aerosol light scattering coefficient. The multi-angle absorption photometer operates at a wavelength of 670 nm; updated measurement guidelines for these instruments are provided in WMO (2011).

Recent improvements in a different approach to determining the aerosol light absorption coefficient, called photoacoustic spectroscopy, offer a promising alternative to filter-based methods. Although not as sensitive, the photoacoustic method allows determination of the aerosol light absorption coefficient while the particles are suspended in air, eliminating the artefacts introduced by depositing the particles on a filter. The photoacoustic method can be used in regions where light absorption levels are moderately high, and as a calibration standard for filter-based instruments.

### 16.6.3 Particle number concentration and size distribution

Condensation nuclei counters, also known as condensation particle counters (CPCs), are used to measure particle concentration for particles of diameter as small as a few nanometres. The technology is well established and is commercially available from different manufacturers. Condensation nuclei can be detected after the condensation of water or other condensable vapour (often an alcohol such as butanol) from a supersaturated atmosphere onto the particle. The supersaturation in CPCs is typically quite elevated, about 150%. The CPC is robust and designed for long-term operations. However, it needs regular QA checks on site, especially in terms of cleaning the saturator and optics. Additionally, annual calibrations of the CPC against a reference instrument are required. If the counting efficiency is not controlled, CPC performance might drift with time causing an unnoticed bias of up to several tens of per cent. Measurements of particle number size distribution complement condensation nuclei counters. Many commercial instruments are now available for both the fine and the coarse modes. They utilize a wide range of physical principles to classify particles according to size. Some of the better-known approaches use the electrical mobility of particles, aerodynamic size, or optical size determined by light scattering. Mobility particle size spectrometers (MPSSs) measure the particle number size distribution of the submicrometer size range from approximately 10 to 800 nm. The technology is well established and is commercially available, but there are also custom-designed measurement systems. An MPSS is robust and designed for long-term operations although it requires regular QA checks on site. Additionally, annual or biannual calibrations of both MPSS and CPC against reference instruments are required. If the MPSS instrument performance is not controlled there may be drift with time, causing unnoticed biases in both particle sizing and particle number concentration of up to several tens of per cent.

For the upper accumulation and coarse mode size ranges, optical and aerodynamic particle size spectrometers (OPSSs and APSSs) are employed. The technology of the APSS is well established and is commercially available. Comparison results of these instruments can be consulted in the report of the APSS workshop 2014. The APSSs are robust and designed for long-term operations. There are several different OPSSs on the market, some of which could be used for long-term measurements. OPSSs include a number of relatively small, low-cost instruments utilizing laser diodes that have to be operated carefully to deliver reliable quantitative measurements. Both APSSs and OPSSs need regular QA sizing checks on site. Additionally, annual or biannual calibrations against traceable standards and reference instruments are required. If OPSSs or APSSs performance is not controlled, both instrument types might drift with time, causing an unnoticed bias of up to several tens of per cent.

### 16.6.4 Cloud condensation nuclei

Measurements of CCN are made to determine the concentration and establish climatology of those particles that have the potential to produce cloud droplets at supersaturations typical of natural clouds, that is, less than about 1%. Past CCN measurements in the GAW Programme have been made predominantly using static thermal-gradient chambers, which are well suited to relatively low-frequency sampling and low-resolution (differential) CCN spectrum determination. Instruments utilizing continuous flow now have established technology and are commercially available, and are becoming the recommended technical approach at a growing number of GAW stations. The CCN counter is designed for long-term operations. However, the instruments need regular six-monthly QA calibrations with a standard aerosol on site. Additionally, annual or biannual calibrations of the CCN counter against a reference instrument are required. If a CCN counter performance is not controlled, flow might change

with time causing an ill-defined supersaturation in the instrument and a bias in the measured number concentration. Because of the complexity of the measurement, it is recommended CCN determinations be undertaken at GAW stations with more highly developed aerosol programmes.

### 16.6.5 Aerosol optical depth

The AOD is retrieved from observations of atmospheric spectral transmission. The solar spectral irradiance $I$ at a given wavelength can be expressed as:

$$I = I_0 \exp\left(-m\delta\right) \tag{16.3}$$

with $I_0$ being the extraterrestrial (top of the atmosphere) irradiance of the sun, $m$ the optical airmass and $\delta$ the total optical depth. The optical airmass equals 1 for a vertical path through the atmosphere and is roughly proportional to 1/cos $z$, with $z$ being the zenith angle of the sun during the observation. The total optical depth $\delta$ at a given wavelength is composed of several components, such as scattering by gas molecules $\delta_R$ (Rayleigh scattering), extinction by aerosol particles $\delta_A$, absorption of trace gases $\delta_G$ (ozone, nitrogen dioxide, and the like), and possible cloud contamination. Thus, the AOD can be obtained from the total optical depth by subtracting modelled estimates of the other components $\delta_A = \delta - \delta_R - \delta_G$.

Because AOD is essentially a difference between two larger numbers, it is sensitive to small calibration errors and, to a minor degree, to the methods chosen to model the other components. A traceable calibration uncertainty of 1.5%, corresponding to an uncertainty of 0.015 optical depths at unit optical airmass, should be maintained for AOD observations (WMO, 2005).

Wavelengths and bandpasses specifically for AOD that are largely free of variable extinction components (water vapour and $NO_x$) and strong ozone extinction have been recommended in WMO (2003). The Baseline Surface Radiation Network (BSRN) and GAW-PFR (a network of AOD observations with precision filter radiometers) are using four AOD channels at 368, 412, 500 and 862 nm. While some other networks have selected different wavelengths based on their specific needs (validation of satellite sensors, modelling efforts), measurements at 500 ±3 nm and 865 ±5 nm are typically available in most networks.

Measurements of the solar spectral irradiance are traditionally taken by sun-pointing radiometers (sun photometers) mounted on a two-axis solar tracker, with a sampling rate of once every minute to allow for objective QC and cloud filtering algorithms. Homogeneous QC is more difficult to achieve with handheld sun photometers.

Rotating shadow-band filter radiometers measure global and diffuse spectral irradiance at several wavelength bands. Direct normal irradiance obtained as the difference between global and diffuse radiation, normalized by the solar zenith angle, can be used to retrieve AOD in the same way as with sun photometers.

More advanced instruments like sky-scanning radiometers can be used to infer additional column aerosol optical properties, including size distribution, single-scattering albedo or phase function, through sophisticated mathematical inversion models.

Sun photometers and shadow-band and sky-scanning radiometers are commercially available from several manufacturers. Centralized data evaluation and calibration services[5] are offered for standardized instruments by global networks, such as the Aerosol Robotic Network (AERONET), GAW-PFR or SKYNET (WMO, 2005).

[5] For more details, see the World Optical Depth Research and Calibration Centre website (at https://www.pmodwrc.ch/en/home/.

### 16.6.6 GAW aerosol lidar

The basic lidar principle is the following: a laser pulse is transmitted into the atmosphere where it encounters gas molecules and particles; a small amount of this energy is backscattered in the direction of the receiver system, typically a telescope, and transferred to a photodetector such as a photomultiplier. The resulting electrical signal is proportional to the optical power received, which depends on the presence, range and concentration of atmospheric scatterers and absorbers in the light path volume. Lidar techniques are able to characterize atmospheric aerosols in terms of vertical profiles of extinction and backscatter coefficients, lidar ratio, optical depth and microphysical properties such as shape, refractive index and size distribution, on timescales as short as minutes and vertical scales as short as metres.

Lidar observations are much more powerful if used in coordinated networks. Lidar networks are fundamental to studying aerosols on a large spatial scale and to investigating transport and modification phenomena. There are several research lidar networks that contribute to GAW: the Asian Dust and Aerosol Lidar Observation Network, Latin American Lidar Network, Commonwealth of Independent States Lidar Network, European Aerosol Research Lidar Network, Micro Pulse Lidar Network, NDACC, and the US NOAA Cooperative Remote Sensing Science and Technology Lidar Network. These networks are coordinated within the GAW Aerosol Lidar Observation Network (WMO, 2008*a*).

Several different lidar techniques exist, depending on the specific instrument design and mainly on the specific laser-atmosphere scattering process.

#### Elastic backscatter lidar

This is the simplest type of aerosol lidar: the backscattered wavelength is identical to the transmitted wavelength, and the magnitude of the received signal at a given range depends on the backscatter cross-section of scatterers along the path to that range. Typical operating wavelengths are 355, 532 and 1 064 nm. The typical product of a backscatter lidar is the vertical profile of the aerosol backscatter coefficient obtained assuming a lidar ratio, that is, the extinction-to-backscatter ratio, that is mostly constant throughout the profile and usually derived from an existing climatology obtained with measurements from a Raman lidar, described later. In this sense, it is necessary to underline that without an a priori assumption about the lidar ratio, this kind of lidar system cannot provide quantitative aerosol backscatter data.

#### Depolarization lidar

These are elastic backscatter lidars equipped with channels for the detection of the two parallel and cross-polarized components of the backscattered radiation. This provides quantitative information about particle shape, strongly contributing to aerosol typing as well as to the identification of thin clouds contaminating the profiles. A depolarization channel allows discrimination of volcanic ash and other aerosol particles. Typical operating wavelengths are 355 and 532 nm. Depolarization lidar systems need accurate calibration.

#### Raman lidar

The Raman lidar technique operates by measuring the inelastic Raman scattering by a specific gas. The Raman backscattered radiation from molecular nitrogen (or oxygen) is typically used for retrieving the vertical profile of the aerosol extinction coefficient that, coupled with the elastic scattering collected at the same emission wavelength, also provides the vertical profile of the aerosol backscatter coefficient without assuming a lidar ratio. Typical operating wavelengths are 355 and 532 nm. Most of the existing Raman lidar instruments are also equipped with a depolarization channel providing data on the particle linear depolarization ratio. Advanced multiwavelength Raman aerosol lidar techniques have been demonstrated to be the only

technique capable of providing range-resolved aerosol microphysical properties. Moreover, rotational Raman lidar systems can be designed for optimizing extinction measurements in daytime conditions.

### High spectral resolution lidar

The high spectral resolution lidar (HSRL) technique provides calibrated measurements of AOD, extinction and backscatter. Measurements are computed from ratios of the particulate scattering to the measured molecular scattering. This provides absolute calibration and makes the calibration insensitive to dirt or precipitation on the output window. A very narrow, angular field-of-view reduces contamination from spurious sources, like multiple scattering contributions. The small field-of-view, coupled with a narrow optical bandwidth, nearly eliminates noise due to scattered sunlight, improving the SNR during daytime operations.

### Ceilometers

Ceilometers are basically elastic backscatter lidars that employ a diode laser source emitting at IR wavelengths (typically 905 or 1 064 nm) using a low energy but a high repetition rate (in units of μJ of energy per pulse and kHz for the rate) and that detect the elastic backscattered radiation by clouds and precipitation. Ceilometers are a self-contained, turnkey, surface-based, active, remote-sensing device designed to measure cloud-base height and potentially the backscatter signals by aerosols. Ceilometers can provide qualitative information about aerosol vertical distribution. Generally, older and typically less powerful instruments are barely able to detect aerosol layers in the atmosphere, while newer instruments can be useful for volcanic ash/dust detection and ash/dust plume tracking.

All of these lidar techniques can provide data products suitable for monitoring the spatial and temporal distribution of aerosol up to the upper troposphere/lower stratosphere region and can characterize them from a dynamical and microphysical point of view. The main lidar limitation is related to the presence of rain, dense fog and thick clouds (optical depths larger than 2–3) that do not allow monitoring of the atmosphere above the cloud-base region. The altitude range covered by lidars is limited at the bottom by the overlap height (altitude where there is a full overlap between the transmitter and the receiver), typically about 250–500 m above the ground level but can be up to 2 km above the ground depending on the specific design. The maximum altitude range strongly depends on the laser power and optical design, reaching 25–30 km for high-power systems. It is difficult to provide general estimates of the accuracy of the different lidar products because these are system specific and also depend on the prevailing meteorological conditions. On average, uncertainties for extinction and backscatter coefficient are about 20% (in the case of Raman lidar or HSRL). The retrieval of microphysical properties is possible only if optical data have uncertainties lower than 20%–30%.

Aerosol lidar products (see Table 16.4 for more details):

(a) Geometrical properties:

  (i) Layer identification (top, bottom and centre of mass);

(b) Profiles of optical properties:

  (i) Extensive optical parameters: aerosol backscatter coefficient ($\beta_a$), aerosol extinction coefficient ($\alpha_a$);

  (ii) Intensive optical parameters: lidar ratio, particle linear depolarization ratio ($\delta_a$), Ångström backscatter-related exponent ($Å_\beta$), Ångström extinction-related exponent ($Å_\alpha$);

**Table 16.4. Lidar products related to specific surface-based lidar techniques (note that (d) = daytime only)**

| *Surface-based lidar techniques* | *Geometrical properties* | $\beta_a$ | $\alpha_a$ | *Lidar ratio*[a] | *AOD* | $\mathring{A}_\beta$ | $\mathring{A}_\alpha$ | *Type*[b] | *Microphysical properties* |
|---|---|---|---|---|---|---|---|---|---|
| Ceilometer[c] | ✓ | ✓[d] | | | | | | | |
| Ceilometer + sun photometer | ✓ | ✓ | ✓(d)[e] | | ✓(d) | | | | |
| Ceilometer + sun photo. + depolarization lidar | ✓ | ✓ | ✓(d)[e] | | ✓(d) | | | ✓ (limited) | |
| 1-wavelength (1-$\lambda$) backscatter lidar | ✓ | ✓ | | | | | | | |
| 1-$\lambda$ backscatter lidar + sun photometer | ✓ | ✓ | ✓(d)[e] | | ✓(d) | | | | |
| 1-$\lambda$ backscatter lidar + sun photo. + depolarization lidar | ✓ | ✓ | ✓(d)[e] | | ✓(d) | | | ✓(d) (limited) | |
| Multiwavelength (m-$\lambda$)[f] backscatter lidar | ✓ | ✓ | | | | | ✓ | | |
| M-$\lambda$[f] backscatter lidar + sun photometer | ✓ | ✓ | ✓(d)[e] | | ✓(d) | ✓(d)[e] | ✓ | | ✓(d)[e] |
| M-$\lambda$[f] backscatter lidar + sun photo. + depolarization lidar | ✓ | ✓ | ✓(d)[e] | | ✓(d) | ✓(d)[e] | ✓ | ✓ | ✓(d)[e] |
| 1-$\lambda$ Raman lidar/ HSRL | ✓ | ✓ | ✓[g] | ✓[g] | ✓[g] | | | ✓[g] (limited) | |
| 1-$\lambda$ Raman lidar/ HSRL + sun photometer | ✓ | ✓ | ✓[g] | ✓[g] | ✓[g] | ✓(d)[e] | ✓(d)[e] | ✓ (limited) | ✓(d)[e] |
| 1-$\lambda$ Raman lidar/ HSRL + sun photo. + depolarization lidar | ✓ | ✓ | ✓[g] | ✓[g] | ✓[g] | ✓(d)[e] | ✓(d)[e] | ✓ | ✓(d)[e] |
| M-$\lambda$[f] Raman lidar | ✓ | ✓ | ✓[g] | ✓[g] | ✓[g] | ✓[g] | ✓ | ✓[g] | ✓[g] |
| M-$\lambda$[f] Raman lidar + sun photometer | ✓ | ✓ | ✓[g] | ✓[g] | ✓[g] | ✓[g] | ✓ | ✓ | ✓[g] |
| M-$\lambda$[f] Raman lidar + sun photo. + depolarization lidar | ✓ | ✓ | ✓[g] | ✓[g] | ✓[g] | ✓[g] | ✓ | ✓ | ✓[g] |

Notes:
a From two independent measurements
b Identification of scattering type (aerosol particles, cloud droplets, ice crystals, some aerosol type information)
c A ceilometer is a single-wavelength, low-power lidar, with lower SNR.
d If calibrated
e Estimate only
f m > 2
g Most Raman lidar systems operate during night-time. Some 24-h Raman lidar systems exist and their operability has been proved. However, few systems nowadays operate Raman channels during daytime; HSRL is independent of daytime.

(c) Optical properties in the identified layer:

  (i) Integrated backscatter, AOD;

  (ii) Mean intensive optical parameters (lidar ratio, particle linear depolarization ratio, Ångström backscatter-related exponent, Ångström extinction-related exponent);

(d) Aerosol typing classification;

(e) Mass concentration estimate;

(f) Microphysical properties retrieved.

## 16.7 NATURAL RADIOACTIVITY

The global distributions of the source/sink terms of the naturally occurring radionuclides ($^{7}$Be, $^{10}$Be, $^{210}$Pb and $^{222}$Rn) and the anthropogenic radionuclides ($^{85}$Kr) are reasonably well known. $^{7}$Be and $^{10}$Be are produced by cosmic-ray interactions in the upper troposphere and lower stratosphere. $^{222}$Rn is exhaled from the Earth's land surface as a result of uranium decay in soil. $^{210}$Pb is produced in the lower troposphere from the decay of $^{222}$Rn. Most of the $^{85}$Kr in the atmosphere is released during nuclear fuel reprocessing. Atoms of $^{7}$Be, $^{10}$Be and $^{210}$Pb attach themselves to submicron-size aerosol particles, and therefore act as aerosol-borne tracers in the atmosphere. $^{222}$Rn and $^{85}$Kr, which are chemically and physically inert, act as noble gases in the atmosphere.

Measurements of radionuclides are not a priority area within the GAW Programme. Some general recommendations can be found in WMO (2001) and WMO (2004*b*).

## ANNEX. GAW CENTRAL FACILITIES

List of GAW central facilities and host institutions (as stated in WMO, 2017a); the World Central Facilities have assumed global responsibilities, unless indicated.

| *Variable* | *Quality Assurance/ Science Activity Centre (QA/SAC)* | *Central Calibration Laboratory (CCL)* | *World Calibration Centre (WCC)* | *Regional Calibration Centre (RCC)* | *World Data Centre (WDC)* |
|---|---|---|---|---|---|
| $CO_2$ | JMA (Asia, South-West Pacific)<br><br>Empa (Americas, Europe, Africa) | NOAA-ESRL | NOAA-ESRL (round robin)<br><br>Empa (audits) | | JMA |
| $CO_2$ isotopes | | MPI-BGC | | | JMA |
| $CH_4$ | Empa (Americas, Europe, Africa)<br><br>JMA (Asia, South-West Pacific) | NOAA-ESRL | Empa (Americas, Europe, Africa)<br><br>JMA (Asia, South-West Pacific) | | JMA |
| $N_2O$ | Empa | NOAA-ESRL | Empa | | JMA |
| $SF_6$ | | NOAA-ESRL | KMA | | JMA |
| CFCs, HCFCs, HFCs | | METAS (HFO-1234yf, HFC-125, CFC-13, HCFC-132b, 1,2-dichloroethane, HFO-1336mzz(Z), HFC-32, HFC-365mfc, $CH_2Cl_2$, $CCl_4$ | | | JMA |
| Surface Ozone | Empa | NIST | Empa | OCBA (South America) | NILU |
| CO | Empa | NOAA-ESRL | Empa | | JMA |
| VOCs | UBA | NPL (ethane, propane, n-butane, isobutane, n-pentane, isopentane, acetylene, toluene, benzene, isoprene)<br><br>NIST (monoterpenes)<br><br>KRISS (DMS) | FZJ/IEK-8 | | NILU |
| $NO_x$ | UBA | NPL | FZJ(IEK-8) | | NILU |
| $SO_2$ | | | | | NILU |

| *Variable* | *Quality Assurance/ Science Activity Centre (QA/SAC)* | *Central Calibration Laboratory (CCL)* | *World Calibration Centre (WCC)* | *Regional Calibration Centre (RCC)* | *World Data Centre (WDC)* |
|---|---|---|---|---|---|
| $H_2$ | | MPI-BGC | | | JMA |
| Precipitation Chemistry/Wet Deposition | NOAA-ARL (Americas) | ISWS | ISWS | | NOAA-ARL |
| Total Ozone | JMA (Asia, South-West Pacific) | NOAA-ESRL (Dobson instruments)<br><br>ECCC (Brewer instruments) | NOAA-ESRL (Dobson instruments)<br><br>ECCC (Brewer instruments) | Dobson instruments:<br><br>(general forum)<br><br>BoM (Australia & Oceania)<br><br>NOAA-ESRL<br><br>JMA (Asia)<br><br>DWD-MOHp (Europe)<br><br>CHMI-SOO-HK (Europe)<br><br>OCBA (South America)<br><br>SAWS (Africa)<br><br>Brewer instruments:<br><br>IARC-AEMET (Europe)<br><br>Filter instruments:<br><br>MGO | ECCC (Ground based observations)<br><br>DLR (Satellite based observations) |
| Ozone Profile | RMI | FZJ(IEK-8) | FZJ(IEK-8) | | ECCC |
| UV Radiation | | | PMOD/WRC | NOAA-ESRL (Americas) | ECCC |
| Aerosol Physical Properties | UBA | | IfT | | NILU (Ground based observations)<br><br>DLR (Satellite based observations) |
| Aerosol Optical Depth | UBA | PMOD/WRC (Precision Filter Radiometers) | PMOD/WRC | | NILU (Ground based observations)<br><br>DLR (Satellite based observations) |

| *Variable* | *Quality Assurance/ Science Activity Centre (QA/SAC)* | *Central Calibration Laboratory (CCL)* | *World Calibration Centre (WCC)* | *Regional Calibration Centre (RCC)* | *World Data Centre (WDC)* |
|---|---|---|---|---|---|
| Aerosol Chemical Properties | | | | | NILU |
| Solar Radiation | | PMOD/WRC | PMOD/WRC | | MGO |

**Host institutions**

| | |
|---|---|
| BoM | Bureau of Meteorology, Melbourne, Australia |
| BSRN | Baseline Surface Radiation Network, Federal Institute of Technology (ETH), Zürich, Switzerland |
| CHMI | Czech Hydrometeorological Institute |
| DLR | Deutsches Zentrum für Luft- und Raumfahrt (German Aerospace Centre), Oberpfaffenhofen, Wessling, Germany |
| DWD | German Meteorological Service (Deutscher Wetterdienst) |
| ECCC | Environment and Climate Change Canada, Toronto, Ontario, Canada |
| EML | Environmental Measurements Laboratory, Department of Energy (DoE), New York City, New York, USA |
| Empa | Swiss Federal Laboratories for Materials Testing and Research, Dübendorf, Switzerland |
| FZJ (IEK-8) | Forschungszentrum Jülich, Institute of Energy and Climate Research: Troposphere (IEK-8), Jülich, Germany |
| IARC-AEMET | Izaña Atmospheric Research Centre - La Agencia Estatal de Meteorología, Tenerife, Spain |
| IfT | Institute for Tropospheric Research, Leipzig, Germany |
| ISWS | Illinois State Water Survey, Champaign, IL, United States |
| JMA | Japan Meteorological Agency, Tokyo, Japan |
| KMA | Korea Meteorological Administration, Seoul, Republic of Korea |
| METAS | Federal Institute of Metrology, Bern, Switzerland |
| MGO | A.I. Voeikov Main Geophysical Observatory, Russian Federal Service for Hydrometeorology and Environmental Monitoring, St. Petersburg, Russian Federation |
| MOHp | Meteorologisches Observatorium Hohenpeissenberg, Hohenpeissenberg, Germany |
| MPI-BGC | Max Planck Institute for Biogeochemistry, Jena, Germany |
| NILU | Norwegian Institute for Air Research, Kjeller, Norway |
| NIST | National Institute of Standards and Technology, Gaithersburg, MD, United States |
| NOAA-ARL | NOAA, Air Resources Laboratory, Silver Spring, MD, United States |
| NOAA-ESRL | NOAA, Earth System Research Laboratory, Global Monitoring Division, Boulder, CO, United States |
| NPL | National Physical Laboratory, Teddington, Middlesex, United Kingdom |
| OCBA | Observatorio Central de Buenos Aires, Buenos Aires, Argentina |
| PMOD/WRC | Physikalisch-Meteorologisches Observatorium Davos/World Radiation Centre, Davos, Switzerland |
| SAWS | South African Weather Service, Pretoria, South Africa |
| SOO-HK | Solar and Ozone Observatory, Hradec Kralove, Czech Republic |
| UBA | Umweltbundesamt (German Environmental Agency), Berlin, Germany |

## REFERENCES AND FURTHER READING


Birch, M.E. and R.A. Cary, 1996: Elemental carbon-based method for monitoring occupational exposures to particulate diesel exhaust. *Aerosol Science and Technology*, 25:221–241.

Cavalli, F., M. Viana, K.E. Yttri, J. Genberg and J.-P. Putaud, 2010: Toward a standardised thermal-optical protocol for measuring atmospheric organic and elemental carbon: the EUSAAR protocol. *Atmospheric Measurement Techniques*, 3:79–89.

Chow, J.C., J.G. Watson, L.-W.A. Chen, G. Paredes-Miranda, M.-C.O. Chang, D. Trimble, K.K. Fung, H. Zhang and J. Zhen Yu, 2005: Refining temperature measures in thermal/optical carbon analysis. *Atmospheric Chemistry and Physics*, 5:2961–2972.

Chow, J.C., J.G. Watson, D. Crow, D.H. Lowenthal and T. Merrifield, 2001: Comparison of IMPROVE and NIOSH carbon measurements. *Aerosol Science and Technology*, 34:23–34.

Chow, J.C., J.G. Watson, L.C. Pritchett, W.R. Pierson, C.A. Frazier and R.G. Purcell, 1993: The DRI thermal/optical reflectance carbon analysis system: Description, evaluation, and applications in U.S. air quality studies. *Atmospheric Environment*, 27A(8):1185–1201.

Coplen, T.B., W.A. Brand, M. Gehre, M. Gröning, H.A.J. Meijer, B. Toman and R.M. Verkouteren, 2006: New Guidelines for $\delta^{13}C$ Measurements. *Analytical Chemistry*, 78(7):2439–2441.

EMEP, 2014: *EMEP Manual for Sampling and Chemical Analysis.* Kjeller, Norwegian Institute for Air Research, available from https://projects.nilu.no/ccc/manual/index.html.

European Committee for Standardization (CEN), 2017: Ambient air - Measurement of elemental carbon (EC) and organic carbon (OC) collected on filters. EN-16909:2017. Comité European de Normalisation.

de Laeter, J.R., J.K. Böhlke, P. De Bièvre, H. Hidaka, H.S. Peiser, J.K.R. Rosman and P.D. Taylor, 2003: Atomic weights of the elements: Review 2000. IUPAC Technical Report. *Pure and Applied Chemistry*, 75:683–800.

Ge, B., Y. Sun, Y. Liu, H. Dong, D. Ji, Q. Jiang, J. Li and Z. Wang, 2013: Nitrogen dioxide measurements by cavity attenuated phase shift spectroscopy (CAPS) and implications in ozone production efficiency and nitrate formation in Beijing, China. *Journal of Geophysical Research: Atmospheres,* 118:9499–9509, doi:10.1002/jgrd.50757.

Götz, F.W.P., A.R. Meetham and G.M.B. Dobson, 1934: The vertical distribution of ozone in the atmosphere. *Proceedings of the Royal Society of London*, A145(855):416–446.

Grant, A., C.S. Witham, P.G. Simmonds, A.J. Manning and S. O'Doherty, 2010: A 15 year record of high-frequency, in situ measurements of hydrogen at Mace Head, Ireland. *Atmospheric Chemistry and Physics*, 10:1203–1214 (available from http://www.atmos-chem-phys.net/10/1203/2010/acp-10-1203-2010.pdf).

Herndon, S.C., M.S. Zahniser, D.D. Nelson Jr., J. Shorter, J.B. McManus, R. Jiménez, C. Warneke and J.A. de Gouw, 2007: Airborne measurements of HCHO and HCOOH during the New England Air Quality Study 2004 using a pulsed quantum cascade laser spectrometer. *Journal of Geophysical Research*, 112(D10S03).

Hönninger, G., C. von Friedeburg and U. Platt, 2004: Multi axis differential optical absorption spectroscopy (MAX-DOAS). *Atmospheric Chemistry and Physics,* 4:231–254, https://doi.org/10.5194/acp-4-231-2004.

International Organization for Standardization/International Electrotechnical Commission, 2008: *Uncertainty of Measurement – Part 3: Guide to the Expression of Uncertainty in Measurement*, ISO/IEC Guide 98-3:2008, Incl. Suppl. 1:2008/Cor 1:2009, Suppl. 1:2008, Suppl. 2:2011. Geneva. (equivalent to: Joint Committee for Guides in Metrology, 2008: *Evaluation of Measurement Data – Guide to the Expression of Uncertainty in Measurement*, JCGM 100:2008, Corrected in 2010).

Jaroslawski, J., 2013: Improvement of the Umkehr ozone profile by the neural network method: analysis of the Belsk (51.80° N, 20.80° E) Umkehr data. *International Journal of Remote Sensing*, 34(15):5541–5550.

Jordan, A. and B. Steinberg, 2011: Calibration of atmospheric hydrogen measurements. *Atmospheric Measurement Techniques,* 4:509–521.

Kelly, T.J., C.W. Spicer and G.F. Ward, 1990: An assessment of the luminol chemiluminescence technique for measurement of $NO_2$ in ambient air. *Atmospheric Environment,* 24A(9):2397–2403.

Kuang, S., Newchurch M.J., Burris J. and Liu X., 2013: Ground-based lidar for atmospheric boundary layer ozone measurements. *Applied Optics*, 52(15):3557–3566, http://dx.doi.org/10.1364/AO.52.003557.

Lebegue, B., M. Schmidt, M. Ramonet, B. Wastine, C. Yver Kwok, O. Laurent, S. Belviso, A. Guemri, C. Philippon, J. Smith and S. Conil, 2016: Comparison of nitrous oxide ($N_2O$) analyzers for high-precision measurements of atmospheric mole fractions. *Atmospheric Measurement Techniques*, 9:1221–1238.

Mateer, C.L. and J.J. DeLuisi, 1992: A new Umkehr inversion algorithm. *Journal of Atmospheric and Terrestrial Physics*, 54(5):537–556.

Mateer, C.L. and H.U. Dütsch, 1964: *Uniform Evaluation of Umkehr Observations from the World Ozone Network, Part I – Proposed Standard Evaluation Technique*. NCAR, Boulder, Colorado.

Nash, T., 1953: The colorimetric estimation of formaldehyde by means of the Hantzsch reaction. *Biochemical Journal*, 55(3):416–421, doi: 10.1042/bj0550416.

Novelli, P., A.M. Crotwell and B.D. Hall, 2009: Application of gas chromatography with a pulsed discharge helium ionization detector for measurements of molecular hydrogen in the atmosphere. *Environmental Science and Technology*, 43(7):2431–2436, doi: 10.1021/es803180g.

Petropavlovskikh, I., P.K. Bhartia and J. DeLuisi, 2005: New Umkehr ozone profile retrieval algorithm optimized for climatological studies. *Geophysical Research Letters*, 32(L16808).

Petzold, A., J.A. Ogren, M. Fiebig, P. Laj, S.-M. Li, U. Baltensperger, T. Holzer-Popp, S. Kinne, G. Pappalardo, N. Sugimoto, C. Wehrli, A. Wiedensohler and X.-Y. Zhang, 2013: Recommendations for reporting "black carbon" measurements. *Atmospheric Chemistry and Physics*, 13:8365–8379.

Platt U. and J. Stutz, 2008: Differential Optical Absorption Spectroscopy (DOAS)—Principles and Applications. 10.1007/978-3-540-75776-4.

Ramanathan, K.R. and J.V. Dave, 1957: The calculation of the vertical distribution of ozone by the Götz Umkehr Effect (method B). *Annals of the International Geophysical Year*, V(1):23–45.

Rella, C. W., H. Chen, A.E. Andrews, A. Filges, C. Gerbig, J. Hatakka, A. Karion, N.L.Miles, S.J. Richardson, M. Steinbacher, C. Sweeney, B. Wastine and C. Zellweger, 2013: High accuracy measurements of dry mole fractions of carbon dioxide and methane in humid air. *Atmospheric Measurement Techniques*, 6:837–860.

Schmid, H., L. Laskus, H.J. Abraham, U. Baltensperger, V. Lavanchy, M. Bizjak, P. Burba, H. Cachier, D. Crow, J. Chow, T. Gnauk, A. Even, H.M. ten Brink, K.P. Giesen, R. Hitzenberger, C. Hueglin, W. Maenhaut, C. Pio, A. Carvalho, J.-P. Putaud, D. Toom-Sauntry and H. Puxbaum, 2001: Results of the "carbon conference" international aerosol carbon round robin test stage I. *Atmospheric Environment*, 35(12):2111–2121.

Schultz, M.G., H. Akimoto, J. Bottenheim, B. Buchmann, I.E. Galbally, S. Gilge, D. Helmig, H. Koide, A.C. Lewis, P.C. Novelli, C. Plass-Dülmer, T.B. Ryerson, M. Steinbacher, R. Steinbrecher, O. Tarasova, K. Torseth, V. Thouret and C. Zellweger, 2015: The Global Atmosphere Watch reactive gases measurement network. *Elementa Science of the Anthropocene*, 3:1–23, https://online.ucpress.edu/elementa/article/doi/10.12952/journal.elementa.000067/112741/The-Global-Atmosphere-Watch-reactive-gases?searchresult=1.

Sofieva, V.F., N. Rahpoe, J. Tamminen, E. Kyrölä, N. Kalakoski, M. Weber, A. Laeng, T. von Clarmann, G. Stiller, S. Lossow, D. Degenstein, A. Bourassa, C. Adams, C. Roth, N. Lloyd, P. Bernath, R.J. Hargreaves, J. Urban, D. Murtagh, A. Hauchecorne, M. van Roozendael, N. Kalb and C. Zehner, 2013: Harmonized dataset of ozone profiles from satellite limb and occultation measurements. *Earth System Science Data Discussions*, 6:189–222.

Tegtmeier, S., M.I. Hegglin, J. Anderson, A. Bourassa, S. Brohede, D. Degenstein, L. Froidevaux, R. Fuller, B. Funke, J. Gille, A. Jones, Y. Kasai, K. Krüger, E. Kyrölä, G. Lingenfelser, J. Lumpe, B. Nardi, J. Neu, D. Pendlebury, E. Remsberg, A. Rozanov, L. Smith, M. Toohey, J. Urban, T. von Clarmann, K.A. Walker, and R. Wang, 2013: SPARC Data Initiative: A comparison of ozone climatologies from international limb satellite sounders. *Journal of Geophysical Research*, 118:12229–12247.

Tuzson, B., K. Zeyer, M. Steinbacher, J.B. McManus, D.D. Nelson, M.S. Zahniser and L. Emmenegger, 2013: Selective measurements of NO, $NO_2$ and $NO_y$ in the free troposphere using quantum cascade laser spectroscopy. *Atmospheric Measurement Techniques*, 6:927–936.

van der A, R. J., M.A.F. Allaart and H.J. Eskes, 2010: Multi sensor reanalysis of total ozone. *Atmospheric Chemistry and Physics*, 10:11277–11294.

Vardag, S.N., S. Hammer, S. O'Doherty, T.G. Spain, B. Wastine, A. Jordan and I. Levin, 2014: Comparisons of continuous atmospheric $CH_4$, $CO_2$ and $N_2O$ measurements – results from a travelling instrument campaign at Mace Head. *Atmospheric Chemistry and Physics,* 14:8403-8418.

Warneke, C., P. Veres, J.S. Holloway, J. Stutz, C. Tsai, S. Alvarez, B. Rappenglueck, F.C. Fehsenfeld, M. Graus, J.B. Gilman and J.A. de Gouw, 2011: Airborne formaldehyde measurements using PTR-MS: calibration, humidity dependence, inter-comparison and initial results. *Atmospheric Measurement Techniques*, 4:2345–2358.

Watson, J.G., J.C. Chow, L.-W. A. Chen and N.H. Frank, 2009: Methods to assess carbonaceous aerosol sampling artifacts for IMPROVE and other long-term networks. *Journal of the Air and Waste Management Association*, 59(8):898–911.

Wisthaler, A., E.C. Apel, J. Bossmeyer, A. Hansel, W. Junkermann, R. Koppmann, R. Meier, K. Müller, S.J. Solomon, R. Steinbrecher, R. Tillmann and T. Brauers, 2008: Technical note: Intercomparison of formaldehyde measurements at the atmosphere simulation chamber SAPHIR. *Atmospheric Chemistry and Physics*, 8:2189–2200.

World Meteorological Organization, 2001: *Global Atmosphere Watch Measurements Guide*. Global Atmosphere Watch Report No. 143 (WMO/TD-No. 1073). Geneva.

———, 2003: *Quality Assurance in Monitoring Solar Ultraviolet Radiation: the State of the Art* (A.R. Webb). Global Atmosphere Watch Report No. 146 (WMO/TD-No. 1180). Geneva.

———, 2004*a*: *Manual for the GAW Precipitation Chemistry Programme a Guidelines, Data Quality Objectives and Standard Operating Procedures* (M.A. Allan, ed.). Global Atmosphere Watch Report No. 160 (WMO/TD-No. 1251). Geneva.

———, 2004*b*: *1st International Expert Meeting on Sources and Measurements of Natural Radionuclides Applied to Climate and Air Quality Studies (Gif sur Yvette, France, 3–5 June 2003)*. Global Atmosphere Watch Report No. 155 (WMO/TD-No. 1201). Geneva.

———, 2005: *WMO/GAW Experts Workshop on a Global Surface-based Network for Long Term Observations of Column Aerosol Optical Properties* (U. Baltensperger, L. Barrie and C. Wehrli, eds.) (Davos, Switzerland, 8–10 March 2004). Global Atmosphere Watch Report No. 162 (WMO/TD-No. 1287). Geneva.

———, 2007: *A WMO/GAW Expert Workshop on Global Long-Term Measurements of Volatile Organic Compounds (VOCs)* (Geneva, Switzerland, 30 January to 1 February 2006). Global Atmosphere Watch Report No. 171 (WMO/TD-No. 1373). Geneva.

———, 2008*a*: *Plan for the Implementation of the GAW Aerosol Lidar Observation Network GALION* (J. Bösenberg and R. Hoff) (Hamburg, Germany, 27–29 March 2007). Global Atmosphere Watch Report No. 178 (WMO/TD-No. 1443). Geneva.

———, 2008*b*: *The Tenth Biennial WMO Consultation on Brewer Ozone and UV Spectrophotometer Operation, Calibration and Data Reporting* (C.T. McElroy and E.W. Hare, eds.) (Northwich, United Kingdom, 4–8 June 2007). Global Atmosphere Watch Report No. 176 (WMO/TD-No. 1420). Geneva.

———, 2008*c*: *Operations Handbook – Ozone Observations with a Dobson Spectrophotometer* (W.D. Komhyr 1980; revised by R.D. Evans). Global Atmosphere Watch Report No. 183 (WMO/TD-No. 1469). Geneva.

———, 2009: *Guidelines for the Measurement of Methane and Nitrous Oxide and their Quality Assurance*. Global Atmosphere Watch Report No. 185 (WMO/TD-No. 1478). Geneva.

———, 2010: *Guidelines for the Measurement of Atmospheric Carbon Monoxide*. Global Atmosphere Watch Report No. 192 (WMO/TD-No. 1551). Geneva.

———, 2011: *WMO/GAW Standard Operating Procedures for In situ Measurements of Aerosol Mass Concentration, Light Scattering and Light Absorption* (J.A. Ogren, ed.). Global Atmosphere Watch Report No. 200. Geneva.

———, 2012: *Standard Operating Procedures (SOPs) for Air Sampling in Stainless Steel Canisters for Non-Methane Hydrocarbons Analysis* (R. Steinbrecher and E. Weiß). Global Atmosphere Watch Report No. 204. Geneva.

———, 2013: *Guidelines for Continuous Measurements of Ozone in the Troposphere* (I.E. Galbally and M.G. Schultz). Global Atmosphere Watch Report No. 209 (WMO-No. 1110). Geneva.

———, 2014: *Quality Assurance and Quality Control for Ozonesonde Measurements in GAW* (H.G.J. Smit and ASOPOS Panel). Global Atmosphere Watch Report No. 201. Geneva.

———, 2015*a*: *Report of the Second Session of the CAS Environmental Pollution and Atmospheric Chemistry Scientific Steering Committee (EPAC SSC)* (Geneva, Switzerland, 18-20 February 2015). Global Atmosphere Watch Report No. 220. Geneva.

———, 2015*b*: *Eighth Intercomparison Campaign of the Regional Brewer Calibration Center for Europe (RBCC-E)*, (El Arenosillo Sounding Station, Heulva, Spain, 10-20 June 2013), Global Atmosphere Watch Report No. 223. Geneva.

———, 2015*c*: *Ninth Intercomparison Campaign of the Regional Brewer Calibration Center for Europe (RBCC-E)*, (Lichtklimatisches Observatorium, Arosa, Switzerland, 14-26 July 2014). Global Atmosphere Watch Report No. 224. Geneva.

———, 2015*d*: *Absorption Cross-Sections of Ozone (ACSO) Status Report as of December 2015*, Global Atmosphere Watch Report No. 218. Geneva.

———, 2015*e*: *Analytical Methods for Atmospheric SF6 Using Gas Chromatography with micro Electron Capture Detector (GC-μECD)*, Global Atmosphere Watch Report No. 222 (KMA Technical Note CCMD 2015-3). Geneva.

———, 2016a: The Global Observing System for Climate: Implementation Needs, GCOS-200 (GOOS-214). Geneva.

———, 2016*b*: *WMO/UNEP Dobson Data Quality Workshop*, (Hradec Kralove, Czech Republic, 14-18 February 2011), Global Atmosphere Watch Report No. 225. Geneva.

———, 2016*c*: *18th WMO/IAEA Meeting on Carbon Dioxide, Other Greenhouse Gases and Related Tracers Measurement Techniques (GGMT-2015)*, (La Jolla, CA, USA, 13-17 September 2015), Global Atmosphere Watch Report No. 229. Geneva.

———, 2016*d*: *WMO/GAW Aerosol Measurement Procedures, Guidelines and Recommendations*, 2nd Edition, Global Atmosphere Watch Report No. 227 (WMO-No. 1177). Geneva.

———, 2017*a*: *WMO Global Atmosphere Watch (GAW) Implementation Plan: 2016-2023*. Global Atmosphere Watch Report No. 228. Geneva.

———, 2017*b*: *Report of the WMO/GAW Expert Meeting on Nitrogen Oxides and International Workshop on the Nitrogen Cycle*, (York, United Kingdom, 12 - 14 April 2016), Global Atmosphere Watch Report No. 232. Geneva.

———, 2018: *WMO/GAW Calibration Methods of GC-μECD for Atmospheric SF6 Measurements, KMA Technical Note CCMD2016-6*, Global Atmosphere Watch Report No. 239. Geneva.

World Meteorological Organization, World Health Organization, UN Environment, International Global Atmospheric Chemistry and the European Monitoring and Evaluation Programme: *Low-cost Sensors for the Measurement of Atmospheric Composition: Overview of Topic and Future Applications* (A.C Lewis, E. von Schneidemesser and R.E. Peltier, eds) (WMO-No. 1215). Geneva.

Wunch, D., G.C.Toon, P.O. Wennberg, S.C. Wofsy, B.B. Stephens, M.L. Fischer, O. Uchino, J.B. Abshire, P. Bernath, S.C. Biraud, J.-F.L.Blavier, C. Boone, K.P.,Bowman, E.V. Browell, T. Campos, B.J. Connor, B.C. Daube, N.M. Deutscher, M. Diao, J.W. Elkins, C. Gerbig, E. Gottlieb, D.W.T. Griffith, D.F. Hurst, R. Jiménez, G. Keppel-Aleks, E.A. Kort, R. Macatangay, T. Machida, H. Matsueda, F. Moore, I. Morino, ,S. Park, J. Robinson, C.M. Roehl, Y. Sawa, V. Sherlock, C. Sweeney, T. Tanaka and M.A. Zondlo, 2010: Calibration of the Total Carbon Column Observing Network using aircraft profile data. *Atmospheric Measurement Techniques*, 3:1351–1362, https://doi.org/10.5194/amt-3-1351-2010.

Zellweger, C., C. Hüglin, J. Klausen, M. Steinbacher, M Vollmer and B. Buchmann, 2009: Inter-comparison of four different carbon monoxide measurement techniques and evaluation of the long-term carbon monoxide time series of Jungfraujoch. *Atmospheric Chemistry and Physics*, 9:3491–3503.

Zellweger, C., M. Steinbacher and B. Buchmann, 2012: Evaluation of new laser spectrometer techniques for in situ carbon monoxide measurements, *Atmospheric Measurement Techniques*, 5:2555–2567.

Zellweger, C., L. Emmenegger, M. Firdaus, J. Hatakka, M. Heimann, E. Kozlova, T.G. Spain, M. Steinbacher, M.V. van der Schoot and B. Buchmann, 2016: Assessment of recent advances in measurement techniques for atmospheric carbon dioxide and methane observations. *Atmos. Meas. Tech.,* 9: 4737-4757, doi:10.5194/amt-9-4737-2016.

For more information, please contact:

**World Meteorological Organization**

7 bis, avenue de la Paix – P.O. Box 2300 – CH 1211 Geneva 2 – Switzerland

**Strategic Communications Office**

Tel.: +41 (0) 22 730 83 14

Email: cpa@wmo.int

**wmo.int**

JN 24602